

ASSESSING THE PHARMACOLOGICAL EFFECTS AND THERAPEUTIC POTENTIAL OF TRADITIONAL CHINESE MEDICINE IN NEUROLOGICAL DISEASE MODELS: AN UPDATE

EDITED BY: Jiahong Lu, Min Li and Juxian Song
PUBLISHED IN: Frontiers in Pharmacology





frontiers

Frontiers eBook Copyright Statement

The copyright in the text of individual articles in this eBook is the property of their respective authors or their respective institutions or funders. The copyright in graphics and images within each article may be subject to copyright of other parties. In both cases this is subject to a license granted to Frontiers.

The compilation of articles constituting this eBook is the property of Frontiers.

Each article within this eBook, and the eBook itself, are published under the most recent version of the Creative Commons CC-BY licence.

The version current at the date of publication of this eBook is CC-BY 4.0. If the CC-BY licence is updated, the licence granted by Frontiers is automatically updated to the new version.

When exercising any right under the CC-BY licence, Frontiers must be attributed as the original publisher of the article or eBook, as applicable.

Authors have the responsibility of ensuring that any graphics or other materials which are the property of others may be included in the CC-BY licence, but this should be checked before relying on the CC-BY licence to reproduce those materials. Any copyright notices relating to those materials must be complied with.

Copyright and source acknowledgement notices may not be removed and must be displayed in any copy, derivative work or partial copy which includes the elements in question.

All copyright, and all rights therein, are protected by national and international copyright laws. The above represents a summary only. For further information please read Frontiers' Conditions for Website Use and Copyright Statement, and the applicable CC-BY licence.

ISSN 1664-8714

ISBN 978-2-88976-191-3

DOI 10.3389/978-2-88976-191-3

About Frontiers

Frontiers is more than just an open-access publisher of scholarly articles: it is a pioneering approach to the world of academia, radically improving the way scholarly research is managed. The grand vision of Frontiers is a world where all people have an equal opportunity to seek, share and generate knowledge. Frontiers provides immediate and permanent online open access to all its publications, but this alone is not enough to realize our grand goals.

Frontiers Journal Series

The Frontiers Journal Series is a multi-tier and interdisciplinary set of open-access, online journals, promising a paradigm shift from the current review, selection and dissemination processes in academic publishing. All Frontiers journals are driven by researchers for researchers; therefore, they constitute a service to the scholarly community. At the same time, the Frontiers Journal Series operates on a revolutionary invention, the tiered publishing system, initially addressing specific communities of scholars, and gradually climbing up to broader public understanding, thus serving the interests of the lay society, too.

Dedication to Quality

Each Frontiers article is a landmark of the highest quality, thanks to genuinely collaborative interactions between authors and review editors, who include some of the world's best academicians. Research must be certified by peers before entering a stream of knowledge that may eventually reach the public - and shape society; therefore, Frontiers only applies the most rigorous and unbiased reviews.

Frontiers revolutionizes research publishing by freely delivering the most outstanding research, evaluated with no bias from both the academic and social point of view. By applying the most advanced information technologies, Frontiers is catapulting scholarly publishing into a new generation.

What are Frontiers Research Topics?

Frontiers Research Topics are very popular trademarks of the Frontiers Journals Series: they are collections of at least ten articles, all centered on a particular subject. With their unique mix of varied contributions from Original Research to Review Articles, Frontiers Research Topics unify the most influential researchers, the latest key findings and historical advances in a hot research area! Find out more on how to host your own Frontiers Research Topic or contribute to one as an author by contacting the Frontiers Editorial Office: frontiersin.org/about/contact

ASSESSING THE PHARMACOLOGICAL EFFECTS AND THERAPEUTIC POTENTIAL OF TRADITIONAL CHINESE MEDICINE IN NEUROLOGICAL DISEASE MODELS: AN UPDATE

Topic Editors:

Jiahong Lu, University of Macau, China

Min Li, Hong Kong Baptist University, Hong Kong, SAR China

Juxian Song, Guangzhou University of Chinese Medicine, China

Citation: Lu, J., Li, M., Song, J., eds. (2022). Assessing the Pharmacological Effects and Therapeutic Potential of Traditional Chinese Medicine in Neurological Disease Models: An Update. Lausanne: Frontiers Media SA.
doi: 10.3389/978-2-88976-191-3

Table of Contents

- 05 Editorial: Assessing the Pharmacological Effects and Therapeutic Potential of Traditional Chinese Medicine in Neurological Disease Models: An Update**
Zhiqiang Deng, Yuxuan Kan, Min Li, Juxian Song and Jia-Hong Lu
- 08 Yuan-Hu Zhi Tong Prescription Mitigates Tau Pathology and Alleviates Memory Deficiency in the Preclinical Models of Alzheimer's Disease**
A. Iyaswamy, S. K. Krishnamoorthi, Y. W. Liu, J. X. Song, A. K. Kammala, S. G. Sreenivasmurthy, S. Malampati, B. C. K. Tong, K. Selvarasu, K. H. Cheung, J. H. Lu, J. Q. Tan, C. Y. Huang, S. S. K. Durairajan and M. Li
- 25 Elaphuri Davidiani Cornu Improves Depressive-Like Behavior in Mice and Increases Neurotrophic Factor Expression in Mouse Primary Astrocytes via cAMP and ERK-Dependent Pathways**
Yue Zhu, Mengqiu Liu, Suchen Qu, Cheng Cao, Chongqi Wei, Xue-er Meng, Qianyin Lou, Dawei Qian, Jin-ao Duan, Yuhua Ding, Zhengxiang Han and Ming Zhao
- 35 Taohong Siwu Decoction Ameliorates Ischemic Stroke Injury Via Suppressing Pyroptosis**
Mengmeng Wang, Zhuqing Liu, Shoushan Hu, Xianchun Duan, Yanyan Zhang, Can Peng, Daiyin Peng and Lan Han
- 44 Berberine Protects Against NLRP3 Inflammasome via Ameliorating Autophagic Impairment in MPTP-Induced Parkinson's Disease Model**
Shuxuan Huang, Hanqun Liu, Yuwan Lin, Muchang Liu, Yanhua Li, Hengxu Mao, Zhiling Zhang, Yunlong Zhang, Panghai Ye, Liuyan Ding, Ziting Zhu, Xinling Yang, Chaojun Chen, Xiaoqin Zhu, Xiaoyun Huang, Wenyan Guo, Pingyi Xu and Lin Lu
- 59 Effect and Mechanism of Catalpol on Remyelination via Regulation of the NOTCH1 Signaling Pathway**
Yaqin Sun, Jing Ji, Zheng Zha, Hui Zhao, Bing Xue, Liangyun Jin and Lei Wang
- 75 The Combination of Aquilaria sinensis (Lour.) Gilg and Aucklandia costus Falc. Volatile Oils Exerts Antidepressant Effects in a CUMS-Induced Rat Model by Regulating the HPA Axis and Levels of Neurotransmitters**
Huiting Li, Yuanhui Li, Xiaofei Zhang, Guilin Ren, Liangfeng Wang, Jianzhe Li, Mengxue Wang, Tao Ren, Yi Zhao, Ming Yang and Xiaoying Huang
- 91 Natural Medicines for the Treatment of Epilepsy: Bioactive Components, Pharmacology and Mechanism**
Li-Ying He, Mei-Bian Hu, Ruo-Lan Li, Rong Zhao, Lin-Hong Fan, Lin He, Feng Lu, Xun Ye, Yong-liang Huang and Chun-Jie Wu
- 119 l-Borneol Exerted the Neuroprotective Effect by Promoting Angiogenesis Coupled With Neurogenesis via Ang1-VEGF-BDNF Pathway**
Rong Ma, Qian Xie, Hongyan Li, Xiaoqing Guo, Jian Wang, Yong Li, Mihong Ren, Daoyin Gong and Tian Gao

- 136 ***Chinese Medicine Formula Kai-Xin-San Ameliorates Neuronal Inflammation of CUMS-Induced Depression-like Mice and Reduces the Expressions of Inflammatory Factors via Inhibiting TLR4/IKK/NF- κ B Pathways on BV2 Cells***
Suchen Qu, Mengqiu Liu, Cheng Cao, Chongqi Wei, Xue-Er Meng, Qianyin Lou, Bin Wang, Xuan Li, Yuyan She, Qingqing Wang, Zhichao Song, Zhengxiang Han, Yue Zhu, Fei Huang and Jin-Ao Duan
- 150 ***Corynoxine Protects Dopaminergic Neurons Through Inducing Autophagy and Diminishing Neuroinflammation in Rotenone-Induced Animal Models of Parkinson's Disease***
Leilei Chen, Yujv Huang, Xing Yu, Jiahong Lu, Wenting Jia, Juxian Song, Liangfeng Liu, Youcui Wang, Yingyu Huang, Junxia Xie and Min Li
- 161 ***Danggui-Shaoyao-San (DSS) Ameliorates Cerebral Ischemia-Reperfusion Injury via Activating SIRT1 Signaling and Inhibiting NADPH Oxidases***
Yunxia Luo, Hansen Chen, Bun Tsoi, Qi Wang and Jiangang Shen
- 173 ***PI3K/AKT Signal Pathway: A Target of Natural Products in the Prevention and Treatment of Alzheimer's Disease and Parkinson's Disease***
Hui-Zhi Long, Yan Cheng, Zi-Wei Zhou, Hong-Yu Luo, Dan-Dan Wen and Li-Chen Gao
- 193 ***Xiaoyao Pills Ameliorate Depression-like Behaviors and Oxidative Stress Induced by Olfactory Bulbectomy in Rats via the Activation of the PIK3CA-AKT1-NFE2L2/BDNF Signaling Pathway***
Yafei Ji, Jie Luo, Jiuseng Zeng, Yang Fang, Rong Liu, Fei Luan and Nan Zeng
- 210 ***Neuroprotective Effect for Cerebral Ischemia by Natural Products: A Review***
Qian Xie, Hongyan Li, Danni Lu, Jianmei Yuan, Rong Ma, Jinxiu Li, Mihong Ren, Yong Li, Hai Chen, Jian Wang and Daoyin Gong
- 235 ***Progress in Borneol Intervention for Ischemic Stroke: A Systematic Review***
Yong Li, Mihong Ren, Jiajun Wang, Rong Ma, Hai Chen, Qian Xie, Hongyan Li, Jinxiu Li and Jian Wang
- 258 ***Jiedu Tongluo Granules Ameliorates Post-stroke Depression Rat Model via Regulating NMDAR/BDNF Signaling Pathway***
Aimei Zhao, Bo Ma, Li Xu, Mingjiang Yao, Yehao Zhang, Bingjie Xue, Junguo Ren, Dennis Chang and Jianxun Liu
- 271 ***Branched-Chain Amino Acids Catabolism Pathway Regulation Plays a Critical Role in the Improvement of Leukopenia Induced by Cyclophosphamide in 4T1 Tumor-Bearing Mice Treated With Lvjiaobuxue Granule***
Jun-sheng Tian, Hui-liang Zhao, Yao Gao, Qi Wang, Huan Xiang, Xiang-ping Xu, Sheng Huang, Dong-lan Yan and Xue-mei Qin



Editorial: Assessing the Pharmacological Effects and Therapeutic Potential of Traditional Chinese Medicine in Neurological Disease Models: An Update

Zhiqiang Deng¹, Yuxuan Kan¹, Min Li^{1*}, Juxian Song^{2*} and Jia-Hong Lu^{3*}

¹School of Chinese Medicine, Mr. And Mrs. Ko Chi Ming Centre for Parkinson's Disease Research, Hong Kong Baptist University, Kowloon, Hong Kong SAR, China, ²Medical College of Acupuncture-Moxibustion and Rehabilitation, Guangzhou University of Chinese Medicine, Guangzhou, China, ³State Key Laboratory of Quality Research in Chinese Medicine, Institute of Chinese Medical Sciences, University of Macau, Taipa, China

Keywords: stroke, epilepsy, multiple sclerosis, dementia, neurodegenerative diseases

Editorial on The Research Topic

Assessing the Pharmacological Effects and Therapeutic Potential of Traditional Chinese Medicine in Neurological Disease Models: An Update

OPEN ACCESS

Edited and Reviewed by:

Michael Heinrich,
University College London,
United Kingdom

*Correspondence:

Min Li
lmin@hkbu.edu.hk
Juxian Song
juxiansong@gmail.com
Jia-Hong Lu
jiahonglu@um.edu.mo

Specialty section:

This article was submitted to
Ethnopharmacology,
a section of the journal
Frontiers in Pharmacology

Received: 31 March 2022

Accepted: 04 April 2022

Published: 27 April 2022

Citation:

Deng Z, Kan Y, Li M, Song J and
Lu J-H (2022) Editorial: Assessing the
Pharmacological Effects and
Therapeutic Potential of Traditional
Chinese Medicine in Neurological
Disease Models: An Update.
Front. Pharmacol. 13:909153.
doi: 10.3389/fphar.2022.909153

Neurological disorders affect the central and peripheral nervous systems by impairing the function of brain, spinal cord and peripheral nerves. As a wide spectrum of disorders, neurological diseases include epilepsy, stroke, multiple sclerosis, and neurodegenerative diseases, such as Parkinson's disease (PD), Alzheimer disease (AD) and other dementias. Currently, these disorders have affected hundreds of millions of people worldwide especially in low- and middle-income countries. Traditional Chinese Medicine (TCM) is an ancient yet still widely used medicinal system in East Asia. TCM is an important source in the development of modern drugs. In the past decades, increasing number of studies have investigated the role of TCM-preparations including medicinal plant extracts or single compounds in neurological disorder models. This Research Topic was launched to summarize the current advances in the application of TCM-originated materials in neurological disorder models and to make a contribution in development of new drugs for the treatment of neurological diseases. The Research Topic has gathered 17 articles consisting of 13 Original Research articles and 4 Reviews articles which have investigated and/or discussed the protective roles of TCM-originated materials in multiple neurological disorders including stroke, depression, multiple sclerosis, epilepsy, and neurodegenerative diseases including PD and AD.

Among the 13 Original Research articles, three have determined the mechanism of TCM effects on stroke. Luo *et al.* investigated the neuroprotective mechanisms of Danggui-Shaoyao-San (DSS), a famous TCM formula including *Angelica sinensis* (Oliv.) Diels (*Umbelliferae*), *Paeonia lactiflora* Pall. (*Paeoniaceae*), *Conioselinum anthriscoides* "Chuanxiong" (syn. *Ligusticum chuanxiong* Hort.) (*Umbelliferae*), *Wolfiporia . extensa* (Peck) Ginns (syn. *Poria cocos* (Schwein.) (*Polyporaceae*), *Atractylodes macrocephala* Koidz. (*Asteraceae*), and *Alisma plantago-aquatica* subsp. *orientale* (Sam.) Sam. (syn. *Alisma orientalis* (Sam.) Juzep. (*Alismataceae*), for the treatment of ischemic stroke (Luo *et al.*). By administrating ethanol extract of DSS into rats which were subjected to 2 h of MCAO (middle cerebral artery occlusion) plus 22 h reperfusion, they found that ethanol extract of DSS can reduce infarct sizes and improve neurological deficit scores in these rats. Mechanistically, they found that ethanol extract of DSS can inhibit the expression of p67^{phox}, a subunit of NADPH.

Meanwhile, DSS up-regulates SIRT1 expression in the cortex and striatum of MCAO ischemic brains which can be ablated by SIRT1 inhibitor EX527. Together, they demonstrated that DSS protects against cerebral ischemic-reperfusion injury through SIRT1-dependent manner. By using the similar MCAO model of stroke, Wang et al. found Taohong Siwu decoction (THSWD) containing Tao Ren (*Prunus persica* (L.) Batsch), Hong Hua (*Carthamus tinctorius* L.), Dang Gui (*Angelica sinensis* (Oliv.), Shu Di Huang (*Rehmannia glutinosa* (Gaertn.)), Chuan Xiong (*Ligusticum chuanxiong* Hort), and Bai Shao (*Paeonia lactiflora* Pall.) can improve the behavioral function and pathological damage of brain in MCAO rats (Wang et al.). They further demonstrated that THSWD could reduce the activity of NLRP3 inflammatory corpuscle by down-regulating the expression of inflammatory factors and inhibit pyroptosis pathway in MCAO rats. As a classical TCM, *l*-borneol has been used to treat stroke in China for thousands of years. Ma et al. investigated a novel mechanism of *l*-borneol's effect on stroke (Ma et al.). They found that *l*-borneol improves the neurological deficits and pathological damage of cerebral ischemia in MCAO rats through promoting angiogenesis and neurogenesis. Mechanistically, they found that *l*-borneol can increase the number of CD34 positive cells and decrease the levels of ACE and Tie2 to promote angiogenesis, and can significantly enhance the expression of VEGF and BDNF while inhibit the expression of TGF- β 1 and MMP9 to promote neurogenesis. They further verified the mechanism by using molecular docking assay showing a very high binding rate between *l*-borneol and the targets above.

Five of 13 Original Research articles have determined the mechanism of TCM effects on depression. Li et al. investigated the curative effect and mechanism of volatile oil from *Aquilaria sinensis* (Lour.) Gilg and *Aucklandia costus* Falc. (CMVO) in the treatment of depression (Li et al.). In chronic unpredictable mild stress (CUMS) rats, a depressive rat model, they found CMVO displayed an antidepressant effect based on the multiple animal behavior tests. They showed that inhalational administration of CMVO to CUMS rats decreased the level of adrenocorticotrophic hormone in serum through down-regulating the expression of corticotropin-releasing hormone mRNA in hypothalamus, whereas CMVO restored the level of 5-hydroxytryptamine (5-HT) in the hippocampus through up-regulating the expression of 5-HT_{1A} mRNA. Qu et al. reported on the role of Kai-Xin-San (KXS), a TCM formula composed of Ginseng Radix et Rhizoma, Polygalae, Acori Tatarinowii Rhizoma, and Poria, in the regulation of neuronal inflammation in mouse model of CUMS (Qu et al.). They confirmed the antidepressant effects of KXS in CUMS mice. In mechanism, they demonstrated that KXS inhibited the activation of microglia by reducing the expression of pro-inflammatory cytokines (IL-1 β , IL-2 and TNG- α) in hippocampus of CUMS mice. Zhu et al. evaluated the antidepressant effect of Elaphuri Davidiani Cornu (EDC) in depression-like mouse model (Zhu et al.). They found that aqueous extracts of EDC can significantly improve depression-like behavior and enhance the expression of nerve growth factors and brain-derived neurotrophic factors in prefrontal cortex and hippocampus. In the primary cultures of astrocyte derived from these depression-like mice, they identified that the EDC aqueous

extracts exerted the antidepressant effect through cAMP- and ERK-dependent pathways. By using an olfactory bulbectomized (OB) rat model of depression, Ji et al. investigated the antidepressant-like effects of Xiaoyao pills (XYW) composed of paeoniflorin, liquiritin, saikosaponin B2, and atractylenolide II. and the underlying mechanism (Ji et al.). According to the results of multiple behavior tests in the OB rats treated with XYW, they found XYW significantly alleviated the depression-like behaviors. They further demonstrated that XYW played these protective roles by inhibiting oxidative stress and enhancing the activation of PIK3CA-AKT1-NF2EL2/BDNF signaling pathways. Zhao et al. determined the protective function of Jiedu Tongluo granules (JDTLG, which was composed of *Panax ginseng* C. A. Mey. (Ren Shen), *Scutellaria baicalensis* Georgi (Huang Qin), *Ginkgo biloba* L. (Yin Xing Ye), *Hypericum perforatum* L. (GuanYe Lian Qiao), *Gardenia jasminoides* J. Ellis (Zhi Zi), *Gastrodia elata* Blume (Tian Ma), *Conioselinum anthriscoides* "Chuanxiong" (Chuan Xiong.) in post-stroke depression (PSD) rat model established by catotid artery embolization combined with chronic sleep deprivation (Zhao et al.). They found that the neurological deficit and depression symptoms of PSD rats can be significantly improved by oral treatment of JDTLG. By performing proteomic analysis of the brain tissue of PSD rats, they identified several processes including N-methyl-D-aspartate receptor (NMDAR) and brain-derived neurotrophic factor (BDNF) signal pathway involved in the regulation of JDTLG on PSD rats.

Three of 13 Original Research articles have determined the effects and mechanisms of TCM on neurodegenerative diseases including PD and AD. Chen et al. reported on the neuroprotective effect of corynoxine, an oxindole alkaloid isolated from the Chinese botanical drug *Uncaria rhynchophylla* (Gouteng in Chinese), on animal models of PD (Chen et al.). They demonstrated that corynoxine can improve motor dysfunction, prevent tyrosine hydroxylase (TH)-positive neuronal loss, and decrease α -synuclein aggregation in rotenone-induced rat and mouse models. These results will provide experimental basis for corynoxine in the treatment of PD. Huang et al. investigated the effects and potential mechanisms of berberine on NLRP3 inflammasome in PD (Huang et al.). By using *in vivo* models (MPTP-induced PD mice), the authors found that berberine enhanced autophagy and mitigated behavioral impairments, neurotoxicity and neuroinflammation. The *in vitro* data confirmed the inhibitory effect of berberine on NLRP3 inflammasome, including the expressions of NLRP3, cleaved caspase 1 (CASP1), and mature interleukin 1 beta (IL1B). In addition, treatment with the autophagy inhibitor 3-Methyladenine (3-MA) blocked the effect of berberine both *in vivo* and *in vitro*. These results supported the neuroprotective effect of berberine on PD, and provided the mechanism by which berberine inhibits NLRP3 inflammasome activation through enhancing autophagy. Iyaswamy et al. reported on the effect of Chinese medicine formula Yuan-Hu Zhi Tong (YZT), composed of *Corydalis yanhusuo* and *Angelica Dahurica*, on AD (Iyaswamy et al.). In P301S tau and 3XTg-AD mice, they found that YZT can reverse motor dysfunction and enhance learning and memory function, respectively. By using Microarray and the Connectivity

Map analysis, the authors determined that YZT reduced tau aggregation by regulating ubiquitin proteasomal system. The study suggests YZT can be a potential drug for the treatment of AD.

Among the 13 Original Research articles, Sun et al. attempted to illuminate the mechanism of catapol in the treatment of multiple sclerosis (Sun et al.). The authors established cuprizone-induced demyelination model and found that catapol improved the motor functions and promoted myelination in the model. Both *in vivo* and *in vitro* data showed that catapol promoted the differentiation of oligodendrocyte precursor cells (OPCs), which are critical for the formation of remyelination in multiple sclerosis. Mechanistically, they found that the effect of catapol on remyelination may be related to the inhibition of NOTCH1 pathway. This study provided a mechanistic rationale for catapol in the treatment of multiple sclerosis. Tian et al. reported on the mechanism of Chinese medicine Lvjiaobuxue granule, an immunomodulator, against acute leukopenia (Tian et al.). The results showed that Lvjiaobuxue granule improved the blood routine parameters and organ index (including spleen, thymus and liver) in cyclophosphamide-induced leucopenia model of 4T1 tumor-bearing mice. According to the analysis of metabolomics and network pharmacology, the regulation of branched-chain amino acids (BCAAs) degradation may play a pivotal role in mice with leukopenia after Lvjiaobuxue granule treatment. This study provided data and theoretical support for further research on its mechanism.

Among the 4 Review articles, two of them reviewed the neuroprotective effects of natural products on ischemic stroke. Xie et al. comprehensively summarized the pharmacological effects and the underlying mechanisms of natural products for cerebral ischemic injury in multiple preclinical models, and discussed their potential applications in neuroprotection (Xie et al.). They proposed the potential role of the structures of natural products in their biological activity in neuroprotection, which have not been determined currently. The other one contributed by Li et al. systematically reviewed the neuroprotective effects of borneol and the mechanisms of the actions in ischemic stroke at different stages including acute stage, subacute stage and late stage (Li et al.). By performing meta-analysis on key indicators in the experiments *in vivo*, they concluded that unlike many other drugs, borneol protects against neuronal injury in ischemic stroke via multiple mechanisms at different stages, hastens self-repair of the body by mobilizing endogenous nutritional factors, and enhances the therapeutic effects of other drugs by promoting them to pass

through the blood-brain-barrier (BBB). Among the 4 Review articles, one of them is related to the treatment of epilepsy by natural medicine (He et al.). In this review article, He et al. reclassified the ingredients of certain natural medicines and discussed their antiepileptic mechanisms, which would provide benefits to drug development for epilepsy treatment. The last review article is contributed by (Long et al.). In this article, they reviewed the role of PI3K/AKT signal pathway in AD and PD, and summarized the natural products which are displayed preventive and therapeutic effects on these two diseases via PI3K/AKT pathway. The review article would provide guidance and reference for the development of novel drugs for the treatment of AD and PD in this field.

In summary, despite the research quality in these studies are improved by using advanced technologies and powerful tools of molecular biology, several issues remain unsolved currently. For instance, the particular molecular mechanisms by which the TCM-preparations exert protective effects against neurological disorders are still unclear. In the future, research can be benefited from applying the promising approaches including but not limited to using unbiased omics-based analysis to comprehensively decipher the mechanism; using transgenic animal models to significantly enhance the disease relevance; and systemically verifying the drug targets in multiple animal models.

AUTHOR CONTRIBUTIONS

ZD and YK wrote and all authors edited the editorial. All authors contributed to the article and approved the submitted version.

Conflict of Interest: The authors declare that the research was conducted in the absence of any commercial or financial relationships that could be construed as a potential conflict of interest.

Publisher's Note: All claims expressed in this article are solely those of the authors and do not necessarily represent those of their affiliated organizations, or those of the publisher, the editors and the reviewers. Any product that may be evaluated in this article, or claim that may be made by its manufacturer, is not guaranteed or endorsed by the publisher.

Copyright © 2022 Deng, Kan, Li, Song and Lu. This is an open-access article distributed under the terms of the Creative Commons Attribution License (CC BY). The use, distribution or reproduction in other forums is permitted, provided the original author(s) and the copyright owner(s) are credited and that the original publication in this journal is cited, in accordance with accepted academic practice. No use, distribution or reproduction is permitted which does not comply with these terms.



Yuan-Hu Zhi Tong Prescription Mitigates Tau Pathology and Alleviates Memory Deficiency in the Preclinical Models of Alzheimer's Disease

OPEN ACCESS

Edited by:

Vincent Kam Wai Wong,
Macau University of Science and
Technology, Macau

Reviewed by:

Young-Ji Shiao,
National Research Institute of Chinese
Medicine, Taiwan
Wenda Xue,
Nanjing University of Chinese
Medicine, China

*Correspondence:

Min Li
limin@hkbu.edu.hk
Siva Sundara Kumar Durairajan
d.sivasundarakumar@cutn.ac.in
Chi-Ying Huang
cyhuang5@ym.edu.tw

†These authors have contributed
equally to this work

Specialty section:

This article was submitted to
Ethnopharmacology,
a section of the journal
Frontiers in Pharmacology

Received: 18 July 2020

Accepted: 25 September 2020

Published: 30 October 2020

Citation:

Iyaswamy A, Krishnamoorthi SK, Liu
YW, Song JX, Kammala AK,
Sreenivasamurthy SG, Malampati S,
Tong BCK, Selvarasu K, Cheung KH,
Lu JH, Tan JQ, Huang CY, Durairajan
SSK and Li M (2020) Yuan-Hu Zhi
Tong Prescription Mitigates Tau
Pathology and Alleviates Memory
Deficiency in the Preclinical Models of
Alzheimer's Disease.
Front. Pharmacol. 11:584770.
doi: 10.3389/fphar.2020.584770

A. Iyaswamy^{1†}, S. K. Krishnamoorthi^{1†}, Y. W. Liu^{2†}, J. X. Song^{1,3}, A. K. Kammala¹,
S. G. Sreenivasamurthy¹, S. Malampati¹, B. C. K. Tong¹, K. Selvarasu⁴, K. H. Cheung¹,
J. H. Lu⁵, J. Q. Tan⁶, C. Y. Huang^{2*}, S. S. K. Durairajan^{1,4*} and M. Li^{1*}

¹Mr. & Mrs. Ko Chi-Ming Centre for Parkinson's Disease Research, School of Chinese Medicine, Hong Kong Baptist University, Hong Kong SAR, China, ²Institute of Biopharmaceutical Sciences, National Yang Ming University, Taipei, Taiwan, ³Medical College of Acupuncture-Moxibustion and Rehabilitation, Guangzhou University of Chinese Medicine, Guangzhou, China, ⁴Division of Mycobiology and Neurodegenerative Disease Research, Department of Microbiology, School of Life Sciences, Central University of Tamil Nadu, Tiruvarur, India, ⁵State Key Lab of Quality Research in Chinese Medicine, University of Macau, Macao SAR, China, ⁶Center for Medical Genetics, School of Life Sciences, Central South University, Changsha, China

Alzheimer's disease (AD) is characterized by memory dysfunction, A β plaques together with phosphorylated tau-associated neurofibrillary tangles. Unfortunately, the present existing drugs for AD only offer mild symptomatic cure and have more side effects. As such, developments of effective, nontoxic drugs are immediately required for AD therapy. Present study demonstrates a novel role of Chinese medicine prescription Yuan-Hu Zhi Tong (YZT) in treating AD, and it has substantiated the *in vivo* effectiveness of YZT in two different transgenic mice models of AD, namely P301S tau and 3XTg-AD mice. Oral treatment of YZT significantly ameliorates motor dysfunction as well as promotes the clearance of aggregated tau in P301S tau mice. YZT improves the cognitive function and reduces the insoluble tau aggregates in 3XTg-AD mice model. Furthermore, YZT decreases the insoluble AT8 positive neuron load in both P301S tau and 3XTg-AD mice. Using microarray and the "Connectivity Map" analysis, we determined the YZT-induced changes in expression of signaling molecules and revealed the potential mechanism of action of YZT. YZT might regulate ubiquitin proteasomal system for the degradation of tau aggregates. The research results show that YZT is a potential drug candidate for the therapy of tau pathogenesis and memory decline in AD.

Keywords: Alzheimer's disease, P301S tau mice, neurofibrillary tangles, Chinese medicine, yuan-hu zhi tong, microarray, connectivity map

INTRODUCTION

Alzheimer disease (AD) is most vulnerable disease affecting the entire elderly population without curable methods. Therefore, there is a serious demand to develop novel and new drugs targeting the vulnerable neurodegenerative disease including AD. Accumulation of insoluble and toxic protein aggregates and phosphorylated tau species is very rarely researched which is the main cause for the neuron loss with cognitive damages in later AD. Even though AD is commonly believed to be a memory disorder, nearly all people identified with AD create neuropsychiatric symptoms (NPS), such as anxiety, motor impairment, hallucinations, and psychosis, at some stages of their disease

(Dillon et al., 2013). Recent A β -based therapies do not prevent cognitive decline, neurofibrillary tangles (NFT) formation or neurodegeneration (Yoshiyama et al., 2013). Recent research have demonstrated a strong correlation between tau pathology, cognitive decline and NPS in the later part of AD (Geerts et al., 2013).

Presently drugs in market can only mitigate some symptoms but cannot alleviate the disease. The key hallmark features of AD are senile plaques (SP) formation in aggregation of amyloid β -peptide (A β) and NFTs formation due to tau-aggregation (Hardy, 2006; Wang and Mandelkow, 2016). Other critical early features of AD include an increase in neuroinflammation, decline in synapse number, dysfunction of axonal transport and loss of microtubule (MT) density and stability. In the present market, drug discovery based on reducing A β plaques has not shown robust clinical efficacy. In contrast, targeting NFTs seems more likely to be successful because NFTs, which comprises hyperphosphorylated, aggregated, misfolded tau protein, are well correlated with cognitive impairment (Bloom, 2014; Wang and Mandelkow, 2016). Thus, reduction of tau aggregation might be further efficient than A β -targeting remedies for AD treatment (Giacobini and Gold, 2013).

The failure of A β -based clinical trials challenges the belief that A β stimulates tau- arbitrated neurodegeneration. Braak and his associates demonstrated (Braak and Braak, 1995; Braak and Braak, 1996) that tau pathology develops separately from A β and tau pathology may possibly the crucial cause for the neurodegeneration in AD. Many studies had supported this hypothesis by finding evidences in AD disease models: A β immunotherapy demonstrated a decrease in extracellular SP and intracellular A β accumulation and did not mitigate phosphorylated tau pathology in 3XTg-AD (amyloid precursor protein (APP), Presenilin and tau) mice (Oddo et al., 2004). Hence, A β focused remedies might be protective in the very initial clinical phases of AD, however when cognitive decline commences with tau pathology, and subsequently tau mitigating drugs may possibly be essential for disease modification.

Traditional Chinese medicine (TCM), is an ancient drug treatment process yet still effective therapeutic approach extensively employed in East Asia, this method holds a greater success for the medication of many neurodegenerative diseases as well as AD for centuries (Geerts et al., 2013). TCM herbs, those showing clinical efficacies, are drawing extensive interest as a source for drug discovering for neurodegenerative diseases including AD. A TCM herbal formula i.e. “Yuan-hu Zhi Tong San” (YZT), is clinically used to treat pain and neuralgia (Yuan et al., 2004); Chinese Clinical Trail Registry (ChiCTR-TRC-10001155). YZT is a relatively simple TCM formula that consists of dried plant material of *Corydalis yanhusuo* (CY) (Y. H. Chou & Chun C. Hsu) W. T. Wang ex Z. Y. Su & C. Y. Wu [Papaveraceae] and *Angelica dahurica* (ADH) (Hoffm.) Benth. & Hook.f. ex Franch. & Sav [Apiaceae], mixed at a ratio of 2:1.

YZT is extensively used for the medication of gastralgia and neuralgia in China (Han and Jiang, 2011). In Australia, YZT capsules are legally allowed to be sold as a pain reliever through

the Australian Register of Therapeutic Goods (ARTG-ID-14480). YZT has an array of experimentally proven activities involving anxiolytic, antinociceptive, spasmolytic, anti-inflammatory and vasorelaxant (Xu et al., 2013). Even though NFTs and SP are distinctive indicators of AD, AD may possibly be a multifactorial illness which originated from intricate genetic and environmental risk elements. In terms of how the two herbs interact, YZT extract have been shown to generate synergistic activities on the analgesic impact by enhancing plasma contents of dl-tetrahydropalmatine (Liao et al., 2010). However, the disease-modifying activity of YZT against AD on tauopathies have never been studied in previous studies.

In the present study, we probed whether YZT can improve cognitive memory function and boost the clearance of pathological aggregated insoluble tau in 3XTg-AD and P301S tau mice models. Additionally, we assessed motor function and tau degradative pathway *in vivo* and *in vitro*.

MATERIALS AND METHODS

Quality Analysis of Herbal Materials

Dried herbal materials of *Corydalis yanhusuo* (CY) and *Angelica dahurica* (ADH) were procured from Mr. & Mrs. Chan Hon Yin Chinese Medicine Specialty Clinic in the Hong Kong Baptist University (HKBU) and identified according to the Chinese Pharmacopeia specifications (2010 Edition). The voucher specimens were deposited at the School of Chinese Medicine, HKBU, Hong Kong, China. YZT extract was prepared by mixing dry materials of the plant's CY and ADH in the ratio of 2:1 and were grinded into powder utilizing a waring mixer. Roughly 1 Kg of powder was immersed in 1 L of 80% alcohol and incubated overnight at room temperature and subsequently obtained extract were steeped. The same process was repeated two times for a complete extraction. Extracted solutions were put together, and around 3–4 L were combined and was condensed under vacuum by rotary evaporation at 50°C. The condensed extract was finally lyophilized (LABCONCO, Laboratory Construction Company, MO, United States) under vacuum of 105×10^{-3} μ bar. The lyophilized powder from different batches were identified for their purity and then stored at 4°C. The chemical ingredients of every single batch of YZT, CY and ADH were tested for its purity using LC-TOF/MS. A detailed method has been described in our previous publications (Durairajan et al., 2017; Iyaswamy et al., 2020).

Animals and Drug Treatment

Animal experiments were approved by the Committee on the Use of Human and Animal Subjects in Teaching and Research (HASC approval # HASC/13-14/0165) in HKBU and the Committee on the Use of Live Animals for Teaching and Research (CULATR #3314), at the University of Hong Kong. Animal experiments performed in agreement with the applicable guidelines and procedures of HASC and CULATR. We utilized P301S and 3XTg-AD mice models for assessing the effectiveness of YZT in tau pathology. “Generation of P301S transgenic mice overexpressing the shortest human four-repeat tau isoform

(0N4R) under the control of a neuron-specific Thy-1.2 promoter element" has been described previously (Allen et al., 2002). Homozygous P301S tau transgenic and age-matched wild type mice ranging from four to six of weeks age were included in the current study. There were three groups, with N = 14 mice per group in P301S study. In brief, P301S mice were treated every day via food admixture with YZT of 2 or 4 g per kg body weight or vehicle. The study protocol was approved by the HASC of HKBU. Triple transgenic mice (3XTg-AD), carrying three mutant transgenes, i.e., amyloid precursor protein (Swedish, K670M/N671L), presenilin-1 (M146V), and tau (P301L), were used as an AD mouse model (Oddo et al., 2003). 3XTg-AD and C57BL/6J were acquired from the Jackson Laboratory (Bar Harbor, ME, United States). Mice were housed in our laboratory animal unit under 12-h light/dark cycles with food and ad libitum. YZT oral administration was started at 6 months of age up to 18 months of age 3XTg-AD mice fed with YZT diet admixture every day with a low dose (1 g/kg/d), a middle dose (2 g/kg/d), a high dose (4 g/kg/d), or vehicle. The body weight and in-cage behavior were monitored throughout the study.

Rotarod Test

To evaluate motor function, mice were tested on the rotarod equipment (Harvard apparatus) as described previously (Monville et al., 2006). The rotarod test has been recognized widely and offers a simple evaluation of whole motor deficits in P301S tau mice and might provide a valuable quantitative test to assess the efficiency of therapeutic approaches (Rozas and Labandeira Garcia, 1997). In this study, we used a rotarod machine with system-controlled timer and sensors controlled in the software (Panlabs, Harvard Apparatus, MA, United States). Before the first training sessions, the mice were acclimated with a period of 3 min on the rotating drum. The fixed speed rotarod (FSRR) and accelerated rotarod (ARR) was described by (Dunham and Miya, 1957) to assess neurological deficits of motor function in mice. This process was reiterated every day for 3 min just prior to subsequent sessions for the training of the experimental animals. The rotation speed of the rod during the training period was increased every day with 4, 8, and 12 rpm during the test period. On the first day, the acceleration mode of rotarod was switched off, and the rotation was set in a fixed mode at a relatively low speed (4 rpm), to make the task easier for the animals as they learned. On the second and third day, the speed was increased to 8 and 12 rpm, respectively. Each mouse was subjected to three trials for everyday training and between each trial the trained mice were given 5 min gap with rest. In the final day, the trained mice were subject to evaluation in the rod that accelerated efficiently from 4 to 40 rpm over a period of 300 s. The latency of fall and the time taken for the latency of fall in the evaluation day was recorded automatically.

Open Field Test

The procedure for the experiment was described previously (Zhang et al., 2014). A square box made of plexiglass (25 cm × 25 cm) was used as the open field apparatus to test the exploratory and locomotor function. The experimental animals were placed in the novel environment of the box and recorded the activities of

the animal through the tracking camera. Locomotor functions such as time spent in central/marginal areas, rearing and fecal bolus were evaluated through an automated animal tracking system (Ethovision XT software Version 3.0, Noldus Information Technology, Leesburg, VA, United States). the (Noldus, Wageningen, The Netherlands).

Morris Water Maze Test

MWM experiment was performed to evaluate the spatial memory, learning and recognition memory functions as described previously in our publications (Durairajan et al., 2017; Iyaswamy et al., 2020). The experimental animals were acclimatized in the behavior room, trained in visible platform, trained for six consecutive days in hidden platform, memory retention was evaluated in seventh day and monitored using the (Ethovision animal tracking software). All experimental animals in the study were included in the experimental training of visible platform for one day with four trials, continued with hidden platform training for 6 days, placing the platform in a constant location and the animals were placed in random spots of the tank for all trials for six consecutive days. In the seventh day the memory retention functions were evaluated in the probe trial using the animal tracking camera to analyze the time taken by the animal to probe the platform location and time spend in the platform quadrant by the experimental animal for the whole 60 min evaluation.

Tau Extraction

The soluble and insoluble phospho tau from the brain homogenate of P301S tau and 3XTg-AD mice were prepared by us as per the procedure explained in our previous publications (Myeku et al., 2016; Iyaswamy et al., 2020). Here we have explained briefly about the different fractions of tau extraction in the following steps, the extracted brain was homogenized in 10 volumes of radioimmunoprecipitation assay (RIPA) buffer mixed with phosphatase inhibitors and protease inhibitors (Roche). The brain homogenate was centrifuged at 20,000 × g for 20 min to divide proteins into soluble fraction (S1) and the supernatant was incubated and rotated in tubes with 1% sarkosyl for 1 h at room temperature. Further to collect the insoluble fraction a high-speed ultracentrifugation (100,000 × g) for 60 min was employed to collect the insoluble proteins in the pellet fraction. The pellet was resuspended in 20 µL of Tris-EDTA, pH 8.0 labeled P2 (sarkosyl-insoluble tau) and supernatant was designated as S2 fraction (sarkosyl-soluble tau).

Western Blot Analysis

The protein levels in the cell or brain homogenate was evaluated by the Western blot experiment as per the procedures explained in our previous publications (Durairajan et al., 2017; Iyaswamy et al., 2020). 5–10 µg of total protein in the brain or cell homogenate were separated on a SDS-PAGE gel as per the required percentage of gel depending on the target protein and blotted onto polyvinylidene difluoride (PVDF) membranes to detect the target protein namely PHF-1 (phospho-tau Ser396/Ser404), HT7 (total tau), AT8 (Phospho-tau Ser202/Thr205), CP13 (Phospho-tau Ser202), MC1 (a disease-specific

TABLE 1 | Specifications of antibodies used in the present study.

Antibody (clone)	Region specificity	Antigen	Source	Use and dilution
Rabbit polyclonal to APP CT695(CT695)	Human, mouse and rat FL-APP and CTFs	C-terminus 22 amino acid residues of β -APP peptide	Thermoscientific, Waltham, MA, United States	WB 1:1000
Biotinylated mouse monoclonal to human A β 17–24 (4G8)	hA β	Amino acids residues 17–24 of hA β peptide	Biolegend, Dedham, MA, United States	IHC 1:500
Rabbit polyclonal to phosphorylated APP (Thr668)	Human phosphorylated APP at Thr668	Phospho epitopes matching to residues neighboring Thr668 of human APP695	Cell signaling, Danvers, MA, United States	WB 1:1000
AT100 monoclonal to phospho tau	Human, mouse and rat phospho tau	Epitopes matching to residues neighboring Thr212, Ser214 phosphorylated sites	Thermoscientific Waltham, MA, United States	IHC 1:500
AT8 monoclonal to phospho tau biotinated	Human, mouse and rat phospho tau	Epitopes matching to residues neighboring Ser 202, Thr 205 phosphorylated sites	Thermoscientific Waltham, MA, United States	IHC 1:500
HT7 monoclonal to total tau biotinated	Human specific	Human tau between residue 159 and 163	Thermoscientific Waltham, MA, United States	IHC 1:500
PHF-1 monoclonal to phospho tau	Human, mouse and rat phospho tau	Epitopes matching to residues neighboring Ser396 and Ser404 phosphorylated sites	Prof. Peter Davies Albert Einstein College of Medicine, Manhasset, NY, United States	WB 1:1000
HT7 monoclonal to total tau	Human specific	Human tau between residue 159 and 163	Thermoscientific Waltham, MA, United States	WB 1:1000
Mouse monoclonal to β -actin (C4)	β -actin	Bird gizzard actin	Santa Cruz, Dallas, TX, United States	WB: 1:1000
ALZ50 monoclonal to phospho tau	Human, mouse and rat phospho tau	Epitopes matching to residues neighboring Phospho Ser phosphorylated sites	Prof. Peter Davies Albert Einstein College of Medicine, Manhasset, NY, United States	WB 1:1000
CP13 monoclonal to phospho tau	Human, mouse and rat phospho tau	Epitopes matching to residues neighboring Ser 202 phosphorylated sites	Prof. Peter Davies Albert Einstein College of Medicine, Manhasset, NY, United States	WB 1:1000
MC1 monoclonal to phospho tau	Human, mouse and rat phospho tau	Epitopes matching to residues neighboring Ser 312-322 phosphorylated sites	Prof. Peter Davies Albert Einstein College of Medicine, Manhasset, NY, United States	WB 1:1000
AT8 monoclonal to phospho tau	Human, mouse and rat phospho tau	Epitopes matching to residues neighboring Ser 202, Thr 205 phosphorylated sites	Thermoscientific Waltham, MA, United States	WB 1:1000
AT180 monoclonal to phospho tau	Human, mouse and rat phospho tau	Epitopes matching to residues neighboring Thr 231 phosphorylated sites	Thermoscientific Waltham, MA, United States	WB 1:1000

conformational modification of tau), ALZ50 (misfolded tau) and β -actin (**Table 1**). The blot was blocked in milk (5%) and further probed with primary antibodies incubating overnight at 4°C in cold room with shaking. Next morning the blots were washed with tris-buffered saline, 0.1% Tween 20 (TBST) and incubated with target secondary antibodies for 2 h. The immunoblots were further enhanced with Supersignal -West Pico (Thermo Fisher Scientific, United States) and developed using X-ray film (Kodak).

Immunohistochemical Analysis

Immunohistochemical analysis was performed as per the procedure described by us in the previous publications (Durairajan et al., 2017; Iyaswamy et al., 2020). The experimental mice were anesthetized and perfused with 1X Phosphate buffered saline (PBS) and then brain was dissected. The extracted brains were fixed with 4% paraformaldehyde at 4°C for 2 days and then cleaned with 1XPBS for two times further soaked in 30% sucrose at 4°C till we finally embedded in optimal cutting temperature (OCT) medium. The cortico-hippocampal region were sectioned using Shandon Cryotome SME Cryostat (Ramsey, MN, United States) at 30 μ m intervals and stored at 4°C with PBS, 0.1% Tween 20 (PBST); further blocked for 2 h at room temperature with 5% normal bovine serum albumin (BSA) in 1 X PBS and then incubated with target primary antibodies namely MC1, AT100 (Phospho-tau Thr212/Ser214) and AT8 for P301S mice and AT8, HT-7, PHF1 and 4G8 ($A\beta$ 17-24) for 3XTg mice (1:100 dilute in 2% BSA) overnight at 4°C. Next day the brain slices were washed in 1XPBS and then for fluorescent staining the brain slices were incubated with secondary fluorescent antibody green or red probes (Dilute as 1:500 blocking buffer) for 2 h. The floating brain slices were fixed in the coated slides, air-dried out and mounted with fluorescence mounting medium (Fluorsave, Sigma-Aldrich).

Cell Culture

SH-SY5Y cell line expressing tau P301L (SH-SY5Y-P301L) was generated using lentiviral gene transfer; this cell line was donated by Dr. Lars Itner (University of Sydney, Australia) (Ke et al., 2012). The SH-SY5Y-P301L cells cultured in DMEM-F12 (Thermo scientific) containing 15% of heat inactivated fetal bovine serum (FBS) and 1X PSN (Invitrogen) with 3–5 μ g/ml of blasticidin (IThermo scientific), a nucleoside antibiotic used as a selection marker of tau P301L. Chinese hamster ovary (CHO) cell line expressing human APP751 with V717F mutation (7PA2) cells was gifted by Dr. Edward Koo, University of California, San Diego. 7PA2 cells secrete $A\beta$ oligomers rapidly after $A\beta$ peptide generation inside particular intracellular vesicles are successively secreted to the medium (Podlisny et al., 1995).

RNA Extraction, Microarray Processing, and Data Analysis

The SH-SY5Y-P301L cells were seeded 1.2×10^6 cells/dish and after incubating for 16–20 h, the SH-SY5Y-P301L cells were then treated by 0.1% dimethyl sulfoxide (DMSO) (vehicle control group) and YZT (100 μ g/ml), respectively, for 6 h. Cells were harvested using Trizol (TRI Reagent Solution, Ambion) and then stored at -80°C overnight, followed by Phalanx array processing (Phalanx Biotech Group's CytoOneArray) in the next day. The

differentially expressed genes with 2-fold changes as compared to vehicle control were used to query Clue (<https://clue.io/>) (Subramanian et al., 2017), which is a gene expression profile-based bioinformatics database. These differentially expressed genes were used as query inputs to reveal the hubs in the network using Ingenuity Pathways Analysis (IPA) and search tool for interactions of chemicals (STITCH (<https://www.qiagenbioinformatics.com/products/ingenuity-pathway-analysis/> and chemical- protein interaction networks, <http://stitch.embl.de>).

The Connectivity Map (CMap) project (Lamb et al., 2006) was established to accommodate a huge number of gene-expression profiles of various studies of bioactive small molecules to give design-matching algorithms to find these data. Briefly, a potent optimistic connectivity score (similarities) suggests that the profile in CMap displays the gene expression like the query. Many herbal medicines have performed microarray profiling and then executed the bioinformatics analysis via CMap to explore the mechanism of actions (Toyoshiba et al., 2009). By using Clue, which is a new CMap database (<https://clue.io/>) (Subramanian et al., 2017), we could obtain a list of small molecules, shRNA and overexpression constructs sharing similar gene expression patterns with YZT-treated cells for us to predict the mechanism of actions of YZT.

Statistical Analysis

All the raw data was processed as per the requirements of group comparison and number of animals per group are presented as mean \pm SEM or SD. Most of the experiments of biochemical assays like immunoblot and immunohistochemistry were evaluated by “one-way ANOVA” assessment. However, Behavior study was evaluated by “2-way analysis of variance (ANOVA)” because at the same time between the groups and different timepoint were compared. “Pair-wise differences between groups were compared using either Bonferroni's or Fisher's least significant difference (FLSD)-post hoc multiple comparisons test”. Graphical demonstration and statistics were performed with “GraphPad Prism 6 (GraphPad Software, San Diego, CA, United States)”.

RESULTS

Quality Analysis of Yuan-Hu Zhi Tong, *Corydalis yanhusuo* and *Angelica dahurica* by LC- QTOF/MS

We first prepared YZT by mixing CY and ADH in the ratio of 2:1. Dried raw material of the herbs were pulverized into powder, steeped in 80% alcohol overnight, filtered, concentrated by rotary evaporation, and then finally subjected to lyophilized powder (**Figure 1A**) and analyzed YZT, CY and ADH by LC-QTOF/MS. The chromatograms of YZT, CY and ADH are shown in **Figures 1B–D**. The highly abundant 14 compounds among the 24 peaks were detected and verified (**Figure 1E**) by comparing to the internal standards with high-resolution MS and MS/MS fragmentation was presented.

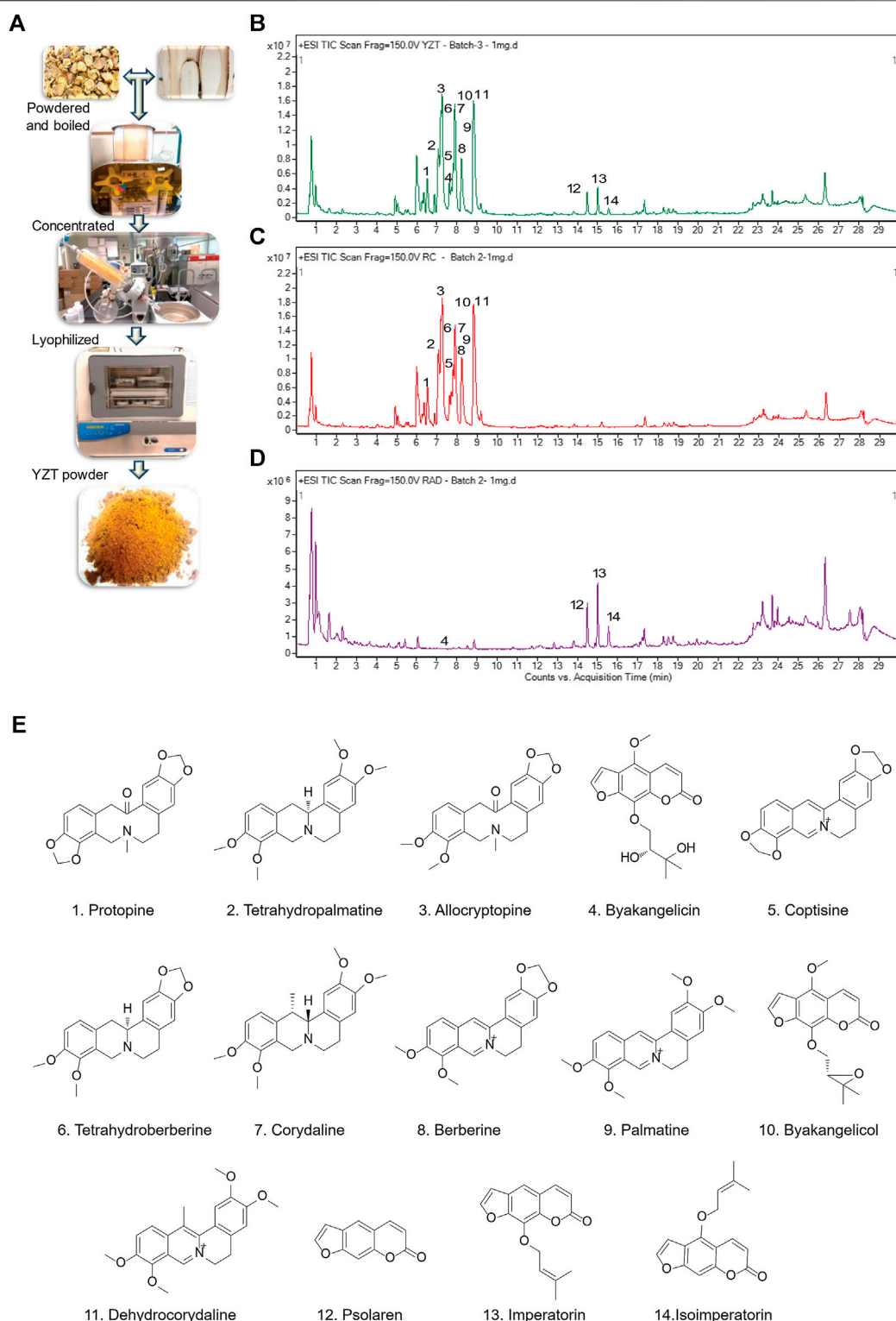


FIGURE 1 | Qualitative analysis and herbal preparation of YZT. **(A)** The herbal materials of YZT were powdered boiled in water; the extract was concentrated and lyophilized to prepare YZT extract powder. LC-ESI-Q/TOF chromatograms (TIC) of **(B)** YZT, **(C)** CY, and **(D)** ADH. **(E)** Peaks: 1. Protopine, 2. Tetrahydropalmatine, 3. α -Allocryptopine, 4. Byakangelicin, 5. Coptisine, 6. Tetrahydroberberine, 7. Corydaline, 8. Berberine, 9. Palmatine, 10. Coptisine, 11. Dehydrocorydaline, 12. Psolaren, 13. Imperatorin, and 14. Isoimperatorin.

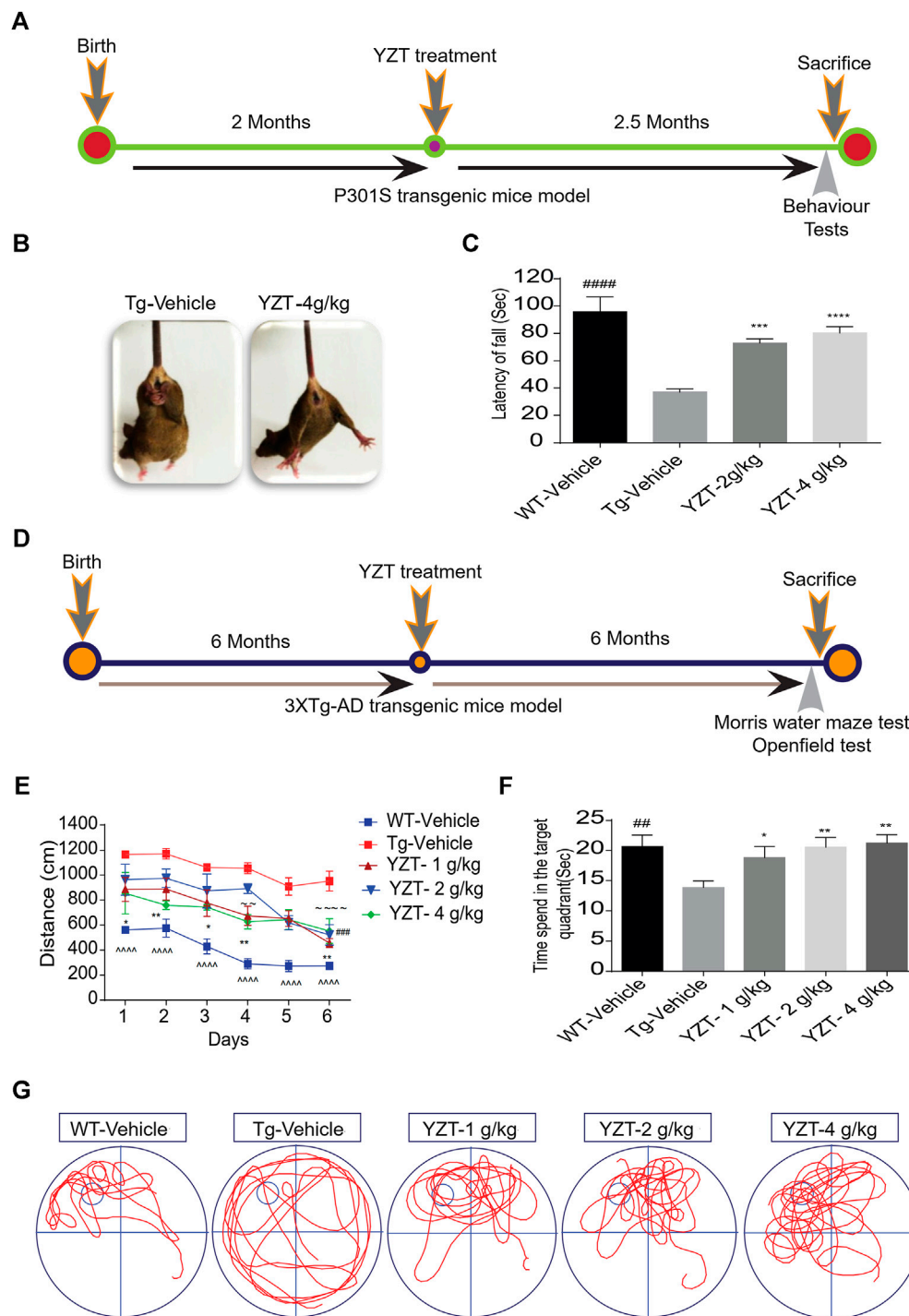


FIGURE 2 | YZT treatment improved motor function and enhances learning and memory function in P301S and 3XTg-AD mice models. **(A)** The timeline schedule of drug administration and behavior tests in P301S tau mice. **(B)** In tail hanging test, YZT improved the motor function of 4 months P301S tau mice when compared to vehicle. **(C)** In rotarod test, regular treatment of 2-month old P301S tau mice with YZT (2 or 4 g/kg) via food admixture for 2 months significantly ameliorated motor function. The average latency of mice ($N = 14$) fall was calculated. #### $p < 0.01$ (WT/Vehicle), *** $p < 0.001$ (YZT 2 g/kg/d), and **** $p < 0.0001$ (YZT 4 g/kg/d) vs Tg-vehicle. **(D)** The timeline schedule of drug administration and behavior tests in 3XTg-AD mice. **(E)** After the visible platform training in Morris water maze test, the experimental mice were trained for 6 days with four trials per day to learn the place and location of hidden platform in the tank. The learning potential of the YZT treatment group improved with the time and days of learning when compared to the Tg-vehicle. Each point represents the mean length values of four trials per day, ($N = 14$). $p < 0.001$ (WT-vehicle vs. Tg-vehicle); #### $p < 0.001$ (YZT -1 g/kg vs. Tg-vehicle), **** $p < 0.0001$ (YZT-2 g/kg vs. Tg-vehicle), ** $p < 0.01$ (YZT-4 g/kg vs. Tg-vehicle). **(F)** On the seventh Day, the probe trial demonstrated that YZT treatment showed improved memory function in probing the platform in target quadrant when compared to the Tg-vehicle. **(G)** The displayed pictures illustrate YZT improved the memory retention in animal's behavior during the probe trial in the animal tracking camera videos.

Yuan-Hu Zhi Tong Treatment Reverses Motor Impairment in P301S Tau Mice and Ameliorates Learning and Memory Functions in 3XTg-AD Mice

We utilized 2-month old P301S tau (N = 14) mice, i.e. before the onset of tau pathology, to evaluate the efficacy of YZT. The timeline indicates the period of drug administration and behavior tests plan in P301S tau mice model (**Figure 2A**). We found that chronic drug-feed administration of YZT (2 or 4 g/kg/d) for nearly 2.5 months until 4.5 months of age, YZT did not substantially alter animal body weight or affect any prominent harmful impacts in P301S tau mice model (**Supplementary Figure S1A**). YZT treatment significantly ameliorated motor impairment compared with control mice, as inferred from the tail hanging test (**Figure 2B**). Further we employed the rotarod experiment to assess the motor function and locomotor activities of vehicle group and YZT treatment group. Substantial changes were detected among the YZT (2 and 4 g/kg/d)-treated mice and vehicle group in the latency to fall (**Figure 2C**). These findings suggest that YZT improved motor function and enhanced locomotor activity.

We tested the long-term effect of YZT in another AD mice model, 3XTg-AD, via food admixture. The timeline for drug administration and behavior tests plan in 3XTg-AD mice is displayed in **Figure 2D**. We found that YZT treatment did not affect the body weight of 3XTg-AD mice (**Supplementary Figure S1B**) during the whole study. Furthermore, in behavioral studies, we found that YZT administration for 6 months significantly reduced the distance traveled by 3XTg-AD mice to detect the platform during the training in the “Morris Water Maze test (MWM)” (**Figure 2E**). The transgenic 3XTg-AD vehicle group (Tg-vehicle) took a lengthier route to find the platform compared to vehicle-treated wild-type (WT) mice (**Figure 2E**). However, YZT treatment in 3XTg-AD mice clearly improved the learning ability, as evidenced by the shorter path on the fourth and sixth days of the learning test (**Figure 2E**). Tg-vehicle mice consistently traveled a longer path [$F(5,15) = 13.22$; $p < 0.0001$] when compared with the vehicle-treated WT mice during all six training sessions (post-hoc, $p < 0.0001$).

To assess memory function after the 6-days learning, we did a probe trial 24 h after the sixth hidden day. During the probe trial, the YZT-treated group spent more time in probing the platform compared to the Tg-vehicle group in the target quadrant (**Figure 2F**). “One-way ANOVA analysis” of the probe test, the search ratio in the target quadrant indicated a significant effect of YZT treatment of 3XTg-AD mice on memory retention compared to the Tg-vehicle [$F(4, 64) = 3.637$; $p < 0.01$]. Altogether, these findings reveal that spatial learning and memory functions of 3XTg-AD mice is improved by YZT administration.

The open field experiment was conducted to assess the exploratory and locomotor activity of Tg-vehicle group and YZT-treated group. There were no significant variations between the Tg-vehicle and YZT-treated group in total moving distance and total ambulatory movement duration,

although YZT-treated groups performed slightly better than the Tg-vehicle group (**Supplementary Figures S1C,D**).

Yuan-Hu Zhi Tong Administration Relieves Tau Pathology and Lowers Phospho Tau Load in P301S Tau and 3XTg-AD Mice Brain

To evaluate the tau pathogenesis in the P301S tau mice model, AT8, AT100 and MC1 monoclonal antibodies were used. The AT8 epitope indicates the phosphorylation site of Thr212/Ser214 signifies internal repeats of “microtubule binding domains (RT-14)”. The epitope AT100 is also located outside the RT-14 and. The epitope MC1 is located in tau 5-15/312-322 all these epitopes imply the development of tau pathogenesis. AT8-positive immunostaining in the cortico-hippocampal brain region of P301S tau mice demonstrated that YZT treatment at doses of 2 and 4 g/kg/d decreased AT8 positive cell count in cortico-hippocampal region by 74% ($p < 0.05$) and 70%, respectively (**Figures 3A,B**). Immunostaining of AT100-positive neurons also revealed that YZT treatment at doses of 2 and 4 g/kg/d decreased AT100 positive cell count in cortico-hippocampal region by 68 and 74%, respectively (**Figures 3A,B**). Immunostaining of MC1-positive neurons also revealed that YZT treatment at doses of 2 and 4 g/kg/d decreased MC1 positive cell count in cortico-hippocampal region by 68% ($p < 0.05$) respectively (**Figures 3A,B**).

3XTg-AD mice brain slice was immune stained with AT8, PHF-1 and HT7 monoclonal antibodies. The epitope PHF-1 is also located outside the RT-14 and requires the phosphorylation of paired helical filaments pSer396/pSer404 and aberrant conformation of tau. The PHF1-positive neuron load in the brain slice of 3XTg-AD mice demonstrated that YZT treatment at doses of 1, 2, and 4 g/kg/d decreased PHF1 positive cell count dose dependent in CA2, CA3 hippocampal region by 44, 55, and 70%, respectively ($p < 0.05$) (**Figures 3C,D**). The AT8, HT7-positive neuron load in the brain slice of 3XTg-AD mice indicated that YZT treatment at doses of 1, 2, and 4 g/kg/d decreased AT8, HT7 positive cell count dose dependent in CA2, CA3 hippocampal region by 48, 58, and 74%, respectively ($p < 0.05$) (**Figures 3C,D**). Long-term YZT treatment did not significantly reduce 4G8 positive neurons in 3XTg-AD mice CA2, CA3 hippocampal brain region are shown in **Supplementary Figures S2C,D**. The quantification of plaque load was performed using ImageJ software.

Yuan-Hu Zhi Tong Decreases the Insoluble Tau Load in the Brain of P301S Tau and 3XTg-AD Mice

The above findings of decreased phospho-tau positive neurons were further corroborated by the differential separation of insoluble tau. The insoluble tau extraction in the brain homogenate of P301S Tau mice model is described previously (Myeku et al., 2016). The brain sample was first extracted with RIPA buffer. The resulting RIPA fraction was further extracted with 1% sarkosyl detergent and ultra-

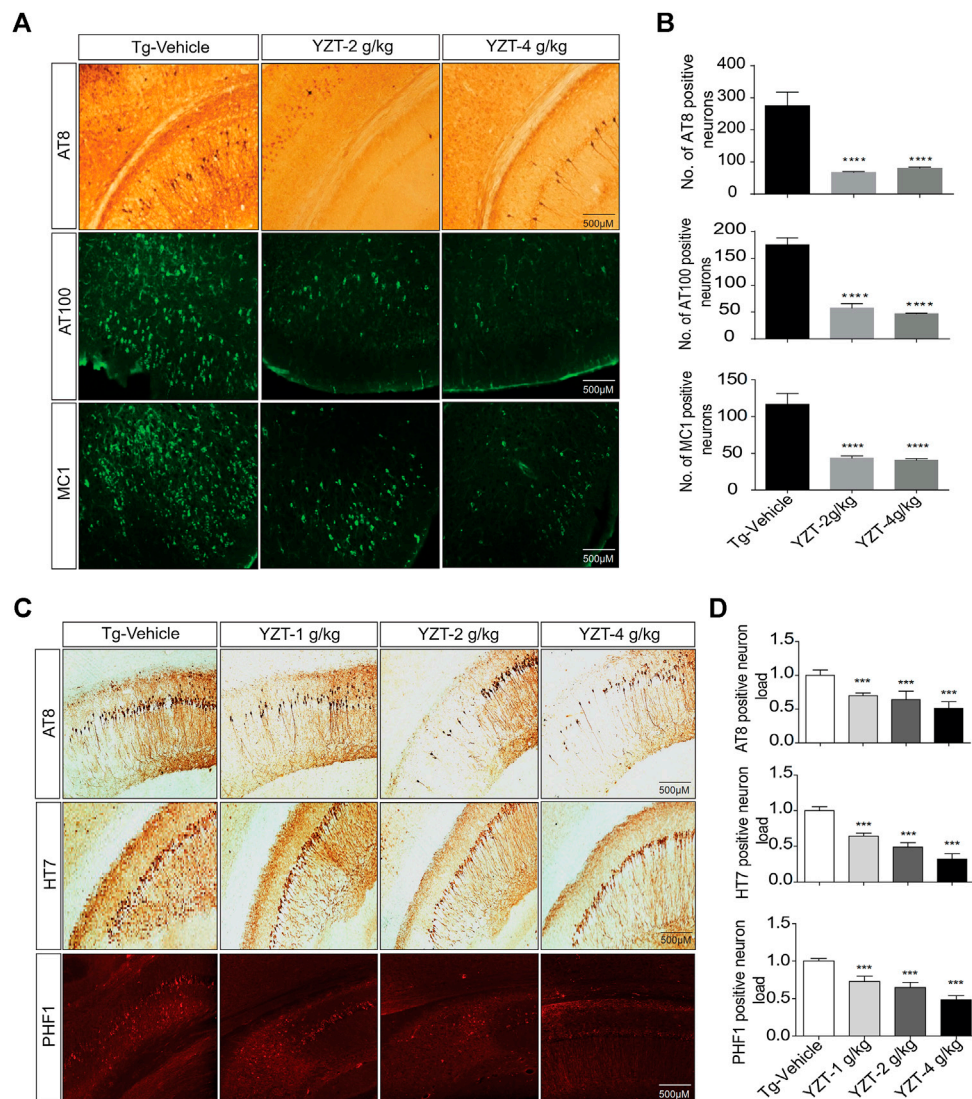
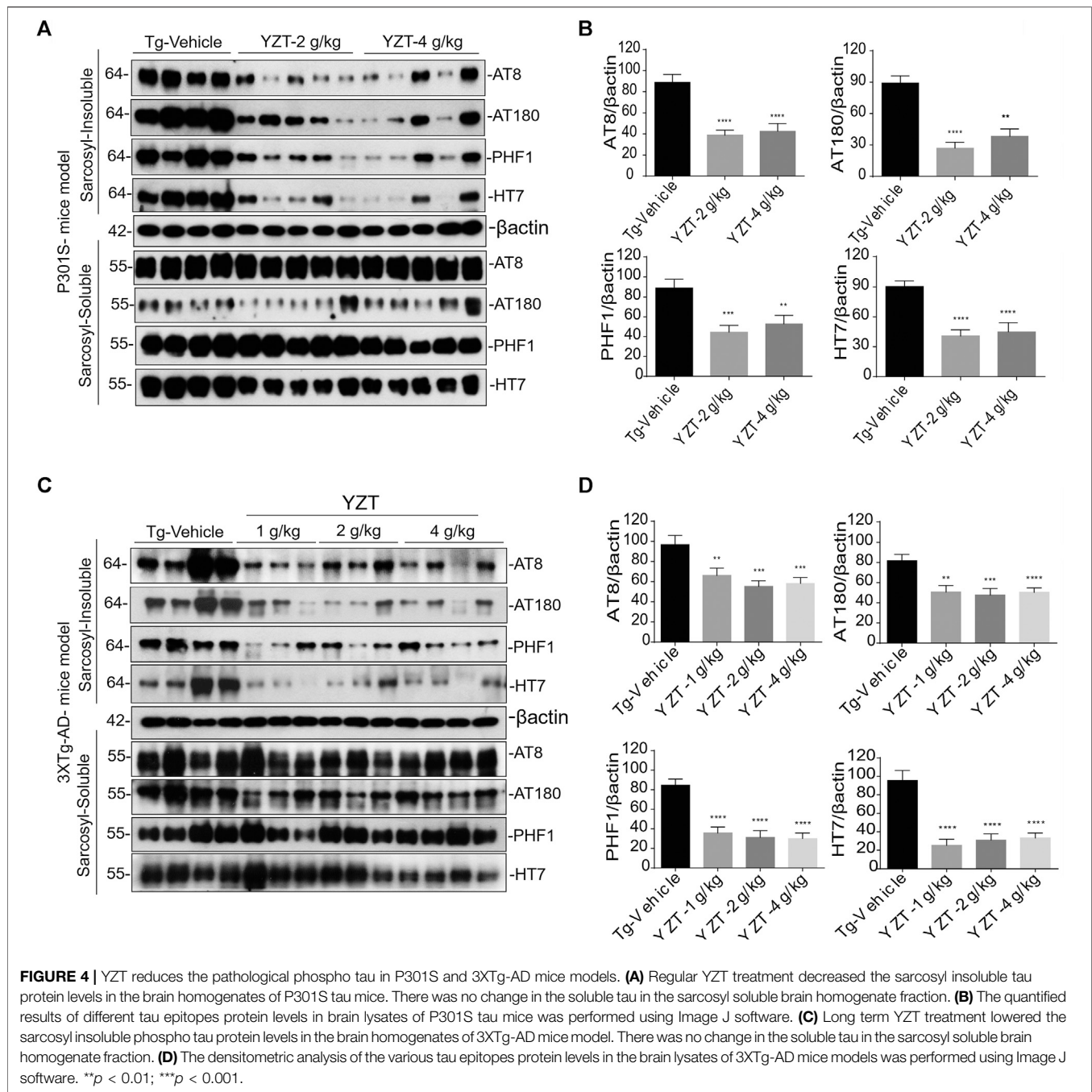


FIGURE 3 | YZT treatment mitigates tau pathology in P301S and 3XTg-AD mice. **(A)** Chronic treatment of YZT reduced AT8, AT100 and MC1 in the cortico-hippocampal brain region of P301S tau mice. The displayed pictures are fluorescent images of brain slice taken in fluorescent detecting microscope. **(B)** The quantified results of AT8, AT100 and MC1 positive neurons in the cortico-hippocampal brain region of P301S tau mice was performed using Image J software N = 14, ** $p < 0.01$; *** $p < 0.001$. **(C)** Chronic treatment of YZT reduced AT8-, PHF- and HT7-positive neurons in the CA2, CA3 hippocampal region of 3XTg-AD mice. **(D)** Quantification of AT8-, HT7- and PHF1 positive neurons in the CA2, CA3 hippocampal brain region of 3XTg-AD mice. The number of phospho and total tau-positive neurons were quantified using ImageJ software N = 4.

centrifuged (100,000 \times g) at least 1 h. Resulting supernatant was marked as soluble tau and pellet was designated as insoluble tau fraction.

AT8, AT180, CP13, PHF-1 antibodies were used to detect the phosphorylated tau in both the fractions of soluble and insoluble toxic protein aggregates. Misfolded conformation tau and total tau were detected using Alz50 and HT7 antibodies. There were no significant differences in phosphorylated, misfolded and total tau in the soluble fraction of the three groups (Figure 4A). In contrast, phosphorylated, misfolded and total tau were significantly reduced in the sarkosyl-insoluble fraction (Figures 4A,B) of YZT-treated groups compared to that in the vehicle-treated group.

To further confirm, we investigated 6 months treatment of YZT in 3XTg-AD mice, treated mice were sacrificed and levels of soluble and insoluble tau in homogenates of their whole brain hemispheres were determined. YZT-treated groups showed significant reduction in levels of insoluble phospho tau when compared with vehicle-treated animals (Figures 4C,D). Notably, there were no significant differences in phosphorylated, misfolded and total tau in the soluble fraction of the three treatment groups (Figure 4C). In contrast, phosphorylated, misfolded and total tau was significantly reduced in the sarkosyl-insoluble fraction (Figures 4C,D) of YZT-treated groups but not in the vehicle-treated group of 3XTg-AD mice. Long-term YZT treatment did not significantly reduce APP,

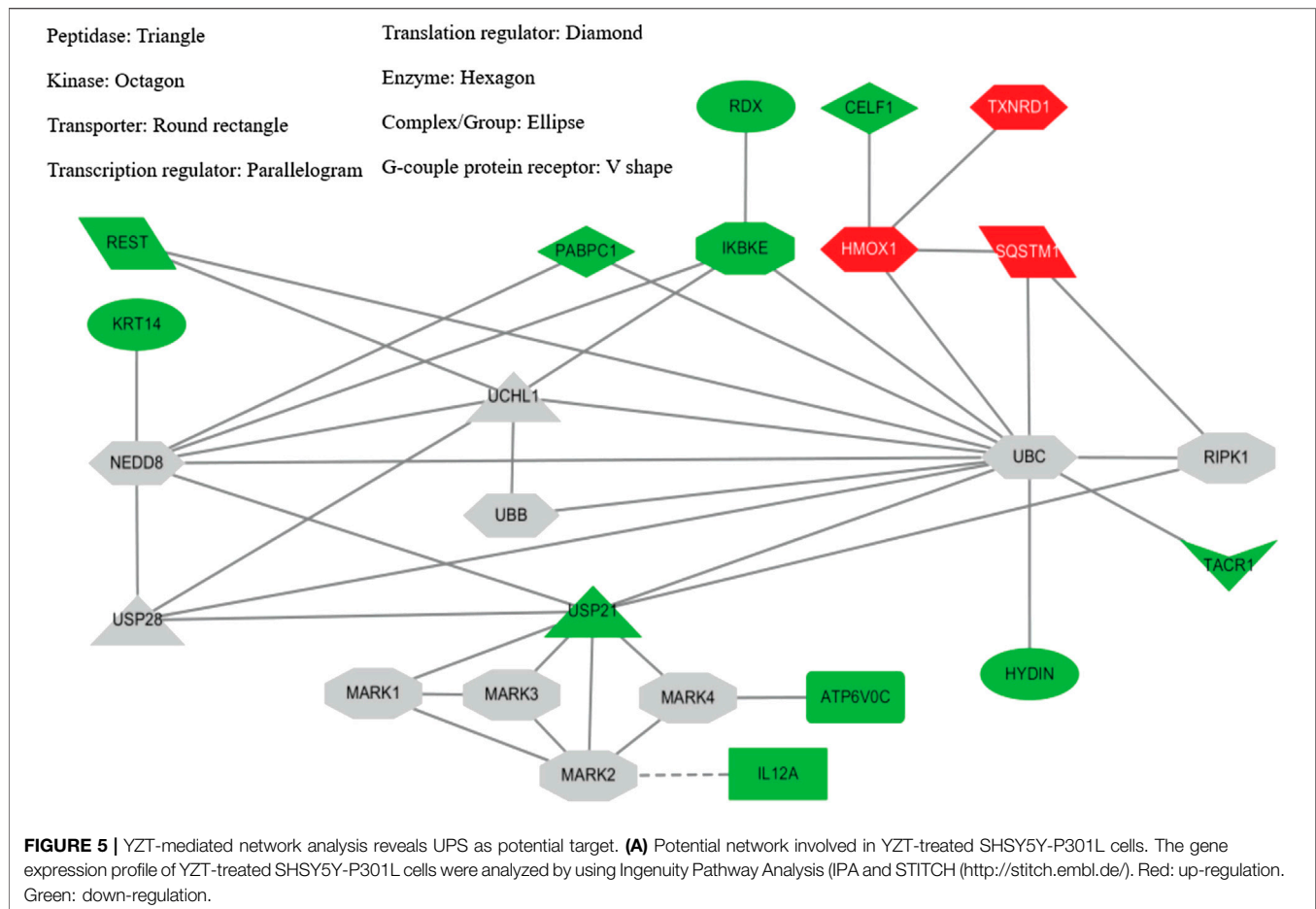


CTFs and its phosphorylated form in the SDS brain fraction of 3XTg-AD mice. Representative figures of APP, CTFs and its phosphorylated form in the SDS brain fraction of 3XTg-AD mice are shown in **Supplementary Figures S2A,B**.

Microarray and Connectivity Maps

In SH-SY5Y-P301L cells, when compared to vehicle control, the YZT treatment of 100 $\mu\text{g/ml}$ in cells demonstrated a 2-fold upregulation of 13 genes with down-regulation 64 genes graphed in a heat map (**Supplementary Figure S3**). The up- and down-regulated genes were used to query Consensus Path Database

(CPDB) (CPDB is an integrative interaction database that gathers molecular interaction data integrated from 32 different public repositories and provides a set of computational methods and visualization tools to explore these data), IPA (Ingenuity Pathway Analysis, QIAGEN), STITCH (search tool for interactions of chemicals), and Clue (This platform provides integrated access to datasets, results from the processing and analysis of these data, and software tools that the community can leverage to advance their research), respectively. From IPA analysis, treatment of YZT generated an upregulated network center on HMOX1 (heme oxygenase 1, an essential enzyme in heme catabolism, cleaves



heme to form biliverdin), SQSTM1 (sequestosome 1 or p62) and TXNRD1 (thioredoxin reductase 1) (**Figure 5**, upper right label in red). Analysis from CPDB suggests that these three hub genes, HMOX1, SQSTM1, and TXNRD1, are involved in the Nuclear Receptors Meta-pathway and Nuclear factor (erythroid-derived 2)-like 2 (NRF2)-mediated oxidative stress response.

Using the gene expression signature from YZT treatment as an input query, Clue analysis gave a connectivity score (or similarity) of 96.51 to upregulation of SQSTM1 and 96.17 to NF- κ B pathway inhibitors (**Figure 5**). In fact, treatment with YZT resulted in the upregulation of SQSTM1, which can bind to ubiquitin (Lee and Wehl, 2017). Using STITCH dataset, an extended protein-protein interaction network (label in gray) was generated (**Figure 5**) and ubiquitination was highlighted from these 24 genes.

Yuan-Hu Zhi Tong Reduces Phospho- Tau via Ubiquitin Proteasomal System *In Vitro* and *In Vivo*

Further to evaluate whether tau-reducing activity of YZT is via ubiquitin proteasomal system (UPS), we carried out experiments *in vitro*. First to confirm the cytotoxicity of the ethanolic extract of YZT, different concentrations of extracts were added to SH-SY5Y P301L and 7PA2 cells for 48 h. The YZT did not show any adverse

effect in the cell morphology and cell viability (**Figure 6A**) as demonstrated by MTT assay in SH-SY5Y-P301L and 7PA2 cells (**Supplementary Figure S4A**).

We further evaluated its tau-reducing activity in SH-SY5Y-P301L cells following YZT treatment with three different doses (25, 50, and 100 μ g/ml final concentration) for 48 h. As expected, the treatment with YZT significantly and dose-dependently reduced the levels of total tau in SH-SY5Y tau-mutant P301L cells (**Figure 6B**) without influencing the viability of cells. The low concentration of YZT (25 μ g/ml) insignificantly reduced the abnormal tau level by 12% in SH-SY5Y P301L cell lysates (**Figure 6B**). At 50 and 100 μ g/ml, abnormal tau was reduced by 33% and by 79%, respectively, compared to the vehicle (0.1% DMSO) control (**Figure 6B**). These data indicate that YZT indeed reduces abnormal tau aggregation in the cell model of tau, and it does so at a concentration-dependent manner YZT treatment did not significantly reduce the level of APP, C-terminal fragments (CTFs), soluble APP (sAPP) $_{\alpha}$ and sAPP $_{\beta}$ in the cell lysate of 7PA2 cells (25, 50, and 100 μ g/ml final concentration), for 48 h (**Supplementary Figure S4B**).

It is well known that the enzyme-determining step in the ubiquitin proteasome system is the ubiquitination of protein substrates and followed by digestion of all ubiquitinated proteins that bind to proteasome. We attempted to investigate whether YZT modulated the total and the K-48 specific ubiquitinated conjugates

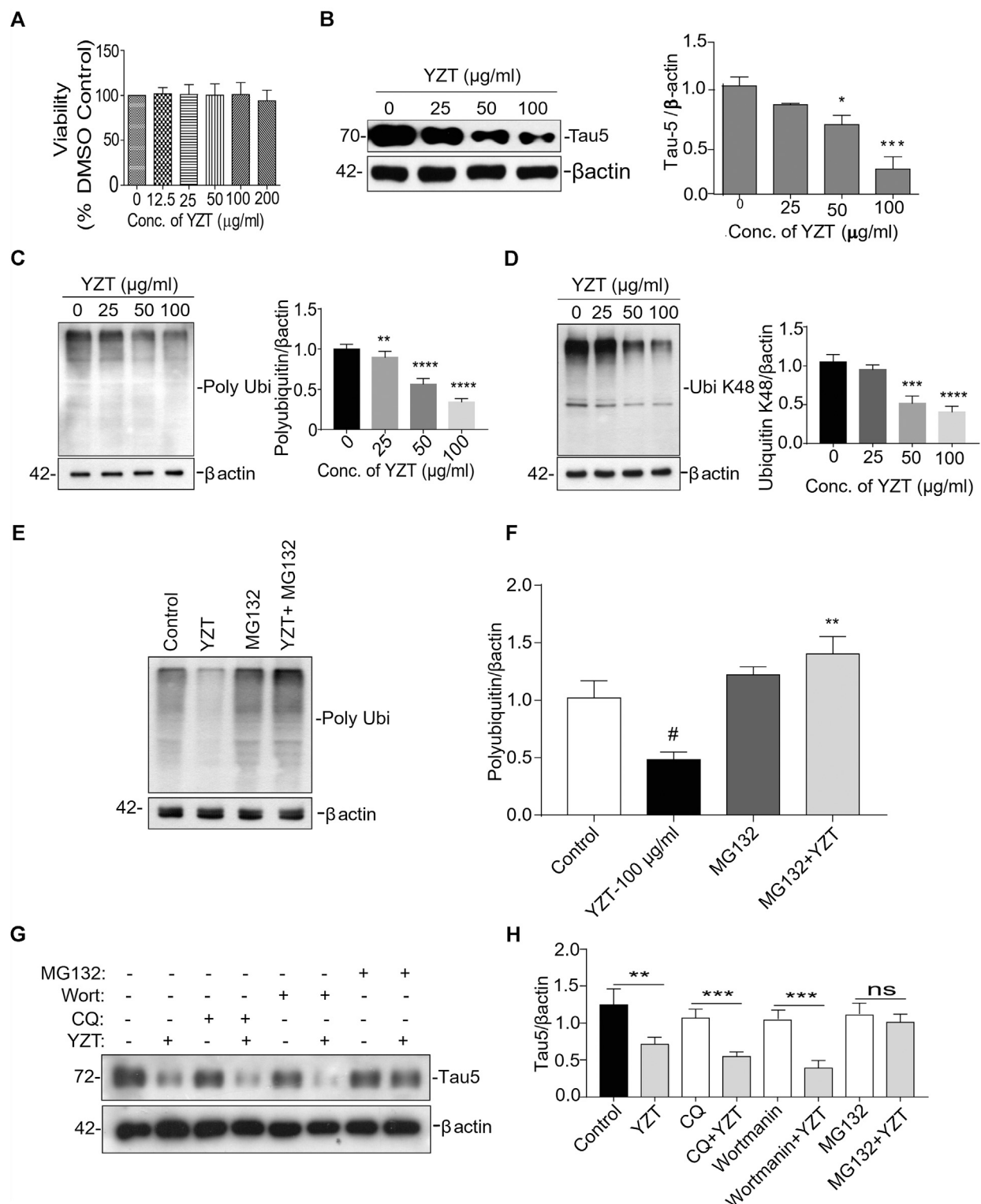
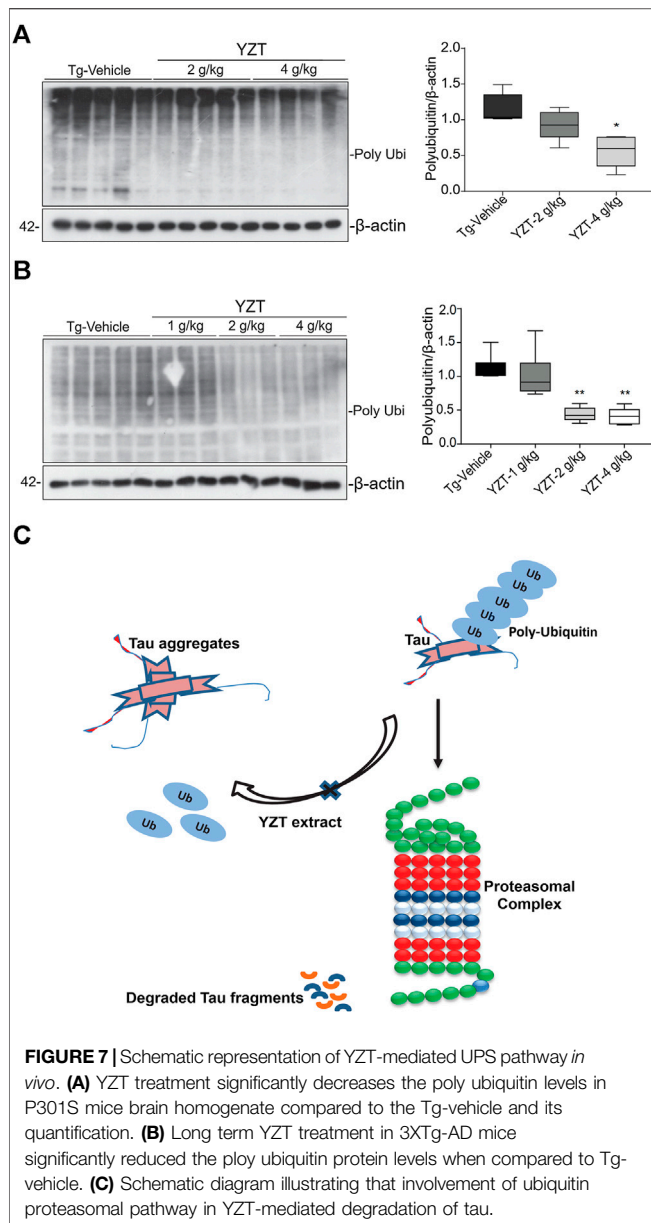


FIGURE 6 | Involvement of UPS in YZT-mediated degradation of tau. **(A)** Viability test of YZT on SH-SY5Y-P301L cells. Cell viability was determined using the MTT assay. **(B)** Effect of YZT on the level of total phospho tau (tau 5) in SH-SY5Y-P301L cells. **(C)** YZT significantly decreased the levels of polyubiquitin in SH-SY5Y-P301L treated cells. **(D)** YZT significantly decreased the levels of ubiquitin K48 in SH-SY5Y-P301L treated cells. **(E,F)** YZT reduces the level of insoluble phosphorylated and misfolded tau via UPS mediated degradation pathway. YZT significantly reduced the levels of polyubiquitin in SH-SY5Y-P301L treated cells. The reduction of polyubiquitin was restored when the cells were pretreated with MG132 (proteasome inhibitor), thus clearly illustrating that involvement of UPS in YZT-mediated degradation of tau. **(G,H)** YZT-treated SH-SY5Y-P301L cells in the presence of autophagy inhibitors (CQ and wortmannin) the tau reducing effect of YZT was not blocked but in the presence of MG132 blocked the YZT's tau reducing effect. All the results were represented as mean \pm SEM of three independent experiments. $N = 3$, ** $p < 0.01$; *** $p < 0.001$.



in SHSY5Y-P301L-tau cells. The amount of both total (Figure 6C) and K-48 ubiquitinated proteins was dose-dependently lowered by the YZT treatment (Figure 6D), which is consistent with the microarray data. Because MG132 (proteasome inhibitor) stopped the effect of YZT on polyubiquitin degradation (Figures 6E,F) and YZT did not influence autophagy as evidenced by the level of light chain 3 (LC3)-II in a time dependent and dose dependent effect (Supplementary Figures S4C,D). Further to evaluate that YZT effect on tau degradation involving UPS and independent of autophagy, we used the inhibitors of Autophagy (chloroquine (CQ) and wortmanin) and UPS (MG132) with YZT treatment to identify the tau degradation pathway. We did not find any increase in the LC3-II levels in the presence of CQ and wortmanin with YZT treatment, which clearly illustrates tau degradation is independent of

autophagy (Supplementary Figure S4E). In addition, in the presence of autophagy inhibitors (CQ and wortmanin) the YZT's tau reducing effect was not blocked but MG132 blocked the YZT's tau reducing effect (Figures 6G,H). Which clearly indicate that proteasomal degradation was exclusively responsible for YZT's effects on ubiquitylated protein degradation of tau. Further illustrating the involvement of UPS in YZT-mediated degradation of tau. Further to correlate this finding with the *in vivo* study, we did the western blot experiment to elucidate the protein expression of UPS proteins in transgenic animal model brain homogenate. Surprisingly, the YZT-treated P301S (Figure 7A) and 3XTg-AD (Figure 7B) brain lysates illustrated a significant decrease in polyubiquitin proteins compared to the Tg-vehicle group, demonstrating YZT degrades the insoluble phospho tau via UPS both *in vitro* and *in vivo*. Further we also evaluated the other degradative pathway proteins in YZT-treated mice brain lysates compared to the Tg-vehicle group, we did not discover any substantial alterations in autophagy proteins and kinases (Supplementary Figures S5A,B) involved in tau degradation. The schematic representation depicts the involvement of UPS in YZT-mediated degradation of tau (Figure 7C).

DISCUSSION

YZT administration to the *in vivo* tau mice model demonstrated a strong tau reducing effect clearly illustrating the therapeutic efficiency of the Chinese herbal medicine. Until now, the actual medicinal value of YZT in curing AD pathology and cognitive deficits is not validated. The present study demonstrates that YZT administration in P301S and 3XTg-AD mice models reduced the tau deposition and improved both motor co-ordination and memory retention, respectively. The herbal composition of YZT is a combination of CY and ADH in a perfect ratio 2:1 and at this specified ratio YZT significantly decreased insoluble phospho tau including misfolded and total tau in brain fractions. Chronic YZT administration boosted the motor function as demonstrated by rotarod experiments and recovered the P301S tau mice hindlimb paralysis compared to the Tg-vehicle. Notably, YZT oral administration improved the motor and memory functions in addition to a substantial reduction in the insoluble tau burden.

Successive extraction of brain homogenates by RIPA and sarkosyl detergent is a method commonly used with different AD mouse models to assess the - total amount of homogenous tau and insoluble tau species in brains (Durairajan et al., 2012; Dillon et al., 2013). During this study, we observed that different doses of YZT significantly reduced sarkosyl-insoluble tau in the brains of P301S tau and 3XTg-AD mice. Overall, the YZT-induced reduction of insoluble tau (65–75%) in the brain hemispheres corresponds well with the decrease in the AT8-positive load (33%) reflecting the overall reduction of tau load in the whole brain. "Since a progressive shift of brain tau from soluble to insoluble pools plays a mechanistic role in the onset and/or progression of AD (Geerts et al., 2013)", YZT mediated decrease in insoluble phospho tau clearly demonstrates its ability to delay the onset of tau pathogenesis in AD.

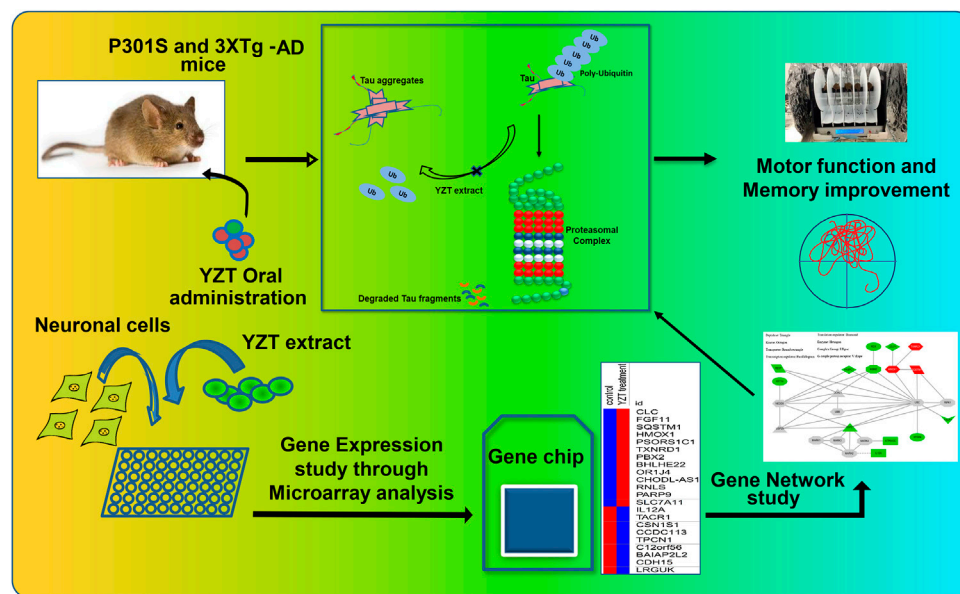


FIGURE 8 | Schematic illustration of YZT's effect on tau pathology and its mechanism of action.

The TCM herbal formula, YZT is clinically used to treat pain and neuralgia (Yuan et al., 2004; Xu et al., 2013). Neuropharmacological studies of YZT and its components have only confirmed the anti-acetylcholine esterase and anti-depressive activities (Xu et al., 2013); for the first time we have found that YZT's components show anti-tau activities. Although "AD is commonly considered a memory disorder, almost all people diagnosed with AD develop neuropsychiatric symptoms" (NPS: anxiety, motor impairment, hallucinations, and psychosis) at some stage during their disease (Podlisny et al., 1995). Recent A β -based therapies do not prevent cognitive decline, NFT formation or neurodegeneration (Dillon et al., 2013). Recent studies have also highlighted the strong correlation between tau pathology, cognitive decline and NPS (Yoshiyama et al., 2013).

Conventional AD drug discovery has taken a great approach in developing many clinical trials to halt the pathogenesis as an established target. Drug discovery for AD based on the cholinergic and β -amyloid hypothesis has not succeeded in that medications anticipated to treat acetylcholine deficiency and β -amyloid accumulation have not been effective (Yoshiyama et al., 2013). Based on these failures, and because NFTs are well correlated with cognitive impairment and NPS (anxiety, motor impairment, hallucinations, and psychosis) (Geerts et al., 2013), current disease-modifying approaches are taking a new approach, focusing on tau-based pathologies. In AD patients many microarray and genetic studies on tau-associated pathogenesis has elucidated the link of psychiatric disorders (markers of psychosis and mood disorders) (Altar et al., 2009).

Traditional Chinese medicine uses a broad way of pharmacological approach in curing neurodegenerative diseases by combining a few herbs with multifactorial disease modifying efficacy. Therefore, TCM typically uses this type of combinational, holistic approach in curing disease and YZT is the

appropriate TCM candidate to tackle multifactorial symptoms of AD including tau aggregation. The disease-modifying activity of YZT against AD and other neurodegenerative disease in general or tauopathies have never been studied. We believe that YZT has the potential to be an effective therapeutic TCM that will both ameliorate the cognitive and psychiatric symptoms and address the underlying biochemical causes of AD.

In an experimental plan primarily designed to identify anti-A β and anti-tau activities of YZT *in vitro* AD models, 7PA2 and SH-SY5Y-P301L cells, we found that YZT did not regulate the protein levels of full length APP (FL-APP) and CTFs. These results indicate that YZT neither influences APP processing nor degrades APP metabolites. Since AD has both A β and tau related abnormalities, we tested the effect of YZT on the levels of tau in SH-SY5Y-P301L cells. Our results show that YZT reduced the levels of total tau in SH-SY5Y-P301L lysates. To confirm the tau-reducing activity of YZT observed in *in vitro* studies, we used P301S tau mice and 3XTg-AD transgenic mice for short-term and long-term *in vivo* studies. The P301S tau mice and 3XTg-AD mice were orally administered YZT (1, 2, or 4 g/kg/day). When we convert the dose used in a mouse to a human dose based on surface area for humans (Tao et al., 2013), 2 g/kg/d of YZT in mouse is equivalent to 0.16 g/kg in human. According to the Chinese pharmacopeia, the daily recommended dose of YZT for human is 0.026 g/kg. The dose used in our animal study is relatively 6 times higher than the dose typically prescribed for human. We used these doses because our cell tests showed no toxicity at this and greater levels; we wished to achieve significant brain levels in order to be able to fully assess the effects of YZT. Indeed, a recent study done elsewhere used even higher doses such as 4 or 8 g/kg/d to assess the *in vivo* effect of YZT with no toxic effects, (Xu et al., 2013). Since YZT components permeates the blood brain barrier (BBB) in acceptable concentrations (Tao

et al., 2013) and we wished to achieve therapeutic effects in the brain, we utilized 1–4 g/kg/d of YZT, which is the dose that had previously used in a pharmacokinetic study to observe the brain permeable components of YZT (Reagan-Shaw et al., 2008).

A possible mechanism by which YZT decreases tau aggregation is by decreasing the phosphorylation of tau. In our experiments, YZT treatment decreased phosphorylated tau, which is the stimulator of tau aggregation (Biernat et al., 1992; Lewis et al., 2000). Although our results evidently demonstrated the capability of YZT to inhibit the advancement of tau aggregation, the underlying mechanism of YZT in reducing tau aggregation is to be disclosed. The p62/SQSTM1-inducing activity of YZT represents an intriguing and interesting finding. Multifunctional role of p62 was observed in several neurodegenerative entities such as tau hyperphosphorylation, association with tau protein and facilitates selective p62 mediated autophagy (Caccamo et al., 2017). Besides, p62 increasing effect of YZT, other antioxidants proteins such as HMOX1 and TXRD1 were also upregulated by YZT probably through the Nrf2-ARE signaling pathway. Upregulation of SLC7A11 in neuronal cells consider as to be the resistance to oxidative stress (Lewerenz et al., 2012). Similarly, HMOX1 also shows the resistance to oxidative stress facilitated cell death (Chen et al., 2000). Higher expression of PBX1, TXNRD1 and bHLHE22 gene shows that, which support neuronal growth, cell differentiation and maturation (Soerensen et al., 2008; Sgado et al., 2012; Dennis et al., 2019). The pathway analysis identified the modulation of ubiquitinylation by targeting deubiquitylating enzyme (DUB), USP21, and its substrates as one of the pathways significantly changed amongst differentially expressed genes in response to YZT treatment (Figure 5). USP21 is a deubiquitinase, which promote deubiquitination process in protein degradation, deubiquitinating enzymes regulates centrosome regulation, chromosomal stability (Urbe et al., 2012). The study on reversible ubiquitination is progressing rapidly. USP21 of USP sub family, prominently regulates several pathway signals to interact with MEK2 and deubiquitinate MEK2 directly, thus promoting the tumor growth in cells inducing stabilization of MEK2 by activating ERK1/2 pathway (Li et al., 2018). In spite, its actual performance in tau stabilization and other proteins involved in neurodegeneration are yet to be established. It is imperative to initiate further studies on this subject to elucidate its participatory role in eradicating neurodegenerative protein. One interesting finding is that the expression of genes nitric oxide synthase one adaptor protein (NOS1AP) also recognized as carboxyl-terminal PDZ ligand of neuronal nitric oxide synthase protein (CAPON); 2) Repressor element-1 binding transcription factor (REST) are involved in tau aggregation and cytoplasmic aggregates formation respectively, were strongly downregulated by YZT (Figure 5). CAPON has recently shown as a molecular linker that connects A β amyloidosis and tau pathology (Hashimoto et al., 2019). Increase of CAPON was observed in the APP mutant knock in (KI) mice brain. Overexpression of CAPON in APP KI mice increased tau phosphorylation in mice whereas the reduction of CAPON decreased tau pathology and neuronal loss in P301S tau transgenic mice. However, CAPON-induced cell death was shown to be only attributed to a A β -dependent mechanism but not tau

(Hashimoto et al., 2019). Ubiquitin-based proteasomal degradation is induced by REST during the neuronal differentiation (Ballas et al., 2005). REST is dormant in mature neurons, however REST can be stimulated by the vulnerable hippocampal neurons in disease like ischemia (Calderone et al., 2003; Formisano et al., 2007) and epileptic seizures (Palm et al., 1998), and also found in Huntington disease (Zuccato et al., 2003; Zuccato et al., 2007).

This study also predicted YZT as an activator of SQSTM1, could be as an antioxidant, and if true, then microarray gene expression profiling could be combined with CMap (Clue) to reveal mechanisms of actions and to identify new health benefits of YZT. In addition, YZT also had connections with aromatase inhibitors (99.27), including exemestane and androsta-1,4-dien-3,17-dione, and FXR antagonist (97.46), including guggulsterone and 15-deoxy-delta(12,14)-prostaglandin J2 (Figure 5). These predictions warrant further characterization. Moreover, it has been shown that the key markers of YZT such as protopine, allocryptopine, tetrahydropalmatine, tetrahydroberberine, corydaline, palmatine, dehydrocorydaline and imperatorin are brain permeable (Tao et al., 2013), which might explicate the tau-reducing effect of YZT in the central nervous system of transgenic AD mice; key markers permeable in brain crossing the blood brain barrier namely. Although YZT components reach the brain, yet it is possible that YZT also exerts therapeutic effects in other areas of the body. Since YZT is encompassed of numerous small molecules, distinguishing the effective compounds and knowing their mechanism of action in disease modification will involve further work.

In conclusion, based on experimental results, we found that YZT had remarkable tau-reducing and cognitive-enhancing activities (Figure 8). Based on the tau-reducing activity, the motor- and memory- enhancing properties and anti-oxidative capacity of YZT, results suggest that YZT can be established as a health supplement or may possibly distributed as a raw material for prescriptions to prevent or cure AD. Present study establishes not only valuable evidence about the disease modifying function of YZT, but also provides a strategy to create TCM into the network pharmacology studies.

DATA AVAILABILITY STATEMENT

The raw data supporting the conclusions of this manuscript will be made available by the authors, without undue reservation, to any qualified researcher.

ETHICS STATEMENT

All animal experiments were approved by the Hong Kong Baptist University Committee on the Use of Human and Animal Subjects in Teaching and Research (HASC approval # HASC/13-14/0165) and by the Committee on the Use of Live Animals for Teaching and Research (CULATR #3314), at the University of Hong Kong. All animal experiments were

performed in accordance with the relevant guidelines and regulations of both HASC and CULATR.

AUTHOR CONTRIBUTIONS

Conceptualization: ML, SSKD, CH. Methodology: AI, SK, YL, AK, SS, SM, BT, SSKD. Investigation: AI, SK, YL, AK, SS, SM. Data curation: SSKD, AI, SK, YL, AK, ML, JS, JL. Writing original draft: AI, SK, YL, SSKD, CH, BT. Writing review and editing: ML, JS, JL, SSKD, CH, JT, and KC. Funding acquisition: ML, SSKD. Resources: ML, SSKD.

FUNDING

This study was supported by the grants of Hong Kong Health and Medical Research Fund (HMRP 12132061, HMRP 14150811, HMRP 15163481, HMRP 17182541, HMRP 17182551), the General Research Fund from Hong Kong Government SAR (GRF/HKBU 12101417, GRF/HKBU 12100618), and research grant from the Hong Kong Baptist University (HKBU/RC-IRCS/17–18/03). This study also supported by the National Natural Science Foundation, China (NSFC 81773926, NSFC 81703487)

REFERENCES

- Allen, B., Ingram, E., Takao, M., Smith, M. J., Jakes, R., Virdee, K., et al. (2002). Abundant tau filaments and nonapoptotic neurodegeneration in transgenic mice expressing human P301S tau protein. *J. Neurosci.* 22, 9340–9351. doi:10.1523/jneurosci.22-21-09340.2002
- Altar, C. A., Vawter, M. P., and Ginsberg, S. D. (2009). Target identification for CNS diseases by transcriptional profiling. *Neuropsychopharmacology* 34, 18–54. doi:10.1038/npp.2008.172
- Ballas, N., Grunseich, C., Lu, D. D., Speh, J. C., and Mandel, G. (2005). REST and its corepressors mediate plasticity of neuronal gene chromatin throughout neurogenesis. *Cell* 121, 645–657. doi:10.1016/j.cell.2005.03.013
- Biernat, J., Mandelkow, E. M., Schröter, C., Lichtenberg-Kraag, B., Steiner, B., Berling, B., et al. (1992). The switch of tau protein to an Alzheimer-like state includes the phosphorylation of two serine-proline motifs upstream of the microtubule binding region. *EMBO J.* 11, 1593–1597. doi:10.1002/j.1460-2075.1992.tb05204.x
- Bloom, G. S. (2014). Amyloid- β and tau. *JAMA Neurol* 71, 505–508. doi:10.1001/jamaneurol.2013.5847
- Braak, H., and Braak, E. (1995). Staging of Alzheimer's disease-related neurofibrillary changes. *Neurobiol. Aging* 16, 271–278; discussion 278–284. doi:10.1016/0197-4580(95)00021-6
- Braak, H., and Braak, E. (1996). Evolution of the neuropathology of Alzheimer's disease. *Acta Neurol. Scand. Suppl.* 94, 3–12. doi:10.1111/j.1600-0404.1996.tb05866.x
- Caccamo, A., Ferreira, E., Branca, C., and Oddo, S. (2017). Retracted article: p62 improves AD-like pathology by increasing autophagy. *Mol. Psychiatr.* 22, 865–873. doi:10.1038/mp.2016.139
- Calderone, A., Jover, T., Noh, K.-m., Tanaka, H., Yokota, H., Lin, Y., et al. (2003). Ischemic insults derepress the gene silencer REST in neurons destined to die. *J. Neurosci.* 23, 2112–2121. doi:10.1523/jneurosci.23-06-02112.2003
- Chen, K., Gunter, K., and Maines, M. D. (2000). Neurons overexpressing heme oxygenase-1 resist oxidative stress-mediated cell death. *J. Neurochem.* 75, 304–313. doi:10.1046/j.1471-4159.2000.0750304.x

and Shenzhen Science and Technology Innovation Commission, China (JCYJ20180507184656626, JCYJ20180302174028790).

ACKNOWLEDGMENTS

We would like to thank Prof. Michel Goedert (MRC Laboratory of Molecular Biology, Cambridge, UK) for his continuous support and supplying the P301S mice to allow us to establish a colony in our animal unit, Prof. Peter Davies (Albert Einstein College of Medicine, Bronx, NY, USA) for his continuous support and providing tau antibodies for the whole research work, Prof. Jian-dong Huang and Prof. Sookja K. Chung in HKU for providing the behavioral facility for the whole research work and Mr. Alan Ho for his technical assistance in the LCMS analysis of the herbal extracts and their pure compounds in HKBU. We would also like to thank Dr. Martha Dahlen for her English editing of this manuscript.

SUPPLEMENTARY MATERIAL

The Supplementary Material for this article can be found online at: <https://www.frontiersin.org/articles/10.3389/fphar.2020.584770/full#supplementary-material>

- Dennis, D. J., Han, S., and Schuurmans, C. (2019). bHLH transcription factors in neural development, disease, and reprogramming. *Brain Res.* 1705, 48–65. doi:10.1016/j.brainres.2018.03.013
- Dillon, C., Serrano, C. M., Castro, D., Heisecke, P. P., Taragano, S. L., and Perez Leguizamon, P. (2013). Behavioral symptoms related to cognitive impairment. *Neuropsychiatr Dis Treat* 9, 1443–1455. doi:10.2147/ndt.s47133
- Dunham, N. W., and Miya, T. S. (1957). A note on a simple apparatus for detecting neurological deficit in rats and Mice**College of pharmacy, university of Nebraska, Lincoln 8. *J. Am. Pharmaceut. Assoc.* 46, 208–209. doi:10.1002/jps.3030460322
- Durairajan, S. S. K., Iyaswamy, A., Shetty, S. G., Kammella, A. K., Malampati, S., Shang, W., et al. (2017). A modified formulation of Huanglian-Jie-Du-Tang reduces memory impairments and beta-amyloid plaques in a triple transgenic mouse model of Alzheimer's disease. *Sci. Rep.* 7, 6238. doi:10.1038/s41598-017-06217-9
- Durairajan, S. S. K., Liu, L.-F., Lu, J.-H., Chen, L.-L., Yuan, Q., Chung, S. K., et al. (2012). Berberine ameliorates β -amyloid pathology, gliosis, and cognitive impairment in an Alzheimer's disease transgenic mouse model. *Neurobiol. Aging* 33, 2903–2919. doi:10.1016/j.neurobiolaging.2012.02.016
- Formisano, L., Noh, K.-M., Miyawaki, T., Mashiko, T., Bennett, M. V. L., and Zukin, R. S. (2007). Ischemic insults promote epigenetic reprogramming of opioid receptor expression in hippocampal neurons. *Proc. Natl. Acad. Sci. U S A* 104, 4170–4175. doi:10.1073/pnas.0611704104
- Geerts, H., Roberts, P., Spiros, A., and Carr, R. (2013). A strategy for developing new treatment paradigms for neuropsychiatric and neurocognitive symptoms in Alzheimer's disease. *Front. Pharmacol.* 4, 47. doi:10.3389/fphar.2013.00047
- Giacobini, E., and Gold, G. (2013). Alzheimer disease therapy-moving from amyloid- β to tau. *Nat. Rev. Neurol.* 9, 677–686. doi:10.1038/nrneurol.2013.223
- Han, Y., and Jiang, L. (2011). Randomized paralleled controlled study on the analgesic effects of neurotrophin in different TCM syndromes. *Chinese Clinical Trial Registry (ChiCTR-TRC-10001155)*
- Hardy, J. (2006). A hundred years of Alzheimer's disease research. *Neuron* 52, 3–13. doi:10.1016/j.neuron.2006.09.016
- Hashimoto, S., Matsuba, Y., Kamano, N., Mihira, N., Sahara, N., Takano, J., et al. (2019). Tau binding protein CAPON induces tau aggregation and neurodegeneration. *Nat. Commun.* 10, 2394. doi:10.1038/s41467-019-10990-1
- Iyaswamy, A., Krishnamoorthi, S. K., Song, J.-X., Yang, C.-B., Kaliyamoorthy, V., Zhang, H., et al. (2020). NeuroDefend, a novel Chinese medicine, attenuates

- amyloid- β and tau pathology in experimental Alzheimer's disease models. *J. Food Drug Anal.* 28, 132–146. doi:10.1016/j.jfda.2019.09.004
- Ke, Y., Dramiga, J., Schütz, U., Kril, J. J., Ittner, L. M., Schröder, H. r., et al. (2012). Correction: tau-mediated nuclear depletion and cytoplasmic accumulation of SFPQ in Alzheimer's and pick's disease. *PLoS One* 7, e35678. doi:10.1371/annotation/6650167a-7567-4c65-931f-4be7145a39fc
- Lamb, J., Crawford, E. D., Peck, D., Modell, J. W., Blat, I. C., Wrobel, M. J., et al. (2006). The connectivity map: using gene-expression signatures to connect small molecules, genes, and disease. *Science* 313, 1929–1935. doi:10.1126/science.1132939
- Lee, Y., and Wehl, C. C. (2017). Regulation of SQSTM1/p62 via UBA domain ubiquitination and its role in disease. *Autophagy* 13, 1615–1616. doi:10.1080/15548627.2017.1339845
- Lewerenz, J., Sato, H., Albrecht, P., Henke, N., Noack, R., Methner, A., et al. (2012). Mutation of ATF4 mediates resistance of neuronal cell lines against oxidative stress by inducing xCT expression. *Cell Death Differ.* 19, 847–858. doi:10.1038/cdd.2011.165
- Lewis, J., McGowan, E., Rockwood, J., Melrose, H., Nacharaju, P., Van Slegtenhorst, M., et al. (2000). Neurofibrillary tangles, amyotrophy and progressive motor disturbance in mice expressing mutant (P301L) tau protein. *Nat. Genet.* 25, 402–405. doi:10.1038/78078
- Li, W., Cui, K., Prochownik, E. V., and Li, Y. (2018). The deubiquitinase USP21 stabilizes MEK2 to promote tumor growth. *Cell Death Dis.* 9, 482. doi:10.1038/s41419-018-0523-z
- Liao, Z.-G., Liang, X.-L., Zhu, J.-Y., Zhao, G.-W., Yang, M., Wang, G.-F., et al. (2010). Correlation between synergistic action of Radix Angelica dahurica extracts on analgesic effects of Corydalis alkaloid and plasma concentration of dl-THP. *J. Ethnopharmacol.* 129, 115–120. doi:10.1016/j.jep.2010.03.005
- Monville, C., Torres, E. M., and Dunnett, S. B. (2006). Comparison of incremental and accelerating protocols of the rotarod test for the assessment of motor deficits in the 6-OHDA model. *J. Neurosci. Methods* 158, 219–223. doi:10.1016/j.jneumeth.2006.06.001
- Myeku, N., Clelland, C. L., Emrani, S., Kukushkin, N. V., Yu, W. H., Goldberg, A. L., et al. (2016). Tau-driven 26S proteasome impairment and cognitive dysfunction can be prevented early in disease by activating cAMP-PKA signaling. *Nat. Med.* 22, 46–53. doi:10.1038/nm.4011
- Oddo, S., Billings, L., Kesslak, J. P., Cribbs, D. H., and Laferla, F. M. (2004). A β immunotherapy leads to clearance of early, but not late, hyperphosphorylated tau aggregates via the proteasome. *Neuron* 43, 321–332. doi:10.1016/j.neuron.2004.07.003
- Oddo, S., Caccamo, A., Shepherd, J. D., Murphy, M. P., Golde, T. E., Kaye, R., et al. (2003). Triple-transgenic model of Alzheimer's disease with plaques and tangles. *Neuron* 39, 409–421. doi:10.1016/s0896-6273(03)00434-3
- Palm, K., Belluardo, N., Metsis, M., and Timmusk, T. ö. (1998). Neuronal expression of zinc finger transcription factor REST/NRSF/XBR gene. *J. Neurosci.* 18, 1280–1296. doi:10.1523/jneurosci.18-04-01280.1998
- Podlisny, M. B., Ostaszewski, B. L., Squazzo, S. L., Koo, E. H., Rydell, R. E., Teplow, D. B., et al. (1995). Aggregation of secreted amyloid -protein into sodium dodecyl sulfate-stable oligomers in cell culture. *J. Biol. Chem.* 270, 9564–9570. doi:10.1074/jbc.270.16.9564
- Reagan-Shaw, S., Nihal, M., and Ahmad, N. (2008). Dose translation from animal to human studies revisited. *Faseb. J.* 22, 659–661. doi:10.1096/fj.07-9574LSF
- Rozas, G., and Labandeira García, J. L. (1997). Drug-free evaluation of rat models of parkinsonism and nigral grafts using a new automated rotarod test. *Brain Res.* 749, 188–199. doi:10.1016/s0006-8993(96)01162-6
- Sgadò, P., Ferretti, E., Grbec, D., Bozzi, Y., and Simon, H. H. (2012). The atypical homeoprotein Pbx1a participates in the axonal pathfinding of mesencephalic dopaminergic neurons. *Neural Dev.* 7, 24. doi:10.1186/1749-8104-7-24
- Soerensen, J., Jakupoglu, C., Beck, H., Förster, H., Schmidt, J., Schmahl, W., et al. (2008). The role of thioredoxin reductases in brain development. *PLoS One* 3, e1813. doi:10.1371/journal.pone.0001813
- Subramanian, A., Narayan, R., Corsello, S. M., Peck, D. D., Natoli, T. E., Lu, X., et al. (2017). A next generation connectivity map: L1000 platform and the first 1,000,000 profiles. *Cell* 171, 1437–1452. doi:10.1016/j.cell.2017.10.049
- Tao, Y., Xu, H., Wang, S., Wang, B., Zhang, Y., Wang, W., et al. (2013). Identification of the absorbed constituents after oral administration of Yuanhu Zhitong prescription extract and its pharmacokinetic study by rapid resolution liquid chromatography/quadrupole time-of-flight. *J. Chromatogr. B* 935, 1–9. doi:10.1016/j.jchromb.2013.07.015
- Toyoshima, H., Sawada, H., Naeshiro, I., and Horinouchi, A. (2009). Similar compounds searching system by using the gene expression microarray database. *Toxicol. Lett.* 186, 52–57. doi:10.1016/j.toxlet.2008.08.009
- Urbé, S., Liu, H., Hayes, S. D., Heride, C., Rigden, D. J., and Clague, M. J. (2012). Systematic survey of deubiquitinase localization identifies USP21 as a regulator of centrosome- and microtubule-associated functions. *MBoC* 23, 1095–1103. doi:10.1091/mbc.e11-08-0668
- Wang, Y., and Mandelkow, E. (2016). Tau in physiology and pathology. *Nat. Rev. Neurosci.* 17, 5–21. doi:10.1038/nrn.2015.1
- Xu, H., Tao, Y., Lu, P., Wang, P., Zhang, F., Yuan, Y., et al. (2013). A computational drug-target network for yuanhu zhitong prescription. *Evid Based Complement Alternat Med* 2013, 658531. doi:10.1155/2013/658531
- Yoshiyama, Y., Lee, V. M. Y., and Trojanowski, J. Q. (2013). Therapeutic strategies for tau mediated neurodegeneration. *J. Neurol. Neurosurg. Psychiatr.* 84, 784–795. doi:10.1136/jnnp-2012-303144
- Yuan, C.-S., Mehendale, S. R., Wang, C.-Z., Aung, H. H., Jiang, T., Guan, X., et al. (2004). Effects of Corydalis yanhusuo and Angelica dahurica on cold pressor-induced pain in humans: a controlled trial. *J. Clin. Pharmacol.* 44, 1323–1327. doi:10.1177/0091270004267809
- Zhang, L., Chung, S. K., and Chow, B. K. C. (2014). The knockout of secretin in cerebellar Purkinje cells impairs mouse motor coordination and motor learning. *Neuropsychopharmacology* 39, 1460–1468. doi:10.1038/npp.2013.344
- Zuccato, C., Belyaev, N., Conforti, P., Ooi, L., Tartari, M., Papadimitou, E., et al. (2007). Widespread disruption of repressor element-1 silencing transcription factor/neuron-restrictive silencer factor occupancy at its target genes in Huntington's disease. *J. Neurosci.* 27, 6972–6983. doi:10.1523/jneurosci.4278-06.2007
- Zuccato, C., Tartari, M., Crotti, A., Goffredo, D., Valenza, M., Conti, L., et al. (2003). Huntingtin interacts with REST/NRSF to modulate the transcription of NRSE-controlled neuronal genes. *Nat. Genet.* 35, 76–83. doi:10.1038/ng1219

Conflict of Interest: The authors declare that the research was conducted in the absence of any commercial or financial relationships that could be construed as a potential conflict of interest.

Copyright © 2020 Iyaswamy, Krishnamoorthi, Liu, Song, Kammala, Sreenivasamurthy, Malampati, Chun-Kit Tong, Selvarasu, CHEUNG, Lu, Tan, Huang, Durairajan and Min. This is an open-access article distributed under the terms of the Creative Commons Attribution License (CC BY). The use, distribution or reproduction in other forums is permitted, provided the original author(s) and the copyright owner(s) are credited and that the original publication in this journal is cited, in accordance with accepted academic practice. No use, distribution or reproduction is permitted which does not comply with these terms.



Elaphuri Davidiani Cornu Improves Depressive-Like Behavior in Mice and Increases Neurotrophic Factor Expression in Mouse Primary Astrocytes via cAMP and ERK-Dependent Pathways

Yue Zhu^{1*}, Mengqiu Liu^{1†}, Suchen Qu^{1†}, Cheng Cao¹, Chongqi Wei¹, Xue-er Meng¹, Qianyin Lou¹, Dawei Qian¹, Jin-ao Duan¹, Yuhua Ding², Zhengxiang Han³ and Ming Zhao^{1*}

OPEN ACCESS

Edited by:

Jiahong Lu,
University of Macau, China

Reviewed by:

Young-Ji Shiao,
National Research Institute of Chinese
Medicine, Taiwan
Feihua Wu,
China Pharmaceutical University,
China

*Correspondence:

Yue Zhu
zhuyue@njucm.edu.cn
Ming Zhao
mingzhao@njucm.edu.cn

[†]These authors have contributed
equally to this work.

Specialty section:

This article was submitted to
Ethnopharmacology,
a section of the journal
Frontiers in Pharmacology

Received: 12 August 2020

Accepted: 14 October 2020

Published: 16 November 2020

Citation:

Zhu Y, Liu M, Qu S, Cao C, Wei C,
Meng X, Lou Q, Qian D, Duan J, Ding
Y, Han Z and Zhao M (2020) Elaphuri
Davidiani Cornu Improves Depressive-
Like Behavior in Mice and Increases
Neurotrophic Factor Expression in
Mouse Primary Astrocytes via cAMP
and ERK-Dependent Pathways.
Front. Pharmacol. 11:593993.
doi: 10.3389/fphar.2020.593993

¹Jiangsu Key Laboratory for High Technology Research of TCM Formulae and Jiangsu Collaborative Innovation Center of Chinese Medicinal Resources Industrialization, Nanjing University of Chinese Medicine, Nan Jing, China, ²Jiangsu Province Dafeng Milu National Nature Reserve, Dafeng, China, ³Department of Neurology and Rehabilitation, Shanghai Seventh People's Hospital, Shanghai University of TCM, Shanghai, China

Elaphuri Davidiani Cornu (EDC) is the natural shedding horn of *Elaphurus davidianus* Millne-Edwards that was used by people in ancient China for maintaining physical and mental health. We evaluated the antidepressant effect of EDC using depression-like animal models and explored possible mechanisms in mouse primary astrocyte cultures. We found that aqueous extracts of EDC significantly improved depression-like behavior in a mouse model of depression. The extracts enhanced expression of nerve growth factor and brain-derived neurotrophic factor neurotrophic factors in mouse prefrontal cortex and hippocampus tissues. In the mouse primary astrocyte cultures, the EDC aqueous extracts significantly increased the neurotrophic factor expression both at the transcriptional and protein levels. EDC extracts might exhibit these functions by regulating matrix metalloprotein-9 of the nerve growth factor and brain-derived neurotrophic factor metabolic pathways and might enhance expression of neurotrophic factors via the cAMP- and ERK-dependent pathways. We confirmed this possibility by showing the effects of related inhibitors, providing scientific evidence that supports the utility of EDC in the development of drugs to treat major depressive disorders.

Keywords: elaphuri davidiani cornu, depression, neurotrophic factor, astrocytes, animal medicine

INTRODUCTION

There are 6,008 Chinese medicinal materials recorded in *Zhong Yao Da Ci Dian* (Great Dictionary of Chinese Medicine) (Zhao et al., 2006). Among them, Elaphuri Davidiani Cornu (EDC) is definitely a special one with a unique fate. It is the natural shedding horn of the Père David's deer, also known as elaphure or Milu (*Elaphurus davidianus* Millne-Edwards). Elaphure is not only the endemic species in China but also a precious medicinal animal. The horn, fat, and meat of elaphure can all be used as medicinal materials; their application history stretches over at least a 1000 years. EDC is the most frequently used medicinal part of the elaphure and was first described by Tao Hong-jing in *Ming Yi*

Bie Lu in 450 A.D. The first formula of EDC was recorded in *Beiji Qianjin Yaofang* by “Medical King” Sun Si-miao in 652 A.D. (Li, 1997). According to the historical records, the function of EDC has been summarized as “warming the kidney and strengthening yang, nourishing ying and supplementing the essence, strengthening bones and muscles, and activating blood circulation” (Song, 2002). However, as elaphure became extinct in China in the 1900s, the medicinal application of EDC ceased. Up to 1986, “the World Wide Fund for Nature (WWF)” donated 39 elaphures (13 males, 26 females) to the Chinese government that been kept in the Jiangsu Dafeng National Nature Reserve to restore elaphure wild populations in their native habitat. Through more than 30 years of efforts by the Chinese government and experts, the elaphure population has increased by nearly 70-fold and now consists of over 6,600 animals. Four wild-elaphure populations and other sporadic groups have formed. The restoration of the elaphure population has made it possible to restore the medical application of EDC.

EDC was used in ancient China to treat various diseases including hypo-immunity, osteoporosis, rheumatoid arthritis, and others. Various studies have been carried out *in vivo* or *in vitro* to validate the EDC function or reveal the mechanism of action. EDC has been reported to induce cellular and humoral immunity and macrophage function. It was also found to induce the transformation of bone marrow cells and the proliferation of hematopoietic progenitor cells in a cyclophosphamide-induced blood deficiency mouse model and increase the bone density, mineral content, and the AKP (alkaline phosphatase) level in the ovariectomized rat model. EDC also exerted an anti-aging effect on D-galactose-induced senescence in mice by increasing the SOD (superoxide dismutase) activity and decreasing the content of MDA (malondialdehyde) and monoamine oxidase in the liver and brain. These modern studies confirmed that EDC could indeed be a valuable medical material.

Based on the ancient medical literature, EDC could also be used to improve depressive mood, however, this function has never been studied and validated (Li, 1997). Therefore, we evaluated the effect of EDC on improving depression mood using in animal and cell models and explored the active substances involved and their mechanisms of action. Here we report the effect of water and ethanol EDC extracts on improving depressive mood using the tail-suspension and forced-swimming mouse models, and on mouse astrocyte primary culture *in vitro* to evaluate the regulation of neurotrophic factors. We separated the EDC extract by ultrafiltration into molecular-weight fractions and treated astrocytes to explore the presence of active substances. Our findings may indicate possible mechanisms of EDC activity in improving depressive mood and offer a scientific basis for EDC drug development.

MATERIALS AND METHODS

Preparation of Extracts

The natural shedding of EDC was collected from Jiangsu Dafeng Milu National Nature Preserves. The morphology of EDC and the voucher number can be found in Supplementary Fig.1 Water and

ethanol extracts of EDC were prepared as follows. Pulverized EDC (15 g) was mixed with distilled water (500 ml) and refluxed for 2 h. The supernatant was removed and the residue was added to 500 ml distilled water for second reflux. The supernatants were combined and concentrated by lyophilization to produce solid material. The ethanol extract was prepared as above but using 85% ethanol. The extracts were characterized using HPLC-MS/MS as previously reported (Li et al., 2013). The representative chromatogram could be found in Supplementary Fig.2. The composition of the extracts is shown in **Supplementary Table S1**. This composition sets up the chemical standards of EDC extracts for further pharmacological and biological studies.

Animals and Housing Conditions

Male ICR mice (7–8 weeks old, 18–22 g) were purchased from Qinglong Mountain experimental Animal Culture Co. Ltd. ICR mice were raised in SPF surroundings in the animal center of Nanjing University of Chinese Medicine. All procedures for treating animals were following the Guide for the Care and Use of Laboratory Animals approved by the Institutional Animal Care and Use Committee. The experimental procedures also conformed to the guidelines of the “Principles of Laboratory Animal Care” (NIH publication No. 80-23, revised 1996).

Drug Treatment

The mice were divided into six treatment groups and contained eight individuals randomly assigned to each group. The control group animals were given saline intragastrically. The positive control group was given fluoxetine (4 mg/kg) (Zhu et al., 2017). The four test groups were given aqueous or ethanol extracts of EDC at dosages (expressed as the crude material) of 2 g/kg/day and 6 g/kg/day, respectively. Animals were treated for 7 days.

For determination of related signaling pathway on astrocyte cultures, PKI (protein kinase A inhibitor, 10 nM) and U0126 (ERK inhibitor, 2 μ M) were treated on astrocytes for 3 h before exposures to EDC extract, forskolin (10 μ M), and TPA (100 nM) (Cao et al., 2018).

Behavioral Tests

The depression-like behavior was evaluated using the tail-suspension tests (TST) and forced-swimming tests (FST). The tail-suspension test was carried out first, with the forced-swimming test performed 24 h later. The experimental details can be found in our previous publication (Cao et al., 2018). In details, individual mouse was suspended in an acoustically and visually isolated chamber. Animal activities were captured by a video camera. The total time of immobility during the last 4 min in a 6 min testing periods was analyzed by software. FST was carried out after 1 day of TST. Similarly, individual mouse was moved in an acoustically and visually isolated chamber and placed in a clear glass tank (40 cm high and 20 cm in diameter) filled with 30 cm of water (22–23°C) and allowed to swim for 6 min. The activities of tested mouse were also recorded by a video camera. The time of mouse floating in the water without struggling were calculated as immobile time and total immobile time during the last 4 min of the 6 min testing period

were analyzed by ANY-maze software (Stoeling Co.Ltd., United States).

Astrocyte Primary Culture

Astrocyte primary culture was prepared from the cortex tissue of postnatal ICR mice at day 1. Cell-culture reagents for astrocytes were purchased from ThermoFisher Scientific (Waltham, MA). The cortex tissues were isolated and trypsinised. The cells were centrifuged and the supernatants were removed. The pellets were suspended and cultured. The cultures were further purified by shaking after 90% of confluence was reached. The cultures were shaken at the speed of 200 rpm/min for 8 h to remove oligodendrocytes and microglia as reported in our previous publication (Zhu et al., 2013).

ELISA Assays

The expression of nerve growth factor (NGF) and brain-derived neurotrophic factor (BDNF) were determined by ELISA assays. The tissues of the prefrontal cortex and the hippocampus were removed from the sacrificed mice and homogenized. After centrifugation, the supernatant was separated and analyzed by mouse NGF ELISA and mouse BDNF ELISA kits (Aviscera Bioscience, Santa Clara, CA). The protein content was expressed in ng/g wet-tissue weight as reported in our earlier publication (Zhu et al., 2017).

Western Blot Analysis

The kinase phosphorylation of signaling pathways was analyzed as follows. The total protein content was extracted from the astrocyte primary culture, separated by 8% polyacrylamide gels, and semi-quantified by SDS (sodium dodecyl sulfate) PAGE (polyacrylamide gel electrophoresis) as reported previously (Zhu et al., 2016a). Primary antibodies used were: rabbit polyclonal anti-Erk (extracellular signal-regulated kinase) (4,695, 1:2,000; Cell Signaling Technology), rabbit polyclonal anti-pErk (4,370, 1:2,000; Cell Signaling Technology), rabbit polyclonal anti-CREB (cAMP response element binding protein) (1:2,000; Cell Signaling Technology), rabbit polyclonal anti-pCREB (1:2,000; Cell Signaling Technology), and rabbit polyclonal anti-GAPDH (glyceraldehyde-3-phosphate dehydrogenase) antibody (1:2,000; Cell Signaling Technology). The secondary antibody used was anti-rabbit IgG antibody conjugated with horseradish peroxidase (1:5,000, Cell Signaling Technology). Immunoreactivity was visualized by ECL (electrochemiluminescence) reagent (Tianneng Co. Ltd., Shanghai, China), and blots were visualized and compared on the imaging system (ChemiDoc™ XRS+, Bio-Rad, Hercules, CA).

Real-Time Quantitative PCR Analysis

Transcriptional levels of kinases accounting for the synthesis and degradation of neurotrophic factors were determined by quantitative PCR analysis. The experimental details can be found in our earlier publications (Zhu et al., 2016b). Firstly, the total RNA from mice astrocyte cultures was extracted by Trizol reagent (Invitrogen, Carlsbad, CA). The concentrations and purity of RNA were determined by DS-11 Spectrophotometer (DeNovix, Wilmington, DE) and the quality of RNA was

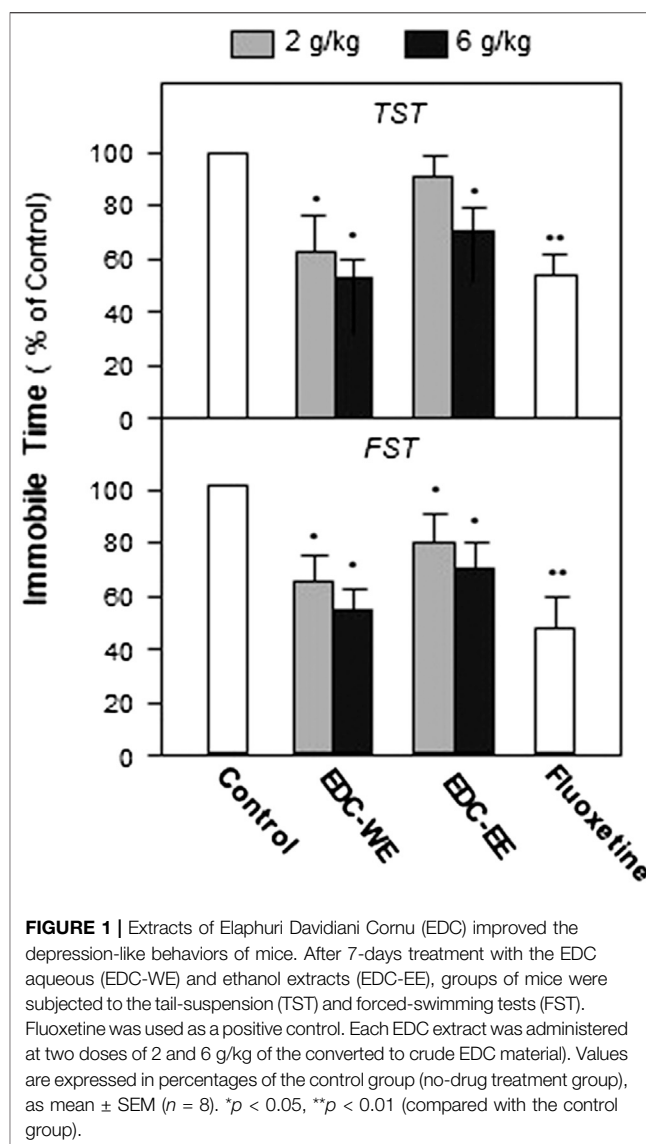


FIGURE 1 | Extracts of Elaphuri Davidiani Cornu (EDC) improved the depression-like behaviors of mice. After 7-days treatment with the EDC aqueous (EDC-WE) and ethanol extracts (EDC-EE), groups of mice were subjected to the tail-suspension (TST) and forced-swimming tests (FST). Fluoxetine was used as a positive control. Each EDC extract was administered at two doses of 2 and 6 g/kg of the converted to crude EDC material). Values are expressed in percentages of the control group (no-drug treatment group), as mean \pm SEM ($n = 8$). * $p < 0.05$, ** $p < 0.01$ (compared with the control group).

evaluated by the ratio of absorbance at 260–280 nm and ranged from 1.9 to 2.1. Total RNA samples were reverse-transcribed using the cDNA obtained using EasyScript One-Step gDNA Removal and cDNA Synthesis SuperMix kit (Transgen Biotech, Beijing, China). Real-time quantitative PCR analysis was carried out by using TransStart Top Green qPCR SuperMix kit (Transgen Biotech, Beijing, China) on Applied Biosystems 7,500 fast real-time PCR system (Thermal Fisher Inc., Foster City, CA). Transcript levels of target genes were quantified by using the $\Delta\Delta C_t$ value method. The primers of genes are listed in **Supplementary Table S2**.

Data Analysis

The comparison of multiple groups was performed by using one-way or two-way ANOVA followed by a Bonferroni post hoc analysis if appropriate (version 13.0, SPSS, IBM Corp., Armonk, NY). Normal-distribution test of data was carried out before the ANOVA. All data are expressed as the mean \pm SEM, where $n = 8$.

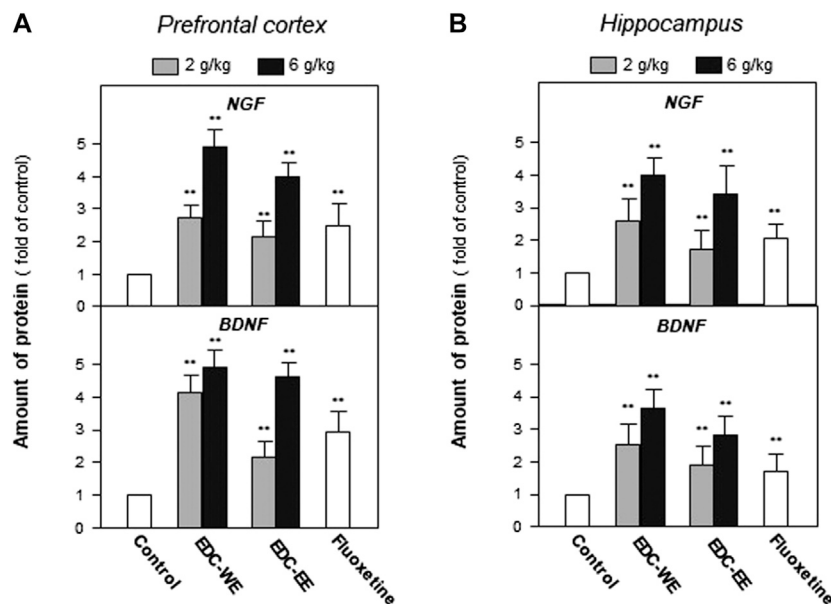


FIGURE 2 | Extracts of Elaphuri Davidiani Cornu (EDC) increased the expressions of neurotrophic factors in the prefrontal cortex and hippocampus tissues of mice.

(A): Mice were given aqueous (EDC-WE) and ethanol extracts (EDC-EE) of EDC by intragastric administration at the stated doses—for 7 days. The amounts of nerve growth factor and brain-derived neurotrophic factor were determined in the tissues of the prefrontal cortex of the sacrificed mice. Fluoxetine was used as a positive control (4 mg/kg/day). **(B):** The samples were the same as in **(A)** and the amounts of nerve growth factor and brain-derived neurotrophic factor were determined in the tissues of the hippocampus of the sacrificed mice. Values are expressed as the percentage of the control group (no drug treatment group), as mean \pm SEM ($n = 8$).

* $p < 0.05$, ** $p < 0.01$ (compared with the control group).

Differences were statistically labeled as significant [*] for $p < 0.05$ or highly significant [**] for $p < 0.01$.

RESULTS

Extracts of Elaphuri Davidiani Cornu Exhibited an Antidepressant Effect on Mice

To evaluate the antidepressant effect and explore the active components of EDC, the aqueous and 70% ethanol extracts were prepared and intragastrically administered to the depression-model animals. TST and FST, two widely used behavioral tests for antidepressant screening, were used to measure the depression-related responses after treatment with EDC extracts for seven consecutive days. As displayed in **Figure 1**, both the aqueous and 70%-ethanol extracts of EDC decreased the immobile time of mice in the FST compared with the control group ($p < 0.05$). The aqueous extract of EDC at two dosages both decreased the immobile time of TST significantly compared with the control group while the ethanol extracts exhibited a positive effect only at the high dose. In the FST, the aqueous and ethanol extracts of EDC at two dosages all significantly decreased the immobile time compared with the control group mice. Therefore, the aqueous extract of EDC exhibited a higher antidepressant effect than the 70% ethanol extract.

Extracts of EDC increased the expression of the neurotrophic factors in the prefrontal cortex and hippocampus tissues of mice.

After the behavioral tests were completed, the expression of NGF and BDNF was determined in the prefrontal cortex and hippocampus of sacrificed mice using ELISA. Treatment with a higher dose of aqueous or 70%-ethanol EDC extracts significantly increased the expressions of NGF and BDNF in the prefrontal cortex and hippocampus compared with the no-drug-treatment control group ($p < 0.01$) (**Figures 2A**). This increase was consistent with the results of the behavioral tests. The aqueous extract of EDC at the higher dose increased up to five-fold the expressions of both NGF and BDNF at a level superior to fluoxetine. The effects of EDC extracts at higher dosages were all higher than at the lower dosage. The aqueous extract exhibited a better effect than the ethanol extract. Similar effects were found in the hippocampus tissue (**Figures 2B**). Taken together, EDC significantly increased the expressions of NGF and BDNF in the prefrontal cortex and hippocampus of mice.

Extracts of EDC increased the expressions of neurotrophic factors in mouse astrocytes.

The mechanism of the EDC effect to increase the expressions of NGF and BDNF was examined further using the astrocyte primary-culture cell model. Though NGF and BDNF can be secreted from neurons and glial cells in brain, EDC aqueous extracts are mainly water-soluble peptides and cannot cross blood brain barrier and affect neurons directly. More realistically, the peptides might be absorbed into blood and act on astrocytes that make up the blood brain barrier. Therefore, we selected astrocytes as the cell model and treated EDC aqueous extract on astrocyte cultures. The EDC aqueous extract was selected for two reasons. Firstly, compared with the EDC ethanol extract, the aqueous

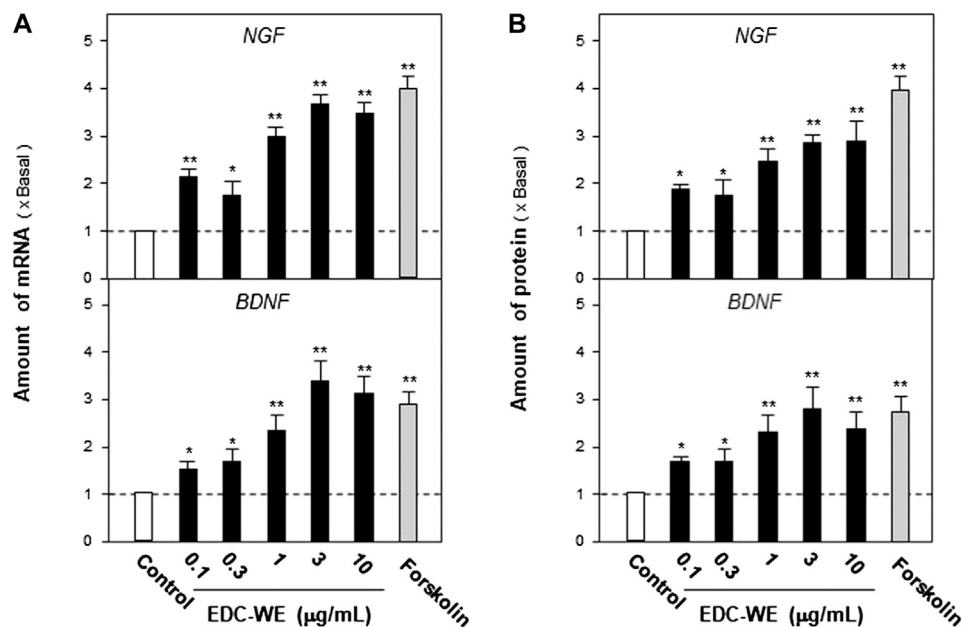


FIGURE 3 | The aqueous extracts of Elaphuri Davidiani Cornu (EDC) increased the neurotrophic factor expression in mouse astrocyte primary cultures. **(A):** The primary mouse astrocyte cultures were treated with the aqueous extract (EDC-WE) at 0.1–10 µg/ml concentrations for 24 h. The mRNA expression levels of nerve growth factor and brain-derived neurotrophic factor were determined by qPCR analysis. **(B):** The drug treatment with EDC-WE was the same as in **(A)** and the expression of nerve growth factor and brain-derived neurotrophic factor was determined by ELISA. Forskolin (10 µM) was used to treat the positive-control group. Data are expressed as a fold-change relative to the positive control group (no-drug treatment) as mean ± SEM, where $n = 5$. * $p < 0.05$, ** $p < 0.01$ (compared with no-treatment control group).

extract showed a stronger effect on promoting the expression of NGF and BDNF in mice. Secondly, the aqueous extract is the major clinical application form of EDC in traditional Chinese medicine.

Astrocyte primary cultures that reached 90% confluence were treated with the EDC aqueous extract at 0.1–10 µg/ml concentration for 48 h and the transcriptional levels of NGF and BDNF were determined. As displayed in **Figures 3A**, the aqueous extract increased the transcriptional levels of NGF and BDNF by more than three-fold compared with no-drug treatment group ($p < 0.01$). The expression of NGF and BDNF was confirmed by the protein levels using ELISA. As displayed in **Figures 3B**, the expression of NGF and BDNF proteins increased up to three-fold after treatment with the EDC aqueous extract. The EDC aqueous extract promoted the expressions of NGF and BDNF in a dose-dependent manner.

The aqueous extract of EDC promotes the expression of neurotrophic factors in mouse astrocyte primary culture via the cAMP- and ERK-dependent pathways.

We explored the possible signaling pathways involved in the effect of the EDC aqueous extract in promoting the expressions of NGF and BDNF in the mouse astrocyte culture. It is well known that both the cAMP- and Erk-dependent signaling pathways are involved in the production of NGF and BDNF. We co-treated astrocytes with the EDC aqueous extract and the inhibitors of cAMP- or Erk-dependent signaling pathway to observe possible changes in the NGF and BDNF expressions and evaluated the

extent of phosphorylation of the critical kinases on the two pathways.

As displayed in **Figures 4A**, the treatment with forskolin, an agonist of the cAMP-dependent pathway, significantly increased the expression of NGF and BDNF compared with the no-drug treatment group ($p < 0.01$). PKA (Protein kinase A) inhibitor significantly reversed the increase induced by forskolin. EDC aqueous extract also significantly induced the expressions of NGF and BDNF. Treatment with PKI weakened the increase of NGF and BDNF expressions in astrocytes treated with the aqueous EDC extract. As shown in **Figures 4B**, application of TPA, or the aqueous EDC extract significantly increased the expressions of NGF and BDNF while the U0126 inhibitor of Erk reversed the increasing trend.

To validate the roles of the signaling pathways, the phosphorylation of CREB and Erk were examined. As displayed in **Figure 5**, forskolin and TPA both significantly increased phosphorylations of CREB and Erk. The antagonist PKI and U0126 significantly inhibited phosphorylations of CREB and Erk. The aqueous EDC extract inhibited the phosphorylation of both CREB and Erk. These data suggest that both cAMP- and Erk-dependent pathways play pivotal roles in the increase by the aqueous EDC extract in the expression of NGF and BDNF in mouse astrocytes.

The aqueous extracts of EDC increase the expression of a neurotrophic factor in mouse astrocyte cultures via regulating MMP-9.

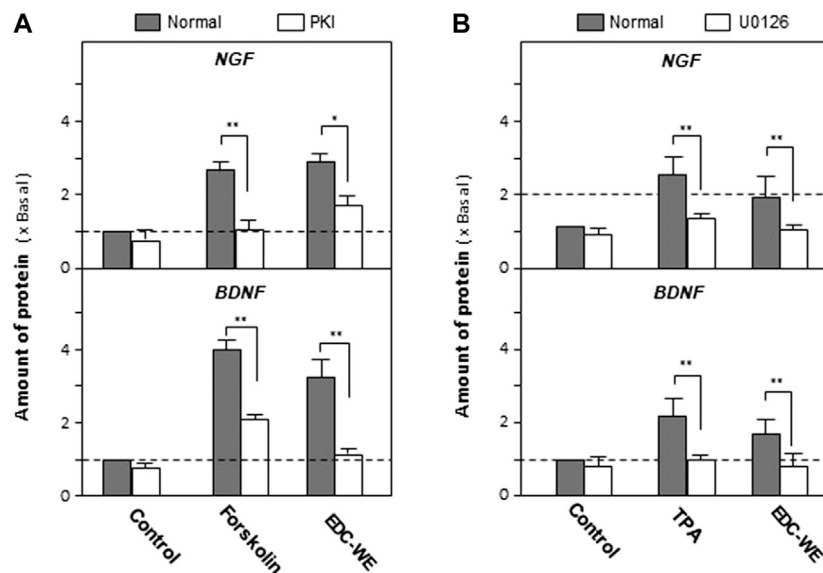


FIGURE 4 | Aqueous extracts of Elaphuri Davidiani Cornu (EDC) increased the expression of nerve growth factor and brain-derived neurotrophic factor in mouse astrocyte primary cultures via the cAMP- and ERK-dependent pathways. **(A):** The mouse astrocyte primary cultures were pre-treated with PKI (10 nM) for 3 h and then treated with forskolin (10 μ M) and EDC-WE (3 μ g/ml) for 24 h. The expression of nerve growth factor and brain-derived neurotrophic factor were determined by ELISA. **(B):** The mouse astrocyte primary cultures were pre-treated with U0126 (2 μ M) for 3 h and then treated with TPA (100 nM) and EDC-WE (3 μ g/ml) for 24 h. The expression of neurotrophic factors was determined by ELISA. Data are expressed as a fold-change relative to the control group (no-drug treatment) in mean \pm SEM, where $n = 5$. * $p < 0.05$, ** $p < 0.01$.

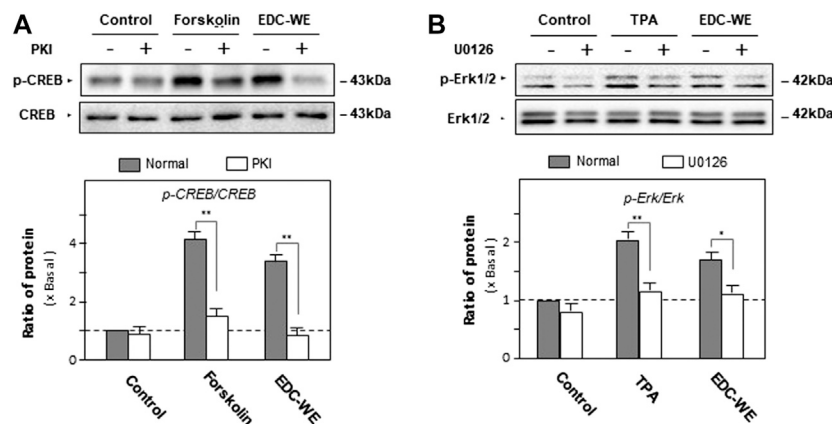
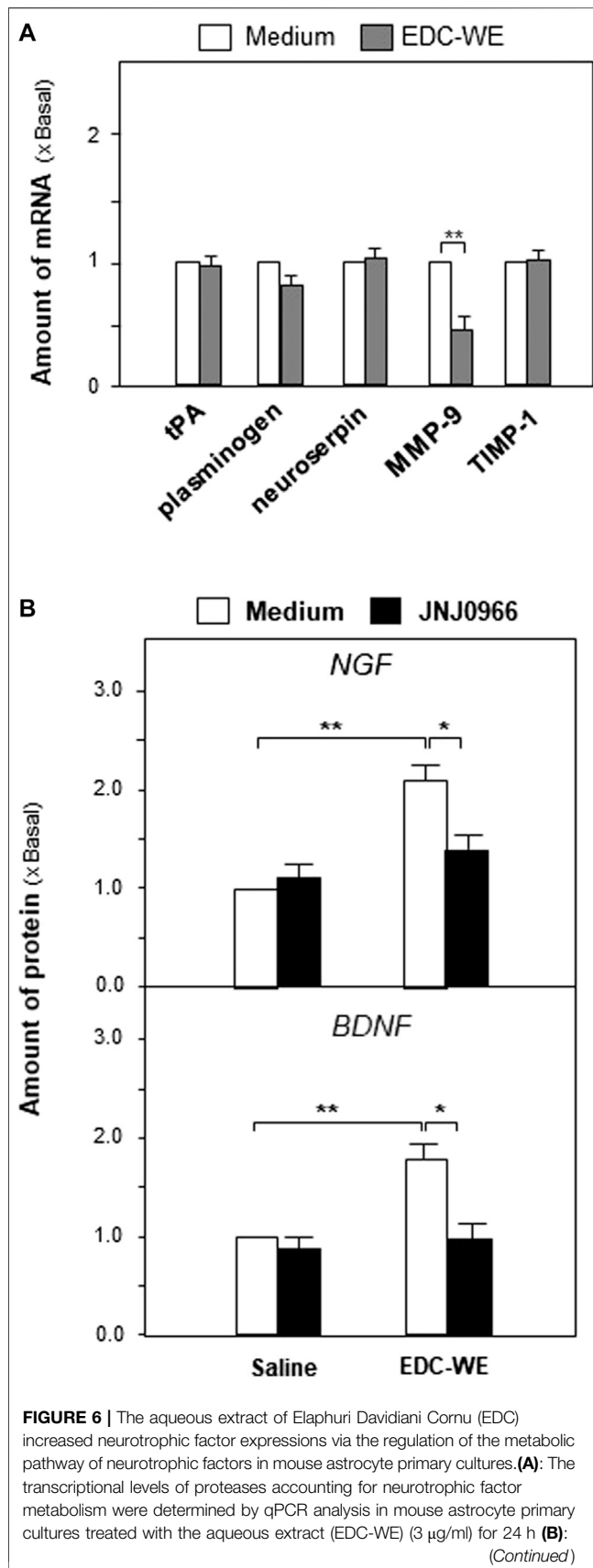


FIGURE 5 | The effect of the aqueous extract of Elaphuri Davidiani Cornu (EDC) on the phosphorylation of kinases of the cAMP- and Erk-dependent pathways in the mouse astrocyte primary cultures. **(A):** Mouse astrocyte primary cultures were pre-treated with PKI (10 nM) for 3 h and then treated with forskolin (10 μ M) and the aqueous extracts (EDC-WE) (3 μ g/ml) for 24 h. Protein-expression levels of p-CREB and CREB in astrocyte primary cultures were determined by western blot analysis. Data are expressed as a fold-change relative to the control group (no-drug treatment) in the ratio of p-CREB to CREB as mean \pm SEM, where $n = 5$. **(B):** Mouse astrocyte primary cultures were pre-treated with U0126 (2 μ M) for 3 h and then treated with TPA (100 nM) and the EDC aqueous extract (EDC-WE) (3 μ g/ml) for 24 h. Protein-expression levels of p-Erk and Erk in astrocyte primary cultures were determined by western blot analysis. Data are expressed as a fold-change relative to the control group (no-drug treatment) in the ratio of p-Erk to Erk as mean \pm SEM, where $n = 5$. * $p < 0.05$, ** $p < 0.01$.

We explored further the possible active targets of the EDC aqueous extract in increasing the expressions of NGF and BDNF. The EDC aqueous extract significantly increased the expression of neurotrophic factors in mouse astrocyte cultures after treatment at 3 μ g/ml concentration for 24 h. The transcriptional levels of the critical enzymes related to the

neurotrophic-factor metabolism were determined. As shown in **Figures 6A**, the EDC aqueous extract exhibited no observable effect on the expressions of synthesizing enzymes such as tissue plasminogen activator (tPA), plasminogen, and neuroserpin. However, the EDC aqueous extract significantly downregulated the transcriptional levels of matrix metalloproteinase 9 (MMP-9)



over two-fold while showing no effect on the level of the tissue inhibitor of metalloproteinase 1 (TIMP-1).

Following up on the results obtained for mRNA levels, we used JNJ0966 (the blocker of MMP-9) to determine whether the EDC aqueous extract regulated the metabolism of neurotrophic factors via MMP-9. As shown in **Figures 6B**, the increased expressions of NGF and BDNF in mouse astrocytes were significantly downregulated by the treatment with JNJ0966, implying that the EDC aqueous extract might regulate the neurotrophic factor metabolism by modulating MMP-9.

DISCUSSION

Studies reported here aimed to re-evaluate and excavate the possible scientific values of EDC using modern technologies. Using several depression-like animal models, we found that EDC exerted antidepressant effect via regulating neurotrophic factors such as NGF and BDNF. In particular, the EDC water extract showed a better effect in increasing neurotrophic factor expression compared with the ethanol extract. The data implied that EDC may exhibit neuronal activities.

Neurotrophic factors are important substances in the maintenance of the physiological function of the brain and the pathological process of neurodegenerative diseases and mood disorders. Neurotrophic factors maintain the survival, differentiation, and synaptic formation of neurons. Neurotrophic factors also play an important role in memory formation and emotion maintenance. NGF maintains the survival of cholinergic neurons, and cholinergic neurons are well-known neurons for the formation and maintenance of memory. BDNF enhances neurogenesis, dendritogenesis, and maintains the synapse stability. It also regulates glutamatergic and GABAergic signaling that play an essential role in long-term memory. In Alzheimer's disease, abnormal regulation and insufficient supply of NGF have been regarded as a crucial pathological process. In major depression disorders, serum BDNF level has been used as a diagnostic parameter and low levels of BDNF were found in the serum of depression patients (Molendijk et al., 2014). Low levels of NGF are also found in the serum of depression patients (Mössner et al., 2007). However, neurotrophic factors are proteins that are easily digested in the gastrointestinal tract and the transcranial administration is not practical in clinically. Therefore, increasing the endocrine supply of neurotrophic factors has become a target for drug development to treat major depressive disorders and Alzheimer's disease (Iulita and Claudio, 2014).

While the available antidepressants such as fluoxetine and venlafaxine are known to elevate the levels of NGF and BDNF

FIGURE 6 | Mouse astrocytes were pre-treated with JNJ0966 (MMP-9 inhibitor, 0.4 μ M) for 24 h and then treated with the EDC aqueous extract (EDC-WE) (3 μ g/ml) for 24 h. The transcriptional levels of neurotrophic factors were determined by qPCR analysis. Data are expressed as a fold-change relative to the control group (no-drug treatment) as mean \pm SEM, where $n = 5$. * $p < 0.05$, ** $p < 0.01$.

both in the serum of depression patients and in depression-like animal models (Mondal and Fatima, 2019), the long-term use of these antidepressants can cause many side effects. The representative tricyclic antidepressants imipramine can cause anticholinergic adverse reactions such as xerostomia and constipation, central nervous system toxicity such as tremor, dyskinesia and epilepsy, and cardiovascular toxicity such as postural hypotension, tachycardia, conduction block, arrhythmia, and cardiac arrest. Compared with TCAs, serotonin reuptake inhibitors (SSRIs) have relatively fewer side effects and toxicity. However, common adverse reactions of SSRIs include insomnia, nausea, irritability, headache, exercise anxiety, mental tension, and tremor. A long-term medication of SSRIs often leads to loss of appetite or loss of sexual function. More seriously, fluoxetine increases the suicide risk in non-adult depression patients. Therefore, the development of antidepressants from natural medicines and with relatively few side effects has become the focus of attention (Cipriani et al., 2018).

Some natural medicines such as *Crocus sativus*, *Curcuma longa*, *Cuscuta* spp., *Hypericum perforatum*, *Lavandula* spp., *Panax ginseng*, and so on (Sarris, 2018) have been shown to have significant antidepressant effects. The types of compounds involved are flavonoid, alkaloid, saponins, monoterpene, and polysaccharide, and others. However, there are very few reports on the antidepressant effects of ingredients from animal medicine (Bahramsoltani et al., 2015). We have found that the powder of EDC significantly improves the depressive behavior in animal models. To study the material basis of the EDC antidepressant activity, we prepared aqueous and alcohol extracts of EDC. We have shown that in animal models, the antidepressant effect of EDC water extract was stronger than that of the alcohol extract. In astrocytes, the main donor of neurotrophic factors in the brain, the enhancing effect of EDC water extract on the expression of neurotrophic factors was significantly higher than that of the alcohol extract. In the current study, we have found that the EDC aqueous extract promotes the expression of neurotrophic factors mainly by inhibiting MMP-9; this differs from the effect of some plant extracts that we have previously found to enhance the expression of neurotrophic factors by promoting the expression of synthase (Zhu et al., 2017). However, MMP-9 plays different role in processing of neurotrophic factors. It degrades mature NGF while converts pro-BDNF to mature BDNF (Mizoguchi et al., 2011). The biological character of pro-neurotrophin is totally different from processed mature neurotrophin. The pro-neurotrophins bind to p75NTR (p75 neurotrophin receptor) to initiate neuronal apoptosis while the mature neurotrophins bind to Trk (tyrosine kinase) receptor to nourish the neurons (Lu et al., 2005). In our studies, EDC down-regulated the expression of MMP-9, which might inhibit degradation of mature NGF and lead to the increase of mature NGF. However, the expressions of mature BDNF was also increased, which was not affected by the down-regulation of MMP-9. For this contradictory phenomenon, we cannot find a reasonable explanation now. We find that most of the studies on

metabolic pathway of neurotrophins are carried out on neuron cultures instead of astrocytes, which implies that the conversion of pro-neurotrophins to its mature form in astrocytes may be different from neurons (Lee et al., 2001; Gärtner and Staiger, 2002; Hwang et al., 2005). In neurons and neuroendocrine cells, people have found that NGF is mainly trafficked through the constitutive secretory pathway, while BDNF is selectively trafficked through the regulated secretory pathway (Griesbeck et al., 1999; Mowla et al., 1999). However, the process and secretory pathway of NGF and BDNF in astrocytes are rarely reported and the possible differences are worth studying in the future. Besides, as a member of the metzincin family of extracellularly operating proteases, MMP-9 has been found to participate in brain physiology and pathology and contributes to a large variety of brain disorders, including epilepsy, schizophrenia, stroke, neurodegeneration, depression, brain tumors, etc. Therefore, the relationship between antidepressant effect of EDC and MMP-9 regulation will be further studied in the future.

According to the ancient records of traditional Chinese medicine, EDC plays a significant role in “warming kidney yang, tonifying essence, and filling marrow.” These statements are supported by modern research. It has been reported that EDC aqueous extracts can correct the dysfunction of the hypothalamus-pituitary-target axis (adrenal cortical axis, thyroid axis, gonadal axis) in the hydrocortisone-induced kidney yang-deficiency rat model (Jiang et al., 2014). In parallel, EDC aqueous extracts also enhanced learning and memory abilities in the mouse D-galactose-induced aging model and inhibited the activity of monoamine oxidase in brain tissues (Qin et al., 2009). These discoveries suggest that the aqueous extract is an important form of EDC to exert anti-aging, memory promoting, and mood-regulating effects. Previous studies found that EDC aqueous extracts contained a large number of water-soluble peptides exhibiting significant biological activities that could be important active components of EDC (Zhai et al., 2017). Therefore, we plan to study extensively the antidepressant effects of water-soluble proteins and peptides present in EDC to provide a more scientific basis for the utilization of this valuable medicine of animal origin. Besides, compared with abundant antidepressant reports of herbal medicine, there are rare reports on animal medicine. We hope that this study will help to compensate for the lack of research in this area.

CONCLUSION

EDC exerted antidepressant effect by improving depression-like behavior in animal models. The effect was linked to the increase in the level of neurotrophic factors in the hippocampus; astrocytes might be the key type of contributing active cells. The aqueous EDC extract was superior to the ethanol extract in promoting the expression of neurotrophic factors. These findings suggest that the

aqueous extract of EDC can be used as an adjuvant treatment for patients with depression.

DATA AVAILABILITY STATEMENT

All datasets presented in this study are included in the article/**Supplementary Material**.

ETHICS STATEMENT

The animal study was reviewed and approved by the Institutional Animal Care and Use Committee of Nanjing University of Chinese Medicine.

AUTHOR CONTRIBUTIONS

YZ and MZ designed the experiments. ML, CC, SQ, XM, CW, and QL performed the experiments including behavioral tests and biochemical analyses. DQ and YD contributed to the preparation of EDC extracts and chemical standardization. ZH and JD contributed to the writing of introduction and discussion. YZ and ML wrote the main manuscript text. YZ and SQ revised the

manuscript. All authors have read and approved the submitted manuscript.

FUNDING

This research was supported by the National Key R&D Program of China “Study on four development modes of new sources of rare and endangered traditional Chinese Medicine resources” (2018YFC1706100), the National Natural Science Foundation of China (81673720, 81973591), the Open Project Program of Jiangsu Key Laboratory for High Technology Research of TCM Formulae and Jiangsu Collaborative Innovation Center of Chinese Medicinal Resources Industrialization (No. FJGS-2015-10), and the fifth phase of the 333 high-level personnel training project of Jiangsu Province (BRA2017463) to YZ.

SUPPLEMENTARY MATERIAL

The Supplementary Material for this article can be found online at: <https://www.frontiersin.org/articles/10.3389/fphar.2020.593993/full#supplementary-material>

REFERENCES

- Bahramsoltani, R., Farzaei, M. H., Farahani, M. S., and Rahimi, R. (2015). Phytochemical constituents as future antidepressants: a comprehensive review. *Rev. Neurosci.* 26, 699–719. doi:10.1515/revneuro-2015-0009
- Cao, C., Xiao, J., Liu, M., Ge, Z., Huang, R., Qi, M., et al. (2018). Active components, derived from Kai-xin-san, a herbal formula, increase the expressions of neurotrophic factor NGF and BDNF on mouse astrocyte primary cultures via cAMP-dependent signaling pathway. *J. Ethnopharmacol.* 224, 554–562. doi:10.1016/j.jep.2018.06.007
- Cipriani, A., Furukawa, T. A., Salanti, G., Chaimani, A., Atkinson, L. Z., Ogawa, Y., et al. (2018). Comparative efficacy and acceptability of 21 antidepressant drugs for the acute treatment of adults with major depressive disorder: a systematic review and network meta-analysis. *Lancet* 391, 1357–1366. doi:10.1016/S0140-6736(17)32802-7
- Gärtner, A., and Staiger, V. (2002). Neurotrophin secretion from hippocampal neurons evoked by long-term-potential-inducing electrical stimulation patterns. *Proc. Natl. Acad. Sci. U. S. A.* 99, 6386–6391. doi:10.1073/pnas.092129699
- Griesbeck, O., Canossa, M., Campana, G., Gärtner, A., Hoener, M. C., Nawa, H., et al. (1999). Are there differences between the secretion characteristics of NGF and BDNF? Implications for the modulatory role of neurotrophins in activity-dependent neuronal plasticity. *Microsc. Res. Tech.* 45 (4-5), 262–275. doi:10.1002/(SICI)1097-0029(19990515/01)45:4/5<262::AID-JEMT10>3.0.CO;2-K
- Hwang, J. J., Park, M. H., Choi, S. Y., and Koh, J. Y. (2005). Activation of the Trk signaling pathway by extracellular zinc. Role of metalloproteinases. *J. Biol. Chem.* 280, 11995–12001. doi:10.1074/jbc.M403172200
- Iulita, M. F., and Claudio, A. C. (2014). Nerve growth factor metabolic dysfunction in Alzheimer's disease and Down syndrome. *Trends Pharmacol. Sci.* 35, 338–348. doi:10.1016/j.tips.2014.04.010
- Jiang, Q., Li, F., Qian, D., Peng, Y., Guo, J., Ouyang, Z., et al. (2014). Effects of different parts of Elaphuri Davidiani Cornu on rats with kidney-yang deficiency syndrome. *Pharmacology and Clinics of Chinese Materia Medica* 30, 84–86. doi:10.13412/j.cnki.zyyj.2014.06.026
- Lee, R., Kerami, P., Teng, K. K., and Hempstead, B. L. (2001). Regulation of cell survival by secreted proneurotrophins. *Science* 294, 1945–1948. doi:10.1126/science.1065057
- Li, F., Duan, J. A., Qian, D., Guo, S., Ding, Y., Liu, X., et al. (2013). Comparative analysis of nucleosides and nucleobases from different sections of Elaphuri Davidiani Cornu and cervi Cornu by UHPLC-MS/MS. *J. Pharm. Biomed. Anal.* 83, 10–18. doi:10.1016/j.jpba.2013.04.022
- Li, J. (1997). *Beiji Qianjin Yaofang*. Beijing, China: People's Medical Publishing House
- Lu, B., Pang, P. T., and Woo, N. H. (2005). The yin and yang of neurotrophin action. *Nat. Rev. Neurosci.* 6, 603–614. doi:10.1038/nrn1726
- Mizoguchi, H., Yamada, K., and Nabeshima, T. (2011). Matrix metalloproteinases contribute to neuronal dysfunction in animal models of drug dependence, Alzheimer's disease, and epilepsy. *Biochem. Res. Int.* 2011, 681385. doi:10.1155/2011/681385
- Molendijk, M. L., Spinhoven, P., Polak, M., Bus, B. A., Penninx, B. W., and Elzinga, B. M. (2014). Serum BDNF concentrations as peripheral manifestations of depression: evidence from a systematic review and meta-analyses on 179 associations (N=9484). *Mol. Psychiatry* 19, 791–800. doi:10.1038/mp.2013.105
- Mondal, A. C., and Fatima, M. (2019). Direct and indirect evidences of BDNF and NGF as key modulators in depression: role of antidepressants treatment. *Int. J. Neurosci.* 129, 283–296. doi:10.1080/00207454.2018.1527328
- Mössner, R., Mikova, O., Koutsilieri, E., Saoud, M., Ehli, A. C., Müller, N., et al. (2007). Consensus paper of the WFSBP task force on biological markers: biological markers in depression. *World J. Biol. Psychiatry* 8, 141–174. doi:10.1080/15622970701263303
- Mowla, S. J., Pareek, S., Farhadi, H. F., Petrecca, K., Fawcett, J. P., Seidah, N. G., et al. (1999). Differential sorting of nerve growth factor and brain-derived neurotrophic factor in hippocampal neurons. *J. Neurosci.* 19, 2069–2080. doi:10.1523/JNEUROSCI.19-06-02069
- Qin, H., Yang, Z., Cheng, H., and Zhu, Q. (2009). Elk antlers ethanolic fluid extract on improvement of cognitive decline in experimental aging model mice. *Chin. J. New Drugs Clin. Remedies* 28, 505–508
- Sarris, J. (2018). Herbal medicines in the treatment of psychiatric disorders: 10-year updated review. *Phytother. Res.* 32, 1147–1162. doi:10.1002/ptr.6055

- Song, L. (2002). *Chinese materia medica*. Shanghai, China: Shanghai Scientific&Technical Publishers
- Zhai, Y., Zhu, Z., Zhu, Y., Qian, D., Liu, R., Peng, Y., et al. (2017). Characterization of collagen peptides in Elaphuri Davidiani Cornu aqueous extract with proliferative activity on osteoblasts using nano-liquid chromatography in tandem with orbitrap mass spectrometry. *Molecules* 22 (1), 166. doi:10.3390/molecules22010166
- Zhao, G., Dai, S., and Chen, R. (2006). *The dictionary of Chinese herbal medicine*. Shanghai, China: Shanghai Scientific&Technical Publishers
- Zhu, K. Y., Xu, S. L., Choi, R. C., Yan, A. L., Dong, T. T., and Tsim, K. W. (2013). Kai-xin-san, a Chinese herbal decoction containing ginseng radix et rhizoma, polygalae radix, acori tatarinowii rhizoma, and poria, stimulates the expression and secretion of neurotrophic factors in cultured astrocytes. *Evid. Based Complement. Alternat. Med.* 2013, 731385. doi:10.1155/2013/731385
- Zhu, Y., Chao, C., Duan, X., Cheng, X., Liu, P., Su, S., et al. (2017). Kai-Xin-San series formulae alleviate depressive-like behaviors on chronic mild stressed mice via regulating neurotrophic factor system on hippocampus. *Sci Rep* 7, 1467. doi:10.1038/s41598-017-01561-2
- Zhu, Y., Duan, X., Cheng, X., Cheng, X., Li, X., Zhang, L., et al. (2016a). Kai-Xin-San, a standardized traditional Chinese medicine formula, up-regulates the expressions of synaptic proteins on hippocampus of chronic mild stress induced depressive rats and primary cultured rat hippocampal neuron. *J. Ethnopharmacol.* 193, 423–432. doi:10.1016/j.jep.2016.09.037
- Zhu, Y., Duan, X., Huang, F., Cheng, X., Zhang, L., Liu, P., et al. (2016b). Kai-Xin-San, a traditional Chinese medicine formula, induces neuronal differentiation of cultured PC12 cells: modulating neurotransmitter regulation enzymes and potentiating NGF inducing neurite outgrowth. *J. Ethnopharmacol.* 193, 272–282. doi:10.1016/j.jep.2016.08.013
- Conflict of Interest:** The authors declare that the research was conducted in the absence of any commercial or financial relationships that could be construed as a potential conflict of interest.

Copyright © 2020 Zhu, Liu, Cao, Qu, Wei, Meng, Lou, Qian, Duan, Ding, Han and Zhao. This is an open-access article distributed under the terms of the Creative Commons Attribution License (CC BY). The use, distribution or reproduction in other forums is permitted, provided the original author(s) and the copyright owner(s) are credited and that the original publication in this journal is cited, in accordance with accepted academic practice. No use, distribution or reproduction is permitted which does not comply with these terms.



Taohong Siwu Decoction Ameliorates Ischemic Stroke Injury Via Suppressing Pyroptosis

Mengmeng Wang^{1,2†}, Zhuqing Liu^{1,2†}, Shoushan Hu^{1,2}, Xianchun Duan¹, Yanyan Zhang³, Can Peng^{1,2}, Daiyin Peng^{1,2,4} and Lan Han^{1,2*}

¹Anhui University of Chinese Medicine, Hefei, China, ²Anhui Province Key Laboratory of Chinese Medicinal Formula, Hefei, China,

³Anhui Medicine College, Hefei, China, ⁴Key Laboratory of Xin'an Medicine, Ministry of Education, Hefei, China

OPEN ACCESS

Edited by:

Jiahong Lu,
University of Macau, China

Reviewed by:

Chun Yang,
Nanjing Medical University, China
Wenda Xue,
Nanjing University of Chinese
Medicine, China

*Correspondence:

Lan Han
hanlan56@ahtcm.edu.cn

[†]These authors have contributed
equally to this work

Specialty section:

This article was submitted to
Ethnopharmacology,
a section of the journal
Frontiers in Pharmacology

Received: 01 August 2020

Accepted: 28 October 2020

Published: 08 December 2020

Citation:

Wang M, Liu Z, Hu S, Duan X, Zhang Y,
Peng C, Peng D and Han L (2020)
Taohong Siwu Decoction Ameliorates
Ischemic Stroke Injury Via
Suppressing Pyroptosis.
Front. Pharmacol. 11:590453.
doi: 10.3389/fphar.2020.590453

Objective: Taohong Siwu decoction (THSWD) is one of the classic prescriptions for promoting blood circulation and removing blood stasis, and it has a good therapeutic effect on ischemic stroke. We sought to explore the therapeutic effects of THSWD on pyroptosis in rats with middle cerebral artery occlusion-reperfusion (MCAO/R).

Methods: MCAO/R model of rats were established by suture-occluded method. MCAO/R rats were randomly divided into five groups, which were model group, nimodipine group, THSWD high, medium and low dose group (18, 9, and 4.5 g/kg, respectively), rats of sham group without thread embolus. All rats were treated by intragastric administration for 7 days. We detected the level of inflammatory factors. NLRP3 and Caspase-1 were detected by immunofluorescence. Western blot was used to detect NLRP3, Caspase-1, ASC, and GSDMD in penumbra. Also, the expression of TXNIP, HMGB1, toll-like receptors (TLR4), NF- κ B, and MAPK were detected.

Results: THSWD treatment improved the behavioral function and brain pathological damage. These results showed that the levels of TNF- α , TGF- β , IL-2, IL-6, IL-1 β , and IL-18 were significantly reduced in THSWD treatment groups. THSWD could significantly decrease the expression levels of NLRP3, Caspase-1, Caspase-1 p10, ASC, TXNIP, GSDMD, HMGB1, TLR4/NF κ B, p38 MAPK, and JNK in penumbra.

Conclusion: Our results showed that THSWD could reduce the activation level of NLRP3 inflammatory corpuscle, down-regulate GSDMD, and inhibit pyroptosis in MCAO/R rats. These may be affected by inhibiting HMGB1/TLR4/NF κ B, MAPK signaling pathways.

Keywords: MAPK, HMGB1/toll-like receptors/NF κ B, pyroptosis, ischemic stroke, Taohong Siwu decoction

INTRODUCTION

In 2016, The Lancet reported that about 90.7% of strokes were related to 10 risk factors, including hypertension, smoking, dyslipidemia, alcohol intake, unhealthy diet, etc (O'Donnell et al., 2016). Although the mortality rate of stroke has shown a downward trend in China (Wang et al., 2017). However, stroke was an important cause of death and disability at present. The prevalence rate continues to increased, and the affected population has shown a younger trend (Fu et al., 2020). Therefore, the prevention and treatment of stroke was a very serious problem in China.

TABLE 1 | Contents of TaoHong SiWu decoction (THSWD).

Latin name	Chinese name	Part used	Weight (g)
<i>Prunus persica</i> (L.) Batsch	Tao Ren	Semen	9
<i>Carthamus tinctorius</i> L.	Hong Hua	Flos	6
<i>Angelica sinensis</i> (Oliv.) Diels	Dang Gui	Radix	9
<i>Rehmannia glutinosa</i> (Gaertn.) DC.	Shu Di Huang	Radix	12
<i>Ligusticum chuanxiong</i> Hort.	Chuan Xiong	Rhizoma	6
<i>Paeonia lactiflora</i> Pall.	Bai Shao	Radix	9

Mitochondrial dysfunction triggers cascade reactions after ischemia stroke, such as the generation of large amounts of endogenous ROS, inflammation, and autophagy. Inflammatory corpuscle and pyroptosis are important in stroke (Fann et al., 2013; Barrington et al., 2017; Dong et al., 2018). The activated NF- κ B pathway up-regulates the gene expression of NLRP3, pro-IL-1 β , and pro-IL-18 (Bauernfeind et al., 2009). The production of endogenous ROS and cathepsin B could stimulate self-assembly of NLRP3 inflammatory corpuscle (Chen and Sun, 2013; Latz et al., 2013). NLRP3, ASC, and pro-Caspase-1 have been assembled to form a protein complex, which promoted cleavage to produce activated Caspase-1. GSDMD is cleaved by mature Caspase-1. GSDMD N-terminal domain assembles membrane pores to induce pyroptosis (Shi et al., 2015; Mulvihill et al., 2018). Mature IL-1 β and IL-18 are released extracellularly through GSDMD membrane pores (He et al., 2015). At the same time, the contents such as HMGB1 are released to the outside of the cell. HMGB1 binds to the transmembrane receptors RAGE and toll-like receptors (TLR4), and further activates the nuclear transcription factor NF- κ B, which further enhances the inflammatory response (Paudel et al., 2019).

Ischemic stroke is considered to be the cerebrovascular disease (Rutten-Jacobs and Rost, 2019). Traditional Chinese medicine has been widely used to treat vascular diseases for nearly 2000 years. Taohong Siwu decoction (THSWD) originated from the traditional Chinese medicine book *Yizong Jinjian* of the Qing Dynasty, which is composed of *Prunus persica* (L.) Batsch, *Carthamus tinctorius* L., *Angelica sinensis* (Oliv.) Diels, *Rehmannia glutinosa* (Gaertn.) DC., *Ligusticum chuanxiong* Hort, *Paeonia lactiflora* Pall. (Table 1). THSWD has been widely used clinically to treat vascular diseases in the past. Our research showed that THSWD could reduce oxidative stress injury, improve learning and memory function, and promote angiogenesis in ischemic stroke (Han et al., 2015; Chen et al., 2020; Wang M. et al., 2020). It is well known that inflammation and pyroptosis are involved in ischemic stroke injury (Barrington et al., 2017; Dong et al., 2018). There is no reported about the effect of THSWD on pyroptosis. The mechanisms whereby THSWD is of value has not been fully elucidated in the treatment of ischemic stroke. Therefore, we hypothesized that THSWD could reduce pyroptosis in ischemic stroke.

In present study, we studied the effect of THSWD on inflammatory factors in rats with middle cerebral artery occlusion-reperfusion (MCAO/R). More importantly, we further explored the effect of THSWD on pyroptosis. This is

more conducive to the research and development of THSWD as a candidate drug for the treatment of stroke.

MATERIALS AND METHODS

Materials

Tao Ren (*Prunus persica* (L.) Batsch, 1702181), Hong Hua (*Carthamus tinctorius* L., 17072135.), Dang Gui (*Angelica sinensis* (Oliv.) Diels, 1611085), Shu Di Huang (*Rehmannia glutinosa* (Gaertn.) DC., 1705312), Chuan Xiong (*Ligusticum chuanxiong* Hort, 17010335), Bai Shao (*Paeonia lactiflora* Pall., 17110114) were purchased from Bozhou Yonggang Pieces Factory Co., Ltd. (Bozhou, China). They were verified by Qingshan Yang (Anhui University of Chinese Medicine, Hefei, China). Nimodipine (State Food and Drug Administration approval number: H14022821) was purchased from Yabao Pharmaceutical Group CO., Ltd. (Yuncheng, China).

Anti-body (GSDMD:ab219800, Caspase-1:ab1872, Caspase-1 p10:ab179515, HMGB1:ab77302, JNK:ab124956, p38:ab45381, TLR4:ab217274) were purchased from Abcam (Cambridge, MA, United States). Anti-body (ASC:sc-514414, TXNIP:sc-271238) were bought from Santa Cruz Biotechnology (Santa Cruz, CA, United States). Anti-NLRP3 (NBP2-12446) was bought from Novus (Colorado, United States). Anti-NF- κ B (bs-0465R) was bought from Bioss (Beijing, China). Anti-GAPDH (19AF0406) was purchased from ZSGB-BIO (Beijing, China). Rat TNF- α , IL-6, IL-1 β , and IL-18 Elisa kits (201903) were purchased from Meimian (Jiangsu, China), rat IL-2, and TGF- β Elisa kits (GR2019-03) were purchased from JYM (Wuhan China).

Preparation of Taohong Siwu Decoction

These THSWD were mixed of six herbs in the proportion of Table 1, soaked in 10 times (v/w) 75% ethanol for 2 h, boiled and refluxed for 2 h. Then the filtrate was collected, and the residue was refluxed with 8 times the amount of 75% ethanol for 2 h. The two filtrates were mixed and concentrate to 1.8 g/ml by rotary evaporation. According to the published standard experimental procedure, UPLC was used to ensure the quality and stability of the THSWD (Han et al., 2017; Chen et al., 2020). The assay chromatogram of THSWD of the same batch number and preparation has been published (Chen et al., 2020).

Animals and Middle Cerebral Artery Occlusion Surgery

Healthy male Sprague-Dawley rats weighing 270 ± 20 g were provided by the Experimental Animal Center of Anhui Medical University (Hefei, China). All rats were housed in a polypropylene cage ($25 \pm 5^\circ\text{C}$, 50–60% relative humidity) under controlled lighting (12 h light/dark cycle), and allowed free access to food and water.

All experimental rats were anesthetized by pentobarbital (50 mg/kg, i.p.). The common carotid artery (CCA), external carotid artery (ECA), and internal carotid artery (ICA) were carefully separated from the middle cervical incision of the rat

neck. To ensure the middle cerebral artery (MCA) was occluded, an incision was made in the CCA, and the nylon suture was inserted to about 18–20 mm through the ICA. The nylon suture was a polylysine coated monofilament nylon with a diameter of 0.285 mm. After 2 h of surgery, the nylon suture was withdrawn from MCA and reperused. After 2 h of surgery, the nylon suture was withdrawn to allow reperused. The sham rats only performed the same process of separating blood vessels. The temperature was kept at 37°C in the experimental process.

After 24 h of ischemia-reperfusion, the behavioral scores were performed according to the method of Zea Longa, and rats were randomly divided into six groups: Sham, MCAO, THSWD (18, 9 and 4.5 g/kg, respectively, equivalent to the dry weight of the raw materials), nimodipine (20 mg/kg) groups, and treated (i.g.) for 7 days.

Functional Outcome Assessment

On the 7th day after the rats were given treatment, all rats completed the Bederson scores. 0, no observable deficit. 1, forelimb flexion when suspended by the tail. 2, decreased resistance to push. 3, counterclockwise circling. 4, unconsciousness, including death within 24 h.

Measurement of Infarct Volume

After killing the rats, brains were isolated and sectioned into five coronal slices in 2 mm thickness. Which were stained with 2,3,5-Triphenyltetrazolium chloride (TTC, 2%, T8170, Solarbio, Beijing, China) for 30 min under dark conditions of 37°C. The coronal slices were taken pictures through digital camera and analyze the infarct volume by Image J (NIH, Bethesda, MD, United States).

Histomorphological Analysis

The brains were fixed in 4% paraformaldehyde, and paraffin sections were prepared for HE staining (BA-4041, BA-4024, BASO, Zhuhai China). After sealed with neutral resin, and images were captured using an optical microscope (SYZX6061, Nikon, Tokyo, Japan). The histomorphological analysis was evaluated by two examiners blinded to the treatment groups.

ELISA

Rat penumbra tissues were separated and homogenized with 10 times PBS (v/w) on ice. The homogenates were centrifuged at 4,000 rpm for 10 min at 4°C, and supernatants were collected, then stored in –80°C until future use. The secretion levels of inflammatory cytokines (TNF- α , IL-2, IL-6, TGF- β , IL-1 β , IL-18) were analyzed by ELISA. According to the manufacturer's protocol above in the ELISA kit instructions, the optical density (OD) at 450 nm was measured by enzyme-labeled instrument (Multiskan GO, Thermo, Waltham, MA, United States).

Immunofluorescence Staining

The brain tissues were quickly removed and frozen, and frozen sections were made. The sections were reacted with a primary antibody and subsequently reacted with a fluorescently labeled secondary antibody. Then, which were sealed with a sealer

containing a quencher. Two examiners blinded to the treatment groups were observed and photographed using a fluorescence microscope (ECLIPSE TI-SR, Nikon, Tokyo, Japan), and analyzed by ImageJ.

Western Blotting

Rat penumbra tissues were separated and homogenized with 10 times ice-cold lysis buffer containing protein inhibitor. The homogenates were centrifuged at 12,000 rpm for 10 min at 4°C, and supernatants were collected. The protein concentration of supernatants were measured by BCA kit (PICPI23223, Thermo, Waltham, MA, United States). In order to denature the protein, the protein samples were added to buffer and boiled for 10 min at 100°C. Equal amounts of proteins were separated by electrophoresis, transferred to NC membranes at low temperatures. After blocking with 5% skimmed milk powder for 2 h, membranes were incubated overnight at 4°C with primary antibodies (anti-NLRP3, anti-ASC, anti-Caspase-1, anti-TXNIP, anti-Caspase-1 p10, anti-GAPDH). The NC membranes were then incubated with the secondary antibody (HRP-conjugated anti-rabbit and anti-mouse secondary antibody, A21010, Abbkine, Wuhan China), and developed with enhanced chemiluminescence (ECL, 32109, Thermo, Waltham, MA, United States).

Statistical Analysis

The data were analyzed with SPSS 23.0 software and expressed as the mean \pm SD. Statistical analyses were performed using one-way ANOVA, followed by LSD tests for the significance of the difference between groups. $p < 0.05$ was considered statistically significant.

RESULTS

Effects of Taohong Siwu Decoction on the Neurological Defect Scores and Infarction Volume in Middle Cerebral Artery Occlusion-Reperfusion Model

As shown in **Figure 1B**, after 7 days of treatment with THSWD and nimodipine, the behavioral function were significantly improved of MCAO/R rats. Compared with model group, the Bederson scores of THSWD and nimodipine groups were significantly reduced ($p < 0.05$, $p < 0.01$). Sham group rats had no behavioral function impairment. TTC staining was used to calculate the infarct volume of rats. The brain of sham group rats had no infarction volume. Compared with model group, the infarct volume were significantly reduced of THSWD and the nimodipine treatment group (**Figures 1C,D**).

Effect of Taohong Siwu Decoction on the Level of Pathological Damage in Brain of Middle Cerebral Artery Occlusion-Reperfusion Rats

The pathological damage of brain tissue was observed by HE staining. The specific results showed in **Figure 2**. The positive cells were intact and abundant, and no infiltration of

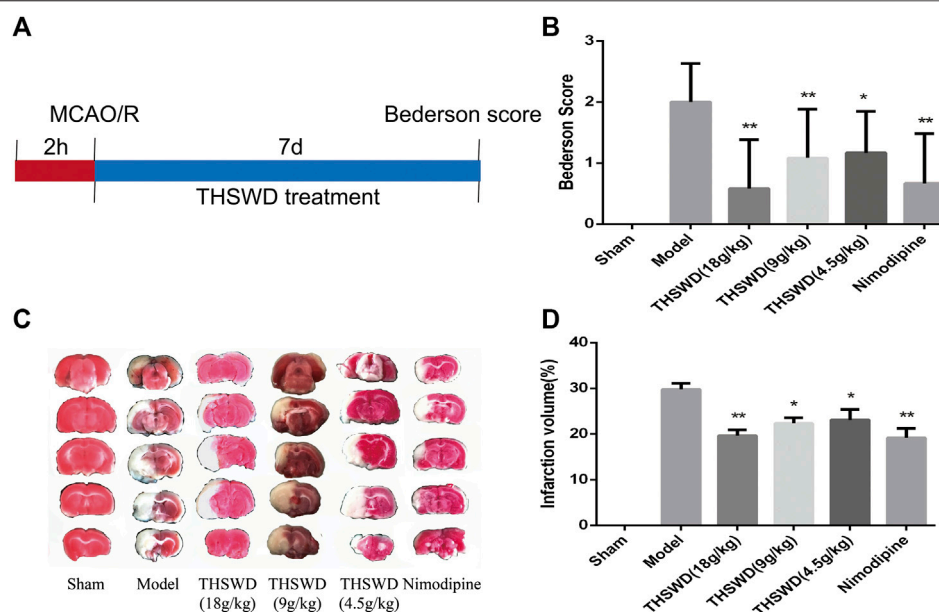


FIGURE 1 | Taohong Siwu decoction (THSWD) alleviated middle cerebral artery occlusion-reperfusion (MCAO/R) induced brain damage. **(A)** The flow diagram of the experiment. **(B)** Neurological deficits scores. **(C)** 2,3,5-Triphenyltetrazolium chloride staining of representative sections. **(D)** Quantification of infarction volume rates. The results were presented as the mean \pm SD ($n = 6$). Compared with sham group, $^{\#}p < 0.05$, $^{##}p < 0.01$. Compared with model group, $^{*}p < 0.05$, $^{**}p < 0.01$.

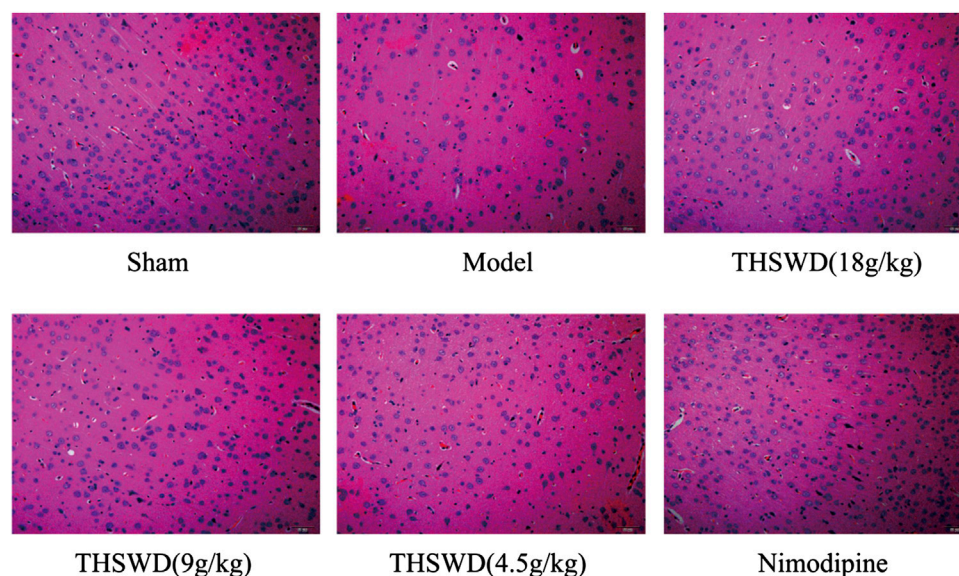
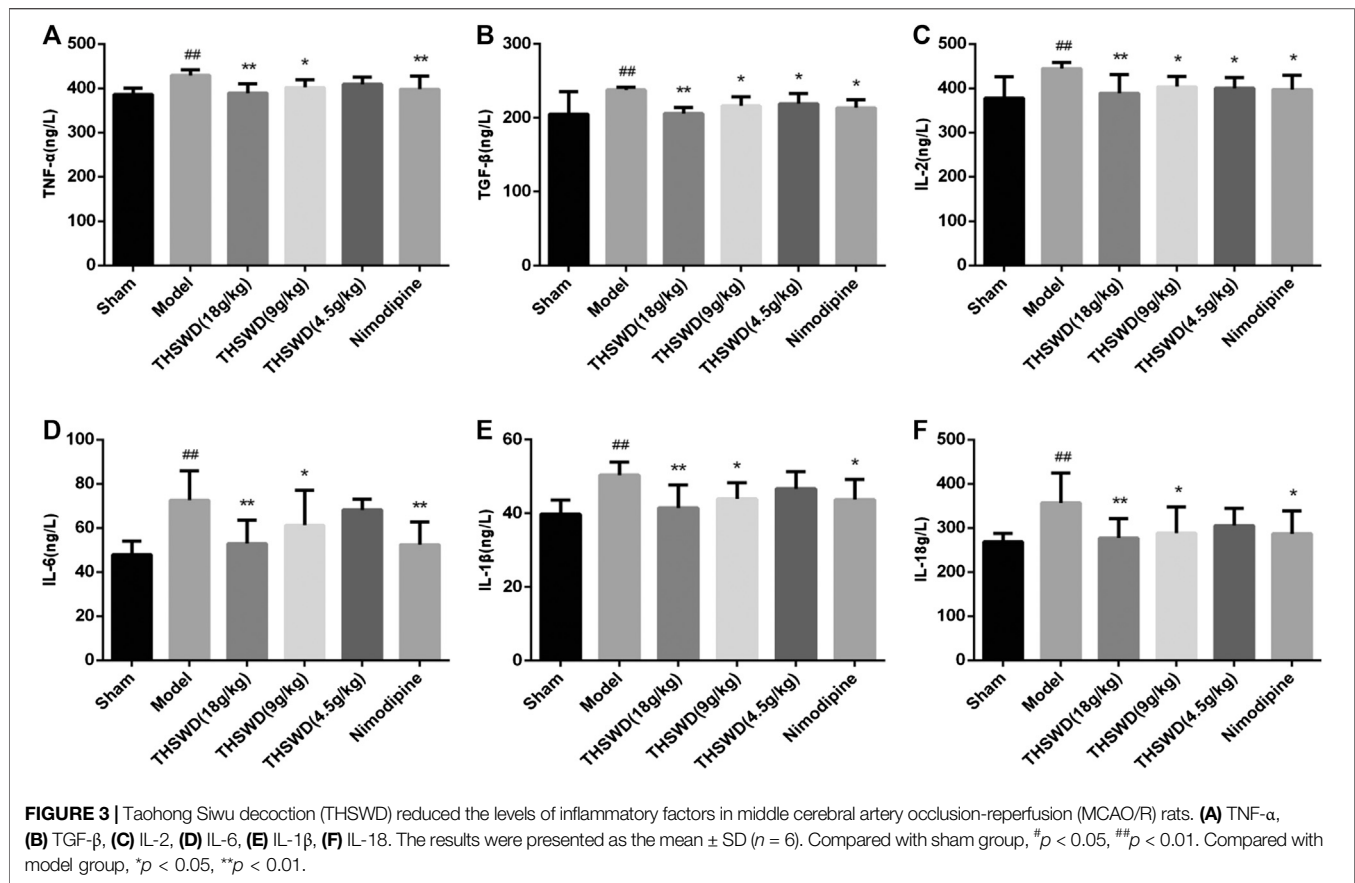


FIGURE 2 | Effect of Taohong Siwu decoction (THSWD) on the level of pathological damage in middle cerebral artery occlusion-reperfusion (MCAO/R) rats ($\times 200$, $n = 3$).

inflammatory cells in sham group. The model group showed that the number of positive cells nuclei were significantly reduced, most cells exhibited visible disorder. There were phenomena, such as nuclear shrinkage, nuclear rupture, and inflammatory cells infiltrated. Advantageously, THSWD treatment group significantly alleviated the abnormal phenomena caused by MCAO/R.

Effect of Taohong Siwu Decoction on Inflammatory Factors in Middle Cerebral Artery Occlusion-Reperfusion Rats

Pro-inflammatory factors increased after a stroke. Besides, plenty of inflammatory factors were detrimental to the function of tissues and cells. We detected the levels of inflammatory factors in penumbra by ELISA. Compared with sham group,



the levels of TNF- α , IL-2, IL-6, TGF- β , IL-1 β , and IL-18 were significantly increased in model group ($p < 0.05$, $p < 0.01$). Compared with model group, THSWD and nimodipine treatment groups significantly reduced the level of inflammatory factors ($p < 0.05$, $p < 0.01$). These showed that THSWD could attenuate inflammatory response of MCAO/R rats (Figure 3). During the occurrence of pyroptosis, IL-1 β and IL-18 were secreted to enhance the inflammatory response. Therefore, we further investigated the effect of THSWD on pyroptosis in MCAO/R rats.

Effect of Taohong Siwu Decoction on Pyroptosis in Middle Cerebral Artery Occlusion-Reperfusion Rats

Immunofluorescence was used to detect the expression of NLRP3 and Caspase-1 in brain. We observed the picture qualitatively and draw the following preliminary results. As shown in Figure 4, compared with sham group, the fluorescence intensity of NLRP3 and Caspase-1 increased significantly in model group. Compared with model group, the fluorescence intensity of NLRP3 and Caspase-1 decreased in THSWD (18 g/kg) treatment groups. We also advanced quantitative analysis of NLRP3 and Caspase-1 by western blot.

We detected the expression levels of NLRP3 inflammatory corpuscle constituent protein and pyroptosis executive protein in penumbra. As shown in Figure 5, these results showed that

compared with sham group, the levels of NLRP3, Caspase-1, Caspase-1 p10, ASC, and GSDMD were significantly increased ($p < 0.01$) in model group. Compared with model group, the levels of NLRP3, Caspase-1, Caspase-1 p10, ASC, and GSDMD were significantly reduced ($p < 0.05$, $p < 0.01$) of THSWD and nimodipine treatment groups in penumbra. Our results indicated that THSWD could inhibit the activation of NLRP3 inflammatory corpuscle and inhibit pyroptosis in MCAO/R rats.

Taohong Siwu Decoction Inhibited the Activity of HMGB1-Toll-Like Receptors-NF κ B and MAPK Signaling Pathways

To explore how THSWD inhibits pyroptosis, western blot was used to detect the signaling pathway in penumbra of the brain. These results showed that compared with sham group, the levels of TXNIP, HMGB1, TLR4 and NF- κ B p65 were significantly increased ($p < 0.01$) in model group. Compared with model group, the levels of TXNIP, HMGB1, TLR4, and NF- κ B p65 were significantly reduced ($p < 0.05$, $p < 0.01$) in THSWD and nimodipine treatment groups (Figures 6B–D). This indicated that THSWD inhibited pyroptosis through down-regulating the HMGB1-TLR4-NF κ B pathway.

In order to study the effect of THSWD on the MAPK pathway of MCAO/R rats, the expression of JNK and p38 MAPK were

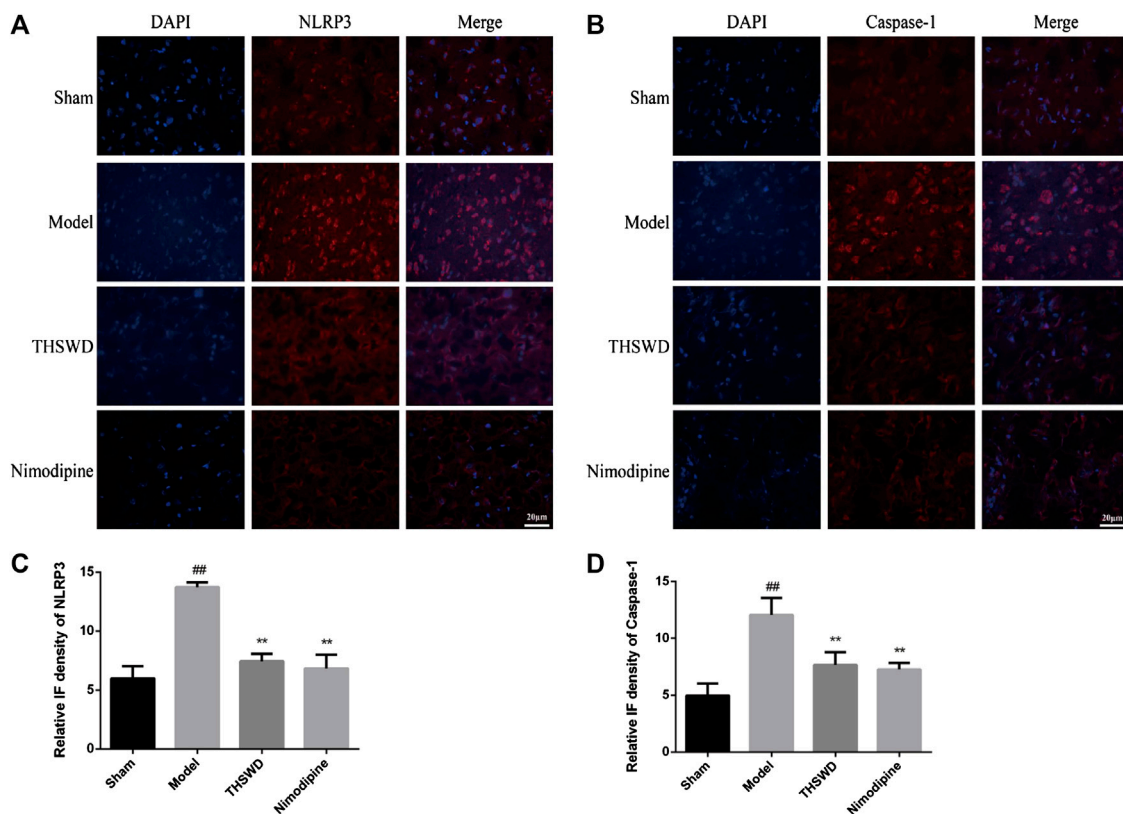


FIGURE 4 | Taohong Siwu decoction (THSWD) inhibited NLRP3 and Caspase-1 expression (x400). **(A)** NLRP3, **(B)** Caspase-1. The nuclei were stained blue by DAPI, and NLRP3 and Caspase-1 were red. **(C,D)** Fluorescence intensity analysis of NLRP3 and Caspase-1 staining ($n = 3$).

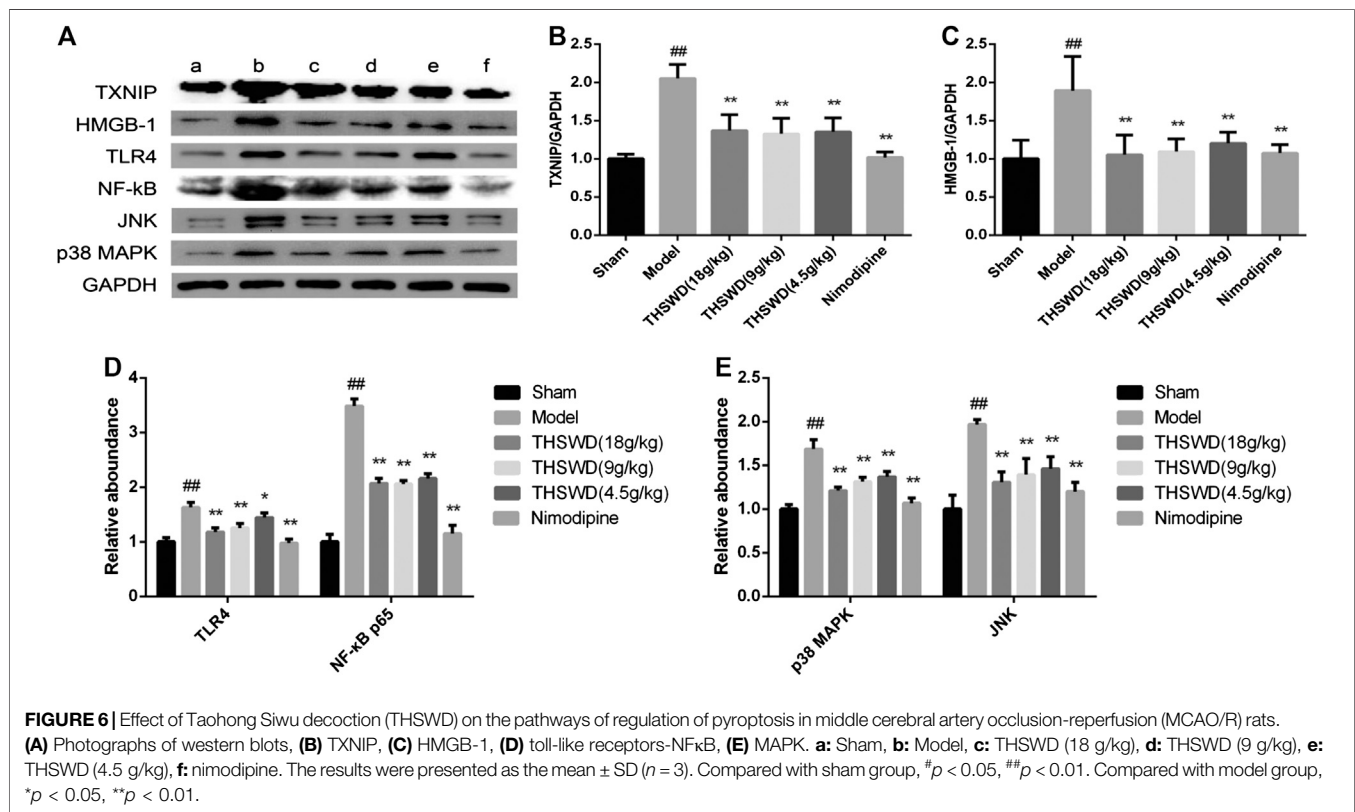
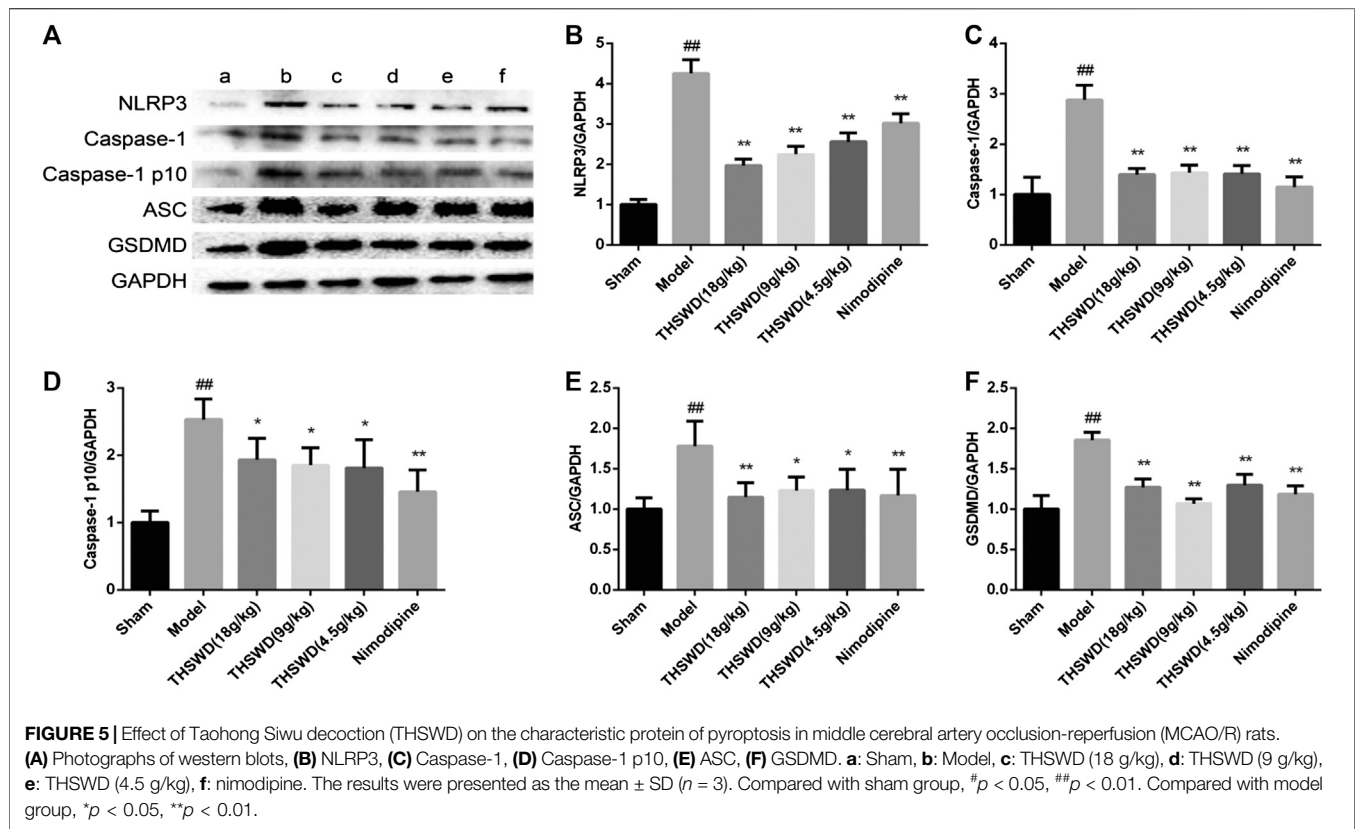
detected in penumbra. These results showed compared with sham group, the levels of JNK and p38 MAPK were significantly increased ($p < 0.01$) in MCAO/R rats. Compared with model group, the levels of JNK and p38 MAPK were significantly reduced ($p < 0.05$, $p < 0.01$) in THSWD and nimodipine treatment groups (Figure 6E). This indicated that THSWD inhibited pyroptosis through down-regulating the MAPK pathway.

DISCUSSION

The inflammatory response is activated due to vascular occlusion in ischemic stroke. Leukocytes are recruited into endothelial cells, which damages the blood-brain barrier (BBB) and a large number of inflammatory mediators are released (Anrather and Iadecola, 2016; De Meyer et al., 2016). Intravascular inflammation is the basis of BBB breakdown and leukocyte invasion. At the same time, the inflammatory cascade process started in brain parenchyma. Microglia are recruited near damaged blood vessels and they are activated quickly (Szalay et al., 2016). Inflammatory factors are released such as IL-1 β and TNF- α and fed back into the inflammatory cascade through other immune cells (Anrather and Iadecola, 2016; Szalay et al., 2016). Our previous research has proved that THSWD has a

good therapeutic effect on MCAO/R. This study also confirms previous conclusions. In this study, the results showed that THSWD could reduce the levels of inflammatory factors in MCAO/R rats. This provides a positive signal for exploring the role of THSWD in pyroptosis.

Pyroptosis is widely involved in central nervous system diseases. Unlike apoptosis, pyroptosis occurred faster and accompanied by the release of a large number of inflammatory factors. Many studies have shown that almost all N-terminal domains of Gasdermin family proteins could induce pyroptosis. GSDMD is the common substrate for activated Caspase-1 and Caspase-4/5/11 (Wang K. et al., 2020). The domain of GSDMD between N-terminal domain and C-terminal domain is cleaved by activated Caspase. GSDMD N-terminal domain specifically is bound to cardiolipin and phosphoinositide, recruited oligomerization on the plasma membrane to form a membrane pore. GSDMD C-terminal domain could inhibit GSDMD N-terminal domain to maintain GSDMD inhibition state (Liu et al., 2018). NLRP3 inflammatory corpuscle is the most widely studied all inflammatory corpuscles. A large number of studies have shown that NLRP3 is expressed among neurons, endothelial cells, and microglia. TXNIP is an endogenous inhibitor of TRX. After cells are stimulated by inflammatory corpuscle activators (ROS), the oxidized TRX causes TXNIP/TRX decomposition. TXNIP is shuttled to cytoplasmic mitochondria



in the ROS-dependent manner, which bound to NLRP3, and activates NLRP3 inflammatory corpuscle (Zhou et al., 2011; Nasoohi et al., 2018). Our direct observation of immunofluorescence results showed that compared with sham group, the expression levels of NLRP3 and Caspase-1 increased in MCAO/R group. Compared with MCAO/R group, the expression of NLRP3 and Caspase-1 decreased in the THSWD (18 g/kg) treatment group. Further research confirmed that THSWD could significantly decrease the expression levels of NLRP3, Caspase-1, GSDMD, TXNIP, ASC. These results proved that pyroptosis is activated by MCAO/R. THSWD could reduce the activation of NLRP3 inflammatory corpuscle and inhibit pyroptosis.

HMGB1 is transferred from the nucleus to the cytoplasm, which is secreted extracellularly by activating inflammatory corpuscles (Vande Walle et al., 2011). Outside the cell, HMGB1 bound to its receptor (TLR2, TLR4, TLR9, RAGE), mediated the production of downstream inflammatory factors and expanded the inflammatory response. Studies have shown that HMGB1 could induce the formation of NLRP3 inflammatory corpuscle through TLRs (Song et al., 2017; Yu et al., 2019). The pro-inflammatory HMGB1-TLR4-NLRP3-GSDMD signal axis could induce Caspase-1 mediated pyroptosis (Dong et al., 2019). Signaling molecules downstream of TLR4/MyD88 pathway include NF- κ B, JNK, p38 MAPK, and ERK1/2. JNK and p38 MAPK are mainly activated by various cellular stress signals and pro-inflammatory cytokines (Kim and Choi, 2015). In ischemic stroke, MAPK and NF- κ B signaling pathways are key links in the expression and activation of NLRP1 and NLRP3 inflammatory corpuscles (Fann et al., 2018). Their involvement is widely recognized in activating inflammatory corpuscles. In this study, we have demonstrated that HMGB1/TLR4/NF κ B and MAPK were activated in the MCAO/R rats. THSWD could inhibit the activation of HMGB1/TLR4/NF κ B and MAPK.

Our team conducted the THSWD fingerprint study by UPLC. A total of fifteen compounds were identified. The six compounds were initially compared by standard product, including hydroxysafflor yellow A, 5-hydroxymethyl furfuraldehyde, ferulic acid, ligustilide, amygdalin and paeoniflorin (Han et al., 2017). The assay chromatogram of THSWD of the same batch number and preparation has been published (Chen et al., 2020). Their respective contents of hydroxysafflor yellow A, amygdalin, paeoniflorin, ferulic acid, verbascoside, and ligustilide in THSWD were identified as 0.198, 0.45, 0.602, 0.031, 0.014, and 0.256 mg ml⁻¹ (Chen et al., 2020). Also, our previous report has investigated the major constituents of THSWD by UPLC-

Q-TOF-MS. A total of 95 components have been identified, including aromatic acids, flavonoids, polysaccharides, volatile oils, monoterpene glycosides, aromatic cyanoglycosides (Duan et al., 2019). Many published articles have confirmed that they are the basis of THSWD inhibitors of pyroptosis (Liu et al., 2017; Ye et al., 2020; Yin et al., 2020).

In summary, the findings showed that THSWD could significantly reduce the level of inflammatory factors. Additionally, this study demonstrated that pyroptosis is involved in MCAO/R rats. THSWD exerts significant effects on ischemic brain injury through a mechanism closely related to reduce the activation of NLRP3 inflammatory corpuscle and inhibit pyroptosis. These may be achieved by down-regulating the HMGB1-TLR4-NF κ B and MAPK pathways. This study is of great significance to verify the main efficacy of traditional Chinese medicine THSWD, as it confirms the mechanism of action of the THSWD on pyroptosis. This work is conducive to the research and development of the stroke candidate drugs of THSWD.

DATA AVAILABILITY STATEMENT

The raw data supporting the conclusions of this article will be made available by the authors, without undue reservation.

ETHICS STATEMENT

The principles of laboratory animal care followed the guiding principles for the care and use of laboratory animals. All experimental procedures were authorized by the Committee on the Ethics of Animal Experiments of Anhui University of Chinese Medicine.

AUTHOR CONTRIBUTIONS

MW, CP, DP, and LH designed and supervised the study. MW and ZL performed the experiments. SH, XD, and YZ analyzed the data. MW and ZL wrote the paper.

FUNDING

This work was supported by grants from the National Natural Science Foundation of China (Nos. 82074152, 81903953, 81503291, and 81473387).

REFERENCES

- Anrather, J. and Iadecola, C. (2016). Inflammation and stroke: an overview. *Neurotherapeutics* 13 (4), 661–670. doi:10.1007/s13311-016-0483-x.
- Barrington, J., Lemarchand, E., and Allan, S. M. (2017). A brain in flame; do inflammasomes and pyroptosis influence stroke pathology? *Brain Pathol.* 27 (2), 205–212. doi:10.1111/bpa.12476.
- Bauernfeind, F. G., Horvath, G., Stutz, A., Alnemri, E. S., Macdonald, K., Speert, D., et al. (2009). Cutting edge: NF- κ B activating pattern recognition and cytokine receptors license NLRP3 inflammasome activation by regulating NLRP3 expression. *J. Immunol.* 183 (2), 787–791. doi:10.4049/jimmunol.0901363
- Chen, F.-F., Wang, M.-M., Xia, W.-W., Peng, D.-Y., and Han, L. (2020). Tao-Hong-Si-Wu decoction promotes angiogenesis after cerebral ischaemia in rats via platelet microparticles. *Chin. J. Nat. Med.* 18 (8), 620–627. doi:10.1016/s1875-5364(20)30074-1.

- Chen, S. and Sun, B. (2013). Negative regulation of NLRP3 inflammasome signaling. *Protein Cell* 4 (4), 251–258. doi:10.1007/s13238-013-2128-8.
- De Meyer, S. F., Denorme, F., Langhauser, F., Geuss, E., Fluri, F., and Kleinschnitz, C. (2016). Thromboinflammation in stroke brain damage. *Stroke* 47 (4), 1165–1172. doi:10.1161/strokeaha.115.011238.
- Dong, W., Zhu, Q., Yang, B., Qin, Q., Wang, Y., Xia, X., et al. (2019). Polychlorinated biphenyl quinone induces caspase 1-mediated pyroptosis through induction of pro-inflammatory HMGB1-TLR4-NLRP3-GSDMD signal axis. *Chem. Res. Toxicol.* 32 (6), 1051–1057. doi:10.1021/acs.chemrestox.8b00376.
- Dong, Z., Pan, K., Pan, J., Peng, Q., and Wang, Y. (2018). The possibility and molecular mechanisms of cell pyroptosis after cerebral ischemia. *Neurosci. Bull.* 34 (6), 1131–1136. doi:10.1007/s12264-018-0294-7.
- Duan, X., Pan, L., Bao, Q., and Peng, D. (2019). UPLC-Q-TOF-MS study of the mechanism of THSWD for breast cancer treatment. *Front. Pharmacol.* 10, 1625. doi:10.3389/fphar.2019.01625.
- Fann, D. Y., Lee, S. Y., Manzanero, S., Tang, S. C., Gelderblom, M., Chunduri, P., et al. (2013). Intravenous immunoglobulin suppresses NLRP1 and NLRP3 inflammasome-mediated neuronal death in ischemic stroke. *Cell Death Dis.* 4, e790. doi:10.1038/cddis.2013.326.
- Fann, D. Y.-W., Lim, Y.-A., Cheng, Y.-L., Lok, K.-Z., Chunduri, P., Baik, S.-H., et al. (2018). Evidence that NF- κ B and MAPK signaling promotes NLRP inflammasome activation in neurons following ischemic stroke. *Mol. Neurobiol.* 55 (2), 1082–1096. doi:10.1007/s12035-017-0394-9.
- Fu, H., Zhang, D., Zhu, R., Cui, L., Qiu, L., Lin, S., et al. (2020). Association between lipoprotein(a) concentration and the risk of stroke in the Chinese Han population: a retrospective case-control study. *Ann. Transl. Med.* 8 (5), 212. doi:10.21037/atm.2020.01.38.
- Han, L., Ji, Z., Chen, W., Yin, D., Xu, F., Li, S., et al. (2015). Protective effects of tao-Hong-si-Wu decoction on memory impairment and hippocampal damage in animal model of vascular dementia. *Evid Based Compl. Alternat. Med.* 2015, 195835. doi:10.1155/2015/195835.
- Han, L., Qiao, O., Wu, H., Wu, S., Zhang, Y., Yao, L., et al. (2017). Chromatographic fingerprint analysis is feasible for comprehensive quality control of Taohongsiwu. *Int. J. Pharmacol.* 13 (5), 488–494. doi:10.3923/ijp.2017.488.494.
- He, W.-T., Wan, H., Hu, L., Chen, P., Wang, X., Huang, Z., et al. (2015). Gasdermin D is an executor of pyroptosis and required for interleukin-1 β secretion. *Cell Res.* 25 (12), 1285–1298. doi:10.1038/cr.2015.139.
- Kim, E. K. and Choi, E.-J. (2015). Compromised MAPK signaling in human diseases: an update. *Arch. Toxicol.* 89 (6), 867–882. doi:10.1007/s00204-015-1472-2.
- Latz, E., Xiao, T. S., and Stutz, A. (2013). Activation and regulation of the inflammasomes. *Nat. Rev. Immunol.* 13 (6), 397–411. doi:10.1038/nri3452.
- Liu, Y.-M., Shen, J.-D., Xu, L.-P., Li, H.-B., Li, Y.-C., and Yi, L.-T. (2017). Ferulic acid inhibits neuro-inflammation in mice exposed to chronic unpredictable mild stress. *Int. Immunopharmacol.* 45, 128–134. doi:10.1016/j.intimp.2017.02.007.
- Liu, Z., Wang, C., Rathkey, J. K., Yang, J., Dubyak, G. R., Abbott, D. W., et al. (2018). Structures of the gasdermin D C-terminal domains reveal mechanisms of autoinhibition. *Structure* 26 (5), 778.e773–784.e773. doi:10.1016/j.str.2018.03.002.
- Mulvihill, E., Sborgi, L., Mari, S. A., Pfreundschuh, M., Hiller, S., and Müller, D. J. (2018). Mechanism of membrane pore formation by human gasdermin-D. *EMBO J.* 37 (14), e98321. doi:10.15252/embj.201798321.
- Nasoohi, S., Ismael, S., and Ishrat, T. (2018). Thioredoxin-interacting protein (TXNIP) in cerebrovascular and neurodegenerative diseases: regulation and implication. *Mol. Neurobiol.* 55 (10), 7900–7920. doi:10.1007/s12035-018-0917-z.
- O'donnell, M. J., Chin, S. L., Rangarajan, S., Xavier, D., Liu, L., Zhang, H., et al. (2016). Global and regional effects of potentially modifiable risk factors associated with acute stroke in 32 countries (INTERSTROKE): a case-control study. *Lancet* 388 (10046), 761–775. doi:10.1016/s0140-6736(16)30506-2.
- Paudel, Y. N., Angelopoulou, E., Piperi, C., Balasubramaniam, V. R. M. T., Othman, I., and Shaikh, M. F. (2019). Enlightening the role of high mobility group box 1 (HMGB1) in inflammation: updates on receptor signalling. *Eur. J. Pharmacol.* 858, 172487. doi:10.1016/j.ejphar.2019.172487.
- Rutten-Jacobs, L. C. A. and Rost, N. S. (2020). Emerging insights from the genetics of cerebral small-vessel disease. *Ann. N. Y. Acad. Sci.* 1471 (1), 5–17. doi:10.1111/nyas.13998.
- Shi, J., Zhao, Y., Wang, K., Shi, X., Wang, Y., Huang, H., et al. (2015). Cleavage of GSDMD by inflammatory caspases determines pyroptotic cell death. *Nature* 526 (7575), 660–665. doi:10.1038/nature15514.
- Song, E., Jahng, J. W., Chong, L. P., Sung, H. K., Han, M., Luo, C., et al. (2017). Lipocalin-2 induces NLRP3 inflammasome activation via HMGB1 induced TLR4 signaling in heart tissue of mice under pressure overload challenge. *Am. J. Transl. Res.* 9 (6), 2723–2735.
- Szalay, G., Martinecz, B., Lenart, N., Kornyei, Z., Orsolits, B., Judak, L., et al. (2016). Microglia protect against brain injury and their selective elimination dysregulates neuronal network activity after stroke. *Nat. Commun.* 7, 11499. doi:10.1038/ncomms11499.
- Vande Walle, L., Kanneganti, T.-D., and Lamkanfi, M. (2011). HMGB1 release by inflammasomes. *Virulence* 2 (2), 162–165. doi:10.4161/viru.2.2.15480.
- Wang, K., Sun, Q., Zhong, X., Zeng, M., Zeng, H., Shi, X., et al. (2020). Structural mechanism for GSDMD targeting by autoprocessed Caspases in pyroptosis. *Cell* 180 (5), 941–955. doi:10.1016/j.cell.2020.02.002.
- Wang, M., Wang, F., Peng, D., Duan, X., Chen, W., Xu, F., et al. (2020). Tao-Hong Si-Wu decoction alleviates cerebral ischemic damage in rats by improving anti-oxidant and inhibiting apoptosis pathway. *Int. J. Pharmacol.* 16 (3), 214–222. doi:10.3923/ijp.2020.214.222.
- Wang, W., Wang, D., Liu, H., Sun, H., Jiang, B., Ru, X., et al. (2017). Trend of declining stroke mortality in China: reasons and analysis. *Stroke Vasc Neurol.* 2 (3), 132–139. doi:10.1136/svn-2017-000098.
- Ye, J.-X., Wang, M., Wang, R.-Y., Liu, H.-T., Qi, Y.-D., Fu, J.-H., et al. (2020). Hydroxysafflor yellow A inhibits hypoxia/reoxygenation-induced cardiomyocyte injury via regulating the AMPK/NLRP3 inflammasome pathway. *Int. Immunopharmacol.* 82, 106316. doi:10.1016/j.intimp.2020.106316.
- Yin, N., Gao, Q., Tao, W., Chen, J., Bi, J., Ding, F., et al. (2020). Paeoniflorin relieves LPS-induced inflammatory pain in mice by inhibiting NLRP3 inflammasome activation via transient receptor potential vanilloid 1. *J. Leukoc. Biol.* 108 (1), 229–241. doi:10.1002/jlb.3ma0220-355r.
- Yu, R., Jiang, S., Tao, Y., Li, P., Yin, J., and Zhou, Q. (2019). Inhibition of HMGB1 improves necrotizing enterocolitis by inhibiting NLRP3 via TLR4 and NF- κ B signaling pathways. *J. Cell. Physiol.* 234 (8), 13431–13438. doi:10.1002/jcp.28022.
- Zhou, R., Yazdi, A. S., Menu, P., and Tschopp, J. (2011). A role for mitochondria in NLRP3 inflammasome activation. *Nature* 469 (7329), 221–225. doi:10.1038/nature09663.

Conflict of Interest: The authors declare that the research was conducted in the absence of any commercial or financial relationships that could be construed as a potential conflict of interest.

Copyright © 2020 Wang, Liu, Hu, Duan, Zhang, Peng, Peng and Han. This is an open-access article distributed under the terms of the Creative Commons Attribution License (CC BY). The use, distribution or reproduction in other forums is permitted, provided the original author(s) and the copyright owner(s) are credited and that the original publication in this journal is cited, in accordance with accepted academic practice. No use, distribution or reproduction is permitted which does not comply with these terms.



Berberine Protects Against NLRP3 Inflammasome via Ameliorating Autophagic Impairment in MPTP-Induced Parkinson's Disease Model

OPEN ACCESS

Edited by:

Juxian Song,
Guangzhou University of Chinese
Medicine, China

Reviewed by:

Yue Li,
Tianjin University of Traditional
Chinese Medicine, China
Chuanbin Yang,
Jinan University, China

*Correspondence:

Lin Lu
lulinc@126.com
Pingyi Xu
pingyixu@sina.com
Wenyuan Guo
guowenyuan1231@163.com

[†]These authors have contributed
equally to this work.

Specialty section:

This article was submitted to
Ethnopharmacology,
a section of the journal
Frontiers in Pharmacology

Received: 18 October 2020

Accepted: 30 December 2020

Published: 27 January 2021

Citation:

Huang S, Liu H, Lin Y, Liu M, Li Y,
Mao H, Zhang Z, Zhang Y, Ye P,
Ding L, Zhu Z, Yang X, Chen C, Zhu X,
Huang X, Guo W, Xu P and Lu L (2021)
Berberine Protects Against NLRP3
Inflammasome via Ameliorating
Autophagic Impairment in MPTP-
Induced Parkinson's Disease Model.
Front. Pharmacol. 11:618787.
doi: 10.3389/fphar.2020.618787

Shuxuan Huang^{1,2†}, Hanqun Liu^{1†}, Yuwan Lin^{1†}, Muchang Liu³, Yanhua Li², Hengxu Mao¹,
Zhiling Zhang¹, Yunlong Zhang⁴, Panghai Ye¹, Liuyan Ding¹, Ziting Zhu¹, Xinling Yang⁵,
Chaojun Chen⁶, Xiaoqin Zhu⁷, Xiaoyun Huang⁸, Wenyuan Guo^{1*}, Pingyi Xu^{1*} and Lin Lu^{1*}

¹Department of Neurology, The First Affiliated Hospital of Guangzhou Medical University, Guangzhou, China, ²Department of Neurology, The People's Hospital of Guangxi Zhuang Autonomous Region, Nanning, China, ³Department of Medical Affairs, The First Affiliated Hospital of Guangzhou Medical University, Guangzhou, China, ⁴Department of Neuroscience, School of Basic Medical Sciences, Guangzhou Medical University, Guangzhou, China, ⁵Department of Neurology, The Second Affiliated Hospital of Xinjiang Medical University, Urumqi, China, ⁶Department of Neurology, Guangzhou Chinese Medical Integrated Hospital (Huadu), Guangzhou, China, ⁷Department of Physiology, School of Basic Medical Sciences, Guangzhou Medical University, Guangzhou, China, ⁸Department of Neurology, The affiliated Houjie Hospital, Guangdong Medical University, Dongguan, China

The NLR family pyrin domain containing 3 (NLRP3) inflammasome was reported to be regulated by autophagy and activated during inflammatory procession of Parkinson's disease (PD). Berberine (BBR) is well-studied to play an important role in promoting anti-inflammatory response to mediate the autophagy activity. However, the effect of Berberine on NLRP3 inflammasome in PD and its potential mechanisms remain unclear. Hence, in this study, we investigated the effects of BBR on 1-Methyl-4-phenyl-1,2,3,6-tetrahydropyridine (MPTP)-induced PD mice, by evaluating their behavioral changes, dopaminergic (DA) neurons loss, neuroinflammation, NLRP3 inflammasome and autophagic activity. BBR was also applied in BV2 cells treated with 1-methyl-4-phenylpyridine (MPP+). The autophagy inhibitor 3-Methyladenine (3-MA) was administrated to block autophagy activity both *in vivo* and *in vitro*. In our *in vivo* studies, compared to MPTP group, mice in MPTP + BBR group showed significant amelioration of behavioral disorders, mitigation of neurotoxicity and NLRP3-associated neuroinflammation, enhancement of the autophagic process in substantia nigra (SN). *In vitro*, compared to MPP+ group, BBR significantly decreased the level of NLRP3 inflammasome including the expressions of NLRP3, PYD and CARD domain containing (PYCARD), cleaved caspase 1 (CASP1), and mature interleukin 1 beta (IL1B), via enhancing autophagic activity. Furthermore, BBR treatment increased the formation of autophagosomes in MPP+-treated BV2 cells. Taken together, our data indicated that BBR prevents NLRP3 inflammasome activation and restores autophagic activity to protect DA neurons against degeneration *in vivo* and *in vitro*, suggesting that BBR may be a potential therapeutic to treat PD.

Keywords: Parkinson's disease, NLRP3, neuroinflammation, autophagy, berberine

INTRODUCTION

Parkinson's disease (PD) is characterized by loss of dopaminergic (DA) neurons and formation of Lewy bodies in substantia nigra (SN), afflicting approximately 1% of the population aged 60 years and older worldwide (Ascherio and Schwarzschild, 2016). At present, there is no radical therapy for PD (Ryan et al., 2019), and it is necessary to elucidate the underlying mechanism of PD to develop novel therapeutic methods. Numerous studies have demonstrated that NLR family pyrin domain containing 3 (NLRP3) inflammasome plays a vital role in the pathogenesis of PD (Haq et al., 2020). The activation of NLRP3 inflammasome triggered by toxins leads to the cleavage of caspase 1 (CASP1) into cleaved CASP1, which results in the secretion of interleukin 1 beta (IL1B) and interleukin 18 (IL18) to induce neuroinflammation and neuron death (Heneka et al., 2018).

NLRP3 inflammasome accumulates in microglia of 1-methyl-4-phenyl-1,2,3,6-tetrahydropyridine (MPTP)-induced mice and leads to DA neurons loss (Lee et al., 2019). 1-methyl-4-phenyl-pyridine (MPP+), a toxic metabolite of MPTP, has been used as a stimulant to mimic PD pathophysiology *in vitro*. Recent studies have also reported that MPP+ can activate NLRP3 inflammasome in microglia (Yao et al., 2019; Zeng et al., 2019; Cheng et al., 2020). Therefore, inhibition of NLRP3 inflammasome activation may be a critical strategy to alleviate PD neuroinflammation.

Autophagy is an evolutionary homeostatic cellular process to degrade damaged organelles and harmful proteins. The multi-step process of autophagy initiated and mediated by a series of autophagy related (Atg) genes such as beclin 1 (BECN1) and microtubule associated protein 1 light chain 3 beta (MAP1LC3B) (Lu et al., 2019; Pohl and Dikic, 2019). Studies have shown that autophagy activation could ameliorate the detrimental effects of neuroinflammation, and thereby protect against chronic inflammatory in PD (Menzies et al., 2017; Ali et al., 2020). Although multiple evidences revealed that autophagy regulates NLRP3 inflammasome thus mitigating inflammatory response (Han et al., 2019; Houtman et al., 2019; Mehto et al., 2019; Fei et al., 2020), although the underlying mechanism of how autophagy affects the activation of NLRP3 inflammasome in PD is not completely understood. Hence, the inhibition of NLRP3 inflammasome via autophagic enhancement may be a potential benefit of PD therapy. Berberine (BBR), an organic isoquinoline alkaloid, has been clinically used in the treatment of various diseases such as cancer, bacterial diarrhea, type 2 diabetes, hypercholesterolemia, inflammation, and cardiac diseases (Neag et al., 2018; Belwal et al., 2020; Song et al., 2020). However, the neuroprotective efficacy and underlying mechanism of BBR in PD remains elusive. Therefore, we implemented MPTP-induced PD *in-vivo* model and MPP+-induced *in-vitro* model, to investigate the neuroprotective and anti-neuroinflammatory effects of BBR in ameliorating PD-like symptoms and to elucidate the role of autophagy in ameliorating neuroinflammation in PD.

MATERIALS AND METHODS

Animals

Eight-weeks-old C57BL/6J male mice (24–31 g) were ordered from Guangdong Medical Experimental Animal Center and housed in a controlled environment in terms of temperature, humidity, and a 12/12-h light/dark cycle, along with food and water *ad libitum*. All the procedures were performed in compliance with the Institute's guidelines and the Guide for the Care and Use of Laboratory Animals. The study was approved by the institutional animal care committee of Guangzhou Medical University.

In-vivo Experimental Design and Drug Treatments

Mice were randomly divided into five groups as control, control + BBR, MPTP, MPTP + BBR, and MPTP + BBR + 3-Methyladenine (3-MA) group, respectively ($N = 12$ per group). BBR, MPTP, and 3-MA were purchased from Sigma-Aldrich Ltd. (Sigma, United States, PHR1502, M0896, M9281, respectively) and dissolved in 0.9% saline. The certified purity of BBR was 88.4%. Prior to MPTP injection for 7 days, 50 mg/kg BBR was intragastrically administered to mice in control + BBR, MPTP + BBR, and MPTP + BBR + 3-MA groups once daily for 21 days, and the same volume of 0.9% saline was intragastrically administered to the control and MPTP groups. For the mice from MPTP, MPTP + BBR, and MPTP + BBR + 3-MA groups, after one week's 0.9% saline or BBR treatment, 30 mg/kg MPTP was subcutaneously injected once a day for 5 consecutive days to establish the MPTP-induced subacute PD model, and the same volume of 0.9% saline were subcutaneously administered to the control and control + BBR groups. In addition, 5 mg/kg 3-MA was intraperitoneally administered in MPTP + BBR + 3-MA group once a day for 21 days. Simultaneously, the same volume of 0.9% saline was intraperitoneally administered to the control, control + BBR, MPTP, and MPTP + BBR groups. BBR and 3-MA were administered in the same day whereas BBR and 3-MA were injected at 8:00 am and 4:00 pm, respectively. The animal behavioral tests including pole, hanging, and swimming tests were performed one day before MPTP injection and the last day after BBR and/or 3-MA treatment separately. All behavioral tests on each mouse were conducted three times at 10-min intervals, and the observer was blinded to all animals. Besides, the body weight of mice was recorded once every 4 days. The timeline of the experimental procedure was shown in **Figure 1A**.

Pole Test

A pole of 50 cm in length and 1 cm in diameter was set upright and a wooden ball wrapped with gauze was adhered to the top of the pole. Mice were placed on the top of the wooden ball and the time until they reached the bottom of the pole was recorded. The average time of three trials was recorded.

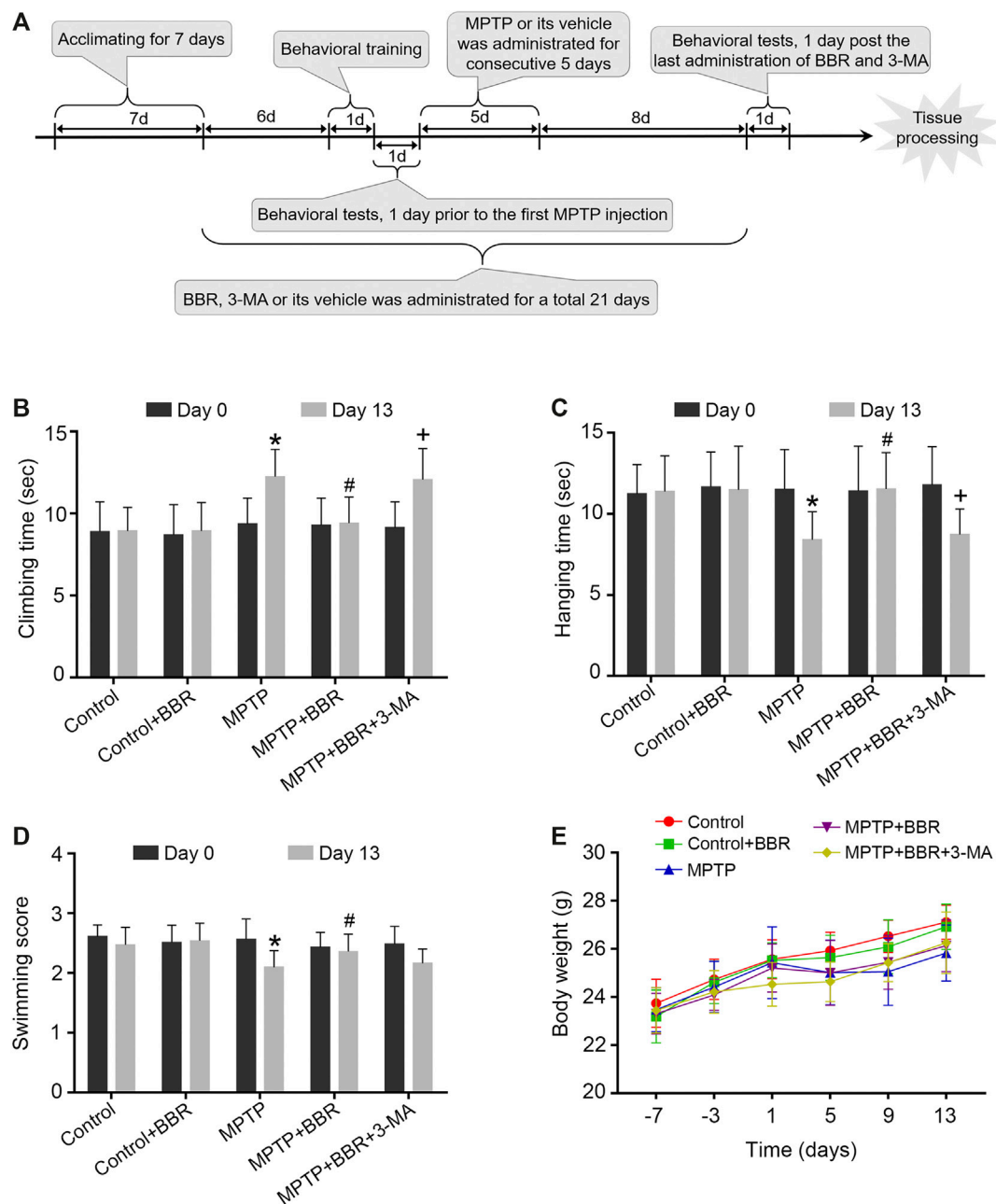


FIGURE 1 | The flowchart of the experimental procedure and neurobehavioral tests in MPTP-induced mice. **(A)** The flowchart of the experimental procedure. **(B)** Time spent in climbing of the pole test. **(C)** Time spent in hanging on the line of the hanging test. **(D)** Swimming scores in the swimming test. **(E)** Body-weight changes at different time points. Data were expressed as the mean \pm SD ($n = 12$). * $p < 0.05$ compared with control group, # $p < 0.05$ compared with MPTP group, + $p < 0.05$ compared with MPTP + BBR group.

Hanging Test

A horizontal wire of 1.5 mm in diameter was suspended 30 cm above a foam carpet. Each mouse was forced to grip the wire with its forelimbs and its hanging time was recorded until the mouse fell onto the foam carpet. The average time of three trials was recorded.

Swimming Test

A container of water (dimensions, 20×30 × 20 cm) was used for swimming test. The depth of the water was 10 cm and the temperature was 22–25 °C. Each mouse was forced to swim for one minute and the swimming scores were determined according to a previous study (Donnan et al., 1987). Briefly, scoring was

based on the following: continuous swimming movements = 3; occasional floating = 2.5; floating > 50% of the time = 2.0; occasional swimming only = 1.5; occasional swimming using hind limbs while floating on side = 1.0; and no use of limbs = 0. The average time of three trials was recorded.

Tissue Preparation

Following the completion of the last behavioral tests, mice were anesthetized, and then transcardially perfused with 4% paraformaldehyde in 0.1 M of phosphate-buffered saline (PBS). The brains were post-fixed in 4% paraformaldehyde overnight at 4°C, then gradually transferred to 10%, 20%, and 30% (w/v) sucrose solutions for cryoprotection. Coronal tissue blocks were cut into 10 µm thickness of sections (Leica CM1950, Heidelberg). The spanning blocks of tissue region were in 0.74 to 0.26 mm from bregma for striatum and -2.92 to -3.64 mm from bregma for SN. Sections were thaw-mounted to adhesive microscope slides and stored at -80°C.

Immunohistochemistry

For immunohistochemical analysis, brain sections were incubated with 3% H₂O₂ for 20 min to block the activity of endogenous peroxidases. After incubating with primary anti-tyrosine hydroxylase (TH) (1:500; Santa Cruz, sc-25269), anti-PYD and CARD domain containing (PYCARD) (1:200; Immunoway, T0365), anti-IL1B (1:200; ABclonal, A13268), and anti-MAP1LC3B (1:1,000; ABclonal, A11282) antibodies overnight at 4°C, sections were incubated with the Two-step Plus Poly-horseradish peroxidase (HRP) Anti-Mouse/Rabbit IgG Detection System (Dako, United States). Finally the tissue sections were treated with 3,3'-diaminobenzidine and hematoxylin. The optical densities (OD) of TH in striatum was calculated by the ImageJ software. The positive cells of TH, MAP1LC3B, PYCARD, and IL1B in SN were manually counted by researchers blinded to the treatment groups.

The immunofluorescence without block of endogenous peroxidases was examined with incubation of primary anti-TH (1:500; Santa Cruz, sc-25269), anti-allograft inflammatory factor 1 (AIF1) (1:200; Abcam, ab178874), anti-glial fibrillary acidic protein (GFAP) (1:200; Abcam, ab7260), anti-NLRP3 (1:200; AdipoGen, AG-20B-0014-C100), anti-PYCARD (1:200; Immunoway, T0365), anti-CASP1 (1:200; ABclonal, A0964) and anti-MAP1LC3B (1:1,000; ABclonal, A11282) antibodies overnight at 4°C. Sections were incubated with Alexa Fluor 568-conjugated goat anti-rabbit IgG (1:1,000; Abcam, ab175471) and Alexa Fluor 488-conjugated goat anti-mouse IgG (1:1,000; Invitrogen, A32723) for 1 h at room temperature. After washing with 0.01 M PBS, sections were stained with 4',6-Diamidino-2'-phenylindole (DAPI) (Sigma,

United States) for nuclear staining, and visualized under fluorescent microscope. GFAP and AIF1 positive cells in SN were manually counted by researchers blinded to the treatment groups. The mean fluorescence intensity (MFI) of NLRP3, PYCARD, and CASP1 were calculated by the ImageJ software. The MAP1LC3B puncta were manually counted by researchers blinded to the treatment groups.

Nissl Staining

Nissl staining was performed according to the manufacturer's instructions of nissl staining solution (Beyotime, Shanghai, China). The positive cells were viewed under a microscope. The number of neurons in SN was manually counted by researchers blinded to the treatment groups.

Transmission Electron Microscopy

For analysis of autophagosome by transmission electron microscopy, mouse SN tissues were cut into a size of 0.5–1.0 mm³ and post-fixed with 2.5% glutaraldehyde overnight at 4°C. These blocks were washed three times with 0.1 M PBS, and post-fixed in 1% osmium tetroxide for 2 h at 4°C. The blocks were microdissected to ultrathin sections (60–70 nm), post-stained with uranyl acetate and lead citrate, then examined under an electron microscope (Philips, Amsterdam, Netherlands).

Quantitative Polymerase Chain Reaction

Total RNA was extracted by using Trizol reagent (Invitrogen, United States) following the manufacturer's instructions. cDNA was synthesized using PrimeScript RT Master Mix (Takara, Japan). qPCR was performed on a Bio-rad Cx96 Detection System (Bio-rad, United States) by using a SYBR green PCR kit (Applied Biosystems, United States). The primers for the targeted genes were shown in **Table 1**. Reaction conditions were 95°C for 5 min, followed by 40 cycles of 95°C for 15 s and 60°C for 1 min mRNA quantification was normalized to ACTB as an internal standard.

Western Blotting Analysis

For western blotting analysis, total proteins were collected from striatum, SN, and BV2 cells and stored at -80°C. 40 µg of total protein lysate was loaded onto a 12% sodium-dodecyl-sulfate polyacrylamide gel in each lane, then transferred onto a polyvinylidene-difluoride membrane (Millipore, United States). The primary antibodies were incubated overnight at 4°C included anti-TH (1:500; Santa Cruz, sc-25269), anti-solute carrier family 6 member 3 (SLC6A3) (1:1,000; ABclonal, A152360), anti-dopamine receptor D2 (DRD2) (1:1,000; ABclonal, A12930), anti-AIF1 (1:1,000; Santa Cruz, sc-32725), anti-GFAP (1:1,000;

TABLE 1 | Primer sequences used for the qPCR analysis.

Gene name	Forward primer sequence (5'-3')	Reverse primer sequence (5'-3')
NLRP3	ATTACCCGCCCGAGAAAGG	TGCGAGCAAGATCCACACAG
IL1B	GAAATGCCACCTTTTGACAGTG	TGGATGCTCTCATCAGGACAG
ACTB	GGCTGTATTCCTCCATCG	CCAGTTGGTAACAATGCCATGT

ABclonal, A14673), anti-NLRP3 (1:200; AdipoGen, AG-20B-0014-C100), anti-PYCARD (1:1,000; Immunoway, T0365), anti-CASP1 (1:1,000; ABclonal, A0964), anti-IL1B (1:1,000; ABclonal, A12688), anti-MAP1LC3B (1:1,000; ABclonal, A11282), anti-BECN1 (1:1,000; Cell Signaling Technology, 3738S) and anti-ACTB (1:3,000; ABclonal, AC026). HRP-conjugated anti-Rabbit antibody (1:5,000; ABclonal, AS014) or anti-Mouse antibody (1:5,000; ABclonal, AS003) was used as secondary antibody. ImageJ software was used to quantify the target bands and ACTB as an internal control.

In-vitro Experiments

BV2 cells were cultured in Dulbecco's modified eagle medium (HyClone) supplemented with 10% fetal bovine serum (Gibco) and 100 U/ml penicillin (Invitrogen) at 37 °C in a humidified atmosphere with 5% CO₂. Cells were treated with MPP+ at 0, 10, 50, 100, 200, and 400 μM concentrations for 24 hours to detect the cells cytotoxicity. Cells treated with BBR at 0, 12.5, 25, 50, 100, and 200 μM concentrations for 24 h were conducted for CCK8 assays. Based on the two batches results, for MPP+ group, cells were treated with MPP+ at 200 μM for 24 h. For MPP+ + BBR groups, cells were incubated with BBR at 0, 12.5, 25, 50 μM concentrations for 3 h respectively, prior to be treated with MPP+ at 200 μM for 24 h. For MPP+ + BBR + 3-MA group, cells were pre-treated with BBR at 25 μM and 3-MA at 10 mM for 3 h, then were treated with 200 μM MPP+ for 24 h. For control group, cells were treated with the same volume of culture medium. All groups of cells, then were collected to examine the activation of NLRP3 inflammasome and autophagic activity.

Enzyme-Linked Immunosorbent Assays

BV2 cells were treated with MPP+ at 0, 10, 50, 100, 200, and 400 μM concentrations for 24 h. The culture supernatants were collected and measured for IL1B via ELISA kits (Invitrogen, United States, BMS6002) according to the manufacturer's instructions. Briefly, supernatants were added in the coated wells with IL1B antibody of 96-well plates and incubated for 2 h at room temperature, then washed five times and incubated with an HRP-linked streptavidin solution for 30 min at room temperature. All samples were tested by duplication, and absorbance at 450 nm was measured by a microplate spectrophotometer (Thermo Scientific, United States).

Monodansylcadaverine (MDC) Staining

MDC, a fluorescent marker of autophagic vacuoles, was used to detect the autophagic activity. BV2 cells were pre-treated with 25 μM BBR with or without 10 mM 3-MA for 3 h, this was followed by addition of 200 μM MPP+ for 24 h. At the end of the incubation period, 50 mM MDC (Sigma, United States, D4008) was added to the cells for 15 min at 37 °C in dark. After washing twice with 0.01 M PBS, cells were examined under a fluorescent microscope (Leica, Solms, Germany). The number of autophagic vacuoles was

manually counted by researchers blinded to the treatment groups.

Statistical Analysis

Data were presented as means ± standard deviations (SDs) and analyzed via SPSS 21.0 software. The differences among groups were compared using one-way analyses of variance (ANOVAs) followed by Tukey's tests for post-hoc comparisons. The differences were established to be statistically significant at $p < 0.05$.

RESULTS

BBR Ameliorates Behavioral Impairments in MPTP-Induced Mice

Compared to the control group, MPTP-induced mice spent significantly longer time in the pole test ($p < 0.05$, **Figure 1B**), shorter time in the hanging test ($p < 0.05$, **Figure 1C**), and achieved lower scores in the swimming test ($p < 0.05$, **Figure 1D**). MPTP + BBR-treated mice showed significantly better performance in behavioral tests including pole test ($p < 0.05$, **Figure 1B**), hanging test ($p < 0.05$, **Figure 1C**) and swimming test ($p < 0.05$, **Figure 1D**) when comparing to MPTP group. While comparing to MPTP + BBR group, mice in MPTP + BBR + 3-MA group showed significantly inferior performance in pole test ($p < 0.05$, **Figure 1B**) and hanging test ($p < 0.05$, **Figure 1C**). Compared to the control group, mice in the other four groups all showed no significant difference in body weight at all time points ($p > 0.05$, **Figure 1E**).

BBR Mitigates Neurotoxicity in MPTP-Induced Mice

Compared to the control group, MPTP-induced mice showed significant loss of TH in striatum ($p < 0.05$, **Figures 2A–D**) and SN ($p < 0.05$, **Figures 2E–H**). Compared to the MPTP group, MPTP + BBR-treated mice showed significant increase of TH in striatum ($p < 0.05$, **Figures 2A–D**) and SN ($p < 0.05$, **Figures 2E–H**). Additionally, mice in MPTP + BBR + 3-MA group showed significant loss of TH both in striatum and SN when compared to those in MPTP + BBR group ($p < 0.05$, **Figures 2A–H**). As shown in **Figures 2I,J**, the number of DA neurons in SN in MPTP and MPTP + BBR + 3-MA groups were decreased by nissl staining ($p < 0.05$), whereas the number of DA neurons in MPTP + BBR group were increased ($p < 0.05$). Additionally, compared to control group, MPTP-induced mice showed lower expression of SLC6A3 and DRD2 in striatum (both $p < 0.05$, **Figures 2K,L**). MPTP + BBR-treated mice showed significant increase of SLC6A3 and DRD2 expressions in striatum when comparing to MPTP group (both $p < 0.05$, **Figures 2K,L**). However, mice in MPTP + BBR + 3-MA group showed significant reduction of SLC6A3 and DRD2 expression in striatum when compared with MPTP + BBR group (both $p < 0.05$, **Figures 2K,L**).

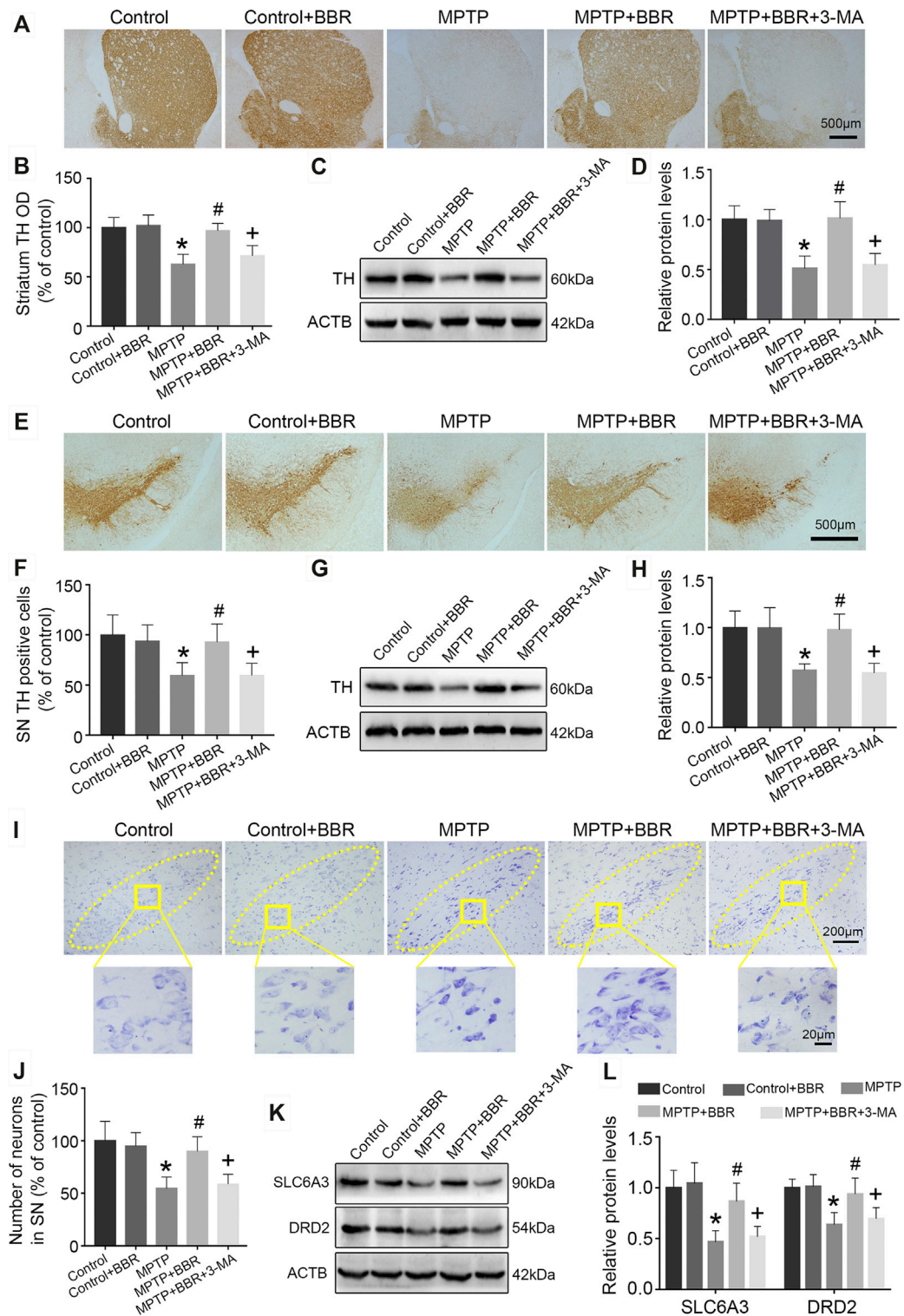


FIGURE 2 | BBR ameliorates dopaminergic neurons degeneration in MPTP-induced mice. **(A)** The representative immunohistochemical staining of TH in striatum. **(B)** The OD of TH staining in striatum. Representative western blot bands **(C)** and the statistical graph **(D)** of TH in striatum. **(E)** The representative immunohistochemical staining of TH in SN. **(F)** The number of TH positive neurons in SN. Representative western blot bands **(G)** and the statistical graph **(H)** of TH in SN. **(I)** Nissl staining for neurons in SN. **(J)** The number of neurons in SN. Representative western blot bands **(K)** and the statistical graph **(L)** of SLC6A3 and DRD2 in striatum. Data were expressed as the mean \pm SD ($n = 6$). * $p < 0.05$ compared with control group, # $p < 0.05$ compared with MPTP group, + $p < 0.05$ compared with MPTP + BBR group. TH, tyrosine hydroxylase; OD, optical densities; SN, substantia nigra; SLC6A3, solute carrier family 6 member 3; DRD2, dopamine receptor D2.

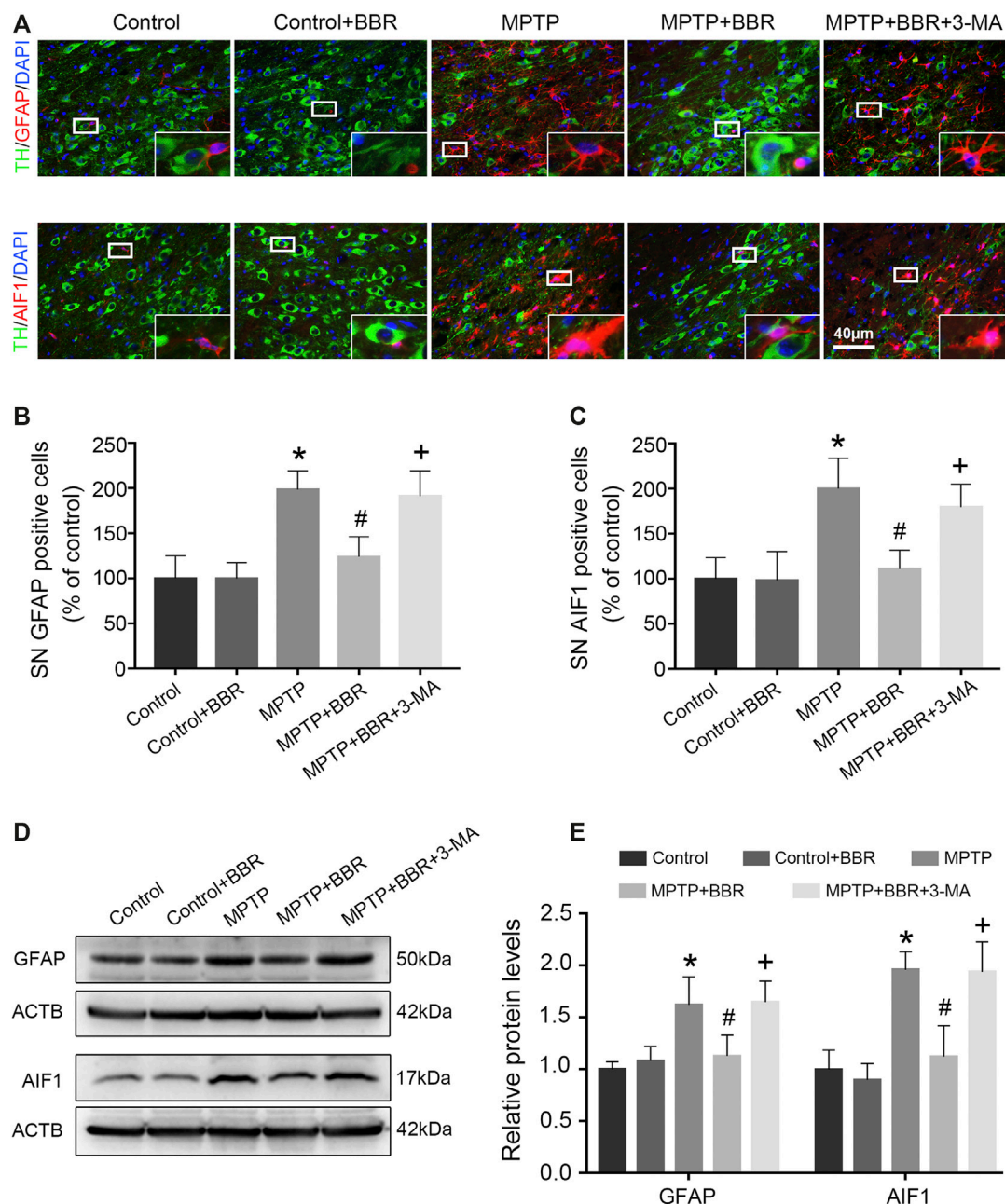


FIGURE 3 | BBR inhibits MPTP-induced neuroinflammation in mice. **(A)** The representative double-immunofluorescent staining of GFAP (red) /TH (green) and AIF1 (red) /TH (green) in SN. The number of GFAP **(B)** and AIF1 **(C)** positive cells in SN. Representative western blot bands **(D)** and the statistical graph **(E)** of GFAP and AIF1 in SN. Data were expressed as the mean \pm SD ($n = 6$). * $p < 0.05$ compared with control group, # $p < 0.05$ compared with MPTP group, + $p < 0.05$ compared with MPTP + BBR group. GFAP, glial fibrillary acidic protein; TH, tyrosine hydroxylase; AIF1, allograft inflammatory factor 1; SN, substantia nigra.

BBR Ameliorates NLRP3-Associated Neuroinflammation in SN of MPTP-Induced Mice

As shown in **Figures 3A–C**, the representative images and statistical graphs of immunofluorescent staining showed that the expressions of AIF1 and GFAP were increased in MPTP and MPTP + BBR + 3-MA groups but not in control, control +

BBR and MPTP + BBR groups (both $p < 0.05$), which indicated the infiltration of microglia and astrocytes in SN of mice from MPTP and MPTP + BBR + 3-MA groups. In accordance, compared to the control group, mice in MPTP + BBR group exhibited a significant reduction in the expression of AIF1 and GFAP in SN (both $p < 0.05$, **Figures 3D,E**). Compared to the MPTP group, MPTP + BBR-treated mice exhibited significantly

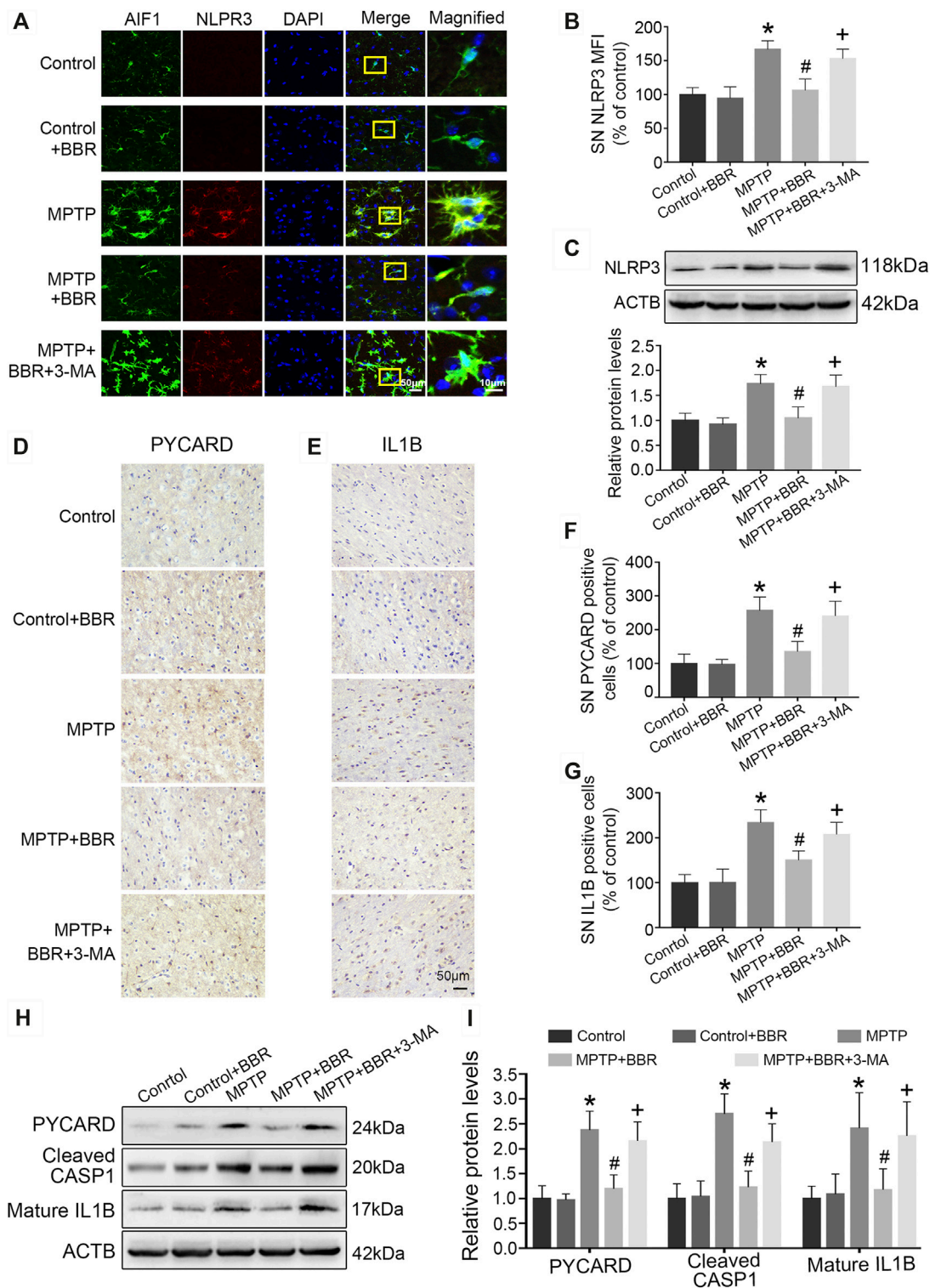
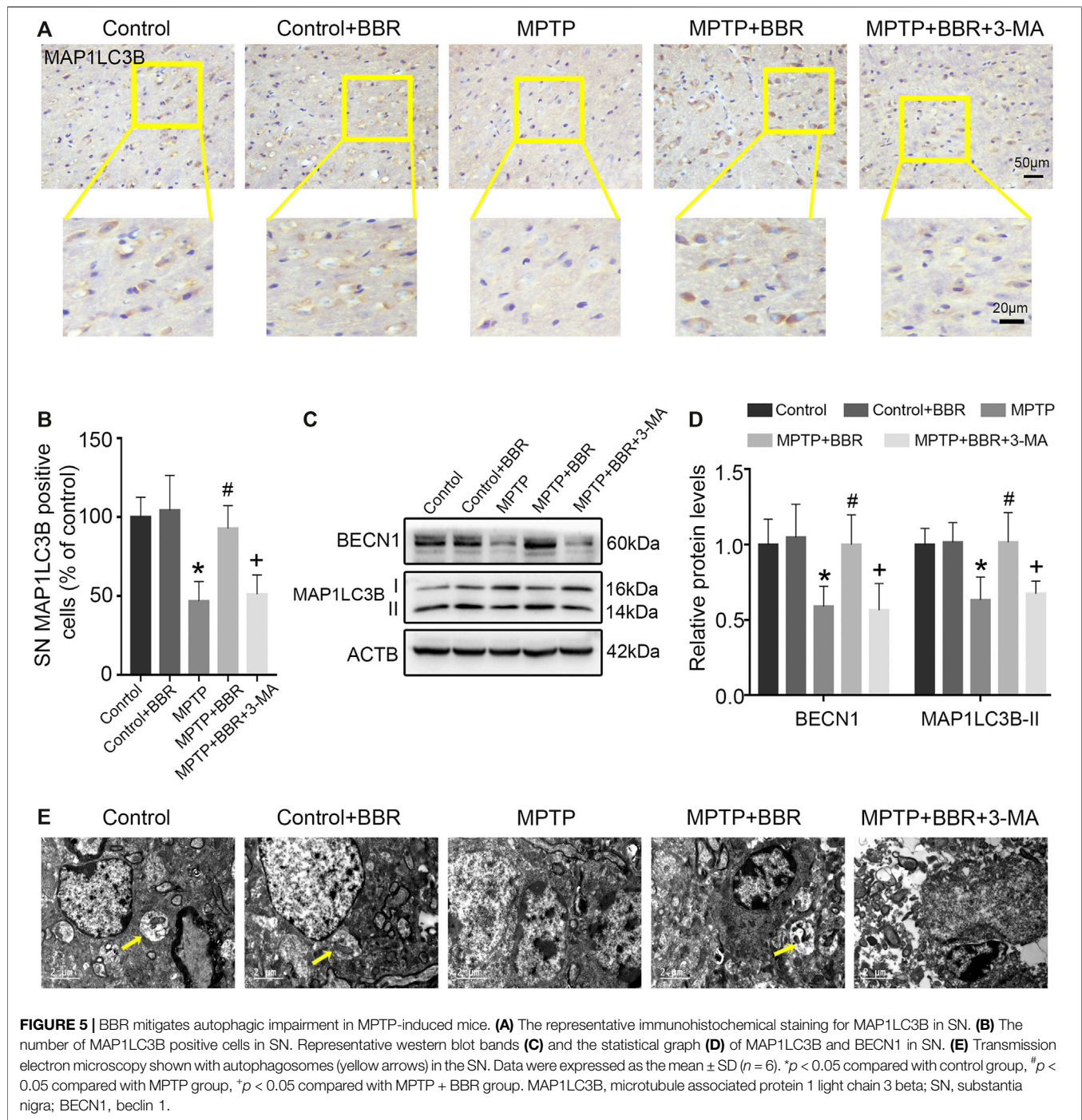


FIGURE 4 | BBR suppresses NLRP3 inflammasome activation in MPTP-induced mice. **(A)** The representative double-immunofluorescent staining of NLRP3 (red) and AIF1 (green) in SN. **(B)** The MFI of NLRP3 in SN. **(C)** Representative western blot bands and the statistical graph of NLRP3 in SN. The representative immunohistochemical staining for PYCARD **(D)** and IL1B **(E)** in SN. The number of PYCARD **(F)** and IL1B **(G)** positive cells in SN. Representative western blot bands **(H)** and the statistical graph **(I)** of PYCARD, cleaved CASP1, and mature IL1B in SN. Data were expressed as the mean \pm SD ($n = 4$ for **Figure 4B**; $n = 6$ for **Figures 4C,F,G,I**). * $p < 0.05$ compared with control group, # $p < 0.05$ compared with MPTP group, + $p < 0.05$ compared with MPTP + BBR group. NLRP3, NLR family pyrin domain containing 3; AIF1, allograft inflammatory factor 1; SN, substantia nigra; MFI, mean fluorescence intensity; PYCARD, PYD and CARD domain containing; IL1B, interleukin 1 beta; CASP1, caspase 1.



lower expression of AIF1 and GFAP in SN (both $p < 0.05$, **Figures 3D,E**), whereas mice in MPTP + BBR + 3-MA group significantly increased the expression of AIF1 and GFAP when compared to those in MPTP + BBR group (both $p < 0.05$, **Figures 3D,E**).

As shown in **Figure 4A**, co-immunostaining revealed NLRP3 and AIF1 were almost overlapping, indicating NLRP3 mainly expressed in microglia of MPTP-induced mice. Statistical graphs of immunofluorescent staining showed that the expressions of NLRP3 were increased in MPTP and MPTP + BBR + 3-MA

groups but not in control, control + BBR and MPTP + BBR groups ($p < 0.05$, **Figure 4B**). Compared to control group, MPTP-induced mice showed significantly higher expression of NLRP3 in SN ($p < 0.05$, **Figure 4C**). Compared to MPTP group, MPTP + BBR-treated mice showed significantly lower expression of NLRP3 ($p < 0.05$, **Figure 4C**). Additionally, mice in MPTP + BBR + 3-MA group significantly increased the expression of NLRP3 when compared to those in MPTP + BBR group ($p < 0.05$, **Figure 4C**). The representative images statistical graphs of

immunohistochemical staining showed the increase in positive cells of PYCARD and IL1B in SN of mice from MPTP and MPTP + BBR + 3-MA groups but not in control, control + BBR and MPTP + BBR groups (both $p < 0.05$, **Figures 4D–G**). Furthermore, compared to control group, MPTP-induced mice exhibited significant increase in the expressions of NLRP3 inflammasome components including PYCARD, cleaved CASP1, and mature IL1B (all $p < 0.05$, **Figures 4H,I**). Compared to MPTP group, MPTP + BBR-treated mice showed significant decrease in the expressions of PYCARD, cleaved CASP1, and mature IL1B (all $p < 0.05$, **Figures 4H,I**), whereas mice in MPTP + BBR + 3-MA group significantly increased the expressions of PYCARD, cleaved CASP1, and mature IL1B when compared to MPTP + BBR group (all $p < 0.05$, **Figures 4H,I**).

BBR Mitigates Autophagic Impairment in SN of MPTP-Induced Mice

As shown in **Figures 5A,B**, the representative images and statistical graphs of immunohistochemical staining results showed the decrease in MAP1LC3B positive cells in SN of mice from MPTP and MPTP + BBR + 3-MA groups but not from control, control + BBR and MPTP + BBR groups ($p < 0.05$). In accordance, compared to control group, MPTP-induced mice showed a significant decrease in the expression of BECN1 and MAP1LC3B-II (both $p < 0.05$, **Figures 5C,D**). Compared to MPTP group, MPTP + BBR-treated mice showed a significant increase in the expression of BECN1 and MAP1LC3B-II (both $p < 0.05$, **Figures 5C,D**), whereas mice in MPTP + BBR + 3-MA group significantly reduced the expression of BECN1 and MAP1LC3B-II when compared to MPTP + BBR group (both $p < 0.05$, **Figures 5C,D**). The representative images of transmission electron microscopy showed the formation of autophagosome in SN of mice from control, control + BBR, and MPTP + BBR groups but not from MPTP and MPTP + BBR + 3-MA groups (**Figure 5E**).

BBR Decreases NLRP3 Inflammasome in MPP+-Treated BV2 Cells

The representative images and statistical graphs of immunofluorescent staining showed that MPP+ at 200 μ M increased the positive cells of NLRP3 in BV2 cells ($p < 0.05$), which was decreased by BBR at the concentrations of 12.5, 25, and 50 μ M (all $p < 0.05$, **Figures 6A,B**). In accordance, compared to untreated group, MPP+ at 200 μ M significantly increased the expression of NLRP3 in BV2 cells ($p < 0.05$), whereas the expression was decreased by BBR in a dose-dependent manner 12.5, 25, and 50 μ M (all $p < 0.05$, **Figures 6C,D**). In addition, MPP+ at 200 μ M significantly increased the positive cells of PYCARD ($p < 0.05$, **Figures 6E,F**) and CASP1 ($p < 0.05$, **Figures 6G,H**) in BV2 cells, which was reduced by BBR at 25 μ M (both $p < 0.05$, **Figures 6E–H**). Furthermore, compared to untreated group, MPP+ at 200 μ M significantly elevated the expressions of PYCARD, cleaved CASP1, and mature IL1B in BV2 cells (all $p < 0.05$, **Figures 6I,J**), whereas were reduced by BBR dose-dependently (all $p < 0.05$, **Figures 6I,J**).

The concentrations of drugs used in BV2 cells were according to the cell survival data as shown in **Supplementary Figure S1**.

BBR Enhances Autophagic Activity in MPP+-Treated BV2 Cells

The representative immunofluorescent images and statistical graphs of MAP1LC3B showed that MPP+ at 200 μ M significantly decreased the positive cells and puncta of MAP1LC3B in BV2 cells ($p < 0.05$), which was increased by BBR at the concentrations of 12.5, 25, and 50 μ M (all $p < 0.05$, **Figures 7A,B**). Compared to untreated group, MPP+ at 200 μ M significantly impaired autophagic activity with a decrease in the expression of BECN1 and MAP1LC3B-II in BV2 cells (both $p < 0.05$, **Figures 7C,D**), which were significantly increased by BBR at the concentration of 12.5, 25, and 50 μ M (all $p < 0.05$, **Figures 7C,D**).

Additionally, immunofluorescence staining results showed that 3-MA could reduce the positive cells and puncta of MAP1LC3B in BV2 cells when treated with MPP+ at 200 μ M plus BBR at 25 μ M ($p < 0.05$, **Figures 7E,F**). Compared to untreated group, MPP+ at 200 μ M reduced the formation of autophagic vesicles in BV2 cells ($p < 0.05$), which was increased by BBR at 25 μ M ($p < 0.05$, **Figures 7G,H**). While 3-MA decreased the formation of autophagic vesicles when BV2 cells were co-treated with MPP+ (200 μ M) and BBR (25 μ M) ($p < 0.05$, **Figures 7G,H**). We further observed that, 3-MA significantly blocked autophagic activity with a decrease in the expression of BECN1 and MAP1LC3B-II in BV2 cells when treated with MPP+ (200 μ M) and BBR (25 μ M) (both $p < 0.05$, **Figures 7I,J**). Besides, 3-MA could also reverse the expressions of NLRP3, PYCARD, cleaved CASP1, and mature IL1B upon co-treated with MPP+ and BBR as shown in **Supplementary Figure S2**.

DISCUSSION

As a housekeeping pathway and mediator of cellular homeostasis, autophagy plays an essential role in regulating the activation of NLRP3 inflammasome (Liu et al., 2020a). Studies have shown that autophagy process is impaired during neuroinflammation (Du et al., 2017; Wang et al., 2017; Ali et al., 2020). Reversing autophagic dysfunction which can block NLRP3 inflammasome may provide a novel therapy against PD (Haque et al., 2020). It was reported that BBR prevents DA neuron from death in SN of MPTP-induced mice (Friedemann et al., 2016), but the underlying mechanism remains unclear. Here our data revealed that BBR ameliorated MPTP/MPP+-induced neurotoxicity by enhancing autophagy activity and inhibiting the activation of NLRP3 inflammasome. Besides, inhibition of autophagy with 3-MA antagonized the neuroprotective effects of BBR on MPTP/MPP+-induced neurotoxicity by activating NLRP3 inflammasome. Taken together, our data revealed that BBR could inhibit the activation of NLRP3 inflammasome by enhancing autophagic functions in PD models.

The NLRP3 inflammasome is a multi-protein complex consisting of NLRP3, PYCARD adaptor and CASP1 (Swanson et al., 2019). Chronic activation of microglia is a characteristic of neuroinflammation in PD (Panicker et al., 2019), which closely

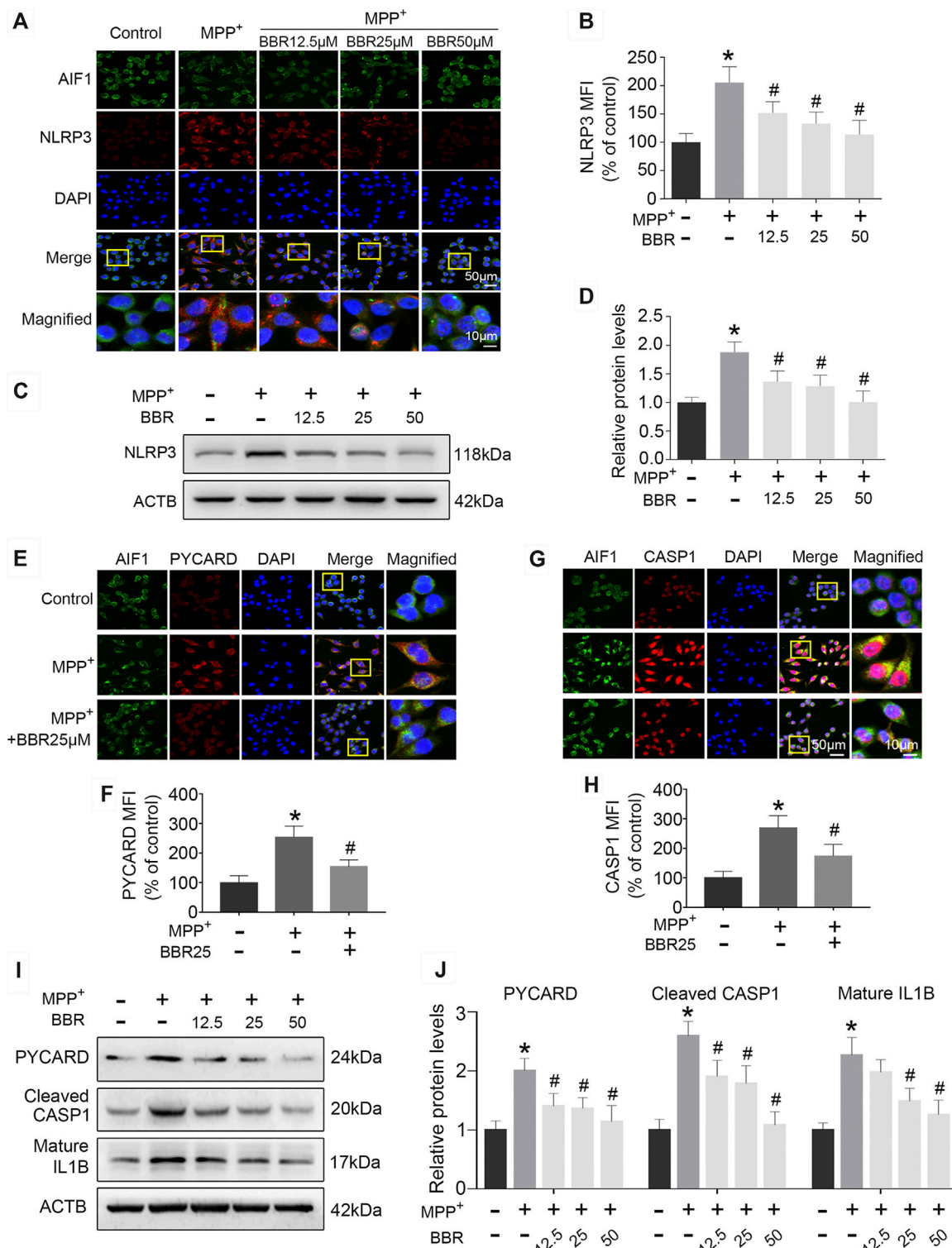


FIGURE 6 | BBR inhibits NLRP3 inflammasome in MPP⁺-treated BV2 cells. The representative double-immunofluorescent staining (A) and MFI (B) of NLRP3 (red) and AIF1 (green) in BV2 cell treated with MPP⁺ at 200 μM and BBR at the concentration of 0, 12.5, 25, and 50 μM. Representative western blot bands (C) and the statistical graph (D) of NLRP3 in BV2 cells treated with MPP⁺ at 200 μM and BBR at the concentration of 0, 12.5, 25, and 50 μM. The representative double-immunofluorescent staining (E) and MFI (F) of PYCARD in BV2 cells treated with MPP⁺ at 200 μM and BBR at 25 μM. The representative double-immunofluorescent staining (G) and MFI (H) of CASP1 in BV2 cells treated with MPP⁺ at 200 μM and BBR at 25 μM. Representative western blot bands (I) and the statistical graph (J) of PYCARD, cleaved CASP1 and mature IL1B in BV2 cell treated with MPP⁺ at 200 μM and BBR at the concentration of 12.5, 25, and 50 μM. Data were expressed as the mean ± SD (n = 3). **p* < 0.05 compared with untreated group, #*p* < 0.05 compared with MPP⁺ group. NLRP3, NLR family pyrin domain containing 3; MFI, mean fluorescence intensity; AIF1, allograft inflammatory factor 1; PYCARD, PYD and CARD domain containing; CASP1, caspase 1; IL1B, interleukin 1 beta.

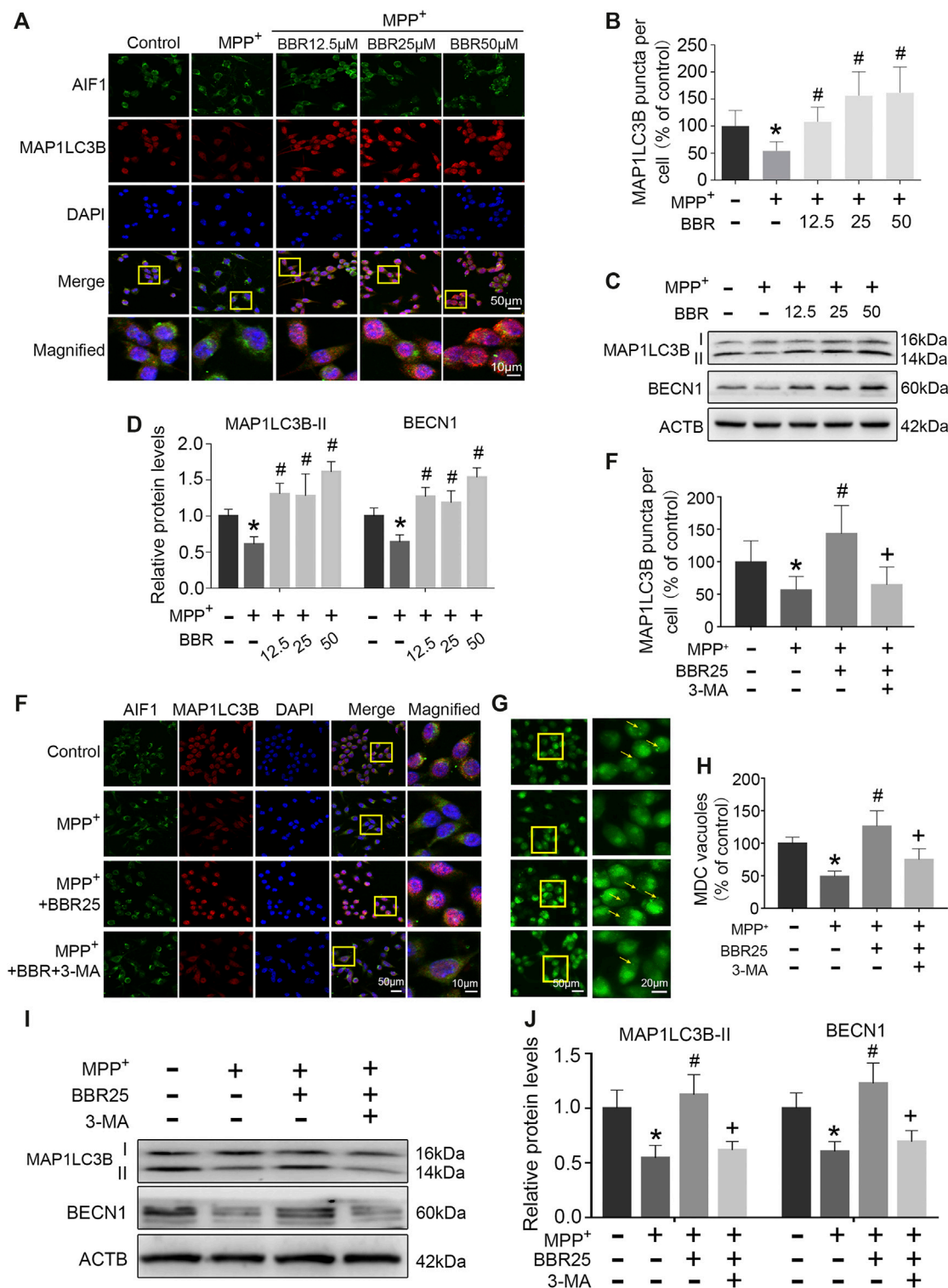


FIGURE 7 | BBR enhances autophagic activity in MPP⁺-treated BV2 cells. The representative immunofluorescent staining (A) and puncta (B) of MAP1LC3B in BV2 cells treated with MPP⁺ at 200 μM and BBR at the concentration of 12.5, 25, and 50 μM (20 cells were analyzed per group for MAP1LC3B puncta counting). Representative western blots (C) and the statistical graph (D) of MAP1LC3B and BECN1 in BV2 cells treated with MPP⁺ at 200 μM and BBR at the concentration of 12.5, 25, and 50 μM. The representative double-immunofluorescent staining (E) and puncta (F) of MAP1LC3B in BV2 cells treated with MPP⁺ at 200 μM, BBR at 25 μM and 3-MA at 10 mM (20 cells were analyzed per group for MAP1LC3B puncta counting). The representative monodansylcadaverine staining (G) and statistical graph (H) of autophagic vesicles in BV2 cells treated with MPP⁺ at 200 μM, BBR at 25 μM and 3-MA at 10 mM. Representative western blot bands (I) and the statistical graph (J) of MAP1LC3B and BECN1 in BV2 cells treated with MPP⁺ at 200 μM, BBR at 25 μM and 3-MA at 10 mM. Data were expressed as the mean ± SD (*n* = 3). **p* < 0.05 compared with untreated group, #*p* < 0.05 compared with MPP⁺ group, +*p* < 0.05 compared with MPP⁺ + BBR group. MAP1LC3B, microtubule associated protein 1 light chain 3 beta; BECN1, beclin 1.

relates to the activation of NLRP3 inflammasome (Nizami et al., 2019). Environmental toxins such as MPTP, rotenone, 6-hydroxydopamine (6-OHDA) or lipopolysaccharide (LPS) were reported to activate NLRP3 inflammasome in microglia and cause DA neuronal death (Zhou et al., 2016; Mao et al., 2017; Haque et al., 2020). In this study, we found that MPTP induced the activation of NLRP3 inflammasome in microglia which led to DA neuron degeneration and behavior dysfunction in mice. Additionally, in line with previous studies (Yao et al., 2019; Zhang et al., 2020), we observed that MPP+ significantly activated NLRP3 inflammasome by increasing the levels of NLRP3, PYCARD, cleaved CASP1, and mature IL1 β . The mechanism of MPP+ activating NLRP3 inflammasome may be explained by that MPP+ stimulates superabundant generation of reactive oxygen species (ROS), which considers as the primary mechanism to activate NLRP3 inflammasome (Groß et al., 2016). Overproduction of ROS dissociates thioredoxin interacting protein (TXNIP), and this dissociation of TXNIP activates NLRP3 inflammasome by directly binding to NLRP3 (Kim et al., 2014; Heo et al., 2019). As a result, the activation of NLRP3 inflammasome releases cleaved CASP1 and also cleaves pro-IL1 β and pro-IL18 into mature IL1 β and mature IL18, triggering inflammatory cascades (Wang et al., 2019) and causing synuclein alpha (SNCA) aggregation in PD (Wang et al., 2016).

Autophagy eliminates damaged organelles, misfolded proteins and stress-related products to maintain cellular homeostasis (Peker and Gozuacik, 2020). During the process of autophagy, MAP1LC3B-I can be conjugated to phosphatidylethanolamine by cysteine proteases and converted into MAP1LC3B-II (Galluzzi et al., 2017; Ruan et al., 2020). The expression of MAP1LC3B-II is widely used to estimate the autophagic activity (Kim et al., 2017; Yuan et al., 2017). BECN1, known as ATG6 or VPS30, regulates lipid kinase vps34 to promote the formation of BECN1-vps34-vps15 complex and initiates the formation of autophagosome (Levine and Kroemer, 2008; Kang et al., 2011). As a crucial molecule, BECN1 is usually used to monitor autophagic activity (Sun et al., 2018b). It was reported that autophagy activity was impaired in both MPTP-induced mice and MPP+-treated cells (Sun et al., 2018a; Chen et al., 2019; Lin et al., 2020). Consistently, we found that MPTP or MPP+ impaired autophagic activity by decreasing MAP1LC3B-II and BECN1 expression, along with reducing the formation of autophagosomes. Previous studies have confirmed that autophagic activity is tightly linked to the activation of NLRP3 inflammasome (Han et al., 2019; Houtman et al., 2019). Enhancing autophagic activity could inhibit NLRP3 inflammasome activation by removal of damaged mitochondria and prevention of ROS release into cytoplasm (Iida et al., 2018; Liu, 2019). On the contrary, inhibition of autophagy and/or lysosome functions may lead to the activation of NLRP3 inflammasome. One recent study reported that autophagy inhibitor 3-MA and lysosome inhibitor chloroquine (CQ) could enhance the activation of the NLRP3 inflammasome in a rat model of chronic cerebral hypoperfusion (Su et al., 2019). Moreover, 3-MA was recently reported to activate NLRP3 inflammasome in influenza virus-infected macrophages (Liu et al., 2020b). CQ could abrogate the inhibitory effect of metformin on NLRP3 expression in a mouse model of acute myocardial infarction (Fei et al., 2020). Thus, induction of autophagy to suppress the activation of NLRP3

inflammasome is important to against NLRP3-associated disorders (Wang et al., 2020). In this study, we found that NLRP3 inflammasome was activated in both MPTP-induced mice and MPP+-treated BV2 cells which accompanied by the impaired autophagy, indicating the activation of NLRP3 inflammasome may ascribe to the autophagy impairment. Additionally, the autophagic flux is the complete process of autophagy, in which the autophagosomes are lysed by lysosomes. It has been found that BBR could activate the autophagic flux process under several pathological conditions such as cholesterol-overloaded liver (Sun et al., 2018), and induced autophagy flux in myocardial tissue in hypoxia/reoxygenation injury (Zhu et al., 2020). Hence, we speculate that BBR may influence the autophagic flux in PD development according to our present results and literature reports, with which further study needs to be verified.

BBR exhibits several protective effects on neural cells (Song et al., 2020), but little to know of its potential mechanisms in PD. In our data, BBR suppressed NLRP3 inflammasome and enhanced autophagic activity in both MPTP-induced mice and MPP+-treated BV2 cells, indicating that NLRP3 inflammasome may be a target of BBR on inhibiting neuroinflammation. It was reported that BBR displays multiple pharmacological effects on modifying autophagy (Song et al., 2020). Zhang et al. demonstrated that BBR enhanced autophagic activity by promoting autophagosome formation and increasing the expression of BECN1 and MAP1LC3B-II (Zhang et al., 2016). In APP/tau/PS1 mouse, BBR promoted autophagic clearance of amyloid β (A β) by enhancing autophagic activity through the class-III phosphoinositide 3-kinase (PI3K)/BECN1 pathway (Huang et al., 2017). Zhou et al. reported a novel mechanism of BBR in protecting insulin resistance by enhancing autophagy to inhibit the activation of NLRP3 inflammasome (Zhou et al., 2017). In our experiments, BBR significantly suppressed the activation of NLRP3 inflammasome and enhanced autophagic activity in PD models. Furthermore, we used the common autophagy inhibitor 3-MA to inhibit autophagy to identify whether the inhibition of autophagy causes the activation of NLRP3 inflammasome in PD. As an autophagic inhibitor, 3-MA inhibits autophagy at the early stage of autophagosome formation by inhibiting class-III PI3K (Zeng et al., 2012). Studies reported that 3-MA inhibited autophagy, reduced the expression of MAP1LC3B-II and caused neuronal death (Zhong et al., 2019; Guo et al., 2020). In the present study, we found that the pharmacological effects of BBR were abolished by 3-MA co-treatment, indicating the mechanism of BBR on inhibiting NLRP3 inflammasome may ascribe to the enhancement of autophagy. Moreover, study has been reported that BBR displayed weak effect on the pro-IL1 β processing in lipopolysaccharide plus palmitate induced bone marrow derived macrophages (Zhou et al., 2017). Enhancing autophagy could promote NLRP3 autophagic degradation to inhibit NLRP3 inflammasome (Han et al., 2019), indicating BBR may inhibit NLRP3 inflammasome by increasing NLRP3 autophagic degradation.

CONCLUSIONS

In this study, we revealed that BBR could ameliorate PD-like pathophysiology by enhancing autophagy process and inhibit the

activation of NLRP3 inflammasome, which provides a novel neuroprotective mechanism of BBR and to be a potential therapeutic agent for PD.

DATA AVAILABILITY STATEMENT

The raw data supporting the conclusion of this article will be made available by the authors, without undue reservation.

ETHICS STATEMENT

The animal study was reviewed and approved by the institutional animal care committee of Guangzhou Medical University.

AUTHOR CONTRIBUTIONS

SH, LL, and HL designed the research. YWL, ML, and YHL performed the cellular experiments. SH, HM, ZZ, YZ, and PY

performed the animal experiments. SH, LD, ZZ, and XH analyzed all experimental data. SH, LL, XY, CC, and XZ drafted and revised the manuscript. LL, PX, and WG supervised this project and revised the manuscript. All authors read and approved the final manuscript.

FUNDING

This work was supported by research grants from National Key R&D Program of China (No. 2016YFC1306601 and 2017YFC1310300), National Natural Science Foundation of China (No. 82071416, 81870992, 81870856, and 81771401), a technology project of Guangzhou (No. 2018-1202-SF-0019 and 2019ZD09).

SUPPLEMENTARY MATERIAL

The Supplementary Material for this article can be found online at: <https://www.frontiersin.org/articles/10.3389/fphar.2020.618787/full#supplementary-material>.

REFERENCES

- Ali, T., Rahman, S., Hao, Q., Li, W., Liu, Z., Ali Shah, F., et al. (2020). Melatonin prevents neuroinflammation and relieves depression by attenuating autophagy impairment through FOXO3a regulation. *J. Pineal Res.* 69 (2), e12667. doi:10.1111/jpi.12667
- Ascherio, A., and Schwarzschild, M. (2016). The epidemiology of Parkinson's disease: risk factors and prevention. *Lancet Neurol.* 15 (12), 1257–1272. doi:10.1016/s1474-4422(16)30230-7
- Belwal, T., Bisht, A., Devkota, H.P., Ullah, H., Khan, H., Pandey, A., et al. (2020). Phytopharmacology and clinical updates of Berberis species against diabetes and other metabolic diseases. *Front Pharmacol.* 11, 41. doi:10.3389/fphar.2020.00041
- Chen, C., Xia, B., Tang, L., Wu, W., Tang, J., Liang, Y., et al. (2019). Echinacoside protects against MPTP/MPP. *Metab. Brain Dis.* 34 (1), 203–212. doi:10.1007/s11011-018-0330-3
- Cheng, X., Xu, S., Zhang, C., Qin, K., Yan, J., and Shao, X. (2020). The BRCC3 regulated by Cdk5 promotes the activation of neuronal NLRP3 inflammasome in Parkinson's disease models. *Biochem. Biophys. Res. Commun.* 522 (3), 647–654. doi:10.1016/j.bbrc.2019.11.141
- Donnan, G. A., Willis, G. L., Kaczmarczyk, S. J., and Rowe, P. (1987). Motor function in the 1-methyl-4-phenyl-1,2,3,6-tetrahydropyridine-treated mouse. *J. Neurol. Sci.* 77 (2-3), 185–191. doi:10.1016/0022-510x(87)90121-3
- Du, D., Hu, L., Wu, J., Wu, Q., Cheng, W., Guo, Y., et al. (2017). Neuroinflammation contributes to autophagy flux blockage in the neurons of rostral ventrolateral medulla in stress-induced hypertension rats. *J. Neuroinflammation* 14 (1), 169. doi:10.1186/s12974-017-0942-2
- Fei, Q., Ma, H., Zou, J., Wang, W., Zhu, L., Deng, H., et al. (2020). Metformin protects against ischaemic myocardial injury by alleviating autophagy-ROS-NLRP3-mediated inflammatory response in macrophages. *J. Mol. Cell. Cardiol.* 145, 1–13. doi:10.1016/j.jmcc.2020.05.016
- Friedemann, T., Ying, Y., Wang, W., Kramer, E. R., Schumacher, U., Fei, J., et al. (2016). Neuroprotective effect of coptis chinensis in MPP+ and MPTP-induced Parkinson's disease models. *Am. J. Chin. Med.* 44 (5), 907–925. doi:10.1142/S0192415X16500506
- Galluzzi, L., Baehrecke, E. H., Ballabio, A., Boya, P., Bravo-San Pedro, J. M., Cecconi, F., et al. (2017). Molecular definitions of autophagy and related processes. *EMBO J.* 36 (13), 1811–1836. doi:10.15252/embj.201796697
- Groß, C., Mishra, R., Schneider, K., Médard, G., Wettmarshausen, J., Dittlein, D., et al. (2016). K efflux-independent NLRP3 inflammasome activation by small molecules targeting mitochondria. *Immunity* 45 (4), 761–773. doi:10.1016/j.immuni.2016.08.010
- Guo, Y., Duan, W., Lu, D., Ma, X., Li, X., Li, Z., et al. (Forthcoming 2020). Autophagy-dependent removal of α -synuclein: a novel mechanism of GM1 ganglioside neuroprotection against Parkinson's disease. *Acta Pharmacol. Sin.* doi:10.1038/s41401-020-0454-y
- Han, X., Sun, S., Sun, Y., Song, Q., Zhu, J., Song, N., et al. (2019). Small molecule-driven NLRP3 inflammation inhibition via interplay between ubiquitination and autophagy: implications for Parkinson disease. *Autophagy* 15 (11), 1860–1881. doi:10.1080/15548627.2019.1596481
- Haque, M., Akther, M., Jakaria, M., Kim, I., Azam, S., and Choi, D. (2020). Targeting the microglial NLRP3 inflammasome and its role in Parkinson's disease. *Movement disord.* 35 (1), 20–33. doi:10.1002/mds.27874
- Heneka, M., McManus, R., and Latz, E. (2018). Inflammasome signalling in brain function and neurodegenerative disease. *Nat. Rev. Neurosci.* 19 (10), 610–621. doi:10.1038/s41583-018-0055-7
- Heo, M. J., Kim, T. H., You, J. S., Blaya, D., Sancho-Bru, P., and Kim, S. G. (2019). Alcohol dysregulates miR-148a in hepatocytes through FoxO1, facilitating pyroptosis via TXNIP overexpression. *Gut* 68 (4), 708–720. doi:10.1136/gutjnl-2017-315123
- Houtman, J., Freitag, K., Gimber, N., Schmoranz, J., Heppner, F., and Jendrach, M. (2019). Beclin1-driven autophagy modulates the inflammatory response of microglia via NLRP3. *EMBO J.* 38 (4). e99430. doi:10.15252/embj.201899430
- Huang, M., Jiang, X., Liang, Y., Liu, Q., Chen, S., and Guo, Y. (2017). Berberine improves cognitive impairment by promoting autophagic clearance and inhibiting production of beta-amyloid in APP/tau/PS1 mouse model of Alzheimer's disease. *Exp. Gerontol.* 91, 25–33. doi:10.1016/j.exger.2017.02.004
- Iida, T., Yokoyama, Y., Wagatsuma, K., Hirayama, D., and Nakase, H. (2018). Impact of autophagy of innate immune cells on inflammatory bowel disease. *Cells* 8 (1), 7. doi:10.3390/cells8010007
- Kang, R., Zeh, H. J., Lotze, M. T., and Tang, D. (2011). The Beclin 1 network regulates autophagy and apoptosis. *Cell Death Differ.* 18 (4), 571–580. doi:10.1038/cdd.2010.191
- Kim, H. J., Cho, M. H., Shim, W. H., Kim, J. K., Jeon, E. Y., Kim, D. H., et al. (2017). Deficient autophagy in microglia impairs synaptic pruning and causes social behavioral defects. *Mol. Psychiatry* 22 (11), 1576–1584. doi:10.1038/mp.2016.103
- Kim, S., Joe, Y., Jeong, S. O., Zheng, M., Back, S. H., Park, S. W., et al. (2014). Endoplasmic reticulum stress is sufficient for the induction of IL-1 β production via activation of the NF- κ B and inflammasome pathways. *Innate Immun.* 20 (8), 799–815. doi:10.1177/1753425913508593

- Lee, E., Hwang, I., Park, S., Hong, S., Hwang, B., Cho, Y., et al. (2019). MPTP-driven NLRP3 inflammasome activation in microglia plays a central role in dopaminergic neurodegeneration. *Cell Death Differ.* 26 (2), 213–228. doi:10.1038/s41418-018-0124-5
- Levine, B., and Kroemer, G. (2008). Autophagy in the pathogenesis of disease. *Cell* 132 (1), 27–42. doi:10.1016/j.cell.2007.12.018
- Lin, C., Wei, P., Chen, C., Huang, Y., Lin, J., Lo, Y., et al. (2020). Lactulose and melibiose attenuate MPTP-induced Parkinson's disease in mice by inhibition of oxidative stress, reduction of neuroinflammation and up-regulation of autophagy. *Front. Aging Neurosci.* 12, 226. doi:10.3389/fnagi.2020.00226
- Liu, D., Zeng, X., Li, X., Cui, C., Hou, R., Guo, Z., et al. (2020a). Advances in the molecular mechanisms of NLRP3 inflammasome activators and inactivators. *Biochem. Pharmacol.* 175, 113863. doi:10.1016/j.bcp.2020.113863
- Liu, H., You, L., Wu, J., Zhao, M., Guo, R., Zhang, H., et al. (2020b). Berberine suppresses influenza virus-triggered NLRP3 inflammasome activation in macrophages by inducing mitophagy and decreasing mitochondrial ROS. *J. Leukoc. Biol.* 108 (1), 253–266. doi:10.1002/JLB.3MA0320-358RR
- Liu, T. (2019). Regulation of inflammasome by autophagy. *Adv. Exp. Med. Biol.* 1209, 109–123. doi:10.1007/978-981-15-0606-2_7
- Lu, S., Guo, Y., Liang, P., Zhang, S., Yin, S., Yin, Y., et al. (2019). Suppression of astrocytic autophagy by α B-crystallin contributes to α -synuclein inclusion formation. *Transl. Neurodegener.* 8, 3. doi:10.1186/s40035-018-0143-7
- Mao, Z., Liu, C., Ji, S., Yang, Q., Ye, H., Han, H., et al. (2017). The NLRP3 inflammasome is involved in the pathogenesis of Parkinson's disease in rats. *Neurochem. Res.* 42 (4), 1104–1115. doi:10.1007/s11064-017-2185-0
- Mehto, S., Chauhan, S., Jena, K. K., Chauhan, N. R., Nath, P., Sahu, R., et al. (2019). IRGM restrains NLRP3 inflammasome activation by mediating its SQSTM1/p62-dependent selective autophagy. *Autophagy* 15 (9), 1645–1647. doi:10.1080/15548627.2019.1628544
- Menzies, F. M., Fleming, A., Caricasole, A., Bento, C. F., Andrews, S. P., Ashkenazi, A., et al. (2017). Autophagy and neurodegeneration: pathogenic mechanisms and therapeutic opportunities. *Neuron* 93 (5), 1015–1034. doi:10.1016/j.neuron.2017.01.022
- Neag, M. A., Mocan, A., Echeverria, J., Pop, R. M., Bocsan, C. I., Crisan, G., et al. (2018). Berberine: Botanical occurrence, traditional uses, extraction methods, and relevance in cardiovascular, metabolic, hepatic, and renal disorders. *Front Pharmacol.* 9, 557. doi:10.3389/fphar.2018.00557
- Nizami, S., Hall-Roberts, H., Warrior, S., Cowley, S. A., and Di Daniel, E. (2019). Microglial inflammation and phagocytosis in Alzheimer's disease: potential therapeutic targets. *Br. J. Pharmacol.* 176 (18), 3515–3532. doi:10.1111/bph.14618
- Panicker, N., Sarkar, S., Harisandra, D., Neal, M., Kam, T., Jin, H., et al. (2019). Fyn kinase regulates misfolded α -synuclein uptake and NLRP3 inflammasome activation in microglia. *J. Exp. Med.* 216 (6), 1411–1430. doi:10.1084/jem.20182191
- Peker, N., and Gozuacik, D. (2020). Autophagy as a cellular stress response mechanism in the nervous system. *J. Mol. Biol.* 432 (8), 2560–2588. doi:10.1016/j.jmb.2020.01.017
- Pohl, C., and Dikic, I. (2019). Cellular quality control by the ubiquitin-proteasome system and autophagy. *Science* 366 (6467), 818–822. doi:10.1126/science.aax3769
- Ruan, C., Wang, C., Gong, X., Zhang, Y., Deng, W., Zhou, J., et al. (2020). An integrative multi-omics approach uncovers the regulatory role of CDK7 and CDK4 in autophagy activation induced by silica nanoparticles. *Autophagy* 1–22. Advance online publication. doi:10.1080/15548627.2020.1763019
- Ryan, M., Eatmon, C. V., and Slevin, J. T. (2019). Drug treatment strategies for depression in Parkinson disease. *Expet Opin. Pharmacother.* 20 (11), 1351–1363. doi:10.1080/14656566.2019.1612877
- Song, D., Hao, J., and Fan, D. (Forthcoming 2020). Biological properties and clinical applications of berberine. *Front. Med.* doi:10.1007/s11684-019-0724-6
- Su, S. H., Wu, Y. F., Lin, Q., Wang, D. P., and Hai, J. (2019). URB597 protects against NLRP3 inflammasome activation by inhibiting autophagy dysfunction in a rat model of chronic cerebral hypoperfusion. *J. Neuroinflammation* 16 (1), 260. doi:10.1186/s12974-019-1668-0
- Sun, H., Liu, Q., Hu, H., Jiang, Y., Shao, W., Wang, Q., et al. (2018). Berberine ameliorates blockade of autophagic flux in the liver by regulating cholesterol metabolism and inhibiting COX2-prostaglandin synthesis. *Cell Death Dis.* 9 (8), 824. doi:10.1038/s41419-018-0890-5
- Sun, S., Han, X., Li, X., Song, Q., Lu, M., Jia, M., et al. (2018a). MicroRNA-212-5p prevents dopaminergic neuron death by inhibiting SIRT2 in MPTP-induced mouse model of Parkinson's disease. *Front. Mol. Neurosci.* 11, 381. doi:10.3389/fnmol.2018.00381
- Sun, Y., Yao, X., Zhang, Q. J., Zhu, M., Liu, Z. P., Ci, B., et al. (2018b). Beclin-1-Dependent autophagy protects the heart during sepsis. *Circulation* 138 (20), 2247–2262. doi:10.1161/CIRCULATIONAHA.117.032821
- Swanson, K., Deng, M., and Ting, J. (2019). The NLRP3 inflammasome: molecular activation and regulation to therapeutics. *Nat. Rev. Immunol.* 19 (8), 477–489. doi:10.1038/s41577-019-0165-0
- Wang, D., Zhang, J., Jiang, W., Cao, Z., Zhao, F., Cai, T., et al. (2017). The role of NLRP3-CASP1 in inflammasome-mediated neuroinflammation and autophagy dysfunction in manganese-induced, hippocampal-dependent impairment of learning and memory ability. *Autophagy* 13 (5), 914–927. doi:10.1080/15548627.2017.1293766
- Wang, S., Yuan, Y. H., Chen, N. H., and Wang, H. B. (2019). The mechanisms of NLRP3 inflammasome/pyroptosis activation and their role in Parkinson's disease. *Int. Immunopharm.* 67, 458–464. doi:10.1016/j.intimp.2018.12.019
- Wang, W., Nguyen, L., Burlak, C., Chagini, F., Guo, F., Chataway, T., et al. (2016). Caspase-1 causes truncation and aggregation of the Parkinson's disease-associated protein α -synuclein. *Proc. Natl. Acad. Sci. U. S. A.* 113 (34), 9587–9592. doi:10.1073/pnas.1610099113
- Wang, Z., Zhang, S., Xiao, Y., Zhang, W., Wu, S., Qin, T., et al. (2020). NLRP3 inflammasome and inflammatory diseases. *Oxid. Med. Cell Longev.* 2020, 4063562. doi:10.1155/2020/4063562
- Yao, S., Li, L., Sun, X., Hua, J., Zhang, K., Hao, L., et al. (2019). FTY720 inhibits MPP(+)-Induced microglial activation by affecting NLRP3 inflammasome activation. *J. Neuroimmune Pharmacol.* 14 (3), 478–492. doi:10.1007/s11481-019-09843-4
- Yuan, B., Shen, H., Lin, L., Su, T., Zhong, L., and Yang, Z. (2017). Autophagy promotes microglia activation through beclin-1-atg5 pathway in intracerebral hemorrhage. *Mol. Neurobiol.* 54 (1), 115–124. doi:10.1007/s12035-015-9642-z
- Zeng, K., Fu, H., Liu, G., and Wang, X. (2012). Aluminum maltolate induces primary rat astrocyte apoptosis via overactivation of the class III PI3K/Beclin 1-dependent autophagy signal. *Toxicol. Vitro* 26 (2), 215–220. doi:10.1016/j.tiv.2011.11.010
- Zeng, R., Luo, D. X., Li, H. P., Zhang, Q. S., Lei, S. S., and Chen, J. H. (2019). MicroRNA-135b alleviates MPP(+)-mediated Parkinson's disease in *in vitro* model through suppressing FoxO1-induced NLRP3 inflammasome and pyroptosis. *J. Clin. Neurosci.* 65, 125–133. doi:10.1016/j.jocn.2019.04.004
- Zhang, Q., Bian, H., Guo, L., and Zhu, H. (2016). Pharmacologic preconditioning with berberine attenuating ischemia-induced apoptosis and promoting autophagy in neuron. *Am. J. Transl. Res.* 8 (2), 1197–1207.
- Zhang, X., Jin, J., and Xie, A. (2020). Laquinimod inhibits MPP+ induced NLRP3 inflammasome activation in human neuronal cells. *Immunopharmacol. Immunotoxicol.* 42 (3), 264–271. doi:10.1080/08923973.2020.1746967
- Zhong, J., Xie, J., Xiao, J., Li, D., Xu, B., Wang, X., et al. (2019). Inhibition of PDE4 by FCPR16 induces AMPK-dependent autophagy and confers neuroprotection in SH-SY5Y cells and neurons exposed to MPP-induced oxidative insult. *Free Radic. Biol. Med.* 135, 87–101. doi:10.1016/j.freeradbiomed.2019.02.027
- Zhou, H., Feng, L., Xu, F., Sun, Y., Ma, Y., Zhang, X., et al. (2017). Berberine inhibits palmitate-induced NLRP3 inflammasome activation by triggering autophagy in macrophages: a new mechanism linking berberine to insulin resistance improvement. *Biomed. Pharmacother.* 89, 864–874. doi:10.1016/j.biopha.2017.03.003
- Zhou, Y., Lu, M., Du, R., Qiao, C., Jiang, C., Zhang, K., et al. (2016). MicroRNA-7 targets Nod-like receptor protein 3 inflammasome to modulate neuroinflammation in the pathogenesis of Parkinson's disease. *Mol. Neurodegener.* 11, 28. doi:10.1186/s13024-016-0094-3
- Zhu, N., Cao, X., Hao, P., Zhang, Y., Chen, Y., Zhang, J., et al. (2020). Berberine attenuates mitochondrial dysfunction by inducing autophagic flux in myocardial hypoxia/reoxygenation injury. *Cell Stress Chaperon.* 25 (3), 417–426. doi:10.1007/s12192-020-01081-5

Conflict of Interest: The authors declare that the research was conducted in the absence of any commercial or financial relationships that could be construed as a potential conflict of interest.

Copyright © 2021 Huang, Liu, Lin, Liu, Li, Mao, Zhang, Zhang, Ye, Ding, Zhu, Yang, Chen, Zhu, Huang, Guo, Xu and Lu. This is an open-access article distributed under the terms of the Creative Commons Attribution License (CC BY). The use, distribution or reproduction in other forums is permitted, provided the original author(s) and the copyright owner(s) are credited and that the original publication in this journal is cited, in accordance with accepted academic practice. No use, distribution or reproduction is permitted which does not comply with these terms.



Effect and Mechanism of Catalpol on Remyelination via Regulation of the NOTCH1 Signaling Pathway

Yaqin Sun¹, Jing Ji¹, Zheng Zha¹, Hui Zhao¹, Bing Xue², Liangyun Jin² and Lei Wang^{1*}

¹School of Traditional Chinese Medicine, Beijing Key Lab of TCM Collateral Disease Theory Research, Capital Medical University, Beijing, China, ²Core Facility Center, Capital Medical University, Beijing, China

OPEN ACCESS

Edited by:

Juxian Song,
Guangzhou University of Chinese
Medicine, China

Reviewed by:

Mingjiang Yao,
Xiyuan Hospital, China
Tan Loh Teng Hern,
Monash University Malaysia, Malaysia

*Correspondence:

Lei Wang
tmwangl@ccmu.edu.cn

Specialty section:

This article was submitted to
Ethnopharmacology,
a section of the journal
Frontiers in Pharmacology

Received: 11 November 2020

Accepted: 21 January 2021

Published: 23 February 2021

Citation:

Sun Y, Ji J, Zha Z, Zhao H, Xue B, Jin L
and Wang L (2021) Effect and
Mechanism of Catalpol on
Remyelination via Regulation of the
NOTCH1 Signaling Pathway.
Front. Pharmacol. 12:628209.
doi: 10.3389/fphar.2021.628209

Promoting the differentiation of oligodendrocyte precursor cells (OPCs) is important for fostering remyelination in multiple sclerosis. Catalpol has the potential to promote remyelination and exert neuroprotective effects, but its specific mechanism is still unclear. Recent studies have shown that the NOTCH1 signaling pathway is involved in mediating OPC proliferation and differentiation. In this study, we elucidated that catalpol promoted OPC differentiation *in vivo* and *in vitro* and explored the regulatory role of catalpol in specific biomolecular processes. Following catalpol administration, better and faster recovery of body weight and motor balance was observed in mice with cuprizone (CPZ)-induced demyelination. Luxol fast blue staining (LFB) and transmission electron microscopy (TEM) showed that catalpol increased the myelinated area and improved myelin ultrastructure in the corpus callosum in demyelinated mice. In addition, catalpol enhanced the expression of CNPase and MBP, indicating that it increased OPC differentiation. Additionally, catalpol downregulated the expression of NOTCH1 signaling pathway-related molecules, such as JAGGED1, NOTCH1, NICD1, RBPJ, HES5, and HES1. We further demonstrated that *in vitro*, catalpol enhanced the differentiation of OPCs into OLs and inhibited NOTCH1 signaling pathway activity. Our data suggested that catalpol may promote OPC differentiation and remyelination through modulation of the NOTCH1 pathway. This study provides new insight into the mechanism of action of catalpol in the treatment of multiple sclerosis.

Keywords: catalpol, multiple sclerosis, remyelination, oligodendrocytes, cuprizone, Notch1 signaling pathway

INTRODUCTION

Multiple sclerosis (MS), a demyelinating disease, affects the central nervous system (CNS), especially the white matter, and is characterized by immune cell infiltration, demyelination, oligodendrocyte (OL) loss and axonal destruction (McQualter and Bernard, 2007; Jurasic et al., 2019). Demyelination caused by immune inflammation results in severe neurological dysfunction in patients with MS (Stanojlovic et al., 2016). Promoting remyelination is important for the restoration of neurological function in MS. During the development of MS, lesions contain enough oligodendrocyte precursor cells (OPCs), which differentiate into myelinating OLs, to form a new myelin sheath around the injured axon. However, this process fails due to interference by various factors. A previous study revealed that activation of the NOTCH1 signaling pathway is one of these factors. The NOTCH1 signaling pathway affects the development and progression of the disease in the CNS by regulating the proliferation, differentiation and apoptosis of stem cells. NOTCH1 binds to the ligand

JAGGED1 to activate downstream signaling pathways and then directly converts extracellular information into changes in nuclear gene expression (Zhang et al., 2009; Paganin and Ferrando, 2011), which may hinder OPC differentiation and remyelination.

Doctors often use glucocorticoids and plasma exchange to alleviate symptoms, shorten the course of the disease, reduce the degree of disability and prevent complications in the acute phase of MS. In the remission phase, teriflunomide, interferon, fingolimod and other disease-modifying therapies (DMTs) are used to control disease progression and reduce recurrence. However, these therapies cannot prevent CNS neurodegeneration (Faissner et al., 2019). Currently, there are no safe and effective strategies to promote remyelination to improve nerve function (Plemel et al., 2017; Katsara and Apostolopoulos, 2018).

Catalpol, also known as catalpinoside, is the main active ingredient of the traditional Chinese herbal medicine *Rehmannia glutinosa* (Gaertn.) DC.. Catalpol has anti-inflammatory and antioxidant properties and exerts neuroprotective effects, improving neurocognitive function (Xia et al., 2017). Administration of 10 mg/kg or 20 mg/kg catalpol for 14 days produces significant antidepressant effects in a mouse model of depression through the serotonin pathway (Wang et al., 2014). The antidepressant effects of catalpol may be related to repair of the hypothalamic-pituitary-adrenal (HPA) axis and increased expression of brain-derived neurotrophic factor (BDNF) (Wang et al., 2015). Catalpol can also protect forebrain neurons from neurodegeneration and enhance memory by increasing BDNF expression (Liu et al., 2006; Wang et al., 2009; Wan et al., 2013). In an experimental model of Parkinson's disease, catalpol increases the concentration of striatal dopamine and the level of glial cell-derived neurotrophic factor (GDNF) (Xu et al., 2010), thereby exerting its neuroprotective functions.

We have found that catalpol can promote remyelination in experimental autoimmune encephalomyelitis (EAE) mice by upregulating the expression of the transcription factors OLIG1 and OLIG2, as well as increasing the proliferation, migration and differentiation of OPCs *in vitro* (Yuan et al., 2015; Yang et al., 2017). However, the mechanism is unclear. Therefore, in this study, we will use a mouse model of demyelination induced by cuprizone (CPZ) and OPCs *in vitro* to explore whether catalpol promotes remyelination by regulating the NOTCH1 signaling pathway.

MATERIALS AND METHODS

Animals

Female specific pathogen-free (SPF) C57BL/6J mice (aged 6–8 weeks) were provided by Beijing Weitong Lihua Experimental Animal Technology Co., Ltd. [SCXK (Beijing) 2016-0006]. The mice were housed in an SPF laboratory at the Experimental Animal Center of Capital Medical University [SYXK (Beijing) 2018-0003] at a stable temperature and humidity and provided solid rodent food and water. Animal experiments were approved by the Animal Experiments and Experimental Animal Welfare Committee of Capital Medical University (AEEI-2015-185).

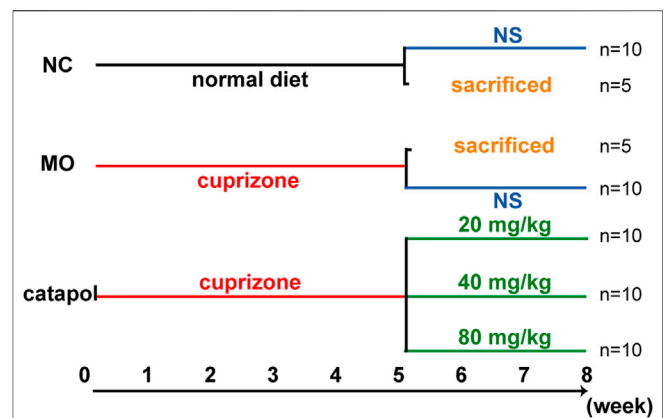


FIGURE 1 | The design scheme of experimental protocol. At the end of the fifth week, five mice in the NC group and MO group were randomly selected and sacrificed; The remaining mice continued to be raised. Black represents a normal diet, red represents a diet containing 0.2% CPZ, blue means a normal diet plus gavage of normal saline, and green represents a normal diet plus gavage of catalpol.

Drugs

Special feed containing 0.2% CPZ (Sigma, United States) produced by Beijing Keao Xieli Feed Co., Ltd. [Beijing Feed Certification (2014) 06054] was used for this experiment after disinfection by cobalt-60 irradiation. For *in vivo* studies, catalpol was purchased from Nanjing Dilge Pharmaceutical Technology Co., Ltd. and used in doses of 20 mg/kg, 40 mg/kg and 80 mg/kg, and its purity was $\geq 85\%$. For *in vitro* studies, the standard substance of catalpol was provided by Target Molecule Corp (T2780) and used in the concentrations of 0–100 μM , and its purity was $\geq 99\%$.

Establishment and Treatment of the CPZ-Induced Demyelination Mouse Model

Sixty mice were randomly divided into five groups: the normal control (NC) group ($n = 15$), the model (MO) group ($n = 15$), and the 20 mg/kg, 40 mg/kg and 80 mg/kg catalpol groups ($n = 10$ /group). The mice in the NC group were given normal feed, and the mice in the other five groups were given feed containing 0.2% CPZ. After 5 weeks, the levels of relevant indicators were assessed in five mice from each of the NC group and the MO group. From the 6th week, the remaining mice were provided normal feed. The catalpol groups were administered the corresponding dose of catalpol daily by gavage, whereas the NC and MO groups were given the same volume of normal saline. Biological materials were collected after 8 weeks (Figure 1).

Body Weight Measurement and the Rotarod Test

From the start of modeling, the body weight of each mouse was measured twice a week. For three days before modeling, the mice were subjected to balance training on a rotating device twice a day. After the mice had been adapted to the device, their motor

abilities were tested twice a week. The rotation speed was slowly increased from 5 rpm to 40 rpm over 3 min. When a mouse fell off or held onto the rotating rod and for two or more rotations, the experiment was ended. The time spent on the rod by the mice was recorded to monitor changes in coordination and balance (Fan et al., 2018).

Luxol Fast Blue Staining

The mice were anesthetized with 4% chloral hydrate and perfused with 40 g/L paraformaldehyde for 30 min, and their tissues were embedded with paraffin. Five-micron -thick coronal slices of the brain located in the corpus callosum were prepared. After being washed with phosphate-buffered saline (PBS), the brain slices were baked at 60°C for 2 h, placed in 1:1 ethanol and chloroform for 4 h, and then transferred to 95% ethanol. After dehydration, the sections were placed in LFB solution overnight, rinsed, and then subjected to color development with 0.05% lithium carbonate and 70% alcohol. After being rinsed, the sections were counterstained with cresyl violet for 5 min, rinsed with water, dehydrated, removed, and sealed for observation.

Primary OPC Culture

Newborn Sprague-Dawley (SD) rats were provided by Beijing Weitong Lihua Experimental Animal Technology Co., Ltd. [SCXK (Beijing) 2016-0006]. OPCs were isolated and purified by a method involving B104-conditioned medium. Mixed glial cells were isolated from the cortices of newborn rats. After being cultured in Dulbecco's modified Eagle medium (DMEM) containing 10% fetal bovine serum (FBS) for 3 days, the mixed glial cells were cultured with modified OPC growth medium (mOGM) containing 15% B104-conditioned medium. The OPCs were isolated and purified by a chemical-based separation procedure when they had proliferated enough.

Cell Counting Kit (CCK)-8 Assay

One hundred microliters of a single-cell suspension containing OPCs (1.5×10^4) was seeded in PPL-coated 96-well plates for 24 h and then treated with catalpol (0, 1, 2.5, 5, 10, 20, 40, 80, or 100 μ M) for 24 h, 48 h or 72 h. Then, cell viability was assessed by a CCK-8 kit according to the manufacturer's instructions. The optical density (OD) values at 450 nm were measured with a microplate reader and normalized to those of the control groups.

Transmission Electron Microscopy

After perfusion, the corpus callosum tissues of the mice were separated on ice, cut into approximately $1 \times 1 \times 3$ mm³ pieces, placed in 2.5% glutaraldehyde for 2 h, and then rinsed with 0.1 M PB three times. Then the corpus callosum tissues were fixed with 1% osmium acid, dehydrated in alcohol, soaked for 20 min, embedded in embedding agent, subjected to melt impregnation and treated with pure embedding agent. The embedded samples were sliced with an ultrathin microtome and then stained and coverslipped. The ultrastructure of the myelin sheath was observed with an electron microscope (JEM-2100, JEOL, Tokyo, Japan). We randomly selected at least 80 axons from each group, used professional image analysis software (Image-Pro Plus, IPP) to measure the diameter of the myelin

sheath and axon in each field of view, and calculated the G-ratio (axon/axon diameter + myelin sheath diameter) to evaluate demyelination.

Immunofluorescence

The mouse brain slices were dewaxed, hydrated, incubated in citric acid for 20 min for antigen repair, cooled to room temperature (RT), and blocked with 10% goat serum at 37°C for 60 min. Goat anti-OLIG2 (1:100; R&D, MN, United States), mouse anti-CNPase (1:200, Abcam, Cambridge, United Kingdom), rabbit anti-MBP (1: 200, Abcam, Cambridge, United Kingdom), and rabbit anti-GFAP (1:400, Abcam, Cambridge, United Kingdom) primary antibodies were added dropwise, and the slices were incubated at 4°C for 48 h. After the slices were rewarmed at 37°C for 60 min, they were incubated with corresponding fluorescently labeled IgG antibodies (Alexa Fluor 488-conjugated donkey anti-rabbit or mouse IgG [1: 200], Cy3-labeled donkey anti-goat IgG [1: 200], or Alexa Fluor 488-conjugated goat anti-rabbit IgG [1: 200]). Then, the slices were sealed with DAPI solution. Representative images were obtained with the Panoramic SCAN digital slice scanner and analysis software (3DHISTECH, Hungary), and ImageJ was used to determine the expression of the abovementioned proteins in the selected area for further data analysis.

A total of 500 μ l of a single-cell suspension containing OPCs (4.5×10^4) was plated in 24-well plates with coated glass coverslips and incubated for 12 h. Then, catalpol (0, 1, 2.5, 5, 10, 20, 40, 80, or 100 μ M) was added. After 24 h, 48 h or 72 , the OPCs on coverslips were fixed with 4% paraformaldehyde for 30 min at RT and treated with 0.5% Triton for 10 min. After being rinsed with PBS, the coverslips were blocked with 5% bovine serum albumin (BSA) for 1 h and then incubated with a rabbit anti-MBP antibody (1:200, Abcam, Cambridge, United Kingdom) at 4°C overnight. Then, the cells were washed with PBS and incubated with Alexa Fluor 488-conjugated donkey anti-rabbit IgG (1:200) at RT for 1 h. The cell nuclei were stained with DAPI for 5 min. Immunoreactivity was observed using a fluorescence microscope. All images were analyzed with ImageJ software.

Western Blot Analysis

OPCs (9×10^5 cells/well in 6-well plates, treated with 40 μ M catalpol according to the method used for immunofluorescence) and mouse brain tissues (containing the corpus callosum, cortex and hippocampus, 30–50 μ g) were lysed with RIPA lysis buffer. The protein concentrations were measured using the Bicinchoninic Acid (BCA) Protein Assay Kit and normalized. The proteins were separated by SDS-PAGE and transferred onto PVDF membranes. After being blocked with 5% skim milk for 1 h, the membranes were incubated with the following primary antibodies overnight at 4°C: rabbit anti-JAGGED1 (1:1,000, CST, 2620), rat anti-NOTCH1 (1:1,000, CST, MA, United States), rabbit anti-NICD1 (1:1,000, CST, MA, United States), rabbit anti-RBPJ (1:1,000, CST, MA, United States), rabbit anti-HES1 (1:1,000, CST, MA, United States), rabbit anti-HES5 (1:1,000, CST, MA, United States), mouse anti-ACTB (1:20,000, Gene Tex, CA, United States), and mouse anti-TUBB (1:20,000, Proteintech,

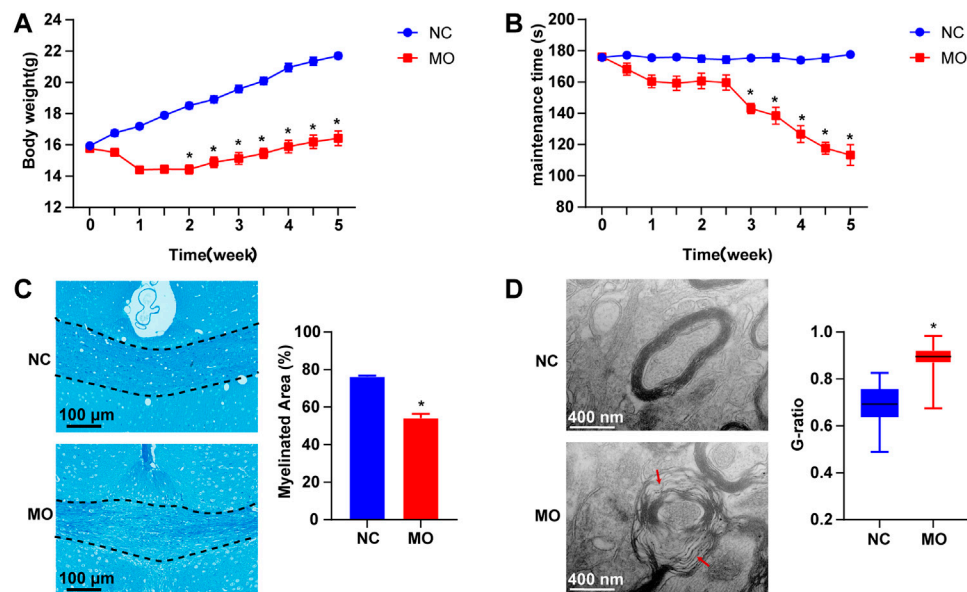


FIGURE 2 | The model of CPZ-induced demyelination. **(A)** Changes in body weight ($n = 15$ /each group), **(B)** rotating rod experiment in mice ($n = 13$ /each group), **(C)** changes in demyelination of the corpus callosum in mice: FLB $\times 200$ times and statistical results of myelinated area ($n = 3$ /each group), **(D)** changes in myelin ultrastructure (TEM $\times 12,000$ times) and myelin sheath G-ratio ($n = 3$, 80 myelin sheaths randomly selected from each group). The data are expressed as mean \pm SEM, compared with the NC group, $*p < 0.05$.

Chicago, United States). After being washed, the membranes were incubated with corresponding IgG antibodies (1:10,000) at RT for 1 h. The proteins were exposed by a gel chemiluminescence imaging analysis system using enhanced chemiluminescence (ECL) reagent. ImageJ software was used to process the images, determine the grayscale values of the bands, and semiquantitatively analyze the relative expression of each protein.

Quantitative RT-PCR

Total RNA was extracted from 50 μ g samples with the One-Step qRT-PCR kit (Toyobo, Osaka, Japan), and then the concentration was measured. RT-PCR mixtures were prepared, and qRT-PCR was performed by the CFX96 TM Real-Time PCR instrument to confirm the mRNA expression levels of the target genes. *Actb* was used as an internal reference for RNA. mRNA expression levels were quantified using the Bio-Rad CFX Real-Time system and analyzed using CFX management software v2.0 (Bio-Rad, Hercules, CA) and the $2^{-\Delta\Delta C_t}$ method.

The sequences of the primers used in this study were as follows: *Notch1*: FWD - GTCCCCTGGGTTTCTCTG and REV - GCAGCGGCACTTGTACTC; *Jag1*: FWD - GACCGTAATCGCATCGTAC and REV - CCTGAGTGAGAAGCCTTTTC; *RBPJ*: FWD - AAGCGGATAAAGGTCATCTC and REV - AAATGCTCCCCACTGTTG; *Hes1*: FWD - AAGCTAGAGAAGGCAGACATTC and REV - GTAGGTCATGGCGTTGATC; *Hes5*: FWD - GGTACAGTTCTTGACCCTGC and REV - AGCAGCAGCAGCCTTAGC; and *Actb*: FWD - TGCCTGACATCAAAGAGAAG and REV - AGAAGGAAGGCTGGAAAAG.

Statistical Analysis

All data are presented as the mean \pm SEM. Statistical analyses were performed by one-way analysis of variance and Tukey's HSD multiple comparison test using GraphPad Prism 7.0 software. For all statistical tests, p -values < 0.05 were considered statistically significant.

RESULTS

Successful Establishment of the CPZ-Induced Demyelination Model

The body weights of the mice in the NC group increased over time. The weights of the mice in the MO (5 weeks) group gradually decreased to the lowest by the end of the second week and then slowly increased. There was a statistically significant difference in body weight between the NC and MO (5 weeks) groups ($p < 0.05$, **Figure 2A**). The results of the rotarod test showed that the time spent on the rod by the mice in the NC group remained basically the same over time. However, from the 3rd week, the time spent on the rod by the mice in the MO (5 weeks) group decreased significantly ($p < 0.05$, **Figure 2B**).

LFB staining indicated that in the mice in the NC group, the myelin sheaths were tight and properly arranged and that there was a large amount of staining; however, in the MO (5 weeks) group, myelin staining in the corpus callosum was notably reduced and sparse, or even absent ($p < 0.05$, **Figure 2C**). According to the results of TEM, in the NC group, the myelin sheaths were clear and dense and no demyelination or axonal atrophy was observed, whereas

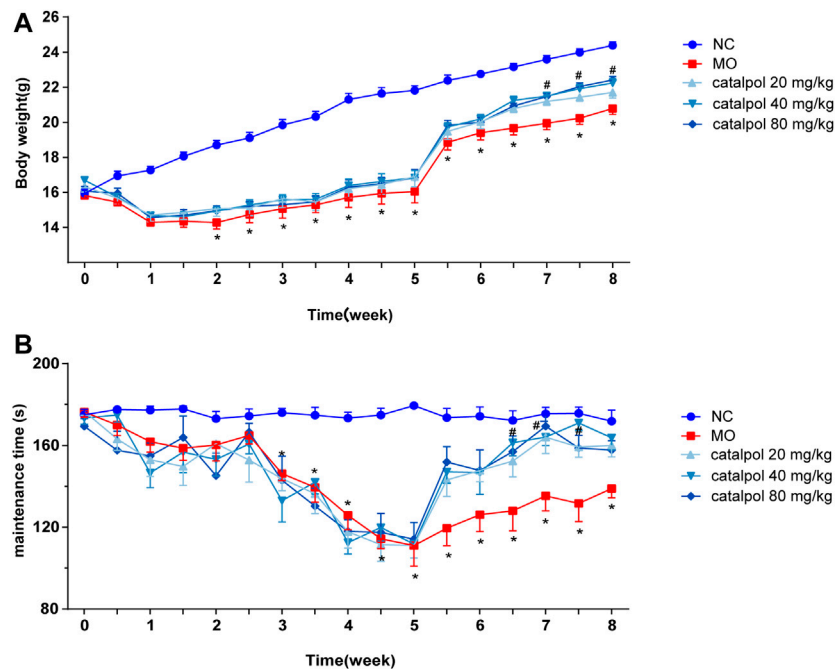


FIGURE 3 | Different concentrations of catalpol improved the body weight and exercise ability of CPZ-induced demyelinated mice. **(A)** Changes in body weight of mice in each group ($n = 10$), **(B)** changes in the time of turning rods of mice in each group ($n = 8$). The data are expressed as mean \pm SEM, compared with the NC group, * $p < 0.05$; compared with MO group, # $p < 0.05$.

loose myelin sheaths with lamellar separation, a decreased ring density, axonal atrophy and significantly higher G-ratios were observed in the MO (5 weeks) group (Figure 2D, $p < 0.05$). Based on the above indicators, the mouse model of CPZ-induced demyelination was successfully established.

Catalpol Increased the Body Weights and Improved the Motor Functions of Demyelinated Mice

After the mice were given normal feed beginning in the 6th week, the body weights of the mice in the NC group continued to increase, and those of the mice in the MO group recovered slightly ($p < 0.05$). The body weights of the mice in the 40 mg/kg and 80 mg/kg catalpol groups recovered quickly. From the 7th week, there were significant differences in body weight between the catalpol groups and the MO group ($p < 0.05$, Figure 3A). The rotarod test results showed from the 6th week, the time spent on the rod by the mice in the NC group remained relatively stable, whereas that spent by the mice in the MO group improved but was still significantly shorter than that spent by the mice in the NC group ($p < 0.05$). The time spent on the rod by the mice in the 20 mg/kg catalpol group was significantly longer than that spent by the mice in the MO group from the 7th week ($p < 0.05$), while the time spent on the rod by the mice in the 40 mg/kg and 80 mg/kg catalpol groups was significantly longer than that spent by the mice in the MO group beginning at six and a half weeks ($p < 0.05$, Figure 3B).

The Effect of Different Concentrations of Catalpol in Reducing Myelination in CPZ-Induced Demyelination Mice

At the 8th week, partial remyelination was observed in the corpus callosum in mice in the MO group. The loss of LFB staining of myelin and myelin lamination was slightly delayed in the MO group, but a significant difference compared with the NC group ($p < 0.001$) was still observed. The stained myelin sheaths were significantly denser and better arranged (Figure 4A), the demyelinated area was significantly smaller (Figure 4B) in the catalpol administration groups than in the MO group ($p < 0.05$). The three catalpol groups exhibited loosening of the lamellar structure of myelin to varying degrees and decreases in ring density. However, these changes were less severe in the three catalpol groups than in the MO group (Figure 4C). The G-ratios were significantly lower in the catalpol groups than in the MO group ($p < 0.05$, $p < 0.001$), with the 40 mg/kg and 80 mg/kg catalpol groups exhibiting more significant changes ($p < 0.05$, $p < 0.001$, Figure 4D).

Catalpol Upregulated the Expression of CNPase and MBP in the Corpus Callosum in Demyelinated Mice

CNPase and MBP are markers of OL differentiation and maturity, respectively. OLIG2, which is essential for cell fate choices, is a transcription factor in OLs (Gouvea-Junqueira

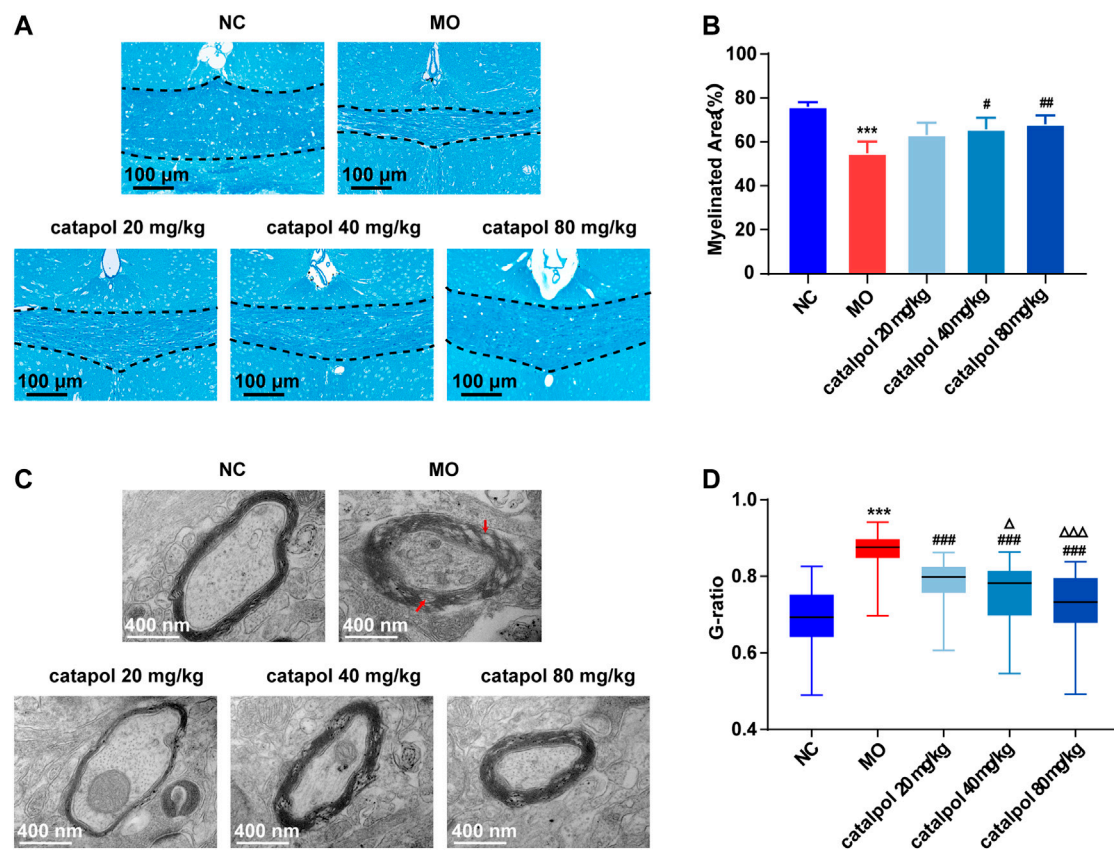


FIGURE 4 | Catalpol at different concentrations significantly promoted myelination in demyelinated mice. **(A)** Changes in demyelination of the corpus callosum in mice (FLB $\times 200$ times, $n = 3$ /each group), **(B)** statistical results of myelinated area of the corpus callosum in each group ($n = 3$), **(C)** changes in the ultrastructure of myelin sheath (TEM $\times 12,000$ times, $n = 3$ /each group), **(D)** changes in G-ratio of myelin sheath in each group ($n = 3$, randomly selecting 80 myelin sheaths each group for statistics). The data are expressed as mean \pm SEM. Compared with NC group, *** $p < 0.001$; compared with MO group, # $p < 0.05$, ## $p < 0.01$, ### $p < 0.001$; compared with 20 mg/kg catalpol group, $\Delta p < 0.05$, $\Delta\Delta p < 0.001$.

et al., 2020). The expression levels of CNPase/OLIG2 and MBP/OLIG2 in the brains of mice in each group were detected by immunofluorescence to evaluate the differentiation and maturation of OPCs. The experimental results indicated that there was no difference in the expression of OLIG2 in the corpus callosum between groups (Figure 5B). This finding further indicates that insufficient differentiation of OPCs, not a lack of OPCs, causes the failure of remyelination in MS. Furthermore, the expression levels of CNPase/OLIG2 in the mice in the MO group were decreased compared to those in the NC group (Figure 5A, $p < 0.001$); CNPase/OLIG2 levels in the catalpol treatment groups were increased to a certain extent. Catalpol had more robust effects at 40 mg/kg and 80 mg/kg than at 20 mg/kg ($p < 0.01$). The expression of CNPase protein was also measured by WB analysis (Figure 5D), and similar results were obtained. The MBP measurement results were basically consistent with those of CNPase. There was no difference in the expression of OLIG2 between groups (Figure 6B), but there were obviously fewer MBP⁺/OLIG2⁺ cells in the MO group than in the NC group and the catalpol groups (Figure 6A, $p < 0.001$). Analysis of MBP protein expression

in the brain further confirmed the effect of catalpol on promoting the differentiation of OPCs (Figure 6D).

Catalpol Downregulated the Expression of GFAP in the Brains of Demyelinated Mice

GFAP is a marker of astrocytes. Studies have found that astrocytes participate in the first line of defense against the early stages of immune inflammation in MS (Farina et al., 2007; Brosnan and Raine, 2013; Ponath et al., 2017) and have neuroprotective effects (Colombo and Farina, 2016). However, the activation of astrocytes during the remyelination stage is harmful (Mayo et al., 2012). Reactive astrocytes form an astroglial scar with recruited chondroitin sulfate proteoglycans, hyaluronic acid and other molecules, the levels of which are upregulated, affecting remyelination (Liddel et al., 2017). On the other hand, a large number of astrocytes produce platelet-derived growth factor α and fibroblast growth factor 2, which inhibit the differentiation of OPCs. In this study, we found that the expression of GFAP was elevated in the MO group compared with the NC group ($p < 0.001$). At the three tested doses, of catalpol decreased GFAP expression in the brain to varying degrees ($p < 0.01$, Figure 7).

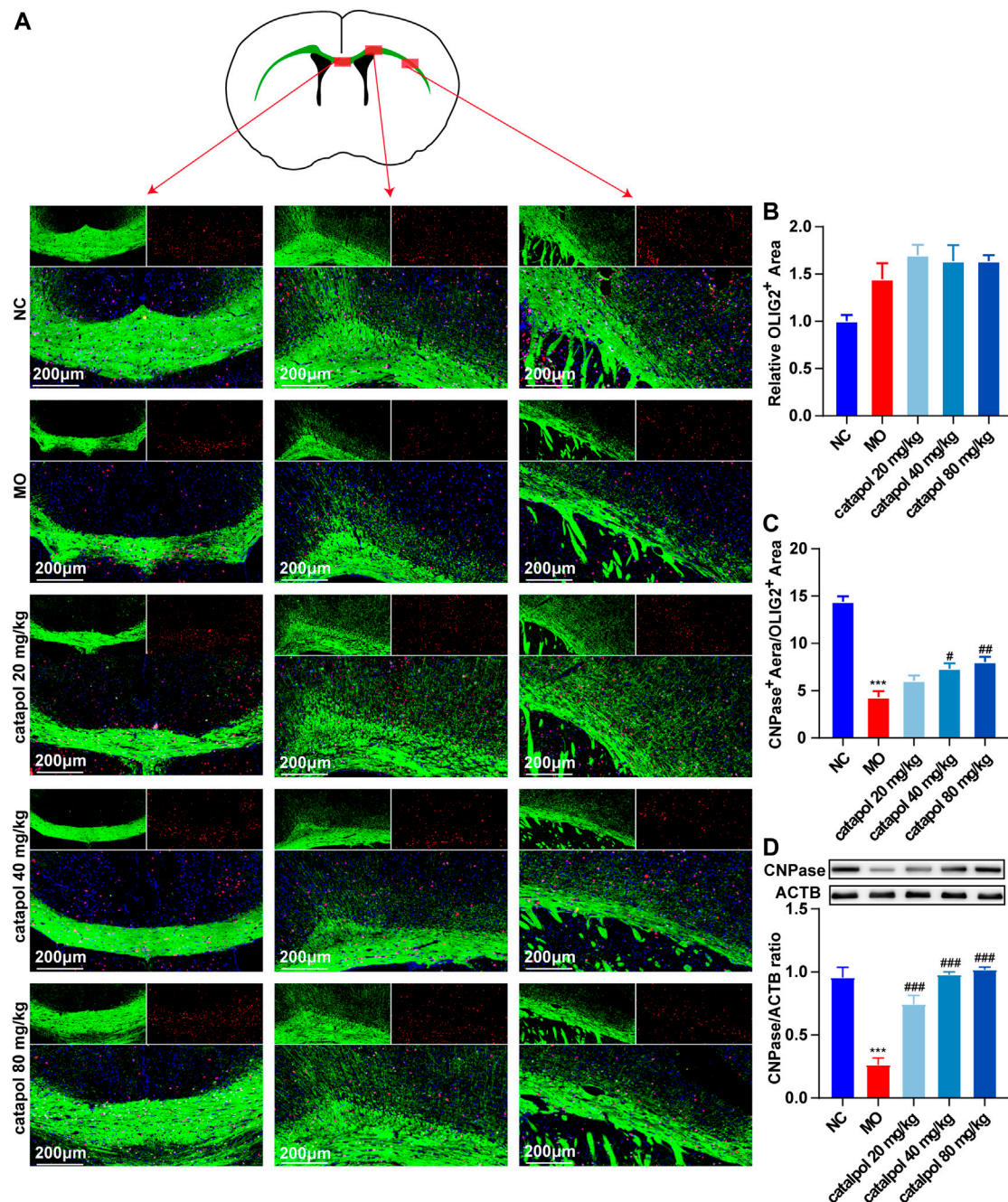


FIGURE 5 | Catalpol at different concentrations up-regulated CNPase in the corpus callosum of demyelinated mice. **(A)** Immunofluorescence localization of CNPase and OLIG2 in the brain. CNPase (green) and OLIG2 (red) were labeled with fluorescent secondary antibodies, and the nuclei were labeled with DAPI. **(B)** Quantitative analysis of the fluorescent expression of OLIG2, **(C)** quantitative analysis of fluorescent expression of CNPase, **(D)** changes of CNPase protein in the brains. The data are expressed as mean \pm SEM ($n = 3$ /each group), compared with NC group, *** $p < 0.001$; compared with MO group, # $p < 0.05$, ## $p < 0.01$, ### $p < 0.001$.

Effects of Catalpol on NOTCH1 Signaling Pathway-Related Proteins and Genes in the Brains of Demyelinated Mice

The NOTCH1 signaling pathway is active in the nervous system throughout life and plays a role in maintaining the steady state of stem or progenitor cells in the developing CNS (Chitnis et al.,

1995; Wettstein et al., 1997). NOTCH1 signaling alters the proliferation and differentiation of differentiated cells through cell-to-cell communication. The activation of NOTCH1 ligands and downstream target genes of the *Hes* family blocks the differentiation of OPCs, causing the failure of myelination by OLs. These findings indicate that the NOTCH1 pathway may be primarily responsible for the failure of remyelination in MS

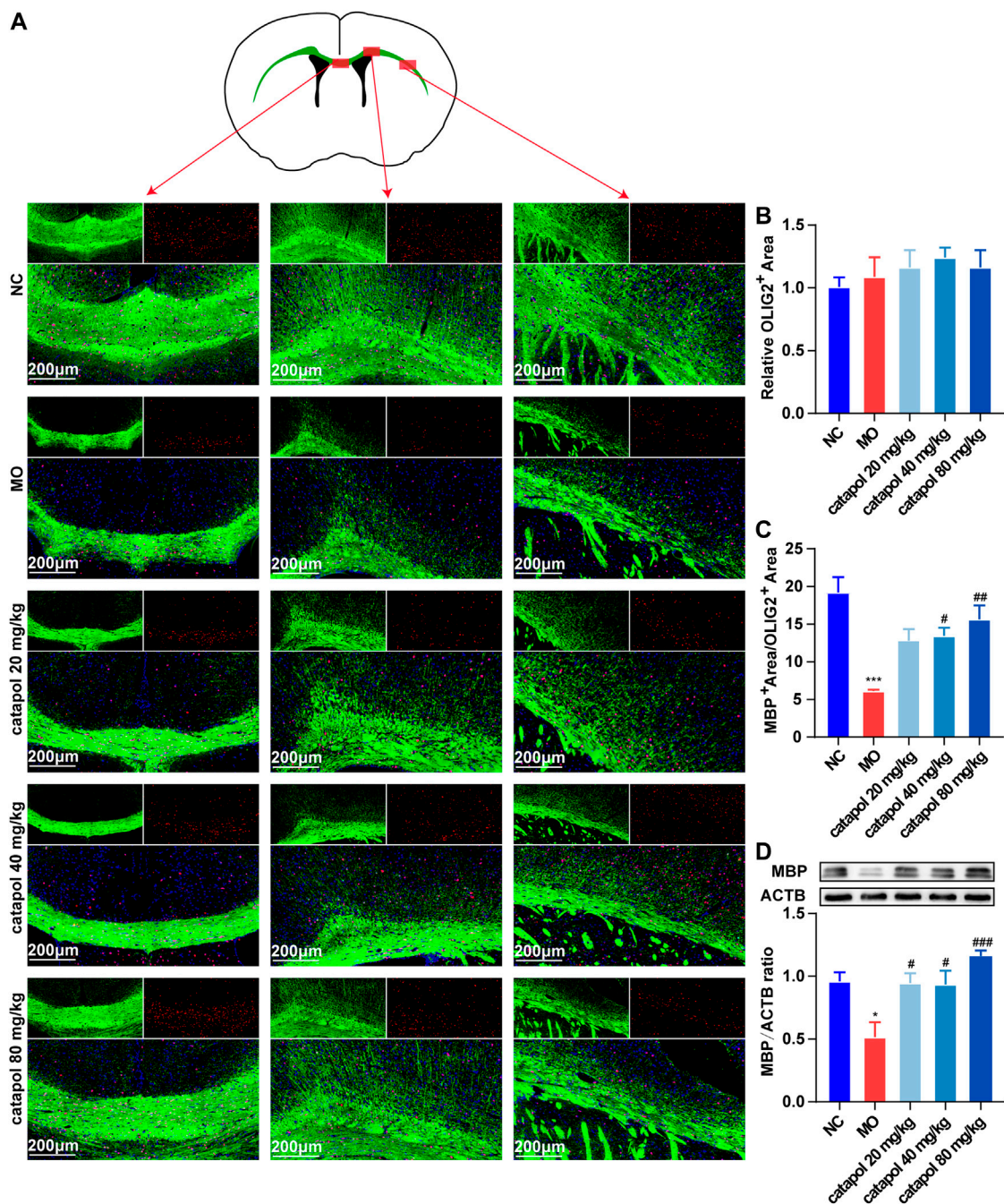


FIGURE 6 | Catalpol at different concentrations up-regulated MBP in the corpus callosum of demyelinated mice. **(A)** Immunofluorescence localization of MBP and OLIG2 in the brain. MBP (green) and OLIG2 (red) were labeled with fluorescent secondary antibodies, and the nuclei were labeled with DAPI. **(B)** Quantitative analysis of the fluorescent expression of OLIG2, **(C)** quantitative analysis of fluorescent expression of MBP, **(D)** changes of CNPase protein in the brains. The data are expressed as mean \pm SEM ($n = 3$ /each group), compared with NC group, * $p < 0.05$, *** $p < 0.001$; compared with MO group, # $p < 0.05$, ## $p < 0.01$, ### $p < 0.001$.

(Mathieu et al., 2019). Therefore, in this experiment, we mainly assessed the levels of several indicators related to the NOTCH1 signaling pathway: the ligand JAGGED1; the transmembrane receptor NOTCH1 (Fortini, 2009; Kovall et al., 2017); Notch intracellular domain (NICD), which is released by γ -secretase; recombination signal binding protein for immunoglobulin kappa

J region (RBPJ), and the downstream transcription factors HES1 and HES5 (Tamura et al., 1995).

We observed that the protein and gene levels of NOTCH1 (*Notch1*), JAGGED1 (*Jag1*), NICD1, RBPJ (*Rbpj*), HES1 (*Hes1*), and HES5 (*Hes5*) were significantly increased in mice in the MO group compared with mice in the NC group

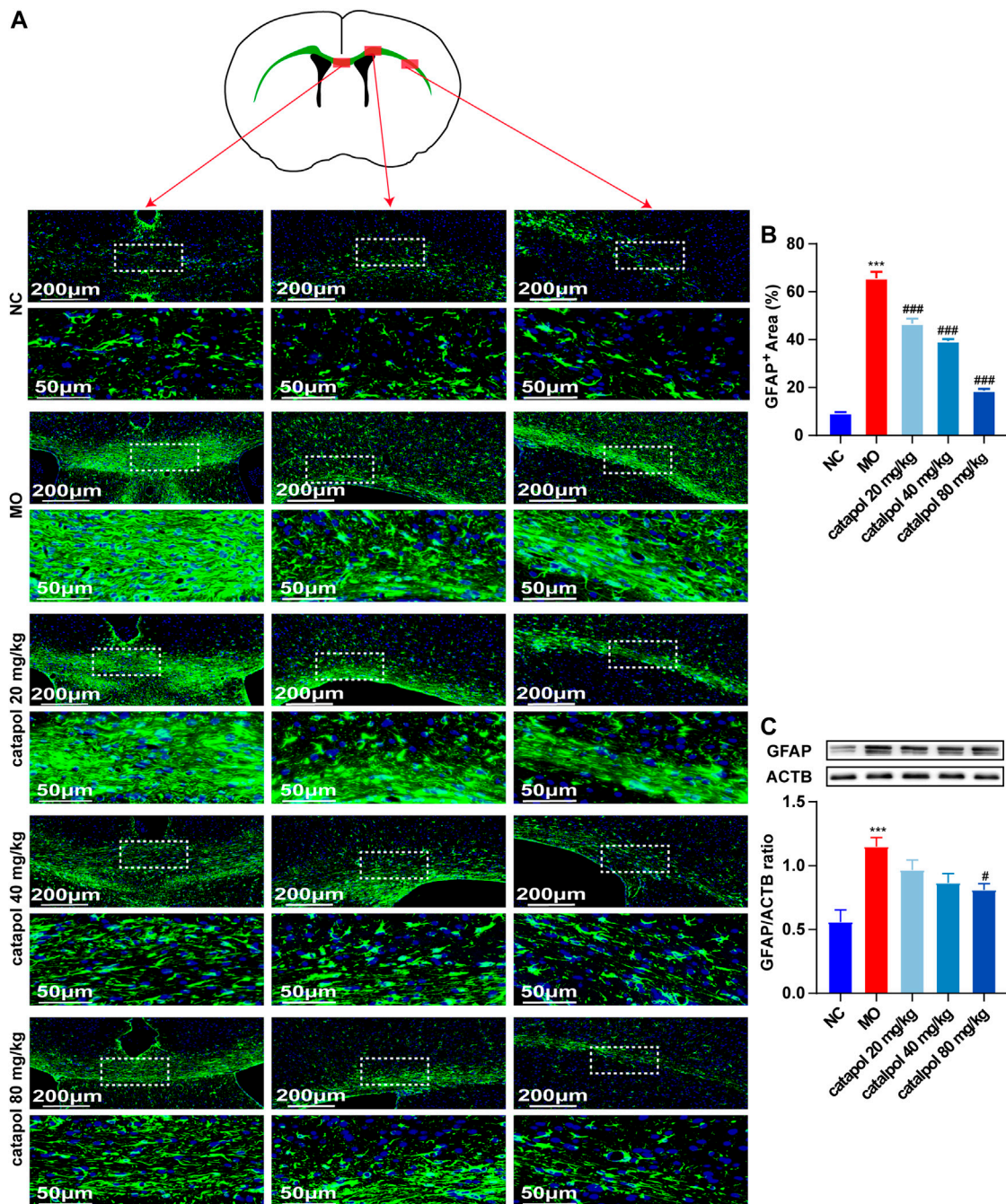


FIGURE 7 | Catalpol at different concentrations down-regulated GFAP in the corpus callosum of demyelinated mice. **(A)** Immunofluorescence localization of GFAP in the brain. GFAP (green) was labeled with fluorescent secondary antibodies, and the nuclei were labeled with DAPI. **(B)** Quantitative analysis of the fluorescent expression of GFAP, **(C)** changes of GFAP protein in the brains. The data are expressed as mean \pm SEM ($n = 3$ /each group), compared with NC group, *** $p < 0.001$; compared with MO group, # $p < 0.05$, ### $p < 0.001$.

($p < 0.01$). Since NICD1 is a digested fragment of the NOTCH1 protein, it cannot be regulated at the gene level. Thus, PCR analysis of this gene was not performed. However, after treatment with different concentrations of catalpol, the levels of the abovementioned markers decreased to varying degrees. The protein and gene expression of JAGGED1 (*Jag1*)

was decreased in all three treatment groups compared to the MO group ($p < 0.05$, $p < 0.001$, **Figure 8A**); 40 mg/kg and 80 mg/kg catalpol reduced the expression of NOTCH1 (*Notch1*), with 80 mg/kg catalpol having the strongest effect ($p < 0.05$, **Figure 8B**); the expression of NICD1 was lower in the brains of mice treated with

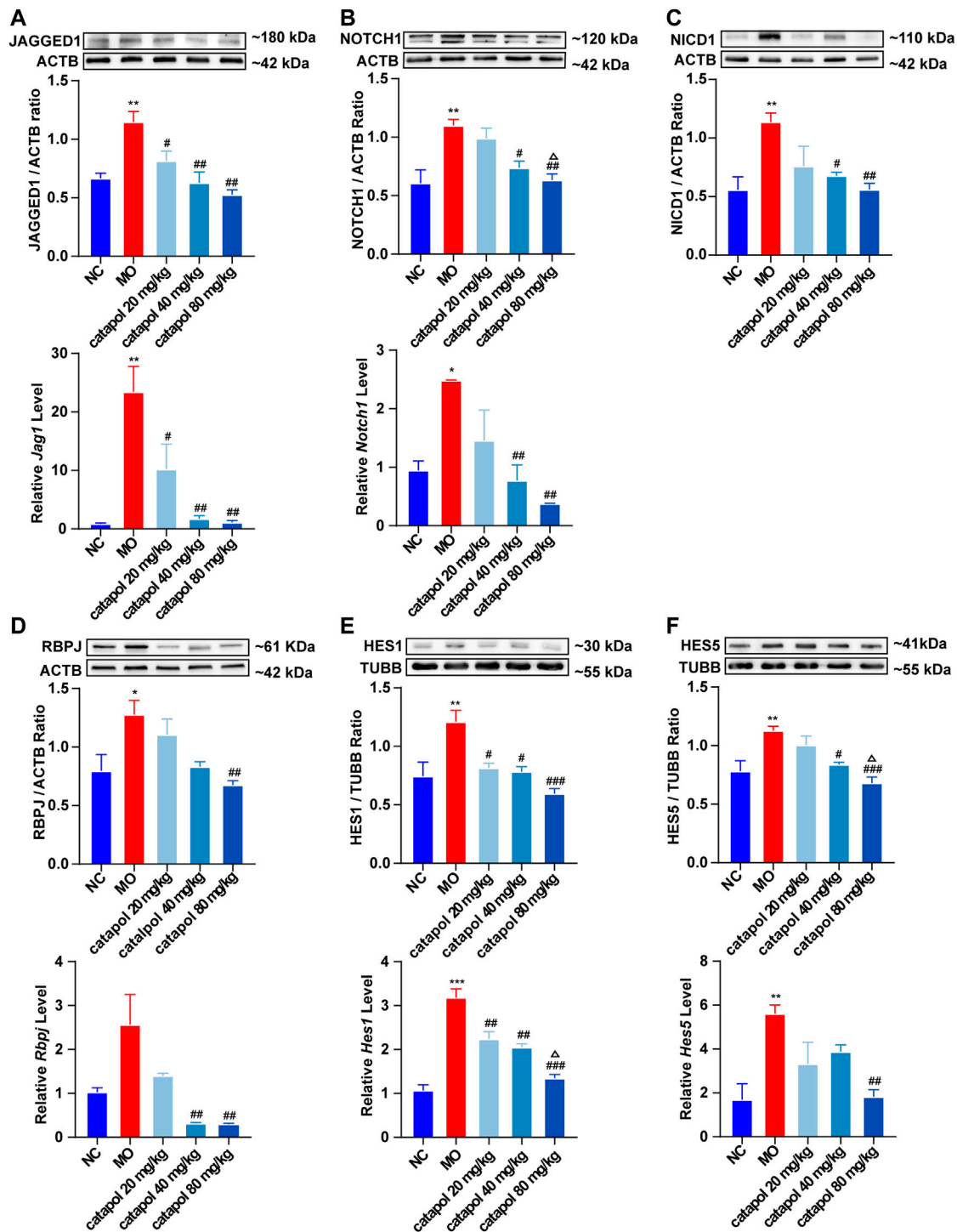


FIGURE 8 | Catalpol at different concentrations down-regulated the expression of NOTCH1 signaling pathway-related proteins and genes in demyelinated mice.

(A) The expression of JAGGED1 protein and *Jag1* gene in the brain, (B) the expression of NOTCH1 protein and *Notch1* gene in the brain, (C) the expression of NICD1 protein in the brain, (D) the expression of RBPJ protein and *Rbpj* gene in the brain, (E) the expression of HES1 protein and *Hes1* gene in the brain, (F) the expression of HES5 protein and *Hes5* gene. The relative expression of gene content was calculated by using $2^{-\Delta\Delta Ct}$ method. The data are expressed as mean \pm SEM ($n = 3$ /each group). Compared with NC group, * $p < 0.05$, ** $p < 0.01$, *** $p < 0.001$; compared with MO group, # $p < 0.05$, ## $p < 0.01$, ### $p < 0.001$; compared with 20 mg/kg catalpol group, $\Delta p < 0.05$.

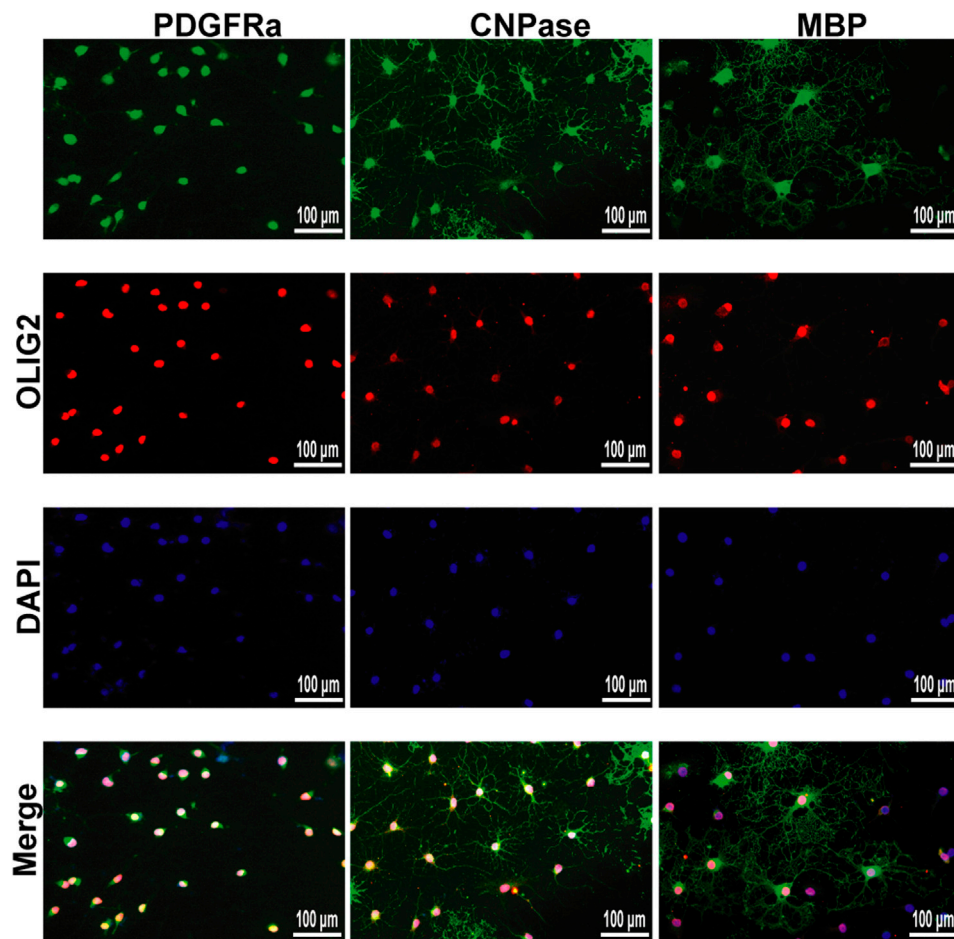


FIGURE 9 | Immunofluorescence localization of PDGFR α , CNPase and MBP in the OPCs and OLs *in vitro*. PDGFR α , CNPase and MBP (green) were labeled with fluorescent secondary antibodies, and the nuclei were labeled with DAPI.

40 mg/kg or 80 mg/kg catalpol than those of mice in the MO group ($p < 0.05$, $p < 0.01$, **Figure 8C**); all doses of catalpol downregulated the expression of RBPJ (*Rbpj*) to a certain extent, with 80 mg/kg catalpol having the most significant effect ($p < 0.05$, **Figure 8D**); the protein and gene levels of HES1 (*Hes1*) in the brain were obviously decreased in the three catalpol treatment groups compared to the MO group, with 80 mg/kg catalpol having the most significant effect ($p < 0.05$, **Figure 8E**); and the downward trend in HES5 (*Hes5*) expression was similar to that of HES1 (*Hes1*) (**Figure 8F**).

Cultivation of OPCs and OLs

We successfully isolated OPCs from the brains of suckling rats and cultured them *in vitro*. We used PDGFR α , a marker of OPCs, to identify the cultured cells. Next, OPCs were cultured in differentiation medium, and the cells at different stages from OPCs to OLs were labeled with markers at different stages to prove that the cultured OPCs had strong differentiation ability (**Figure 9**).

Catalpol Increased the Viability of Primary OPCs

To study the effect of catalpol on the activity of OPCs, cells were treated with catalpol (1, 2.5, 5, 10, 20, 40, 80, or 100 μ M) for 24, 48 or 72, and cell viability was measured by the CCK-8 assay. Catalpol increased the viability of OPCs to different extents (**Figure 10A**).

Catalpol Promoted the Formation of Mature OLs *In Vitro*

MBP is a marker of mature OLs. Catalpol significantly increased the number of MBP⁺ cells. The results revealed that treatment with 0–100 μ M catalpol for 24–72 h promoted the differentiation of OPCs into OLs (**Figure 10B**).

According to the findings related to the viability of and MBP expression in OPCs, catalpol had the best effect at a concentration of 40 μ M for 48 h (**Figure 10C**). Therefore, we chose treatment with 40 μ M catalpol for 48 h for further experiments *in vitro*.

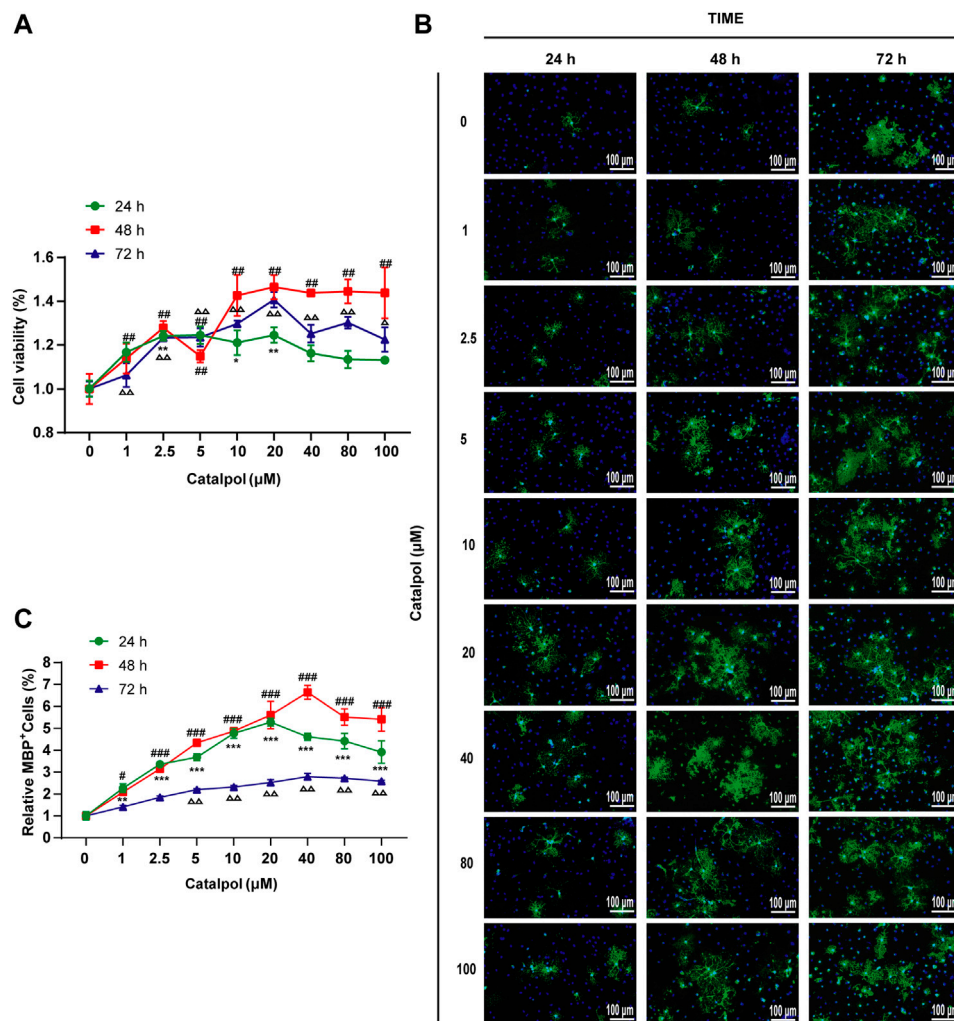


FIGURE 10 | Catalpol promoted the proliferation and differentiation of OPCs *in vitro*. **(A)** OPCs were treated with catalpol (0, 1, 2.5, 5, 10, 20, 40, 80, 100 μM) for 24, 48 and 72 h. Cell viability was analyzed by CCK-8 assay. **(B)** Immunofluorescence localization of MBP. MBP (green) was labeled with fluorescent secondary antibodies, and the nuclei were labeled with DAPI. **(C)** The ratio of quantitative analysis of the fluorescent expression of MBP in each group to the untreated (Catalpol, 0 μM) group. The data are expressed as the mean ± SEM of three independent experiments, compared with catalpol 0 μM for 24 h group, * $p < 0.05$, ** $p < 0.01$, *** $p < 0.001$; compared with catalpol 0 μM for 48 h group, # $p < 0.05$, ## $p < 0.01$, ### $p < 0.001$; compared with catalpol 0 μM for 72 h group, $\Delta p < 0.05$, $\Delta\Delta p < 0.001$.

Catalpol Promoted the Differentiation of OPCs *In Vitro* via the NOTCH1 Signaling Pathway

To investigate whether the NOTCH1 signaling pathway can influence the differentiation of OPCs, OPCs were seeded in 6-well plates and treated with 40 μM catalpol in the absence or presence of the NOTCH1 signaling pathway agonist JAGGED1 polypeptide for 48 h. Treatment with 5 μM JAGGED1 for 24 h blocked the formation of MBP⁺ OLs, and the addition of catalpol reversed this effect (Figure 11F). The protein levels of NICD1, RBPJ, HES1 and HES5 effectively increased in OPCs in the JAGGED1 group (JAG1). The expression of the above indicators was significantly lower in cells treated with catalpol in the presence of JAGGED1 than in cells in JAG1 group (Figures 11A–E). Taken together, our findings indicate that the

stimulation of OL formation by catalpol is in part due to the suppression of the NOTCH1 signaling pathway.

DISCUSSION

Establishment of the CPZ-Induced Demyelination Model

CPZ is a copper ion-chelating agent that targets many metalloenzymes (such as ceruloplasmin), impairs the activity of copper-dependent cytochrome oxidase, and reduces oxidative phosphorylation, leading to degenerative changes in OLs (Cammer, 1999). These changes result in the apoptosis of mature OLs, causing extensive demyelination of the corpus callosum, internal capsule, thalamus and other white matter bundles (Blakemore, 1972; Clarner et al., 2015). However, after

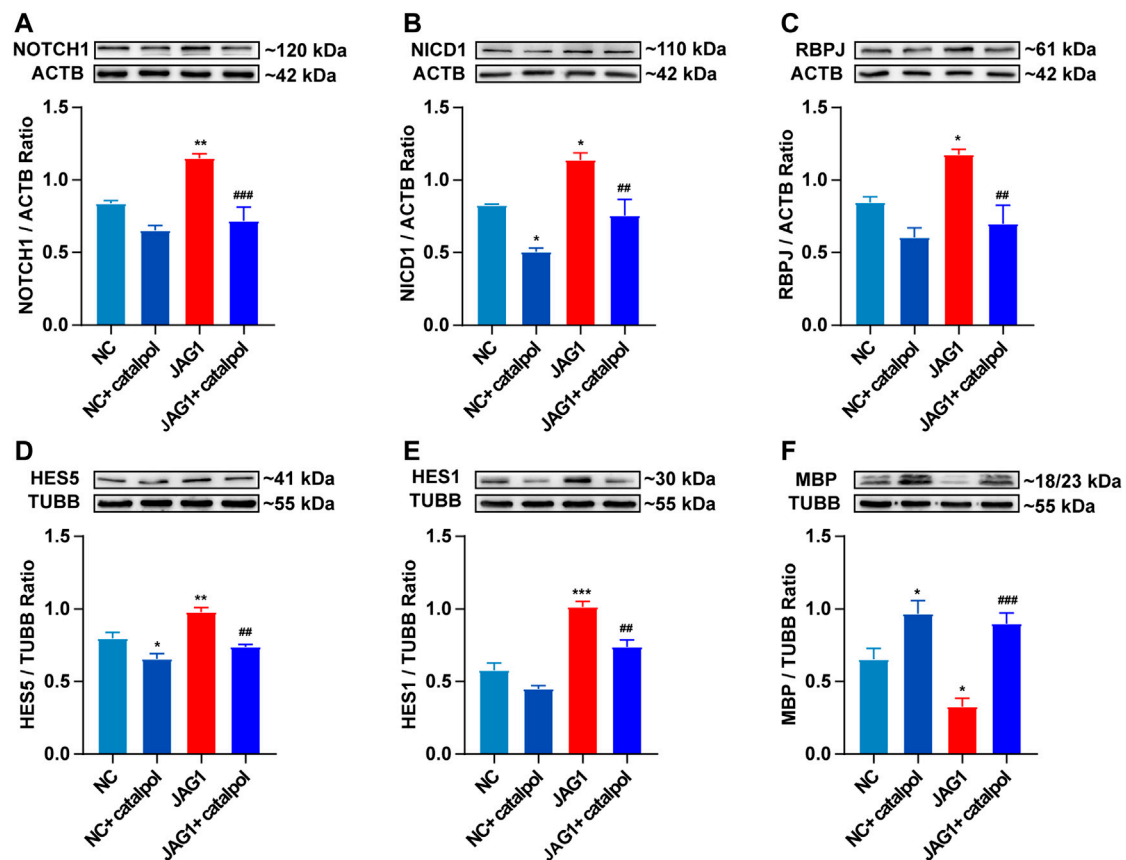


FIGURE 11 | Catalpol promoted the differentiation of OPCs *in vitro* by inhibiting NOTCH1 signaling pathway (A) The expression of NOTCH1 protein in OPCs *in vitro*, (B) the expression of NICD1 protein in OPCs, (C) the expression of RBPJ protein in OPCs, (D) the expression of HES5 protein in OPCs, (E) the expression of HES1 protein in OPCs, (F) the expression of MBP protein in OPCs. The data are expressed as mean \pm SEM of three independent experiments. Compared with NC group, * $p < 0.05$, ** $p < 0.01$, *** $p < 0.001$; compared with JAG1 group, ## $p < 0.01$, ### $p < 0.001$.

CPZ administration is stopped, the myelin protein is re-expressed. Therefore, although pathological changes in autoimmunity observed in MS can be stimulated by the EAE model, the demyelination model induced by the addition of CPZ to the diet, which also mimics the important histological features of demyelinating diseases (van der Star et al., 2012), is the ideal model for researching myelination in MS (Gudi et al., 2014). The exact dosage of CPZ has been determined by several studies. The most common protocol involves feeding 6-to 8-week-old mice with 0.2% CPZ for 5–6 weeks (Vega-Riquer et al., 2019). When 0.2%–0.6% CPZ is mixed with standard rodent food, a significant decrease in myelin protein is observed (Carlton, 1967). Studies have shown that increasing the dose of CPZ from 0.2% to 0.3% can significantly increase the degree of demyelination (Lindner et al., 2008) but increases the mortality rate of mice by more than 5%–10% (Torkildsen et al., 2008). Therefore, 0.2% CPZ is the most suitable concentration because it can cause extensive demyelination and fewer side effects (Liñares et al., 2006; Hesse et al., 2010; Skripuletz et al., 2011).

This experiment mainly studied the effect of catalpol on promoting myelination and neuroprotection, so the CPZ-induced demyelination model was selected. The results showed

that after mice were fed a special diet containing 0.2% CPZ for 5 weeks, the mice exhibited a substantial decrease in weight, deficits in motor ability, and a reduction in LFB staining of myelin in the corpus callosum. The lamellar structure of the myelin sheath was obviously loose and separated, and the G-ratio value was increased. We found that after the demyelinated mice were fed a normal diet for 3 weeks beginning during the 6th week, the weights and motor abilities of the mice slowly recovered, LFB staining of myelin in the corpus callosum increased, and the loosening of the myelin layers decreased, indicating that some myelin sheaths had regenerated.

Neuroprotective Effects of Catalpol

When demyelinating injury occurs in MS, the damaged myelin fragments activate the immune inflammatory response and recruit a large amount of infiltrating immune inflammatory cells. Excessive inflammatory responses cause neuronal damage and severe neurological dysfunction in MS patients (Paganin and Ferrando, 2011). Catalpol exerts a strong neuroprotective effect and improves neurocognitive function (Xia et al., 2017) by reducing the level of proinflammatory cytokines and reducing oxidative stress in the nervous system,

thereby slowing chronic inflammation and neurodegeneration (Wang et al., 2019). Previous studies have found that catalpol decreases immune inflammation and improves nerve damage in EAE mice (Yang et al., 2017). The results of this experiment revealed that at different doses, catalpol slowed the loss of myelin and the loosening of the myelin structure in the corpus callosum in mice, improved the body weight of the mice and increased the time spent on the rod by the mice in the rotarod test, showing that catalpol exerts good neuroprotective effects in mice with CPZ-induced demyelination. Catalpol had a better effect at 40 mg/kg and 80 mg/kg than at 20 mg/kg.

Catalpol Promoted Remyelination

When demyelination occurs, axonal conduction is blocked (Waxman, 1977), and this effect is closely related to the functional defects observed after inflammatory demyelination in MS patients (Smith and McDonald, 1999; Jenkins et al., 2010). Therefore, prevention of demyelination and promotion of remyelination are the basic neuroprotective strategies for MS (Plemel et al., 2017; Villoslada and Steinman, 2020). In the mouse model of CPZ-induced demyelination, the regeneration of myelin in the injured area is closely related to functional recovery (Mozafari et al., 2010), which is extensive and rapid. The proliferation and recruitment of OPCs after injury to the mature CNS is very effective. Neural stem cells or progenitor cells from the subependymal zone rapidly produce OPCs that contribute to myelination (Xing et al., 2014), and OLs newly formed by OPCs undergo remyelination (Crawford et al., 2016). Studies have shown that the change between the average density of OPCs in chronically damaged sites in MS and normal sites is not obvious, which indicates that the number of OPCs may not be the limiting factor for remyelination in chronic injury, proving the importance of the differentiation of OPCs during remyelination (Hughes et al., 2013).

During the process of myelination in MS, OLIG2 acts as a cell transcription factor throughout the differentiation of OL lineage cells and can simultaneously label OPCs and OLs. The experimental results showed that the expression of OLIG2 in the corpus callosum increased slightly in all demyelinated mice, but there was no significant difference between the groups, indicating that OPCs in the demyelinated area were not lacking. CNPase is expressed in the middle stage of differentiation, while MBP is a marker of mature OLs. Early *in vitro* studies have found that catalpol increases the expression of OLIG1 in isolated OPCs and promotes the differentiation and maturation of OPCs (Yuan et al., 2015). This experiment revealed that catalpol increased the number of CNPase⁺/OLIG2⁺ and MBP⁺/OLIG2⁺ cells in the demyelination site and that 40 μ M catalpol promoted the differentiation of OPCs *in vitro*. The results provide an objective basis for catalpol to promote myelination.

Catalpol Promoted Remyelination by Regulating the NOTCH1 Signaling Pathway

In MS, remyelination is always insufficient. The failure of myelination appears to be the result of a variety of pathological processes that interfere with the maturation of OPCs. The activation of the NOTCH1 signaling pathway is one of these processes (Mathieu

et al., 2019). It has been reported that the NOTCH1 signaling axis is activated in response to TGF- β in the brains of MS patients and in cocultured astrocytes and OPCs *in vitro*. As in normal development, JAGGED1 is expressed in astrocytes and neurons in chronic demyelinating lesions, and the receptor NOTCH1 on OPCs combines with activated JAGGED1 and undergoes a conformational change. Subsequently, ADAM metalloprotease mediates the first protein cleavage, producing an intermediate protein hydrolysate called Notch EXtracellular Truncation (NEXT). NEXT is the substrate for the γ -secretase complex, which releases NICD. NICD passes through the cytoplasm from the inner membrane of the plasma membrane to the nucleus. In the cell nucleus, after NICD combines with RBPJ, RBPJ is converted into a transcription activator that recruits acetyltransferase p300 and activates the downstream transcription factors HES1 and HES5 (Tamura et al., 1995). The transcription factors HES1 and HES5 inhibit the maturation of OPCs and maintain their differentiation status. Therefore, blocking NOTCH1 signaling may enhance remyelination.

In EAE mice, the γ -secretase inhibitor MW167 can effectively inhibit the NOTCH1 pathway and promote remyelination (Jurynczyk et al., 2008). In mice with focal demyelination caused by injection of lysophosphatidylcholine, specific knockout of *NOTCH1* in OPCs can significantly improve myelin repair (Zhang et al., 2009). *NOTCH1* siRNA can obviously promote OPC differentiation and promote remyelination to improve the symptoms of nerve injury in CPZ mice (Fan et al., 2018). The above studies revealed that inhibiting the NOTCH1 signaling pathway can improve the disease pathology of MS in animal models and enhance the regeneration of the myelin sheath. Other studies have found that when the expression of jagged1 in astrocytes is induced by TGF β 1, OL differentiation increases (Zhang et al., 2010). Adding 10 μ M DAPT (a γ -secretase inhibitor) to an OPC and astrocyte coculture system for 6 h can significantly inhibit the expression of NICD and promote cell differentiation (Wang et al., 2017). This study showed that *in vivo*, catalpol significantly promoted remyelination in CPZ-treated mice and decreased the expression of the NOTCH1 signaling pathway proteins JAGGED1, NOTCH1, NICD1, and RBPJ and the downstream target genes *Hes1* and *Hes5* and 80 mg/kg catalpol had the best therapeutic effect. Multiple studies have proven that inhibition of the NOTCH1 signaling pathway can promote the differentiation and maturation of OPCs *in vivo* and *in vitro* and promote the remyelination of demyelinated mice. Furthermore, this study revealed that the NOTCH1 pathway is strongly activated in OPCs upon treatment with 5 μ M JAGGED1 polypeptide for 24 h. The number of MBP⁺ cells was also significantly reduced. Treatment with 40 μ M catalpol for 48 h greatly reversed this effect. Catalpol (40 μ M) downregulated the expression of NOTCH1 pathway-related proteins, such as NOTCH1, NICD1, RBPJ, HES1, and HES5, and promoted the differentiation of OPCs. Therefore, our results clearly indicated that the effect of catalpol in promoting remyelination may be related to downregulation of the expression of NOTCH1 signaling pathway-related indicators.

In conclusion, catalpol exerts obvious neuroprotective effects in mice with CPZ-induced demyelination, promoting remyelination. Its mechanism may involve regulation of the NOTCH1 signaling pathway. However, further in-depth exploration of the mechanism is required.

DATA AVAILABILITY STATEMENT

The original contributions presented in the study are included in the article/Supplementary Material, further inquiries can be directed to the corresponding author.

ETHICS STATEMENT

The animal study was reviewed and approved by the Animal Experiments and Experimental Animal Welfare Committee of Capital Medical University (AEEI-2015-185).

REFERENCES

- Blakemore, W. F. (1972). Observations on oligodendrocyte degeneration, the resolution of status spongiosus and remyelination in cuprizone intoxication in mice. *J. Neurocytol.* 1 (4), 413–426. doi:10.1007/BF01102943
- Brosnan, C. F., and Raine, C. S. (2013). The astrocyte in multiple sclerosis revisited. *Glia* 61 (4), 453–465. doi:10.1002/glia.22443
- Cammer, W. (1999). The neurotoxicant, cuprizone, retards the differentiation of oligodendrocytes *in vitro*. *J. Neurol. Sci.* 168 (2), 116–120. doi:10.1016/s0022-510x(99)00181-1
- Carlton, W. W. (1967). Studies on the induction of hydrocephalus and spongy degeneration by cuprizone feeding and attempts to antidote the toxicity. *Life Sci.* 6 (1), 11–19. doi:10.1016/0024-3205(67)90356-6
- Chitnis, A., Henrique, D., Lewis, J., Ish-Horowicz, D., and Kintner, C. (1995). Primary neurogenesis in *Xenopus* embryos regulated by a homologue of the *Drosophila* neurogenic gene Delta. *Nature* 375 (6534), 761–766. doi:10.1038/375761a0
- Clarner, T., Janssen, K., Nellessen, L., Stangel, M., Skripuletz, T., Krauspe, B., et al. (2015). CXCL10 triggers early microglial activation in the cuprizone model. *J. Immunol.* 194 (7), 3400–3413. doi:10.4049/jimmunol.1401459
- Colombo, E., and Farina, C. (2016). Astrocytes: key regulators of neuroinflammation. *Trends Immunol.* 37 (9), 608–620. doi:10.1016/j.it.2016.06.006
- Crawford, A. H., Tripathi, R. B., Foerster, S., McKenzie, I., Kougioumtzidou, E., Grist, M., et al. (2016). Pre-existing mature oligodendrocytes do not contribute to remyelination following toxin-induced spinal cord demyelination. *Am. J. Pathol.* 186 (3), 511–516. doi:10.1016/j.ajpath.2015.11.005
- Faissner, S., Plemel, J. R., Gold, R., and Yong, V. W. (2019). Progressive multiple sclerosis: from pathophysiology to therapeutic strategies. *Nat. Rev. Drug Discov.* 18 (12), 905–922. doi:10.1038/s41573-019-0035-2
- Fan, H., Zhao, J. G., Yan, J. Q., Du, G. Q., Fu, Q. Z., Shi, J., et al. (2018). Effect of Notch1 gene on remyelination in multiple sclerosis in mouse models of acute demyelination. *J. Cell Biochem.* 119 (11), 9284–9294. doi:10.1002/jcb.27197
- Farina, C., Aloisi, F., and Meinel, E. (2007). Astrocytes are active players in cerebral innate immunity. *Trends Immunol.* 28 (3), 138–145. doi:10.1016/j.it.2007.01.005
- Fortini, M. E. (2009). Notch signaling: the core pathway and its posttranslational regulation. *Dev. Cell.* 16 (5), 633–647. doi:10.1016/j.devcel.2009.03.010
- Gouvêa-Junqueira, D., Falvella, A. C. B., Antunes, A. S. L. M., Seabra, G., Bran-dão-Teles, C., Martins-de-Souza, D., et al. (2020). Novel treatment strategies targeting myelin and oligodendrocyte dysfunction in schizophrenia. *Front. Psychiatry* 11, 379. doi:10.3389/fpsy.2020.00379
- Gudi, V., Gingele, S., Skripuletz, T., and Stangel, M. (2014). Glial response during cuprizone-induced de- and remyelination in the CNS: lessons learned. *Front. Cell. Neurosci.* 8, 73. doi:10.3389/fncel.2014.00073
- Hesse, A., Wagner, M., Held, J., Brück, W., Salinas-Riester, G., Hao, Z., et al. (2010). In toxic demyelination oligodendroglial cell death occurs early and is FAS independent. *Neurobiol. Dis.* 37 (2), 362–369. doi:10.1016/j.nbd.2009.10.016
- Hughes, E. G., Kang, S. H., Fukaya, M., and Bergles, D. E. (2013). Oligodendrocyte progenitors balance growth with self-repulsion to achieve homeostasis in the adult brain. *Nat. Neurosci.* 16 (6), 668–676. doi:10.1038/nn.3390
- Jenkins, T., Ciccarelli, O., Toosy, A., Miszkil, K., Wheeler-Kingshott, C., Altmann, D., et al. (2010). Dissecting structure-function interactions in acute optic neuritis to investigate neuroplasticity. *Hum. Brain Mapp.* 31 (2), 276–286. doi:10.1002/hbm.20863
- Jurasic, M. J., Basic, K. V., and Zavoreo, I. (2019). Multiple sclerosis and Fabry disease-diagnostic "mixup". *Mult. Scler. Relat. Disord.* 34, 112–115. doi:10.1016/j.msard.2019.06.008
- Jurynczyk, M., Jurewicz, A., Bielecki, B., Raine, C. S., and Selmaj, K. (2008). Overcoming failure to repair demyelination in EAE: gamma-secretase inhibition of Notch signaling. *J. Neurol. Sci.* 265 (1-2), 5–11. doi:10.1016/j.jns.2007.09.007
- Katsara, M., and Apostolopoulos, V. (2018). Editorial: multiple sclerosis: pathogenesis and therapeutics. *Med. Chem.* 14 (2), 104–105. doi:10.2174/157340641402180206092504
- Kovall, R. A., Gebelein, B., Sprinzak, D., and Kopan, R. (2017). The canonical Notch signaling pathway: structural and biochemical insights into shape, sugar, and force. *Dev. Cell.* 41 (3), 228–241. doi:10.1016/j.devcel.2017.04.001
- Liddel, S. A., Guttenplan, K. A., Clarke, L. E., Bennett, F. C., Bohlen, C. J., Schirmer, L., et al. (2017). Neurotoxic reactive astrocytes are induced by activated microglia. *Nature* 541 (7638), 481–487. doi:10.1038/nature21029
- Liñares, D., Taconis, M., Mañá, P., Correcha, M., Fordham, S., Staykova, M., et al. (2006). Neuronal nitric oxide synthase plays a key role in CNS demyelination. *J. Neurosci.* 26 (49), 12672–12681. doi:10.1523/JNEUROSCI.0294-06.2006
- Lindner, M., Heine, S., Haastert, K., Garde, N., Fokuhl, J., Linsmeier, F., et al. (2008). Sequential myelin protein expression during remyelination reveals fast and efficient repair after central nervous system demyelination. *Neuropathol. Appl. Neurobiol.* 34 (1), 105–114. doi:10.1111/j.1365-2990.2007.00879.x
- Liu, J., He, Q. J., Zou, W., Wang, H. X., Bao, Y. M., Liu, Y. X., et al. (2006). Catalpol increases hippocampal neuroplasticity and up-regulates PKC and BDNF in the aged rats. *Brain Res.* 1123 (1), 68–79. doi:10.1016/j.brainres.2006.09.058
- Mathieu, P. A., Almeida, G. M., Rodríguez, D., Gómez, P. L., Calcagno, M. L., and Adamo, A. M. (2019). Demyelination-remyelination in the central nervous system: ligand-dependent participation of the Notch signaling pathway. *Toxicol. Sci.* 6, kfz130. doi:10.1093/toxsci/kfz130
- Mayo, L., Quintana, F. J., and Weiner, H. L. (2012). The innate immune system in demyelinating disease. *Immunol. Rev.* 248 (1), 170–187. doi:10.1111/j.1600-065X.2012.01135.x
- McQuarrel, J. L., and Bernard, C. C. (2007). Multiple sclerosis: a battle between destruction and repair. *J. Neurochem.* 100 (2), 295–306. doi:10.1111/j.1471-4159.2006.04232.x
- Mozafari, S., Sherfat, M. A., Javan, M., Mirnajafi-Zadeh, J., and Tiraihi, T. (2010). Visual evoked potentials and MBP gene expression imply endogenous myelin repair in adult rat optic nerve and chiasm following local lysolecithin induced demyelination. *Brain Res.* 1351, 50–56. doi:10.1016/j.brainres.2010.07.026
- Paganin, M., and Ferrando, A. (2011). Molecular pathogenesis and targeted therapies for NOTCH1-induced T-cell acute lymphoblastic leukemia. *Blood Rev.* 25 (2), 83–90. doi:10.1016/j.blre.2010.09.004
- Plemel, J. R., Liu, W. Q., and Yong, V. W. (2017). Remyelination therapies: a new direction and challenge in multiple sclerosis. *Nat. Rev. Drug Discov.* 16 (9), 617–634. doi:10.1038/nrd.2017.115

AUTHOR CONTRIBUTIONS

YS and LW designed this study. YS and JJ performed the experiments. YS, ZZ, and LW analyzed the data. YS wrote the manuscript. HZ, BX, LJ and YS revised the manuscript. All authors approved the final manuscript. LW supported the funding.

FUNDING

The study was supported by the National Natural Science Foundation of China (81873252, 81573898) and Beijing Natural Science Foundation (No. 7182020).

- Ponath, G., Ramanan, S., Mubarak, M., Housley, W., Lee, S., Sahinkaya, F. R., et al. (2017). Myelin phagocytosis by astrocytes after myelin damage promotes lesion pathology. *Brain* 140 (2), 399–413. doi:10.1093/brain/aww298
- Skipuletz, T., Gudi, V., Hackstette, D., and Stangel, M. (2011). De- and remyelination in the CNS white and grey matter induced by cuprizone: the old, the new, and the unexpected. *Histol. Histopathol.* 26 (12), 1585–1597. doi:10.14670/HH-26.1585
- Smith, K. J., and McDonald, W. I. (1999). The pathophysiology of multiple sclerosis: the mechanisms underlying the production of symptoms and the natural history of the disease. *Philos. Trans. R. Soc. Lond. B. Biol. Sci.* 354 (1390), 1649–1673. doi:10.1098/rstb.1999.0510
- Stanojlovic, M., Pang, X., Lin, Y., Stone, S., Cvetanovic, M., and Lin, W. (2016). Inhibition of vascular endothelial growth factor receptor 2 exacerbates loss of lower motor neurons and axons during experimental autoimmune encephalomyelitis. *PLoS One* 11 (7), e0160158. doi:10.1371/journal.pone.0160158
- Tamura, K., Taniguchi, Y., Minoguchi, S., Sakai, T., Tun, T., Furukawa, T., et al. (1995). Physical interaction between a novel domain of the receptor Notch and the transcription factor RBP-J kappa/Su(H). *Curr. Biol.* 5 (12), 1416–1423. doi:10.1016/s0960-9822(95)00279-x
- Torkildsen, O., Brunborg, L. A., Myhr, K. M., and Bø, L. (2008). The cuprizone model for demyelination. *Acta Neurol. Scand., Suppl.* 188, 72–76. doi:10.1111/j.1600-0404.2008.01036.x
- van der Star, B. J., Vogel, D. Y., Kipp, M., Puentes, F., Baker, D., and Amor, S. (2012). *In vitro* and *in vivo* models of multiple sclerosis. *CNS Neurol. Disord. Drug Targets* 11 (5), 570–588. doi:10.2174/187152712801661284
- Vega-Riquer, J. M., Mendez-Victoriano, G., Morales-Luckie, R. A., and Gonzalez-Perez, O. (2019). Five decades of cuprizone, an updated model to replicate demyelinating diseases. *Curr. Neuropharmacol.* 17 (2), 129–141. doi:10.2174/1570159X15666170717120343
- Villoslada, P., and Steinman, L. (2020). New targets and therapeutics for neuroprotection, remyelination and repair in multiple sclerosis. *Expert Opin. Investig. Drugs* 29 (5), 443–459. doi:10.1080/13543784.2020.1757647
- Wan, D., Xue, L., Zhu, H., and Luo, Y. (2013). Catalpol induces neuroprotection and prevents memory dysfunction through the cholinergic system and BDNF. *Evid. Based Complement Alternat. Med.* 2013, 134852. doi:10.1155/2013/134852
- Wang, C., Zhang, C. J., Martin, B. N., Bulek, K., Kang, Z., Zhao, J., et al. (2017). IL-17 induced NOTCH1 activation in oligodendrocyte progenitor cells enhances proliferation and inflammatory gene expression. *Nat. Commun.* 8, 15508. doi:10.1038/ncomms15508
- Wang, J., Cui, Y., Feng, W., Zhang, Y., Wang, G., Wang, X., et al. (2014). Involvement of the central monoaminergic system in the antidepressant-like effect of catalpol in mice. *Biosci. Trends.* 8 (5), 248–252. doi:10.5582/bst.2014.01029
- Wang, J. M., Yang, L. H., Zhang, Y. Y., Niu, C. L., Cui, Y., Feng, W. S., et al. (2015). BDNF and COX-2 participate in anti-depressive mechanisms of catalpol in rats undergoing chronic unpredictable mild stress. *Physiol. Behav.* 151, 360–368. doi:10.1016/j.physbeh.2015.08.008
- Wang, L. Y., Yu, X., Li, X. X., Zhao, Y. N., Wang, C. Y., Wang, Z. Y., et al. (2019). Catalpol exerts a neuroprotective effect in the MPTP mouse model of Parkinson's disease. *Front. Aging Neurosci.* 11, 316. doi:10.3389/fnagi.2019.00316
- Wang, Z., Liu, Q., Zhang, R., Liu, S., Xia, Z., and Hu, Y. (2009). Catalpol ameliorates beta amyloid-induced degeneration of cholinergic neurons by elevating brain-derived neurotrophic factors. *Neuroscience* 163 (4), 1363–1372. doi:10.1016/j.neuroscience.2009.07.041
- Waxman, S. G. (1977). Conduction in myelinated, unmyelinated, and demyelinated fibers. *Arch. Neurol.* 34 (10), 585–589. doi:10.1001/archneur.1977.00500220019003
- Wettstein, D. A., Turner, D. L., and Kintner, C. (1997). The *Xenopus* homolog of *Drosophila* Suppressor of Hairless mediates Notch signaling during primary neurogenesis. *Development* 124 (3), 693–702.
- Xia, Z., Wang, F., Zhou, S., Zhang, R., Wang, F., Huang, J. H., et al. (2017). Catalpol protects synaptic proteins from beta-amyloid induced neuron injury and improves cognitive functions in aged rats. *Oncotarget* 8 (41), 69303–69315. doi:10.18632/oncotarget.17951
- Xing, Y. L., Röth, P. T., Stratton, J. A., Chuang, B. H., Danne, J., Ellis, S. L., et al. (2014). Adult neural precursor cells from the subventricular zone contribute significantly to oligodendrocyte regeneration and remyelination. *J. Neurosci.* 34 (42), 14128–14146. doi:10.1523/JNEUROSCI.3491-13.2014
- Xu, G., Xiong, Z., Yong, Y., Wang, Z., Ke, Z., Xia, Z., et al. (2010). Catalpol attenuates MPTP induced neuronal degeneration of nigral-striatal dopaminergic pathway in mice through elevating glial cell derived neurotrophic factor in striatum. *Neuroscience* 167 (1), 174–184. doi:10.1016/j.neuroscience.2010.01.048
- Yang, T., Zheng, Q., Wang, S., Fang, L., Liu, L., Zhao, H., et al. (2017). Effect of catalpol on remyelination through experimental autoimmune encephalomyelitis acting to promote Olig1 and Olig2 expressions in mice. *BMC Complement Altern. Med.* 17 (1), 240. doi:10.1186/s12906-017-1642-2
- Yuan, C. X., Chu, T., Liu, L., Li, H. W., Wang, Y. J., Guo, A. C., et al. (2015). Catalpol induces oligodendrocyte precursor cell-mediated remyelination *in vitro*. *Am. J. Transl. Res.* 7 (11), 2474–2481.
- Zhang, Y., Argaw, A. T., Gurfein, B. T., Zameer, A., Snyder, B. J., Ge, C., et al. (2009). Notch1 signaling plays a role in regulating precursor differentiation during CNS remyelination. *Proc. Natl. Acad. Sci. U.S.A.* 106 (45), 19162–19167. doi:10.1073/pnas.0902834106
- Zhang, Y., Zhang, J., Navrazhina, K., Argaw, A. T., Zameer, A., Gurfein, B. T., et al. (2010). TGFbeta1 induces Jagged1 expression in astrocytes via ALK5 and Smad3 and regulates the balance between oligodendrocyte progenitor proliferation and differentiation. *Glia* 58 (8), 964–974. doi:10.1002/glia.20978

Conflict of Interest: The authors declare that the research was conducted in the absence of any commercial or financial relationships that could be construed as a potential conflict of interest.

Copyright © 2021 Sun, Ji, Zha, Zhao, Xue, Jin and Wang. This is an open-access article distributed under the terms of the Creative Commons Attribution License (CC BY). The use, distribution or reproduction in other forums is permitted, provided the original author(s) and the copyright owner(s) are credited and that the original publication in this journal is cited, in accordance with accepted academic practice. No use, distribution or reproduction is permitted which does not comply with these terms.



The Combination of *Aquilaria sinensis* (Lour.) Gilg and *Aucklandia costus* Falc. Volatile Oils Exerts Antidepressant Effects in a CUMS-Induced Rat Model by Regulating the HPA Axis and Levels of Neurotransmitters

OPEN ACCESS

Edited by:

Vincent Kam Wai Wong,
Macau University of Science and
Technology, Macau

Reviewed by:

Sookja Chung,
Macau University of Science and
Technology, Macau
Qiong Liu,
Fudan University, China
Xinmin Liu,
Chinese Academy of Medical
Sciences and Peking Union Medical
College, China

*Correspondence:

Ming Yang
mingyang26@126.com
Xiaoying Huang
8842100@qq.com

Specialty section:

This article was submitted to
Ethnopharmacology,
a section of the journal
Frontiers in Pharmacology

Received: 06 October 2020

Accepted: 31 December 2020

Published: 24 February 2021

Citation:

Li H, Li Y, Zhang X, Ren G, Wang L,
Li J, Wang M, Ren T, Zhao Y, Yang M
and Huang X (2021) The Combination
of *Aquilaria sinensis* (Lour.) Gilg and
Aucklandia costus Falc. Volatile Oils
Exerts Antidepressant Effects in a
CUMS-Induced Rat Model by
Regulating the HPA Axis and
Levels of Neurotransmitters.
Front. Pharmacol. 11:614413.
doi: 10.3389/fphar.2020.614413

Huiling Li¹, Yuanhui Li², Xiaofei Zhang³, Guilin Ren⁴, Liangfeng Wang², Jianzhe Li²,
Mengxue Wang², Tao Ren², Yi Zhao³, Ming Yang^{1,2*} and Xiaoying Huang^{2*}

¹College of Pharmacy, Chengdu University of traditional Chinese Medicine, Chengdu, China, ²Ministry of Education, Key Laboratory of Modern Preparation of Traditional Chinese Medicine, Jiangxi University of Traditional Chinese Medicine, Nanchang, China, ³College of Pharmacy, Shaanxi University of Chinese Medicine, Xianyang, China, ⁴Southwest Medical University Affiliated Hospital of Traditional Chinese Medicine, Luzhou, China

The *Aquilaria sinensis* (Lour.) Gilg (CX)–*Aucklandia costus* Falc. (MX) herbal pair is frequently used in traditional Chinese medicine prescriptions for treating depression. The volatile oil from CX and MX has been shown to have good pharmacological activities on the central nervous system, but its curative effect and mechanism in the treatment of depression are unclear. Therefore, the antidepressant effect of the volatile oil from CX–MX (CMVO) was studied in chronic unpredictable mild stress (CUMS) rats. The suppressive effects of CMVO (25, 50, 100 μ L/kg) against CUMS-induced depression-like behavior were evaluated using the forced swimming test (FST), open field test (OFT) and sucrose preference test (SPT). The results showed that CMVO exhibited an antidepressant effect, reversed the decreased sugar preference in the SPT and prolongation of immobility time in the FST induced by CUMS, increased the average speed, time to enter the central area, total moving distance, and enhanced the willingness of rats to explore the environment in the OFT. Inhalational administration of CMVO decreased levels of adrenocorticotrophic hormone and corticosterone in serum and the expression of corticotropin-releasing hormone mRNA in the hypothalamus, which indicated regulation of over-activation of the hypothalamic–pituitary–adrenal (HPA) axis. In addition, CMVO restored levels of 5-hydroxytryptamine (5-HT), dopamine, norepinephrine and acetylcholine in the hippocampus. The RT-PCR and immunohistochemistry results showed that CMVO up-regulated the expression of 5-HT_{1A} mRNA. This study demonstrated the antidepressant effect of CMVO in CUMS rats, which was possibly mediated via modulation of monoamine and cholinergic neurotransmitters and regulation of the HPA axis.

Keywords: *Aquilaria sinensis* (Lour.) Gilg, *Aucklandia costus* Falc., volatile oil, depression, chronic unpredictable mild stress, monoamine neurotransmitter, hypothalamic-pituitary-adrenal axis, cholinergic neurotransmitter

INTRODUCTION

Depression is an emotional rhythm disorder that has significant and lasting depressed mood as the main symptom (Difrancesco et al., 2019). It may be accompanied by insomnia, addiction, neurodegenerative diseases and other complications (Chen et al., 2019), and it seriously affects the physical and mental health of patients. The incidence of depression is increasing year by year. Currently, about 15% of people in the world are suffering from depression (Global Burden of Disease Study 2013, Collaborators, 2015). The World Health Organization predicted that it will become the second leading cause of disability after heart disease by 2020 (Holden, 2000). Based on the monoamine neurotransmitter deficiency hypothesis, the commonly used antidepressants are mainly chemical medicines such as selective serotonin reuptake inhibitors or norepinephrine reuptake inhibitors. However, these medicines have shortcomings that include poor curative effect, long duration of treatment and recurrence after drug withdrawal, and adverse reactions such as sexual dysfunction, nausea, tremor and insomnia (Zhuo et al., 2020). Studies (Antunes et al., 2015; Li et al., 2020b) have shown that one-third of patients do not respond to initial treatment, and almost half have only a secondary response. Therefore, it is very meaningful to look for natural medicines with better curative effects and suitability. Many studies have shown that volatile oils from aromatic herbs are potential natural medicines for the treatment of depression.

Aromatic herbs mainly contain volatile components, which are considered by traditional Chinese medicine (TCM) to relieve anxiety and other complications such as insomnia caused by depression. Fragrant traditional Chinese herbs have historically been used to regulate emotion and relieve depressive symptoms (Chen et al., 2019; Li et al., 2020a). Recent studies have shown that the volatile oils of clove (Mehta et al., 2013), fennel (Perveen et al., 2017), Cang-ai compound (Chen et al., 2019) and other aromatic traditional Chinese herbs can exert antidepressant effects by regulating the levels of monoamine neurotransmitters and activity of the hypothalamic-pituitary-adrenal (HPA) axis, or by improving immune function. Similarly, aromatherapy is also widely used in Western countries, exemplified by the use of lavender volatile oil to treat depression (López et al., 2017). Compared with other chemical components, volatile components more easily pass through the blood-brain barrier, which is advantageous in the treatment of central nervous system diseases (Zheng et al., 2018). Aromatherapy is not only effective, but also provides a pleasant treatment experience. It has unique advantages and broad development prospects for depression and other emotion-related chronic diseases.

Depression has complex etiologies and complications, so drug combinations are often used for treatment to exploit synergistic effects, improve efficacy or reduce adverse reactions, such as the combination of fluoxetine and olanzapine (Brunner et al., 2014).

There is a similar mode of drug use in TCM, the herbal pair, which is the simplest form of compatibility in traditional Chinese herbal medicine (Wang et al., 2019b). *Aquilaria sinensis* (Lour.) Gilg (Chen-Xiang, CX) and *Aucklandia costus* Falc. (Mu-Xiang, MX), an ancient and classic herbal pair, has been commonly used to treat Yu-syndrome (Depression and Anxiety) in many traditional prescriptions, such as Er-xiang Powder recorded in “Jiyang Compendium.” Traditional Chinese medicine believes that the main causes of depression are stagnation of liver qi and dysfunction of spleen in transportation. Clinically, herbs with the effects of invigorating the spleen and soothing the liver qi are mainly used to treat depression. CX has the effects of activating qi and relieving pain, warming the stomach and relieving vomiting. It has a long history of clinical application, and is often used as a sedative, analgesic and digestive aid (Tan et al., 2019) in TCM. MX has the effects of invigorating qi and relieving pain, invigorating the spleen and eliminating food. These two herbs relieve depression, indigestion and other symptoms by soothing the liver, regulating qi and recuperating the spleen. Many proprietary Chinese medicines that relieve anxiety and irritability and reduce appetite contain both CX and MX, such as Chen xiang shu yu tablets, Chen xiang shu qi pills and Chen xiang hua qi tablets. Studies have shown that the volatile oil is one of the main active components in these two herbs. It has been demonstrated that the volatile oil from CX exerts antidepressant effects, possibly by inhibition of corticotropin-releasing hormone (CRH) and hyperactivity of the HPA axis (Wang et al., 2018). Other studies have suggested that the volatile oil of MX has potential neuroprotective activities, due to the regulation of apoptotic pathways (Zhao et al., 2016). Its main active ingredient, dehydrocostus lactone, elicited protective effects against hippocampal oxygen-glucose deprivation/reoxygenation injury by inhibiting apoptosis (Zhao et al., 2018). Besides, MX volatile oil and its main components have been proved to have immunosuppressive (Na et al., 2013), gastrointestinal regulation (Dong et al., 2018), anti-inflammatory (Woo et al., 2019) and other pharmacological effects, while CX volatile oil has a variety of pharmacological activities, such as antioxidation (Wang et al., 2018a), sedation (Wang et al., 2017), and anti-inflammation (Gao et al., 2019). However, the mechanism of CMVO in the treatment of depression is still unclear. Thus, it is of great significance to unravel its fundamental mechanisms, which may provide a novel and effective medicine and therapeutic method for depression.

The antidepressant effect of CMVO *in vivo* was therefore investigated in this study. The CUMS depression model is recognized as reliable and practical, and is widely used to study the mechanism of depression (Willner, 1997; Zhuo et al., 2020). Accordingly, body weight assessment, sucrose preference test (SPT), forced swimming test (FST) and open

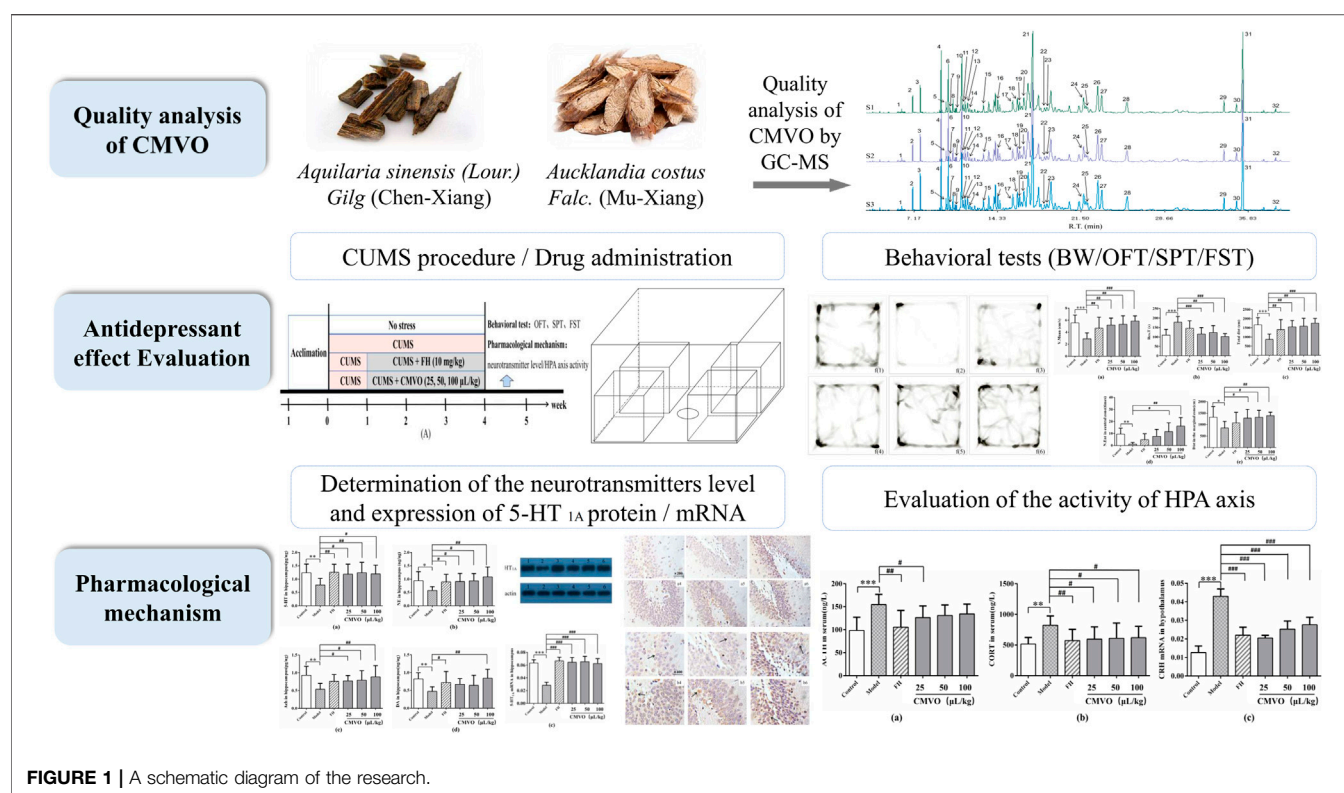


FIGURE 1 | A schematic diagram of the research.

field test (OFT) were executed in CUMS-induced rats to analyze the antidepressant effects of CMVO after inhalational administration. Previously, it was shown that CX volatile oil exerts an antidepressant effect by regulating hyperactivity of the HPA axis (Wang et al., 2018b), while the main active component of MX volatile oil exerts a neuroprotective effect on the hippocampus (Zhao et al., 2018). In addition, abnormal function of the HPA axis and deficiency of hippocampal monoamine neurotransmitters have been implicated in the pathogenesis of depression (Chen et al., 2019; Xing et al., 2019). Therefore, the possible effects of CMVO inhalational administration on depression were studied from the perspective of regulation of the HPA axis and neurotransmitters levels. The technical strategy of this study is shown in Figure 1.

MATERIALS AND METHODS

Animals

All experimental procedures were approved by the Animal Ethics Committee of Jiangxi University of TCM. All efforts were made to minimize suffering and the number of animals used to produce reliable data.

Male Sprague Dawley rats weighing 180–220 g were supplied by Hunan Shrek Jingda Experimental Animal Co., Ltd. (Animal license No.: SCXK (Xiang) 2019-0004). The rats were housed at a constant temperature ($23 \pm 2^\circ\text{C}$), maintained

on a 12 h light/dark cycle (lights on 8:00–20:00) and had free access to food and water. All rats were acclimatized for 7 days before the experiment.

Materials and Reagents

The volatile oil of CX was obtained from Guangzhou Aroma Master Chenxiang Technology Co., Ltd. (Guangzhou, China) and the volatile oil of MX was obtained from Changshengyuan Medicinal Materials Development Co., Ltd. (Mianyang, China). Fluoxetine hydrochloride (FH) was purchased from Lilly Suzhou Pharmaceutical Co., Ltd. (Suzhou, China). The commercial enzyme-linked immunosorbent assay (ELISA) kits for adrenocorticotrophic hormone (ACTH), corticosterone (CORT), 5-hydroxytryptamine (5-HT), dopamine (DA), norepinephrine (NE) and acetylcholine (ACh) were purchased from Jiangsu Enzymatic Immunity Industry Co., Ltd. (Yancheng, China). β -Actin and 5-HT_{1A} antibodies were purchased from Abcam (Cambridge, UK). The reagents (i.e., ethanol, chloroform, isopropanol, H₂O₂ and xylene) were of analytical reagent grade and were obtained from Sinopharm Chemical Reagent Co., Ltd. (Shanghai, China). Horseradish peroxidase (HRP)-conjugated secondary antibodies were obtained from Biyuntian Biotechnology Co., Ltd. (Shanghai, China). The SYBR Green PCR kit was purchased from Thermo Fisher Scientific (China) Co., Ltd. Neutral gum and phosphate buffered saline (PBS) solution were obtained from Beijing Solarbio Science & Technology Co., Ltd. (Beijing, China).

Quality Analysis of ChenXiang-MuXiang Volatile Oil

Gas chromatography-mass spectrometry (GC-MS) was used to control the quality of CMVO. The gas chromatographic conditions were as follows: an Agilent HP-5MS (30 m × 250 μm × 0.25 μm) capillary column was used, the carrier gas was high purity He (99.999%), the sample volume was 1 μL, the shunt ratio was 10:1, and the flow rate was 1 mL/min. The temperature program was as follows: an initial temperature of 70°C, increased by 15°C/min up to 110°C, increased by 7°C/min up to 154°C (held for 5 min), increased by 1°C/min up to 155°C (held for 5 min), increased by 1°C/min up to 157°C (held for 5 min), increased by 2°C/min up to 165°C, and then increased by 10°C/min up to 300°C (held for 5 min). The mass spectrometry conditions were as follows: an EI ion source, the electron energy was 70 eV, the ion source temperature was 230°C, the MS quadrupole temperature was 150°C, the interface temperature was 250°C, the solvent delay was 3.0 min, the quality scan pattern was full scan, and the scan range was 30–650 amu. The chemical components were identified using the NIST 17.0 mass spectrometry database. The retention index (relative to C7–C40 n-alkanes, under the same gas chromatographic conditions) of each compound was calculated and compared with literature values to verify each compound identity.

Chronic Unpredictable Mild Stress Procedure

The CUMS procedure was conducted as previously described (Willner, 1997; Dong et al., 2014) with minor modification. The rats in the control group were housed without interference, and were given food and water normally, except that water was withheld for 24 h before the SPT. The CUMS-induced rats were isolated in individual cages and randomly exposed to various stressors: restraint stress for 45 min, 1.5 min of tail nip (0.5–1 cm from the end of the tail), swimming in cold (4°C) water for 5 min, swimming in hot (40°C) water for 5 min, strange object stimulation, inversion of light/dark cycle for 24 h, food deprivation for 24 h, water deprivation for 24 h, level shaking for 5 min (1 time/s), wet bedding for 24 h (200 mL of water per individual cage to make the bedding wet), odor stimulation (ammonia or acetic acid) or cage tilting for 8 h (45°). The 12 types of stimulation (1 type per day) were applied randomly. Each stimulus appeared discontinuously, and the animals could not predict the occurrence of the stimulation, which lasted for 28 days.

Drug Administration and Treatment

Before the modeling, the body weight and sucrose preference of each rat were tested. According to the results, the rats were divided into 6 groups and ensured that there was no significant difference in body weight and sucrose preference among all groups. The six groups are as follows: control group, CUMS model group, FH group (10 mg/kg), CMVO low, middle and high dose groups (25, 50, 100 μL/kg), with eight rats in each group. The main body of the aromatherapy inhalational administration device consists of a large transparent plexiglass box (measures 80 × 80 × 65 cm, covered) and four small transparent plexiglass boxes (measuring 30 × 30 × 30 cm). The small boxes were evenly

placed at the bottom of the large box, and the aromatherapy atomizer that holds the volatile oil was placed in the middle of the large box. The CMVO was diluted into 10 ml of distilled water and was released into the glass box in the form of spray through an atomizer.

All rats were subjected to CUMS for 1 week (except the blank group), and then the CMVO groups were given aromatherapy for 1 h every day for 3 weeks with the continued CUMS procedure. The control and CUMS groups were given 0.9% saline every day, and the FH group received intragastric administration of FH at a dose of 10 mg/kg, for 3 weeks. The experimental procedure is shown in **Figure 2A** and the aromatherapy box used for administration is shown in **Figure 2B**.

Behavioral Tests

Depression-like behavior in rats was determined using the body weight (BW) test, OFT, SPT and FST.

Sucrose Preference Test and Body Weight

The SPT was carried out with reference to the previous literature (Daodee et al., 2019). The rats were trained to adapt to sucrose solution (1%, w/v) before the test. Two bottles of 1% sugar water were placed in each cage, and one of them was replaced with pure water 24 h later. After adaption, the rats were deprived of water and food for 24 h. Animals were then kept in separate cages with free access to two bottles, one filled with 200 mL sucrose solution (1%, w/v) and the other with 200 mL water. The positions of the bottles were balanced, and the two bottles were interchanged after 30 min to avoid side preference. The test was finished 1 h later and the sucrose preference was calculated by the following formula: sucrose preference (%) = sucrose consumption/(water consumption + sucrose consumption). All rats were weighed before and after treatment, and the BW change was assessed from the week-4 weight minus week-0 weight.

Open Field Test

The OFT was carried out with reference to the previous literature (Yi et al., 2013) with slight modification. The experiment was carried out in a square open black box. The laboratory was kept quiet, with constant light, a room temperature of 24 ± 1°C and humidity of 60–70%. A camera was installed directly above the central area of the black box. The rats were placed in the middle of the open field to explore freely, and the video analysis system was immediately activated to capture video automatically. The measuring time was 5 min for each rat, and the environment in the box was cleared after the end of measurement. The single-subject tracking mode of the system was used to measure average speed (V.mean), rest time (Res.T), number of times to enter the central area (N.Ent), total moving distance (Total dist) and Dist in the marginal zone of each rat.

Forced Swimming Test

The FST was carried out with reference to the previous literature (Wang et al., 2019a). The rats were placed in a cylinder with a height of 46 cm, a diameter of 45 cm, a depth of 41 cm, and a water temperature of 24 ± 1°C. The rats were exposed to a pre-test for 15 min, and the next day underwent the FST. The immobility

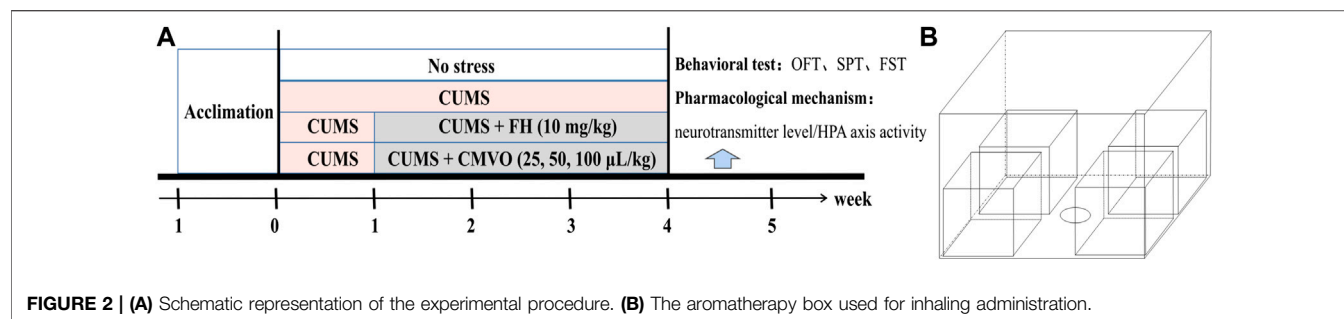


FIGURE 2 | (A) Schematic representation of the experimental procedure. **(B)** The aromatherapy box used for inhaling administration.

time of the rats was observed for 5 min. The immobility time refers to the time it takes for the rats to float in the water without struggling, but only to keep their heads above the surface.

Tissue Preparation

After 28 days of administration, the rats were killed and serum and brain tissue were collected. Blood was collected from the femoral artery, and the serum was separated by centrifugation after 30 min (3500 r/min centrifugation for 10 min at 4°C), and then stored in a refrigerator at -80°C. The hippocampus and hypothalamus of each rat were removed onto ice and stored in a refrigerator at -80°C after freezing with liquid nitrogen.

Quantification of 5-Hydroxytryptamine, Dopamine, Norepinephrine, Acetylcholine in Hippocampus, and Adrenocorticotrophic Hormone and Corticosterone in Serum by Enzyme-Linked Immunosorbent Assay

The rat hippocampi were used to determine the levels of neurotransmitters associated with CUMS-induced depression-like behavior. The serum was used to evaluate activity of the HPA axis associated with CUMS-induced depression-like behavior. The levels of 5-HT, DA, NE and ACh in hippocampus and the levels of ACTH and CORT in serum of rats were measured using ELISA kits. The operation was strictly in accordance with the corresponding instructions, and the concentration was normalized according to the standard curve.

Detection of 5-HT_{1A} Content in Hippocampus by Western Blot

The total protein was extracted from fresh hippocampal tissue. A sample (20 μg) was separated by electrophoresis and transferred onto polyvinylidene difluoride membranes. After blocking with 5% skimmed milk powder at room temperature for 1 h, the membrane was incubated with primary antibody (5-HT_{1A}, 1:1,000) at 4°C overnight, rinsed three times with tris-buffered saline/Tween 20 (TBST) for 5 min, and incubated with HRP-conjugated secondary antibody (1:1,000) for 1 h at 37°C. The membrane was rinsed with TBST for 5 min three times, and then analyzed using a chemiluminescence imaging system. Relative expression of protein = grayscale of target protein band/grayscale of β-actin band. The mean value of the intensity was obtained from three independent experiments.

TABLE 1 | Primer information for the RT-PCR experiment.

Gene name	Primer sequence (5' → 3')
5-HT _{1A}	Primer F: TCTCGCTCACTTGGCTCATTTG Primer R: TCCTGACAGTCTTGCGGATTC
CRH	Primer F: CTCACCTTCCACCTTCTGAG Primer R: GGCCAAGCGCAACATTTTC
β-actin	Primer F: CGGTCAGGTCATCACTATC Primer R: CAGGGCAGTAATCTCCTTC

Detection of 5-HT_{1A} mRNA in Hippocampus and Corticotropin-Releasing Hormone mRNA in Hypothalamus by Reverse Transcription-Polymerase Chain Reaction

The RT-PCR reaction was conducted according to the SYBR Green PCR kit instructions. The expression levels of 5-HT_{1A} mRNA in hippocampus and CRH mRNA in hypothalamus were determined. The sequences of the primers used for real-time PCR are shown in Table 1. The set amplification procedure was as follows: 95°C, 10 min (95°C, 15 s; 55°C, 45 s) × 40; 95°C, 15 s; 60°C, 1 min; 95°C, 15 s; 60°C, 15 s. The data were analyzed by ABI Prism 7300 SDS software and the expression levels of 5-HT_{1A} and CRH mRNA were determined.

Immunohistochemical Detection of 5-HT_{1A} in Hippocampus

The tissues were embedded, fixed and made into sections. Sections were deparaffinized and then hydrated with different concentrations of alcohol in double distilled water. The antigen was retrieved in 0.01 M trisodium citrate buffer and washed with 0.02 M PBS. The sections were incubated with 3% H₂O₂ for 10 min. Non-immune and normal goat serum were added to block non-specific antigen, followed by incubation in a wet box for 30 min at 37°C. The primary antibody was added and incubated overnight at 4°C. The sections were then incubated with HRP-conjugated secondary antibody (goat-anti rabbit) for 1 h at 37°C and visualized with 3,3'-diaminobenzidine. After washing, the sections were counterstained with hematoxylin, differentiated with 0.1% hydrochloric acid-alcohol and observed under a microscope to control the degree of staining. Finally, the sections were dehydrated in alcohol solution at different concentrations, cleared with xylene and sealed with neutral gum. A DM2500B microscope (Leica Corp., Wetzlar, Germany) was used to capture images and analyze the samples.

TABLE 2 | The components of CMVO.

Peak No.	Identification	RT (min)	RI ^a	RI ^b	Area pct
1	Terpinen-4-ol	6.1047	1215	1180	0.154
2	Benzylacetone	7.043	1279	1257	0.9063
3	Anethole	7.6871	1321	/	1.4285
4	β -Elemen	9.4867	1430	1394	3.0074
5	Dihydro- α -ionone	9.9068	1452	1417	0.6224
6	Caryophyllene	10.0958	1462	1446	2.9496
7	trans- α -Bergamotene	10.2709	1471	1433	0.2446
8	Geranylacetone	10.502	1484	/	0.7454
9	Humulene	10.789	1499	1464	0.2634
10	β -Agarofuran	11.2582	1517	/	5.4282
11	β -Ionone	11.3772	1521	1516	0.5671
12	(+)- β -Selinene	11.5382	1527	1509	0.8105
13	(-)- α -Selinene	11.7413	1535	1493	1.2873
14	(3R,5aR,9S,9aS)-2,2,5a,9-Tetramethyloctahydro-2H-3,9a-methanobenzo[b]oxepine	11.9374	1542	/	0.4209
15	α -Elemol	13.1137	1586	1546	0.9187
16	Caryophyllene oxide	14.346	1622	1588	1.1901
17	2-((2S,4aR)-4a,8-Dimethyl-1,2,3,4,4a,5,6,7-octahydronaphthalen-2-yl)propan-2-ol	15.6414	1655	/	2.0584
18	(+)- γ -Eudesmol	16.0405	1665	1633	2.0719
19	Agarospirol	16.2156	1669	1645	1.5116
20	8,8,9,9-Tetramethyl-3,4,5,6,7,8-hexahydro-2H-2,4a-methanonaphthalene	16.5866	1679	/	3.1942
21	Aplotaxene	17.3569	1698	/	13.3124
22	Aromandendrene	18.3652	1716	1826	0.7836
23	α -Costal	18.5682	1720	1767	0.9397
24	(+)-4,11(13)-Eudesmadien-12-ol	21.7261	1774	/	2.5602
25	Phenol,2-ethyl-4,5-dimethyl-	22.0412	1780	/	0.9532
26	Costol	22.9445	1795	1734	5.1089
27	(-)- α -Costol	23.2735	1801	/	3.2934
28	Dehydrofukinone	25.4511	1829	/	2.8459
29	Dihydrodehydrocostus lactone	33.7695	1972	/	1.1565
30	n-Hexadecanoic acid	34.8548	2000	1985	0.9052
31	Dehydrocostus lactone	35.3939	2026	2007	8.5016
32	9-Octadecenoic acid	38.2158	2267	/	0.2981

RI, retention indices; RT, retention time.

^aRI calculated from RTs in relation to those of a series C₇-C₄₀ of n-alkanes.

^bRI from the literatures (Feng et al., 2016; Chen, 2019; Han et al., 2019; Huang et al., 2018; Shang, 2018; Geng, 2020; Song et al., 2020; Sun et al., 2020).

Statistical Analysis

The experimental data were expressed as mean \pm standard error of the mean (SEM) ($\bar{x} \pm s$). The experimental data were statistically analyzed and plotted with SPSS 21.0 (SPSS Inc., Chicago, IL, United States) and GraphPad Prism 6 software (GraphPad Software Inc., San Diego, CA, United States). One-way analysis of variance (ANOVA) was used for comparison between groups, LSD method was used for homogeneity of variance, Games-Howell method was used for heterogeneity of variance, where $p < 0.05$ indicated a significant difference and $p < 0.01$ indicated a very significant difference.

RESULTS

Composition Analysis of ChenXiang-MuXiang Volatile Oil

The components of CMVO were determined by GC-MS. Finally, 32 chemical constituents were identified. The GC-MS chromatogram and the 32 components are shown in **Table 2** and **Figure 3**. The highest content of which is Aplotaxene

(peak21, 13.3124%), followed by Dehydrocostus lactone (peak31, 8.5016%), β -Agarofuran (peak10, 5.4282%), Costol (peak26, 5.1089%), (-)- α -Costol (peak27, 3.2934%), etc. The GC-MS detection results of CMVO were compared with the previous studies, and it was found that Dehydrocostus lactone (peak31), Aplotaxene (peak21), Terpinen-4-ol (peak1), trans- α -Bergamotene (peak7) were the main characteristic components of the MX volatile oil (Yan et al., 2020), while Benzylacetone (peak2) (Miyoshi et al., 2013), β -Agarofuran (peak10), Agarospirol (peak19) were the unique components of CX volatile oil (Monggoot et al., 2018).

Effects of Inhaling ChenXiang-MuXiang Volatile Oil on Depression-like Behavior Induced by Chronic Unpredictable Mild Stress in Rats

The depression-like behavior in CUMS rats was assessed to examine the antidepressant effects of CMVO using the OFT, FST and SPT. The body weights of all rats before and after modeling were measured.

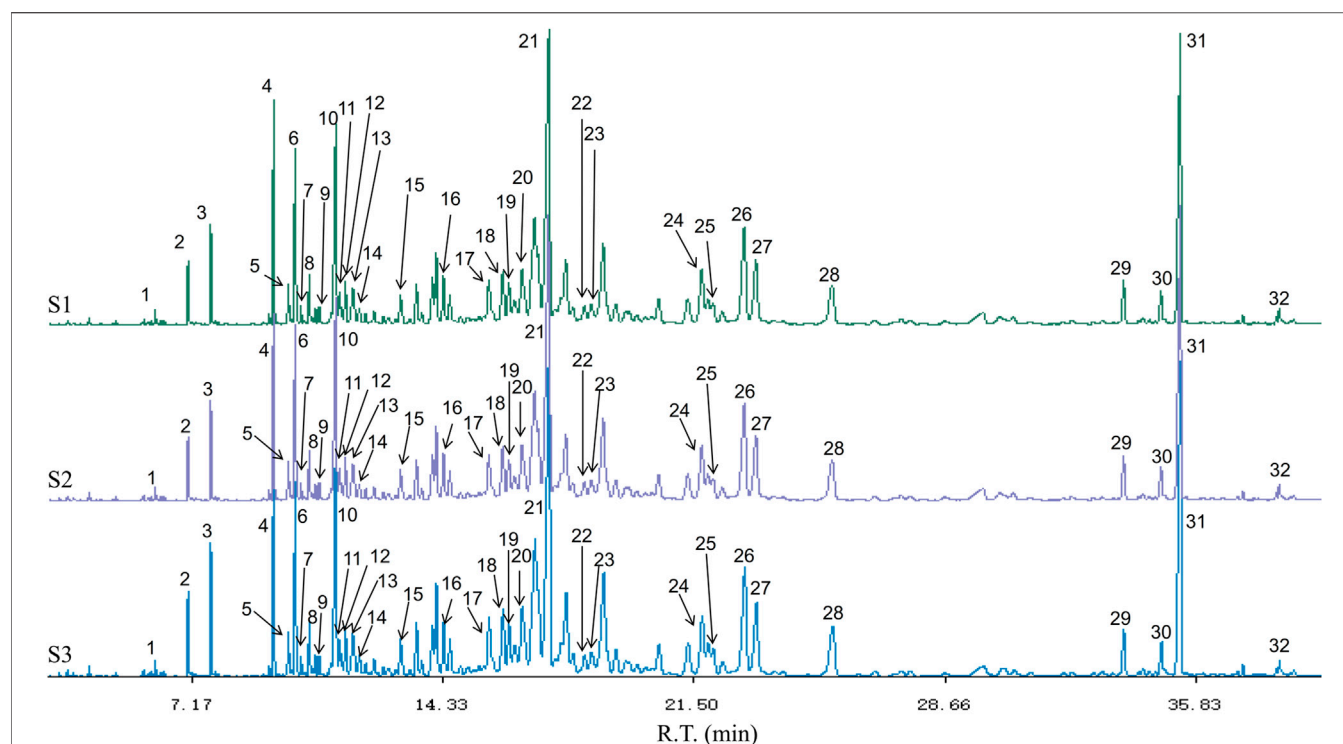


FIGURE 3 | The GC-MS chromatogram of CMVO. S1-S3 represents three GC-MS chromatograms of CMVO samples, and three times GC-MS analysis were carried out to show the repeatability. The 32 components identified are numbered in the figure, which matches the serial numbers of each component in **Table 2**.

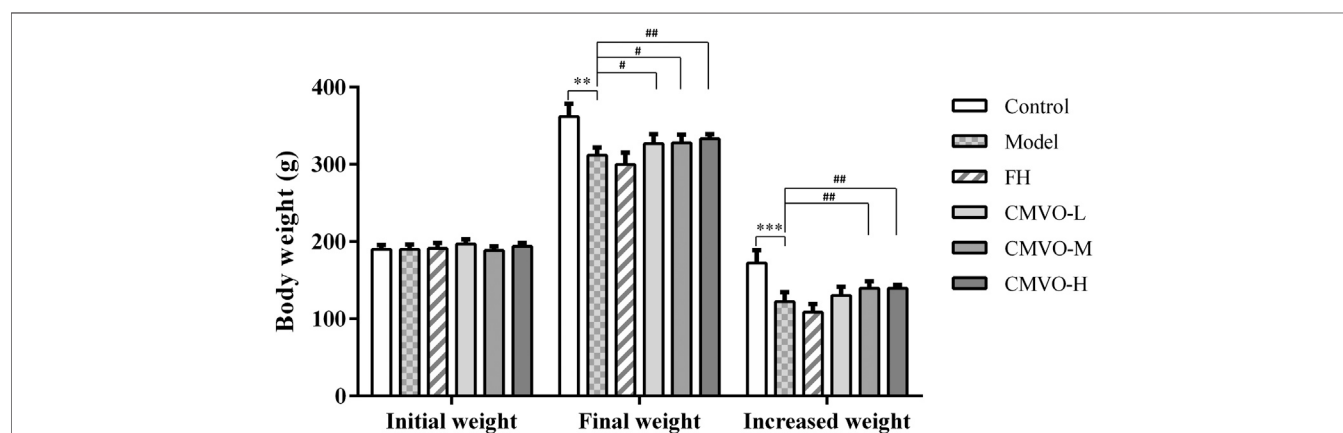


FIGURE 4 | The BW in each group at weeks 0 and 4 (Mean \pm SD, $n = 8$). The BW was recorded at weeks 0 and 4, and the increased weight is expressed as the BW at week 4 minus the BW at week 0. * $p < 0.05$, ** $p < 0.01$, *** $p < 0.001$ vs. control group. # $p < 0.05$, ## $p < 0.01$, ### $p < 0.001$ vs. CUMS group.

Effects of ChenXiang-MuXiang Volatile Oil on Body Weight and Sucrose Preference Test

Before the CUMS modeling process, there were no significant differences in the baseline BW, as shown in **Figure 4**. After treatment for 4 weeks, differences in BW showed statistical significance among the groups ($F_{5,42} = 23.617$, $p < 0.01$). Compared with the control group, the BW of the model group increased slowly and decreased

significantly after modeling ($p < 0.01$), which suggests that CUMS may cause gastrointestinal dysfunction in rats, resulting in loss of appetite and individual growth retardation. Compared with the model group, the weights in the CMVO-L, CMVO-M and CMVO-H groups significantly increased ($p < 0.05$ or $p < 0.01$).

Before the modeling process, there were no significant differences in the baseline sucrose preference, as shown in

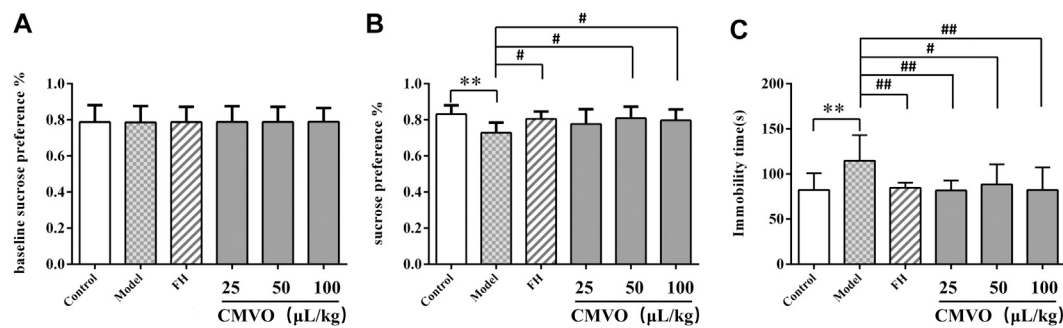


FIGURE 5 | Effects of CUMS and CMVO treatment (25, 50, 100 $\mu\text{L/kg}$) on baseline sucrose preference (A), SPT (B) and FST (C). Values are expressed as (Mean \pm SD, $n = 8$). * $p < 0.05$, ** $p < 0.01$, *** $p < 0.001$ vs. control group. # $p < 0.05$, ## $p < 0.01$, ### $p < 0.001$ vs. CUMS group.

Figure 5A. In the SPT (Figure 5B), the results showed that there were significant differences in sucrose preference among different groups ($F_{5,42} = 2.777$, $p < 0.05$). Compared with the control group, the sucrose preference rate in the model group decreased significantly ($p < 0.01$). Compared with the model group, the sucrose preference rate of other groups increased, and there were significant differences in the fluoxetine hydrochloride (FH), CMVO-M and CMVO-H groups ($p < 0.05$).

Effects of ChenXiang-MuXiang Volatile Oil on the Immobility Time in Forced Swimming Test

The effect of CMVO on FST in CUMS rats is shown in Figure 5C. There were significant differences in immobility time among the groups ($F_{5,42} = 3.281$, $p < 0.05$). The immobility time during forced swimming in the model group was significantly increased compared with that in the control group ($p < 0.01$). In the FST, lower immobility time was observed in FH- and CMVO-treated CUMS rats, and there were significant differences in the FH, CMVO-L and CMVO-H groups ($p < 0.01$), and in the CMVO-M group ($p < 0.05$).

Effects of ChenXiang-MuXiang Volatile Oil on Open Field Test

Figures 6A–E show the effects of CMVO on the OFT in CUMS rats. The results of one-way ANOVA showed that there were significant differences in V.mean, Dist, Res.T, N.Ent and Dist in the marginal zone among the groups ($F_{5,42} = 5.289$, $p < 0.01$; $F_{5,42} = 5.314$, $p < 0.01$; $F_{5,42} = 6.295$, $p < 0.01$; $F_{5,42} = 7.006$, $p < 0.01$; $F_{5,42} = 5.314$, $p < 0.01$). Compared with the control group, V.mean, Total Dist, Dist in the marginal zone and N.Ent decreased significantly ($p < 0.05$ or $p < 0.01$), and Res.T increased significantly ($p < 0.001$), which indicated that the activity and curiosity about the novel environment of the model group rats were decreased (Cao et al., 2019b). Compared with the model group, V.mean and Dist in the FH group and all CMVO dose groups increased significantly ($p < 0.01$), while Res.T in all CMVO dose groups decreased significantly ($p < 0.01$) and N.Ent in CMVO-M and CMVO-H groups increased significantly ($p < 0.05$ or $p < 0.01$). This showed that the willingness of rats in

the treatment groups to explore the environment was enhanced, indicating that CMVO exerted an antidepressant effect. Figures 6F (1–6) show heat maps of the rat's movement trajectory for 5 min in the open field.

Effect on Hypothalamic–Pituitary–Adrenal Axis Activity in Rats

In order to observe the regulatory effect of CMVO on the HPA axis in CUMS rats, the levels of ACTH and CORT in serum were determined by ELISA and the expression level of CRH mRNA in hypothalamus was measured by RT-PCR. Significant differences among the groups were observed on ACTH and CORT levels in serum, and CRH mRNA expression level in hypothalamus ($F_{5,42} = 4.715$, $p < 0.01$; $F_{5,42} = 2.572$, $p < 0.05$; $F_{5,12} = 21.467$, $p < 0.01$).

The serum levels of ACTH and CORT in the CUMS group were significantly higher than those in the control group ($p < 0.01$). Compared with the model group, treatment with FH and CMVO remarkably decreased ACTH levels. There were significant differences in the FH group ($p < 0.01$) and CMVO-L group ($p < 0.05$). In addition, FH or CMVO treatment also reversed the increase of serum CORT induced by CUMS. There were significant differences in the FH and all CMVO dose groups ($p < 0.01$ or $p < 0.05$). The RT-PCR results showed that CUMS significantly increased hypothalamus expression of CRH mRNA in the model group ($p < 0.001$). The expression of CRH mRNA decreased significantly after treatment with FH, CMVO-L, CMVO-M and CMVO-H compared with the model group ($p < 0.001$). The results are shown in Figures 7A–C. These results suggest that CUMS can lead to overexcitation of the HPA axis, increasing expression of ACTH, CORT and CRH mRNA in rats. The overexcitation of the HPA axis was regulated by inhalation of CMVO, which may be a mechanism for the action of CMVO in the treatment of depression.

Effects on the Levels of Neurotransmitters (5-Hydroxytryptamine, Norepinephrine, Acetylcholine and Dopamine)

The levels of neurotransmitters in the hippocampus were assessed to reveal the role of CMVO in treatment of

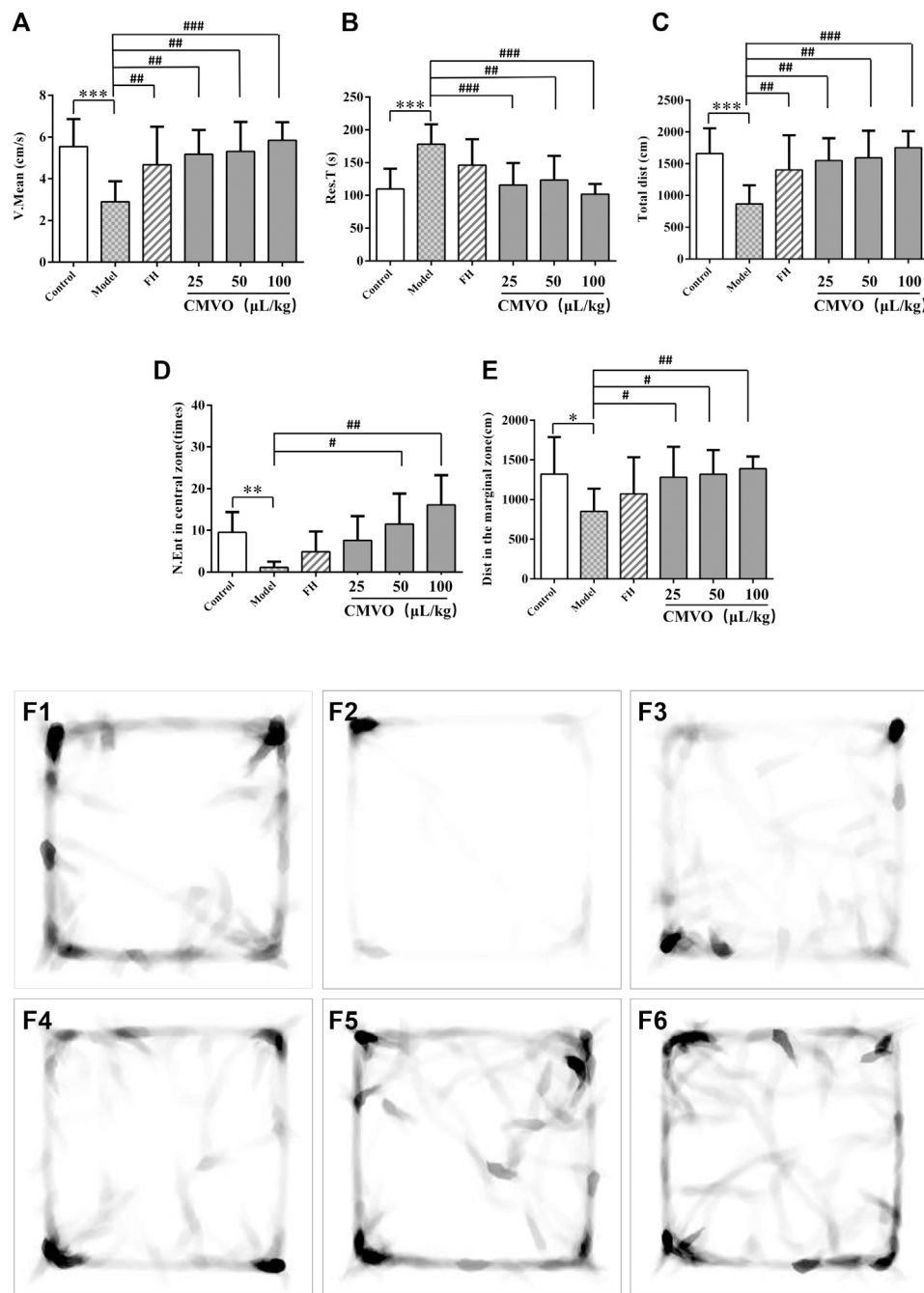


FIGURE 6 | The V.mean, Res.T, Total dist, N.Ent in central zone and Dist in the marginal zone of rats on OFT (A,B,C,D,E) and the heat map (F1-F6) of the rat's movement trajectory for 5 min in the open field (f1-f6). Values are expressed as (Mean \pm SD, $n = 8$). * $p < 0.05$, ** $p < 0.01$, *** $p < 0.001$ vs. control group. # $p < 0.05$, ## $p < 0.01$, ### $p < 0.001$ vs. CUMS group.

depression. Significant effects were observed on 5-HT, NE, ACh and DA in the hippocampus ($F_{5,42} = 2.449$, $p < 0.05$; $F_{5,42} = 2.636$, $p < 0.05$; $F_{5,42} = 2.781$, $p < 0.05$; $F_{5,42} = 2.855$, $p < 0.05$). The levels of 5-HT, NE, ACh and DA in the hippocampus of CUMS-induced rats were significantly

decreased compared with the control group ($p < 0.01$ or $p < 0.05$) (Figures 8A–D and Table 3). Treatment with CMVO reversed the decrease of neurotransmitters induced by the CUMS procedure. Compared with the model group, the levels of 5-HT in the FH, CMVO-L, CMVO-M and

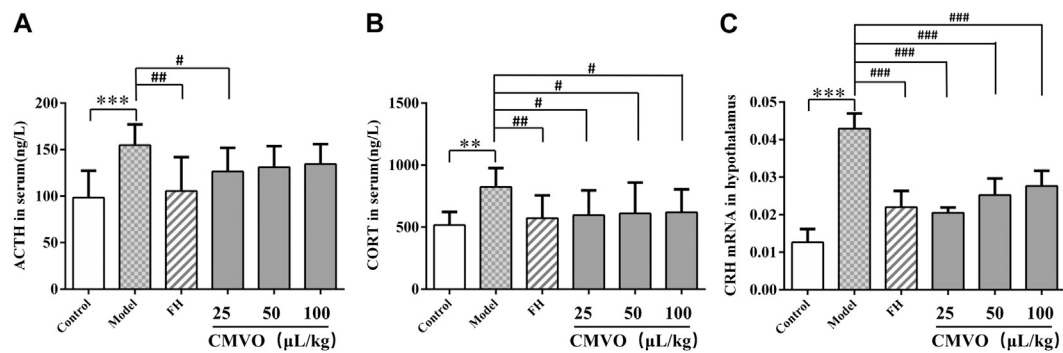


FIGURE 7 | Effects of CMVO treatment on ACTH (A) and CORT (B) levels ($n = 8$) and CRH mRNA expression (C) ($n = 3$). The levels of ACTH and CORT in the hippocampus of rats were tested by ELISA, and the CRH mRNA in the hypothalamus was tested by RT-PCR. Values are expressed as (Mean \pm SD). * $p < 0.05$, ** $p < 0.01$, *** $p < 0.001$ vs. control group. # $p < 0.05$, ## $p < 0.01$, ### $p < 0.001$ vs. CUMS group.

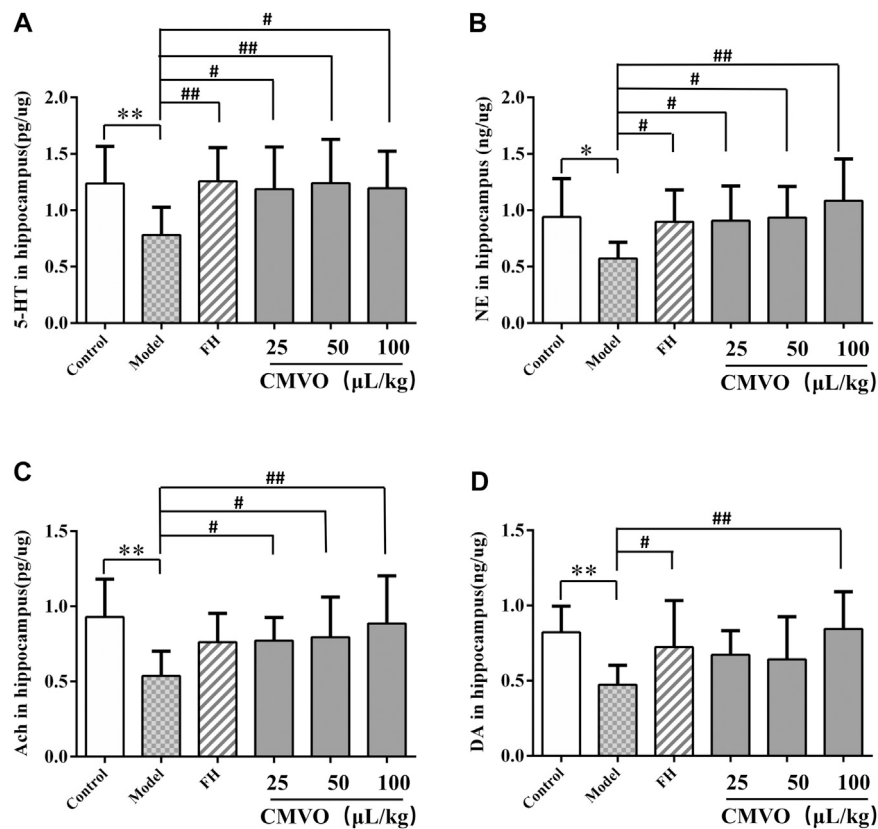


FIGURE 8 | Effects of CMVO treatment on 5-HT, NE, Ach and DA levels in hippocampus (A,B,C,D). The levels of 5-HT, NE, Ach and DA in the hippocampus of rats were tested by ELISA. Values are expressed as (Mean \pm SD, $n = 8$). * $p < 0.05$, ** $p < 0.01$, *** $p < 0.001$ vs. control group. # $p < 0.05$, ## $p < 0.01$, ### $p < 0.001$ vs. CUMS group.

CMVO-H groups were significantly increased ($p < 0.01$ or $p < 0.05$). The levels of NE in each group were also increased by varying degrees, with significant differences in the FH, CMVO-L and CMVO-M groups ($p < 0.05$) and the CMVO-H group ($p < 0.01$). After treatment with FH and

CMVO, the levels of ACh significantly increased compared with the model group, with significant differences in all CMVO dose groups ($p < 0.01$ or $p < 0.05$). Compared with the model group, the DA levels increased significantly in the FH group ($p < 0.05$) and CMVO-H group ($p < 0.01$).

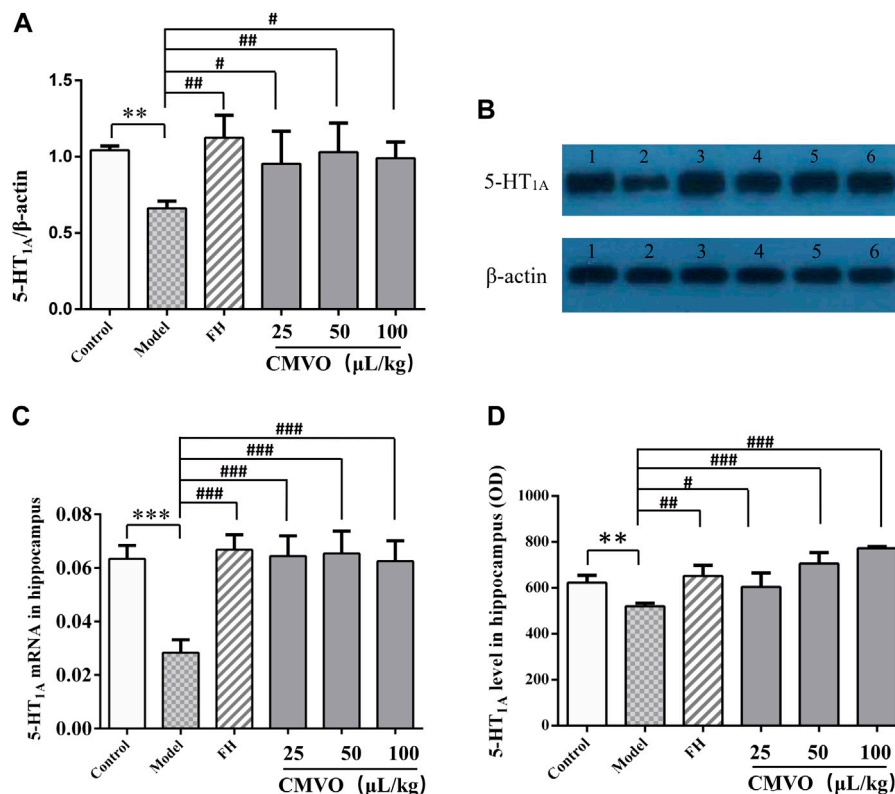


FIGURE 9 | (A,B) Effects of CMVO on the level of 5-HT_{1A} protein in the hippocampus (Mean \pm SD, $n = 3$). The results of Western blot are shown in **Figures 9A,B** (1: control group, 2:CUMS group, 3:FH group, 4:CMVO-L group, 5:CMVO-M group, 6: CMVO-H group). **(C)** Effects of CMVO on the level of 5-HT_{1A} mRNA in the hippocampus (Mean \pm SD, $n = 3$). The results of the RT-PCR are shown in **Figure 9C**. (Mean \pm SD, $n = 3$). **(D)** Effect of CMVO on the expression of 5-HT_{1A} in the hippocampus by immunohistochemistry (Mean \pm SD, $n = 3$). The results of immunohistochemical staining are shown in **Figure 9D** (OD: optical density). Values are expressed as mean \pm SEM. * $p < 0.05$, ** $p < 0.01$, *** $p < 0.001$ vs. control group. # $p < 0.05$, ## $p < 0.01$, ### $p < 0.001$ vs. CUMS group.

Effect of ChenXiang-MuXiang Volatile Oil on the Level of 5-HT_{1A} Protein in the Hippocampus

The expression level of 5-HT_{1A} in hippocampus of rats was semi-quantitatively analyzed by calculating the ratio of the gray value of 5-HT_{1A} bands to β -actin bands. The results showed that 5-HT_{1A} gene transcription in hippocampus was significantly decreased in the CUMS group compared with the control group ($F_{5,12} = 3.953$, $p < 0.01$) (**Figures 9A,B**). The expression of 5-HT_{1A} was significantly increased in the FH and CMVO-M groups ($p < 0.01$), CMVO-L and CMVO-H groups ($p < 0.05$) compared with the CUMS group.

Effect of ChenXiang-MuXiang Volatile Oil on the Expression of 5-HT_{1A} mRNA in the Hippocampus

Similarly, RT-PCR analysis showed that expression of 5-HT_{1A} mRNA in the hippocampus of the model group was significantly decreased compared with the control group ($p < 0.001$), while the expression of 5-HT_{1A} mRNA in the CMVO treatment groups was significantly reversed ($p < 0.001$) (**Figure 9C**).

Effect of ChenXiang-MuXiang Volatile Oil on the Expression of 5-HT_{1A} in the Hippocampus

5-HT_{1A} positive cells in the hippocampus of each group were examined by immunohistochemistry (**Figures 9D, 10A,10B**). The OD value of the 5-HT_{1A} positive cells in the hippocampus was analyzed (**Figure 9D**). Compared with the control group, the expression of 5-HT_{1A} positive cells in the CUMS group was significantly reduced ($p < 0.01$). Compared with the CUMS group, the expression of 5-HT_{1A}-positive cells was significantly increased in the FH ($p < 0.01$) and CMVO groups ($p < 0.05$ or $p < 0.001$).

DISCUSSION

In the CUMS model, the state of reduced interest and lack of pleasure shown by animals is similar to the clinical symptoms of depression. Lack of pleasure is an important manifestation of depression and the SPT is widely used to evaluate the degree of pleasure deficiency in depressed animals (Xu et al., 2011). In this study, the sucrose preference index in the CUMS group decreased significantly, indicating that the response of

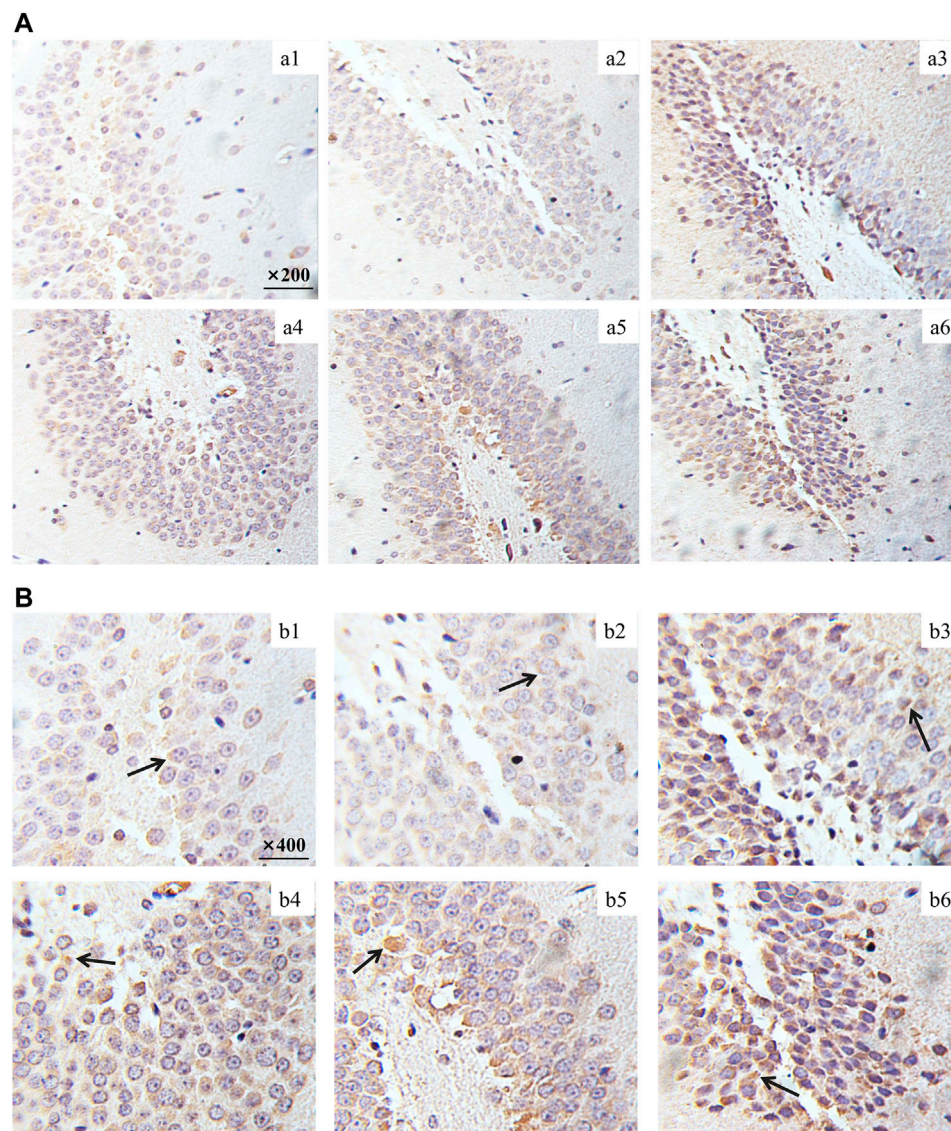


FIGURE 10 | Effect of CMVO on the expression of 5-HT_{1A} in the hippocampus. The immunohistochemical staining pictures taken by microscope are shown in **Figure 10A** (Magnification:×200) and **Figure 10B** (Magnification:×400).

animals to reward decreased and that the depression model was established successfully. The treatment with CMVO increased the sucrose preference index and showed an antidepressant effect. The efficacy of antidepressants is widely evaluated using FST, in which the immobility time reflects the degree of despair in the rats (Porsolt et al., 1978; Xing et al., 2015). Consistent with previous studies, CUMS significantly prolonged the immobility time in the FST, while CMVO administration shortened the immobility time. The OFT is based on the phenomenon that rats are afraid to enter the open or bright field to reflect their emotions, and depressive behavior is evaluated by the desire of the rats to explore in the open field (Xing et al., 2015). The desire to explore in the open field decreased in the model group, total moving distance

and the number of times to enter the central area decreased, immobility time was prolonged and movement was slower. After administration of CMVO, these indexes were reversed. Analysis of BW, and OFT, FST and SPT results showed that the rats in the model group exhibited obvious depressive behavior, indicating successful establishment of the model. Treatment with different doses of CMVO reversed these depressive behaviors and showed an obvious antidepressant effect. Although there was an obvious antidepressant effect in the FH group according to the behavioral experiments (OFT, FST, SPT), the body weights of rats decreased slightly compared with the model group, which was not consistent with some experimental results reported previously (Xing et al., 2019; Li et al., 2020c). On the one hand, according to

the literature (Willner, 1997), although the commonly used chronic antidepressant drugs can normalize sucrose intake, they may not reverse CUMS-induced weight loss (Willner et al., 1987). In the CUMS model, there is no obvious positive correlation between sucrose preference index and body weight, which is consistent with the report of the founder of the model (Willner, 1997; Zhang et al., 2018). On the other hand, the results showed that FH did not improve the appetite or digestive function of depressed rats in the short term, but that CMVO significantly improved the body weight of the rats, suggesting that CMVO may have a better effect on anorexia caused by depression.

Depression is a disease involving a variety of neurotransmitters and brain regions, and its pathogenesis has not been fully elucidated. However, it is generally recognized that chronic stress plays an important role in the development of depression. Long-term chronic stress can lead to dysfunction of the HPA axis and increased secretion of corticosteroids, both of which are considered to be closely involved in the pathogenesis of human depression (Jozuka et al., 2003; Xing et al., 2015). The HPA axis is one of the complex neurobiological mechanisms contributing to the occurrence and development of depression (Xing et al., 2015). During the stress process, CRH is released from the paraventricular nucleus of the hypothalamus and promotes the release of ACTH from the pituitary. This results in the release of glucocorticoids from the adrenal cortex, providing feedback to the HPA axis through the glucocorticoid receptor (Zhang et al., 2019). In patients suffering from depression, the activity of the HPA axis is abnormally increased. The concentrations of cortisol are generally increased, which eventually destroys the negative feedback regulation of the HPA axis. Therefore, the concentrations of ACTH and CORT in serum and the expression of CRH mRNA in the hypothalamus were measured after the CUMS procedure. It was found that ACTH and CORT levels and the expression of CRH mRNA were increased significantly in CUMS rats, which was consistent with published literature (Song et al., 2003; Li et al., 2020b) that chronic stress can activate the HPA axis. The administration of CMVO significantly decreased the levels of ACTH and CORT in the serum of CUMS rats. These results suggest that the inhibition of hyperfunction of the HPA axis and restoration of the negative feedback loop may be an important mechanism of the CMVO antidepressant effect.

Moreover, there is a close relationship between the HPA axis and neurotransmitters. Overexcitation of the HPA axis may damage monoaminergic neurons in the hippocampus, resulting in decreased release of monoamine neurotransmitters (Zhang et al., 2019). Studies proved that the disruption of negative feedback regulation of the HPA axis will further impair the function of the hippocampus, which is closely involved in memory and emotion, and eventually lead to lower levels of neurotransmitters and aggravate depression (Mahar et al., 2014; Cao, 2019a). Through inhaled administration, volatile compounds can bind to olfactory receptors, trigger electrophysiological responses, stimulate the brain and alleviate depression-like behavior (Park et al., 2015;

Zhang et al., 2019). In addition, it may prevent excessive activation of the HPA axis and stimulate the brain to achieve antidepressant effects by increasing concentrations of neurotransmitters (Watanabe et al., 2011; Lv et al., 2013; Zhang et al., 2019).

The hippocampus plays an important role in emotional regulation and is an important region that mediates the stress response (Peng et al., 2015; Sheline et al., 2019). The causes of depression are thought to be associated with the serotonergic system, norepinephrine, and dopamine (Li et al., 2020c). The monoamine hypothesis is the first neurobiochemical theory of depression, which holds that deficiency of NE, 5-HT or DA in the synaptic space *in vivo* is the main cause of depression (Duffey et al., 2013). In fact, most of the commonly used antidepressants are 5-HT reuptake inhibitors. Anhedonia, the core clinical feature of depression, is most likely linked to abnormality of the DA-reward pathway (Chen et al., 2019). The imbalance between acetylcholine and adrenergic neurons may lead to depression (Janowsky et al., 1972), and studies have shown that ACh-NE signals can mediate behaviors related to anxiety and depression through the interaction between β_2 nAChRs and α_2 -norepinephrine receptors (Mineur et al., 2018; Meng et al., 2020). Therefore, we determined the levels of monoamine neurotransmitters (5-HT, NE and DA) and cholinergic neurotransmitter (ACh) in the hippocampus of rats. In the CUMS group, the levels of 5-HT, NE, DA and ACh were significantly decreased. Their levels were significantly increased after intervention with FH and CMVO, indicating that CMVO may exert an antidepressant effect by regulating the levels of neurotransmitters. The levels of ACh and NE in the CUMS model group decreased significantly, and both levels were significantly increased by CMVO intervention, indicating that CMVO can regulate the interaction of the ACh-NE signal. The 5-HT_{1A} receptor subtype is considered to be an important mediator for the stimulatory influence of 5-HT on stress HPA activity (Goel et al., 2014). The 5-HT_{1A} receptor is closely involved in emotional disorders, and its blockade can lead to spontaneous antidepressant behavior in mice (Stewart et al., 2014). In order to further explore the mechanism of CMVO, we evaluated the change of 5-HT_{1A} levels by immunohistochemistry, RT-PCR and western blot. The results showed that 5-HT_{1A} decreased significantly in the model group, and CMVO administration increased the level, indicating that CMVO may regulate levels of 5-HT by up-regulating the expression of 5-HT_{1A}. The results of our study suggest that CMVO can regulate the metabolism of neurotransmitters in the hippocampus, which may underlie its mechanism of action, and its effect is similar to that of the established drug, fluoxetine hydrochloride.

32 components of CMVO were identified by GC-MS analysis, of which sesquiterpenes were the main components. We speculate that CMVO may play a comprehensive antidepressant effect through these components. In recent years, many literatures have reported the effects of the components in the CX and MX volatile oil on the central nervous system. At present, the most concerned compounds with potential antidepressant activity in CX essential oil are agarofuran-like derivatives, among which buagafuran is the most

TABLE 3 | Contents of 5-HT, Ach, DA, NE in the hippocampus ($\bar{x} \pm s$, $n = 8$).

Groups	5-HT (pg/ug)	Ach (pg/ug)	DA (ng/ug)	NE (ng/ug)
Control group	1.24 \pm 0.33	0.93 \pm 0.25	0.82 \pm 0.17	0.94 \pm 0.34
CUMS group	0.78 \pm 0.25**	0.54 \pm 0.17**	0.47 \pm 0.13**	0.57 \pm 0.14*
FH group	1.26 \pm 0.30##	0.76 \pm 0.19	0.72 \pm 0.31#	0.90 \pm 0.28#
CMVO-L group	1.19 \pm 0.37#	0.77 \pm 0.15#	0.67 \pm 0.16	0.91 \pm 0.31#
CMVO-M group	1.24 \pm 0.39##	0.79 \pm 0.27#	0.64 \pm 0.28	0.94 \pm 0.28#
CMVO-H group	1.20 \pm 0.33#	0.89 \pm 0.32##	0.84 \pm 0.25##	1.08 \pm 0.37##

potential and phase II clinical trials are being conducted on it (Wang et al., 2018c). Its potential mechanism might be through modulating central neurotransmitters, such as dopamine (Zhang et al., 2004). The CX volatile oil has definite sedative effect by inhalational administration, in which agarospirol (Okugawa et al., 1996; Okugawa et al., 2000), benzylacetone, α -gurjunene, and (+)-calarene are the main components (Takemoto et al., 2008). Study (Okugawa et al., 2000) have shown that agarospirol in CX essential oil and dehydrocostus lactone in MX essential oil were found to be the principle products evaluated as analgesics in pharmacological studies. In addition, the two components has shown to be potent as an antagonist of dopamine D₂ and serotoninine 5-HT_{2A} receptor binding (Okugawa et al., 2000). Based on the above research results, it can be concluded that the components such as dehydrocostus lactone in MX volatile oil, β -Agarofuran, agarospirol and benzylacetone in CX volatile oil may have comprehensive effects on the central nervous system by regulating neurotransmitters such as 5-HT and DA. Similarly, our results also show that CMVO can regulate the level of neurotransmitters such as 5-HT and DA, thus playing an antidepressant effect. Besides, apilotaxene is the most abundant component in CMVO, study have shown that it has a good immune function, and has been proved to be a novel immunotherapeutic agent for immunological diseases related to the overactivation of T cells. On the other hand, study (Yamahara et al., 1990) have shown that sesquiterpenes such as β -eudesmol and hinesol can clearly enhanced intestinal charcoal transport in mice. It has been found that benzylacetone, the main active compound in the CX volatile oil, has the effect of boosting appetite (Okugawa et al., 2016a; Okugawa et al., 2016b). As mentioned in the experimental results, CMVO significantly increased the body weight of rats within the 21 days' administration, showing a better effect compared with positive drug FH. Depression is common symptoms such as loss of appetite, and CMVO is likely to play a role in gastrointestinal regulation through these compounds. Symptoms such as loss of appetite are common in patients with depression, and CMVO is likely to improve gastrointestinal function through these components. To sum up, various components of CMVO may play antidepressant effect by regulating neurotransmitters' levels, immunity and gastrointestinal function.

CONCLUSION

In conclusion, this study demonstrated that CMVO inhalational administration exerts antidepressant effects in CUMS rats. Its

potential mechanism of action is related to inhibition of the hyperactive HPA axis and regulation of monoamine neurotransmitter levels in the hippocampus. This study may provide medicines with definite curative effect and suitability for long-term administration in patients with depression. CX and MX are two classical aromatic traditional Chinese herbs which are frequently used in antidepressant prescriptions, but most of the studies have focused on the efficacy of their oral administration, and the antidepressant effects and mechanisms of the combination of the two volatile oils have not been studied. In this study, a self-made aromatherapy device was used to study the antidepressant effect and mechanism of CMVO through inhalational administration. At present, most of the antidepressants are oral drugs, and there are some deficiencies in the treatment of depression, a long-term chronic disease. This study explored a new administration method for CX-MX, a traditional herbal pair, to play an antidepressant effect, and it can also provide a reference for others to study the antidepressant effect of aromatic traditional Chinese herbs by inhalational administration.

DATA AVAILABILITY STATEMENT

The original contributions presented in the study are included in the article, further inquiries can be directed to the corresponding authors.

ETHICS STATEMENT

The animal study was reviewed and approved by Animal Ethics Committee of Jiangxi University of Traditional Chinese Medicine.

AUTHOR CONTRIBUTIONS

HL wrote the original draft; XZ and GR designed the experiments; YL reviewed and edited the paper; LW analyzed the data; JL, TR and MW performed the experiments; YZ provided experimental equipment; MY and XH are project administrator. All authors have given approval to the final version of the manuscript.

FUNDING

This work was supported by the National key R & D program of China (2018YFC1706404), Major scientific and technological research and development projects of Jiangxi Province (20194ABC28009), Innovative training program of Jiangxi University of TCM (201910412071 and 201910412065).

REFERENCES

- Antunes, M. S., Ruff, J. R., de Oliveira Espinosa, D., Piegas, M. B., de Brito, M. L., and Rocha, K. A. (2015). Neuropeptide Y administration reverses tricyclic antidepressant treatment-resistant depression induced by ACTH in mice. *Horm. Behav.* 73, 56–63. doi:10.1016/j.yhbeh.2015.05.018
- Brunner, E., Tohen, M., Osuntokun, O., Landry, J., and Thase, M. E. (2014). Efficacy and safety of olanzapine/fluoxetine combination vs fluoxetine monotherapy following successful combination therapy of treatment-resistant major depressive disorder. *Neuropsychopharmacology* 39, 2549–2559. doi:10.1038/npp.2014.101
- Cao, C. (2019a). Study of anti-depressive material basis of Kai-Xin-San on regulation of brain-gut axis. Master's dissertation. Nanjing (China): Nanjing University of Chinese Medicine.
- Cao, L.-H., Qiao, J.-Y., Huang, H.-Y., Fang, X.-Y., Zhang, R., and Miao, M.-S. (2019b). PI3K-AKT signaling activation and icariin: the potential effects on the perimenopausal depression-like rat model. *Molecules* 24, 3700. doi:10.3390/molecules24203700
- Chen, B. J., Li, J. J., Xie, Y. H., Ming, X., Li, G., Wang, J., et al. (2019). Cang-ai volatile oil improves depressive-like behaviors and regulates DA and 5-HT metabolism in the brains of CUMS-induced rats. *J. Ethnopharmacol.* 244, 112088. doi:10.1016/j.jep.2019.112088
- Chen, H. Q. (2011). Preliminary evaluation of the use of artificial liquid transfusion technology in inducing agarwood formation in the whole body of cultivated. *Aquilaria sinensis* (Lour.). Gilg Trees. Beijing, China: Chinese Academy of Medical Sciences Peking Union Medical College.
- Daodee, S., Monthakantirak, O., Ruengwinitwong, K., Gatenakorn, K., Maneenet, J., Khamphukdee, C., et al. (2019). Effects of the ethanol extract of dipterocarpus alatus leaf on the unpredictable chronic mild stress-induced depression in ICR mice and its possible mechanism of action. *Molecules* 24, 3396. doi:10.3390/molecules24183396
- Difrancesco, S., Lamers, F., Riese, H., Merikangas, K. R., Beekman, A. T. F., and van Hemert, A. M. (2019). Sleep, circadian rhythm, and physical activity patterns in depressive and anxiety disorders: a 2-week ambulatory assessment study. *Depress. Anxiety* 36, 975–986. doi:10.1002/da.22949
- Dong, H. Y., Gao, Z. Y., Rong, H., Jin, M., and Zhang, X. J. (2014). β -asarone reverses chronic unpredictable mild stress-induced depression-like behavior and promotes hippocampal neurogenesis in rats. *Molecules* 19, 5634–5649. doi:10.3390/molecules19055634
- Dong, S., Ma, L. Y., Liu, Y. T., Yu, M., Jia, H. M., and Zhang, H. W. (2018). Pharmacokinetics of costunolide and dehydrocostuslactone after oral administration of *Radix Aucklandiae* extract in normal and gastric ulcer rats. *J. Asian Nat. Prod. Res.* 20, 1055–1063. doi:10.1080/10286020.2018.1489379
- Duffey, K. C., Shih, O., Wong, N. L., Drisdell, W. S., Saykally, R. J., and Cohen, R. C. (2013). Evaporation kinetics of aqueous acetic acid droplets: effects of soluble organic aerosol components on the mechanism of water evaporation. *Phys. Chem. Chem. Phys.* 15, 11634–11639. doi:10.1039/c3cp51148k
- Feng, G. B., and Fang, H. Z. (2016). Analyze on the essential oil of drug pair coptis-radix aucklandiae. *Guangdong Chemical Industry* 43 (23), 14–16.
- Gao, X. L., Zhang, Q. H., Hui, X., Zhu, Z. X., Zhao, Y. F., and Tu, P. F. (2019). Anti-inflammatory effect of Chinese agarwood essential oil via inhibiting p-STAT3 and IL-1 β /IL-6. *Chin Pharm J* 54, 1951–1957. doi:10.11669/cpj.2019.23.008
- Geng, T. Y. (2020). Study on extraction and biological activity of Agarwood essential oil. Chongqing, China: Southwest University.
- Global Burden of Disease Study 2013 Collaborators (2015). Global, regional, and national incidence, prevalence, and years lived with disability for 301 acute and chronic diseases and injuries in 188 countries, 1990–2013: a systematic analysis for the global burden of disease study 2013. *Lancet* 386, 743–800. doi:10.1016/S0140-6736(15)60692-4
- Goel, N., Innala, L., and Viau, V. (2014). Sex differences in serotonin (5-HT) 1A receptor regulation of HPA axis and dorsal raphe responses to acute restraint. *Psychoneuroendocrinology* 40, 232–241. doi:10.1016/j.psyneuen.2013.11.020
- Han, Q. Q., Yang, S. H., Chen, X. Y., Zhong, Z. J., Zhou, X., Zhang, W. M., et al. (2019). Analysis and comparison of chemical constituents of volatile oil from aloes. *Journal of Chinese Medicinal Materials* 42 (07), 1566–1571. doi:10.13863/j.issn1001-4454.2019.07.022
- Holden, C. (2000). Mental health. Global survey examines impact of depression. *Science* 288, 39–40. doi:10.1126/science.288.5463.39
- Huang, Y. Q., Guo, X., Chen, X. Y., Zhong, Z. J., Li, H. H., Zhang, W. M., et al. (2018). Analysis of secondary metabolites of artificial agarwood induced by *Pseudomonas oryzae* A8. *Journal of Chinese Medicinal Materials* 42 (07), 1662–1667. doi:10.13863/j.issn1001-4454.2018.07.031
- Janowsky, D. S., El-Youcef, M. K., Davis, J. M., and Sekerke, H. J. (1972). A cholinergic-adrenergic hypothesis of mania and depression. *Lancet* 2, 632–635. doi:10.1016/S0140-6736(72)93021-8
- Jozuka, H., Jozuka, E., Takeuchi, S., and Nishikaze, O. (2003). Comparison of immunological and endocrinological markers associated with major depression. *J. Int. Med. Res.* 31, 36–41. doi:10.1177/147323000303100106
- Li, C., Huang, J., Cheng, Y. C., and Zhang, Y. W. (2020a). Traditional Chinese medicine in depression treatment: from molecules to systems. *Front. Pharmacol.* 11, 586. doi:10.3389/fphar.2020.00586
- Li, K. W., Yan, L., Zhang, Y. P., Yang, Z. Y., Zhang, C., and Li, Y. J. (2020b). Seahorse treatment improves depression-like behavior in mice exposed to CUMS through reducing inflammation/oxidants and restoring neurotransmitter and neurotrophin function. *J. Ethnopharmacol.* 250, 112487. doi:10.1016/j.jep.2019.112487
- Li, Y. B., Wu, L. L., Chen, C., Wang, L. W., Guo, C., Zhao, X. Q., et al. (2020c). Serum metabolic profiling reveals the antidepressive effects of the total iridoids of *Valeriana jatamansi* Jones on chronic unpredictable mild stress mice. *Front. Pharmacol.* 11, 338. doi:10.3389/fphar.2020.00338
- López, V., Nielsen, B., Solas, M., Ramírez, M. J., and Jäger, A. K. (2017). Exploring pharmacological mechanisms of lavender (*Lavandula angustifolia*) essential oil on central nervous system targets. *Front. Pharmacol.* 8, 280. doi:10.3389/fphar.2017.00280
- Lv, X. N., Liu, Z. J., Zhang, H. J., and Tzeng, C. M. (2013). Aromatherapy and the central nerve system (CNS): therapeutic mechanism and its associated genes. *Curr. Drug Targets* 14, 872–879. doi:10.2174/1389450111314080007
- Mahar, I., Bambico, F. R., Mechawar, N., and Nobrega, J. N. (2014). Stress, serotonin, and hippocampal neurogenesis in relation to depression and antidepressant effects. *Neurosci. Biobehav. Rev.* 38, 173–192. doi:10.1016/j.neubiorev.2013.11.009
- Mehta, A. K., Halder, S., Khanna, N., Tandon, O. P., and Sharma, K. K. (2013). The effect of the essential oil of *Eugenia caryophyllata* in animal models of depression and locomotor activity. *Nutr. Neurosci.* 16, 233–238. doi:10.1179/1476830512Y.0000000051
- Meng, M. D., Feng, Y., Wang, P., Feng, J. Y., Qin, X. M., and Gao, X. X. (2020). Regulatory effect of polar extract of *Poria cocos* on neurotransmitter and circadian rhythm disorder in CUMS rats. *Chin. Tradit. Herb. Drugs* 51, 118–126. doi:10.7501/j.issn.0253-2670.2020.01.017
- Mineur, Y. S., Cahuzac, E. L., Mose, T. N., Benthall, M. P., Plantenga, M. E., and Thompson, D. C. (2018). Interaction between noradrenergic and cholinergic signaling in amygdala regulates anxiety- and depression-related behaviors in mice. *Neuropsychopharmacology* 43, 2118–2125. doi:10.1038/s41386-018-0024-x
- Miyoshi, T., Ito, M., Kitayama, T., Isomori, S., and Yamashita, F. (2013). Sedative effects of inhaled benzylacetone and structural features contributing to its activity. *Biol. Pharm. Bull.* 36 (9), 1474–1481. doi:10.1248/bpb.b13-00250
- Monggoot, S., Kulsing, C., Wong, Y. F., and Pripdeevech, P. (2018). Incubation of *Aquilaria subintegra* with microbial culture supernatants enhances production of volatile compounds and improves quality of agarwood oil. *Indian J. Microbiol.* 58 (2), 201–207. doi:10.1007/s12088-018-0717-1
- Na, B. R., Kim, H. R., Kwon, M. S., Lee, H. S., Piragyte, I., and Choi, E. J. (2013). Apoptase blocks T cell activation by modulation of protein kinase C- θ -dependent pathway. *Food Chem. Toxicol.* 62, 23–31. doi:10.1016/j.fct.2013.08.016
- Ogawa, K., and Ito, M. (2016a). Appetite-enhancing effects of trans-cinnamaldehyde, benzylacetone and 1-Phenyl-2-butanone by inhalation. *Planta Med.* 82, 84–88. doi:10.1055/s-0035-1558087
- Ogawa, K., and Ito, M. (2016b). Appetite-Enhancing effects: the influence of concentrations of benzylacetone and trans-cinnamaldehyde and their inhalation time, as well as the effect of aroma, on body weight in mice. *Biol. Pharm. Bull.* 39 (5), 794–798. doi:10.1248/bpb.b15-00937
- Okugawa, H., Ueda, R., Matsumoto, K., Kawanishi, K., and Kato, A. (1996). Effect of jinkoh-eremol and agarospirol from agarwood on the central nervous system in mice. *Planta Med.* 62, 2–6. doi:10.1055/s-2006-957784
- Okugawa, H., Ueda, R., Matsumoto, K., Kawanishi, K., and Kato, K. (2000). Effects of sesquiterpenoids from "oriental incenses" on acetic acid-induced writhing and D₂ and 5-HT_{2a} receptors in rat brain. *Phytomedicine* 7, 417–422. doi:10.1016/S0944-7113(00)80063-X

- Park, H. J., Lim, E. J., Zhao, R. J., Oh, S. R., Jung, J. W., and Ahn, E. M. E. M. (2015). Effect of the fragrance inhalation of essential oil from *Asarum heterotropoides* on depression-like behaviors in mice. *BMC Compl. Alternative Med.* 15, 43. doi:10.1186/s12906-015-0571-1
- Peng, D. H., Shi, F., Li, G., Fralick, D., Shen, T., and Qiu, M. H. (2015). Surface vulnerability of cerebral cortex to major depressive disorder. *PLoS One* 10, e0120704. doi:10.1371/journal.pone.0120704
- Perveen, T., Emad, S., Ahmad, S., Batool, Z., Yousuf, S., Sheikh, S., et al. (2017). Fennel oil treatment mimics the anti-depressive and anxiolytic effects of fluoxetine without altering the serum cholesterol levels in rats. *Pjz* 49, 2291. doi:10.17582/journal.pjz/2017.49.6.2291.2297
- Porsolt, R. D., Anton, G., Blavet, N., and Jalfre, M. (1978). Behavioural despair in rats: a new model sensitive to antidepressant treatments. *Eur. J. Pharmacol.* 47, 379–391. doi:10.1016/0014-2999(78)90118-8
- Shang, L. L. (2018). Establishment and application of chromatographic fingerprints of Agarwood. Beijing, China: Chinese Academy of Forestry.
- Sheline, Y. I., Liston, C., and McEwen, B. S. (2019). Parsing the Hippocampus in depression: chronic stress, hippocampal volume, and major depressive disorder. *Biol. Psychiatr.* 85, 436–438. doi:10.1016/j.biopsych.2019.01.011
- Song, C., Phillips, A. G., and Leonard, B. (2003). Interleukin 1 beta enhances conditioned fear memory in rats: possible involvement of glucocorticoids. *Eur. J. Neurosci.* 18, 1739–1743. doi:10.1046/j.1460-9568.2003.02886.x
- Song, S., Chang, Y., Jin, X. D., Qiu, R. L., Yao, W., Yu, S., et al. (2020). Experimental study on rapid discrimination of raw *Aucklandia Radix* and its roasted products by HS-GC-MS combined with chemometrics analysis. *Journal of Pharmaceutical Analysis*. 40(05), 916–926. doi:10.1615/j.0254-1793.2020.05.20
- Stewart, A., Maity, B., Wunsch, A. M., Meng, F., Wu, Q., and Wemmie, J. A. (2014). Regulator of G-protein signaling 6 (RGS6) promotes anxiety and depression by attenuating serotonin-mediated activation of the 5-HT_{1A} receptor-adenylyl cyclase axis. *FASEB J.* 28, 1735–1744. doi:10.1096/fj.13-235648
- Sun, Y. A., Zhang, H., Li, Z., Yu, W., Zhao, Z., Wang, K., et al. (2020). Determination and comparison of agarwood from different origins by comprehensive two-dimensional gas chromatography–quadrupole time-of-flight mass spectrometry. *J. Sep. Sci.* 43 (7), 1284–1296. doi:10.1002/jssc.201901008
- Takemoto, H., Ito, M., Shiraki, T., Yagura, T., and Honda, G. (2008). Sedative effects of vapor inhalation of agarwood oil and spikenard extract and identification of their active components. *J. Nat. Med.* 62, 41–46. doi:10.1007/s11418-007-0177-0
- Tan, C. S., Isa, N. M., Ismail, I., and Zainal, Z. (2019). Agarwood induction: current developments and future perspectives. *Front. Plant Sci.* 10, 122. doi:10.3389/fpls.2019.00122
- Wang, S., Wang, C., Peng, D., Liu, X., Wu, C., and Guo, P. (2017). Agarwood essential oil displays sedative-hypnotic effects through the GABAergic system. *Molecules*. 22 (12). doi:10.3390/molecules22122190
- Wang, M.-R., Li, W., Luo, S., Zhao, X., Ma, C.-H., and Liu, S.-X. (2018a). GC-MS study of the chemical components of different *Aquilaria sinensis* (lour.) gilgorgans and agarwood from different asian countries. *Molecules* 23 (9), 2168. doi:10.3390/molecules23092168
- Wang, S., Wang, C., Yu, Z., Wu, C., Peng, D., Liu, X., et al. (2018b). Agarwood essential oil ameliorates restrain stress-induced anxiety and depression by inhibiting HPA Axis hyperactivity. *Ijms* 19, 3468. doi:10.3390/ijms19113468
- Wang, S., Yu, Z., Wang, C., Wu, C., Guo, P., and Wei, J. (2018c). Chemical constituents and pharmacological activity of agarwood and *Aquilaria* plants. *Molecules* 23 (2), 342. doi:10.3390/molecules23020342
- Wang, C. Z., Lin, H. Q., Yang, N., Wang, H., Zhao, Y., Li, P. Y., et al. (2019a). Effects of platycodins folium on depression in mice based on a UPLC-Q/TOF-MS serum assay and hippocampus metabolomics. *Molecules* 24, 1712. doi:10.3390/molecules24091712
- Wang, X. P., Wang, P. F., Bai, J. Q., Gao, S., Wang, Y. H., and Quan, L. N. (2019b). Investigating the effects and possible mechanisms of danshen- honghua herb pair on acute myocardial ischemia induced by isoproterenol in rats. *Biomed. Pharmacother.* 118, 109268. doi:10.1016/j.biopha.2019.109268
- Watanabe, T., Fujihara, M., Murakami, E., Miyoshi, M., Tanaka, Y., and Koba, S. S. (2011). Green odor and depressive-like state in rats: toward an evidence-based alternative medicine? *Behav. Brain Res.* 224, 290–296. doi:10.1016/j.bbr.2011.06.001
- Willner, P. (1997). Validity, reliability and utility of the chronic mild stress model of depression: a 10-year review and evaluation. *Psychopharmacology (Berl)* 134, 319–329. doi:10.1007/s002130050456
- Willner, P., Towell, A., Sampson, D., Sophokleous, S., and Muscat, R. (1987). Reduction of sucrose preference by chronic unpredictable mild stress, and its restoration by a tricyclic antidepressant. *Psychopharmacology (Berl)* 93, 358–364. doi:10.1007/BF00187257
- Woo, J. H., Ahn, J. H., Jang, D. S., and Choi, J. H. (2019). Effect of dehydrocostus lactone isolated from the roots of *Aucklandia lappa* on the apoptosis of endometriotic cells and the alternative activation of endometriosis-associated macrophages. *Am. J. Chin. Med.* 47, 1289–1305. doi:10.1142/S0192415X19500666
- Xing, H., Zhang, K., Zhang, R., Shi, H., Bi, K., and Chen, X. (2015). Antidepressant-like effect of the water extract of the fixed combination of *Gardenia jasminoides*, *Citrus aurantium* and *Magnolia officinalis* in a rat model of chronic unpredictable mild stress. *Phytomedicine* 22, 1178–1185. doi:10.1016/j.phymed.2015.09.004
- Xing, H., Zhang, X., Xing, N., Qu, H., and Zhang, K. (2019). Uncovering pharmacological mechanisms of Zhi-Zi-Hou-Po decoction in chronic unpredictable mild stress induced rats through pharmacokinetics, monoamine neurotransmitter and neurogenesis. *J. Ethnopharmacol.* 243, 112079. doi:10.1016/j.jep.2019.112079
- Xu, F., Peng, D., Tao, C., Yin, D., Kou, J., and Zhu, D. D. N. (2011). Anti-depression effects of Danggui-Shaoyao-San, a fixed combination of Traditional Chinese Medicine, on depression model in mice and rats. *Phytomedicine* 18, 1130–1136. doi:10.1016/j.phymed.2011.05.002
- Yamahara, J., Matsuda, H., Huang, Q., Li, Y., and Fujimura, H. (1990). Intestinal motility enhancing effect of *Atractylodes lancea* rhizome. *J. Ethnopharmacol.* 29 (3), 341–344. doi:10.1016/0378-8741(90)90044-t
- Yan, X., Wang, W., Chen, Z., Xie, Y., Li, Q., and Yu, Z. W. (2020). Quality assessment and differentiation of *Aucklandia radix* and *Vladimiria radix* based on GC-MS fingerprint and chemometrics analysis: basis for clinical application. *Anal. Bioanal. Chem.* 412 (7), 1535–1549. doi:10.1007/s00216-019-02380-2
- Yi, L. T., Li, J., Geng, D., Liu, B. B., Fu, Y., and Tu, J. Q. (2013). Essential oil of *Perilla frutescens*-induced change in hippocampal expression of brain-derived neurotrophic factor in chronic unpredictable mild stress in mice. *J. Ethnopharmacol.* 147, 245–253. doi:10.1016/j.jep.2013.03.015
- Zhang, L.-L., Yang, Z.-Y., Fan, G., Ren, J.-N., Yin, K.-J., and Pan, S.-Y. (2019). Antidepressant-like effect of *Citrus sinensis* (L.) Osbeck essential oil and its main component limonene on mice. *J. Agric. Food Chem.* 67, 13817–13828. doi:10.1021/acs.jafc.9b00650
- Zhang, T. Y., Li, Y. T., and Liu, P. (2018). Effects of Yiyuping capsules on hippocampal neuron apoptosis and BDNF in CUMS stress rats. *Pharm. J. Chin. People's Liberation Army* 34, 105–109. doi:10.3969/j.issn.1008-9926.2018.02.002
- Zhang, Y., Wang, W., and Zhang, J. (2004). Effects of novel anxiolytic 4-butyl-alpha-agarofuran on levels of monoamine neurotransmitters in rats. *Eur. J. Pharmacol.* 504, 39–44. doi:10.1016/j.ejphar.2004.09.051
- Zhao, Q., Chen, A., Wang, X., Zhang, Z., Zhao, Y., and Huang, Y. Y. (2018). Protective effects of dehydrocostuslactone on rat hippocampal slice injury induced by oxygen-glucose deprivation/reoxygenation. *Int. J. Mol. Med.* 42, 1190–1198. doi:10.3892/ijmm.2018.3691
- Zhao, Q., Cheng, X., Wang, X., Wang, J., Zhu, Y., and Ma, X. (2016). Neuroprotective effect and mechanism of Mu-Xiang-You-Fang on cerebral ischemia-reperfusion injury in rats. *J. Ethnopharmacol.* 192, 140–147. doi:10.1016/j.jep.2016.07.016
- Zheng, Q., Tang, Y., Hu, P. Y., Liu, D., Zhang, D., and Yue, P. P. (2018). The influence and mechanism of ligustilide, senkyunolide I, and senkyunolide A on echinacoside transport through MDCK-MDR1 cells as blood-brain barrier *in vitro* model. *Phytother. Res.* 32, 426–435. doi:10.1002/ptr.5985
- Zhuo, J. Y., Chen, B. Y., Sun, C. Y., Jiang, T., Chen, Z. W., and Liu, Y. L. (2020). Patchouli alcohol protects against chronic unpredictable mild stress-induced depressant-like behavior through inhibiting excessive autophagy via activation of mTOR signaling pathway. *Biomed. Pharmacother.* 127, 110115. doi:10.1016/j.biopha.2020.110115

Conflict of Interest: The authors declare that the research was conducted in the absence of any commercial or financial relationships that could be construed as a potential conflict of interest.

Copyright © 2021 Li, Li, Zhang, Ren, Wang, Li, Wang, Ren, Zhao, Yang and Huang. This is an open-access article distributed under the terms of the Creative Commons Attribution License (CC BY). The use, distribution or reproduction in other forums is permitted, provided the original author(s) and the copyright owner(s) are credited and that the original publication in this journal is cited, in accordance with accepted academic practice. No use, distribution or reproduction is permitted which does not comply with these terms.



Natural Medicines for the Treatment of Epilepsy: Bioactive Components, Pharmacology and Mechanism

Li-Ying He^{1†}, Mei-Bian Hu^{2†}, Ruo-Lan Li¹, Rong Zhao¹, Lin-Hong Fan¹, Lin He¹, Feng Lu¹, Xun Ye¹, Yong-liang Huang^{3*} and Chun-Jie Wu^{1*}

¹College of Pharmacy, Chengdu University of Traditional Chinese Medicine, Chengdu, China, ²Institute of Pharmaceutical and Food engineering, Shanxi University of Chinese Medicine, Jinzhong, China, ³Hospital of Chengdu University of Traditional Chinese Medicine, Chengdu, China

OPEN ACCESS

Edited by:

Jiahong Lu,
University of Macau, China

Reviewed by:

Lei Wang,
University of Pittsburgh, United States
Song-Lin Li,
Jiangsu Provincial Hospital of
Traditional Chinese Medicine, China

*Correspondence:

Yong-liang Huang
ld10000@126.com
Chun-Jie Wu
wucjcdtcm@163.com

[†]These authors contributed equally to
this manuscript

Specialty section:

This article was submitted to
Ethnopharmacology,
a section of the journal
Frontiers in Pharmacology

Received: 08 September 2020

Accepted: 05 January 2021

Published: 04 March 2021

Citation:

He L-Y, Hu M-B, Li R-L, Zhao R,
Fan L-H, He L, Lu F, Ye X, Huang Y and
Wu C-J (2021) Natural Medicines for
the Treatment of Epilepsy: Bioactive
Components, Pharmacology
and Mechanism.
Front. Pharmacol. 12:604040.
doi: 10.3389/fphar.2021.604040

Epilepsy is a chronic disease that can cause temporary brain dysfunction as a result of sudden abnormal discharge of the brain neurons. The seizure mechanism of epilepsy is closely related to the neurotransmitter imbalance, synaptic recombination, and glial cell proliferation. In addition, epileptic seizures can lead to mitochondrial damage, oxidative stress, and the disorder of sugar degradation. Although the mechanism of epilepsy research has reached up to the genetic level, the presently available treatment and recovery records of epilepsy does not seem promising. Recently, natural medicines have attracted more researches owing to their low toxicity and side-effects as well as the excellent efficacy, especially in chronic diseases. In this study, the antiepileptic mechanism of the bioactive components of natural drugs was reviewed so as to provide a reference for the development of potential antiepileptic drugs. Based on the different treatment mechanisms of natural drugs considered in this review, it is possible to select drugs clinically. Improving the accuracy of medication and the cure rate is expected to compensate for the shortage of the conventional epilepsy treatment drugs.

Keywords: natural herbal medicines, epilepsy, bioactive components, mechanisms, therapy

INTRODUCTION

Epilepsy, which is also commonly known as “goatopathy,” was first recognized in 1997, since when the global campaign against epilepsy (GCAE) has been working on the strategy of “improving access, treatment, services, and prevention of epilepsy worldwide” (Saxena and Li, 2017). As per the World Health Organization data on epilepsy for 2006–2015, the number of people with epilepsy continues to remain high. Epilepsy is a common, severe, chronic neurological disease that affects >70 million people across the world. In fact, it affects individuals irrespective of their ages, gender, ethnic background, or the geographic location (Khan et al., 2020).

The known causes of epilepsy has been reclassified as hereditary, structural, infectious, immunological, metabolic, or unknown (Singh and Trevick, 2016). Increasing attention is being paid to the treatment of epilepsy, and the combination of Chinese and western medicine treatment may be more favored (Li, 2012). On one hand, Western medicine treatment for epilepsy can be mainly categorized as etiological treatment, drug treatment, or surgical treatment (Fu and Qu, 2019), example, levetiracetam and phenytoin sodium carbamazepine. On the other hand, natural drugs have been reported to play an important role in the clinical treatment of epilepsy (Piazzi and Berio,

2015). The effect of natural drugs on epilepsy treatment through different mechanisms has been reported in many articles, and the improvement effect is better.

Presently, the conventional drugs that are commonly used for the treatment of epilepsy include carbamazepine, valproate sodium, phenobarbital sodium, phenytoin sodium, and prelampona, among others (Fu and Qu, 2019). These drugs also regulate excitatory and inhibitory discharge in the brain and indirectly regulate the excitatory and inhibitory discharge by regulating the ion concentration. Among these, phenytoin sodium has an outstanding curative effect; however, after treatment, adverse reactions such as anemia after reproduction and acute cerebellar ataxia may occur. Carbamazepine treatment is likely to cause rashes, neurotoxic side effects, diplopia, dermatomyositis, blood and respiratory system damage, and other different types of adverse syndromes. In the recent years, new drugs have been proposed to treat epilepsy, including topiramate, lamotrigine, levetiracetam, and gabapentin. When compared with the conventional drugs, the advantages of these natural drugs include a broad spectrum of antiepileptic, involving less adverse reactions, higher safety, and lesser drug interaction. However, for some refractory epilepsy and epilepsy patients with other comorbidities, the use of these drugs obviously cannot meet their needs. Natural medicines retain the natural and biological activities of their constituents (Guo et al., 2015). Natural drugs have limited or no toxic side-effects. In addition, animals do not possess the advantages of drug resistance, hence the use of natural drugs in animals generally leave no drug residue and causes no health hazards. When compared with the conventional medicine used for the treatment of epilepsy, the composition of natural drugs is complex. Although the use of a single drug may not produce outstanding cure rate, it induces slight toxic side-effects, which can reduce a patient's level of discomfort. The combination of natural and conventional medicines may not only reduce the resultant adverse reactions but also improve the overall comprehensive efficacy (Yuan et al., 2019). Therefore, the present study reviewed the active components of natural drugs and the conventional antiepileptic drugs.

The use of Western medicine alone to treat epilepsy has been reported to induce more adverse reactions. For instance, the use of phenytoin sodium alone can cause gastrointestinal irritation, and its long-term use can cause gingival hyperplasia, nervous system dysfunction, and hematopoietic system disorders. The use of carbamazepine alone may induce dizziness, nausea, vomiting, and ataxia as well as occasional aplastic anemia and granulocytopenia. Valproate alone can cause nausea, vomiting, lethargy, tremor, hair loss, and hepatotoxicity. The use of an antiepileptic alone may induce anorexia, nausea, dizziness, and drowsiness.

The present paper reviewed the effects of active components of natural drugs on epilepsy, including flavonoids, alkaloids, glycosides, coumarins, and terpenoids. Among the monomer components, flavonoids, alkaloids, and terpenoids demonstrated significant activity against epilepsy. We have summarized the methods for the prevention and treatment of epilepsy by balancing excitatory and inhibitory neurotransmitters and inhibiting neuroinflammation, oxidative stress, and

mitochondrial dysfunction. In addition, we innovatively summarized the combined methods of natural drug monomer compounds and natural drug compound as well as conventional antiepileptic drugs, expecting to bring hope to epileptic patients and provide them with a credible reference for improving the epilepsy cure rate.

THE PATHOGENESIS OF EPILEPSY

One of the main causes of epileptic seizures is believed to be the abnormal activity of cortical neurons, and the abnormal discharge of these neurons has mostly been related to the loss of specific subarea inhibitory and excitatory neurons, neurotransmitter transmission and imbalance, synaptic recombination, axonal germination, as well as the change in the glial cell functioning and structure. Glial cells and axons in the white matter content may play a secondary role in this situation (Xue, 2005; Zhu et al., 2014). Recurrent seizures can lead to abnormal synaptic protein expression, synaptic remodeling, and abnormal neuronal network formation, which is one of the pathophysiological mechanisms of refractory epilepsy (Yang et al., 2017). In addition, with the development of molecular biology, the study of epilepsy mechanism has shifted from phenotype to genotype, with dozens of genes or candidate genes found. The occurrence of epilepsy can be attributed to primary genetic abnormality or secondary definite structure or metabolic disorder (Depondt, 2006; Thijs et al., 2019). Genealogy and genetic analysis have indicated that epilepsy can be inherited in one or more genes, dominant or recessive, or even concomitantly. Therefore, innate genetic factors and acquired environmental factors can lead to the occurrence and development of epilepsy.

Synapses and Receptors

GABA is a major inhibitory neurotransmitter in the cerebral cortex that maintains the inhibitory tension to balance nerve excitation (Hirose, 2014). If this balance is disturbed, seizures follow. The enzyme glutamic acid decarboxylase (GAD) can promote the synthesis of neuronal GABA from glutamic acid, which is encoded by two different genes, *GAD2* and *GAD1* (Obata, 2013). *GAD1* plays the major role for GABA production in the embryonic brain, whereas the contribution of *GAD2* begins to increase after birth. *GAT-1* and *GAT-3* are GABA-transporters (GATs), and high level of GAT content has been associated with seizures. GABA receptors can be categorized into three types based on their different pharmacological characteristics as GABA-A, GABA-B, and GABA-C receptors (Pham et al., 2016). GABA-type A receptor (GABA-A R) has been found to be the major genetic target of heritable human epilepsy (Chen et al., 2017). GABA-A induces epilepsy mainly in the following ways: through controlling the chloride ion flow or by impairing GABAergic inhibitory input that lead to synchronous excitatory activity in the neuronal population and, ultimately, seizures (Beenhakker and Huguenard, 2009). GABAB, which increases potassium conductance, reduces the Ca^{2+} entry and inhibits the release of other presynaptic

transmitters. Presently, reduced or abnormal GABA function has been detected in both genetic and acquired animal models of epilepsy and in the human epileptic brain tissues (Treiman, 2001).

Glutamate (Glu) acts on various membrane receptors, which form cation-permeable ion channel receptors. It can be categorized into three families: alpha-amino-3-hydroxy-5-methyl-4-isoxazole-propionate (AMPA) receptors (AMPA), kainate receptors (KARs), and NMDA receptors (NMDARs) (Paoletti et al., 2013). The high levels of Glu causes nerve damage or death, mainly due to increased NMDAR activity and Ca^{2+} influx through the NMDAR channels. Excessive NMDAR activity may also form the basis for epileptic seizures, which are characterized by neuronal hyperexcitability or sensitivity. In addition, nicotinic acetylcholinergic receptors (nAChRs) in the vertebrates are pentamer ligands-gated ion channels assembled from homologous subunits (Adams et al., 2012). Central nAChRs can influence the onset of epilepsy through the regulation of the release of other neurotransmitters, such as glutamate, GABA, dopamine, and norepinephrine (Sinkus et al., 2015). Several past studies have suggested that nNOS can facilitate seizure generation during SE. The mechanism involved in this event is that NO reduces the blood-brain barrier opening after trauma by improving the vascular permeability (Gangar and Bhatt, 2020). The 5-HT receptor-related changes have also been reported in the study of epilepsy mechanisms (Zhao et al., 2018).

Ion Channels and Epilepsy

Mutations in the sodium channels are responsible for the development of genetic epilepsy syndromes with a wide range of severity. Mutations in the NaV1.1 channels have severely impaired sodium currents and the action potential firing in the hippocampal GABAergic inhibitory neurons, which can cause hyperexcitability, contributing to seizures (William et al., 2010). SCN1A gene, which encodes NaV1.1 subunit expressed in inhibitory GABA neurons, has also been implicated in the mutations of SCN1A in epilepsy patients (Duflocq et al., 2008). In addition, SCN1B, SCN2A, and SCN8A mutations have been found to be associated with epilepsy (Tang and Mei, 2016). Potassium channels are the most diverse group of ion channels and they play an important role in countless cellular processes, for example, in regulating the potassium outflow, current and action potential, and neurotransmitter release (Contet et al., 2016). The K^+ channels control the resting membrane potential and enable rapid repolarization of the action potential by producing outward K^+ currents, which limits neuronal excitability. Among the numerous genes that encode potassium channels, mutations in KCNMA1 were first reported in large families with autosomal-dominant totipotent epilepsy and parasympathetic dysmotility. Subsequently, mutations in KCNQ2, KCNT1, and KCNQ3 were reported in familial neonatal epilepsy (Tang et al., 2016).

A large amount of Ca^{2+} influx not only causes excitatory amino acid poisoning but also increases the concentration of Ca^{2+} in the cells, thereby inducing neuronal damage. The plasmids become overcharged with negative Ca^{2+} influx for a long time.

The Ca^{2+} imbalance and the malfunctioning of mitochondria form a vicious cycle make the brain organization of ATP production insufficient, the release of mPTP leads to fine cytosolic edema, and results in intracellular Ca^{2+} overload of the nerve cells, which eventually causes nerve cell death. In addition, the overload leads to excessive production of NO in the regulatory neurons, which can be combined with superoxygenated substances to produce ONOO⁻ in the nervous cells; this event is highly toxic to the white matter, membrane lipids, and DNA as well as leads to oxidative stress. Therefore, the increase in Ca^{2+} concentration affects the occurrence of epilepsy from different aspects. Currently, numerous experimental data suggest that CACNA1A mutation plays a significant role in human epilepsy (Alexander et al., 2016). Moreover, the CLCN2 channel plays a critical role near GABA-A receptors at the GABAergic inhibitory synapses (Agostino et al., 2004). CLCN2 mutations in multiphenotypic families (Martin et al., 2009) and in primary systemic epilepsy have also been identified. The mechanism of epilepsy induced by the imbalance of the CLC channels or gene mutation may be related to its regulation of excitability of the cell membrane and the transport functions of electrolytes, water, and nutrients (Wei et al., 2017). Highly polarized activated cyclic nucleotide gating (HCN) channels encoded by 4 genes (HCN1-4) have been reported to undergo transcriptional changes in patients with epilepsy, with the possible mechanism of influencing excitability in patients with epilepsy (DiFrancesco and DiFrancesco, 2015).

Immune System

Impaired immune function and inflammatory response are both the cause of occurrence and development of epilepsy as well as the result of partial epilepsy. Past studies have demonstrated that CD3, CD4, and $\text{CD4}^+/\text{CD8}^+$ count of helper T-cells decrease and the CD8^+ value of inhibitory T-cells increase significantly in the peripheral blood of epileptic patients (DiFrancesco and DiFrancesco, 2015; Arreola et al., 2017). In addition, several past scholars have studied the changes in the values of IgG, IgA, IgM, IgG1, IgG2, IgG3, and IgE in epileptic patients (Callenbach et al., 2003; Godhwani and Bahna, 2016). A weakened immune system often acts as an accomplice in the onset of epilepsy, along with other trigger factors (Matin et al., 2015). Moreover, cytokines involved in the regulatory effects of the immune system have been found to be involved in epilepsy in patients with partially overexpressed states. A major portion of this process is the inflammatory response, and changes in the inflammatory factors to a certain extent indicate that the occurrence of epilepsy can also induce a certain inflammatory response. For instance, IL-1 β , IL-6, IL-10, IL-2, IL-17 (Kumar et al., 2019), IL-4, and TNF- α were abnormally expressed in patients, whose elevated levels can lead to neuronal degeneration and induce epilepsy (Ravizza et al., 2006). Another mechanism by which IL-1 participates in epilepsy is through the upregulation of NMDA receptors on postsynaptic cells through the activation of GluN2B subunits of NMDA receptors (Ravizza et al., 2006). TNF- α increases the number of Glu receptors and induces the ingestion of GABA, which in turn reduces the inhibitory drive and induces

neuronal excitation, which leads to the development of epilepsy (Liu et al., 2015).

Glioma-Associated Epilepsy

Glial cells regulate excitatory and inflammatory responses that affect the occurrence of epilepsy (Devinsky et al., 2013). Astrogliosis is a common pathological hallmark of idiopathic and acquired forms of epilepsy. L-glutamic acid, D-serine, GABA, and kynurenic acid released from astrocytes are mostly involved in the epileptic process (Yamamura et al., 2013). In addition, GS is a cytoplasmic enzyme present in astrocytes that regulates the Glu acid levels. In a past study, the GS levels were significantly reduced in the hippocampus and the amygdala of TLE patients, which suggests that this enzyme is associated with the occurrence of epilepsy (Devinsky et al., 2013). Microglia activation not only increases the levels of brain inflammatory factors and TNF- α but also enhances the activities of induced nitric oxide synthase (iNOS) and cyclooxygenase-2 (COX-2), which can enhance the induction of epilepsy induced by neurogenesis (Akin et al., 2011; Yuan and Liu, 2020). The activated astrocytes induce the release of inflammatory factors such as IL-1 β . Therefore, glial cells are not only involved in the imbalance of neurotransmitters in the process of epilepsy but also in the process of inflammation.

Mitochondrial Dysfunction and Oxidative Stress

Mitochondrial oxidative stress and dysfunction may trigger epileptic seizures arising from mitochondrial DNA (mtDNA) or nuclear DNA mutations and temporal lobe epilepsy (Rowley and Patel, 2013). Myoclonic epilepsy has been shown to be associated with mtDNA mutations. Two such targets of oxidation related to episodes of epilepsy are the glial glutamate transporters GLT-1 and GLAST (Liang et al., 2012). In addition, oxidative stress and mitochondrial dysfunction result from prolonged duration of seizure. The depolarization pattern during intense epileptic activity of neurons in response to external stimuli leads to mitochondrial depolarization and mitochondrial Ca²⁺ accumulation, which in turn induces mitochondrial apoptotic pathways or oxidative stress that accelerate energy failure and mitochondrial superoxide production (Kudin et al., 2002). Superoxide is a moderately active free radical and its production leads to the formation of more active ROS, which lead to lipid peroxidation and subsequent membrane destruction that are reflected in the increased content of MDA as a product of lipid peroxidation. This event thus promotes the intrinsic pathway toward triggering of cell apoptosis and death. The content of SOD, CAT, and glutathione peroxidase in the mitochondria also changes in this situation. The degradation pathways of superoxide and hydrogen peroxide (H₂O₂) involved in SOD and CAT were also affected with the change in the upstream products. The time-dependent generation of H₂O₂ in the hippocampal mitochondria as well as the frequency of mtDNA damage also increases in epileptic patients (Smith and Patel, 2017).

Glycogen Degradation

Glycogen is involved in the neurotransmission of glutamate as well as in the degradation of glycogen to promote glutamate transport in the astrocytes. Furthermore, glycogen in astrocytes can be used to synthesize glutamine, which is a precursor of glutamate (Bark et al., 2018). In addition, glycogen is involved in promoting the removal of K⁺ from the extracellular space, and excessive neuronal activity has been associated with K⁺ efflux (Walls et al., 2009). Moreover, decreased glycogen degradation is believed to be associated with epileptic seizures.

Glucocorticoids

Glucocorticoids have been reported to be involved in the regulation of various activities of the nervous system through the GR (Kanner, 2009). Glucocorticoids have also been reported to affect people with epilepsy. Some of the reported results demonstrate that the level of glucocorticoids increases in epilepsy models. However, only a few studies have been reported in this field, although this conclusion needs further verification. The possible pathogenesis of epilepsy is displayed in Table 1.

PHARMACOLOGICAL EFFECTS OF NATURAL MEDICINES FOR THE MANAGEMENT OF EPILEPSY

Despite the increasing number of researches on natural medicine, the ingredients of natural medicine remain complex, such as alkaloids, flavonoids, saccharides, glycosides, quinones, coumarins, lignans, terpenes, volatile oils, saponins, and cardiac glycosides (Kim, 2016). Several ingredients have been reported to possess antiepileptic activity, with the main therapeutic mechanisms including regulating synapse and receptor pathways (i.e., GABA, Glu, NMDAR, and 5-HT), ion channels (i.e., Ca²⁺, K⁺, and Na⁺), immune system (i.e., CD3, CD4, IgG, IgA, TNF- α , IL-1 β , IL-2, IL-4, IL-6, and IL-10), glial cells (i.e., glial cell proliferation and potassium uptake ability) and mitochondrial dysfunction and oxidative stress (i.e., oxidation markers, accumulation of Ca²⁺, cell death, and apoptosis). Presently, we can reclassify these ingredients in accordance to the difference in the mechanisms of action.

NATURAL MEDICINES IMPROVES EPILEPSY BY REGULATING SYNAPSES AND RECEPTORS

Flavonoids share similar structures to benzodiazepines (Nilsson and Sterner, 2011), and play an anti-epileptic role through the regulation of the GABAA-Cl-channel complex (Xiang et al., 2014). Several flavonoids that can be used to treat epilepsy through different receptor signaling pathways are known. Tanshinone IIA is a hydrophobic ketone extracted from *Salvia miltiorrhiza*. Past studies have shown that the reduced c-fos expression in the brains of PTZ-exposed zebrafish larvae plays a therapeutic role in epilepsy through the activation of the GABA

TABLE 1 | Possible mechanisms involved in epilepsy.

Component	Specific factors	References
Neurotransmitters	Imbalance of Glu and GABA	Hirose (2014)
Synapses and Receptor	GABA-A, NMDA, 5-HT, AMPA receptor, acetylcholine receptor Enzyme, modulator, transporter, axonal burst bud	Hirose (2014); Paoletti et al. (2013); Thijs et al. (2019)
Ion channels	Sodium channel; Potassium channel; HCN channel; Calcium channel; Chloride channel	Alexander et al. (2016); Contet et al. (2016); Duflocq et al. (2008); Tang et al. (2016)
Inflammatory cytokines	IL-1 β , IL-2, IL-4, IL-6, IL-10, TNF- α , cyclooxygenase-2, Platelet-activating factor, Prostaglandin E2, Adhesion molecules, MMP-9; TLR-1, -2, -3; Chemokines were increased	Godhwani and Bahna (2016); Kumar et al. (2019)
Immune system	Both cellular and humoral immunity are affected. Increasing IgA, IgG, CD8, CD54; Decreasing CD3, CD4, CD4/CD8	Ravizza et al. (2006); Roseti et al. (2015); Liu et al. (2015)
Glial cell	Astrocytes and microglia proliferated and the ability of astrocytes to absorb potassium ions decreased	Bark et al. (2018)
Oxidative stress and apoptosis	ROS was increased, the ratio of Bcl-2/Bax was decreased, and the expression levels of apoptotic proteins cytochrome C and Caspase-3 were significantly increased	Liang et al. (2012); Kudin et al. (2002)
Mitochondrial dysfunction	Increasing Ca ²⁺ and ATP consumption	Rowley and Patel (2013); Liang et al. (2012); Kudin et al. (2002); Smith and Patel (2017)
Genetic factors	SCN1A, SCN2A, SCN8A and other mutations	Pal et al. (2010)
Glycogen metabolism	Decreased glycogen degradation, abnormal expression of glucocorticoid	Walls et al. (2009)

MMP-9, Matrix metalloproteinase-9; TLR, Toll-like receptors.

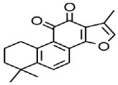
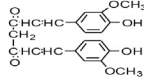
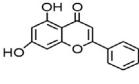
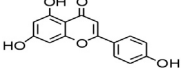
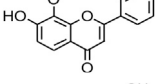
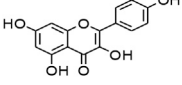
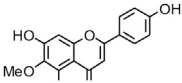
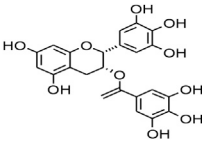
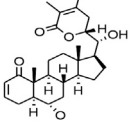
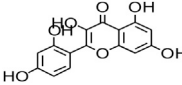
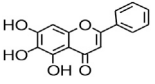
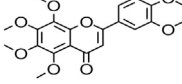
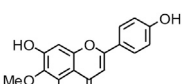
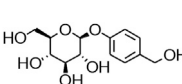
signaling pathway (Buenafe et al., 2013). Curcumin can improve depressive behavior and cognitive functioning through inhibition of acetylcholinesterase and by mediating monoaminergic regulation, which significantly reduces the number and degree of seizures by via inhibition of the activation of mechanistic target of the rapamycin complex 1 (mTORC1) (Kiasalari et al., 2013). Amentoflavone can improve the activity of hippocampal acetylcholinesterase as well as the learning and memory functions of rats (Yuan, 2016). However, amentoflavone has no regulating effect on the GABAR channel current in insular neurons induced by GABA. Luteolin is one of the main isolates of resveratrol, which is a natural flavonoid (Shen et al., 2016). Past studies have demonstrated that luteolin can increase the seizure threshold, and the mechanism may be to enhance the activation of GABAA receptors, thereby promoting the opening of GABA-mediated chlorine channels (Tambe et al., 2016; Tambe et al., 2017). (-)-Epigallocatechin-3-Gallate (EGCG) plays a therapeutic role in lithium-pilocarpine-induced epilepsy through the inhibition of the Toll-like receptor 4 (TLR4)/nuclear factor- κ B (NF- κ B) signaling pathway (Qu et al., 2019). Nobiletin significantly upregulated the expression of GAD65 and GABAA. Bupleuronin inhibited the current generated by NMDA receptor activation (Yang et al., 2018).

Glycosides have been reported to exert a therapeutic effect on epilepsy. Paeoniflorin (PF) plays an antiepileptic role through the inhibition of glutene-induced Ca²⁺ influx, activation of the metabotropic Glu receptor 5 (mGluR5), membrane depolarization, and neuronal death induced by Glu (Hino et al., 2012). Gastrodin mainly involves antioxidants and regulates the release of neurotransmitters. It has been reported to decrease GABA-T, GAD65, and GAD67 (Yuan et al., 2019). Sclerosylglucoside usulate (UASG) significantly prolonged the incubation period and reduced the seizure duration in animal models of INH-induced epilepsy by increasing GABA release (Kazmi et al., 2012).

Recently, the application of terpenoids in epilepsy has attracted much attention. (+)-Dehydrofukinone (DHF), an active ingredient in *Acorus tatarinowii*, is believed to possess anticonvulsant properties and may act as a potential antiepileptic drug through the induction of sedation and anesthesia via modulation of GABAA receptors (Garlet et al., 2017). In addition, 1-nitro-2-phenylethane is an active component that is isolated from volatile oil of *Aniba canelilla*. In a past study, mice injected with 1-nitro-2-phenylethane flumazine showed prolonged sleep pattern, and this hypnotic effect was possibly due to the upregulation of GABA in the central nervous system (Oyemitan et al., 2013). Tetrahydrocannabinol (THC) has been the primary focus of cannabis research until date. Delta9-THC (Δ 9-THC) exerts antioxidant effects in α -amino-3-hydroxy-5-methyl-4-isoxazolepropionic acid models and NMDA-mediated cytotoxicity models. Moreover, Δ 9-THC also desensitizes and transiently activates the transient receptor potential (TRP) channels TRPA1, TRPV1, and TRPV2 (Bahr et al., 2019). Borneol can easily cross the blood-brain barrier and exert a certain GABA regulating effect (Xiang et al., 2014). Isopulegol exhibited anticonvulsive effects through the positive modulation of benzodiazepine-sensitive GABAA receptors and antioxidant properties.

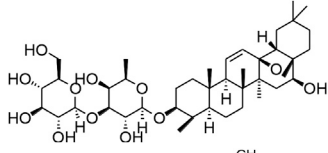
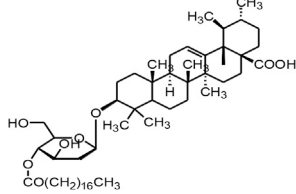
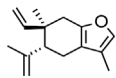
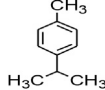
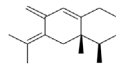
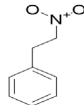
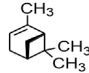
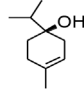
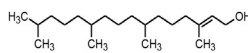
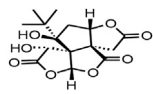
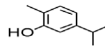
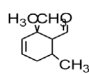
Alkaloids have been reported to regulate different receptors. Rhynchophylline (RIN) is an alkaloid isolated from *Uncaria rhynchophylla* (Ho et al., 2014). On one hand, RIN decreases neuronal hyperexcitability by inhibiting NMDA receptor current, and further decreases the expression of N-methyl-D-aspartate receptor 2B (NR2B) protein induced by pilocarpin (Shao et al., 2016). On the other hand, RIN inhibits the synaptic transmission. Sanjoinine A is an alkaloid active ingredient isolated from *Zizyphi Spinosi Semen* (Ma et al., 2008). Sanjoinine A not only blocks NMDA-induced epileptoid electroencephalography changes and reduces cerebellar granulos cell damage but also inhibits intracellular Ca²⁺ influx in NMDA-induced models. Tetrahydropalmatine (THP) is an alkaloid

TABLE 2 | Natural drugs used to treat epilepsy by regulating neurotransmitters and synaptic function.

Natural drugs	Compounds	Chemical structure	Animal models	Mechanisms	References
<i>Salvia miltiorrhiza</i> Bunge (<i>Lamiaceae</i>)	Tanshinone IIA		PTZS in rats; 4-APS in mice	Activating GABA signaling pathway; Decreasing MEK activity and Glu, C-fos expressions	Buenafe et al. (2013); Tan et al. (2014)
<i>Curcuma longa</i> L. ("turmeric," <i>Zingiberaceae</i>)	Curcumin		PTZS and KAS in mice	Inhibiting acetylcholinesterase and mediating monoaminergic regulation	Kiasalari et al. (2013)
<i>Passiflora coerulea</i> L. var. <i>Hort.</i>	Chrysin		PTZS in rats	Myorelaxant action agonizing the benzodiazepine receptor	Xiang et al. (2014)
<i>Matricaria chamomilla</i> L. (<i>Chamomile</i>)	Apigenin		PTXS in mice	Curbing benzodiazepine agonist	Xiang et al. (2014)
<i>Scutellaria baicalensis</i> Georgi. (<i>Lamiaceae</i>)	Wogonin		Mice	Enhancing expression of GABAA receptors	Diniz et al. (2015)
<i>Bupleurum chinense</i> (<i>Umbelliferae</i>)	Quercetin		KAS	Influencing ionotropic GABA receptors	Xiang et al. (2014)
<i>Plantago asiatica</i> L. (<i>Plantaginaceae</i>)	Hispidulin		Rat	Decreasing Glu	Diniz et al. (2015)
Green tea (<i>Camellia sinensis</i> (L.) Kuntze)	EGCG		L&PS in rats	Increasing impression of GABA	Qu et al. (2019)
<i>Withania somnifera</i> (L.) Dunal (<i>Solanaceae</i>)	Withanolide A		PTZS in rats	Recovering distorted NMDA receptor solidity; Regulating AMPA receptor function	Xiang et al. (2014)
<i>Maclura tinctoria</i> (<i>Moraceae</i>)	Morin		PTZS in mouse	Modulating the concentrations of GABA	Lee et al. (2018)
<i>Radix astragali</i> (<i>Astragalus species</i>)	Baicalin		PTZS in rats	Increasing impression of GABA	Diniz et al. (2015)
<i>Citrus reticulata</i> Blanco (<i>Rutaceae</i>)	Nobiletin		PTZS in mice	Modulating expression of GABAA and GAD65; Recovering Glu and GABA balance	Yang et al. (2018)
Smoke tree (<i>Cotinus coggygria</i>)	Fisetin		Iron-induced experimental model in rats	Increasing GABA level in brain	Diniz et al. (2015)
<i>Gastrodia elata</i> Blume (<i>Orchidaceae</i>)	Gastrodin		NMDAS in rat	Decreasing GABA-T, Glu, Increasing GAD65, GAD67	Liu et al. (2018)

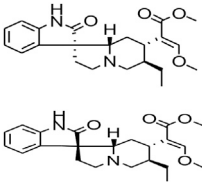
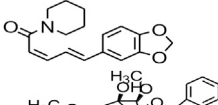
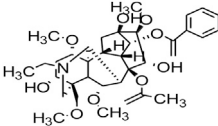
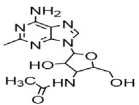
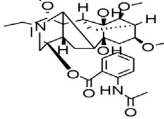
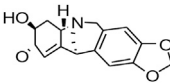
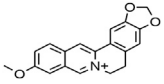
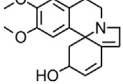
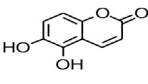
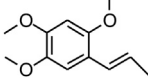
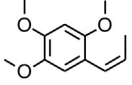
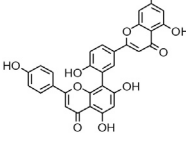
(Continued on following page)

TABLE 2 | (Continued) Natural drugs used to treat epilepsy by regulating neurotransmitters and synaptic function.

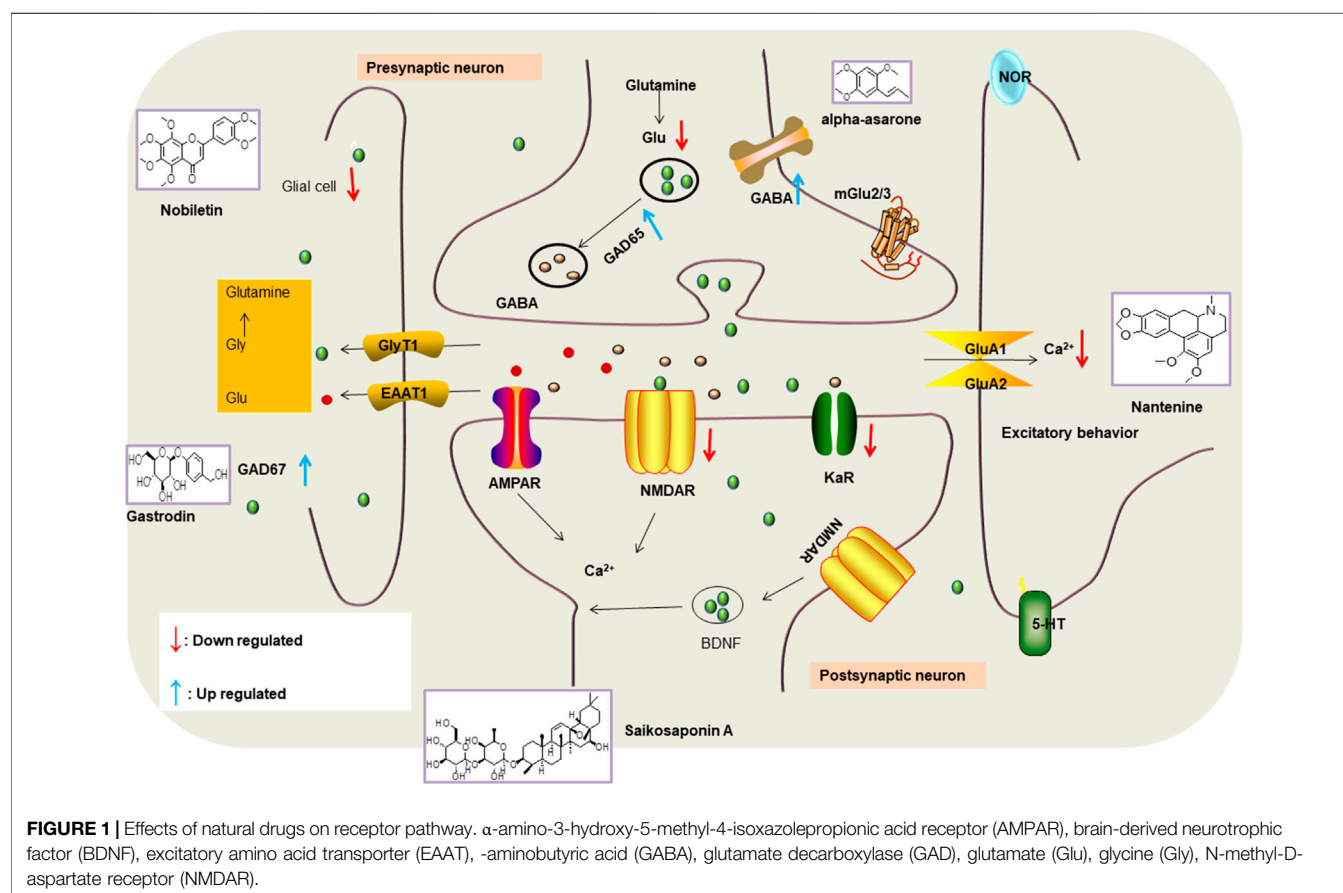
Natural drugs	Compounds	Chemical structure	Animal models	Mechanisms	References
<i>Radix bupleuri</i> (<i>Bupleurum</i> L.)	Saikosaponin A		L&PS in rats	Decreasing protein of p-gp, NMDAR	Xiang et al. (2014); Xie et al. (2013)
<i>Lantana camara</i> L. (<i>Verbenaceae</i>)	Ursolic acid Stearoyl glucoside		MES in mice	Increasing the GABA level in central nervous system	Kazmi et al. (2012)
<i>Curcuma longa</i> L. (<i>Zingiberaceae</i>)	Curzerene		PTZS in mice	Effecting GABAergic and opioid systems	Abbasi et al. (2017)
<i>Rhododendron tomentosum</i> (<i>Ledum palustre</i>)	P-Cymene		MES in mice	Mediating an increase in GABAergic response	Abbasi et al. (2017)
<i>Matricaria chamomilla</i> L. (<i>Lauraceae</i>)	(+)-Dehydrofukinone		GABAA RM in mice	Facilitating GABAergic neuronal	Garlet et al. (2017)
<i>Dennettia tripetala</i> Baker f (<i>Pepperfruit</i>)	1-nitro-2-phenylethane		PTZS in mice	Associated with GABA neurons	Oyemitan et al. (2013)
<i>Nigella sativa</i> (<i>N. sativa</i>) L. (<i>Ranunculaceae</i>)	Alpha-Pinene		PTZS in mice	Mediating GABAergic response	Bahr et al. (2019)
<i>Thymus vulgaris</i> L. (<i>Lamiaceae</i>)	Terpinen-4-ol		PTZS in mice	Regulating GABAergic neurotransmission	Bahr et al. (2019)
<i>Various medicinal plants</i>	Phytol		PTZS in mice	Interacting with GABAA receptor	Xiang et al. (2014)
<i>Ginkgo biloba</i> L. (<i>Ginkgoaceae</i>)	Bilobalide		L&PS in rats	Increasing GABA levels by potentiation	Xiang et al. (2014)
<i>Capsicum annuum</i> L. (<i>Solanaceae</i>)	Carvacrol		PTZS, MES in mice	Enhancing GABAA BZD receptor	Xiang et al. (2014)
<i>Saffron</i> (<i>Crocus sativus</i> L.)	Safranal		PTZS in rats	Regulating the GABAA benzodiazepine receptor	Xiang et al. (2014)

(Continued on following page)

TABLE 2 | (Continued) Natural drugs used to treat epilepsy by regulating neurotransmitters and synaptic function.

Natural drugs	Compounds	Chemical structure	Animal models	Mechanisms	References
<i>Uncaria rhynchophylla</i> (Miq.) Miq. ex Havil. (<i>Uncaria Schreber nom. cons.</i>)	Rhynchophylline isorhynchophylline		KAS in mice	Decreasing central nervous system synaptic transmission	Shao et al. (2016); Wang and Cai (2018)
<i>Piper nigrum</i> L. (<i>Piperaceae</i>)	Piperine		PTZS in both zebrafish and mice	Increasing GABA; Inhibit the TRPV1 receptor	Diniz et al. (2015)
<i>Aconitum carmichaeli</i> Debx. (<i>Ranunculaceae</i>)	Aconitine		Male Wistar rats	Blocking GABAA mediated	Zhao et al. (2020)
<i>Aconitum carmichaeli</i> Debx. (<i>Ranunculaceae</i>)	3-Acetylaconitine		Male Wistar rats	Promoting GABAA activity	Zhao et al. (2020)
<i>Aconitum carmichaeli</i> Debx. (<i>Ranunculaceae</i>)	Lappaconitine		Male Wistar rats	Promoting the release of GABAA	Xiang et al. (2014)
<i>Aconitum carmichaeli</i> Debx. (<i>Ranunculaceae</i>)	Montanine		PTZS in rats	Modulating neurotransmitter receptor systems; including GABAA receptors	Xiang et al. (2014)
<i>Coptis chinensis</i> Franch., C. (<i>Ranunculaceae</i>)	Berberine		PTZS in Zebrafish	Reducing convulsions and mortality and NMDA	Yang et al. (2018)
<i>Erythrina mulungu</i> Mart ex Benth (<i>Leguminosae-Papilionaceae</i>)	Erysotrine		PTZS in mice BCLS in rats	Related to NMDA	Xiang et al. (2014)
<i>Cortex fraxini</i> (<i>Fraxinus rhynchophylla</i> Hance)	Esculetin		EMS in mice	Probably through the GABAergic neuron	Xiang et al. (2014)
<i>Acorus tatarinowii</i> Schott (<i>Acorus L. Araceae</i>)	α -asarone		L&PS in rats	Decreasing GABA-T and NMDAR1 mRNA. Increasing GAD65, GAD67	Miao et al. (2011); Yuan and Liu (2020)
<i>Acorus tatarinowii</i> Schott (<i>Acorus L. Araceae</i>)	β -asarone		PTZS in rats	Modulating the excitatory transmitter glutamate	Yuan et al. (2019)
<i>Nandina domestica</i> Thunb (<i>Berberidaceae</i>)	Amentoflavone		L&PS in rats	Improving the activity of acetylcholinesterase	Yuan (2016)

4-AP induced seizures; EGCG, (-)-Epigallocatechin gallate; BCLS, bicuculline induced seizure; GABAA RM, GABAA Receptor mutation; KAS, Kainic acid (KA)-induced seizures; L&PS, Lithium & pilocarpine induced seizures; MES, Maximal electroshock-induced seizures; NMDAS, NMDA induced seizures; PTZS, PTZ-induced seizures; PTXS, Picrotoxin induced seizures.



component isolated from *Rhizoma corydalis*. When THP was injected into the epileptic model, dopamine secretion was reduced in parallel with the enhancement in GABA receptor function and cholinergic receptor function and the kindling process was inhibited (Lin et al., 2002). Tetramethylpyrazine (TMP) is the main bioactive alkaloid in *Chuanxiong Rhizoma* (*Conioselinum anthriscoides* 'Chuanxiong'). The therapeutic effect of TMP on epilepsy may be attributed to its inhibitory excitatory synaptic transmission (Jin et al., 2019). Berberine acts as an anticonvulsant through the regulation of the neurotransmitter system. It can reduce the hyperexcitatory movement and abnormal movement trajectory of the larvae in a concentration-dependent manner, which slows down excessive photosensitive epileptiform swimming and helps restore the STX1B expression level to balance (Zheng et al., 2018).

Coumarin is the general name of o-hydroxycinnamate lactones, which possess an effect of anticoagulant, photosensitive, antibacterial, cytotoxic, antioxidant, and neuroprotective activities. The anticonvulsant effects of coumarin have been found to be related to the regulation of GABA receptors. For example, esculetin (6,7-dihydroxycoumarin) has been reported in animal models to induce an antiepileptic effect through the regulation of GABA neurons. However, this effect needs to be tested further to comprehend how such high concentrations of the substance cross the blood-brain barrier into the brain. The mechanism of coumarins in epilepsy is

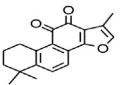
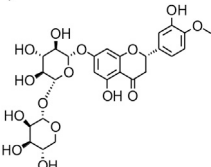
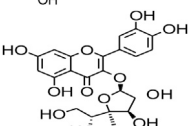
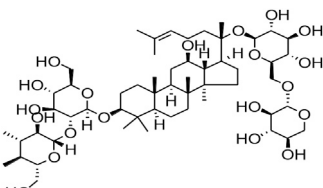
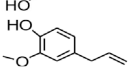
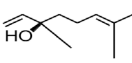
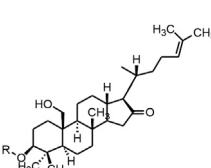
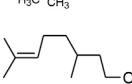
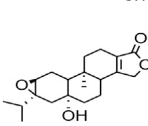
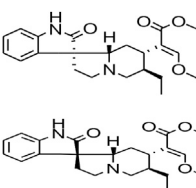
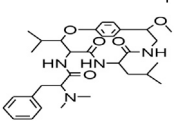
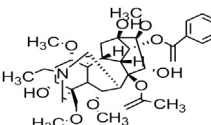
hence not considered may be not entirely through the GABAA receptors (Xiang et al., 2014).

Various anti-epileptic mechanisms of α -asarum have been reported, which may be mainly related to neurotransmitters and apoptotic factors. α -Asarum decreased the activity of GABA-T, while the expression of GAD 67 and GABAA receptors were increased (Miao et al., 2011). In addition, the α -asarum level can obviously reduce the expression of NMDA receptor-1 level in the hippocampus CA1 and CA3 areas, thereby inhibiting the activity of NMDAR1 and excitatory neurotoxicity (Liu et al., 2013). We noted that flavonoids, terpenoids, and alkaloids play an important role in the treatment of epilepsy through the receptor pathways. The main receptors affected are the Glu receptor pathway and the GABA receptor pathway. More natural compounds that play antiepileptic roles through the regulation of receptors and synaptic pathways are displayed in Table 2. The effects of natural drugs on the receptor pathways are depicted in Figure 1.

NATURAL MEDICINES IMPROVES EPILEPSY BY REGULATING ION CHANNELS

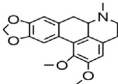
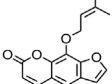
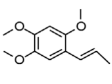
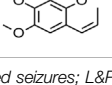
Tanshinone IIA, a flavonoid compound, activates the potassium channels by increasing the presynaptic Ca^{2+} influx and improves

TABLE 3 | Natural drugs used to treat epilepsy by regulating the concentration of ions.

Natural drugs	Compounds	Chemical structure	Animal models	Mechanisms	References
<i>Salvia miltiorrhiza</i> Bunge (<i>Lamiaceae</i>)	Tanshinone IIA		PTZS in rats; 4-APS in mice	Increasing presynaptic Ca^{2+} inflow	Tan et al. (2014); Lin et al. (2013)
<i>Crataegus pinnatifida</i> Bunge. Var. <i>major</i> (<i>Crataegus</i> L.)	Hesperidin		PTZS in mice	Blocking the effects of enhanced Ca^{2+}	Xiang et al. (2014)
<i>Abelmoschus manihot</i> (Linn.) (<i>Malvaceae</i>)	Isoquercitrin		PTZS, MES in mice	Modulating the $\text{GABA}_A\text{-Cl}^-$ channel	Xiang et al. (2014)
<i>Panax ginseng</i> C. A. Meyer (<i>Panax</i> L.)	Ginsenoside Rb3		L&PS in rats	Decreasing influx of Ca^{2+}	Kim and Rhim (2004)
<i>Syzygium aromaticum</i> , L. (<i>Syzygium oblata</i> Lindl.)	Eugenol		Granule cell	Depressing the transient and late components of Na^+ in the neurons	Kim (2016)
Green tea (<i>Camellia sinensis</i> (L.) Kuntze)	Linalool		Scn1lab-/- in zebrafish	Improving Na^+ channels	Kim (2016)
<i>Portulaca oleracea</i> L. (<i>purslane</i>)	Baccoside A		<i>C. Elegans</i> at higher temperatures	Regulating T-type calcium channel (CCA-1) protein	Xiang et al. (2014)
<i>Curculigo orchioides</i> Gaertn. (<i>Hypoxidaceae</i>)	Citronellol		PTXS in mice	Inhibiting neuronal excitability by regulating voltage dependent Na^+ channels	Xiang et al. (2014)
<i>Tripterygium wilfordii</i> Hook F. (<i>Celastraceae</i>)	Triptolide		KAS in microglia	Increasing Kv1.1 expression of neurons in hippocampus CA3	Sun et al. (2018); Pan et al. (2012)
<i>Uncaria rhynchophylla</i> (Miq.) Miq. ex Havil (<i>Rubiacaceae</i>)	Rhynchophylline isorhynchophylline		KAS in mice	Decreasing Ca^{2+} internal flow	Ho et al. (2014); Wang and Cai (2018)
<i>Ziziphus jujuba</i> Mill. var. <i>spinosa</i> (Bunge) Hu ex H. F. Chou (<i>Rhamnaceae</i>)	Sanjoinine		NMDAS in rats	Blocking of intracellular Ca^{2+} influx	Ma et al. (2008)
<i>Aconitum carmichaeli</i> Debx. (<i>Ranunculaceae</i>)	Aconitine		Male Wistar rats	Blocking sodium channels, low Mg^{2+}	Zhao et al. (2020)

(Continued on following page)

TABLE 3 | (Continued) Natural drugs used to treat epilepsy by regulating the concentration of ions.

Natural drugs	Compounds	Chemical structure	Animal models	Mechanisms	References
<i>Platycodon grandiflorus</i> (Platycodon)	Nantenine		PTZS, MES in mice	Decreasing Ca ²⁺ influx into the cell	Xiang et al. (2014)
<i>Cnidium monnieri</i> (L.) Cuss (umbellifera)	Osthole		MES in mice	Increasing Kv1.2 expression of neurons in hippocampus CA3	Xiang et al. (2014)
<i>Acorus tatarinowii</i> Schott (Araceae)	α -asarone		PTZS in mice	Regulating voltage gated sodium ion channel (NAV1.2 channel)	Yuan et al. (2019)
<i>Acorus tatarinowii</i> Schott (Araceae)	β -asarone		PTZS in mice	Inhibiting of Ca ²⁺ influx	Yuan et al. (2019)

4-APS, 4-AP induced seizures; KAS, Kainic acid (KA)-induced seizures; L&PS, Lithium & pilocarpine induced seizure; MES, Maximal electroshock-induced seizures; NMDAS, NMDA induced seizures; PTZS, PTZ-induced seizures; PTXS, Picrotoxin induced seizure.

the cognitive function of epileptic rats (Lin et al., 2013; Tan et al., 2014).

Glycosides and saponins can play some roles by regulating the ion channels. For example, ginsenoside Rg3 can inhibit seizure-induced Ca²⁺ influx with spontaneous recurrent epileptiform discharges (SRED) and further attenuate SREDs-induced neuronal death (He et al., 2019). PF is a water-soluble monoterpenoid glycoside extracted and isolated from *Paeonia lactiflora* Pall. The anti-epilepsy mechanism of PF may be involved in inhibiting the increase of intracellular Ca²⁺ influx (Hino et al., 2012).

Terpenoids can also play a role by regulating the ion channels. For example, triptolide (TL) exerts neuroprotective effects in epileptic rats, possibly by increasing the expression of kv1.1 in the hippocampus CA3 (Pan et al., 2012). The specific effect of eugenol on the ionic current has been shown to increase the degree of voltage-gated Na⁺ current inactivation and inhibiting the non-inactivated (Kim, 2016).

The ionic regulation of alkaloids has been reported in several articles. RIN decreased neuronal hyperexcitability by inhibiting continuous sodium current (INaP) and further decreased pilocarpin-induced Nav1.6 (Shao et al., 2016). RIN also inhibits the Ca²⁺ influx in the central nervous system. Aconitine is an important active ingredient in aconitum that acts directly on the sodium ion channel, which not only changes the voltage sensitivity and ion selectivity of a sodium ion channel but also reduces the hyperpolarization potential caused by Na⁺ current activation as well as reduces the maximum inward current (Zhao et al., 2020). In addition, 3-acetylaconitine has been reported to inhibit the excitation through mediation of sodium channels. Tetramethylpyrazine has also been reported to inhibit the calcium channels (Jin et al., 2019).

β -Asarone, which is an effective component of acorus tatarinowii, has been demonstrated to play neuroprotective roles *in vitro* studies through the inhibition of the Ca²⁺ influx. In addition, α -asarum has been reported to inhibit voltage-gated sodium channels (NAV1.2 channels) (Yuan and Liu, 2020). In

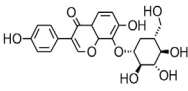
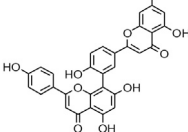
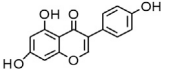
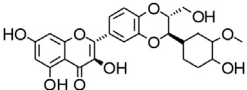
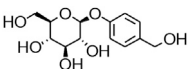
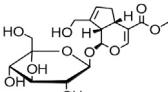
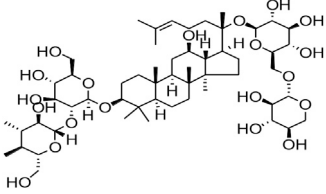
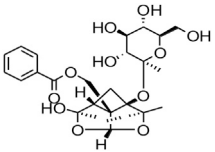
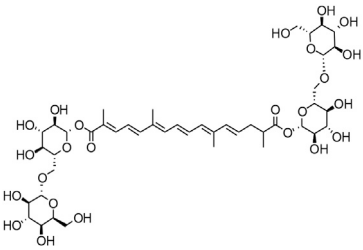

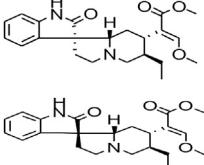
summary, most of the natural compounds can be applied to the treatment of epilepsy mainly because they can affect the Ca²⁺ and Na⁺ activities. More natural compounds that regulate ion concentration and ion channels are given in Table 3.

NATURAL MEDICINES IMPROVES EPILEPSY THROUGH THE IMMUNE SYSTEM

Flavonoids have also been often reported to exert immunomodulatory effects. For example, carbenoxolone (CBX) exhibits anti-inflammatory effects through the stimulation of the adrenal glands or by enhancing the effects of endogenous corticosteroids. In a study, the degree of seizure in an epileptic rat was reduced and the incubation period was prolonged after CBX treatment. This effect may be related to the decreased expression of glial fibrillary acidic protein and ligand 43 in cortical rats with epilepsy (Chen et al., 2013). Morin can be extracted from several herbs and fruits. Past studies have demonstrated that morin can reduce the susceptibility to seizures, the expression levels of apoptotic molecules, and the activities of inflammatory cytokines and mammalian target of rapamycin complex 1 (mTORC1) in a seizure model (Lee et al., 2018).

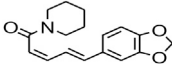
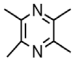
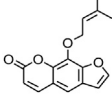
Saponins and glycosides can inhibit inflammation and play an indirect therapeutic role via regulating the content of inflammatory factors. For example, saikosaponin A is an effective monomer extracted from *Radix Bupleuri*. Xie noted that saikosaponin A can dose-dependently decrease the expression of multi-drug resistant protein P-glycoprotein (P-GP) in the temporal cortex and hippocampus, thereby reducing the level of refractory epilepsy caused by picrocarbine (Yu et al., 2012; Xie et al., 2013). Ginsenoside can induce a decrease in the level of IL-1 β . Pueraria flavone can regulate the NF-KB mRNA and IL-10 mRNA expressions in the hippocampus of epileptic rats (He et al., 2019). Gastrodin can decrease the levels of

TABLE 4 | Natural drugs that treats epilepsy by regulating the immune system and inflammatory factors.

Natural drugs	Compounds	Chemical structure	Animal models	Mechanisms	References
<i>Radix Puerariae lobatae</i> (<i>Pueraria DC.</i>)	Puerarin		PTZ & PS in rats	Decreasing IL-10	He et al. (2019)
<i>Nandina domestica Thunb</i> (<i>Berberidaceae</i>)	Amentoflavone		L&PS in rats	Decreasing IL-1 β , TNF- α	Zhang et al. (2015)
<i>Soybean (Glycine max (L.))</i>	Genistein		DHPGS in rats	Effecting both cell-mediated and humoral components of the adaptive immune system	Diniz et al. (2015)
<i>Milk thistle (Silybum marianum)</i>	Silibinin		L&PS in mouse	Decreasing TNF- α , IL-1 β , and IL-6	Kim et al. (2017)
<i>Gastrodia elata Blume</i> (<i>Orchidaceae</i>)	Gastrodin		NMDAS in rat	Decreasing, IL-1 β and TNF- α	Liu et al. (2018)
<i>Gardenia jasminoides J. Ellis</i> (<i>Fructus Gardenia</i>)	Geniposide		EMS in mouse	Decreasing TNF- α , IL-1 β levels and plasma expression of vascular pseudohemophilia factor	Wei et al. (2018)
<i>Gardenia jasminoides J. Ellis</i> (<i>Fructus Gardenia</i>)	Ginsenoside Rb3		L&PS in rats	Decreasing IL-1 β	Kim and Rhim (2004)
<i>Herbaceous peony (Paeonia lactiflora Pall.)</i>	Paeoniflorin		MCC in rats	Inhibiting the inflammatory response; protecting neuronal activity	Hino et al. (2012)
<i>Crocus sativus L. (saffron)</i>	Crocin		HRKS in mice	Suppressing formation of advanced glycation products and brain inflammatory mediators IL-1 β , TNF- α	Mazumder et al. (2017)
<i>The fragrant camphor tree (Cinnamomum camphora)</i>	Borneol		PTZS in mice	Anti-inflammatory; anti-bacterial; protecting central nervous	Tambe et al. (2016)
<i>Uncaria rhynchophylla (Miq.) Miq. ex Havil</i> (<i>Rubiaceae</i>)	Rhynchophylline isorhynchophylline		KAS in mice	Decreasing IL-1 β	Shao et al. (2016); Wang and Cai (2018)

(Continued on following page)

TABLE 4 | (Continued) Natural drugs that treats epilepsy by regulating the immune system and inflammatory factors.

Natural drugs	Compounds	Chemical structure	Animal models	Mechanisms	References
<i>Piper nigrum</i> L. (pepper berries)	Piperine		PTZS in both zebrafish and mice	Decreasing TNF- α	Diniz et al. (2015)
<i>Ligusticum chuanxiong</i> hort (Umbelliferae)	Tetramethylpyrazine		Epileptic Sprague Dawley rats	Decreasing IL-2, IL-6, TNF- α , Bim	Jin et al. (2019)
<i>Peucedanum praeruptorum</i> Dunn (Radix Peucedani)	Imperatorin		MES in mice	Decreasing TNF- α and IL-6 levels	Chowdhury et al. (2018)

Asp, aspartic acid; 4-APS, 4-AP induced seizures; AS, Audiogenic induced seizures; DHPGS, (S)-3,5-dihydroxyphenylglycine induced models; HRKS, Hippocampus rapid kindling model was established in C57BL/6J; KAS, Kainic acid (KA)-induced seizures; L&PS, Lithium & pilocarpine induced seizure; MES, Maximal electroshock-induced seizures; MCC, Metallic cobalt to the cerebral cortex; NMDAS, NMDA induced seizures; PTZS, PTZ-induced seizures.

IL-1 β and TNF- α (Yuan et al., 2019). Moreover, ginsenoside possesses the ability of inhibiting microglial cell activation and polarization (Kim and Rhim, 2004).

Some alkaloids have also been reported to possess anti-inflammatory effects. For example, RIN can regulate immune response and neurotrophic factor signaling pathways, such as brain-derived neurotrophin associated with neuronal survival and inflammatory factor IL-1 β (Shao et al., 2016). TMP can simultaneously reduce the production of IL-2, IL-6, and TNF- α to counter pentaerythritol-induced epileptic seizures in experimental rats (Liu et al., 2010).

A few coumarins have also been studied *in vivo* in epilepsy patients. For instance, pretreatment of imperata (IMP) has been shown to not only improve the L&PS-induced behavior and memory disorders but also significantly reduce the associated oxidative stress and pain levels. Moreover, it can also reduce the TNF- α and IL-6 levels, leading to significant upregulation of the BDNF levels (Chowdhury et al., 2018).

Ursolic acid (UA), which is found in many human diets and cosmetics, can be used as an antioxidant, anti-inflammatory drugs (Nieoczym et al., 2018). Trans-caryophyllene (TC) applied in epilepsy may be attributed to its ability to reduce the expression of pro-inflammatory cytokines, such as TNF- α and IL-1 β (Liu et al., 2015). Several compounds can play a therapeutic role by affecting the immune system, of which flavonoids and saponins are the main components. More natural compounds are displayed in **Table 4**, and the effects of natural drugs on the immune system is shown in **Figure 2**.

NATURAL MEDICINES IMPROVES EPILEPSY BY CORRECTING THE GLIAL CELLS

Amentoflavone can significantly inhibit the expression of COX2 and iNOS, as well as inhibit the activation of BV-2 microglia

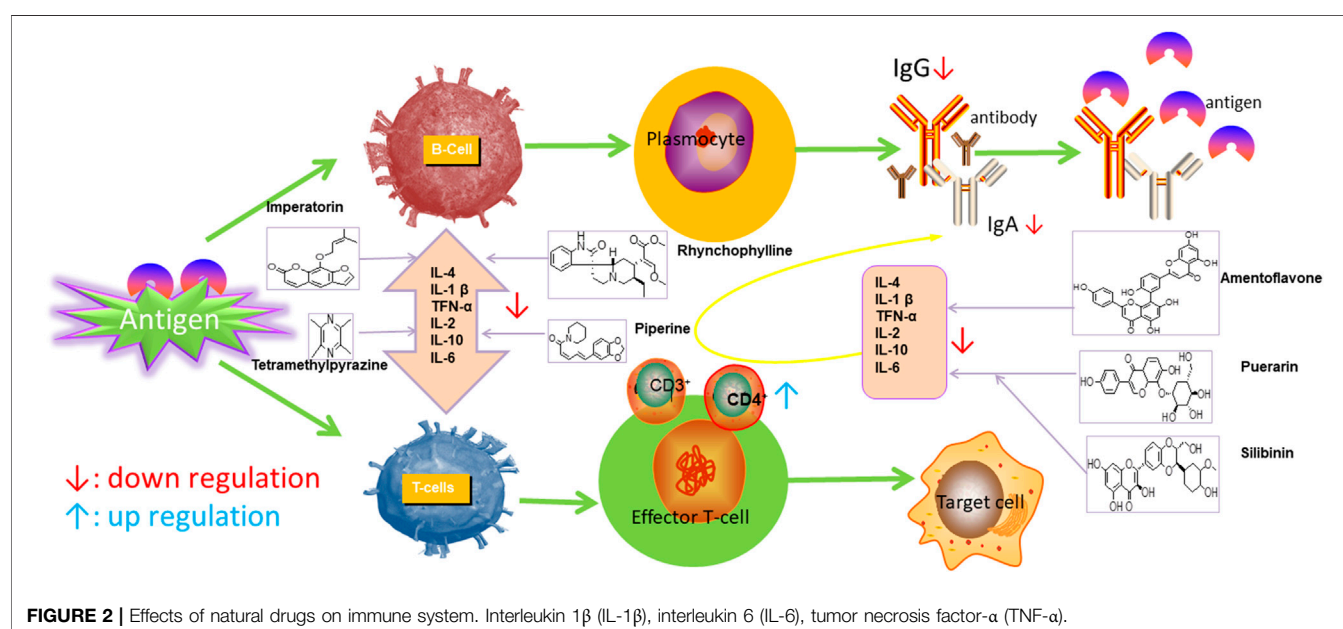
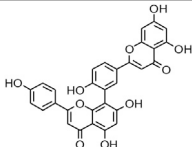
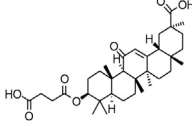
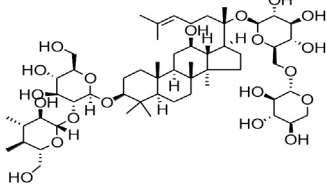
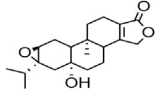
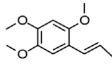


TABLE 5 | Natural drugs used to treat epilepsy by regulating glial cells.

Natural drugs	Compounds	Chemical structure	Animal models	Mechanisms	References
<i>Nandina domestica</i> Thunb (Berberidaceae)	Amentoflavone		L&PS in rats	Inhibition of microglial activation and reactive proliferation of astrocytes	Reng et al. (2020)
<i>Glycyrrhiza glabra</i> L. (Fabaceae)	Carbenoxolone		Rat model of ferric ion-induced posttraumatic epilepsy	Reduced cortical glial fibrillary acidic protein and connexin 43 expression	Chen et al. (2013)
<i>Panax quinquefolius</i> L. (Araliaceae)	Ginsenoside Rb3		L&PS in rats	Inhibiting microglial cell activation and polarization	Kim and Rhim (2004)
<i>Tripterygium wilfordii</i> Hook F.(Celastraceae)	Triptolide		KAS in microglia	Inhabiting expression of IIMHC II	Sun et al. (2018)
<i>Acorus tatarinowii</i> Schott (Araceae)	α -asarone		PTZS in rats	Inhibiting microglia cell activation in rat brain tissue	Yuan and Liu (2020)

IIMHC, major histocompatibility complex class; L&PS, Lithium & pilocarpine induced seizure.

(Reng et al., 2020). Carbenoxolone pretreatment or treatment could significantly reduce the connexin expression in the cortex, inhibit glial fibrillary acidic protein expression, and ameliorate the extent of seizure in the experimental rats (Chen et al., 2013). In the persistent epileptic mode induced by pilocarpine, α -asarone inhibited the activation of microglia cells in rat brain tissues (Yuan and Liu, 2020). TL may exert suppressive effects on the expression of major histocompatibility complex class (MHC II) in KA-activated microglia; this mechanism may involve the regulation of the AP-1 activity (Sun et al., 2018). More natural compounds also play a therapeutic role in epilepsy through the regulation of glial cells (Table 5).

NATURAL MEDICINES IMPROVES EPILEPSY BY CORRECTING MITOCHONDRIAL DYSFUNCTION AND OXIDATIVE STRESS

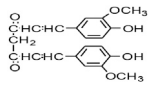
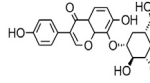
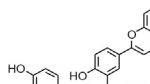
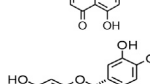
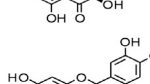
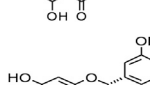
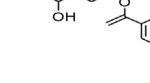
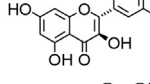
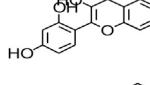
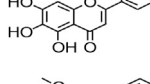
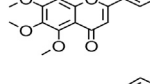
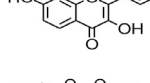
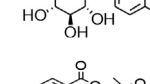
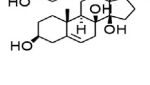
The role of flavonoids in epilepsy treatment involves regulating oxidative stress (Diniz et al., 2015), such as glutathione and superoxide dismutase (SOD) (Oliveira et al., 2018). Curcumin, extracted from *Radix curcumae*, reduces the expression of COX-2, 5-lipoxygenase mRNA and protein in the hippocampal neurons of epileptic rats through the regulation of free radicals and carbon monoxide synthase and improves the anti-oxidative stress effect, hippocampal neuron damage, and cognitive function of pilocarp-induced epileptic in experimental rats (Kiasalari et al.,

2013). Another study reported that nobiletin can markedly decrease the expression of caspase-3, Bad, Bax, Glu, and PTEN and activate the PI3K/Akt pathway while upregulating the expression of phosphorylated Akt, GSK-3, mTORC-1, and mTORC-2 (Yang et al., 2018).

Glycosides have been reported to exert antioxidant activity. Otophyllloside N (OtoN) is one of the ginseng saponins extracted from *Cynanchum otophyllum* Schneid. OtoN can downregulate the Bax/Bcl-2 ratio and increase the level of c-Fos and play an anti-epileptic role (Sheng et al., 2016). Moreover, otophyllloside A, B and two c-21 steroidal saponins have also been reported as the main active ingredients for the treatment of epilepsy (Zhao et al., 2013). Ginsenoside, a partially purified extract from *American ginseng*, has been shown to exert anticonvulsant activity. Rb1 can ameliorate cognitive deficits induced by PTZ as well as dose-dependently increase the GSH levels, decrease the MDA levels, and alleviated neuronal injury. In addition, under Mg^{2+} -free condition, Rb1 can increase the cell activity and reduce neuronal apoptosis as well as demonstrate a certain dose-dependence mechanism. An *in vitro* and *in vivo* study revealed that Rb1 can also enhance the Nrf2 and HO-1 expressions (Wei et al., 2017). Crocin can significantly increase the activity of SOD, decrease the level of reactive oxygen species (ROS), and reduce the level of nuclear factor- κ B (NF- κ B) in the hippocampus of PTZ-induced animal models (Mazumder et al., 2017). Gastrodin can increase the expression of CAT, GSH, and SOD (Liu et al., 2018).

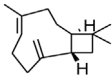
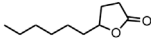
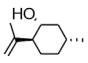
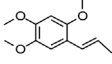
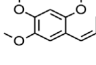
In the study on epilepsy, some alkaloids were noted to exert antioxidant activities. For example, RIN was reported to increase

TABLE 6 | Natural drugs used to treat epilepsy by regulating mitochondrial damage and oxidative stress.

Natural drugs	Compounds	Chemical structure	Animal models	Mechanisms	References
<i>Curcuma longa</i> L. (turmeric)	Curcumin		PTZS and KAS in mice	Anti-oxidative stress; Decreasing COX-2, 5-LOX, acetylcholinesterase	Kiasalari et al. (2013)
<i>Radix Puerariae lobatae</i> (<i>Pueraria</i> DC.)	Puerarin		PTZ & PS in rats	Decreasing NF-κB; Antioxidant and anti-apoptotic mechanisms	He et al. (2019)
<i>Nandina domestica</i> Thunb. (Berberidaceae)	Amentoflavone		L&PS in rats	Decreasing COX-2, NF-κB p65	Zhang et al. (2015)
Green tea (<i>Camellia sinensis</i> (L.) Kuntze)	Catechin		PTZS in rats	Ameliorating cognitive impairment and oxidative stress	Ahmad et al. (2020)
<i>Eclipta prostrata</i> L. (Asteraceae)	Luteolin		PTZS in mice	Inhibiting oxidative stress	Tambe et al. (2016)
Green tea (<i>Camellia sinensis</i> (L.) Kuntze)	EGCG		L&PS in rats	Inhibiting TLR4, NF-κB signaling pathway; Antioxidant	Qu et al. (2019)
Milk thistle (<i>Silybum marianum</i>)	Silibinin		L&PS in mouse	Decreasing Hif-1α	Kim et al. (2019)
<i>Chlorophora tinctoria</i> (L.)	Morin hydrate		PTZS in mouse	Modulating the concentrations Na ⁺ /K ⁺ -ATP; Antioxidant status	Lee et al. (2018)
<i>Astragalus</i> spp. (<i>Radix Astragal</i>)	Baicalin		PTZS in rats	Decreasing Bcl-2, GSH, SOD, IL-1β, Bax, caspase-3, TNF-α, Lipid peroxidation, nitrite	Diniz et al. (2015)
<i>Citrus reticulata</i> Blanco (Rutaceae)	Nobiletin		PTZS in mice	Antiapoptotic	Yang et al. (2018)
Smoke tree (<i>Cotinus coggygria</i>)	Fisetin		Iron-induced experimental model in rats	Inhibiting oxidative injury	Diniz et al. (2015)
<i>Gastrodia elata</i> Blume (Orchidaceae)	Gastrodin		NMDAS in rat	Increasing CAT, GSH, SOD	Liu et al. (2018)
<i>Cynanchum otophyllum</i> Schneid (Asclepiadaceae)	Otophyllside		PTZS in mice	Downregulating Bax/Bcl-2 ratio; Increasing the expression level of c-fos	Sheng et al. (2016)
<i>Panax quinquefolius</i> L. (Araliaceae)	Rb1 ginsenosides		PTZS in rat	Increased GSH levels, decreased MDA levels, enhanced both the Nrf2 and HO-1 expressions	Shi et al. (2018)

(Continued on following page)

TABLE 6 | (Continued) Natural drugs used to treat epilepsy by regulating mitochondrial damage and oxidative stress.

Natural drugs	Compounds	Chemical structure	Animal models	Mechanisms	References
<i>Syringa oblata</i> Lindl. (Oleaceae)	Trans-Caryophyllene		KAS in mice	Preserving the activity of gpx, SOD, and CAT	Liu et al. (2015)
Strawberries (<i>Fragaria X ananassa</i> , Duch.)	l-Decanolactone		PTZS in mice	Protecting oxidative stress and DNA damage in mice	Xiang et al. (2014)
<i>Eucalyptus citriodora</i> Hook. (Myrtaceae)	Isopulegol		PTZS in mice	Decreasing in lipid peroxidation; preserving catalase activity in normal levels; preventing loss of GSH	Xiang et al. (2014)
<i>Acorus tatarinowii</i> Schott (Araceae)	α -asarone		PTZS in mice	Regulating the abnormal expression of neuronal apoptotic factors Bax and Bcl-2	Liu et al. (2013)
<i>Acorus tatarinowii</i> Schott (Araceae)	β -asarone		PTZS in mice	Stabilizing mitochondrial membrane potential	Yuan et al. (2019)

KAS, Kainic acid (KA)-induced seizures; L&PS, Lithium & pilocarpine induced seizure; NMDAS, NMDA induced seizures; PTZS, PTZ-induced seizures.

the activity of serum SOD. In addition, tricholonin has been reported to reduce the levels of hippocampal mitochondrial MDA and scavenge-free radicals, thereby reducing oxidative stress induced by PTZ kindling.

Terpenoids are mostly detected in volatile oils, which has been reported to demonstrate some antioxidant activities. UA, which is

detected in several human diets and cosmetics, can be used as an antioxidant. TC is a component that can be isolated from volatile oils of several flowering plants. Pretreatment of TC can preserve the activity of SOD, GPx, and CAT in the mitochondria as well as reduce the resultant oxidative damage (Liu et al., 2014). After borneol treatment, the levels of SOD, GSH, and CAT in a PTZ-

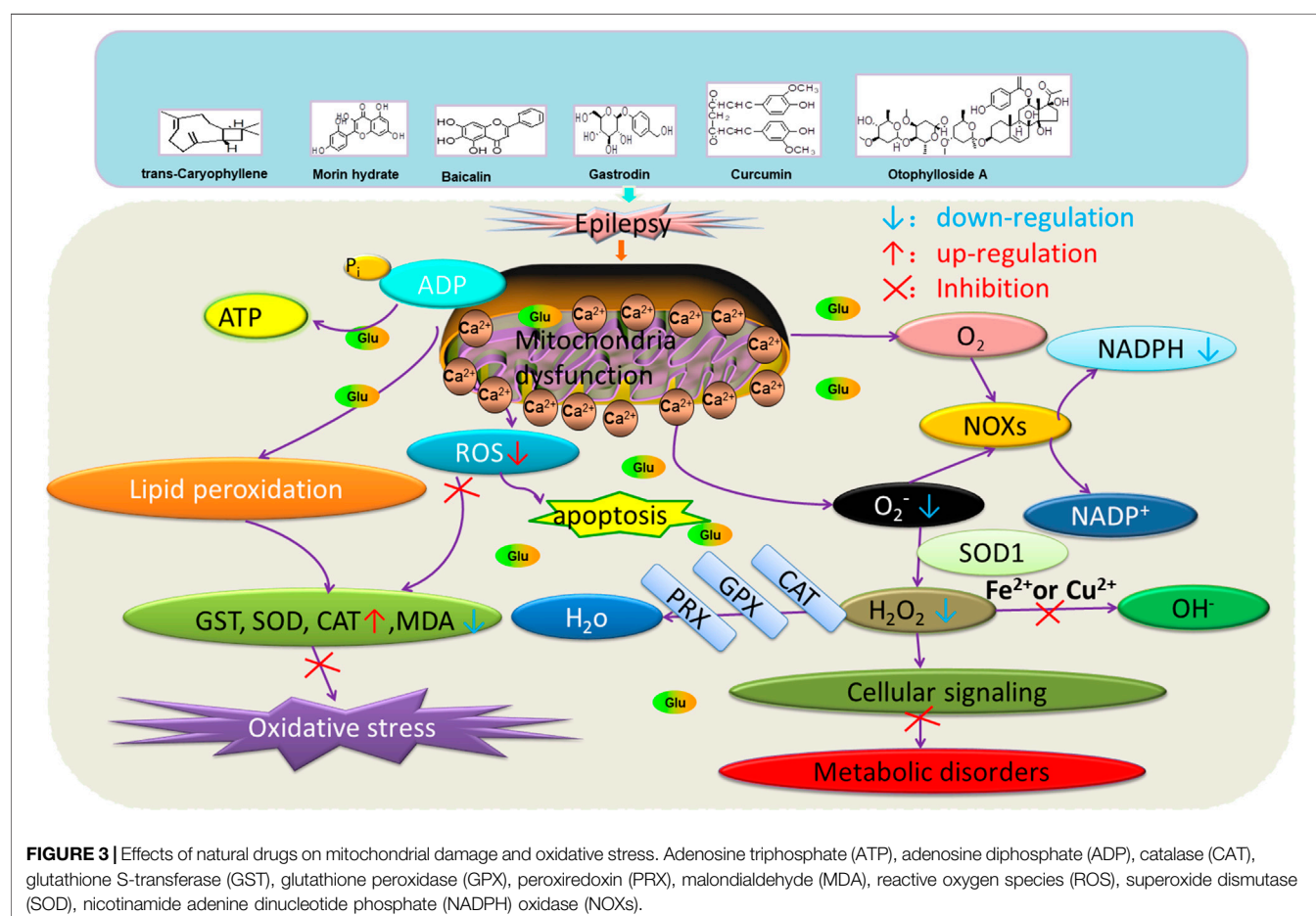


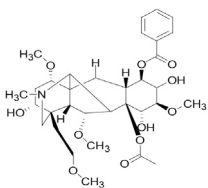
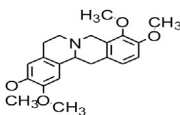
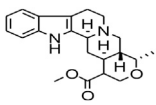
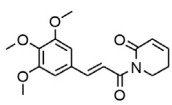
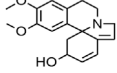
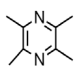
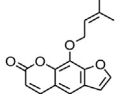
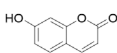
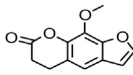
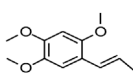
FIGURE 3 | Effects of natural drugs on mitochondrial damage and oxidative stress. Adenosine triphosphate (ATP), adenosine diphosphate (ADP), catalase (CAT), glutathione S-transferase (GST), glutathione peroxidase (GPX), peroxiredoxin (PRX), malondialdehyde (MDA), reactive oxygen species (ROS), superoxide dismutase (SOD), nicotinamide adenine dinucleotide phosphate (NADPH) oxidase (NOXs).

TABLE 7 | he other.

Natural drugs	Compounds	Chemical structure	Animal models	Mechanisms	References
<i>Curcuma longa</i> L. (turmeric)	Curcumin		PTZS and KAS in mice	Inhibit MTORC1 activation; Reduce the damage of hippocampal neurons and cognitive dysfunction	Kiasalari et al. (2013)
<i>Citrus aurantium</i> L. (Rutaceae)	Naringin		KAS in mice	Reducing GCD and mtorc1 activation	Diniz et al. (2015)
<i>Sophora japonica</i> L. (Fabaceae)	Rutin		PTZS in zebrafish; KAS in mice	Improving epileptoid action	Diniz et al. (2015)
<i>Folium Sennae</i> (Senna)	Vitexin		PTZ-CS	Neuroprotective effects	Diniz et al. (2015)
<i>Achillea millefolium</i> L. (Yarrow)	Kaempferol		Epileptic <i>drosophila</i>	Inhibition of DNA topoisomerase I enzyme	Diniz et al. (2015)
Smoke tree (<i>Cotinus coggygria</i>)	Fisetin		Iron-induced experimental model in rats	Protecting endogenous enzyme level	Diniz et al. (2015)
<i>Dendranthema morifolium</i> (Ramat.) Tzvelev	Linarin		PTZS in mice	Preventing CNS excitation or stress	Diniz et al. (2015)
<i>Cannabis sativa</i> L. (Moraceae, hemp)	Cannabidiol		Patients	Inhabiting neuronal excitability	Xiang et al. (2014)
<i>Herba Menthae Haplocalycis</i> (<i>Mentha haplocalyx</i> Briq.)	Carvone		PTZS in mice	Inhibiting central nervous system	Xiang et al. (2014)
<i>Origanum vulgare</i> L. (Lamiaceae Martinov)	l-terpinene		PTZS, MES in mice	Raising the threshold of convulsion	Xiang et al. (2014)
Norway spruce (<i>Picea abies</i> (L.) Karst.) trees	Verbenone		PTZS in mice	Related to RNA expression of COX-2, BDNF, and C-fos	Bahr et al. (2019)
<i>Cannabis sativa</i> (marihuana)	Delta9-tetrahydrocannabinol		PTZS in mice	Improving seizures in children	Bahr et al. (2019)
<i>Nepeta cataria</i> L. var. <i>citriodora</i> (Lamiaceae)	Ursolic acid		PTZS in mice	Unknown	Nieoczym et al. (2018)
<i>Moschus moschiferus</i> L.	Muscone		Rat	Inhibiting the central nervous system excitability	Bahr et al. (2019)
The fragrant camphor tree (<i>Cinnamomum camphora</i>)	Borneol		PTZS in mice	Anti-bacterial; protecting central nervous	Tambe et al. (2016)

(Continued on following page)

TABLE 7 | (Continued) the other.

Natural drugs	Compounds	Chemical structure	Animal models	Mechanisms	References
<i>Aconitum carmichaeli</i> Debx. (Ranunculaceae)	Mesaconitine		Wistar rats	Regulating the noradrenergic system	Zhao et al. (2020)
<i>Rhizoma Corydalis</i> (Papaveraceae)	DL-Tetrahydropalmatine		Electrical kindling in rats	Reducing dopamine output	Lin et al. (2002)
<i>Rauwolfia serpentina</i> (Sarpagandha)	Raubasine		PTZS in mice	Interacting at benzodiazepine sites with a benzodiazepine agonist-type activity	Xiang et al. (2014)
<i>Piper nigrum</i> L. (Pepper berries)	Piperlongumine		PTZS in mice	Decreasing the latency to death in mice	Xiang et al. (2014)
<i>Erythrina mulungu</i> Mart ex Benth (Papilionaceae)	Erythravine		BCLS in Wistar rats	Unclear	Xiang et al. (2014)
<i>Ligusticum chuanxiong</i> hort (Umbelliferae)	Tetramethylpyrazine		Epileptic Sprague Dawley rats	Increasing neuron cell adhesion molecule -140	Jin et al. (2019)
<i>Peucedanum praeruptorum</i> dunn (Umbelliferae)	Imperatorin		MES in mice	Upregulating of BDNF levels	Chowdhury et al. (2018)
<i>Heracleum mantegazzianum</i> s.l. (Giant hogweed)	Umbelliferone		MES in mice	Unclear	Zagaja et al. (2015)
<i>Zanthoxylum schinifolium</i> Sieb. et Zucc. (Rutaceae)	Xanthotoxin		MES in mice	Unclear	Zagaja et al. (2016)
<i>Acorus tatarinowii</i> Schott (Araceae)	α -asarum		Caco -2 cells	Decreased expression of P glycoprotein and multidrug resistance gene	Yuan and Liu. (2020)

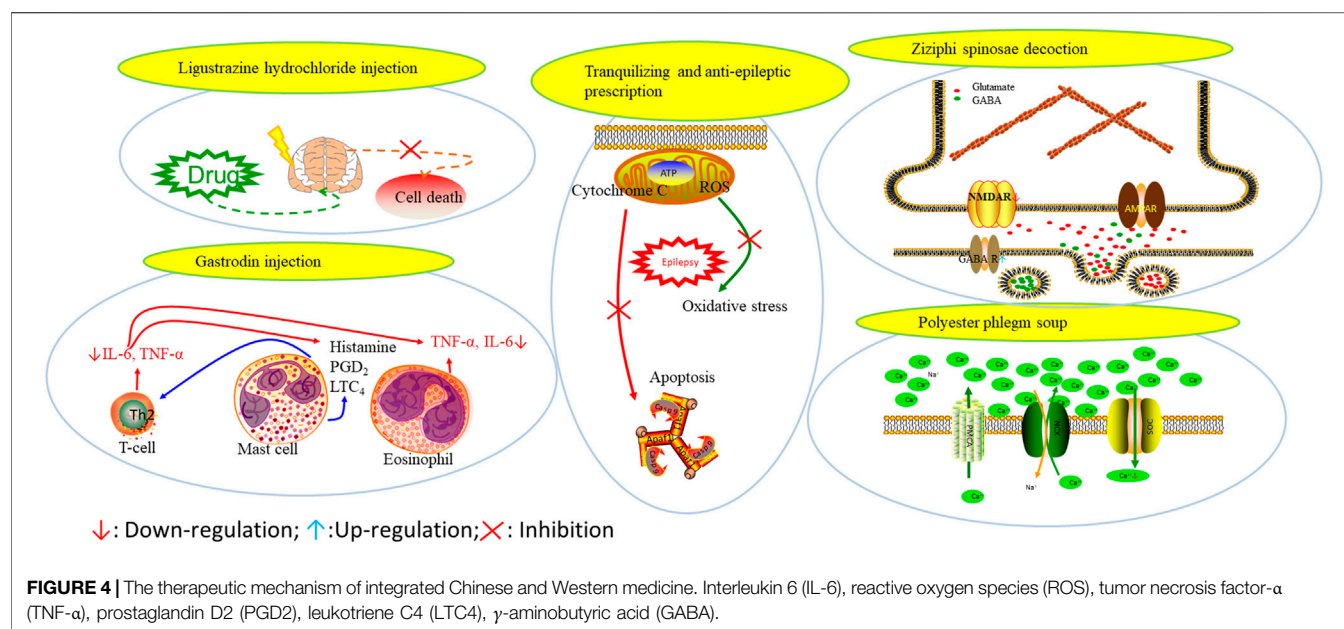
BCLS, bicuculline induced seizure; KAS, Kainic acid (KA)-induced seizures; MES, Maximal electroshock-induced seizures; PTZS, PTZ-induced seizures; PTZ-CS, PTZ induced chronic seizures.

kindling model increases, demonstrating certain antioxidant effects.

Beta-asarone plays a neuroprotective role through the stabilization of the mitochondrial membrane potential to reduce Glu damage to neurons. α -Asarum reduces the neuronal injury of epilepsy by adjusting the neuron apoptosis factor Bax and the abnormal expression of Bcl-2 (Ma et al., 2011; Wang et al., 2014). More natural compounds also play a therapeutic role in epilepsy through the regulation of SOD or oxidation levels (Table 6). The effects of natural drugs on mitochondrial damage and oxidative stress are illustrated in Figure 3.

NATURAL MEDICINES FOR EPILEPSY TREATMENT THROUGH OTHER MECHANISMS

Several natural compounds have been reported with antiepileptic effects, and their mechanisms are complex. Silibinin, the main active ingredient isolated from *Silybum marianum* (L.), has been reported to administrate dramatically inhibited KA-induced GCD and mTORC1 activation, while the phosphorylation levels of the mTORC1 substrate 4E-BP1 and p70S6K were also altered (Kim et al., 2017).



Terpenoids can also play a therapeutic role through other mechanisms. UA, which is detected in several human diet components and cosmetics, can be used as an antioxidant, anti-inflammatory, antibacterial, and anti-tumor agent. In addition, its anticonvulsant effects were demonstrated in the 6-Hz-induced psychomotor seizure threshold test. This effect was further validated in the maximum electroconvulsive threshold test and time-sharing intravenous injection of pentaerythrazol (Nieoczym et al., 2018). Pathological studies indicated that borneol had a neuroprotective effect at an appropriate dose, which was manifested as decreased GFAP level on immunostaining (Tambe et al., 2016).

Alkaloids are also widely applied in the treatment of epilepsy. RIN downregulate the expression of TLR4 in hippocampal tissues and exert a protective effect on the brain injury of rats caused by the persistent state of convulsion (Wang and Cai, 2018). Mesaconitine (MA) can also reduce the excitability by inhibiting the norepinephrine uptake [3H] within a certain concentration range. TMP can enhance the expression of adhesion molecule-140 in hippocampal neurons and reduce the expression of apoptotic factor Bim, thereby playing a protective role on the neurons (Yu et al., 2010; Fang and Zhang, 2013).

The synergistic effect of xanthotoxin combined with oxacipine and topiramate in the maximum electroshock-induced epilepsy test suggests that xanthocyanin may play a role similar to that of an antiepileptic drug at certain level. However, there are only limited data available on this aspect, thus requiring further verification of this hypothesis (Zagaja et al., 2016).

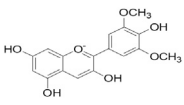
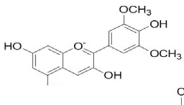
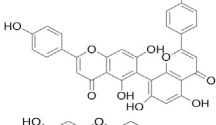
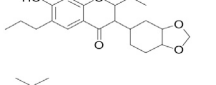
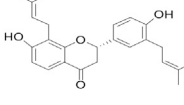
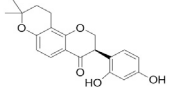
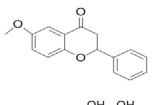
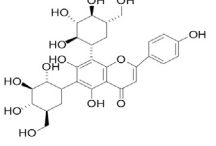
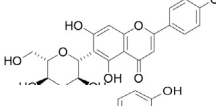
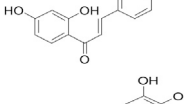
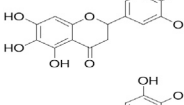
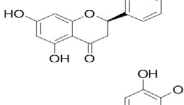
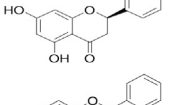
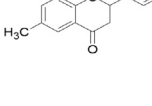
Gardenoside is one of the main active components of *G. jasminoides Ellis*, and past studies have demonstrated its applicability in treating epilepsy. The main mechanism of treatment may be to reduce the expression of COX-2 and AP-1 and regulate the apoptosis of nerve cells by the PI3K/Akt/GSK-3 signaling pathway (Wei et al., 2017).

Subtilisin A has been reported to exert an antiepileptic effect through the mediation of rho-activated coiled-coil kinase. In addition, it can regulate neurotransmitters and apoptotic factors. Moreover, α -asarum plays a protective role in cases of treatment-resistant epilepsy that induced neuronal cell membrane damage through the inhibition of the laminin-1 expression (Huang et al., 2013). Other compounds have been found to exert antiepileptic effects in pharmacological studies, such as umbelliferone (UMB; Zagaja et al., 2015), erysothrine (Rosa et al., 2012), resveratrol, and catechin (Ahmad et al., 2020). In addition, the anticonvulsant and epileptic effects of some protein components have also been studied. Some other natural compounds are shown in Table 7.

COMBINED USE OF NATURAL MEDICINES AND ANTI-EPILEPTIC CONVENTIONAL DRUGS

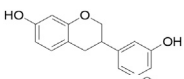
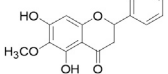
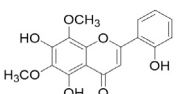
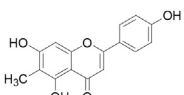
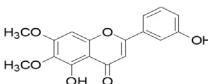
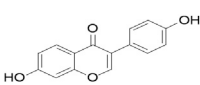
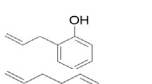
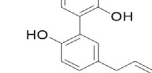
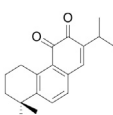
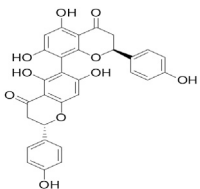
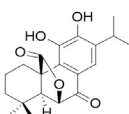
Drug therapy remains the dominant mode of epilepsy control. The efficacy of Western medicine in epilepsy control is clear, with several known adverse reactions, such as anorexia, damaged liver function, dizziness, headache, decrease of white blood cells, cognitive function decline, and a decrease in life quality (Zhu et al., 2017). Especially for pediatric patients, the physical damage through these Western medicine is even greater (Tang et al., 2016). On the other hand, natural drugs have little toxic and side effects with lesser discomfort to patients than that by Western drugs. In the recent years, past studies have recorded that the combination of conventional Chinese and Western medicine can bring hope to epilepsy patients who cannot be otherwise treated with Western medicine (Qu and Zhang, 2019). Moreover, conventional Chinese medicine and the conventional Chinese medicine prescriptions can effectively improve the efficacy of Western medicine as well as effectively reduce the adverse reactions

TABLE 8 | A monomer compound derived from a natural drug that modulated ionotropic GABA receptors.

Compound	Structure	Application	References
Malvidin		Osteoarthritis, Premature senescence, Myocardial infarction	Johnston (2015)
Taxifolin		Osteoclastogenesis, Antioxidant, Alzheimer's disease, hyperuricemic	Johnston (2015)
Agathisflavone		Protecting nerve; anti-oxidative damage and anti-viral	Shrestha et al. (2012)
2-Ethyl-7-hydroxy-3',4'-methylenedioxy-6-propylisoflavone		Unclear	Hanrahan et al. (2015)
Glabrol		Antibacterial	Hanrahan et al. (2015)
Glabridin		Muscle atrophy, Cardiovascular	Hanrahan et al. (2015)
6-methoxyflavone		Neuropathic allodynia and hypoalgesia, anti-inflammatory	Hall et al. (2014)
Vicenin		Prostate cancer, vascular inflammation, Radiation protection	Oliveira et al. (2018)
Isovitexin		Various activities, such as anti-oxidant [12], anti-inflammatory, anti-AD effects	Oliveira et al. (2018)
Isoliquiritigenin		Cervical cancer, breast cancer, hepatoma cancer, colon cancer, prostate cancer, human leukemia, oral carcinoma, Cardioprotective, Hepatoprotective, Antiangiogenic, anti-microbial, anti-anorexia	Wasowski and Marder (2012)
Dihydromyricetin		Antioxidant, anti-inflammatory, protecting cells, regulating lipid and glucose metabolism	Wasowski and Marder (2012)
Eriodictyol		Antioxidant, anti-inflammatory, anti-cancer, neuroprotective, cardioprotective, anti-diabetic, anti-obesity, hepatoprotective, and miscellaneous	Wasowski and Marder (2012)
Hesperetin		Cancer, anti-inflammatory, cataracts, antioxidant and anti-inflammatory	Wasowski and Marder (2012)
6-methylflavanone		Antioxidant and anticancer	Wasowski and Marder (2012)

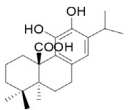
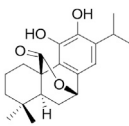
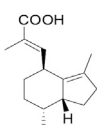
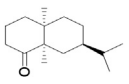
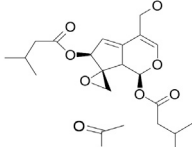
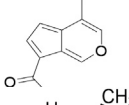
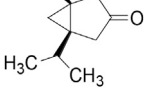
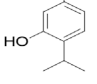
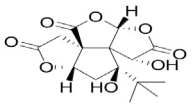
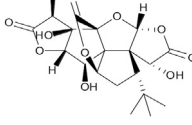
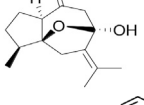
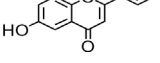
(Continued on following page)

TABLE 8 | (Continued) A monomer compound derived from a natural drug that modulated ionotropic GABA receptors.

Compound	Structure	Application	References
3,7-Dihydroxyisoflavan		Anti-oxidant, anti-estrogenic, anti-cancerous and anti-inflammatory	Wasowski and Marder (2012)
Oroxylin A		Anti-cancer, antiinflammation, neuroprotective, anti-coagulation	Wasowski and Marder (2012)
2,5,7,-trihydroxy-6,8-dimethoxyflavone		Antioxidant	Wasowski and Marder (2012)
6-methylapigenin		Sedative, sleep-enhancing properties, anxiolytic	Nilsson and Sterner (2011)
Skrofullein		Anti-proliferative, anti-cancer, anti-inflammatory, breast cancer, antioxidative and antiplatelet	Nilsson and Sterner (2011)
Daidzein		Against various neuropathological conditions mainly by its interaction with the cerebrovascular system, anti-tumor, inhibits choriocarcinoma proliferation	Nilsson and Sterner (2011)
Honokiol		Antioxidant, alzheimer, anticancer, antineoplastic, anti-inflammatory	Nilsson and Sterner (2011)
Magnolol		Anti-inflammatory, inflammatory bowel disease, Lung cancer, Hepatocellular carcinoma, Antidepressant	Nilsson and Sterner (2011)
Miltirone		Antileukemic, anti-inflammatory, anti-platelet, resistant lung cancer	Nilsson and Sterner (2011)
Rhusflavone		Inducing sleep	Shen et al. (2016)
Galdosol		Antioxidant, Cytostatic and antibacterial	Nilsson and Sterner (2011)

(Continued on following page)

TABLE 8 | (Continued) A monomer compound derived from a natural drug that modulated ionotropic GABA receptors.

Compound	Structure	Application	References
Carnosic acid		Antioxidant, anti-inflammatory, anticancer activities, antimicrobial, protecting mitochondria	Nilsson and Sterner (2011)
Carnosol		Anti-carcinogenic, atopic dermatitis, gastric tumor, chronic stress, improved lifespan, healthspan	Nilsson and Sterner (2011)
Valerenic acid		Anxiety, sleep disturbances, postpartum blues, depression, anti-inflammatory	Nilsson and Sterner (2011)
Valeranone		Sedative, tranquilizing antihypertensive properties, hyperkinetic behavior disorders	Nilsson and Sterner (2011)
Valtrate		Breast cancer, ovarian cancer, anti-HIV	Nilsson and Sterner (2011)
Baldrinal		Anticonvulsant effects	Nilsson and Sterner (2011)
(-)- α -thujone		Polycystic ovary syndrome, malignant glioblastoma, Pro-apoptotic and anti-angiogenic	Nilsson and Sterner (2011)
Thymol		Antibacterial, antifungal, anticancer, Dermanyssus gallinae, anthelmintic, antioxidant, against geotrichum citri-aurantii	Nilsson and Sterner (2011)
Bilobalide		Gastric ulcer, abates inflammation, insulin resistance and secretion of angiogenic factors, alleviates depression	Nilsson and Sterner (2011)
Ginkgolide B		Ischemic stroke, anti-inflammatory and chondroprotective	Nilsson and Sterner (2011)
Isocurcumenol		Antitumour, anti-androgenic	Nilsson and Sterner (2011)
6-hydroxyflavone		Anxiolytic	Ren et al. (2010)

resultant from the usage of Western medicine (Huang et al., 2013). Chinese medicine in the remission of conditioning tonic enhances patients' anti-epilepsy and anti-convulsion states, reduces the nerve damage in patients during the course of epilepsy, and make patients more conducive to the recovery from the disease.

Nobiletin and Clonazepam

Nobiletin and clonazepam significantly reduce seizure severity. The administration of clonazepam and nobiletin can downregulate seizure-induced increases in apoptotic protein expression and apoptotic cell count, restore the Glu/GABA balance, and modulate the expression of GABAA and GAD 65. Moreover, the administration of nobiletin and clonazepam can significantly upregulate the phosphoinositide 3-kinase/protein kinase B (PI3K/Akt) signaling (Yang et al., 2018).

UMB, Valproate, and Phenobarbital

Systemic intraperitoneal (ip) administration of UMB at a dosage of 150 mg/kg could significantly elevate the threshold for EMS in mice. The selective potentiation of the anticonvulsant potency of phenobarbital and valproate by UMB and the lack of any pharmacokinetic interactions between the drugs make the combinations of UMB with phenobarbital or valproate worthy of consideration for refractory epileptic patients (Zagaja et al., 2015).

Naringin and Phenytoin

Naringin in combination with phenytoin has demonstrated a protective effect against seizures as well as improved the conditioned avoidance response in PTZ-induced kindling model. This combination can improve the neurochemical balance by elevating the levels of GABA and dopamine, decrease the levels of Glu and MDA, and increase the levels of antioxidants GSH, SOD, CAT, and total thiol. Therefore, the co-administration of naringin with phenytoin offers a potential treatment option for epilepsy (Phani et al., 2018).

Gastrodin and Carbamazepine

Gastrodin combined with carbamazepine can improve the treatment progression of epilepsy patients with a significant clinical efficacy as well as improve the electroencephalogram abnormalities and the overall treatment effects (Guo, 2017), with fewer complications, which is cumulatively conducive to improve the prognosis of patients and their quality of life (Liu et al., 2018).

Compound Preparation

Prescriptions are more widely used in the clinical practice, and the resultant therapeutic effect is also recognized by more patients (Tian, 2015; Yang et al., 2015). The right combination of two drugs can not only reduce the toxicity and enhance the efficacy of a single drug use but also provide a more pleasant treatment experience to the patients (Roseti et al., 2015). For example, ziziphi spinosae decoction (*Ligusticum chuanxiong hort*, *Glycyrrhiza glabra L*, *Semen ziziphi spinosae*, *Anemarrhena asphodeloides Bunge*) decreased has been

reported to decrease the expression of glu and NMDAR1 (Lu et al., 2020). In addition, polyester phlegm soup (*Curcuma rchenyujin Y*, *H. Chenet C. Ling*, *Ligusticum chuanxiong hort*, *Angelica sinensis (Oliv.) Diels*, *Prunus persica (L.) Batsch*, *Pinellia ternata (Thunb.) Breit*, *Paeonia lactiflora Pall*, *Pericarpium citri reticulatae*, and *Carthamus tinctorius L.*) has been reported to decrease the levels of Na⁺ and Ca²⁺ (Li, 2018). Moreover, Tongqiao Dingxian Soup (*Bombyx Batryticatus*, *Agkistrodon*, *Gastrodia elata Bl*, *Polygala tenuifolia Willd*, *Acorus tatarinowii Schott*, *Pheretima*, *Androctonus crassicauda*, *Scolopendridae*, *Albizia julibrissin Durazz*, and *Gardenia jasminoides Ellis*) can reportedly decrease the serum neuropeptide Y, BDNF, and glial fibrino acid protein (Zhou, 2018). Several types of drugs play different roles in the body simultaneously; this special approach of compatibility has achieved the effect of enhancing the curative effect and reducing the toxic and side-effects, for example, with the use of drugs such as ligustrazine hydrochloride injection, tranquilizing and antiepileptic prescription, wild jujube seed decoction, and gastrodin injection. These proprietary drugs have been widely applied, and their therapeutic mechanisms are displayed in **Figure 4**.

In the past, studies have been performed on the "Dictionary of Traditional Chinese Medicine Prescriptions" for the treatment of epilepsy 532 prescription law analysis (Wu and Zhao, 2017). The drugs with a single drug use frequency of >15% included *Cinnabaris*, *Glycyrrhiza glabra L*, *Panax ginseng C. A. Meyer*, *Calculus bovis*, *Moschus*, *Polygala tenuifolia Willd*, *Rheum officinale Baill*, *Poria cocos (Schw.) Wolf*, *Rehmannia glutinosa (Gaertn.) DC*, *Scutellaria baicalensis Georgi*, and *Aconitum carmichaeli Debx*. The drugs are mainly used to calm the liver and quench the wind, fill the deficiency and calm the mind, clear the heat and dissolve phlegm, and open the body to awaken the mind, which are all suitable for the etiology, pathogenesis, and treatment of epilepsy. Based on the analysis of drugs, the most frequently used anti-spasmodic drugs for calming the liver wind include *Calculus bovis*, *Gastrodia elata Bl*, *Bombyx Batryticatus*, *Androctonus crassicauda*, and *Paeonia lactiflora Pall*. The most common drugs for deficiency include qi tonic, blood tonic, and Yin tonic. The representative drugs include *Glycyrrhiza glabra L*, *Panax ginseng C. A. Meyer*, *Angelica sinensis (Oliv.) Diels*, *Paeonia lactiflora Pall*, and *Ophiopogon japonicus (Linn. f.) Ker-Gawl*. The main tranquilizers are the important and mind-nourishing ones. The representative tranquilizers include *Cinnabaris*, *Dens draconis*, *Polygala tenuifolia Willd*, and *Semen ziziphi spinosae*. Heat-clearing drugs mainly include the heat-clearing and dampness drugs, the heat-clearing and purging gunpowder, and the heat-clearing and blood-cooling drugs; the representative drugs include *Radix scutellariae*, *Rhizoma coptidis*, *Gypsum fibrosum*, and *Radix Rehmanniae*. The frequency of *Moschus* was the highest among the prescription drugs. Phlegm-reducing drugs are mainly to warm cold phlegm drugs; the representative drugs include *Rehmannia glutinosa (Gaertn.) DC* and *Arisaema heterophyllum Blume*.

OTHER FORMS OF EPILEPSY TREATMENT

Nursing intervention (Dong, 2018) and neural stem cell transplantation has also been gaining increasing attention as a treatment approach (Thodeson et al., 2018). In addition, there is an extremely interesting report that regular consumption of bacopa monniera tea can improve the epilepsy condition as well as alleviate dementia, psychosis, and other neurological disorders, which may be linked to improved learning and reasoning abilities among adults and children (Krishnakumar et al., 2009). In addition, based on the epileptic comorbid embarks, the new guideline on the exploration of epileptic treatment can be regarded as a new way. Among these, the GABA receptor pathway plays an important role in various mental diseases (Johnston, 2015). We have summarized here the drugs utilized that showed GABA excitatory effects (Table 8).

CONCLUSION

Based on our cumulative review, it seems that the occurrence of epilepsy is not only related to the nervous system but also to the body's immune and metabolic systems, for instance, neurodegenerative protein accumulation, neurotransmitter imbalance, glial cell proliferation, nerve excitability, synaptic changes, neurons voltage, ion channel mutations or variants of ligand, inflammatory reaction, oxidative stress, mitochondria damage, and glycogen metabolism disorders. Natural medicines are precious resources that promises establishment of reliable candidate drugs with low toxicity and presents several effective monomers that possess specific pharmacological activities; these natural medicines include such as artemisinin (Tu, 2016), emodin (Zhang Q et al., 2020), and berberine (Wang et al., 2019). In addition, it has been reported that natural medicines are beneficial in controlling the manifestations of psychiatric disorders (Zhang Y et al., 2020). According to the pathogenesis and symptoms of patients with epilepsy, different ways of treatment have been considered. The outcomes with the use of natural medicine has been superior in this respect. Natural drugs are thus believed to improve the release of neurotransmitters and in relation to the synaptic structure and functions, in the improvement of the imbalance of ion channels, reduction in the release of inflammatory factors, and enhancement in the activity of antioxidant enzymes and in modulating immune responses. Most natural drugs possess therapeutic effects through the regulation of inhibitory neurotransmitters, and anti-inflammatory and oxidative stress pathways, while some drugs have multiple pathways rather than a single target. Moreover, the most surprising aspect is that the combination of natural medicine and western medicine can not only reduce the potential side-effects but also improve the overall therapeutic effect. The combined use of natural medicine and western medicine thus plays a synergistic role with better outcomes (Guo et al., 2015;

Kang et al., 2015; Yang et al., 2015). For several patients, a comprehensive treatment approach is thus a reasonable and effective treatment option.

We noted some limitation in the study. For instance, epilepsy pathogenesis research is mostly limited to some animal models. In addition, whether the data from the epilepsy model are directly applicable to humans is also questionable. The pathogenesis of epilepsy is quite complex, and the model of epilepsy induced by a single drug cannot completely simulate the pathogenesis of epilepsy, which brings its own set of difficulties to the treatment approach of epilepsy. Moreover, which of the conclusions drawn from the epileptic model can form the basis of the occurrence of epilepsy requires further comprehension. Therefore, on one hand, it has been suggested that scholars develop new and more vivid comprehensive epilepsy model so as to achieve the same effect of drug application in an epilepsy model and clinical patients. Future studies thus suggest that a combination of clinical practice and theory should be considered for such cases. On the other hand, gene therapy as a new treatment should attract academic attention. The theory that changes in a single gene can induce epilepsy needs, requiring further verification to enable future research to focus on the whole genome. In addition, neural stem cell transplantation, as a new technique, has achieved good outcomes in the field of epilepsy.

AUTHOR CONTRIBUTIONS

LH prepared the draft manuscript. MH supplemented the framework of the paper and collated the data with RL. RZ, LF, and LH summarized all the tables. FL and XY revised the figure. YH and CW revised the manuscript. All authors read and approved the manuscript.

FUNDING

This work was supported by National Natural Science Foundation of China (No. 81773906); Xinglin Scholars in Chengdu University of Traditional Chinese Medicine (QNXZ2019018); Chengdu University of Traditional Chinese Medicine informatization research project (MIEC1803); Science and Technology Development Fund Project of Hospital of Chengdu University of Traditional Chinese Medicine (Y2019128); Science and Technology Development Fund project of Hospital of Chengdu University of Traditional Chinese Medicine (Y2019114).

SUPPLEMENTARY MATERIAL

The Supplementary Material for this article can be found online at: <https://www.frontiersin.org/articles/10.3389/fphar.2021.604040/full#supplementary-material>.

REFERENCES

- Abbasi, N., Mohammadpour, S., Karimi, E., Aidy, A., Karimi, P., Azizi, M., et al. (2017). Protective effects of smyrnium cordifolium boiss essential oil on pentylenetetrazol-induced seizures in mice: involvement of benzodiazepine and opioid antagonists. *J. Biol. Regul. Homeost. Agents* 31, 683–689. PMID: 28956418.
- Adams, C. E., Yonchek, J. C., Schulz, K. M., Graw, S. L., and Stevens, K. E. (2012). Reduced chrna7 expression in mice is associated with decreases in hippocampal markers of inhibitory function: implications for neuropsychiatric diseases. *Neuroscience* 207, 274–282. doi:10.1016/j.neuroscience.2012.01.033
- Agostino, D. D., Bertelli, M., Gallo, S., Cecchin, S., Albiero, E., Garofalo, P. G., et al. (2004). Mutations and polymorphisms of the CLCN2 gene in idiopathic epilepsy. *Neurology* 63, 1500–1502. doi:10.1212/01.wnl.0000142093.94998.1a
- Ahmad, N., Ahmad, R., Alrasheed, R. A., Almatar, H. M. A., Sami, A. A., Amir, M., et al. (2020). Quantification and evaluations of catechin hydrate polymeric nanoparticles used in brain targeting for the treatment of epilepsy. *Pharmaceutics* 12, 203. doi:10.3390/pharmaceutics12030203
- Akin, D., Ravizza, T., Maroso, M., Carcak, N., Eryigit, T., Vanzulli, I., et al. (2011). IL-1 β is induced in reactive astrocytes in the somatosensory cortex of rats with genetic absence epilepsy at the onset of spike-and-wave discharges, and contributes to their occurrence. *Neurobiol. Dis.* 44, 259–269. doi:10.1016/j.nbd.2011.05.015
- Alexander, S. P., Catterall, W. A., Kelly, E., Marrion, N., Peters, J. A., Benson, H. E., et al. (2016). CGTP collaborators, the concise guide to PHARMACOLOGY 2015/16: voltage-gated ion channels. *Pharmacology* 172, 5904–5941. doi:10.1111/bph.13349
- Arreola, J. C., West, R. M., Torreblanca, J. M., Hernandez, E. M., Pacheco, J. S., Gonzalez, M. M., et al. (2017). The role of innate immune system receptors in epilepsy research. *CNS Neurol. Disord. Drug Targets* 16 (7), 749–762. doi:10.2174/1871527316666170725145549
- Bahr, T. A., Rodriguez, D., Beaumont, C., and Allred, K. (2019). The effects of various essential oils on epilepsy and acute seizure: a systematic review. *Evid. Based. Complement. Alternat. Med.* 2019, 6216745. doi:10.1155/2019/6216745
- Bark, L. K., Walls, A. B., Schousboe, A., and Waagepetersen, H. S. (2018). Astrocytic glycogen metabolism in the healthy and diseased brain. *J. Biol. Chem.* 293, 7108–7116. doi:10.1074/jbc.R117.803239
- Beenhakker, M. P., and Huguenard, J. R. (2009). Neurons that fire together also conspire together: is normal sleep circuitry hijacked to generate epilepsy?. *Neuron* 62, 612–632. doi:10.1016/j.neuron.2009.05.015
- Buenafe, O. E., Paucar, A. O., Maes, J., Huang, H., Ying, X. H., Borggraeve, W. D., et al. (2013). Tanshinone IIA exhibits anticonvulsant activity in zebrafish and mouse seizure models. *ACS Chem. Neurosci.* 4, 1479–1487. doi:10.1021/cn400140e
- Callenbach, P. M. C., Van Der Zijde, C. M. J., Geerts, A. T., Arts, W. F. M., Van Donselaar, C. A., and Peters, A. C. B. (2003). Dutch study of epilepsy in childhood immunoglobulins in children with epilepsy: the dutch study of epilepsy in childhood. *Clin. Exp. Immunol.* 132, 144–151. doi:10.1046/j.1365-2249.2003.02097.x
- Chen, W., Gao, Z., and Ni, Y. (2013). Carbenoxolone pretreatment and treatment of posttraumatic epilepsy. *Neural. Regen. Res.* 8, 169–176. doi:10.3969/j.issn.1673-5374.2013.02.010
- Chen, X. M., Durisic, N., Lynch, J. W., and Keramidas, A. (2017). Inhibitory synapse deficits caused by familial α 1 GABA A receptor mutations in epilepsy. *Neurobiol. Dis.* 108, 213–224. doi:10.1016/j.nbd.2017.08.020
- Chowdhury, A. A., Gawali, N. B., Shinde, P., Munshi, R., and Juvekar, A. R. (2018). Imperatorin ameliorates lipopolysaccharide induced memory deficit by mitigating proinflammatory cytokines, oxidative stress and modulating brain-derived neurotrophic factor. *Cytokine* 110, 78–86. doi:10.1016/j.cyt.2018.04.018
- Contet, C., Goulding, S. P., Kuljis, D. A., and Barth, A. L. (2016). BK channels in the central nervous system. *Int. Rev. Neurobiol.* 128, 281–342. doi:10.1016/bs.irm.2016.04.001
- Depondt, C. (2006). The potential of pharmacogenetics in the treatment of epilepsy. *Eur. J. Paediatr. Neurol.* 10, 57–65. doi:10.1016/j.ejpn.2005.11.009
- Devinsky, O., Vezzani, A., Najjar, S., Lanerolle, N. C. D., and Rogawsk, M. A. (2013). Glia and epilepsy: excitability and inflammation. *Trends Neurosci.* 36, 174–184. doi:10.1016/j.tins.2012.11.008
- DiFrancesco, J. C., and DiFrancesco, D. (2015). Dysfunctional HCN ion channels in neurological diseases. *Front. Cell. Neurosci.* 6, 174. doi:10.3389/fncel.2015.00071
- Diniz, T. C., Silva, J. C., Saraiva, S. R. G. D. L., Ribeiro, F. P. R. D. A., Pacheco, A. G. M., Freitas, R. M. D., et al. (2015). The role of flavonoids on oxidative stress in epilepsy. *Oxid. Med. Cell. Longev.* 2015, 171756. doi:10.1155/2015/171756
- Dong, Z. T. (2018). Application of empathy nursing in treatment of refractory epilepsy in children with ketogenic diet therapy. *Doctor* 15, 104–105.
- Duflocq, A., Bras, B. L., Bullier, E., Couraud, F., and Davenne, M. (2008). Nav1.1 is predominantly expressed in nodes of Ranvier and axon initial segments. *Mol. Cell. Neurosci.* 39, 180–192. doi:10.1016/j.mcn.2008.06.008
- Fang, Y. L., and Zhang, D. L. (2013). Expression of Bim in rat neurons induced by penicillin induced by ligustrazine. *J. Mathematical Med.* 26, 27.
- Fu, D. T., and Qu, M. (2019). Western medicine for epilepsy. *Chin. J. Clin.* 10, 1142–1145. CNKI:SUN:ZLYS.0.2019-10-006
- Gangar, K., and Bhatt, L. K. (2020). Therapeutic targets for the treatment of comorbidities associated with epilepsy. *Curr. Mol. Pharmacol.* 13, 85–93. doi:10.2174/1874467212666191203101606
- Garlet, Q. I., Pires, L. D. C., Milanesi, L. H., Marafija, J. R., Baldisserotto, B., Mello, C. F., et al. (2017). (+)-Dehydrofukinone modulates membrane potential and delays seizure onset by GABA α receptor-mediated mechanism in mice. *Toxicol. Appl. Pharmacol.* 332, 52–63. doi:10.1016/j.taap.2017.07.010
- Godhwani, N., and Bahna, S. L. (2016). Antiepilepsy drugs and the immune system. *Ann. Allergy Asthma Immunol.* 117, 634–640. doi:10.1016/j.anai.2016.09.443
- Guo, Q. (2017). Effect of gastrodin combined with carbamazepine in the treatment of epilepsy. *Chin. Minkang. Med.* 29, 30–31. doi:10.3969/j.issn.1672-0369.2017.21.015
- Guo, X. Y., Zhou, P. P., Xia, C. Q., Lin, H., and Song, P. (2015). Clinical observation of combined Traditional Chinese and Western medicine in the treatment of epilepsy after stroke. *China Health Stand. Manage.* 6, 144–145. doi:10.3969/j.issn.1674-9316.2015.23.105
- Hall, B. J., Karim, N., Chebib, M., Johnston, G. A. R., and Hanrahan, J. R. (2014). Modulation of ionotropic GABA receptors by 6-methoxyflavanone and 6-methoxyflavone. *Neurochem. Res.* 39, 1068–1078. doi:10.1007/s11064-013-1157-2
- Hanrahan, J. R., Chebib, M., and Johnston, G. A. R. (2015). Interactions of flavonoids with ionotropic GABA receptors. *Adv. Pharmacol.* 72, 189–200. doi:10.1016/bs.apha.2014.10.007
- He, X. Q., Huang, J. M., Liu, G. J., Li, J., and Fu, X. P. (2019). Effect of pueraria flavone on NF- κ B mRNA and il-10mRNA expression in hippocampus of epileptic rats. *Chin. Foreign Med. Res.* 17, 13–15. CNKI:SUN:YJZY.0.2019-10-004
- Hino, H., Takahashi, H., Suzuki, Y., Tanaka, J., Ishii, E., and Fukuda, M. (2012). Anticonvulsive effect of paeoniflorin on experimental febrile seizures in immature rats: possible application for febrile seizures in children. *PLoS One* 7, e42920. doi:10.1371/journal.pone.0042920
- Hirose, S. (2014). Mutant GABA(A) receptor subunits in genetic (idiopathic) epilepsy. *Prog. Brain Res.* 213, 55–85. doi:10.1016/B978-0-444-63326-2.00003-X
- Ho, T. Y., Tang, N. Y., Hsiang, C. Y., and Hsieh, C. L. (2014). Uncaria rhynchophylla and rhynchophylline improved kainic acid-induced epileptic seizures via IL-1 β and brain-derived neurotrophic factor. *Phytomedicine* 21, 893–900. doi:10.1016/j.phymed.2014.01.011
- Huang, C., Li, W. G., Zhang, X. B., Wang, L., Xu, T. L., Wu, D. Z., et al. (2013). α -asarone from Acorus gramineus alleviates epilepsy by modulating A-type GABA receptors. *Neuropharmacology* 65, 1–11. doi:10.1016/j.neuropharm.2012.09.001
- Jin, Y., Cai, S., Jiang, Y. P., Zhong, K., Wen, C. P., Ruan, Y. P., et al. (2019). Tetramethylpyrazine reduces epileptogenesis progression in electrical kindling models by modulating hippocampal excitatory neurotransmission. *ACS Chem. Neurosci.* 10, 4854–4863. doi:10.1021/acschemneuro.9b00575

- Johnston, G. A. R. (2015). Flavonoid nutraceuticals and ionotropic receptors for the inhibitory neurotransmitter GABA. *Neurochem. Int.* 89, 120–125. doi:10.1016/j.neuint.2015.07.013
- Kang, Y. G., Yang, L. S., Yu, L. P., Kong, W., Li, W. Q., et al. (2015). Clinical effect of Tongluo Dingxian Decoction combined with phenobarbital in the treatment of epileptic persistent state and its cerebral protective effect analysis. *Guide. Trad. Chin. Med.* 21, 64–68. doi:10.13862/j.cnki.cn43-1446/r.2015.23.023
- Kanner, A. M. (2009). Depression and epilepsy: do glucocorticoids and glutamate explain their relationship? *Curr. Neurol. Neurosci. Rep.* 9, 307–312. doi:10.1007/s11910-009-0046-1
- Kazmi, I., Afzal, M., Gupta, G., and Anwar, F. (2012). Antiepileptic potential of ursolic acid stearyl glucoside by GABA receptor stimulation. *CNS Neurosci. Ther.* 18, 799–800. doi:10.1111/j.1755-5949.2012.00369.x
- Khan, A. U., Akram, M., Daniyal, M., Akhter, N., Riaz, M., and Akhtar, N. (2020). Awareness and current knowledge of epilepsy. *Metab. Brain Dis.* 35, 45–63. doi:10.1007/s11011-019-00494-1
- Kiasalari, Z., Roghani, M., Khalili, M., Rahmati, B., and Baluchnejadmojarad, T. (2013). Antiepileptogenic effect of curcumin on kainate-induced model of temporal lobe epilepsy. *Pharm. Biol.* 51, 1572–1578. doi:10.3109/13880209.2013.803128
- Kim, S. R. (2016). Control of granule cell dispersion by natural materials such as eugenol and naringin: a potential therapeutic strategy against temporal lobe epilepsy. *J. Med. Food* 19, 730–736. doi:10.1089/jmf.2016.3712
- Kim, S., and Rhim, H. (2004). Ginsenosides inhibit NMDA receptor-mediated epileptic discharges in cultured hippocampal neurons. *Arch. Pharm. Res.* 27, 524–530. doi:10.1007/BF02980126
- Kim, S., Jung, U. J., Oh, Y. S., Jeon, M. T., Kim, H. J., Shin, W. H., et al. (2017). Beneficial effects of silibinin against kainic acid-induced neurotoxicity in the hippocampus *in vivo*. *Exp. Neurobiol.* 26, 266–277. doi:10.5607/en.2017.26.5.266
- Kudin, A. P., Kudina, T. A., Seyfried, J., Vielhaber, S., Beck, H., Elger, C. E., et al. (2002). Seizure-dependent modulation of mitochondrial oxidative phosphorylation in rat hippocampus. *Eur. J. Neurosci.* 15, 1105–1114. doi:10.1046/j.1460-9568.2002.01947.x
- Kumar, P., Shih, D. C. W., Lim, A., Paleja, B., Ling, S., and Yun, L. L. (2019). Pro-inflammatory, IL-17 pathways dominate the architecture of the immunome in pediatric refractory epilepsy. *JCI Insight.* 5, e126337. doi:10.1172/jci.insight.126337
- Krishnakumar, A., Abraham, P. M., Paul, J., and Paulose, C. S. (2009). Down-regulation of cerebellar 5-HT(2C) receptors in pilocarpine-induced epilepsy in rats: therapeutic role of Bacopa monnieri extract. *J. Neurol. Sci.* 284, 124–8. doi:10.1016/j.jns.2009.04.032
- Lee, J. M., Hong, J., Moon, G. J., Jung, U. J., Won, S. Y., and Kim, S. R. (2018). Morin prevents granule cell dispersion and neurotoxicity via suppression of mTORC1 in a kainic acid-induced seizure model. *Exp. Neurobiol.* 27, 226–237. doi:10.5607/en.2018.27.3.226
- Li, C. Q. (2018). Clinical efficacy of SCR decoction combined with Topiramate in the treatment of epilepsy secondary to cerebral infarction. *Electron. J. Integr. Chin. West. Med. Cardiovasc. Dis.* 6, 175–177. doi:10.16282/j.cnki.cn11-9336/r.2018.06.121
- Li, X. H. (2012). Advances in the treatment of epilepsy. *J. Clin. Ration. Drug Use* 5, 155. doi:10.3969/j.issn.1674-3296.2012.06.129
- Liang, L. P., Waldbaum, S., Rowley, S., Huang, T. T., Day, B. J., and Patel, M. (2012). Mitochondrial oxidative stress and epilepsy in SOD2 deficient mice: attenuation by a lipophilic metalloporphyrin. *Neurobiol. Dis.* 45, 1068–1076. doi:10.1016/j.nbd.2011.12.025
- Lin, M. T., Wang, J. J., and Young, M. S. (2002). The protective effect of dl-tetrahydropalmatine against the development of amygdala kindling seizures in rats. *Neurosci. Lett.* 320, 113–116. doi:10.1016/s0304-3940(01)02508-3
- Lin, T. Y., Lu, C. W., and Huang, S. K. (2013). Tanshinone II A, a constituent of Danshen, inhibits the release of glutamate in rat cerebrocortical nerve terminals. *J. Ethnopharmacol.* 147, 488–496. doi:10.1016/j.jep.2013.03.045
- Liu, C. Y., Donf, S. X., and Zhang, T. (2010). Immunological mechanism of ligustrazine in antiepileptics. *Chin. Gerontol.* 30, 1848. doi:10.3969/j.issn.1005-9202.2010.13.032
- Liu, H., Song, Z., Liao, D. G., Zhang, T. Y., Liu, F., Zhuang, K., et al. (2014). Neuroprotective effects of trans-caryophyllene against kainic acid induced seizure activity and oxidative stress in mice. *Neurochem. Res.* 40, 118–123. doi:10.1007/s11064-014-1474-0
- Liu, Q. D., Liu, X. X., and Wu, Y. (2013). Effects of α -asarum on Bax and Bcl-2 in hippocampus of KA epileptic rats. *Stroke Neurological. Dis.* 30, 312. doi:10.19845/j.cnki.zfysjbjzz.2013.04.007
- Liu, Y., Gao, J. L., Peng, M., Meng, H. Y., Ma, H. B., Cai, P. P., et al. (2018). A review on central nervous system effects of gastrodin. *Front. Pharmacol.* 9, 24. doi:10.3389/fphar.2018.00024
- Liu, Y. Z., Xie, W., Ren, Z. J., Zhou, Y., and Zheng, Y. H. (2015). Modernization of traditional Chinese medicine and materia medica. *World Sci. Technol.* 17, 850–855. doi:10.11842/wst.2015.04.017
- Lu, W., Wang, W. H., Xu, M., Jing, X. G., Wang, J., and Chen, L. (2020). Clinical effect analysis of Zizyphus jujube kernel soup combined with sodium valproate in the treatment of traumatic epilepsy. *Epilepsy* 6, 108–112. CNKI:SUN:DXZA.0.2020-02-006
- Ma, M. G., Wu, Y., and Wu, Y. J. (2011). Effects of α -asarine on cell models of refractory epilepsy and Laminin β 1. *Shi. Zhen. Chin. Med.* 22, 1059.
- Ma, Y., Yun, S. R., Nam, S. Y., Kim, Y. B., Hong, J. T., Kim, Y., et al. (2008). Protective effects of sanjoinine A against N-methyl-D-aspartate-induced seizure. *Biol. Pharm. Bull.* 31, 1749–1754. doi:10.1248/bpb.31.1749
- Martin, C. S., Gauvain, G., Teodorescu, G., An, I. G., Fedirko, E., Weber, Y. G., et al. (2009). Christel Depienne Two novel CLCN2 mutations accelerating chloride channel deactivation are associated with idiopathic generalized epilepsy. *Hum. Mutat.* 30, 397–405. doi:10.1002/humu.20876
- Matin, N., Tabatabaie, O., Falsaperla, R., Lubrano, R., Pavone, P., and Mahmood, F. (2015). Epilepsy and innate immune system: a possible immunogenic predisposition and related therapeutic implications. *Hum. Vaccines Immunother.* 11, 2021–2029. doi:10.1080/21645515.2015.1034921
- Mazumder, A. G., Sharma, P., Patial, V., and Singh, D. (2017). Crocin attenuates kindling development and associated cognitive impairments in mice via inhibiting reactive oxygen species-mediated NF- κ B activation. *Basic Clin. Pharmacol. Toxicol.* 120, 426–433. doi:10.1111/bcpt.12694
- Miao, J. K., Chen, Q. X., and Wu, X. M. (2011). Regulation effect of Acorus gramineus α -asarum ether on GABA system in Epilepsy model of Lithium- Pi- Locarpine. *Chin. Pharmacol. Bull.* 27, 1067–1078.
- Nieoczym, D., Socala, K., and Wlaż, P. (2018). Assessment of the anticonvulsant potency of ursolic acid in seizure threshold tests in mice. *Neurochem. Res.* 43, 995–1002. doi:10.1007/s11064-018-2505-z
- Nilsson, J., and Sterner, O. (2011). Modulation of GABA(A) receptors by natural products and the development of novel synthetic ligands for the benzodiazepine binding site. *Curr. Drug Targets* 12, 1674–1688. doi:10.2174/138945011798109509
- Obata, K. (2013). Synaptic inhibition and γ -aminobutyric acid in the mammalian central nervous system. *Proc. Jpn. Acad. Ser. B Phys. Biol. Sci.* 89, 139–156. doi:10.2183/pjab.89.139
- Oliveira, D. R. D., Todo, A. H., Rêgo, G. M., Cerutti, J. M., Cavalheiro, A. J., Rando, D. G. G., et al. (2018). Flavones-bound in benzodiazepine site on GABA A receptor: concomitant anxiolytic-like and cognitive-enhancing effects produced by Isovitetexin and 6-C-glycoside-Diosmetin. *Eur. J. Pharmacol.* 831, 77–86. doi:10.1016/j.ejphar.2018.05.004
- Oyemitan, I. A., Elusiyan, C. A., Akanmu, M. A., and Hypnotic, T. A. O. (2013). Anticonvulsant and anxiolytic effects of 1-nitro-2-phenylethane isolated from the essential oil of *Dennettia tripetala* in mice. *Phytomedicine* 20, 1315–1322. doi:10.1016/j.phymed.2013.07.005
- Pal, D. K., Pong, A. W., and Chung, W. K. (2010). Genetic evaluation and counseling for epilepsy. *Nat. Rev. Neurol.* 6, 445–453. doi:10.1038/nrneurol.2010.92
- Pan, X., Zou, S. F., Zeng, C. X., Cui, J. H., Hu, B., and Li, Y. W. (2012). Effects of tripterolide on kv1.1 expression of voltage gated potassium channels in epileptic rats. *J. Internat. Neurol. Neurosurg.* 39, 108–113. doi:10.7666/d.y2150841
- Paoletti, P., Bellone, C., and Zhou, Q. (2013). NMDA receptor subunit diversity: impact on receptor properties, synaptic plasticity and disease. *Nat. Rev. Neurosci.* 14, 383–400. doi:10.1038/nrn3504
- Pham, V. D., Somasundaram, S., Park, S. J., Lee, S. H., and Hong, S. H. (2016). Co-localization of GABA shunt enzymes for the efficient production of gamma-aminobutyric acid via GABA shunt pathway in *Escherichia coli*. *J. Microbiol. Biotechnol.* 26, 710–716. doi:10.4014/jmb.1511.11037
- Phani, K. K., Annapurna, A., Lakshmi, S. N. R., Ravi, C. S. R. D., Abutalaha, M., and Srikanth, I. (2018). Naringin in a combined therapy with phenytoin on

- pentylentetrazole-induced kindling in rats. *Epilepsy Behav.* 89, 159–168. doi:10.1016/j.yebeh.2018.10.006
- Piazzini, A., and Berio, A. (2015). Activity of drugs and components of natural origin in the severe myoclonic epilepsy of infancy (Dravet syndrome). *Cent. Nerv. Syst. Agents Med. Chem.* 15, 95–98. doi:10.2174/1871524915666150430161321
- Qu, S. X., and Zhang, L. F. (2019). Clinical observation of treating epilepsy with phlegm quenching and wind combined with Western medicine. *Chin. Foreign Women's Health Study*, 58–59. CNKI:SUN:ZWVJ.0..
- Qu, Z. Z., Jia, L. J., Xie, T., Zhen, J. L., Si, P. P., Cui, Z. Q., et al. (2019). (-)-Epigallocatechin-3-Gallate protects against lithium-pilocarpine-induced epilepsy by inhibiting the toll-like receptor 4 (TLR4)/nuclear factor- κ B (NF- κ B) signaling pathway. *Med. Sci. Mon. Int. Med. J. Exp. Clin. Res.* 25, 1749–1758. doi:10.12659/MSM.915025
- Ravizza, T., Boer, K., Redeker, S., Spliet, W. G. M., Rijen, P. C. V., and Troost, D. (2006). The IL-1 β system in epilepsy-associated malformations of cortical development. *Neurobiol. Dis.* 24, 128–143. doi:10.1016/j.brainres.2016.12.006
- Ren, L. H., Wang, F., Xu, Z. W., Chan, W. M., Zhao, C. Y., and Xue, H. (2010). GABA(A) receptor subtype selectivity underlying anxiolytic effect of 6-hydroxyflavone. *Biochem. Pharmacol.* 79, 1337–1344. doi:10.1016/j.bcp.2009.12.024
- Reng, X. P., Zhang, Q. P., Rong, S. K., Zuo, D., Wang, F., and Liu, K. M. (2020). Amantodiflone inhibited IPS-induced inflammatory response in mouse BV-2 microglia. *J. Cell. Mol. Immunol.* 1. doi:10.13423/j.cnki.cjcmi.008950
- Rosa, D. S., Faggion, S. A., Gavin, A. S., Souza, M. A. D., Fachim, H. A., Santos, W. F. D., et al. (2012). Erysothrine, an alkaloid extracted from flowers of *Erythrina mulungu* Mart. Ex Benth: evaluating its anticonvulsant and anxiolytic potential. *Epilepsy Behav.* 23, 205–212. doi:10.1016/j.yebeh.2012.01.003
- Roseti, C., Vliet, E. A. V., Cifelli, P., Ruffolo, G., Baayen, J. C., Castro, M. A. D., et al. (2015). GABAA currents are decreased by IL-1 β in epileptogenic tissue of patients with temporal lobe epilepsy: implications for ictogenesis. *Neurobiol. Dis.* 82, 311–320. doi:10.1016/j.nbd.2015.07.003
- Rowley, S., and Patel, M. (2013). Mitochondrial involvement and oxidative stress in temporal lobe epilepsy. *Free Radic. Biol. Med.* 62, 121–131. doi:10.1016/j.freeradbiomed.2013.02.002
- Saxena, S., and Li, S. (2017). Defeating epilepsy: a global public health commitment. *Epilepsia Open* 2, 153–155. doi:10.1002/epi4.12010
- Shao, H., Yang, Y., Mi, Z., Zhu, G. X., Qi, A. P., Ji, W. G., et al. (2016). Anticonvulsant effect of Rhynchophylline involved in the inhibition of persistent sodium current and NMDA receptor current in the pilocarpine rat model of temporal lobe epilepsy. *Neuroscience* 19 (337), 355–369. doi:10.1016/j.neuroscience.2016.09.029
- Shen, M. L., Wang, C. H., Lin, C. H., Zhou, N., Kao, S. T., and Wu, D. C. (2016). Luteolin attenuates airway mucus overproduction via inhibition of the GABAergic system. *Sci. Rep.* 6, 32756. doi:10.1038/srep32756
- Sheng, F. Y., Chen, M. T., Tan, Y., Xiang, C., Zhang, M., Li, B. C., et al. (2016). Protective effects of otophyllolide N on pentylentetrazol-induced neuronal injury *in vitro* and *in vivo*. *Front. Pharmacol.* 7, 224. doi:10.3389/fphar.2016.00224
- Shi, Y., Miao, W., Teng, J. F., and Zhang, L. L. (2018). Ginsenoside Rb1 protects the brain from damage induced by epileptic seizure via Nrf2/ARE signaling. *Cell. Physiol. Biochem.* 45, 212–225. doi:10.1159/000486768
- Shrestha, S., Park, J., Lee, D. Y., Cho, J. G., Cho, S., Yang, H. J., et al. (2012). Rhus parviflora and its biflavonoid constituent, rhusflavone, induce sleep through the positive allosteric modulation of GABA(A)-benzodiazepine receptors. *J. Ethnopharmacol.* 142, 213–220. doi:10.1016/j.jep.2012.04.047
- Singh, A., and Trevick, S. (2016). The epidemiology of global epilepsy. *Neurol. Clin.* 34, 837–847. doi:10.1016/j.ncl.2016.06.015
- Sinkus, M. L., Graw, S., Freedman, R., Ross, R. G., Lester, H. A., and Leonard, S. (2015). The human CHRNA7 and CHRFA7A genes: a review of the genetics, regulation, and function. *Neuropharmacology* 96, 274–288. doi:10.1016/j.neuropharm.2015.02.006
- Smith, J. N. P., and Patel, M. (2017). Metabolic dysfunction and oxidative stress in epilepsy. *Int. J. Mol. Sci.* 18, 2365. doi:10.3390/ijms18112365
- Sun, Z., Du, M., Lu, Y., and Zeng, C. Q. (2018). Effects of triptolide on the expression of MHC II in microglia in kainic acid-induced epilepsy. *Mol. Med. Rep.* 17, 8357–8362. doi:10.3892/mmr.2018.8891
- Tambe, R., Jain, P., Patil, S., Ghumatkar, P., and Sathaye, S. (2016). Antiepileptogenic effects of borneol in pentylentetrazole-induced kindling in mice. *Naunyn-Schmiedeberg's Arch. Pharmacol.* 389, 467–475. doi:10.1007/s00210-016-1220-z
- Tambe, R., Patil, A., Jain, P., Sancheti, J., Somani, G., and Sathaye, S. (2017). Assessment of luteolin isolated from *Eclipta alba* leaves in animal models of epilepsy. *Pharm. Biol.* 55, 264–268. doi:10.1080/13880209.2016.1260597
- Tan, X. Q., Cheng, X. L., Yang, Y., Li, Y., Gu, J. L., Li, H., et al. (2014). Tanshinone IIA sodium sulfonate (DS-201) enhances human BKCa channel activity by selectively targeting the pore-forming a subunit. *Acta Pharmacol. Sin.* 35, 1351.
- Tang, Z. F., and Mei, Q. X. (2016). Contraindications for the compatibility of nervous system western medicine and traditional Chinese medicine. *Chin. Pharm.* 27, 2446–2448. doi:10.6039/j.issn.1001-0408.2016.17.49
- Tang, Q. Y., Zhang, F. F., Xu, J., Wang, R., Chen, J., Logothetis, D. E., et al. (2016). Epilepsy-related slack channel mutants lead to channel over-activity by two different mechanisms. *Cell. Rep.* 14, 129–139. doi:10.1016/j.celrep.2015.12.019
- Thijs, R. D., Surges, R., O'Brien, T. J., and Sander, J. W. (2019). Epilepsy in adults. *Lancet* 393, 689–701. doi:10.1016/S0140-6736(18)32596-0
- Thodeson, D. M., Brulet, R., and Hsieh, J. (2018). Neural stem cells and epilepsy: functional roles and disease-in-a-dish models. *Cell Tissue Res.* 371, 47–54. doi:10.1007/s00441-017-2675-z
- Tian, Y. (2015). Observation on the curative effect of integrated Chinese and western medicine in treating epilepsy after apoplexy. *World Latest. Med. Informat.* 96, 131–132. doi:10.3969/j.issn.1671-3141.2015.96.089
- Treiman, D. M. (2001). GABAergic mechanisms in epilepsy. *Epilepsia* 42, 8–12. doi:10.1046/j.1528-1157.2001.042suppl.3008.x
- Tu, Y. (2016). Artemisinin – a gift from traditional Chinese medicine to the world (Nobel Lecture). *Angew Chem. Int. Ed. Engl.* 55, 10210–10226. doi:10.1002/anie.201601967
- Walls, A. B., Heimbürger, C. M., Bouman, S. D., Schousboe, A., and Waagepetersen, H. S. (2009). Robust glycogen shunt activity in astrocytes: effects of glutamatergic and adrenergic agents. *Neuroscience* 158, 284–292. doi:10.1016/j.neuroscience.2008.09.058
- Wang, C. P., and Cai, X. P. (2018). Effects of uncinnigenin on serum SOD level and TLR4 expression in hippocampal tissue of juvenile rats with convulsion persisting state. *New Medical.* 50, 6. doi:10.13457/j.cnki.jncm.2018.03.002
- Wang, J., Wang, L., Lou, G. H., Zeng, H. R., Hu, J., Huang, Q. W., et al. (2019). Coptidis Rhizoma: a comprehensive review of its traditional uses, botany, phytochemistry, pharmacology and toxicology. *Pharm. Biol.* 57, 193–225. doi:10.1080/13880209.2019.1577466
- Wang, Z. J., Levinson, S. R., Sun, L., and Heinbockel, T. (2014). Identification of both GABAA receptors and voltage-activated Na⁺ channels as molecular targets of anticonvulsant α -asarone. *Front. Pharmacol.* 5, 40. doi:10.3389/fphar.2014.00040
- Wasowski, C., and Marder, M. (2012). Flavonoids as GABAA receptor ligands: the whole story?. *J. Exp. Pharmacol.* 23, 9–24. doi:10.2147/JEP.S23105
- Wei, F., Yan, L. M., Su, T., He, N., Lin, Z. J., and Wang, J. (2017). Ion channel genes and epilepsy: functional alteration, pathogenic potential, and mechanism of epilepsy. *Neurosci. Bull.* 33, 455–477. doi:10.1007/s12264-017-0134-1
- Wei, H. T., Duan, G. H., He, J. X., Meng, Q. L., Liu, Y. X., Chen, W. Q., et al. (2018). Geniposide attenuates epilepsy symptoms in a mouse model through the PI3K/Akt/GSK-3 β signaling pathway. *Exp. Ther. Med.* 15, 1136–1142.
- William, A., Catterall, F. K., and Oakley, J. C. (2010). NaV1.1 channels and epilepsy. *J. Physiol.* 588, 1849–1859. doi:10.1113/jphysiol.2010.187484
- Wu, F. X., and Zhao, W. G. (2017). Exploration of the law of epilepsy medication based on data mining. *Chin. J. E. Tradit. Med. Formulae* 23, 1005–9903.
- Xiang, C., Wan, J. B., Wang, Y. T., Zhu, H. L., Li, B. C., He, J., et al. (2014). Medicinal compounds with antiepileptic/anticonvulsant activities. *Epilepsia* 55, 3–16. doi:10.1111/epi.12463
- Xie, W., Chen, W. J., and Meng, C. X. (2013). Effect of Bupleuronin A on p-glycoprotein expression in multidrug resistant epileptic rats. *Chin. J. E. Formulol.* 19, 229–9903.
- Xue, F. Y. (2005). The pathogenesis of epilepsy. *Guangxi Med. Dent. J.* 27, 624–626. doi:10.3969/j.issn.0253-4304.2005.05.005
- Yamamura, S., Hoshikawa, M., Dai, K., Saito, H., Suzuki, N., Niwa, O., et al. (2013). ONO-2506 inhibits spike-wave discharges in a genetic animal model without

- affecting traditional convulsive tests via gliotransmission regulation. *Br. J. Pharmacol.* 168, 1088–1100. doi:10.1111/j.1476-5381.2012.02132.x
- Yang, B. W., Wang, J., and Zhang, N. (2018). Effect of nobiletin on experimental model of epilepsy. *Transl. Neurosci.* 9, 211–219. doi:10.1515/tnsci-2018-0031
- Yang, H. J., Guo, A. C., and Wang, Q. (2017). Study on the pathogenesis of epilepsy. *J. Epilepsy* 2, 40–44. doi:10.7507/2096-0247.20170019
- Yang, X. J., Chai, T. Q., Yu, H. B., Chen, X. C., Huang, X. X., and Liu, Y. F. (2015). Meta-analysis on the clinical efficacy of traditional Chinese medicine combined with western medicine in treating epilepsy after stroke. *J. Liaoning. U. Tradit. Chin. Med.* 6, 133–136.
- Yu, X. H., Zhang, L. H., and Zhang, D. L. (2010). Effect of ligustrazine on the expression of adhesion molecule -140 in neurons induced by penicillin in rats. *Chin. J. Hosp. Pharm.* 30, 665. CNKI:SUN:ZGYZ.0.2010-08-014
- Yu, Y. H., Wei, X., Yong, B., Hui-Ming, L., San-Jue, H., and Jun-Ling, X. (2012). Saikosaponin a mediates the an-ticonvulsant properties in the HNC models of AE and SE by in-hibiting NMDA receptor current and persistent sodium current. *PloS One* 7, e50694. doi:10.1371/journal.pone.0050694
- Yuan, C. C. (2016). Discussion on the mechanism of amantol diflavone on epilepsy and cognition. *Ningxia Med. U.* 33, 1253–1255. doi:10.4324/9781315757919
- Yuan, S. Y., and Liu, J. M. (2020). Advances in the pharmacology of α -asarum. *J. Integrat. Chin. West. Med. Cardio Cerebrovascul. Dis.* 18, 67–69. CNKI:SUN:ZYYY.0.2020-08-016
- Yuan, X., Li, Z., Wang, X. T., Li, X. Y., Hua, H., Li, X. C., et al. (2019). Roles and mechanisms of traditional Chinese medicine and its active ingredients in treating epilepsy. *Zhongguo Zhong. Yao. Za. Zhi.* 44, 9–18. doi:10.19540/j.cnki.cjcm.20181012.006
- Zagaja, M., Andres-Mach, M., Woźniak, K. S., Rękas, A. R., Kondrat-Wróbel, M. W., Gleńsk, M., et al. (2015). Assessment of the combined treatment with umbelliferone and four classical antiepileptic drugs against maximal electroshock-induced seizures in mice. *Pharmacology* 96, 175–180. doi:10.1159/000438704
- Zagaja, M., Mach, M. A., Patrzylas, P., Pyrka, D., Szpringer, M., Łuszczki, M. F., et al. (2016). Influence of xanthotoxin (8-methoxypsoralen) on the anticonvulsant activity of various novel antiepileptic drugs against maximal electroshock-induced seizures in mice. *Fitoterapia* 115, 86–91. doi:10.1016/j.fitote.2016.09.020
- Zhang, Q., Liu, J., Li, R., Zhao, R., Zhang, M., Wei, S., et al. (2020). A network pharmacology approach to investigate the anticancer mechanism and potential active ingredients of *Rheum palmatum* L. against lung cancer via induction of apoptosis. *Front. Pharmacol.* 11, 528308. doi:10.3389/fphar.2020.528308
- Zhang, Y., Long, Y., Yu, S., Li, D., Yang, M., Guan, Y., et al. (2020). Natural volatile oils derived from herbal medicines: a promising therapy way for treating depressive disorder. *Pharmacol. Res.* 164, 105376. doi:10.1016/j.phrs.2020.105376
- Zhang, Z., Sun, T., Niu, J. G., He, Z. Q., Liu, Y., and Wang, F. (2015). Amentoflavone protects hippocampal neurons: anti-inflammatory, antioxidative, and antiapoptotic effects. *Neural. Regen. Res.* 10, 1125–1133. doi:10.4103/1673-5374.160109
- Zhao, H. Y., Lin, Y., Chen, S. R., Li, X., and Huo, H. L. (2018). 5-HT₃ receptors: a potential therapeutic target for epilepsy. *Curr. Neuropharmacol.* 16, 29–36. doi:10.2174/1570159X15666170508170412
- Zhao, L. H., Sun, Z. H., Yang, L. M., Cui, R. J., Yang, W., and Li, B. J. (2020). Neuropharmacological effects of aconiti lateralis radix praeparata. *Clin. Exp. Pharmacol. Physiol.* 47, 531–542. doi:10.1111/1440-1681.13228
- Zhao, Z. M., Sun, Z. H., Chen, M. H., Liao, Q., Tan, M., Zhang, X. W., et al. (2013). Neuroprotective polyhydroxypregnane glycosides from *Cynanchum otophyllum*. *Steroids* 78, 1015–1020. doi:10.1016/j.steroids.2013.06.007
- Zheng, Y. M., Chen, B., Jiang, J. D., and Zhang, J. P. (2018). Syntaxin 1B mediates berberine's roles in epilepsy-like behavior in a pentylenetetrazole-induced seizure zebrafish model. *Front. Mol. Neurosci.* 26, 378. doi:10.3389/fnmol.2018.00378
- Zhou, B. F. (2018). Clinical study of carbamazepine combined with Tongqiao Dingxian decoction in the treatment of epilepsy. *J. Integrated. Chinese. Western. Med. Cardio-Cerebrovascul. Dis.* 16, 2392–2395. doi:10.12102/j.issn.1672-1349.2018.16.033
- Zhu, D. Y., Lu, Z. Y., Lu, L. D., Xu, Q., and Zhao, H. (2017). Progress in western and traditional Chinese medicine treatment of epilepsy. *J. Neurol. Neurorehabil.* 13, 221–226. doi:10.12022/jnnr.2017-0052
- Zhu, H. L., Wan, J. B., Wang, Y. T., Li, B. C., Cheng, X., He, J., et al. (2014). Medicinal compounds with antiepileptic/anticonvulsant activities. *Epilepsia* 55, 3–16. doi:10.1111/epi.12463

Conflict of Interest: The authors declare that the research was conducted in the absence of any commercial or financial relationships that could be construed as a potential conflict of interest.

Copyright © 2021 He, Hu, Li, Zhao, Fan, He, Lu, Ye, Huang and Wu. This is an open-access article distributed under the terms of the Creative Commons Attribution License (CC BY). The use, distribution or reproduction in other forums is permitted, provided the original author(s) and the copyright owner(s) are credited and that the original publication in this journal is cited, in accordance with accepted academic practice. No use, distribution or reproduction is permitted which does not comply with these terms.



I-Borneol Exerted the Neuroprotective Effect by Promoting Angiogenesis Coupled With Neurogenesis via Ang1-VEGF-BDNF Pathway

Rong Ma^{1,2†}, Qian Xie^{1,2†}, Hongyan Li^{1,2}, Xiaoqing Guo^{1,2}, Jian Wang^{1,2*}, Yong Li^{1,2}, Mihong Ren^{1,2}, Daoyin Gong^{3*} and Tian Gao^{3,4}

¹State Key Laboratory of Southwestern Chinese Medicine Resources, Chengdu, China, ²School of Pharmacy, Chengdu University of Traditional Chinese Medicine, Chengdu, China, ³Department of Pathology, Hospital of Chengdu University of Traditional Chinese Medicine, Chengdu, China, ⁴Adverse Reaction Monitoring Center, Hospital of Chengdu University of Traditional Chinese Medicine, Chengdu, China

OPEN ACCESS

Edited by:

Jiahong Lu,
University of Macau, China

Reviewed by:

Maria Luisa Del Moral,
University of Jaén, Spain
Amit Krishna De,
Indian Science Congress Association,
India

*Correspondence:

Jian Wang
jianwang08@163.com
Daoyin Gong
269095483@qq.com

[†]These authors have contributed
equally to this work

Specialty section:

This article was submitted to
Ethnopharmacology,
a section of the journal
Frontiers in Pharmacology

Received: 15 December 2020

Accepted: 25 January 2021

Published: 05 March 2021

Citation:

Ma R, Xie Q, Li H, Guo X, Wang J, Li Y,
Ren M, Gong D and Gao T (2021)
I-Borneol Exerted the Neuroprotective
Effect by Promoting Angiogenesis
Coupled With Neurogenesis via Ang1-
VEGF-BDNF Pathway.
Front. Pharmacol. 12:641894.
doi: 10.3389/fphar.2021.641894

At present, Stroke is still one of the leading causes of population death worldwide and leads to disability. Traditional Chinese medicine plays an important role in the prevention or treatment of stroke. *I*-borneol, a traditional Chinese medicine, has been used in China to treat stroke for thousands of years. However, its mechanism of action is unclear. After cerebral ischemia, promoting angiogenesis after cerebral ischemia and providing nutrition for the infarct area is an important strategy to improve the damage in the ischemic area, but it is also essential to promote neurogenesis and replenish new neurons. Here, our research shows that *I*-borneol can significantly improve the neurological deficits of pMCAO model rats, reduce cerebral infarction, and improve the pathological damage of cerebral ischemia. and significantly increase serum level of Ang-1 and VEGF, and significantly decrease level of ACE and Tie2 to promote angiogenesis. PCR and WB showed the same results. Immunohistochemistry also showed that *I*-borneol can increase the number of CD34 positive cells, further verifying that *I*-borneol can play a neuroprotective effect by promoting angiogenesis after cerebral ischemia injury. In addition, *I*-borneol can significantly promote the expression level of VEGF, BDNF and inhibit the expression levels of TGF- β 1 and MMP9 to promote neurogenesis. The above suggests that *I*-borneol can promote angiogenesis coupled neurogenesis by regulating Ang1-VEGF-BDNF to play a neuroprotective effect. Molecular docking also shows that *I*-borneol has a very high binding rate with the above target, which further confirmed the target of *I*-borneol to improve cerebral ischemic injury. These results provide strong evidence for the treatment of cerebral ischemia with *I*-borneol and provide reference for future research.

Keywords: *I*-borneol, cerebral ischemia, pMCAO, angiogenesis, neurogenesis

Abbreviations: t-PA, Tissue plasminogen activator; FDA, Food and Drug Administration; VEGF, vascular endothelial growth factor; Ang, angiopoietin; BDNF, Brain derived neurotrophic factor; SVZ, subventricular zone; LPS, lipopolysaccharide; BBB, blood brain-barrier; MCAO, middle cerebral artery occlusion; SD, Sprague Dawley; TTC, 2,3,5-Triphenyltetrazolium chloride; ELISA, Enzyme-linked immunosorbent assay; Hematoxylin-eosin, HE; IHC, immunohistochemical; ACE, angiotensin-converting enzyme; PBS, Phosphate buffer solution; SDS, Sodium dodecyl sulfate; PDB, Protein Data Bank; TGF- β 1, Transforming growth factor, MMP9, Matrix metalloprotein 9; qRT-PCR, quantitative real-time polymerase chain reaction; VEGFR, vascular endothelial growth factor receptor; MVD, Microvessel density; eNOS, endothelial nitric oxide synthases, NO, nitric oxide

INTRODUCTION

Stroke which caused by interruption to flow of blood in brain vessels results in the insufficient blood supplement. Stroke is still one of the leading causes of population death worldwide and leads to disability at present (Phipps and Cronin, 2020). It has the characteristics of high morbidity, high lethality rate, and high disability rate, and there is a tendency of rejuvenation (Boot et al., 2020). The outcomes of ischemic stroke damage are far-reaching, generating immense burden to both the family and society (Roth et al., 2018). So far, ideal drugs or strategies for ischemic stroke are still unavailable. Present strategies for treatment of stroke include recanalization by means of pharmacologic or mechanical thrombolysis and neuroprotective agents (Alim et al., 2019). Tissue plasminogen activator (t-PA) intravenous thrombolysis has been approved as the principal recommended strategy for the treatment of acute stroke by US Food and Drug Administration (FDA) (Dirnagl et al., 1999; Donnan et al., 2008). The reports stated intravenous thrombolysis within 6 h after the onset of stroke is the only treatment to reduce the disability of stroke patients (Miller et al., 2012; Wardlaw et al., 2012; Demaerschalk et al., 2016; Furie and Jayaraman 2018). However, its activation of the fibrinolytic system caused bleeding and limited its application (Külkens and Hacke, 2014; Henderson et al., 2018). According to reports, only 9.9% of patients can receive thrombolytic therapy, and there are some patients with unsuccessful thrombolysis. Hence, there is necessary to explore novel neuroprotective strategies for ischemic stroke treatment. Further research is needed to identify neuroprotective drugs and their mechanisms, which will prevent or ameliorate brain injury.

Emerging evidence suggests the cerebral ischemia injury caused a sophisticated cascade of pathophysiologic events (Kahles and Brandes 2013; Ludewig et al., 2019). After cerebral ischemia, brain parenchyma cells, intercellular stroma and microvascular regeneration is inhibited, which leads to the edema and death of glial cells and vascular cells in the acute phase, and even causes the injured neurons to lose timely nutritional support and die. Therefore, vascular reconstruction is very important to save reversible nerve injury of ischemic penumbra and promote regeneration and repair after injury (Wang et al., 2019). Recent studies have shown that angiogenesis plays an important role in neuroprotection (Seevinck et al., 2010; Benedek et al., 2019). Ischemia can cause neuronal ischemia and hypoxia death, so it is also essential to promote neurogenesis and replenish damaged neurons (Zhang et al., 2020). The ideal strategies are to promote angiogenesis, improve microcirculation, increase cerebral blood flow, and promote neurogenesis, replenish damaged neurons, repair brain tissue injury in ischemic area, further to improve neurological dysfunction (Lunardi and Lehmann 2019). In fact, angiogenesis and neurogenesis often go hand in hand. The new neurons can guide the development of the vascular tree to the infarct area and improve the tissue perfusion in the infarct area and penumbra. The new blood vessels can provide nutrients for the new neurons, promote their maturation, and promote their migration to the infarct area.

Vascular endothelial growth factor (VEGF) is considered to be the most powerful and specific angiogenic factor, while angiopoietin (Ang) is the first one that has been determined to

have the effect of promoting angiogenesis. VEGF and Ang coordinate with each other and jointly regulate angiogenesis (Zhang and Chopp 2002). Another study showed that VEGF-Ang/Tie pathway has important regulatory significance in cerebral ischemia (Hori et al., 2004). Brain derived neurotrophic factor (BDNF) is a kind of neurotrophic factor formed in the brain, which is involved in the survival, differentiation, and maturation of neurons (Liu et al., 2020; Müller et al., 2020). What's more, BDNF is the possible mechanism by exercise exerts positive effects in the brain (Amin et al., 2020). VEGF also has the effect of promoting neurogenesis, especially in the hippocampus and subventricular zone (SVZ) area (Greenberg and Jin, 2013). VEGF can stimulate axon growth, promote the proliferation and differentiation of neuron precursors, and promote the release of BDNF from endothelial cells (Sun et al., 2003). Simultaneously, VEGF-BDNF pathway could improve the cognitive dysfunction (Jeong et al., 2019). TGF- β 1 also played an important role for ischemic cerebrovascular disorders (Rehab et al., 2020). Therefore, angiogenesis and neurogenesis might be a potential mechanism to improve cerebral ischemia injury.

Borneol is a traditional Chinese medicine, which has been used to treat stroke for a long history in China. In recent years, it was reported that borneol has many pharmacological effects, such as, anti-inflammatory, analgesic, sedative, and anti-bacterial, anti-tumor (Sousa et al., 2007; Chen et al., 2019; Cao et al., 2020; Ji et al., 2020; Xin et al., 2020). Our previous studies showed that borneol could reduce the temperature of lipopolysaccharide (LPS) induced fever rats (Luo et al., 2016). Both *l*-borneol and synthetic borneol had a brain protection effect and regulated the permeability of blood brain-barrier (BBB), and the effect of *l*-borneol was better than synthetic borneol (Ni et al., 2011a; Ni et al., 2011b; Tian et al., 2013; Zhou et al., 2014). Simultaneously, we found that borneol could significantly increase the serum VEGF in the middle cerebral artery occlusion (MCAO) rats, and reduce the TNF- α level, and borneol could improve the neuron BBB ultrastructure to protect neurovascular units (Dong et al., 2018). However, the mechanism of *l*-borneol has not been elucidated. Therefore, it is the first time to investigate the mechanism of *l*-borneol by angiogenesis and neurogenesis. This study might provide a novel view on the neuroprotective effect of *l*-borneol on stroke. The graphical abstract of this study is shown in **Figure 1**.

MATERIALS AND METHODS

Animals

Male Sprague Dawley (SD) rats weighing (8–10 weeks old, 250 ± 10 g) were obtained from SPF (Beijing) Biotechnology Co., Ltd. (Beijing, China), permit number: SCXK (Jing) 2019-0010. All animals were handled in keeping with institutional guidelines and ethics. Rats were housed at $22 \pm 2^\circ\text{C}$ with a 12 h light/12 h dark cycle. The animals had free access to food and water. Randomization was used to allocated animals to various experimental groups and the data analysis were performed by a blinded investigator. The experimental processing is approved by ethics committee of Affiliated Hospital of Chengdu University of Traditional Chinese Medicine, number: DL2019002.

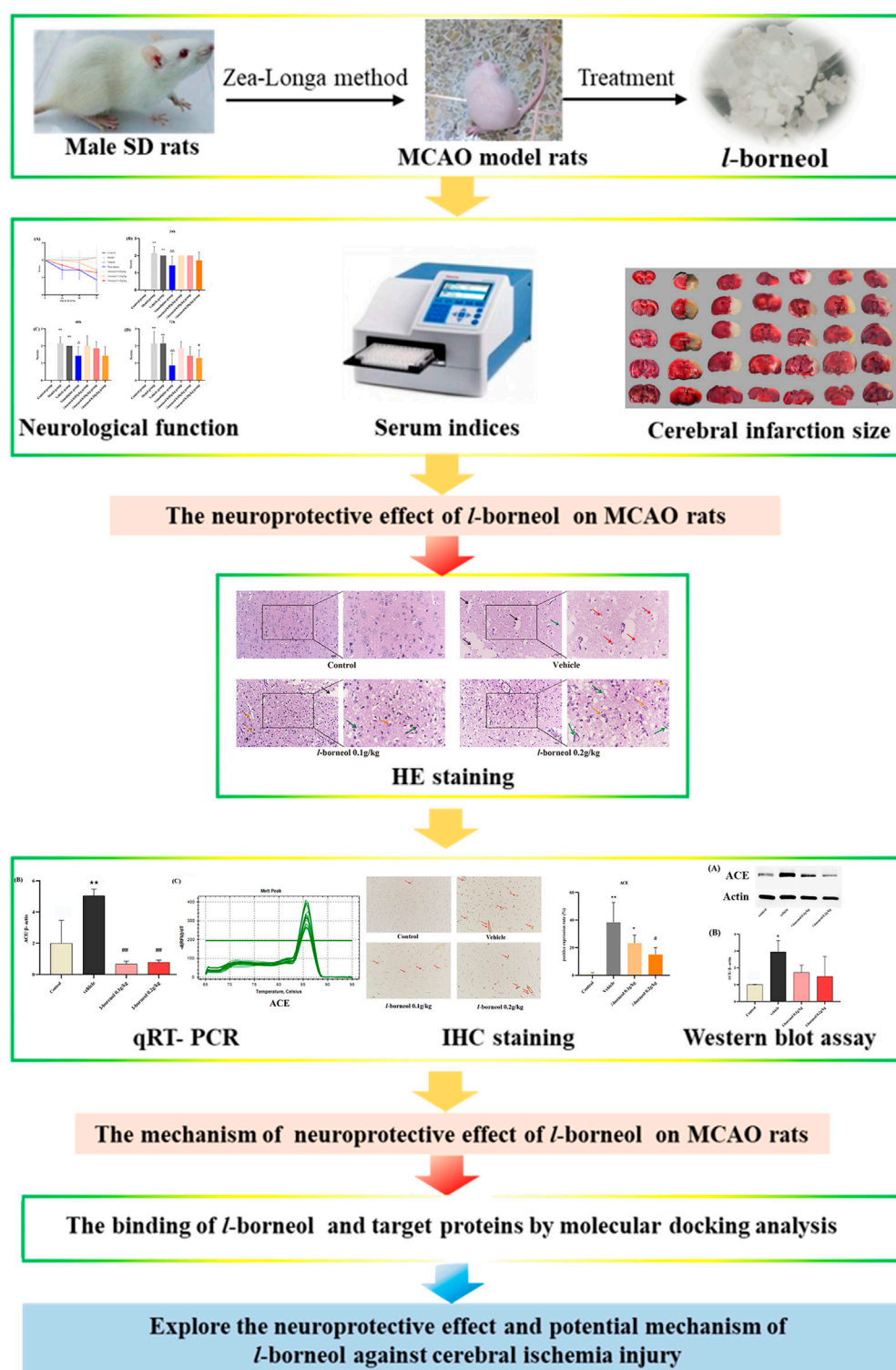


FIGURE 1 | The graphical abstract of this study.

Experimental Drugs and Reagents

The *l*-borneol was purchased from Luodian, Guizhou, China, which is a high-quality production area for *l*-borneol. According to the method

specified in the Pharmacopoeia of the People's Republic of China, 88.6% of the *l*-borneol in this study meets the requirement of no less than 85.0%. Nimodipine was obtained from Yabao Pharmaceutical

TABLE 1 | Zea-Longa neurological function score.

Grade	Rat behavior	Neurological function
0	No neurological deficit	Normal
1	The forelimb on the paralyzed side cannot be fully extended	Mild neurological deficit
2	The rat turns to the paralyzed side while walking	Moderate neurological deficit
3	The rat falls to the paralyzed side while walking	Severe neurological deficit
4	Can't go spontaneously, lose consciousness	Very severe neurological deficit

Group Co., Ltd. (Shanxi, China). Hematoxylin (batch number, G1140) and Eosin (G1100) was purchased from Solarbio co., Ltd. (Beijing, China). 2,3,5-Triphenyltetrazolium chloride (TTC) was purchased from Kelong co. (Chengdu, China). Brain derived neurotrophic factor (BDNF) (Lot No. 9ZFHS54AQT), Tie2 (Lot No. M6RQRBWEEN), Matrix metalloprotein 9 (MMP 9) (Lot No. YU5E7JW4UR) and Ang-1 (Lot No. JNS67D5Z7W) kits were purchased from Elabscience Biotech Co., Ltd. (Wuhan, China). Vascular endothelial growth factor (VEGF) (Lot No. A38381252) and TGF- β 1 (Lot No. A18181155) kits were purchased from MultiSciences (Lianke) Biotech Co., Ltd. (Hangzhou, China).

Drug Preparation

The borneol dosing was calculated according to the dose conversion table of experimental animals. The 10 times of an adult's (60 kg) daily consumption (0.3 g) is as equivalent dosing (0.05 g/kg). The 1, 2, four time(s) of equivalent dose were used as low dosing (0.05 g/kg), medium dosing (0.1 g/kg) and high dosing (0.2 g/kg). Every group were dissolved in 5% tween 80 solution. The concentration of nimodipine was 0.012 g/kg, which is dissolved in pure water.

Permanent MCAO Surgery, Neurological Deficit Determination and Drug Treatments

Rats were adaptively fed for 5 days. A total of 54 male rats were divided into two parts of the experiment. The first part included the sham operation group, model group, vehicle group, nimodipine group, and *l*-borneol 0.05 g/kg group, *l*-borneol 0.1 g/kg group, *l*-borneol 0.2 g/kg group, with six rats in each group. The second part includes sham operation group, vehicle group, *l*-borneol 0.1 g/kg group, *l*-borneol 0.2 g/kg group, with three rats in each group. The rats were subjected to permanent MCAO surgery as described in previous study (Dong et al., 2018; Ma et al., 2020). The rat body temperature was kept at 37°C during surgery. The skin incision and blood vessel dissection only were performed in the sham operation (Control) group, and the rest of the operation was the same as the other groups. Perform neurobehavioral testing by the classic neurologic deficit score method Zea-Longa to determine the neurological deficit after MCAO (Table 1). For the first part of the experiment, then grade 2 of MCAO animals were randomly divided into six group: model group, vehicle group, nimodipine group, *l*-borneol 0.05 g/kg group, *l*-borneol 0.1 g/kg group, *l*-borneol 0.2 g/kg group. All of rats were treated by intragastric administration with 10 ml/kg. The control group and model group were given the same volume of pure water. The vehicle group was given the same volume of 5% tween 80 solutions. The nimodipine group, *l*-borneol 0.05, 0.1, 0.2 g/kg group were given the same volume of the

TABLE 2 | Semi-quantitative injury score standards.

Scores	0	1	2	3
Liquefying necrosis of infarct	–	+	++	+++
Red neuron	–	+	++	+++
Inflammatory cell infiltration	–	+	++	+++

TABLE 3 | Semi-quantitative repair score standards.

Scores	0	1	2
Vessels number	–	+	++
Phagocyte	–	+	++

corresponding drug solution. All rats were given continuous intervention for 3 days, and neurobehavioral tests were performed at 24, 48, and 72 h after MACO. In the second part of the experiment, rat brain tissue is used for IHC and PCR.

Serum and Brain Tissue Preparation

After neurological test, the rats were anesthetized and decapitated under anesthesia. Thereafter, the serum was obtained from abdominal aortathe and centrifuged 3,000 rpm after standing. The supernatant was collected and frozen at –80°C. The rat brains were promptly obtained and the olfactory bulb, lower brain stem and cerebellum were removed.

Cerebral Infarction Assessment

The brain was frozen at –20°C for 15 min. Five coronal brain sections of 2 mm thickness were stained with TTC at 37°C for 30 min in darkness. After TTC staining, those pieces were fixed with 4% formaldehyde for 24 h in the dark. The cerebral infarction rate was analyzed.

Enzyme-Linked Immunosorbent Assay (ELISA) Detection

The supernatant serum had been obtained. levels of VEGF, Ang1, BDNF, Tie2, TGF- β 1, MMP9 were detected according ELISA kits complied with the manufacturer's protocol.

Hematoxylin-Eosin (HE) Staining

The brain tissue was fixed in 4% paraformaldehyde and embedded in paraffin. The paraffin-embedded brain tissue was cut into slices. The slices were dehydrated and dewaxed and then stained with HE for morphological evaluation. Each slice was observed under $\times 200$ and $\times 400$ microscopy. According to the

TABLE 4 | Sequence of primers.

Primer	Sequence (5'→3')
ACE	F: TTCACATCCCAAGCGTGACA, R: CTGAACCCAGCAGGTCCTTC
CD 34	F: CAGTCTGAGGTTAGCCCGA, R: CTGGGTCACATTGGCCTTTC
HIF 1α	F: GCGGCGAGAACGAGAAGAAA, R: AGATGGGAGCTCACGTTGTG

scoring standards of semi-quantitative injury and repair in **Table 2** and **Table 3**, the pathological conditions of brain tissue in each group were analyzed.

According to the degree of pathological changes from light to heavy, the semi-quantitative results are as follows: slight or very small "-" marked 0, slight or small "+" marked 1, moderate "+" marked 2, severe or large "+" marked 3.

According to the degree of repair from bad to good, the semi-quantitative results are as followed: slight or very small "-" marked 0, slight or small "+" marked 1, moderate or medium "+" marked 2.

Quantitative Real-Time Polymerase Chain Reaction (qRT-PCR)

Total RNA was obtained with the Trizol Reagent, which was reverse transcribed to cDNA with the Servicebio® RT First Strand cDNA Synthesis Kit (Servicebio. Co., Ltd., G3330, Wuhan, China). The CFX96 real-time PCR detection system (Bio-Rad Laboratories Ltd., Hertfordshire, United Kingdom) was used to perform qRT-PCR. The specific primers and according sequences were displayed in **Table 4**. In the reaction, 1 μL cDNA of each sample was mixed with Servicebio® 2 × SYBR Green qPCR Master Mix (None ROX) (Servicebio. Co., Ltd., G3320, Wuhan, China) according to the manufacture's protocol. The PCR conditions were listed as follow: 30 s at 95°C, then 40 cycles at 95°C for 15 s, followed by 60°C for 30 s. Results were normalized to Actin mRNA level and presented as the fold change ($2^{-\Delta\Delta Ct}$).

Immunohistochemical (IHC) Staining

IHC was used to determine the expression of anti-angiotensin-converting enzyme (ACE) and CD34 protein. In brief, the brain sections with paraffin-embedded (4 μm) were rinsed with 3% H₂O₂ for 10 min to block endogenous peroxide activity and incubated with 10% goat serum albumin for 30 min to block nonspecific binding. Then, the sections were incubated with the primary antibodies (ACE, abcam, No. ab254222, United Kingdom, 1:100) and anti-CD34 (1:200) overnight at 4°C, after incubation, sections were incubated with corresponding secondary antibody (anti-rabbit IgG-HRP, 1:200). Counterstaining was performed using hematoxylin. For the semiquantitative analysis of the immunohistochemical results, three sections from each brain, with each section containing three microscopic fields from the ischemic cerebral cortex, were digitized under a ×200 objective. The immunoreactivity of the target proteins was quantified based on the integrated optical density of immunostaining per field using Image J software.

Western Blot Assay

The brains were prepared, washed with cold phosphate buffer solution (PBS), resuspended in a lysis buffer, and sonicated the

lysate. The proteins were separated on 10% sodium dodecyl sulfate (SDS) gels and transferred to poly-vinylidene fluoride membranes. After incubation with 1:1,000 primary antibody-ACE dilution buffer for 1 h, Goat Anti-Rabbit IgG (H + L) HRP (1:3,000, absin) was used as secondary antibody and developed by enhanced chemiluminescence.

Molecular Docking Analysis

Molecular docking analysis between *l*-borneol and were performed using Discovery Studio 3.5. The human X-ray crystal structures of VEGF, Ang1, BDNF, Tie2, TGF-β1, MMP9 were obtained from the Protein Data Bank (PDB) archives and used as target for molecular docking. **Table 5** showed that the information about those targets PDB ID. The structure of *l*-borneol was drawn by ChemDraw. The active site was searched via "Receptor - Ligand interactions - Define and Edit Bind Site". The interactions between *l*-borneol and target proteins were detected to obtain the score using LibDock function.

Statistical Analysis

Data are expressed as mean ± SD. GraphPad Prism 8 (GraphPad Software Inc., San Diego, CA, United States) was used to analyze all data. Two or multiple groups were compared using Student's unpaired *t*-test or one-way ANOVA followed by Bonferroni *post hoc* test with *F* at *p* < 0.05 and no significant variance inhomogeneity. *p* < 0.05 was considered statistically significant.

RESULTS

Effect of *l*-Borneol Interventions on Neurological Function Score

Neurological function score was performed by Zea - Longa methods. The results showed in **Figure 2**. The trend of neurological score after MCAO is shown in **Figure 2A**, which suggested *l*-borneol post treatment could gradually improve the neurological function. In the day of MCAO, the rats in the control group had no neurological damage, so the score was 0, and the rats in the other groups were scored 2, indicating a successful modeling. The model and vehicle group had no significant difference, it is suggested that 5% Tween solution as a solvent has no significant effect on neurological function after cerebral ischemia. Compared with model group, nimodipine could significantly improve neurological function scores after 24 h, 48 h and 72 h (*p* < 0.05 or *p* < 0.01). Compared with vehicle

TABLE 5 | The information of target proteins.

Gene	Name	PDB ID
Ang1	Angiotensin-1	4epu
BDNF	Brain-derived neurotrophic factor	1b8m
VEGF	Vascular endothelial growth factor	1wq9
TGF-β1	Transforming growth factor-1β	5vqp
Tie2	TEK tyrosine kinase, endothelial	3l8p
MMP9	Matrix metalloproteinase 9	4h82

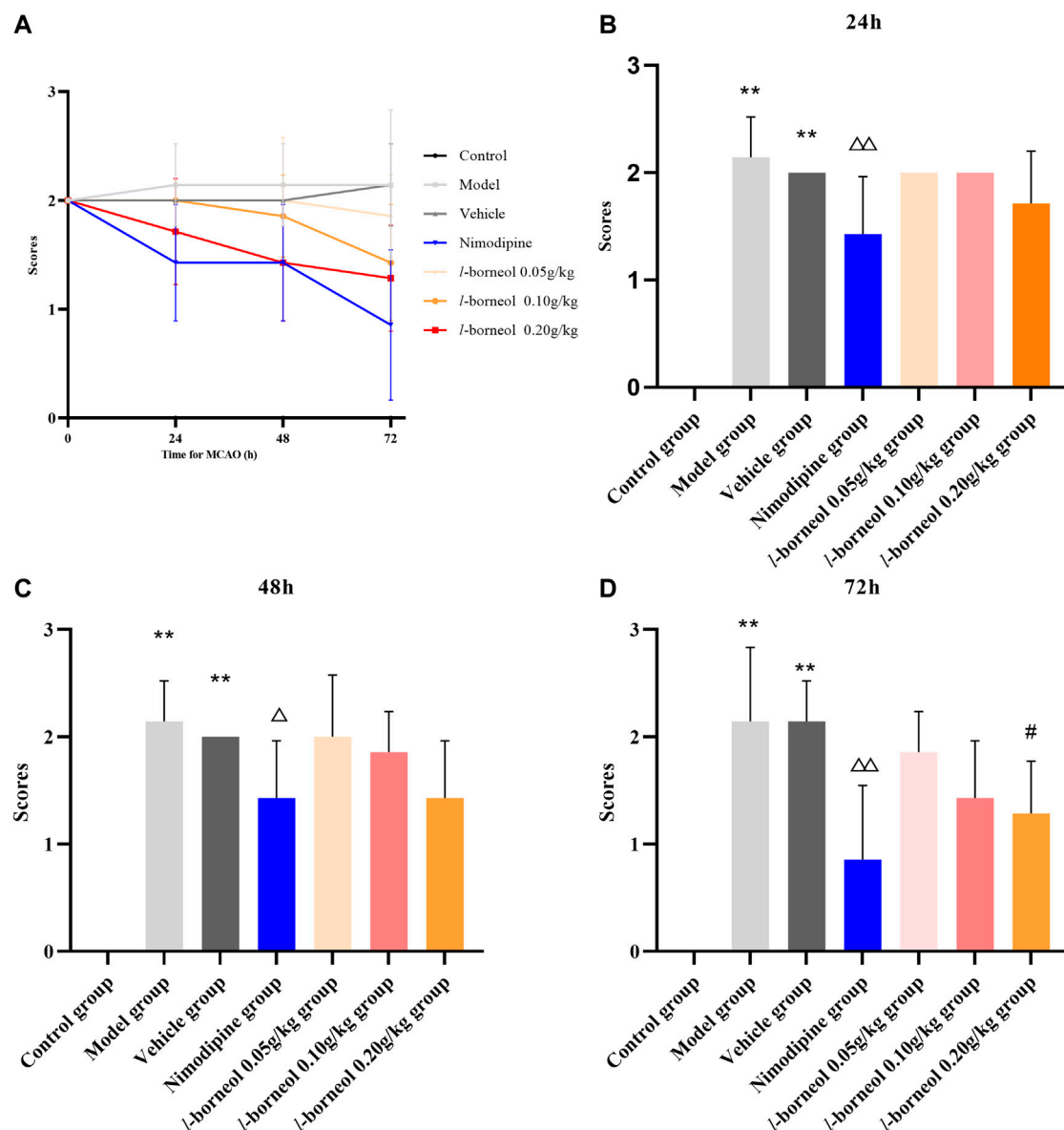


FIGURE 2 | Illustration of neurological function score using Zea-Longa methods ($n = 6$). **(A)** the trend after MCAO; **(B)** neurological function score after 24h; **(C)** neurological function score after 48h; **(D)** neurological function score after 72 h. ** $p < 0.01$, compared with the control group; $\Delta p < 0.05$, $\Delta\Delta p < 0.01$, compared with the model group; # $p < 0.05$, compared with the vehicle group.

group, *l*-borneol 0.2 g/kg could significantly reduce the neurological function scores after 72 h ($p < 0.05$). The other time points had the trend of improving the neural function, but there was no significant difference ($p > 0.05$). The results suggest that *l*-borneol can significantly reduce neurological deficits caused by cerebral ischemia.

Effect of *l*-Borneol Interventions on Cerebral Infarction

For the assessment of infarction, TTC staining was used. TTC is converted to red formazone pigment by NAD and

dehydrogenase and there of stained the viable cells deep red. The infarcted cells have lost the enzyme and cofactor and thus remained unstained dull yellow or white. The results showed in **Figure 3**, the rats in the control group had no significant infarct volume, the infarction of the model group and vehicle group showed significantly different from that of the control group ($p < 0.01$). The model and vehicle group had no significant difference. Cerebral infarct size was obviously reduced in the nimodipine group compared with the model group ($p < 0.01$). Compared with the vehicle group, *l*-borneol could reduce the cerebral infarction rate ($p < 0.05$ or $p < 0.01$), showing the dose dependent relationship.

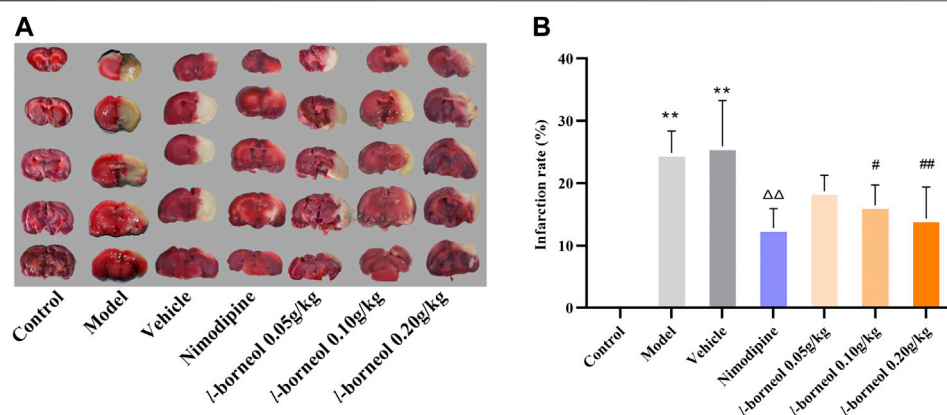


FIGURE 3 | Illustration of cerebral infarction by TTC staining ($n = 6$). The infarcted cells showed white or yellow, the normal side was red. ** $p < 0.01$, compared with the control group; $\Delta\Delta p < 0.01$, compared with the model group; # $p < 0.05$, ## $p < 0.01$, compared with the vehicle group.

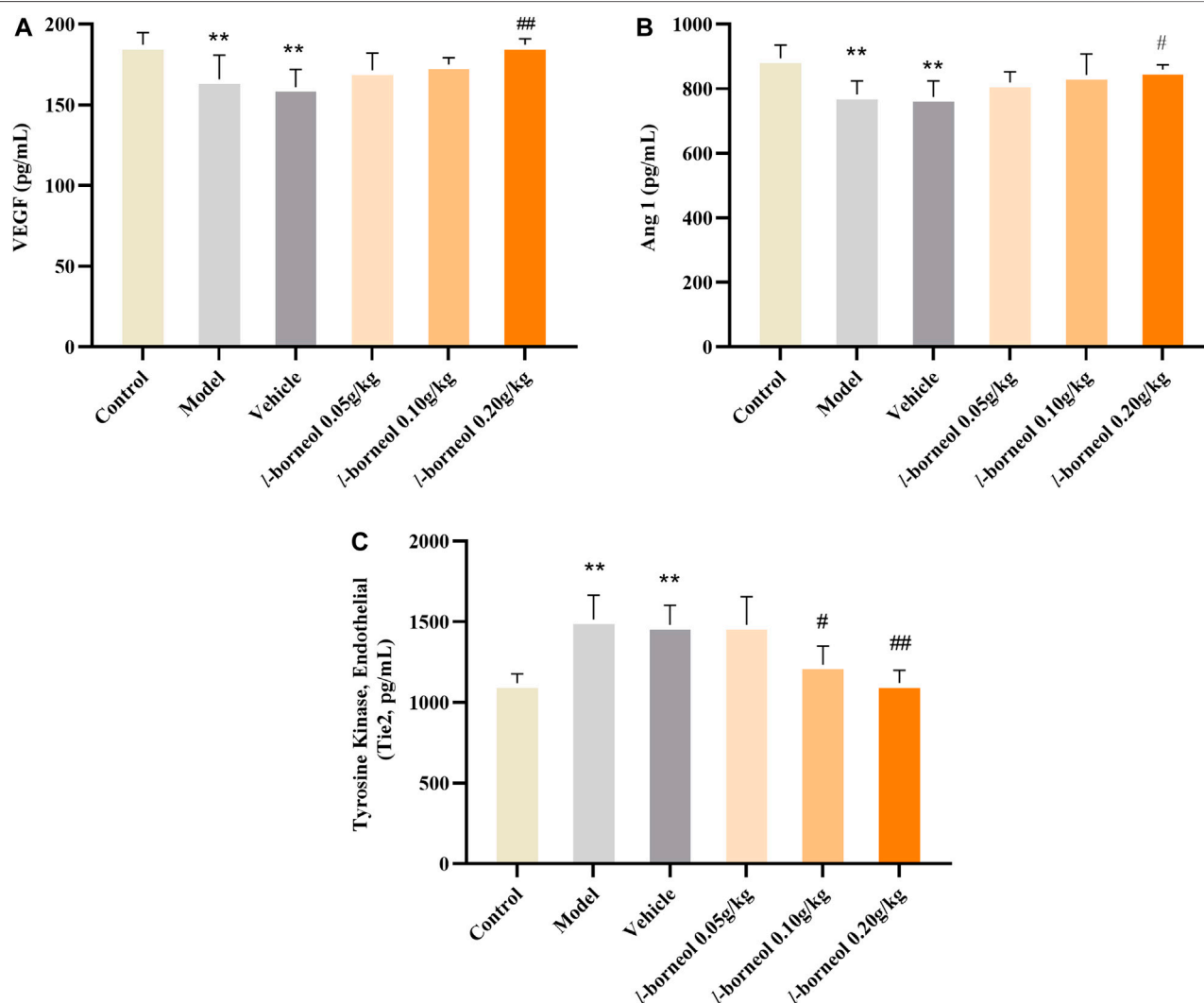
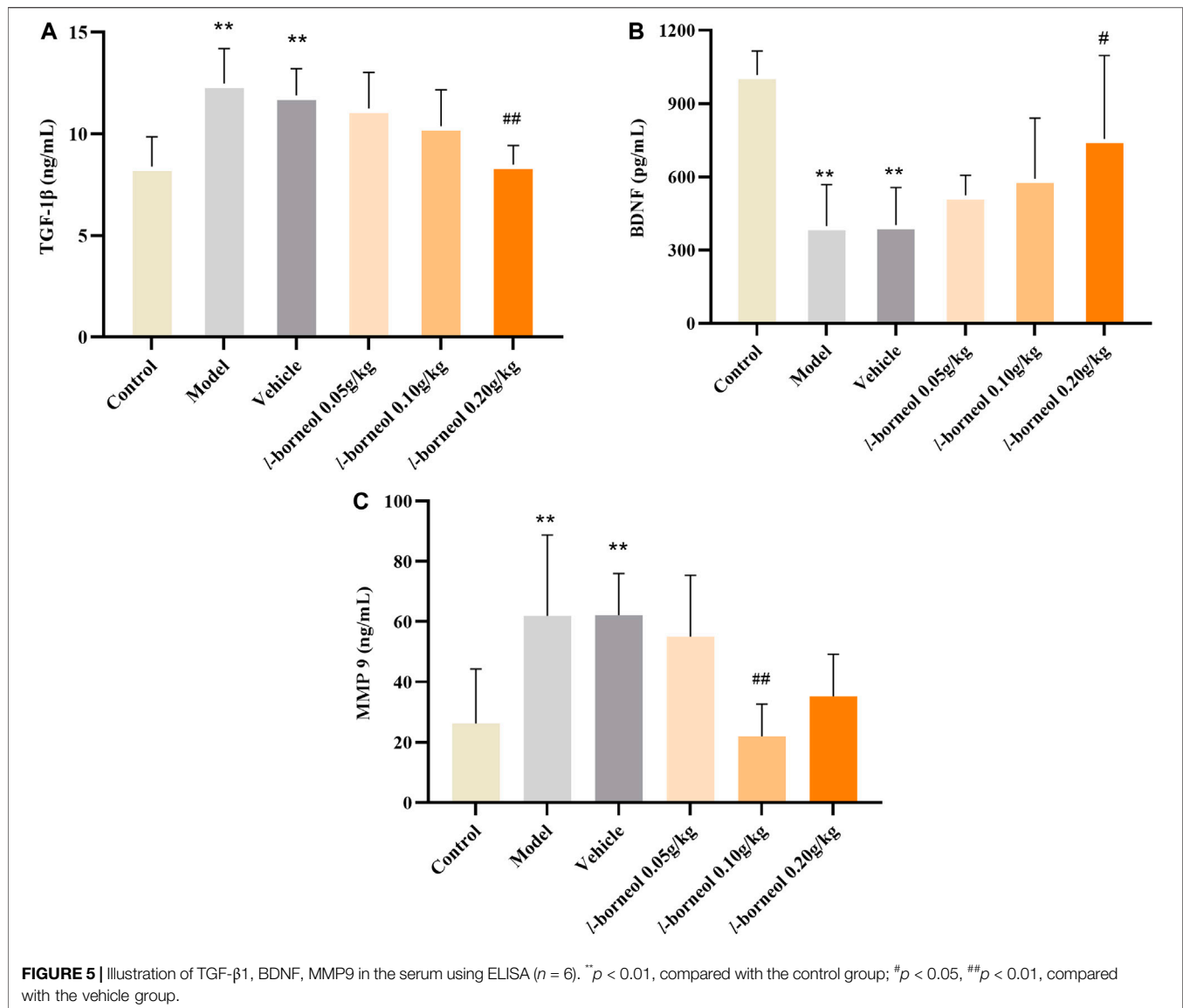


FIGURE 4 | Illustration of VEGF, Ang1 and Tie two in the serum using ELISA ($n = 6$). ** $p < 0.01$, compared with the control group; # $p < 0.05$, ## $p < 0.01$, compared with the vehicle group.



Effect of *l*-Borneol Interventions on VEGF, Ang1 and Tie two in the Serum

The levels of VEGF, Ang1 and Tie two in the serum were performed by ELISA methods. The results showed in **Figure 4**. The expressions of angiogenic growth factors including VEGF and Ang-1 in the model and vehicle group were significantly decreased, while the expression of Tie two was significantly increased as compared with those in the control group ($p < 0.01$). The model and vehicle group had no significant difference. Compared with the vehicle group, VEGF and Ang-1 expression levels significantly increased in the *l*-borneol 0.2 g/kg groups ($p < 0.01$ or $p < 0.05$), Tie two expression in the *l*-borneol 0.1 and 0.2 g/kg group was significantly decreased ($p < 0.05$ or $p < 0.01$). These results demonstrate that *l*-borneol could promote angiogenesis in a dose-dependent manner against ischemic brain injury.

Effect of *l*-Borneol Interventions on TGF-β1, BDNF, MMP9 in the Serum

The levels of TGF-β1, BDNF, MMP9 in the serum were performed by ELISA methods. The results showed in **Figure 5**. Compared with control group, the expressions TGF-β1 and MMP9 were significantly increased in the model and vehicle group, the expressions level of BDNF was significantly decreased in the model and vehicle group ($p < 0.01$). The model and vehicle group had no significant difference. While, the expressions of TGF-β1 in the *l*-borneol 0.2 g/kg group was significantly decreased ($p < 0.01$), and the BDNF was significantly increased as compared with those in the vehicle control group ($p < 0.05$), and presenting dosing dependent. The expressions level of MMP9 was significantly decreased in *l*-borneol 0.1 g/kg group ($p < 0.01$). It suggested *l*-borneol could promote neurogenesis against ischemic brain injury.

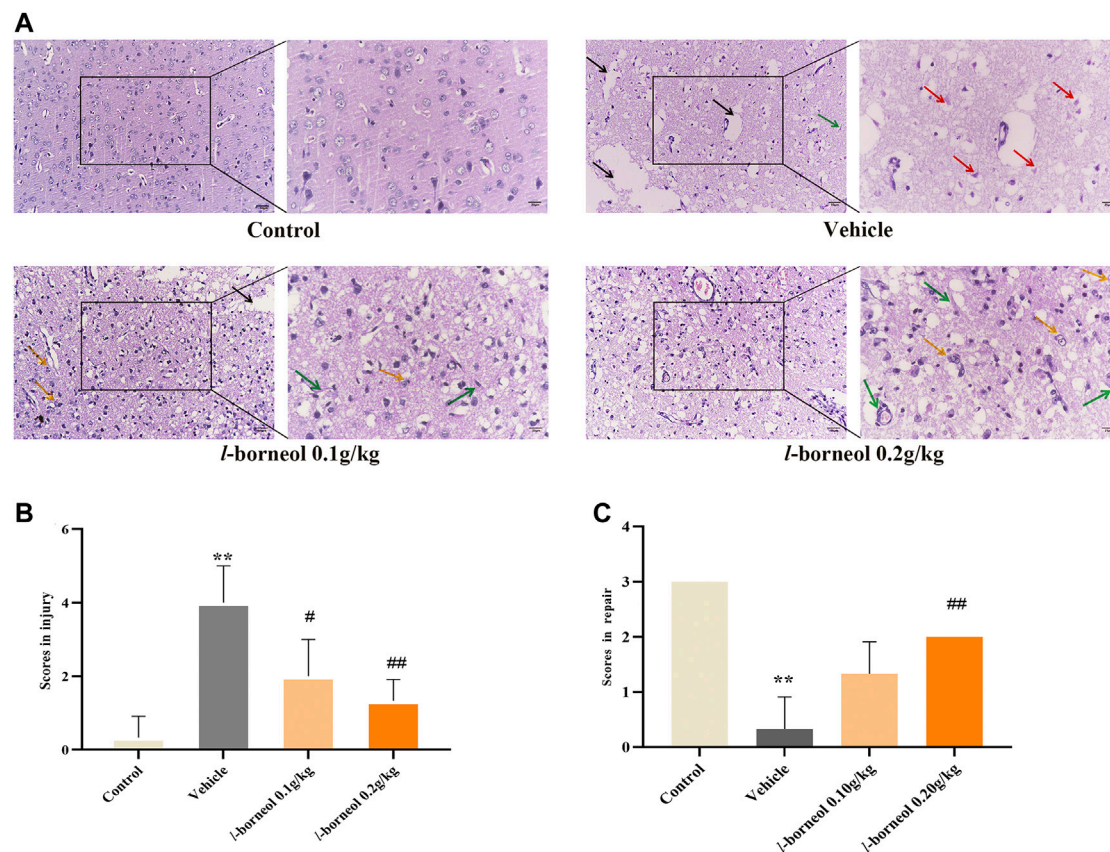


FIGURE 6 | Illustration of pathological changes using HE staining ($n = 3$). **(A)** HE results of each group, **(B)** Semi-quantitative analysis of pathological injury, **(C)** Semi-quantitative analysis of pathological repair. Red arrow represents red neuron, black arrow represents liquefied and necrotic nerve tissue, yellow arrow represents microglia clears out necrotic neurons, green arrows represents new blood vessels, ** $p < 0.01$, compared with the control group; # $p < 0.05$, ## $p < 0.01$, compared with the vehicle group.

Effect of *l*-Borneol Interventions on Pathological Changes in Brain

HE staining was performed to observe the pathological changes under light microscope with $\times 200$ and $\times 400$ magnification. The morphology and structure of the cerebral cortex were normal without obvious pathological changes in the control group. And there were many blood vessels full of red blood cells in some fields (**Figure 6A**). There was obvious infarct, the homogenized cells, liquefied and necrotic nerve tissue to form a cribriform focus in the vehicle group. And shows a large number of red neurons, which is a sign of acute ischemic injury. What's more, the cell density was obviously reduced and there was swelling phenomenon, which is different from control group. Infarct size were found in *l*-borneol 0.1 and 0.2 g/kg, while the degree of ischemic damage was relatively light (**Figure 6A**). It was found that there was the decrease of liquefied necrosis area, rare red neurons, more capillaries, higher cell density and obvious phagocytosis of proliferative glial cells than the vehicle group. According to the results of semi-quantitative scoring of tissue injury and tissue repair (**Figures 6B,C**), the brain injury was significant reduced in *l*-borneol 0.1 and 0.2 g/kg group ($p < 0.01$, $p < 0.05$), *l*-borneol 0.2 g/kg group had more brain repair effect

than vehicle group ($p < 0.01$), presenting vessels production and glial cells clear out necrotic neurons.

Effect of *l*-Borneol Interventions on ACE, CD34, HIF 1 α mRNA in Brain

The ACE, CD34, HIF 1 α mRNA expression was detected by qRT-PCR (**Figure 7**). Compared with control group, the expression of ACE mRNA was obviously increased in the vehicle group ($p < 0.01$), the expression of HIF1 α mRNA showed an increasing trend, and the expression of CD34 mRNA showed a decreasing trend. Compared with vehicle group, *l*-borneol 0.1 and 0.2 g/kg could significantly reduce ACE expression ($p < 0.01$) and *l*-borneol 0.2 g/kg also increased CD 34 expression ($p < 0.05$). The expression of HIF1 α mRNA in the *l*-borneol 0.1 and 0.2 g/kg groups showed a downward trend.

Effect of *l*-Borneol Interventions on ACE in Brain

The effect of *l*-borneol interventions on blood vessels was measured by IHC staining using ACE antibody to mark

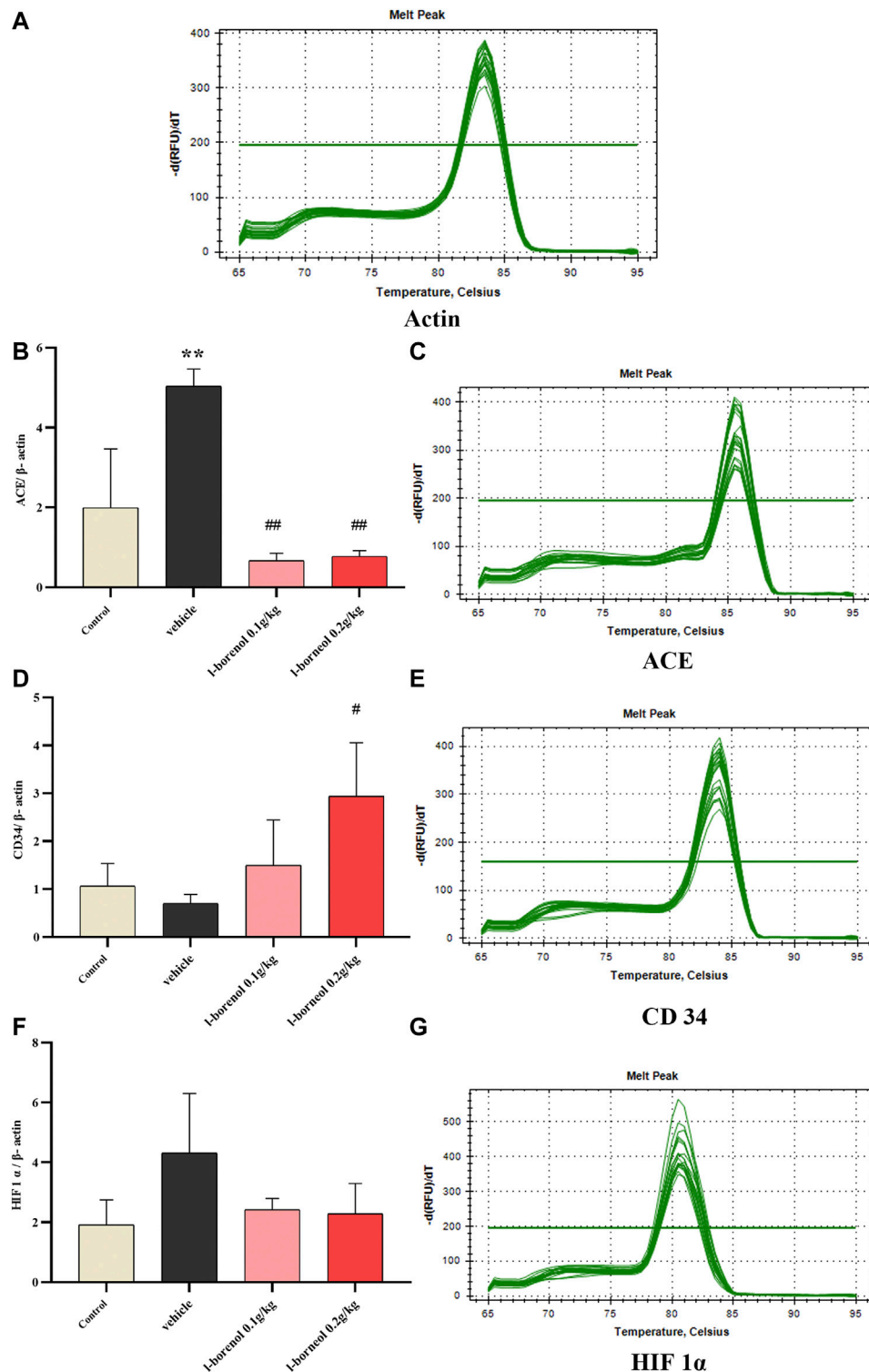


FIGURE 7 | Illustration of ACE, CD34, HIF 1α mRNA using qRT-PCR ($n = 3$). ** $p < 0.01$, compared with the control group; # $p < 0.05$, ## $p < 0.01$, compared with the vehicle group.

vessels. The results showed that the number of ACE -positive cells was markedly elevated after MCAO than those of control group. However, the increased number of ACE -positive cells were

attenuated by *l*-borneol (**Figure 8A**). The results of western blot also showed, *l*-borneol had a trend of reducing ACE expression compared with vehicle group (**Figure 8B**).

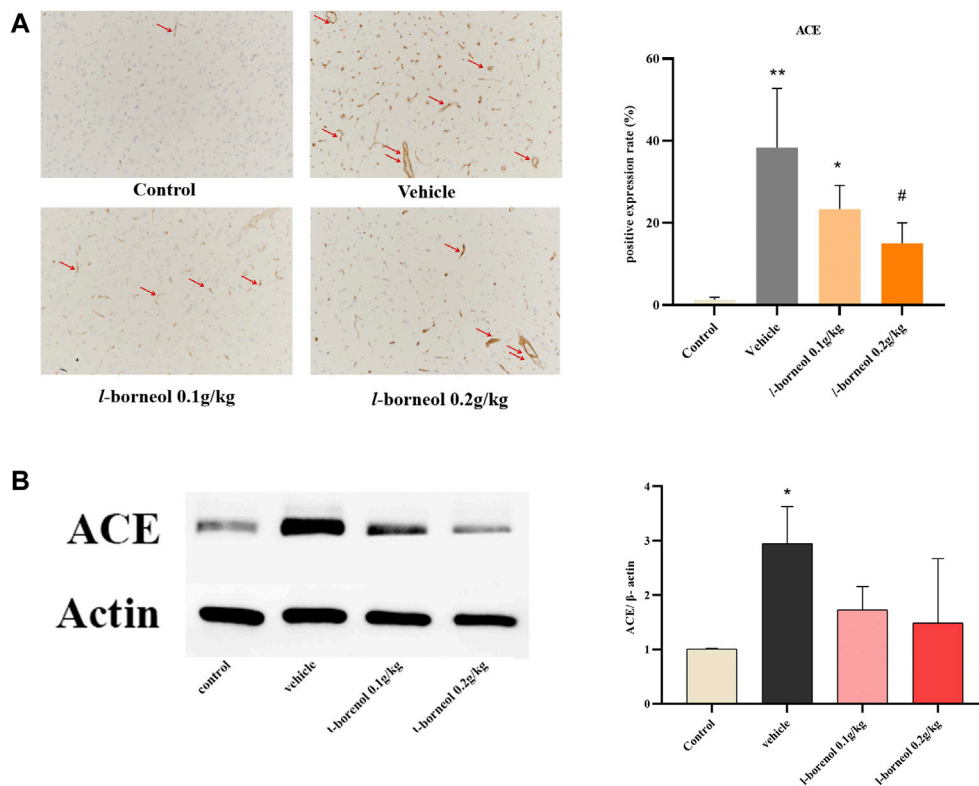


FIGURE 8 | Illustration of ACE expression using IHC staining and western blot ($n = 3$). ** $p < 0.01$, compared with the control group; * $p < 0.05$, ## $p < 0.01$, compared with the vehicle group, red arrow indicates positive expression.

Effect of *L*-Borneol Interventions on VEGFR and CD 34 in Brain

The effect of *L*-borneol interventions on vascular endothelial growth factor receptor (VEGFR) was measured by IHC staining using VEGFR antibody. The results showed that the number of VEGFR -positive cells was markedly reduced after MCAO than those of control group. However, the number of VEGFR -positive cells were increased by *L*-borneol (**Figure 9A**). In addition, we use CD34 antibody to mark blood vessels by IHC staining. CD34 staining was performed as an indicator of microvessel density (MVD). The results showed the number of CD34-positive cells was increased after MCAO than that of control group. This suggests that ischemia activates the endogenous angiogenesis compensatory improvement of ischemic damage. The number of CD34-positive cells was still markedly increased after MCAO with *L*-borneol interventions than that of control group (**Figure 9B**), suggesting *L*-borneol increased the number of the MVD, further promotes angiogenesis.

The Overall Effect of L-Borneol Intervention on Cerebral Ischemia Related Factors

The heat map can visualize the data, and integrate the indicators to intuitively compare the strength of their expression. The heat map shows the overall regulation of

L-borneol on cerebral ischemia and mechanism factors (**Figure 10**). *L*-borneol promotes angiogenesis and neurogenesis by increasing the levels of Ang 1, VEGF and BDNF after cerebral ischemia. The increase of CD34 protein confirms this result. *L*-borneol can also inhibit neuronal apoptosis and enhance the stability of neovascularization by inhibiting the levels of ACE, MMP9, HIF1 α , TGF- β 1 and Tie2, thereby improving the neurological deficit in ischemic rats, reducing the rate of cerebral infarction, and exerting neuroprotective effects.

Molecular Docking Analysis

The 3D and 2D binding graphs of the small molecule and the target protein after docking are shown in **Figure 11**, and the binding scores are shown in **Table 6**. The results showed that *L*-borneol has certain binding effect with VEGF, Tie2, Ang1, TGF- β 1, BDNF, MMP9, mainly through hydrogen bonding.

DISCUSSION

Stroke is a disease caused by insufficient blood supply and vascular embolism, which has the characteristics of high incidence rate, high mortality rate, high recurrence rate and high disability rate. In 2015, according to the World Health Organization, stroke which is the second leading cause of

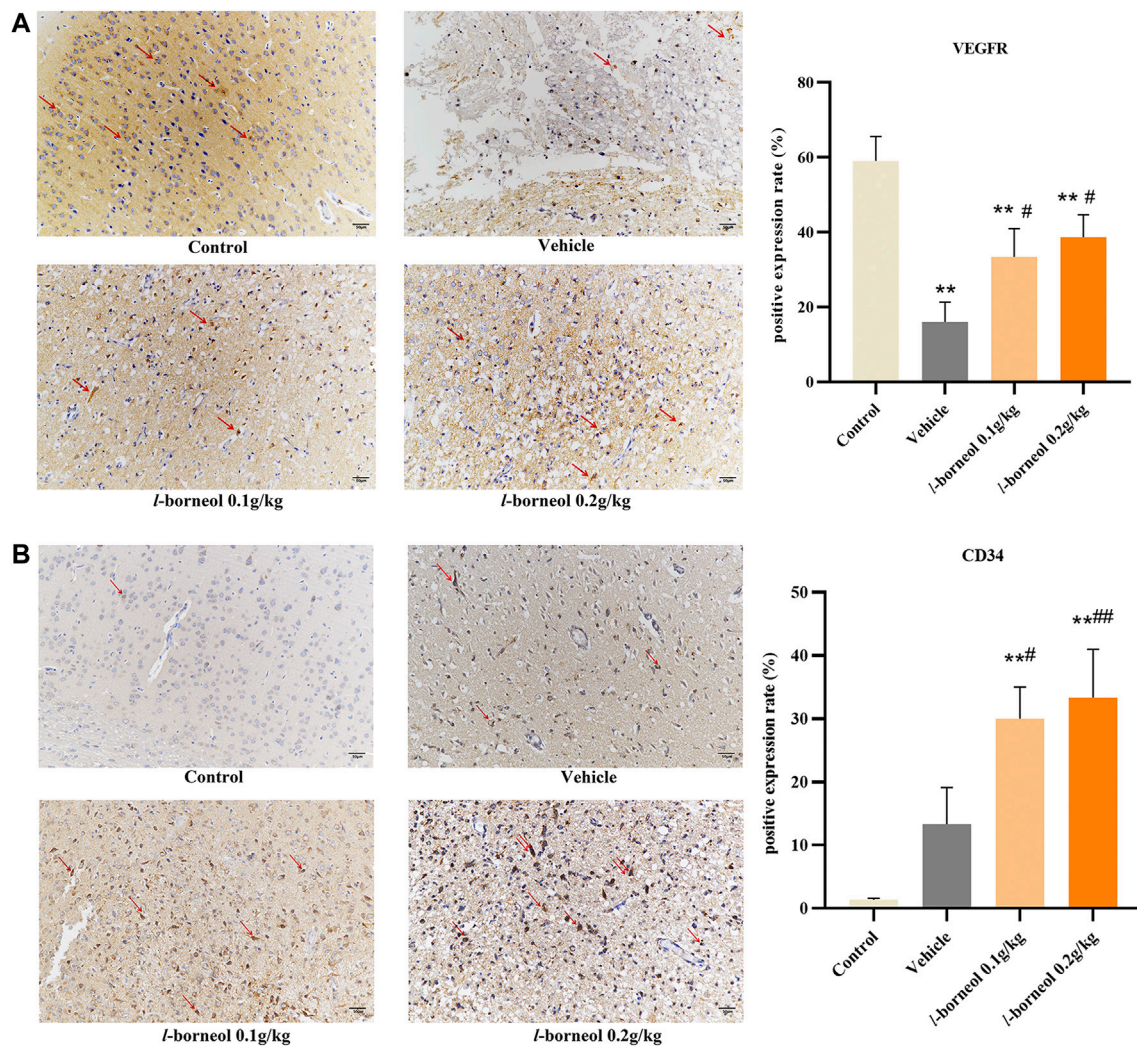
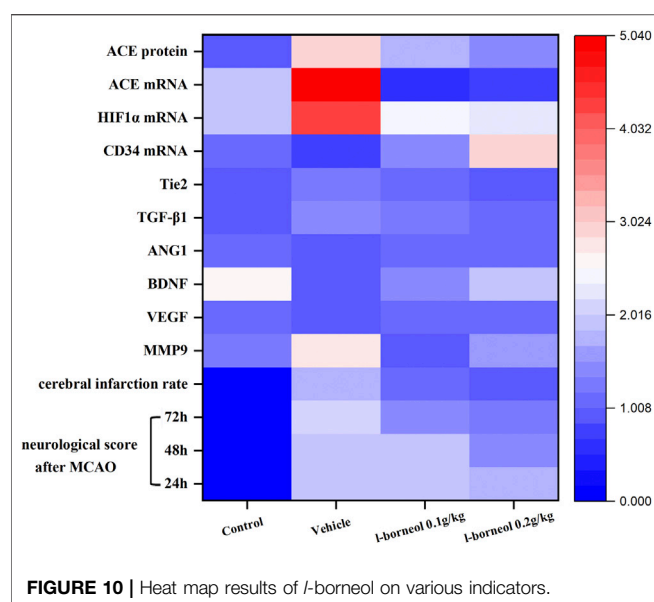


FIGURE 9 | Illustration of VEGFR and CD34 expression using IHC staining ($n = 3$). ** $p < 0.01$, compared with the control group; # $p < 0.05$, ## $p < 0.01$, compared with the vehicle group, red arrow indicates positive expression.

death caused 6.2 million deaths globally. With the aging of the population, the incidence rate is increasing year by year. Moreover, with the rapid development of modern life and the gradual increase of modern pressure, the incidence of stroke tends to encroach on young people and bring a heavy burden to society and families (Boot et al., 2020). At present, there is no ideal treatment strategy. Therefore, the development of new drugs and new treatment strategies is still an urgent problem in the treatment of stroke. Borneol is a traditional Chinese medicine, which has the effect of resuscitation and restoring the spirit. The Chinese patent medicine containing borneol is commonly used in the treatment of cerebrovascular diseases, and even has better therapeutic effect than other therapies (Liu et al., 2019; Ma et al., 2018 and 2017). *L*-borneol comes from *Blumea balsamifera* (L.) DC, which is safe and easy to obtain (Luo et al., 2018). Its curative effect is equivalent to that of natural borneol. The previous study showed that the order of the efficacy against cerebral ischemia injury was *L*-borneol, natural borneol, synthetic borneol (Dong

et al., 2018). Therefore, this study is to investigate the angiogenesis and neurogenesis mechanism of *L*-borneol against cerebral ischemia.

In the current study, we explored the neuroprotection of *L*-borneol, a natural small molecule, against cerebral ischemia injury and endeavored to elucidate its underlying mechanisms. Our findings demonstrated that *L*-borneol effectively protected against outcomes of cerebral ischemia injury as evidenced by reduced MCAO-induced neurological deficits, cerebral infarction size. Therefore, it is reasonable to believe that *L*-borneol might be certain brain protective effect against cerebral ischemia injury. Hypertension is a high risk factor for stroke. ACE is an important metabolic enzyme in the RAS system that regulates blood pressure. It can convert inactive Ang I into Ang II, which in turn acts on the AT1R, inducing vasoconstriction, increasing blood pressure and aggravates ischemic damage. It's reported that ACE was significantly increased in the acute stage of cerebral ischemic stroke (Lu et al., 2013), thus reducing ACE levels can



alleviate ischemic injury. Regarding clinical studies, treatment with ACE inhibitors and AT1 receptor antagonists exert preventive and therapeutic effects on stroke (Kangussu et al., 2019). In addition, Ang II can induce the expression and activation of MMP9 via NF-KappaB dependent pathway. In turn, it may lead to instability and rupture of atherosclerotic plaque or cerebral aneurysm, thereby triggering stroke. It also degrades the extracellular matrix after stroke, promotes BBB leakage, causes vasogenic edema, and destroys the stability of new blood vessels. Therefore, reducing the level of MMP9 helps to reduce the permeability of new blood vessels and strengthen the stability of the vessel wall (Turner and Sharp, 2016). In our study, the results showed that *l*-borneol can significantly inhibit the

activity of ACE and reduce the level of MMP9, suggesting that *l*-borneol can reduce ischemic damage and strengthen the stability of new blood vessels.

As noted, angiogenesis and neurogenesis play important roles in neuroprotection (Seevinck et al., 2010; Benedek et al., 2019; Zhang et al., 2020). HIF-1 α can be activated after ischemia, which is the earliest cytokine involved in the specific response of cells to hypoxia. It can regulate the expression of various factors such as Ang and VEGF to promote angiogenesis, so that the body can better adapt to hypoxia environment. However, in the early stage of ischemia, overexpression of HIF-1 α can induce cell apoptosis. Studies have shown that HIF1 α knockout mice show better survival rates and improved neurological function in the early stage of ischemia. Therefore, the early inhibition of HIF1 α has a certain anti-apoptotic effect and reduces nerve function damage (Barteczek et al., 2017). HIF-1 α can induce the release of Ang1, VEGF and BDNF from vascular endothelial cells, and promote angiogenesis and neurogenesis. However, Ang1 and VEGF have different effects in inducing angiogenesis. VEGF is a powerful endothelial cell mitogen, which can promote the proliferation and aggregation of vascular endothelial cells to form a lumen. However, VEGF is also known as vascular permeability factor. The neovascularization induced by VEGF is usually immature and leaking, which may cause brain edema and aggravate brain damage (Couvelard et al., 2000; Lena, 2016; Jin et al., 2017). Therefore, it needs to cooperate with Ang one to induce angiogenesis. Tie two is the specific receptor of Ang1 (Dixit et al., 2007; Saharinen et al., 2017), Ang-1 promotes endothelial cell budding, migration and chemotaxis by activating Tie 2 (Saharinen et al., 2017), and reduce the vascular permeability caused by VEGF, MMP9 and other factors. It can also maintain the stability of the vascular structure by promoting the interaction between cells and cells, cells and substrates

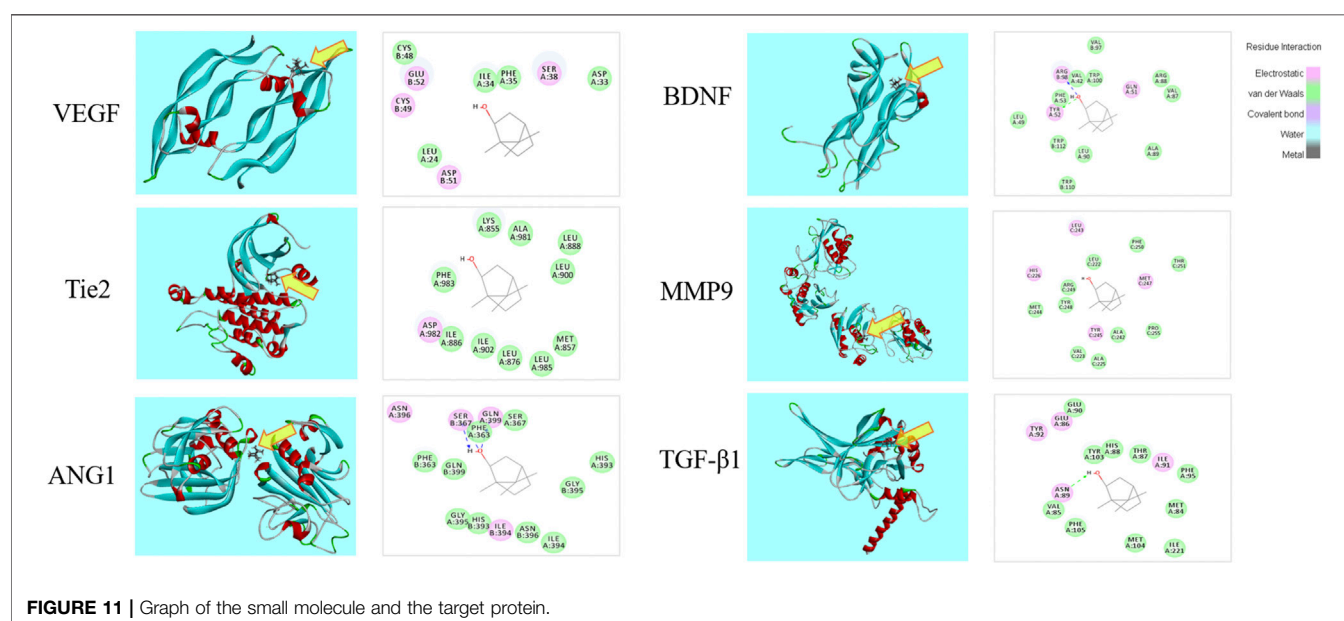


TABLE 6 | The scores of the small molecule and the target protein.

Gene	PDB ID	Score	Gene	PDB ID	Score
VEGF	1wq9	40.12	BDNF	1b8m	66.68
Tie2	3l8p	45.14	MMP9	4h82	63.46
ANG1	4epu	69.06	TGF- β 1	5vqp	72.49

(Shen et al., 2011). VEGF and Ang one promote angiogenesis and maintain vascular stability through coordinate with each other (Zhang and Chopp, 2002).

CD34 antigen is a stage-specific leukocyte differentiation antigen, which is selectively expressed on the surface of human stem cell, progenitor cell and vascular endothelial cells. Because its expression in neovascular endothelium is much greater than that in non-neovascular endothelium, it becomes the most sensitive vascular endothelial marker. It is often used to count the density of neovascularization to determine angiogenesis. (Solmaz and Guvena, 2016). In our study, *l*-borneol can effectively increase the levels of VEGF in serum

and VEGF mRNA in tissues, and increase the expression of VEGFR in the cortex of brain tissue, while regulating the Ang1/Tie2 pathway, synergistically VEGF promotes angiogenesis and stabilizes the structure of blood vessels. CD34 mRNA expression and CD34 positive cells in brain tissue increased significantly after *l*-borneol administration, indicating the increasing number of MVD, which further confirmed the angiogenesis effect of *l*-borneol. In addition, *l*-borneol can significantly inhibit cell apoptosis induced by HIF-1 α transcription, and can significantly inhibit the levels of ACE and MMP9 in brain tissue to further alleviate cerebral ischemic damage.

Cerebral ischemia induced the death of neurons is the main cause of neuron dysfunction. Therefore, increasing neurons survival and regeneration in cerebral penumbra is an important means to improve the neuron function (Puig et al., 2018). TGF- β 1 is an important regulator in the transformation and growth of cells and angiogenesis (Lupo et al., 2014). It could stimulate neuron to secrete cell growth factors, such as VEGF, BDNF, and promote the survival and differentiation of neurons (Guan and Sun, 2002).

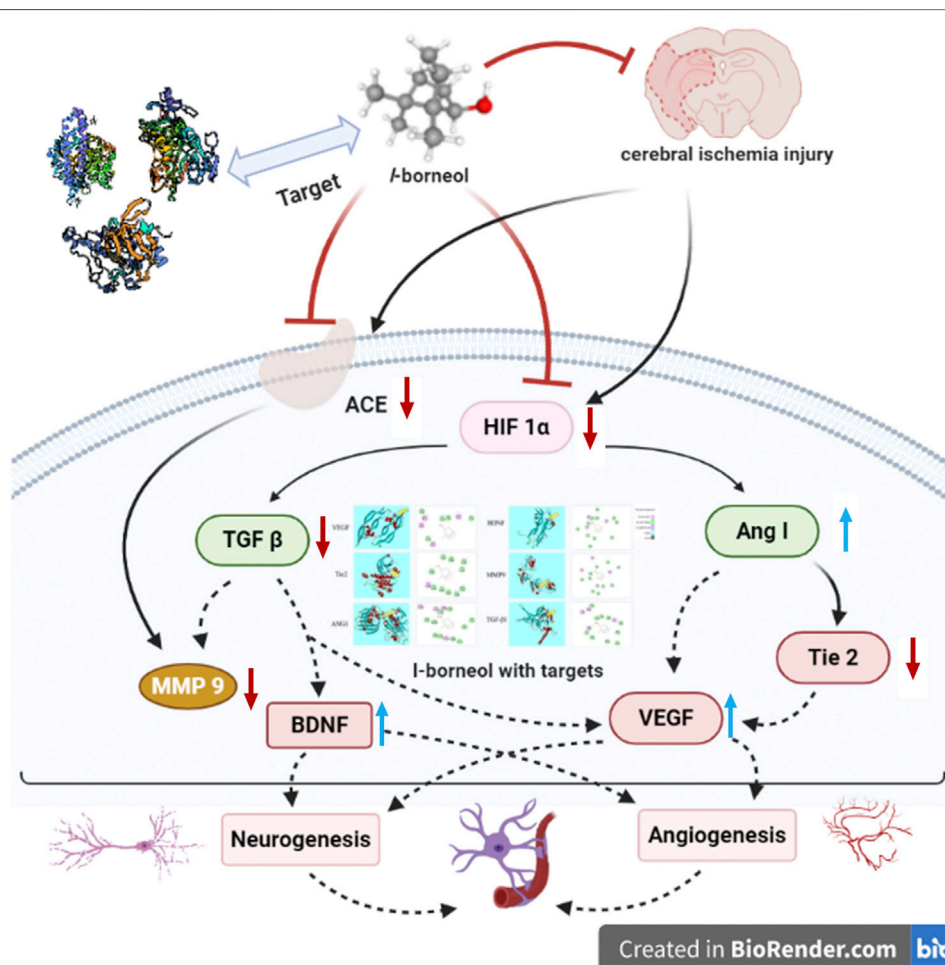


FIGURE 12 | Schematic presentation of a proposed mechanism for the protective role of *l*-borneol against cerebral ischemia injury (<https://app.biorender.com/>). Red arrows represent an inhibition effect; Blue arrows represent an enhancement effect.

Studies have demonstrated that BDNF can promote the proliferation, differentiation and migration of neural stem cells (NSC), promote the growth of axons and dendrites in the process of neuron growth, and participate in the formation and maturation of synapses. As a principle of mitosis, VEGF can directly promote the proliferation of neural precursor cells, and stimulate the proliferation and differentiation of neural precursor cells by promoting the establishment of vascular niches. In addition, VEGF can further induce neurogenesis by stimulating endothelial cells to release BDNF. Exogenously induced VEGF overexpression can increase the conversion rate of neurons, enhance neurogenesis and neural migration rate (Wang et al., 2007a; Wang et al., 2007b). VEGF and BDNF can mediate the coupling loop of neurogenesis and angiogenesis. NSC induces endothelial cells to release VEGF and BDNF by promoting the up-regulation of nitric oxide (NO). VEGF and BDNF activate VEGFR and TrkB on endothelial cells to induce angiogenesis through autocrine and paracrine methods. VEGF and BDNF can also promote the phosphorylation of eNOS (endothelial nitric oxide synthases) on NSC, continue to produce NO and stimulate the proliferation of NSC, and promote neurogenesis, thereby forming a feedback loop of angiogenesis coupled neurogenesis with VEGF and BDNF as targets.

In our study, *l*-borneol significantly increased the levels of VEGF and BDNF, and increased the number of VEGFR in the cortex of brain tissue, suggesting that *l*-borneol can promote neurogenesis by increasing the expression of VEGF and BDNF. In addition, the results show that *l*-borneol can significantly reduce the level of TGF- β 1. Studies have shown that TGF- β 1 has a two-way effect, and low concentrations of TGF- β 1 have a positive synergistic effect on angiogenesis. The high concentration of TGF- β 1 can reduce the VEGF-mediated pro-angiogenesis effect (Dobolyi et al., 2012), and has the effect of inducing MMP9 activity. *l*-borneol may reduce the concentration of TGF- β 1, enhance angiogenesis, reduce the level of MMP9, and stabilize vascular permeability. In conclusion, our research shows that *l*-borneol can improve ischemic injury by inhibiting the expression of HIF-1 α , ACE, TGF- β 1 and MMP9, and regulate the Ang1-VEGF-BDNF pathway to promote angiogenesis coupled neurogenesis to exert neuroprotective effects. Molecular docking also confirmed that the above factors may be the targets of *l*-borneol to exert neuroprotective effects.

CONCLUSION

Our study indicated that *l*-borneol had a significant effect on improving neurological function scores and infarction size. Simultaneously, *l*-borneol alleviated the pathological changes in the brain tissue. The neuroprotective effect of *l*-borneol against cerebral ischemia might be associated with angiogenesis and neurogenesis. *l*-borneol could promote Ang-1, VEGF, BDNF expression and enhance micro vessels density, inhibit TGF- β 1, Tie 2, MMP9 and ACE, which is the biological basis of the neuroprotective effect of *l*-borneol (Figure 12). Certainly, the mechanisms of injury are complicated, and the pathway on angiogenesis and neurogenesis is various, other mechanisms

remains to be evaluated in future studies. In addition, the long-term therapeutic effect of *l*-borneol also needs to be verified in future studies.

DATA AVAILABILITY STATEMENT

The datasets presented in this study can be found in online repositories. The names of the repository/repositories and accession number(s) can be found in the article/Supplementary Material.

ETHICS STATEMENT

The animal study was reviewed and approved by the Ethics Committee of the Affiliated Hospital of Chengdu University of Traditional Chinese Medicine (number: DL2019002). Written informed consent was obtained from the owners for the participation of their animals in this study.

AUTHOR CONTRIBUTIONS

Conceived and designed the experiments: RM and JW. Performed the experiments: QX, XG and RM. Analysis and interpretation, data collection: HL, DG. Wrote the manuscript: QX, RM, YL and MR. Critically reviewed the article: JW, TG. The authors have read and agreed to the published version of the manuscript.

FUNDING

This work was supported by the National Natural Science Foundation of China (Nos. 81873023, 81473371, 81873073), the Innovation Team in Chengdu University of Traditional Chinese Medicine (CXTD2018004), the Open Research Fund of the Key Laboratory of Southwestern Characteristic Chinese Medicine Resources, Chengdu University of Traditional Chinese Medicine (2020XSOG025). “Hundred Talents Program” of the Hospital of Chengdu University of Traditional Chinese Medicine (grant nos. 20-Q18).

ACKNOWLEDGMENTS

The authors are grateful to DG (Affiliated Hospital of Chengdu University of TCM) for providing the guidance to HE and IHC staining.

SUPPLEMENTARY MATERIAL

The Supplementary Material for this article can be found online at: <https://www.frontiersin.org/articles/10.3389/fphar.2021.641894/full#supplementary-material>.

REFERENCES

- Alim, I., Caulfield, J. T., Chen, Y., Swarup, V., Geschwind, D. H., Ivanova, E., et al. (2019). Selenium drives a transcriptional adaptive program to block ferroptosis and treat stroke. *Cell* 177 (5), 1262–1279. doi:10.1016/j.cell.2019.03.032
- Amin, M. Z., Saadat, S., Marefati, N., Hosseini, M., and Boskabady, M. H. (2020). Treadmill exercise restores memory and hippocampal synaptic plasticity impairments in ovalbumin-sensitized juvenile rats: involvement of brain-derived neurotrophic factor (BDNF). *Neurochem. Int.* 135, 104691. doi:10.1016/j.neuint.2020.104691
- Bartczek, P., Li, L., Ernst, A. S., Böhrer, L. I., Marti, H. H., and Kunze, R. (2017). Neuronal HIF-1 α and HIF-2 α deficiency improves neuronal survival and sensorimotor function in the early acute phase after ischemic stroke. *J. Cereb. Blood Flow Metab.* 37 (1), 291–306. doi:10.1177/0271678X15624933
- Benedek, A., Cernica, D., Mester, A., Opincariu, D., Hodas, R., Rodean, I., et al. (2019). Modern concepts in regenerative therapy for ischemic stroke: from stem cells for promoting angiogenesis to 3D-bioprinted scaffolds customized via carotid shear stress analysis. *Int. J. Mol. Sci.* 20 (10), 2574. doi:10.3390/ijms20102574
- Boot, E., Ekker, M. S., Putaala, J., Kittner, S., De Leeuw, F., and Tuladhar, A. M. (2020). Ischaemic stroke in young adults: a global perspective. *J. Neurol. Neurosurg. Psychiatry* 91 (4), 411–417. doi:10.1136/jnnp-2019-322424
- Cao, W., Zhai, X., Ma, J., Fu, X., Zhao, B., Zhang, P., et al. (2020). Natural borneol sensitizes human glioma cells to cisplatin-induced apoptosis by triggering ROS-mediated oxidative damage and regulation of MAPKs and PI3K/AKT pathway. *Pharm. Biol.* 58 (1), 72–79. doi:10.1080/13880209.2019.1703756
- Chen, Z., Xu, Q., Shan, C., Shi, Y., Wang, Y., Chang, R. C., et al. (2019). Borneol for regulating the permeability of the blood-brain barrier in experimental ischemic stroke: preclinical evidence and possible mechanism. *Oxidative Med. Cell Longevity* 2019, 1–15. doi:10.1155/2019/2936737
- Couvelard, A., Paraf, F. O., Gratio, V. R., Scoazec, J., Hénin, D., Degott, C., et al. (2000). Angiogenesis in the neoplastic sequence of Barrett's oesophagus. Correlation with VEGF expression. *J. Pathol.* 192, 14–18. doi:10.1002/1096-9896(2000)9999:9999::AID-PATH709>3.0.CO;2-F
- Demaerschalk, B. M., Kleindorfer, D. O., Adeoye, O. M., Demchuk, A. M., Fugate, J. E., Grotta, J. C., et al. (2016). Scientific rationale for the inclusion and exclusion criteria for intravenous alteplase in acute ischemic stroke. *Stroke* 47 (2), 581–641. doi:10.1161/STR.0000000000000086
- Dirnagl, U., Iadecola, C., and Moskowitz, M. A. (1999). Pathobiology of ischaemic stroke: an integrated view. *Trends Neurosci.* 22 (9), 391–397. doi:10.1016/S0166-2236(99)01401-0
- Dixit, M., Bess, E., Fisslthaler, B., Hartel, F. V., Noll, T., Busse, R., et al. (2007). Shear stress-induced activation of the AMP-activated protein kinase regulates FoxO1 α and angiotensin-2 in endothelial cells. *Cardiovasc. Res.* 77 (1), 160–168. doi:10.1093/cvr/cvm017
- Dobolyi, A., Vincze, C., Pál, G., and Lovas, G. (2012). The neuroprotective functions of transforming growth factor beta proteins. *Int. J. Mol. Sci.* 13 (7), 8219–8258. doi:10.3390/ijms13078219
- Dong, T., Chen, N., Ma, X., Wang, J., Wen, J., Xie, Q., et al. (2018). The protective roles of L-borneol, D-borneol and synthetic borneol in cerebral ischaemia via modulation of the neurovascular unit. *Biomed. Pharmacother.* 102, 874–883. doi:10.1016/j.biopha.2018.03.087
- Donnan, A., Fisher, M., Malcolm, M., and Davis, S. (2008). Stroke. *Lancet* 371 (9624), 1612–1623. doi:10.1016/S0140-6736(08)60694-7
- Furie, K. L., and Jayaraman, M. V. (2018). Guidelines for the early management of patients with acute ischemic stroke. *Stroke* 49 (3), 509–510. doi:10.1161/STROKEAHA.118.020176
- Greenberg, D. A., and Jin, K. (2013). Vascular endothelial growth factors (VEGFs) and stroke. *Cell Mol. Life Sci.* 70 (10), 1753–1761. doi:10.1007/s00018-013-1282-8
- Guan, J., and Sun, S. (2002). Cytokines and ischemic brain injury. *Stroke Nervous Dis.* 9 (4), 255–257. doi:10.3969/j.issn.1007-0478.2002.04.029
- Henderson, S. J., Weitz, J. I., and Kim, P. Y. (2018). Fibrinolysis: strategies to enhance the treatment of acute ischemic stroke. *J. Thromb. Haemost.* 16 (10), 1932–1940. doi:10.1111/jth.14215
- Hori, S., Ohtsuki, S., Hosoya, K., Nakashima, E., and Terasaki, T. (2004). A pericyte-derived angiotensin-1 multimeric complex induces occludin gene expression in brain capillary endothelial cells through Tie-2 activation *in vitro*. *J. Neurochem.* 89 (2), 503–513. doi:10.1111/j.1471-4159.2004.02343.x
- Jeong, H., Chung, J., Ko, I., Kim, S., Jin, J., Hwang, L., et al. (2019). Effect of polydeoxyribonucleotide on lipopolysaccharide and sevoflurane-induced postoperative cognitive dysfunction in human neuronal SH-SY5Y cells. *Int. Neurology J.* 23 (Suppl. 2), S93–S101. doi:10.5213/inj.1938218.109
- Ji, J., Zhang, R., Li, H., Zhu, J., Pan, Y., and Guo, Q. (2020). Analgesic and anti-inflammatory effects and mechanism of action of borneol on photodynamic therapy of acne. *Environ. Toxicol. Pharmacol.* 75, 103329. doi:10.1016/j.etap.2020.103329
- Jin, D., Zhu, D., Fang, Y., Chen, Y., Yu, G., Pan, W., et al. (2017). Vegfa signaling regulates diverse artery/vein formation in vertebrate vasculatures. *J. Genet. Genomics* 44 (10), 483–492. doi:10.1016/j.jgg.2017.07.005
- Kahles, T., and Brandes, R. P. (2013). Which NADPH oxidase isoform is relevant for ischemic stroke? The case for nox 2. *Antioxid. Redox Signaling* 18 (12), 1400–1417. doi:10.1089/ars.2012.4721
- Kangussu, L. M., Marzano, L., Souza, C. F., Dantas, C. C., Miranda, A. S., and Simões e Silva, A. C. (2019). The renin-angiotensin system and the cerebrovascular diseases: experimental and clinical evidence. *Protein Pept. Lett.* 27, 463–475. doi:10.2174/0929866527666191218091823
- Külkens, S., and Hacke, W. (2014). Thrombolysis with alteplase for acute ischemic stroke: review of SITS-MOST and other Phase IV studies. *Expert Rev. Neurotherapeutics* 7 (7), 783–788. doi:10.1586/14737175.7.7.783
- Lena, C. (2016). VEGF receptor signal transduction – a brief update. *Vasc. Pharmacol.* 86, 14–17. doi:10.1016/j.vph.2016.05.011
- Liu, H., Yan, Y., Pang, P., Mao, J., Hu, X., Li, D., et al. (2019). Angong Niuhuang Pill as adjuvant therapy for treating acute cerebral infarction and intracerebral hemorrhage: a meta-analysis of randomized controlled trials. *J. Ethnopharmacology* 237, 307–313. doi:10.1016/j.jep.2019.03.043
- Liu, W., Wang, X., O'Connor, M., Wang, G., and Han, F. (2020). Brain-derived neurotrophic factor and its potential therapeutic role in stroke comorbidities. *Neural Plasticity* 2020, 1–13. doi:10.1155/2020/1969482
- Lu, J., Jiang, T., Wu, L., Gao, L., Wang, Y., Zhou, F., et al. (2013). The expression of angiotensin-converting enzyme 2-angiotensin-(1–7)-Mas receptor axis are upregulated after acute cerebral ischemic stroke in rats. *Neuropeptides* 47 (5), 289–295. doi:10.1016/j.npep.2013.09.002
- Ludewig, P., Winneberger, J., and Magnus, T. (2019). The cerebral endothelial cell as a key regulator of inflammatory processes in sterile inflammation. *J. Neuroimmunology* 326, 38–44. doi:10.1016/j.jneuroim.2018.10.012
- Lunardi, S., and Lehmann, C. (2019). Microcirculatory changes in experimental models of stroke and CNS-injury induced immunodepression. *Int. J. Mol. Sci.* 20 (20), 5184. doi:10.3390/ijms20205184
- Luo, S., Jian, W., Jing, W., Chuan, C., and Qian, X. (2016). Monitoring the impact of three borneol temperature fever rats dynamic concept based on TCM. *Lishizhen Med. Materia Med. Res.* 27 (3), 521–523. doi:10.3969/j.issn.1008-0805.2016.03.004
- Luo, S., Li, L., Qiongfang, Z., and Xueying, B. (2018). Research progress of borneol. *Chin. J. Ethnomed. Ethnopharm.* 27 (5), 73–76.
- Lupo, G., Motta, C., Salmeri, M., Spina-Purrello, V., Alberghina, M., and Anfuso, C. D. (2014). An *in vitro* retinoblastoma human triple culture model of angiogenesis: a modulatory effect of TGF- β . *Cancer Lett.* 354 (1), 181–188. doi:10.1016/j.canlet.2014.08.004
- Ma, R., Ma, X., Wen, J., Wang, J., Xie, Q., Chen, N., et al. (2018). Preclinical evidence and mechanism of xingnaojing injection for cerebral ischemia: a systematic review and meta-analysis of animal studies. *Evidence-Based Complement. Altern. Med.* 2018, 1–12. doi:10.1155/2018/9624175
- Ma, R., Xie, Q., Li, Y., Chen, Z. P., Ren, M. H., Chen, H., et al. (2020). Animal models of cerebral ischemia: a review. *Biomed. Pharmacother.* 131, 110686. doi:10.1016/j.biopha.2020.110686
- Ma, X., Yang, Y. X., Chen, N., Xie, Q., Wang, T., He, X., et al. (2017). Meta-analysis for clinical evaluation of xingnaojing injection for the treatment of cerebral infarction. *Front. Pharmacol.* 8, 486. doi:10.3389/fphar.2017.00485
- Miller, J., Hartwell, C., and Lewandowski, C. (2012). Stroke treatment using intravenous and intra-arterial tissue plasminogen activator. *Curr. Treat. Options. Cardiovasc. Med.* 14 (3), 273–283. doi:10.1007/s11936-012-0176-7
- Müller, P., Duderstadt, Y., Lessmann, V., and Müller, N. G. (2020). Lactate and BDNF: key mediators of exercise induced neuroplasticity? *J. Clin. Med.* 9 (4), 1136. doi:10.3390/jcm9041136

- Ni, C., Nan, Z., Fuhui, X., Ling, G., Jinwei, L., Jian, W., et al. (2011a). Effects of aromatic resuscitation drugs on blood brain barrier in cerebral ischemia-reperfusion injury model rats. *China J. Chin. Materia Med.* (18), 2562–2566. doi:10.4268/cjcm20111824
- Ni, C., Zeng, N., Qi, T., Yongxin, T., Jian, W., and Houlin, X. (2011b). The effect of aromatics on the permeability of blood-brain barrier in normal mice. *Jiangsu J. Traditional Chin. Med.* 43 (2), 88–89. doi:10.3969/j.issn.1672-397X.2011.02.058
- Phipps, M. S., and Cronin, C. A. (2020). Management of acute ischemic stroke. *BMJ* 398, 16983. doi:10.1136/bmj.16983
- Puig, B., Brenna, S., and Magnus, T. (2018). Molecular communication of a dying neuron in stroke. *Int. J. Mol. Sci.* 19 (9), 2834. doi:10.3390/ijms19092834
- Rehab, A., Alqasoumi, S., Ogaly, H., Abd-Elsalam, R., El-Banna, H., and Soliman, G. (2020). Propolis ameliorates cerebral injury in focal cerebral ischemia/reperfusion (I/R) rat model via upregulation of TGF- β 1. *Saudi Pharm. J.* 28 (1), 116–126. doi:10.1016/j.jsps.2019.11.013
- Roth, G. A., Abate, D., Abate, K. H., Abay, S. M., Abbafati, C., Abbasi, N., et al. (2018). Global, regional, and national age-sex-specific mortality for 282 causes of death in 195 countries and territories, 1980–2017: a systematic analysis for the Global Burden of Disease Study 2017. *Lancet* 392 (10159), 1736–1788. doi:10.1016/S0140-6736(18)32203-7
- Saharinen, P., Eklund, L., and Alitalo, K. (2017). Therapeutic targeting of the angiopoietin - TIE pathway. *Nat. Rev. Drug Discov.* 9 (16), 1–27. doi:10.1038/nrd.2016.278
- Seevinck, P. R., Daddens, L. H., and Dijkhuizen, R. M. (2010). Magnetic resonance imaging of brain angiogenesis after stroke. *Angiogenesis* 13 (2), 101–111. doi:10.1007/s10456-010-9174-0
- Shen, F., Walker, E. J., Jiang, L., Degos, V., Li, J., Sun, B., et al. (2011). Coexpression of angiopoietin-1 with VEGF increases the structural integrity of the blood-brain barrier and reduces atrophy volume. *J. Cereb. Blood flow Metab.* 31 (12), 2343–2351. doi:10.1038/jcbfm.2011.97
- Solmaz, H. P., and Guvena, T. (2016). Borderline ovarian tumors" A contemporary review of clinicopathological characteristics, diagnostic methods and therapeutic options. *J. BUON* 21 (4), 780–786.
- Sousa, D. P., Raphael, E., Brocksom, U., and Brocksom, T. J. (2007). Sedative effect of monoterpene alcohols in mice: a preliminary screening. *J. Biosci.* 62 (7–8), 563. doi:10.1515/znc-2007-7-816
- Sun, Y., Jin, K., Xie, L., Childs, J., Mao, X. O., Logvinova, A., et al. (2003). VEGF-induced neuroprotection, neurogenesis, and angiogenesis after focal cerebral ischemia. *J. Clin. Invest.* 111 (12), 1843–1851. doi:10.1172/JCI17977
- Tian, H., Wang, J., Tian, G., Xiao, M., Jing, W., Limei, W., et al. (2013). Protective effect of L-borneol and borneol syntheticum on cerebral ischemia and anoxia in mice. *Pharmacol. Clin. Chin. Materia Med.* 29 (2), 53–56. doi:10.13412/j.cnki.zyyj.2013.02.021
- Turner, R. J., and Sharp, F. R. (2016). Implications of MMP9 for blood brain barrier disruption and hemorrhagic transformation following ischemic stroke. *Front. Cell Neurosci.* 10, 56. doi:10.3389/fncel.2016.00056
- Wang, S., Wang, Z., Xu, T., Cheng, M., Li, W., and Miao, C. (2019). Cerebral organoids repair ischemic stroke brain injury. *Translational Stroke Res.* 11, 983–1000. doi:10.1007/s12975-019-00773-0
- Wang, Y., Guo, X., Qiu, M., Feng, X., and Sun, F. (2007a). VEGF overexpression enhances striatal neurogenesis in brain of adult rat after a transient middle cerebral artery occlusion. *J. Neurosci. Res.* 85 (1), 73–82. doi:10.1002/jnr.21091
- Wang, Y., Jin, K., Mao, X. O., Xie, L., Banwait, S., Marti, H. H., et al. (2007b). VEGF-overexpressing transgenic mice show enhanced post-ischemic neurogenesis and neuromigration. *J. Neurosci. Res.* 85 (4), 740–747. doi:10.1002/jnr.21169
- Wardlaw, J. M., Murray, V., Berge, E., Del Zoppo, G., Sandercock, P., Lindley, R. L., et al. (2012). Recombinant tissue plasminogen activator for acute ischaemic stroke: an updated systematic review and meta-analysis. *Lancet* 379 (9834), 2364–2372. doi:10.1016/S0140-6736(12)60738-7
- Xin, Y., Zhao, H., Xu, J., Xie, Z., Li, G., Gan, Z., et al. (2020). Borneol-modified chitosan: antimicrobial adhesion properties and application in skin flora protection. *Carbohydr. Polym.* 228, 115378. doi:10.1016/j.carbpol.2019.115378
- Zhang, N., Zhang, Z., He, R., Li, H., and Ding, S. (2020). GLAST-CreERT2 mediated deletion of GDNF increases brain damage and exacerbates long-term stroke outcomes after focal ischemic stroke in mouse model. *Glia* 68 (11), 2395–2414. doi:10.1002/glia.23848
- Zhang, Z., and Chopp, M. (2002). Vascular endothelial growth factor and angiopoietins in focal cerebral ischemia. *Trends Cardiovasc. Med.* 12 (2), 62–66. doi:10.1016/S1050-1738(01)00149-9
- Zhou, Z., Jian, W., Hui, T., Xiao-hua, L., Du, J., and Qiao-lin, F. (2014). Comparison of the brain-protect effects on middle cerebral artery occlusion rats model and factors influencing between L-borneolum and borneolum syntheticum. *Lishizhen Med. Materia Med. Res.* 25 (10), 2349–2351. doi:10.3969/j.issn.1008-0805.2014.10.016

Conflict of Interest: The authors declare that the research was conducted in the absence of any commercial or financial relationships that could be construed as a potential conflict of interest.

Copyright © 2021 Ma, Xie, Li, Guo, Wang, Li, Ren, Gong and Gao. This is an open-access article distributed under the terms of the Creative Commons Attribution License (CC BY). The use, distribution or reproduction in other forums is permitted, provided the original author(s) and the copyright owner(s) are credited and that the original publication in this journal is cited, in accordance with accepted academic practice. No use, distribution or reproduction is permitted which does not comply with these terms.



OPEN ACCESS

Edited by:

Jiahong Lu,
University of Macau, China

Reviewed by:

Feihua Wu,
China Pharmaceutical University,
China
Gang Chen,
Jinan University, China

*Correspondence:

Yue Zhu
zhuyue@njucm.edu.cn
Fei Huang
szhuangfei@126.com
Jin-Ao Duan
dja@njucm.edu.cn

[†]These authors have contributed
equally to this work

Specialty section:

This article was submitted to
Ethnopharmacology,
a section of the journal
Frontiers in Pharmacology

Received: 07 November 2020

Accepted: 25 January 2021

Published: 11 March 2021

Citation:

Qu S, Liu M, Cao C, Wei C, Meng X-E,
Lou Q, Wang B, Li X, She Y, Wang Q,
Song Z, Han Z, Zhu Y, Huang F and
Duan J-A (2021) Chinese Medicine
Formula Kai-Xin-San Ameliorates
Neuronal Inflammation of CUMS-
Induced Depression-like Mice and
Reduces the Expressions of
Inflammatory Factors via Inhibiting
TLR4/IKK/NF- κ B Pathways on
BV2 Cells.
Front. Pharmacol. 12:626949.
doi: 10.3389/fphar.2021.626949

Chinese Medicine Formula Kai-Xin-San Ameliorates Neuronal Inflammation of CUMS-Induced Depression-like Mice and Reduces the Expressions of Inflammatory Factors via Inhibiting TLR4/IKK/NF- κ B Pathways on BV2 Cells

Suchen Qu^{1†}, Mengqiu Liu^{1†}, Cheng Cao¹, Chongqi Wei¹, Xue-Er Meng¹, Qianyin Lou¹,
Bin Wang¹, Xuan Li¹, Yuyan She¹, Qingqing Wang¹, Zhichao Song¹, Zhengxiang Han²,
Yue Zhu^{1*}, Fei Huang^{3*} and Jin-Ao Duan^{1*}

¹Jiangsu Key Laboratory for High Technology Research of TCM Formulae and Jiangsu Collaborative Innovation Center of Chinese
Medicinal Resources Industrialization, Nanjing University of Chinese Medicine, Nanjing, China, ²Department of Neurology and
Rehabilitation, Shanghai Seventh People's Hospital, Shanghai University of TCM, Shanghai, China, ³Department of
Endocrinology, Suzhou TCM Hospital Affiliated to Nanjing University of Chinese Medicine, Suzhou, China

Kai-Xin-San (KXS) is a traditional Chinese medicinal formula composed of Ginseng Radix et Rhizoma, Polygalae Radix, Acori Tatarinowii Rhizoma, and Poria for relieving major depressive disorder and Alzheimer's disease in traditional Chinese medicine (TCM) clinics. Previous studies on the antidepressant mechanism of KXS mainly focused on neurotransmitter and neurotrophic factor regulation, but few reports exist on neuronal inflammation regulation. In the current study, we found that KXS exerted antidepressant effects in chronic unpredictable mild stress-induced depression-like mice according to the results of behavioral tests. Meanwhile, KXS also inhibited the activation of microglia and significantly reduced the expression of pro-inflammatory cytokines such as IL-1 β , IL-2, and TNF- α in the hippocampus of mice. In mice BV2 microglia cell lines, KXS extract reduced the expression of inflammatory factors in BV2 cells induced by lipopolysaccharide via inhibiting TLR4/IKK/NF- κ B pathways, which was also validated by the treatment of signaling pathway inhibitors such as TAK-242 and JSH-23. These data implied that the regulation of pro-inflammatory cytokines in microglia might account for the antidepressant effect of KXS, thereby providing more scientific information for the development of KXS as an alternative therapy for major depressive disorder.

Keywords: Kai-Xin-San, neuronal inflammation, toll like receptor 4, NF- κ B, Chinese medicine formulae

INTRODUCTION

Major depressive disorder (MDD), a widespread mental disorder characterized by the presence of sadness, pleasure loss, and somatic and cognitive changes, has become a serious public health problem (Malhi and Mann, 2018). Its pathogenesis is extremely complex, and various pathogenesis hypotheses, such as neurotransmitter imbalance, deficient supply of neurotrophic factors, and over-stimulation of the hypothalamus-pituitary gland-adrenal gland (HPA) axis, have been proposed (Otte et al., 2016). In recent years, an increasing number of studies have shown that chronic inflammation of the central nervous system (CNS) is crucial to the occurrence of depression. Patients with inflammatory autoimmune diseases such as multiple sclerosis, diabetes, and rheumatoid arthritis have been found to have a higher incidence of depression. The levels of interleukin-1 beta (IL-1 β), interleukin-6 (IL-6), and tumor necrosis factor alpha (TNF- α) in the serum of patients with depression are also significantly higher than those of normal people (Pape et al., 2019). Animal studies also confirmed that persistent chronic stress activates the HPA axis, damages neurons in the hippocampus, and reduces the release of chemokine CX3CL1, which inhibits microglial activation. Microglia are principal immune cells located in the brain responsible for the upregulation of pro-inflammatory mediators upon activation, which is critical for the development of neuronal inflammation in the brain. Chronic overstimulation of microglia can lead to pro-inflammatory mediator release, including pathogenic proteins, cytokines, and chemokines,

which significantly and adversely affect neurobiological structure and function. It has been clinically found that patients with depression have obvious signs of inflammation in the brain, accompanied by blood-brain barrier dysfunction. Concurrently, intracerebral necropsy of depressive suicide victims also revealed an abnormal increase in microglia density. Therefore, decreasing the levels of inflammatory cytokines in the brain and reducing neuronal inflammatory damage might be another target for the development of antidepressants (Dantzer, 2018).

Chinese medicine formulae are usually composed of several herbs, which can achieve synergistic effects through multiple targets. Kai-Xin-San (KXS) is comprised of four herbs, namely Ginseng Radix (GR), Polygalae Radix (PR), Acori Tatarinowii Rhizoma (ATR), and Poria (PO), and is used to relieve psychological diseases. According to the different symptoms of patients, the ratios of these four herbs (GR:PR:ATR:PO) are varied and three ratios are frequently used: 3:2:2:3 (D-652), 1:1:1:2 (K-984), and 1:1:4:8 (K-1640). The details can be found in **Supplementary Table S1**. At present, KXS is still used for treating MDD and Alzheimer's disease in clinical settings. In our previous studies, we found that KXS exerts antidepressant effects by increasing the supply of neurotransmitters and neurotrophic factors. In addition, KXS could exert an antidepressant effect by regulating the gut-brain axis, which included modification of gut microbiota distribution, suppression of the hypothalamus-pituitary-adrenal axis, and down-regulation of pro-inflammatory cytokines in the brain in chronic unpredictable mild stress (CUMS)-induced depression-like mice (Cao et al., 2018; Cao

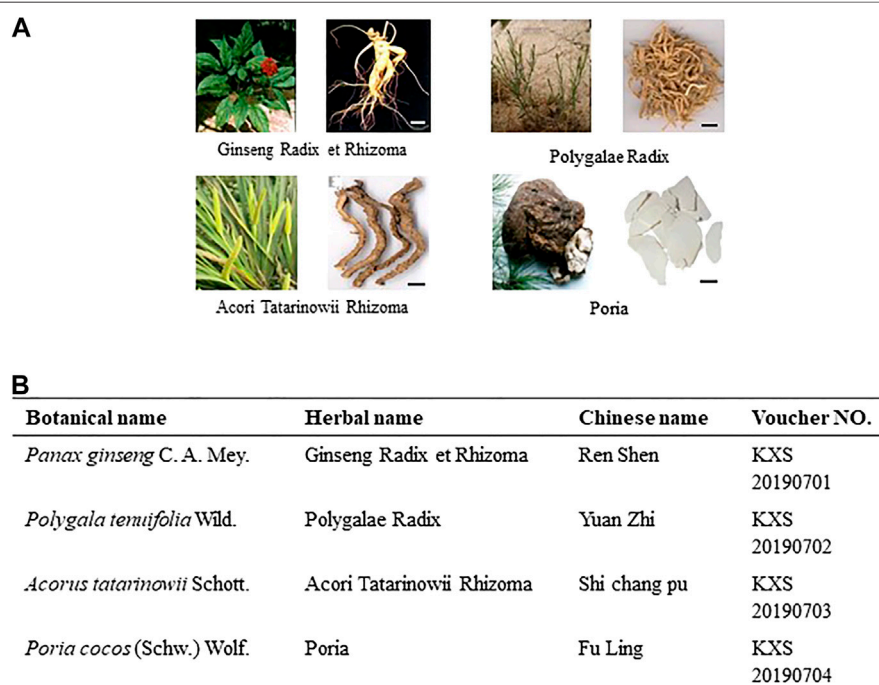


FIGURE 1 | Information of components in KXS formula. **(A)**: Morphology of herbs in KXS. Bar = 1 cm. **(B)**: List of botanical, herbal, Chinese name, and voucher number of the corresponding herb in KXS.

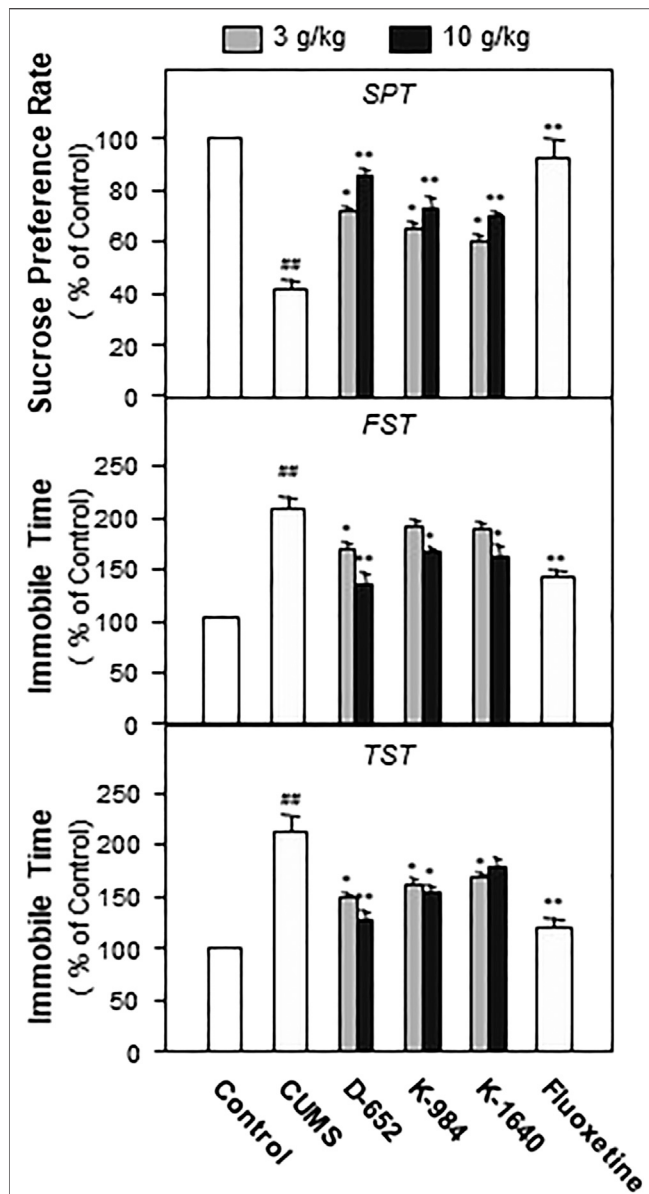


FIGURE 2 | KXS extracts alleviate depressive-like behaviors in CUMS-exposed mice. The effects of KXS extracts on the sucrose consumption test (SPT), immobility time of forced swimming test (FST) and tail suspension test (TST) of CUMS-exposed mice. Values are expressed as mean \pm SEM ($n = 8$). Comparisons between groups were carried out by a one-way ANOVA followed by a post-hoc Bonferroni test. $^{###}p < 0.01$ (compared with the normal control group), $^{*}p < 0.05$, $^{**}p < 0.01$ (compared with the CUMS vehicle group).

et al., 2020). In the current study, we aimed to elucidate the details and relationship between KXS exerting an antidepressant effect and suppressing the expression of pro-inflammatory cytokines in the brain. First, CUMS-induced depression-like mice were used as the animal model. Different compatible ratios of KXS were applied to treat the mice and behavioral tests were used to evaluate its antidepressant effect. In addition, the expression of pro-inflammatory cytokines in the brain and the status of microglia were determined. Second, KXS extracts were treated

with lipopolysaccharide (LPS)-induced inflammatory mice BV2 microglia cell lines to evaluate the effect of suppressing pro-inflammatory cytokine expression, and the possible signaling pathway was explored. This study might be helpful for the elucidation of the antidepressant effect of KXS, which is beneficial for the development of KXS as an alternative therapy for patients with MDD.

MATERIALS AND METHODS

Preparation of KXS Extract

The four herbs comprising KXS, namely Ginseng Radix, Polygalae Radix, Acori Tatarinowii Rhizoma, and Poria, were purchased from Suzhou Tianling Chinese Herbal Medicine Co. Ltd. They were identified as authentic medicinal materials by Prof. Hui Yan of Nanjing University of Chinese Medicine (NJUCM) according to their morphological characteristics. The details of the herbs are listed in **Figure 1**. According to the different compatibility ratios of KXS (**Supplementary Table S1**), the four herbs were mixed, weighing 100 g in total. They were soaked in 1,000 ml water, refluxed, and filtered. The residue was repeated for the same extraction procedures. The extraction solutions were combined and freeze-dried to obtain powders. The quality control procedures of KXS extracts can be found in our previous publication (Cao et al., 2020). The representative chromatograms of KXS extracts are displayed in **Supplementary Figure S1**, and the quantification results of the chemical amounts are listed in **Supplementary Table S2**.

Animals and Housing Conditions

Male Institute of Cancer Research mice (body weight 22–25 g) were purchased from GemPharmatech (China). The animals were raised in the SPF environment of the experimental animal center of NJUCM). They were raised in a routine way, under a 12-h light/dark cycle, in a temperature of 22–25°C and a humidity of 40%–70%. The development of the CUMS animal model and behavioral and biochemical tests on the animals were approved by the Animal Experimental Ethics Committee of NJUCM and conformed to the guidelines of the “Public Health Service Policy on Human Care and Use of Laboratory Animals” published by the Department of Health and Human Services (United States) (2015 revised edition). In addition, procedures were performed to minimize the number of experimental animals and possible injuries.

CUMS Model Development and Drug Treatment

All mice were adapted to the environment for 5 days. Based on the comprehensive scores acquired from a series of screening tests, including the open field experiment, sucrose preference test (SPT), and body weight determination, 90 mice with similar scores were selected. Ten mice were randomly selected and raised under normal conditions, which was set as the normal group. The other mice underwent CUMS procedures. The CUMS procedures were as follows: five mice were raised in one cage, and given two

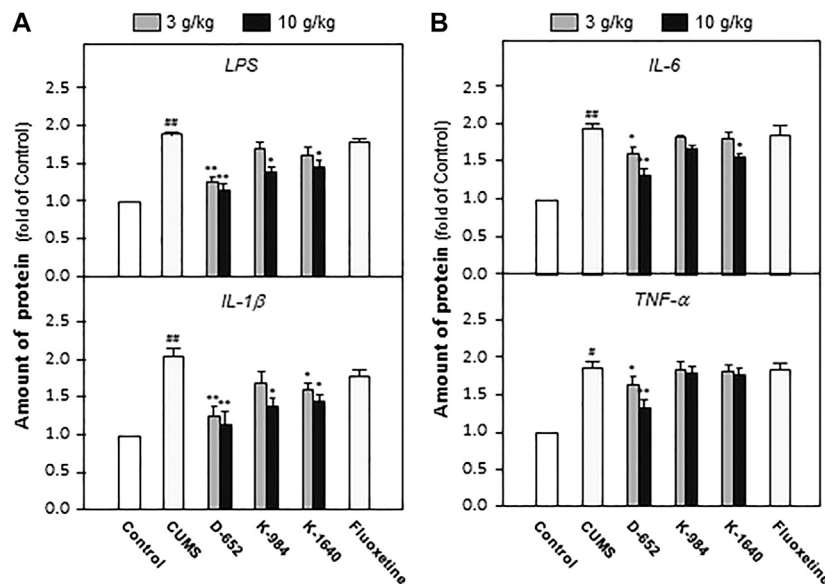


FIGURE 3 | KXS extracts reduce the expression of inflammatory factors in hippocampus of CUMS-exposed mice. **(A):** The effects of KXS on the expression of inflammatory factors LPS and IL-1 β in hippocampus of CUMS-exposed mice; **(B):** The effects of KXS on the expression of inflammatory factors IL-6 and TNF- α in hippocampus of CUMS-exposed mice. Values are expressed as the percentage of the control group (normal mice), as Mean \pm SEM ($n = 8$). Comparisons between groups were carried out by a one-way ANOVA followed by a post-hoc Bonferroni test. # $p < 0.05$, ## $p < 0.01$ (compared with control group), * $p < 0.05$, ** $p < 0.01$ (compared with CUMS vehicle group).

or three different kinds of stressors every day, and each stressor could not be repeated within three days. The stressors included: 1) food deprivation for 24 h; 2) water deprivation for 24 h; 3) inclined cage for 24 h; 4) overnight illumination; 5) restraint for 6 h; 6) wet cage for 24 h; 7) empty cage for 24 h (i.e. without cushion material); 8) stroboscopic; 9) day night reversal; (10) horizontal vibration for 30 min; 11) electric shock for 1 min; 12) foreign objects. In the first week, in order to control the mortality of mice, mild stimulation was used as far as possible. The sucrose preference test of mice was tested every week, and the specific methods of modeling were adjusted according to the sugar water preference rate and the state of mice. After 8 weeks of CUMS procedures, the CUMS model mice were randomly separated into different groups and treated with different drugs for 7 days. The groups and treatments were set as follows: normal group (0.9% saline); CUMS vehicle group (0.9% saline); D-652 at low dosage (3 g/kg/d) and high dosage (10 g/kg/d); K-984 at low dosage (3 g/kg/d) and high dosage (10 g/kg/d); K-1640 at low dosage (3 g/kg/d) and high dosage (10 g/kg/d); and fluoxetine group (positive drug group, 7.2 mg/kg/d) (Tunc-Ozcan et al., 2019; Shuto et al., 2020).

Behavioral Evaluation

The depression-like behaviors of mice were examined using the sucrose preference test (SPT), tail suspension test (TST) and forced swimming test (FST).

The details of SPT were as follows: All mice were trained to adapt to 1% sucrose solution (w/v) 72 h before the test, where two bottles of 1% sucrose solution were placed in each cage. After 24 h, 1% sucrose in one bottle was replaced with tap water. After a

24 h adaptation period, mice were deprived of food and water for another 24 h. Then the mice were housed in individual cages with free access to two bottles containing either 100 ml of sucrose solution (1%, w/v) or 100 ml of tap water. During the test, the position of the water bottle was exchanged for 1 h to prevent the position preference. After 3 h, the weights of the consumed sucrose solution and tap water were separately recorded, and the sucrose preference was calculated using the following formula: sucrose preference = sucrose consumption/(tap water consumption + sucrose consumption) \times 100%.

The details of FST and FST were as follows. In TST, individual mice were suspended in an acoustically and visually isolated chamber. Animal activities were captured using a video camera. The total time of immobility during the last 4 min in a 6-min testing period was analyzed using ANY-maze software (Stoeling Co. Ltd., United States). In FST, mice were forced to swim in a transparent glass vessel (20 cm high, 14 cm in diameter, filled with 10 cm of water at 24–26°C) placed in a cabinet. The mobilities of mice were recorded with a camera and the mice were considered immobile when they made no attempts to escape, except for the movements necessary to keep their heads above the water. The total duration of immobile time (seconds) was recorded during the last 4 min of a single 6-min test session, while the initial 2 min was applied for mouse adaptation.

Cell Culture and Treatments

Mice microglial cell lines (BV2) were purchased from the American Type Culture Collection. The culture medium consisted of Minimum Essential Medium-Eagle (88%), fetal bovine serum (10%), penicillin/streptomycin (1%), and sodium

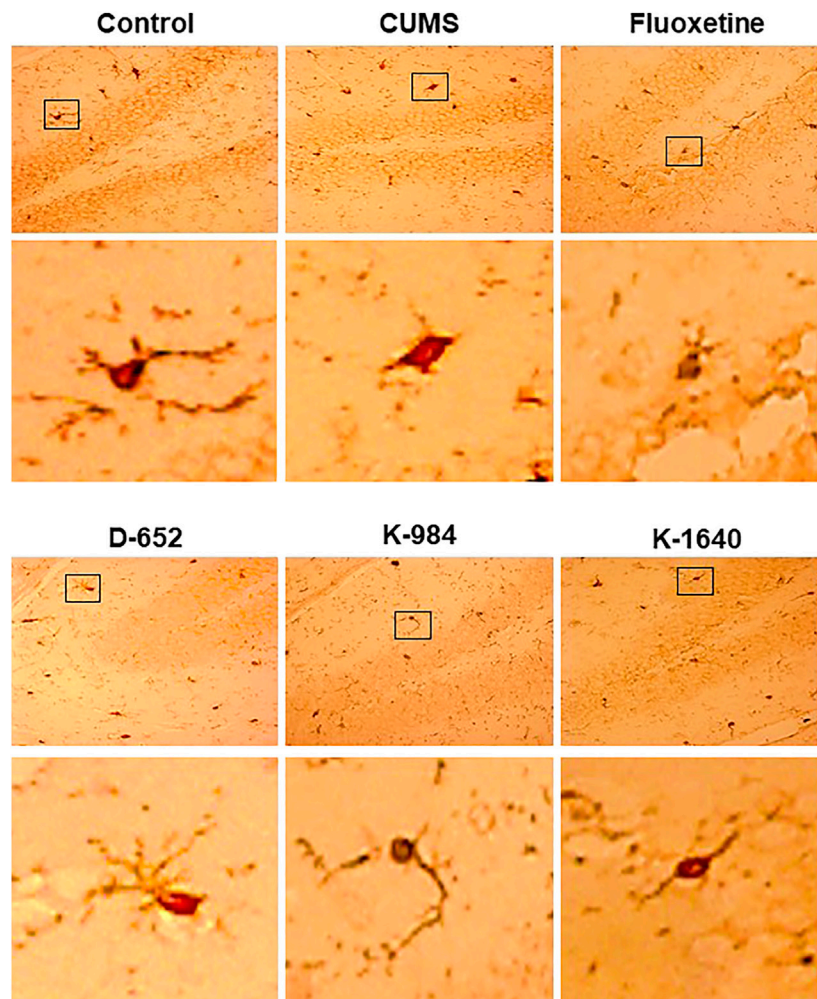


FIGURE 4 | KXS extracts affect the morphology of microglia in mice. The morphologies of microglia in dentate gyrus of mice in normal control group, CUMS vehicle group, D-652 administration group, K-984 administration group, K-1640 administration group, and fluoxetine administration group, were determined by immunoperoxide method. The doses of D-652 administration group, K-984 administration group, K-1640 administration group were set as 10 g/kg/d ($n = 3$). Correspondingly, the larger images of microglia in normal control group, CUMS vehicle group, D-652 administration group, K-984 administration group, K-1640 administration group, and fluoxetine administration group were displayed.

pyruvate solution (1%). The culture medium was changed every 48 h. When the cell density reached 70%, the cells were sub-cultured. All reagents used for cell culture were purchased from Thermo Fisher Scientific (Invitrogen, Carlsbad, CA). LPS was purchased from CST (China) and 10 mg was dissolved in 10 ml sterile Phosphate-buffered saline (PBS) to prepare the stock solution (1 mg/ml). TAK-242, a TLR4 blocker, was purchased from Selleck (China) and the stock solution was 50 mM in Dimethyl sulfoxide (DMSO) (Kim et al., 2018; Gu et al., 2020). JSH-23, a transcriptional inhibitor of NF- κ B, was purchased from Selleck (China) and the stock solution was 10 mM in DMSO (Cai et al., 2018; Su et al., 2020).

ELISA Assays

After the behavioral tests, the mice were sacrificed and the hippocampal tissues were dissected. The amounts of IL-1 β , IL-

6, and TNF- α were determined using ELISA kits. The ELISA kits were purchased from Nanjing Jin Yibai Biological Technology Co. Ltd., and the procedures were carried out according to the manufacturer's instructions. The detection range of the kit was 20–500 pg/ml.

Western Blot Analysis

The experimental details of Sodium dodecyl sulfate polyacrylamide gel electrophoresis and western blot analysis can be found in our previous publication (Zhu et al., 2017). Briefly, total protein samples were loaded on 10% polyacrylamide gels and separated. The primary antibodies used were mouse polyclonal anti-TLR4 (AF7017, 1:1,000, Affinity Biosciences), rabbit polyclonal anti-NF- κ B (4,764, 1:1,000, CST), rabbit polyclonal anti-p-NF- κ B (5,801, 1:1,000, CST), rabbit polyclonal anti-histone H3 (4,499, 1:1,000, CST), and rabbit

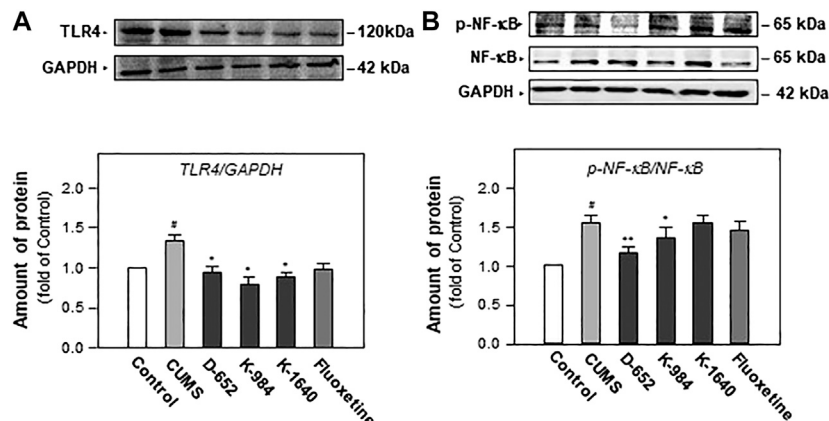


FIGURE 5 | KXS extracts regulate the expression of proteins of TLR4/NF- κ B signaling pathway in the hippocampus of CUMS-exposed mice. **(A):** The effects of KXS extract (10 g/kg/d) on TLR4 protein expression in the hippocampus of CUMS-exposed mice; **(B):** The effects of KXS extracts on expressions of p-NF- κ B and NF- κ B in the hippocampus of CUMS-exposed mice; Values are expressed as the percentage of the control group (normal mice), as Mean \pm SEM ($n = 8$). Comparisons between groups were carried out by a one-way ANOVA followed by a post-hoc Bonferroni test. [#] $p < 0.05$, (compared with control group), ^{*} $p < 0.05$, ^{**} $p < 0.01$ (compared with CUMS group).

polyclonal anti-GAPDH (5,174, 1:1,000, CST). The secondary antibody used was anti-rabbit IgG and HRP-linked antibody (7,074, 1:5,000, CST). The bands were compared on an image analyzer, and relative quantification was performed with Image-J Digital Imaging System (Bio-Rad, Hercules, California). Gel documentation and relative quantification were performed using the Image-J Digital Imaging System.

Real-Time Quantitative Polymerase Chain Reaction Analysis

Total RNA extraction was carried out according to the instructions listed in the TRIzol RNA extraction kit (15596-026, Thermo Fisher, United States). cDNA was acquired according to the instructions of the reverse transcription kit (AE311, Transgen Company, China). The transcriptional expression of pro-inflammatory cytokines was determined by quantitative PCR according to the instructions of the SYBR fluorescence real-time quantitative kit (AQ132, TransGen, Transgen Company, China). The primer sequences used are shown in **Supplementary Table S2**. Gene expression was calculated by the $\Delta\Delta C_t$ method, and GAPDH was set as the internal reference gene.

Immunohistochemistry

The mice were sacrificed after the behavioral tests. Entire brains were dissected and fixed in 4% paraformaldehyde (PFA) fixative solution at room temperature. Conventional dehydration and paraffin embedding were carried out afterward. Mice brain slices were dewaxed with xylene, dehydrated with an ethanol gradient, and then placed in a sodium citrate buffer solution for 15 min. The slices were cooled for 30 min and then treated with 3% hydrogen peroxide for dehydrogenation. The slices were blocked for 1 h with 5% bovine serum albumin (BSA) added

with PBS-T (Triton). The primary antibody used was rabbit anti-Iba1 (19,741, 1:1,000, Wako, Japan). The secondary antibody was horseradish peroxidase labeled goat anti-rabbit IgG (H+L) antibody (1:50, Beyotime, China). DAB Horseradish Peroxidase Color Development Kit (Beyotime, China) was used to develop the color in dark for 15 min. The slices were washed with running water, dried, dehydrated and transparent, sealed with Neutral balsam (Solarbio) and photographed under microscope.

BV2 cells were washed three times with pre-cooled PBS, fixed with PBS containing 4% PFA for 30 min, and perforated with PBS permeation membrane containing 0.2% TritonX-100 for 15 min. To prevent nonspecific binding, cells were blocked with 5% BSA for 2 h at room temperature. Cells were incubated with NF- κ B p65 subunit antibody (4,764, 1:1,000, CST) at 4°C overnight and then removed from the refrigerator and incubated at room temperature for 2 h. After three washes, the cells were incubated with the secondary antibody labeled with Alexa Fluor® 488 anti-rabbit antibody (1:1,000, Invitrogen) for 1 h at room temperature. DAPI (1:10,000) staining was performed for 5 min. Fluorescence images were generated by confocal microscopy.

Fluorescence images were all taken with a fluorescence microscope (X5, Zeiss, Swiss) at the corresponding excitation and emission wavelengths, and the images were processed by ZEN2012 image processing software.

Data Analysis

Statistical tests were performed using one-way or two-way ANOVA analysis (version 13.0, SPSS, IBM Corp., Armonk, NY) followed by a Bonferroni post hoc analysis if appropriate. Before ANOVA analysis, a normal distribution test was carried out. The control group was varied in different experiments, as specified in the figure legends. Data are expressed as mean \pm

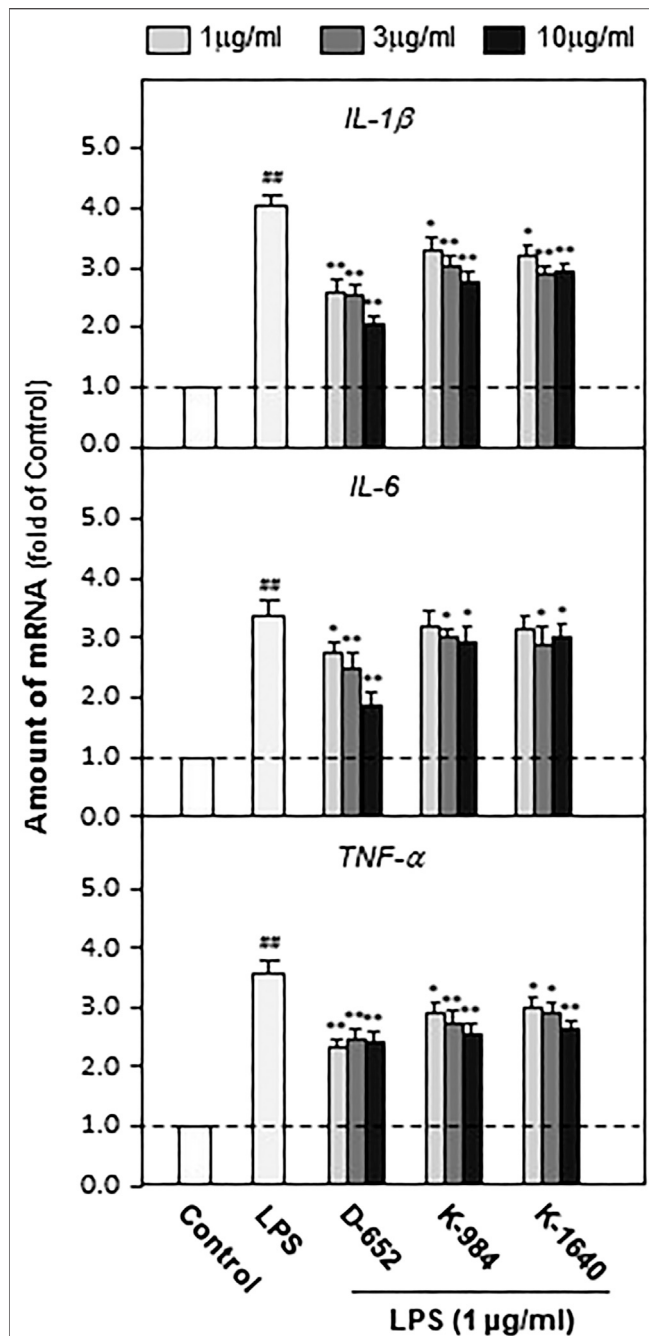


FIGURE 6 | KXS extracts decrease the expressions of pro-inflammatory factors in LPS-treated BV2 cells. BV2 cells were treated with LPS (1 μ g/ml) and different compatibility ratios of KXS extracts simultaneously. The expressions of IL-1 β , IL-6, TNF- α were determined by qPCR. Values are expressed as the percentage of the control group (no drug treatment) as Mean \pm SEM (n = 5). Comparisons between groups were carried out by a one-way ANOVA followed by a post-hoc Bonferroni test. *** p < 0.01 (compared with control group), * p < 0.05, ** p < 0.01 (compared with LPS treatment group).

standard error of the mean, where $n = 3-8$. For behavior test, the number was set as 8. For immunohistochemistry, the number was set as 3. For western analysis, the number was set as 5. Statistically

significant changes were classed as significant [*] where $p < 0.05$, highly significant [***], where $p < 0.01$.

RESULTS

KXS Extracts Ameliorated Depressive-like Behaviors on CUMS-Induced Depression Mice

Seven days after the administration of KXS, all mice underwent behavioral tests including the SPT, FST, and tail suspension test (TST). Statistical results showed that the consumption of sucrose in the model group was significantly lower than that in the normal control group ($p < 0.01$), and the immobile time in FST and TST was significantly higher than that in the normal group ($p < 0.01$). Compared with the CUMS vehicle group, KXS increased the sucrose preference rate and decreased the immobile time of the model animals in the FST and TST ($p < 0.05$). Among the different ratios of KXS, D-652 had the strongest effect in alleviating depression-like behaviors in animals, and its active trend was similar to that of the positive drug fluoxetine (Figure 2).

KXS Extracts Reduced the Expressions of Inflammatory Factors in the Hippocampus of Mice

After behavioral tests, the groups of mice were sacrificed, and the hippocampal tissues were isolated. The levels of LPS, IL-1 β , IL-6, and TNF- α were measured using an ELISA kit. The experimental results showed that the levels of LPS, IL-1 β , IL-6, and TNF- α in the hippocampus of CUMS model mice were significantly upregulated compared with those of the normal control group ($p < 0.01$). KXS significantly downregulated the expression of LPS, IL-1 β , IL-6, and TNF- α in the hippocampus of CUMS model animals compared with the untreated CUMS vehicle group ($p < 0.05$). In line with the behavioral tests, D-652 treatment at high dosage showed the strongest active trend (Figure 3).

Effect of KXS Extracts on Microglia in Mouse hippocampus

After the animals were sacrificed, the entire brains of the mice were isolated. Morphological changes in microglia in hippocampal tissues were observed by fluorescence microscopy. The results showed that the microglia in the hippocampus of mice in the normal control group were in a branching state, suggesting that they were inactivated. Meanwhile, the microglia in the hippocampus of mice in the CUMS vehicle group were in a circular state, suggesting that they were activated. The morphology of microglia in the KXS-treated group was similar to that in the normal group, indicating that their activation status could be inhibited by KXS treatment, especially in the D-652 treatment group. The positive drug fluoxetine group had no obvious inhibitory effect on microglial activation (Figure 4).

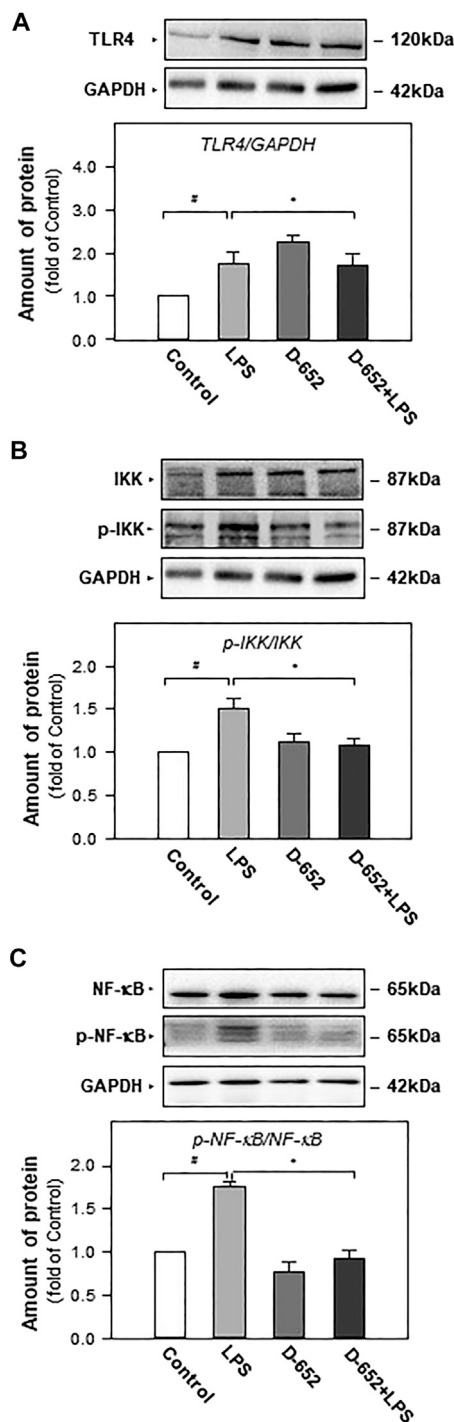


FIGURE 7 | KXS extracts regulate the expression of proteins of TLR4/NF-κB signaling pathway in LPS-treated BV2 cells. **(A):** The effect of KXS extracts D-652 on the TLR4 expression in LPS-treated BV2 cells at 2 h; **(B):** The effect of KXS extracts D-652 on the proteins of p-IKK and IKK in LPS-treated BV2 cells at 2 h; **(C):** The effect of KXS extracts D-652 on the proteins of p-NF-κB and NF-κB in LPS-treated BV2 cells at 2 h; Values are expressed as the percentage of the control group (no drug treatment) as Mean ± SEM (n = 5). Comparisons between groups were carried out by a one-way ANOVA followed by a post-hoc Bonferroni test. ## $p < 0.01$ (compared with control group), * $p < 0.05$ (compared with LPS treatment group).

KXS Extracts Decreased the Expressions of TLR4 Receptor and Inhibited NF-κB Phosphorylation in the Hippocampus of Mice

After behavioral tests, the expression of TLR4 and NF-κB phosphorylation in the hippocampus of mice, two proteins closely related to the NF-κB signaling pathway, were studied. As shown in **Figures 5A,B**, the expression of TLR4 and the phosphorylation level of NF-κB protein increased in the hippocampus of CUMS vehicle group mice compared with those of the normal control group ($p < 0.05$). These phenomena suggest that chronic unpredictable stress promotes NF-κB protein entry into the nucleus by activating the phosphorylation of the NF-κB protein in the hippocampus of mice. Compared with the CUMS vehicle group, D-652 decreased the expression of TLR4 ($p < 0.05$) and inhibited the phosphorylation level of the NF-κB protein ($p < 0.01$), thus inhibiting the expression of inflammatory factors in the hippocampus of CUMS model mice.

KXS Extracts Decreased the Expressions of Pro-Inflammatory Cytokines by Regulating the TLR4/IKK/NF-κB Signaling Pathway and Inhibiting Nuclear Translocation of NF-κB on BV2 Cells

We constructed an *in vitro* cell model mimicking central nervous system inflammation by treating the microglial cell line (BV2) with LPS to stimulate pro-inflammatory cytokine expression. Subsequently, the effects of KXS on the expression levels of IL-1β, IL-6, and TNF-α were evaluated. As shown in **Figure 6**, LPS at 1 μg/ml significantly promoted the expression of inflammatory factors in BV2 cells compared with that in the untreated control group ($p < 0.01$), and KXS extracts significantly inhibited the expression of pro-inflammatory factors in BV2 cells stimulated by LPS ($p < 0.01$). In addition, KXS extracts had no effect on the expression of inflammatory factors in BV2 cells (data were not shown). Based on the animal and cell experiments, the D-652 compatibility ratio exerting the best active trend in improving depression-like behaviors and suppressing pro-inflammatory cytokine expression was selected for further study on the mechanism of KXS pro-inflammatory cytokine expression.

When BV2 cells were treated with LPS, the expression of TLR4 was significantly increased compared to that in the normal control group. This increasing trend was significantly reversed by treatment with D-652 (**Figure 7A**). A similar active trend was found in both the IKK phosphorylation levels and NF-κB phosphorylation levels (**Figures 7B,C**). As shown in **Figures 8A,B**, we further found that LPS treatment significantly promoted the nuclear translocation of NF-κB ($p < 0.01$) and D-652 significantly inhibited the nuclear translocation of NF-κB ($p < 0.01$).

Furthermore, TAK-242 (the inhibitor of TLR4) and JSH-23 (an inhibitor of NF-κB nuclear translocation) were simultaneously treated with D-652 on BV2 cells to verify whether KXS simultaneously decreased pro-inflammatory cytokine expression

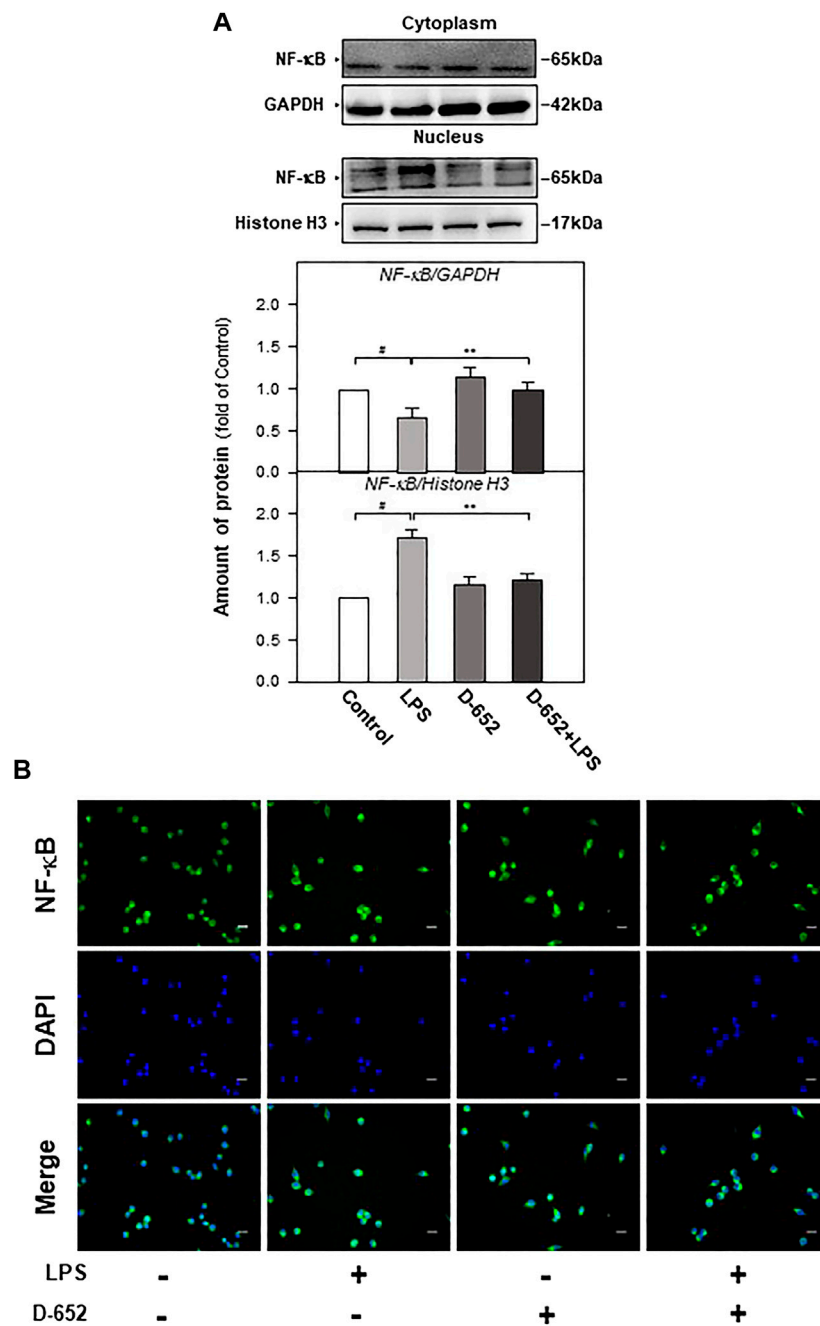


FIGURE 8 | KXS extracts regulate the nucleus translocation of the NF- κ B protein in LPS-treated BV2 cells. **(A):** The effect of KXS extracts D-652 on the expressions of NF- κ B in nucleus and cytoplasm in LPS-treated BV2 cells at 2 h; **(B):** The immunofluorescent images of the NF- κ B nucleus translocation were observed with fluorescent microscopy in LPS-treated BV2 cells at 2 h; Green, NF- κ B; blue, DAPI; scale bar = 5 μ m. Values are expressed as the percentage of the control group (no drug treatment) as Mean \pm SEM (n = 5). Comparisons between groups were carried out by a one-way ANOVA followed by a post-hoc Bonferroni test. $^{##}p < 0.01$ (compared with control group), $^{*}p < 0.05$ (compared with LPS treatment group).

by regulating the TLR4/IKK/NF- κ B signaling pathway. As shown in **Figures 9A,B**, single D-652 treatment and single TAK-242 treatment both significantly decreased the expression of pro-inflammatory cytokines in LPS-treated BV2 cells. However, the combined treatment of TAK-242 and D-652 exerted no significant effects on the expression of pro-inflammatory cytokines compared with single

D-652 or TAK-242 treatment groups. Therefore, the downregulated expression of pro-inflammatory cytokines of D-652 and TAK-242 co-treatment was exerted mainly by TAK-242 instead of D-652. In other words, the downregulation effect of D-652 on pro-inflammatory cytokine expression was attenuated. A similar effect was also found in the combined treatment of JSH-23 and D-652.

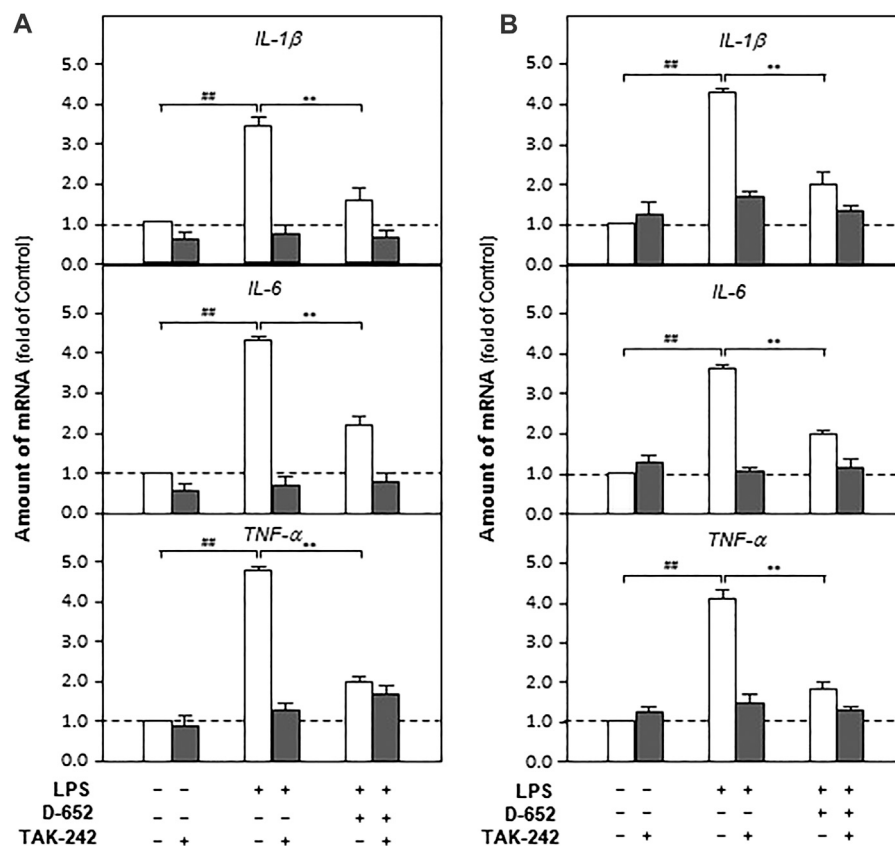


FIGURE 9 | Effect of KXS extracts on the expressions of pro-inflammatory factors in LPS-treated BV2 cells after administration of TAK-242 and JSH-23. **(A):** Effect of KXS extracts on the expressions of pro-inflammatory factors in LPS-treated BV2 cells after administration of TAK-242. **(B):** Effect of KXS extracts on the expressions of pro-inflammatory factors in LPS-treated BV2 cells after administration of JSH-23. Values are expressed as the percentage of the control group (no drug treatment) as Mean \pm SEM ($n = 5$). Comparisons between groups were carried out by a two-way ANOVA followed by a post-hoc Bonferroni test. * $p < 0.05$.

We also evaluated the effect of TAK-242 on TLR4 expression in D-652 treated LPS-exposed BV2 cells. As shown in **Figure 10**, TAK-242 significantly inhibited LPS-induced increase in TLR4 expression. The downregulation effect of D-652 on TLR4 was also attenuated by simultaneous treatment with TAK-242. Similarly, the inhibition of D-652 on nucleus translocation of NF- κ B was also attenuated by JSH-23 (**Figures 11A–C**).

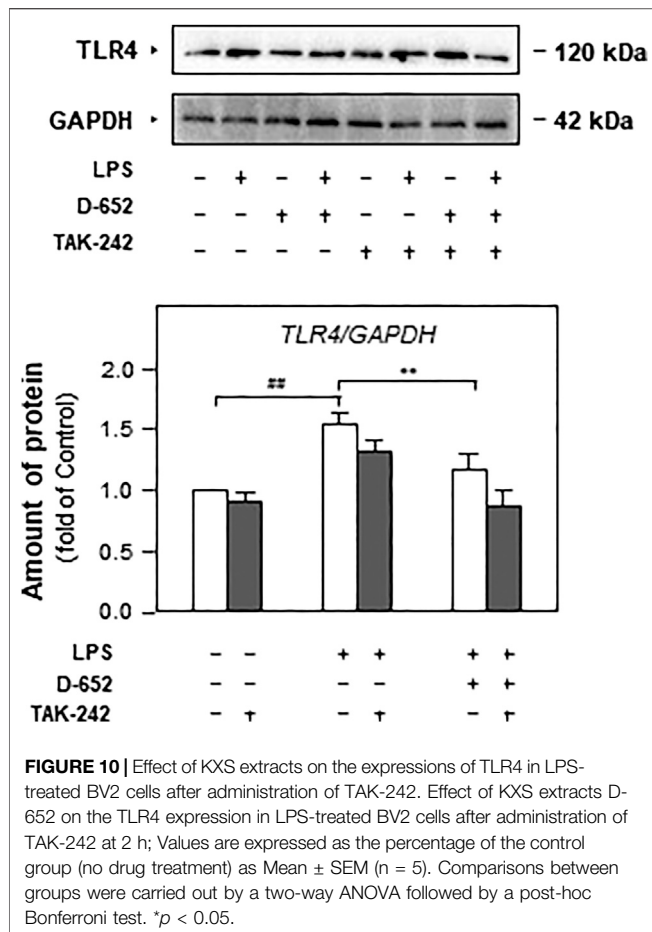
DISCUSSION

In the current study, we found that KXS significantly alleviated depression-like behaviors, decreased the LPS and pro-inflammation factors, and suppressed the activation of microglia in the hippocampus of CUMS-exposed depression-like mice. In BV2 microglia cell lines, KXS extracts significantly decreased the expression of IL-1 β , IL-2, and TNF- α induced by LPS and inhibited TLR4/IKK/NF- κ B signaling pathways, which might be indispensable in the antidepressant effect of KXS.

At present, central neuronal inflammation has been recognized to play an important role in the pathogenesis and development of MDD. Clinical findings showed that the serum levels of inflammatory cytokines IL-1 β , IL-6, and TNF- α in patients with

MDD were significantly higher than those in normal people. Microglia are the main cells responsible for inflammation in the brain. Animal studies have also confirmed that sustained chronic stress stimulates the HPA axis and activates microglia to secrete inflammatory cytokines, which impairs the survival and development of neurons. The impairment of neurons leads to decreased CX3CL1 release, which further activates microglia to induce pro-inflammatory cytokine release, which further aggravates neuronal inflammation. In addition, neuronal inflammation also stimulates the tryptophan-kynurenine acid metabolic pathway, which reduces serotonin synthesis and leads to insufficient supply of serotonin. In neuronal inflammation, the activated NF- κ B signaling pathway is the principal pathway that promotes the expression of pro-inflammatory cytokines in microglia, and LPS is an important inducer of this signaling pathway. LPS acts on TLR4 receptors in microglia, promotes NF- κ B in the cytoplasm to enter the nucleus, exerts transcriptional regulation, and promotes the synthesis and secretion of pro-inflammatory cytokines. Therefore, relieving neuronal inflammation and inhibiting activated TLR4/NF- κ B should be included in new-generation antidepressant development (Yirmiya et al., 2015; Zhang et al., 2017; Deczkowska et al., 2018).

At present, the available antidepressants in clinics are monoamine neurotransmitter reuptake inhibitors. No antidepressant has been



developed to suppress central nervous system inflammation. Studies have shown that the serotonin reuptake inhibitors fluoxetine and escitalopram can significantly reduce the expression of IL-1 β , IL-6, TNF- α , and inducible nitric oxide synthase in BV2 cells and primary microglia induced by the combination of LPS and interferon- γ (Su et al., 2015; Xiaoling et al., 2018). The serotonin and norepinephrine reuptake inhibitors venlafaxine can downregulate the expression of inflammatory factors IL-1 β , IL-6, and TNF- α induced by morphine in mice, thus exerting the effects of anti-neuroinflammation. However, these antidepressants are ineffective in 40% of patients with MDD and cause side effects such as gastrointestinal discomfort and sexual dysfunction. In addition, in view of the complex pathological networks of MDD, single compounds with limited action targets may not be suitable for this sophisticated disease, while Chinese medicine formulae composed of multiple components and action targets might be an effective alternative therapy for MDD (Degner et al., 2004).

Traditional Chinese medicine has rich experience in the prevention and treatment of depression. At present, the number of compound Chinese medicine in the stage of new drug development is increasing year by year. Among them, Yueju pill, Ganmai Dazao decoction, Chaihu Shugan powder, Sini Powder, KXS and so on are representative Chinese herbal compound. Animal experiments showed that the petroleum ether extract of Yueju pill could alleviate the depressive behavior of mice by

promoting the release of BDNF and the activation of TrkB (Xue et al., 2013). Clinical studies have shown that Ganmai Dazao decoction can exert antidepressant effect by affecting the content of monoamine neurotransmitters in brain regions (Ma et al., 2014). Animal experiments show that Chaihu Shugan powder can alleviate the depressive behavior of rats by increasing the expression of BDNF and TrkB in hippocampus, amygdala and frontal lobe (Zhan et al., 2004). Animal experiments show that Sinisan can reduce the increase of serum corticosterone and plasma ACTH by inhibiting the over activation of HPA axis, thus exerting the antidepressant effect (Wei et al., 2016). KXS is an effective treatment for mild and moderate depression. Studies have shown that KXS can significantly alleviate the depression like behavior of CUMS mice, and play an antidepressant role by promoting the release of neurotransmitters and neurotrophic factors in the brain of mice and inhibiting the excessive activation of HPA axis. And KXS is rich in anti-inflammatory active ingredients, such as ginsenoside and Ginsenoside Rg3, which can inhibit the activation of HPA axis in chronic stress depression rats, reduce the levels of IL-1 β , IL-6 and TNF- α in hippocampus, and improve the level of 5-hydroxytryptamine in hippocampus by inhibiting the metabolism of tryptophan to kynuric acid. Ginseng, as the main component of KXS, can significantly alleviate the central nervous system inflammation, which also reveals the application prospect of KXS in regulating central nervous system inflammation and alleviating depression. KXS has extensive research value in relieving depression because of its multi-component, multi-target and multi-channel pharmacological action.

KXS is one of the most frequently applied formulae for treating MDD in Chinese medicine clinics. The components contained in KXS have been confirmed to regulate neuronal inflammation. The total ginsenoside and ginsenoside Rg3 in Radix Ginseng can inhibit HPA axis activation in rats with chronic stress-induced depression. They reduce the levels of IL-1 β , IL-6, and TNF- α in the hippocampus, and increase the level of 5-HT in the hippocampus by inhibiting the metabolism of tryptophan into canine uric acid (Kang et al., 2011; Kang et al., 2017; Xu et al., 2018). In the current study, we also found that D-652, with a higher content of Ginseng Radix, exerted the strongest antidepressant effect. Alfa-asarone in Rhizoma Acori Tatarinowii extract can inhibit the expression of inflammatory factors, regulate NF- κ B transcription levels, and block the release of inflammatory factors in senile rats and primary cultured microglia by blocking the ubiquitination of I κ B- α and β kinases, thereby playing a role in resisting neuroinflammation. It has been reported that β -asarone, also an active ingredient of Rhizoma Acori Tatarinowii, can improve the damage of cognitive and synaptic plasticity by regulating the excessive release of pro-inflammatory cytokines and the activation of microglia (Lim et al., 2014; Liu et al., 2017). Although there are no direct reports of compounds from Polygalae Radix and Poria on the regulation of central neuronal inflammation, senegenin in Polygalae Radix et Rhizoma can reduce the symptoms of colitis by regulating IFN- γ and IL-4 (Hong et al., 2002; Cheong et al., 2011). Total triterpenoids of Poria can fight against acute inflammation in mice with auricle swelling and an increase in abdominal cavity capillary permeability caused by xylene. Poria neonate C was also found to inhibit the expression

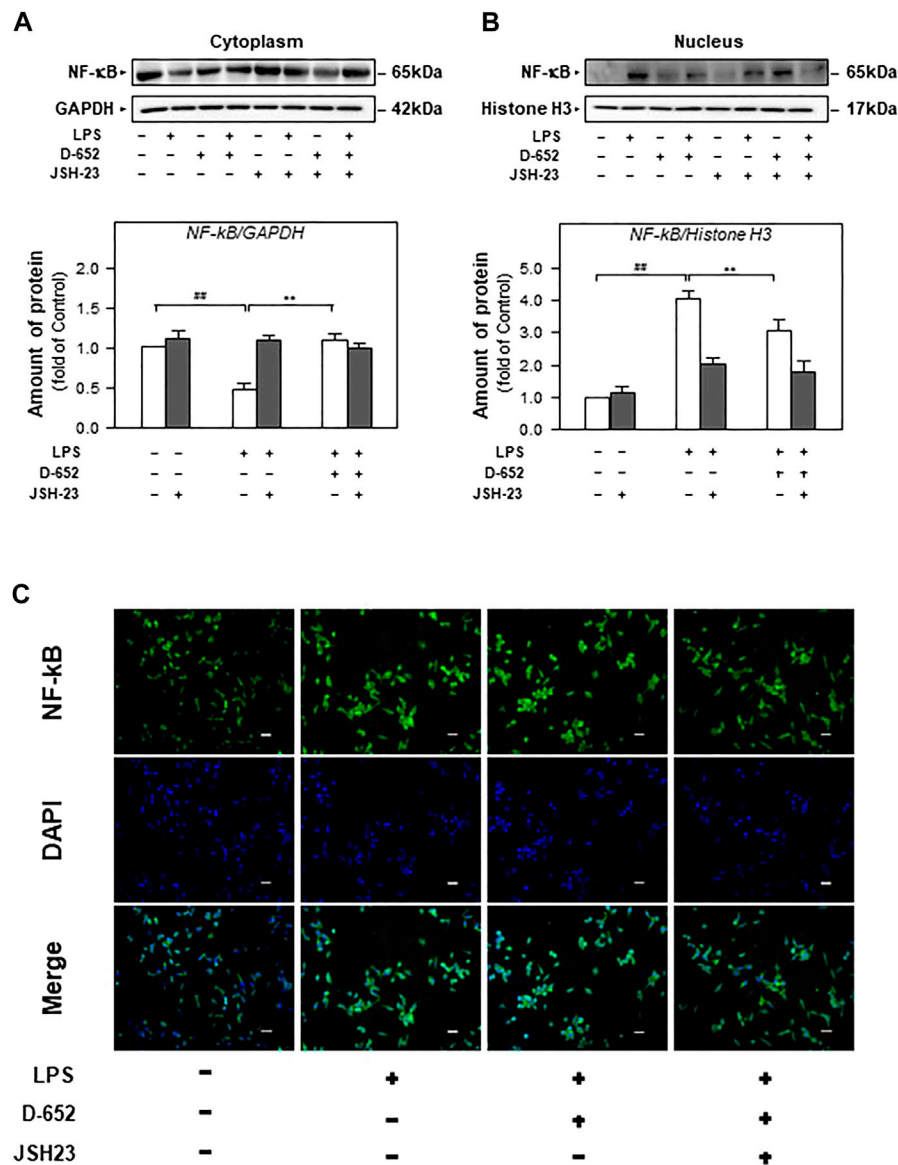


FIGURE 11 | Effect of KXS extracts on the nucleus translocation of the NF-κB protein in LPS-treated BV2 cells after administration of JSH-23. **(A)**: Effect of KXS extracts D-652 on the NF-κB expression in cytoplasm of LPS-treated BV2 cells after administration of JSH-23 at 2 h; **(B)**: Effect of KXS extracts D-652 on the NF-κB expression in nucleus of LPS-treated BV2 cells after administration of JSH-23 at 2 h; **(C)**: The immunofluorescent images of the NF-κB nucleus translocation were observed with fluorescent microscopy in LPS-treated BV2 cells after administration of JSH-23 of D-652 at 2 h; Green, NF-κB; blue, DAPI; scale bar = 5 μm. Values are expressed as the percentage of the control group (no drug treatment) as Mean ± SEM (n = 5). Comparisons between groups were carried out by a two-way ANOVA followed by a post-hoc Bonferroni test. ##*p* < 0.01 (compared with control group), **p* < 0.05 (compared with LPS treatment group).

of INOS and COX-2 by downregulating the expression of NF-κB protein to play an anti-inflammatory role (Ríos, 2011). Therefore, the antidepressant effect of KXS might be due to the synergistic effect of the multiple compounds of the four herbs.

In addition to KXS, some Chinese medicine formulae also exerted antidepressant effects by regulating neuronal inflammation. The Ban-Xia-Hou-Pu decoction plays an antidepressant role by inhibiting the activation of NLRP3 inflammasomes and the production of IL-1β in the liver, hypothalamus, hippocampus, or prefrontal cortex of CUMS-induced depression rats (Jia et al., 2017). Si-Ni-San reduces the release of inflammatory factors IL-1β, IL-6, IL-

2, and TNF-α in the peripheral fluid of patients with post-stroke depression and regulates the over-activation of the HPA axis, thereby exerting an antidepressant effect (Guo et al., 2009; Li et al., 2013). Chang-Yu-Xiao-Yao-San can reduce the expression of inflammatory factors IL-6, IL-8, and TNF-α in the serum of patients with chronic hepatitis B combined with depression, and relieve the symptoms of depression in patients. Animal experimental results also show that Chang-Yu-Xiao-Yao-San inhibits an over-expression of serum IL-6, IL-8, and TNF-α in LPS-induced depression model rats and increased the content of hippocampal 5-HT in rats (Qi et al., 2013; Jing et al., 2015). However, the above-mentioned study on

the inhibition of central nervous inflammation by traditional Chinese medicine compounds is often limited to the determination of inflammatory factors, and there is a lack of in-depth research on the mechanism. In addition, the differences in the antidepressant regulation networks between these formulae are worth elucidating.

Besides, we found that D-652 increased TLR4 expressions in BV2 cells alone while decreased TLR4 expressions both in LPS treated BV2 cells and CUMS depressive mice. Interestingly, this contradictory phenomenon is also reported in Radix Ginseng. *In vitro*, ginsenosides is reported to activate phagocytosis on macrophage RAW264.7 cells through regulating TLR2/4 and NF- κ B signaling pathways and the enhancement of TLR4 expression is also found (Xu et al., 2018; Gao et al., 2020). *In vivo*, Radix Ginseng is also reported to down-regulate the TLR4 expressions in disease-like animal models like cerebral Ischemia rats (Cheng et al., 2019; Li et al., 2020). These findings support that Radix Ginseng exert bi-directional function in regulating immunity by enhancing phagocytosis in normal condition while inhibiting abnormal stimulation of phagocytes in pathological condition. Since Radix Ginseng is the major herb of D-652, we hypothesize that Radix Ginseng might contribute to the enhanced expressions of TLR4 in BV2 cells. However, we will further investigate the details in the future. Besides, we will further study the functional material basis and the in-depth mechanism of KXS suppression of central neuronal inflammation, which will provide more scientific evidence for the development of new antidepressants or alternative therapies from this Chinese medicine formula.

CONCLUSION

KXS extracts play an antidepressant role by improving depression-like behaviors on CUMS-exposed mice. This effect may be related to the inhibition of the release of inflammatory factors in microglia of hippocampus and regulation of TLR4/IKK/NF- κ B signaling pathway on BV2 cells. This study will be helpful for the antidepressant alternative therapies or drug developments (Zhu et al., 2012).

DATA AVAILABILITY STATEMENT

The raw data supporting the conclusions of this article will be made available by the authors, without undue reservation.

REFERENCES

- Cai, B., Seong, K. J., Bae, S. W., Chun, C., Kim, W. J., and Jung, J. Y. (2018). A synthetic diosgenin primary amine derivative attenuates LPS-stimulated inflammation via inhibition of NF- κ B and JNK MAPK signaling in microglial BV2 cells. *Int. Immunopharmacol.* 61, 204–214. doi:10.1016/j.intimp.2018.05.021
- Cao, C., Liu, M., Qu, S., Huang, R., Qi, M., Zhu, Z., et al. (2020). Chinese medicine formula Kai-Xin-San ameliorates depression-like behaviours in chronic unpredictable mild stressed mice by regulating gut microbiota-inflammation-stress system. *J. Ethnopharmacol.* 261, 113055. doi:10.1016/j.jep.2020.113055

ETHICS STATEMENT

The animal study was reviewed and approved by the Animal Experimental Ethics Committee of NJUCM.

AUTHOR CONTRIBUTIONS

YZ and SQ designed the experiments. SQ, CC, ML, QW, X-EM, QL performed the experiments including behavioral tests and biochemical analyses. YS, QW and ZS contributed to the preparation of KXS extracts and chemical standardisation. FH, J-AD and ZH contributed to the writing of introduction and discussion. SQ wrote the main manuscript text and YZ revised the manuscript. All authors have read and approved the submitted manuscript.

FUNDING

This research was supported by the National Natural Science Foundation of China (81673720, 81973591), the Open Project Program of Jiangsu Key Laboratory for High Technology Research of TCM Formulae and Jiangsu Collaborative Innovation Centre of Chinese Medicinal Resources Industrialization (No. FJGJS-2015-10), and the fifth phase of the 333 high-level personnel training project of Jiangsu Province (BRA2017463) to YZ; Innovation projects of scientific research for the graduate student in Jiangsu province to Suchen QU (KYCX20_1598). the 2020 Jiangsu University Students Innovation and Entrepreneurship Training Program Project (202010315043Y) to YS; Suzhou people's livelihood Science and Technology demonstration Project (SS202006) and Jiangsu province official health research project (BJ19009) to FH.

The funders have no role in the design of the study and the collection, analyses, or interpretation of data, in the preparation of the manuscript, or the publication of the results.

SUPPLEMENTARY MATERIAL

The Supplementary Material for this article can be found online at: <https://www.frontiersin.org/articles/10.3389/fphar.2021.626949/full#supplementary-material>.

- Cao, C., Xiao, J., Liu, M., Ge, Z., Huang, R., Qi, M., et al. (2018). Active components, derived from Kai-xin-san, a herbal formula, increase the expressions of neurotrophic factor NGF and BDNF on mouse astrocyte primary cultures via cAMP-dependent signaling pathway. *J. Ethnopharmacol.* 224, 554–562. doi:10.1016/j.jep.2018.06.007
- Cheng, Z., Zhang, M., Ling, C., Zhu, Y., Ren, H., Hong, C., et al. (2019). Neuroprotective effects of ginsenosides against cerebral ischemia. *Molecules* 24, 1102. doi:10.3390/molecules24061102
- Cheong, M. H., Lee, S. R., Yoo, H. S., Jeong, J. W., Kim, G. Y., Kim, W. J., et al. (2011). Anti-inflammatory effects of Polygala tenuifolia root through inhibition of NF- κ B activation in lipopolysaccharide-induced BV2 microglial cells. *J. Ethnopharmacol.* 137, 1402–1408. doi:10.1016/j.jep.2011.08.008

- Dantzer, R. (2018). Neuroimmune interactions: from the brain to the immune system and vice versa. *Physiol. Rev.* 98, 477–504. doi:10.1152/physrev.00039.2016
- Deczkowska, A., Keren-Shaul, H., Weiner, A., Colonna, M., Schwartz, M., and Amit, I. (2018). Disease-associated microglia: a universal immune sensor of neurodegeneration. *Cell* 173, 1073–1081. doi:10.1016/j.cell.2018.05.003
- Degner, D., Grohmann, R., Kropp, S., R  ther, E., Bender, S., Engel, R. R., et al. (2004). Severe adverse drug reactions of antidepressants: results of the German multicenter drug surveillance program AMSPP. *Pharmacopsychiatry* 37 (1), S39–S45. doi:10.1055/s-2004-815509
- Gao, H., Kang, N., Hu, C., Zhang, Z., Xu, Q., Liu, Y., et al. (2020). Ginsenoside Rb1 exerts anti-inflammatory effects in vitro and in vivo by modulating toll-like receptor 4 dimerization and NF-  B/MAPKs signaling pathways. *Phytomedicine* 69, 153197. doi:10.1016/j.phymed.2020.153197
- Gu, H., Wang, C., Li, J., Yang, Y., Sun, W., Jiang, C., et al. (2020). High mobility group box-1-toll-like receptor 4-phosphatidylinositol 3-kinase/protein kinase B-mediated generation of matrix metalloproteinase-9 in the dorsal root ganglion promotes chemotherapy-induced peripheral neuropathy. *Int. J. Cancer* 146, 2810–2821. doi:10.1002/ijc.32652
- Guo, J. Y., Huo, H. R., Li, L. F., Guo, S. Y., and Jiang, T. L. (2009). Sini tang prevents depression-like behavior in rats exposed to chronic unpredictable stress. *Am. J. Chin. Med.* 37, 261–272. doi:10.1142/S0192415X0900693X
- Hong, T., Jin, G. B., Yoshino, G., Miura, M., Maeda, Y., Cho, S., et al. (2002). Protective effects of Polygalae root in experimental TNBS-induced colitis in mice. *J. Ethnopharmacol.* 79, 341–346. doi:10.1016/s0378-8741(01)00399-3
- Jia, K. K., Zheng, Y. J., Zhang, Y. X., Liu, J. H., Jiao, R. Q., Pan, Y., et al. (2017). Banxia-houpu decoction restores glucose intolerance in CUMS rats through improvement of insulin signaling and suppression of NLRP3 inflammasome activation in liver and brain. *J. Ethnopharmacol.* 209, 219–229. doi:10.1016/j.jep.2017.08.004
- Jing, L. L., Zhu, X. X., Lv, Z. P., and Sun, X. G. (2015). Effect of Xiaoyaosan on major depressive disorder. *Chin. Med.* 10, 18. doi:10.1186/s13020-015-0050-0
- Kang, A., Hao, H., Zheng, X., Liang, Y., Xie, Y., Xie, T., et al. (2011). Peripheral anti-inflammatory effects explain the ginsenosides paradox between poor brain distribution and anti-depression efficacy. *J. Neuroinflammation* 8, 100. doi:10.1186/1742-2094-8-100
- Kang, A., Xie, T., Zhu, D., Shan, J., Di, L., and Zheng, X. (2017). Suppressive effect of ginsenoside Rg3 against lipopolysaccharide-induced depression-like behavior and neuroinflammation in mice. *J. Agric. Food Chem.* 65, 6861–6869. doi:10.1021/acs.jafc.7b02386
- Kim, S. M., McIlwraith, E. K., Chalmers, J. A., and Belsham, D. D. (2018). Palmitate induces an anti-inflammatory response in immortalized microglial BV-2 and IMG cell lines that decreases TNF   levels in mHypoE-46 hypothalamic neurons in Co-culture. *Neuroendocrinology* 107, 387–399. doi:10.1159/000494759
- Li, Y., Liang, W., Guo, C., Chen, X., Huang, Y., Wang, H., et al. (2020). Renshen Shouwu extract enhances neurogenesis and angiogenesis via inhibition of TLR4/NF-  B/NLRP3 signaling pathway following ischemic stroke in rats. *J. Ethnopharmacol.* 253, 112616. doi:10.1016/j.jep.2020.112616
- Li, Y., Sun, Y., Ma, X., Xue, X., Zhang, W., Wu, Z., et al. (2013). Effects of Sini San used alone and in combination with fluoxetine on central and peripheral 5-HT levels in a rat model of depression. *J. Tradit. Chin. Med.* 33, 674–681. doi:10.1016/s0254-6272(14)60041-8
- Lim, H. W., Kumar, H., Kim, B. W., More, S. V., Kim, I. W., Park, J. I., et al. (2014).   -Asarone (cis-2,4,5-trimethoxy-1-allyl phenyl), attenuates pro-inflammatory mediators by inhibiting NF-  B signaling and the JNK pathway in LPS activated BV-2 microglia cells. *Food Chem. Toxicol.* 72, 265–272. doi:10.1016/j.fct.2014.07.018
- Liu, H. J., Lai, X., Xu, Y., Miao, J. K., Li, C., Liu, J. Y., et al. (2017).   -Asarone attenuates cognitive deficit in a pilocarpine-induced status epilepticus rat model via a decrease in the nuclear factor-  B activation and reduction in microglia neuroinflammation. *Front. Neurol.* 8, 661. doi:10.3389/fneur.2017.00661
- Ma, X. J., Zhao, J., Feng, Z. Y., Chang, J. M., Meng, S., Liu, H. Z., et al. (2014). Effects of modified Ganmai Dazao decoction on neuroendocrine system in patients with climacteric depression. *Zhongguo Zhong Yao Za Zhi* 39, 4680–4684.
- Malhi, G. S., and Mann, J. J. (2018). Depression. *Lancet* 392, 2299–2312. doi:10.1016/S0140-6736(18)31948-2
- Otte, C., Gold, S. M., Penninx, B. W., Pariante, C. M., Etkin, A., Fava, M., et al. (2016). Major depressive disorder. *Nat. Rev. Dis. Primers* 2, 16065. doi:10.1038/nrdp.2016.65
- Pape, K., Tamouza, R., Leboyer, M., and Zipp, F. (2019). Immunoneuropsychiatry—novel perspectives on brain disorders. *Nat. Rev. Neurol.* 15, 317–328. doi:10.1038/s41582-019-0174-4
- Qi, F. H., Wang, Z. X., Cai, P. P., Zhao, L., Gao, J. J., Kokudo, N., et al. (2013). Traditional Chinese medicine and related active compounds: a review of their role on hepatitis B virus infection. *Drug Discov. Ther.* 7, 212–224. doi:10.5582/ddt.2013.v7.6.212
- R  os, J. L. (2011). Chemical constituents and pharmacological properties of *Poria cocos*. *Planta. Med.* 77, 681–691. doi:10.1055/s-0030-1270823
- Shuto, T., Kuroiwa, M., Sotogaku, N., Kawahara, Y., Oh, Y. S., Jang, J. H., et al. (2020). Obligatory roles of dopamine D1 receptors in the dentate gyrus in antidepressant actions of a selective serotonin reuptake inhibitor, fluoxetine. *Mol. Psychiatry* 25, 1229–1244. doi:10.1038/s41380-018-0316-x
- Su, F., Yi, H., Xu, L., and Zhang, Z. (2015). Fluoxetine and S-citalopram inhibit M1 activation and promote M2 activation of microglia in vitro. *Neuroscience* 294, 60–68. doi:10.1016/j.neuroscience.2015.02.028
- Su, Y., Ko, M. E., Cheng, H., Zhu, R., Xue, M., Wang, J., et al. (2020). Multi-omic single-cell snapshots reveal multiple independent trajectories to drug tolerance in a melanoma cell line. *Nat. Commun.* 11, 2345. doi:10.1038/s41467-020-15956-9
- Tunc-Ozcan, E., Peng, C. Y., Zhu, Y., Dunlop, S. R., Contractor, A., and Kessler, J. A. (2019). Activating newborn neurons suppresses depression and anxiety-like behaviors. *Nat. Commun.* 10, 3768. doi:10.1038/s41467-019-11641-8
- Wei, S. S., Yang, H. J., Huang, J. W., Lu, X. P., Peng, L. F., and Wang, Q. G. (2016). Traditional herbal formula Sini Powder extract produces antidepressant-like effects through stress-related mechanisms in rats. *Chin. J. Nat. Med.* 14, 590–598. doi:10.1016/S1875-5364(16)30069-3
- Xiaoling, Z., Yunping, H., and Yingdong, L. (2018). Analysis of curative effect of fluoxetine and escitalopram in the depression treatment based on clinical observation. *Pak J. Pharm. Sci.* 31, 1115–1118.
- Xu, J. N., Chen, L. F., Su, J., Liu, Z. L., Chen, J., Lin, Q. F., et al. (2018). The anxiolytic-like effects of ginsenoside Rg3 on chronic unpredictable stress in rats. *Sci. Rep.* 8, 7741. doi:10.1038/s41598-018-26146-5
- Xue, W., Zhou, X., Yi, N., Jiang, L., Tao, W., Wu, R., et al. (2013). Yueju pill rapidly induces antidepressant-like effects and acutely enhances BDNF expression in mouse brain. *Evid. Based Complement. Alternat. Med.* 2013, 184367. doi:10.1155/2013/184367
- Yirmiya, R., Rimmerman, N., and Reshef, R. (2015). Depression as a microglial disease. *Trends Neurosci.* 38, 637–658. doi:10.1016/j.tins.2015.08.001
- Zhan, C. E., Chen, J. Y., and Pan, F. (2004). Effect of modified chaihushugan powder in treating patients with functional dyspepsia accompanied with depression. *Zhongguo Zhong Xi Yi Jie He Za Zhi* 24, 1119–1121.
- Zhu, K. Y., Mao, Q. Q., Ip, S. P., Choi, R. C., Dong, T. T., Lau, D. T., et al. (2012). A standardized chinese herbal decoction, kai-xin-san, restores decreased levels of neurotransmitters and neurotrophic factors in the brain of chronic stress-induced depressive rats. *Evid Based Complement Alternat Med* 2012, 149256. doi:10.1155/2012/149256
- Zhu, Y., Chao, C., Duan, X., Cheng, X., Liu, P., Su, S., et al. (2017). Kai-Xin-San series formulae alleviate depressive-like behaviors on chronic mild stressed mice via regulating neurotrophic factor system on hippocampus. *Sci. Rep.* 7, 1467. doi:10.1038/s41598-017-01561-2
- Zhang, Q., Lenardo, M. J., and Baltimore, D. (2017). 30 Years of NF-  B: a Blossoming of relevance to human pathobiology. *Cell* 168, 37–57. doi:10.1016/j.cell.2016.12.012

Conflict of Interest: The authors declare that the research was conducted in the absence of any commercial or financial relationships that could be construed as a potential conflict of interest.

Copyright    2021 Qu, Liu, Cao, Wei, Meng, Lou, Wang, Li, She, Wang, Song, Han, Zhu, Huang and Duan. This is an open-access article distributed under the terms of the Creative Commons Attribution License (CC BY). The use, distribution or reproduction in other forums is permitted, provided the original author(s) and the copyright owner(s) are credited and that the original publication in this journal is cited, in accordance with accepted academic practice. No use, distribution or reproduction is permitted which does not comply with these terms.



Corynoxine Protects Dopaminergic Neurons Through Inducing Autophagy and Diminishing Neuroinflammation in Rotenone-Induced Animal Models of Parkinson's Disease

Leilei Chen^{1,2,3*}, Yujv Huang^{1,2,3}, Xing Yu⁴, Jiahong Lu⁵, Wenting Jia^{1,2,3}, Juxian Song^{4,6}, Liangfeng Liu⁴, Youcui Wang^{1,2,3}, Yingyu Huang⁴, Junxia Xie^{1,2,3*} and Min Li^{4*}

¹Institute of Brain Science and Disease, Qingdao University, Qingdao, China, ²Shandong Provincial Collaborative Innovation Center for Neurodegenerative Disorders, Qingdao University, Qingdao, China, ³Shandong Provincial Key Laboratory of Pathogenesis and Prevention of Neurological Disorders, Qingdao University, Qingdao, China, ⁴Mr. and Mrs. Ko Chi Ming Centre for Parkinson's Disease Research, School of Chinese Medicine, Hong Kong Baptist University, Kowloon Tong, Hong Kong, ⁵State Key Laboratory of Quality Research in Chinese Medicine, Institute of Chinese Medical Sciences, University of Macau, Macau, China, ⁶Medical College of Acupuncture-Moxibustion and Rehabilitation, Guangzhou University of Chinese Medicine, Macau, China

OPEN ACCESS

Edited by:

Luca Rastrelli,
University of Salerno, Italy

Reviewed by:

Betty Yuen Kwan Law,
Macau University of Science and
Technology, Macau
Ina Yosifova Aneva,
Bulgarian Academy of Sciences,
Bulgaria

*Correspondence:

Leilei Chen
leileichen2019@qdu.edu.cn
Junxia Xie
jiaxie@163.com
Min Li
limin@hkbu.edu.hk

Specialty section:

This article was submitted to
Ethnopharmacology,
a section of the journal
Frontiers in Pharmacology

Received: 17 December 2020

Accepted: 10 February 2021

Published: 13 April 2021

Citation:

Chen L, Huang Y, Yu X, Lu J, Jia W, Song J, Liu L, Wang Y, Huang Y, Xie J and Li M (2021) Corynoxine Protects Dopaminergic Neurons Through Inducing Autophagy and Diminishing Neuroinflammation in Rotenone-Induced Animal Models of Parkinson's Disease. *Front. Pharmacol.* 12:642900. doi: 10.3389/fphar.2021.642900

Recent studies have shown that impairment of autophagy is related to the pathogenesis of Parkinson's disease (PD), and small molecular autophagy enhancers are suggested to be potential drug candidates against PD. Previous studies identified corynoxine (Cory), an oxindole alkaloid isolated from the Chinese herbal medicine *Uncaria rhynchophylla* (Miq.) Jacks, as a new autophagy enhancer that promoted the degradation of α -synuclein in a PD cell model. In this study, two different rotenone-induced animal models of PD, one involving the systemic administration of rotenone at a low dosage in mice and the other involving the infusion of rotenone stereotactically into the *substantia nigra* pars compacta (SNpc) of rats, were employed to evaluate the neuroprotective effects of Cory. Cory was shown to exhibit neuroprotective effects in the two rotenone-induced models of PD by improving motor dysfunction, preventing tyrosine hydroxylase (TH)-positive neuronal loss, decreasing α -synuclein aggregates through the mechanistic target of the rapamycin (mTOR) pathway, and diminishing neuroinflammation. These results provide preclinical experimental evidence supporting the development of Cory into a potential delivery system for the treatment of PD.

Keywords: parkinson's disease, corynoxine, rotenone, autophagy, α -synuclein, neuroinflammation

INTRODUCTION

Parkinson's disease (PD) is the second most common neurodegenerative disease, affecting more than 1% of the population over the age of 60 years. In 2005, it was predicted that the number of individuals (age > 50 years) with PD would double by 2030, and this number increased by approximately 10% in 2018 (Rossi et al., 2018). Usually, both selective degeneration of dopaminergic neurons in the *substantia nigra* pars compacta (SNpc) and the appearance of Lewy bodies, whose main component is aggregated α -synuclein, in the remaining neurons are thought to be the major pathological

hallmarks of PD (Przedborski, 2017; Johnson et al., 2019). Although the pathogenic factors of PD have been comprehensively investigated since the first detailed description by James Parkinson in 1817, the pathogenesis of this disease has not been fully elucidated and there are no effective drugs for its cure.

The autophagy-lysosome pathway is one of the major pathways that clear disordered, especially long-lived proteins, such as α -synuclein (Hou et al., 2020). Impaired autophagy is thought to exacerbate the aggregation of α -synuclein, thereby contributing to the pathological development of PD in patients and animal models (Xilouri et al., 2016; Chen et al., 2019; Hou et al., 2020). Therefore, autophagy enhancers, which could promote the clearance of aggregated α -synuclein, are suggested to be a new therapeutic measure for PD. A previous study conducted by our research group identified corynoxine (Cory), an indole alkaloid isolated from the Chinese herb *Uncaria rhynchophylla* (Chen et al., 2014; Chen et al., 2017), as a new autophagy enhancer that promoted the clearance of α -synuclein in a cell model of PD. However, the microenvironment between *in vitro* and *in vivo* cells is quite different, and the information obtained from cells models is limited. Therefore, it is necessary to evaluate the neuroprotective properties of Cory in animal models of PD prior to commencing clinical trials.

The impairment of mitochondrial complex I was reported to be a major factor that contributed to neurodegeneration (Betarbet et al., 2000). Consequently, inhibitors of mitochondrial complex I, such as rotenone (Xiong et al., 2012; Miyazaki et al., 2020), are widely used to reproduce Parkinson-like symptoms in animals. In this study, two animal models of PD were employed, one of which involved stereotactically injecting rotenone into the SNpc of rats to establish rat models of PD with acute toxicity (Xiong et al., 2009; Anusha et al., 2017), and the other one involved systemically exposing C57BL/6J mice to a low dose of rotenone to establish mouse models of PD with chronic toxicity (Miyazaki et al., 2020). The neuroprotective effects of Cory in the two PD models were evaluated, and the results provided experimental evidence to support the development of Cory for use in the treatment of PD.

MATERIALS AND METHODS

Reagents

Apomorphine (Y0001465) and rotenone (R8875) were purchased from Sigma; Cory was purchased from Aktin Chemicals Inc. (Chengdu, China); anti-TH antibody (AB152) was purchased from Merck Millipore; anti-Iba-1 (019-19741) was purchased from Wako Pure Chemical Industries; anti- β -actin (sc-47778) was purchased from Santa Cruz Biotechnology; anti-LC3 (2775), anti-p62 (5114), anti-phospho-p70S6K (Thr389) (9234), anti-phospho-mTOR (Ser2448) (2971), and anti- α -syn (2628) were purchased from Cell Signaling Technology; goat anti-rabbit IgG (H + L) secondary antibody, Alexa Fluor® 594 conjugate (R37117), goat anti-mouse (626520), and goat anti-rabbit (G21234) secondary antibodies were purchased from Invitrogen; and VECTASTAIN Elite ABC Kit (PK-6101) was

purchased from Vector Lab. ELISA kits were purchased from Beijing 4A Biotech Co., Ltd.

Animals

C57BL/6J mice (25~30 g) and SD rat (220~250 g) were purchased from Beijing Weitong Lihua Experimental Animal Technology Co., Ltd.

Dopamine Level Detection

Detection of the dopamine level in the striatum is followed with previous report (Li et al., 2018). Briefly, striatum was weighted and homogenized in 0.5 ml ice cold 0.1 M HCl, 30 s, 50 Hz. After adding 1 ml methanol with 0.1 M HCl, homogenization was performed at 50 Hz, 1 min. Lysates were centrifuged 16,000 rpm, for 10 min at 4°C. 1 ml supernatant was taken out to freeze-dry for 48 h. Then, 30 μ l 0.1 M HCl was added to dissolve the sample. 70 μ l methanol with 0.1 M HCl was added to precipitate the protein. Centrifugation with 16,000 rpm for 10 min at 4°C was performed. The supernatant was subject to be analyzed with liquid chromatography (Agilent 1290, San Jose, CA, United States) coupled with electrospray ionization on a triple quadrupole mass spectrometer (Agilent 6460, San Jose, CA, United States).

TH Immunostaining

The protocol is followed the VECTASTAIN Elite ABC Kit. Working solution was prepared before staining. Frozen brain sections (SNpc: 30 μ m, striatum: 25 μ m) were prepared with Cryostat Series (7721.160 GB, SHANDON). Sections were rinsed with PBS for 3 times (3 min/time). After incubating with 3% H₂O₂ for 10 min, sections were rinsed with PBS for another 3 times (3 min/time). Then, sections were blocked with normal serum for 30 min, and rinsed with PBS for 3 times (3 min/time). Sections were incubated with primary antibody (1:500) overnight at 4°C. Then, after rinsing with PBS for 3 times (3 min/time), sections were incubated with Elite second antibody for 30 min at room temperature. After rinsing with PBS for 3 times (3 min/time), sections were incubated with Elite ABC reagent for another 30 min at room temperature. Sections were rinsed with PBS for 3 times (3 min/time), and incubated with DAB reagent for 2 min. At last, the slides were mounted and images were taken with confocal.

Fluoresce Immunostaining

Working solution was prepared before staining. Frozen brain sections (SNpc: 30 μ m, striatum: 25 μ m) were prepared with Cryostat Series (7721.160 GB, SHANDON). Sections were rinsed with PBS for 3 times (3 min/time). After incubating with 3% H₂O₂ for 10 min, sections were rinsed with PBS for 3 times (3 min/time). Sections were blocked with normal serum for 30 min and rinsed with PBS for 3 times (3 min/time). Sections were incubated with primary antibody overnight at 4°C. Then, sections were rinsed with PBS for 3 times (3 min/time) and incubated them with Alexa Fluor 594 s antibody for 30 min at room temperature. At last, sections were rinsed with PBS for 3 times (3 min/time), slides were mounted, and images were taken with confocal.

TABLE 1 | Experiment data of Cory acute toxicity.

Test sequence	Animal ID	Dose (mg/kg)	Short-term result	Long-term result
1	1	80	O	O
2	2	105	X	X
3	3	80	O	O
4	4	105	X	X
5	5	80	O	O

O, survived; X, died; short-term, 48 h; long-term, 14 days.

Western Blotting Analysis

Tissues were lysed with RIPA lysis buffer (150 mM NaCl, 50 mM Tris-HCl, 0.35% sodium deoxycholate, 1 mM EDTA, 1% NP40, 1 mM PMSF, 5 mg/ml aprotinin, and 5 mg/ml leupeptin). The boiled samples (each containing 10–20 µg of protein) were subjected to SDS-PAGE on a 10–15% acrylamide gel and transferred to PVDF membranes (GE Healthcare, RPN303F). The membranes were blocked for 1 h in TBST containing 5% nonfat milk and then probed with the appropriate primary and secondary antibodies. The desired bands were visualized using the ECL kit (Pierce, 32106). The band density was quantified using the ImageJ program and normalized to that of the control group.

Statistical Analysis

Statistical significance was assessed by using one-way ANOVA with the Newman–Keuls' multiple comparison tests. Calculations were performed using ImageJ and Prism (version 5) software. Statistical significance was considered when $p < 0.05$.

RESULTS

Determining the Toxicity of Cory

At the beginning of this study, an acute toxicity study was performed to confirm the safe dosage of Cory. Five female Sprague–Dawley (SD) rats (8 weeks old) weighing 200 ± 10 g were used in the study. The rats were placed separately in laboratory animal houses at 20–25°C with 50–60% humidity and 12 h light/dark cycle with the lights off at 7 PM. The rats were fed with standard diet from Lab Diet, allowed to access distilled water ad libitum, and acclimated to laboratory conditions for 7 days. Test up-and-down procedure followed the OECD guideline. Acute Oral Toxicity (Guideline 425) Statistical Program (AOT425StatPgm) developed by the US Environmental Protection Agency was used. The assumed dose progression factor of 1.2 was used in the study. Whether the dosing will continue depends on the 48-h outcomes after dosing. Test will be stopped when one of the following stopping criteria first is met: 1) 3 consecutive animals survive at the upper bound; 2) 5 reversals occur in any 6 consecutive animals tested; or 3) at least 4 animals have followed the first reversal and the specified likelihood ratios exceed the critical value.

Cory was directly dissolved in the normal saline. The final injection volume for each rat was 1.0 ml. Before dosing, each rat was fasted overnight. It has been reported that the intravenous

(IV) dose required to kill half the members of a tested population after a specified test duration (LD_{50}) of rhynchophylline, which is an isomer of Cory, is 105 mg/kg in mice (Ozaki, 1989). Therefore, based on this information, the limit test using a dosage of 2000 mg/kg was skipped, and the main test with first dosage of 80 mg/kg was performed immediately. The data generated from this study (Table 1) show that the IV LD_{50} of Cory in rats was approximately 96.89 mg/kg, which was calculated by the Acute Oral Toxicity (Guideline 425) Statistical Program (AOT425StatPgm).

Establishing the Rotenone-Induced Acute and Chronic Toxicity Models of PD

In this study, both the rotenone-induced acute toxicity rat model and rotenone-induced chronic toxicity mouse models of PD were employed to evaluate the neuroprotective effects of Cory. The classic mTOR inhibitor, rapamycin, acted as a positive control of autophagy induction, and Sinemet® and Madopar®, which are widely used in clinical practice (Chen and Xie, 2018a), acted as positive controls for the treatment of PD. Every tablet of Sinemet® contains 200 mg of levodopa and 50 mg of carbidopa, and every tablet of Madopar® contains 200 mg of levodopa and 50 mg of benserazide.

The rotenone-induced acute toxicity rat models of PD were established in male SD rats that were 8 weeks old. The SD rats were randomly divided into 5 groups (16 rats/group). The detailed groups were as follows: vehicle control group (Vehicle group), rotenone-induced PD rat group (Rotenone group, 3 µg/µl * 1 µl), Sinemet® group (Rot + Sinemet group, 0.975 mg Sinemet/rat), low-dose Cory group (Rot + Cory-L, 2.5 mg/kg), and high-dose Cory group (Rot + Cory-H group, 5 mg/kg). Rotenone (3 µg/µl) was dissolved in dimethyl sulfoxide (DMSO) and was kept away from light before use. According to Bao's rat cerebral stereotaxic atlas, rotenone (1 µl) was injected into the right-side substantia nigra compacta (SNpc) (AP: −5.3 mm; ML: 2.0 mm; DV: −8.0 mm). The Sham/Vehicle group was injected with the same amount of DMSO. Cory or Sinemet® was orally administered to the rats based on their group allocations. Before the injection of rotenone, rats were pretreated with Cory or Sinemet® for 1 week, and the treatment was continued for 4 weeks after the model was established.

The chronic toxicity models of PD were established in 10-week-old male C57BL/6J mice that were orally administered with rotenone for 8 weeks. The C57BL/6J mice were randomly divided into 6 groups (20 mice/group). The detailed groups were as

follows: the vehicle control group (Vehicle group), rotenone-induced PD mice group (Rotenone group, 30 mg/kg), Madopar® group (Rot + Madopar group, 1.95 mg Madopar/mouse), rapamycin group (Rot + Rapamycin group, 10 mg/kg), low-dose Cory group (Rot + Cory-L, 5 mg/kg), and high-dose Cory group (Rot + Cory-H group, 10 mg/kg). All of the drugs or compounds, including Cory, were orally administered to the C57BL/6J mice. Before the administration of rotenone, the mice were pretreated with Madopar®, rapamycin, or Cory for 1 week, and the administration coupled with rotenone was continued for another 8 weeks.

Effects of Cory on Motor Dysfunction in the Rotenone-Induced Animal Models of PD

Apomorphine is a nonselective dopamine agonist that activates both D1-like and D2-like receptors, and apomorphine-induced rotation in a rat model of PD is usually used to estimate the motor impairment (Xiong et al., 2009; Carbone et al., 2019; Gunaydin et al., 2019). At the end of the fourth week after rotenone-induced rat models of PD were established, a rotation test induced by apomorphine was performed. Totally, 2.5 mg/kg of apomorphine (i.p.) was intraperitoneally injected, and 35 min of video footage was recorded for each rat. After 5 min of adaptation, rotations were calculated for 30 min. In the rotenone-induced rat model group, the number of rotations induced by apomorphine significantly increased and reached 320 per 30 min. Similar to Sinemet® treatment, both low and high doses of Cory significantly decreased the rotations (Figure 1A). At the end of the eighth week after rotenone-induced mouse models of PD were established (chronic toxicity models), both the rotarod test and the pole test were performed, and the latency time on the rotarod, locomotion activity time, and time to turn on the pole were recorded. The movement time on the rotating rod was significantly shortened in the rotenone group than in the vehicle control group (Figure 1C), and both the climbing time and turning time on the pole were significantly longer in the rotenone group than in the vehicle control group (Figure 1D). Confirming its validity as a widely used drug for the treatment of PD, treatment in clinic, Madopar® significantly improved the motor dysfunction induced by rotenone as shown by the increased latency time on the rotarod, decreased locomotion activity time, and decreased turning time (Figures 1C,D). Cory also contributed toward motor improvements with increased latency time on the rotarod and decreased turning time, although there was no significant difference in the locomotion activity time between the Cory-treated and rotenone groups (Figures 1C–E). At the same time, striatal dopamine levels decrease in both rotenone-induced rat and mouse models (Figures 1B–F). Supplementary of levodopa, which is a precursor of dopamine, significantly increased the dopamine levels in the striatum of the animals in the Sinemet® and Madopar® groups compared to the levels in the animals in the rotenone groups. In addition, a high dose of Cory increased the striatal dopamine levels in the rotenone-induced rat models of PD (Figure 1B), while both the low and high doses of Cory increased striatal dopamine levels in the rotenone-induced mouse models of PD (Figure 1F).

Effects of Cory on Tyrosine Hydroxylase-Positive Neuronal Loss in the Rotenone-Induced Animal Models of PD

TH is the enzyme responsible for catalyzing the conversion of the amino acid L-tyrosine to L-3, 4-dihydroxyphenylalanine (Nagatsu, 1995). It is a rate-limiting enzyme that controls the first step of dopamine biosynthesis. The expression of TH in the right-side brain tissue of SNpc was detected by Western blotting, and the quantification density of TH was analyzed by image J. Lower expression of TH was observed in the right side of SNpc in the rotenone group than in the vehicle group (Figures 2B,C), while Cory significantly increased the levels of TH in these models (Figures 2B,C). Consistent with the Western blotting results, significant loss of TH-positive neurons was found in the right-side brain tissue of the SNpc and striatum in the rotenone-induced rat models (Figure 2A, Supplementary Figure S1). However, the loss of TH-positive neurons in the SNpc and striatum was diminished by treatment with Cory (Figure 2A, Supplementary Figure S1). In the rotenone-induced chronic toxicity mouse models of PD, immunostaining results revealed that rotenone also induced a TH-positive neuronal loss in the SNpc compared to the vehicle group, and Madopar® and Cory showed neuroprotective effects that prevented TH-positive neuronal loss (Figures 2D–E).

Effect of Cory on Autophagy Induction and Neuroinflammation in Rotenone-Induced Animal Models of PD

Prior to conducting the neuroprotective mechanism study, an herbal search of Cory was performed on the SymMap database (<http://www.symmap.org/>). The search generated 130 Cory-related symptoms and 1700 targets. Since it has been deduced that Cory can promote the clearance of α -synuclein through the autophagy pathway in a cell model of PD, the symptoms of PD and targets involved in autophagy, including CSTB, HSPA5, PRKCA, and AHSA1, as well as targets involved in neuroinflammation, including TNF, IL-6, IL1B, and IL1A, were all selected from the SymMap integrated network, which indicated the neuroprotective mechanism of Cory in PD (Figure 3).

In the acute toxicity rat models of PD induced by rotenone, immunostaining results on the brain tissue revealed that the number of α -synuclein aggregates significantly increased in the right side of the SNpc, while the number of α -synuclein aggregates significantly decreased after treatment with Cory (Figures 4A,B). The expression levels of α -synuclein in the right-side brain tissue of SNpc, which were detected by Western blotting, were consistent with the immunostaining results (Figures 4C,D). However, no significant aggregates of α -synuclein were found in the striatum of rats (Supplementary Figure S2). Moreover, the autophagy marker proteins, including LC3 and p62, were detected using Western blotting, with significantly increased p62 levels being observed in the right-side tissue of SNpc in the rotenone group (Figures 4E,G). When compared to the

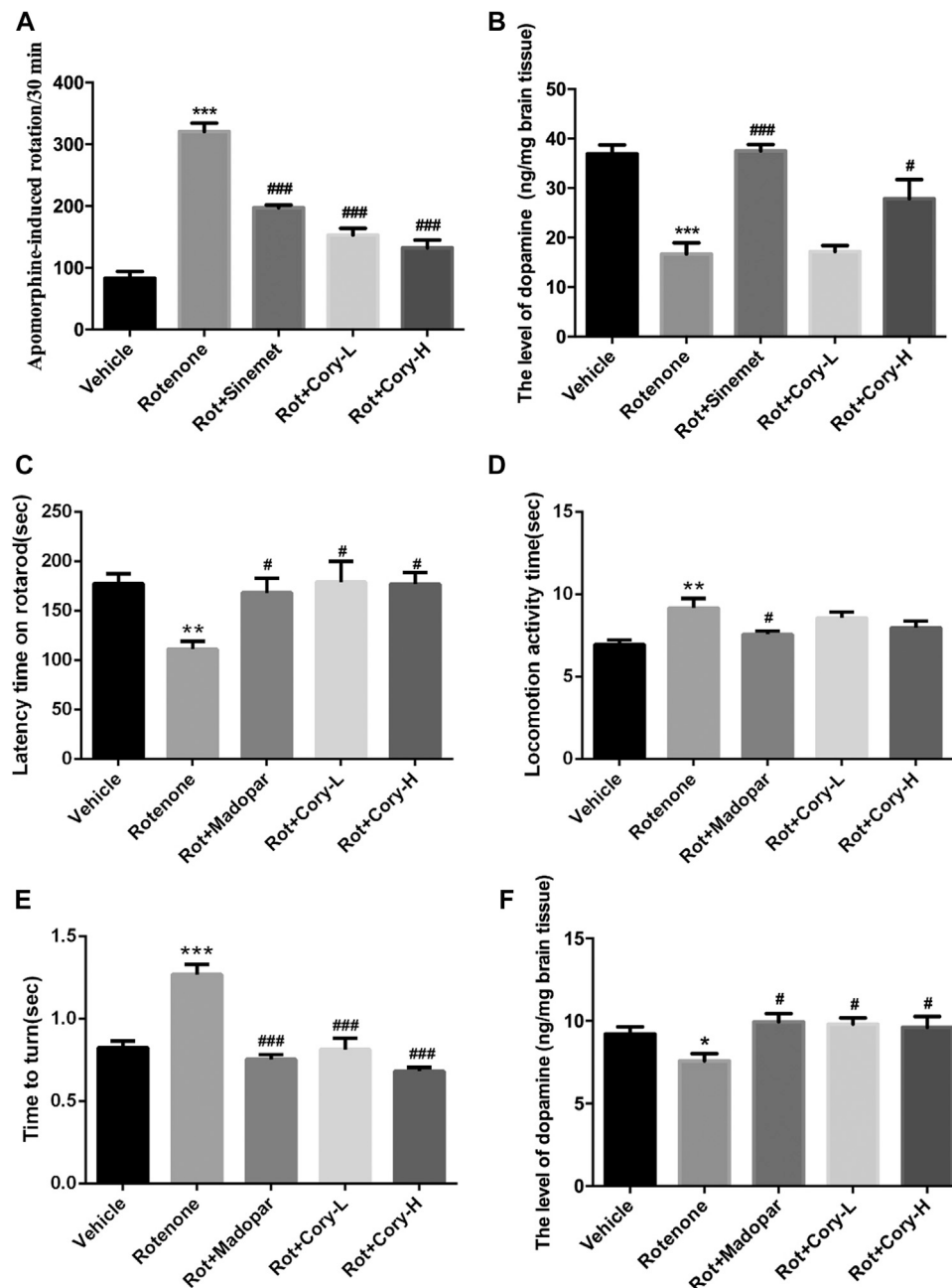


FIGURE 1 | Cory improves the motor dysfunction and increases the striatal dopamine level in the rotenone-induced rat and mice models. **(A–B)** Tests in the rotenone-induced rat model of PD, and **(C–F)** tests in the rotenone-induced mice model of PD. **(A)** Rotation test induced by apomorphine (2.5 mg/kg) was performed at the end of the fourth week after rotenone rat model establishment. Rotations of 30 min were totaled. Cory increases the level of dopamine in the striatum in both of the PD rat **(B)** and mice **(F)** models. In the rotarod test, Cory increases the movement time of rotenone-induced PD mice maintained on the rotarod **(C)**. In the pole test, although the effect of Cory to shorten the locomotion activity time is not significant **(D)**, Cory significantly shortens the turning time **(E)**. Dosage of Cory in the rotenone-induced rat model of PD: Cory-L: 2.5 mg/kg, Cory-H: 5 mg/kg. Dosage of Cory in the rotenone-induced mice model of PD: Cory-L: 5 mg/kg, Cory-H: 10 mg/kg. Data were presented as mean \pm SEM. (* $p < 0.05$, *** $p < 0.001$ compared with the Sham or Vehicle group, # $p < 0.05$, ### $p < 0.001$ compared with the Rotenone group, $n \geq 6$; one-way ANOVA with Newman–Keuls' multiple test.)

vehicle or rotenone group, Cory increased the level of LC3II and decreased the levels of p62, indicating that Cory was responsible for the induction of the autophagy pathway (Figures 4E–G, Supplementary Figure S3). Furthermore,

decreased p-mTOR and p-p70 levels (Figures 4H–J) were observed in the Cory treatment groups, indicating that Cory induces autophagy through the mTOR pathway in the rotenone-induced rat models of PD.

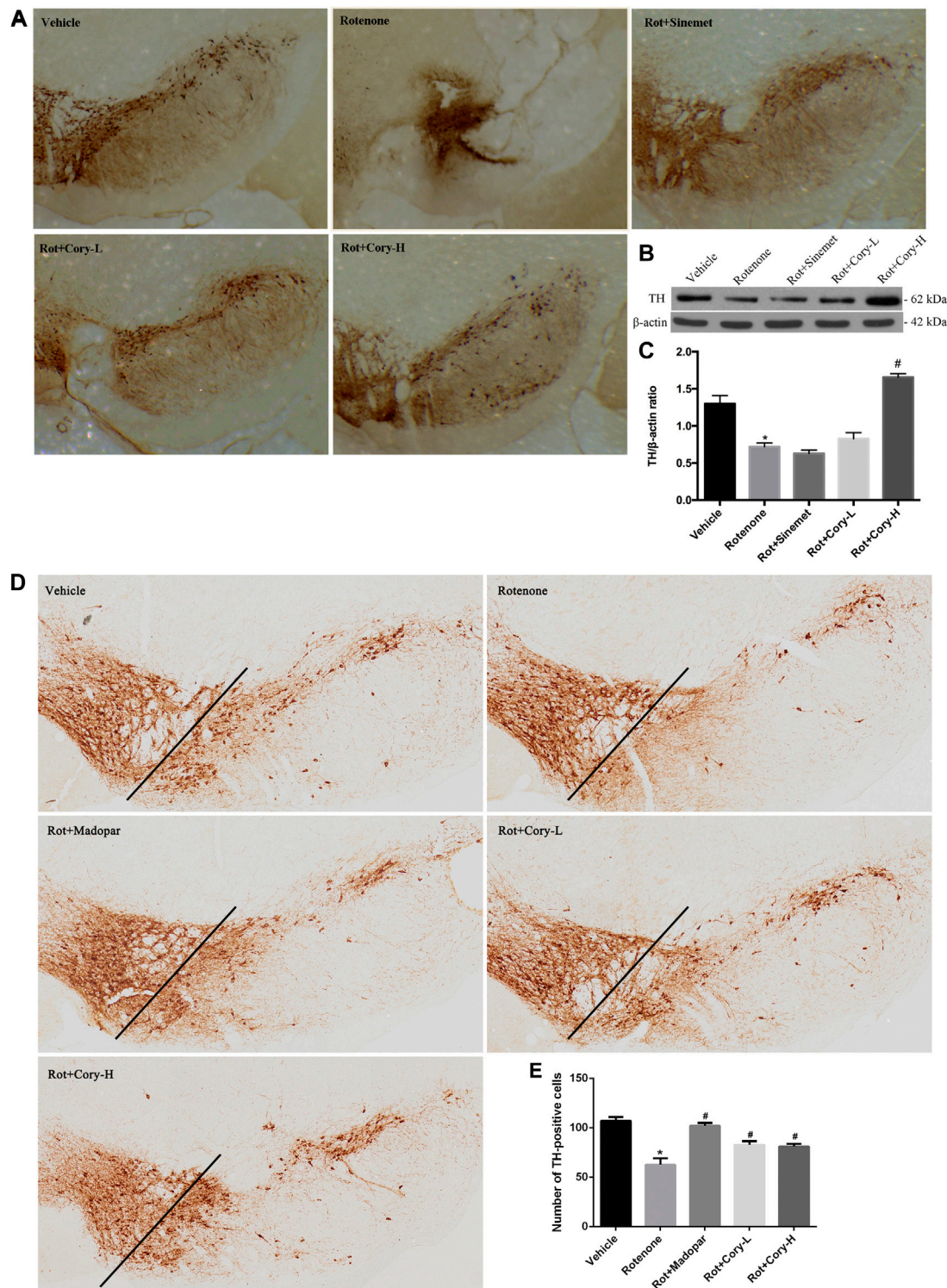


FIGURE 2 | Cory prevents the loss of tyrosine hydroxylase-positive neurons in the SNpc. **(A–C)** Tests in the rotenone-induced rat model of PD, and **(D–E)** tests in the rotenone-induced mice model of PD. Immunostaining results reveal that Cory prevents the loss of tyrosine hydroxylase-positive neurons in the SNpc of the PD rat **(A)** and mice **(D–E)** models. **(B, C)** Cory increases the level of tyrosine hydroxylase. The right side of SNpc was isolated from the brain tissue of the PD rat model. After protein extraction, samples were subjected to Western blotting assay. Dosage of Cory in the rotenone-induced rat model of PD: Cory-L: 2.5 mg/kg, Cory-H: 5 mg/kg. Dosage of Cory in the rotenone-induced mice model of PD: Cory-L: 5 mg/kg, Cory-H: 10 mg/kg. Data were presented as mean \pm SEM. (* $p < 0.05$ compared with Sham or Vehicle group, # $p < 0.05$ compared with the Rotenone group, $n \geq 6$; one-way ANOVA with Newman-Keuls' multiple test.)

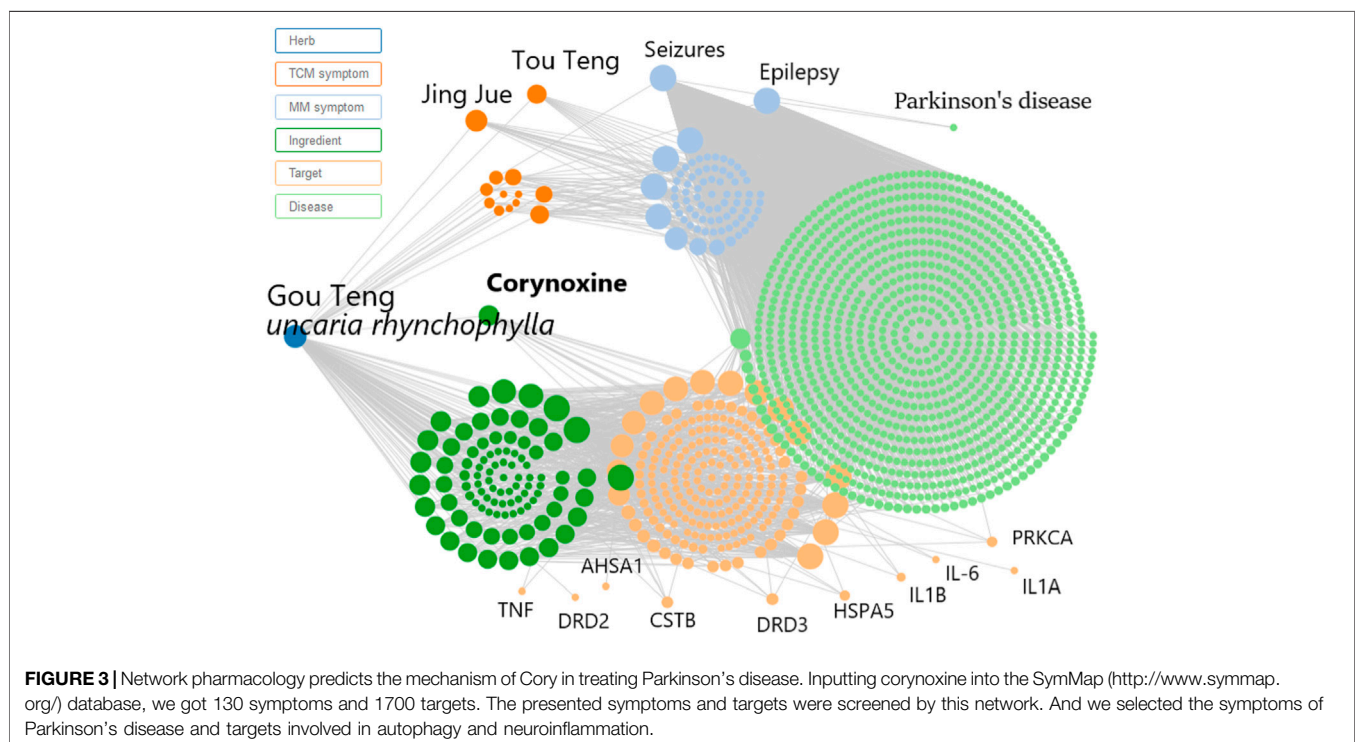
Neuroinflammation, which is characterized by the activation of glial cells and release of pro-inflammatory cytokines, is considered as a detrimental factor in PD. In this study, immunostaining was performed on the brain sections from the SNpc region using the Iba-1 antibody, a marker of microglial cells. The rotenone groups of the two PD models had significantly higher number of active microglial cells than the Vehicle groups (Figures 5A–D). However, after treatment with Cory, the active microglial cells were in the former groups (Figures 5A–D). The level of pro-inflammatory cytokines that were indicated in Figure 3, such as TNF and IL-6, was also detected. In the rotenone-induced chronic toxicity mouse models, the levels of TNF- α significantly increased in the rotenone group, and a high dose of Cory decreased the levels of TNF- α in the serum (Figure 5E). Furthermore, overexpression of α -synuclein induced by doxycycline increased the release of IL-8, and Cory was shown to inhibit an inflammatory response induced by doxycycline in inducible PC12 cells (Figure 5F). However, no significant change of IL-6 release was observed in the inducible PC12 cells (Supplementary Figure S4). The aforementioned results indicate that Cory diminishes neuroinflammation in the mouse and cell models of PD.

DISCUSSION

In the year 2000, rotenone was first reported to show features of PD following chronic systemic exposure (Betarbet et al., 2000). These effects were reported to be similar to those produced by 1-methyl-4-phenyl-1,2,3,6-tetrahydropyridine (MPTP), and since then, animal models induced by

rotenone have been investigated. Due to the lipophilic nature, rotenone crosses the blood–brain barrier and cell membranes with relative ease in comparison to MPTP. The behavioral, central, and peripheral neurodegenerative features of PD, such as dopaminergic neuronal cell loss in the SNpc, lesioned nerve terminals in the striatum, as well as increased α -synuclein aggregates in the SNpc, dorsal motor nucleus of the vagus, and intestinal myenteric plexus, are all well reproduced by rotenone treatment (Miyazaki et al., 2020). However, the PD model established with systemic administration of rotenone usually caused a high mortality rate and various neuropathological changes (Richardson et al., 2019). To avoid these disadvantages of mouse models with systemic administration of rotenone, a rat model with stereotaxical infusion of rotenone into the SNpc was also employed in this study. Two safe doses of Cory were also administered to the animals to evaluate the neuroprotective properties of the alkaloid.

Due to the dopaminergic neuronal impairment induced by rotenone in the SNpc and striatum, motor dysfunction symptoms, evaluated by apomorphine-induced rotation, the rotarod test, and the pole test, were present in the rotenone-treated rats and mice (Figures 1, 2). Similar to Sinemet® and Madopar® treatment, Cory increased dopamine levels in the striatum and latency time on the rotarod, and decreased the rotations induced by apomorphine and turning time in the pole test, indicating that Cory may play a protective role in motor dysfunction by increasing dopamine (Figure 1). Dopaminergic neuronal loss and significantly decreased TH levels in the SNpc were reflected in the rotenone-treated rats or mice (Figure 2). However, Cory treatments had a neuroprotective effect by



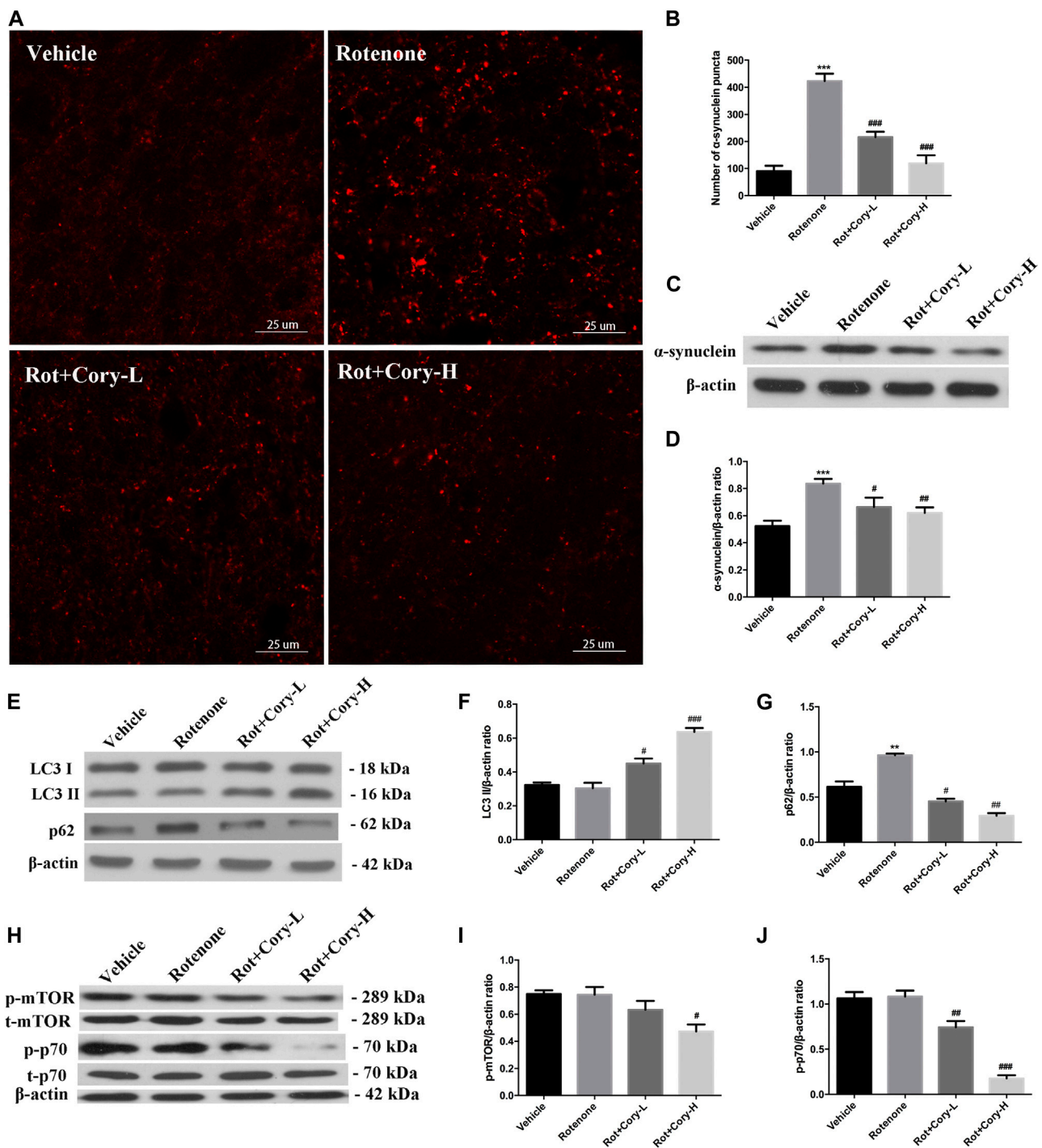


FIGURE 4 | Cory induces autophagy via the mTOR pathway and promotes the clearance of α-synuclein aggregation in the rotenone-induced rat model of PD. **(A, B)** Cory decreases the number of α-synuclein aggregations in the right side of SNpc. **(C, D)** Cory decreases α-synuclein expression in the right side of SNpc. The right side of SNpc was isolated from the brain tissue. After protein extraction, samples were subjected to Western blotting assay. **(E–G)** Cory increases LC3 II level and decreases p62 level in the right side of SNpc. **(H–J)** Cory decreases p-mTOR and p-p70 levels in the right side of SNpc. The right side of SNpc was isolated from the brain tissue. After protein extraction, samples were subjected to Western blotting assay. Dosage of Cory in the rotenone-induced rat model of PD: Cory-L: 2.5 mg/kg, Cory-H: 5 mg/kg. Data were presented as mean ± SEM of three independent experiments. (***) $p < 0.001$ compared with Sham model, # $p < 0.05$, ## $p < 0.01$, ### $p < 0.001$ compared with Rotenone group, one-way ANOVA with Newman-Keuls multiple test.)

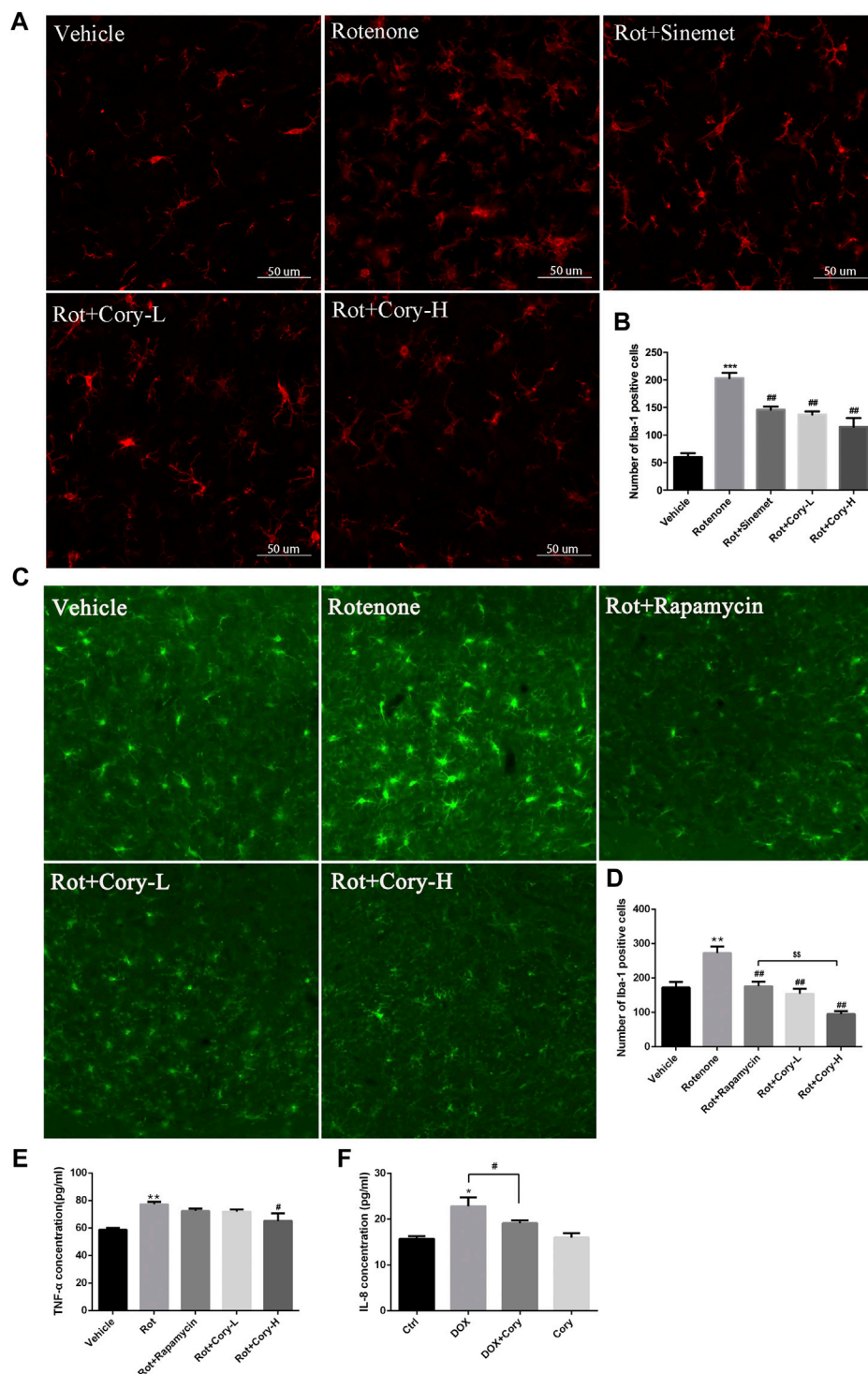


FIGURE 5 | Cory decreases the neuroinflammation *via* inhibiting the activation of microglia and decreasing TNF- α . Cory significantly decreases the number of active microglia cells both in the right-side SNpc of the PD rat model (**A, B**) and in the SNpc of the PD mice model (**C, D**). (**E**) In the rotenone-induced mice model of PD, Cory significantly decreases the level of TNF- α in the serum. (**F**) Cory diminishes the release of IL-8 in inducible PC12 with overexpression of mutant α -synuclein (A53T). Inducible PC 12 cells were treated with doxycycline for 24 h and further treated with Cory (25 μ M) for another 24 h. Supernatant was collected, and the level of IL-8 was analyzed by ELISA. Dosage of Cory in the rotenone-induced rat model of PD: Cory-L: 2.5 mg/kg, Cory-H: 5 mg/kg. Dosage of Cory in the rotenone-induced mice model of PD: Cory-L: 5 mg/kg, Cory-H: 10 mg/kg. Data were presented as mean \pm SEM. (** p < 0.01, *** p < 0.001 compared with Sham or Vehicle group; # p < 0.05, ## p < 0.01 compared with Rotenone group; \$\$ p < 0.01, Rot + Rapamycin v.s. Rot + Cory-H; * p < 0.05 compared with Ctrl, # p < 0.05 compared with Dox; $n \geq 6$, one-way ANOVA with Newman-Keuls' multiple test.)

preventing the TH-positive neuronal loss and increasing TH levels (**Figure 2**). All these data indicate that Cory protects the nigrostriatum dopaminergic system and improves the motor dysfunction and dopaminergic neuronal loss induced by rotenone.

The genus *Uncaria* is an important folk medicine to be widely used in China, Malaysia, the Philippines, Africa, and Southeast America (Zhang et al., 2015). Up to now, more than 200 compounds, including indole alkaloids, triterpenes, flavonoids, phenols, and phenylpropanoids, have been isolated from *Uncaria*. As the characteristic constituents, indole alkaloids isolated from *Uncaria* are reported to be efficacy for PD, Alzheimer's disease, hypertension, and epilepsy, and depressant (Zhang et al., 2015; Zhao et al., 2019a; Zhao et al., 2019b; Zheng et al., 2020; Zhao et al., 2021). Cory is an oxindole alkaloid isolated from *Uncaria rhynchophylla*. Previously, we provided evidences that Cory induced autophagy and promoted the clearance of α -synuclein through the Akt/mTOR pathway in neuronal cells, including N2a, SH-SY5Y, and PC12 cells. Meanwhile, Cory induced autophagy in Cg-GAL4 > UAS-GFP-Atg8a *Drosophila* larvae fat body (Chen et al., 2014). In order to identify the key protein kinase, a novel network-based algorithm of *in silico* kinome activity profiling, which was named iKAP, was developed, and MAP2K2 was found to play an essential role in the progress of Cory-induced autophagy (Chen et al., 2017; Chen et al., 2018; Chen and Xie, 2018b). In this study, increased α -synuclein aggregates were found in the lesioned side of the SNpc in the rotenone group (**Figures 4A–D**), which is consistent with previous reports (Ramalingam et al., 2019; Richardson et al., 2019). Decreased p62, a substrate of autophagy, and increased LC3II indicated that the aforementioned alkaloid induced autophagy in the rotenone rat models of PD (**Figures 4E,G**). Furthermore, decreased levels of p-mTOR and p-p70 indicated that Cory induced autophagy through the mTOR pathway (**Figures 4H–J**) in the animal models, which is consistent with the results obtained from cell modes. Induction of autophagy by Cory, which is considered to be an effective route to clear aggregated α -synuclein, resulted in a significant decrease in the aggregation and expression of α -synuclein after Cory treatment (**Figures 4A–D**). Therefore, Cory may promote the clearance of α -synuclein *via* autophagy in a rotenone-induced rat model of PD.

Recently, neuroinflammation, which is induced by the activation of microglia and the release of pro-inflammatory cytokines, was reported to play an important role in the degeneration of dopaminergic neurons in PD (Ho, 2019; Liu et al., 2019). In patients who were at early stages of PD, both microglial activation and dopaminergic terminal loss were observed in the midbrains and thalamus (Ouchi et al., 2005). Heightened levels of pro-inflammatory cytokines, such as TGF- β 1, IL-6, and IL-1 β , were also found in the cerebrospinal fluid of these PD patients (Chen et al., 2018). A rat model of PD with overexpression of human α -synuclein

displayed microglial activation and neuroinflammation, which were coupled with early alterations, including reduced striatal dopamine outflow and motor dysfunction, prior to nigral degeneration. Prevention of the central and peripheral inflammation by resolving D1 improves the neuronal dysfunction and motor deficits (Krashia et al., 2019). Recent reports have shown that microglia can clear the α -synuclein released by neurons through TLR4-NF- κ B-p62-mediated synucleinphagy (Choi et al., 2020). In the present study, both the activated microglia and increased pro-inflammatory cytokines induced by rotenone, as well as increased IL-8 levels induced by α -synuclein overexpression, were diminished by Cory (**Figure 5**). In addition, the effects of Cory on microglia activation and TNF- α secretion were better than those of rapamycin, which has been reported to suppress microglial activation and TNF- α expression induced by intracerebral hemorrhage (Li et al., 2016; Karunakaran et al., 2019). All these reports support the link between microglia and α -synuclein in contributing to dopaminergic degeneration in PD. However, the potential anti-neuroinflammatory effects of Cory highlighted in this study may also be responsible for its neuroprotective abilities in PD.

Collectively, these study findings indicated that Cory possessed neuroprotective effects in rotenone-induced rat and mouse models of PD by improving motor dysfunction, preventing TH-positive neuronal loss, decreasing α -synuclein aggregates through the mTOR pathway, and diminishing neuroinflammation. This provides experimental data to support the development of Cory for the treatment of PD.

AUTHOR CONTRIBUTIONS

All authors listed have made a substantial, direct, and intellectual contribution to the work and approved it for publication.

FUNDING

This work was supported by grants from the Natural Science Foundation of China (31800893, 31771124, 31671054, and 31900745) and the Shandong Provincial Natural Science Foundation (ZR2020YQ23 and ZR2019BC008). This study was also partly supported by the grants from the Health Medical Research Fund, Food and Health Bureau, Hong Kong SAR (HMRP 17182541 and HMRP 17182551).

SUPPLEMENTARY MATERIAL

The Supplementary Material for this article can be found online at: <https://www.frontiersin.org/articles/10.3389/fphar.2021.642900/full#supplementary-material>.

REFERENCES

- Anusha, C., Sumathi, T., and Joseph, L. D. (2017). Protective role of apigenin on rotenone induced rat model of Parkinson's disease: suppression of neuroinflammation and oxidative stress mediated apoptosis. *Chem. Biol. Interact.* 269, 67–79. doi:10.1016/j.cbi.2017.03.016
- Betarbet, R., Sherer, T. B., Mackenzie, G., Garcia-Osuna, M., Panov, A. V., and Greenamyre, J. T. (2000). Chronic systemic pesticide exposure reproduces features of Parkinson's disease. *Nat. Neurosci.* 3, 1301–1306. doi:10.1038/81834
- Carbone, F., Djamshidian, A., Seppi, K., and Poewe, W. (2019). Apomorphine for Parkinson's disease: efficacy and safety of current and new formulations. *CNS Drugs* 33, 905–918. doi:10.1007/s40263-019-00661-z
- Chen, L. L., Huang, Y. J., Cui, J. T., Song, N., and Xie, J. (2019). Iron dysregulation in Parkinson's disease: focused on the autophagy-lysosome pathway. *ACS Chem. Neurosci.* 10, 863–871. doi:10.1021/acschemneuro.8b00390
- Chen, L. L., Song, J. X., Lu, J. H., Yuan, Z. W., Liu, L. F., Durairajan, S. S., et al. (2014). Corynoxine, a natural autophagy enhancer, promotes the clearance of alpha-synuclein via Akt/mTOR pathway. *J. Neuroimmune Pharmacol.* 9, 380–387. doi:10.1007/s11481-014-9528-2
- Chen, L. L., Wang, Y. B., Song, J. X., Deng, W. K., Lu, J. H., Ma, L. L., et al. (2017). Phosphoproteome-based kinase activity profiling reveals the critical role of MAP2K2 and PLK1 in neuronal autophagy. *Autophagy* 13, 1–12. doi:10.1080/15548627.2017.1371393
- Chen, L., and Xie, J. (2018a). Dopamine in Parkinson's disease: precise supplementation with motor planning. *Neurosci. Bull.* 34, 873–874. doi:10.1007/s12264-018-0245-3
- Chen, L., and Xie, J. (2018b). Identification of neuronal autophagy regulators: combined use of iKAP and THANATOS. *Mov. Disord.* 33, 580–581. doi:10.1002/mds.27354
- Chen, X., Hu, Y., Cao, Z., Liu, Q., and Cheng, Y. (2018). Cerebrospinal fluid inflammatory cytokine aberrations in alzheimer's disease, Parkinson's disease and amyotrophic lateral sclerosis: a systematic review and meta-analysis. *Front. Immunol.* 9, 2122–2131. doi:10.3389/fimmu.2018.02122
- Choi, I., Zhang, Y., Seegobin, S. P., Pruvost, M., Wang, Q., Purtell, K., et al. (2020). Microglia clear neuron-released alpha-synuclein via selective autophagy and prevent neurodegeneration. *Nat. Commun.* 11, 1386–1399. doi:10.1038/s41467-020-15119-w
- Gunaydin, C., Avci, B., Bozkurt, A., Onger, M. E., Balci, H., and Bilge, S. S. (2019). Effects of agomelatine in rotenone-induced Parkinson's disease in rats. *Neurosci. Lett.* 699, 71–76. doi:10.1016/j.neulet.2019.01.057
- Ho, M. S. (2019). Microglia in Parkinson's disease. *Adv. Exp. Med. Biol.* 1175, 335–353. doi:10.1007/978-981-13-9913-8_13
- Hou, X., Watzlawik, J. O., Fiesel, F. C., and Springer, W. (2020). Autophagy in Parkinson's disease. *J. Mol. Biol.* 2, a009357. doi:10.1101/cshperspect.a009357
- Johnson, M. E., Stecher, B., Labrie, V., Brundin, L., and Brundin, P. (2019). Triggers, facilitators, and aggravators: redefining Parkinson's disease pathogenesis. *Trends Neurosci.* 42, 4–13. doi:10.1016/j.tins.2018.09.007
- Karunakaran, I., Alam, S., Jayagopi, S., Frohberger, S. J., Hansen, J. N., Kuehlwein, J., et al. (2019). Neural sphingosine 1-phosphate accumulation activates microglia and links impaired autophagy and inflammation. *Glia* 67, 1859–1872. doi:10.1002/glia.23663
- Krashia, P., Cordella, A., Nobili, A., La Barbera, L., Federici, M., Leuti, A., et al. (2019). Blunting neuroinflammation with resolvin D1 prevents early pathology in a rat model of Parkinson's disease. *Nat. Commun.* 10, 3945–3963. doi:10.1038/s41467-019-11928-w
- Li, D., Liu, F., Yang, T., Jin, T., Zhang, H., Luo, X., et al. (2016). Rapamycin protects against neuronal death and improves neurological function with modulation of microglia after experimental intracerebral hemorrhage in rats. *Cell Mol. Biol. (Noisy-le-grand)* 62, 67–75.
- Li, Y., Jiao, Q., Du, X., Bi, M., Han, S., Jiao, L., et al. (2018). Investigation of behavioral dysfunctions induced by monoamine depletions in a mouse model of Parkinson's disease. *Front. Cell Neurosci.* 12, 241. doi:10.3389/fncel.2018.00241
- Liu, C. Y., Wang, X., Liu, C., and Zhang, H. L. (2019). Pharmacological targeting of microglial activation: new therapeutic approach. *Front. Cell Neurosci.* 13, 514–532. doi:10.3389/fncel.2019.00514
- Miyazaki, I., Isooka, N., Imafuku, F., Sun, J., Kikuoka, R., Furukawa, C., et al. (2020). Chronic systemic exposure to low-dose rotenone induced central and peripheral neuropathology and motor deficits in mice: reproducible animal model of Parkinson's disease. *Int. J. Mol. Sci.* 21, 3254. doi:10.3390/ijms21093254
- Nagatsu, T. (1995). Tyrosine hydroxylase: human isoforms, structure and regulation in physiology and pathology. *Essays Biochem.* 30, 15–35.
- OECD (2008). *Guideline for the testing of chemical 425, Acute oral toxicity- up-and-down procedure (UDP)*. Paris, France: OECD.
- Ouchi, Y., Yoshikawa, E., Sekine, Y., Futatsubashi, M., Kanno, T., Ogosu, T., et al. (2005). Microglial activation and dopamine terminal loss in early Parkinson's disease. *Ann. Neurol.* 57, 168–175. doi:10.1002/ana.20338
- Ozaki, Y. (1989). Pharmacological studies of indole alkaloids obtained from domestic plants, *Uncaria rhynchophylla* Miq. and *Amsonia elliptica* Roem. et Schult. *Nippon Yakurigaku Zasshi* 94, 17–26. doi:10.1254/fpj.94.17
- Przedborski, S. (2017). The two-century journey of Parkinson disease research. *Nat. Rev. Neurosci.* 18, 251–259. doi:10.1038/nrn.2017.25
- Ramalingam, M., Huh, Y. J., and Lee, Y. I. (2019). The impairments of alpha-synuclein and mechanistic target of rapamycin in rotenone-induced SH-SY5Y cells and mice model of Parkinson's disease. *Front. Neurosci.* 13, 1028. doi:10.3389/fnins.2019.01028
- Richardson, J. R., Fitsanakis, V., Westerink, R. H. S., and Kanthasamy, A. G. (2019). Neurotoxicity of pesticides. *Acta Neuropathol.* 138, 343–362. doi:10.1007/s00401-019-02033-9
- Rossi, A., Berger, K., Chen, H., Leslie, D., Mailman, R. B., and Huang, X. (2018). Projection of the prevalence of Parkinson's disease in the coming decades: revisited. *Mov. Disord.* 33, 156–159. doi:10.1002/mds.27063
- Xilouri, M., Brekk, O. R., and Stefanis, L. (2016). Autophagy and alpha-synuclein: relevance to Parkinson's disease and related synucleopathies. *Mov. Disord.* 31, 178–192. doi:10.1002/mds.26477
- Xiong, N., Huang, J., Zhang, Z., Zhang, Z., Xiong, J., Liu, X., et al. (2009). Stereotaxical infusion of rotenone: a reliable rodent model for Parkinson's disease. *PLoS One* 4, e7878. doi:10.1371/journal.pone.0007878
- Xiong, N., Long, X., Xiong, J., Jia, M., Chen, C., Huang, J., et al. (2012). Mitochondrial complex I inhibitor rotenone-induced toxicity and its potential mechanisms in Parkinson's disease models. *Crit. Rev. Toxicol.* 42, 613–632. doi:10.3109/10408444.2012.680431
- Zhang, Q., Zhao, J. J., Xu, J., Feng, F., and Qu, W. (2015). Medicinal uses, phytochemistry and pharmacology of the genus *Uncaria*. *J. Ethnopharmacol.* 173, 48–80. doi:10.1016/j.jep.2015.06.011
- Zhao, W., Li, C., Zhang, H., Zhou, Q., Chen, X., Han, Y., et al. (2021). Dihydrotanshinone I attenuates plaque vulnerability in apolipoprotein E-deficient mice: role of receptor-interacting protein 3. *Antioxid. Redox Signal.* 34, 351–363. doi:10.1089/ars.2019.7796
- Zhao, W., Yuan, Y., Zhao, H., Han, Y., and Chen, X. (2019a). Aqueous extract of *Salvia miltiorrhiza* Bunge-*Radix Puerariae* herb pair ameliorates diabetic vascular injury by inhibiting oxidative stress in streptozotocin-induced diabetic rats. *Food Chem. Toxicol.* 129, 97–107. doi:10.1016/j.fct.2019.04.018
- Zhao, W., Zeng, X., Meng, F., Bi, X., Xu, D., Chen, X., et al. (2019b). Structural characterization and in vitro-in vivo evaluation of effect of a polysaccharide from *Sanguisorba officinalis* on acute kidney injury. *Food Funct.* 10, 7142–7151. doi:10.1039/c9fo01891c
- Zheng, H., Feng, H., Zhang, W., Han, Y., and Zhao, W. (2020). Targeting autophagy by natural product Ursolic acid for prevention and treatment of osteoporosis. *Toxicol. Appl. Pharmacol.* 409, 115271. doi:10.1016/j.taap.2020.115271

Conflict of Interest: The authors declare that the research was conducted in the absence of any commercial or financial relationships that could be construed as a potential conflict of interest.

Copyright © 2021 Chen, Huang, Yu, Lu, Jia, Song, Liu, Wang, Huang, Xie and Li. This is an open-access article distributed under the terms of the Creative Commons Attribution License (CC BY). The use, distribution or reproduction in other forums is permitted, provided the original author(s) and the copyright owner(s) are credited and that the original publication in this journal is cited, in accordance with accepted academic practice. No use, distribution or reproduction is permitted which does not comply with these terms.



Danggui-Shaoyao-San (DSS) Ameliorates Cerebral Ischemia-Reperfusion Injury via Activating SIRT1 Signaling and Inhibiting NADPH Oxidases

Yunxia Luo^{1,2,3,4}, Hansen Chen², Bun Tsoi², Qi Wang^{1,4*} and Jiangang Shen^{1,2*}

¹Science and Technology Innovation Center, Guangzhou University of Chinese Medicine, Guangzhou, China, ²School of Chinese Medicine, Li Ka Shing Faculty of Medicine, The University of Hong Kong, Hong Kong, China, ³Department of Endocrinology, Fourth Clinical Medical College, Guangzhou University of Chinese Medicine, Shenzhen, China, ⁴Institute of Clinical Pharmacology, Guangzhou University of Chinese Medicine, Guangzhou, China

OPEN ACCESS

Edited by:

Min Li,
Hong Kong Baptist University,
Hong Kong

Reviewed by:

Maria Luisa Del Moral,
University of Jaén, Spain
Zhipeng Li,
Binzhou Medical University, China
Xinchun Jin,
Soochow University, China

*Correspondence:

Jiangang Shen
shenjg@hkucc.hku.hk
Qi Wang
wangqi@gzucm.edu.cn

Specialty section:

This article was submitted to
Ethnopharmacology,
a section of the journal
Frontiers in Pharmacology

Received: 15 January 2021

Accepted: 22 March 2021

Published: 15 April 2021

Citation:

Luo Y, Chen H, Tsoi B, Wang Q and Shen J (2021) Danggui-Shaoyao-San (DSS) Ameliorates Cerebral Ischemia-Reperfusion Injury via Activating SIRT1 Signaling and Inhibiting NADPH Oxidases.
Front. Pharmacol. 12:653795.
doi: 10.3389/fphar.2021.653795

Danggui-Shaoyao-San (DSS) is a famous Traditional Chinese Medicine formula that used for treating pain disorders and maintaining neurological health. Recent studies indicate that DSS has neuroprotective effects against ischemic brain damage but its underlining mechanisms remain unclear. Herein, we investigated the neuroprotective mechanisms of DSS for treating ischemic stroke. Adult male Sprague-Dawley (S.D.) rats were subjected to 2 h of middle cerebral artery occlusion (MCAO) plus 22 h of reperfusion. Both ethanol extract and aqueous extract of DSS (12 g/kg) were orally administrated into the rats at 30 min prior to MCAO ischemic onset. We found that 1) ethanol extract of DSS, instead of aqueous extract, reduced infarct sizes and improved neurological deficit scores in the post-ischemic stroke rats; 2) Ethanol extract of DSS down-regulated the expression of the cleaved-caspase 3 and Bax, up-regulated bcl-2 and attenuated apoptotic cell death in the ischemic brains; 3) Ethanol extract of DSS decreased the production of superoxide and peroxynitrite; 4) Ethanol extract of DSS significantly down-regulated the expression of p67^{phox} but has no effect on p47^{phox} and iNOS statistically. 5) Ethanol extract of DSS significantly up-regulated the expression of SIRT1 in the cortex and striatum of the post-ischemic brains; 6) Co-treatment of EX527, a SIRT1 inhibitor, abolished the DSS's neuroprotective effects. Taken together, DSS could attenuate oxidative/nitrosative stress and inhibit neuronal apoptosis against cerebral ischemic-reperfusion injury via SIRT1-dependent manner.

Keywords: Danggui-Shaoyao-San, stroke, peroxynitrite, SIRT1, oxidative stress

INTRODUCTION

Stroke is a major disease burden with high mortality and disability in which ischemic stroke accounts for 87% (Feigin et al., 2014; Feigin et al., 2015; Benjamin et al., 2017). To date, tissue plasminogen activator (t-PA) is the only United States Food and Drug Administration approved drug for acute ischemic stroke. With the narrow therapeutic window within 4.5 h and the risk of hemorrhagic

transformation, less than 10% ischemic stroke patients benefit from t-PA treatment (Mozaffarian et al., 2016). Seeking new therapeutic approaches is timely important for ischemic stroke.

Reactive oxygen species (ROS) and reactive nitrogen species (RNS) are important players in cerebral ischemia-reperfusion injury. Superoxide (O_2^-) is representative ROS whereas nitric oxide (NO) and peroxynitrite ($ONOO^-$) are typical RNS. During cerebral ischemia-reperfusion injury, the production of O_2^- is mainly from the activations of NADPH oxidase (Miller et al., 2006), xanthine oxidase (McCord, 1985), and cyclooxygenase (COX) (Fabian et al., 1995; Kawano et al., 2006). NO is generated by the activation of endothelial nitric oxide synthase (eNOS), neuronal NOS (nNOS) inducible NOS (iNOS). The simultaneous presentation of NO and O_2^- rapidly produces $ONOO^-$ in a diffusion-limited rate (Chen et al., 2013). Peroxynitrite could mediate neural apoptotic cell death, and aggravate the blood-brain barrier (BBB) disruption, infarction enlargement and neurological deficit in cerebral ischemia-reperfusion injury (Chen et al., 2013). Peroxynitrite induces protein tyrosine nitration by the addition of a nitro group to the hydroxyl group of the tyrosine residue to form 3-nitrotyrosine (3-NT), a footprint marker for $ONOO^-$ production (Kuhn et al., 2004). Plasma 3-NT level was positively correlated with the magnitude of the brain injury in ischemic stroke patients (Bas et al., 2012). $ONOO^-$ could be a promising therapeutic target to attenuating neural cell death, protecting the BBB integrity, and reducing thrombolysis-mediated hemorrhage transformation for improving ischemic stroke outcome (Gong et al., 2015; Chen et al., 2018; Chen et al., 2020). Peroxynitrite decomposition catalysts reduce 3-NT expression and MMPs activation, attenuate hemorrhagic transformation and improve neurological outcome in ischemic rat brains with delayed t-PA treatment (Chen et al., 2015). Therefore, antioxidant therapy could be a promising therapeutic strategy for ischemic stroke treatment.

Silent information regulator 2 homolog 1 (SIRT1) plays crucial roles in the molecular regulations under oxidative/nitrosative stress related brain damages. SIRT1 is a protein deacetylase to regulating endothelium-dependent relaxation of the cerebral vasculature (Tajbakhsh and Sokoya, 2012). SIRT1 could be a therapeutic target in vascular-related diseases for restoring endothelial function. Under bilateral common carotid artery stenosis (~50% stenosis), overexpression of SIRT1 preserves cerebral blood flow (CBF) via the deacetylation of eNOS (Hattori et al., 2014; Hattori et al., 2015). In bilateral common carotid artery occlusion (BCAO) mouse model, sirt1-overexpression significantly lessens ischemic brain damage with the preserved CBF up to 45–50% of the baseline level (Hattori et al., 2015). In a rat model of right-sided endovascular middle cerebral artery occlusion, activating SIRT1 decreased the infarct volume by targeting p53/microRNA-22 signaling pathway (Lu and Wang, 2017). Many antioxidants activate SIRT1 signaling for their neuroprotective effects (Wang et al., 2009; He et al., 2017; Ren et al., 2019; Teertam et al., 2020). Therefore, SIRT1 could be a promising therapeutic target for ischemic stroke.

Traditional Chinese Medicine (TCM) practice provides valuable sources for stroke treatment with relatively low- or non-toxicity (Wu et al., 2007; Seto et al., 2016). Danggui-Shaoyao-San (DSS), also called Tokishakuyaku-san (TJ-23) or Dangguijakyak-san (DJS), is a classic herbal formula including *Angelica sinensis* (Oliv.) Diels (Umbelliferae), *Paeonia lactiflora* Pall. (Paeoniaceae), *Conioselinum anthriscoides* “Chuanxiong” (syn. *Ligusticum chuanxiong* Hort.) (Umbelliferae), *Wolfiporia extensa* (Peck) Ginns (syn. *Poria cocos* (Schwein.) (Polyporaceae), *Atractylodes macrocephala* Koidz. (Asteraceae), and *Alisma plantago-aquatica* subsp. *orientale* (Sam.) Sam. (syn. *Alisma orientalis* (Sam.) Juzep.) (Alismataceae) which forms a TCM formula mixed in a ratio of 3:16:8:4:4:8. DSS was originally used for gynecological diseases (Wang et al., 2015; Lee et al., 2016). Previous studies indicate the potentials of DSS for improving neurological functions in post stroke treatment (Goto et al., 2011; REN et al., 2013). DSS exerts various neuroprotective effects by ameliorating oxidative stress in a permanent ischemic stroke rat model and reducing inflammation in a global ischemia-reperfusion model (Lin et al., 2008; Kim et al., 2016). DSS treatment also promotes focal angiogenesis and neurogenesis, attenuates neurological deficit scores, and improves memory functions in experimental rat models of cerebral ischemic reperfusion injury (Izzettin et al., 2007; Song et al., 2013; Ren et al., 2015). However, the underlying mechanisms of DSS for neuroprotection remain largely unknown. In the present study, we tested the hypothesis that DSS could protect against cerebral ischemic-reperfusion injury via attenuating oxidative/nitrosative stress and inhibiting neuronal apoptosis in a SIRT1-dependent manner.

MATERIALS AND METHODS

DSS Extraction Preparation

Herbal materials including *Angelica sinensis* (Oliv.) Diels (Umbelliferae), *Paeonia lactiflora* Pall. (Paeoniaceae), *Conioselinum anthriscoides* “Chuanxiong” (syn. *Ligusticum chuanxiong* Hort.) (Umbelliferae), *Wolfiporia extensa* (Peck) Ginns (syn. *Poria cocos* (Schwein.) (Polyporaceae), *Atractylodes macrocephala* Koidz. (Asteraceae), and *Alisma plantago-aquatica* subsp. *orientale* (Sam.) Sam. (syn. *Alisma orientalis* (Sam.) Juzep. (Alismataceae) were purchased from native sources from Mainland China through School of Chinese Medicine, The University of Hong Kong, and these herbs were mixed in a ratio of 3:16:4:8:4:8 for extract preparation. We prepared both aqueous and ethanol extract to compare their effects in treating ischemic brain injury. The aqueous extract of DSS was prepared with the following procedure. The DSS was soaked in eight times of distilled water for 40 min following by decocted 1 h. After that, the filtrate was collected, and the filter residue was decocted with six volumes of distilled water for another 1 h. The filtrate was collected again and the two filtrates were mixed, lyophilized, and stored for usage. Ethanol extract of DSS preparation was made with the following procedures: Raw materials of DSS were ground into powder, macerated overnight and repeatedly ultrasound-extracted with 70% ethanol/water (1:10 w/v, 1:8 w/v, 1:5 w/v,

respectively) for 1 h each time. The extracted solutions were evaporated under vacuum (45 °C) to remove ethanol, and the remained aqueous solution was frozen and freeze-dried to obtain DSS ethanol extract powder.

Quality Control Analysis for DSS Ethanol Extract

Ethanol extract of DSS was analyzed by using high-performance liquid chromatography system (HPLC) in which paeoniflorin, alibiflorin, and ferulic acid were used as quantitative stands. Briefly, DSS power (200 mg) was accurately weighed, dissolved in 2 ml methanol proceed by sonication for 20 min and filtrated with 0.22 µm filter for quantitative analysis. DSS solution (5 µl) was injected into an apparatus with an autosampler. Chromatographic separation was achieved at a flow rate of 1.0 ml/min with an Agilent Eclipse Plus C18 column (4.6 × 250 mm, 5 µm). The details of mobile phase are shown in **Supplementary Table S1**. The separation temperature was 25°C, with a detection wavelength of 230 nm.

We detected the linearity, sensitivity, precision, accuracy, and stability for the validation of the quantitative methodology (Li et al., 2018) with a mini modification. In briefly, stock solutions of paeoniflorin (5,000 µg/ml), alibiflorin (620 µg/ml) and ferulic acid (180 µg/ml) were prepared in methanol. To prepare calibration curves, we analyzed seven concentrations of paeoniflorin, alibiflorin, and ferulic acid standers by using HPLC. The accuracy and precision were evaluated by measuring the intraday variabilities and recovery of those standard compounds. Stability was examined by analyzing DSS over a period of 0, 3, 6, 9, 12, and 24 h. The limits of detection (LOD) and limits of quantitation (LOQ) under the present conditions were determined at an S/N (signal/noise) of about 3 and 10, respectively. The data were monitored, recorded and analyzed by Agilent 1260 (United States).

Cerebral Ischemia Reperfusion Injury Model

Adult male Sprague-Dawley (S.D.) rats (270–290 g) were obtained from the Laboratory Animal Unit, the University of Hong Kong. All procedures for animal care and experimental were approved by the University Committee on the Use of Live Animals in Teaching and Research (CULATR). The rats were kept in a temperature and humidity-controlled environment for 12 h dark/light cycles with free access to food and water.

Rats were subjected to middle cerebral artery occlusion (MCAO) to induce experimental cerebral ischemia-reperfusion model with the protocols as described previously with minor modification (Chen et al., 2015). Briefly, rats were anesthetized firstly with 4% isoflurane and maintained at 2% isoflurane through inhalation. A middle incision was made in the neck, followed by careful exposure of the left common carotid artery (CCA), external carotid artery (ECA), and internal carotid artery (ICA) under the microscope. A silicon-coated suture (Doccol, Redlands, CA, United States), with the diameter is 0.38 mm, was inserted from ECA to ICA, and advanced to occlude the middle cerebral artery (MCA). After 2 h of occlusion, the suture was removed and CCA was released to allow reperfusion. Sham group

rats underwent the same surgical procedure without MCA occlusion. Rats body temperature were monitored during and after surgery. Rats were temporarily transferred to a cage with a heating lamp from recovery. 2,3,5-triphenyl-2H-tetrazolium chloride (TTC) staining was performed to evaluate the success of the MCAO model (Chen et al., 2020).

Experimental Design and Drug Treatment

We investigated the neuroprotective effects of DSS ethanol extract (DSS/E) and aqueous extract (DSS/W) against cerebral ischemia-reperfusion injury. Rats were randomly divided into the following four groups: Sham control, MCAO, and MCAO plus DSS/W (12 g/kg wt), MCAO + DSS/E (12 g/kg wt). The dosage of 12 g/kg was equivalent to human doses of raw materials (Zhang, 2005). DSS/W or DSS/E (12 g/kg) was orally administered to the rats at 30 min before reperfusion. For sham and MCAO vehicle groups, rats were orally given the same volume of double-distilled water. Secondly, in order to elucidate whether the neuroprotective effects of DSS/E were SIRT1-dependent, rats were randomly divided into the following three groups: MCAO, MCAO plus DSS/E, MCAO plus EX527 and DSS/E. The rats in the MCAO vehicle and MCAO plus DSS groups were given the same treatment as described in the first experiment. For MCAO + EX527 + DSS group, the rats were intraperitoneally injected with EX527 at the dose of 5 mg/kg every 2 days for four times before MCAO surgical procedure (Kou et al., 2017).

Neurological Deficit Cores

We used the modified Neurological Severity Score (mNSS) method to measure neurological deficits. The mNSS score was graded from 0 to 18, representing various levels of neurological dysfunction involving motor, sensory and reflex (Chen et al., 2001). The higher the score, the more severe neurological deficits. An investigator blind to the experimental design performed the mNSS test.

Infarct Size Measurement

We evaluated cerebral infarct size by using 2,3,5-triphenyl-2H-tetrazolium chloride (TTC) method (Feng et al., 2018). Rats were anesthetized and perfused with PBS and then brain tissue harvest. Tissue sample was cut into 2-mm thick coronal slices, which were immediately immersed into 0.5% TTC (T8877, Sigma) solution at room temperature in the dark for 20 min. Digital images of the brain slices were captured using a camera, and the infarct size was measured and analyzed by using Image J software. To reduce the bias of brain edema, we calculated the infarct size with the following formula: Infarct size percentage = (right hemisphere – red size of left hemisphere)/right hemisphere size × 100%.

TUNEL Staining

Apoptotic cell death was determined by using terminal deoxynucleotidyl transferase-mediated dUTP nick end labeling (TUNEL) assay. Briefly, rat brain samples were fixed with 4% paraformaldehyde (PFA) and then immersed in 30% sucrose until it sank. Samples were then embedded in O.C.T. and cut into a section of 25 µm. TUNEL staining was conducted referring to the manufacturer's instructions in the TUNEL assay kit

(Shanghai YEASEN Biotechnology Co.). Hoechst staining was used to visualize the cell nucleus. A fluorescence microscope (Carl Zeiss) with Axio Vision digital imaging system was applied to obtain the fluorescence images.

Immunostaining

Immunostaining assay was performed to visualize the expressions of SIRT1, 3-nitrotyrosine (3-NT), and cleaved caspase-3. Brain samples were prepared as described in “TUNEL Staining” section. Samples were blocked with 5% goat serum (Thermo Fisher Scientific) in PBS and incubated with the primary antibodies including SIRT1 (1:200, Abcam), 3-NT (1:100, Abcam), and cleaved caspase-3 (1:100, Immunoway), at appropriate dilution overnight at 4°C. Then sections were incubated with secondary antibody Alexa Fluor 568 Goat anti-mouse (Invitrogen), Alexa Fluor 488 Goat anti-rabbit, and Alexa Fluor 647 Goat anti-mouse at room temperature for 2 h. DAPI ((4',6-diamidino-2-phenylindole) was used for cell nucleus visualization. Immunofluorescent figures were obtained by a confocal microscope Carl Zeiss LSM 780.

Western Blot Analysis

Western blot analysis was performed according to standard protocol. Briefly, brain tissues were lysed in RIPA buffer containing 1% protease and phosphorylate inhibitor cocktail (Sigma-Aldrich). To determine protein concentration, an equal amount of total protein was separated by 10% sodium dodecyl sulfate polyacrylamide (SDS-PAGE) gel electrophoresis and transferred to polyvinylidene fluoride membranes (IPVH00010, EMD Millipore, Germany). Membranes were blocked with 5% bovine serum albumin and then probed with a primary antibodies including β -actin (Mouse, 1:3,000, Sigma), iNOS (Rabbit, 1:200, Abcam), nNOS (Rabbit, 1:1,000, Abcam), Cleaved-caspase3 (Rabbit polyclonal, 1:1,000, Millipore), caspase3 (Rabbit, 1:500, Abcam) or 3-NT (Mouse, 1:1,000, Millipore) overnight at 4°C. The membranes were washed by using TBS-Tween 20 buffer and incubated with the secondary antibody (1:2,000) for 2 h at room temperature. The immunoblots were enhanced using chemiluminescent ECL select kit (GE Healthcare, IL, United States), detected by Gel-Doc system (Bio-Rad, CA, United States) and analyzed with Image Lab software (Bio-Rad, CA, United States).

Superoxide Detection

We detected the superoxide production by using hydroethidine (HET) and HKSOX-1, a newly developed high specific and sensitive fluorescent probe (Hu et al., 2015). The isolated brains were immediately made into frozen sections, and the brain slice at 6 mm from the frontal tip was stained with the probe solutions of HET (20 μ M, DMF) or HKSOX-1 (20 μ M, DMF) for 10 min in the dark. Fluorescence was immediately detected by using Carl Zeiss LSM 780 Confocal Microscopy.

Statistical Analysis

Data were represented as Mean \pm SEM. Statistical analysis was performed by using one-way analysis of variance (ANOVA)

followed by Dunnett's multiple-comparison test. Neurological severity scores were analyzed by using non-parametric Kruskal-Wallis tests, followed by Dunnett's multiple comparison test. $p < 0.05$ was considered as statistically significant.

RESULTS

Ethanol Extract of DSS had Better Neuroprotective Effects than Aqueous Extract in Cerebral Ischemia-Reperfusion Injury

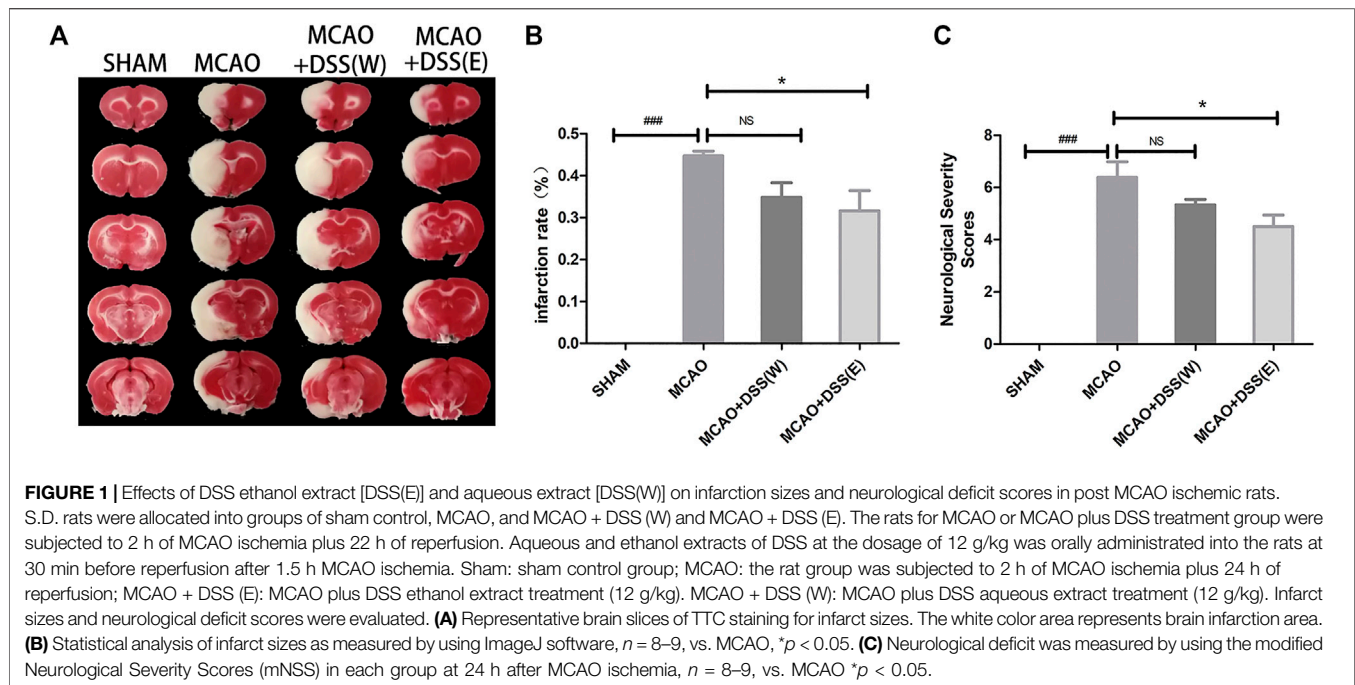
We firstly compared the neuroprotective effects of DSS with ethanol extract [DSS(E)] and aqueous extract [DSS(W)]. Rats were subjected to 2 h MCAO ischemia plus 22 h reperfusion. We analyzed infarct size and examined neurological deficit scores in the MCAO ischemia-reperfusion rats with or without DSS treatment. As shown in **Figure 1**, DSS(E) treatment significantly reduced the infarct sizes and neurological deficit mNSS scores whereas DSS(W) treatment had no neuroprotective effects. Therefore, the ethanol extract of DSS, instead of aqueous extract, has neuroprotective effects against cerebral ischemic-reperfusion injury.

DSS Ethanol Extract Inhibited Cleaved-Caspase3 and Bax, and Attenuated Apoptotic Cell Death in Ischemia-Reperfused Rat Brains

We then investigated the effects of the DSS ethanol extract on apoptotic cell death in acute MCAO ischemia reperfusion brains. We used the DSS ethanol extract for the rest of the experiments whose name was simplified as DSS accordingly. TUNEL staining was used to evaluate apoptotic cell death in the ischemic brain tissues at 22 h after 2 h of MCAO ischemia. As shown in **Figure 2**, DSS treatment significantly decreased apoptotic cell death in both cortex and striatum of the ischemia-reperfusion brains. In line with the result of TUNEL staining, western blot analysis showed that DSS down-regulated the expression of the cleaved-caspase 3 and Bax but up-regulated the expression of bcl-2 in the ischemic brains. These results suggest that DSS ethanol extract inhibits apoptotic cell death in cerebral ischemia-reperfusion injury.

DSS Ethanol Extract Decreased Superoxide Level and Inhibited 3-Nitrotyrosine Expression in Ischemia-Reperfused Rat Brains

We then investigated the antioxidant properties of DSS to scavenging O_2^- and $ONOO^-$ in the rat brains after subjected to 2 h MCAO ischemia plus 22 h reperfusion. The production of O_2^- were detected by using HET and HKSOX-1 (Hu et al., 2015). The production of $ONOO^-$ was examined by the immunostaining of 3-NT, a footprint protein of $ONOO^-$. As shown in **Figure 3**, the DSS treatment group had a significantly lower expression level of 3-NT and lower fluorescent staining of HET and HKSOX-1 in the



ischemic brains than the MCAO vehicle treatment group. Those results suggest that DSS could inhibit the productions of superoxide and peroxynitrite in cerebral ischemia-reperfusion injury.

DSS Ethanol Extract Inhibited NADPH Oxidase and Up-Regulated SIRT1 Expression in Ischemic-Reperfusion Rat Brains

NADPH oxidase and iNOS are major enzymes for the productions of superoxide and nitric oxide respectively in cerebral ischemia-reperfusion injury (Robinson et al., 2011; Winterbourn et al., 2016). Meanwhile, SIRT1 exerts neuroprotective effects by attenuating oxidative stress in ischemic brain injury (Shin et al., 2012; Fu et al., 2014). SIRT1 could be also a promising therapeutic target for ischemic stroke (He et al., 2017; Lu and Wang, 2017; Ren et al., 2019; Teertam et al., 2020). Thus, we detected NADPH oxidase subtypes p47^{phox} and p67^{phox}, and iNOS and SIRT1 in the post-ischemic brains. As shown in **Figure 4**, the expression levels of p47^{phox} and p67^{phox} was significantly up-regulated, indicating that activation of NADPH oxidases in the ischemic brains. However, the expression level of iNOS had a trend of increase in the MCAO ischemia-reperfused group but it was not statistically different from the sham control group. The increased expression of p67^{phox} was significantly inhibited by DSS treatment ($p < 0.05$). The expression of p47^{phox} and iNOS had no statistical difference between the MCAO plus vehicle group and MCAO plus DSS treatment. Meanwhile, the expression level of SIRT1 was down-regulated in the post-ischemic brains which was reserved by the DSS treatment ($p < 0.05$). Consistently, immunofluorescent staining showed that the expression of SIRT1 was increased in the cortex and striatum of the post-ischemic brains after receiving the DSS treatment (**Figure 5**). These results suggest that the antioxidant effects of

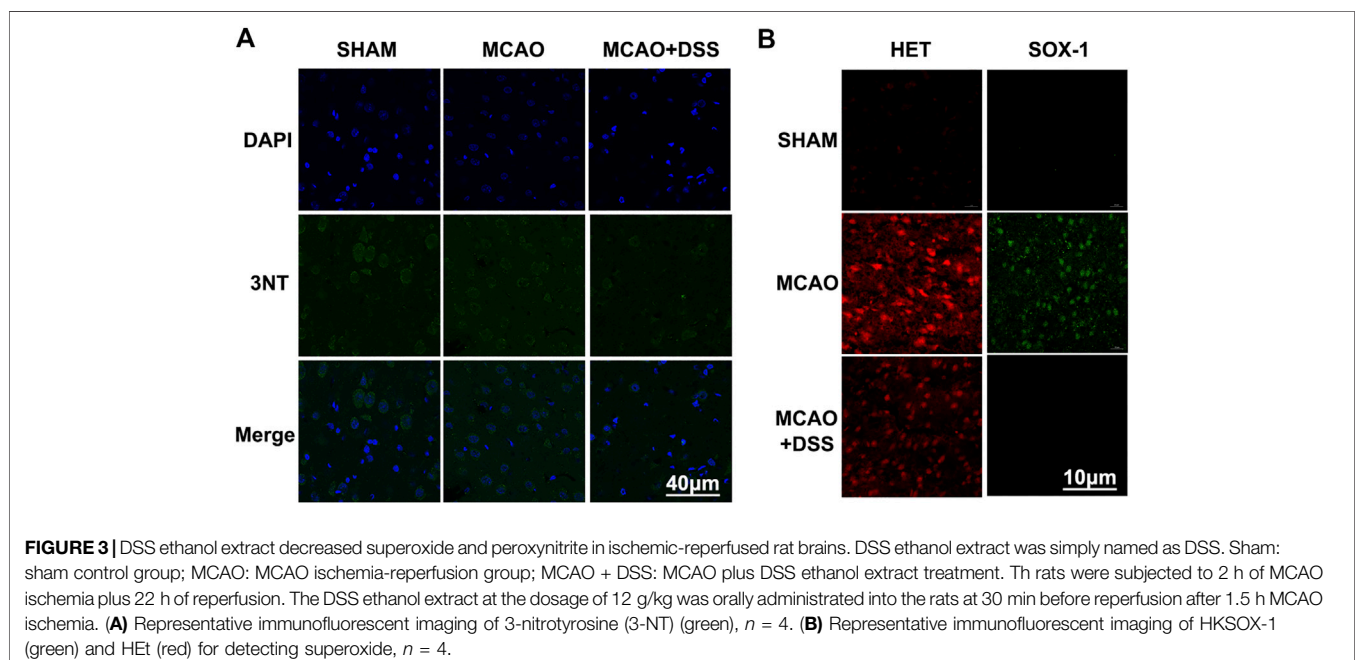
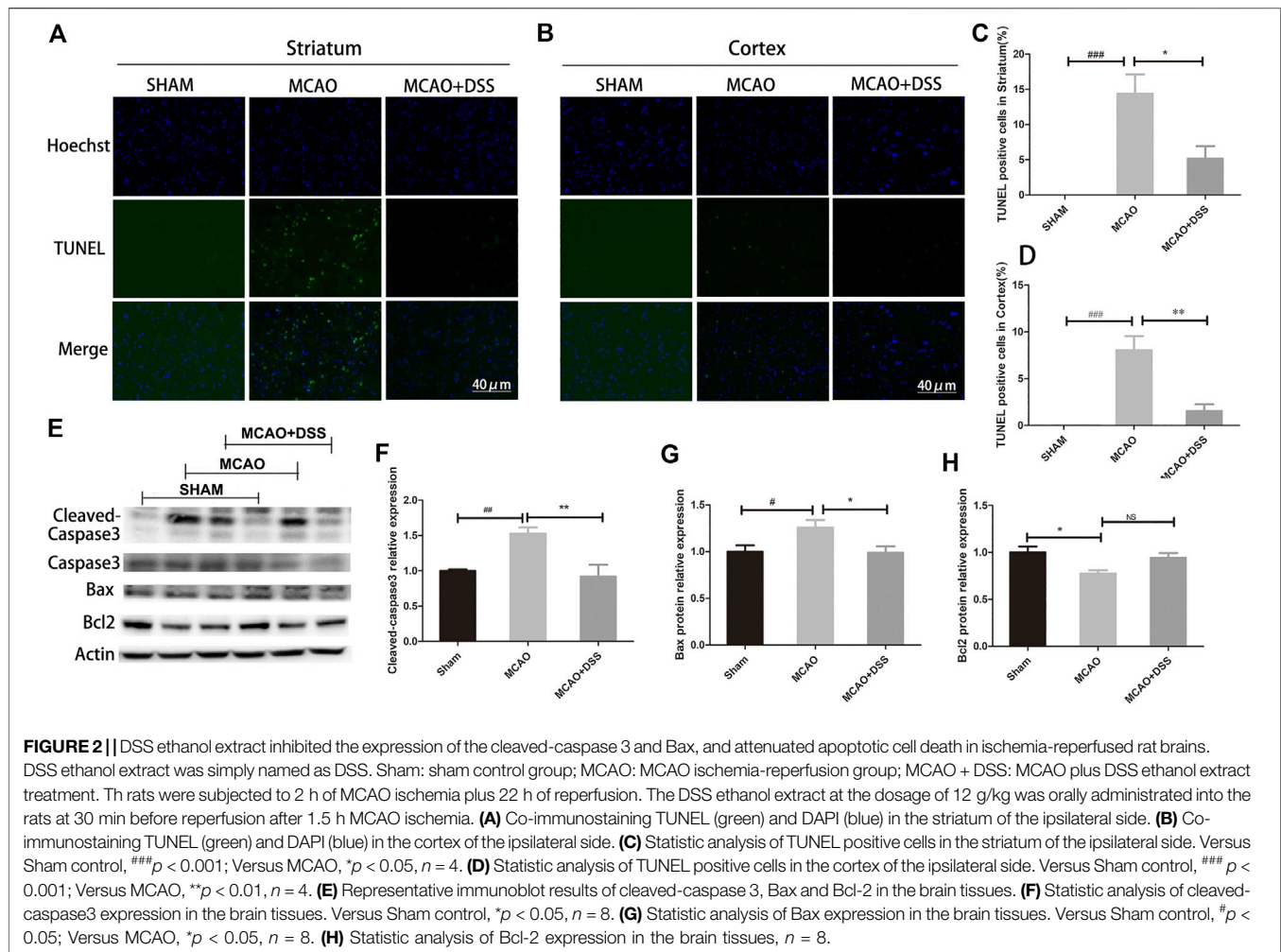
DSS ethanol extract could be attributed to inhibiting NADPH oxidase and activate SIRT1 signaling in post-ischemic brains.

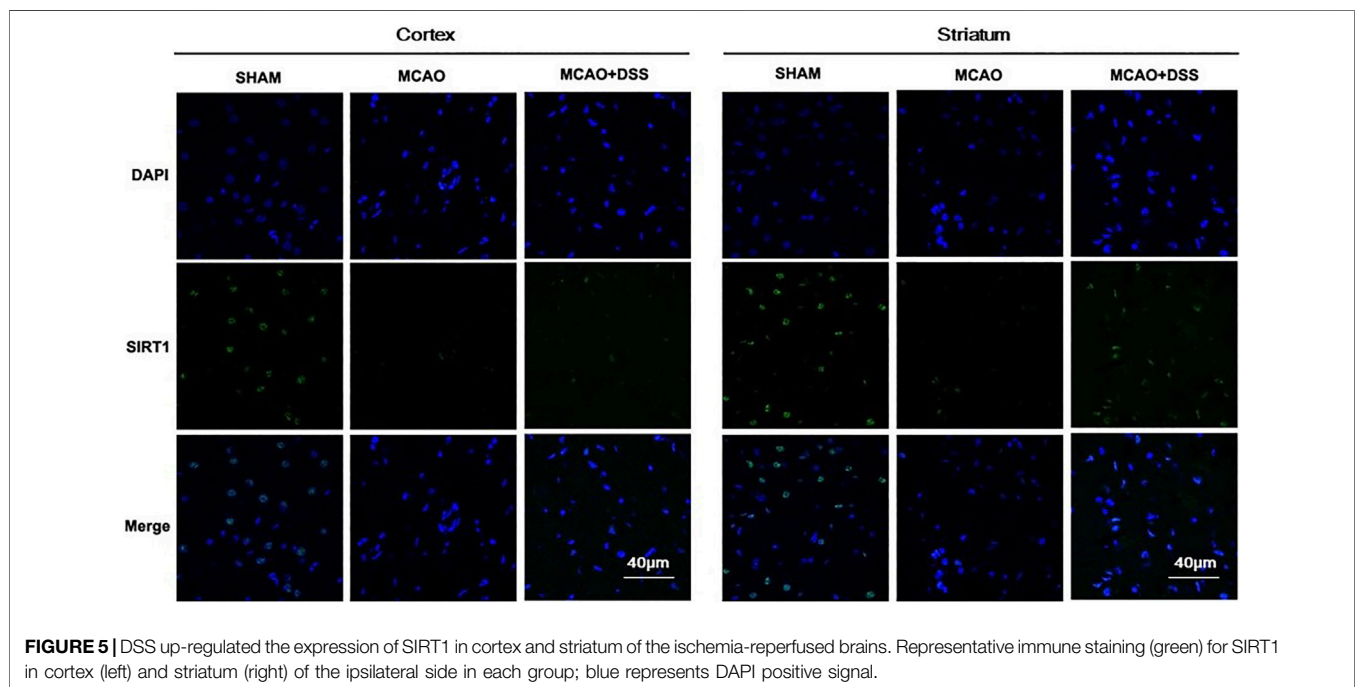
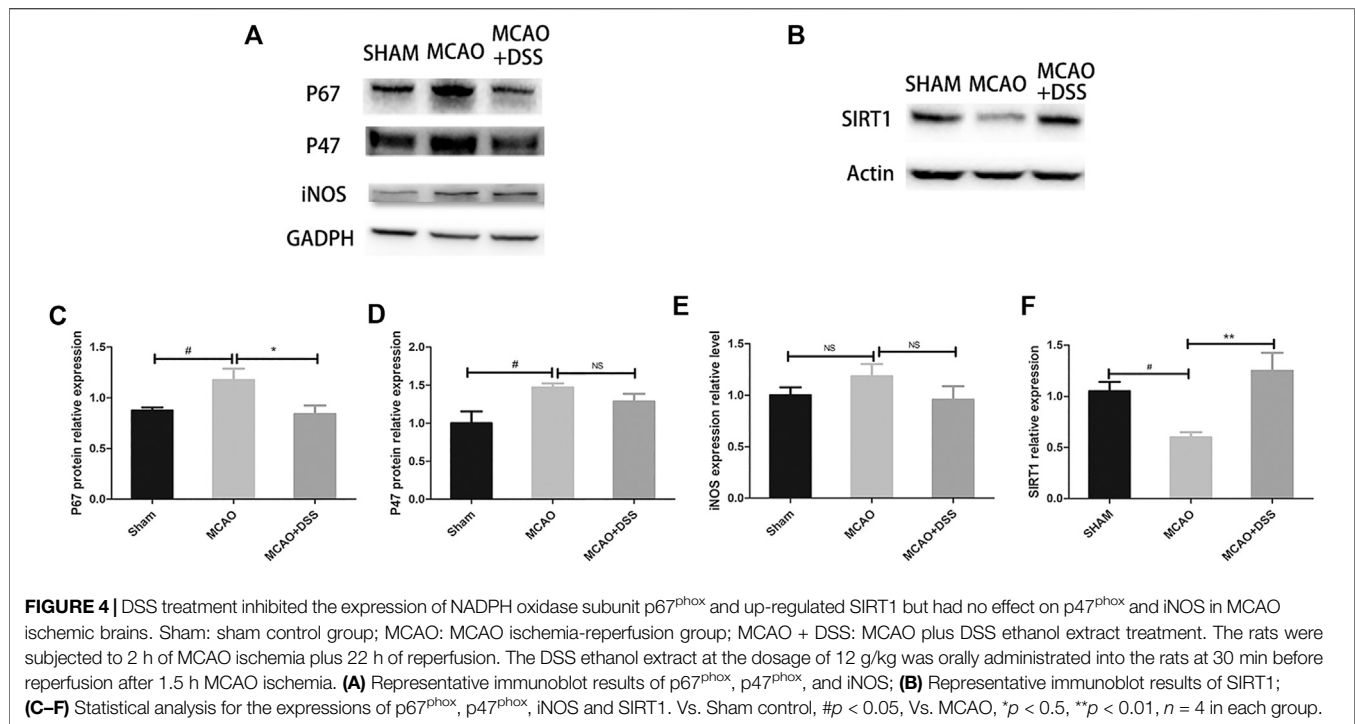
SIRT1 Inhibitor EX527 Ablated Neuroprotective Effects of DSS Ethanol Extract Against Cerebral Ischemia-Reperfusion Injury

We further explored whether the therapeutic effect of DSS is SIRT1-dependent. We injected SIRT1 specific inhibitor EX527 at 5 mg/kg into rat brains intraperitoneally prior to MCAO operation. DSS treatment reduced infarct size and improved neurological functions whose effects were abolished by EX527 (**Figures 6**). Thus, SIRT1 signaling could be one of the therapeutic targets of DSS against cerebral ischemia-reperfusion injury.

Qualitative and Quantitative Analysis of DSS Ethanol Extract

For the quality control of DSS/E, we identified three ingredients as the standard for HPLC analysis, including paeoniflorin, alibiflorin, and ferulic acid. The chromatographic condition was optimized and a well-separated fingerprint was obtained (**Figure 7**). The linearity, precision, stability, and accuracy were measured in the HPLC system (**Table 1**). The linearities of the standard curves for paeoniflorin, alibiflorin, and ferulic acid were $y = 6.903x - 98.718$ with correlation coefficients (r) 1, $y = 6.903x - 17.161$ with correlation coefficients 0.9994, $y = 17.906x + 9.819$ with correlation coefficients 1, respectively. The precisions of paeoniflorin, alibiflorin, and ferulic acid were assayed by intra-day variations (RSD) at one concentration with six replicates, which were 1.8, 1.8, and 1.6%, respectively. The stability was assessed by the RSD values of peak areas which had 1.0, 0.1, and 2.3% for

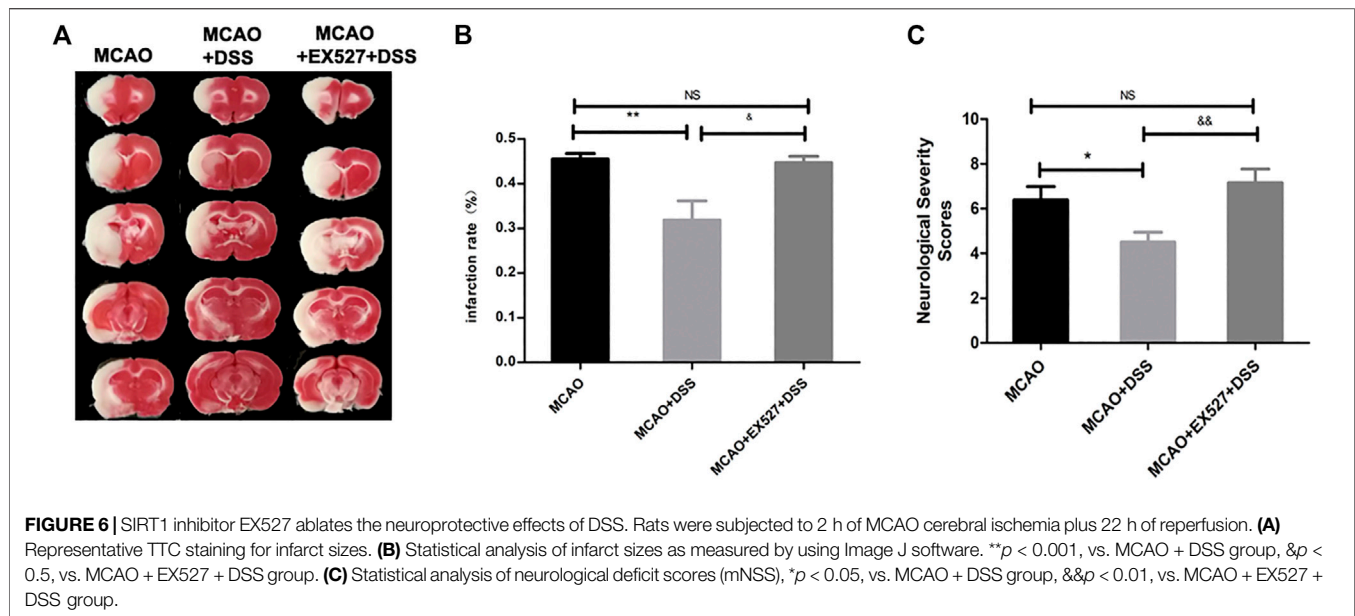




paeoniflorin, alibiflorin, and ferulic acid respectively. The accuracy of the analytical method was confirmed with the overall recovery of 99.5–108.5%. These results suggest that the HPLC-UV method has good sensitivity, accuracy, and stability. With the validated HPLC-UV method, the concentrations of paeoniflorin, alibiflorin, and ferulic acid were identified to be 39.7412, 5.3411, and 0.8221 µg/mg, respectively, in DSS ethanol extract.

DISCUSSION

In the present study, we investigated the efficacies of aqueous and ethanol extract of Danggui-Shaoyao-San (DSS) against cerebral ischemia-reperfusion injury. Ethanol extract of DSS, instead of aqueous extract, significantly reduced infarct sizes and improved neurological deficit mNSS scores in the transient MCAO



ischemia rats. The DSS ethanol extract inhibited the expression of NADPH oxidase subunit p67^{phox} and up-regulated SIRT1, decreased the productions of superoxide and peroxynitrite, attenuated infarct sizes and improved neurological functions in the transient MCAO ischemic rats. Those results indicate that ethanol extract of DSS has much better neuroprotective effects than the aqueous extract. The results could be used for the application of DSS in the TCM treatment for ischemic stroke.

DSS was firstly documented to be prepared with “wine” to enhance its therapeutic effects in *Essentials from the Golden Cabinet*, a classic TCM textbook written in the Eastern Han Dynasty by Master Zhongjing Zhang. A previous study reported that the organic solvent extract of DSS had higher concentrations of paeoniflorin and alibiflorin than the aqueous extract (Liu et al., 2010). Paeoniflorin has antioxidant and anti-inflammation activities and neuroprotective effects against cerebral ischemia-reperfusion injury (Tang et al., 2010; Guo et al., 2012; Zhang et al., 2015; Zhang Y. et al., 2017). Paeoniflorin increased blood supply to the ischemic hemisphere in an experimental focal cerebral ischemia-reperfusion animal model (Rao et al., 2014). Albiflorin has the capacity to pass through the BBB and protect the BBB integrity in cerebral ischemia-reperfusion injury (Li et al., 2015). Ferulic acid exerts antioxidant properties and has neuroprotective effects against cerebral ischemia/reperfusion-induced injury (Cheng et al., 2008; Cheng et al., 2016; Ren et al., 2017; Cheng et al., 2019). Thus, we used paeoniflorin, alibiflorin, and ferulic acid as marker compounds for quality control whose concentrations were 39.7412, 5.3411, and 0.8221 $\mu\text{g}/\text{mg}$ in DSS ethanol extract respectively.

ROS and RNS play important roles in the pathological process of cerebral ischemic-reperfusion injury (Chen et al., 2013; Chen et al., 2016; Chen et al., 2018). NADPH oxidase is a major pro-oxidant enzyme for O_2^- generation whereas iNOS activation produces high concentration of NO. Our previous studies

indicate that ischemia-reperfusion significantly up-regulated NADPH oxidase subunits p47^{phox} and p67^{phox}, and iNOS and increased the production of O_2^- and NO, subsequently inducing the production of ONOO⁻ and aggravating cerebral ischemia-reperfusion injury (Chen et al., 2015; Chen et al., 2020). Peroxynitrite has much higher toxicity and penetrating capacity across the lipid membrane than O_2^- (Moro et al., 2005; Pacher et al., 2007). The levels of ONOO⁻ and its footprint marker 3-NT were confirmed in the cerebrospinal fluid (CSF) and plasma of stroke patients (Nanetti et al., 2007; Isobe et al., 2009). The increased ONOO⁻ production, mediates DNA damage, protein nitration and lipid peroxidation, activates matrix metalloproteinases (MMPs), degrades tight junction proteins, and aggravates the BBB disruption in ischemic brain injury (Salgo et al., 1995; Virag et al., 2003; Kuhn et al., 2004; Tajés et al., 2013; Ding et al., 2014). Thus, we used HET and HKSOX1 to directly visualize and detected 3-NT expression in the ischemic brain tissues after the rats were exposed to 2 h of MCAO ischemia plus 22 h of reperfusion. The levels of O_2^- and 3-NT were increased in the ischemic brains which were reduced by treatment of DSS. The expression levels of p47^{phox} and p67^{phox} were significantly increased in the ischemia-reperfused brains. The expression of iNOS had a trend of increase but without statistical differences. Treatment of DSS significantly down-regulated the expression of p67^{phox} but has no effect on the expression of p47^{phox} and iNOS statistically. Those results suggest that DSS could inhibit the production of O_2^- and ONOO⁻ through inhibiting NADPH oxidases in the MCAO ischemic brains.

Notably, DSS ethanol extract up-regulated the expression of Silent information regulator 1 (SIRT1) in ischemic brains whose effect was abolished by EX527, a SIRT1 inhibitor. SIRT1 is a NAD⁺ dependent histone deacetylase. SIRT1 plays an essential roles in multiple cellular events including cellular stress resistance

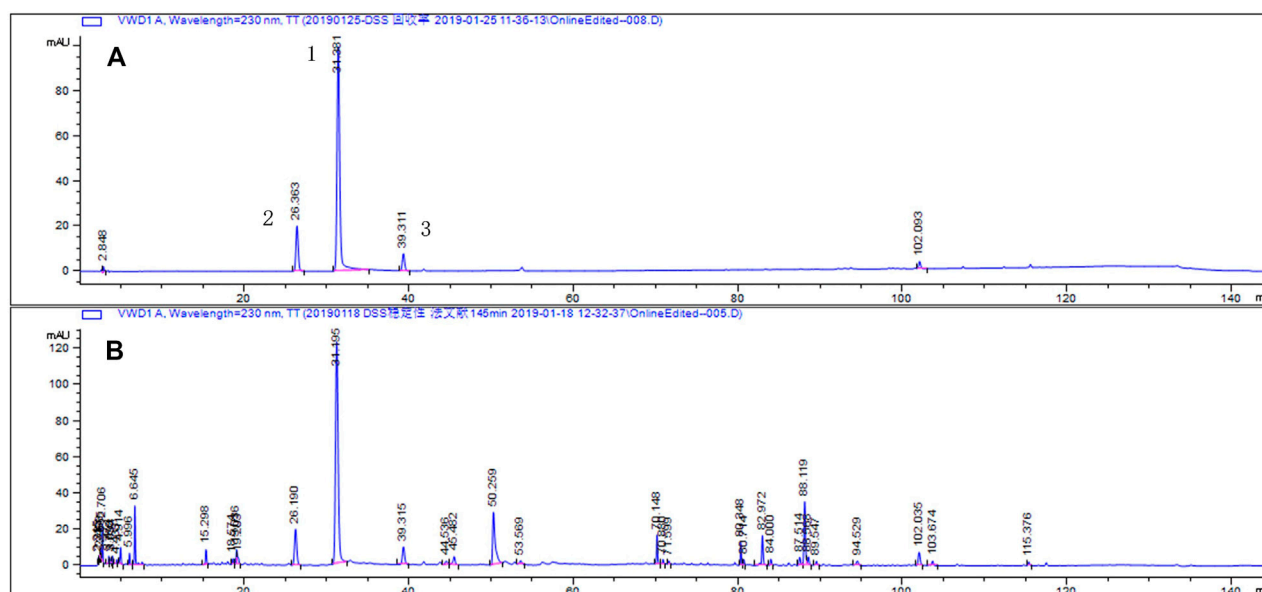


FIGURE 7 | Representative chromatograms of standard compounds **(A)** and DSS ethanol extract **(B)** analyzed by HPLC-UV. 1) paeoniflorin; 2) alibiflorin; 3) ferulic acid.

TABLE 1 | The linearity, precision, stability results of standard compounds paeoniflorin, alibiflorin, and ferulic acid.

Standard compounds	Regression equation (R^2) of the linearity	RSD indicator of the precision assay (%)	RSD indicator of the stability assay (%)
Paeoniflorin	$Y = 6.903X - 98.718$ (1)	1.8	1.0
Alibiflorin	$Y = 6.903X - 17.161$ (0.994)	1.8	0.1
Ferulic acid	$Y = 17.906X + 9.819$ (1)	1.6	2.3

Correlation coefficients, R^2 .

(Brunet et al., 2004; Han et al., 2017), energy metabolism (Purushotham et al., 2009; Cao et al., 2016), oxidation stress (Singh et al., 2017; Rada et al., 2018), inflammation (Yang et al., 2015), and apoptosis (Zhang M. et al., 2017; Chen et al., 2019). SIRT1 has antioxidant activity in vascular endothelial cells by modulating multiple molecular targets including FOXOs, NF- κ B, NOX, SOD, and eNOS, etc. (Zhang W. et al., 2017). For example, SIRT1 inhibits NADPH oxidase activation and protects endothelial function (Zarzuelo et al., 2013). SIRT1 knockout mice had larger infarct sizes than wild-type mice after exposed to MCAO cerebral ischemia (Hernandez-Jimenez et al., 2013; Liu et al., 2013). Treatment of resveratrol, a SIRT1 activator, decreased infarct size, lessened brain edema, attenuated the BBB disruption, and improved neurological functional outcomes (Huang et al., 2001; Gao et al., 2006; Tsai et al., 2007; Cheng et al., 2009; Yousuf et al., 2009) whereas SIRT1 inhibitors aggravated ischemic brain injury (Hernandez-Jimenez et al., 2013). Thus, the antioxidant property of SIRT1 might contribute to the neuroprotective effects of DSS against cerebral ischemia-

reperfusion injury. With multiple active gradients in the DSS formula, it is of interesting to explore the active compounds with the properties of regulating SIRT1 signaling. A recent study revealed that paeoniflorin attenuated ox-LDL-induced apoptosis and inhibited adhesion molecule expression via upregulating SIRT1 in endothelial cells (Wang et al., 2019). Of note, DSS has multiple constituents (Fu et al., 2016) with complex network regulating mechanisms in ischemic brain injury, the exact molecular targets and mechanisms remain to be further elucidated.

In conclusion, DSS ethanol extract could protect against cerebral ischemic-reperfusion injury via attenuating oxidative/nitrosative stress and inhibiting neuronal apoptosis via inhibiting NADPH oxidases and activating SIRT1 signaling.

DATA AVAILABILITY STATEMENT

The raw data supporting the conclusions of this article will be made available by the authors, without undue reservation.

ETHICS STATEMENT

The animal study was reviewed and approved by The Committee on the Use of Live Animals for Teaching and Research (CULATR), University of Hong Kong.

AUTHOR CONTRIBUTIONS

JS and QW conceived the idea; JS received fund to support the study; YL and HC performed the experiments; YL and JS wrote the manuscript; HC, BT, and JS revised the manuscript.

REFERENCES

- Bas, D. F., Topcuoglu, M. A., Gursay-Ozdemir, Y., Saatci, I., Bodur, E., and Dalkara, T. (2012). Plasma 3-nitrotyrosine estimates the reperfusion-induced cerebrovascular stress, whereas matrix metalloproteinases mainly reflect plasma activity: a study in patients treated with thrombolysis or endovascular recanalization. *J. Neurochem.* 123 (Suppl. 2), 138–147. doi:10.1111/j.1471-4159.2012.07952.x
- Benjamin, E. J., Blaha, M. J., Chiuve, S. E., Cushman, M., Das, S. R., Deo, R., et al. (2017). Heart disease and stroke statistics-2017 update: a report from the American heart association. *Circulation* 135, e146–e603. doi:10.1161/cir.0000000000000485
- Brunet, A., Sweeney, L. B., Sturgill, J. F., Chua, K. F., Greer, P. L., Lin, Y., et al. (2004). Stress-dependent regulation of FOXO transcription factors by the SIRT1 deacetylase. *Science* 303, 2011–2015. doi:10.1126/science.1094637
- Cao, Y., Jiang, X., Ma, H., Wang, Y., Xue, P., and Liu, Y. (2016). SIRT1 and insulin resistance. *J. Diabetes its Complications* 30, 178–183. doi:10.1016/j.jdiacomp.2015.08.022
- Chen, D. Z., Wang, W. W., Chen, Y. L., Yang, X. F., Zhao, M., and Yang, Y. Y. (2019). miR128 is upregulated in epilepsy and promotes apoptosis through the SIRT1 cascade. *Int. J. Mol. Med.* 694–704. doi:10.3892/ijmm.2019.4223
- Chen, H.-S., Chen, X.-M., Feng, J.-H., Liu, K.-J., Qi, S.-H., and Shen, J.-G. (2015). Peroxynitrite decomposition catalyst reduces delayed thrombolysis-induced hemorrhagic transformation in ischemia-reperfusion rat brains. *CNS Neurosci. Ther.* 21, 585–590. doi:10.1111/cns.12406
- Chen, H., Guan, B., Chen, X., Chen, X., Li, C., Qiu, J., et al. (2018). Baicalin attenuates blood-brain barrier disruption and hemorrhagic transformation and improves neurological outcome in ischemic stroke rats with delayed t-PA treatment: involvement of ONOO⁻-MMP-9 pathway. *Transl. Stroke Res.* 9, 515–529. doi:10.1007/s12975-017-0598-3
- Chen, H., Guan, B., Wang, B., Pu, H., Bai, X., Chen, X., et al. (2020). Glycyrrhizin prevents hemorrhagic transformation and improves neurological outcome in ischemic stroke with delayed thrombolysis through targeting peroxynitrite-mediated HMGB1 signaling. *Transl. Stroke Res.* 11, 967–982. doi:10.1007/s12975-019-00772-1
- Chen, J., Sanberg, P. R., Li, Y., Wang, L., Lu, M., Willing, A. E., et al. (2001). Intravenous administration of human umbilical cord blood reduces behavioral deficits after stroke in rats. *Stroke* 32, 2682–2688. doi:10.1161/hs1101.098367
- Chen, X.-m., Chen, H.-s., Xu, M.-j., and Shen, J.-g. (2013). Targeting reactive nitrogen species: a promising therapeutic strategy for cerebral ischemia-reperfusion injury. *Acta Pharmacol. Sin.* 34, 67–77. doi:10.1038/aps.2012.82
- Cheng, C.-Y., Ho, T.-Y., Lee, E.-J., Su, S.-Y., Tang, N.-Y., and Hsieh, C.-L. (2008). Ferulic acid reduces cerebral infarct through its antioxidative and anti-inflammatory effects following transient focal cerebral ischemia in rats. *Am. J. Chin. Med.* 36, 1105–1119. doi:10.1142/s0192415x08006570
- Cheng, C.-Y., Kao, S.-T., and Lee, Y.-C. (2019). Ferulic acid exerts anti-apoptotic effects against ischemic injury by activating HSP70/bcl-2- and HSP70/autophagy-mediated signaling after permanent focal cerebral ischemia in rats. *Am. J. Chin. Med.* 47, 39–61. doi:10.1142/s0192415x19500034
- Cheng, C. Y., Tang, N. Y., Kao, S. T., and Hsieh, C. L. (2016). Ferulic acid administered at various time points protects against cerebral infarction by activating p38 MAPK/p90RSK/CREB/Bcl-2 anti-apoptotic signaling in the subacute phase of cerebral ischemia-reperfusion injury in rats. *PLoS One* 11, e0155748. doi:10.1371/journal.pone.0155748
- Cheng, G., Zhang, X., Gao, D., Jiang, X., and Dong, W. (2009). Resveratrol inhibits MMP-9 expression by up-regulating PPAR α expression in an oxygen glucose deprivation-exposed neuron model. *Neurosci. Lett.* 451, 105–108. doi:10.1016/j.neulet.2008.12.045
- Ding, R., Chen, Y., Yang, S., Deng, X., Fu, Z., Feng, L., et al. (2014). Blood-brain barrier disruption induced by hemoglobin *in vivo*: involvement of up-regulation of nitric oxide synthase and peroxynitrite formation. *Brain Res.* 1571, 25–38. doi:10.1016/j.brainres.2014.04.042
- Fabian, R. H., Dewitt, D. S., and Kent, T. A. (1995). *In vivo* detection of superoxide anion production by the brain using a cytochrome c electrode. *J. Cereb. Blood Flow Metab.* 15, 242–247. doi:10.1038/jcbfm.1995.30
- Feigin, V. L., Forouzanfar, M. H., Krishnamurthi, R., Mensah, G. A., Connor, M., Bennett, D. A., et al. (2014). Global and regional burden of stroke during 1990–2010: findings from the global burden of disease study 2010. *The Lancet* 383, 245–255. doi:10.1016/s0140-6736(13)61953-4
- Feigin, V. L., Krishnamurthi, R. V., Parmar, P., Norrving, B., Mensah, G. A., Bennett, D. A., et al. (2015). Update on the global burden of ischemic and hemorrhagic stroke in 1990–2013: the GBD 2013 study. *Neuroepidemiology* 45, 161–176. doi:10.1159/000441085
- Feng, J., Chen, X., Lu, S., Li, W., Yang, D., Su, W., et al. (2018). Naringin attenuates cerebral ischemia-reperfusion injury through inhibiting peroxynitrite-mediated mitophagy activation. *Mol. Neurobiol.* 55(12):9029–9042. doi:10.1007/s12035-018-1027-7
- Fu, B., Zhang, J., Zhang, X., Zhang, C., Li, Y., Zhang, Y., et al. (2014). Alpha-lipoic acid upregulates SIRT1-dependent PGC-1 α expression and protects mouse brain against focal ischemia. *Neuroscience* 281, 251–257. doi:10.1016/j.neuroscience.2014.09.058
- Fu, X., Wang, Q., Wang, Z., Kuang, H., and Jiang, P. (2016). Danggui-shaoyao-san: new hope for Alzheimer's disease. *A&D* 7, 502–513. doi:10.14336/ad.2015.1220
- Gao, D., Zhang, X., Jiang, X., Peng, Y., Huang, W., Cheng, G., et al. (2006). Resveratrol reduces the elevated level of MMP-9 induced by cerebral ischemia-reperfusion in mice. *Life Sci.* 78, 2564–2570. doi:10.1016/j.lfs.2005.10.030
- Gong, J., Sun, F., Li, Y., Zhou, X., Duan, Z., Duan, F., et al. (2015). Momordica charantia polysaccharides could protect against cerebral ischemia/reperfusion injury through inhibiting oxidative stress mediated c-Jun N-terminal kinase 3 signaling pathway. *Neuropharmacology* 91, 123–134. doi:10.1016/j.neuropharm.2014.11.020
- Goto, H., Satoh, N., Hayashi, Y., Hikiami, H., Nagata, Y., Obi, R., et al. (2011). A Chinese herbal medicine, tokishakuyakusan, reduces the worsening of impairments and independence after stroke: a 1-year randomized, controlled Trial. *Evidence-based Complementary and alternative medicine* 2011:194046, doi:10.1093/ecam/nep026
- Guo, R. B., Wang, G. F., Zhao, A. P., Gu, J., Sun, X. L., and Hu, G. (2012). Paeoniflorin protects against ischemia-induced brain damages in rats via

FUNDING

This work was supported by General Research Fund (GRF No. 17118717, No 17105220), Research Grant Council, AoE/P-705/16 Areas of Excellence Scheme, Research Grant Council; Hong Kong SAR, China. Seed Fund for Basic Research (No. 201811159037), University of Hong Kong.

SUPPLEMENTARY MATERIAL

The Supplementary Material for this article can be found online at: <https://www.frontiersin.org/articles/10.3389/fphar.2021.653795/full#supplementary-material>.

- inhibiting MAPKs/NF-kappaB-mediated inflammatory responses. *PLoS One* 7, e49701. doi:10.1371/journal.pone.0049701
- Han, C., Gu, Y., Shan, H., Mi, W., Sun, J., Shi, M., et al. (2017). O-GlcNAcylation of SIRT1 enhances its deacetylase activity and promotes cytoprotection under stress. *Nat. Commun.* 8, 1491. doi:10.1038/s41467-017-01654-6
- Hattori, Y., Okamoto, Y., Maki, T., Yamamoto, Y., Oishi, N., Yamahara, K., et al. (2014). Silent information regulator 2 homolog 1 counters cerebral hypoperfusion injury by deacetylating endothelial nitric oxide synthase. *Stroke* 45, 3403–3411. doi:10.1161/strokeaha.114.006265
- Hattori, Y., Okamoto, Y., Nagatsuka, K., Takahashi, R., Kalaria, R. N., Kinoshita, M., et al. (2015). SIRT1 attenuates severe ischemic damage by preserving cerebral blood flow. *Neuroreport* 26, 113–117. doi:10.1097/wnr.0000000000000308
- He, Q., Li, Z., Wang, Y., Hou, Y., Li, L., and Zhao, J. (2017). Resveratrol alleviates cerebral ischemia/reperfusion injury in rats by inhibiting NLRP3 inflammasome activation through Sirt1-dependent autophagy induction. *Int. Immunopharmacology* 50, 208–215. doi:10.1016/j.intimp.2017.06.029
- Hernandez-Jimenez, M., Hurtado, O., Cuartero, M. I., Ballesteros, I., Moraga, A., Pradillo, J. M., et al. (2013). Silent information regulator 1 protects the brain against cerebral ischemic damage. *Stroke* 44, 2333–2337. doi:10.1161/strokeaha.113.001715
- Hu, J. J., Wong, N.-K., Ye, S., Chen, X., Lu, M.-Y., Zhao, A. Q., et al. (2015). Fluorescent probe HKSOX-1 for imaging and detection of endogenous superoxide in live cells and in vivo. *J. Am. Chem. Soc.* 137, 6837–6843. doi:10.1021/jacs.5b01881
- Huang, S. S., Tsai, M. C., Chih, C. L., Hung, L. M., and Tsai, S. K. (2001). Resveratrol reduction of infarct size in Long-Evans rats subjected to focal cerebral ischemia. *Life Sci.* 69, 1057–1065. doi:10.1016/s0024-3205(01)01195-x
- Isobe, C., Abe, T., and Terayama, Y. (2009). Remarkable increase in 3-nitrotyrosine in the cerebrospinal fluid in patients with lacunar stroke. *Brain Res.* 1305, 132–136. doi:10.1016/j.brainres.2009.09.108
- Izzettin, H.-a.-K., Bölükbaş, H. F., Yoshitaka, Y., Katsunori, I., Nobuaki, E., An-Xin, L., et al. (2007). Effect of Toki-shakuyaku-san on acetylcholine level and blood flow in dorsal *Hippocampus* of intact and twice-repeated ischemic rats. *Phytotherapy Res.* 21, 291–294. doi:10.1002/ptr.2050
- Kawano, T., Anrather, J., Zhou, P., Park, L., Wang, G., Frys, K. A., et al. (2006). Prostaglandin E2 EP1 receptors: downstream effectors of COX-2 neurotoxicity. *Nat. Med.* 12, 225–229. doi:10.1038/nm1362
- Kim, S.-H., Chung, D.-K., Lee, Y. J., Song, C.-H., and Ku, S.-K. (2016). Neuroprotective effects of Danggui-Jakyak-San on rat stroke model through antioxidant/antiapoptotic pathway. *J. Ethnopharmacology* 188, 123–133. doi:10.1016/j.jep.2016.04.060
- Kou, D.-Q., Jiang, Y.-L., Qin, J.-H., and Huang, Y.-H. (2017). Magnolol attenuates the inflammation and apoptosis through the activation of SIRT1 in experimental stroke rats. *Pharmacol. Rep.* 69, 642–647. doi:10.1016/j.pharep.2016.12.012
- Kuhn, D. M., Sakowski, S. A., Sadidi, M., and Geddes, T. J. (2004). Nitrotyrosine as a marker for peroxynitrite-induced neurotoxicity: the beginning or the end of the end of dopamine neurons? *J. Neurochem.* 89, 529–536. doi:10.1111/j.1471-4159.2004.02346.x
- Lee, H. W., Jun, J. H., Kil, K.-J., Ko, B.-S., Lee, C. H., and Lee, M. S. (2016). Herbal medicine (Danggui Shaoyao San) for treating primary dysmenorrhea: a systematic review and meta-analysis of randomized controlled trials. *Maturitas* 85, 19–26. doi:10.1016/j.maturitas.2015.11.013
- Li, D., Ke, Y., Zhan, R., Liu, C., Zhao, M., Zeng, A., et al. (2018). Trimethylamine-N-oxide promotes brain aging and cognitive impairment in mice. *Aging Cell* 17, e12768. doi:10.1111/acel.12768
- Li, H., Ye, M., Zhang, Y., Huang, M., Xu, W., Chu, K., et al. (2015). Blood-brain barrier permeability of Gualou Guizhi granules and neuroprotective effects in ischemia/reperfusion injury. *Mol. Med. Rep.* 12, 1272–1278. doi:10.3892/mmr.2015.3520
- Lin, Z., Zhu, D., Yan, Y., and Yu, B. (2008). Herbal formula FBD extracts prevented brain injury and inflammation induced by cerebral ischemia-reperfusion. *J. Ethnopharmacology* 118, 140–147. doi:10.1016/j.jep.2008.03.023
- Liu, A.-J., Guo, J.-M., Liu, W., Su, F.-Y., Zhai, Q.-W., Mehta, J. L., et al. (2013). Involvement of arterial baroreflex in the protective effect of dietary restriction against stroke. *J. Cereb. Blood Flow Metab.* 33, 906–913. doi:10.1038/jcbfm.2013.28
- Liu, Z., Song, X., Wang, M. Y., and Xu, F. (2010). Comparative study on the content of paeoniflorin and ferulic acid of dangguishao Yao San by different extraction methods. *Asia-Pacific Traditional Med.* 006, 20–22. doi:10.3969/j.issn.1003-1634.2004.05.017
- Lu, H., and Wang, B. (2017). SIRT1 exerts neuroprotective effects by attenuating cerebral ischemia/reperfusion-induced injury via targeting p53/microRNA-22. *Int. J. Mol. Med.* 39, 208–216. doi:10.3892/ijmm.2016.2806
- Mccord, J. M. (1985). Oxygen-derived free radicals in postischemic tissue injury. *N. Engl. J. Med.* 312, 159–163. doi:10.1056/NEJM198501173120305
- Miller, A. A., Dusting, G. J., Roulston, C. L., and Sobey, C. G. (2006). NADPH-oxidase activity is elevated in penumbral and non-ischemic cerebral arteries following stroke. *Brain Res.* 1111, 111–116. doi:10.1016/j.brainres.2006.06.082
- Moro, M., Almeida, A., Bolanos, J., and Lizasoain, I. (2005). Mitochondrial respiratory chain and free radical generation in stroke. *Free Radic. Biol. Med.* 39, 1291–1304. doi:10.1016/j.freeradbiomed.2005.07.010
- Mozaffarian, D., Benjamin, E. J., Go, A. S., Arnett, D. K., Blaha, M. J., Cushman, M., et al. (2016). Executive summary: heart disease and stroke statistics-2016 update. *Circulation* 133, 447–454. doi:10.1161/cir.0000000000000366
- Nanetti, L., Taffi, R., Vignini, A., Moroni, C., Raffaelli, F., Bacchetti, T., et al. (2007). Reactive oxygen species plasmatic levels in ischemic stroke. *Mol. Cell Biochem.* 303, 19–25. doi:10.1007/s11010-007-9451-4
- Pacher, P., Beckman, J. S., and Liaudet, L. (2007). Nitric oxide and peroxynitrite in health and disease. *Physiol. Rev.* 87, 315–424. doi:10.1152/physrev.00029.2006
- Purushotham, A., Schug, T. T., Xu, Q., Surapureddi, S., Guo, X., and Li, X. (2009). Hepatocyte-specific deletion of SIRT1 alters fatty acid metabolism and results in hepatic steatosis and inflammation. *Cel Metab.* 9, 327–338. doi:10.1016/j.cmet.2009.02.006
- Rada, P., Pardo, V., Mobasher, M. A., García-Martínez, I., Ruiz, L., González-Rodríguez, Á., et al. (2018). SIRT1 controls acetaminophen hepatotoxicity by modulating inflammation and oxidative stress. *Antioxid. Redox Signaling* 28, 1187–1208. doi:10.1089/ars.2017.7373
- Rao, M. L., Tang, M., He, J. Y., and Dong, Z. (2014). [Effects of paeoniflorin on cerebral blood flow and the balance of PGI2/TXA2 of rats with focal cerebral ischemia-reperfusion injury]. *Yao Xue Xue Bao* 49, 55–60. doi:10.16438/j.0513-4870.2014.01.008
- Ren, C., Wang, B., Li, N., Jin, K., and Ji, X. (2015). Herbal formula dangguishao Yao San promotes neurogenesis and angiogenesis in rat following middle cerebral artery occlusion. *A&D* 6, 245–253. doi:10.14336/ad.2014.1126
- Ren, Q., Hu, Z., Jiang, Y., Tan, X., Botchway, B. O. A., Amin, N., et al. (2019). SIRT1 protects against apoptosis by promoting autophagy in the oxygen glucose deprivation/reperfusion-induced injury. *Front. Neurol.* 10, 1289. doi:10.3389/fneur.2019.01289
- Ren, Y., Zhao, Y., and Lu, S. (2013). Clinical observation on effect of Danggui shaoyao powder combined with rehabilitation technique in treatment of 60 cases cerebral infarction. *J. Liaoning Univ. Traditional Chin. Med.* 8, 087.
- Ren, Z., Zhang, R., Li, Y., Li, Y., Yang, Z., and Yang, H. (2017). Ferulic acid exerts neuroprotective effects against cerebral ischemia/reperfusion-induced injury via antioxidant and anti-apoptotic mechanisms *in vitro* and *in vivo*. *Int. J. Mol. Med.* 40, 1444–1456. doi:10.3892/ijmm.2017.3127
- Robinson, M. A., Baumgardner, J. E., and Otto, C. M. (2011). Oxygen-dependent regulation of nitric oxide production by inducible nitric oxide synthase. *Free Radic. Biol. Med.* 51, 1952–1965. doi:10.1016/j.freeradbiomed.2011.08.034
- Salgo, M. G., Squadrito, G. L., and Pryor, W. A. (1995). Peroxynitrite causes apoptosis in rat thymocytes. *Biochem. Biophysical Res. Commun.* 215, 1111–1118. doi:10.1006/bbrc.1995.2578
- Seto, S.-W., Chang, D., Jenkins, A., Bensoussan, A., and Kiat, H. (2016). Angiogenesis in ischemic stroke and angiogenic effects of Chinese herbal medicine. *Jcm* 5, 56. doi:10.3390/jcm5060056
- Shin, J. A., Lee, K.-E., Kim, H.-S., and Park, E.-M. (2012). Acute resveratrol treatment modulates multiple signaling pathways in the ischemic brain. *Neurochem. Res.* 37, 2686–2696. doi:10.1007/s11064-012-0858-2
- Singh, P., Hanson, P. S., and Morris, C. M. (2017). SIRT1 ameliorates oxidative stress induced neural cell death and is down-regulated in Parkinson's disease. *BMC Neurosci.* 18, 46. doi:10.1186/s12868-017-0364-1
- Song, M. D., Kim, D. H., Kim, J. M., Lee, H. E., Park, S. J., Ryu, J. H., et al. (2013). Danggui-Jakyak-San ameliorates memory impairment and increase neurogenesis

- induced by transient forebrain ischemia in mice. *BMC Complement. Altern. Med.* 13, 324. doi:10.1186/1472-6882-13-324
- Tajbakhsh, N., and Sokoya, E. M. (2012). Regulation of cerebral vascular function by sirtuin 1. *Microcirculation* 19, 336–342. doi:10.1111/j.1549-8719.2012.00167.x
- Tajes, M., Ill-Raga, G., Palomer, E., Ramos-Fernandez, E., Guix, F. X., Bosch-Morato, M., et al. (2013). Nitro-oxidative stress after neuronal ischemia induces protein nitrotyrosination and cell death. *Oxid. Med. Cel Longev* 2013, 826143. doi:10.1155/2013/826143
- Tang, N.-Y., Liu, C.-H., Hsieh, C.-T., and Hsieh, C.-L. (2010). The anti-inflammatory effect of paeoniflorin on cerebral infarction induced by ischemia-reperfusion injury in Sprague-Dawley rats. *Am. J. Chin. Med.* 38, 51–64. doi:10.1142/s0192415x10007786
- Teertam, S. K., Jha, S., and Prakash Babu, P. (2020). Up-regulation of Sirt1/miR-149-5p signaling may play a role in resveratrol induced protection against ischemia via p53 in rat brain. *J. Clin. Neurosci.* 72, 402–411. doi:10.1016/j.jocn.2019.11.043
- Tsai, S.-K., Hung, L.-M., Fu, Y.-T., Cheng, H., Nien, M.-W., Liu, H.-Y., et al. (2007). Resveratrol neuroprotective effects during focal cerebral ischemia injury via nitric oxide mechanism in rats. *J. Vasc. Surg.* 46, 346–353. doi:10.1016/j.jvs.2007.04.044
- Virág, L., Szabó, É., Gergely, P., and Szabó, C. (2003). Peroxynitrite-induced cytotoxicity: mechanism and opportunities for intervention. *Toxicol. Lett.* 140–141, 113–124. doi:10.1016/s0378-4274(02)00508-8
- Wang, T., Gu, J., Wu, P.-F., Wang, F., Xiong, Z., Yang, Y.-J., et al. (2009). Protection by tetrahydroxystilbene glucoside against cerebral ischemia: involvement of JNK, SIRT1, and NF- κ B pathways and inhibition of intracellular ROS/RNS generation. *Free Radic. Biol. Med.* 47, 229–240. doi:10.1016/j.freeradbiomed.2009.02.027
- Wang, Y., Che, J., Zhao, H., Tang, J., and Shi, G. (2019). Paeoniflorin attenuates oxidized low-density lipoprotein-induced apoptosis and adhesion molecule expression by autophagy enhancement in human umbilical vein endothelial cells. *J. Cel Biochem.* 120, 9291–9299. doi:10.1002/jcb.28204
- Wang, Y. L., Ru, S. Y., Fang, Q., Li, G. Q., Pan, Y. F., Yao, Y., et al. (2015). [Mechanism study on Danggui shaoyao san and guizhi fuling wan for treating primary dysmenorrheal based on biological network]. *Zhong Yao Cai* 38, 2348–2352. doi:10.13863/j.issn1001-4454.2015.11.028
- Winterbourn, C. C., Kettle, A. J., and Hampton, M. B. (2016). Reactive oxygen species and neutrophil function. *Annu. Rev. Biochem.* 85, 765–792. doi:10.1146/annurev-biochem-060815-014442
- Wu, B., Liu, M., Liu, H., Li, W., Tan, S., Zhang, S., et al. (2007). Meta-analysis of traditional Chinese patent medicine for ischemic stroke. *Stroke* 38, 1973–1979. doi:10.1161/strokeaha.106.473165
- Yang, H., Bi, Y., Xue, L., Wang, J., Lu, Y., Zhang, Z., et al. (2015). Multifaceted modulation of SIRT1 in cancer and inflammation. *Crit. Rev. Oncog* 20, 49–64. doi:10.1615/critrevoncog.2014012374
- Yousuf, S., Atif, F., Ahmad, M., Hoda, N., Ishrat, T., Khan, B., et al. (2009). Resveratrol exerts its neuroprotective effect by modulating mitochondrial dysfunctions and associated cell death during cerebral ischemia. *Brain Res.* 1250, 242–253. doi:10.1016/j.brainres.2008.10.068
- Zarzuelo, M. J., López-Sepúlveda, R., Sánchez, M., Romero, M., Gómez-Guzmán, M., Ungvary, Z., et al. (2013). SIRT1 inhibits NADPH oxidase activation and protects endothelial function in the rat aorta: implications for vascular aging. *Biochem. Pharmacol.* 85, 1288–1296. doi:10.1016/j.bcp.2013.02.015
- Zhang, M., Zhang, Q., Hu, Y., Xu, L., Jiang, Y., Zhang, C., et al. (2017a). miR-181a increases FoxO1 acetylation and promotes granulosa cell apoptosis via SIRT1 downregulation. *Cell Death Dis.* 8, e3088. doi:10.1038/cddis.2017.467
- Zhang, W., Huang, Q., Zeng, Z., Wu, J., Zhang, Y., and Chen, Z. (2017b). Sirt1 inhibits oxidative stress in vascular endothelial cells. *Oxid. Med. Cel Longev* 2017, 7543973. doi:10.1155/2017/7543973
- Zhang, Y., Li, H., Huang, M., Huang, M., Chu, K., Xu, W., et al. (2015). Paeoniflorin, a monoterpene glycoside, protects the brain from cerebral ischemic injury via inhibition of apoptosis. *Am. J. Chin. Med.* 43, 543–557. doi:10.1142/s0192415x15500342
- Zhang, Y., Qiao, L., Xu, W., Wang, X., Li, H., Xu, W., et al. (2017c). Paeoniflorin attenuates cerebral ischemia-induced injury by regulating Ca(2+)/CaMKII/CREB signaling pathway. *Molecules* 22. doi:10.3390/molecules22030359
- Zhang, Z. J. (2005). *Synopsis of prescriptions of the golden chamber*. Chicago. People's sanitary publishing press.

Conflict of Interest: The authors declare that the research was conducted in the absence of any commercial or financial relationships that could be construed as a potential conflict of interest.

Copyright © 2021 Luo, Chen, Tsoi, Wang and Shen. This is an open-access article distributed under the terms of the Creative Commons Attribution License (CC BY). The use, distribution or reproduction in other forums is permitted, provided the original author(s) and the copyright owner(s) are credited and that the original publication in this journal is cited, in accordance with accepted academic practice. No use, distribution or reproduction is permitted which does not comply with these terms.



PI3K/AKT Signal Pathway: A Target of Natural Products in the Prevention and Treatment of Alzheimer's Disease and Parkinson's Disease

Hui-Zhi Long^{1,2}, Yan Cheng^{1,2}, Zi-Wei Zhou^{1,2}, Hong-Yu Luo^{1,2}, Dan-Dan Wen¹ and Li-Chen Gao^{1,2*}

¹Department of Pharmacy, Cancer Institute, Phase I Clinical Trial Centre, Changsha Central Hospital Affiliated to University of South China, School of Pharmacy, University of South China, Changsha, China, ²Hunan Provincial Key Laboratory of Tumor Microenvironment Responsive Drug Research, Hengyang, China

OPEN ACCESS

Edited by:

Jiahong Lu,
University of Macau, China

Reviewed by:

Young-Ji Shiao,
National Research Institute of Chinese
Medicine, Taiwan
Gao Zhu Ye,
China Academy of Chinese Medical
Sciences, China

*Correspondence:

Li-Chen Gao
89206346@qq.com

Specialty section:

This article was submitted to
Ethnopharmacology,
a section of the journal
Frontiers in Pharmacology

Received: 01 January 2021

Accepted: 08 March 2021

Published: 15 April 2021

Citation:

Long H-Z, Cheng Y, Zhou Z-W,
Luo H-Y, Wen D-D and Gao L-C (2021)
PI3K/AKT Signal Pathway: A Target of
Natural Products in the Prevention and
Treatment of Alzheimer's Disease and
Parkinson's Disease.
Front. Pharmacol. 12:648636.
doi: 10.3389/fphar.2021.648636

Alzheimer's disease (AD) and Parkinson's disease (PD) are two typical neurodegenerative diseases that increased with aging. With the emergence of aging population, the health problem and economic burden caused by the two diseases also increase. Phosphatidylinositol 3-kinases/protein kinase B (PI3K/AKT) signaling pathway regulates signal transduction and biological processes such as cell proliferation, apoptosis and metabolism. According to reports, it regulates neurotoxicity and mediates the survival of neurons through different substrates such as forkhead box protein Os (FoxOs), glycogen synthase kinase-3 β (GSK-3 β), and caspase-9. Accumulating evidences indicate that some natural products can play a neuroprotective role by activating PI3K/AKT pathway, providing an effective resource for the discovery of potential therapeutic drugs. This article reviews the relationship between AKT signaling pathway and AD and PD, and discusses the potential natural products based on the PI3K/AKT signaling pathway to treat two diseases in recent years, hoping to provide guidance and reference for this field. Further development of Chinese herbal medicine is needed to treat these two diseases.

Keywords: PI3K/Akt signal pathway, neurodegenerative diseases, Alzheimer's disease, Parkinson's disease, natural products, nerve protection

INTRODUCTION

Neurodegenerative diseases are a kind of diseases that gradually lose the structure or function of neurons, including Parkinson's disease (PD), Alzheimer's disease (AD) and Amyotrophic lateral sclerosis (ALS) and so on. These diseases are characterized by progressive degeneration and neuronal necrosis, resulting in cognitive, emotional and behavioral abnormalities (Hetman et al., 2020). With the acceleration of population ages, the number of people suffering from AD and PD is increasing year by year. Up to now, the current treatment strategies of these diseases aim to alleviate symptoms and/or inhibit disease progression without radical cure, posing a serious threat to the quality of patients' life, hence becoming a global health problem. The high cost of treatment and nursing not only brings great trouble to patients and their families, but also causes great social and economic burden (Batista and Pereira, 2016), making the development of this kind of new drugs an urgent problem in the field of medicine. In addition, abnormal injuries caused by chemotherapy drugs give rise to different degrees of impact on patients' physical and mental health and quality of life, which

have become the direct cause of dosage restriction or discontinuation of some drugs (Vaz and Silvestre, 2020). A systematic review showed that Chinese herbal medicine and its natural active ingredients are of good safety and tolerance in protecting the central nervous system injury, and so that it gets increasing attention by the medical community (Yang et al., 2017).

Phosphatidylinositol 3-kinase/protein kinase B (PI3K/AKT) signal pathway has been proved to play an important role in the central nervous system (Matsuda et al., 2019). It has been diffusely studied for its involvement in the physiological processes of central nervous system, such as cell survival, autophagy, neurogenesis, neuronal proliferation and differentiation, and synaptic plasticity. In recent years, a growing number of studies have found that many natural products based on PI3K/AKT signal pathway protect dopaminergic neurons, hippocampal neurons, cortical neurons, and inhibit the activation of microglia, thus playing a role in the prevention and treatment of AD and PD. In this paper, we obtain relevant literature through Pubmed, Web of Science, China National Knowledge Infrastructure (CNKI) and other extensive databases. And we systematically summarize the related studies of natural products for the prevention and treatment of AD and PD based on PI3K/AKT signal pathway.

PI3K/AKT SIGNAL PATHWAY: OVERVIEW

PI3K: The Key Component Upstream of the Pathway

PI3Ks, a family of intracellular lipid kinases, are key elements in the upstream of the PI3K/AKT signaling pathway. PI3Ks are divided into three classes (I-III) according to their structure and substrate selectivity. The most generally studied class I isoforms that are activated by cell surface receptors are heterodimers composed of a regulatory subunit (P85) and a catalytic subunit (P110). The amino terminus of P85 contains a Src Homology 3 (SH3) domain and two proline-rich regions, while the basal terminus contains two SH2 domains and a non-coding region that combine with P110. Besides, class I isoforms are further segmented into class IA (PI3K α , β and δ) and class IB (PI3K γ) based on their modes of regulation (Thorpe et al., 2015). Class IA consists of catalytic subunits p110 α , β , δ and regulatory subunits p85 α , β , γ . Class IB are constituted by a p110 γ catalytic subunit coupled with the regulatory isoforms p101 or p87. The differences lie in the way of the activation between the two kinases. PI3K α , β and δ are activated when extracellular ligands bind to a transmembrane glycoprotein receptor tyrosine kinase (RTK) with enzyme activity, while PI3K γ is activated by G protein coupled receptors (GPCRs) and Ras family GTP enzymes (Dobbin and Landen, 2013). There are three class II isoforms, PI3K ζ 2 α , 2 β , 2 γ , which may constitutively bind to membranes and require additional activation signals. And the single class III PI3K, vacuolar protein sorting 34 (VPS34), is significant for membrane traffic from the plasma membrane to early endosomes (Sugiyama et al., 2019).

AKT: The Core Site of the Pathway

Protein kinase B (PKB), a serine/threonine kinase, is considered as one of the most important effector kinase downstream of PI3K and the core of PI3K/AKT signal pathway. Different genes encode three highly homologous subtypes of AKT: AKT1/PKB α , AKT2/PKB β , and AKT3/PKB γ . Each isoform contains a conserved N-terminal pleckstrin homology (PH) domain, a central fragment, and a C-terminal regulatory domain (Hemmings et al., 2004). Membrane translocation in AKT activation is mediated by the PH domain, and AKT activity is weakened due to its mutation or deletion. The structure of the catalytic domain includes an ATP binding site and a threonine residue Thr308 (AKT1-Thr308, AKT2-Thr309, AKT3-Thr305), which is the necessary phosphorylation site for AKT activation. The C-terminal regulatory domain consists of 40 amino acids, holding a hydrophobic region, which containing the second phosphorylation site needed to activate AKT, namely the serine residue Ser473 (AKT1-Ser473, AKT2-Ser474, AKT3-Ser472). Although the three AKT subtypes are highly homologous, each exerts unique physiological functions. AKT1 is broadly distributed in all tissues of the body, mainly involved in cell growth, proliferation, angiogenesis and tumor cell invasiveness (Petrik et al., 2016). Found in Mammalian skeletal muscle, and adipose tissue, AKT2 are confirmed participate in cell growth and proliferation, and mediate glucose homeostasis (Garofalo et al., 2003). Relatively little is known about AKT3, it is crucial for brain development and the survival of malignant glioma cells (Ghoneum and Said, 2019).

Signal Regulation of PI3K/AKT Pathway

Activation of PI3K/AKT Pathway

The activation of PI3K/AKT pathway begins with the activation of PI3K by RTK. Numerous cytokines or growth factors, such as fibroblast growth factor (FGF) and platelet-derived growth factor (PDGF), bind to the plasma membrane receptor RTK in response to stimulation by extracellular ligands, inducing receptor dimerization and cross-phosphorylation of tyrosine residues in intracellular domains. The regulatory subunit P85 binds to the phosphorylated tyrosine residue on the activated receptor through its SH2 domain. The catalytic subunit p110 is then recruited to form a fully active PI3K enzyme. Also, P110 subunit could be recruited independently of p85, like Ras-GTP, even other cohesive molecules as insulin receptor substrate (IRS). Besides, activation of G α subunit could activate Src-dependent integrin signal transduction in PI3K. By unifying with the signal protein AKT and phosphatidylinositol dependent protein kinase 1 (PDK1) containing PH domain, Phosphatidylinositol (3,4,5)-trisphosphate (PIP3), the second messenger phosphorylated from Phosphatidylinositol (4,5)-disphosphate (PIP2) by P110, recruits inactive AKT and PDK1 from the cytoplasm to the cell membrane, thus enabling PDK1 to obtain catalytic activity. At the same time, the conformational change of AKT structure exposes the phosphorylation sites of Thr308 and Ser473, resulting the phosphorylation of Thr308 residues by PDK1 (Altomare et al., 2005; Wei et al., 2019). And the second phosphorylation at Ser473 at the carboxyl terminal is essential and mainly carried out by

mechanistic target of rapamycin complex 2 (mTORC2) (Zeng et al., 2007). Many other kinases are known to phosphorylate AKT at Ser473, including PDK-1, integrin-linked kinase (ILK) or ILK-related kinases, and AKT itself (Memmott and Dennis, 2009). Binding proteins such as actin, extracellular signal-regulated kinase (ERK)1/2, heat shock protein (Hsp) 90 or Hsp27 are able to regulate the activity of AKT (Shanu and Komal, 2015). In addition, members of the family of PI3K-associated kinases, including DNA-dependent protein kinases (DNA-PK), can also phosphorylate AKT in Ser473 (Bellacosa et al., 2005).

As a downstream member of AKT, mTOR in turn acts as an activator for AKT activation. mTOR is linked to a regulatory-associated protein of mTOR (Raptor), and mammalian lethal with SEC13 protein 8 (mLST8) to form two multiprotein complexes with different functions, namely mTORC1 and mLST8 (Soliman, 2013). mTORC2 directly phosphorylates the hydrophobic motif Ser473 of AKT, and therefore enhances the activity of AKT kinase and promotes the phosphorylation of Thr308 by PDK1 (Laplane and Sabatini, 2012).

Negative Regulation of PI3K/AKT Pathway

Tumor suppressor, phosphatase and tensin homolog (PTEN) is a specific phosphatase with double activity (Satoru et al., 2018). Inactivation of AKT is mediated by the lipid phosphatase PTEN through dephosphorylation of PI(3,4,5)P₃ to PI(4,5)P₂, and by Src homology domain-containing inositol 5'-phosphatase 1 (SHIP1) due to conversion of PIP₃ to PIP₂. Negative regulation also be done by PH domain and leucine rich repeat protein phosphatase (PHLPP) and protein phosphatase 2 A (PP2A) which in turn dephosphorylate AKT at Ser473 and Thr308 respectively (Bertacchini, 2015).

Downstream Regulation of PI3K/AKT Pathway

After phosphorylated by the upstream signal, PI3K/AKT executes diverse biological actions by phosphorylating or forming complexes for a range of downstream molecules, such as the FoxO family members, GSK-3 β , mTOR, and actin-related protein, among others (Mirdamadi et al., 2017; Matsuo et al., 2018). The activation of this signaling pathway and its downstream regulation are basically illustrated in **Supplementary Figures S1** or **S2**. mTOR is the main downstream target of PI3K/AKT signal transduction and a key regulatory factor of cellular metabolism. AKT affects cell cycle progression by phosphorylating and inhibiting cyclin-dependent kinase inhibitors p21 and p27. And it modulates apoptosis through inhibiting Bcl2-antagonist of cell death (Bad), bcl-2-like protein 11 (BIM), caspase-9 and forkhead box protein O1 (FoxO1). Nuclear factor erythroid 2 related factor 2 (Nrf2) is the main regulator of oxidative stress, which can promote the transcription of detoxification enzyme and antioxidant enzyme protein genes. Some drugs have been proved to activate PI3K/AKT/Nrf2 signaling, thereby reducing cognitive impairment and neurological dysfunction (Liang et al., 2018). In simple terms, PI3K/AKT pathway has been implicated in cell proliferation, glucose metabolism, cell survival, cell cycle, protein synthesis, and participates in neuronal morphology and plasticity through

adjusting several downstream molecules. Imbalanced expression in solid tumors, immune-mediated diseases, cardiovascular diseases, diabetes, nervous system diseases and other diseases, PI3K/AKT pathway arouses the interest of many scholars act as a meaningful therapeutic target, worthy of a further exploration.

ROLES OF PI3K/AKT PATHWAY IN ALZHEIMER'S DISEASE

AD is a neurodegenerative disease positively concerned with age and associated with memory, cognitive impairment and behavioral changes (Martins et al., 2019). Two chiefly pathological features as following: senile plaque (SP) with amyloid protein (A β) as the core and abnormal high phosphorylation of Tau protein in brain nerve cells to form neurofibrillary tangles (NFT). With the aging of the population, the incidence of AD is increasing year by year, which brings a heavy burden to the society and families. Distinctly, the major problem facing researchers is to prevent and treat AD available.

Although several hypotheses have been proposed after decades of research, the specific pathogenesis of AD is still obscure. The most common amyloid deposition hypothesis proposes that the self-assembly of misfolded amyloid peptides affects the structure and function of neurons, stimulates apoptosis, leading to synaptic dysfunction and neurodegeneration. It has been found that PI3K/AKT signal pathway is involved in the formation of two special pathological structures in AD (Do et al., 2014), so that activating the PI3K/AKT pathway may conduce to delay the progression of AD (**Supplementary Figure S1**). The activation of PI3K/AKT signal pathway is capable of protecting neurons against A β -induced neurotoxicity. Various targets downstream of this pathway are closely related to the occurrence and development of the disease. For example, the increase of GSK-3 β activity is directly related to the increase of A β production and deposition, hyperphosphorylation of tau and the formation of NFT. During AKT phosphorylation, the phosphorylated protein of GSK-3 β is inactivated at the Ser9 site, and therefore weakens the hyperphosphorylation of Tau protein, and inhibits the formation of NFT (Kitagishi et al., 2014).

Different from normal people, there is an evidently decrease in the number of neurons in some brain regions of AD patients. These changes were mainly caused by apoptosis induced by oxidative stress response and the excitatory toxicity of glutamate, and eventually lead to the occurrence of nervous system diseases. Studies have shown that cell death in AD is related to the changes in the expression of anti-apoptotic proteins (Bcl-2, Bcl-xL), which play an anti-apoptotic role by stabilizing the permeability of mitochondrial membrane and preventing the release of mitochondrial cytochrome C. Interestingly, the PI3K/AKT signaling pathway can regulate the expression of mitochondrial membrane permeability protein Bcl-2, Bax and other proteins (Zeng et al., 2011). Other studies have shown that the repression of PI3K/AKT induces neuronal apoptosis through the mediation of P38 activation. In addition, overexpression of PTEN associated with the apoptosis, and the survival or death of

neuronal cells may be partly attributed to the variations in PTEN expression (Satoru et al., 2018). Accordingly, the down-regulation of PTEN to promote the activation of AKT might be of great significance in maintaining its neuroprotective effects.

What else, synaptic plasticity of neurons could be adjusted by the PI3K/AKT pathway. In the animal model of AD, inhibition of PTEN is beneficial for preserving normal synaptic function and thereby improving cognition (Cui et al., 2017b). Some studies have confirmed that mTOR protein pathway in PI3K/AKT signaling is also involved in the development of neuronal dendrites and the formation of dendritic spines. The increase in synaptic plasticity is characterized by long term potentiation (LTP) (Shane et al., 2019), which requires the activation of N-methyl-D-aspartic acid (NMDA) receptors, thereby promoting the insertion of α -amino-3-hydroxy-5-methyl-4-isoxazolpropionic acid (AMPA) receptors into the postsynaptic membrane. On the one hand, mTOR increases the expression of LTP-related proteins, and PI3K also binds to AMPA receptors and guides its distribution on the membrane (Parkinson and Hanley, 2018). On the other hand, NMDA receptor activation also promotes PI3K activation. In addition, AKT immobilizes phosphatidylinositol (PI) to the postsynaptic membrane to recruit the docking protein of AMPA receptor and promote the fixation of AMPA receptor in the postsynaptic membrane (Spinelli et al., 2019). As a result, PI3K/AKT/mTOR signaling pathway regulates neuronal synaptic plasticity at multiple nodes.

ROLES OF PI3K/AKT PATHWAY IN PARKINSON'S DISEASE

PD is the second largest neurodegenerative disease after AD, also known as idiopathic tremor paralysis. It is characterized by the degeneration and deletion of dopaminergic neurons in substantia nigra (SN) and the formation of eosinophilic inclusion body (Lewy bodies, LBs), as well as the production of neuroinflammation. For decades, though, there has been a great deal of research on PD, drugs on effectively inhibiting or reversing the development of PD are still an assumption except the treatment of temporary improvement of symptoms, so the treatment of PD is more difficult than it seems. As for the pathogenesis of PD, scientists have successively proposed hypotheses including oxidative stress mitochondrial damage, excitatory amino acid toxicity, inflammatory response, and abnormal deposition of α synuclein. However, most of the pathogenic factors have not been confirmed. At present, the abnormal aggregation of fibrillation and α -synuclein is considered to be the key factor for the cascade of pathological events in PD. LBs is mainly composed of misfolded proteins, such as synuclein, tubulin, and amyloid precursor protein. Mitogen-activated protein kinases (MAPKs) like AKT/ERK, found in cells, participate in the removal of these proteins through phosphorylation and dephosphorylation. Intracellular deposition of alpha synuclein leads to neuronal degeneration and apoptosis. Autophagy degrade synuclein and resist the deposition of synuclein in Lewy, so it is usually increased in PD patients (Chen et al., 2017).

The loss of dopaminergic neurons in the SN and striatum caused by apoptosis is an important cause of PD. Scholars manifested that AKT and phosphorylated AKT are significantly reduced in the substantia nigra compacta (SNpc) of PD patients (Luo et al., 2019). GSK-3 is widely expressed in the central nervous system, but abnormally in PD (Zhang et al., 2016b). Caspase-3 plays a key role in apoptosis and as a key effector in all apoptosis pathways. During the pathogenesis of PD, GSK-3 activation up-regulates the content of caspase-3 in the dopaminergic nerve, leading the apoptosis of dopaminergic neurons. Experiments show that AKT could inhibit the activity of GSK-3 by phosphorylating Ser21 of GSK-3 α or Ser9 of GSK-3 β (Liying et al., 2018). As a downstream pathway of AKT, IKK/I κ Ba/NF- κ B pathway is one of the vital pathways for cell survival (Yan et al., 2019). Consequently, the activation of PI3K/AKT pathway facilitates the survival and growth of dopamine neurons by inhibiting apoptosis. Besides, knockout of PTEN make a contribution to neuroprotection and promotion of the rapid growth of dopaminergic (DA) neurons (Wang et al., 2017).

Oxidative stress, inducing neuronal cell death and apoptosis through intracellular calcium overload lipid peroxidation DNA damage and excitatory toxicity, also contributes to the onset of PD. The PI3K/AKT pathway influences oxidative stress by modulating downstream molecular targets such as GSK-3, mTOR and FoxO3a. Decreasing the mTOR activity may lead to neurodegeneration. The stress response protein regulated in development and DNA damage responses 1 (REDD1) is up-regulated in dopaminergic neurons in PD patients and can modulate the activity of mTOR (Chong et al., 2012). When Parkin (a mutation-prone gene associated with PD) is abnormally expressed, the PI3K/AKT/FoxO3a pathway is blocked, resulting in the imbalance of oxidative stress and ultimately the occurrence of PD (Gong et al., 2018). Additionally the relationship between the above mentioned PI3K/AKT signaling pathway and PD is clearly sorted out in **Supplementary Figure S2**.

NATURAL PRODUCTS FOR PREVENTION AND TREATMENT OF ALZHEIMER'S DISEASE BASED ON PI3K/AKT PATHWAY

Natural products have attracted the attention of researchers by virtue of their natural advantages such as wide variety, wide source and wide function spectrum. Structurally classified into flavonoids, alkaloids, phenylpropanoids, glycosides, and others, natural products are widely distributed in nature and commonly found in herbs, fruits and vegetables. Interestingly, almost every natural product has a variety of pharmacological properties, covering anti-tumor, antioxidant, antibacterial, anti-inflammatory, anti-diabetic, hypoglycemic, neuroprotective, etc. Additionally, natural products are generally less toxic and very safe, hence becoming an important alternative source of many types of drugs. Over the years, AD has become the fourth leading cause of death after cardiovascular disease, cancer and stroke. Under the circumstance of poor progress in synthetic drug

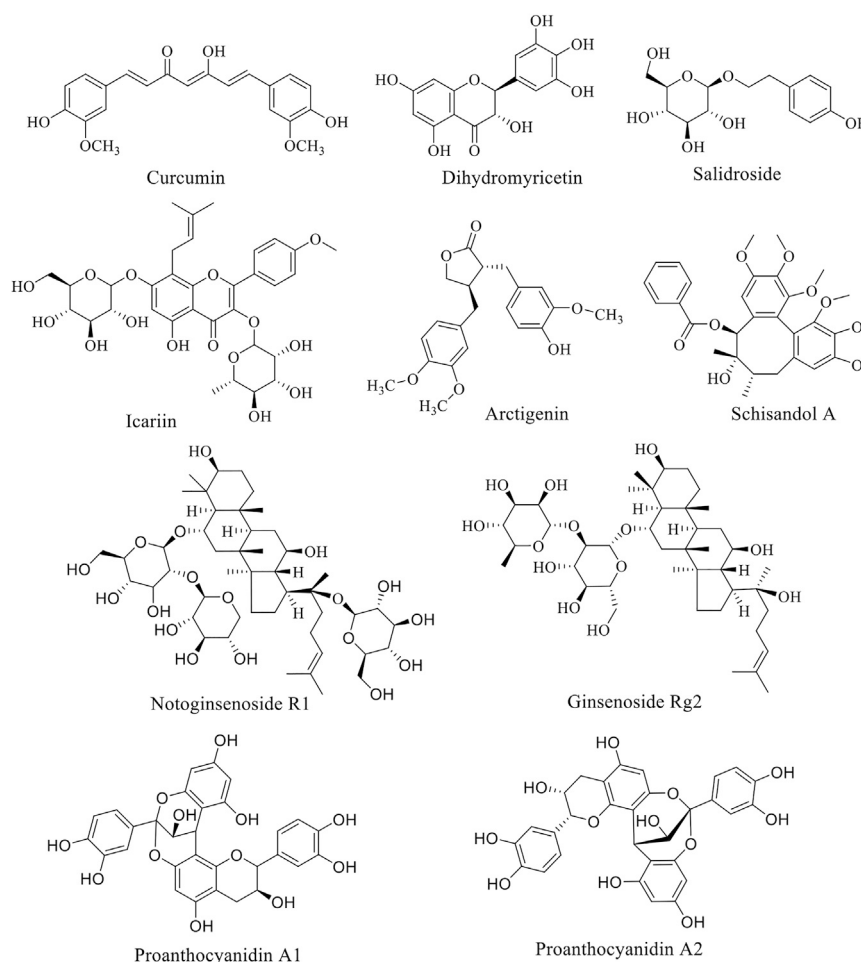


FIGURE 1 | Structure of anti-PD natural compounds.

research, natural product anti-AD therapy has become an attractive direction of exploration. Natural products such as curcumin, dihydromyricetin and salidroside have been found to have eminently preventive and therapeutic effects on AD through PI3K/AKT pathway. These natural products are summarized below, and the structure of natural products is listed (**Figure 1**). The experimental cell, animals, dose and time used in natural product research were summarized in **Table 1**, providing reference for readers.

Flavonoids

Curcumin is a rare diketone compound in the plant kingdom, mainly extracted from the rhizomes of some plants in Zingiberaceae and Araceae (Mario et al., 2016). The protective property of curcumin on neuronal degeneration caused by mitochondrial dysfunction and the resulting oxidative stress, inflammation and apoptosis of nerve cells has been demonstrated. And the neuroprotection pathogenesis of curcumin is mediated by two momentous signaling pathways, PI3K/AKT/GSK-3 or PI3K/AKT/cAMP response element-binding protein (CREB)/brain-derived neurotrophic factor

(BDNF) (Kandezi et al., 2020). By regulating above pathway, curcumin inhibits the glutamate-induced release of mitochondrial cytochrome C, the activation of caspase-3, a key enzyme for cell apoptosis, as well as reduces pro-inflammatory biomarkers (interferon- α (IFN- α), tumor necrosis factor- α (TNF- α), interleukin (IL)-8) and increases anti-inflammatory cytokines/compounds (IL-10, IL-1) (Wolkmer et al., 2013). It is noteworthy that the increasing clinical data indicate that curcumin is expected to be a standard candidate for neuroprotective agent (Voulgaropoulou et al., 2019). Yet not all clinical trials are positive. Some clinical studies show that curcumin has a beneficial effect on cognitive improvement of AD (Cox et al., 2015; Small et al., 2018). Whereas another suggest that curcumin has no cognitive-enhancing properties (Ringman et al., 2012). Curcumin reduces A β deposition in the brain, which is supported by neuroimaging (Small et al., 2018). While in another clinical trial, the results are misty (Ringman et al., 2012).

Dihydromyricetin (DHM), also called ampelopsin, is a dihydroflavonol compound, has been found to markedly rescued apoptosis of neurons in hippocampus of D-gal-induced brain aging model of rats, improving learning and

TABLE 1 | Summary of some natural products with AD and PD therapeutic potential.

Natural products	Diseases	<i>In-vitro/vivo</i> models/human trial	Dose and period of treatment	Treatment time	Mechanism	Activation or inhibition of PI3K/ AKT pathway	References
Curcumin	AD PD	N2a/WT cells APP/PS1 transgenic mice	5 μ M for cell line and 1or 0.16 g/kg for animals	6 months	Decrease in Caveolin-1, inactivation of GSK-3 and inhibition of abnormal excessive tau phosphorylation, bax and increase in Bcl-2	Activation	Sun et al. (2017)
Dihydromyricetin	AD PD	D-gal-induced aging rat model Sprague-dawley rats	The doses of 100 and 200 mg/kg	5 weeks	Decrease the expression of caspase-3, p53 and p62, up-regulate Bcl-2 and SIRT1 activity, suppress aging-related astrocyte activation and inhibiting mTOR signal pathway as well as down-regulate miR-34a	Activation	Kou et al. (2016)
Salidroside	AD	Transgenic drosophila AD models	Concentration of 50,100,200 μ M	24 h	Decrease a β levels and a β deposition, increase AKT phosphorylation level p-mTOR or p-p70S6K level	Activation	Zhang et al., (2016a)
		C57BL mice APP/PS1 transgenic mice	Concentration of 0.3 mg/ml	2–12 months	Reduce the aggregation of a β and improve synaptic structure. Activation of PI3K/AKT/mTOR signaling pathway		Wang et al. (2020)
Arctigenin	AD	ICR mice	The doses of 10, 40, or 150 mg/kg for animals	16 days	Inhibit the production of phosphorylated tau, and inhibition of the PI3K/akt/ gsk-3 β signaling pathway	Activation	Qi et al. (2017)
Schizandrol A	AD	SH-SY5Y cells or primary hippocampal neurons	Concentration of 2 μ g/ml	24 h	Suppress the ratio of Bax/ Bcl-2 and caspase-3, increase of p62, and decrease of LC3-II/LC3-I, Beclin-1, decreased ratios of p-Tau/Tau	Activation	Song et al. (2020)
Ginsenoside Rg2	AD	Male sprague-dawley rats	The doses of 25,50,100 mg/kg/day	6 days	Increase the Bcl-2/Bax ratio, attenuate the cleavage of caspase-3, and enhance the phosphorylation of AKT.	Activation	Cui et al., (2020)
Notoginsenoside R1	AD	C57BL/6J mice and APP/PS1 mice	Dose of 5 mg/kg/day	6 months	Improve cell viability, reduce the cleavage of Navb2 by BACE1 suppression, and also correct the abnormal distribution of Nav1.1a	Activation	Hu et al. (2020)
Fructus broussonetiae	AD	APP/PS1 double- transgenic mice Rabbits	0.1, 0.15,0.3 g/ml for mice, and 150 mg/kg for rabbits	2 months	Increase p-AKT and β - catenin signaling, decrease caspase-3,caspase-9, and levels of a β and	Activation	Li Y.-h. et al. (2020)
				10 days	phosphorylate tau proteins		
Icariin	AD	SAMP8 mice model of AD	The doses of 60 mg/kg	22 days	Down-regulate the expression of BACE1 to reduce the expression of cytotoxic A β ₁₋₄₂ , and increase the Bcl-2/Bax ratio	Activation	Wu et al. (2020)
	PD	Ovariectomized PD mice, dopaminergic MES23.5 cells	The doses of 50/100/ 200 mg/kg	13 days	Increase the DA content, the Bcl-2 and attenuate the increase of bax and caspase-3 protein levels, active PI3K/AKT or MEK/ ERK signaling pathway		Chen et al. (2017)

(Continued on following page)

TABLE 1 | (Continued) Summary of some natural products with AD and PD therapeutic potential.

Natural products	Diseases	<i>In-vitro/vivo</i> models/human trial	Dose and period of treatment	Treatment time	Mechanism	Activation or inhibition of PI3K/ AKT pathway	References
Baicalein	AD	PC12 cells	Concentration of 40/ 60/80 μ M	2 days	Increase the cell viability and niacin level. Inhibit $A\beta_{25-35}$ -induce cytotoxicity by restraining the levels of ROS, and increasing the level of MMP and mitochondrial respiratory complex I	Activation	Gao et al. (2020)
	PD	Sprague-dawley rats	The doses of 30 mg/kg/day	7 days 9 days	Reduce procaspase-1, caspase-3 and elevate active caspase-1 levels		Zhao et al. (2017)
Baicalin	PD	Sprague-dawley rats	The doses of 25 mg/kg	4 weeks	Increase the expression of mTOR, <i>p</i> -mTOR, AKT, <i>p</i> -AKT, GSK-3 β , and <i>p</i> -GSK-3 β	Activation	Zhai et al. (2019)
Apigenin	PD	SH-SY5Y cells, C57BL/6 mice	10,20,40,100 μ M for cells and 50 mg/kg/day for mice	2h and 15 days	Upregulate the p-PI3K/PI3K ratio and <i>p</i> -AKT/AKT ratio while downregulate Bax/Bcl-2 ratio and caspase-3 activity, improve the lesioned neurobehavior	Activation	Hu et al. (2018)
Amentoflavone	PD	C57BL/6 mice	The doses of 50 mg/kg/day	15 days	Elevate the viability and alleviate apoptosis, restore the decreased TH expression, inhibit the activation of caspase-3 and p21 but increase the Bcl-2/Bax ratio, activate PI3K/AKT and ERK signaling pathways	Activation	Cao et al. (2017)
Puerarin	PD	SH-SY5Y cells, sprague-Dawley rats	10,50,100,150,200 μ M for cells and 50 mg/kg for animal	12 h, 7 days	Elevate the viability, mitigate intracellular oxidative stress and ROS, up-regulate TH and VMAT2 expressions, and dopamine levels, alleviate behavioral defects of PD.	Activation	Zhang et al. (2014)
Tovophyllin A	PD	Primary cortical neurons, C57BL/6 mice	The doses of 40 mg/kg	24 h	Alleviate MPTP-induced behavioral dysfunctions and DA neuron loss, increase the phosphorylation of AKT and GSK-3 β	Activation	Huang et al. (2020)
Berberine	PD	SH-SY5Y neuroblastoma cells	Concentration of 10^{-5} , 10^{-4} , 10^{-3} , 10^{-2} , 10^{-1} , 1, 10, and 100 μ M	24 h	Up-regulate the Bcl-2, downregulate the bax and caspase-3, activate PI3K/AKT signaling pathway	Activation	Deng et al. (2020)
Schisantherin	AD	Differentiated rat pheochromocytoma PC12 cells	SCH (50 μ M) and NKT (10 μ M)	24 h	Activate the PI3K/AKT/GSK-3 β /mTOR pathway, and inflammatory related proteins such as NF- κ B, IKK, IL-1 β , IL-6 and TNF- α are decreased	Activation	Qi et al. (2020)

(Continued on following page)

TABLE 1 | (Continued) Summary of some natural products with AD and PD therapeutic potential.

Natural products	Diseases	<i>In-vitro/vivo</i> models/human trial	Dose and period of treatment	Treatment time	Mechanism	Activation or inhibition of PI3K/ AKT pathway	References
Schisandrol A	PD	C57BL/6J mice	The doses of 10,20,30 mg/kg	2 weeks	Decrease the focal encephalomalacia and inhibite the striatal degeneration, enhance the PI3K/AKT pathway, inhibit the IKK/I κ B α /NF- κ B pathway, reduce neuronal inflammation and oxidative stress, and enhance the survival of DA neurons in the brain of mice	Activation	Yan et al. (2019)
Paeniflorin	PD	C57BL/6 mice	The doses of 7.5,15,30 mg/kg	1 week	Prevent the TH and DAT protein decrease induced by MPTP, prevent the striatal p-AKT (Ser473) protein decrease, attenuate caspase-3 and caspase-9 activation	Activation	Zhao et al. (2017)
Cannabidiol	PD	The human neuroblastoma cell line SH-SY5Y	Concentration of 10 μ M	24 or 48 h	Decrease LC3-II levels, activate the ERK and AKT/ mTOR pathways and modulate autophagy	Activation	Gugliandolo et al. (2020)
Lycium barbarum polysaccharide	PD	C57BL/6 mice	The doses of 100 or 200 mg/kg	21 days	Up-regulate the TH level, inhibit the oxidative stress in the midbrain, and inhibit the aggregation of α -synuclein, downregulated LC3-II and beclin expression, activate the AKT/mTOR pathway through inhibiting PTEN.	Activation	Wang et al. (2018b)
<i>Astragalus</i> polysaccharides	PD	PC12 cell	Concentration of 50,100,200 μ M	24 h	Promote the phosphorylation of AKT and mTOR, and up-regulate the expression of PTEN.	Activation	Tan et al. (2020)
Crocin	PD	Adult male wistar rats	The doses of 30 mg/ml/day	1 month	Increase active form of AKT, reduce expression and activity of FoxO3 and GSK- 3 β , elevate miRNA-221 expression, decrease pro- apoptotic caspase-9 and enhance anti-apoptotic Bcl-2	Activation	Salama et al. (2020)
Asiatic acid	PD	C57BL/6 mice	The doses of 25,50,100 mg/kg		Increase the phosphorylation of PI3K, AKT, GSK-3 β and mTOR, inhibition of JNK, ERK and P38 MAPK-mediated signaling pathways	Activation	Nataraj et al. (2017)

A β , amyloid- β ; AKT, protein kinase B; BACE1, amyloid precursor protein cleaving enzyme one; Bad, Bcl-xL/Bcl-2-associated death promoter homologue; caspase-3, cysteine protease protein; ERK, extracellular signal-regulated kinase; GSK-3 β , glycogen synthase kinase-3 β ; HO-1, heme oxygenase-1; IKK, I κ B kinase; IL-1 β , interleukin-1 β ; IL-6, interleukin-6; JNK, c-Jun NH(2)-terminal kinase; LC3-II/LC3-I, the autophagosome-associated protein; MAPK, mitogen-activated protein kinases; MMP, mitochondrial membrane potential; MPTP, 1-methyl-4-phenyl-1,2,3,6-tetrahydropyridine; mTOR, mammalian target of rapamycin; NF- κ B, nuclear factor-kappa B; p53, tumor suppressor gene; p62, the atypical protein kinase C-interacting protein; PI3K, phosphoinositide 3-kinase; PTEN, phosphatase and tensin homolog; SD, Sprague-Dawley; SIRT1, Silent mating type information regulation two homolog-1; TNF- α , tumor necrosis factor-alpha.

memory impairment (Kou et al., 2016). It activates hemeoxygenase-1 (HO-1) in pheochromocytoma 12 (PC 12) cells, and increases the expression of HO-1 or enzyme activity, thus againsts H₂O₂ and 6-OHDA-induced neurotoxicity in PC12

cells. The protection of amelopsin is link to inhibition of rwactive oxygen species (ROS) formation, expression of poly ADP-ribose polymerase (PARP) and caspase-3, inhibition of p38, MAPK phosphorylation and up-regulation of HO-1 expression.

Interestingly, the increase in HO-1 expression is mainly due to increased phosphorylation levels of ERK and AKT (Kou et al., 2012). Based on AKT and ERK1/2 signaling, DHM also dose-dependently attenuated sodium nitroprusside induced PC12 cell damage (Liao et al., 2014). In addition, DHM up-regulates Bcl-2, down-regulates cleaved caspase3 and Bax, increases antioxidant capacity and inhibits apoptosis (Mu et al., 2016). In another study, DMY improves glucose metabolism of PC12 cells stimulated by endogenous toxic compound methylglyoxal through AMPK/glucose transporter 4 (GLUT4) signaling pathway, inhibiting oxidative stress, and protecting mitochondria of cells (Jiang et al., 2014a). Moreover, DHM has been confirmed to execute its protective function through GSK-3 β /Nrf2/antioxidant response element (ARE) signal pathways (Kou et al., 2015).

Icariin (ICA), a flavonol isolated from *Epimedium perralderianum* Coss (family Berberidaceae, genus *Epimedium*), is the main active component of *Epimedium perralderianum*. It had previously been observed that ICA alleviated symptoms in AD model animals, which may be caused by increased expression of insulin-like growth factor (IGF) and BDNF, thereby activating PI3K/AKT pathway, inhibiting production of A β and tau protein phosphorylation (Wu et al., 2012). A recent *in vivo* study suggested that the promotion effect of ICA on proliferation and differentiation of hippocampal neural stem cells in AD model is related to the BDNF-tyrosine kinase B (TrkB)-ERK/AKT signaling pathway (Lu et al., 2020). Moreover, ICA treatment significantly enhanced proteasome-dependent degradation of PTEN and protected SK-N-MC cells from A β -induced insulin resistance (Zou et al., 2020). In addition, by down-regulating the expression of β -site amyloid precursor protein (APP) cleavage enzyme 1, icariin could decrease the deposition of β -amyloid peptide (Wu et al., 2020).

Phenylpropanoids

Phenylpropanoid compounds incorporate simple phenylpropanoid, coumarin and lignans. Salidroside (Sal), belonging to phenylpropanoid glycoside, is a bioactive substance mainly extracted from traditional herbs such as *Rhodiola coccinea* (Royle) Boriss., be of a species in the genus *Rhodiola* (family Crassulaceae). In recent years, Sal has been reported to exhibit great neuroprotection, including antioxidant, anti-inflammatory, anti-apoptosis and regulation of multiple signal pathways and key molecules (Fan et al., 2020). Zhang et al., in their study on the therapeutic potential of Sal for AD, pointed out that Sal alleviate pathological progression in AD models by reducing amyloidosis and activating PI3K/AKT signaling, suggesting the potential role of Sal in the prevention and treatment of AD due to its neuroprotective property. In addition, mTOR has been found to be a mammalian target that plays an important role in the formation of AD related memories (Zhang et al., 2016a). In a subsequently study, results are similar to Bei et al. However, the alteration of mTOR might be influenced by different animal models or drug delivery methods, and the exact mechanisms remain to be investigated (Wang et al., 2020). Additionally, Sal reduces inflammation and brain injury after middle cerebral artery occlusion in rats via PI3K/PKB/Nrf2/

NF κ B signaling pathway (Zhang et al., 2019a). In an experiment to test the cognitive effect of Sal on AD mice, the researchers demonstrated that Sal reduced the expression of TNF- α and IL-6 cytokine inflammatory factors, improving cognitive function in AD mice. The authors suggested that this protective effect may be related to changes in the level of free radicals in the hippocampus (Li et al., 2018). But it only limited to the guess rather than further inquiry. Structurally, Sal is linked by a glycosidic group to an aglycon (tyrosol) via a β -glycosidic bond. The polyhydroxyl structure of Sal gives it a strong polarity, thereby limiting its diffusion and absorption through the body (Cheng et al., 2012). In order to overcome the above problems, Yang et al. synthesized twenty-six novel derivatives of Sal and evaluated their cell protective effects in CoCl₂-treated PC12 cells (Yang et al., 2021). Among the twenty-six salidroside derivatives, five of them showed stronger cell protective effect than Sal (EC₅₀, 0.30 μ M) under the same condition. Among them, pOBz had a more significant protective effect (EC₅₀, 0.038 μ M). Although the mechanism studies found that pOBz reduced monoamine oxidase (MAO) activity and played a neuroprotective role after MCAO reperfusion in rats, and also inhibited the expression of C3 protein in the brain after cerebral ischemia reperfusion injury, these studies were obviously insufficient. Whether the action mechanism of pOBz and other derivatives is the same as Sal remain to be further studied, and their molecular targets also need to be further studied.

Arctigenin is a phenylpropanoid dibenzylbutyrolactone lignan compound, naturally found in *Arctium lappa* L. (family Compositae, genus *Arctium*). Qi et al. firstly elucidated that arctigenin (10, 40, or 150 mg/kg, orally) attenuates the level of phosphorylated tau protein expression in the hippocampus through PI3K/AKT/GSK-3 β signaling pathway in A β -induced AD mice, hence successfully providing protection against learning and memory deficits (Qi et al., 2017). However, different routes of administration affect the bioavailability of arctigenin *in vivo*. Pharmacokinetic investigations have shown that the oral administration of arctigenin will cause large amounts of primary metabolism, which would affect its *in vivo* and clinical efficacy. So it is suggested that Arctigenin should be administered through the intranasal route for the treatment of central nervous system dysfunction (Gao et al., 2018). This suggests that monitoring pharmacokinetics is crucial for better understanding the role of arctigenin. Due to the few researches, clinical trials of arctigenin are rather limited. Therefore the anti-AD effect of arctigenin has not been clinically confirmed. In brief, sufficient research data is required to justify the need for clinical trials. Schizandrol A (SchA), a type of lignans, is a natural active ingredient extracted from *Schisandra chinensis* (Turcz.) Baill. (family Schisandraceae, genus *Schisandra*), the Chinese herb fruit. In a study of the neuroprotective effects of SchA in AD cell models, researchers demonstrated that SchA swimmingly reduces the decrease of living cells, the increase of the number of apoptotic cells, the expression of pro-apoptotic proteins and the changes of oxidative stress markers induced by A β ₁₋₄₂. Moreover, SchA inhibited the increase of microtubule-

associated protein 1A/1B-light chain 3 (LC3)-II/LC3-I and Beclin-1 and the decrease of p62. It revealed that SchA perhaps to be a new drug for the prevention and treatment of AD (Song et al., 2020). SchA has been shown to inhibit ischemia-induced neuronal autophagy via AMPK/mTOR pathway (Wang et al., 2019). A comparative experiment was carried out that SchA (50 μ M) combined with norepinephrine (NE, 10 μ M) work better than alone (Qi et al., 2020).

Saponins

Ginsenosides are the main bioactive components of *Panax ginseng* C.A.Mey. (family Araliaceae, genus *Panax*) with the functions of eliminating free radicals, anti-oxidation, delaying cell aging, protecting nervous system, and improving memory of the elderly, becoming the hot candidate drugs for the treatment of central nervous system diseases. Investigators have showed that ginsenosides enhance the expression of synaptic-related proteins and synaptic plasticity, up-regulate the expression of CREB and BDNF, reduce apoptosis and AD pathology-like protein expression, scavenge free radicals and protect nerve cells (Lulin et al., 2017). A study on HT22 cells and APPSW SH-SY5Y cells demonstrated that Rg1 promoted α -secretase cleavage of APP by activating ERK/MAPK and PI3K/AKT pathway (Shi et al., 2012). Li et al. also illustrated via experiments that ginsenosides improve memory and reduce the content of $A\beta_{1-42}$ and p-tau in AD mice, and the anti-AD effect of ginsenoside is mediated by activating PI3K/AKT signal pathway (Li et al., 2016). Other studies have confirmed that ginsenoside Rg2, one of the most important active components of ginsenosides, significantly inhibits the apoptosis of $A\beta$ treated PC12 cells by up-regulating the PI3K/AKT signaling pathway, which may be caused by the decrease of ROS and intracellular Ca^{2+} concentration by ginsenoside, the activation of autophagy pathway, the up-regulation of Bcl-2 and the down-regulation of Bax (Cui et al., 2017a). Taken together, ginsenosides are deemed as potential new drugs for the treatment of AD (Cui et al., 2020).

Notoginsenoside R1 also possesses a certain repair effect on AD (Hu et al., 2020). Notoginseng R1 as reported conspicuously improved the cell damage induced via $A\beta_{25-35}$ by increasing cell activity, inhibiting oxidative stress and the activation of MAPK signaling pathway (Ma, 2014). Meng et al. have found that the neuroprotection of notoginsenoside R1 is related to estrogen receptor dependence, and the up-regulation of antioxidant enzymes is associated to AKT and ERK1/2, as well as Nrf2 pathway (Meng et al., 2014).

Non-flavonoid Polyphenols

Being a naturally occurring stilbene, piceatannol (PT) has been reported to possess antioxidant, anti-inflammatory, anti-diabetic and neuroprotective effects (Zhang et al., 2018). In an early study, the effects of PT and pterostilbene (PS) against $A\beta$ -induced apoptosis in PC12 cells were evaluated. The results show that PT and PS have obvious anti-apoptotic activity. PT up-regulates the PI3K/AKT/BAD signaling pathway, further inhibits the expression of Bcl-2/Bax, the cleavage of caspase-9, caspase-3 and PARP. While PS promotes phosphorylation of AKT

without affecting other factors (Fu et al., 2016). What's more, the active fraction derived from *Litchi chinensis* Sonn. (family Sapindaceae, genus *Litchi*) seed can improve the cognitive function and behavior of AD model rats through decreasing $A\beta$ fibril formation and Tau hyperphosphorylation. Catechin, proanthocyanidin A1 and proanthocyanidin A2 polyphenols isolated from seed of *Litchi chinensis* Sonn. inhibit hyperphosphorylated Tau protein by up-regulating IRS-1/PI3K/AKT and down-regulating GSK-3 (Fu et al., 2016).

Others

Being commonly used spices, *Zanthoxylum bungeanum* Maxim. (*Z. bungeanum*) (family Rutaceae, genus *Zanthoxylum*) and its ingredients possess anti-inflammatory, antioxidant and neuroprotective effects (Deng et al., 2019). Zhao et al. demonstrated for the first time that *Zanthoxylum bungeanum* Maxim water extract (WEZ) and volatile oil extract (VOZ) inhibit apoptosis and oxidative stress by activating PI3K/AKT/Nrf2 signal pathway, attenuating impairment of D-galactose-induced aging mice. Unfortunately, the specific active ingredients have not been reported (Zhao et al., 2020). Evaluated the functions of *Broussonetia papyrifera* (L.) L'Hér. ex Vent. (family Moraceae, genus *Broussonetia*) in both mouse and cell models of AD, Li and colleagues found that *Broussonetia papyrifera* (L.) L'Hér. ex Vent. up-regulates AKT and β -catenin signaling pathways in the pretreated PC12 cells (Li Y.-h. et al., 2020). Same as other traditional Chinese herbal medicine with a variety of components, which component plays a critical role in AD is unclear.

NATURAL PRODUCTS FOR PREVENTION AND TREATMENT OF PARKINSON'S DISEASE BASED ON PI3K/AKT PATHWAY

Due to the complex pathogenesis of PD, there is no specific drug for it so far. The research and development of anti-PD drugs have attracted great attention from the medical community all over the world. In recent years, with the deepening of the research on neurophysiology, biochemical and pharmacology of the elderly, the research on the development of natural products against PD is in hot progress. Thanks to the efforts of many scholars, many natural products have been proved to have good effects on the treatment of PD. Natural flavonoids products, such as icariin, baicalein, other products like berberine, paeoniflorin, etc. have achieved great success in PD model animals and *in vitro* cell experiments.

Flavonoids

Baicalein is a bioactive flavonoid monomer compound isolated from *Scutellaria baicalensis* Georgi (family Lamiaceae, genus *Scutellaria*). Evidences suggest that baicalein have neuroprotective functions in addition to antioxidation such as alleviate the symptoms of AD and PD (Li et al., 2017). According to previous studies, baicalein was found to have a neuroprotective effect on acrolein-induced neurotoxicity at multiple levels (Zhao et al., 2017). And baicalein pretreatment significantly inhibited 6-

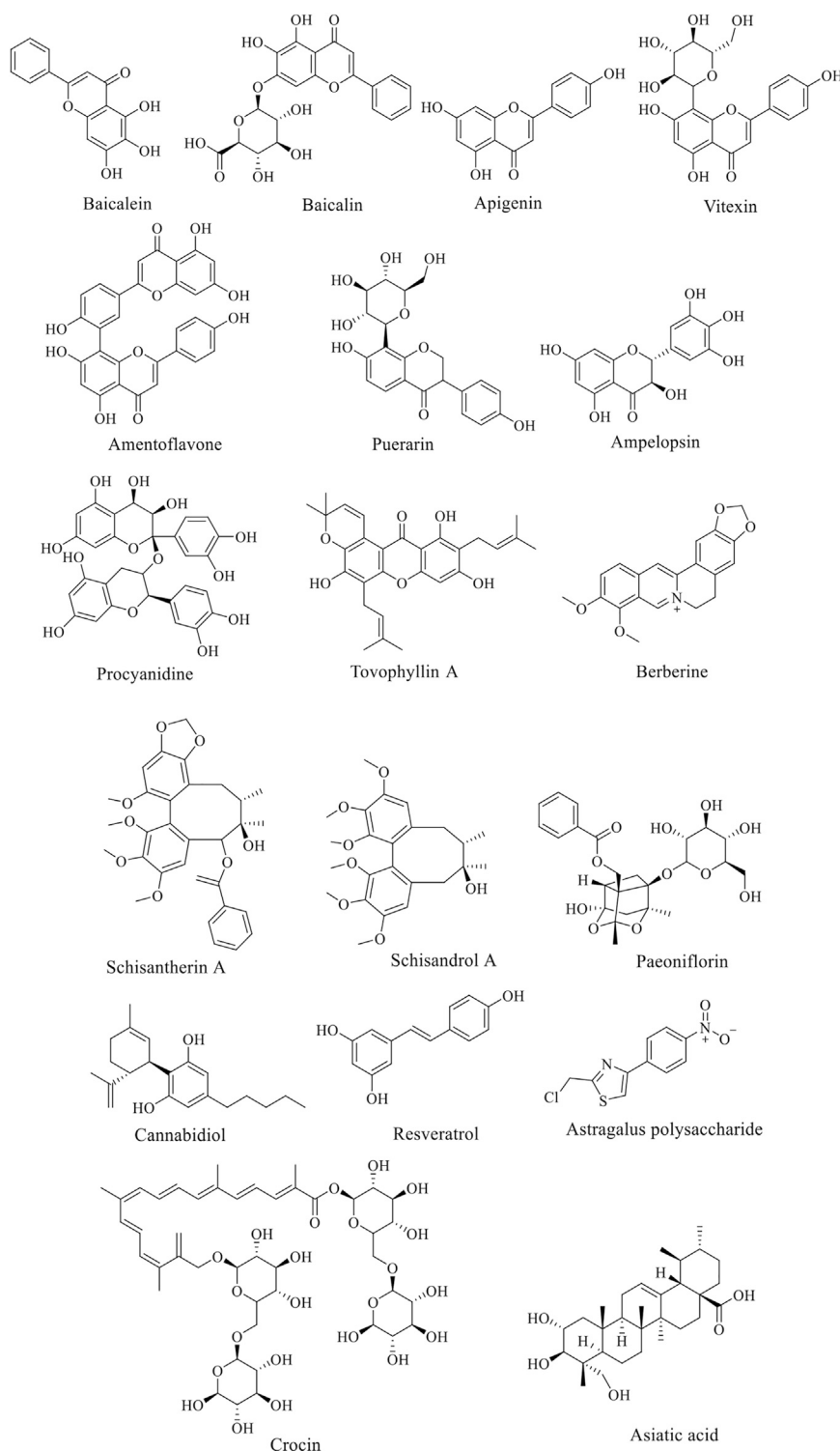


FIGURE 2 | Structure of anti-AD natural compounds.

hydroxydopamine (6-OHDA)-induced apoptosis (Zhu et al., 2019). Zhang et al. showed that the anti-PD function of baicalein is probably related to the activation of Nrf2/HO-1, protein kinase C (PKC) and PI3K/AKT signaling pathways

(Zhang et al., 2012). Baicalin has one more glucuronide in the seven hydroxyl group than baicalein (Figure 2), which inhibit 6-OHDA-induced apoptosis of substantia nigra neurons in PD rats through mTOR/AKT/GSK-3 β pathway (Zhai et al., 2019).

Apigenin has been shown to remarkably reduce the effects of 1-methyl-4-phenylpyridine (MPP⁺)-induced apoptosis in experimental models of PD. Furthermore, the glucoside derivative Vitexin of apigenin and several other flavonoid species showed similar protective effects on PD cells and mouse models (Ming et al., 2018).

Amentoflavone (AF) is an effective component of *Selaginella tamariscina* (P.Beauv.) Spring (family Selaginellaceae, genus *Selaginella*). In an *in vitro* of PD model study by Cao et al., AF enhanced PI3K phosphorylation, and reduced the loss of cell viability induced by MPP⁺, without obvious cytotoxicity. It also inhibits the activation of caspase-3 and p21, but increases the ratio of Bcl-2/Bax. *In vivo*, AF significantly reduces the loss of dopaminergic neurons in SNpc and striatal fibers induced by 1-methyl-4-phenyl-1,2,3,6-tetrahydropyridine (MPTP), and enhances the activation of PI3K and AKT and the ratio of Bcl-2/Bax in SN (Cao et al., 2017). Similarly, the PD mouse experiment of icariin obtained a similar conclusion as AF (Chen et al., 2017). Puerarin (PUE) is a vital isoflavone compound in traditional Chinese medicine *Pueraria lobata*. Zhang et al. have shown that PUE could reduce the protection of dopaminergic neurons from rotenone toxicity in PD animal model of PD by activating PI3K/AKT signal pathway, and decrease the overexpression of abnormal proteins in PD animal model (Zhang et al., 2014).

According to the reports, Ampelopsin increases the antioxidant and anti-apoptotic activity of cells through ERK1/2 and AKT signaling pathways, thus protecting neurons (Coria et al., 2019; Guo et al., 2020). Likewise, Procyanidine (PC), widely found in *Vitis vinifera* L. (family Vitaceae, genus *Vitis*) and other plants, tellingly scavenge free radicals, inhibits neuronal apoptosis and protects mitochondria (Zhang et al., 2019b). In recent years, Tovophyllin A (TA) has been reported to play a useful role in the treatment of neurodegenerative diseases. Some studies have found that TA has significant neuroprotective effects on primary cortical neurons injured by MPP⁺/paraquat and PD mouse model induced by MPTP. The mechanism is confirmed to be related to the apoptosis signal pathway of AKT/GSK-3 cells, but it still need a further explored (Huang et al., 2020). It has also been reported that curcumin inhibits the activation of astrocytes and microglia (Fu et al., 2015), and protects mitochondrial membrane potential from oxidative damage to dopaminergic neurons (Ma and Guo, 2017). Curcumin could conspicuously improve the oxidative damage of dopaminergic neurons induced by oxidative stress in the compact part of substantia nigra of rats via activating AKT/Nrf2 signal pathway, demonstrating great therapeutic impact on the experimental model of PD (Cui et al., 2016).

Alkaloids

Berberine (BBR), an alkaloid in the medicinal plants such as *Coptis chinensis* Franch. (family Ranunculaceae, genus *Coptis*) and *Phellodendron amurense* Rupr. (family Rutaceae, genus *Phellodendron*), is proved to be of anti-oxidative stress and anti-apoptotic role in central nervous system diseases. The low concentration of BBR can significantly reduce apoptosis induced by Cytomegalovirus in cultured spiral ganglion cells via

NMDAR1/Nox3, decreasing mitochondrial ROS generation (Zhuang et al., 2018). It have be reported that BBR inhibits ROS levels, mitochondrial dysfunction and mitochondrial autophagy by PI3K/AKT/mTOR signal pathway, thus protecting PC12 cells from oxidative damage (Zhang et al., 2017). In another research, a new concept emerged that BBR can attenuate the cytotoxicity induced by tert-butyl peroxide (t-BHP) (Deng et al., 2020). Han et al. demonstrated once again that berberine protects SH-SY5Y cells treated with rotenone through antioxidant and activation of the PI3K/AKT signaling pathway (Li Z. et al., 2020).

Phenylpropanoids

Lignans are natural compounds polymerized from 2-molecular phenylpropanoid derivatives. Schisandra chinensis lignans (SCL) of include Schisandra Ester A, B, C and D. Previous studies have suggested that the protective effect of SCL on cerebral ischemic nerve injury may be achieved through PI3K/AKT pathway. Meso-dihydroguaiaretic acid, schiarsanrin A and heteroclitin D, lignans isolated from the root of *Kadsura coccinea* (Lem.) A.C.Sm. (family Schisandraceae, genus *Kadsura*), significantly inhibit LPS-induced neuronal injury through the same signal pathway (Jiang et al., 2014b). Schisantherin A has been reported to enhance antioxidant stress, inhibit the overproduction of nitric oxide and prevent the loss of dopaminergic neurons stimulated by 6-OHDA in zebrafish (Zhang et al., 2015). On the side, schisandrol A, by activating the PI3K/AKT pathway, inhibits the IKK/I κ B/ $\text{NF-}\kappa\text{B}$ pathway, reduces neuronal inflammation and oxidative stress, and improves the survival of dopamine neurons in the brain of mice, showing promising prospects in the treatment of PD (Yan et al., 2019). In MPTP-induced PD mice, treatment with high dose of schisandrol A (40 mg/kg) significantly reduce cytokines, such as IL-1 β or TNF- α , and inhibit the activity of MDA, but increase SOD, improving antioxidant defences. While low dose of schisandrol A (20 mg/kg) showed no above effect. Additionally, autophagy-related proteins LC3-II, Beclin1, Parkin, Pink1, and mTOR were expressed after schisandrol A treatment (Zhi et al., 2019).

Glycosides

Paeoniflorin (PF), a bicyclic monoterpene glycoside (Figure 2), is the main active component of *Paeonia lactiflora* Pall. (family Paeoniaceae, genus *Paeonia*). In addition to anti-inflammation and anti-oxidation, PF also has neuroprotective effects and can be used in the treatment of cerebral ischemia, epilepsy and PD (Gu et al., 2016). Zheng et al. found that PF plays a neuroprotective role through the Bcl-2/Bax/caspase-3 pathway *in vitro* cell experiments. In PD mouse models, PF treatment protected dopaminergic neurons by preventing MPTP-induced declines in the levels of striatal and melanotic dopaminergic transporters (DAT) and tyrosine hydroxylase (TH) proteins and altering dopamine catabolism (Zheng et al., 2017).

Non-flavonoid Polyphenols

Resveratrol is an antitoxin produced by many plants when they are stimulated. The experiment results showed that resveratrol

delay the progression of PD symptoms by activating SIRT1/AKT1 and PI3K/AKT signal pathway (Wang et al., 2018a; Huang et al., 2019). As a compound extracted from *Cannabis sativa* L. (family Cannabaceae, genus *Cannabis*), Cannabidiol (CBD) has a series of physiological functions, such as blocking breast cancer metastasis, treating epilepsy, anti-insomnia and so on. It also has a good effect on the treatment of nervous system diseases. A study suggested that the prevention and protection of CBD on PD seem to be mediated by activating ERK and AKT/mTOR pathways. This protective effect could be eliminated by AKT1/2 inhibitors and mTOR inhibitors (Gugliandolo et al., 2020). In 2020, a Brazilian team published a paper discussing the biological basis for the potential role of CBD, as well as the team's preclinical and clinical studies of CBD in Parkinson's disease. The three clinical studies include open label studies (six patients), case series (four patients), and randomized controlled trials (twenty-one patients) (Zuardi et al., 2009; Chagas et al., 2014; Ferreira-Junior et al., 2020). Although these studies have shown beneficial results, they are limited by the small sample size and short follow-up time, which make the results inconclusive. Recently, a first clinical trial of the efficacy of relatively high doses of CBD (20 mg/kg/day) on PD patients examined the tolerability and effectiveness of a range of doses in the PD population (Leehey et al., 2020). However, the study is limited due to the lack of a placebo arm and a small group of participants. And adverse reactions were found at high doses. Therefore, a large number of studies on CBD are still needed to explore the in-depth mechanism of CBD on PD and its biosafety for patients.

Others

Crocin is a carotenoid found in *Crocus sativus* L. (family Iridaceae, genus *Crocus*), which shows beneficial effects on neurodegenerative diseases through anti-apoptosis, anti-inflammatory and antioxidant activities. However, the exact molecular pathway of the neuroprotective effect of safflower has not been fully elucidated. In rotenone (ROT)-induced rat PD model, crocin visibly stimulated PI3K/AKT pathway and decreased the expression of GSK-3, FoxO3a and downstream caspase-9, presenting a good neuroprotective function (Salama et al., 2020). Astaxanthin (AST), as a lipid-soluble pigment, inhibits apoptosis and neuronal injury by up-regulating phosphorylation of PI3K and AKT *in vivo* and *in vitro*, and it is considered for the treatment of AD and PD (Zarneshan et al., 2020). Moreover, asiatic acid (AA), a pentacyclic triterpene obtained from *Centella asiatica* (L.) Urb. (family Apiaceae, genus *Centella*), has been shown to effectively provide neuroprotection for MPTP-induced neuron cell loss through ERK and PI3K/AKT/mTOR/GSK-3 pathway (Nataraj et al., 2017). The phosphorylation levels of AKT and mTOR could be increased by both *Lycium barbarum* polysaccharide (LBP) (Wang et al., 2018b) and *Astragalus* polysaccharides (APS) (Tan et al., 2020), effectively alleviate the nigral striatal system degeneration and regulation of cell autophagy, thereby affecting the occurrence and development of PD.

DISCUSSION

The PI3K/AKT signaling pathway plays an important role in maintaining homeostasis throughout the life cycle. This pathway is triggered by the expression or abnormal regulation of many genes and has been found to be associated with numerous human diseases (Mengqiu et al., 2019). On the one hand, the excessive activation of PI3K/AKT pathway associated with diseases such as cancers and diabetes. On the other hand, deregulating its action might be relevant to cardiovascular diseases, and neurological diseases like AD and PD. Therefore, the study of PI3K/AKT signaling pathway and its upstream and downstream molecular mechanisms is of great significance for the prevention and treatment of various diseases. According to existing studies, many natural compounds have shown symptomatic alleviating effects on neurological diseases AD or PD, and such effects have been found to be related to the regulation of PI3K/AKT signaling pathway. However, it is not certain that whether this pathway plays a key role in this process. In other words, more evidence is needed to determine if this pathway be able to a target for drugs acting on AD or PD. Moreover the complex pathogenesis of these diseases and the multifactorial effects of natural products also bring challenges to explore the synergistic effects of various mechanisms, so that the molecular mechanisms of the neuroprotective effects of natural products also need to be further elucidated.

It is known that numerous natural products with medicinal potential are derived from a wide variety of vegetables, fruits and Chinese herbs, some scholars believe that dietary adjustments might be help for the prevention and treatment of diseases. (Kitagishi et al., 2014). For instance, multiple clinical trials have investigated the effect of curcumin on AD. But in most of these trials, curcumin was used as a dietary supplement, like an ongoing clinical trial in India about the efficacy and safety of curcumin formulation in Alzheimer's disease (Bhat et al., 2019). Even though there are no clinical reports of true dietary supplements for the treatment of neurological diseases, preclinical and clinical studies have demonstrated in some respects that diet still has merit as an adjunct preventive approach.

In reviewing the literature, we found that a variety of common natural polyphenols possess neuroprotective effects, including flavonoids and non-flavonoids, such as curcumin, icariin, baicalein and cannabidiol. However, it is a pity that many natural compounds, including natural flavonoids, are often limited in their application due to bioavailability and other defects. Consequently, using natural products as lead compounds and key pharmacophore targets to develop more effective and safer derivatives with high bioavailability may be a promising strategy for new drug development. For instance, curcumin is eliminated *in vivo* easily as its hydrophobicity and low bioavailability (Gupta et al., 2012; De Oliveira et al., 2016; Mirzaei et al., 2017), but such problems can be solved by modifying the structure of curcumin and synthesizing a series of derivatives (Bagheri et al., 2020). And the low solubility of baicalein is able to improve by nano-loading, that is, the oral bioavailability of baicalein is improved by nano-emulsion or nano-crystal loaded with baicalein (Liu et al., 2016; Yin et al., 2017). We summarize the natural products mentioned above that

have the potential to treat AD and PD, as shown in **Supplementary Figures S1 and S2**. The structure of the active ingredients is shown in **Figure 1** and **Figure 2**, and so do some relevant information for reference (**Table 1**). It can be learned that the treatment of natural products is a relatively long process, and some natural products could exert better effects at lower doses. But some are ineffective at low doses and require high concentrations to be effective. The therapeutic effects are connected with the dosage, time, and mode of administration. For instance, at low concentrations (0.12–16 μ M), BBR dramatically reduces 6-OHDA-induced cytotoxicity through the activation of PI3K/AKT/Bcl-2 cell survival and Nrf2/HO-1 antioxidative signaling pathways. However, treatment with high concentrations (16 μ M) BBR did not show protective effect (Zhang et al., 2017). A study investigated the role of curcumin and erythropoietin in an ICV-STZ rat model (a model for sporadic dementia of the Alzheimer's type (SDAT)) (Samy et al., 2016). The experimental animals were given vehicle, oral administration of curcumin (80 mg/kg/day), an intraperitoneal injection of erythropoietin (500 IU/kg every other day) as well as combined curcumin and erythropoietin for 3 months. The results showed that curcumin and/or erythropoietin were beneficial in restoring the behavioral, histological, and biochemical changes induced by ICV-STZ. And the long-term adverse effects of curcumin were lower than those of erythropoietin. In contrast, Bassani et al. found no beneficial effect in short-term spatial memory in ICV-STZ rats by evaluating extended oral curcumin (doses of 25, 50, and 100 mg/kg) (Bassani et al., 2017). But improvements were found in short-term cognitive memory. In addition, the combination of natural products with existing drugs is also a direction worth exploring. A report indicates that combination treatment of icariin and L-3,4-dihydroxyphenylalanine (L-DOPA) are beneficial for the treatment of dopamine neurotoxicity in 6-OHDA injury (Lu et al., 2018).

Each new drug should be clinically tested after developed but before used in humans. Practically, the fact that the results of animal and human are not exactly consistent is worrisome. In animal studies, certain natural products have shown great promise in treating Alzheimer's disease and cognitive aging, but this has not been observed in all clinical trials. After all, there is no animal model at the moment really reproduces all the symptoms observed in human pathology. In contrast to animal studies, the number of confirmed human studies is limited, and many of the results remain controversial. However, natural products are widely available, relatively safe and easy to obtain, making the research still extraordinary significance. Consequently, it is essential to conduct more long-term studies to assess the possibility of side effects from chronic administration in humans.

PROSPECT

Scientists have never stopped exploring the complex pathogenesis of AD and PD. It is exciting that great progress has been made in

recent years, which supply more possibilities to overcome these diseases. However, we also note that a small number of new drugs have been developed for the treatment of AD and PD over the years, and most of them are still in the stage of basic research. The pathological changes associated with the onset of neurodegenerative diseases are irreversible. When cognitive impairment shows up in patients, the course of the disease are often in the middle or late stage, as a result, the treatment can only slow down rather than reverse the development of the disease. Undoubtedly, it is particularly important for early prevention and diagnosis of neurodegenerative diseases. Further research into its pathogenesis is needed to develop drugs to reverse the progression of AD and PD. Substantial amounts of studies on natural products with multiple activities have proved to be of positive significance for the treatment of such diseases. In-depth research on natural products will bring more hope for the treatment of diseases, and at the same time promote the development of traditional Chinese herbal medicine. The direction for the continued research of natural products has also been proposed in the previous discussion: (I) the diseases prevention and control mechanisms of natural products are worthy of further investigation; (II) structural modification as a lead compound; (III) application of nanotechnology for decoration; (IV) combination with other drugs. Finally, it should be noted that the key to determining the safety and effectiveness of the final drug lies in conduct extensive clinical trials.

AUTHOR CONTRIBUTIONS

H-ZL completed the manuscript. YC, Z-WZ, D-DW and H-YL helped in searching for related articles. The revision of the manuscript was collaboratively finished by H-ZL, YC, Z-WZ, H-YL, D-DW and L-CG. All authors contributed to the article and finally the submitted version is approved by L-CG.

FUNDING

This work was supported by Science and Technology Key Program of Hunan Province Grants (2016SK 2066), Key Projects of Hunan Health Committee (B2017207), Hunan Province Chinese Medicine Research Program Grants (201940), Changsha City Science and Technology Program Grants (kq1801144), Changsha Central Hospital Affiliated to University of South China Foundation of key Program (YNKY201901), Hunan Province Foundation of High-level Health Talent (225 Program), and Science and Technology Key Program of Hunan Provincial Health Committee (20201904).

SUPPLEMENTARY MATERIAL

The Supplementary Material for this article can be found online at: <https://www.frontiersin.org/articles/10.3389/fphar.2021.648636/full#supplementary-material>.

REFERENCES

- Altomare, D. A., Testa, J. R., Testa, A., and Joseph, R. (2005). Perturbations of the AKT signaling pathway in human cancer. *Oncogene*. 24 (50), 7455–7464. doi:10.1038/sj.onc.1209085
- Bagheri, H., Ghasemi, F., Barreto, G. E., Rafiee, R., Sathyapalan, T., and Sahebkar, A. (2020). Effects of curcumin on mitochondria in neurodegenerative diseases. *Biofactors*. 46 (1), 5–20. doi:10.1002/biof.1566
- Bassani, T. B., Turnes, J. M., Moura, E. L. R., Bonato, J. M., Cópola-Segovia, V., Zanata, S. M., et al. (2017). Effects of curcumin on short-term spatial and recognition memory, adult neurogenesis and neuroinflammation in a streptozotocin-induced rat model of dementia of Alzheimer's type. *Behav. Brain Res.* 335, 41–54. doi:10.1016/j.bbr.2017.08.014
- Batista, P., and Pereira, A. (2016). Quality of life in patients with neurodegenerative diseases. *J. Neurol. Neurosci.* 7 (1). doi:10.21767/2171-6625.100074
- Bellacosa, A., Kumar, C. C., Cristofano, A. D., and Testa, J. R. (2005). Activation of AKT kinases in cancer: implications for therapeutic targeting. *Adv. Cancer Res.* 94 (1), 29–86. doi:10.1016/S0065-230X(05)94002-5
- Bertacchini, J., Heidari, N., Mediani, L., Capitani, S., Shahjehani, M., Ahmadvadeh, A., et al. (2015). Targeting PI3K/AKT/mTOR network for treatment of leukemia. *Cell. Mol. Life Sci.* 72 (12), 2337–2347. doi:10.1007/s00018-015-1867-5
- Bhat, A., Mahalakshmi, A. M., Ray, B., Tuladhar, S., Hediya, T. A., Manthiannem, E., et al. (2019). Benefits of curcumin in brain disorders. *Biofactors* 45 (5), 666–689. doi:10.1002/biof.1533
- Cao, Q., Qin, L., Huang, F., Wang, X., Yang, L., Shi, H., et al. (2017). Amentoflavone protects dopaminergic neurons in MPTP-induced Parkinson's disease model mice through PI3K/Akt and ERK signaling pathways. *Toxicol. Appl. Pharmacol.* 319, 80–90. doi:10.1016/j.taap.2017.01.019
- Chagas, M. H. N., Zuardi, A. W., Tumas, V., Pena-Pereira, M. A., Sobreira, E. T., Bergamaschi, M. M., et al. (2014). Effects of cannabidiol in the treatment of patients with Parkinson's disease: an exploratory double-blind trial. *J. Psychopharmacol.* 28 (11), 1088–1098. doi:10.1177/0269881114550355
- Chen, W.-F., Wu, L., Du, Z.-R., Chen, L., Xu, A.-L., Chen, X.-H., et al. (2017). Neuroprotective properties of icariin in MPTP-induced mouse model of Parkinson's disease: involvement of PI3K/Akt and MEK/ERK signaling pathways. *Phytomedicine*. 25, 93–99. doi:10.1016/j.phymed.2016.12.017
- Cheng, Q., Zhang, S., and Ding, F. (2012). Determination of salidroside in rats and its pharmacokinetic profile. *Lishizhen Med. Materia Med. Res.* 10, 2422–2424.
- Chong, Z. Z., Shang, Y. C., Wang, S., and Maiese, K. (2012). A critical kinase cascade in neurological disorders: PI3K, Akt and mTOR. *Future Neurol.* 7 (6), 733–748. doi:10.2217/fnl.12.72
- Coria, H. M., Mendoza Rojas, M. X., Arrieta Cruz, I., and Valdés, H. E. L. (2019). Preclinical research of dihydromyricetin for brain aging and neurodegenerative diseases. *Front. Pharmacol.* 10, 1334. doi:10.3389/fphar.2019.01334
- Cox, K. H., Pipingas, A., and Scholey, A. B. (2015). Investigation of the effects of solid lipid curcumin on cognition and mood in a healthy older population. *J. Psychopharmacol.* 29 (5), 642–651. doi:10.1177/0269881114552744
- Cui, J., Shan, R., Cao, Y., Zhou, Y., Liu, C., and Fan, Y. (2021). Protective effects of ginsenoside Rg2 against memory impairment and neuronal death induced by Aβ25–35 in rats. *J. Ethnopharmacology* 266, 113466. doi:10.1016/j.jep.2020.113466
- Cui, J., Wang, J., Zheng, M., Gou, D., and Zhou, Y. (2017a). Ginsenoside Rg2 protects PC12 cells against β-amyloid 25–35 -induced apoptosis via the phosphoinositide 3-kinase/Akt pathway. *Chem. Biol. Interact.* 275, 152–161. doi:10.1016/j.cbi.2017.07.021
- Cui, W., Wang, S., Wang, Z., Wang, Z., Sun, C., Zhang, Y., et al. (2017b). Inhibition of PTEN attenuates endoplasmic reticulum stress and apoptosis via activation of PI3K/AKT pathway in Alzheimer's disease. *Neurochem. Res.* 42 (11), 3052–3060. doi:10.1007/s11064-017-2338-1
- Cui, Q., Li, X., and Zhu, H. (2016). Curcumin ameliorates dopaminergic neuronal oxidative damage via activation of the Akt/Nrf2 pathway. *Mol. Med. Rep.* 13 (2), 1381–1388. doi:10.3892/mmr.2015.4657
- De Oliveira, M. R., Jardim, F. R., Setzer, W. N., Nabavi, S. M., and Nabavi, S. F. (2016). Curcumin, mitochondrial biogenesis, and mitophagy: exploring recent data and indicating future needs. *Biotechnol. Adv.* 34, 813–826. doi:10.1016/j.biotechadv.2016.04.004
- Deng, H., Jia, Y., Pan, D., and Ma, Z. (2020). Berberine alleviates rotenone-induced cytotoxicity by antioxidation and activation of PI3K/Akt signaling pathway in SH-SY5Y cells. *Neuroreport*. 31 (1), 41–47. doi:10.1097/WNR.0000000000001365
- Deng, S., Rong, H., Tu, H., Zheng, B., Mu, X., Zhu, L., et al. (2019). Molecular basis of neurophysiological and antioxidant roles of Szechuan pepper. *Biomed. Pharmacother.* 112, 108696. doi:10.1016/j.biopha.2019.108696
- Do, T. D., Economou, N. J., Chamas, A., Buratto, S. K., Shea, J.-E., Bowers, M. T., et al. (2014). Interactions between amyloid-β and tau fragments promote aberrant aggregates: implications for amyloid toxicity. *J. Phys. Chem. B*. 118 (38), 11220–11230. doi:10.1021/jp506258g
- Dobbin, Z., and Landen, C. (2013). The importance of the PI3K/AKT/mTOR pathway in the progression of ovarian cancer. *Int J Mol Sci.* 14 (4), 8213–8227. doi:10.3390/ijms14048213
- Fan, F., Yang, L., Li, R., Zou, X., Li, N., Meng, X., et al. (2020). Salidroside as a potential neuroprotective agent for ischemic stroke: a review of sources, pharmacokinetics, mechanism and safety. *Biomed. Pharmacother.* 129, 110458. doi:10.1016/j.biopha.2020.110458
- Ferreira-Junior, N. C., Campos, A. C., Guimarães, F. S., Del-Bel, E., Zimmermann, P. M. d. R., Brum Junior, L., et al. (2020). Biological bases for a possible effect of cannabidiol in Parkinson's disease. *Braz. J. Psychiatry* 42 (2), 218–224. doi:10.1590/1516-4446-2019-0460
- Fu, W., Zhuang, W., Zhou, S., and Wang, X. (2015). Plant-derived neuroprotective agents in Parkinson's disease. *Am. J. Transl Res.* 7 (7), 1189–1202.
- Fu, Z., Yang, J., Wei, Y., and Li, J. (2016). Effects of piceatannol and pterostilbene against β-amyloid-induced apoptosis on the PI3K/Akt/Bad signaling pathway in PC12 cells. *Food Funct.* 7 (2), 1014–1023. doi:10.1039/c5fo01124h
- Gao, L., Zhou, F., Wang, K.-x., Zhou, Y.-z., Du, G.-h., Qin, X.-m., et al. (2020). Baicalein protects PC12 cells from Aβ25–35-induced cytotoxicity via inhibition of apoptosis and metabolic disorders. *Life Sci.* 248, 117471. doi:10.1016/j.lfs.2020.117471
- Gao, Q., Yang, M., and Zuo, Z. (2018). Overview of the anti-inflammatory effects, pharmacokinetic properties and clinical efficacies of arctigenin and arctiin from *Arctium lappa* L. *Acta Pharmacol. Sin.* 39 (5), 787–801. doi:10.1038/aps.2018.32
- Garofalo, R. S., Orena, S. J., Rafidi, K., Torchia, A. J., Stock, J. L., Hildebrandt, A. L., et al. (2003). Severe diabetes, age-dependent loss of adipose tissue, and mild growth deficiency in mice lacking Akt2/PKBβ. *J. Clin. Invest.* 112 (2), 197–208. doi:10.1172/jci16885
- Ghoneum, A., and Said, N. (2019). PI3K-AKT-mTOR and NFκB pathways in ovarian cancer: implications for targeted therapeutics. *Cancers* 11 (7), 949. doi:10.3390/cancers11070949
- Gong, J., Zhang, L., Zhang, Q., Li, X., Xia, X.-J., Liu, Y.-Y., et al. (2018). Lentiviral vector-mediated SHC3 silencing exacerbates oxidative stress injury in nigral dopamine neurons by regulating the PI3K-AKT-FoxO signaling pathway in rats with Parkinson's disease. *Cell. Physiol. Biochem.* 49 (3), 971–984. doi:10.1159/000493228
- Gu, X.-S., Wang, F., Zhang, C.-Y., Mao, C.-J., Yang, J., Yang, Y.-P., et al. (2016). Neuroprotective effects of paeoniflorin on 6-OHDA-lesioned rat model of Parkinson's disease. *Neurochem. Res.* 41 (11), 2923–2936. doi:10.1007/s11064-016-2011-0
- Gugliandolo, A., Pollastro, F., Bramanti, P., and Mazzon, E. (2020). Cannabidiol exerts protective effects in an *in vitro* model of Parkinson's disease activating AKT/mTOR pathway. *Fitoterapia* 143, 104553. doi:10.1016/j.fitote.2020.104553
- Guo, C.-h., Cao, T., Zheng, L.-t., Waddington, J. L., and Zhen, X.-c. (2020). Development and characterization of an inducible Dicer conditional knockout mouse model of Parkinson's disease: validation of the antiparkinsonian effects of a sigma-1 receptor agonist and dihydromyricetin. *Acta Pharmacol. Sin.* 41 (4), 499–507. doi:10.1038/s41401-020-0379-5
- Gupta, S. C., Patchva, S., Koh, W., and Aggarwal, B. B. (2012). Discovery of curcumin, a component of golden spice, and its miraculous biological activities. *Clin. Exp. Pharmacol. Physiol.* 39 (3), 283–299. doi:10.1111/j.1440-1681.2011.05648.x
- Hanada, M., Feng, J., and Hemmings, B. A. (2004). Structure, regulation and function of PKB/AKT—a major therapeutic target. *Biochim. Biophys. Acta* 1697 (1), 3–16. doi:10.1016/j.bbapap.2003.11.009
- Hetman, M., Chen, W. T., Kuo, Y. Y., Lin, G. B., Lu, C. H., Hsu, H. P., et al. (2020). Thermal cycling protects SH-SY5Y cells against hydrogen peroxide and

- β -amyloid-induced cell injury through stress response mechanisms involving Akt pathway. *PLoS One* 15 (10), e0240022. doi:10.1371/journal.pone.0240022
- Hu, M., Li, F., and Wang, W. (2018). Vitexin protects dopaminergic neurons in MPTP-induced Parkinson's disease through PI3K/Akt signaling pathway. *Drug Des. Devel. Ther.* 12, 565–573. doi:10.2147/dddt.s156920
- Hu, T., Li, S., Liang, W.-Q., Li, S.-S., Lu, M.-N., Chen, B., et al. (2020). Notoginsenoside R1-induced neuronal repair in models of Alzheimer disease is associated with an alteration in neuronal hyperexcitability, which is regulated by Nav. *Front. Cel. Neurosci.* 14, 280. doi:10.3389/fncel.2020.00280
- Huang, N., Zhang, Y., Chen, M., Jin, H., Nie, J., Luo, Y., et al. (2019). Resveratrol delays 6-hydroxydopamine-induced apoptosis by activating the PI3K/Akt signaling pathway. *Exp. Gerontol.* 124, 110653. doi:10.1016/j.exger.2019.110653
- Huang, Y., Sun, L., Zhu, S., Xu, L., Liu, S., Yuan, C., et al. (2020). Neuroprotection against Parkinson's disease through the activation of akt/gsk3 β signaling pathway by Tovophyllin A. *Front. Neurosci.* 14, 723. doi:10.3389/fnins.2020.00723
- Jiang, B., Le, L., Pan, H., Hu, K., Xu, L., Xiao, P., et al. (2014a). Dihydromyricetin ameliorates the oxidative stress response induced by methylglyoxal via the AMPK/GLUT4 signaling pathway in PC12 cells. *Brain Res. Bull.* 109, 117–126. doi:10.1016/j.brainresbull.2014.10.010
- Jiang, E. P., Wang, S. Q., Wang, Z., Yu, C. R., Chen, J. G., Yu, C. Y., et al. (2014b). [Effect of Schisandra chinensis lignans on neuronal apoptosis and p-AKT expression of rats in cerebral ischemia injury model]. *Zhongguo Zhong Yao Za Zhi* 39 (9), 1680–1684. doi:10.4268/cjcm.20140927
- Kandezi, N., Mohammadi, M., Ghaffari, M., Gholami, M., Motaghinejad, M., Safari, S., et al. (2020). Novel insight to neuroprotective potential of curcumin: a mechanistic review of possible involvement of mitochondrial biogenesis and PI3/akt/GSK3 or PI3/akt/CREB/BDNF signaling pathways. *Int. J. Mol. Cel Med.* 9 (1), 1–32. doi:10.22088/IJCMC.BUMS.9.1.1
- Kitagishi, Y., Nakanishi, A., Ogura, Y., and Matsuda, S. (2014). Dietary regulation of PI3K/AKT/GSK-3 β pathway in Alzheimer's disease. *Alzheimers Res. Ther.* 6 (3), 35. doi:10.1186/alzrt265
- Kou, X., Li, J., Bian, J., Yang, Y., Yang, X., Fan, J., et al. (2015). Ampelopsin attenuates 6-OHDA-induced neurotoxicity by regulating GSK-3 β /NRF2/ARE signalling. *J. Funct. Foods* 19, 765–774. doi:10.1016/j.jff.2015.10.010
- Kou, X., Liu, X., Chen, X., Li, J., Yang, X., Fan, J., et al. (2016). Ampelopsin attenuates brain aging of D-gal-induced rats through miR-34a-mediated SIRT1/mTOR signal pathway. *Oncotarget* 7 (46), 74484–74495. doi:10.18632/oncotarget.12811
- Kou, X., Shen, K., An, Y., Qi, S., Dai, W.-X., Yin, Z., et al. (2012). Ampelopsin inhibits H₂O₂-induced apoptosis by ERK and akt signaling pathways and up-regulation of heme oxygenase-1. *Phytother. Res.* 26 (7), 988–994. doi:10.1002/ptr.3671
- Laplanche, M., and Sabatini, D. M. (2012). mTOR signaling in growth control and disease. *Cell* 149 (2), 274–293. doi:10.1016/j.cell.2012.03.017
- Leehey, M. A., Liu, Y., Hart, F., Epstein, C., Cook, M., Sillau, S., et al. (2020). Safety and tolerability of cannabidiol in Parkinson disease: an open label, dose-escalation study. *Cannabis Cannabinoid Res.* 5 (4), 326–336. doi:10.1089/can.2019.0068
- Li, H., Kang, T., Qi, B., Kong, L., Jiao, Y., Cao, Y., et al. (2016). Neuroprotective effects of ginseng protein on PI3K/Akt signaling pathway in the hippocampus of D-galactose/AlCl₃ inducing rats model of Alzheimer's disease. *J. Ethnopharmacology* 179, 162–169. doi:10.1016/j.jep.2015.12.020
- Li, Q., Wang, J., Li, Y., and Xu, X. (2018). Neuroprotective effects of salidroside administration in a mouse model of Alzheimer's disease. *Mol. Med. Rep.* 17, 7287–7292. doi:10.3892/mmr.2018.8757
- Li, Y.-h., Jin, Y., Wang, X.-s., Chen, X.-l., Chen, H.-b., Xu, J., et al. (2020). Neuroprotective effect of fructus broussonetiae on APP/PS1 mice via upregulation of AKT/ β -Catenin signaling. *Chin. J. Integr. Med.* 27, 115. doi:10.1007/s11655-019-3178-4
- Li, Y., Zhao, J., and Hölscher, C. (2017). Therapeutic potential of baicalein in Alzheimer's disease and Parkinson's disease. *CNS Drugs* 31 (8), 639–652. doi:10.1007/s40263-017-0451-y
- Li, Z., Jiang, T., Lu, Q., Xu, K., He, J., Xie, L., et al. (2020). Berberine attenuated the cytotoxicity induced by t-BHP via inhibiting oxidative stress and mitochondria dysfunction in PC-12 cells. *Cell. Mol. Neurobiol.* 40 (4), 587–602. doi:10.1007/s10571-019-00756-7
- Liang, J., Wu, Y., Yuan, H., Yang, Y., Xiong, Q., Liang, C., et al. (2019). Dendrobium officinale polysaccharides attenuate learning and memory disabilities via anti-oxidant and anti-inflammatory actions. *Int. J. Biol. Macromolecules* 126, 414–426. doi:10.1016/j.ijbiomac.2018.12.230
- Liao, S. F., Wang, H. T., Yan, F. X., Zheng, Y. X., Zeng, Z. W., Zheng, W. H., et al. (2014). [Protective effect and mechanisms of dihydromyricetin on PC12 cells induced by oxidative injury]. *Zhong Yao Cai* 37 (6), 1014–1020.
- Liu, W., Zhai, Y., Heng, X., Che, F. Y., Chen, W., Sun, D., et al. (2016). Oral bioavailability of curcumin: problems and advancements. *J. Drug Target* 24 (8), 694–702. doi:10.3109/1061186x.2016.1157883
- Zhu, Q., Zhuang, X., and Lu, J. (2019). Neuroprotective effects of baicalein in animal models of Parkinson's disease: a systematic review of experimental studies. *Phytomedicine* 55, 302–309. doi:10.1016/j.phymed.2018.09.215
- Liyang, Y., Hongyan, W., Lijun, L., and Anmu, X. (2018). The role of insulin/IGF-1/PI3K/Akt/GSK3 β signaling in Parkinson's disease dementia. *Front. Neurosci.* 12, 73. doi:10.3389/fnins.2018.00073
- Lu, D.-S., Chen, C., Zheng, Y.-X., Li, D.-D., Wang, G.-Q., Liu, J., et al. (2018). Combination treatment of icariin and L-DOPA against 6-OHDA-lesioned dopamine neurotoxicity. *Front. Mol. Neurosci.* 11, 155. doi:10.3389/fnmol.2018.00155
- Lu, Q., Zhu, H., Liu, X., and Tang, C. (2020). Icarin sustains the proliferation and differentiation of A β 25-35-treated hippocampal neural stem cells via the BDNF-TrkB-ERK/Akt signaling pathway. *Neurol. Res.* 42 (11), 936–945. doi:10.1080/01616412.2020.1792701
- Lulin, N., Junxia, X., Honglian, L., Zaijun, Z., Ying, Y., Xinfeng, H., et al. (2017). Ginsenoside Rg1 ameliorates behavioral abnormalities and modulates the hippocampal proteomic change in triple transgenic mice of Alzheimer's disease. *Oxid Med. Cel Longev.* 2017, 1–17. doi:10.1155/2017/6473506
- Luo, S., Kang, S. S., Wang, Z.-H., Liu, X., Day, J. X., Wu, Z., et al. (2019). Akt phosphorylates NQO1 and triggers its degradation, abolishing its antioxidative activities in Parkinson's disease. *J. Neurosci.* 39 (37), 7291–7305. doi:10.1523/JNEUROSCI.0625-19.2019
- Ma, B., Meng, X., Wang, J., Sun, J., Ren, X., Qin, M., et al. (2014). Notoginsenoside R1 attenuates amyloid- β -induced damage in neurons by inhibiting reactive oxygen species and modulating MAPK activation. *Int. Immunopharmacology* 22(1), 151–159. doi:10.1016/j.intimp.2014.06.018
- Ma, X.-W., and Guo, R.-Y. (2017). Dose-dependent effect of Curcuma longa for the treatment of Parkinson's disease. *Exp. Ther. Med.* 13 (5), 1799–1805. doi:10.3892/etm.2017.4225
- Mario, P. M., Jorge, M. F., Cesar, R. T., and Mcarmen, R. T. (2016). Curcumin and health. *Molecules* 21 (3), 264. doi:10.3390/molecules21030264
- Martins, A. C., Morcillo, P., Ijomone, O. M., Venkataramani, V., Harrison, F. E., Lee, E., et al. (2019). New insights on the role of manganese in Alzheimer's disease and Parkinson's disease. *Int J Environ Res Public Health* 16 (19), 3546. doi:10.3390/ijerph16193546
- Matsuda, S., Ikeda, Y., Murakami, M., Nakagawa, Y., Tsuji, A., Kitagishi, Y., et al. (2019). Roles of PI3K/AKT/GSK3 pathway involved in psychiatric illnesses. *Diseases* 7 (1), 22. doi:10.3390/diseases7010022
- Matsuo, F. S., Andrade, M. F., Loyola, A. M., da Silva, S. J., Silva, M. J. B., Cardoso, S. V., et al. (2018). Pathologic significance of AKT, mTOR, and GSK3 β proteins in oral squamous cell carcinoma-affected patients. *Virchows Arch.* 472, 983. doi:10.1007/s00428-018-2318-0
- Memmott, R. M., and Dennis, P. A. (2009). Akt-dependent and -independent mechanisms of mTOR regulation in cancer. *Cell Signal* 21 (5), 656–664. doi:10.1016/j.cellsig.2009.01.004
- Meng, X., Sun, G., Ye, J., Xu, H., Wang, H., Sun, X., et al. (2014). Notoginsenoside R1-mediated neuroprotection involves estrogen receptor-dependent crosstalk between Akt and ERK1/2 pathways: a novel mechanism of Nrf2/ARE signaling activation. *Free Radic. Res.* 48 (4), 445. doi:10.3109/10715762.2014.885117
- Mengqiu, S., Ann, B., Zigang, D., and Mee-Hyun, I. (2019). AKT as a therapeutic target for cancer. *Cancer Res.* 79, 1019. doi:10.1158/0008-5472.CAN-18-2738
- Ming, H., Fangming, L., and Weidong, W. (2018). Vitexin protects dopaminergic neurons in MPTP-induced Parkinson's disease through PI3K/Akt signaling pathway. *Drug Des. Dev. Ther.* 12, 565–573. doi:10.2147/DDDT.S156920
- Mirdamadi, Y., Bommhardt, U., Goihl, A., Guttek, K., Zouboulis, C. C., Quist, S., et al. (2017). Insulin and Insulin-like growth factor-1 can activate the phosphoinositide-3-kinase/Akt/FoxO1 pathway in T cells *in vitro*. *Dermato-Endocrinology* 9(1), e1356518. doi:10.1080/19381980.2017.1356518

- Mirzaei, H., Shakeri, A., Rashidi, B., Jalili, A., Banikazemi, Z., Sahebkar, A., et al. (2017). Phytosomal curcumin: a review of pharmacokinetic, experimental and clinical studies. *Biomed. Pharmacother.* 85, 102–112. doi:10.1016/j.biopha.2016.11.098
- Mu, S., Li, Y., Liu, B., Wang, W., Chen, S., Wu, J., et al. (2016). Dihydromyricetin ameliorates 3NP-induced behavioral deficits and striatal injury in rats. *J. Mol. Neurosci.* 60, 267. doi:10.1007/s12031-016-0801-0
- Nataraj, J., Manivasagam, T., Justin Thenmozhi, A., and Essa, M. M. (2017). Neurotrophic effect of asiatic acid, a triterpene of *Centella asiatica* against chronic 1-methyl 4-phenyl 1, 2, 3, 6-tetrahydropyridine hydrochloride/probenecid mouse model of Parkinson's disease: the role of MAPK, PI3K-Akt-GSK3 β and mTOR signalling pathways. *Neurochem. Res.* 42 (5), 1354–1365. doi:10.1007/s11064-017-2183-2
- Parkinson, G. T., and Hanley, J. G. (2018). Mechanisms of AMPA receptor endosomal sorting. *Front. Mol. Neurosci.* 11. doi:10.3389/fnmol.2018.00440
- Petrik, L., Santry, L., Moorehead, R., Jücker, M., and Petrik, J. (2016). Akt isoform specific effects in ovarian cancer progression. *Oncotarget* 7 (46), 74820–74833. doi:10.18632/oncotarget.11204
- Qi, Y., Cheng, X., Gong, G., Yan, T., Du, Y., Wu, B., et al. (2020). Synergistic neuroprotective effect of schisandrin and nootkatone on regulating inflammation, apoptosis and autophagy via the PI3K/AKT pathway. *Food Funct.* 11 (3), 2427–2438. doi:10.1039/c9fo02927c
- Qi, Y., Dou, D.-Q., Jiang, H., Zhang, B.-B., Qin, W.-Y., Kang, K., et al. (2017). Arctigenin attenuates learning and memory deficits through PI3k/akt/GSK-3 β pathway reducing tau hyperphosphorylation in $\alpha\beta$ -induced AD mice. *Planta Med.* 83 (1–2), 51–56. doi:10.1055/s-0042-107471
- Ringman, J. M., Frautschy, S. A., Teng, E., Begum, A. N., Bardens, J., Beigi, M., et al. (2012). Oral curcumin for Alzheimer's disease: tolerability and efficacy in a 24-week randomized, double blind, placebo-controlled study. *Alzheimers Res. Ther.* 4 (5), 43. doi:10.1186/alzrt146
- Salama, R. M., Abdel-Latif, G. A., Abbas, S. S., El Magdoub, H. M., and Schaalán, M. F. (2020). Neuroprotective effect of crocin against rotenone-induced Parkinson's disease in rats: interplay between PI3K/Akt/mTOR signaling pathway and enhanced expression of miRNA-7 and miRNA-221. *Neuropharmacology* 164, 107900. doi:10.1016/j.neuropharm.2019.107900
- Samy, D. M., Ismail, C. A., Nassra, R. A., Zeitoun, T. M., and Nomair, A. M. (2016). Downstream modulation of extrinsic apoptotic pathway in streptozotocin-induced Alzheimer's dementia in rats: erythropoietin versus curcumin. *Eur. J. Pharmacol.* 770, 52–60. doi:10.1016/j.ejphar.2015.11.046
- Satoru, M., Yuki, N., Ai, T., Yasuko, K., Atsuko, N., Toshiyuki, M., et al. (2018). Implications of PI3K/AKT/PTEN signaling on superoxide dismutases expression and in the pathogenesis of Alzheimer's disease. *Diseases* 6 (2), 28
- Shane, M., and Aggleton, J. P. (2019). Space and memory (far) beyond the *Hippocampus*: many subcortical structures also support cognitive mapping and mnemonic processing. *Front. Neural Circu.* 13, 52. doi:10.3389/fncir.2019.00052
- Shanu, M., and Komal, J. (2015). Ganetespib: research and clinical development. *Oncotargets Ther.* 8, 1849. doi:10.2147/OTT.S65804
- Shi, C., Zheng, D.-d., Fang, L., Wu, F., Kwong, W. H., Xu, J., et al. (2012). Ginsenoside Rg1 promotes nonamyloidogenic cleavage of APP via estrogen receptor signaling to MAPK/ERK and PI3K/Akt. *Biochim Biophys Acta.* 1820 (4), 453–460. doi:10.1016/j.bbagen.2011.12.005
- Small, G. W., Siddarth, P., Li, Z., Miller, K. J., Ercoli, L., Emerson, N. D., et al. (2018). Memory and brain amyloid and tau effects of a bioavailable form of curcumin in non-demented adults: a double-blind, placebo-controlled 18-month trial. *Am. J. Geriatr. Psychiatry* 26 (3), 266–277. doi:10.1016/j.jagp.2017.10.010
- Soliman, G. (2013). The role of mechanistic target of rapamycin (mTOR) complexes signaling in the immune responses. *Nutrients* 5 (6), 2231–2257. doi:10.3390/nu5062231
- Song, L., Yao, L., Zhang, L., Piao, Z., and Lu, Y. (2020). Schizandrol A protects against A β 1-42-induced autophagy via activation of PI3K/AKT/mTOR pathway in SH-SY5Y cells and primary hippocampal neurons. *Naunyn-Schmiedeberg's Arch. Pharmacol.* 393 (9), 1739–1752. doi:10.1007/s00210-019-01792-2
- Spinelli, M., Fusco, S., and Grassi, C. (2019). Brain insulin resistance and hippocampal plasticity: mechanisms and biomarkers of cognitive decline. *Front. Neurosci.* 13, 788. doi:10.3389/fnins.2019.00788
- Sugiyama, M. G., Fairn, G. D., and Antonescu, C. N. (2019). Akt-ing up just about everywhere: compartment-specific akt activation and function in receptor tyrosine kinase signaling. *Front. Cel Dev. Biol.* 7, 70. doi:10.3389/fcell.2019.00070
- Sun, J., Zhang, X., Wang, C., Teng, Z., and Li, Y. (2017). Curcumin decreases hyperphosphorylation of tau by down-regulating caveolin-1/GSK-3 β in N2a/APP695swe cells and APP/PS1 double transgenic Alzheimer's disease mice. *Am. J. Chin. Med.* 45, 1667–1682. doi:10.1142/S0192415X17500902
- Tan, Y., Yin, L., Sun, Z., Shao, S., Chen, W., Man, X., et al. (2020). Astragalus polysaccharide exerts anti-Parkinson via activating the PI3K/AKT/mTOR pathway to increase cellular autophagy level *in vitro*. *Int. J. Biol. Macromolecules* 153, 349–356. doi:10.1016/j.jbiomac.2020.02.282
- Thorpe, L. M., Yuzugullu, H., and Zhao, J. J. (2015). PI3K in cancer: divergent roles of isoforms, modes of activation and therapeutic targeting. *Nat. Rev. Cancer* 15 (1), 7–24. doi:10.1038/nrc3860
- Vaz, M., and Silvestre, S. (2020). Alzheimer's disease: recent treatment strategies. *Eur. J. Pharmacol.* 887, 173554. doi:10.1016/j.ejphar.2020.173554
- Voulgaropoulou, S. D., van Amelsvoort, T. A. M. J., Prickaerts, J., and Vingerhoets, C. (2019). The effect of curcumin on cognition in Alzheimer's disease and healthy aging: a systematic review of pre-clinical and clinical studies. *Brain Res.* 1725, 146476. doi:10.1016/j.brainres.2019.146476
- Wang, G., Wang, T., Zhang, Y., Li, F., Yu, B., Kou, J., et al. (2019). Schizandrin protects against OGD/R-Induced neuronal injury by suppressing autophagy: involvement of the AMPK/mTOR pathway. *Molecules* 24 (19), 3624. doi:10.3390/molecules24193624
- Wang, H., Dong, X., Liu, Z., Zhu, S., Liu, H., Fan, W., et al. (2018a). Resveratrol suppresses rotenone-induced neurotoxicity through activation of SIRT1/akt1 signaling pathway. *Anat. Rec.* 301 (6), 1115–1125. doi:10.1002/ar.23781
- Wang, H., Li, Q., Sun, S., and Chen, S. (2020). Neuroprotective effects of salidroside in a mouse model of Alzheimer's disease. *Cel. Mol. Neurobiol.* 40 (7), 1133–1142. doi:10.1007/s10571-020-00801-w
- Wang, R., Yang, S., Nie, T., Zhu, G., Feng, D., Yang, Q., et al. (2017). Transcription factors: potential cell death markers in Parkinson's disease. *Neurosci. Bull.* 33 (5), 552–560. doi:10.1007/s12264-017-0168-4
- Wang, X., Pang, L., Zhang, Y., Xu, J., Ding, D., Yang, T., et al. (2018b). Lycium barbarum polysaccharide promotes nigrostriatal dopamine function by modulating PTEN/AKT/mTOR pathway in a methyl-4-phenyl-1,2,3,6-tetrahydropyridine (MPTP) murine model of Parkinson's disease. *Neurochem. Res.* 43 (4), 938–947. doi:10.1007/s11064-018-2499-6
- Wei, Y., Zhou, J., Yu, H., and Jin, X. (2019). AKT phosphorylation sites of Ser473 and Thr308 regulate AKT degradation. *Biosci. Biotechnol. Biochem.* 83 (3), 429–435. doi:10.1080/09168451.2018.1549974
- Wolkmer, P., da Silva, C. B., Paim, F. C., Duarte, M. M. F., Castro, V., Palma, H. E., et al. (2013). Pre-treatment with curcumin modulates acetylcholinesterase activity and proinflammatory cytokines in rats infected with *Trypanosoma evansi*. *Parasitol. Int.* 62 (2), 144–149. doi:10.1016/j.parint.2012.11.004
- Wu, B., Chen, Y., Huang, J., Ning, Y., Bian, Q., Shan, Y., et al. (2012). Icaritin improves cognitive deficits and activates quiescent neural stem cells in aging rats. *J. Ethnopharmacology* 142 (3), 746–753. doi:10.1016/j.jep.2012.05.056
- Wu, J., Qu, J.-Q., Zhou, Y.-J., Zhou, Y.-J., Li, Y.-Y., Huang, N.-Q., et al. (2020). Icaritin improves cognitive deficits by reducing the deposition of β -amyloid peptide and inhibition of neurons apoptosis in SAMP8 mice. *Neuroreport* 31, 663. doi:10.1097/WNR.00000000000001466
- Yan, T., Sun, Y., Gong, G., Li, Y., Fan, K., Wu, B., et al. (2019). The neuroprotective effect of schisandrol A on 6-OHDA-induced PD mice may be related to PI3K/AKT and IKK/I κ B/NF- κ B pathway. *Exp. Gerontol.* 128, 110743. doi:10.1016/j.exger.2019.110743
- Yang, W.-t., Zheng, X.-w., Chen, S., Shan, C.-s., Xu, Q.-q., Zhu, J.-Z., et al. (2017). Chinese herbal medicine for Alzheimer's disease: clinical evidence and possible mechanism of neurogenesis. *Biochem. Pharmacol.* 141, 143–155. doi:10.1016/j.bcp.2017.07.002
- Yang, Z., Huang, X., Lai, W., Tang, Y., Liu, J., Wang, Y., et al. (2021). Synthesis and identification of a novel derivative of salidroside as a selective, competitive inhibitor of monoamine oxidase B with enhanced neuroprotective properties. *Eur. J. Med. Chem.* 209, 112935. doi:10.1016/j.ejmech.2020.112935
- Yin, J., Xiang, C., Wang, P., Yin, Y., and Hou, Y. (2017). Biocompatible nanoemulsions based on hemp oil and less surfactants for oral delivery of baicalein with enhanced bioavailability. *Int J Nanomedicine*. Vol. 12, 2923. doi:10.2147/IJN.S131167

- Zarneshan, S. N., Fakhri, S., Farzaei, M. H., Khan, H., and Saso, L. (2020). Astaxanthin targets PI3K/Akt signaling pathway toward potential therapeutic applications. *Food Chem. Toxicol.* 145, 111714. doi:10.1016/j.fct.2020.111714
- Zeng, K. W., Wang, X. M., Ko, H., Kwon, H. C., Cha, J. W., Yang, H. O., et al. (2011). Hyperoside protects primary rat cortical neurons from neurotoxicity induced by amyloid β -protein via the PI3K/Akt/Bad/Bcl(XL)-regulated mitochondrial apoptotic pathway. *Eur. J. Pharmacol.* 672, 45. doi:10.1016/j.ejphar.2011.09.177
- Zeng, Z., Sarbassov, D. D., Samudio, I. J., Yee, K. W. L., Munsell, M. F., Ellen Jackson, C., et al. (2007). Rapamycin derivatives reduce mTORC2 signaling and inhibit AKT activation in AML. *Blood* 109 (8), 3509–3512. doi:10.1182/blood-2006-06-030833
- Zhai, H., Kang, Z., Zhang, H., Ma, J., and Chen, G. (2019). Baicalin attenuated substantia nigra neuronal apoptosis in Parkinson's disease rats via the mTOR/AKT/GSK-3 β pathway. *J. Integr. Neurosci.* 18 (4), 423–429. doi:10.31083/j.jin.2019.04.192
- Zhang, B., Wang, Y., Li, H., Xiong, R., Zhao, Z., Chu, X., et al. (2016a). Neuroprotective effects of salidroside through PI3K/Akt pathway activation in Alzheimer's disease models. *Drug Des. Devel. Ther.* 10, 1335. doi:10.2147/DDDT.S99958
- Zhang, C., Li, C., Chen, S., Li, Z., Jia, X., Wang, K., et al. (2017). Berberine protects against 6-OHDA-induced neurotoxicity in PC12 cells and zebrafish through hormetic mechanisms involving PI3K/AKT/Bcl-2 and Nrf2/HO-1 pathways. *Redox Biol.* 11 (C), 1–11. doi:10.1016/j.redox.2016.10.019
- Zhang, L. Q., Sa, F., Chong, C. M., Wang, Y., Zhou, Z. Y., Chang, R. C. C., et al. (2015). Schisantherin A protects against 6-OHDA-induced dopaminergic neuron damage in zebrafish and cytotoxicity in SH-SY5Y cells through the ROS/NO and AKT/GSK3 β pathways. *J. Ethnopharmacology* 170, 8–15. doi:10.1016/j.jep.2015.04.040
- Zhang, W., He, H., Song, H., Zhao, J., Li, T., Wu, L., et al. (2016b). Neuroprotective effects of salidroside in the MPTP mouse model of Parkinson's disease: involvement of the PI3K/Akt/GSK3 β pathway. *Parkinson's Dis.* 2016, 1. doi:10.1155/2016/9450137
- Zhang, X., Lai, W., Ying, X., Xu, L., Chu, K., Brown, J., et al. (2019a). Salidroside reduces inflammation and brain injury after permanent middle cerebral artery occlusion in rats by regulating PI3K/PKB/Nrf2/NF κ B signaling rather than complement C3 activity. *Inflammation* 42 (5), 1830–1842. doi:10.1007/s10753-019-01045-7
- Zhang, X., Xiong, J., Liu, S., Wang, L., Huang, J., Liu, L., et al. (2014). Puerarin protects dopaminergic neurons in Parkinson's disease models. *Neuroscience* 280, 88–98. doi:10.1016/j.neuroscience.2014.08.052
- Zhang, Y., Huang, N., Chen, M., Jin, H., Nie, J., Shi, J., et al. (2019b). Procyanidin protects against 6-hydroxydopamine-induced dopaminergic neuron damage via the regulation of the PI3K/Akt signalling pathway. *Biomed. Pharmacother.* 114, 108789. doi:10.1016/j.biopha.2019.108789
- Zhang, Y., Zhang, L.-H., Chen, X., Zhang, N., and Li, G. (2018). Piceatannol attenuates behavioral disorder and neurological deficits in aging mice via activating the Nrf2 pathway. *Food Funct.* 9(1), 371–378. doi:10.1039/c7fo01511a
- Zhang, Z., Cui, W., Li, G., Yuan, S., Xu, D., Hoi, M. P. M., et al. (2012). Baicalein protects against 6-OHDA-induced neurotoxicity through activation of keap1/nrf2/HO-1 and involving PKC α and PI3K/AKT signaling pathways. *J. Agric. Food Chem.* 60 (33), 8171–8182. doi:10.1021/jf301511m
- Zhao, M., Tang, X., Gong, D., Xia, P., Wang, F., Xu, S., et al. (2020). Bungeanum improves cognitive dysfunction and neurological deficits in D-galactose-induced aging mice via activating PI3K/Akt/Nrf2 signaling pathway. *Front. Pharmacol.* 11, 71. doi:10.3389/fphar.2020.00071
- Zhao, W.-Z., Wang, H.-T., Huang, H.-J., Lo, Y.-L., and Lin, A. M.-Y. (2017). Neuroprotective effects of baicalein on acrolein-induced neurotoxicity in the nigrostriatal dopaminergic system of rat brain. *Mol. Neurobiol.* 55 (1), 130–137. doi:10.1007/s12035-017-0725-x
- Zheng, M., Liu, C., Fan, Y., Yan, P., Shi, D., Zhang, Y., et al. (2017). Neuroprotection by Paeoniflorin in the MPTP mouse model of Parkinson's disease. *Neuropharmacology* 116, 412–420. doi:10.1016/j.neuropharm.2017.01.009
- Zhi, Y., Jin, Y., Pan, L., Zhang, A., and Lin, F. (2019). Schisandrin A ameliorates MPTP-induced Parkinson's disease in a mouse model via regulation of brain autophagy. *Arch. Pharm. Res.* 42(11), 1012–1020. doi:10.1007/s12272-019-01186-1
- Zhuang, W., Li, T., Wang, C., Shi, X., Li, Y., Zhang, S., et al. (2018). Berberine exerts antioxidant effects via protection of spiral ganglion cells against cytomegalovirus-induced apoptosis. *Free Radic. Biol. Med.* 121, 127–135. doi:10.1016/j.freeradbiomed.2018.04.575
- Zou, X., Feng, X., Fu, Y., Zheng, Y., Ma, M., Wang, C., et al. (2020). Icaritin attenuates amyloid- β (A β)-Induced neuronal insulin resistance through PTEN downregulation. *Front. Pharmacol.* 11. doi:10.3389/fphar.2020.00880
- Zuardi, A., Crippa, J., Hallak, J., Pinto, J., Chagas, M., Rodrigues, G., et al. (2009). Cannabidiol for the treatment of psychosis in Parkinson's disease. *J. Psychopharmacol.* 23 (8), 979–983. doi:10.1177/0269881108096519

Conflict of Interest: The authors declare that the research was conducted in the absence of any commercial or financial relationships that could be construed as a potential conflict of interest.

Copyright © 2021 Long, Cheng, Zhou, Luo, Wen and Gao. This is an open-access article distributed under the terms of the Creative Commons Attribution License (CC BY). The use, distribution or reproduction in other forums is permitted, provided the original author(s) and the copyright owner(s) are credited and that the original publication in this journal is cited, in accordance with accepted academic practice. No use, distribution or reproduction is permitted which does not comply with these terms.

GLOSSARY

6-OHDA	6-hydroxydopamine	LBP	Lycium barbarum polysaccharide
AA	asiatic acid	I-DOPA	L-3,4-dihydroxyphenylalanine
AD	Alzheimer's disease	LSF	Active fraction of lychee seed
AF	amentoflavone	LTP	Long term potentiation
AKT	protein kinase B	MAO	Monoamine oxidase
AMPA	α -amino-3-hydroxy-5-methyl-4-isoxazolpropionic acid	mLST8	SEC13 protein 8
APP	amyloid precursor protein	MMP	Mitochondrial membrane potential
APS	astragalus polysaccharides	MMP+	1-methyl-4-phenyl-pyridine
ARE	antioxidant response element	MPTP	1-methyl-4-phenyl-1,2,3,6-tetrahydropyridine
AST	astaxanthin	mTOR	Mammalian target of rapamycin
Aβ	amyloid protein	mTORC2	Mechanistic target of rapamycin complex 2
BACE1	β -secretase 1	NE	Norepinephrine
Bad	Bcl2-antagonist of cell death	NFT	Neurofibrillary tangles
Bax	BCL2-associated X protein	NF-κB	Nuclear factor kappa-light-chain-enhancer of activated B cells
Bcl-2	B-cell lymphoma 2	NMDA	N-methyl-d-aspartic acid
BDNF	Brain-derived neurotrophic factor	Nrf2	Nuclear factor erythrocyte 2-related factor 2
BIM	Bcl-2-like protein 11	PARP	Poly ADP-ribose polymerase
CBD	Cannabidiol	PC	Procyanidine
CNKI	China national knowledge infrastructure	PC12	Pheochromocytoma 12
CREB	cAMP response element-binding protein	PD	Parkinson's disease
DA	Dopaminergic	PDGF	Platelet-derived growth factor
DAT	Dopaminergic transporters	PDK1	Phosphatidylinositol dependent protein kinase 1
DHM	Dihydromyricetin	PF	Paeoniflorin
DNA-PK	DNA-dependent protein kinases	PHLPP	PH domain and leucine rich repeat protein phosphatase
ERK	Extracellular signal-regulated kinase	PI3K	Phosphoinositide 3-kinase
FB	Fructus broussonetiae	PIP2	Phosphatidylinositol (4,5)-disphosphate
FGF	Fibroblast growth factor	PIP3	Phosphatidylinositol (3,4,5)-trisphosphate
FoxO1	Caspase-9 and forkhead box protein	PKB	Protein kinase B
GLUT4	Glucose transporter 4	PKC	Protein kinase C
GPCR	G protein coupled receptors	PP2A	Protein phosphatase 2 A
GSK-3β	Glycogen synthase kinase-3 β	PS	Pterostilbene
HO-1	Heme oxygenase 1	PT	Piceatannol
Hsp	Heat shock protein	PTEN	Phosphatase and tensin homolog
ICA	Icariin	PUE	Puerarin
IFN-α	Interferon- α ; α TrkB, tyrosine kinase B	REDD1	DNA damage responses 1
IGF	Insulin-like growth factor	ROS	Reactive oxygen species
IKK	I κ B kinase	ROT	Rotenone
IL1β	Interleukin-1 β	RTK	Receptor tyrosine kinase
ILK	Integrin-linked kinase	Sal	Salidroside
IRS	Insulin receptor substrate	SchA	Schizandrol A
JNK	c-Jun NH(2)-terminal kinase	SCL	Schisandra chinensis lignans
		SDAT	Sporadic dementia of the Alzheimer's type
		SH	Src Homology

SHIP1 Src homology domain-containing inositol 5'-phosphatase 1

SIRT1 Silent mating type information regulation 2 homolog-1

SN Substantia nigra

SNpc Substantia nigra compacta

SP Senile plaque

TA Tovophyllin A

t-BHP Tert-butyl peroxide

TH Tyrosine hydroxylase

TNF- α Tumor necrosis factor- α

VOZ Zanthoxylum bungeanum volatile oil extract

VPS34 Vacuolar protein sorting 34

WEZ Zanthoxylum bungeanum water extract



Xiaoyao Pills Ameliorate Depression-like Behaviors and Oxidative Stress Induced by Olfactory Bulbectomy in Rats via the Activation of the PIK3CA-AKT1-NFE2L2/BDNF Signaling Pathway

Yafei Ji^{1,2†}, Jie Luo^{2†}, Jiuseng Zeng², Yang Fang², Rong Liu², Fei Luan^{2*} and Nan Zeng^{1,2*}

OPEN ACCESS

Edited by:

Juxian Song,
Guangzhou University of Chinese
Medicine, China

Reviewed by:

Minyi Zhang,
Guangzhou University of Chinese
Medicine, China
Chun Zhou,
Southern Medical University, China

*Correspondence:

Nan Zeng
19932015@cdutcm.edu.cn
Fei Luan
luanfeiren@163.com

[†]These authors have contributed
equally to this work

Specialty section:

This article was submitted to
Ethnopharmacology,
a section of the journal
Frontiers in Pharmacology

Received: 18 December 2020

Accepted: 02 March 2021

Published: 15 April 2021

Citation:

Ji Y, Luo J, Zeng J, Fang Y, Liu R,
Luan F and Zeng N (2021) Xiaoyao Pills
Ameliorate Depression-like Behaviors
and Oxidative Stress Induced by
Olfactory Bulbectomy in Rats via the
Activation of the PIK3CA-AKT1-
NFE2L2/BDNF Signaling Pathway.
Front. Pharmacol. 12:643456.
doi: 10.3389/fphar.2021.643456

¹State Key Laboratory of Southwestern Chinese Medicine Resources, Chengdu University of Traditional Chinese Medicine, Chengdu, China, ²Department of Pharmacology, School of Pharmacy, Chengdu University of Traditional Chinese Medicine, Chengdu, China

Numerous studies have revealed that oxidative stress is closely associated with the occurrence and development of depression. Xiaoyao Pills (XYW) are included in the Chinese Pharmacopoeia and are frequently used for treating anxiety and depression by smoothing the liver, strengthening the spleen, and nourishing the blood. However, the antidepressant effects of XYW have not yet been thoroughly investigated. The objective of our study was to investigate the antidepressant-like effects of XYW and the underlying molecular mechanism in the olfactory bulbectomized (OB) rat model of depression using the open field test (OFT), sucrose preference test (SPT), splash test (ST), and novelty suppressed feeding test (NSFT). Results showed that XYW (0.93 and 1.86 g·kg⁻¹) significantly alleviated depression-like behaviors in rats, which was indicated by increased sucrose preference in the SPT, prolonged grooming time in the ST, decreased horizontal movement in the OFT, and shorter feeding latency in the NSFT. In addition, XYW treatment dramatically reversed the reduced activity of superoxide dismutase and the decreased level of glutathione, while also lowering levels of malondialdehyde, an inflammatory mediator (nitric oxide), and pro-inflammatory cytokines (interleukin-6 and 1 β) in the serum and cortex of OB rats. Mechanistically, XYW induced marked upregulation of mRNA and protein expression levels of NFE2L2, KEAP1, GPX3, HMOX1, SOD1, NQO1, OGG1, PIK3CA, p-AKT1/AKT1, NTRK2, and BDNF, and downregulation of ROS in the cortex and hippocampus via the activation of the

Abbreviations: ACTB, actin beta; AKT1, Akt1 serine/threonine kinase 1; BDNF, brain derived neurotrophic factor; CREB1, cAMP responsive element binding protein 1; FLX, fluoxetine hydrochloride; GAPDH, glyceraldehyde-3-phosphate dehydrogenase; GPX3, glutathione peroxidase 3; GSH, glutathione; GSSH, glutathione (Oxidized); HMOX1, heme oxygenase 1; IL6, interleukin 6; IL1B, interleukin 1 beta; KEAP1, kelch like ECH associated protein 1; MDA, malondialdehyde; NO, nitric oxide; MAPK1, mitogen-activated protein kinase 1; NFE2L2, nuclear factor, erythroid 2 like 2; NQO1, NAD(P)H quinone dehydrogenase 1; NLRP3, NLR family pyrin domain containing 3; NSFT, novelty suppressed feeding test; OFT, open field test; OGG1, 8-oxoguanine DNA glycosylase; PIK3CA, phosphatidylinositol-4,5-bisphosphate 3-kinase catalytic subunit alpha; ROS, reactive oxygen species; ST, splash test; SPT, sucrose preference test; SOD, superoxide dismutase; NTRK2, neurotrophic receptor tyrosine kinase 2; XYW, xiaoyao pills.

NFE2L2/KEAP1, PIK3CA/AKT1, and NTRK2/BDNF pathways. These findings suggest that XYW exert antidepressant-like effects in OB rats with depression-like symptoms, and these effects are mediated by the alleviation of oxidative stress and the enhancement of neuroprotective effects through the activation of the PIK3CA-AKT1-NFE2L2/BDNF signaling pathways.

Keywords: xiaoyao pills, depression, olfactory bulbectomized rats, oxidative stress, inflammatory response

INTRODUCTION

Depression is one of the most common mental illnesses and is characterized by low mood, sleep disturbances, loss of energy, change in appetite, constipation, decreased concentration, and risk of suicide (Cui, 2015). It has become increasingly clear that oxidative stress may play a crucial role in the activation of intracellular signaling pathways that are thought to be involved in various psychiatric disorders (Michael et al., 2011). Long-term exposure to stress may lead to changes in the structure and function of the brain, which can lead to cognitive deficits and an increased risk of developing a psychiatric disorder (Lupien et al., 2009; Dragana et al., 2016). It has been suggested that environmental stressors may have a significant impact on the generation of reactive oxygen species (ROS) in the brain (Manoli et al., 2000; Fontella et al., 2005) disruptions in the balance between the clearance and production of active free radicals (i.e., ROS) in the body induce an oxidative stress reaction, which leads to macromolecular oxidation (e.g., lipids, DNA, and proteins) (Tanja et al., 2012), oxidation defense system damage (e.g. glutathione [GSH], and superoxide dismutase [SOD]) (Herbet et al., 2017), and inflammation (Hovatta et al., 2010). Increased levels of ROS in the blood have been reported in patients with major depression (Bilici et al., 2001). Moreover, previous studies have confirmed that there is a close relationship between excessive elevation of ROS levels and the pathogenesis of depression (Du et al., 2016; Herbet et al., 2017).

Clinically, traditional Chinese medicines (TCMs) are commonly used as complementary and alternative therapies for the treatment of depression. Recently, numerous studies have demonstrated that TCMs are effective in relieving symptoms of depression in both patients and animal models via various complex mechanisms (Wang Y. et al., 2017). Xiaoyao Pills (XYW) are a modified form of the commonly prescribed Xiaoyao powder, which contains eight herbs in various ratios (*Bupleurum chinense* DC., *Angelica sinensis* Diels., *Paeonia lactiflora* Pall., *Atractylodes macrocephala* Koidz., *Mentha haplocalyx* Briq., *Poria cocos* Wolf., *Glycyrrhiza uralensis* Fisch., *Zingiber officinale* Rosc. in ratios of 9:9:9:1.5:9:4.5:9, respectively). Because it is included in the China Pharmacopoeia Commission, 2020 Edition, XYW has the advantages of an established preparation technology and strict quality control compared with Xiaoyao powder. According to the TCM theory, the pathogenesis of depression is linked to liver-qi stagnation, blood stasis, and a deficiency of the spleen-qi (Zhang et al., 2005). Xiaoyao powder is thought to treat and prevent

depressive syndromes by effectively smoothing the liver, nourishing blood, and strengthening the spleen. In our previous studies, we demonstrated that Xiaoyao powder exerts definitive anti-depressive effects by regulating the level and function of serotonin (Xiong et al., 2007a; Xiong et al., 2007b), improving neuroinflammation (Shi et al., 2019a; Fang et al., 2020), promoting synaptic plasticity (Shi et al., 2018; Shi et al., 2019a; Shi et al., 2019b; Shi B. et al., 2019), reversing decreases in neurotrophic factor (Wang et al., 2018c), and reducing neuronal apoptosis (Li et al., 2010; Jiang et al., 2014, 2015). Although XYW has been confirmed to affect multiple pathways that are targeted by antidepressants, the effect on oxidative stress remains unclear.

The NFE2L2/Kelch-like ECH associated protein-1 (KEAP1) pathway is a major regulator of redox homeostasis (Baird and Dinkova, 2011). NFE2L2 is usually retained in the cytosol, where it is tethered to its cytosolic repressor, KEAP1. A recent study has shown that NFE2L2 antioxidant signaling pathways are inhibited in the prefrontal cortex of patients with severe depression (Martín-Hernández et al., 2018). Furthermore, NFE2L2 gene knockout increases susceptibility to depression (Bouvier et al., 2017). NFE2L2 is also thought to be involved in the mechanisms underlying the antidepressant effect of serotonin reuptake inhibitors (Mendez-David et al., 2015). Taken together, it is evident that NFE2L2 plays an important role in the pathogenesis of depression (Martín-Hernández et al., 2016; Yao et al., 2016). Based on these findings, we hypothesize that long-term olfactory absence results in chronic stress and suppression of the NFE2L2 signaling pathway, which leads to the development of depression. However, the association between oxidative stress and the pathogenesis of depression is poorly understood, and there are currently no recognized therapies that effectively halt or slow the progression of depression. Therefore, using the OB rat model, we investigated whether XYW attenuated depression-like behaviors and oxidative stress. We also explored the mechanisms underlying these effects.

MATERIALS AND METHODS

Xiaoyao Pills Quality Control

Xiaoyao Pills is composed of eight Chinese herbal medicines with the characteristics of complex composition. However, the Chinese Pharmacopoeia only provides content determination for paeoniflorin (C₂₃H₂₈O₁₁). According to previous literature (Liu et al., 2018; Zhao et al., 2018), they analyzed the composition

of XYW, including paeoniflorin, liquiritin, saikosaponin B2 and atractylenolide II. In the present study, we determined the components of paeoniflorin ($C_{23}H_{28}O_{11}$), liquiritin ($C_{21}H_{22}O_9$), saikosaponin B2 ($C_{42}H_{68}O_{13}$) and atractylenolide II ($C_{15}H_{20}O_2$).

The analysis was performed by high-performance liquid chromatography (HPLC) (Thermo, US). Hypersil GOLDTM C₁₈ chromatographic column (250 mm × 4.6 mm, 5 μm, Thermo SCIENTIFIC) was used and the chromatographic separation conditions were as follows: mobile phase: 0.05% (V/V) phosphoric acid (A) + acetonitrile (B) (0~30 min, 10~25% B; 30~40 min, 25~44% B; 40~60 min, 44~50% B; 60~70 min, 50~60% B; 70~80 min, 60~75% B; 80~90 min, 75~10% B; 90~100 min, 10% B); detection wavelength: 230 nm (10~16 min, paeoniflorin), 210 nm (16~20 min, liquiritin), 210 nm (43~47 min, saikosaponin B2), 230 nm (58~62 min, atractylenolide II); column temperature: 30°C; flow rate: 1.0 ml·min⁻¹; injection volume: 10 μL. Stock solutions of XYW was prepared by dissolving 1.0 g of analyte in 100 ml dilute methanol. The content of paeoniflorin ($C_{23}H_{28}O_{11}$), liquiritin ($C_{21}H_{22}O_9$), saikosaponin B2 ($C_{42}H_{68}O_{13}$) and atractylenolide II ($C_{15}H_{20}O_2$) in XYW was determined.

Drugs and Reagents

The XYW (Tai Ji, China, batch number 1707029) and fluoxetine hydrochloride (FLX) (Patheon, France, 7686 A) were dissolved in pure water solution preparation (SOD, batch number 20180,309), malondialdehyde (MDA, batch number 20180,313) (GSH, batch number 20180,621), and GSH/glutathione disulfide (GSH/GSSG, batch number 20180,726) levels were assessed using commercially available kits (Nanjing Jiancheng Bioengineering Institute, Nanjing, China). Nitric oxide (NO) assay kit (Biyuntian, 0,72117,171,110, China). Rat interleukin 6 (IL6) ELISA Kit (MULTI SCIENCES, A30680231), rat interleukin 1β (IL1B) ELISA Kit (ExCell Bio, 21H183), rabbit anti-NTRK2 antibody (Cell Signaling Technology; Cat. No. #4603), rabbit anti-AKT1 antibody (Cell Signaling Technology; Cat. No. #4691S), rabbit anti-p-AKT1 antibody (Cell Signaling Technology; Cat. No. #4060S), rabbit anti-HMOX1 antibody (Cell Signaling Technology; Cat. No. #S2206S), rabbit anti-PIK3CA antibody (Servicebio; Cat. No. #LS190932), rabbit anti-GAPDH antibody (Servicebio; Cat. No. #GB11002), rabbit anti-SOD1 antibody (Novus Biologicals; Cat. No. #03253462C2B), rabbit anti-NFE2L2 antibody (Invitrogen; Cat. No. #TK2668681A), rabbit anti-brain-derived neurotrophic factor (BDNF) antibody (Abcam; Cat. No. #ab108319) and anti-rabbit IgG HRP-linked antibody (Servicebio; Cat. No. #GB23303).

Animals

Male Sprague-Dawley rats weighing 180–200 g were purchased from Chengdu Dashuo Biotechnology Company (Chengdu, China, Qualified number: SCXK-[Chuan]-2015-030). Before commencing the experiment, the animals were randomly housed in cages at room temperature (25 ± 2°C) with a 12-h light/dark cycle. They had full access to food and water and were acclimatized to the environment for 3 days. The experiments were conducted in accordance with the guidelines of the Committee

for Animal Care and Use of Laboratory Animals, College of Pharmacy, Chengdu University of Traditional Chinese Medicine (Chengdu, China).

Olfactory Bulbectomy Surgery

Olfactory bulbectomy was performed according to previously used methods (Van, 1990; Freitas et al., 2013) but with minor modifications. Briefly, rats were anesthetized, and the skull covering the olfactory bulbs was exposed using a midline incision. Then, 2 mm burr holes were drilled 8 mm anterior to the bregma and 2 mm lateral to the midline. The top of the rats' heads was shaved and fixed to a brain stereotaxic instrument. The incisor bar was set at 4.5 mm below the interaural line. Both olfactory bulbs were obliterated and aspirated, the holes were filled with glass-ionomer cement, and the scalp was subsequently sutured. Sham-operated rats underwent the same procedure but without the bulb obliteration/aspiration. The animals received daily intramuscular injections of penicillin (8 × 10⁵ U, 0.1 ml/200 g) for 3 days post-surgery to prevent infection and were subsequently housed individually in polypropylene cages. The experiments were continued after 15 days of recovery, after which the OB rats were selected using the open field test. The experimental procedure is illustrated in **Figure 1A**.

Drug Treatment

Animals in the XYW group (0.93 and 1.86 g·kg⁻¹) were intragastrically administered XYW daily for 30 days after the 15-days recovery from surgery. Animals in the FLX group (0.01 g·kg⁻¹) were intragastrically administered FLX daily for 30 days after the 15-days recovery from surgery. Animals in the sham and OB groups received equivalent volumes of water daily to ensure isocaloric intake.

Behavioral Studies

Open Field Test

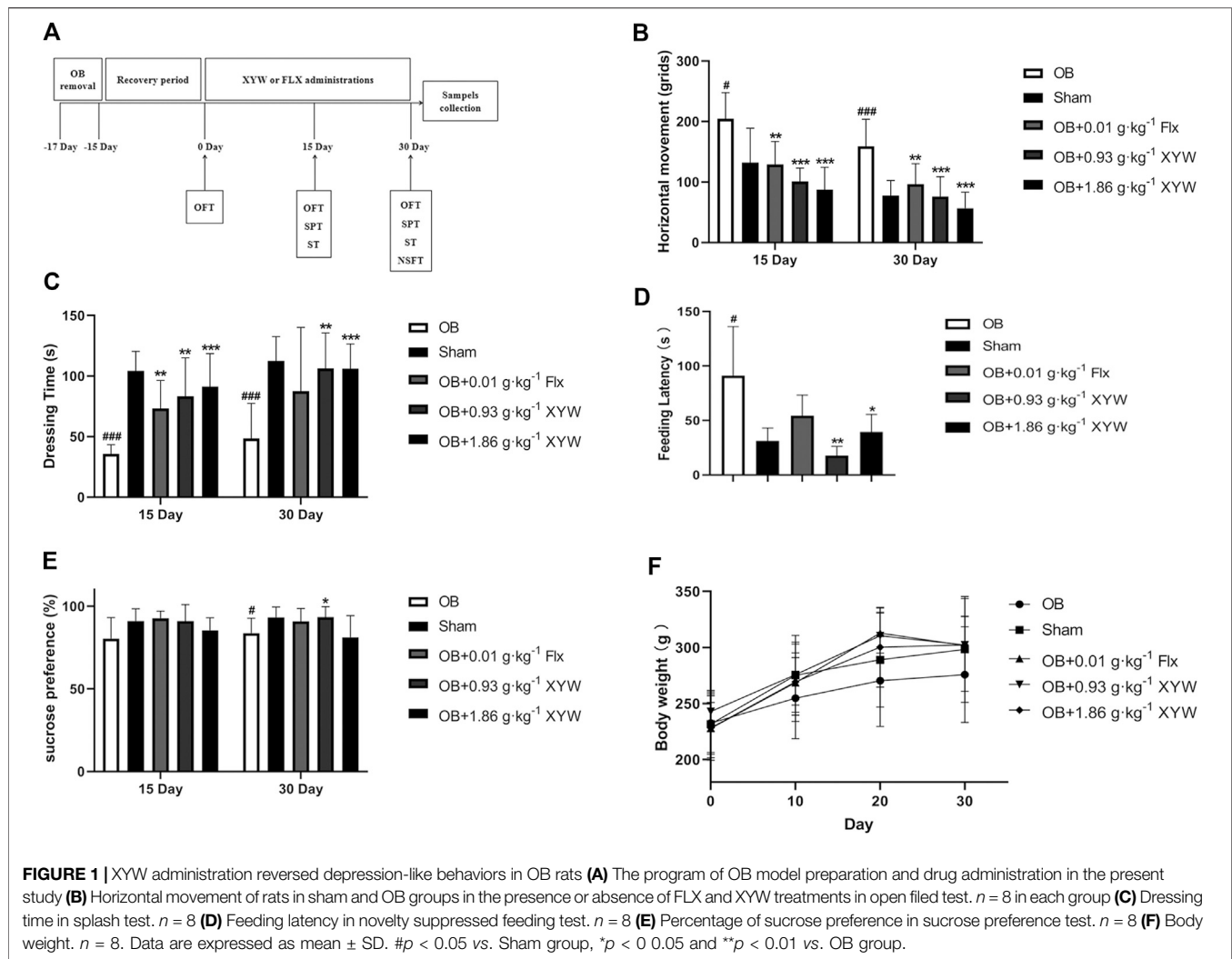
The rats from each treatment group were put into the corner of an open box. After 2 min of adaptation, we observed and recorded the total distance traveled during a 4-min period (Zueger et al., 2005).

Sucrose Preference Test

Two water bottles were placed in each cage during feeding to eliminate the effect of animal habits on the experiment. Before testing, all rats were fasted and water-deprived for 24 h. On the day of testing, drinking water and a 2% sucrose solution were placed in the home cage for 6 h. At the end of testing, the fluid content was measured, and sucrose preference was calculated using the following equation: sucrose preference (%) = sucrose intake/(sucrose intake + water intake) × 100%

Splash Test

The splash test was performed in a standard rat cage with no bedding. The rats were sprayed with a 2 ml 10% sucrose solution on the dorsal while in their home cage to induce grooming behavior. We recorded the total grooming time during a 5-min period (Surget et al., 2008).



Novelty Suppressed Feeding Test

The rats were deprived of food for 48 h before testing. For the test, the rats were placed in an open field (60 \times 60 \times 20 cm) that had a small amount of food placed at the center. The time taken for the rat to bite the food was recorded as the feeding latency where rats were given up to 5 min (Wang et al., 2018b).

Tissue Sample Collection

After the behavioral tests were completed, abdominal aorta bleeds were performed, and plasma was collected by centrifugation at 3,000 rpm for 15 min. Both the hippocampus and cortex tissues were immediately dissected on an ice-plate and frozen with liquid nitrogen. All tissue samples were then stored at -80°C .

Oxidative Stress Assays

The levels of SOD, MDA, GSH, and GSH/GSSG in the serum and cortex were assessed using commercially available kits according to manufacturer instructions. Briefly, the cortex tissue was homogenized with 0.9% saline in an ice-bath and centrifuged (12,000 g, 4°C , 10 min). The supernatant and serum were applied to estimate the antioxidant content.

Inflammatory Markers Assays

The levels of NO in the serum were determined using a commercially available NO assay kit according to manufacturer instructions. The optical density was measured at 540 nm using a micro-plate reader. The levels of IL6 and IL1B in the serum and cortex were determined using commercially available ELISA kits according to manufacturer instructions. Briefly, the cortex tissue was homogenized with 0.9% saline in an ice-bath and centrifuged (12,000 g, 4°C , 10 min). The supernatant and serum were applied to estimate the IL6 and IL1B content. Optical density was measured at 450 nm using a micro-plate reader.

RNA Isolation and Gene Expression Assessment

Total RNA was used to synthesize complementary DNA using a FastQuant RT kit (Tiangen, Beijing, China). The amplification reactions were performed in 96-well reaction plates with a 20 μL reaction volume (Bio-Rad, Hercules, CA, United States). The gene primer sequences for Actb, Nfe2l2, Keap1, Gpx3, Hmox1,

TABLE 1 | Gene primer sequence.

Gene	Prime	Primer sequence (5' to 3')	Product size (bp)
Actb	Forward primer	CACCCGCGAGTACAACCTTC	207
	Reverse primer	CCCATACCCACCATCACACC	
Nfe2l2	Forward primer	ATTCAGCCAGCGTTGAGAG	128
	Reverse primer	TCCTGCCAAACTTGTCCAT	
Keap1	Forward primer	TCCATTGAAGGCATCCACCC	117
	Reverse primer	GTACATGACTGCCCGTTCA	
Nqo1	Forward primer	CTCAGGTGGCCTGGGATATG	139
	Reverse primer	ACAAGTGGGTGGAGGATTGG	
Gpx3	Forward primer	CGTGAACGGGGAGAAAGAGC	198
	Reverse primer	CTGACTGTGGTCCGGTGGTA	
Hmox1	Forward primer	CCATCCCTTACACACCAGCC	245
	Reverse primer	GCGAGCACGATAGAGCTGTT	
Ogg1	Forward primer	CCCTCTGGCCAAACAAGAAC	167
	Reverse primer	GATCCCTTTTTCGCGTTTGC	

Nqo1, and Ogg1 used in this study are listed in **Table 1**. Data were normalized using the $2^{-\Delta\Delta Ct}$ method.

Western Blot Analysis

RIPA lysate buffer containing 1 mM phenylmethanesulfonyl fluoride and 1 mM phosphatase inhibitor cocktail was added to each sample to collect the total protein. The total protein concentration of each sample was determined using the bicinchoninic acid assay method, and all samples were adjusted to have the same concentration. The protein samples were mixed with a 5× loading buffer and denatured at 95°C. The proteins were separated using sodium dodecylsulfonate-polyacrylamide gel electrophoresis and electrophoretically transferred onto polyvinylidene fluoride membranes. The membranes were probed with rabbit anti-NTRK2 (1:1000; Cell Signaling Technology; Cat. No. #4603), rabbit anti-AKT1 (1:1000; Cell Signaling Technology; Cat. No. #4691S), rabbit anti-p-AKT1 (1:1000-*Ak*; Cell Signaling Technology; Cat. No. #4060S), rabbit anti-HMOX1 (1:1000; Cell Signaling Technology; Cat. No. #S2206S), rabbit anti-PIK3CA (1:1000; Servicebio; Cat. No. #LS190932), rabbit anti-GAPDH (1:1000; Servicebio; Cat. No. #GB11002), rabbit anti-SOD1 (1:1000; Novus Biologicals; Cat. No. #03253462C2B), rabbit anti-NFE2L2 (1:1000; Invitrogen; Cat. No. #TK2668681A), and rabbit anti-BDNF (1:1000; Abcam; Cat. No. #ab108319) antibodies overnight at 4°C and then incubated with anti-rabbit IgG HRP-linked antibody (1:3000; Servicebio; Cat. No. #GB23303) at 37°C for 1.5 h. Detection was performed using a ChemiDoc XRS+ (BioRad, United States) image analysis system.

Immunofluorescence Staining

The brain tissues were sliced into frozen sections (Thermo, Cryotome E), and the tissue sections were subsequently rewarmed. The tissue slides were incubated for 30 min at 37°C in the dark with DHE (Sigma, D7008) stain, which was diluted with phosphate-buffered saline. The slides were placed on a shaker and washed three times for 5 min each time. After drying the slide slightly, the DAPI dye solution was added dropwise, and the core was stained for 10 min at room temperature. The sections were observed under a fluorescence microscope (ECLIPSE TI-SR, Nikon, Japan), and the images were

captured. The nucleus was stained blue, and the level of ROS in the cells was judged based on the intensity of red fluorescence. Image acquisition was performed at ×200 magnification. The relative expression of ROS was calculated according to the relative cumulative optical density (IOD), which was calculated by the formula: IOD = ROS cumulative optical density/nuclear stain cumulative optical density.

Statistical Analyses

All statistical analyses were performed using SPSS 21 (IBM Corporation, Armonk, NY, United States). Data are presented as means ± standard deviations. All analyses were performed using a one-way analysis of variance (SNK was used for pairwise between group comparisons) or *t*-test. Differences were considered statistically significant at $p < 0.05$.

RESULTS

Content of Paeoniflorin, Liquiritin, Saikosaponin B2 and Atractylenolide II in Xiaoyao Pills

According to National Pharmacopoeia Committee (2020 edition), the content of paeoniflorin should not be less than 4.0 mg in 1.0 g of condensed pills. The characteristic map (chromatogram) of Xiaoyao Pills is shown in **Figure 2**, peak 1 represents peak characteristic of paeoniflorin, and the content of paeoniflorin in 1.0 g Xiaoyao Pills was 8.48 mg. Moreover, peak 2, 3, 4 represent peak characteristic of liquiritin, saikosaponin B2, atractylenolide II, respectively. The content of liquiritin, saikosaponin B2, and atractylenolide II in 1.0 g XYW is 1.31, 0.63, and 0.05 mg, respectively.

Xiaoyao Pills Partially Reversed Depression-like Behaviors of Olfactory Bulbectomized Rats

On day 15, OB rats showed a significant increase in horizontal movements in the OFT (**Figure 1B**, $p < 0.05$) and a significant

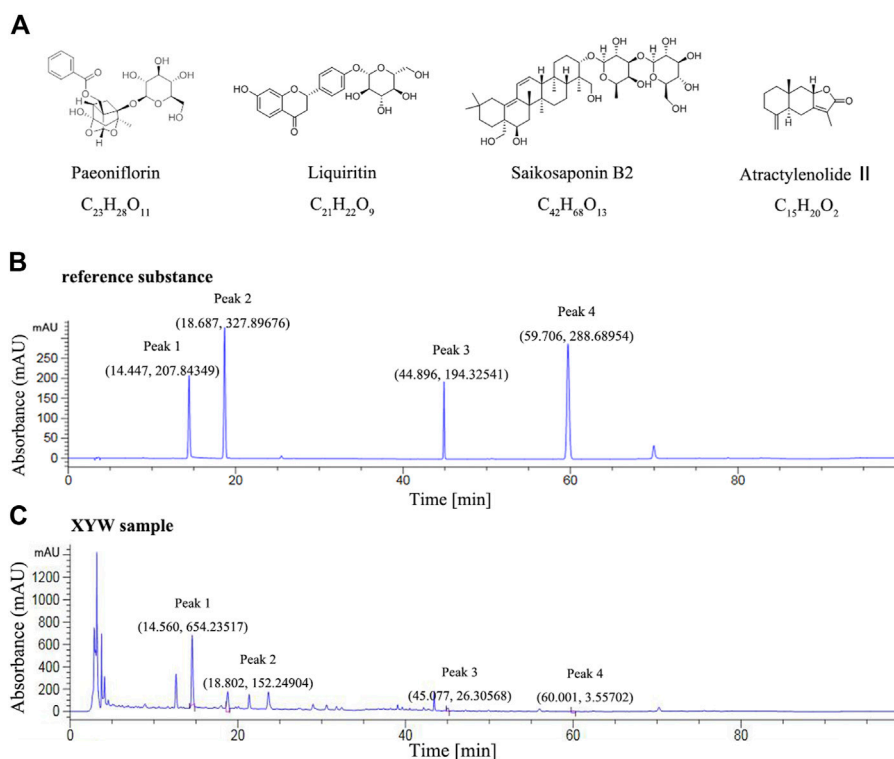


FIGURE 2 | The quality control map of Xiaoyao Pills **(A)** The chemical structure formula of paeoniflorin, liquiritin, saikosaponin B2 and atractylenolide II **(B)** High performance liquid chromatography map of reference substance (Peak 1, 2, 3, 4 represent peak characteristic of paeoniflorin, liquiritin, saikosaponin B2, atractylenolide II, respectively) **(C)** High performance liquid chromatography map of Xiaoyao Pills sample (Peak 1, 2, 3, 4 represent peak characteristic of paeoniflorin, liquiritin, saikosaponin B2, atractylenolide II, respectively).

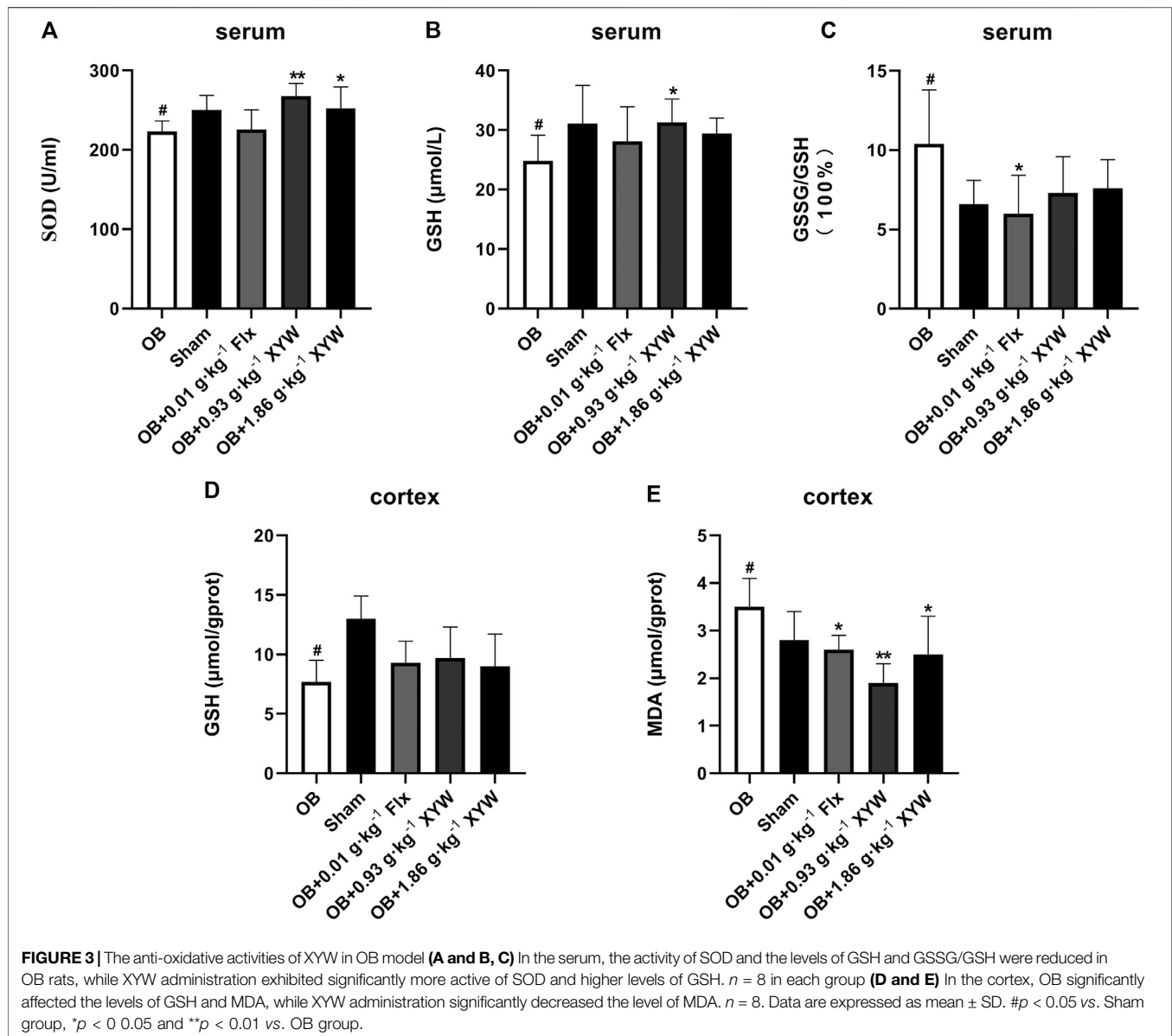
decrease in grooming time in the ST (**Figure 1C**, $p < 0.001$) compared with the sham group, whereas the FLX and XYW (0.93 and $1.86 \text{ g}\cdot\text{kg}^{-1}$) treatment groups showed a dramatic reversal of depression-like behaviors ($p < 0.01$ and $p < 0.001$, respectively).

In contrast with the sham group, on day 30, OB rats showed a significant increase in both horizontal movements in the OFT (**Figure 1B**, $p < 0.001$) and feeding latency in the NSFT (**Figure 1D**, $p < 0.05$), whereas grooming time in the ST (**Figure 1C**, $p < 0.001$) and sucrose preference in the SPT (**Figure 1E**, $p < 0.05$) decreased, which suggested that olfactory bulbectomy induced continuous depression-like behaviors. However, FLX treatment significantly alleviated the depression-like behavior of OB rats in the OFT only (**Figure 1B**, $p < 0.05$), whereas XYW (0.93 and $1.86 \text{ g}\cdot\text{kg}^{-1}$) treatment significantly reversed the depression-like behaviors in the OFT, ST, NSFT, and SPT (**Figures 1B–E**, $p < 0.05$, $p < 0.01$, and $p < 0.001$). Moreover, the trend of weight gain in OB rats was less than that in the sham rats, whereas the drugs restored that (**Figure 1F**). The behavioral results indicate that XYW (0.93 and $1.86 \text{ g}\cdot\text{kg}^{-1}$) can significantly improve the depression-like behaviors of rat caused by olfactory bulbectomy, suggesting that it has anti-depression-like effects.

Xiaoyao Pills Mitigated Oxidative Stress and Neuroinflammation Caused by Olfactory Bulbectomy

To investigate whether olfactory bulbectomy caused oxidative stress, we assessed the relevant antioxidants. As shown in **Figures 3A–C**, both the SOD activity and GSH level in the serum of OB rats were significantly lower than those of the sham rats ($p < 0.05$), whereas the ratio of GSSG/GSH was significantly higher ($p < 0.05$); these were significantly alleviated by treatment with FLX and XYW (0.93 and $1.86 \text{ g}\cdot\text{kg}^{-1}$). Similarly, the OB rats exhibited lower GSH activity ($p < 0.05$) and higher MDA ($p < 0.05$) levels in the cortex (**Figures 3D,E**); treatment with FLX ($p < 0.05$) and XYW ($1.86 \text{ g}\cdot\text{kg}^{-1}$, $p < 0.05$; $0.93 \text{ g}\cdot\text{kg}^{-1}$, $p < 0.01$) effectively reduced MDA levels without reversing the levels of GSH. Our examination of the production of cytokines to detect whether further inflammation occurred due to oxidative stress revealed significant elevation in the levels of NO, IL6, and IL1B in both the serum and cortex of OB rats. Moreover, treated rats also showed alleviation and enhanced expression of the inflammatory mediator, NO, and proinflammatory cytokines, IL6 and IL1B (**Figures 4A–E**).

Taken together, these results confirm that XYW (0.93 and $1.86 \text{ g}\cdot\text{kg}^{-1}$) administration can restore the damage caused by central and peripheral oxidative stress and minimize further inflammation, which demonstrates the neuroprotective effect of XYW.



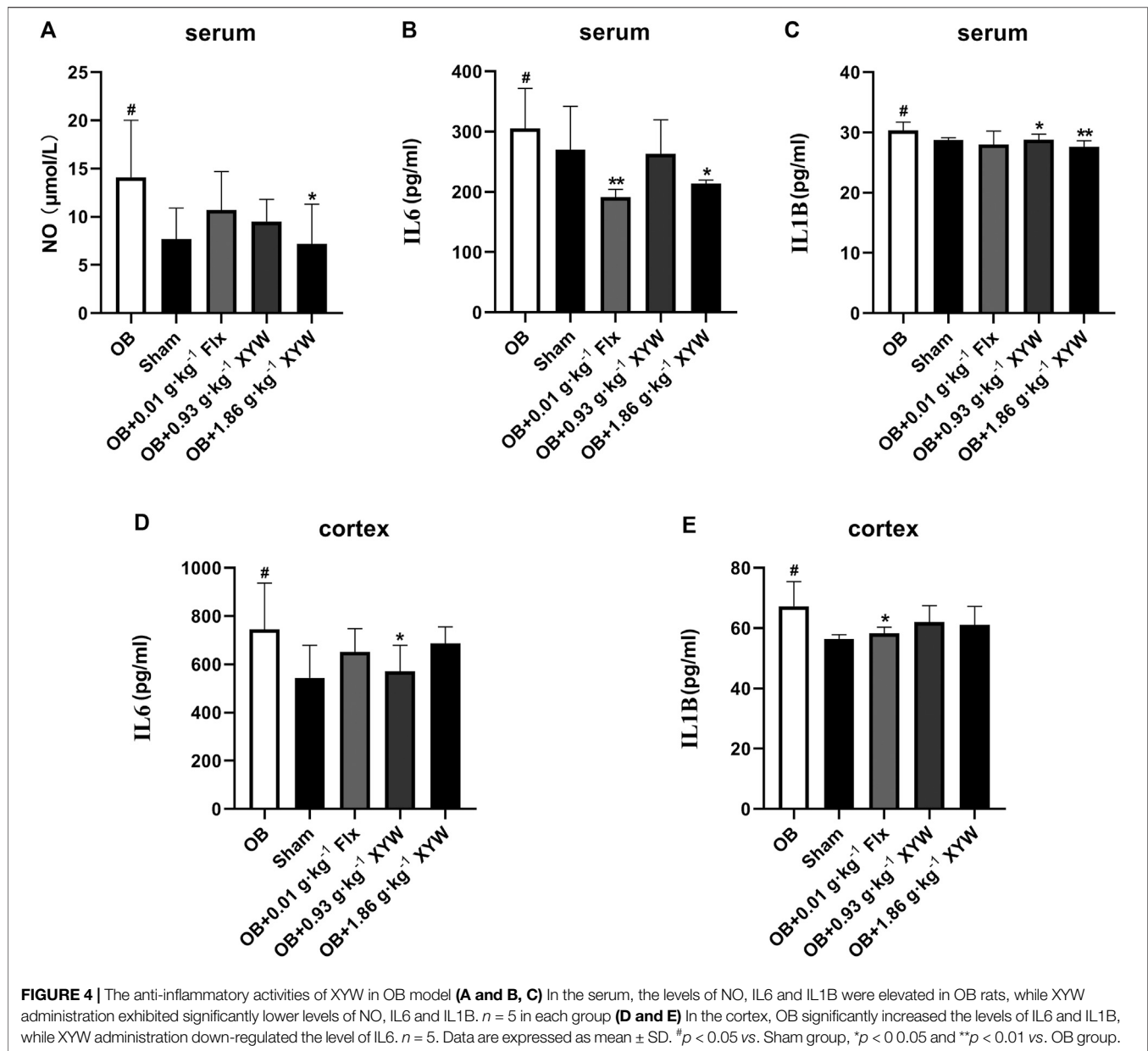
Xiaoyao Pills Reduced the Production of ROS in the Cortex and Hippocampus of Olfactory Bulbectomized Rats

An increased ROS level is an important indicator of oxidative stress. To visually observe oxidative stress levels, we conducted immunofluorescence detection of ROS in the cortex and CA3 and DG regions of the hippocampus. A DHE dye solution was used to tag superoxide anion (O_2^-), which is shown by the red ROS staining in **Figures 5A–C**. As shown in **Figure 5D**, OB rats showed slightly more ROS fluorescence in the cortex and hippocampal CA3 region than the sham rats and had significantly stronger ROS fluorescence signals in the hippocampal DG region ($p < 0.01$). Similarly, XYW ($1.86 \text{ g} \cdot \text{kg}^{-1}$) and FLX treated rats showed distinctly less red fluorescence in the cortex and

hippocampal CA3 and DG regions ($p < 0.01$). Our results further indicate that high doses of XYW eliminate ROS to reduce the oxidative stress level in the cortex and hippocampus of OB rats.

Xiaoyao Pills Restored the Gene Transcription and Protein Expression of Nfe2l2/Keap1 Pathway in Olfactory Bulbectomized Rats

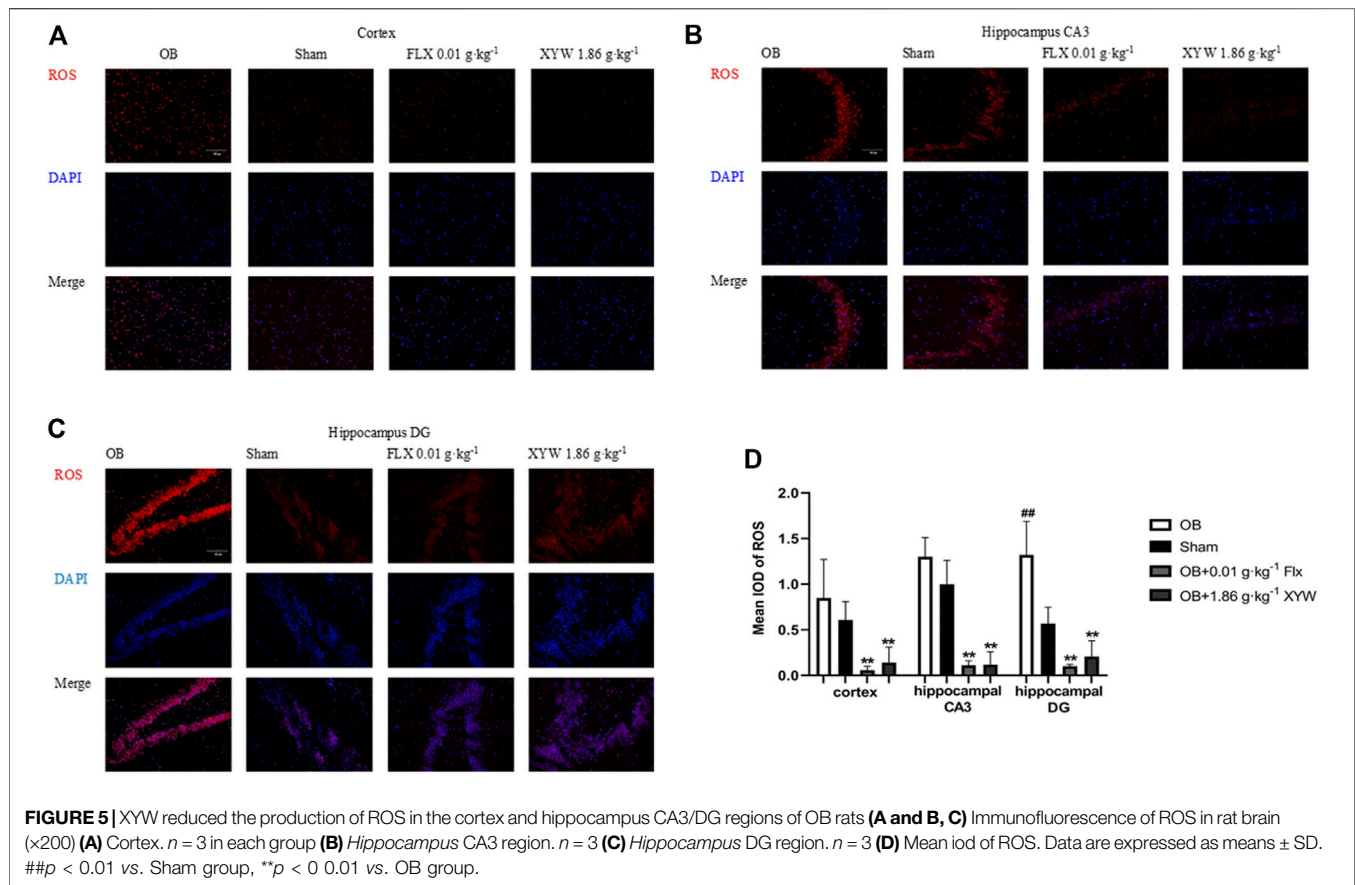
It is well known that the Nfe2l2/Keap1 pathway, which promotes transcription of antioxidants and reduces oxidative stress damage, is of vital importance for the antioxidative system. Therefore, we further studied gene transcription and protein expression of the Nfe2l2/Keap1 pathway in the OB rats.



As shown in **Figures 6A–E**, the messenger RNA (mRNA) levels of Nfe2l2 and Keap1 as well as the downstream Hmox1, Nqo1 and Gpx3 ($p < 0.05$) were significantly downregulated ($p < 0.05$) in the cortex of OB rats. Consistent with previous findings, treatment with FLX and XYW (0.93 and 1.86 g·kg⁻¹) showed marked antioxidant effects. FLX treatment significantly restored transcription of Nfe2l2, Hmox1, Nqo1 and Gpx3 mRNA ($p < 0.05$), and XYW (0.93 and 1.86 g·kg⁻¹) treatment restored transcription of Nfe2l2, Keap1, Hmox-1, Nqo1 and CPX3 mRNA ($p < 0.05$). In the hippocampus of OB rats (**Figures 6G–K**), there was a significant reduction of Nfe2l2, Hmox1 and Nqo1 mRNA ($p < 0.05$), whereas the downregulated Hmox1 and Nfe2l2 mRNA were restored by XYW (0.93 and 1.86 g·kg⁻¹) treatment ($p < 0.05$). Furthermore, Ogg1 (**Figures 6F,L**), a

specific enzyme that repairs DNA oxidative damage, was decreased in both the cortex and hippocampus of OB rats and was significantly improved by XYW (1.86 g·kg⁻¹) treatment ($p < 0.05$).

In terms of protein level, HMOX1 and SOD1 were significantly reduced in the cortex and hippocampus of OB rats ($p < 0.05$), whereas FLX and XYW (0.93 and 1.86 g·kg⁻¹) treatments accelerated the production of HMOX1 and SOD1 ($p < 0.05$; **Figures 7A–G**). As shown in **Figures 7A,B**, the downregulation of NFE2L2 in the cortex was reversed by XYW (1.86 g·kg⁻¹) treatment; however, this was not statistically significant. These findings suggest that during states of excessive oxidative stress, the NFE2L2/KEAP1 pathway is suppressed, so that downstream antioxidants, such



as HMOX1, NQO1, GPX3 and SOD1 are reduced, which heightens the risk for DNA damage. Moreover, XYW treatments reverse the downregulated NFE2L2/KEAP1 pathway to produce central antioxidant effects.

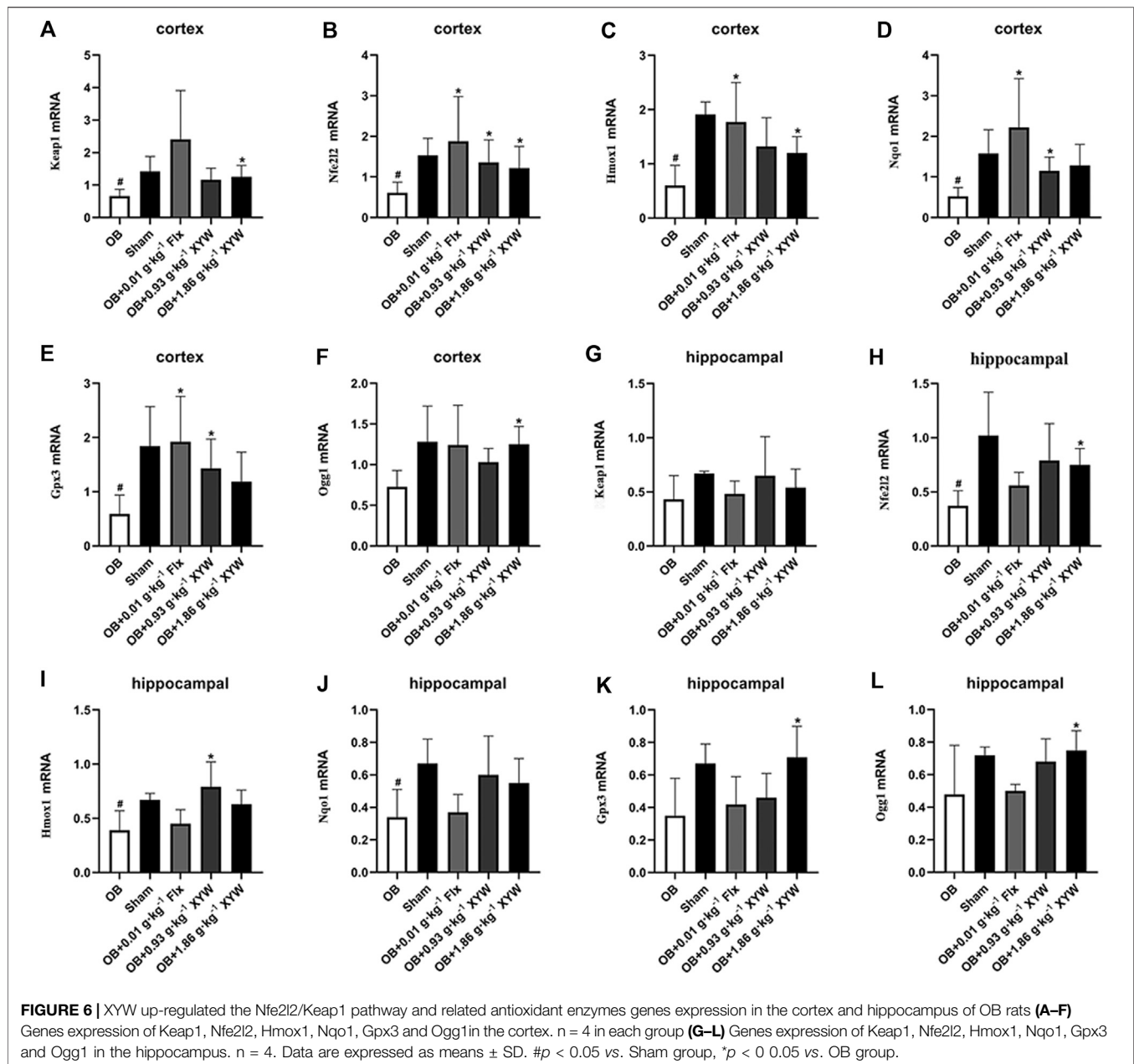
Xiaoyao Pills Restored the Suppressed Upstream Protein Expression of the PIK3CA/AKT1 Pathway in Olfactory Bulbectomized Rats

With mild levels of oxidative stress, the production of ROS activates the PIK3CA/AKT1 pathway and promotes the cleavage of NFE2L2/KEAP1 and nuclear translocation of NFE2L2, which activates the production of downstream antioxidant enzymes, reducing ROS levels to achieve an antioxidant effect (Cameron et al., 2018; Li et al., 2018). However, many investigations have found that ROS inhibit the activation of the PIK3CA/AKT1 pathway, which exacerbates oxidative stress and inflammation, leading to excessive oxidative damage (Wang K. S. et al., 2017; Jiang et al., 2018). In the present study, olfactory bulbectomy led to the suppression of the NFE2L2/KEAP1 pathway, so we assessed protein expression of the PIK3CA/AKT1 pathway to study whether changes in the PIK3CA/AKT1 pathway were similar to those in the downstream NFE2L2/KEAP1 pathway. As shown in **Figures 8A–C**, the expression of PIK3CA in the cortex of OB

rats was significantly lower than that of the sham rats ($p < 0.05$), whereas the expression of AKT1 showed a decreasing trend. Similarly, PIK3CA in the hippocampus of OB rats showed a decreasing trend and AKT1 was significantly lower ($p < 0.05$) compared with the sham rats (**Figures 8D–F**). We also found that administering FLX and XYW (0.93 and 1.86 g·kg⁻¹) improved the protein levels of PIK3CA and AKT1 to some extent (**Figures 8D–F**). Our results show that the PIK3CA/AKT1 pathway is upstream of the ROS and NFE2L2/KEAP1 pathways is suppressed as well in the central because of the damage due to the oxidative stress caused by olfactory bulbectomy; however, this could be restored by XYW treatment.

Xiaoyao Pills Restored the Decreased Protein Expression of the NTRK2/BDNF Pathway in Olfactory Bulbectomized Rats

BDNF has been well established as a specific indicator of depression-related diseases. Furthermore, the production of BDNF is closely related to the activation of the PIK3CA/AKT1 and CREB1/BDNF pathways (Mohammadi et al., 2018; Rai et al., 2019). The activation of PIK3CA induces the phosphorylation of AKT1, which activates CREB1, resulting in the elevation in the expression of BDNF. Moreover, the binding of NTRK2 and BDNF activates the PIK3CA/AKT1 pathway, which promotes synaptic plasticity and enhances long-term potentiation to

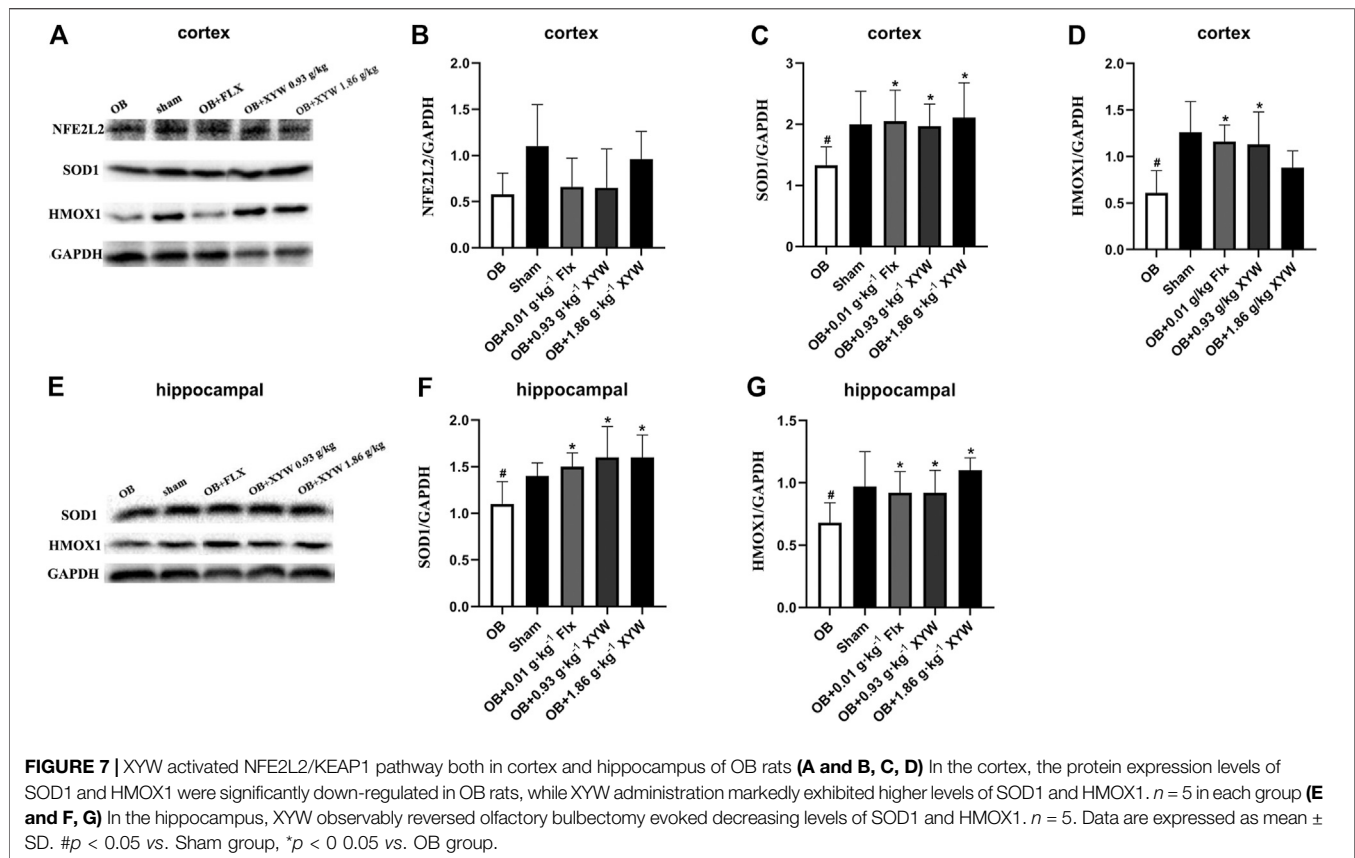


alleviate depression. Because the PIK3CA/AKT1 pathway was suppressed due to excessive oxidative stress, we tested whether the expression of BDNF and the activity of the downstream pathway were also inhibited. As shown in **Figures 9A–F**, the protein levels of NTRK2 and BDNF in both the cortex and hippocampus of the OB rats were significantly downregulated compared with that of the sham rats ($p < 0.05$). FLX and XYW (0.93 and 1.86 g/kg⁻¹) treatment dramatically restored the reduction in protein expression of NTRK2 and BDNF ($p < 0.05$), which demonstrated the neuroprotective effects of the treatments. Our results suggest that oxidative stress damage caused by olfactory bulbectomy is accompanied by the suppression of the NTRK2/BDNF pathway, and XYW is able

to reverse this effect to promote the expression of BDNF and provide neuroprotection.

DISCUSSION

Depression is a common chronic disease, which seriously affects the physical health and quality of life of patients. XYW, a clinically prescribed medication, has been shown to induce specific antidepressant effects; however, the underlying mechanism remains unclear. Olfactory bulbectomy is a recognized animal model of depression that induces changes in physiological functions and behaviors in the animal that

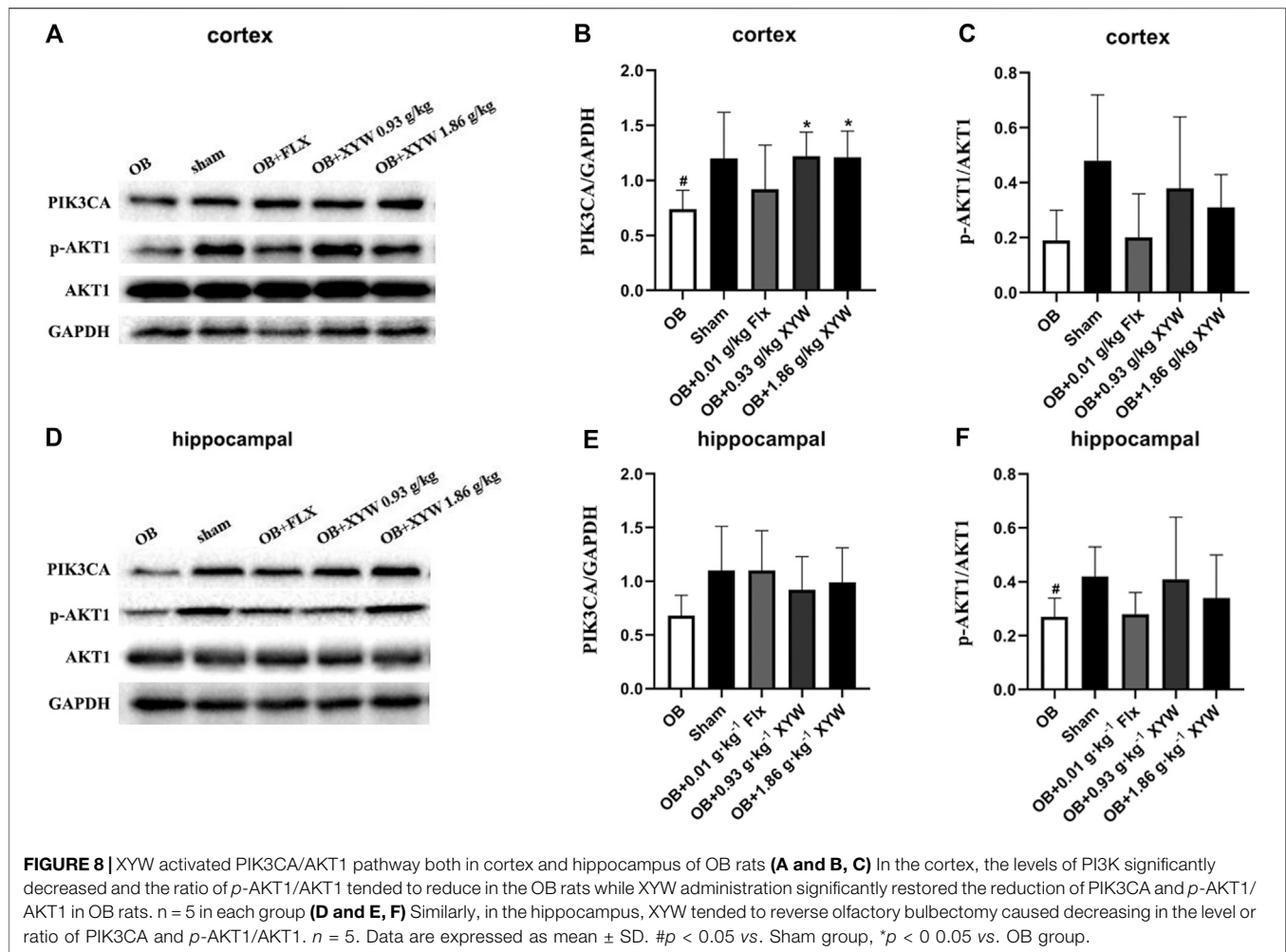


resemble symptoms commonly observed in patients with depression (Czéh et al., 2016). Our findings reveal that XYW effectively ameliorate the behavioral dysfunctions induced by olfactory bulbectomy through the attenuation of oxidative stress and neuroinflammation by activating the PI3CA-AKT1-NFE2L2/BDNF pathways in the cortex and hippocampus. A schematic representation of the underlying mechanism of the antidepressant effects of XYW are illustrated in **Figure 10**.

Previous reports have confirmed that neuroinflammation is involved in the pathogenesis of depression and may be a potential therapeutic target for depression (Dowlati et al., 2010; Marc et al., 2014). In our OB rats, high levels of ROS expression were found in the hippocampal DG and CA3 regions and cortex, and MDA levels were elevated in the cortex, which suggests that the OB rats experienced oxidative damage. In addition, the high GSSG/GSH ratio and reduced activity of SOD in the serum indicated that OB rats had an impaired antioxidant system, which weakened their ability to scavenge for oxygen-free radicals. Moreover, the imbalance of redox homeostasis correlated with depression. Evidence has confirmed that high levels of ROS can act as upstream messengers to activate the NLRP3 (Suárez and Buelvas, 2015) and NF- κ B inflammatory signaling pathways (Formentini et al., 2017; Gan et al., 2017). Furthermore, the production of caspase-1 induces the maturation of the inflammatory mediator IL1B (Du et al., 2016). Consequently, oxidative stress in the central may

cause neuroinflammation, which is an important factor that contributes to neuronal damage.

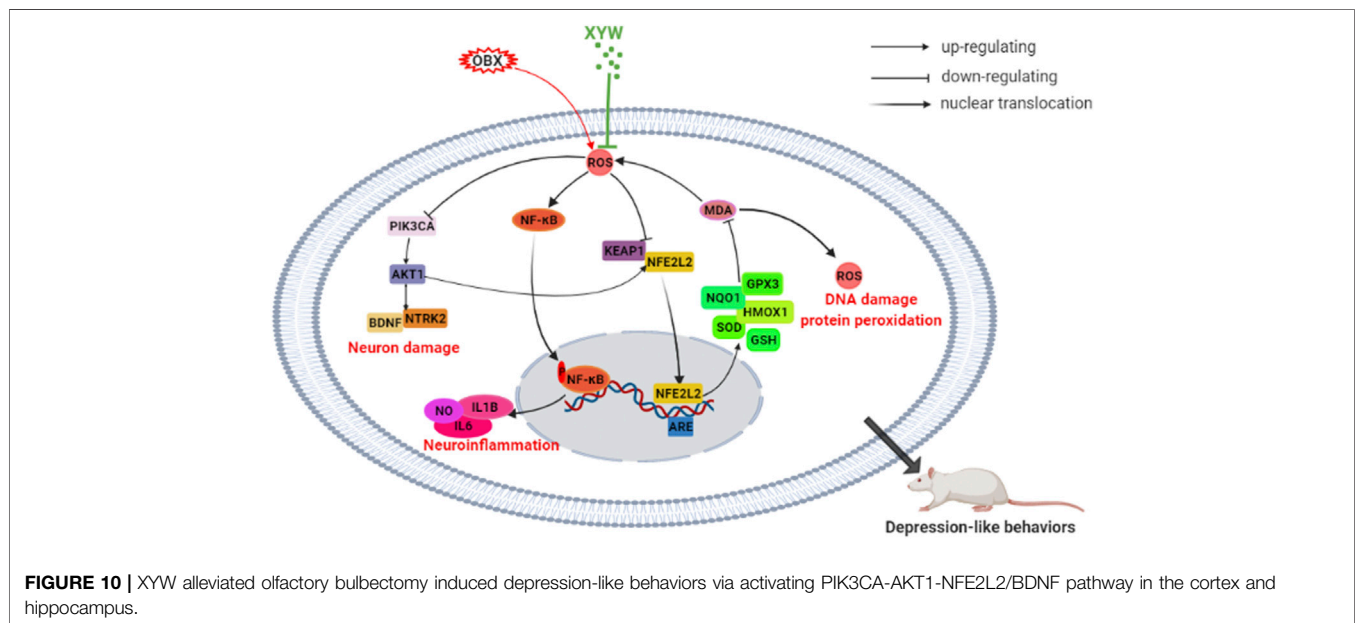
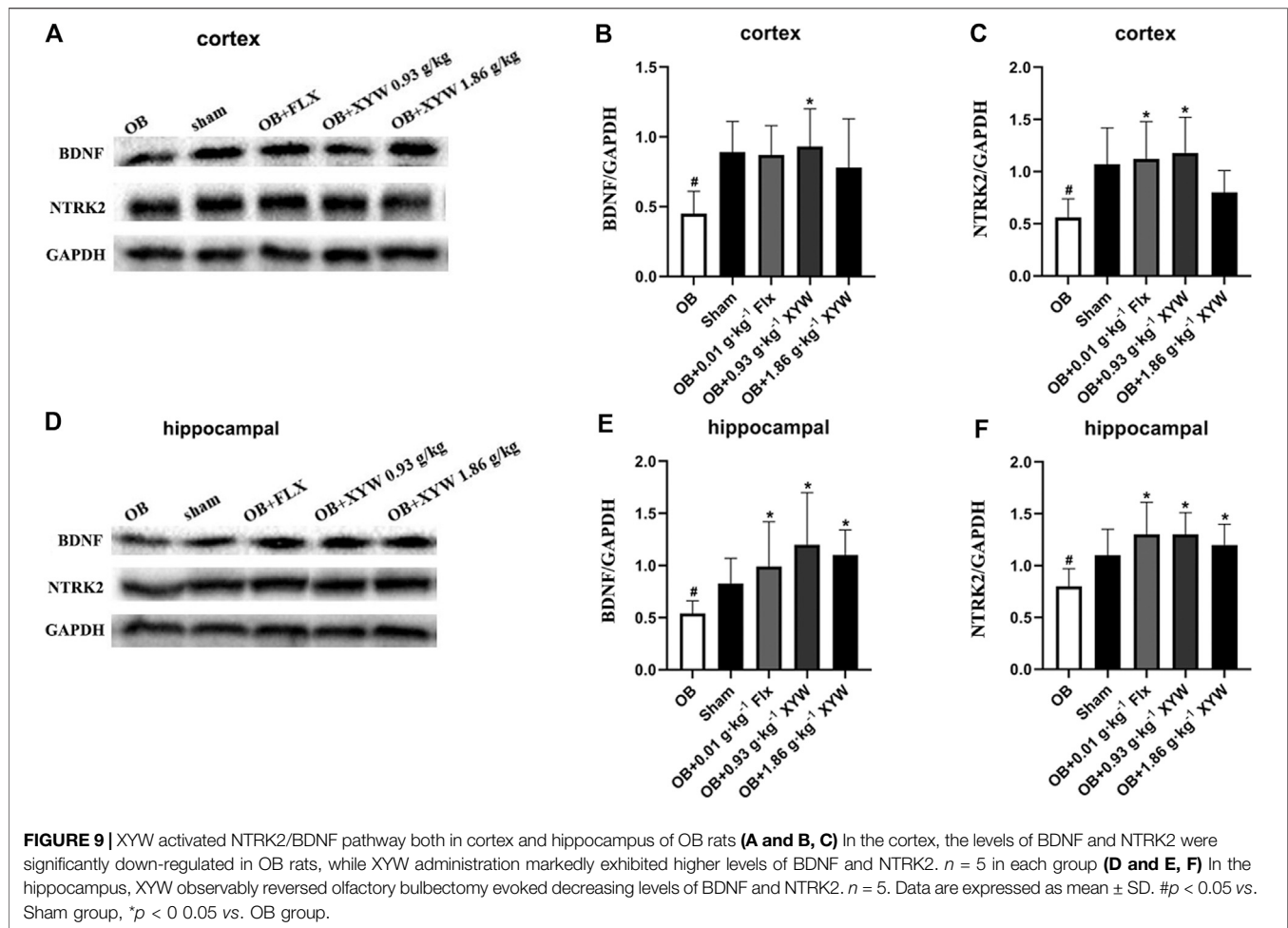
As mentioned earlier, NFE2L2 has been implicated in various psychiatric disorders, such as depression and anxiety (Hashimoto, 2018; Perić et al., 2017). Activation of the NFE2L2 signaling pathway can improve the lipopolysaccharide (LPS)-induced inflammatory response and reduce damage due to oxidative stress (Ren et al., 2019). In the LPS and chronic unpredictable mild stress-induced depression models, NFE2L2 signals were found to play key roles (Huang et al., 2013; Yang et al., 2018b). The NFE2L2-ARE pathway is an intrinsic mechanism of defense against oxidative stress. Moreover, NFE2L2 is a transcription factor that induces the expression of a large number of cytoprotective and detoxification genes (Buendia et al., 2016). During states of adequate oxidative stress, the NFE2L2 detaches from KEAP1 (an endogenous inhibitor of NFE2L2) and transfers to the nucleus to combine with ARE, which promotes the translation of antioxidants, such as SOD and HMOX1 (Tu et al., 2019). In the present study, the expression of NFE2L2 and KEAP1 as well as downstream antioxidant enzymes (e.g., GPX3, NQO1, and HMOX1) were significantly reduced in OB rats. We also observed a simultaneous increase in IL6 and IL1B levels in both the serum and cortex, which indicated that sustained olfactory bulbectomy-induced oxidative stress triggered an inflammatory response, which inhibited the activation of the NFE2L2 antioxidant signaling pathway. Notably, XYW treatment significantly lowered the



levels of MDA, ROS, NO, IL6, and IL1B, elevated the levels of GSH, SOD, GPX, NQO1, HMOX1, NFE2L2, and KEAP1, and ameliorated the behavioral deficits that resulted from olfactory bulbectomy. Recent studies have confirmed that XYW mitigates LPS-induced neuroinflammation, synaptic damage, and neuron deficiency both *in vivo* and *in vitro* (Shi et al., 2019a; Fang et al., 2020). These results suggest that XYW regulates oxidative stress and neuroinflammation via the NFE2L2/KEAP1 pathway.

The PIK3CA/AKT1 pathway is a core component in the pathogenesis of depression. Firstly, the PIK3CA/AKT1 pathway plays an essential role in the uptake and transport of serotonin, glutamate, and acetylcholine, and thus regulates the level and function of neurotransmitter receptors. Secondly, PIK3CA catalyzes PIP2 into PIP3, which induces the phosphorylation of AKT1. Subsequently *p*-AKT1 activates several downstream pathways, such as the mTOR, FoxO, GSK-3 β , and NF- κ B pathways, thereby regulating protein synthesis, cell proliferation, differentiation, autophagy, and apoptosis (Magariños et al., 1996; Polter et al., 2009; Li et al., 2010; Beurel et al., 2011; Dou et al., 2015). Thirdly, the PIK3CA/AKT1 pathway can cease ROS production by facilitating the synthesis of SOD and promoting appropriate mitochondrial

autophagy, leading to an improvement mitochondrial function (Cunningham et al., 2007; Bellot et al., 2009). In our study, we found that olfactory bulbectomy caused mass production of ROS in the cortex and hippocampus, which inhibited the PIK3CA-AKT1-NFE2L2/KEAP1 pathway, leading to reduced production of antioxidant enzymes and weakened clearing capacity of ROS in the central. Finally, the PIK3CA/AKT1 pathway interacts with BDNF, as was demonstrated in our study. On the one hand, phosphorylation of AKT1 can activate CREB, which further promotes the synthesis of BDNF (Jiang et al., 2017). On the other hand, when BDNF binds with NTRK2, a BDNF specific receptor, the PIK3CA/AKT1 pathway is activated (Jiang et al., 2017), which retrigger the physiological process. We also found that there was reduced expression of BDNF and NTRK2 in the cortex and hippocampus of OB rats, which may have been due to oxidative damage, and indicated that the development and nutrition of neurons were compromised. Overall, our study verified that during states of excessive oxidative stress, the PIK3CA/AKT1-NFE2L2/KEAP1 and PIK3CA/AKT1/BDNF/NTRK2 signaling pathways are suppressed, which induced OB rats to exhibit phenotypic behaviors of depression.



In recent decades, there has been limited improvement in the drugs used to treat depression, with selective serotonin reuptake inhibitors (SSRIs) continuing to be the most widely used class of antidepressants (Berton and Nestler, 2006). However, SSRIs generally take several weeks to achieve a therapeutic effect. It has been reported that about a third of patients do not respond to SSRIs; moreover, SSRIs can have side effects in some patients (Rush et al., 2006; Holtzheimer and Mayberg, 2011). The disadvantages of SSRI treatment are mainly attributed to the unclear pathogenesis of depression. Therefore, further studies on the pathogenesis of depression is necessary to develop more effective treatments. Several studies to date have shown that the pathogenesis of depression is complex and involves multi-target and multi-pathway regulation. Complex components and difficulties in identifying effective components are the disadvantages of traditional Chinese medicine; although, they are also the advantages of the treatment of depression. For example, there are numerous representative effective constituents of XYW that have antidepressant effects: Total Saikosaponins, which has anti-inflammation, anti-apoptosis, and synaptic protein expression promoting effects (Lixing et al., 2018; Sun et al., 2018); Glycyrrhizic acid, which has an antidepressant effect by modulating autophagy, promoting anti-inflammation, and ameliorating the kynurenine pathway (Wang et al., 2018a; Yang et al., 2018a; Cao et al., 2020); and Paeoniflorin, which exerts a neuroprotective effect by inhibiting oxidative stress and Ca^{2+} overload, promotes neurogenesis in the hippocampal dentate gyrus, and activates the MAPK1-CREB1 pathway (Mao et al., 2010; Chen et al., 2019; Zhong et al., 2019). These three components have varying mechanisms of action to induce the antidepressant effect, which suggests that the advantage of TCM compounds as depression treatments lies in the complexity of its components; therefore, TCMs have the potential to restore molecular imbalances at different levels in a multi-component and multi-target manner. As shown in our previous studies, Xiaoyao powder and XYW may offer an effective form of depression treatment by improving neurotransmission, neuroinflammation, neurogenesis, and other aspects in multi-component, multi-target and multi-pathway ways. Moreover, XYW can be extensively used to treat a variety of uncomfortable symptoms caused by depression, such as decreased gastrointestinal function, decreased sexual desire, and insomnia (Gong, 2014; Cao et al., 2019; Xian, 2007). These benefits are related to its effects of smoothing the liver, nourishing the blood, and strengthening the spleen, which are effects that cannot be achieved by FLX.

Both the cortex and hippocampus are two important brain regions that are associated with the pathogenesis of depression. The cortex is a significant nerve center that regulates thinking and behavior, whereas the hippocampus is responsible for memory formation, storage, and emotional adjustment (Treadway et al., 2015; Hainmueller and Bartos, 2018). Recent studies have shown that stress and depression have an impact on cortical and hippocampal morphology (Belleau et al., 2019) and function, such as suppressed neuroplasticity, decreased spine density, downregulation of neurotrophic factors, and increased neuroinflammation (Lanz et al., 2019; Zhang et al., 2014; Giridharan et al., 2019). In the present study, we found that XYW promoted transcription of KEAP1/NFE2L2 pathway genes and

upregulated protein expression of NFE2L2, SOD1, HMOX1, p-PIK3CA, p-AKT1, BDNF, and NTRK2 in both the cortex and hippocampus, which suggests that XYW has antioxidative and neuroprotective effects on both regions.

Overall, we demonstrated that by removing the olfactory bulb, it is possible to induce continuous oxidative stress in the cortex and hippocampus, which results in increased levels of ROS and MDA, reduced activity of SOD, HMOX1, NQO1, GSH, and GPX3, and increased lipid peroxidation. Moreover, we find that the PIK3CA/AKT1, NFE2L2/KEAP1, and NTRK2/BDNF pathways are suppressed, whereas XYW induces the clearance of excessive ROS and enhances the activation of the PIK3CA-AKT1/NFE2L2/BDNF pathway, which results in antidepressant and neuroprotective effects. Although determining the underlying mechanisms requires further investigation, our research highlights that NFE2L2 antioxidant signaling is important in depression and raises the possibility that the Chinese herbal compound, XYW, has promise as an effective treatment for depression.

CONCLUSION

Since there may be a risk of non-specific effects at this dose level, it will be important to further study this extract at lower dose levels.

DATA AVAILABILITY STATEMENT

The raw data supporting the conclusions of this article will be made available by the authors, without undue reservation, to any qualified researcher.

ETHICS STATEMENT

The animal study was reviewed and approved by the guidelines of the Committee for Animal Care and Use of Laboratory Animals, College of Pharmacy, Chengdu University of Traditional Chinese Medicine.

AUTHOR CONTRIBUTIONS

YFJ, JL, JSZ, YF, RL, FL and NZ conceived and designed the experiments; YFJ, JL, JSZ, YF and RL carried out the experiments; YFJ, JL, JSZ, YF, RL, FL and NZ analyzed the datum and drafted relevant text; YFJ and JL wrote the manuscript. All authors have read and approved the final version of this manuscript.

FUNDING

This work was supported by the National Natural Science Foundation of China (Grant No. 82074094), the Applied Basic Research Project of Science and Technology Department of Sichuan Province (20YYJC0640), the Open Research Fund of

Chengdu University of Traditional Chinese Medicine Key Laboratory of Systematic Research of Distinctive Chinese Medicine Resources in Southwest China (Grant No.

2020XSGG002), and the Xinglin Scholar Research Promotion Project of Chengdu University of Traditional Chinese Medicine (Grant No. CDTD2018014).

REFERENCES

- Baird, L., and Dinkova-Kostova, A. T. (2011). The cytoprotective role of the Keap1-Nrf2 pathway. *Arch. Toxicol.* 85 (4), 241–272. doi:10.1007/s00204-011-0674-5
- Belleau, E. L., Treadway, M. T., and Pizzagalli, D. A. (2019). The impact of stress and major depressive disorder on hippocampal and medial prefrontal cortex morphology. *Biol. Psychiatry* 85 (6), 443–453. doi:10.1016/j.biopsych.2018.09.031
- Bellot, G., Garcia-Medina, R., Gounon, P., Chiche, J., Roux, D., Pouyssegur, J., Mazure, M., et al. (2009). Hypoxia-induced autophagy is mediated through hypoxia-inducible factor induction of BNIP3 and BNIP3L via their BH3 domains. *Mol. Cell. Biol.* 29 (10), 2570–2581. doi:10.1038/nrn184610.1128/mcb.00166-09
- Berton, O., and Nestler, E. J. (2006). New approaches to antidepressant drug discovery: beyond monoamines. *Nat. Rev. Neurosci.* 7 (2), 137–151. doi:10.1038/nrn1846
- Beurel, E., Song, L., and Jope, R. S. (2011). Inhibition of glycogen synthase kinase-3 is necessary for the rapid antidepressant effect of ketamine in mice. *Mol. Psychiatry* 16 (11), 1068–1070. doi:10.1038/mp.2011.47
- Bilici, M., Efe, H., Köroğlu, M. A., Uydu, H. A., Bekaroğlu, M., and Değer, O. (2001). Antioxidative enzyme activities and lipid peroxidation in major depression: alterations by antidepressant treatments. *J. Affective Disord.* 64 (1), 43–51. doi:10.1016/s0165-0327(00)00199-3
- Bouvier, E., Brouillard, F., Molet, J., Claverie, D., Cabungcal, J.-H., Cresto, N., et al. (2017). Nrf2-dependent persistent oxidative stress results in stress-induced vulnerability to depression. *Mol. Psychiatry* 22 (12), 1701–1713. doi:10.1038/mp.2016.144
- Buendia, I., Michalska, P., Navarro, E., Gameiro, I., Egea, J., and León, R. (2016). Nrf2-ARE pathway: an emerging target against oxidative stress and neuroinflammation in neurodegenerative diseases. *Pharmacol. Ther.* 157, 84–104. doi:10.1016/j.pharmthera.2015.11.003
- Cameron, B. D., Sekhar, K. R., Ofori, M., and Freeman, M. L. (2018). The role of Nrf2 in the response to normal tissue radiation injury. *Radiat. Res.* 190 (2), 99–106. doi:10.1667/RR15059.1
- Cao, J., Zhou, D. S., Zhang, Y., Zhu, G. D., Yuan, N. H., and Yu, C. (2019). Clinical observation of amitriptyline combined with Xiaoyao powder in the treatment of postpartum depression. *Chin. J. Prim. Med. Pharm.* 26 (19), 2332–2335.
- Cao, Z. Y., Liu, Y. Z., Li, J. M., Ruan, Y. M., Yan, W. J., Zhong, S. Y., et al. (2020). Glycyrrhizic acid as an adjunctive treatment for depression through anti-inflammation: a randomized placebo-controlled clinical trial. *J. Affective Disord.* 265, 247–254. doi:10.1016/j.jad.2020.01.048
- Chen, L. B., Qiu, F. M., Zhong, X. M., Hong, C., and Huang, Z. (2019). Promoting neurogenesis in hippocampal dentate gyrus of chronic unpredictable stress-induced depressive-like rats with paeoniflorin. *J. Integr. Neurosci.* 18 (1), 43–49. doi:10.31083/j.jin.2019.01.116
- China Pharmacopoeia Commission (2020). *Chinese pharmacopoeia*. Beijing, China: China Medical Science Press, 1462.
- Cui, R. (2015). Editorial (thematic selection: a systematic review of depression). *Curr. Neuropsychopharmacol.* 13 (4), 480. doi:10.2174/1570159x1304150831123535
- Cunningham, J. T., Rodgers, J. T., Arlow, D. H., Vazquez, F., Mootha, V. K., and Puigserver, P. (2007). mTOR controls mitochondrial oxidative function through a YY1-PGC-1 α transcriptional complex. *Nature* 450 (7170), 736–740. doi:10.1038/nature06322
- Czeh, B., Fuchs, E., Wiborg, O., and Simon, M. (2016). Animal models of major depression and their clinical implications. *Prog. Neuro-Psychopharmacol. Biol. Psychiatry* 64, 293–310. doi:10.1016/j.pnpb.2015.04.004
- Dou, L., Wang, S., Sui, X., Meng, X., Shen, T., Huang, X., et al. (2015). MiR-301a mediates the effect of IL-6 on the AKT/GSK pathway and hepatic glycogenesis by regulating PTEN expression. *Cell. Physiol. Biochem.* 35 (4), 1413–1424. doi:10.1159/000373962
- Dowlati, Y., Herrmann, N., Swardfager, W., Liu, H., Sham, L., Reim, E. K., et al. (2010). A meta-analysis of cytokines in major depression. *Biol. Psychiatry* 67 (5), 446–457. doi:10.1016/j.biopsych.2009.09.033
- Dragana, F., Nevena, T., Rick, E. B., and Peter, G. (2016). Oxidative and nitrosative stress pathways in the brain of socially isolated adult male rats demonstrating depressive- and anxiety-like symptoms. *Brain Struct. Funct.* 222, 1–20. doi:10.1007/s00429-016-1218-9
- Du, R.-H., Wu, F.-F., Lu, M., Shu, X.-d., Ding, J.-H., Wu, G., et al. (2016). Uncoupling protein 2 modulation of the NLRP3 inflammasome in astrocytes and its implications in depression. *Redox Biol.* 9 (C), 178–187. doi:10.1016/j.redox.2016.08.006
- Fang, Y., Shi, B., Liu, X., Luo, J., Rao, Z., Liu, R., et al. (2020). Xiaoyao Pills attenuate inflammation and nerve injury induced by lipopolysaccharide in hippocampal neurons in vitro. *Neural Plasticity* 2020, 1–12. doi:10.1155/2020/8841332
- Fontella, F. U., Siqueira, I. R., Vasconcellos, A. P. S., Tabajara, A. S., Netto, C. A., and Dalmaz, C. (2005). Repeated restraint stress induces oxidative damage in rat *Hippocampus*. *Neurochem. Res.* 30 (1), 105–111. doi:10.1007/s11064-004-9691-6
- Formentini, L., Santacatterina, F., de Arenas, C. N., Stamatakis, K., López-Martínez, D., Logan, A., et al. (2017). Mitochondrial ROS production protects the intestine from inflammation through functional M2 macrophage polarization. *Cell Rep.* 19 (6), 1202. doi:10.1016/j.celrep.2017.04.036
- Gan, Z., Kang, F. J., Hai, C. W., Chang, W. Q., Gan, Z. D., and Xiu, L. P. (2017). Polydatin reduces *Staphylococcus aureus* lipoteichoic acid-induced injury by attenuating reactive oxygen species generation and TLR2-NF κ B signalling. *J. Cell Mol. Med.* 21 (11), 2796–2808. doi:10.1111/jcmm.13194
- Giridharan, V. V., Réus, G. Z., Selvaraj, S., Scaini, G., Barichello, T., and Quevedo, J. (2019). Maternal deprivation increases microglial activation and neuroinflammatory markers in the prefrontal cortex and hippocampus of infant rats. *J. Psychiatr. Res.* 115, 13–20. doi:10.1016/j.jpsychires.2019.05.001
- Gong, X. P. (2014). *Effect of Xiaoyao powder on gastrointestinal function and regulation mechanism of 5-HT system in CUMS model rats*. Chengdu, China: Chengdu University of Traditional Chinese Medicine.
- Hainmueller, T., and Bartos, M. (2018). Parallel emergence of stable and dynamic memory engrams in the hippocampus. *Nature* 558 (7709), 292–296. doi:10.1038/s41586-018-0191-2
- Hashimoto, K. (2018). Essential role of keap1-nrf2 signaling in mood disorders: overview and future perspective. *Front. Pharmacol.* 9, 1182. doi:10.3389/fphar.2018.01182
- Herbet, M., Korga, A., Gawrońska-Grzywacz, M., Izdebska, M., Piątkowska-Chmiel, I., Polesza, E., et al. (2017). Chronic variable stress is responsible for lipid and DNA oxidative disorders and activation of oxidative stress response genes in the brain of rats. *Oxid. Med. Cell. Longev.* 2017 (174), 7313090. doi:10.1155/2017/7313090
- Holtzheimer, P. E., and Mayberg, H. S. (2011). Stuck in a rut: rethinking depression and its treatment. *Trends Neurosciences* 34 (1), 1–9. doi:10.1016/j.tins.2010.10.004
- Hovatta, I., Juhila, J., and Donner, J. (2010). Oxidative stress in anxiety and comorbid disorders. *Neurosci. Res.* 68 (4), 261–275. doi:10.1016/j.neures.2010.08.007
- Huang, Q., Chu, S. F., Zhang, J. T., and Chen, N. H. (2013). Effects of Ginsenoside Rg1 on anti-depression and synaptic ultrastructure. *Chin. Pharmacol. Bull.* 29 (8), 1124–1127.
- Jiang, K., Guo, S., Yang, C., Yang, J., Chen, Y., Shaukat, A., et al. (2018). Barbaloin protects against lipopolysaccharide (LPS)-induced acute lung injury by inhibiting the ROS-mediated PI3K/AKT/NF- κ B pathway. *Int. Immunopharmacol.* 64, 140–150. doi:10.1016/j.intimp.2018.08.023
- Jiang, T., Wang, X.-Q., Ding, C., and Du, X.-I. (2017). Genistein attenuates isoflurane-induced neurotoxicity and improves impaired spatial learning and memory by regulating cAMP/CREB and BDNF-TrkB-PI3K/Akt signaling. *Korean J. Physiol. Pharmacol.* 21 (6), 579–589. doi:10.4196/kjpp.2017.21.6.579
- Jin, P., and Jiang, Y. C. (2014). Clinical study on apoptosis of depression cells after stroke and the treatment of Xiaoyao powder. *Shandong J. Traditional Chin. Med.* 10 (11), 880–882.

- Jin, P., and Jiang, Y. C. (2015). Clinical study on the adjustment of Xiaoyao powder to poststroke depression. *Hebei. J. TCM*. 37 (2), 226–228.
- Lanz, T. A., Reinhart, V., Sheehan, M. J., Rizzo, S. J. S., Bove, S. E., James, L. C., et al. (2019). Postmortem transcriptional profiling reveals widespread increase in inflammation in schizophrenia: a comparison of prefrontal cortex, striatum, and hippocampus among matched tetrads of controls with subjects diagnosed with schizophrenia, bipolar or major depressive disorder. *Transl. Psychiatry* 9 (1), 151. doi:10.1038/s41398-019-0492-8
- Li, N., Lee, B., Liu, R.-J., Banasr, M., Dwyer, J. M., Iwata, M., et al. (2010). mTOR-dependent synapse formation underlies the rapid antidepressant effects of NMDA antagonists. *Science* 329 (5994), 959–964. doi:10.1126/science.1190287
- Li, H., Tang, Z., Chu, P., Song, Y., Yang, Y., Sun, B., et al. (2018). Neuroprotective effect of phosphocreatine on oxidative stress and mitochondrial dysfunction induced apoptosis *in vitro* and *in vivo*: involvement of dual PI3K/Akt and Nrf2/HO-1 pathways. *Free Radic. Biol. Med.* 120, 228–238. doi:10.1016/j.freeradbiomed.2018.03.014
- Liu, Y. B., Lian, Y. L., Cui, Y. H., and Li, M. S. (2018). Simultaneous determination of five chemical components in Xiaoyao pill by HPLC. *Drug Stand. China* 19 (3), 230–234.
- Lixing, X., Zhouye, J., Liting, G., Ruyi, Z., Rong, Q., and Shiping, M. (2018). Saikosaponin-d-mediated downregulation of neurogenesis results in cognitive dysfunction by inhibiting Akt/Foxg-1 pathway in mice. *Toxicol. Lett.* 284, 79–85. doi:10.1016/j.toxlet.2017.11.009
- Lupien, S. J., McEwen, B. S., Gunnar, M. R., and Heim, C. (2009). Effects of stress throughout the lifespan on the brain, behaviour and cognition. *Nat. Rev. Neurosci.* 10 (6), 434. doi:10.1038/nrn2639
- Magariños, A. M., McEwen, B. S., Flügge, G., and Fuchs, E. (1996). Chronic psychosocial stress causes apical dendritic atrophy of hippocampal CA3 pyramidal neurons in subordinate tree shrews. *J. Neurosci.* 16 (10), 3534–3540. doi:10.1523/JNEUROSCI.16-10-03534.1996
- Manoli, L. P., Gamaro, G. D., Silveira, P. P., and Dalmaz, C. (2000). Effect of chronic variate stress on thiobarbituric-acid reactive species and on total radical-trapping potential in distinct regions of rat brain. *Neurochem. Res.* 25 (7), 915. doi:10.1023/a:1007592022575
- Mao, Q.-Q., Zhong, X.-M., Feng, C.-R., Pan, A.-J., Li, Z.-Y., and Huang, Z. (2010). Protective effects of paeoniflorin against glutamate-induced neurotoxicity in PC12 cells via antioxidant mechanisms and Ca²⁺ antagonism. *Cell. Mol. Neurobiol.* 30 (7), 1059–1066. doi:10.1007/s10571-010-9537-5
- Marc, U., Diego, H., Ricard, N., Xavier, F., Ricard, S., Magi, F., et al. (2014). Prophylactic antidepressant treatment of interferon-induced depression in chronic hepatitis C: a systematic review and meta-analysis. *J. Clin. Psychiatry* 75 (10), 1113–1121. doi:10.4088/JCP.13r08800
- Martín-Hernández, D., Bris, Á. G., MacDowell, K. S., García-Bueno, B., Madrigal, J. L. M., Leza, J. C., et al. (2016). Modulation of the antioxidant nuclear factor (erythroid 2-derived)-like 2 pathway by antidepressants in rats. *Neuropharmacology*. 103(11), 79–91. doi:10.1016/j.neuropharm.2015.11.029
- Martín-Hernández, D., Caso, J. R., Meana, J. J., Callado, L. F., Madrigal, J. L. M., García-Bueno, B., et al. (2018). Intracellular inflammatory and antioxidant pathways in postmortem frontal cortex of subjects with major depression: effect of antidepressants. *J. Neuroinflamm.* 15(1), 250. doi:10.1186/s12974-018-1294-2
- Mendez-David, I., Tritschler, L., El Ali, Z., Damiens, M. H., Pallardy, M., David, D. J., et al. (2015). Nrf2-signaling and BDNF: a new target for the antidepressant-like activity of chronic fluoxetine treatment in a mouse model of anxiety/depression. *Neurosci. Lett.* 597, 121–126. doi:10.1016/j.neulet.2015.04.036
- Michael, M., Piotr, G., Yong, S. C., and Michael, B. (2011). A review on the oxidative and nitrosative stress (O&NS) pathways in major depression and their possible contribution to the (neuro)degenerative processes in that illness. *Prog. Neuropsychopharmacol. Biol. Psychiatry* 35 (3), 676–692. doi:10.1016/j.pnpb.2010.05.004
- Mohammadi, A., Amooeian, V. G., and Rashidi, E. (2018). Dysfunction in brain-derived neurotrophic factor signaling pathway and susceptibility to schizophrenia, Parkinson's and alzheimer's diseases. *Curr. Gene. Ther.* 18 (1), 45–63. doi:10.2174/1566523218666180302163029
- Perić, I., Stanisavljević, A., Gass, P., and Filipović, D. (2017). Fluoxetine reverses behavior changes in socially isolated rats: role of the hippocampal GSH-dependent defense system and proinflammatory cytokines. *Eur. Arch. Psychiatry Clin. Neurosci.* 267 (8), 1–13. doi:10.1007/s00406-017-0807-9
- Polter, A., Yang, S., Zmijewska, A. A., van Groen, T., Paik, J.-H., Depinho, R. A., et al. (2009). Forkhead box, class O transcription factors in brain: regulation and behavioral manifestation. *Biol. Psychiatry* 65 (2), 150–159. doi:10.1016/j.biopsych.2008.08.005
- Rai, S. N., Dilmashin, H., Birla, H., Singh, S. S., Zahra, W., Rathore, A. S., et al. (2019). The role of PI3K/akt and ERK in neurodegenerative disorders. *Neurotox. Res.* 35 (3), 775–795. doi:10.1007/s12640-019-0003-y
- Ren, J., Li, L., Wang, Y., Zhai, J., Chen, G., and Hu, K. (2019). Gambogic acid induces heme oxygenase-1 through Nrf2 signaling pathway and inhibits NF-κB and MAPK activation to reduce inflammation in LPS-activated RAW264.7 cells. *Biomed. Pharmacother.* 109, 555–562. doi:10.1016/j.biopha.2018.10.112
- Rush, A. J., Trivedi, M. H., Wisniewski, S. R., Nierenberg, A. A., Stewart, J. W., Warden, D., et al. (2006). Acute and longer-term outcomes in depressed outpatients requiring one or several treatment steps: a STAR*D report. *Am. J. Psychiatry*. 163 (11), 1905–1917. doi:10.1176/ajp.2006.163.11.1905
- Shi, B. Y., Luo, J., Rao, Z. L., Liu, X. B., Liu, R., Ye, X. L., et al. (2018). Study on the intervention effect and mechanism of Xiaoyao Powder on Depression-like rats induced by LPS. *Pharmacol. Clin. Chin. Mater. Med.* 34 (6), 3–7.
- Shi, B., Luo, J., Fang, Y., Liu, X., Rao, Z., Liu, R., et al. (2019). Xiaoyao Pills prevent lipopolysaccharide-induced depression by inhibiting inflammation and protecting nerves. *Front. Pharmacol.* 10, 1324. doi:10.3389/fphar.2019.01324
- Shi, B. Y., Liu, R., Rao, Z. L., Liu, X. B., Luo, J., Ji, Y. F., et al. (2019a). Protective effects of Xiaoyao Powder on rat neuron injury induced by LPS. *Chin. J. Exp. Formulation* 25 (5), 50–56.
- Shi, B. Y., Rao, Z. L., Luo, J., Liu, X. B., Fang, Y., Cao, H. J., et al. (2019b). Study on the protective effect and mechanism of Xiaoyao Powder on hippocampal neuron cell injury induced by LPS. *J. Chin. Materia Med.* 44 (4), 781–786.
- Suárez, R., and Buelvas, N. (2015). Inflammasome: activation mechanisms. *Invest. Clin.* 56 (1), 74.
- Surget, A., Saxe, M., Leman, S., Ibarguen-Vargas, Y., Chalon, S., Griebel, G., et al. (2008). Drug-Dependent requirement of hippocampal neurogenesis in a model of depression and of antidepressant reversal. *Biol. Psychiatry* 64 (4), 293–301. doi:10.1016/j.biopsych.2008.02.022
- Sun, X., Li, X., Pan, R., Xu, Y., Wang, Q., and Song, M. (2018). Total Saikosaponins of Bupleurum yinchowense reduces depressive, anxiety-like behavior and increases synaptic proteins expression in chronic corticosterone-treated mice. *BMC. Complement. Altern. Med.* 18 (1), 117. doi:10.1186/s12906-018-2186-9
- Tanja, M. M., Dietrich, P., and Johannes, T. (2012). The role of oxidative stress in depressive disorders. *Curr. Pharm. Des.* 18 (36), 5890–5899. doi:10.2174/138161212803523554
- Treadway, M. T., Waskom, M. L., Dillon, D. G., Holmes, A. J., Park, M. T. M., Chakravarty, M. M., et al. (2015). Illness progression, recent stress, and morphometry of hippocampal subfields and medial prefrontal cortex in major depression. *Biol. Psychiatry* 77 (3), 285–294. doi:10.1016/j.biopsych.2014.06.018
- Tu, W., Wang, H., Li, S., Liu, Q., and Sha, H. (2019). The anti-inflammatory and anti-oxidant mechanisms of the keap1/nrf2/ARE signaling pathway in chronic diseases. *Aging Dis.* 10 (3), 637–651. doi:10.14336/AD.2018.0513
- Wang, K. S.Lv, Y., Wang, Z., Ma, J., Mi, C., Li, X., et al. (2017). Imperatorin efficiently blocks TNF-α-mediated activation of ROS/PI3K/Akt/NF-κB pathway. *Oncol. Rep.* 37 (6), 3397–3404. doi:10.3892/or.2017.5581
- Wang, Y.Li, M., Liang, Y., Yang, Y., Liu, Z., Yao, K., et al. (2017). Chinese herbal medicine for the treatment of depression: applications, efficacies and mechanisms. *Curr. Pharm. Des.* 23 (34), 5180–5190. doi:10.2174/1381612823666170918120018
- Wang, B., Lian, Y.-J., Dong, X., Peng, W., Liu, L.-L., Su, W.-J., et al. (2018a). Glycyrrhizic acid ameliorates the kynurenine pathway in association with its antidepressant effect. *Behav. Brain Res.* 353, 250–257. doi:10.1016/j.bbr.2018.01.024
- Wang, J. J., Hodes, G. E., Zhang, H., Zhang, S., Zhao, W., Golden, S. A., et al. (2018b). Epigenetic modulation of inflammation and synaptic plasticity promotes resilience against stress in mice. *Nat. Commun.* 9 (1), 477. doi:10.1038/s41467-017-02794-5
- Wang, X., Liu, R., Luo, J., Liu, X. B., Shi, B. Y., Ye, X. L., et al. (2018c). Study on antidepressant effect and BDNF/HPA mechanism of modified Xiaoyao Powder based on CUMS rats. *Pharmacol. Clin. Chin. Mater. Med.* 34 (1), 14–19.

- Xian, H. (2007). *Clinical study on the treatment of depression by soothing liver and invigorating spleen [D]*. Chaoyang, China: Beijing University of Chinese Medicine.
- Xiong, J. Y., Zeng, N., Zhang, C. Y., Yang, J., and Liu, X. S. (2007a). Effect of Xiaoyao Powder on behavior and monoamine neurotransmitters in brain of CUMS model rats. *Prog. Mod. Biomed.* 7 (11), 1635–1639.
- Xiong, J. Y., Zeng, N., Zhang, C. Y., Yang, J., and Liu, X. S. (2007b). Study on antidepressant effect of Xiaoyao. *Powder. Pharmacol. Clin. Chin. Mater. Med.* 23 (1), 3–5007.
- Yang, G., Li, J., Cai, Y., Yang, Z., Li, R., and Fu, W. (2018a). Glycyrrhizic acid alleviates 6-hydroxydopamine and corticosterone-induced neurotoxicity in SH-SY5Y cells through modulating autophagy. *Neurochem. Res.* 43 (10), 1914–1926. doi:10.1007/s11064-018-2609-5
- Yang, M., Dang, R., Xu, P., Guo, Y., Han, W., Liao, D., et al. (2018b). DL-3-n-Butylphthalide improves lipopolysaccharide-induced depressive-like behavior in rats: involvement of Nrf2 and NF- κ B pathways. *Berl* 235 (9), 2573–2585. doi:10.1007/s00213-018-4949-x
- Yao, W., Zhang, J. C., Ishima, T., Dong, C., Yang, C., Ren, Q., et al. (2016). Role of Keap1-Nrf2 signaling in depression and dietary intake of glucoraphanin confers stress resilience in mice. *Sci. Rep.* 6, 30659. doi:10.1038/srep30659
- Zhang, H. L., Wang, T. F., Guo, W., Tian, R. P., and Ma, Y. P. (2005). Literature analysis of TCM syndromes of depression in recent 10 years. *J. Beijing Univ. Traditional Chin. Med.* 28 (3), 79–81.
- Zhang, J. C., Wu, J., Fujita, Y., Yao, W., Ren, Q., Yang, C., et al. (2015). Antidepressant effects of TrkB ligands on depression-like behavior and dendritic changes in mice after inflammation. *Int. J. Neuropsychopharmacol.* 18 (4), pyu077. doi:10.1093/ijnp/pyu077
- Zhao, W., Wang, Z. Y., and Wu, Z. A. (2018). Determination of six active components in Xiaoyao pill by wavelength transform high performance liquid chromatography. *Her. Med.* 37 (8), 1000–1003.
- Zhong, X., Li, G., Qiu, F., and Huang, Z. (2019). Paeoniflorin ameliorates chronic stress-induced depression-like behaviors and neuronal damages in rats via activation of the ERK-CREB pathway. *Front. Psychiatry* 9, 772. doi:10.3389/fpsyt.2018.00772
- Zueger, M., Urani, A., Chourbaji, S., Zacher, C., Roche, M., Harkin, A., et al. (2005). Olfactory bulbectomy in mice induces alterations in exploratory behavior. *Neurosci. Lett.* 374 (2), 142–146. doi:10.1016/j.neulet.2004.10.040

Conflict of Interest: The authors declare that the research was conducted in the absence of any commercial or financial relationships that could be construed as a potential conflict of interest.

Copyright © 2021 Ji, Luo, Zeng, Fang, Liu, Luan and Zeng. This is an open-access article distributed under the terms of the Creative Commons Attribution License (CC BY). The use, distribution or reproduction in other forums is permitted, provided the original author(s) and the copyright owner(s) are credited and that the original publication in this journal is cited, in accordance with accepted academic practice. No use, distribution or reproduction is permitted which does not comply with these terms.



Neuroprotective Effect for Cerebral Ischemia by Natural Products: A Review

Qian Xie^{1,2†}, Hongyan Li^{1,2†}, Danni Lu^{1,2}, Jianmei Yuan^{1,2}, Rong Ma^{1,2}, Jinxiu Li^{1,2}, Mihong Ren^{1,2}, Yong Li^{1,2}, Hai Chen^{1,2}, Jian Wang^{1,2*} and Daoyin Gong^{3*}

¹State Key Laboratory of Southwestern Chinese Medicine Resources, Chengdu, China, ²School of Pharmacy, Chengdu University of Traditional Chinese Medicine, Chengdu, China, ³Hospital of Chengdu University of Traditional Chinese Medicine, Chengdu, China

OPEN ACCESS

Edited by:

Min Li,
Hong Kong Baptist University,
Hong Kong

Reviewed by:

Hsu-Shan Huang,
Taipei Medical University, Taiwan
Xiang Lin,
The University of Hong Kong,
Hong Kong

*Correspondence:

Jian Wang
jianwang08@163.com
Daoyin Gong
269095483@qq.com

[†]These authors have contributed
equally to this work

Specialty section:

This article was submitted to
Ethnopharmacology,
a section of the journal
Frontiers in Pharmacology

Received: 17 September 2020

Accepted: 08 March 2021

Published: 22 April 2021

Citation:

Xie Q, Li H, Lu D, Yuan J, Ma R, Li J,
Ren M, Li Y, Chen H, Wang J and
Gong D (2021) Neuroprotective Effect
for Cerebral Ischemia by Natural
Products: A Review.
Front. Pharmacol. 12:607412.
doi: 10.3389/fphar.2021.607412

Natural products have a significant role in the prevention of disease and boosting of health in humans and animals. Stroke is a disease with high prevalence and incidence, the pathogenesis is a complex cascade reaction. In recent years, it's reported that a vast number of natural products have demonstrated beneficial effects on stroke worldwide. Natural products have been discovered to modulate activities with multiple targets and signaling pathways to exert neuroprotection via direct or indirect effects on enzymes, such as kinases, regulatory receptors, and proteins. This review provides a comprehensive summary of the established pharmacological effects and multiple target mechanisms of natural products for cerebral ischemic injury *in vitro* and *in vivo* preclinical models, and their potential neuro-therapeutic applications. In addition, the biological activity of natural products is closely related to their structure, and the structure-activity relationship of most natural products in neuroprotection is lacking, which should be further explored in future. Overall, we stress on natural products for their role in neuroprotection, and this wide band of pharmacological or biological activities has made them suitable candidates for the treatment of stroke.

Keywords: natural products, cerebral ischemia, neuroprotection, therapeutic application, mechanisms

Abbreviations: t-PA, tissue plasminogen activator; BBB, blood-brain barrier; NVU, neurovascular unit; CNKI, China National Knowledge Internet; FDA Food and Drug Administration; Mcl 1, myeloid cell leukemia 1; Bcl 2, B-cell lymphoma-2; SOD, superoxide dismutase; MDA, malondialdehyde; MCAO, middle cerebral artery occlusion; NF- κ B, nuclear factor kappa B; TLR2/4, toll like receptor 2/4; NOD2, nucleotide-binding oligomerization domain protein 2; TNF α , tumor necrosis factor α ; MAPK, mitogen-activated protein kinase; p-ERK1/2, phosphorylation extracellular regulated kinase 1/2; VEGF, vascular endothelial growth factor; bFGF, basic fibroblast growth factor, NOX2, nicotinamide adenine dinucleotide phosphate oxidase 2; BCCAO, bilateral common carotid arteries; iNOS, inducible nitric oxide synthase; eNOS, endothelial nitric oxide synthase; mTOR, mechanistic target of rapamycin; p-JNK, phosphorylation c-Jun N-terminal kinase; ACE, angiotensin-converting enzyme; AT1R, Ang II type 1 receptor; TNF- α , tumor necrosis factor α ; IL-6, interleukin-6; IL-1 β , interleukin-1 β ; PARP, poly (ADPribose) polymerase; NAD, nicotinamide adenine dinucleotide; OGD, oxygen-glucose deprivation; I/R, ischemic reperfusion; HBMVECs, human brain microvessel endothelial cells; I κ B, inhibitory κ B; PPAR α , peroxisome proliferator-activated receptor α ; PPAR γ , peroxisome proliferator-activated receptor γ ; IRE1, inositol requiring enzyme 1; XBP1 X-Box Binding Protein 1; BDNF, brain-derived neurotrophic factor; RASD1, dexamethasone-induced Ras-related protein 1; ER, estrogen receptor; p Akt, phospho-Akt; GSK 3 β , glycogen synthase kinase 3- β ; CREB, cAMP response element binding protein; HIF-1 α , hypoxia inducible factor-1- α ; GSH-Px, glutathione peroxidase; TJ, tight junction; MMP 9, matrix metalloprotein 9; AQP4, aquaporin 4; Cyt-C, cytochrome C; Sirt 1, silent information regulator 1; HI, hypoxic-ischemia; PAR 1, protease-activated receptor-1; SNpc, substantia nigra pars compacta; PGE2, prostaglandin E2; COX-2, cyclooxygenase; GSH, glutathione; STAT, signal transducer and activator of transcription; Nrf2, nuclear factor erythroid 2-related factor 2; HO-1, heme oxygenase-1; ET-1, endothelin-1; mPTP, mitochondrial permeability transition pore; PAR 1, protease-activated receptor-1; CECs, cerebral endothelial cells; GLT-1, glutamate transporter-1; ERK, extracellular signal-regulated kinase.

INTRODUCTION

Stroke is a disease with high prevalence and incidence (Benjamin et al., 2018). Strokes can be divided into two categories: ischemic and hemorrhagic stroke, and over 80% are ischemic stroke (Zhou et al., 2018). Ischemic stroke is a pathological condition characterized by blood vessels occlusion and insufficient of blood supply. Stroke which is one of the most common causes of disability and death worldwide, seriously endangers human health and brings heavy burden to society and family (Donnan et al., 2008; Kalogeris et al., 2016). The pathological mechanism of cerebral ischemia is a complex cascade reaction, and its severity is related to the time of cerebral ischemia and the depth of the ischemic site (Steliga et al., 2020). The occurrence and development of cerebral ischemia included neuron excitotoxicity, mitochondrial dysfunction, neuroinflammatory damage, oxidative stress, etc. It is generally believed that glutamate excitotoxicity, energy metabolism disorder, and Ca^{2+} overload happened within 24 h of the onset of stroke, accompanied by the generation of free radicals (Guo, Li and Wang, 2009; Manzanero, Santro, Arumugam, 2013). Apoptosis and necrosis also occurred within a few hours of ischemia (Wang, C. et al., 2015). In the subacute phase, brain edema and blood-brain barrier (BBB) destruction happened. Endothelial cells, pericytes, astrocytes, etc are activated and inflammatory factors are released, accompanied with the proliferation of reactive glial cells (Stanimirovic and Satoh, 2000; Liebner et al., 2018). There exists endogenous repair in the late stage of cerebral ischemia, and neurogenesis, glial scars, angiogenesis could be observed (Steliga et al., 2020). Therefore, the occurrence and development of stroke is complicated, which makes its treatment very difficult. Tissue plasminogen activator (t-PA) is the only therapeutic medicine for ischemic stroke approved by Food and Drug Administration (FDA). However, t-PA has a restricted time window of 6 h, and delayed t-PA infusion increases the risk of hemorrhagic transformation and carries high mortality (Group 1995; Hacke et al., 2008). Despite constantly increasing understanding of ischemic stroke pathophysiology through laboratory and clinical studies, the treatment strategy is still not ideal. Therefore, there is an urgent medical need to identify new molecules that can provide neuroprotection against cerebral ischemic or ischemic reperfusion (I/R) injury.

Natural products obtained from natural sources, including plants, animals, fungi and microorganisms. Natural products have played an important role in ancient traditional medicine systems, such as Unani, Chinese and Ayurveda which are still in common use today. Natural products are known to exert additive, synergistic or antagonistic effects on the body. With the pharmacology technology developing, the administration forms of natural products are various, which has drawn much attention for the treatment of stroke from drug discovery to drug delivery (Hermann et al., 2019; Long et al., 2020; Williams et al., 2020). The pathogenesis of stroke is a complex cascade reaction, including neuro-inflammatory damage, oxidative stress, mitochondrial dysfunction, neurotoxicity, blood-brain barrier (BBB) disruption, neurovascular unit (NVU) damage and other factors. In recent years, it's reported that a vast number

of natural products have demonstrated beneficial effects on stroke worldwide (Fei et al., 2020). The neuroprotection of natural products has been discovered to modulate activities via multiple targets and signaling pathways with direct or indirect effects on enzymes, such as kinases, receptors and proteins (Bagli et al., 2016). This wide band of pharmacological or biological activities has made them suitable candidates for the treatment of stroke (Cai et al., 2019; Zhang, C. et al., 2020; Zhong et al., 2020). As a requirement of novel drug development for stroke, there is a focus on the neuroprotection of natural products via multi-targets. Hence, we stress on natural products for their role in neuroprotection (**Figure 1**). This review provides a comprehensive summary of the pharmacological effects and multiple target mechanisms of natural products for cerebral ischemic or I/R injury.

METHODOLOGY

Database searches using Google scholar, PubMed, and China National Knowledge Internet (CNKI) were conducted until July 2020 to include up to date documented information in the present review. For data mining, the following words were used in the databases mentioned above: neuroprotection, natural product, phytoconstituents, natural products cerebral ischemic injury, natural products cerebral ischemic reperfusion injury, *in vivo* and *in vitro* studies for prevention and treatment of stroke. In almost all cases, the original articles or abstracts were obtained and the relevant data was extracted.

Neuroprotective Role of Flavonoids in Ischemic Brain Injury

Flavonoids, a natural bioactive compound found abundant in vegetables, fruits and traditional herbal medicine. Prevention and/or treatment with flavonoids such as baicalin, apigenin, vitexin, quercetin and other flavonoid compounds have shown promising neuroprotective effects against ischemic-induced injury by through increasing neuronal viability, cerebral blood flow and reducing ischemic-related apoptosis (Putteeraj et al., 2018).

Baicalin

Baicalin, mainly derived from the root of *Scutellaria baicalensis* Georgi, is one kind of a crucial flavonoid (**Figure 2A**). This medicinal plant is widely distributed in China, Russia, Mongolia, North Korea and Japan, and has the functions of clearing away heat and dampness, purging fire and detoxification (Zhao et al., 2019). In recent years, baicalin has also been found to have a wide range of neuroprotective effects (Liang et al., 2017; Sowndhararajan et al., 2018). Middle cerebral artery occlusion (MCAO) induced cerebral ischemic injury *in vivo* and oxygen-glucose deprivation (OGD) induced hypoxia injury *in vitro* were implemented. Baicalin at doses ranging from 50 to 200 mg/kg could significantly improve neurological deficit and reduce infarct volume via inhibiting apoptotic and oxidative pathway, including myeloid cell leukemia 1 (Mcl 1), B-cell

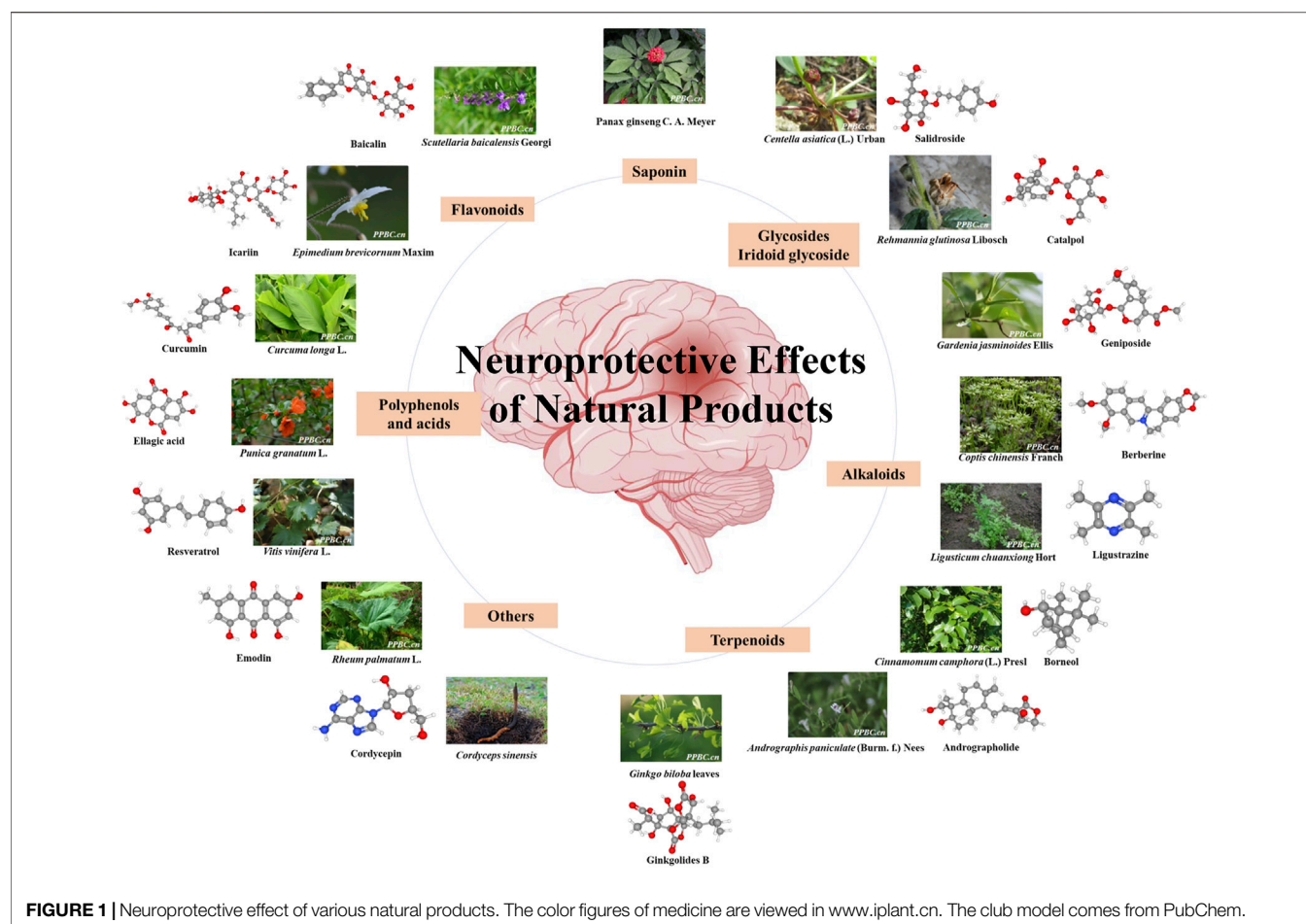


FIGURE 1 | Neuroprotective effect of various natural products. The color figures of medicine are viewed in www.iplant.cn. The club model comes from PubChem.

lymphoma-2 (Bcl 2), superoxide dismutase (SOD), malondialdehyde (MDA), and so on (Cao et al., 2011; Zheng et al., 2015). Neuroprotective activity was also confirmed in another study. Baicalin could decrease nuclear factor kappa B (NF- κ B) p 65 to exert neuroprotection (Xue et al., 2010). In addition, baicalin 100 mg/kg inhibits toll like receptor 2/4 (TLR2/4) signaling pathway in cerebral ischemia rats (Tu et al., 2011). Baicalin down-regulated nucleotide-binding oligomerization domain protein 2 (NOD2) receptor and tumor necrosis factor α (TNF α) expression of neurons with OGD *in vitro* and cerebral ischemia-reperfusion *in vivo* (Li, F et al., 2010). These findings suggested baicalin could afford neuroprotection through multiple pathways.

Scutellarin and Scutellarein

Scutellarin (Figure 2B) and scutellarein (Figure 2C), is the major active component extracted from *Erigeron breviscapus* (Vant.) Hand-Mazz, a Chinese herbal medicine (Zhang et al., 2009). Accumulated data have demonstrated the effectiveness and benefits of breviscapine and scutellarin in treating cerebrovascular disease and cardiovascular disease in clinic and in experimental study (Cao et al., 2008; Wang et al., 2015a; Gao et al., 2017). It has demonstrated that scutellarin is benefit to brain injury caused by cerebral ischemia/reperfusion

due to its anti-oxidation and anti-inflammatory effects and ability to attenuate neuronal damage (Wang and Ma 2018). Scutellarin could effectively suppress the inflammatory response in activated microglia/brain macrophage in experimentally induced cerebral ischemia, whose underlying mechanism was associated with suppressing the phosphorylation c-Jun N-terminal kinase (p-JNK) and p-p38 mitogen-activated protein kinase (MAPK), increasing phosphorylation extracellular regulated kinase 1/2 (p-ERK1/2) (Chen H.-L et al., 2020). In MCAO rats given scutellarin 100 mg/kg treatment, neurological scores were significantly improved coupled with a marked decrease in infarct size, which was found that scutellarin had a neuroprotective effect, amplified TNC1 astrogliosis and activated microglia to remodel injured tissue via notch pathway (Fang et al., 2015; Fang et al., 2016). Pretreated with scutellarin 50 or 75 mg/kg has protective effects for cerebral injury through upregulating endothelial nitric oxide synthase (eNOS) expression and downregulating of vascular endothelial growth factor (VEGF), basic fibroblast growth factor (bFGF), and inducible nitric oxide synthase (iNOS) expression (Hu et al., 2005). Another study also proved scutellarin protected against ischemic injury through regulation of nicotinamide adenine dinucleotide phosphate oxidase 2 (NOX2) and connexin 43 to decrease oxidative damage and apoptotic cell death (Sun, J. B.

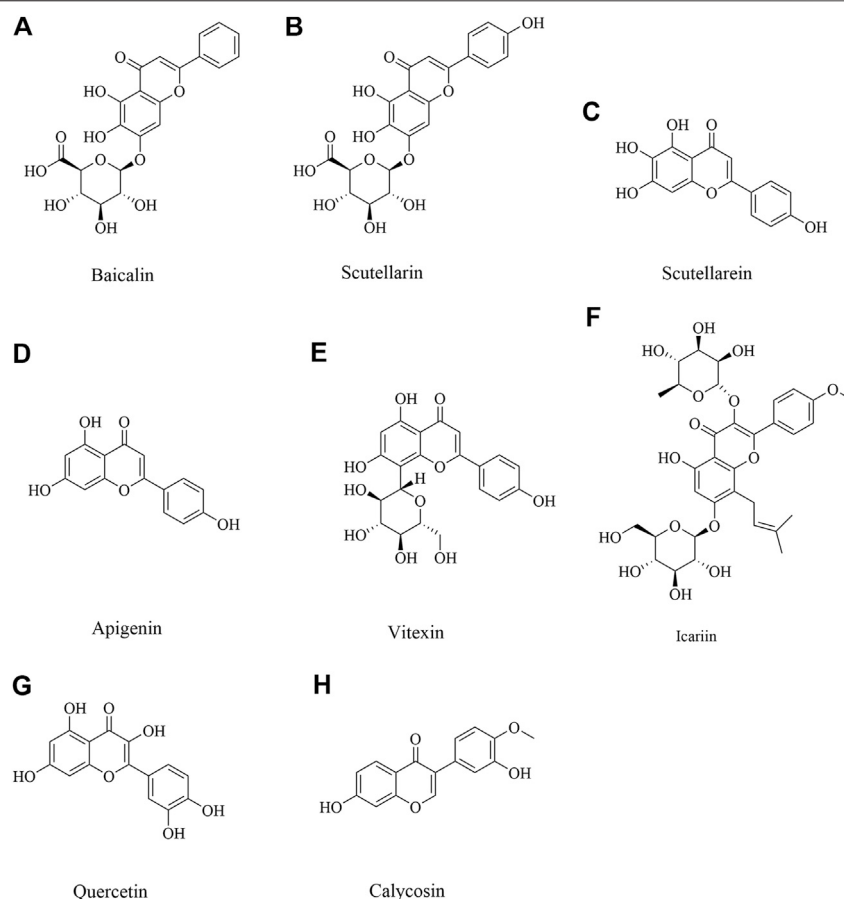


FIGURE 2 | The flavonoids for cerebral ischemia injury.

et al., 2018; Zhang et al., 2009). Scutellarin and scutellarein could improve neuronal injury, and scutellarein had better protective effect than scutellarin through improving the Ca^{2+} -ATPase and Na^+ , K^+ -ATPase activity in rat cerebral ischemia with bilateral common carotid arteries (BCCAO) (Tang et al., 2014). Scutellarin protects brain from acute ischemic injury probably through its inhibitory effect on the angiotensin-converting enzyme (ACE) and Ang II type 1 receptor (AT1R), also TNF- α , interleukin-6 (IL-6), and interleukin-1 β (IL-1 β) (Wang et al., 2016).

Apigenin and Vitexin

Apigenin (**Figure 2D**) is a natural flavonoid and vitexin (**Figure 2E**) is an apigenin flavone glycoside, which were found in several dietary plant foods as vegetables and fruits, and had a variety of pharmacological effects (Babaei et al., 2020). It has been reported that apigenin and vitexin played a protective role in diseases associated with the oxidative process, such as cardiovascular and neurological disorders (Ayoobi et al., 2017; Che et al., 2020; Li, S. et al., 2017). Angiogenesis is one of the ways to repair brain injury. It's reported that apigenin could promote cell proliferation, tube formation, and cell migration while inhibiting apoptosis and autophagy by affecting caveolin-1/VEGF, Bcl-2, caspase-3, Beclin-1, and mechanistic target of

rapamycin (mTOR) expression. What's more, apigenin significantly reduced neurobehavioral scores and volume of cerebral infarction while promoting vascular endothelial cell proliferation by upregulating VEGFR2 to affect caveolin-1, VEGF, and eNOS expression in brain tissue of I/R rats (Pang et al., 2018). Vitexin could also play a protective role by suppressing oxidative stress (Cui et al., 2019). In addition, vitexin regulated cell apoptosis and autophagy via MAPK and mTOR/Ulk1 pathway to attenuate cerebral I/R injury (Wang et al., 2015b; Jiang et al., 2018). Apigenin also showed long-term therapeutic effect in cognitive impairments after cerebral I/R injury (Tu et al., 2017). Above all, it suggested apigenin and vitexin had neuroprotective effect through inflammation, angiogenesis, apoptosis and autophagy pathways with multi-targets.

Icariin

Icariin (**Figure 2F**), an active flavonoid extracted from *Epimedium brevicornum* Maxim, has been proven to possess a wide range of efficacy including anti-tumor, anti-oxidant, anti-bacterial and anti-inflammatory, etc (Luo et al., 2007; Zhou et al., 2011). It has been also reported to alleviate brain injury and attenuate cognitive deficits (Li, H. et al., 2010; Li et al., 2005).

Xiong et al. and Deng et al. found that pretreatment with Icariin and Icariside II, a metabolite of icariin, could decrease neurological deficit score, diminish the infarct volume, and reduce IL-1 β and transforming growth factor- β (TGF- β 1). Moreover, Icariin suppressed inhibitory κ B (I κ B)- α degradation and NF- κ B activation and up-regulated peroxisome proliferator-activated receptor α (PPAR α) and peroxisome proliferator activated receptor γ (PPAR γ) levels in I/R model (Deng et al., 2016; Xiong et al., 2016). Moreover, a study by Mo et al. found that Icariin can inhibit apoptosis and inflammatory in neurons after OGD/R through inositol requiring enzyme 1 (IRE1)- X-Box Binding Protein 1 (XBP1) signaling pathway (Mo et al., 2020).

Quercetin

Quercetin (Figure 2G), is a common flavonoid found in many fruits and vegetables (Lee et al., 2003). It has been reported that quercetin has an anti-oxidative property, anti - inflammation and immunity, anti-cancer, etc (Costa et al., 2016; Li, W. et al., 2016; Shafabakhsh and Asemi 2019; Xu, D. et al., 2019). A study by Jin et al. found that quercetin could increase the expression of ZO-1, Claudin-5, β -catenin, and LEF1, and decrease the expression of MMP-9, GSK-3 β and axin to reduce brain edema and BBB leakage and improve BBB dysfunction, which suggested the neuroprotection of quercetin was related to Wnt/ β -catenin pathway (Jin et al., 2019). Calcium acts as a second messenger that mediates physiologic functions. It's reported that quercetin exerted a preventative effect through attenuation of intracellular calcium overload and restoration of down-regulated hippocampal expression during ischemic injury (Park et al., 2020). Moreover, quercetin alleviated the increase of protein tyrosine and serine/threonine phosphatase activity, along with the reduction of ERK and Akt phosphorylation in cerebral I/R injury (Wang, Y. Y. et al., 2020). In addition, iso-quercetin protected against oxidative stress and neuronal apoptosis via Nrf2-mediated inhibition of the NOX4/ROS/NF- κ B signaling pathway in cerebral ischemic stroke (Dai et al., 2018).

Calycosin

Calycosin (Figure 2H), an isoflavone phytoestrogen isolated from *Astragalus membranaceus*, is found to possess various potential pharmacological activities, such as, anti-tumorigenesis, anti-oxidation, anti-virus and apoptosis-modulation effects (Chen, J et al., 2015; Wang and Zhao, 2016; Zhao, Y. et al., 2016). It was also demonstrated that calycosin 30 mg/kg could ameliorate both the neurological deficit and infarct volume in experimental cerebral ischemia reperfusion injury, and the mechanism might be attributed to its antioxidant effects (Guo et al., 2012). Post-stroke calycosin 30 mg/kg therapy increased brain-derived neurotrophic factor (BDNF)/TrkB to ameliorate the neurological injury due to switching the microglia from the activated amoeboid state to the resting ramified state in ischemic stroke rats (Hsu et al., 2020). Calycosin exhibited a downregulation of dexamethasone-induced Ras-related protein 1 (RASD1), and an upregulation of estrogen receptor (ER)- α and Bcl-2 (Wang, X. et al., 2014). A study by Wang et al. found that calycosin pretreatment for 14 days dramatically upregulated p62, neighbor

of BRCA1 gene 1 (NBR1) and Bcl-2, and downregulated TNF- α to ameliorate neurological scores in cerebral I/R rats (Wang, L. et al., 2018).

Neuroprotective Role of Alkaloids in Ischemic Brain Injury

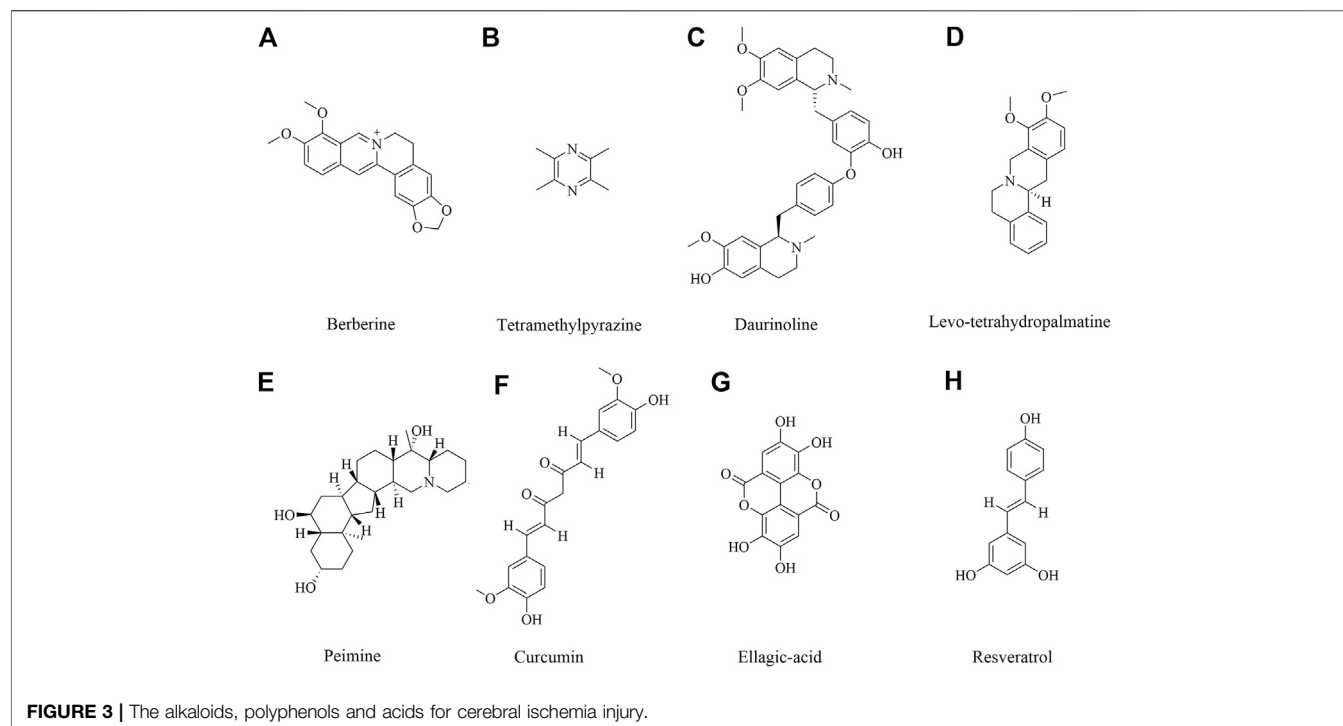
Alkaloids are rated as among the most-investigated plant secondary metabolites with versatile biological activity (Qiu et al., 2014). Recent investigations have pointed out the dynamic role of alkaloids as antibacterial, antidepressant, antioxidant, anti-inflammation (Perviz et al., 2016; Li et al., 2020; Liu et al., 2020; Rosales et al., 2020). Accordingly, alkaloids are emerging as pharmaceutical tools for neuroprotective effects (An et al., 2020). Alkaloids were investigated on neuroprotective effects including berberine, ligustrazine, tetrahydropalmatine and others.

Berberine

Berberine (Figure 3A) is an isoquinoline alkaloid isolated from traditional herbal medicine. It is widely present in the roots, rhizomes, stems or bark of various natural plants, such as *Coptis chinensis* Franch., *Phellodendron chinense* Schneid., etc. These plants have been used for thousands of years (Wang et al., 2019a; Fan et al., 2019). Studies have shown that berberine has a variety of pharmacological activities, including anti-microbial, anti-tumor, lowering glucose, lowering cholesterol, anti-inflammatory, antioxidant, immunomodulatory and neuroprotective effects (Asemi et al., 2020; Song et al., 2020). So far, the neuroprotective effect of berberine has been involved (Lin and Zhang 2018). Berberine could improve the survival rate in OGD/R cells and improve the neurological deficiency in cerebral ischemic injury, which was involved in reducing the expression of cleave caspase 3 and up-regulating the expression of p-Bad to inhibit cell apoptosis via TrkB-PI3K/Akt pathway to promote neuron growth (Hu et al., 2012; Chai et al., 2013; Yang et al., 2018a). Other studies also showed berberine 40 mg/kg preconditioning had neuroprotective effects by promoting autophagy, reducing cell apoptosis via PI3K/Akt signaling pathway (Zhang et al., 2016a; Zhang et al., 2016b). In addition, berberine exerted the neuroprotective effects by regulating I/R-induced peripheral lymphocytes early immunoactivation (Song et al., 2012). A study by Zhang et al. found that neuroprotection of early and short-time applying berberine could upregulate p-Akt, p-GSK 3 β and phosphor cAMP response element binding protein (p-CREB) and downregulate NF- κ B expression to ameliorate BBB permeability in the acute phase of cerebral ischemia (Zhang et al., 2012).

Tetramethylpyrazine

Tetramethylpyrazine (Figure 3B), also called ligustrazine, is a kind of alkaloids identified in *Ligusticum chuanxiong* Hort, which has been used to treat cardiovascular and cerebrovascular diseases for hundreds of years in ancient China (Zhao, X. et al., 2016; Zheng, J. S. et al., 2018). In recent study, *Ligusticum chuanxiong* Hort and its main active compound ligustrazine have been



studied and had anti-inflammatory, anti-oxidant and analgesic effect (Kao et al., 2006; Zou et al., 2018). Tetramethylpyrazine treatment with 20 mg/kg suppressed hypoxia inducible factor-1- α (HIF-1 α), TNF- α , and activated caspase-3 expression in MCAO-induced brain ischemia in rats (Chang et al., 2007). Tetramethylpyrazine 20 mg/kg inhibited neutrophil activation via elevating nuclear related factor 2 (Nrf2) and heme oxygenase-1 (HO-1) expression and inhibiting high-mobility group box-1 protein (HMGB1)/toll-like receptor-4 (TLR4), Akt, and ERK pathway following cerebral ischemia rats (Chang et al., 2015). Tetramethylpyrazine analogues were also investigated to induce p-eNOS by activation of PI3K/Akt and TLR-4/NF- κ B signaling pathway and regulate the expression of tight junction (TJ) proteins, matrix metalloprotein 9 (MMP-9) and aquaporin 4 (AQP4) under cerebral I/R injury (Yan et al., 2015; Xu et al., 2017; Zhou et al., 2019). The similar finds of PI3K/Akt pathway also were shown in another study (Ding et al., 2019). What's more, the synergistic effect of drugs has also been shown to have good therapeutic effect. Ligustrazine accompanied with borneol could attenuate I/R injury by downregulating IL-1 β , IL-6, and TNF- α , upregulating SOD, GSH-Px and regulating apoptosis and autophagy (Yu, B. et al., 2017; Yu et al., 2016).

Daurinoline

Daurinoline (Figure 3C) is a kind of dibenzyl tetrahydroisoquinoline alkaloid, isolated from *menispermum dauricum* DC., which has a variety of pharmacological activities, including neuroprotective effect (Zhang et al., 2011). Daurinoline 10 mg/kg and 20 mg/kg could enhance of SOD activity and the ability of scavenging oxygen free radicals (Lan and Lianjun 2020). Daurinoline reduced the level of MDA in

brain tissue and increase the activity of SOD to prevent and ameliorated energy metabolism disturbance of cortex and mitochondria of brain induced by repeatedly cerebral ischemia reperfusion (Li and Gong 2004). In addition, daurinoline 5 and 10 mg/kg could inhibit cytochrome c (Cyt-C) release and caspase-3 and caspase-9 to inhibit neuronal cells apoptosis in the penumbra after cerebral ischemia (Yang et al., 2009).

Levo-tetrahydropalmatine

Levo-tetrahydropalmatine (Figure 3D) are a series of alkaloids, isolated from a Chinese analgesic medicine, called *Corydalis yanhusuo* W. T. Wang. *L*-Tetrahydropalmatine, one of its main active ingredients, has been demonstrated to have potent analgesic effects and has been used in Chinese clinical practice for this purpose for many years (Chu et al., 2008; Han et al., 2012; Kang et al., 2016). Recent work showed that *L*-tetrahydropalmatine suppressed the central excitatory effects of amphetamine (Chang and Lin 2001), and played a protective role against neuronal injury in animal models (Liu et al., 2005; Mantsch et al., 2007; Chen et al., 2012). Levo-tetrahydropalmatine could regulate Src and c-Abl expression to inhibit neuron apoptosis and attenuate BBB injury in cerebral ischemic animals (Mao et al., 2015; Sun, J. B et al., 2018).

Peimine

Peimine (Figure 3E) is a major biologically active component of *Fritillaria ussuriensis*. Recent studies have shown that isosteroidal alkaloids in *Fritillaria* had a wide range of pharmacological activities besides its role in cough remedies (Li, J. et al., 2019; Li et al., 2020a; Zhang et al., 2020a; Zhao et al., 2018). It's also reported that peimine had protective effects on cerebral I/R injury

in rats. The mechanism of neuroprotective effect might be related to inhibition of apoptosis, oxidative stress and inflammatory response, reduction of pathological damage and neurological dysfunction through regulation of the PI3K/Akt/mTOR pathway (Guo et al., 2019; Duan et al., 2020).

Neuroprotective Role of Polyphenols and Acids in Ischemic Brain Injury

Polyphenols, a bioactive compound, were found abundant in vegetables, fruits and medical plant. Neuroprotection of polyphenols in medical plants is getting attention in the world. Curcumin, ellagic acid, resveratrol has been extensively studied and show multi-function. They are neuroprotectants, antioxidants, anti-inflammatory and antithrombic agents. It's reported that the neuroprotective efficacy of these compounds was involved in mitigating brain infarction and global ischemia, improving cerebral blood circulation (Lin 2011).

Curcumin

Curcumin (Figure 3F), a polyphenolic compound extracted from *Curcuma longa* L., has potential anti-inflammatory, cardiovascular protective effect and neuroprotection. Recent studies demonstrated the neuroprotective effect of curcumin against cerebral ischemic injury through oxidation, apoptosis, autophagy pathways (Eghbaliferiz et al., 2020; Forouzanfar et al., 2020; Ułamek-Kozioł et al., 2020). Rats or mice with cerebral ischemic injury that received curcumin at 10–400 mg/kg exhibited significantly alleviated brain injury. Moreover, a more SOD, GSH-Px and glutathione (GSH) and a lower MDA, NO contents were found in curcumin administrated animals (Thiyagarajan and Sharma 2004; Li, Y. et al., 2016), which suggested the mechanism of curcumin was related to antioxidative activity. In addition, curcumin was proven to suppress the release of inflammatory cytokines via NF- κ B, signal transducer and activator of transcription (STAT), Akt/mTOR, ERK signaling pathways (Huang et al., 2018; Li et al., 2015; Mukherjee et al., 2019; Xu, H. et al., 2018). Moreover, Bax, Bcl 2, caspase 3, LC3 II activity and other autophagy and apoptosis cytokines were also reversed by curcumin (Hou et al., 2019; Huang et al., 2018; Wang et al., 2005; Xie, C. J. et al., 2018; Xu, L. et al., 2019; Zhang et al., 2018a). Furthermore, curcumin promoted neuron survival *in vitro* to exert neuroprotective effects against ischemia injury (Lu et al., 2018; Xie, W. et al., 2018; Zhang, X. et al., 2018).

Resveratrol

Resveratrol (Figure 3G), also named 3,4,5-trihydroxy-trans-stilbene, a natural polyphenolic compound, occurs naturally in grapes and a variety of medicinal plants, and possesses multiple biological activities (Santos et al., 2019; Thapa et al., 2019). The effect of resveratrol on cerebral ischemic injury was also explored. Resveratrol dosage at 10–100 mg/kg marked improved neurological deficiency and protected against cerebral ischemic injury through PI3K/Akt, NF- κ B and other pathways (Lei et al., 2020; Simao et al., 2012a; Simao et al., 2012a; Yu, P. et al., 2017). Resveratrol treatment could obviously upregulate nuclear factor

erythroid 2-related factor 2 (Nrf2) and heme oxygenase-1 (HO-1) to ameliorate oxidative damage in cerebral ischemic injury (Ren et al., 2011; Yang et al., 2018b; Gao et al., 2018). Furthermore, MDA, NO, SOD could be reversed by resveratrol administration (Jie et al., 2020; Tsai et al., 2007; Xu, J. et al., 2018). Silent information regulator 1 (Sirt 1) is a NAD + dependent deacetylase, which plays an important role in cerebral I/R injury (She et al., 2017). It's reported that resveratrol protected against cerebral ischemic injury by inhibiting NLRP3 inflammasome activation, improving alterations in mitochondrial and glycolytic function through Sirt1 pathway (Della-Morte et al., 2009; Koronowski et al., 2015; He et al., 2017; Koronowski et al., 2017). Moreover, resveratrol could inhibit inflammatory response, including prostaglandin E2 (PGE2), cyclooxygenase (COX)-2, NOS and MMP 9 to alleviate neurological deficits (Candelario-Jalil et al., 2007; Simao et al., 2012b; Wei et al., 2015). In addition, resveratrol could improve brain energy metabolism via inhibiting xanthine oxidase activity and preventing the production of hypoxanthine, xanthine and oxygen radicals (Li et al., 2011). These findings suggested resveratrol could reduce cerebral ischemia injury through multiple pathways.

Ellagic Acid

Ellagic acid (Figure 3H), an important cell protective and antioxidant compound, is a low molecular weight polyphenol derived from several fruits, vegetables and nuts (De Oliveira, 2016). Ellagic acid are recently more taken into accounts since their promising pharmacological effects, such as, anti-inflammation, anti-oxidant and anti-cancer (Ceci et al., 2018; Baradaran Rahimi et al., 2020). In recent study, ellagic acid is investigated as a potential endowed with multi-target pharmacological properties on central nervous system (Alfei et al., 2019). BCCAO was carried out to make global cerebral ischemic injury. Ellagic acid pretreatment with 100 mg/kg could reduce MDA level and restore the heart rate to normal level (Nejad et al., 2015). In addition, ellagic acid 100 mg/kg could activate PI3K/Akt/NOS pathway to alleviate brain injury and protect brain tissue in MCAO model (Kaihua and Jiyu 2020). Furthermore, ellagic acid administration with 10–90 mg/kg could improve brain injury outcomes and increase the proliferation of NSCs through the Wnt/ β -catenin signaling pathway (Liu, Q. S. et al., 2017). The upregulation of zonula occludens-1 (ZO-1) and down-regulation of AQP 4 and MMP-9 in injured brain tissues after being treated ellagic acid 10–50 mg/kg (Wang et al., 2019b).

Neuroprotective Role of Glycosides in Ischemic Brain Injury

Asiaticoside

Asiaticoside (Figure 4A) is isolated from *Centella asiatica* (L.), which has been using as a memory enhancing and psychoactive drug for a long time in Asia (Zheng and Qin 2007). Many studies have shown that *C. asiatica* indeed has many biological activities in central nervous system (Mook-Jung et al., 1999; Zheng and Qin 2007; Dhanasekaran et al., 2009; Orhan 2012). A report demonstrated asiaticoside showed anti-inflammation effect via

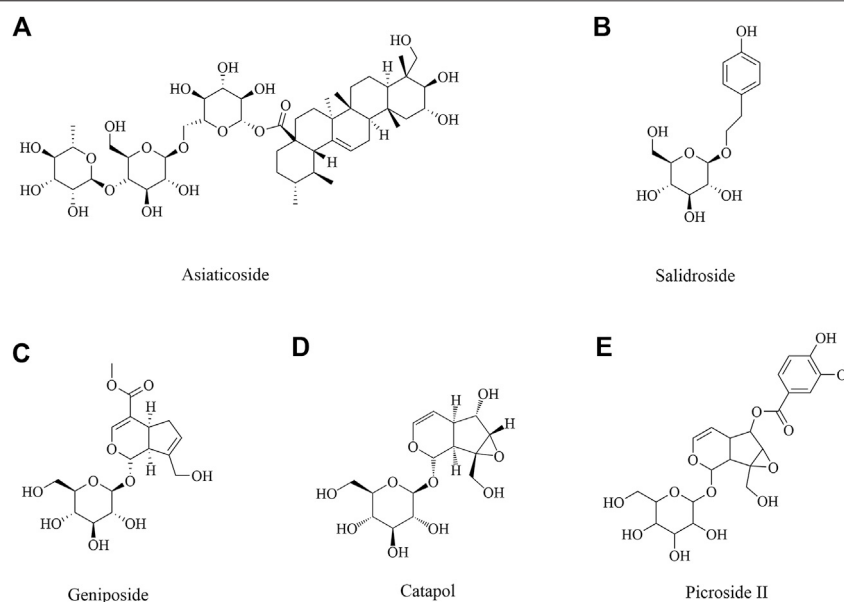


FIGURE 4 | The glucosides for cerebral ischemia injury.

inhibiting overactivation of p38 MAPK pathway against cerebral I/R mice (Chen et al., 2014). Another study found asiaticoside showed a protective effect against cerebral I/R injury via the NOD2/MAPK/NF- κ B signaling pathway (Zhang et al., 2020b).

Salidroside

Salidroside (Figure 4B), the major phenylpropanoid glycoside extract from medicinal Tibetan plant *Rhodiola rosea* L, has diverse pharmacological activities. Many recent reports and reviews have highlighted that salidroside may exert anti-inflammatory, neuroprotective effects and improve cognitive function (Li, M. et al., 2018; Xu, N. et al., 2019). Salidroside may involve the modulation of monoamine metabolism in the striatum and substantia nigra pars compacta (SNpc), which may be related to the function of the dopaminergic system in the cerebral I/R brain (Zhong et al., 2019). Many studies reported salidroside protected against cerebral I/R injury via PI3K/Akt pathway, accompanying with Nrf2/NF- κ B pathway (Wei et al., 2017; Zhang, Y. et al., 2018; Zhang, J. et al., 2019; Zuo et al., 2018). Salidroside exhibited neuroprotective effects against hypoxia/reperfusion injury by activating the SIRT1/FOXO3 α pathway (Xu, L. et al., 2018). In addition, salidroside is an effective treatment for ischemic stroke that functions via the fibroblast growth factor 2 (FGF2)-mediated cAMP/PKA/CREB pathway to promote dendritic and synaptic plasticity (Li et al., 2020b). Salidroside treatment reduced the expression of M1 microglia/macrophage markers and increased the expression of M2 microglia/macrophage markers after stroke and induced primary microglia from M1 phenotype to M2 phenotype (Liu et al., 2018). What's more, salidroside reduced the markers of endothelial activation and neutrophilic infiltration after I/R injury by inhibition of complement, restoring an anti-inflammatory endothelial

phenotype after oxidative stress and inhibiting classical complement activation, in association with anti-apoptotic effects (Wang, Y. et al., 2020).

Neuroprotective Role of Iridoid Glycosides in Ischemic Brain Injury

Iridoid glycosides are special glycosides. Iridoid glycoside exists broadly in plants of many families and has a wide variety of biological activities including purgative, liver protective, anti-microbial, analgesic, antitumor, sedative and anti-inflammatory activities (Ismailoglu et al., 2002). Geniposide, Catalpol and Picroside II were investigated in depth as iridoid glycosides, which had a neuroprotective effect.

Geniposide

Geniposide (Figure 4C), as an iridoid glycoside, was initially isolated from the herb *Gardenia jasminoides* Ellis (Wang et al., 1992), which has been noted for its variable pharmacological effects, including anti-oxidation, anti-inflammation, and anti-diabetes effects, among others (Koo et al., 2006; Wu et al., 2009). Previous studies showed that geniposide induced neuronal differentiation and attenuated cell injury (Liu et al., 2009; Yin et al., 2010). To date, there were some studies about the cerebral ischemia injury. Geniposide treatment after neonatal hypoxic-ischemia (HI) insult attenuated cell apoptosis, IgG leakage, microgliosis, astrogliosis, pericytes loss and junction protein degradation, which might be through the activation of PI3K/Akt pathway (Liu, F. et al., 2019). Geniposide attenuated inflammatory response by suppressing P2Y₁₄ receptor and downstream ERK1/2 pathway in brain microvascular endothelial cells (BMECs) with OGD (Huang et al., 2017; Li, Y. et al., 2016). What's more, geniposide in neuroprotection by

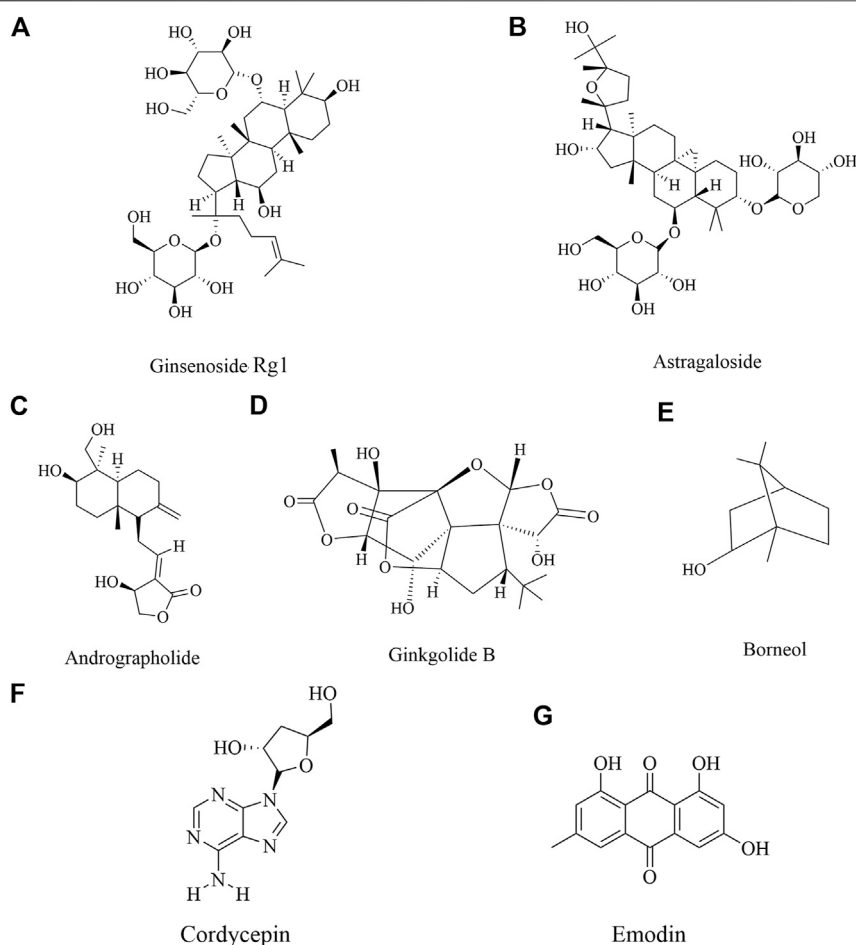


FIGURE 5 | The saponin, terpenoids and others for cerebral ischemia injury.

activating autophagy and inhibiting NLRP3 inflammasome in microglial cells (Fu et al., 2020).

Catalpol

Catalpol (**Figure 4D**) is the main active component of the radix from *Rehmannia glutinosa* Libosch, and it belongs to the iridoid monosaccharide glycoside family (Ismailoglu et al., 2002; Zhang et al., 2008), which has pleiotropic protective effects on many diseases, including neurodegenerative diseases (Xia et al., 2012), ischemic stroke (Zhu et al., 2010), metabolic disorders (Zhu et al., 2010) and others. It's reported that the efficacy of catalpol pretreatment on cerebral I/R injury may be attributed to reduction of free radicals and inhibition of lipid peroxidation and endothelin-1 (ET-1) production (Liu, H. et al., 2014). Additionally, a study by Li et al. found catalpol also exerted the most significant cytoprotective effect on astrocytes by suppressing the production of free radicals and elevating antioxidant capacity (Li et al., 2008). What's more, catalpol significantly inhibited apoptosis by modulating Bcl-2 and Bax (Li et al., 2006). Catalpol affected angiogenesis via the JAK2/STAT3 signaling pathway and VEGF expression (Dong, W et al., 2016).

Picroside II

Picrorhiza scrophulariflora belongs to the plant family composed of picroside I, II and III, of which picroside II (**Figure 4E**) is one of the most effective components extracted from the dried rhizome and roots of *Picrorhiza kurrooa* Royle ex Benth and *Picrorhiza scrophulariae flora* Pennell (Stuppner and Wagner 1989; Wang et al., 1993). Current researches on picroside II are focused on its neuroprotective, anti-apoptotic, anti-cholestatic, anti-oxidant, anti-inflammation, immunomodulating activities (Cao et al., 2007; Li et al., 2007; He et al., 2009). It has been confirmed that picroside II 25 mg/ml could enhance nerve growth factor - induced PC12 cell axon growth, reduce H₂O₂ induced PC12 cell damage and improve cell survival *in vitro* (Cao et al., 2007). Picroside II attenuated cerebral I/R injury via inhibiting apoptosis and inflammation, included COX2, TLR4/NF- κ B and MEK-ERK1/2 pathway (Guo et al., 2010; Wang, F. et al., 2015; Wang, L. Y. et al., 2015). Picroside II could protect BBB possibly through reducing oxidative stress factors (ROS, NOX2 ROCK, MLCK, and MMP-2) and enhancing BBB function factors, claudin-5 (Zhai et al., 2017). Furthermore, picroside II exerted a neuroprotective

effect by inhibiting the mitochondria Cyt C signal pathway and decreasing the permeability of mitochondrial permeability transition pore (mPTP) following I/R injury in rats (Zhang et al., 2017; Li, Q et al., 2018).

Neuroprotective Role of Saponin in Ischemic Brain Injury

Ginsenoside Rg1 (Figure 5A) is the representative components in saponin. Ginsenoside Rg1 is one of the main active ingredients of ginseng (Zhang and Zhao 2014; Chuang et al., 2015). It has been shown that as a small molecular substance, ginsenoside Rg1 easily passes through the blood brain barrier. Moreover, ginsenoside Rg1 could promote stem cell orientation transformation, induce stem cell proliferation and played a neuroprotective role in brain repair (Cheng et al., 2005; Tang et al., 2017; Xie, C. J. et al., 2018). It's reported that ginsenoside Rg1 could relieve the I/R injury through multiple pathways. Ginsenoside Rg1 could improve neurological injury, regulate BBB disruption and permeability and downregulate AQP 4 and protease-activated receptor-1 (PAR 1) (Zhou et al., 2014; Xie et al., 2015). Ginsenoside Rg1 alleviated oxidative stress after I/R through inhibiting miR-144 activity and subsequently promoting the Nrf2/ARE pathway (Chu et al., 2019). What's more, a study by Li et al. found that ginsenoside Rg1 may exert its neuroprotective action on cerebral I/R injury through the activation of PPAR γ signaling (Li et al., 2017). In addition, it's also shown that ginsenoside Rg1 treatment obviously decreased cell apoptosis, while the transplanted cells could be differentiated into neurons and glial cells, which also improved cerebral ischemia (Bao et al., 2015). Other studies showed that ginsenoside Rg1 40 mg/kg was attributed to a decrease in ubiquitinated aggregates and a suppression of the inflammatory response and increased in the expression of BDNF in the hippocampal CA1 region after I/R insult (Wang, Y. et al., 2018; Zheng et al., 2019).

Astragaloside IV

Astragaloside IV (Figure 5B) is a triterpenoid saponin existing in the root of *Astragalus membranaceus*. Astragaloside IV also has a variety of pharmacological effects, such as anti-inflammatory, anti-cancer, anti-fibrosis, anti-oxidation stress, immunomodulatory through multiple signals (Ren et al., 2013; Zhang, X. et al., 2019). Meanwhile, it showed that astragaloside IV could inhibit neuroinflammation by reducing BBB permeability and lymphocyte infiltration, and played a neuroprotective role through mitochondrial pathway, antioxidant, anti-inflammatory and anti-apoptotic effects (Costa et al., 2018; Song et al., 2018), which mainly regulated JNK3, FAS, FasL, caspase-8, Bid, caspase-3 and cyto C, p62, Bax/Bcl-2, LC3II/LC3I (Li et al., 2019; Liu et al., 2013; Yin et al., 2020; Zhang, J. et al., 2019). In addition, astragaloside IV could also inhibit neutrophil adhesion related molecules (TNF- α , NF κ B, IL-1 β , etc.) to play an anti-inflammatory role, and had neuroprotective effect on cerebral I/R injury (Li et al., 2012).

NEUROPROTECTIVE ROLE OF TERPENOID IN ISCHEMIC BRAIN INJURY

Andrographolide

Andrographolide (Figure 5C), a labdane diterpene lactone, is the most active and important constituent isolated from the leaves of *Andrographis paniculata* (Burm. f.) Nees (Acanthaceae) (Coon and Ernst 2004). Recent studies demonstrated that andrographolide possesses anticancer, anti-inflammatory and hepatoprotective activities, also neuroprotective effect (Negi et al., 2008; Bao et al., 2009). Andrographolide reduced NOX2 and iNOS expression possibly by modulating PI3K/AKT-dependent NF- κ B and HIF-1 α activation, which mediated the protective effect in the cerebral I/R mice (Chern et al., 2011). Studies by Yen et al. found andrographolide could play an important role to cerebral endothelial cells (CECs). Furthermore, andrographolide increased Nrf2/HO-1 expression through p38 MAPK regulation, which provided protection against I/R injury (Yen et al., 2013; Yen et al., 2016).

Ginkgolides

Ginkgolide B (Figure 5D) were one of ten kinds of diterpene lactone compounds, which were isolated from *Ginkgo biloba* leaves. It's reported that exact of *Ginkgo biloba* had a broad range of pharmacological effects, such as anti-inflammation, antioxidant, anti-depressant (Chen, C et al., 2017; Hu et al., 2018; Jin, G et al., 2014; Ran et al., 2014; Saini et al., 2014; Wan et al., 2016). Ginkgolides B upregulated the levels of antioxidant proteins through Akt/Nrf2 pathway to protect neurons from oxidative stress injury (Liu, Q. et al., 2019). In addition, ginkgolide B improved neurological function by promoting the proliferation and differentiation of neural stem cells in rats with cerebral I/R injury (Zheng et al., 2018b).

Borneol

Borneol (Figure 5E) is a terpene and bicyclic organic compound, a resin from *Cinnamomum camphora* (L.) Presl, a traditional Chinese medicine (Yin et al., 2017; Zheng et al., 2018a). As a traditional Chinese medicine, borneol has been used for thousands of years in the treatment of cardiovascular and cerebrovascular diseases. Modern pharmacological studies have shown that borneol had anti-inflammatory, antioxidant stress, anti-apoptosis and other pharmacological effects (Almeida et al., 2013). Borneol protected against cerebral I/R injury through multifunctional cytoprotective pathways, involving in the alleviation of intracellular ROS and iNOS/NO pathway, inhibition of inflammatory factor and depression of caspase-related apoptosis. Additionally, the inhibition of I κ B α /NF- κ B pathway might play a significant role in the neuroprotection of borneol (Liu et al., 2011). Another study by Dong et al. found that borneol could alleviate cerebral ischemic injury, most likely executed via anti-apoptosis and anti-inflammation effects and maintenance of the BBB stability and TJs to comprehensively improve NVU function (Dong et al., 2018). Additionally, the protection of OGD induced

BMECs by tetramethylpyrazine phosphate and borneol combination involved anti-oxidation, apoptosis inhibition, and angiogenesis (Yu et al., 2019).

NEUROPROTECTIVE ROLE OF OTHER COMPOUNDS IN ISCHEMIC BRAIN INJURY

Emodin

Emodin (**Figure 5F**), 1,3,8-trihydroxy-6-methylantraquinone, is a naturally occurring anthraquinone derivative and an active component from *Polygonum multiflorum* Thunb. *Rheum palmatum* L. etc, which have been used widely in Asia in treatment of multiple diseases (Dong, X. et al., 2016). Emodin has been demonstrated to possess a wide spectrum of pharmacological effects, such as anti-viral, anti-bacterial, anti-allergic, anti-osteoporotic, immunosuppressive, neuroprotective activities (Dong, W. et al., 2016; Leung et al., 2020; Xue et al., 2020). In fact, the neuroprotective effect of *Polygonum multiflorum* Thunb was first published in 2000 (Gu et al., 2000) and the neuroprotective effect of emodin was published in 2005 when its ability to interfere with the release of glutamate was identified as a method of neuroprotection (Gu et al., 2005). Additionally, emodin might afford a significant neuroprotective effect against glutamate-induced apoptosis through the critical role including Bcl-2/Bax, active caspase-3, p-Akt, p-CREB, and mature BDNF for potent neuroprotective effects of emodin to subsequently enhance behavioral function in cerebral ischemia (Ahn et al., 2016). Another study by Leung et al. found emodin had neuroprotective effects against I/R or OGD injury both *in vitro* and *in vivo*, which may be increase Bcl-2 and glutamate transporter-1 (GLT-1) expression but suppress activated-caspase 3 levels through activating ERK1/2 pathway (Leung et al., 2020).

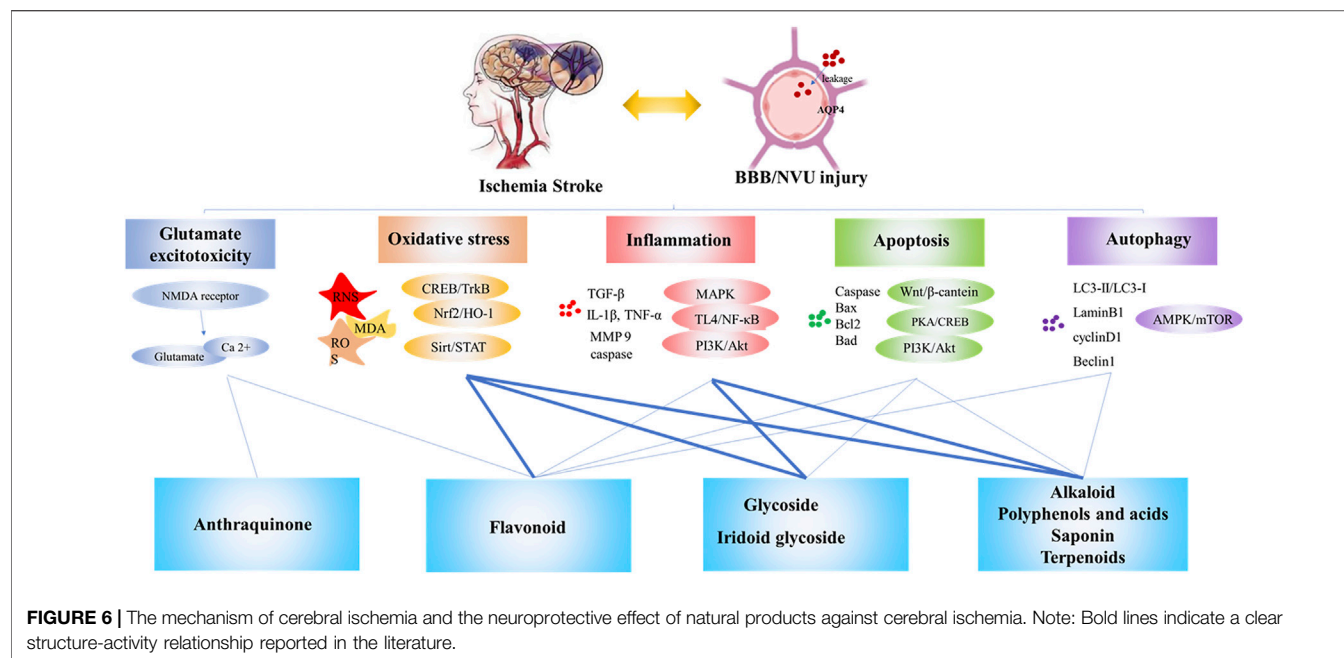
Cordycepin

Cordycepin (**Figure 5G**) is a derivative of nucleoside adenosine and one of the main active components of *Cordyceps sinensis*, which is mainly distributed in Europe, North America and Asia (Tuli et al., 2013; Wang, Y. et al., 2015). Cordycepin has a variety of pharmacological activities, such as anti-inflammatory, anti-tumor, antioxidant, anti-inflammatory microorganism, anti-hyperlipidemia, anti-hepatotoxicity, anti-depressant and neuroprotective activities (Ryu et al., 2014; Wang et al., 2015a; Qin et al., 2019). It was shown that cordycepin had an important neuroprotective effect on hypoxic injury by improving the electrophysiological function of neurons (Chen, K. et al., 2017; Liu, Z. B et al., 2015). It is confirmed that cordycepin could significantly reduce glutamic acid and aspartic acid, increase SOD activity and down-regulate MDA and MMP-3 to alleviate cerebral ischemic injury or hypoxia injury, suggesting cordycepin could inhibit oxidative damage to exert neuroprotection (Hwang et al., 2008; Cheng et al., 2011). Cordycepin regulated adenosine A1 receptor to improve long-term potentiation formation and neuronal survival through p38/JNK/ERK pathway in BCCAO model and

glutamate-induced HT22 neuronal cell death (Dong et al., 2019; Jin, M. L et al., 2014).

Polysaccharides

Polysaccharides are considered to have a wide range of pharmacological effects, such as scavenging free radicals, immune regulation, anti-tumor, anti-oxidation, anti-viral, anti-inflammatory, lowering blood sugar, anti-depression, liver protection, etc (Jin et al., 2012; Kwok et al., 2019; Fang et al., 2020). Panax notoginseng polysaccharide is a kind of heteroglycan derived from the medicinal plant *Panax notoginseng*, which could increase the ratio of Bcl-2/Bax and reduce caspase-3 in cerebral ischemic brain tissue (Jia et al., 2014). What's more, it could enhance GSH-Px, SOD activity and IL 10 level, while downregulate MDA, TNF- α , IL-1 β level to reduce cerebral infarction size and cell apoptosis to afford neuroprotective effect (Jia et al., 2014; Sy et al., 2015). Angelica polysaccharide is the main active ingredient of *Angelica sinensis* (Oliv.) Diels, which could also enhance the activities of SOD, GSH and GSH-PX, and reduce MDA, IL-1 β , TNF- α and NF- κ B in cerebral ischemia-reperfusion injury rats (Yan and Xie, 2018; Dai et al., 2020), in addition, enhance angiopoietin 1, angiopoietin 2, VEGF to promote angiogenesis (Hu et al., 2006; Li, J. et al., 2019). Ginkgo biloba polysaccharides could also play a neuroprotective effect by inhibiting oxidative stress and inflammation to improve neurological deficits in cerebral ischemic animals (Yang et al., 2013). Black fungus polysaccharide is the main active ingredient of *Auricularia auricula* (Lex Hook.) Underw in China. Studies have found that fungus polysaccharides could reduce the production of ROS, MDA, and NO in rats with acute or chronic cerebral ischemia injury, enhance the activity of SOD and played an anti-oxidant effect. In addition, it can inhibit neuronal apoptosis and improve cerebral ischemia-reperfusion injury. (Lu et al., 2010; Qian and Min 2010; Ye et al., 2010). Fucose is a marine sulfated polysaccharide extracted from brown algae and some marine invertebrates (Apostolova et al., 2020; Oliveira et al., 2020). Experimental studies have shown that fucose can significantly reduce the levels of pro-inflammatory factors IL-1 β , IL-6, MPO and TNF- α in cerebral ischemia model animals, reduce the levels of oxidative stress-related proteins SOD and MDA, and could also regulate cell apoptosis via inhibiting the MAPK pathway to play a neuroprotective effect in cerebral ischemia reperfusion study (Che et al., 2017). Other studies have shown that fucose could also play a neuroprotective effect by inhibiting neuronal apoptosis, glial cell activation and anti-oxidative stress properties (Ahn et al., 2019; Kim et al., 2019). Codonopsis pilosula polysaccharide is a kind of polysaccharide extracted from *Codonopsis pilosula*. Studies have shown that *Codonopsis pilosula* polysaccharide could reduce LDH, NO and MDA, increase the content of AChE, SOD and GSH-Px, and inhibit the expression of Beclin-1 to regulate autophagy in the cerebral ischemia-reperfusion injury model (Chen, W. et al., 2015; Ma et al., 2019). It could also inhibit the expression of GFAP protein (Li, S. et al., 2018). *Codonopsis pilosula* polysaccharides can also reduce the expression of Bax, up-regulate the expression of Bcl-2 and inhibit apoptosis to exert



neuroprotective effects through mediating the Nrf2/HO-1 pathway (Ma et al., 2019). Lycium barbarum polysaccharide, astragalus polysaccharide, aloe polysaccharide, yam polysaccharide, etc. also have a certain protective effect on cerebral ischemia (Ge et al., 2017; Liu, H. et al., 2014; Lu et al., 2012; Peng et al., 2019; Wang, Y. et al., 2014; Yan and Zhou, 2012).

Structure-Activity Relationship Between Natural Products and Neuroprotection

Many studies have confirmed the neuroprotective effect of natural products on cerebral ischemia and clarified its preliminary mechanism of action. Different natural products have different mechanisms of anti-cerebral ischemia, which are closely related to the different structures of the compounds. **Figure 6** shows the mechanism of cerebral ischemia and the role of different types of natural products in this process. The research on the structure-activity relationship of the biological activity of natural products is mainly related to the basic nucleus of the compound, the number and position of double bonds, and the position of functional groups. They have a great influence on the biological activity of the compound (Aljahdali et al., 2020; Zhou et al., 2021). The flavonoids are based on 2-phenylchromone as the skeleton, which has ortho-dihydroxyl in the structure. The hydroxyl substituent on the basic skeleton is the key functional group for scavenging oxygen free radicals. At the same time, a conjugated system is also the key active site to scavenging oxygen free radicals (Chen et al., 2013). Therefore, flavonoids have unique advantages in scavenging free radicals and inhibiting lipid peroxidation. In addition, flavonoids had anti-inflammatory effects. It is believed that when the C-5 and 7 positions of the A ring of flavonoids have hydroxyl groups at the same time, they will affect the secretion process, mitosis and cell

interactions of cells, and then produce strong anti-inflammatory effect (Ying and Chi, 2007).

Alkaloids are quite different in structure. For example, berberine has a methylenedioxy ring structure and is the main functional group for anti-bacterial and hypoglycemic activity (Han et al., 2020; Wu and Fang, 2020). This may also be the key structure of its antioxidant effect, which needs further research to confirm. Ligustrazine has a simple structure and a wide range of pharmacological effects. Use it as a lead compound to synthesize various derivatives, which has a variety of biological activities (Wang et al., 2013), and the derivative is more stable than ligustrazine, such as ligustrazine hydrochloride injection has better curative effect in the treatment of ischemic cerebrovascular disease (Li and Zhang, 2020; You et al., 2020). Dauricine is a kind of bisbenzyltetrahydro isoquinoline alkaloid. It has a phenolic hydroxyl group and a conjugated system that is easy to form hydrogen bonds. It may be similar to flavonoids and is considered to be a key structure for antioxidant effects. Studies have shown that phenolic acids have a strong antioxidant effect, which is due to the existence of carboxyl, carbonyl and other structures (Bialecka-Florjanczyk et al., 2018; Wang, Y. et al., 2019). Glycoside components are compounds formed by non-sugar substances and sugars or sugar derivatives, which have the active characteristics both sugar substances and non-sugar substances. For example, flavonoid glycosides and flavonoid aglycones have anti-oxidative biological activity (Xue et al., 2001; Gao et al., 2008; Shao et al., 2013). In addition, most studies believe that glycoside compounds mainly exerted neuroprotective effects by improving the body's immunity (Brito-Arias, 2007). Iridoid glycosides are a special glycoside chemical. The core of iridoid glycosides is hemiacetal-enether cyclopentane, which is an important structural basis. Anti-oxidant stress is the manifestation of its biological activity (Wang et al., 2019a). Some studies also believe that the double

bond on the cyclopentane in iridoid glycosides, the C-11 substituent, and the way of forming the bond after ring opening also have important effects on the anti-inflammatory activity (Mao et al., 2019). For example, loganin, morroniside, and sorgenin all contain several electron-donating groups-hydroxyl groups. The hydroxyl groups release hydrogen atoms and combine with free radicals to block the chain reaction mediated by reactive oxygen species and reduce the body's oxidative stress. Stimulus levels, which weaken the phosphorylation of inflammatory signal pathway related factors, thereby inhibiting the inflammatory response, improving insulin resistance and liver damage (Li et al., 2014). Studies believe that tetracyclic triterpene saponins are the leading compounds for the treatment of neurological diseases, and can show strong neurological activity after proper structural modification and modification. Among them, C-7 and C-9 of lanolin triterpenoids The diene bond connected at the position may be the key group for nerve extension promoting activity (Liu, Y. et al., 2015). The research on the structure-activity relationship of tetracyclic triterpenes is mainly focused on the study of the binding sites related to the action of NMDAR antagonists, indicating that the structural modification and optimization of its aglycon and side chain sugar groups can obtain a new type of neuroactive monomer with high efficiency and low toxicity drug. Tetracyclic triterpene dammarane compounds as NMDAR antagonists will be an effective way to treat neurological diseases (Lee et al., 2006; Ryoo et al., 2020). Studies believe that ginkgolides can improve cerebral blood circulation and energy metabolism through specific inhibition of PAFR, and show a good market prospect in the prevention and treatment of cardiovascular and cerebrovascular diseases. The main differences in their effects are: the number and positions of hydroxyl groups contained in ginkgolides are different, PAF and ginkgolide ligands can be combined, and the introduction of benzyl derivatives at position C-10 is more beneficial for antagonistic activity; In addition, the presence of C, D ring and tert-butyl group also plays an important role in activity (Hui et al., 2013). Some scholars have studied the structure-activity relationship of andrographolide and found that the position of the double bond determines the anti-inflammatory effect of andrographolide and its derivatives, and the anti-inflammatory effects of compounds with double bonds in the ring are stronger than those with double bonds outside the ring (Tian et al., 2015). As a natural component of polycarbonyl and polyhydroxyl groups, emodin can coordinate and chelate with the zinc ions of type IV collagenase to inactivate type IV collagenase, thereby preventing type IV collagenase (MMP-2, MMP-9) degradation of basement membrane and extracellular matrix of normal tissue cells, play a role in anti-invasion and anti-metastasis (Wang, 2006). As a nucleoside antibiotic, cordycepin has a good application prospect in regulating immunity and scavenging free radicals (Lee et al., 2020).

In summary, the activity of natural products has an important relationship with the structure of the substance itself. The active functional groups of natural products are the key to their functions. Moreover, the bioavailability of many natural products is very low, which limits their use, the

structural modifications, changes in dosage forms or improvements in pharmacokinetic parameters can improve their bioavailability. Because the pathogenesis of cerebral ischemia is complex, and cascade reactions occur cross-over. The anti-cerebral ischemia effects of individual natural products are often weak. Therefore, a full understanding of the mechanism of the cerebral ischemia cascade can provide the possibility for the development of specific mechanisms or targeted compounds, and the combined use of different natural products to play a multi-target neuroprotective effect may be a promising therapy. However, it is very important to combine animal models with clinical practice (Ma et al., 2020). Choose appropriate experimental models according to actual conditions to provide a solid foundation for the clinical transformation of natural products.

CONCLUSIONS AND OUTLOOK

Stroke is one of the most common causes of disability and death worldwide, seriously endangers human health and brings heavy burden to society and family. Till now, there is no effective therapy which is available for the treatment of cerebral ischemia. Recombinant plasminogen activator is the only medicament utilized clinically and its use is restricted due to short therapy time windows and the risk of bleeding. Natural products from plants have been used to treat the cure of numerous disorders through the previous practice of therapeutics (Fan et al., 2020; Li Y. et al., 2017; Savopoulos et al., 2009; Chen, S. et al., 2020). Nowadays, many attempts have been made to explore the neuroprotective effects of natural products with the advance of technology. Hence, this review summarizes recent studies on the biological activities and mechanisms of recognized compounds for cerebral ischemia injury prevention or/and treatment (Table 1). Through the literatures, three aspects should be noted with special focus. First, multiple types of natural products, including flavonoids, alkaloids, saponin, terpene, iridoid glycosides, polyphenols and others, are proven to have a definite effect on cerebral ischemia injury. In fact, the clinical efficacy still requires further confirmation and to study. Second, animal models and cell experiments were used to investigate the neuroprotective effect of natural product on cerebral ischemia injury. Animal models including MCAO, BCCAO and other occlusion methods were used to induce cerebral ischemia injury. Due to the diversity of brain cells, a variety of cell lines are used in the study of neurological diseases, for example, HT22, BV2, BMEC and others. Due to the limitations of cell models, the neuroprotective effects of many natural products in cell models still need to be verified by *in vivo* experiments. Third, most of the compounds show neuroprotective effects through multiple targets or signaling pathways. These natural products work by comprehensive regulation, inhibiting excitotoxicity, influencing free radicals, anti-apoptosis, impairing blood-brain barrier disruption, anti-inflammation, influencing astrocytic activation and proliferation. The

TABLE 1 | Summary a few natural products and their targets of action imparting neuroprotective activity.

Categories	Natural products	Dosage	Targets/pathway	References
Flavonoid	Baicalin	50, 100, 200 mg/kg (<i>in vivo</i>), 10 µg/ml (<i>in vitro</i>)	MDA, SOD, GSH, GSH-Px, caspase-3, BDNF, NOD2, TNFα, IL-1β, COX-2, iNOS, NO, PGE2, TLR2/4, NF-κB p65, MCL-1, Bcl-2, MRTF-A, PI3K, ERK1/2	(Cao et al., 2011; Li, F et al., 2010; Tu et al., 2011; Xue et al., 2010; Zheng et al., 2015)
	Scutellarin/scutellarein	50, 100 mg/kg (<i>in vivo</i>), 0.54 mM (<i>in vitro</i>)	TNF-α, IL-1β, JNK, ERK, p38, iNOS, eNOS, nNOS, ROS, NOX2, Cx43, SOD, MDA, NO, caspase-3, Notch-1, NICD, HES-1, VEGF, bFGF, ACE, ANG II, AT1R, IL-6	(Chen, S et al., 2020; Fang et al., 2016; Fang et al., 2015; Hu et al., 2005; Sun, R et al., 2018; Tang et al., 2014; Wang et al., 2016)
	Apigenin/Vitexin	2–40 mg/kg (<i>in vivo</i>), 2.5, 5, 10 µM and 0.5, 2.5, 10 nM (<i>in vitro</i>)	IL-1β, IL-6, TNF-α, IL-10, LDH, SOD, MDA, NO, eNOS, iNOS, bax, Bcl-2, Caspase-3, PARP, MMP-2, MMP-9, ROCK2, RhoA, VEGF, BDNF, PI3K/Akt, ERK, JNK, p38, mTOR, PPAR-γ, Caveolin-1, Beclin1, p62, LC3I, LC3II, NKCC1, Ulk1, Keap1, HO-1, Nrf2, CREB	(Cui et al., 2019; Jiang et al., 2018; Pang et al., 2018; Tu et al., 2017; Wang et al., 2015b; Zhang, X. et al., 2019)
	Icariin	10, 30 mg/kg (<i>in vivo</i>), 0.25, 0.5, 1 mg/L (<i>in vitro</i>)	IL-1 β, IL-6, TNF-α, TGF-β1, NF-κB p65, PPARα, PPARγ, IκB-α, IRE1α, XBP1u, XBP1s, caspase-3, Bcl-2, bax	(Deng et al., 2016; Xiong et al., 2016; Mo et al., 2020; Yang et al., 2020)
	Quercetin	5–25 mg/kg (<i>in vivo</i>), 10 µM (<i>in vitro</i>)	TNF-α, IL-1β, LDH, ERK, akt, EGF, MMP-9, Claudin-5, ZO-1, β-catenin, GSK-3β, Axin, LEF1, MDA, SOD, CAT, caspase-3, Bcl-2, Nrf2, NOX4, IκBα, p65	(Dai et al., 2018; Jin et al., 2019; Park et al., 2020; Wang, Y et al., 2020)
	Calycosin	5–30 mg/kg	BDNF/TrkB, TNF-α, Bcl-2, NBR1, p62, caveolin-1, claudin-5, NO, ZO-1, MMP-2, MMP-9, ROS, ER-α, RASD1, Bcl-2, SIRT1, FOXO1, Bcl-2, bax, PGC-1α	(Guo et al., 2012; Hsu et al., 2020; Wang, Y et al., 2014; Wang, Y. et al., 2018)
Alkaloid	Berberine	0.002–100 mg/kg (<i>in vivo</i>), 0.5 µg/ml (<i>in vitro</i>)	PI3K/Akt, p53, cyclin D1, caspase 3, bad, p55γ, BDNF, TrkB, GSK3β, CREB, claudin-5, NF-κB, HIF-1α	(Hu et al., 2012; Song et al., 2012; Zhang et al., 2012; Chai et al., 2013; Zhang et al., 2016b; Yang et al., 2018b)
	Ligustrazine	10–100 mg/kg (<i>in vivo</i>), 1, 10, 100 mM (<i>in vitro</i>)	IL-1β, IL-6, TNF-α, IL-10, SOD, GSH-Px, MDA, p53, Caspase-3, Bcl-2, bax, mTOR, ULK1, BNIP3, Beclin1, LC3 II/I, Bax/Bcl-2, HIF-1α, MPO, Nrf2, HO-1, ERK, IFN-γ, TLR4, HMGB1, occludin, JAM-1, AQP4, MMP9, NO, iNOS, eNOS, akt, MCP-1, ICAM-1, TLR-4/NF-κB p65	(Chang et al., 2015; Chang et al., 2007; Ding et al., 2019; Xu et al., 2017; Yan et al., 2015; Yu, P. et al., 2017; Yu et al., 2016; Zhou et al., 2019)
	Daurisoline	5, 10, 20 mg/kg	Cyt-C, Caspase 3, Caspase 9, SOD, MDA, GSH-Px	(Li and Gong 2004; Yang et al., 2009; Lan and Lianjun 2020)
	Tetrahydropalmatine	10, 20, 40 mg/kg	MPO, NO, ONOO2-, iNOS, p85, eNOS, akt, HIF-1, VEGF, TNF-α, occludin, ZO-1, claudin-5, caveolin-1, MMP-2/9, src, MLCK, p-MLC, p38, bax, caspase-3, Bcl-2, PRAP	(Han et al., 2012; Mao et al., 2015; Sun, R et al., 2018)
	Peimine	1–5 mg/kg	SOD, MDA, LDH, IL-6, IL-10, IL-18, ICAM-1, IL-1β, caspase-9, caspase-3, bax, bcl-2, LC3II/LC3I, beclin1, p62, PI3K, Akt, mTOR, TNF-α, β-arrestin	(Guo et al., 2019; Duan et al., 2020)
	Curcumin	30–300 mg/kg (<i>in vivo</i>), 1.25–20 µM (<i>in vitro</i>)	MDA, GSH, GSH-Px, SOD, NF-κB p65, Nrf2, IL-1β, IL-8, JAK2, STAT3, akt, mTOR, LC3-II, LC3-I, p62, TLR4, p-38, IL-1, IL-6, TNF-α, iNOS, caspase-3, bax, Bcl-2, Bcl-XL, COX-2, Nrf2, NO, HO-1, MEK, ERK, CREB, LDH, MnSOD, AIF, caspase-9/-3, Trx-2, MPT, MMP-9, ZO1, occludin, HIF-1α, JNK	(Huang et al., 2018; Li et al., 2015; Li et al., 2016; Lu et al., 2018; Xie, C. J. et al., 2018; Xu, N. et al., 2019)

(Continued on following page)

TABLE 1 | (Continued) Summary a few natural products and their targets of action imparting neuroprotective activity.

Categories	Natural products	Dosage	Targets/pathway	References
Glycoside	Resveratrol	20–40 mg/kg (<i>in vivo</i>), 1–50 μ M (<i>in vitro</i>)	NF- κ B p65, NO, iNOS, eNOS, nNOS, JNK, GFAP, PI3K/Akt, GSK-3 β , CREB, PGE, COX-1, COX-2, LDH, Bcl-2, Caspase-3, NQO-1, Sirt1, UCP2, LC3B-II/I, p62, NLRP3, caspase-1, IL-18, Nrf2/HO-1, Caspase-3, GSH-Px, SOD, CAT, MDA, TNF- α , IL-1 β , IL-6, LDH, MMP-9, TIMP-1, shh	(Candelario-Jalil et al., 2007; Simao et al., 2012b; Wei et al., 2015; He et al., 2017; Koronowski et al., 2017; Yang et al., 2018b)
	Ellagic acid	10–100 mg/kg	Bax, bcl 2, cyt C, caspase 3, PI3K/Akt, NOS, MDA, wnt/ β -catenin, ZO-1, AQP 4, MMP-9	(Kaihua and JiYu 2020; Liu, Z. B. et al., 2017; Nejad et al., 2015; Wang, F. et al., 2019)
	Asiaticoside	20, 40, 60 mg/kg	TNF- α , IL-6, IL-1 β , MCP1, ROS, MDA, LDH, SOD, bcl 2, bax, caspase3, NOD2, p38 MAPK, NF- κ B p65, JNK, ERK, I κ B α	(Chen et al., 2014; Zhang et al., 2020b)
	Salidroside	25, 50, 100 mg/kg (<i>in vivo</i>), 1, 10, 100 μ M (<i>in vitro</i>)	Caspase-3, Bcl-2, bax, ROS, iNOS, LDH, PARP, FGF2, cAMP/PKA/CREB, TNF- α , IL-1 β , IL-6, Arg1, TGF β , IL-2, IL-8, akt, HIF-1 α , HIF- 2 α , HIF- 3 α , EPO, nrf2/HO-1, NF- κ B p50, PI3K/PKB, cyt-c, MMP9, Claudin 5, occludin	(Li et al., 2020; Liu et al., 2018; Wei et al., 2017; Zhang, Y. et al., 2018; Zhang X. et al., 2019; Zhong et al., 2019; Zuo et al., 2018)
Iridoid glycoside	Geniposide	5, 10, 20 mg/kg	LDH, TNF- α , IL-1 β , IL-6, IL-8, IL-18, NLRP3, ASC, caspase-1, raf/mek1/2/ erk1/2, MCP-1, ZO-1, occludin, Claudin-5, β -catenin, PI3K/Akt, Bcl-2/Bax, AchE, NOS, MDA, SOD	(Fu et al., 2020; Huang et al., 2017; Li, W. et al., 2016; Liu, Q et al., 2019)
	Catalpol	5, 10, 20 mg/kg (<i>in vivo</i>) 0.3 mM, 2.8 mM, 27.6 mM, 275.9 mM (<i>in vitro</i>)	ET-1, SOD, MDA, CGRP, EPO, STAT3, VEGF, JAK2/STAT3, bax, Bcl-2, ROS, NO, iNOS, GSH-Px, GSH	(Dong, X. et al., 2016; Li et al., 2006; Li et al., 2008; Liu, Y. R et al., 2014)
	Picroside II	10, 20 mg/kg	TLR4, TNF- α , NF- κ B p65, ERK1/2, ROS, NOX2, Rac-1 ROCK, MLCK, MMP-2, claudin-5, MEK/erk1/2-cox2, ROS, caspase 3, cyt C	(Guo et al., 2010; Li, S. et al., 2018; Wang, C. et al., 2015; Zhai et al., 2017; Zhang et al., 2017)
Saponin	Ginsenoside Rg1	10, 20, 40 mg/kg	PAR-1, akt, nrf2/HO-1, ppar γ /HO-1, ERK, JNK, caspase-3/rock1/mlc, IL-1 β , IL-6, TNF- α , I κ B, NF- κ B p65, AQP4, p38 MAPK, MPO, SOD, CAT, HMGB1, Nrf2/ARE, AMPK/mTOR, AMP/AMPK-GLUT	(Li, S. et al., 2017; Xie, W. et al., 2018; Zheng et al., 2019; Zhou et al., 2014)
	Astragaloside IV	10–50 mg/kg (<i>in vivo</i>), 0.1–10 μ M (<i>in vitro</i>)	STAT-3/TNF- α /IL-1 β , JNK3, MPO/TNF- α /IL-1 β , NF- κ B, akt, LC3II/LC3I, p62, Fas, FasL, Caspase-8, bax, Bcl-2, bid, cyt C, Caspase-3, PI3K/Akt, ICAM-1	(Li et al., 2012; Li, J et al., 2019; Yin et al., 2020)
Terpenoids	Andrographolide	5 mg/kg	LDH, caspase-3, ERK1/2, p38 MAPK, JNK1/2, nrf2/HO-1, Lamin B1	(Chern et al., 2011; Yen et al., 2013; Yen et al., 2016)
	Ginkgolide B	1, 2, 4 mg/kg	LDH, IL-1 β , TNF- α , TLR4, NF- κ B, nrf2/HO-1, NQO1, SOD, akt, BDNF, EGF, NGF	(Liu, Q et al., 2019; Zheng et al., 2018b)
	Borneol	200 mg/kg	Bax, Bcl-2, Claudin-5, VEGF, TNF- α , ROS, NO, iNOS, caspase-3, caspase-9, ICAM-1, NF- κ B p65	(Liu et al., 2011; Dong et al., 2018)
Others	Emodin	15, 50 mg/kg	ERK-1/2, GLT-1, caspase-3, ERK-1/2, LDH, Bcl-2, bax, akt, CREB, BDNF, TNF- α , IL-1 β , IL-6, NF- κ B p65, I κ B α	(Ahn et al., 2016; Leung et al., 2020)
	Cordycepin	5, 10, 20 mg/kg (<i>in vivo</i>), 5, 10, 20, 40, 80 μ M (<i>in vitro</i>)	Bcl-2, bax, Caspase-3, p53, MAPK	(Chen, K. et al., 2017; Cheng et al., 2011; Dong et al., 2019; Hwang et al., 2008; Jin, G. et al., 2014)
	Panax notoginseng polysaccharide	100, 300 mg/kg	Bcl-2/Bax, caspase-3, GSH-Px, SOD, IL 10, MDA, TNF- α , IL-1 β	(Jia et al., 2014; Sy et al., 2015)
	Angelica polysaccharide	30, 45, 60 mg/kg	SOD, GSH, GSH-PX, MDA, IL-1 β , TNF- α , NF- κ B	(Dai et al., 2020; Yan and Xie, 2018; Hu et al., 2006; Li, Y. et al., 2019)
	Ginkgo biloba polysaccharides	100, 200, 400 mg/kg	SOD, GSH, GSH-PX, MDA, IL-1 β , TNF- α	(Yang et al., 2013)
	Black fungus polysaccharide	50, 100 mg/kg	ROS, MDA, NO; SOD	(Lu et al., 2010; Qian and Min, 2010; Ye et al., 2010)

(Continued on following page)

TABLE 1 | (Continued) Summary a few natural products and their targets of action imparting neuroprotective activity.

Categories	Natural products	Dosage	Targets/pathway	References
	Fucose	80, 160 mg/kg	MAPK; SOD; MDA; IL-1 β , IL-6, MPO; TNF- α	(Che et al., 2017; Ahn et al., 2019; Kim et al., 2019)
	Codonopsis pilosula polysaccharide	1, 2 g/kg	Nrf2/HO-1; Bcl-2; bax; bax; AChE, SOD; GSH-Px	(Chen, J. et al., 2015; Ma et al., 2019; Li et al., 2018)

mechanism by which natural products has multiple targets and diverse signaling pathways. Therefore, natural products would be very valuable when seeking novel therapeutic agents for stroke.

In conclusion, this review summarizes that the facts are comprehensive and deeply informative about the neuroprotective activities of natural products *in vitro* and *in vivo* experiment. For prophylactic and therapeutic management of stroke, they are promising candidates. Therefore, this review would provide as a reference for current advances in the study on natural products for neuroprotection.

AUTHOR CONTRIBUTIONS

QX and HL are equally contributed to the article and supervised as a whole and finalized the manuscript. DL, JY, and DG carried out various literature survey studies. RM, JL, and JW prepared the

initial draft and graphical representation for figures. MR, HC and YL provided significant input into the chemistry part.

FUNDING

The authors are grateful to National Natural Science Foundation of China (Grant Numbers 81873023, 81473371, 81873073), and Hundred Talents Program of the Hospital of Chengdu University of Traditional Chinese Medicine (Grant No. 20-Q18).

ACKNOWLEDGMENTS

The authors are grateful to National Natural Science Foundation of China (Grant Numbers: 81873023, 81473371, 81873073), and Hundred Talents Program of the Hospital of Chengdu University of Traditional Chinese Medicine (Grant No. 20-Q18).

REFERENCES

- Ahn, J. H., Shin, M. C., Kim, D. W., Kim, H., Song, M., Lee, T. K., et al. (2019). Antioxidant properties of fucoidan alleviate acceleration and exacerbation of hippocampal neuronal death following transient global cerebral ischemia in high-fat diet-induced obese gerbils. *Int. J. Mol. Sci.* 20, 114. doi:10.3390/ijms20030554
- Ahn, S. M., Kim, H. N., Kim, Y. R., Choi, Y. W., Kim, C. M., Shin, H. K., et al. (2016). Emodin from polygonum multiflorum ameliorates oxidative toxicity in HT22 cells and deficits in photothrombotic ischemia. *J. Ethnopharmacology* 188, 13–20. doi:10.1016/j.jep.2016.04.058
- Alfei, S., Turrini, F., Catena, S., Zunin, P., Grilli, M., Pittaluga, A. M., et al. (2019). Ellagic acid a multi-target bioactive compound for drug discovery in CNS? A narrative review. *Eur. J. Med. Chem.* 183, 111724. doi:10.1016/j.ejmech.2019.111724
- Aljahdali, A. Z., Foster, K. A., and O'Doherty, G. A. (2020). Synthesis and biological study of the phomopsolid and phomopsolidone natural products. *Chem. Commun.* 56, 12885–12896. doi:10.1039/d0cc04069j
- Almeida, J. R., Souza, G. R., Silva, J. C., Saraiva, S. R., Júnior, R. G., Quintans, J. de S., et al. (2013). Borneol, a bicyclic monoterpene alcohol, reduces nociceptive behavior and inflammatory response in mice. *Sci. World J.* 2013, 808460. doi:10.1155/2013/808460
- An, J., Chen, B., Kang, X., Zhang, R., Guo, Y., Zhao, J., et al. (2020). Neuroprotective effects of natural compounds on LPS-induced inflammatory responses in microglia. *Am. J. Transl. Res.* 12, 2353–2378.
- Apostolova, E., Lukova, P., Baldzhieva, A., Katsarov, P., Nikolova, M., Iliev, I., et al. (2020). Immunomodulatory and anti-inflammatory effects of fucoidan: a review. *Polymers (Basel)* 12, 2338. doi:10.3390/polym12102338
- Asemi, Z., Behnam, M., Pourattar, M. A., Mirzaei, H., Razavi, Z. S., and Tamtaji, O. R. (2020). Therapeutic potential of berberine in the treatment of glioma: insights into its regulatory mechanisms. *Cell Mol. Neurobiol.* 11, 23. doi:10.1007/s10571-020-00903-5
- Ayoobi, F., Shamsizadeh, A., Fatemi, I., Vakilian, A., Allahtavakoli, M., Hassanshahi, G., et al. (2017). Bio-effectiveness of the main flavonoids of *Achillea millefolium* in the pathophysiology of neurodegenerative disorders - a review. *Iran J. Basic Med. Sci.* 20, 604–612. doi:10.22038/IJBMS.2017.8827
- Babaei, F., Moafizad, A., Darvishvand, Z., Mirzababaei, M., Hosseinzadeh, H., and Nassiri-Asl, M. (2020). Review of the effects of vitexin in oxidative stress-related diseases. *Food Sci. Nutr.* 8, 2569–2580. doi:10.1002/fsn3.1567
- Bagli, E., Goussia, A., Moschos, M. M., Agnantis, N., and Kitsos, G. (2016). Natural compounds and neuroprotection: mechanisms of action and novel delivery systems. *In Vivo* 30, 535–547. doi:10.1002/9780470134931.ch3
- Bao, C., Wang, Y., Min, H., Zhang, M., Du, X., Han, R., et al. (2015). Combination of ginsenoside Rg1 and bone marrow mesenchymal stem cell transplantation in the treatment of cerebral ischemia reperfusion injury in rats. *Cell Physiol. Biochem.* 37, 901–910. doi:10.1159/000430217
- Bao, Z., Guan, S., Cheng, C., Wu, S., Wong, S. H., Kemeny, D. M., et al. (2009). A novel antiinflammatory role for andrographolide in asthma via inhibition of the nuclear factor-kb pathway. *Am. J. Respir. Crit. Care Med.* 179, 657–665. doi:10.1164/rccm.200809-1516oc
- Baradaran Rahimi, V., Ghadiri, M., Ramezani, M., and Askari, V. R. (2020). Antiinflammatory and anti-cancer activities of pomegranate and its constituent, ellagic acid: evidence from cellular, animal, and clinical studies. *Phytotherapy Res.* 34, 685–720. doi:10.1002/ptr.6565
- Benjamin, E. J., Virani, S. S., Callaway, C. W., Chamberlain, A. M., Chang, A. R., Cheng, S., et al. (2018). Heart disease and stroke statistics-2018 update: a report from the American heart association. *Circulation* 137, e67–e492. doi:10.1161/CIR.0000000000000558
- Bialecka-Florjanczyk, E., Fabiszewska, A., and Zieniuk, B. (2018). Phenolic acids derivatives - biotechnological methods of synthesis and bioactivity. *Curr. Pharm. Biotechnol.* 19, 1098–1113. doi:10.2174/1389201020666181217142051
- Brito-Arias, M. (2007). *Synthesis and characterization of glycosides*. Berlin, Germany: Springer Science+Business Media.
- Cai, D., Qi, J., Yang, Y., Zhang, W., Zhou, F., Jia, X., et al. (2019). Design, synthesis and biological evaluation of diosgenin-amino acid derivatives with dual

- functions of neuroprotection and angiogenesis. *Molecules* 24, 113. doi:10.3390/molecules24224025
- Candelario-Jalil, E., de Oliveira, A., Gräf, S., Bhatia, H. S., Hüll, M., Muñoz, E., et al. (2007). Resveratrol potentially reduces prostaglandin E2 production and free radical formation in lipopolysaccharide-activated primary rat microglia. *J. Neuroinflammation* 4, 25. doi:10.1186/1742-2094-4-25
- Cao, W., Liu, W., Wu, T., Zhong, D., and Liu, G. (2008). Dengzhanhua preparations for acute cerebral infarction. *Cochrane Database Syst. Rev.* 11, CD005568. doi:10.1002/14651858.CD005568.pub2
- Cao, Y., Liu, J. W., Yu, Y. J., Zheng, P. Y., Zhang, X. D., Li, T., et al. (2007). Synergistic protective effect of picoside II and NGF on PC12 cells against oxidative stress induced by H₂O₂. *Pharmacol. Rep.* 59, 573–579. doi:10.7324/japs.2019.90403
- Cao, Y., Mao, X., Sun, C., Zheng, P., Gao, J., Wang, X., et al. (2011). Baicalin attenuates global cerebral ischemia/reperfusion injury in gerbils via anti-oxidative and anti-apoptotic pathways. *Brain Res. Bull.* 85, 396–402. doi:10.1016/j.brainresbull.2011.05.002
- Ceci, C., Lacal, P. M., Tentori, L., De Martino, M. G., Miano, R., and Graziani, G. (2018). Experimental evidence of the antitumor, antimetastatic and antiangiogenic activity of ellagic acid. *Nutrients* 10, 1756. doi:10.3390/nu1011756
- Chai, Y.-S., Hu, J., Lei, F., Wang, Y.-G., Yuan, Z.-Y., Lu, X., et al. (2013). Effect of berberine on cell cycle arrest and cell survival during cerebral ischemia and reperfusion and correlations with p53/cyclin D1 and PI3K/Akt. *Eur. J. Pharmacol.* 708, 44–55. doi:10.1016/j.ejphar.2013.02.041
- Chang, C.-K., and Lin, M.-T. (2001). DL-Tetrahydropalmatine may act through inhibition of amygdaloid release of dopamine to inhibit an epileptic attack in rats. *Neurosci. Lett.* 307, 163–166. doi:10.1016/s0304-3940(01)01962-0
- Chang, C.-Y., Kao, T.-K., Chen, W.-Y., Ou, Y.-C., Li, J.-R., Liao, S.-L., et al. (2015). Tetramethylpyrazine inhibits neutrophil activation following permanent cerebral ischemia in rats. *Biochem. Biophys. Res. Commun.* 463, 421–427. doi:10.1016/j.bbrc.2015.05.088
- Chang, Y., Hsiao, G., Chen, S.-h., Chen, Y.-c., Lin, J.-h., Lin, K.-h., et al. (2007). Tetramethylpyrazine suppresses HIF-1 α , TNF- α , and activated caspase-3 expression in middle cerebral artery occlusion-induced brain ischemia in rats. *Acta Pharmacologica Sinica* 28, 327–333. doi:10.1111/j.1745-7254.2007.00514.x
- Che, D. N., Cho, B. O., Kim, J. S., Shin, J. Y., Kang, H. J., and Jang, S. I. (2020). Luteolin and apigenin attenuate LPS-induced astrocyte activation and cytokine production by targeting MAPK, STAT3, and NF- κ B signaling pathways. *Inflammation* 43, 1716–1728. doi:10.1007/s10753-020-01245-6
- Che, N., Ma, Y., and Xin, Y. (2017). Protective role of fucoidan in cerebral ischemia-reperfusion injury through inhibition of MAPK signaling pathway. *Biomolecules Ther.* 25, 272–278. doi:10.4062/biomolther.2016.098
- Chen, C., Liu, X.-P., Jiang, W., Zeng, B., Meng, W., Huang, L.-P., et al. (2017). Anti-effects of cordycepin to hypoxia-induced membrane depolarization on hippocampal CA1 pyramidal neuron. *Eur. J. Pharmacol.* 796, 1–6. doi:10.1016/j.ejphar.2016.12.021
- Chen, H.-L., Jia, W.-J., Li, H.-E., Han, H., Li, F., Zhang, X.-L., et al. (2020). Scutellarin exerts anti-inflammatory effects in activated microglia/brain macrophage in cerebral ischemia and in activated BV-2 microglia through regulation of MAPKs signaling pathway. *Neuromol Med.* 22, 264–277. doi:10.1007/s12017-019-08582-2
- Chen, J., Lin, C., Yong, W., Ye, Y., and Huang, Z. (2015). Calycosin and genistein induce apoptosis by inactivation of HOTAIR/p-Akt signaling pathway in human breast cancer MCF-7 cells. *Cel Physiol. Biochem.* 35, 722–728. doi:10.1159/000369732
- Chen, K., Sun, W., Jiang, Y., Chen, B., Zhao, Y., Sun, J., et al. (2017). Ginkgolide B suppresses TLR4-mediated inflammatory response by inhibiting the phosphorylation of JAK2/STAT3 and p38 MAPK in high glucose-treated HUVECs. *Oxid Med. Cel Longev* 2017, 9371602. doi:10.1155/2017/9371602
- Chen, S., Yin, Z.-J., Jiang, C., Ma, Z.-Q., Fu, Q., Qu, R., et al. (2014). Asiaticoside attenuates memory impairment induced by transient cerebral ischemia-reperfusion in mice through anti-inflammatory mechanism. *Pharmacol. Biochem. Behav.* 122, 7–15. doi:10.1016/j.pbb.2014.03.004
- Chen, W., Tang, Y., Liu, L., and Jiao, Y. (2015). Influence of Codonopsis pilosula polysaccharide on brain Tissues, Oxygen free radicals and beclin-1 level of rats with ischemia-reperfusion. *Mil. Med. J. South China* 29, 886–888+923. doi:10.1016/j.carbpol.2012.07.062
- Chen, Y.-J., Liu, Y.-L., Zhong, Q., Yu, Y.-F., Su, H.-L., Toque, H. A., et al. (2012). Tetrahydropalmatine protects against methamphetamine-induced spatial learning and memory impairment in mice. *Neurosci. Bull.* 28, 222–232. doi:10.1007/s12264-012-1236-4
- Chen, Y., Long, X., Pan, S., An, X., and Chen, S. L. (2013). Advances in pharmacodynamic mechanisms and SAR studies of flavonoids. *Chin. J. Exp. Trad. Med. Formulae* 19, 337–344. doi:10.1201/9781420041781.ch29
- Cheng, Y., Shen, L.-h., and Zhang, J.-t. (2005). Anti-amnesic and anti-aging effects of ginsenoside Rg1 and Rb1 and its mechanism of action. *Acta Pharmacologica Sinica* 26, 143–149. doi:10.1111/j.1745-7254.2005.00034.x
- Cheng, Z., He, W., Zhou, X., Lv, Q., Xu, X., Yang, S., et al. (2011). Cordycepin protects against cerebral ischemia/reperfusion injury in vivo and in vitro. *Eur. J. Pharmacol.* 664, 20–28. doi:10.1016/j.ejphar.2011.04.052
- Chen, S., Chen, H., Du, Q., and Shen, J. (2020). Targeting myeloperoxidase (MPO) mediated oxidative stress and inflammation for reducing brain ischemia injury: potential application of natural compounds. *Front. Physiol.* 11 (undefined), 433. doi:10.3389/fphys.2020.00433
- Chern, C.-M., Liou, K.-T., Wang, Y.-H., Liao, J.-F., Yen, J.-C., and Shen, Y.-C. (2011). Andrographolide inhibits PI3K/AKT-dependent NOX2 and iNOS expression protecting mice against hypoxia/ischemia-induced oxidative brain injury. *Planta Med.* 77, 1669–1679. doi:10.1055/s-0030-1271019
- Chu, H., Jin, G., Friedman, E., and Zhen, X. (2008). Recent development in studies of tetrahydropyridoberberines: mechanism in antinociception and drug addiction. *Cel Mol Neurobiol* 28, 491–499. doi:10.1007/s10571-007-9179-4
- Chu, S.-f., Zhang, Z., Zhou, X., He, W.-b., Chen, C., Luo, P., et al. (2019). Ginsenoside Rg1 protects against ischemic/reperfusion-induced neuronal injury through miR-144/Nrf2/ARE pathway. *Acta Pharmacol. Sin* 40, 13–25. doi:10.1038/s41401-018-0154-z
- Chuang, J.-H., Tung, L. C., and Lin, Y. (2015). Neural differentiation from embryonic stem cells in vitro: an overview of the signaling pathways. *Wjsc* 7, 437–447. doi:10.4252/wjsc.v7.i2.437
- Coon, J. T., and Ernst, E. (2004). Andrographis paniculata in the treatment of upper respiratory tract infections: a systematic review of safety and efficacy. *Planta Med.* 70, 293–298. doi:10.1055/s-2004-818938
- Costa, I. M., Vieira Lima, F., Fernandes, L., Norrara, B., Neta, F., Alves, R., et al. (2018). Astragaloside IV supplementation promotes A neuroprotective effect in experimental models of neurological disorders: a systematic review. *Curr. Neuropharmacol.* 17, 648–665. doi:10.2174/1570159X16666180911123341
- Costa, L. G., Garrick, J. M., Roqué, P. J., and Pellacani, C. (2016). Mechanisms of neuroprotection by quercetin: counteracting oxidative stress and more. *Oxid Med. Cel Longev* 11, 2986796. doi:10.1155/2016/2986796
- Cui, Y.-h., Zhang, X.-q., Wang, N.-d., Zheng, M.-d., and Yan, J. (2019). Vitexin protects against ischemia/reperfusion-induced brain endothelial permeability. *Eur. J. Pharmacol.* 853, 210–219. doi:10.1016/j.ejphar.2019.03.015
- Dai, Y., Zhang, H., Zhang, J., and Yan, M. (2018). Isoquercetin attenuates oxidative stress and neuronal apoptosis after ischemia/reperfusion injury via Nrf2-mediated inhibition of the NOX4/ROS/NF- κ B pathway. *Chemico-Biol. Interact.* 284, 32–40. doi:10.1016/j.cbi.2018.02.017
- Dai, Z., Zhu, Y., and Wang, Z. (2020). Effects of Angelica polysaccharides on the expression of IL-1 β , TNF- α , NF- κ B in rats with cerebral ischemia reperfusion injury. *Chin. Trad. Patent Med.* 42, 2176–2178. doi:10.1016/b978-0-12-374530-9.00013-9
- de Oliveira, M. R. (2016). The effects of ellagic acid upon brain cells: a mechanistic view and future directions. *Neurochem. Res.* 41, 1219–1228. doi:10.1007/s11064-016-1853-9
- Della-Morte, D., Dave, K. R., DeFazio, R. A., Bao, Y. C., Raval, A. P., and Perez-Pinzon, M. A. (2009). Resveratrol pretreatment protects rat brain from cerebral ischemic damage via a sirtuin 1-uncoupling protein 2 pathway. *Neuroscience* 159, 993–1002. doi:10.1016/j.neuroscience.2009.01.017
- Deng, Y., Xiong, D., Yin, C., Liu, B., Shi, J., and Gong, Q. (2016). Icariside II protects against cerebral ischemia-reperfusion injury in rats via nuclear factor- κ B inhibition and peroxisome proliferator-activated receptor up-regulation. *Neurochem. Int.* 96, 56–61. doi:10.1016/j.neuint.2016.02.015
- Dhanasekaran, M., Holcomb, L. A., Hitt, A. R., Tharakan, B., Porter, J. W., Young, K. A., et al. (2009). Centella asiatica extract selectively decreases amyloid β levels

- in hippocampus of Alzheimer's disease animal model. *Phytother. Res.* 23, 14–19. doi:10.1002/ptr.2405
- Ding, Y., Du, J., Cui, F., Chen, L., and Li, K. (2019). The protective effect of ligustrazine on rats with cerebral ischemia-reperfusion injury via activating PI3K/Akt pathway. *Hum. Exp. Toxicol.* 38, 1168–1177. doi:10.1177/0960327119851260
- Dong, T., Chen, N., Ma, X., Wang, J., Wen, J., Xie, Q., et al. (2018). The protective roles of L- borneolum, D- borneolum and synthetic borneol in cerebral ischaemia via modulation of the neurovascular unit. *Biomed. Pharmacother.* 102, 874–883. doi:10.1016/j.biopha.2018.03.087
- Dong, W., Xian, Y., Yuan, W., Huifeng, Z., Tao, W., Zhiqiang, L., et al. (2016). Catalpol stimulates VEGF production via the JAK2/STAT3 pathway to improve angiogenesis in rats' stroke model. *J. Ethnopharmacology* 191, 169–179. doi:10.1016/j.jep.2016.06.030
- Dong, X., Fu, J., Yin, X., Cao, S., Li, X., Lin, L., et al. (2016). Emodin: a review of its pharmacology, toxicity and pharmacokinetics. *Phytother. Res.* 30, 1207–1218. doi:10.1002/ptr.5631
- Dong, Z.-S., -W., Cao, Z.-P., Shang, Y.-J., Liu, Q.-Y., Wu, B.-Y., Liu, W.-X., et al. (2019). Neuroprotection of cordycepin in NMDA-induced excitotoxicity by modulating adenosine A1 receptors. *Eur. J. Pharmacol.* 853, 325–335. doi:10.1016/j.ejphar.2019.04.015
- Donnan, G. A., Fisher, M., Macleod, M., and Davis, S. M. (2008). Stroke. *The Lancet* 371, 1612–1623. doi:10.1016/s0140-6736(08)60694-7
- Duan, J., Kang, K., Huang, C.-r., Chen, L.-g., Wan, W.-f., Peng, T.-m., et al. (2020). Protective effect of peimine on cerebral ischemia-reperfusion injury in rats. *Chin. J. New Drugs Clin. Rem* 39, 240–246. doi:10.3724/sp.j.1008.2010.00238
- Eghbaliferiz, S., Farhadi, F., Barreto, G. E., Majeed, M., and Sahebkar, A. (2020). Effects of curcumin on neurological diseases: focus on astrocytes. *Pharmacol. Rep.* 72, 769–782. doi:10.1007/s43440-020-00112-3
- Fan, D., Liu, L., Wu, Z., and Cao, M. (2019). Combating neurodegenerative diseases with the plant alkaloid berberine: molecular mechanisms and therapeutic potential. *Cn* 17, 563–579. doi:10.2174/1570159x16666180419141613
- Fan, Q., Zhou, J., Wang, Y., Xi, T., Ma, H., Wang, Z., et al. (2020). Chip-based serum proteomics approach to reveal the potential protein markers in the sub-acute stroke patients receiving the treatment of Ginkgo Diterpene Lactone Meglumine Injection. *J. Ethnopharmacol.* 260, 112964. doi:10.1016/j.jep.2020.112964
- Fang, J., Wang, Z., Wang, P., and Wang, M. (2020). Extraction, structure and bioactivities of the polysaccharides from Ginkgo biloba: a review. *Int. J. Biol. Macromol.* 162, 1897–1905. doi:10.1016/j.ijbiomac.2020.08.141
- Fang, M., Yuan, Y., Lu, J., Li, H. E., Zhao, M., Ling, E.-A., et al. (2016). Scutellarin promotes microglia-mediated astrogliosis coupled with improved behavioral function in cerebral ischemia. *Neurochem. Int.* 97, 154–171. doi:10.1016/j.neuint.2016.04.007
- Fang, M., Yuan, Y., Rangarajan, P., Lu, J., Wu, Y., Wang, H., et al. (2015). Scutellarin regulates microglia-mediated TNF1 astrocytic reaction and astrogliosis in cerebral ischemia in the adult rats. *BMC Neurosci.* 16, 84. doi:10.1186/s12868-015-0219-6
- Fei, F., Su, N., Li, X., and Fei, Z. (2020). Neuroprotection mediated by natural products and their chemical derivatives. *Neural Regen. Res.* 15, 2008–2015. doi:10.4103/1673-5374.282240
- Forouzanfar, F., Read, M. I., Barreto, G. E., and Sahebkar, A. (2020). Neuroprotective effects of curcumin through autophagy modulation. *IUBMB Life* 72, 652–664. doi:10.1002/iub.2209
- Fu, C., Zhang, X., Lu, Y., Wang, F., Xu, Z., Liu, S., et al. (2020). Geniposide inhibits NLRP3 inflammasome activation via autophagy in BV-2 microglial cells exposed to oxygen-glucose deprivation/reoxygenation. *Int. Immunopharmacol.* 84, 106547. doi:10.1016/j.intimp.2020.106547
- Group T. N. I. O. N. D. A. S. r.-P. S. S. (1995). Tissue plasminogen activator for acute ischemic stroke. *N. Engl. J. Med.* 333, 1581–1587. doi:10.1056/NEJM199512143332401
- Gao, J., Chen, G., He, H., Liu, C., Xiong, X., Li, J., et al. (2017). Therapeutic effects of breviscapine in cardiovascular diseases: a review. *Front. Pharmacol.* 8, 289. doi:10.3389/fphar.2017.00289
- Gao, R., Zhao, X., Zheng, Y., and Liu, C. (2008). Study on immune function of soy isoflavone glycoside and aglycon. *Cereals Oils*, 14, 43–44. doi:10.1007/springerreference_135032
- Gao, Y., Fu, R., Wang, J., Yang, X., Wen, L., and Feng, J. (2018). Resveratrol mitigates the oxidative stress mediated by hypoxic-ischemic brain injury in neonatal rats via Nrf2/HO-1 pathway. *Pharm. Biol.* 56, 440–449. doi:10.1080/13880209.2018.1502326
- Ge, J. B., Lu, H. J., Song, X. J., Li, M., Chen, D. D., and Wu, F. (2017). [Protective effects of LBP on cerebral ischemia reperfusion injury in mice and mechanism of inhibiting NF- κ B, TNF- α , IL-6 and IL-1 β]. *Zhongguo Zhong Yao Za Zhi* 42, 326–331. doi:10.19540/j.cnki.cjcm.20161222.016
- Gu, J.-W., Hasuo, H., Takeya, M., and Akasu, T. (2005). Effects of emodin on synaptic transmission in rat hippocampal CA1 pyramidal neurons *in vitro*. *Neuropharmacology* 49, 103–111. doi:10.1016/j.neuropharm.2005.02.003
- Gu, J., Zhang, X., Fei, Z., Wen, A., Qin, S., and Yi, S. (2000). [Rhubarb Extracts in Treating Complications of Severe Cerebral Injury]. *Chin. Med. J.* 113 (6), 529–531.
- Guo, C., Tong, L., Xi, M., Yang, H., Dong, H., and Wen, A. (2012). Neuroprotective effect of calycosin on cerebral ischemia and reperfusion injury in rats. *J. Ethnopharmacology* 144, 768–774. doi:10.1016/j.jep.2012.09.056
- Guo, S., Li, J., and Xiao, S. (2019). Effects of peimine a on inflammatory response and autophagy in mice with cerebral ischemia-reperfusion injury. *Chin. J. Gerontol.* 39, 5347–5350. doi:10.5353/th_b5328058
- Guo, Y., Xu, X., Li, Q., Li, Z., and Du, F. (2010). Anti-inflammation effects of picoside 2 in cerebral ischemic injury rats. *Behav. Brain Functions* 6, 43. doi:10.1186/1744-9081-6-43
- Guo, Z.-H., Li, F., and Wang, W.-Z. (2009). The mechanisms of brain ischemic insult and potential protective interventions. *Neurosci. Bull.* 25 (3), 139–152. doi:10.1007/s12264-009-0104-3
- Hacke, W., Kaste, M., Bluhmki, E., Brozman, M., Dávalos, A., Guidetti, D., et al. (2008). Thrombolysis with alteplase 3 to 4.5 hours after acute ischemic stroke. *N. Engl. J. Med.* 359, 1317–1329. doi:10.1056/nejmoa0804656
- Han, Y., Liu, H., Li, K., Wang, T., and Ge, X. (2020). Research progress on antifungal activity of berberine and synthesis of its molecular probes. *Chem. World* 61, 83–91. doi:10.31830/2348-7542.2019.107
- Han, Y., Zhang, W., Tang, Y., Bai, W., Yang, F., Xie, L., et al. (2012). l-Tetrahydropalmatine, an active component of *Corydalis yanhusuo* W.T. Wang, protects against myocardial ischaemia-reperfusion injury in rats. *PLoS One* 7, e38627. doi:10.1371/journal.pone.0038627
- He, L. J., Liang, M., Hou, F. F., Guo, Z. J., Xie, D., and Zhang, X. (2009). Ethanol extraction of *Picrorhiza scrophulariiflora* prevents renal injury in experimental diabetes via anti-inflammation action. *J. Endocrinol.* 200, 347–355. doi:10.1677/joe-08-0481
- He, Q., Li, Z., Wang, Y., Hou, Y., Li, L., and Zhao, J. (2017). Resveratrol alleviates cerebral ischemia/reperfusion injury in rats by inhibiting NLRP3 inflammasome activation through Sirt1-dependent autophagy induction. *Int. Immunopharmacol.* 50, 208–215. doi:10.1016/j.intimp.2017.06.029
- Hermann, D. M., Popa-Wagner, A., Kleinschnitz, C., and Doeppner, T. R. (2019). Animal models of ischemic stroke and their impact on drug discovery. *Expert Opin. Drug Discov.* 14, 315–326. doi:10.1080/17460441.2019.1573984
- Hou, Y., Wang, J., and Feng, J. (2019). The neuroprotective effects of curcumin are associated with the regulation of the reciprocal function between autophagy and HIF-1 α in cerebral ischemia-reperfusion injury. *Dddt* 13, 1135–1144. doi:10.2147/dddt.s194182
- Hsu, C.-C., Kuo, T.-W., Liu, W.-P., Chang, C.-P., and Lin, H.-J. (2020). Calycosin preserves BDNF/TrkB signaling and reduces post-stroke neurological injury after cerebral ischemia by reducing accumulation of hypertrophic and TNF- α -containing microglia in rats. *J. Neuroimmune Pharmacol.* 15, 326–339. doi:10.1007/s11481-019-09903-9
- Hu, J., Chai, Y., Wang, Y., Kheir, M. M., Li, H., Yuan, Z., et al. (2012). PI3K p55y promoter activity enhancement is involved in the anti-apoptotic effect of berberine against cerebral ischemia-reperfusion. *Eur. J. Pharmacol.* 674, 132–142. doi:10.1016/j.ejphar.2011.11.014
- Hu, Q., Shen, P., Bai, S., Dong, M., Liang, Z., Chen, Z., et al. (2018). Metabolite-related antidepressant action of diterpene ginkgolides in the prefrontal cortex. *Ndt* 14, 999–1011. doi:10.2147/ndt.s161351
- Hu, X.-m., Zhou, M.-m., Hu, X.-m., and Zeng, F.-d. (2005). Neuroprotective effects of scutellarin on rat neuronal damage induced by cerebral ischemia/reperfusion. *Acta Pharmacol. Sinica* 26, 1454–1459. doi:10.1111/j.1745-7254.2005.00239.x

- Hu, X., Liao, W., Yang, W., Jiang, C., Zhou, Q., Chen, M., et al. (2006). Effect of Angelica polysaccharide on the expression of angiopoietin after the ischemic brain injury in rats. *Chin. J. Rehabil. Med.* 11, 204–206+230. doi:10.26226/morressier.57d034cfd462b80292383365
- Huang, B., Chen, P., Huang, L., Li, S., Zhu, R., Sheng, T., et al. (2017). Geniposide attenuates post-ischaemic neurovascular damage via GluN2A/AKT/ERK-dependent mechanism. *Cel Physiol. Biochem.* 43, 705–716. doi:10.1159/000480657
- Huang, L., Chen, C., Zhang, X., Li, X., Chen, Z., Yang, C., et al. (2018). Neuroprotective effect of curcumin against cerebral ischemia-reperfusion via mediating autophagy and inflammation. *J. Mol. Neurosci.* 64, 129–139. doi:10.1007/s12031-017-1006-x
- Hui, A., Wu, Z., Yuan, Y., Zhou, A., and Pan, J. (2013). Progress in synthesis and antagonistic activities towards PAFR and GlyR of ginkgolide derivatives and analogs. *Chin. J. Org. Chem.* 33, 1263–1272. doi:10.6023/cjoc201209028
- Hwang, I., Lim, S., Yoo, K.-Y., Lee, Y., Kim, H., Kang, I.-J., et al. (2008). A Phytochemically characterized extract of Cordyceps militaris and cordycepin protect hippocampal neurons from ischemic injury in gerbils. *Planta Med.* 74, 114–119. doi:10.1055/s-2008-1034277
- Ismailoglu, U. B., Saracoglu, I., Harput, U. S., and Sahin-Erdemli, I. (2002). Effects of phenylpropanoid and iridoid glycosides on free radical-induced impairment of endothelium-dependent relaxation in rat aortic rings. *J. Ethnopharmacol.* 79, 193–197. doi:10.1016/s0378-8741(01)00377-4
- Jia, D., Deng, Y., Gao, J., Liu, X., Chu, J., and Shu, Y. (2014). Neuroprotective effect of Panax notoginseng polysaccharides against focal cerebral ischemia reperfusion injury in rats. *Int. J. Biol. Macromol.* 63, 177–180. doi:10.1016/j.ijbiomac.2013.10.034
- Jiang, J., Dai, J., and Cui, H. (2018). Vitexin reverses the autophagy dysfunction to attenuate MCAO-induced cerebral ischemic stroke via mTOR/Ulk1 pathway. *Biomed. Pharmacother.* 99, 583–590. doi:10.1016/j.biopha.2018.01.067
- Jie, L., Yu, R., Yue, C., Jing, L., Qin, X., and Qin, Y. (2020). Effects of resveratrol on microglia polarization after oxygen glucose deprivation/reoxygenation injury in vitro. *Acta Anatomica Sinica* 51, 320–325. doi:10.16098/j.issn.0529-1356.2020.03.002
- Jin, M., Zhao, K., Huang, Q., Xu, C., and Shang, P. (2012). Isolation, structure and bioactivities of the polysaccharides from Angelica sinensis (Oliv.) Diels: a review. *Carbohydr. Polym.* 89, 713–722. doi:10.1016/j.carbpol.2012.04.049
- Jin, Z., Ke, J., Guo, P., Wang, Y., and Wu, H. (2019). Quercetin improves blood-brain barrier dysfunction in rats with cerebral ischemia reperfusion via Wnt signaling pathway. *Am. J. Transl. Res.* 11, 4683–4695. doi:10.1002/brb3.1911/v2/review1
- JinGHe, X. R., and Chen, L. P. (2014). The protective effect of ginkgo bilboa leaves injection on the brain dopamine in the rat model of cerebral ischemia/reperfusion injury. *Afr. Health Sci.* 14, 725–728. doi:10.4314/ahs.v14i3.31
- JinM. L., Park, S. Y., Kim, Y. H., Oh, J.-I., Lee, S. J., and Park, G. (2014). The neuroprotective effects of cordycepin inhibit glutamate-induced oxidative and ER stress-associated apoptosis in hippocampal HT22 cells. *Neurotoxicology* 41, 102–111. doi:10.1016/j.neuro.2014.01.005
- Kaihua, Z., and Jiayu, L. (2020). Neuroprotective effect of ellagic acid on cerebral ischemia-reperfusion injury in rats based on PI3K/Akt/NOS pathway. *Chin. J. Pract. Nervous Dis.* 23, 33–39. doi:10.1007/s12031-020-01703-8
- Kalogeris, T., Baines, C. P., Krenz, M., and Korthuis, R. J. (2016). Ischemia/reperfusion. *Compr. Physiol.* 7, 113–170. doi:10.1002/cphy.c160006
- Kang, D. W., Moon, J. Y., Choi, J. G., Kang, S. Y., Ryu, Y., Park, J. B., et al. (2016). Antinociceptive profile of levo-tetrahydropalmatine in acute and chronic pain mice models: role of spinal sigma-1 receptor. *Sci. Rep.* 6, 37850. doi:10.1038/srep37850
- Kao, T.-K., Ou, Y.-C., Kuo, J.-S., Chen, W.-Y., Liao, S.-L., Wu, C.-W., et al. (2006). Neuroprotection by tetramethylpyrazine against ischemic brain injury in rats. *Neurochem. Int.* 48, 166–176. doi:10.1016/j.neuint.2005.10.008
- Kim, H., Ahn, J. H., Song, M., Kim, D. W., Lee, T.-K., Lee, J.-C., et al. (2019). Pretreated fucoidan confers neuroprotection against transient global cerebral ischemic injury in the gerbil hippocampal CA1 area via reducing of glial cell activation and oxidative stress. *Biomed. Pharmacother.* 109, 1718–1727. doi:10.1016/j.biopha.2018.11.015
- Koo, H.-J., Lim, K.-H., Jung, H.-J., and Park, E.-H. (2006). Anti-inflammatory evaluation of gardenia extract, geniposide and genipin. *J. Ethnopharmacology* 103, 496–500. doi:10.1016/j.jep.2005.08.011
- Koronowski, K. B., Dave, K. R., Saul, I., Camarena, V., Thompson, J. W., Neumann, J. T., et al. (2015). Resveratrol preconditioning induces a novel extended window of ischemic tolerance in the mouse brain. *Stroke* 46, 2293–2298. doi:10.1161/strokeaha.115.009876
- Koronowski, K. B., Khoury, N., Saul, I., Loris, Z. B., Cohan, C. H., Stradecki-Cohan, H. M., et al. (2017). Neuronal SIRT1 (silent information regulator 2 homologue 1) regulates glycolysis and mediates resveratrol-induced ischemic tolerance. *Stroke* 48, 3117–3125. doi:10.1161/strokeaha.117.018562
- Kwok, S. S., Bu, Y., Lo, A. C., Chan, T. C., So, K. F., Lai, J. S., et al. (2019). A systematic review of potential therapeutic use of lycium barbarum polysaccharides in disease. *Biomed. Res. Int.* 2019, 4615745. doi:10.1155/2019/4615745
- Lan, N., and Lianjun, G. (2020). Neuroprotective effect of daurinoline on focal cerebral ischemia in rats. *China Pharmacist* 23, 1029–1031. doi:10.1016/j.lfs.2003.06.042
- Lee, C., Huang, K., Shaw, J., Chen, J., Kuo, W., Shen, G., et al. (2020). Cordyceps militaris Trends in the immunomodulatory effects of : total extracts, polysaccharides and cordycepin. *Front. Pharmacol.* 11, 575704. doi:10.3389/fphar.2020.575704
- Lee, E., Kim, S., Chul Chung, K., Choo, M.-K., Kim, D.-H., Nam, G., et al. (2006). 20(S)-ginsenoside Rh2, a newly identified active ingredient of ginseng, inhibits NMDA receptors in cultured rat hippocampal neurons. *Eur. J. Pharmacol.* 536, 69–77. doi:10.1016/j.ejphar.2006.02.038
- Lee, J.-C., Kim, J., Park, J.-K., Chung, G.-H., and Jang, Y.-S. (2003). The antioxidant, rather than prooxidant, activities of quercetin on normal cells: quercetin protects mouse thymocytes from glucose oxidase-mediated apoptosis. *Exp. Cel Res.* 291, 386–397. doi:10.1016/s0014-4827(03)00410-5
- Lei, W., Huojun, H., Jinyang, M., Yuanxun, D., Song, H., Changtao, F., et al. (2020). Role of cell autophagy in protection of resveratrol against cerebral ischemia-reperfusion injury in rats. *Chin. J. Clin. Neurosurg.* 25, 303–307. doi:10.1016/j.jneuroim.2017.11.015
- Leung, S. W., Lai, J. H., Wu, J. C., Tsai, Y. R., Chen, Y. H., Kang, S. J., et al. (2020). Neuroprotective effects of emodin against ischemia/reperfusion injury through activating ERK-1/2 signaling pathway. *Int. J. Mol. Sci.* 21, 114. doi:10.3390/ijms21082899
- Li, D.-Q., Bao, Y.-M., Li, Y., Wang, C.-F., Liu, Y., and An, L.-J. (2006). Catalpol modulates the expressions of Bcl-2 and Bax and attenuates apoptosis in gerbils after ischemic injury. *Brain Res.* 1115, 179–185. doi:10.1016/j.brainres.2006.07.063
- Li, F., Gong, Q.-H., Wu, Q., Lu, Y.-F., and Shi, J.-S. (2010). Icaritin isolated from Epimedium brevicornum Maxim attenuates learning and memory deficits induced by d-galactose in rats. *Pharmacol. Biochem. Behav.* 96, 301–305. doi:10.1016/j.pbb.2010.05.021
- Li, F., Lang, F., Zhang, H., Xu, L., Wang, Y., Zhai, C., et al. (2017). Apigenin alleviates endotoxin-induced myocardial toxicity by modulating inflammation, oxidative stress, and autophagy. *Oxidative Med. Cell Longevity* 2017, 1–10. doi:10.1155/2017/2302896
- Li, F., Li, W., Li, X., Li, F., Zhang, L., Wang, B., et al. (2016). Geniposide attenuates inflammatory response by suppressing P2Y14 receptor and downstream ERK1/2 signaling pathway in oxygen and glucose deprivation-induced brain microvascular endothelial cells. *J. Ethnopharmacology* 185, 77–86. doi:10.1016/j.jep.2016.03.025
- Li, H., Hu, J., Ma, L., Yuan, Z., Wang, Y., Wang, X., et al. (2010). Comprehensive study of baicalin down-regulating NOD2 receptor expression of neurons with oxygen-glucose deprivation in vitro and cerebral ischemia-reperfusion in vivo. *Eur. J. Pharmacol.* 649, 92–99. doi:10.1016/j.ejphar.2010.09.023
- Li, H., Hung, A., Li, M., and Yang, A. W. H. (2019). Fritillariae thunbergii bulbosus: traditional uses, phytochemistry, pharmacodynamics, pharmacokinetics and toxicity. *Int. J. Mol. Sci.* 20, 121. doi:10.3390/ijms20071667
- Li, H., Yan, Z., Zhu, J., Yang, J., and He, J. (2011). Neuroprotective effects of resveratrol on ischemic injury mediated by improving brain energy metabolism and alleviating oxidative stress in rats. *Neuropharmacology* 60, 252–258. doi:10.1016/j.neuropharm.2010.09.005
- Li, L., Li, H., and Li, M. (2015). Curcumin protects against cerebral ischemia-reperfusion injury by activating JAK2/STAT3 signaling pathway in rats. *Int. J. Clin. Exp. Med.* 8, 14985–14991. doi:10.1002/brb3.1911/v2/review1

- Li, L., Zhou, Q. X., and Shi, J. S. (2005). Protective effects of icariin on neurons injured by cerebral ischemia/reperfusion. *Chin. Med. J.* 118, 1637–1643. doi:10.5353/th_b4414290
- Li, L., and Zhang, H. (2020). Clinical study on Ligustrazine Hydrochloride Injection combined with ticagrelor in treatment of angina pectoris of coronary heart disease. *Drugs Clinic* 35, 1968–1972. doi:10.31525/ct1-nct04022031
- Li, M., Liu, X., Wang, Y., and Ju, X. (2020). *In vitro* effects of peimoin on the activity of cytochrome P450 enzymes. *Xenobiotica* 50, 1202–1207. doi:10.1080/00498254.2020.1761572
- Li, M., Qu, Y. Z., Zhao, Z. W., Wu, S. X., Liu, Y. Y., Wei, X. Y., et al. (2012). Astragaloside IV protects against focal cerebral ischemia/reperfusion injury correlating to suppression of neutrophils adhesion-related molecules. *Neurochem. Int.* 60, 458–465. doi:10.1016/j.neuint.2012.01.026
- Li, Q., Wang, J., Li, Y., and Xu, X. (2018). Neuroprotective effects of salidroside administration in a mouse model of Alzheimer's disease. *Mol. Med. Rep.* 7, 139. doi:10.3892/mmr.2018.8757
- Li, S., Jiao, Y., Wang, H., Shang, Q., Lu, F., Huang, L., et al. (2017). Sodium tanshinone IIA sulfate adjunct therapy reduces high-sensitivity C-reactive protein level in coronary artery disease patients: a randomized controlled trial. *Sci. Rep.* 7, 17451. doi:10.1038/s41598-017-16980-4
- Li, S., Liu, X., Chen, X., and Bi, L. (2020a). Research progress on anti-inflammatory effects and mechanisms of alkaloids from Chinese medical herbs. *Evid. Based Complement. Alternat Med.* 2020, 1303524. doi:10.1155/2020/1303524
- Li, S., Lu, Y., Ding, D., Ma, Z., Xing, X., Hua, X., et al. (2020b). Fibroblast growth factor 2 contributes to the effect of salidroside on dendritic and synaptic plasticity after cerebral ischemia/reperfusion injury. *Aging* 12, 10951–10968. doi:10.18632/aging.103308
- Li, S., Wang, T., Zhai, L., Ge, K., Zhao, J., Cong, W., et al. (2018). Picroside II exerts a neuroprotective effect by inhibiting mPTP permeability and EndoG release after cerebral ischemia/reperfusion injury in rats. *J. Mol. Neurosci.* 64, 144–155. doi:10.1007/s12031-017-1012-z
- Li, T., Liu, J.-W., Zhang, X.-D., Guo, M.-C., and Ji, G. (2007). The neuroprotective effect of picroside II from hu-huang-lian against oxidative stress. *Am. J. Chin. Med.* 35, 681–691. doi:10.1142/s0192415x0700517x
- Li, W., Suwanwela, N. C., and Patumraj, S. (2016). Curcumin by down-regulating NF- κ B and elevating Nrf2, reduces brain edema and neurological dysfunction after cerebral I/R. *Microvasc. Res.* 106, 117–127. doi:10.1016/j.mvr.2015.12.008
- Li, X., Ye, J., Zhao, L., Xia, P., Peng, X., and Yu, X. (2014). Effect of Gentiana officinalis from total secoiridoid glucoside on interleukin-1 β (IL-1 β)-induced rat chondrocytes. *Chin. Pharm. J.* 49, 1121–1125. doi:10.1016/j.biopha.2018.06.154
- Li, Y., Guan, Y., Wang, Y., Yu, C. L., Zhai, F. G., and Guan, L. X. (2017). Neuroprotective effect of the ginsenoside Rg1 on cerebral ischemic injury in vivo and in vitro is mediated by ppar γ -regulated antioxidative and anti-inflammatory pathways. *Evid. Based Complement. Alternat Med.* 2017, 7842082. doi:10.1155/2017/7842082
- Li, Y., Bao, Y., Jiang, B., Wang, Z., Liu, Y., Zhang, C., et al. (2008). Catalpol protects primary cultured astrocytes from *in vitro* ischemia-induced damage. *Int. J. Dev. Neurosci.* 26, 309–317. doi:10.1016/j.jdevneu.2008.01.006
- Li, Y. H., and Gong, P. L. (2004). The protective effect of dauricine on cerebral ischemia in mice. *Chin. Pharmacol. Bull.* 20, 564–566. doi:10.4268/cjcm20140626
- Li, Y., Yang, Y., Zhao, Y., Zhang, J., Liu, B., Jiao, S., et al. (2019). Astragaloside IV reduces neuronal apoptosis and parthanatos in ischemic injury by preserving mitochondrial hexokinase-II. *Free Radic. Biol. Med.* 131, 251–263. doi:10.1016/j.freeradbiomed.2018.11.033
- Li, Y., Yao, J., Han, C., Yang, J., Chaudhry, M., Wang, S., et al. (2016). Quercetin, inflammation and immunity. *Nutrients* 8, 167. doi:10.3390/nu8030167
- Liang, W., Huang, X., and Chen, W. (2017). The effects of baicalin and baicalein on cerebral ischemia: a review. *A&D* 8, 850–867. doi:10.14336/ad.2017.0829
- Liebner, S., Dijkhuizen, R. M., Reiss, Y., Plate, K. H., Agalliu, D., and Constantin, G. (2018). Plate karl H., agalliu dritan., constantin Gabriela.Functional morphology of the blood-brain barrier in health and disease. *Acta Neuropathol.* 135 (3), 311–336. doi:10.1007/s00401-018-1815-1
- LijLei, T., Lin, J., and Liao, W. (2019). Protective effects of Angelica polysaccharides on cerebral ischemia reperfusion injury in rats. *Chin. Arch. Trad. Chin. Med.* 37, 2272–2276+2317. doi:10.3724/sp.j.1008.2010.00238
- LiM.Li, J., Liu, S., and Li, W. (2018). Codonopsis pilosula polysaccharide on cerebral ischemia-reperfusion injury model mice brain protection and its effect on GFAP expression. *Acta Neuroparmacologica* 8, 42–43. doi:10.1016/j.carbpol.2012.07.062
- Lin, B. (2011). Polyphenols and neuroprotection against ischemia and neurodegeneration. *Mini Rev. Med. Chem.* 11, 1222–1238. doi:10.2174/138955711804586784
- Lin, X., and Zhang, N. (2018). Berberine: pathways to protect neurons. *Phytotherapy Res.* 32, 1501–1510. doi:10.1002/ptr.6107
- Liu, F., Wang, Y., Yao, W., Xue, Y., Zhou, J., and Liu, Z. (2019). Geniposide attenuates neonatal mouse brain injury after hypoxic-ischemia involving the activation of PI3K/Akt signaling pathway. *J. Chem. Neuroanat.* 102, 101687. doi:10.1016/j.jchemneu.2019.101687
- Liu, G., Song, J., Guo, Y., Wang, T., and Zhou, Z. (2013). Astragalus injection protects cerebral ischemic injury by inhibiting neuronal apoptosis and the expression of JNK3 after cerebral ischemia reperfusion in rats. *Behav. Brain Functions* 9, 36. doi:10.1186/1744-9081-9-36
- Liu, G., Wu, X., and Tang, W. (2015). Study on the chemical constituents and physiological activity of Poria cocos. *J. Qiqihar University(Natural Sci. Edition)* 31, 50–54. doi:10.4268/cjcm20140615
- Liu, H., Bai, J., Tan, J., and Weng, X. (2014). Cerebral protective effect of astragalus polysaccharide pretreatment on focal cerebral ischemia-reperfusion injury in rats. *J. Pract. Diabetology* 10, 31–32. doi:10.3724/sp.j.1008.2010.00238
- Liu, J.-h., Yin, F., Guo, L.-x., Deng, X.-h., and Hu, Y.-h. (2009). Neuroprotection of geniposide against hydrogen peroxide induced PC12 cells injury: involvement of PI3 kinase signal pathway. *Acta Pharmacol. Sin* 30, 159–165. doi:10.1038/aps.2008.25
- Liu, Q., Jin, Z., Xu, Z., Yang, H., Li, L., Li, G., et al. (2019). Antioxidant effects of ginkgolides and bilobalide against cerebral ischemia injury by activating the Akt/Nrf2 pathway *in vitro* and *in vivo*. *Cell Stress and Chaperones* 24, 441–452. doi:10.1007/s12192-019-00977-1
- Liu, R., Zhang, L., Lan, X., Li, L., Zhang, T.-T., Sun, J.-H., et al. (2011). Protection by borneol on cortical neurons against oxygen-glucose deprivation/reperfusion: involvement of anti-oxidation and anti-inflammation through nuclear transcription factor kappaB signaling pathway. *Neuroscience* 176, 408–419. doi:10.1016/j.neuroscience.2010.11.029
- Liu, X., Wen, S., Yan, F., Liu, K., Liu, L., Wang, L., et al. (2018). Salidroside provides neuroprotection by modulating microglial polarization after cerebral ischemia. *J. Neuroinflammation* 15, 39. doi:10.1186/s12974-018-1081-0
- Liu, Y.-l., Liang, J.-h., Yan, L.-d., Su, R.-b., Wu, C.-f., and Gong, Z.-h. (2005). Effects of l-tetrahydropalmatine on locomotor sensitization to oxycodone in mice. *Acta Pharmacol. Sin* 26, 533–538. doi:10.1111/j.1745-7254.2005.00101.x
- Liu, Y.-r., Li, P.-w., Suo, J.-j., Sun, Y., Zhang, B.-a., Lu, H., et al. (2014). Catalpol provides protective effects against cerebral ischaemia/reperfusion injury in gerbils. *J. Pharm. Pharmacol.* 66, 1265–1270. doi:10.1111/jphp.12261
- Liu, Y., Cui, Y., Lu, L., Gong, Y., Han, W., and Piao, G. (2020). Natural indole-containing alkaloids and their antibacterial activities. *Arch. Pharm. (Weinheim)* 23, e2000120. doi:10.1002/ardp.202000120
- Liu, Y., Wang, J., Wang, W., Zhang, H., Zhang, X., and Han, C. (2015). The chemical constituents and pharmacological actions of Cordyceps sinensis. *Evidence-Based Complement. Altern. Med.* 2015, 1–12. doi:10.1155/2015/575063
- LiuQ. S.Li, S. R., Li, K., Li, X., Yin, X., and Pang, Z. (2017). Ellagic acid improves endogenous neural stem cells proliferation and neurorestoration through Wnt/ β -catenin signaling *in vivo* and *in vitro*. *Mol. Nutr. Food Res.* 61, 113. doi:10.1002/mnfr.201600587
- LiuZ.-B.Liu, C., Zeng, B., Huang, L.-P., and Yao, L.-H. (2017). Modulation effects of cordycepin on voltage-gated sodium channels in rat hippocampal CA1 pyramidal neurons in the presence/absence of oxygen. *Neural Plasticity* 2017, 1–9. doi:10.1155/2017/2459053
- Long, Y., Yang, Q., Xiang, Y., Zhang, Y., Wan, J., Liu, S., et al. (2020). Nose to brain drug delivery - a promising strategy for active components from herbal medicine for treating cerebral ischemia reperfusion. *Pharmacol. Res.* 159, 104795. doi:10.1016/j.phrs.2020.104795
- Lu, S., Sun, L., Shen, J., Su, F., Wang, H., Ye, Z., et al. (2010). Protective effects of auricularia auricular polysaccharide on chronic cerebral ischemia injury in rats. *Chin. J. Pathophysiology* 26, 721–724. doi:10.3892/mmr.2018.9579

- Lu, Z.-Q., Deng, Y.-J., and Lu, J.-X. (2012). Effect of aloe polysaccharide on caspase-3 expression following cerebral ischemia and reperfusion injury in rats. *Mol. Med. Rep.* 6, 371–374. doi:10.3892/mmr.2012.927
- Lu, Z., Liu, Y., Shi, Y., Shi, X., Wang, X., Xu, C., et al. (2018). Curcumin protects cortical neurons against oxygen and glucose deprivation/reoxygenation injury through flotillin-1 and extracellular signal-regulated kinase1/2 pathway. *Biochem. Biophysical Res. Commun.* 496, 515–522. doi:10.1016/j.bbrc.2018.01.089
- Luo, Y., Nie, J., Gong, Q.-H., Lu, Y.-F., Wu, Q., and Shi, J.-S. (2007). Protective effects of icariin against learning and memory deficits induced by aluminium in rats. *Clin. Exp. Pharmacol. Physiol.* 34, 792–795. doi:10.1111/j.1440-1681.2007.04647.x
- Ma, J., He, W., Gao, C., Yu, D., Xue, P., and Niu, Y. (2019). Antioxidant and neuroprotective effects of Codonopsis pilosula polysaccharides on hypoxic-ischemic brain injury induced by Nrf2 pathway. *Chin. J. Clin. Anat.* 37, 403–408. doi:10.4077/cjp.2011.amm059
- Ma, R., Xie, Q., Li, Y., Chen, Z., Ren, M., Chen, H., et al. (2020). Animal models of cerebral ischemia: a review. *Biomed. Pharmacother.* 131, 110686. doi:10.1016/j.biopha.2020.110686
- Mantsch, J. R., Li, S.-J., Risinger, R., Awad, S., Katz, E., Baker, D. A., et al. (2007). Levo-tetrahydropalmatine attenuates cocaine self-administration and cocaine-induced reinstatement in rats. *Psychopharmacology* 192, 581–591. doi:10.1007/s00213-007-0754-7
- Manzanero, S., Santoro, T., and Arumugam, T. V. (2013). Neuronal oxidative stress in acute ischemic stroke: sources and contribution to cell injury. *Neurochem. Int.* 62 (5), 712–718. doi:10.1016/j.neuint.2012.11.009
- Mao, G., Zhang, L., Qian, F., Chen, K., Xu, J., Xu, J., et al. (2019). Research progress on anti-inflammatory activity of three kinds of iridoid glycosides in Chinese materia medica. *Chin. Trad. Herbal Drugs* 50, 225–233. doi:10.21203/rs.3.rs-58802/v1
- Mao, X. W., Pan, C. S., Huang, P., Liu, Y. Y., Wang, C. S., Yan, L., et al. (2015). Levo-tetrahydropalmatine attenuates mouse blood-brain barrier injury induced by focal cerebral ischemia and reperfusion: involvement of Src kinase. *Sci. Rep.* 5, 11155. doi:10.1038/srep11155
- Mo, Z.-t., Liao, Y.-l., Zheng, J., and Li, W.-n. (2020). Icariin protects neurons from endoplasmic reticulum stress-induced apoptosis after OGD/R injury via suppressing IRE1 α -XBP1 signaling pathway. *Life Sci.* 255, 117847. doi:10.1016/j.lfs.2020.117847
- Mook-Jung, I., Shin, J.-E., Yun, S. H., Huh, K., Koh, J. Y., Park, H. K., et al. (1999). Protective effects of asiaticoside derivatives against beta-amyloid neurotoxicity. *J. Neurosci. Res.* 58, 417–425. doi:10.1002/(sici)1097-4547(19991101)58:3<417::aid-jnr7>3.0.co;2-g
- Mukherjee, A., Sarkar, S., Jana, S., Swarnakar, S., and Das, N. (2019). Neuroprotective role of nanocapsulated curcumin against cerebral ischemia-reperfusion induced oxidative injury. *Brain Res.* 1704, 164–173. doi:10.1016/j.brainres.2018.10.016
- Negi, A. S., Kumar, J. K., Luqman, S., Shanker, K., Gupta, M. M., and Khanuja, S. P. S. (2008). Recent advances in plant hepatoprotectives: a chemical and biological profile of some important leads. *Med. Res. Rev.* 28, 746–772. doi:10.1002/med.20115
- Nejad, K. H., Dianat, M., Sarkaki, A., Naseri, M. K., Badavi, M., and Farbood, Y. (2015). Ellagic acid improves electrocardiogram waves and blood pressure against global cerebral ischemia rat experimental models. *Electron. Physician* 7, 1153–1162. doi:10.14661/2015.1153-1162
- Oliveira, C., Neves, N. M., Reis, R. L., Martins, A., and Silva, T. H. (2020). A review on fucoidan antitumor strategies: from a biological active agent to a structural component of fucoidan-based systems. *Carbohydr. Polym.* 239, 116131. doi:10.1016/j.carbpol.2020.116131
- Orhan, I. E. (2012). Centella asiatica (L.) urban: from traditional medicine to modern medicine with neuroprotective potential. *Evid. Based Complement. Alternat Med.* 2012, 946259. doi:10.1155/2012/946259
- Pang, Q., Zhao, Y., Chen, X., Zhao, K., Zhai, Q., and Tu, F. (2018). Apigenin protects the brain against ischemia/reperfusion injury via caveolin-1/VEGF in vitro and in vivo. *Oxid Med. Cel Longev* 2018, 7017204. doi:10.1155/2018/7017204
- Park, D.-J., Jeon, S.-J., Kang, J.-B., and Koh, P.-O. (2020). Quercetin reduces ischemic brain injury by preventing ischemia-induced decreases in the neuronal calcium sensor protein hippocalcin. *Neuroscience* 430, 47–62. doi:10.1016/j.neuroscience.2020.01.015
- Peng, X., Shi, Z., Liang, C., Ren, Y., and Tan, R. (2019). Protective effect of Chinese Yam polysaccharides on cerebral ischemia-reperfusion injury in mice. *Pharmacol. Clin. Chin. Materia Med.* 35, 60–63. doi:10.4268/cjcm.20140327
- Perviz, S., Khan, H., and Pervaiz, A. (2016). Plant alkaloids as an emerging therapeutic alternative for the treatment of depression. *Front. Pharmacol.* 7, 28. doi:10.3389/fphar.2016.00028
- Putteeraj, M., Lim, W., Teoh, S. L., and Yahaya, M. (2018). Flavonoids and its neuroprotective effects on brain ischemia and neurodegenerative diseases. *Curr. Drug Targets* 19, 115. doi:10.2174/1389450119666180326125252
- Qian, G., and Min, L. (2010). Protective effect of black fungus polysaccharide on hypoxic-ischemic brain damage in neonatal rats. *Chin. J. Trad. Med. Sci. Technol.* 17, 129–130. doi:10.1109/hhbe.2011.6027979
- Qin, P., Li, X., Yang, H., Wang, Z. Y., and Lu, D. (2019). Therapeutic potential and biological applications of cordycepin and metabolic mechanisms in cordycepin-producing fungi. *Molecules* 24, 2231. doi:10.3390/molecules24122231
- Qiu, S., Sun, H., Zhang, A.-H., Xu, H.-Y., Yan, G.-L., Han, Y., et al. (2014). Natural alkaloids: basic aspects, biological roles, and future perspectives. *Chin. J. Nat. Medicines* 12, 401–406. doi:10.1016/s1875-5364(14)60063-7
- Ran, K., Yang, D.-L., Chang, Y.-T., Duan, K.-M., Ou, Y.-W., Wang, H.-P., et al. (2014). Ginkgo biloba extract postconditioning reduces myocardial ischemia reperfusion injury. *Genet. Mol. Res.* 13, 2703–2708. doi:10.4238/2014.april.8.14
- Ren, J., Fan, C., Chen, N., Huang, J., and Yang, Q. (2011). Resveratrol pretreatment attenuates cerebral ischemic injury by upregulating expression of transcription factor Nrf2 and HO-1 in rats. *Neurochem. Res.* 36, 2352–2362. doi:10.1007/s11064-011-0561-8
- Ren, S., Zhang, H., Mu, Y., Sun, M., and Liu, P. (2013). Pharmacological effects of Astragaloside IV: a literature review. *J. Trad. Chin. Med.* 33, 413–416. doi:10.1016/s0254-6272(13)60189-2
- Rosales, P. F., Bordin, G. S., Gower, A. E., and Moura, S. (2020). Indole alkaloids: 2012 until now, highlighting the new chemical structures and biological activities. *Fitoterapia* 143, 104558. doi:10.1016/j.fitote.2020.104558
- Ryoo, N., Rahman, M. A., Hwang, H., Ko, S. K., Nah, S.-Y., Kim, H.-C., et al. (2020). Ginsenoside Rk1 is a novel inhibitor of NMDA receptors in cultured rat hippocampal neurons. *J. Ginseng Res.* 44, 490–495. doi:10.1016/j.jgr.2019.04.002
- Ryu, E., Son, M., Lee, M., Lee, K., Cho, J. Y., Cho, S., et al. (2014). Cordycepin is a novel chemical suppressor of Epstein-Barr virus replication. *Oncoscience* 1, 866–881. doi:10.18632/oncoscience.110
- Saini, A., Taliyan, R., and Sharma, P. (2014). Protective effect and mechanism of Ginkgo biloba extract-EGb 761 on STZ-induced diabetic cardiomyopathy in rats. *Phcog Mag.* 10, 172–178. doi:10.4103/0973-1296.131031
- Santos, A. C., Pereira, I., Pereira-Silva, M., Ferreira, L., Caldas, M., Collado-González, M., et al. (2019). Nanotechnology-based formulations for resveratrol delivery: effects on resveratrol in vivo bioavailability and bioactivity. *Colloids Surf. B: Biointerfaces* 180, 127–140. doi:10.1016/j.colsurfb.2019.04.030
- Savopoulos, C., Ntaios, G., and Hatzitolios, A. (2009). Is there a geographic variation in the seasonal distribution of acute myocardial infarction and sudden cardiac death?. *Int. J. Cardiol.* 135, 253–254. doi:10.1016/j.ijcard.2008.03.019
- Shafabakhsh, R., and Asemi, Z. (2019). Quercetin: a natural compound for ovarian cancer treatment. *J. Ovarian Res.* 12, 55. doi:10.1186/s13048-019-0530-4
- Shao, J., Jin, H., Zhu, H., and Liu, J. (2013). Optimization of the technological parameters for the alcohol extraction of ginkgo flavonoid glycosides and the in vitro antioxidant study. *J. China Univ. Mining Technol.* 42, 663–669. doi:10.1016/j.phytochem.2016.05.005
- She, D. T., Jo, D. G., and Arumugam, T. V. (2017). Emerging roles of sirtuins in ischemic stroke. *Transl Stroke Res.* 12, 147. doi:10.1007/s12975-017-0544-4
- Simão, F., Matté, A., Pagnussat, A. S., Netto, C. A., and Salbego, C. G. (2012b). Resveratrol preconditioning modulates inflammatory response in the rat hippocampus following global cerebral ischemia. *Neurochem. Int.* 61, 659–665. doi:10.1016/j.neuint.2012.06.009
- Simão, F., Matté, A., Pagnussat, A. S., Netto, C. A., and Salbego, C. G. (2012a). Resveratrol prevents CA1 neurons against ischemic injury by parallel modulation of both GSK-3 β and CREB through PI3-K/Akt pathways. *Eur. J. Neurosci.* 36, 2899–2905. doi:10.1111/j.1460-9568.2012.08229.x
- Song, B., Tang, X., Wang, X., Huang, X., Ye, Y., Lu, X., et al. (2012). Berberine induces peripheral lymphocytes immune regulations to realize its

- neuroprotective effects in the cerebral ischemia/reperfusion mice. *Cell Immunol.* 276, 91–100. doi:10.1016/j.cellimm.2012.04.006
- Song, D., Hao, J., and Fan, D. (2020). Biological properties and clinical applications of berberine. *Front. Med.* 4, 144. doi:10.5194/fmed-2020-1-rc1
- Song, M.-t., Ruan, J., Zhang, R.-y., Deng, J., Ma, Z.-q., and Ma, S.-p. (2018). Astragaloside IV ameliorates neuroinflammation-induced depressive-like behaviors in mice via the PPAR γ /NF- κ B/NLRP3 inflammasome axis. *Acta Pharmacol. Sin.* 39, 1559–1570. doi:10.1038/aps.2017.208
- Sowndhararajan, K., Deepa, P., Kim, M., Park, S. J., and Kim, S. (2018). Neuroprotective and cognitive enhancement potentials of baicalin: a review. *Brain Sci.* 8, 137. doi:10.3390/brainsci8060104
- Stanimirovic, D., and Satoh, K. (2000). Inflammatory mediators of cerebral endothelium: a role in ischemic brain inflammation. *Brain Pathol.* 10 (1), 113–126. doi:10.1111/j.1750-3639.2000.tb00248.x
- Steliga, A., Kowiański, P., Czuba, E., Wąskow, M., Moryś, J., and Lietzau, G. (2020). Neurovascular unit as a source of ischemic stroke biomarkers-limitations of experimental studies and perspectives for clinical application. *Transl. Stroke Res.* 11 (4), 553–579. doi:10.1007/s12975-019-00744-5
- Stuppner, H., and Wagner, H. (1989). New cucurbitacin glycosides from *Picrorhiza kurroo*. *Planta Med.* 55, 559–563. doi:10.1055/s-2006-962095
- Sun, J. B., Li, Y., Cai, Y. F., Huang, Y., Liu, S., Yeung, P. K., et al. (2018). Scutellarin protects oxygen/glucose-deprived astrocytes and reduces focal cerebral ischemic injury. *Neural Regen. Res.* 13, 1396–1407. doi:10.4103/1673-5374.235293
- Sun, R., Song, Y., Li, S., Ma, Z., Deng, X., Fu, Q., et al. (2018). Levotetrahydropalmatine attenuates neuron apoptosis induced by cerebral ischemia-reperfusion injury: involvement of c-abl activation. *J. Mol. Neurosci.* 65, 391–399. doi:10.1007/s12031-018-1063-9
- Sy, L., Xie, Y., and Yu, Z. (2015). Notoginseng polysaccharide on rat ischemia-reperfusion injury of protection. *J. Apoplexy Nervous Dis.* 32, 996–998. doi:10.1007/978-3-0348-8988-9_25
- Tang, B., Wang, D., Li, M., Wu, Q., Yang, Q., Shi, W., et al. (2017). An *in vivo* study of hypoxia-inducible factor-1 α signaling in ginsenoside Rg1-mediated brain repair after hypoxia/ischemia brain injury. *Pediatr. Res.* 81, 120–126. doi:10.1038/pr.2016.178
- Tang, H., Tang, Y., Li, N., Shi, Q., Guo, J., Shang, E., et al. (2014). Neuroprotective effects of scutellarin and scutellarein on repeatedly cerebral ischemia-reperfusion in rats. *Pharmacol. Biochem. Behav.* 118, 51–59. doi:10.1016/j.pbb.2014.01.003
- Thapa, S. B., Pandey, R. P., Park, Y. I., and Kyung Sohng, J. (2019). Biotechnological advances in resveratrol production and its chemical diversity. *Molecules* 24, 2571. doi:10.3390/molecules24142571
- Thiyagarajan, M., and Sharma, S. S. (2004). Neuroprotective effect of curcumin in middle cerebral artery occlusion induced focal cerebral ischemia in rats. *Life Sci.* 74, 969–985. doi:10.1016/j.lfs.2003.06.042
- Tian, Y., Liu, A., Su, J., Xu, S., Dai, G., and Xue, H. (2015). Theoretical study on the structure-activity relationship of andrographolide derivatives. *J. Zhengzhou University(Natural Sci. Edition)* 47, 103–106. doi:10.3109/14756361003724760
- Tsai, S.-K., Hung, L.-M., Fu, Y.-T., Cheng, H., Nien, M.-W., Liu, H.-Y., et al. (2007). Resveratrol neuroprotective effects during focal cerebral ischemia injury via nitric oxide mechanism in rats. *J. Vasc. Surg.* 46, 346–353. doi:10.1016/j.jvs.2007.04.044
- Tu, F., Pang, Q., Huang, T., Zhao, Y., Liu, M., and Chen, X. (2017). Apigenin ameliorates post-stroke cognitive deficits in rats through histone acetylation-mediated neurochemical alterations. *Med. Sci. Monit.* 23, 4004–4013. doi:10.12659/msm.902770
- Tu, X. K., Yang, W. Z., Shi, S. S., Chen, Y., Wang, C. H., Chen, C. M., et al. (2011). Baicalin inhibits TLR2/4 signaling pathway in rat brain following permanent cerebral ischemia. *Inflammation* 34, 463–470. doi:10.1007/s10753-010-9254-8
- Tuli, H. S., Sandhu, S., and Sharma, A. (2013). Pharmacological and therapeutic potential of Cordyceps with special reference to Cordycepin. *Biotech* 4, 1–12. doi:10.1007/s13205-013-0121-9
- Ułamek-Kozioł, M., Czuczwar, S. J., Januszewski, S., and Pluta, R. (2020). Substantiation for the use of curcumin during the development of neurodegeneration after brain ischemia. *Int. J. Mol. Sci.* 21, 517. doi:10.3390/ijms21020517
- Wan, W., Zhang, C., Danielsen, M., Li, Q., Chen, W., Chan, Y., et al. (2016). EGB761 improves cognitive function and regulates inflammatory responses in the APP/PS1 mouse. *Exp. Gerontol.* 81, 92–100. doi:10.1016/j.exger.2016.05.007
- Wang, C., Li, Y., Gao, S., Cheng, D., Zhao, S., and Liu, E. (2015). Breviscapine injection improves the therapeutic effect of western medicine on angina pectoris patients. *PLoS One* 10, e0129969. doi:10.1371/journal.pone.0129969
- Wang, D. Q., He, Z. D., Feng, B. S., and Yang, C. R. (1993). Chemical constituents from *Picrorhiza scrophulariiflora*. *Acta Botanica Yunnanica* 15, 83–88.
- Wang, F., Zhang, Y., Zheng, X., Dai, Z., Liu, B., and Ma, S. (2019). Research progress of the structure and biological activities of iridoids compounds. *Chin. Pharm. Aff.* 33, 323–330. doi:10.1159/000391383
- Wang, J., Wang, L., Lou, G.-H., Zeng, H.-R., Hu, J., Huang, Q.-W., et al. (2019a). *Coptidis Rhizoma*: a comprehensive review of its traditional uses, botany, phytochemistry, pharmacology and toxicology. *Pharm. Biol.* 57, 193–225. doi:10.1080/13880209.2019.1577466
- Wang, J., Xu, J., Gong, X., Yang, M., Zhang, C., and Li, M. (2019b). Biosynthesis, chemistry, and pharmacology of polyphenols from Chinese salvia species: a review. *Molecules* 24, 59. doi:10.3390/molecules24010155
- Wang, L.-Y., Liu, J., Li, Y., Li, B., Zhang, Y.-Y., Jing, Z.-W., et al. (2015). Time-dependent variation of pathways and networks in a 24-hour window after cerebral ischemia-reperfusion injury. *BMC Syst. Biol.* 9 (1), 11. doi:10.1186/s12918-015-0152-4
- Wang, L., and Ma, Q. (2018). Clinical benefits and pharmacology of scutellarin: a comprehensive review. *Pharmacol. Ther.* 190, 105–127. doi:10.1016/j.pharmthera.2018.05.006
- Wang, L., Wang, P., Xu, K., Chen, Y., Li, Q., and Lei, H. (2013). Research progress on structure-activity relationship of ligustrazine derivatives. *Chin. Trad. Herbal Drugs* 44, 2766–2771. doi:10.21873/anticancerres.11635
- Wang, L., Zhao, H., Zhai, Z.-z., and Qu, L.-x. (2018). Protective effect and mechanism of ginsenoside Rg1 in cerebral ischaemia-reperfusion injury in mice. *Biomed. Pharmacother.* 99, 876–882. doi:10.1016/j.biopha.2018.01.136
- Wang, Q., Sun, A. Y., Simonyi, A., Jensen, M. D., Shelat, P. B., Rottinghaus, G. E., et al. (2005). Neuroprotective mechanisms of curcumin against cerebral ischemia-induced neuronal apoptosis and behavioral deficits. *J. Neurosci. Res.* 82, 138–148. doi:10.1002/jnr.20610
- Wang, S.-W., Lai, C.-Y., and Wang, C.-J. (1992). Inhibitory effect of geniposide on aflatoxin B1-induced DNA repair synthesis in primary cultured rat hepatocytes. *Cancer Lett.* 65, 133–137. doi:10.1016/0304-3835(92)90157-q
- Wang, T., Zhai, L., Zhang, H., Zhao, L., and Guo, Y. (2015a). Picroside II inhibits the MEK-ERK1/2-COX2 signal pathway to prevent cerebral ischemic injury in rats. *J. Mol. Neurosci.* 57, 335–351. doi:10.1007/s12031-015-0623-5
- Wang, T., Zhao, L., Guo, Y., Zhang, M., and Pei, H. (2015b). Picroside II inhibits neuronal apoptosis and improves the morphology and structure of brain tissue following cerebral ischemic injury in rats. *PLoS One* 10, e0124099. doi:10.1371/journal.pone.0124099
- Wang, W., Ma, X., Han, J., Zhou, M., Ren, H., Pan, Q., et al. (2016). Neuroprotective effect of scutellarin on ischemic cerebral injury by down-regulating the expression of angiotensin-converting enzyme and AT1 receptor. *PLoS One* 11, e0146197. doi:10.1371/journal.pone.0146197
- Wang, X. (2006). *Research on the design, synthesis, biological activity and quantitative structure-activity relationship of emodin derivatives targeting matrix metalloproteinases*. Jinan, China: Shandong University.
- Wang, X., Chen, L., Tan, C., and Xie, D. (2014). Protective effect of lycium barbarum polysaccharides on cerebral ischemia-reperfusion injury model rats. *China Pharm.* 25, 1365–1367. doi:10.5353/th_b5328058
- Wang, X., and Zhao, L. (2016). Calycosin ameliorates diabetes-induced cognitive impairments in rats by reducing oxidative stress via the PI3K/Akt/GSK-3 β signaling pathway. *Biochem. Biophys. Res. Commun.* 473, 428–434. doi:10.1016/j.bbrc.2016.03.024
- Wang, Y., Dong, X., Li, Z., Wang, W., Tian, J., and Chen, J. (2014). Downregulated RASD1 and upregulated miR-375 are involved in protective effects of calycosin on cerebral ischemia/reperfusion rats. *J. Neurol. Sci.* 339, 144–148. doi:10.1016/j.jns.2014.02.002
- Wang, Y., Ren, Q., Zhang, X., Lu, H., and Chen, J. (2018). Neuroprotective mechanisms of calycosin against focal cerebral ischemia and reperfusion injury in rats. *Cel Physiol. Biochem.* 45, 537–546. doi:10.1159/000487031
- Wang, Y., Su, Y., Lai, W., Huang, X., Chu, K., Brown, J., et al. (2020). Salidroside restores an anti-inflammatory endothelial phenotype by selectively inhibiting endothelial complement after oxidative stress. *Inflammation* 43, 310–325. doi:10.1007/s10753-019-01121-y

- Wang, Y., Wu, Y., Liang, C., Tan, R., Tan, L., and Tan, R. (2019). Pharmacodynamic effect of ellagic acid on ameliorating cerebral ischemia/reperfusion injury. *Pharmacology* 104, 320–331. doi:10.1159/000502401
- Wang, Y., Zhen, Y., Wu, X., Jiang, Q., Li, X., Chen, Z., et al. (2015). Vitexin protects brain against ischemia/reperfusion injury via modulating mitogen-activated protein kinase and apoptosis signaling in mice. *Phytomedicine* 22, 379–384. doi:10.1016/j.phymed.2015.01.009
- Wang, F., Yin, P., Lu, Y., Zhou, Z., Jiang, C., Liu, Y., et al. (2015). Cordycepin prevents oxidative stress-induced inhibition of osteogenesis. *Oncotarget* 6, 117. doi:10.18632/oncotarget.6072
- Wang, Y.-Y., Chang, C.-Y., Lin, S.-Y., Wang, J.-D., Wu, C.-C., Chen, W.-Y., et al. (2020). Quercetin protects against cerebral ischemia/reperfusion and oxygen glucose deprivation/reoxygenation neurotoxicity. *J. Nutr. Biochem.* 83, 108436. doi:10.1016/j.jnutbio.2020.108436
- Wei, H., Wang, S., Zhen, L., Yang, Q., Wu, Z., Lei, X., et al. (2015). Resveratrol attenuates the blood-brain barrier dysfunction by regulation of the MMP-9/TIMP-1 balance after cerebral ischemia reperfusion in rats. *J. Mol. Neurosci.* 55, 872–879. doi:10.1007/s12031-014-0441-1
- Wei, Y., Hong, H., Zhang, X., Lai, W., Wang, Y., Chu, K., et al. (2017). Salidroside inhibits inflammation through PI3K/Akt/HIF signaling after focal cerebral ischemia in rats. *Inflammation* 40, 1297–1309. doi:10.1007/s10753-017-0573-x
- Williams, E. I., Betterton, R. D., Davis, T. P., and Ronaldson, P. T. (2020). Transporter-mediated delivery of small molecule drugs to the brain: a critical mechanism that can advance therapeutic development for ischemic stroke. *Pharmaceutics* 12, 63. doi:10.3390/pharmaceutics12020154
- Wu, L., and Fang, F. (2020). Advances in structural modification and structure-activity relationship of berberine. *Chin. J. New Drugs* 29, 1257–1264. doi:10.1001/archneur.1968.00470320053006
- Wu, S.-y., Wang, G.-f., Liu, Z.-q., Rao, J.-j., Lü, L., Xu, W., et al. (2009). Effect of geniposide, a hypoglycemic glucoside, on hepatic regulating enzymes in diabetic mice induced by a high-fat diet and streptozotocin. *Acta Pharmacol. Sin* 30, 202–208. doi:10.1038/aps.2008.17
- Xia, Z., Zhang, R., Wu, P., Xia, Z., and Hu, Y. (2012). Memory defect induced by beta-amyloid plus glutamate receptor agonist is alleviated by catalpol and donepezil through different mechanisms. *Brain Res.* 1441, 27–37. doi:10.1016/j.brainres.2012.01.008
- Xie, C.-L., Li, J.-H., Wang, W.-W., Zheng, G.-Q., and Wang, L.-X. (2015). Neuroprotective effect of ginsenoside-Rg1 on cerebral ischemia/reperfusion injury in rats by downregulating protease-activated receptor-1 expression. *Life Sci.* 121, 145–151. doi:10.1016/j.lfs.2014.12.002
- Xie, C. J., Gu, A. P., Cai, J., Wu, Y., and Chen, R. C. (2018). Curcumin protects neural cells against ischemic injury in N2a cells and mouse brain with ischemic stroke. *Brain Behav.* 8, e00921. doi:10.1002/brb3.921
- Xie, W., Zhou, P., Sun, Y., Meng, X., Dai, Z., Sun, G., et al. (2018). Protective effects and target network analysis of ginsenoside Rg1 in cerebral ischemia and reperfusion injury: a comprehensive overview of experimental studies. *Cells* 7, 114. doi:10.3390/cells7120270
- Xiong, D., Deng, Y., Huang, B., Yin, C., Liu, B., Shi, J., et al. (2016). Icarin attenuates cerebral ischemia-reperfusion injury through inhibition of inflammatory response mediated by NF- κ B, PPAR α and PPAR γ in rats. *Int. Immunopharmacology* 30, 157–162. doi:10.1016/j.intimp.2015.11.035
- Xu, D., Hu, M. J., Wang, Y. Q., and Cui, Y. L. (2019). Antioxidant activities of quercetin and its complexes for medicinal application. *Molecules* 24, 119. doi:10.3390/molecules24061123
- Xu, H., Hua, Y., Zhong, J., Li, X., Xu, W., Cai, Y., et al. (2018). Resveratrol delivery by albumin nanoparticles improved neurological function and neuronal damage in transient middle cerebral artery occlusion rats. *Front. Pharmacol.* 9, 1403. doi:10.3389/fphar.2018.01403
- Xu, L., Ding, L., Su, Y., Shao, R., Liu, J., and Huang, Y. (2019). Neuroprotective effects of curcumin against rats with focal cerebral ischemia-reperfusion injury. *Int. J. Mol. Med.* 43, 1879–1887. doi:10.3892/ijmm.2019.4094
- Xu, N., Huang, F., Jian, C., Qin, L., Lu, F., Wang, Y., et al. (2019). Neuroprotective effect of salidroside against central nervous system inflammation-induced cognitive deficits: a pivotal role of sirtuin 1-dependent Nrf-2/HO-1/NF- κ B pathway. *Phytotherapy Res.* 33, 1438–1447. doi:10.1002/ptr.6335
- Xu, S.-H., Yin, M.-S., Liu, B., Chen, M.-L., He, G.-w., Zhou, P.-P., et al. (2017). Tetramethylpyrazine-2'-O-sodium ferulate attenuates blood-brain barrier disruption and brain oedema after cerebral ischemia/reperfusion. *Hum. Exp. Toxicol.* 36, 670–680. doi:10.1177/0960327116657401
- Xue, D., Jiang, H., Xiao, K., and Xuan, L. (2001). Isolation, identification and antioxidant effect of soy isoflavones. *J. Nanjing Agric. Univ.*, 89–92. doi:10.1186/isrctn98074661
- Xue, X., Qu, X.-J., Yang, Y., Sheng, X.-H., Cheng, F., Jiang, E.-N., et al. (2010). Baicalin attenuates focal cerebral ischemic reperfusion injury through inhibition of nuclear factor κ B p65 activation. *Biochem. Biophysical Res. Commun.* 403, 398–404. doi:10.1016/j.bbrc.2010.11.042
- Xue, X., Quan, Y., Gong, L., Gong, X., and Li, Y. (2020). A review of the processed Polygonum multiflorum (Thunb.) for hepatoprotection: clinical use, pharmacology and toxicology. *J. Ethnopharmacol.* 261, 113121. doi:10.1016/j.jep.2020.113121
- Xu, L., Kong, X., Xiu, H., Dou, Y., Wu, Z., and Sun, P. (2018). Combination of curcumin and vagus nerve stimulation attenuates cerebral ischemia/reperfusion injury-induced behavioral deficits. *Biomed. Pharmacother.* 103, 614–620. doi:10.1016/j.biopha.2018.04.069
- Xu, L., Jia, L., Wang, Q., Hou, J., Li, S., and Teng, J. (2018). Salidroside attenuates hypoxia/reoxygenation-induced human brain vascular smooth muscle cell injury by activating the SIRT1/FOXO3 α pathway. *Exp. Ther. Med.* 15, 822–830. doi:10.3892/etm.2017.5446
- Yan, A., and Xie, Y. (2018). Effect of angelica sinensis radix polysaccharide on oxidative stress level and inflammatory cytokine expression of brain tissues in rats with cerebral ischemia reperfusion injury. *Chin. J. Exp. Trad. Med. Formulae* 24, 123–127. doi:10.1159/000418069
- Yan, L., and Zhou, Q. H. (2012). Study on neuroprotective effects of astragalin in rats with ischemic brain injury and its mechanisms. *Zhongguo Ying Yong Sheng Li Xue Za Zhi* 28, 373–377. doi:10.1016/j.jalz.2010.05.551
- Yan, S., Chen, L., Wei, X., Cheng, L., Kong, L., Liu, X., et al. (2015). Tetramethylpyrazine analogue CXCI95 ameliorates cerebral ischemia-reperfusion injury by regulating endothelial nitric oxide synthase phosphorylation via PI3K/Akt signaling. *Neurochem. Res.* 40, 446–454. doi:10.1007/s11064-014-1485-x
- Yang, J., Huang, J., Shen, C., Cheng, W., Yu, P., Wang, L., et al. (2018a). Resveratrol treatment in different time-attenuated neuronal apoptosis after oxygen and glucose deprivation/reoxygenation via enhancing the activation of nrf-2 signaling pathway in vitro. *Cel Transpl.* 27, 1789–1797. doi:10.1177/0963689718780930
- Yang, J., Yan, H., Li, S., and Zhang, M. (2018b). Berberine ameliorates MCAO induced cerebral ischemia/reperfusion injury via activation of the BDNF-TrkB-PI3K/Akt signaling pathway. *Neurochem. Res.* 43, 702–710. doi:10.1007/s11064-018-2472-4
- Yang, X., Zhang, L., Jiang, S., Gong, P., and Zeng, F. (2009). Effect of dauricine on apoptosis and expression of apoptogenic protein after transient focal cerebral ischemia-reperfusion injury in rats. *Zhongguo Zhong Yao Za Zhi* 34, 78–83. doi:10.31083/jin-170047
- Yang, Y., Liu, P., Chen, L., Liu, Z., Zhang, H., Wang, J., et al. (2013). Therapeutic effect of Ginkgo biloba polysaccharide in rats with focal cerebral ischemia/reperfusion (I/R) injury. *Carbohydr. Polym.* 98, 1383–1388. doi:10.1016/j.carbpol.2013.07.045
- Yang, Y., Liu, Y., Liu, M., Hu, W., Yang, X., Deng, Y., et al. (2020). The neuroprotective effects of icaritin on focal cerebral ischemia reperfusion injured rats during early recovery period. *Trad. Chin. Drug Res. Clin. Pharmacol.* 31, 662–667. doi:10.3892/ijmm.2019.4094
- Ye, T. M., Sun, L. N., Su, F., Shen, J., Wang, H. P., Ye, Z. G., et al. (2010). Study of the effects of Auricularia auricular polysaccharide on local ischemia/reperfusion injury in rat. *Zhongguo Ying Yong Sheng Li Xue Za Zhi* 26, 423–426. doi:10.14711/thesis-b878059
- Yen, T.-L., Chen, R.-J., Jayakumar, T., Lu, W.-J., Hsieh, C.-Y., Hsu, M.-J., et al. (2016). Andrographolide stimulates p38 mitogen-activated protein kinase-nuclear factor erythroid-2-related factor 2-heme oxygenase 1 signaling in primary cerebral endothelial cells for definite protection against ischemic stroke in rats. *Translational Res.* 170, 57–72. doi:10.1016/j.trsl.2015.12.002
- Yen, T.-L., Hsu, W.-H., Huang, S. K.-H., Lu, W.-J., Chang, C.-C., Lien, L.-M., et al. (2013). A novel bioactivity of andrographolide from Andrographis paniculata on cerebral ischemia/reperfusion-induced brain injury through induction of cerebral endothelial cell apoptosis. *Pharm. Biol.* 51, 1150–1157. doi:10.3109/13880209.2013.782051

- Yin, F., Liu, J., Zheng, X., Guo, L., and Xiao, H. (2010). Geniposide induces the expression of heme oxygenase-1 via PI3K/Nrf2-signaling to enhance the antioxidant capacity in primary hippocampal neurons. *Biol. Pharm. Bull.* 33, 1841–1846. doi:10.1248/bpb.33.1841
- Yin, F., Zhou, H., Fang, Y., Li, C., He, Y., Yu, L., et al. (2020). Astragaloside IV alleviates ischemia reperfusion-induced apoptosis by inhibiting the activation of key factors in death receptor pathway and mitochondrial pathway. *J. Ethnopharmacology* 248, 112319. doi:10.1016/j.jep.2019.112319
- Yin, Q., Wang, R., Yang, S., Wu, Z., Guo, S., Dai, X., et al. (2017). Influence of temperature on transdermal penetration enhancing mechanism of borneol: a multi-scale study. *Int. J. Mol. Sci.* 18, 195. doi:10.3390/ijms18010195
- Ying, L., and Chi, Y. (2007). Research progress on the separation and structure-activity relationship of flavonoid glycosides from botanicals. *Chin. J. Inf. Trad. Chin. Med.* 100–102. doi:10.4268/jcmm.20131120
- You, X., Yang, M., Ming, X., Li, Q., Qian, L., Liu, Y., et al. (2020). Efficacy of ligustrazine hydrochloride injection combined with butylphthalide capsule in the treatment of acute cerebral infarction and the effect of hemorrhage. *Shaanxi J. Trad. Chin. Med.* 41, 743–745+757. doi:10.4314/tpj.v17i9.28
- Yu, B., Ruan, M., Zhang, Z. N., Cheng, H. B., and Shen, X. C. (2016). Synergic effect of borneol and ligustrazine on the neuroprotection in global cerebral ischemia/reperfusion injury: a region-specificity study. *Evid. Based Complement. Alternat Med.* 2016, 4072809. doi:10.1155/2016/4072809
- Yu, B., Zhong, F. M., Yao, Y., Deng, S. Q., Xu, H. Q., Lu, J. F., et al. (2019). Synergistic protection of tetramethylpyrazine phosphate and borneol on brain microvascular endothelium cells injured by hypoxia. *Am. J. Transl. Res.* 11, 2168–2180. doi:10.1093/chromsci/46.5.395
- Yu, B., Ruan, M., Liang, T., Huang, S. W., Liu, S. J., Cheng, H. B., et al. (2017). Tetramethylpyrazine phosphate and borneol combination therapy synergistically attenuated ischemia-reperfusion injury of the hypothalamus and striatum via regulation of apoptosis and autophagy in a rat model. *Am. J. Transl. Res.* 9, 4807–4820. doi:10.1007/978-3-7091-6837-0_3
- Yu, P., Wang, L., Tang, F., Zeng, L., Zhou, L., Song, X., et al. (2017). Resveratrol pretreatment decreases ischemic injury and improves neurological function via sonic hedgehog signaling after stroke in rats. *Mol. Neurobiol.* 54, 212–226. doi:10.1007/s12035-015-9639-7
- Zhai, L., Liu, M., Wang, T., Zhang, H., Li, S., and Guo, Y. (2017). Picric acid II protects the blood-brain barrier by inhibiting the oxidative signaling pathway in cerebral ischemia-reperfusion injury. *PLoS One* 12, e0174414. doi:10.1371/journal.pone.0174414
- Zhang, C., Chen, S., Zhang, Z., Xu, H., Zhang, W., Xu, D., et al. (2020). Asiaticoside alleviates cerebral ischemia-reperfusion injury via NOD2/mitogen-activated protein kinase (MAPK)/Nuclear factor kappa B (NF- κ B) signaling pathway. *Med. Sci. Monit.* 26, e920325. doi:10.12659/msm.920325
- Zhang, H.-F., Hu, X.-M., Wang, L.-X., Xu, S.-Q., and Zeng, F.-D. (2009). Protective effects of scutellarin against cerebral ischemia in rats: evidence for inhibition of the apoptosis-inducing factor pathway. *Planta Med.* 75, 121–126. doi:10.1055/s-0028-1088368
- Zhang, H., Zhai, L., Wang, T., Li, S., and Guo, Y. (2017). Picric acid II exerts a neuroprotective effect by inhibiting the mitochondria cytochrome C signal pathway following ischemia reperfusion injury in rats. *J. Mol. Neurosci.* 61, 267–278. doi:10.1007/s12031-016-0870-0
- Zhang, J., Wu, C., Du, G., and Qin, X. (2019). Astragaloside IV derived from *Astragalus membranaceus*: a research review on the pharmacological effects. *Adv. Pharmacol.* 87, 89–112. doi:10.1016/bs.apha.2019.08.002
- Zhang, J., Yang, L., and Guo, L. J. (2011). Effects of daurinoline on microcirculation of cerebral pia mater in mice. *Med. J. Wuhan Univ.* 32, 187. doi:10.1080/10739680601139153
- Zhang, L., Cui, M., and Chen, S. (2020a). Identification of the molecular mechanisms of peimine in the treatment of cough using computational target fishing. *Molecules* 25, 1105. doi:10.3390/molecules25051105
- Zhang, L., Li, F., Hou, C., Zhu, S., Zhong, L., Zhao, J., et al. (2020b). Design, synthesis, and biological evaluation of novel stachydrine derivatives as potent neuroprotective agents for cerebral ischemic stroke. *Naunyn-Schmiedeberg's Arch. Pharmacol.* 393, 2529–2542. doi:10.1007/s00210-020-01868-4
- Zhang, Q., Bian, H., Guo, L., and Zhu, H. (2016b). Pharmacological preconditioning with berberine attenuating ischemia-induced apoptosis and promoting autophagy in neuron. *Am. J. Transl. Res.* 8, 1197–1207. doi:10.4016/14162.01
- Zhang, Q., Bian, H., Guo, L., and Zhu, H. (2016a). Berberine preconditioning protects neurons against ischemia via sphingosine-1-phosphate and hypoxia-inducible factor-1 α . *Am. J. Chin. Med.* 44, 927–941. doi:10.1142/s0192415x16500518
- Zhang, Q., and Zhao, Y.-H. (2014). Therapeutic angiogenesis after ischemic stroke: Chinese medicines, bone marrow stromal cells (BMSCs) and their combinational treatment. *Am. J. Chin. Med.* 42, 61–77. doi:10.1142/s0192415x14500049
- Zhang, R.-X., Li, M.-X., and Jia, Z.-P. (2008). *Rehmannia glutinosa*: review of botany, chemistry and pharmacology. *J. Ethnopharmacology* 117, 199–214. doi:10.1016/j.jep.2008.02.018
- Zhang, X., Du, Q., Yang, Y., Wang, J., Liu, Y., Zhao, Z., et al. (2018). Salidroside alleviates ischemic brain injury in mice with ischemic stroke through regulating BDNF mediated PI3K/Akt pathway. *Biochem. Pharmacol.* 156, 99–108. doi:10.1016/j.bcp.2018.08.015
- Zhang, X., Zhang, X., Wang, C., Li, Y., Dong, L., Cui, L., et al. (2012). Neuroprotection of early and short-time applying berberine in the acute phase of cerebral ischemia: up-regulated pAkt, pGSK and pCREB, down-regulated NF- κ B expression, ameliorated BBB permeability. *Brain Res.* 1459, 61–70. doi:10.1016/j.brainres.2012.03.065
- Zhang, Y., Fang, M., Sun, Y., Zhang, T., Shi, N., Li, J., et al. (2018). Curcumin attenuates cerebral ischemia injury in Sprague-Dawley rats and PC12 cells by suppressing overactivated autophagy. *J. Photochem. Photobiol. B: Biol.* 184, 1–6. doi:10.1016/j.jphotobiol.2018.05.010
- Zhang, X., Lai, W., Ying, X., Xu, L., Chu, K., Brown, J., et al. (2019). Salidroside reduces inflammation and brain injury after permanent middle cerebral artery occlusion in rats by regulating PI3K/PKB/Nrf2/NF κ B signaling rather than complement C3 activity. *Inflammation* 42, 1830–1842. doi:10.1007/s10753-019-01045-7
- Zhao, B., Shen, C., Zheng, Z., Wang, X., Zhao, W., Chen, X., et al. (2018). Peiminine inhibits glioblastoma *in vitro* and *in vivo* through cell cycle arrest and autophagic flux blocking. *Cel. Physiol. Biochem.* 51, 1566–1583. doi:10.1159/000495646
- Zhao, T., Tang, H., Xie, L., Zheng, Y., Ma, Z., Sun, Q., et al. (2019). *Scutellaria baicalensis* Georgi. (Lamiaceae): a review of its traditional uses, botany, phytochemistry, pharmacology and toxicology. *J. Pharm. Pharmacol.* 71, 1353–1369. doi:10.1111/jphp.13129
- Zhao, X., Li, X., Ren, Q., Tian, J., and Chen, J. (2016). Calycosin induces apoptosis in colorectal cancer cells, through modulating the ER β /MiR-95 and IGF-1R, PI3K/Akt signaling pathways. *Gene* 591, 123–128. doi:10.1016/j.gene.2016.07.012
- Zhao, Y., Liu, Y., and Chen, K. (2016). Mechanisms and clinical application of tetramethylpyrazine (an interesting natural compound isolated from *Ligusticum wallicii*): current status and perspective. *Oxid. Med. Cel. Longev.* 2016, 2124638. doi:10.1155/2016/2124638
- Zheng, C., and Qin, L.-P. (2007). Chemical components of *Centella asiatica* and their bioactivities. *Zhong Xi Yi Jie He Xue Bao* 5, 348–351. doi:10.3736/jcim20070324
- Zheng, J.-S., Zheng, P.-D., Mungur, R., Zhou, H.-J., Hassan, M., and Jiang, S.-N. (2018). Ginkgolide B promotes the proliferation and differentiation of neural stem cells following cerebral ischemia/reperfusion injury, both *in vivo* and *in vitro*. *Neural Regen. Res.* 13, 1204–1211. doi:10.4103/1673-5374.232476
- Zheng, Q., Chen, Z.-X., Xu, M.-B., Zhou, X.-L., Huang, Y.-Y., Zheng, G.-Q., et al. (2018a). Borneol, a messenger agent, improves central nervous system drug delivery through enhancing blood-brain barrier permeability: a preclinical systematic review and meta-analysis. *Drug Deliv.* 25, 1617–1633. doi:10.1080/10717544.2018.1486471
- Zheng, Q., Huang, Y. Y., Zhu, P. C., Tong, Q., Bao, X. Y., Zhang, Q. H., et al. (2018b). Ligustrazine exerts cardioprotection in animal models of myocardial ischemia/reperfusion injury: preclinical evidence and possible mechanisms. *Front. Pharmacol.* 9, 729. doi:10.3389/fphar.2018.00729
- Zheng, T., Jiang, H., Jin, R., Zhao, Y., Bai, Y., Xu, H., et al. (2019). Ginsenoside Rg1 attenuates protein aggregation and inflammatory response following cerebral ischemia and reperfusion injury. *Eur. J. Pharmacol.* 853, 65–73. doi:10.1016/j.ejphar.2019.02.018
- Zheng, W.-x., Cao, X.-L., Wang, F., Wang, J., Ying, T.-z., Xiao, W., et al. (2015). Baicalin inhibiting cerebral ischemia/hypoxia-induced neuronal apoptosis via

- MRTF-A-mediated transactivity. *Eur. J. Pharmacol.* 767, 201–210. doi:10.1016/j.ejphar.2015.10.027
- Zhong, Y., Gao, Y., Xu, Y., Qi, C., and Wu, B. (2020). Synthesis of novel aryloxyethylamine derivatives and evaluation of their *in Vitro* and *in Vivo* neuroprotective activities. *Chem. Biodivers.* 7, 33. doi:10.1080/10739680600777599
- Zhong, Z. F., Han, J., Zhang, J. Z., Xiao, Q., Chen, J. Y., Zhang, K., et al. (2019). Neuroprotective effects of salidroside on cerebral ischemia/reperfusion-induced behavioral impairment involves the dopaminergic system. *Front. Pharmacol.* 10, 1433. doi:10.3389/fphar.2019.01433
- Zhou, J., Wen, B., Xie, H., Zhang, C., Bai, Y., Cao, H., et al. (2021). Advances in the preparation and assessment of the biological activities of chitosan oligosaccharides with different structural characteristics. *Food Funct.* 12, 926–951. doi:10.1039/d0fo02768e
- Zhou, J., Wu, J., Chen, X., Fortenbery, N., Eksioğlu, E., Kodumudi, K. N., et al. (2011). Icariin and its derivative, ICT, exert anti-inflammatory, anti-tumor effects, and modulate myeloid derived suppressive cells (MDSCs) functions. *Int. Immunopharmacology* 11, 890–898. doi:10.1016/j.intimp.2011.01.007
- Zhou, P., Du, S., Zhou, L., Sun, Z., Zhuo, L. H., He, G., et al. (2019). Tetramethylpyrazine2'-O-sodium ferulate provides neuroprotection against neuroinflammation and brain injury in MCAO/R rats by suppressing TLR-4/NF- κ B signaling pathway. *Pharmacol. Biochem. Behav.* 176, 33–42. doi:10.1016/j.pbb.2018.08.010
- Zhou, Y., Li, H.-q., Lu, L., Fu, D.-l., Liu, A.-j., Li, J.-h., et al. (2014). Ginsenoside Rg1 provides neuroprotection against blood brain barrier disruption and neurological injury in a rat model of cerebral ischemia/reperfusion through downregulation of aquaporin 4 expression. *Phytomedicine* 21, 998–1003. doi:10.1016/j.phymed.2013.12.005
- Zhou, Z., Lu, J., Liu, W.-W., Manaenko, A., Hou, X., Mei, Q., et al. (2018). Advances in stroke pharmacology. *Pharmacol. Ther.* 191, 23–42. doi:10.1016/j.pharmthera.2018.05.012
- Zhu, H.-F., Wan, D., Luo, Y., Zhou, J.-L., Chen, L., and Xu, X.-Y. (2010). Catalpol increases brain angiogenesis and up-regulates VEGF and EPO in the rat after permanent middle cerebral artery occlusion. *Int. J. Biol. Sci.* 6, 443–453. doi:10.7150/ijbs.6.443
- Zou, J., Gao, P., Hao, X., Xu, H., Zhan, P., and Liu, X. (2018). Recent progress in the structural modification and pharmacological activities of ligustrazine derivatives. *Eur. J. Med. Chem.* 147, 150–162. doi:10.1016/j.ejmech.2018.01.097
- Zuo, W., Yan, F., Zhang, B., Hu, X., and Mei, D. (2018). Salidroside improves brain ischemic injury by activating PI3K/Akt pathway and reduces complications induced by delayed tPA treatment. *Eur. J. Pharmacol.* 830, 128–138. doi:10.1016/j.ejphar.2018.04.001

Conflict of Interest: The authors declare that the research was conducted in the absence of any commercial or financial relationships that could be construed as a potential conflict of interest.

Copyright © 2021 Xie, Li, Lu, Yuan, Ma, Li, Ren, Li, Chen, Wang and Gong. This is an open-access article distributed under the terms of the Creative Commons Attribution License (CC BY). The use, distribution or reproduction in other forums is permitted, provided the original author(s) and the copyright owner(s) are credited and that the original publication in this journal is cited, in accordance with accepted academic practice. No use, distribution or reproduction is permitted which does not comply with these terms.



Progress in Borneol Intervention for Ischemic Stroke: A Systematic Review

Yong Li, Mihong Ren, Jiajun Wang, Rong Ma, Hai Chen, Qian Xie, Hongyan Li, Jinxiu Li and Jian Wang*

College of Pharmacy, Chengdu University of Traditional Chinese Medicine, Chengdu, China

Background: Borneol is a terpene and bicyclic organic compound that can be extracted from plants or chemically synthesized. As an important component of proprietary Chinese medicine for the treatment of stroke, its neuroprotective effects have been confirmed in many experiments. Unfortunately, there is no systematic review of these studies. This study aimed to systematically examine the neuroprotective effects of borneol in the cascade reaction of experimental ischemic stroke at different periods.

Methods: Articles on animal experiments and cell-based research on the actions of borneol against ischemic stroke in the past 20 years were collected from Google Scholar, Web of Science, PubMed, ScienceDirect, China National Knowledge Infrastructure (CNKI), and other biomedical databases. Meta-analysis was performed on key indicators *in vivo* experiments. After sorting the articles, we focused on the neuroprotective effects and mechanism of action of borneol at different stages of cerebral ischemia.

Results: Borneol is effective in the prevention and treatment of nerve injury in ischemic stroke. Its mechanisms of action include improvement of cerebral blood flow, inhibition of neuronal excitotoxicity, blocking of Ca^{2+} overload, and resistance to reactive oxygen species injury in the acute ischemic stage. In the subacute ischemic stage, borneol may antagonize blood-brain barrier injury, intervene in inflammatory reactions, and prevent neuron excessive death. In the late stage, borneol promotes neurogenesis and angiogenesis in the treatment of ischemic stroke.

Conclusion: Borneol prevents neuronal injury after cerebral ischemia via multiple action mechanisms, and it can mobilize endogenous nutritional factors to hasten repair and regeneration of brain tissue. Because the neuroprotective effects of borneol are mediated by various therapeutic factors, deficiency caused by a single-target drug is avoided. Besides, borneol promotes other drugs to pass through the blood-brain barrier to exert synergistic therapeutic effects.

Keywords: L-borneol, D-borneol, DL-borneol, ischemic stroke, cascade reaction, neuroprotection

INTRODUCTION

Borneol is a bicyclic terpenoid with strong fat solubility (Lv et al., 2012). The 2020 edition of Chinese Pharmacopoeia contains three commercial borneol products: D-borneol (Chinese name “Tianranbingpian”), L-borneol (Chinese name “Aipian”), and Synthetic borneol (Chinese name “Bingpian”). D-borneol are extracted from fresh branches and leaves of *Cinnamomum camphora* (L.)

OPEN ACCESS

Edited by:

Jiahong Lu,
University of Macau,
China

Reviewed by:

He-Hui Xie,
Shanghai Jiao Tong University, China
Ziying Wang,
Jinan University, China

*Correspondence:

Jian Wang
jianwang08@163.com

Specialty section:

This article was submitted to
Ethnopharmacology,
a section of the journal
Frontiers in Pharmacology

Received: 15 September 2020

Accepted: 14 April 2021

Published: 04 May 2021

Citation:

Li Y, Ren M, Wang J, Ma R, Chen H,
Xie Q, Li H, Li J and Wang J (2021)
Progress in Borneol Intervention for
Ischemic Stroke: A Systematic Review.
Front. Pharmacol. 12:606682.
doi: 10.3389/fphar.2021.606682

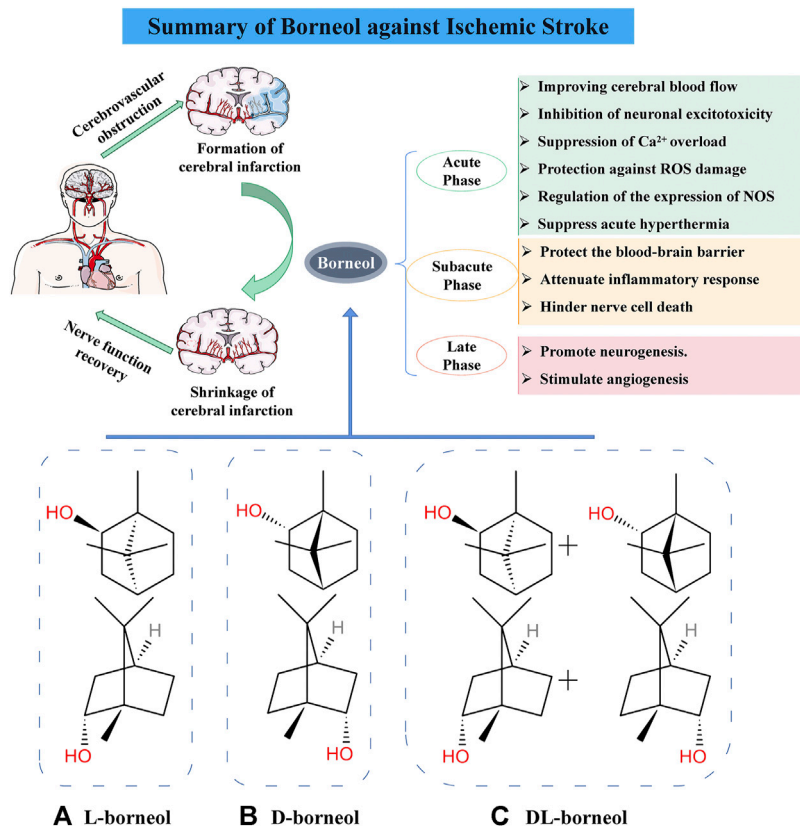


FIGURE 1 | Mechanism of borneol against cerebral ischemia injury and chemical structure of three borneols. **(A)** Levorotatory borneol (endo-(1 S)-1,7,7-trimethylbicyclo [2.2.1] heptan-2-ol, (–)-borneol), which is extracted from fresh leaves of *Blumea balsamifera* (L.) DC. **(B)** Dextrorotatory borneol (endo-(1 R)-1,7,7-trimethylbicyclo [2.2.1] heptan-2-ol, (+)-borneol), which is extracted from fresh branches and leaves of *Cinnamomum camphora* (L.) Presl. **(C)** Synthetic borneol (DL-borneol) is an optically inactive (\pm) borneol that is mainly a mixture of (\pm) borneol and is obtained via the chemical transformation of camphor and turpentine oil.

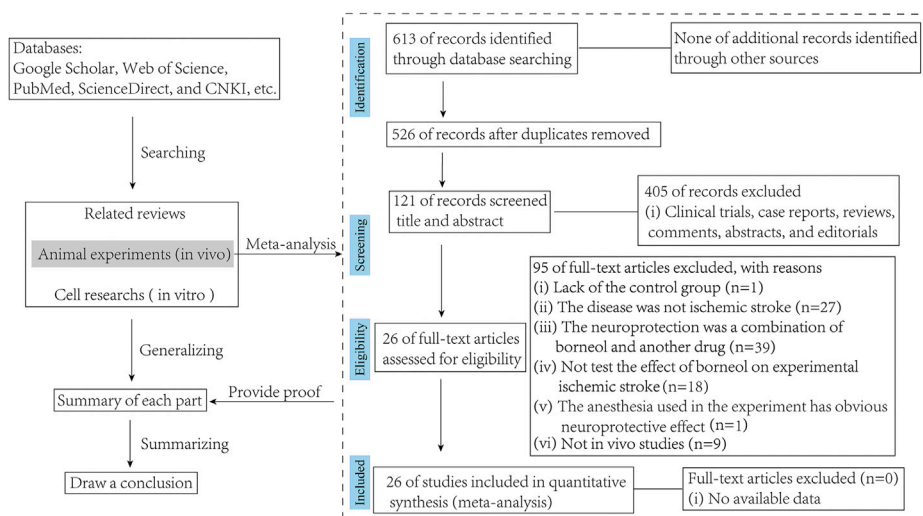


FIGURE 2 | Flow diagram of the search process.

Presl. or *Dryobalanops aromatica Gaertn.f* (Yang et al., 2018; Wang and Wang, 2018). L-borneol is processed from the sublimation of *Blumea balsamifera* (L.) DC (Islam et al., 2010). Synthetic borneol is a racemic borneol (A mixture with D-borneol and L-borneol as the main components) prepared by chemical synthesis of turpentine and camphor (Chinese Pharmacopoeia Committee, 2020) (Figure 1). Borneol has been used in China for more than 1600 years (Li et al., 2013). In Traditional Chinese Medicine (TCM) theory, borneol is an upper ushering drug that guides herbs to their target organs, especially in the upper part of the body, including the brain (Chen et al., 2019). In addition, borneol is suitable for the treatment of mental diseases accompanied by signs of heat syndrome because the herbal medicine has the property of being “cold” (Zou et al., 2017; Wang and Wang, 2018). Several proprietary Chinese medicine preparations such as Angong Niuhuang pills and Xingnaojing injection contain borneol and are widely used in the clinical treatment of stroke (Guo et al., 2014; Zhang et al., 2019).

Cerebral stroke is a disorder of cerebral blood circulation of the central nervous system and may either be ischemic or hemorrhagic. Ischemic stroke accounts for approximately 80% of stroke cases (Fan et al., 2017). Ischemic stroke is accompanied by extremely complex physiological and pathological processes. The acute stage of ischemic stroke is characterized by glutamate excitotoxicity, intracellular Ca^{2+} overload, oxidative stress, and production of free radicals. The subacute stage is characterized by apoptosis and necrosis, blood-brain barrier damage, brain edema, and an inflammatory response. The late stage of ischemic stroke is characterized by reactive astrocyte proliferation, glial scar formation, angiogenesis, and neurogenesis (Steliga et al., 2020). These processes occur at different time points, overlap with each other, and eventually lead to brain injury and repair after ischemia.

In the study of brain diseases, the regulatory effect of borneol on blood-brain barrier has always been the focus of relevant practitioners. In fact, there are also abundant studies have shown that borneol has a neuroprotective effect on cerebral ischemic. Unfortunately, the neuroprotective mechanism of borneol is complex and involves many aspects, and only few reviews have focused on the protective mechanism of borneol at different periods of cerebral ischemia. Therefore, we take the review of borneol intervention in cerebral ischemia as the main content of the article, and supplement the meta-analysis of key indicators *in vivo* studies, hoping to provide some valuable references for borneol's experimental research and clinical application.

METHODS

Search Strategy

A comprehensive search strategy was conducted in several databases, including Google Scholar, Web of Science, ScienceDirect, PubMed, and CNKI from their inception to March 2021. For data mining, the following words were used in the databases mentioned above: “borneol” or “D-borneol” or

“L-borneol” or “synthetic borneol” and “cerebral ischemic” or “ischemic stroke” or “neuroprotection.” In almost all cases, the original articles or abstracts were obtained and the relevant data was extracted.

Eligibility and Exclusion Criteria

Both animal experiments (*in vivo*) and cell studies (*in vitro*) on borneol intervention in ischemic stroke have been included in the review. But all studies accepted for meta-analysis should be met the following eligibility criteria: 1) The drugs used must be borneol, whether D-borneol, L-borneol, or synthetic borneol, it should be noted that the literature on combination of drugs, which sets borneol alone as a group to compare with the model group, can also be included in this study; 2) The animal model used must be a cerebral ischemia model, whether permanent or cerebral ischemia-reperfusion; and 3) the control group receiving vehicle or no adjunct intervention was included in the studies. Exclusion criteria were as follows: 1) the study was a case report, clinical trial, review, or *in vitro* study; 2) lack of the control group; 3) the targeting disease was not ischemic stroke; 4) the intervention was a combination of borneol and another agent with potential effect on ischemic stroke; 5) the anesthesia used in the experiment has obvious neuroprotective effect (Figure 2).

Statistical Analysis

To evaluate the effect of borneol on cerebral ischemia in animal experiments, Revman version 5.3 was performed for statistical analysis. If statistical heterogeneity was found ($p < 0.1$, $I^2 > 50\%$), a model of random effect (RE) was applied to evaluate pooled effect with 95% CI; and if no statistical evidence of heterogeneity existed ($p \geq 0.1$, $I^2 \leq 50\%$), a model of fixed effect (FE) was set with 95% CI. If the outcomes were applied at the same scale, the weighted mean difference (WMD) was calculated as a summary statistic; and if the same results were measured in different ways, the standardized mean differences (SMD) were used. Heterogeneity was assessed by standard chi-square test and I^2 statistics. A probability value less than 0.05 was considered statistically significant. To minimize bias and human error, the meta-analysis was performed by 2 independent reviewers and disagreements reconciled by a third independent reviewer.

RESULTS

Mechanism of Borneol Intervention in the Acute Stage of Ischemic Stroke

Decreased cerebral blood flow in the acute phase of ischemic stroke (within 24 h of human cerebral ischemia) causes a decrease in oxygen and metabolic substrates to neurons. Subsequently, The lack of oxygen interrupts oxidative phosphorylation by the mitochondria and drastically reduces cellular ATP production. Inhibition of the Na^+/K^+ -ATPase function causes a profound loss of ionic gradients and depolarization of regulated neurons, which leads to excessive release of excitatory amino acids-particularly glutamate-to the extracellular compartment. The presence of excessive amounts of free glutamate into the synapses and extrasynaptic sites can lead eventually to neuronal death.

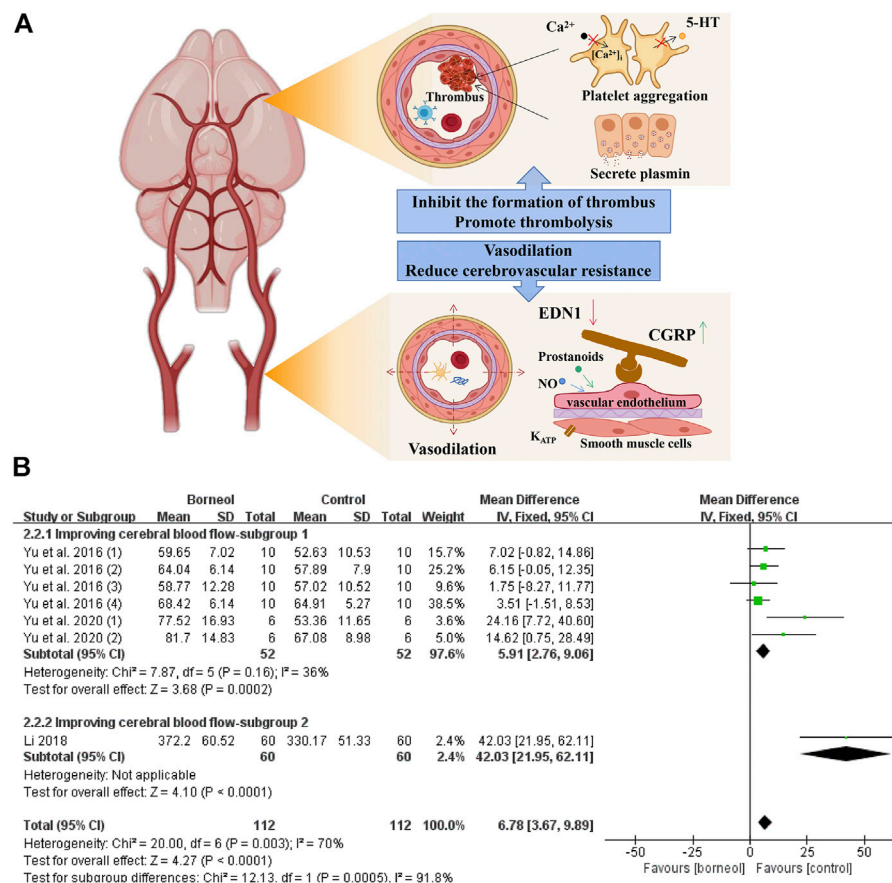


FIGURE 3 | (A) Borneol reduces platelet aggregation by blocking the release of 5-HT and the increasing of intracellular Ca^{2+} levels, and interferes with thrombus formation by inhibiting thrombin activity. In addition, borneol activates the fibrinolytic system to promote the dissolution of plasma euglobulin. Borneol also improve cerebral blood flow under ischemia by regulating vascular neuropeptides. **(B)** The forest plots: the borneol group vs. the control group on cerebral blood flow. Subgroup 1 measures the cerebral blood flow in a certain brain area such as the hypothalamus or hippocampus in a tGCIR rodent model, showing that borneol significant increase of cerebral blood flow in the treatment of cerebral ischemic injury ($n_T/n_C = 52/52$, MD 5.91, 95% CI: 2.76~9.06, $p = 0.0002$; heterogeneity $\chi^2 = 7.87$, $df = 5$, $I^2 = 36\%$). In subgroup 2, the cerebral blood flow of bilateral parietal cortex was monitored, and the model was induced by photochemical method, which also showed that borneol could improve the cerebral blood flow.

Excitotoxicity leads to a number of deleterious consequences, including impairment of cellular calcium homeostasis, generation of free radicals and oxidative stress, mitochondrial damage, and activation of transcription factors. All these mechanisms' acting synergy can cause acute neuron death by apoptosis (Rama and Garcia, 2016). Borneol participates in multiple physiological and pathological processes in the acute phase of ischemic stroke and impedes disease progression by antagonizing the damage in the initial stage of ischemic stroke.

Improving Cerebral Blood Flow

Disordered energy metabolism is required in the development of cerebral ischemia. Stenosis and occlusion of blood vessels lead to the interruption of local blood flow and alters blood circulation. Cerebral infarction occurs when the supply of nutrients provided by local blood circulation does not meet the energy metabolism needs of brain cells beyond a certain time limit. Therefore, timely improvement of the blood supply to the brain is the primary goal of the clinical treatment of ischemic stroke. Borneol has the

pharmacological effects of relaxing blood vessels, reducing blood pressure and cerebral vascular resistance, inhibiting thrombosis, and promoting thrombolysis, thereby improving cerebral blood flow after cerebral ischemia.

Regulation of Vascular Neuropeptide

In an *in vivo* canine study, DL-borneol reduced abdominal aortic blood pressure, increased common carotid blood flow, and reduced cerebrovascular resistance (Shang et al., 2015). L-borneol has a vasorelaxant effect that depends on the presence of vascular endothelium and the participation of nitric oxide (NO) and prostanooids. In addition, L-borneol directly relaxed vascular smooth muscle, which is dependent on K_{ATP} channels (Santos et al., 2018). Under pathological conditions, D-borneol increased blood flow in the cortex in photochemical-mediated cerebral ischemia model rats and DL-borneol increased blood flow in the cortex and striatum in transient global cerebral ischemia reperfusion (tGCIR) animal models (Yu et al., 2016; Li, 2018; Wang et al., 2018; Yu et al.,

2020). The meta-analysis results of three studies jointly suggested that borneol could improve the blood microcirculation in different brain regions (**Figure 3**).

Endothelin 1 (EDN1/ET) and calcitonin gene-related peptide (CGRP) are neuropeptides that contract and dilate blood vessels, respectively. Cerebral ischemia/reperfusion injury induces increased EDN1 secretion, promotes vascular smooth muscle contraction, and aggravates low perfusion. Conversely, CGRP is a strong neuropeptide vasodilator that serves as an endogenous endothelin antagonist to reverse vasospasms and improve blood circulation. Stroke leads to increased EDN1 and decreased CGRP levels (Yuan et al., 2006; Giannopoulos et al., 2008). Borneol can effectively reduce EDN1 levels and tends to increase CGRP levels (Huang, 2018), suggesting that it can dilate blood vessels and improve cerebral blood flow during cerebral ischemia.

Regulation of the Fibrinolytic System and Anti-Thrombosis

The thrombus causing cerebral ischemia is mainly composed of platelets, leukocytes, erythrocytes, and fibrin (Michael et al., 2016). The dissolution time of plasma euglobulin reflects the activity of fibrinolytic enzymes. Borneol significantly shortens the euglobulin lysis time in rats, reduces the weight of the whole blood clot in mice, and inhibits ADP-induced platelet aggregation in rabbits (He, 2005). Furthermore, borneol inhibits venous thrombosis and arteriovenous shunt in a concentration-dependent manner and exerts anticoagulant activity by prolonging prothrombin time and thrombin time (Li et al., 2008). 5-hydroxytryptamine (5-HT), secreted and released by platelets, plays an important role in platelet aggregation and thrombosis. Ca^{2+} , as the second messenger, also plays a key role in the process of platelet activation. The deformation, aggregation and release of platelets are accompanied by the increase in the level of intracellular Ca^{2+} (Wöckel et al., 2008). Borneol inhibits FeCl_3 -induced arterial thrombosis in rats, which involves inhibition of platelet 5-HT release and platelet aggregation, as well as the decrease of cytoplasmic Ca^{2+} level in platelet (Yang et al., 2010). The mechanisms of borneol improves cerebral blood flow and the results of meta-analysis of cerebral blood flow are shown in **Figure 3**.

Inhibition of Neuronal Excitotoxicity

The excessive release of glutamate and the drastic disruption of glutamate transporters, that occurs early after the cerebral ischemic is toxic to neurons, mainly through the activation of ionotropic receptors and intracellular calcium overload that trigger detrimental cascades causing excitotoxic neuronal death (Lai et al., 2014). Conversely, Some *in vitro* studies showed that activation of GABA_A and GABA_B receptors played a neuroprotective role (Costa et al., 2004; Xu et al., 2008). The expression of GABA_A receptors after ischemia is decreased in distinct brain regions of rodents subjected to transient MCAO (Huang and Zhao, 2017). And the disruption of GABA-mediated neurotransmission early during reperfusion may also contribute to ongoing neuronal excitability (Mele et al., 2014). Neuroprotection is achieved in the preclinical setting by GABAergic drugs acting through multiple mechanisms, such as GABA receptors agonists or positive modulators. Borneol

plays a neuroprotective role by reducing glutamate (Glu) levels, activating GABA_A receptor, and then blocking the necrosis and apoptosis of neurons.

In one study, D-borneol and L-borneol enhanced the actions of γ -aminobutyric acid (GABA) at recombinant GABA_A receptor and had moderate direct action on these receptors (Granger et al., 2005). D-borneol has neuroprotective effects after primary neuronal injury induced by glutamate at low concentrations, and this effect is consistent with the activation of GABA_A receptor (Cheng et al., 2006; Chen et al., 2013). In addition, borneol reduces Glu levels in the hippocampus and hypothalamus in a tGCIR rat model (Yu et al., 2019a). The inhibitory effects of borneol on Glu secretion were also confirmed in a transient bilateral carotid occlusion (tBCO) rodent model (Huang, 2018). The meta-analysis results of the above two studies further suggested that borneol could reduce glutamate levels with small heterogeneity (**Figure 4**). Borneol promoted glutamate clearance in hypoxia/reoxygenation astrocytes and improved astrocyte viability during hypoxia (Chai et al., 2019). Borneol, combined with echinacoside, artificial moschus, *Ligusticum chuanxiong*, and other drugs, can also improve the content of Glu after cerebral ischemia (Liu et al., 2002a; Zhong et al., 2012; Yu et al., 2019b). The mechanisms by which borneol attenuates the toxicity of excitatory amino acid and the meta-analysis results of glutamate level are shown in **Figure 4**.

Protection Against Damage Caused by Reactive Oxygen Species

The reactive oxygen species (ROS) causing cerebral ischemic injury include superoxide anion ($\text{O}_2^{\cdot-}$), hydroxyl radical (OH^{\cdot}), and hydrogen peroxide (H_2O_2). Brain tissue is rich in iron ions that catalyze the formation of free radicals, which makes the brain more vulnerable to ROS (González-Ibarra et al., 2011). When thrombolysis exceeds the therapeutic time window, a large amount of ROS is produced by dysfunctional mitochondria, the neutrophil respiratory burst, increased xanthine oxidase formation in capillary endothelial cells, and catecholamine self-oxidation after cerebral ischemia/reperfusion (Huang and Zhao, 2017). Furthermore, cerebral ischemia decreases the ability of the antioxidant system to scavenge ROS. The antioxidant system is composed of glutathione peroxidase (GSH-Px), superoxide dismutase (SOD), catalase (CAT), and other antioxidant enzymes. Improving antioxidant enzymes activity or activating related pathways is an important way to combat ischemic brain injury. Borneol improves the body's ability to resist ROS by increasing the activity of antioxidant enzymes and activating the nuclear factor erythroid 2-related factor 2 (Nrf2)-antioxidant response element (ARE) signaling pathway.

Several studies have shown that borneol injection reduces malondialdehyde (MDA) levels and increases SOD and GSH-Px activity to accelerate the scavenging of superoxide anion free radicals after pMCAO in a rodent model (He et al., 2006; He et al., 2007). Borneol also increases SOD and GSH-Px activity and decreases MDA levels in the cerebral cortex, hippocampus, hypothalamus, and striatum of rats subjected to tGCIR (Yu et al., 2016). L-borneol and DL-borneol increase SOD and decrease MDA in ischemic brain tissue and the serum in a

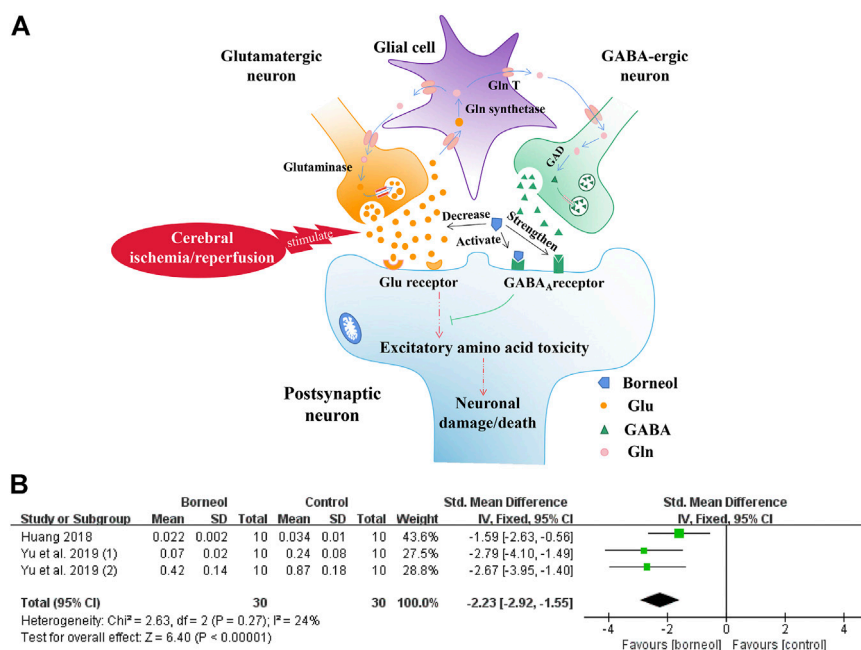


FIGURE 4 | (A) Borneol inhibits the increase of extracellular glutamate levels in the ischemic state and strengthens the binding of GABA to GABA_A receptors. The direct activation of the GABA_A receptor by borneol could also inhibit glutamate-mediated excitatory amino acid toxicity. **(B)** The forest plots: the borneol group vs. the control group on glutamate levels. Meta-analysis of two studies with three comparisons showed that animals in the borneol group had statistically significant lower glutamate levels than the control group ($n_T/n_C = 30/30$, SMD -2.23, 95% CI: -2.92~ -1.55, $p < 0.00001$, heterogeneity $\chi^2 = 2.63$, $df = 2$, $I^2 = 24\%$).

rodent model of tMCAO (Tian, 2013). The meta-analysis results of related studies further suggested that borneol could resist free radical damage by reducing MDA levels and increasing the activities of GSH-PX and SOD (Figure 5). Borneol, combined with musk, *Ligusticum chuanxiong*, and other drugs, can also attenuate ROS injury after cerebral ischemia (Liu et al., 2002b; Wang, 2011; Yu et al., 2017a). Besides, DL-borneol increases SOD and CAT activity, and D-Borneol increases SOD and GSH-Px activity in OGD/R-treated PC12 cells (Huang et al., 2020).

Borneol may protect against free radical damage by activating the Nrf2-ARE signaling pathway. Nrf2, an anti-oxidative stress nuclear transcription factor, translocates from the cytoplasm to the nucleus and binds to the ARE receptor to activate the Nrf2-ARE signaling pathway when cells are exposed to ROS. The activation of this pathway induces the expression of downstream antioxidant enzymes to reduce cell damage caused by ROS and maintain the dynamic cellular redox balance (Wang et al., 2015). Circulating macrophages will enter the core area of cerebral ischemia through the blood-brain barrier to remove damaged cells after organic injury occurs in the brain. An *in vitro* cell experiment demonstrated that D-borneol promotes the expression of Nrf2 in RAW 264.7 macrophages stimulated with lipopolysaccharide (LPS) (Sun et al., 2019). It is also worth mentioning that L-borneol and D-borneol protected human neuroblastoma cells (SH-SY5Y) against β -amyloid induced toxicity, exerted an antioxidative effect by increasing the expression and nuclear translocation of Nrf2 (Hur et al., 2013). Borneol, combined with *Salvia miltiorrhiza*, not only increased SOD levels and decreased MDA levels but also

upregulated the expression of Nrf2 and inhibited the oxidative stress. The combination of these two drugs is more effective than *Salvia miltiorrhiza* alone, suggesting that borneol plays a synergistic role by activating the Nrf2-ARE signaling pathway *in vivo* (Liang et al., 2016). The actions of borneol against ROS damage and the meta-analysis results of related indicators are detailed in Figure 5.

Regulation of the Expression of NOS to Protect Against NO Damage

NO plays a dual role in neuroprotection and neurotoxicity. Nitric oxide synthase (NOS) isoforms are crucial in determining the role of NO in cerebral ischemia. There are three isoforms of NOS: neuronal NOS (nNOS/NOS1), inducible NOS (iNOS/NOS2), and endothelial NOS (eNOS/NOS3) (Chen et al., 2017). The transient increase of NO after cerebral ischemia is mainly mediated by eNOS and nNOS. NO synthesized by eNOS can dilate blood vessels, inhibit platelet aggregation, reduce leukocyte adhesion, and enhance collateral circulation to play a short-term neuroprotective effect (Ito et al., 2010). NO synthesized by nNOS participates in glutamate-induced neuronal Ca^{2+} overload, mediates early glutamate excitotoxicity (Zhou and Zhu, 2009). Also, nNOS activation contributes to microvascular damage and decreased cerebral perfusion early after reoxygenation and worsens brain damage (Hsu et al., 2014). The slow upregulation of iNOS in the late stage of cerebral ischemia leads to delayed neuronal injury by producing excessive NO, increasing microvascular permeability, and inducing brain edema (Liu and Mu, 2014). Therefore,

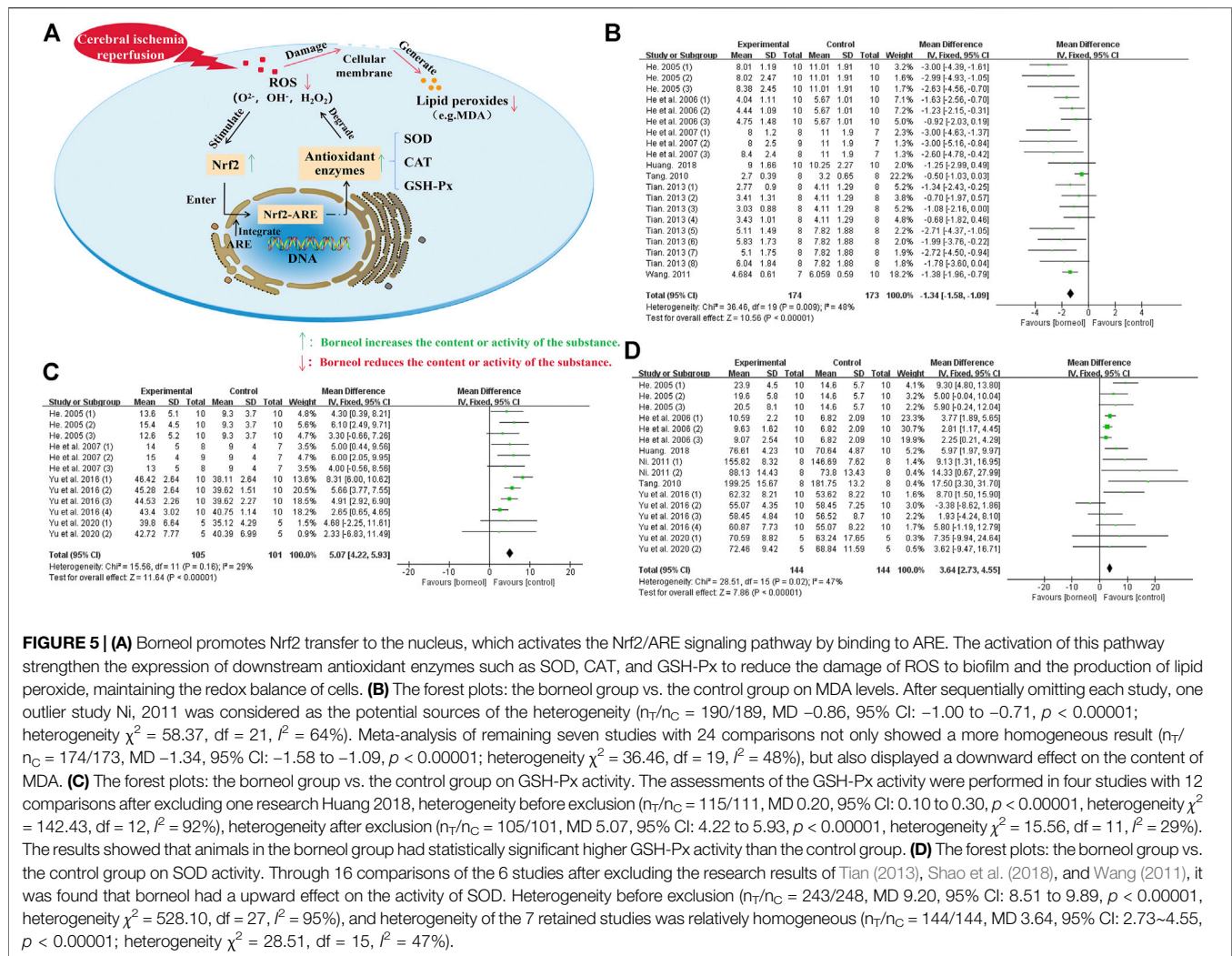


FIGURE 5 | (A) Borneol promotes Nrf2 transfer to the nucleus, which activates the Nrf2/ARE signaling pathway by binding to ARE. The activation of this pathway strengthens the expression of downstream antioxidant enzymes such as SOD, CAT, and GSH-Px to reduce the damage of ROS to biofilm and the production of lipid peroxide, maintaining the redox balance of cells. (B) The forest plots: the borneol group vs. the control group on MDA levels. After sequentially omitting each study, one outlier study Ni, 2011 was considered as the potential sources of the heterogeneity ($n_T/n_C = 190/189$, MD -0.86 , 95% CI: -1.00 to -0.71 , $p < 0.00001$; heterogeneity $\chi^2 = 58.37$, df = 21, $I^2 = 64\%$). Meta-analysis of remaining seven studies with 24 comparisons not only showed a more homogeneous result ($n_T/n_C = 174/173$, MD -1.34 , 95% CI: -1.58 to -1.09 , $p < 0.00001$; heterogeneity $\chi^2 = 36.46$, df = 19, $I^2 = 48\%$), but also displayed a downward effect on the content of MDA. (C) The forest plots: the borneol group vs. the control group on GSH-Px activity. The assessments of the GSH-Px activity were performed in four studies with 12 comparisons after excluding one research Huang 2018, heterogeneity before exclusion ($n_T/n_C = 115/111$, MD 0.20 , 95% CI: 0.10 to 0.30 , $p < 0.00001$, heterogeneity $\chi^2 = 142.43$, df = 12, $I^2 = 92\%$), heterogeneity after exclusion ($n_T/n_C = 105/101$, MD 5.07 , 95% CI: 4.22 to 5.93 , $p < 0.00001$, heterogeneity $\chi^2 = 15.56$, df = 11, $I^2 = 29\%$). The results showed that animals in the borneol group had statistically significant higher GSH-Px activity than the control group. (D) The forest plots: the borneol group vs. the control group on SOD activity. Through 16 comparisons of the 6 studies after excluding the research results of Tian (2013), Shao et al. (2018), and Wang (2011), it was found that borneol had an upward effect on the activity of SOD. Heterogeneity before exclusion ($n_T/n_C = 243/248$, MD 9.20 , 95% CI: 8.51 to 9.89 , $p < 0.00001$, heterogeneity $\chi^2 = 528.10$, df = 27, $I^2 = 95\%$), and heterogeneity of the 7 retained studies was relatively homogeneous ($n_T/n_C = 144/144$, MD 3.64 , 95% CI: 2.73 to 4.55 , $p < 0.00001$; heterogeneity $\chi^2 = 28.51$, df = 15, $I^2 = 47\%$).

promoting the expression of eNOS in the early stage or inhibiting the expression of iNOS in the latter stage is a good therapeutic strategy for treating cerebral ischemia. Studies have found that borneol plays a neuroprotective effect by increasing eNOS expression and reducing iNOS expression, but the effect of borneol on nNOS is not clear.

Intravenous administration of D-borneol inhibits iNOS expression in rodent brain tissue and, consequently, reduces peroxynitrite (ONOO⁻) levels after tMCAO and pMCAO (Wu et al., 2014b; Chang et al., 2017). L-borneol and DL-borneol also reduce the expression level of iNOS in a pMCAO rodent model (Tian, 2013). In an *in vitro* oxygen-glucose deprivation-reperfusion (OGD/R) ischemia model, borneol inhibited the activity and expression of iNOS in primary cortical neurons and, therefore, reduced the production of iNOS-derived NO (Liu et al., 2011). In addition, borneol promotes the synthesis of eNOS-derived NO under both physiological and brain contusion conditions and has a stronger effect on the synthesis of NO by endothelial cells in the pathological state (Zhao et al., 2001). Borneol, combined with catalpol and puerarin, increases the expression of eNOS in rats

with MCAO (Wu et al., 2016). The combination of borneol and musk promotes the synthesis of NO in vascular endothelial cells and inhibits the expression of iNOS in a global cerebral ischemia/reperfusion rat model (Zhang et al., 2002; Liu et al., 2011).

Inhibition of Intracellular Ca²⁺ Overload

Calcium overload is considered being the last common pathway of neuronal injury during cerebral ischemia/reperfusion (Vannucci et al., 2001; Shi, 2014). The ways of calcium entering neurons following cerebral ischemia include glutamate receptors; voltage-dependent calcium channel; transient receptor potential channels; acid-sensing ion channels; sodium-calcium exchanger operating in entry mode; inward excitotoxic injury current calcium permeable channels; mitochondria and endoplasmic reticulum calcium release, etc. And the pathways of calcium exit into neurons include Ca²⁺-ATPase pump; Na⁺-Ca²⁺ exchanger operating in exit mode, etc (Singh et al., 2019).

It was found that both L-borneol and DL-borneol significantly reduced Ca²⁺ concentration in ischemic ipsilateral brain tissue of rats subjected to tMCAO (Ni, 2011; Tian, 2013). DL-borneol

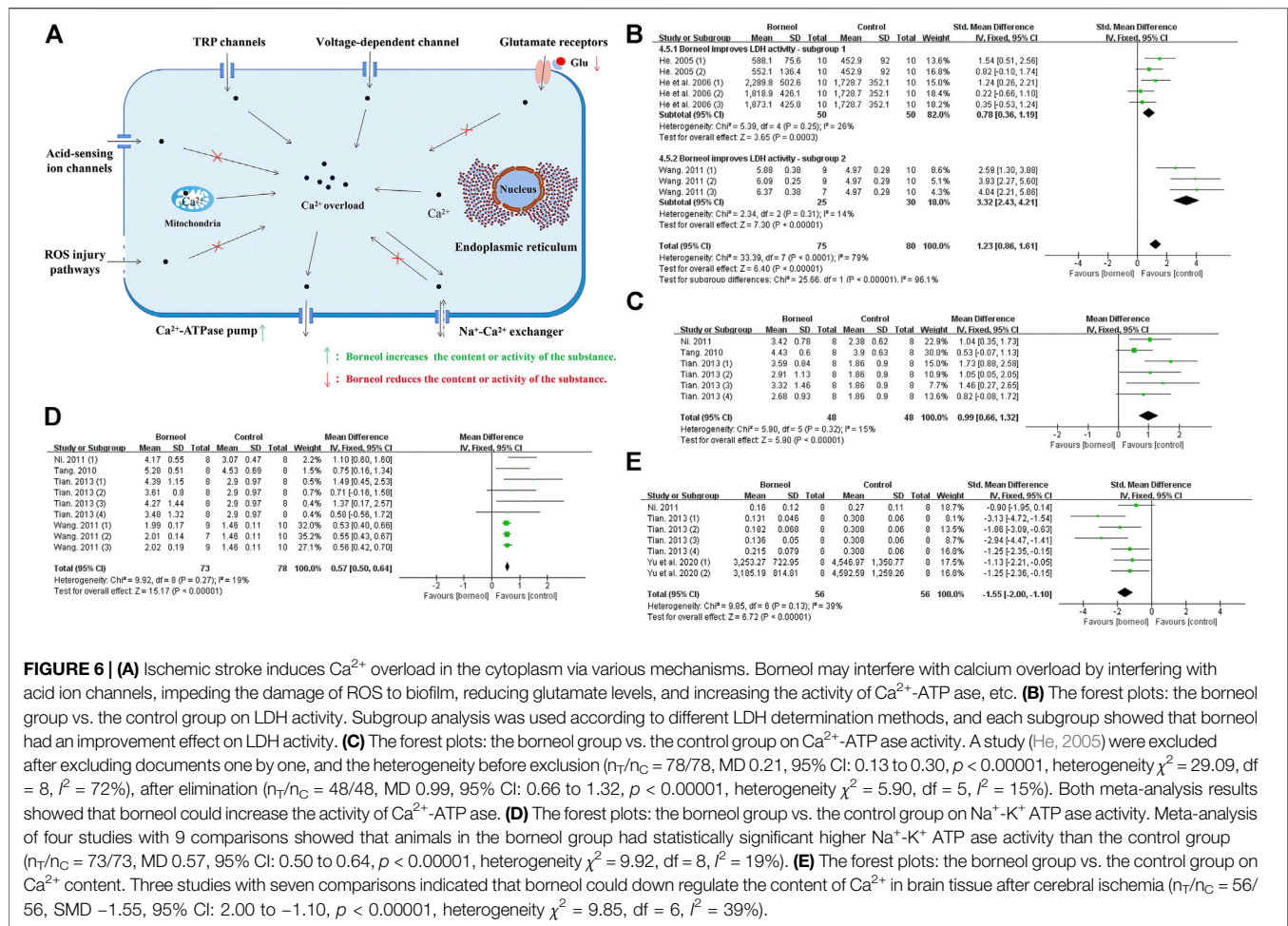


FIGURE 6 | (A) Ischemic stroke induces Ca^{2+} overload in the cytoplasm via various mechanisms. Borneol may interfere with calcium overload by interfering with acid ion channels, impeding the damage of ROS to biofilm, reducing glutamate levels, and increasing the activity of Ca^{2+} -ATPase, etc. **(B)** The forest plots: the borneol group vs. the control group on LDH activity. Subgroup analysis was used according to different LDH determination methods, and each subgroup showed that borneol had an improvement effect on LDH activity. **(C)** The forest plots: the borneol group vs. the control group on Ca^{2+} -ATPase activity. A study (He, 2005) were excluded after excluding documents one by one, and the heterogeneity before exclusion ($n_T/n_C = 78/78$, MD 0.21, 95% CI: 0.13 to 0.30, $p < 0.00001$, heterogeneity $\chi^2 = 29.09$, $df = 8$, $I^2 = 72\%$), after elimination ($n_T/n_C = 48/48$, MD 0.99, 95% CI: 0.66 to 1.32, $p < 0.00001$, heterogeneity $\chi^2 = 5.90$, $df = 5$, $I^2 = 15\%$). Both meta-analysis results showed that borneol could increase the activity of Ca^{2+} -ATPase. **(D)** The forest plots: the borneol group vs. the control group on Na^{+} -K $^{+}$ ATPase activity. Meta-analysis of four studies with 9 comparisons showed that animals in the borneol group had statistically significant higher Na^{+} -K $^{+}$ ATPase activity than the control group ($n_T/n_C = 73/73$, MD 0.57, 95% CI: 0.50 to 0.64, $p < 0.00001$, heterogeneity $\chi^2 = 9.92$, $df = 8$, $I^2 = 19\%$). **(E)** The forest plots: the borneol group vs. the control group on Ca^{2+} content. Three studies with seven comparisons indicated that borneol could down regulate the content of Ca^{2+} in brain tissue after cerebral ischemia ($n_T/n_C = 56/56$, SMD -1.55, 95% CI: 2.00 to -1.10, $p < 0.00001$, heterogeneity $\chi^2 = 9.85$, $df = 6$, $I^2 = 39\%$).

significantly decreased the concentration of Ca^{2+} in hippocampal and hypothalamic neurons after cerebral ischemia reperfusion (CIR) in rats (Yu et al., 2019a). Previous studies have found that borneol significantly increased the activity of lactate dehydrogenase (LDH) in ischemic brain tissue to inhibit the accumulation of lactic acid, which may interfere with Ca^{2+} entering cells through acid-sensitive ion channels (He, 2005; He et al., 2006; Wang, 2011). Besides, borneol reduces cytoplasmic Na^{+} levels by increasing Na^{+} -K $^{+}$ ATPase activity, which prevent Ca^{2+} from entering neurons via sodium-calcium exchange (He, 2005). ROS increase cytoplasmic Ca^{2+} concentration by destroying the integrity of the biofilm, but borneol prevents the damage of biofilm by accelerating the scavenging of ROS. Glutamate mediates calcium influx in neurons by activating glutamate receptors, while borneol reduces the level of glutamate (Huang, 2018; Yu et al., 2019b). In addition, L-borneol and DL-borneol increased the expression and activity of Ca^{2+} -Mg $^{2+}$ -ATPase, promoting the outflow of intracellular Ca^{2+} (Ni, 2011; Tian, 2013). The meta-analysis results also suggested that borneol could reduce the calcium content and increase the activities of LDH, Ca^{2+} -ATPase and Na^{+} -K $^{+}$ -ATPase (Figure 6). Overall, these publications show that borneol can improve the concentration of intracellular Ca^{2+} ,

block the pathological injury caused by Ca^{2+} overload, and interfere with the process of neuronal apoptosis in the cascade reaction. Mechanism of borneol inhibiting cytoplasmic Ca^{2+} overload and the meta-analysis results of related indicators are showed in Figure 6.

Suppress Acute Hyperthermia

During the acute stage of cerebral ischemia, fever increases the mortality and disability rates by aggravating neuronal damage (Wrotek et al., 2012). The leukocytes gather in the core area of cerebral infarction and release endogenous heat generators, and these cytokines raise the hypothalamic thermoregulation set point by triggering the release of arachidonic acid and activating cyclooxygenase to produce prostaglandins (Blatteis et al., 2005). Correlation analysis of clinical data and models of cerebral ischemia show that the harmful effects of fever after stroke are mediated by the increased excitotoxicity by glutamate, and the protective effect of hypothermia is also closely related to decreased glutamate release (Campos et al., 2012; Campos et al., 2013). Through feedback regulation, fever can further aggravate cerebral ischemic injury by promoting the secretion of excitatory neurotransmitters, increasing the production of ROS, accelerating the metabolic rate, and aggravating the

degradation of neuronal cytoskeleton proteins (Ginsberg and Busto, 1998). Researchers accidentally found that both L-borneol and DL-borneol significantly inhibited the elevation of rats body temperature after pMCAO or tMCAO (Ni, 2011; Tian, 2013). We know that infection can also induce elevated body temperature in stroke patients. Studies have also shown that the three borneols reduced LPS-induced elevation of body temperature and reduced fever due to inflammation (Luo et al., 2016; Zou et al., 2017). These suggest that borneol can inhibit acute fever of ischemic stroke, and this process may involve the inhibition of glutamate excitotoxicity and reduction in the release of endogenous febrile factors.

Mechanisms of Borneol Intervention in the Subacute Stage of Ischemic Stroke

The physiological and pathological responses in the subacute stage of ischemic stroke (within 2–7 days after the occurrence of human cerebral ischemia) play a key role in the transformation of brain injury in the infarcted area. Apoptosis and necrosis occur in the first few hours after ischemic stroke and reach a peak after 24 h (Wang et al., 2015b). Structural damage to the blood-brain barrier and the high expression of astrocyte aquaporins continue to aggravate brain edema and reach a peak 3–4 days after ischemia (Badaut et al., 2002; Badaut et al., 2007). Compared with the treatment of primary injury after arterial occlusion, secondary injury caused by inflammation may have a longer treatment time window. Intervening in the inflammatory response is an important means of treatment (Kawabori and Yenari, 2015). Therefore, the therapeutic use of borneol for blood-brain barrier damage, different types of cell death, and the inflammatory response in the subacute stage of ischemic stroke have important consequences for the treatment and rehabilitation of stroke patients.

Intervention of Inflammatory Cytokine Expression

Tumor necrosis factor alpha (TNF- α), interleukin-1 β (IL-1 β), and interleukin-6 (IL-6) are key inflammatory factors in cerebral ischemic injury. Nuclear factor kappa B (NF- κ B) also plays an important role in the inflammatory process (Sun et al., 2014). All kinds of borneol significantly reduce TNF- α levels, while D-borneol and DL-borneol reduce IL-1 β levels and DL-borneol reduces IL-6 in cerebral ischemia/reperfusion models (Ni, 2011; Chang et al., 2017; Wen, 2017; Yu et al., 2017b; Dong et al., 2018). Myeloperoxidase (MPO) is a specific marker of neutrophils (Tu et al., 2010). D-borneol inhibits MPO activity, and inhibits neutrophil infiltration in the brain tissue of rats subjected to pBCO (Shao et al., 2018). Inhibition of cyclooxygenase-2 (COX-2) and 5-lipoxygenase (5-LOX) showed a neuroprotective effect in ischemic stroke rat model (Singh and Chopra, 2014). Cerebral ischemia/reperfusion induces the upregulation of COX-2 expression, resulting in the aggravation of the cerebral injury (Zhang et al., 2019). Cysteinyl leukotriene receptor 2 (CYSLTR2) is a subtype of cysteinyl leukotriene receptor, an inflammatory mediator (Zhang, 2013). Borneol inhibits the activities of 5-LOX and COX-2 of rats subjected to tMCAO and blocks CYSLTR2

expression in the hippocampus (Duan et al., 2012; Liu et al., 2018). As shown in **Figure 7**, the meta-analysis results suggested that borneol played an anti-inflammatory role by reducing the levels of TNF- α , IL-1 β and IL-6, and inhibiting the expression of 5-LOX and COX-2 in serum or brain tissue of cerebral ischemic animals. What's more, borneol inhibits proinflammatory factor release and cytoplasmic inhibitor of kappa B alpha (I κ B α) degradation, and blocks NF- κ B p65 nuclear translocation induced by OGD/R. Borneol also inhibits the release of TNF- α and the expression of intercellular adhesion molecule-1 (ICAM1), reverses OGD/R-induced neuronal injury, nuclear pyknosis, ROS production, and the disappearance of mitochondrial membrane potential (Liu et al., 2011). Microglia-mediated neuroinflammation plays a crucial role in the pathophysiological process of multiple neurological disorders. Both LPS treatment and oxygen-glucose deprivation of neurons lead to the activation of microglia. Borneol has a direct inhibitory effect on the activation of microglia mediated by LPS *in vitro*. There was an increase in neuronal death after the addition of activated microglia culture supernatant, but the microglia culture medium treated with borneol reduced the toxicity of microglia to neurons with the decrease of TNF- α , IL-1 β , and IL-6 levels, and the increase of interleukin-10 (IL-10) levels (Wang et al., 2019). Taken together, these studies described above suggest that borneol protects against acute brain cell injury by attenuating inflammation. The mechanism of borneol attenuating inflammatory injury and the meta-analysis of related indicators are shown in **Figure 7**.

Resistance to Damage of the Blood-Brain Barrier

The blood-brain barrier (BBB) is a selective structural and functional barrier between the brain tissue and blood. The structural barrier is composed of vascular endothelial cells, pericytes, basal lamina, and astroglial terminal feet (Ueno, 2009). The functional barrier depends on P-glycoprotein (P-gp), which can expel specific substances that enter the endothelial cells back into the bloodstream (Ueno et al., 2010). The protective effect of borneol on the BBB is achieved by structurally up-regulating the expression of tight junction proteins in vascular endothelial cells, inhibiting structural destruction of the BBB mediated by metalloproteinases, and functionally inhibiting the efflux of P-gp on neuroprotective drugs.

Direct Protective Effect on BBB

The meta-analysis results of several studies confirmed that borneol could reduce the infiltration of Evans blue (EB) into the brain and decrease the brain water content after cerebral ischemia (Jia, 2014; Liu et al., 2017; Dong et al., 2018; Wang, 2011; Yao et al., 2011) (**Figure 8**). The mechanism of borneol inhibits BBB structural damage may involve the downregulation of matrix metalloproteinase 2 (MMP2) and matrix metalloproteinase 9 (MMP9), and the upregulation of TIMP metalloproteinase inhibitor 1 (TIMP1). MMP9 and MMP2 are proteases that promote the opening of the BBB and the formation of brain edema by degrading the basal lamina of cerebral vessels. TIMP1 antagonizes MMP2 and MMP9 activity. DL-borneol increases

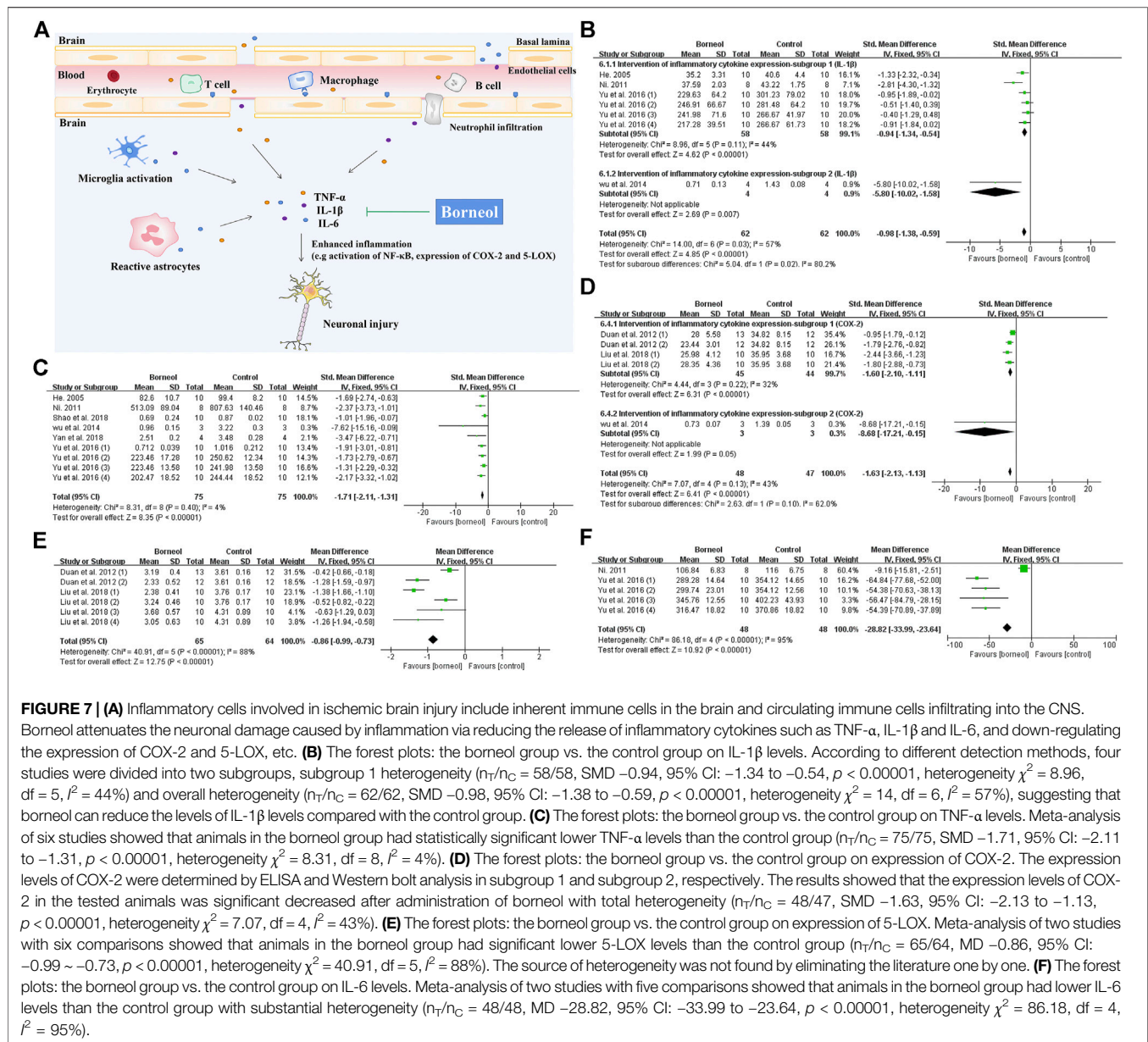


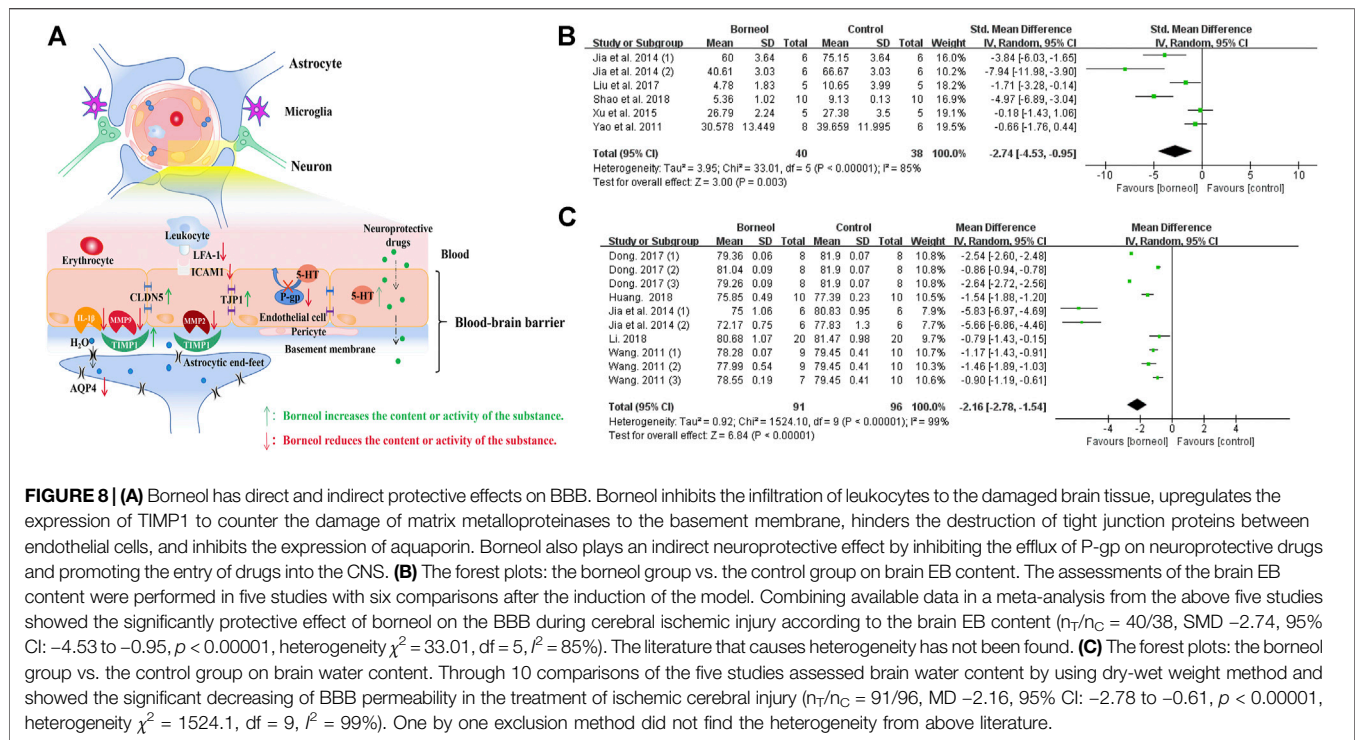
FIGURE 7 | (A) Inflammatory cells involved in ischemic brain injury include inherent immune cells in the brain and circulating immune cells infiltrating into the CNS. Borneol attenuates the neuronal damage caused by inflammation via reducing the release of inflammatory cytokines such as TNF- α , IL-1 β and IL-6, and down-regulating the expression of COX-2 and 5-LOX, etc. **(B)** The forest plots: the borneol group vs. the control group on IL-1 β levels. According to different detection methods, four studies were divided into two subgroups, subgroup 1 heterogeneity ($n_T/n_C = 58/58$, SMD -0.94, 95% CI: -1.34 to -0.54, $p < 0.00001$, heterogeneity $\chi^2 = 8.96$, $df = 5$, $I^2 = 44\%$) and overall heterogeneity ($n_T/n_C = 62/62$, SMD -0.98, 95% CI: -1.38 to -0.59, $p < 0.00001$, heterogeneity $\chi^2 = 14$, $df = 6$, $I^2 = 57\%$), suggesting that borneol can reduce the levels of IL-1 β levels compared with the control group. **(C)** The forest plots: the borneol group vs. the control group on TNF- α levels. Meta-analysis of six studies showed that animals in the borneol group had statistically significant lower TNF- α levels than the control group ($n_T/n_C = 75/75$, SMD -1.71, 95% CI: -2.11 to -1.31, $p < 0.00001$, heterogeneity $\chi^2 = 8.31$, $df = 8$, $I^2 = 4\%$). **(D)** The forest plots: the borneol group vs. the control group on expression of COX-2. The expression levels of COX-2 in the tested animals was significant decreased after administration of borneol with total heterogeneity ($n_T/n_C = 48/47$, SMD -1.63, 95% CI: -2.13 to -1.13, $p < 0.00001$, heterogeneity $\chi^2 = 7.07$, $df = 4$, $I^2 = 43\%$). **(E)** The forest plots: the borneol group vs. the control group on expression of 5-LOX. Meta-analysis of two studies with six comparisons showed that animals in the borneol group had significant lower 5-LOX levels than the control group ($n_T/n_C = 65/64$, MD -0.86, 95% CI: -0.99 ~ -0.73, $p < 0.00001$, heterogeneity $\chi^2 = 40.91$, $df = 5$, $I^2 = 88\%$). The source of heterogeneity was not found by eliminating the literature one by one. **(F)** The forest plots: the borneol group vs. the control group on IL-6 levels. Meta-analysis of two studies with five comparisons showed that animals in the borneol group had lower IL-6 levels than the control group with substantial heterogeneity ($n_T/n_C = 48/48$, MD -28.82, 95% CI: -33.99 to -23.64, $p < 0.00001$, heterogeneity $\chi^2 = 86.18$, $df = 4$, $I^2 = 95\%$).

TIMP1 mRNA expression in rats subjected to tMCAO (Liu et al., 2007). D-borneol downregulates MMP2 and MMP9 expression in rats subjected to pMCAO, and DL-borneol inhibits *MMP9* mRNA and protein in a tMCAO rat model (Liu et al., 2009; Wang et al., 2018).

In addition to the effects on metalloproteinases, borneol may also downregulate the expression of ICAM1 and lymphocyte function-associated antigen 1 (LFA-1). ICAM1 is a transmembrane protein expressed on vascular endothelial cells that binds to LFA-1 in inflammatory site. The combination of LFA-1 and ICAM1 facilitate leukocyte adherence to, or passage through vascular endothelial cells to reach the focal area of ischemia. Borneol inhibits the adhesion and penetration of leukocytes to endothelial cells by inhibiting the expression of ICAM1 and LFA-1 (Liu et al., 2009; Kong et al., 2013; Liu et al., 2011).

Borneol upregulates claudin 5 (CLDN5) and tight junction protein 1 (TJP1) expression. CLDN5 and TJP1 are key components of tight junctions between cerebral microvascular endothelial cells, and their expression is significantly decreased in ischemic brain tissue (Li et al., 2017). Previous studies have confirmed that D-borneol upregulates CLDN5 and TJP1 expression in tMCAO model rats and brain microvascular endothelial cells with OGD/R treatment (Xu and Zhang, 2015; Xu and Zhang et al., 2016). L-borneol and DL-borneol increased the expression of CLDN5 in an animal model of permanent cerebral ischemia (Xu et al., 2016; Wen, 2017; Dong et al., 2018; Wang et al., 2018).

In addition, aquaporin 4 (AQP4) is concentrated at the foot processes of astrocytes. The outer surface of blood vessels is almost surrounded (85%) by the end feet of glial cells. Thus, increased expression of this protein can induce brain edema (Hu



et al., 2012). Borneol inhibits brain edema after cerebral ischemia, which may be related to the downregulation of AQP4 mRNA expression (Liu et al., 2009).

Indirect Protective Effect on BBB

The anatomy of the BBB protects the central nervous system (CNS) from toxins and variations in blood composition, and maintains the consistency of the brain's micro-environment (Abbott and Friedman, 2012). Although considerable advancements have been made in drug delivery to the CNS, the clinical application of CNS drugs is still limited by their poor bioavailability due to the BBB (Denora et al., 2009). Borneol promotes the penetration and accumulation of neuroprotective drugs such as gastrodin, puerarin, kaempferol, and nimodipine, increases the bioavailability of these drugs, thereby exerting an indirect neuroprotective effect (Cai et al., 2008; Gao et al., 2010; Wu et al., 2014a; Zhang et al., 2015). The mechanism of this effect is closely related to the regulation of P-gp.

One study showed that P-gp was expressed 30 min after focal cerebral ischemia in rats and lasted for 24 h (Xing et al., 2007). Borneol downregulates the expression of P-gp both physiological and pathological conditions. L-borneol inhibits P-gp expression in rats subjected to tMCAO (Yu et al., 2011; Tian, 2013). P-gp, which is encoded by *Mdr1a*, is expressed on the luminal membrane of brain microvascular endothelial cell (BMEC) and confers multidrug resistance to various chemotherapeutic agents (Chen et al., 2003). In an *in vitro* BBB model composed of rat brain BMECs and astrocytes, L-borneol downregulated the efflux function of P-gp by inhibiting the expression of *mdr1a* mRNA and P-gp, and this process was related to the transient activation of NF- κ B (Fan et al., 2015).

Borneol also affects 5-HT, a known BBB neurotransmitter (Ke et al., 2000). Borneol can mediate BBB opening by increasing 5-HT in the hypothalamus of rats (Hui et al., 2009). Since P-gp is a lipophilic protein (Abbott et al., 2010), borneol easily binds to P-gp after passing through the BBB and inhibits the binding of 5-HT to P-gp, which results in a reduction in P-gp-mediated efflux of 5-HT and a consequent increase in 5-HT in cerebral vascular endothelial cells (Yuan et al., 2006). The mechanism of borneol protecting BBB and results of meta-analysis of related indicators are shown in Figure 8.

Regulation of Various Forms of Cell Death

Previous studies applied TTC staining to evaluate cerebral infarction area, showing that borneol had significant differences in alleviating cerebral infarction (Wen, 2017; Dong et al., 2018). The cytotoxic effects of excitatory amino acid toxicity, oxidative stress, and ROS damage in the acute stage of cerebral ischemia lead to rapid disintegration and necrosis of neurons. Delayed neuronal injury after several days of ischemia exhibits characteristics of apoptosis. Cellular injury in the central necrotic area of the cerebral infarction is irreversible, but the peripheral ischemic penumbra is salvageable (Guo, 2000). BCL2 apoptosis regulator (BCL2) and BCL2 associated X, apoptosis regulator (BAX) are typical BCL-2 family apoptosis-inhibiting protein and apoptosis-inducing protein, respectively. Regulating the balance between BAX and BCL2 can hinder the expansion of infarct area (Xu et al., 2016). Previous reports demonstrated that D-borneol and L-borneol reduced the BAX/BCL2 ratio in rats subjected to pMCAO and DL-borneol reduced the BAX/BCL2 ratio in both pMCAO and tMCAO models (Huang, 2018; Wen, 2017). Caspase-3 (CASP3) induces neuronal apoptosis in

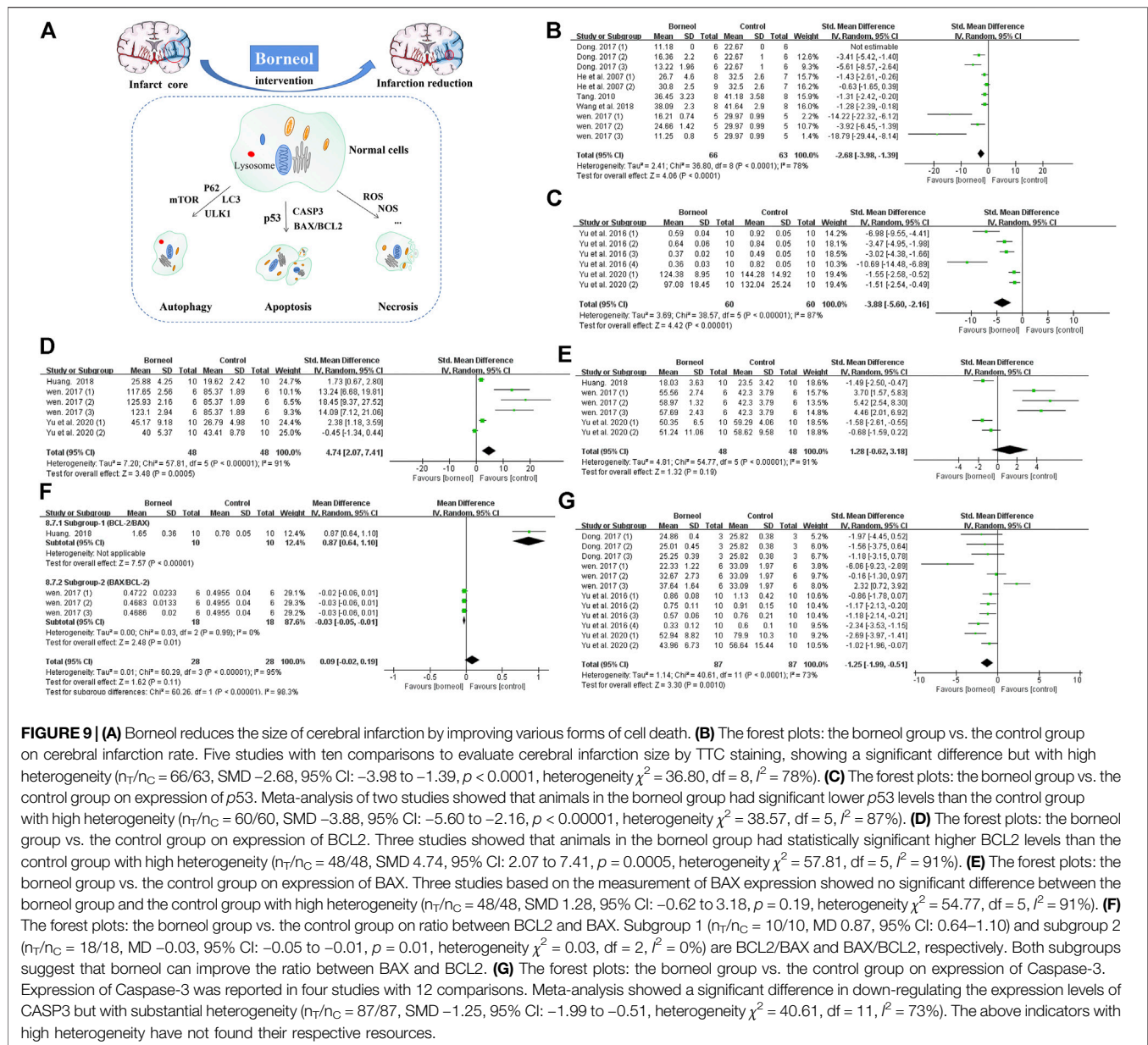


FIGURE 9 | (A) Borneol reduces the size of cerebral infarction by improving various forms of cell death. **(B)** The forest plots: the borneol group vs. the control group on cerebral infarction rate. Five studies with ten comparisons to evaluate cerebral infarction size by TTC staining, showing a significant difference but with high heterogeneity ($n_T/n_C = 66/63$, SMD -2.68 , 95% CI: -3.98 to -1.39 , $p < 0.0001$, heterogeneity $\chi^2 = 36.80$, $df = 8$, $I^2 = 78\%$). **(C)** The forest plots: the borneol group vs. the control group on expression of p53. Meta-analysis of two studies showed that animals in the borneol group had significant lower p53 levels than the control group with high heterogeneity ($n_T/n_C = 60/60$, SMD -3.88 , 95% CI: -5.60 to -2.16 , $p < 0.00001$, heterogeneity $\chi^2 = 38.57$, $df = 5$, $I^2 = 87\%$). **(D)** The forest plots: the borneol group vs. the control group on expression of BCL2. Three studies showed that animals in the borneol group had statistically significant higher BCL2 levels than the control group with high heterogeneity ($n_T/n_C = 48/48$, SMD 4.74 , 95% CI: 2.07 to 7.41 , $p = 0.0005$, heterogeneity $\chi^2 = 57.81$, $df = 5$, $I^2 = 91\%$). **(E)** The forest plots: the borneol group vs. the control group on expression of BAX. Three studies based on the measurement of BAX expression showed no significant difference between the borneol group and the control group with high heterogeneity ($n_T/n_C = 48/48$, SMD 1.28 , 95% CI: -0.62 to 3.18 , $p = 0.19$, heterogeneity $\chi^2 = 54.77$, $df = 5$, $I^2 = 91\%$). **(F)** The forest plots: the borneol group vs. the control group on ratio between BCL2 and BAX. Subgroup 1 ($n_T/n_C = 10/10$, MD 0.87 , 95% CI: 0.64 – 1.10) and subgroup 2 ($n_T/n_C = 18/18$, MD -0.03 , 95% CI: -0.05 to -0.01 , $p = 0.01$, heterogeneity $\chi^2 = 0.03$, $df = 2$, $I^2 = 0\%$) are BCL2/BAX and BAX/BCL2, respectively. Both subgroups suggest that borneol can improve the ratio between BAX and BCL2. **(G)** The forest plots: the borneol group vs. the control group on expression of Caspase-3. Expression of Caspase-3 was reported in four studies with 12 comparisons. Meta-analysis showed a significant difference in down-regulating the expression levels of CASP3 but with substantial heterogeneity ($n_T/n_C = 87/87$, SMD -1.25 , 95% CI: -1.99 to -0.51 , heterogeneity $\chi^2 = 40.61$, $df = 11$, $I^2 = 73\%$). The above indicators with high heterogeneity have not found their respective resources.

ischemic stroke, and which is interrupted by L-borneol and D-borneol after cerebral ischemia/reperfusion (Wen, 2017; Yu et al., 2020). Tumor protein 53 (p53) is mainly expressed in the mitochondria and contributes to cell apoptosis (Wang et al., 2017b). Borneol reduces p53 expression in the cortex and striatum (Yu et al., 2020). Meta-analysis results also suggested that borneol had anti-apoptotic effects by down-regulating the expression levels of p53 and caspase-3, and regulating the ratio of BAX and BCL-2 (Figure 9). Furthermore, borneol enhances the neuron protective autophagy in the cortex and striatum by modulating beclin1, mTOR, and LC3II/I (Yu et al., 2017c; Yu et al., 2020). L-camphor is one of the metabolic products of borneol in the body (Jiang et al., 2008). Several studies have demonstrated that L-camphor upregulates cell adhesion molecule 2 (CADM2) expression to promote neurite outgrowth by

targeting microRNA-125a and microRNA-140 and upregulates heterogeneous nuclear ribonucleoprotein A1 (HNRNPA1) expression to promote the expression of stress granules. At the same time, L-camphor can improve apoptosis and autophagy by regulating the autophagy-related proteins, p62 and LC3, and apoptosis-related proteins BCL-XL and CASP3 (Li, 2016; Liu, 2017; Ren, 2018). The mechanism of borneol intervention in various forms of neuronal death and related meta-analysis results are shown in Figure 9.

Mechanism of Borneol Intervention in the Late Stage of Ischemic Stroke

In the late stage of ischemic stroke (one week after the occurrence of cerebral ischemia in humans), reactive glial cell hyperplasia

and glial scar formation limit the expansion of brain damage and separate the necrotic infarct core from the surrounding normal tissues (Sims and Yew, 2017). The reconstruction of the glial cell groups, the neovascularization of the blood vessels, and the regeneration of the nerve myelin sheath play leading roles in the repair process at this stage. Borneol helps the body recover to a healthy physiological state more quickly by promoting angiogenesis and accelerating the repair of damaged neurons in the late stage of stroke.

Promoting the Growth and Repair of Neurons and Angiogenesis

Animal experiments confirmed that borneol improved the neurological function score and reduced the cerebral infarction area (Wu et al., 2014b; Dong et al., 2018). Immunofluorescence staining showed that borneol also lowered neuronal mortality and promoted neurogenesis (Zhang et al., 2017b; Yu et al., 2020). Tanshinol borneol ester (DBZ) is a novel synthetic compound derived from Dantonice®. DBZ plays a role in inducing angiogenesis in both *in vivo* and *in vitro* experiments (Liao et al., 2019). Borneol promotes neurogenesis and angiogenesis in the brain, possibly through the upregulation of endogenous neurotrophic factors and regulation of the Wnt/ β -catenin pathway.

Increasing Endogenous Neurotrophic Factors

Ischemic brain injury destroys nerves and cerebral vessels and induces compensatory neonatal reactions in brain tissue, including nerve regeneration and vascular remodeling. Borneol regulates brain derived neurotrophic factor (BDNF), nerve growth factor (NGF), vascular endothelial growth factor (VEGF), fibroblast growth factor 2 (FGF2/bFGF), and glial cell derived neurotrophic factor (GDNF), and promotes repair of nerves as well as remodeling of blood vessels by activating the Wnt/ β -catenin pathway.

In a tMCAO rodent model, DL-borneol significantly decreased *VEGF* mRNA on the first day after cerebral ischemia but increased *VEGF* mRNA levels on the second and third days (Hu et al., 2005; Ni, 2011). Three kinds of borneol can upregulate the expression of VEGF in a pMCAO rat model after ischemia (Dong et al., 2018). Under physiological conditions, endothelial cells express approximately 10 times less fms related receptor tyrosine kinase 1 (FLT1/VEGFR1) than kinase insert domain receptor (KDR/VEGFR2) (DeVal and Black, 2009). Binding of VEGF to VEGFR2 activates intracellular tyrosine kinases and multiple downstream signals that induce angiogenesis. The inhibition of VEGFR2 signaling disturbs endothelial cell proliferation after stroke (Shimotake et al., 2010). On the contrary, VEGFR1 negatively regulates cell proliferation and reduces angiogenesis (Mendes et al., 2018). Increasing evidence suggests that cerebral ischemia upregulates VEGFR1 expression, which positively correlates with the degree of damage (Yoo et al., 2010; Causey et al., 2012). In a BMECs model treated with OGD, borneol increased the expression of VEGF, reduced the expression of VEGFR1, and tended to increase the expression of VEGFR2 (Yu et al., 2019a). The latest research confirms that L-borneol can promote

angiogenesis coupled neurogenesis by regulating Ang1-VEGF-BDNF to play a neuroprotective effect (Ma et al., 2021). In a tMCAO rat model, borneol significantly enhanced the expression of *NGF*, *BDNF*, *GDNF*, and *VEGF* mRNA after 48 h of reperfusion. Borneol not only increased the expression of *NGF*, *GDNF*, and *VEGF* mRNA but also significantly increased the level of *bFGF* mRNA after 72 h of reperfusion (Hu, 2004).

Regulation of the Wnt/ β -Catenin Pathway

The Wnt/ β -catenin pathway regulates neuronal differentiation and microangiogenesis, and this pathway is crucial for endothelial cell maintenance of the BBB homeostasis and normal neural function. The Wnt/ β -catenin pathway participates in the proliferation and differentiation of neural stem cells, the formation of axons, the occurrence of cortical patterns, vascular regeneration and remodeling in the nervous system, and the formation of the BBB. Wnt family member 3A (WNT3A), β -catenin, disheveled (Dsh), and lymphoid enhancer binding factor 1 (LEF1) are positive regulatory molecules of the Wnt/ β -catenin pathway, while glycogen synthase kinase 3 beta (GSK3B) and APC regulator of WNT signaling pathway (APC) are negative regulators of this pathway (Wen et al., 2016). Three kinds of borneol activate the Wnt/ β -catenin signal pathway by regulating the expression of positive and negative regulatory molecules in rats subjected to pMCAO, performing the neuroprotective effect of CNS (Wen, 2017). In another study, the combination of borneol, astragaloside IV, and *Panax notoginseng* saponins promotes the proliferation of neurons and repairs damaged neurons, enhancing the resistance of rats to cerebral ischemia/reperfusion injury, which is also associated with the regulation of the Wnt/ β -catenin signaling pathway (Yang et al., 2019).

DISCUSSION

Summary of Results

Ischemic brain injury is an extremely complex process, but the neuroprotective effect of many drugs is more likely to play a single role in the ischemic cascade reaction. In summary, borneol has protective effects at all three stages of cerebral ischemic injury. In the acute stage of cerebral ischemia, borneol improves cerebral blood flow by relaxing blood vessels and eliciting anti-thrombotic effects, inhibits neuronal excitotoxicity by reducing Glu levels and activating GABA_A receptors, improves the ability of the body to resist ROS injury by increasing the activity of antioxidant enzymes, regulates the activity of different types of NOS and antagonizes the neurotoxic effect of NO, reduces the content of intracellular Ca²⁺, interferes with the process of neuron death, and antagonizes the symptoms of acutely elevated body temperature. In the subacute phase of ischemia stroke, borneol interferes with the expression of inflammatory cytokines, the destruction of BBB, and multiple forms of neuron death. In the late stage of brain injury, borneol promotes neuronal repair and angiogenesis. Furthermore, borneol mobilizes endogenous nutritional factors to hasten self-repair of the body, avoiding

TABLE 1 | Summary of borneol intervention for ischemic stroke.

Study	Drug	Dosage and delivery way	Animal	Model	Ischemia/reperfusion	Time of	Outcome measures	Conclusion/possible mechanisms of neuroprotection
Li (2018)	D-borneol	ip, 10 mg/kg	Kunming mice	Photochemical cerebral ischemia model		24 h	(1) Zea-Longa neurological function score (2) Cerebral blood flow (3) Cerebral infarction rate (4) Brain water content (5) Neuronal viability (6) Caspase-3 (7) MMP-9	(1) Improve neurological deficits (2) Reduce brain edema and cerebral infarction size (3) Increase blood perfusion (4) Attenuate neuronal apoptosis by downregulating the expression of Caspase-3 (5) Protect the BBB by downregulating the expression of MMP-9
Wang et al. (2018)	D-borneol	ig, 30 mg/kg	Male, SD rats	pMCAO 2 h		7 day	(1) Longa neurological function score (2) Cerebral blood flow (3) Cerebral infarction rate (4) Cerebral histopathology with H&E staining (5) MMP-2 (6) MMP-9 and MMP-9 mRNA (7) Claudin-5 mRNA (8) ZO-1	(1) Reduce cerebral infarction size (2) Increase cerebral blood flow (3) Improve the brain histopathological morphology (4) Protect the BBB by downregulating the expression of MMP-2, MMP-9 and MMP-9 mRNA and increasing the expression of ZO-1 and Claudin-5 mRNA.
Yu et al. (2020)	DL-borneol	ig, 80 mg/kg	SD rats (sex in half)	GOIR 60s		7 day	(1) Cerebral blood flow (2) SOD, CAT, GSH-Px, MDA, ROS, iNOS and NO (3) Apoptosis-related genes: p53, Caspase-3, Bcl-2, bax (4) Apoptosis rate with TUNEL staining (5) Autophagy-related proteins: pAMPK, mTOR, ULK1, LC3 I/II, Beclin1 and BNIP3 (6) Ca ²⁺ content	(1) Improve microcirculation (2) Promote autophagy by increasing the expression of LC3 I/II and Beclin1 (3) Inhibit apoptosis in cortex by regulating the expression of p53, Caspase-3, Bcl-2 and bax (4) Inhibit Ca ²⁺ overload
Yu et al. (2016)	DL-borneol	ig, 160 g/kg	Male, SD rats	IGIR 10min		7 day	(1) Cerebral blood flow (2) Inflammation indicators: IL-1 β , IL-6, TNF- α (3) Antioxidant ability: SOD, GSH-Px, and MDA (4) Apoptosis-related genes: p53, Caspase-3 (5) Score of hist staining (1) Ca ²⁺ content (2) The ultrastructure of BBB (3) Apoptosis rate with TUNEL staining (4) Levels of glycine, glutamate, and γ -aminobutyric acid	(1) Improve microcirculation (2) Inhibit inflammatory response by decreasing the expression of IL-1 β , IL-6, TNF- α (3) Antioxidative damage by increasing the activity of SOD and GSH-Px, and decreasing the MDA content (4) Antiapoptosis by decreasing the expression of p53 and Caspase-3 (1) Reduce glutamate levels and Ca ²⁺ content in hippocampus and hypothalamus (2) Inhibit nerve cell apoptosis and protect BBB ultrastructure
Yu et al. (2019c)	DL-borneol	ig, 160 mg/kg	Male, SD rats	IGIR 20min		7 day	(1) Ca ²⁺ content (2) The ultrastructure of BBB (3) Apoptosis rate with TUNEL staining (4) Levels of glycine, glutamate, and γ -aminobutyric acid	(1) Reduce cerebral infarction rate (2) Improve neurological deficits and memory ability
He 2005 (1)	DL-borneol	iv, 2.0, 1.0, 0.5 mg/kg	Kunming mice (sex in half)	IMCAO 15 min		22 h	(1) Cerebral infarction rate (2) Neurological function score (3) Step-down test and avoidance reaction experiment	Anti-inflammation by decreasing the expression of TNF- α , IL-1 β , and ICAM-1
He 2005 (2)	DL-borneol	iv, 1.4 mg/kg	Male and female, Wistar rats	IMCAO 2 h		22 h	(1) Cerebral infarction rate (2) Neurological function score (3) ICAM-1, IL-1 β , TNF- α	Improve the energy metabolism disorder by upregulating the activity of Na ⁺ -K ⁺ -ATPase, Ca ²⁺ -ATPase, Mg ²⁺ -ATPase, and LDH
He 2005 (3)	DL-borneol	iv, 2.0, 1.0, 0.5 mg/kg	Kunming mice (sex in half)	IMCAO 30 min		2 h	(1) LDH (2) Na ⁺ -K ⁺ -ATPase (3) Ca ²⁺ -ATPase and Mg ²⁺ -ATPase	(1) Reduce cerebral infarction rate (2) Improve neurological deficits and memory ability
He et al. (2006)	DL-borneol	iv, 0.35, 0.7, 1.4 mg/kg	Kunming mice (sex in half)	IMCAO 3 h		3 h	(1) Neurological function score	Reduce oxidative reactions by increasing the activity of SOD and decreasing MDA levels
He et al. (2007)	DL-borneol	iv, 2.0, 1.0, 0.5 mg/kg	Kunming mice (sex in half)	pBCO		6 h	(2) MDA, SOD, LDH (1) Cerebral infarction rate (2) GSH-Px, MDA	(2) Improve the energy metabolism disorder by upregulating the activity of LDH Reduce oxidative reactions by increasing the activity of GSH-Px and decreasing MDA levels
Huang (2018)	DL-borneol	ig, 100 mg/kg	SD rats (sex in half)	IMCAO 2 h		24 h	(1) Brain water content (2) Bax and Bcl-2 (3) ET and CGRP (4) SOD, MDA, and GSH-Px (5) Levels of glycine, glutamate, aspartic acid, and γ -aminobutyric acid	(1) Antiapoptosis by modulating the Bax/Bcl-2 expression (2) Reduce oxidative reactions by increasing the activity of SOD and GSH-Px, and decreasing the concentration of MDA (3) Dilate blood vessels by increasing CGRP content and reducing ET content (4) Anti-excitatory amino acid neurotoxicity by decreasing levels of glutamate and aspartic acid
Tian (2013)	L-borneol	ig, 133.3, 200 mg/kg	Male, SD rats	IMCAO 2 h		22 h	(1) Rate of cerebral edema (2) Rectal temperature (3) MDA, SOD	(1) Improve the energy metabolism disorder by upregulating the activity of Na ⁺ -K ⁺ -ATPase, Ca ²⁺ -Mg ²⁺ -ATPase, and T-ATPase (2) Alleviate the pathological BBB disruption by alleviating the damage of the BBB tight junction integrity (3) Reduce oxidative reactions by increasing the activity of SOD and decreasing MDA levels
Tian (2013)	DL-borneol	ig, 133.3, 200 mg/kg	Male, SD rats	IMCAO 2 h		22 h	(4) P-GP, MDRI mRNA (5) The ultrastructure of BBB (6) NO, iNOS, iNOS (7) T-ATPase, Na ⁺ -K ⁺ -ATPase, Ca ²⁺ -Mg ²⁺ -ATPase, Ca ²⁺ levels	(4) Neuroprotection via P-GP signaling pathway (5) Neuroprotection via NO signaling pathway

(Continued on following page)

TABLE 1 | (Continued) Summary of borneol intervention for ischemic stroke.

Study	Drug	Dosage and delivery way	Animal	Model	Time of ischemia/reperfusion	Outcome measures	Conclusion/possible mechanisms of neuroprotection
Ni (2011)	DL-borneol	ig, 200 mg/kg	Male, SD rats	IMCAO 2 h	22 h	(1) The ultrastructure of BBB (2) SOD, MDA (3) IL-1 β , IL-6, TNF- α (4) NO, NOS, Ca ²⁺ levels (5) Na ⁺ -K ⁺ -ATPase, Ca ²⁺ -Mg ²⁺ -ATPase (6) MMP-9, VEGF (1) Cerebral infarction rate	(1) Alleviate the pathological BBB disruption by downregulating VEGF and MMP-9 (2) Reduce oxidative reactions by increasing the activity of SOD and decreasing MDA levels (3) Anti-inflammation by decreasing the expression of TNF- α , IL-1 β , and IL-6 (4) Neuroprotection via NO signaling pathway (5) Improve the energy metabolism disorder by upregulating the activity of Na ⁺ -K ⁺ -ATPase and Ca ²⁺ -Mg ²⁺ -ATPase (1) Reduce oxidative reactions by increasing the activity of SOD and decreasing MDA and NO levels (2) Improve the energy metabolism disorder by upregulating the activity of Na ⁺ -K ⁺ -ATPase and Ca ²⁺ -Mg ²⁺ -ATPase
Tang (2010)	DL-borneol	ig, 200 mg/kg	Male, SD rats	pMCAO	6 h	(2) Zea-longa neurological function score (3) Cerebral histopathology with HE staining (4) SOD, MDA, NO (5) Na ⁺ -K ⁺ -ATPase, Ca ²⁺ -Mg ²⁺ -ATPase (1) Zea-longa neurological function score	(1) Antiapoptosis by modulating the Bax/Bcl-2 and Caspase-3 expression at both the mRNA and protein levels (2) Protect nerve vascular unit by activating Wnt/ β -catenin signaling pathway (3) Anti-inflammation by decreasing the expression of TNF- α
Wan (2017)	D-borneol, L-borneol, DL-borneol	ig, D-borneol (600 mg/kg), L-borneol (200 mg/kg), DL-borneol (200 mg/kg)	Male, SD rats	pMCAO	24 h	(2) Brain water content (3) Cerebral infarction rate (4) The ultrastructure of BBB (5) Cerebral histopathology with HE staining (6) VEGF, NGF, TNF- α , IL-1 β (7) Bax, Bcl-2, Caspase-3 mRNA and protein (8) APC, Dsh1, LEF1, Wnt3a, GSK-3 β β -catenin mRNA and protein (1) Zea-longa neurological function score (2) Brain water content (3) Cerebral infarction rate	(1) Anti-inflammation by decreasing the expression of TNF- α (2) Antiapoptosis by modulating the Bax/Bcl-2 expression at both the mRNA and protein levels (3) Alleviate the pathological BBB disruption by upregulating tight junction proteins Claudin-5 (4) Accelerate the proliferation of vascular endothelial cells by initiating angiogenesis
Dong et al. (2018)	D-borneol, L-borneol, DL-borneol	ig, D-borneol (600 mg/kg), L-borneol (200 mg/kg), DL-borneol (200 mg/kg)	Male, SD rats	pMCAO	24 h	(1) mNSS neurological function score (2) Brain water (3) Cerebral infarction rate (4) TNF- α , IL-1 β and COX-2 (5) iNOS, ONOO ⁻ (1) Brain EB content (2) ZO-1 mRNA and protein (3) Claudin-5 mRNA and protein (1) Brain EB content (2) Brain water content (3) Number of ZO-1 positive cells (4) Expression of ZO-1 protein	(1) Anti-inflammation by decreasing the expression of TNF- α and IL-1 β (2) anti-free radical injury by decreasing the expression of iNOS and ONOO ⁻
Wu et al. (2014b)	D-borneol	iv, 0.3 mg/kg, 0.8 mg/kg	SD rats	IMCAO 2 h	24 h	(1) mNSS neurological function score (2) Brain water (3) Cerebral infarction rate (4) TNF- α , IL-1 β and COX-2 (5) iNOS, ONOO ⁻ (1) Brain EB content (2) ZO-1 mRNA and protein (3) Claudin-5 mRNA and protein (1) Brain EB content (2) Brain water content (3) Number of ZO-1 positive cells (4) Expression of ZO-1 protein	Reduces BBB permeability by increasing protein and mRNA expression of ZO-1 and Claudin-5 Reduces BBB permeability by increasing protein expression of ZO-1
Xu et al. (2016)	D-borneol	ig, 28 mg/kg	SD rats	IMCAO 2 h	24 h	(1) Cerebral infarction rate (2) Neurological function score (3) Grid-walking task and cylinder task (4) dendrite spine length and number (5) TNF- α and iNOS (1) SOD (2) MPO and TNF- α (3) Brain EB content (1) SOD (2) MPO and TNF- α (3) Brain EB content	(1) Anti-inflammation by decreasing the expression of TNF- α and IL-1 β (2) anti-free radical injury by decreasing the expression of iNOS and ONOO ⁻
Jia (2014)	D-borneol	ig, 200 mg/kg	Wistar rats (sex in half)	IGCIR 20 min	3 day	(1) Cerebral infarction rate (2) Neurological function score (3) Grid-walking task and cylinder task (4) dendrite spine length and number (5) TNF- α and iNOS (1) SOD (2) MPO and TNF- α (3) Brain EB content (1) SOD (2) MPO and TNF- α (3) Brain EB content	Reduces BBB permeability by increasing protein and mRNA expression of ZO-1 and Claudin-5 Reduces BBB permeability by increasing protein expression of ZO-1
Chang et al. (2017)	D-borneol	iv, 1 mg/kg	Male, SD rats	Photochemical cerebral ischemia model	24 h	(1) Cerebral infarction rate (2) Neurological function score (3) Grid-walking task and cylinder task (4) dendrite spine length and number (5) TNF- α and iNOS (1) SOD (2) MPO and TNF- α (3) Brain EB content (1) SOD (2) MPO and TNF- α (3) Brain EB content	(1) Anti-inflammation by decreasing pro-inflammatory molecules such as iNOS and TNF- α (2) Produce long-term beneficial effect on sensorimotor functions by ameliorating degeneration of dendrites (1) Anti-inflammation by decreasing the expression of TNF- α and MPO (2) Reduce oxidative reactions by increasing the activity of SOD
Shao et al. (2018)	D-borneol	ig, 500 mg/kg	Rats	IMCAO 2 h	24 h	(1) SOD (2) MPO and TNF- α (3) Brain EB content (1) SOD (2) MPO and TNF- α (3) Brain EB content	(1) Reduce oxidative reactions by increasing the activity of SOD (2) Anti-inflammation by decreasing the expression of TNF- α and MPO
Yan et al. (2018)	DL-borneol	ig, 500 mg/kg	Rats	BCO 0.5 h	24 h	(1) SOD (2) MPO and TNF- α (3) Brain EB content (1) NO (2) lipid peroxidation (3) SOD	(1) Reduce oxidative reactions by increasing the activity of SOD (2) Anti-inflammation by decreasing the expression of TNF- α and MPO
Huang et al. (2001)	DL-borneol	ig, 1000 mg/kg	SD rats (sex in half)	IBCO 40 min	1 h	(1) NO (2) lipid peroxidation (3) SOD	Reduce oxidative reactions decreasing the levels of NO and lipid peroxidation and increasing SOD activity

(Continued on following page)

TABLE 1 | (Continued) Summary of borneol intervention for ischemic stroke.

Study	Drug	Dosage and delivery way	Animal	Model	Time of ischemia/reperfusion	Outcome measures	Conclusion/possible mechanisms of neuroprotection
Wang (2011)	DL-borneol	lg, 66.67 mg/kg, 133.34 mg/kg, 200 mg/kg	SD rats (sex in half)	pBCO	3 h	(1) Brain water content (2) SOD and MDA (3) LDH and Na ⁺ -K ⁺ -ATPase	(1) Reduce oxidative reactions by increasing the activity of SOD and decreasing the concentration of MDA (2) Improve the energy metabolism disorder by upregulating the activity of Na ⁺ -K ⁺ -ATPase and improving the activity of LDH
Duan et al. (2012)	DL-borneol	lg, 25 g/kg, 50 mg/kg	Male, SD rats	IMCAO 2 h	24 h	(1) Neurological function score (2) COX-2 (3) 5-LOX	Anti-inflammation by decreasing the activity of COX-2 and 5-LOX
Liu et al. (2018)	DL-borneol	lg, 25 g/kg, 50 mg/kg	Male, SD rats	pMCAO	1 day, 3 day	(1) Zea-longa Neurological function score (2) COX-2 (3) 5-LOX (4) OysLT2	Anti-inflammation by decreasing the activity of COX-2, 5-LOX and OysLT2
Liu et al. (2007)		lg, 3 mg/kg	Male and female, SD rats	IMCAO 2 h	24 h	(1) Brain water content (2) Brain EB content	Reduce cerebral water content and permeability of BBB
Yao et al. (2011)		lg, 66.67 mg/kg	Male and female, Kunming mice	BCO 20 min	20 min	Brain EB content	Reduce the permeability of BBB

tMCAO, temporary middle cerebral artery occlusion; pMCAO, permanent middle cerebral artery occlusion; BCO, bilateral common carotid artery occlusion; GPCR, global cerebral ischemia and reperfusion; Ip, intraperitoneal administration; Ig, intragastric administration; Iv, intravenous administration.

the defect of single-target therapeutic agents. Moreover, borneol can promote other drugs to pass through the BBB to enhance their therapeutic effects and play a synergistic neuroprotective effect. Hence, borneol can interfere with neuronal injury after cerebral ischemia through multiple channels.

Implications

Borneol is a naturally occurring product in a class of “orifice-opening” agents used in TCM for resuscitative purpose, and is widely used as an upper ushering drug for various brain diseases in many Chinese herbal formulae (Zhang et al., 2017a; Chen et al., 2019). This is consistent with the findings of many scholars that borneol has a beneficial effect on increasing the bioavailability, tissue distribution, and blood concentration of other drugs, and making other drugs transport through BBB easier (Xiao et al., 2007; Cai et al., 2008; Lu et al., 2011).

Heat-clearing is a traditional effect of borneol as a resuscitation-inducing aromatic medicine (Zou et al., 2017; Wang and Wang, 2018). Some researchers found that oral administration of borneol had a certain improvement effect on fever in the acute phase of stroke, which is consistent with the understanding of “inducing resuscitation with drugs of pungent flavor and cool nature” of borneol in TCM clinical practice. But the time-effect, dose-effect relationships, and mechanisms of borneol inhibiting stroke hyperpyrexia deserve a more thorough study.

Oral administration is the most common route in the clinical use of borneol. Borneol is absorbed rapidly into the brain and has the same concentration in the brain as in the blood within 5 min of oral administration (Pan et al., 2014). In mice, a single oral dose of borneol accumulates in organs in this order: lung < muscle < spleen < heart < kidney < brain < liver (Huang et al., 2009). The distribution of borneol in the brain also shows regional specificity, with the highest concentration in the cortex, moderate concentrations in the hippocampus and hypothalamus, and lowest concentration in the striatum (Yu et al., 2013). Besides, the biphasic half-life and elimination of D-borneol and DL-borneol in the plasma were 0.7–8.5 h and 0.8–8.0 h, respectively, (Cheng et al., 2013). Another study found that 10 h after a single dose of 2 g L-borneol, about 81% of borneol is excreted in the form of glucuronic acid binding in urine (Bhatia et al., 2008). These studies suggest that while borneol is easily absorbed, it does not easily accumulate in the body.

Outlooks

In **Table 1**, we found that borneol administration in ischemic stroke was mainly oral, with some instances of intravenous administration being recorded. However, it has been reported that intranasal administration of borneol had rapid absorption into the blood and brain compared with oral administration while having similar bioavailability compared to intravenous administration (Zhao et al., 2012). Therefore, it is necessary to pay more attention to the nasal administration of borneol in the future research of brain diseases.

It is undeniable that only few patients receive thrombolysis within 6–8 h in the treatment of cerebral ischemia, which results in most patients developing permanent cerebral ischemia

TABLE 2 | Quality assessment of included studies.

Study years	A	B	C	D	E	F	G	Total
Li (2018)	+	+	+		+	+	+	6
Wang et al. (2018)	+	+			+		+	4
Yu et al. (2020)	+	+			+	+	+	5
Yu et al. (2016)	+	+			+	+	+	5
Yu et al. (2019a)	+	+			+		+	4
He (2005)	+	+			+		+	4
He et al. (2006)	+	+			+	+	+	5
He et al. (2007)	+	+			+	+	+	5
Huang (2018)	+	+			+	+	+	5
Tian (2013)	+	+			+	+	+	5
Ni (2011)	+	+			+	+	+	5
Tang (2010)	+	+			+	+	+	5
Wen (2017)	+	+			+	+	+	5
Dong et al. (2018)	+	+			+	+	+	5
Wu et al. (2014)	+	+	+		+	+	+	6
Xu et al. (2016)	+	+			+		+	4
Jia (2014)	+	+			+	+	+	5
Chang et al. (2017)	+	+	+		+	+	+	6
Shao et al. (2018)	+	+			+		+	4
Yan et al. (2018)	+	+			+		+	4
Huang et al. (2001)	+	+					+	3
Wang (2011)	+	+			+	+	+	5
Duan et al. (2012)	+	+			+		+	4
Liu et al. (2018)	+	+					+	3
Liu et al. (2007)	+	+			+		+	4
Yao et al. (2011)	+	+			+		+	4

A, peer-reviewed publication; B, random allocation; C, blinded conduct of the Experiments; D, blinded assessment of outcome; E, use of anesthetic without significant neuroprotection; F, compliance with animal welfare regulations; G, detailed description of animals and models.

(Chalela et al., 2007). Regrettably, most experimental studies being focused on transient ischemic stroke (Mcbride and Zhang, 2017; Ma et al., 2020). This phenomenon can also be seen in **Table 1**. Thus, the comparative study between permanent cerebral ischemia model and ischemia-reperfusion model has far-reaching clinical value for the differential medication of borneol in the treatment of stroke.

As we all know, there are pharmacodynamic differences between the compounds which are optically active isomers (Wermuth, 2015). Borneol is a bicyclic compound with three chiral carbon atoms and several optical isomers. L-borneol and D-borneol are a pair of optical isomers, and their neuroprotective effects in ischemic injury may be different. Consequently, the comparison of pharmacodynamic differences of different borneols in the intervention of ischemic stroke should be one of the focuses of later work. Besides, it is worth noting that there are many commercial species or isomers of borneol, and the botanical taxonomic names used by researchers are not the same, which makes it difficult to compare the experimental results. Therefore, it is also necessary to clarify the botanical source, spatial structure and drug purity of borneol in future experimental studies.

Limitations

The mechanisms of ischemic brain damage in humans and experimental animals cannot be equal because of species differences. This paper is based on the injury mechanism in

humans at different periods (acute stage, subacute stage, and late stage) as a clue to sort out the neuroprotective effect of borneol in experimental models. Therefore, whether borneol can exert the same protective mechanism in clinical practice requires further study.

Some meta-analysis results have high heterogeneity due to experimental animals, the types and doses of borneol, animal models, and other factors. Therefore, exploring the reason that causes substantial heterogeneity and conducting more detailed data analysis will be issues that need to be addressed by relevant practitioners later.

The quality scores for the included studies shown in **Table 2**. The average quality score of *in vivo* animal studies for meta-analysis was 4.6. Twenty-six studies were peer-reviewed publications, among them, nine studies were published master's thesis or PhD thesis. Twenty-six studies declared the random allocation. Three studies reported the masked conduct of experiments. None of the included studies described the blinded assessments of outcome. Twenty-four studies described the use of anesthetic without significant intrinsic neuroprotective activity. Fifteen studies stated they compliance with animal welfare regulations. Twenty-six studies described the experimental animals and the model preparation process in comparatively detail. According to the above quality assessment results, we call for more high-quality studies to confirm the neuroprotective effect and mechanism of borneol in the future.

CONCLUSION

Although borneol is rarely used alone in the clinical treatment of brain diseases, it cannot be ignored that borneol exerts a significant neuroprotective effect even when used alone *in vivo* and *in vitro* studies. The meta-analysis results of various animal experiments further indicated that borneol has an intervention effect in energy metabolism, inflammatory reaction, apoptosis, and necrosis as well as other processes of cerebral ischemic cascade reaction. This possible explanation for the benefits and the success of borneol in preventing enlargement of infarction and improving neurological function score. Overall, the previous review excessively focused on the regulation of borneol on BBB and ignored its overall effect on the treatment of cerebral ischemia. But this review comprehensively highlights the potential application of borneol as a neuroprotective agent against cerebral ischemia. We strongly believe that the research field of borneol anti-ischemic stroke is still promising.

AUTHOR CONTRIBUTIONS

YL, MR, JW (3rd author), QX, HL, and JL of our team are responsible for collecting relevant documents, YL is responsible for writing the first draft of the paper, JW (9th author), RM and HC are responsible for reviewing the manuscript, and YL is responsible for submitting the final manuscript.

FUNDING

This work is financially supported by grants from National Natural Science Foundation of China (81873023 and 81473371).

REFERENCES

- Abbott, N. J., and Friedman, A. (2012). Overview and Introduction: the Blood-Brain Barrier in Health and Disease. *Epilepsia*. 53, 1–6. doi:10.1111/j.1528-1167.2012.03696.x
- Abbott, N. J., Patabendige, A. A. K., Dolman, D. E. M., Yusof, S. R., and Begley, D. J. (2010). Structure and Function of the Blood-Brain Barrier. *Neurobiol. Dis.* 37 (1), 13–25. doi:10.1016/j.nbd.2009.07.030
- Badaut, J., Lasbennes, F., Magistretti, P. J., and Regli, L. (2002). Aquaporins in Brain: Distribution, Physiology, and Pathophysiology. *J. Cereb. Blood Flow Metab.* 22, 367–378. doi:10.1097/00004647-200204000-00001
- Badaut, J., Ashwal, S., Tone, B., Regli, L., Tian, H. R., and Obenaus, A. (2007). Temporal and Regional Evolution of Aquaporin-4 Expression and Magnetic Resonance Imaging in a Rat Pup Model of Neonatal Stroke. *Pediatr. Res.* 62 (3), 248–254. doi:10.1203/PDR.0b013e3180db291b
- Bhatia, S. P., McGinty, D., Letizia, C. S., and Api, A. M. (2008). Fragrance Material Review on L-Borneol. *Food Chem. Toxicol.* 46 (Suppl. 1111), S81–S84. doi:10.1016/j.fct.2008.06.054
- Blatteis, C. M., Li, S., Li, Z., Feleder, C., and Perlik, V. (2005). Cytokines, PGE2 and Endotoxin Fever: a Re-assessment. *Prostaglandins Other Lipid Mediat.* 76 (1), 1–18. doi:10.1016/j.prostaglandins.2005.01.001
- Cai, Z., Hou, S., Li, Y., Zhao, B., Yang, Z., Xu, S., et al. (2008). Effect of Borneol on the Distribution of Gastrodin to the Brain in Mice via Oral Administration. *J. Drug Target.* 16 (2), 178–184. doi:10.1080/10611860701794395
- Campos, F., Pérez-Mato, M., Agulla, J., Blanco, M., Barral, D., Almeida, Á., et al. (2012). Glutamate Excitotoxicity Is the Key Molecular Mechanism Which Is Influenced by Body Temperature during the Acute Phase of Brain Stroke. *Plos One*. 7 (8), e44191. doi:10.1371/journal.pone.0044191
- Campos, F., Sobrino, T., Vieites-Prado, A., Pérez-Mato, M., Rodríguez-Yáñez, M., Blanco, M., et al. (2013). Hyperthermia in Human Ischemic and Hemorrhagic Stroke: Similar Outcome, Different Mechanisms. *PLoS ONE*. 8, e78429. doi:10.1371/journal.pone.0078429
- Causey, M. W., Salgar, S., Singh, N., Martin, M., and Stallings, J. D. (2012). Valproic Acid Reversed Pathologic Endothelial Cell Gene Expression Profile Associated with Ischemia-Reperfusion Injury in a Swine Hemorrhagic Shock Model. *J. Vasc. Surg.* 55 (4), 1096–1103. doi:10.1016/j.jvs.2011.08.060
- Chai, L. J., Xu, Y., Huang, J. Y., Li, R. L., Guo, H., and Wang, S. X. (2019). Xingnaojing Injection Components Promote Glutamate Clearance in Hypoxia/reoxygenation Astrocytes and Improve Cell Viability in Hypoxia Neurons. *Tianjin J. Traditional Chin. Med.* 36 (3), 283–287. doi:10.11656/j.issn.1672-1519.2019.03.19
- Chalela, J. A., Kidwell, C. S., Nentwich, L. M., Luby, M., Butman, J. A., Demchuk, A. M., et al. (2007). Magnetic Resonance Imaging and Computed Tomography in Emergency Assessment of Patients with Suspected Acute Stroke: a Prospective Comparison. *The Lancet* 369 (9558), 293–298. doi:10.1016/S0140-6736(07)60151-2
- Chang, L., Yin, C. Y., Wu, H. Y., Tian, B. B., Zhu, Y., Luo, C. X., et al. (2017). (+)-borneol Is Neuroprotective against Permanent Cerebral Ischemia in Rats by Suppressing Production of Proinflammatory Cytokines. *J. Biomed. Res.* 31 (004), 306–314. doi:10.7555/JBR.31.20160138
- Chen, C., Liu, X., and Smith, B. (2003). Utility of Mdr1-Gene Deficient Mice in Assessing the Impact of P-Glycoprotein on Pharmacokinetics and Pharmacodynamics in Drug Discovery and Development. *Curr Drug Metab.* 4 (4), 272–291. doi:10.2174/1389200033489415
- Chen, J. J., Liu, J. C., Chang, L., Zhu, D. Y., and Li, T. Y. (2013). Neuroprotective Effects of Borneol and its Analogues on Glutamate Acid Induced Neuron Injury. *J. Nanjing Med. Univ. (Natural Sci. Edition)* 33 (5), 630–635. doi:10.7655/NYDXBNS20130513
- Chen, Z. Q., Mou, R. T., Feng, D. X., Wang, Z., and Chen, G. (2017). The Role of Nitric Oxide in Stroke. *Med. Gas Res.* 7 (3), 194–203. doi:10.4103/2045-9912.215750
- Chen, Z. X., Xu, Q. Q., Shan, C. S., Shi, Y. H., Wang, Y., Chang, R. C. C., et al. (2019). Borneol for Regulating the Permeability of the Blood-Brain Barrier in Experimental Ischemic Stroke: Preclinical Evidence and Possible Mechanism. *Oxidative Med. Cell Longevity*. 2019, 1–15. doi:10.1155/2019/2936737
- Cheng, C., Liu, X. W., Du, F. F., Li, M. J., Xu, F., Wang, F. Q., et al. (2013). Sensitive Assay for Measurement of Volatile Borneol, Isoborneol, and the Metabolite Camphor in Rat Pharmacokinetic Study of Borneolum (Bingpian) and Borneolum Syntheticum (Synthetic Bingpian). *Acta Pharmacol. Sin.* 34, 1337–1348. doi:10.1038/aps.2013.86
- Cheng, X. P., Sun, H., and Yu, X. H. (2006). Effect of Borneolum Syntheticum on GABA_A Receptor-Mediated Currents in Rat Hippocampal Neurons. *Pharmacol. Clin. Matetia Medica* 22 (5), 14–16. doi:10.3969/j.issn.1001-859X.2006.05.008
- Chinese Pharmacopoeia Committee (2020). *The Pharmacopoeia of People's Republic of China*. Beijing, China: China Medical Science Press
- Costa, C., Leone, G., Saulle, E., Pisani, F., Bernardi, G., and Calabresi, P. (2004). Coactivation of GABA A and GABA B Receptor Results in Neuroprotection during *In Vitro* Ischemia. *Stroke*. 35 (2), 596–600. doi:10.1161/01.STR.0000113691.32026.06
- De Val, S., and Black, B. L. (2009). Transcriptional Control of Endothelial Cell Development. *Developmental Cell* 16, 180–195. doi:10.1016/j.devcel.2009.01.014
- Denora, N., Trapani, A., Laquintana, V., Lopodota, A., and Trapani, G. (2009). Recent Advances in Medicinal Chemistry and Pharmaceutical Technology-Strategies for Drug Delivery to the Brain. *Curr Top Med Chem.* 9 (2), 182–196. doi:10.2174/156802609787521571
- Dong, T., Chen, N., Ma, X., Wang, J., Wen, J., Xie, Q., et al. (2018). The Protective Roles of L- Borneolum, D- Borneolum and Synthetic Borneol in Cerebral Ischaemia via Modulation of the Neurovascular Unit. *Biomed. Pharmacother.* 102, 874–883. doi:10.1016/j.biopha.2018.03.087
- Duan, S. W., Wang, X., Wang, B., Li, Y. W., and Wang, Y. J. (2012). Effect of Musk, Borneol, Diosgenin and Geniposide on Inflammatory Injury in Cerebral Ischemia and Reperfusion Rats. *Pharmacol. Clin. Chin. Materia Med.* 28 (03), 43–46. doi:10.13412/j.cnki.zyyl.2012.03.038
- Fan, X., Chai, L., Zhang, H., Wang, Y., Zhang, B., and Gao, X. (2015). Borneol Depresses P-Glycoprotein Function by a NF- κ B Signaling Mediated Mechanism in a Blood Brain Barrier *In Vitro* Model. *Int J Mol Sci.* 16 (11), 27576–27588. doi:10.3390/ijms161126051
- Fan, J. J., Li, Y., Fu, X. Y., Li, L. J., Hao, X. T., and Li, S. S. (2017). Nonhuman Primate Models of Focal Cerebral Ischemia. *Neural Regen. Res.* 12 (2), 321–328. doi:10.4103/1673-5374.200815
- Gao, C., Li, X., Li, Y., Wang, L., and Xue, M. (2010). Pharmacokinetic Interaction between Puerarin and Edaravone, and Effect of Borneol on the Brain Distribution Kinetics of Puerarin in Rats. *J. Pharm. Pharm.* 62, 360–367. doi:10.1211/jpp.62.03.0011
- Giannopoulos, S., Kosmidou, M., Hatzitolios, A. I., Savopoulos, C. G., Ziakas, A., and Karamouzis, M. (2008). Measurements of Endothelin-1, C-Reactive Protein and Fibrinogen Plasma Levels in Patients with Acute Ischemic Stroke. *Neurol. Res.* 30 (7), 727–730. doi:10.1179/174313208X297904
- Ginsberg, M. D., and Busto, R. (1998). Combating Hyperthermia in Acute Stroke. *Stroke*. 29 (2), 529–534. doi:10.1161/01.STR.29.2.529
- González-Ibarra, F. P., Varon, J., and López-Meza, E. G. (2011). Therapeutic Hypothermia: Critical Review of the Molecular Mechanisms of Action. *Front. Neur. 2*, 4. doi:10.3389/fneur.2011.00004
- Granger, R. E., Campbell, E. L., and Johnston, G. A. R. (2005). (+)- and (–)-borneol: Efficacious Positive Modulators of GABA Action at Human Recombinant

ACKNOWLEDGMENTS

YL gratefully acknowledges the support provided by all the members of the scientific research team during the preparation of this manuscript. Special thanks to JW and RM.

- $\alpha 1\beta 2\gamma 2L$ GABAA Receptors. *Biochem. Pharmacol.* 69 (7), 1101–1111. doi:10.1016/j.bcp.2005.01.002
- Guo, Y. P. (2000). Pathophysiological Progress of Ischemic Brain Injury and Suggestions for Prevention and Treatment of Cerebral Infarction. *Chin. J. Geriatr. Heart Brain Vessel Dis.* 002 (006), 368–371. doi:10.3969/j.issn.1009-0126.2000.06.002
- Guo, Y., Yan, S., Xu, L., Zhu, G., Yu, X., and Tong, X. (2014). Use of Angong Niu Huang in Treating Central Nervous System Diseases and Related Research. *Evidence-Based Complement. Altern. Med.* 2014, 1–9. doi:10.1155/2014/346918
- He, X. J. (2005). *Study on the Pharmacodynamics of Borneol against Cerebral Ischemia and its Related Mechanism*. Shenyang: Shenyang Pharmaceutical University
- He, X. J., Zhao, L. M., and Liu, Y. L. (2006). The Protective Effect of Borneol on Experimental Cerebral Ischemia. *J. Guangdong Coll. Pharm.* 22 (2), 171–173. doi:10.3969/j.issn.1006-8783.2006.02.025
- He, X. J., Qin, X. H., and Liu, Y. L. (2007). Effect of Borneol Injection on Cerebral Ischemia. *Shanxi Med. J.* 036 (09), 794–795. doi:10.3969/j.issn.0253-9926.2007.17.009
- Hsu, Y.-C., Chang, Y.-C., Lin, Y.-C., Sze, C.-I., Huang, C.-C., and Ho, C.-J. (2014). Cerebral Microvascular Damage Occurs Early after Hypoxia-Ischemia via nNOS Activation in the Neonatal Brain. *J. Cereb. Blood Flow Metab.* 34 (4), 668–676. doi:10.1038/jcbfm.2013.244
- Hu, L. M. (2004). *Influence of Borneol to Drug Permeability of BBB and Neuroprotective Mechanism of Borneol Combined with Salvianolic Acid B and Saponins of Panax Notoginseng*. Tianjin: Tianjin University of Traditional Chinese Medicine
- Hu, H., Lu, H., He, Z., Han, X., and Tu, R. (2012). Gene Interference Regulates Aquaporin-4 Expression in Swollen Tissue of Rats with Cerebral Ischemic Edema: Correlation with Variation in Apparent Diffusion Coefficient. *Neural Regen. Res.* 7 (21), 1659–1666. doi:10.3969/j.issn.1673-5374.2012.21.009
- Hu, L. M., Zhang, Y. J., Wang, W., Wu, Y., Fan, X., Gao, X. M., et al. (2005). Influence of Borneol or Combined with Salvianolic Acid B and Saponins of Panax Notoginseng on the Expression of Vascular Endothelial Growth Factor mRNA in Brain Tissue of Rats with Cerebral Ischemia/reperfusion. *Chin. J. Integrated Traditional West. Med. Intensive Crit. Care* 12 (05), 263–266. doi:10.3321/j.issn:1008-9691.2005.05.002
- Huang, L., Li, Q., Wen, R., Yu, Z., Li, N., Ma, L., et al. (2017). Rho-kinase Inhibitor Prevents Acute Injury against Transient Focal Cerebral Ischemia by Enhancing the Expression and Function of Gaba Receptors in Rats. *Eur. J. Pharmacol.* 797, 134–142. doi:10.1016/j.ejphar.2017.01.021
- Huang, J. Y., Wang, Z. X., Wang, S. X., Guo, H., Chai, L. J., and Hu, L. M. (2020). Protection of Active Pharmaceutical Ingredients in the Xingnaojing Injection against Oxygen Glucose Deprivation/re-Oxygenation-Induced PC12 Cells Injury. *Chin. J. Clin. Pharmacol.*
- Huang, L. (2018). *The Same Effect of Beta-Asarone, Borneol, Muscone and Styrax Naphtha about in Inducing Resuscitation and Protecting the Brain*. Guangzhou: Guangzhou University of Chinese Medicine
- Huang, N., and Zhao, J. (2017). *Pathophysiology*. second Edition. Bei Jing: Bei Jing Science Press
- Huang, P., Jiang, X. F., Zou, J. L., Yuan, Y. M., Yao, M. C., and Lu, Y. S. (2009). A Novel GC-MS Bioanalytical Method for Natural Borneol and its Application in Investigating Natural Borneol Distribution in Mice Mode. *Tradit. Chin. Med. Mater. Med.* 11, 821–827. doi:10.3969/j.issn.1674-3849.2009.06.012
- Hur, J., Pak, S. C., Koo, B.-S., and Jeon, S. (2013). Borneol Alleviates Oxidative Stress via Upregulation of Nrf2 and Bcl-2 in Sh-Sy5y Cells. *Pharm. Biol.* 51 (1), 30–35. doi:10.3109/13880209.2012.700718
- Islam, B. M. N., Uddin, C. J., and Jaripa, B. (2010). Chemical Components in Volatile Oil from Blumea Balsamifera (L.) Dc. *Bangladesh J. Bot.* 38 (1), 107–109. doi:10.3329/bjb.v38i1.5132
- Ito, Y., Ohkubo, T., Asano, Y., Hattori, K., Shimazu, T., Yamazato, M., et al. (2010). Nitric Oxide Production during Cerebral Ischemia and Reperfusion in eNOS- and nNOS-Knockout Mice. *Curr. Neurovasc. Res.* 7 (1), 23–31. doi:10.2174/156720210790820190
- Jia, Y. L. (2014). *Effects of Borneol on Rat's Blood Brain Barrier and Zonula Occludens-1 after Global Cerebra Ischemia-Reperfusion Injury*. Xinxiang: Xinxiang Medical University
- Jiang, X. F., Zou, J. L., Yuan, Y. M., Francis, C. P. Law., Qiao, Y. J., and Yao, M. C. (2008). Preliminary Study: Biotransformation of Borneol to Camphor in Mice, Rats, and Rabbits. *World Sci. Technology.* 10 (3), 27–36. doi:10.1016/S1876-3553(09)60013-2
- Kawabori, M., and Yenari, M. (2015). Inflammatory Responses in Brain Ischemia. *Curr. Med. Chem.* 22 (10), 1258–1277. doi:10.2174/0929867322666150209154036
- Ke, Y. Q., Xu, R. X., and Chen, C. C. (2000). Effect of 5-Hydroxytryptamine Level Changes on Permeability of Blood-Brain Barrier Following Brain Injury. *Chin. J. Clin. Neurosurg.* 5 (z1), 40–42. doi:10.3969/j.issn.1009-153X.2000.z1.015
- Kong, Q., Wu, Z., Chu, X., Liang, R., Xia, M., and Li, L. (2013). Study on the Anti-cerebral Ischemia Effect of Borneol and its Mechanism. *Afr. J. Trad. Compl. Alt. Med.* 11 (1), 161–4. doi:10.4314/ajtcam.v11i1.25
- Lai, T. W., Zhang, S., and Wang, Y. T. (2014). Excitotoxicity and Stroke: Identifying Novel Targets for Neuroprotection. *Prog. Neurobiol.* 115, 157–188. doi:10.1016/j.pneurobio.2013.11.006
- Li, J. M., Hu, S. X., and Li, H. Q. (2013). The Commodity Types and Historical Origins of Traditional Chinese Medicine Borneol. *Modern Chinese Medicine.* doi:10.3969/j.issn.1673-4890.2013.06.023
- Li, Y. J. (2016). *The Molecular Mechanisms of Left-Handed Camphor Prevents Autophagy by Targeting miR-140 in PC12 Cells*. Guangzhou: Guangzhou University of Chinese Medicine
- Li, Y. (2018). *Mechanism Study of Natural Borneol in Treatment of Ischemic Stroke*. Tai'an: Taishan Medical University. doi:10.27353/d.cnki.gtsyc.2018.000151
- Li, Y. H., Sun, X. P., Zhang, Y. Q., and Wang, N. S. (2008). The Antithrombotic Effect of Borneol Related to its Anticoagulant Property. *Am. J. Chin. Med.* 36 (04), 719–727. doi:10.1142/S0192415X08006181
- Li, X., Wan, X., Gao, J. J., Zhao, C. S., Liu, X. F., Yang, L. J., et al. (2017). *Effects of Huazhuo Jiedu Huoxue Tongluo Prescription on Expression of Tight Junction ZO-1 and Occludin in Rats with Cerebral Ischemia Reperfusion Injury*. Global Traditional Chinese Medicine. doi:CNKI:SUN:HQZY.0.2017-07-005
- Liang, Z. W., Dong, Q. F., Wang, M. M., Gao, K., Li, J. K., and Yang, L. (2016). Protective Effects of Borneol “Meridian Guiding” Salvia Miltiorrhiza in Treatment of Cerebral Ischemia/Reperfusion. *Prog. Mod. Biomed.* 16 (13), 2430–2433. doi:10.13241/j.cnki.pmb.2016.13.007
- Liao, S., Han, L., Zheng, X., Wang, X., Zhang, P., Wu, J., et al. (2019). Tanshinol Borneol Ester, a Novel Synthetic Small Molecule Angiogenesis Stimulator Inspired by Botanical Formulations for Angina Pectoris. *Br. J. Pharmacol.* doi:10.1111/bph.14714
- Liu, H. T., and Mu, D. Z. (2014). [Inducible Nitric Oxide Synthase and Brain Hypoxic-Ischemic Brain Damage]. *Zhongguo Dang Dai Er Ke Za Zhi.* 16 (9), 962–967. Chinese. doi:10.7499/j.issn.1008-8830.2014.09.022
- Liu, Y. Q. (2017). *L-camphor Target MicroRNA-125-3p on the Mechanism of Cerebral Ischemia Reperfusion Injury*. Guangzhou University of Traditional Chinese Medicine
- Liu, Y. M., Zhang, C. A., Xu, Q. Y., and Peng, S. Q. (2002a). Effect of Moschus and Borneol on the Content of Aminoacid Neurotransmitter in Brain Tissue of Rats with Cerebral Ischemia and Reperfusion Injury. *Traditional Chin. Drug Res. Clin. Pharmacol.* (04), 231–233. doi:10.3321/j.issn:1003-9783.2002.04.013
- Liu, Y. M., Zhang, Z. A., Xu, Q. Y., Zeng, Z. L., and Peng, S. Q. (2002b). The Influence on the Brain Edema, SOD and MDA of Ischemia Reperfusion Rat by Using Inducing Resuscitation Method. *Chin. J. Inf. Traditional Chin. Med.* 009 (7), 22–24. doi:10.3969/j.issn.1005-5304.2002.07.010
- Liu, Y. M., Zhao, G. F., Xia, X. H., Xu, Q. Y., and Shen, Q. (2009). Influence of Muskiness Compounded with Borneol on Blood Brain Barrier after Ischemic Reperfusion Injury. *Beijing J. Traditional Chin. Med.* 28 (06), 459–462. doi:CNKI:SUN:BJZO.0.2009-06-025
- Liu, R., Zhang, L., Lan, X., Li, L., Zhang, T.-T., Sun, J.-H., et al. (2011). Protection by Borneol on Cortical Neurons against Oxygen-Glucose Deprivation/reperfusion: Involvement of Anti-oxidation and Anti-inflammation through Nuclear Transcription Factor kappaB Signaling Pathway. *Neuroscience.* 176, 408–419. doi:10.1016/j.neuroscience.2010.11.029
- Liu, Y. M., Xia, X. H., Zhao, G. F., Peng, S. Q., Xu, Q. Y., and Shen, Q. (2007). Effect of Moschus Combined with Borneol on Brain Water Content and Blood-Brain Barrier Permeability in Rat Model of Cerebral Focal Ischemia with Reperfusion. *J. Guangzhou Univ. Traditional Chin. Med.* 24 (6), 498–501. doi:10.3969/j.issn.1007-3213.2007.06.016
- Liu, L., Wei, H., and Xu, Li. (2018). Effects of Different Doses of Musk and Borneol on the Neurological Deficit Score, activities of COX-2 and 5-LOX in Brain and

- CysLT2 Expression in the hippocampus of Cerebral IR Model. *J. Clin. Exp. Med.* 17 (12), 1241–1244. doi:10.3969/j.issn.1671-4695.2018.12.003
- Lu, Y., Du, S.-y., Chen, X.-l., Wu, Q., Song, X., Xu, B., et al. (2011). Enhancing Effect of Natural Borneol on the Absorption of Geniposide in Rat via Intranasal Administration. *J. Zhejiang Univ. Sci. B.* 12 (2), 143–148. doi:10.1631/jzus. B1000121
- Luo, S. L., Wang, J., Wen, J., Cao, C., and Xie, Q. (2016). Monitoring the Impact of Three Borneol Temperature Fever Rats Dynamic Concept Based on TCM. *Lishizhen Med. Materia Med. Res.* 27 (3), 521–523. doi:10.3969/j.issn.1008-0805.2016.03.004
- Lv, X. X., Sun, M. J., and Sun, F. Z. (2012). [Research of Borneol Promote Drugs through Blood-Brain Barrier]. *Zhongguo Zhong Yao Za Zhi.* 37 (7), 878–881. doi:10.4268/cjcm20120702
- Ma, R., Xie, Q., Li, H., Guo, X., Wang, J., Li, Y., et al. (2021). I-Borneol Exerted the Neuroprotective Effect by Promoting Angiogenesis Coupled with Neurogenesis via Ang1-VEGF-BDNF Pathway. *Front. Pharmacol.* 12. doi:10.3389/fphar. 2021.641894
- Ma, R., Xie, Q., Li, Y., Chen, Z., Ren, M., Chen, H., et al. (2020). Animal Models of Cerebral Ischemia: a Review. *Biomed. Pharmacother.* 131, 110686. doi:10.1016/j.biopha.2020.110686
- Mcbride, D. W., and Zhang, J. H. (2017). Precision Stroke Animal Models: the Permanent MCAO Model Should Be the Primary Model, Not Transient MCAO. *Transl. Stroke Res.* 8 (5), 397–404. doi:10.1007/s12975-017-0554-2
- Mele, M., Ribeiro, L., Inácio, A. R., Wieloch, T., and Duarte, C. B. (2014). GABAA Receptor Dephosphorylation Followed by Internalization Is Coupled to Neuronal Death in Vitro Ischemia. *Neurobiol. Dis.* 65, 220–232. doi:10.1016/j.nbd.2014.01.019
- Mendes, R. T., Nguyen, D., Stephens, D., Pamuk, F., Fernandes, D., Hasturk, H., et al. (2018). Hypoxia-induced Endothelial Cell Responses - Possible Roles during Periodontal Disease. *Clin. Exp. Dent Res.* 4, 241–248. doi:10.1002/cre2.135
- Michael, S., Ignaz, G., Christoph, K., and Peter, K. (2016). Immunohistochemical Analysis of Cerebral Thrombi Retrieved by Mechanical Thrombectomy from Patients with Acute Ischemic Stroke. *Int. J. Mol. Sci.* 17 (3), 298. doi:10.3390/ijms17030298
- Ni, C. X. (2011). *The Effects of Aromatic Resuscitation Drugs on Anti-brain Ischemia and the Function of Blood-Brain Barrier*. Chengdu: Chengdu University of traditional Chinese Medicine
- Pan, X. U., Ying, L. I., Shou-Ying, D. U., Yang, L. U., Bai, J., and Guo, Q. L. (2014). Comparative Pharmacokinetics of Borneol in Cerebral Ischemia-Reperfusion and Sham-Operated Rats. *J. Zhejiang University B.* 15 (1), 84–91. doi:10.1631/jzus.B1300141
- Rama, R., and Garcia, J. C. (2016). *Excitotoxicity and Oxidative Stress in Acute Stroke. Excitotoxicity and Oxidative Stress in Acute Stroke. Acute Ischemic Stroke*. InTech
- Ren, Z. X. (2018). *miR-140-HnnpAl Inhibits Stress Granule Formation and L-Camphor Intervention*. Guangzhou: Guangzhou University of Chinese Medicine
- Santos, S. E., Ribeiro, F. P. R. A., Menezes, P. M. N., Duarte Filho, L. A. M., Quintans, J. S. S., Quintans Junior, L. J., et al. (2018). New Insights on Relaxant Effects of (-)-borneol Monoterpene in Rat Aortic Rings. *Fundam. Clin. Pharmacol.* 33. doi:10.1111/fcp.12417
- Shang, K., Sui, D. J., Liu, Q. M., Wang, D. Y., Zhang, X., and Qiu, Z. D. (2015). Effects of Pair Herbs “Yanhusuo-bingpian” on Cerebral Blood Flow Dynamics in Anesthetized Dogs. *Chin. J. Vet. Sci.* (06), 153–156. doi:CNKI:SUN: ZSYX.0.2015-06-030
- Shao, X. R., Cai, K. R., Jia, R., Zhao, H., Li, L., Zhou, X., et al. (2018). Effects of Borneol on Inflammatory Reaction and Permeability of Blood-Brain Barrier in Rats with Cerebral Ischemic Injury. *Chin. J. Clin. Pharmacol.* 34 (13), 1558–1560. doi:10.13699/j.cnki.1001-6821.2018.13.020
- Shi, Y. M. (2014). Research Progress of Calcium Channels in the Neuron after Cerebral Ischemia/Reperfusion Injury. *Med. Recapitulate* 20 (14), 2507–2509. doi:10.3969/j.issn.1006-2084.2014.14.005
- Shimotoke, J., Derugin, N., Wendland, M., Vexler, Z. S., and Ferriero, D. M. (2010). Vascular Endothelial Growth Factor Receptor-2 Inhibition Promotes Cell Death and Limits Endothelial Cell Proliferation in a Neonatal Rodent Model of Stroke. *Stroke.* 41, 343–349. doi:10.1161/STROKEAHA.109.564229
- Sims, N. R., and Yew, W. P. (2017). Reactive Astrogliosis in Stroke: Contributions of Astrocytes to Recovery of Neurological Function. *Neurochem. Int.* 107, 88–103. doi:10.1016/j.neuint.2016.12.016
- Singh, D. P., and Chopra, K. (2014). Flavocoxid, Dual Inhibitor of Cyclooxygenase-2 and 5-lipoxygenase, Exhibits Neuroprotection in Rat Model of Ischaemic Stroke. *Pharmacol. Biochem. Behav.* 120, 33–42. doi:10.1016/j.pbb.2014.02.006
- Singh, V., Mishra, V. N., Chaurasia, R. N., Joshi, D., and Pandey, V. (2019). Modes of Calcium Regulation in Ischemic Neuron. *Ind. J. Clin. Biochem.* 34 (2), 246–253. doi:10.1007/s12291-019-00838-9
- Steliga, A., Kowiański, P., Czuba, E., Waśkow, M., Moryś, J., and Lietzau, G. (2020). Neurovascular Unit as a Source of Ischemic Stroke Biomarkers-Limitations of Experimental Studies and Perspectives for Clinical Application. *Transl. Stroke Res.* 11, 553–579. doi:10.1007/s12975-019-00744-5
- Sun, B. Z., Chen, L., Wu, Q., Wang, H. L., Wei, X. B., Xiang, Y. X., et al. (2014). Suppression of Inflammatory Response by Flurbiprofen Following Focal Cerebral Ischemia Involves the NF-Kb Signaling Pathway. *Int. J. Clin. Exp. Med.* 7 (9), 3087–3095.
- Sun, S. P., Du, Y. Y., Suo, X. G., Wang, Y., Zhang, J. H., Wu, C. G., et al. (2019). Effect of Borneol on Lipopolysaccharide-Induced RAW264.7 Macrophage Inflammation Model. *J. Tonghua Normal Univ.* 40 (4)
- Tang, Y. X. (2010). *The Experimental Study on the Anti-Acute Brain Ischemia Effect of Four Aromatic Resuscitation Drugs and the Initial Exploring The Drug Property*. Chengdu: Chengdu University of traditional Chinese Medicine
- Tian, H. (2013). *Comparative Research on Mechanism of Neuroprotective Effect and Influence of Blood-Brain Barrier between L-Borneolum and Borneolum Syntheticum*. Chengdu: Chengdu University of Traditional Chinese Medicine
- Tu, X.-k., Yang, W.-z., Shi, S.-s., Wang, C.-h., Zhang, G.-l., Ni, T.-r., et al. (2010). Spatio-Temporal Distribution of Inflammatory Reaction and Expression of TLR2/4 Signaling Pathway in Rat Brain Following Permanent Focal Cerebral Ischemia. *Neurochem. Res.* 35 (8), 1147–1155. doi:10.1007/s11064-010-0167-6
- Ueno, M. (2009). Mechanisms of the Penetration of Blood-Borne Substances into the Brain. *Curr. Neuropharmacol.* 7 (2), 142–149. doi:10.2174/157015909788848901
- Ueno, M., Nakagawa, T., Wu, B., Onodera, M., Huang, C.-l., Kusaka, T., et al. (2010). Transporters in the Brain Endothelial Barrier. *Curr. Med. Chem.* 17, 1125–1138. doi:10.2174/092986710790827816
- Vannucci, R. C., Brucklacher, R. M., and Vannucci, S. J. (2001). Intracellular Calcium Accumulation during the Evolution of Hypoxic-Ischemic Brain Damage in the Immature Rat. *Developmental Brain Res.* 126 (1), 117–20. doi:10.1016/s0165-3806(00)00135-8
- Wang, Y. (2011). *The Effect of Musk, Borneol and Compatibility of Them Onn the Animal Models of Cerebral Ischemia*. Chengdu: Chengdu University of Traditional Chinese Medicine
- Wang, L. Y., Liu, J., Li, Y., Li, B., Zhang, Y. Y., Jing, Z. W., et al. (2015a). Time-dependent Variation of Pathways and Networks in a 24-hour Window after Cerebral Ischemia-Reperfusion Injury. *BMC Syst. Biol.* 9 (1), 11. doi:10.1186/s12918-015-0152-4
- Wang, N., Ma, H. P., Qi, X. Z., Meng, P., and Jia, Z. P. (2015b). Progression of Nrf2-ARE Signaling Pathway in Protection of Oxidative Stress Injury of the Body. *Med. Pharm. J. Chin. People's Liberation Army* 27 (12), 21–27. doi:10.3969/j.issn.2095-140X.2015.12.005
- Wang, Z.-P., Tian, Y., and Lin, J. (2017b). Role of Wild-type P53-Induced Phosphatase 1 in Cancer. *Oncol. Lett.* 14, 3893–3898. doi:10.3892/ol.2017.6685
- Wang, J., Qu, X. L., Fan, C. D., and Gao, H. L. (2018). Study on Action Mechanism of Borneol Combined with Safflower on Cerebral Ischemia Injury in Rats. *Chin. J. Hosp. Pharm.* 038 (023), 2410–2415. doi:10.13286/j.cnki.chinhosppharmacj. 2018.23.06
- Wang, L., Liang, Q., Lin, A., Wu, Y., Min, H., Song, S., et al. (2019). Borneol Alleviates Brain Injury in Sepsis Mice by Blocking Neuronal Effect of Endotoxin. *Life Sci.* 232, 116647. doi:10.1016/j.lfs.2019.116647
- Wang, J., and Wang, S. Y. (2018). *Chinese Herbal Medicine*. Beijing: China Medical Science Press
- Wen, J. (2017). *Research on Protection Mechanism of Aromatic Resuscitation Drug against Neurovascular Unit in Permanent Cerebral Ischemia Model Rats*. Chengdu: Chengdu University of traditional Chinese Medicine

- Wen, J., Wang, J., Luo, S. L., Peng, W., and Ren, Y. M. (2016). Advances in Studies on Regulating Effects of Wnt/ β -Catenin Signaling Pathway on Neurovascular Unit after Cerebral Ischemia and Related Medicine. *Chin. Pharmacol. Bull.* 32 (03), 310–314. doi:10.3969/j.issn.1001-1978.2016.03.003
- Wermuth, C. G. (2015). *Chapter 18 - Optical Isomerism in Drugs. The Practice of Medicinal Chemistry (Fourth Edition)*. Salt Lake: Academic Press, 429–447.
- Wöckel, L., Koch, S., Stadler, C., Meyer-Keitel, A.-E., and Schmidt, M. (2008/2008). Serotonin-induced Platelet Intracellular Ca^{2+} Response in Patients with Anorexia Nervosa. *Pharmacopsychiatry* 41 (1), 10–16. doi:10.1055/s-2007-992145
- Wrotek, S. E., Kozak, W. E., Hess, D. C., and Fagan, S. C. (2011). Treatment of Fever after Stroke: Conflicting Evidence. *Pharmacotherapy* 31 (11), 1085–1091. doi:10.1592/phco.31.11.1085
- Wu, C., Liao, Q., Yao, M., Xu, X., Zhou, Y., Hou, X., et al. (2014a). Effect of Natural Borneol on the Pharmacokinetics and Distribution of Nimodipine in Mice. *Eur. J. Drug Metab. Pharmacokinet.* 39, 17–24. doi:10.1007/s13318-013-0135-z
- Wu, H.-Y., Tang, Y., Gao, L.-Y., Sun, W.-X., Hua, Y., Yang, S.-B., et al. (2014b). The Synergetic Effect of Edaravone and Borneol in the Rat Model of Ischemic Stroke. *Eur. J. Pharmacol.* 740, 522–531. doi:10.1016/j.ejphar.2014.06.035
- Wu, J. J., Wang, H. J., Yang, S., Liu, Y., and Xu, X. Y. (2016). [Borneol Promotes Catalpol and Puerarin Crossing through Blood-Brain Barrier in Focal Cerebral Ischemic Rats]. *Zhongguo Zhong Yao Za Zhi* 41 (21), 3988–3995. doi:10.4268/cjcm20162117
- Xiao, Y. Y., Ping, Q. N., and Chen, Z. P. (2007). The Enhancing Effect of Synthetical Borneol on the Absorption of Tetramethylpyrazine Phosphate in Mouse. *Int. J. Pharm.* 337 (1–2), 74–79. doi:10.1016/j.ijpharm.2006.12.034
- Xing, H. Y., Sun, S. G., Mei, Y. W., Shi, J., and Dirk, M. H. (2007). Inhibition of P-Glycoprotein Potentiates Neuroprotection of FK506 on Ischemic Brain Injury. *CHINESE JOURNAL NEUROLOGY* 40 (2), 112–115. doi:10.3760/j.issn:1006-7876.2007.02.011
- Xu, J., Li, C., Yin, X.-H., and Zhang, G.-Y. (2008). Additive Neuroprotection of Gaba A and Gaba B Receptor Agonists in Cerebral Ischemic Injury via Pi-3k/akt Pathway Inhibiting the Ask1-Jnk Cascade. *Neuropharmacology* 54 (7), 1029–1040. doi:10.1016/j.neuropharm.2008.01.014
- Xu, L., and Zhang, T. J. (2016). Effects of Borneolum Synthetium Combined with Brevescapine on Blood-Brain Barrier Permeability Induced by Hypoxia/Reoxygenation Injury. *Chin. J. Inf. Traditional Chin. Med.* 23 (02), 76–78. doi:10.3969/j.issn.1005-5304.2016.02.021
- Xu, L., and Zhang, T. J. (2015). Effects of Borneol Combined with Brevescapine on Blood-Brain Barrier Permeability after Ischemia Reperfusion Injury in Rats. *Pharmacol. Clin. Chin. Materia Med.* 31 (1), 74–76. doi:CNKI:SUN:ZYLL.0.2015-01-025
- Xu, Y. B., Mao, X. N., Xu, G. C., Tao, L. D., Zhang, J., and Zhang, P. J. (2016). The Role of Apoptosis Proteins Bcl-2, Bax in Hepatic Ischemia-Reperfusion Injury Model. *Chin. J. Clinicians (Electronic Edition)* 010 (13), 1968–1971. doi:10.3877/cma.j.issn.1674-0785.2016.13.026
- Yan, L., Hu, J. P., Shao, X. R., Sun, X. D., and C, K. R. (2018). Effects of Icaritin Combined with Borneol on Antioxidant Activity Inflammatory Reaction and Permeability of Blood-Brain Barrier in Rats Following Cerebral Ischemic Injury. *Shaanxi J. Tradit. Chin. Med.* 39 (12), 5–8. doi:CNKI:SUN: SXZY.0.2018-12-001
- Yang, L., Li, W. R., Kui, S. Q., and Wang, N. S. (2010). Inhibitory Effects and Mechanism of Borneol on Arterial Thrombosis Induced by FeCl_3 in Rat. *Chin. J. Exp. Traditional Med. Formulae* 16 (006), 164–166. doi:10.3969/j.issn.1005-9903.2010.06.052
- Yang, X. Q., Ding, H., Liu, X. D., Tang, S., Yang, R. Y., Deng, C. Q., et al. (2019). Study on Borneol Combined with Astragaloside IV and Panax Notoginseng Saponins Promoting Nerve Repair after Cerebral Ischemia-Reperfusion. *China J. Traditional Chin. Med. Pharm.*
- Yang, Z., Guo, P., Han, R., Wu, S., and Gao, J.-M. (2018). Gram-scale Separation of Borneol and Camphor from *Cinnamomum Camphora* (L.) Presl by Continuous Counter-current Chromatography. *Sep. Sci. Plus* 1, 144–153. doi:10.1002/sscp.201700041
- Yao, H. W., Wang, J., Liu, Y., and Wang, D. D. (2011). Effect of Moschus and Borneol Camphor in Different Proportion on Bloodbrain Barrier Permeability of Acute Cerebral Ischemic Model Mice. *J. Chengdu Univ. Traditional Chin. Med.*
- Yoo, K.-Y., Hwang, I. K., Lee, C. H., Choi, J. H., Kwon, S.-H., Kang, I.-J., et al. (2010). Difference of Fibroblast Growth Factor Receptor 1 Expression Among CA1-3 Regions of the Gerbil hippocampus after Transient Cerebral Ischemia. *J. Neurol. Sci.* 296, 13–21. doi:10.1016/j.jns.2010.06.018
- Yu, B., Lu, G. H., Sun, Y., Lin, X., and Fang, T. H. (2011). Effect of Electroacupuncture Combined with Intragastric Administration of Borneol on the Permeability of Blood-Brain Barrier in the Mouse. *Acupuncture Res.* 36 (05), 335–340.
- Yu, B., Ruan, M., Cui, X. B., Guo, J. M., Xu, L., and Dong, X. P. (2013). Effects of Borneol on the Pharmacokinetics of Geniposide in Cortex, hippocampus, Hypothalamus and Striatum of Conscious Rat by Simultaneous Brain Microdialysis Coupled with UPLC-MS. *J. Pharm. Biomed. Anal.* 77, 128–132. doi:10.1016/j.jpba.2013.01.017
- Yu, B., Ruan, M., Zhang, Z. N., Cheng, H. B., and Shen, X. C. (2016). Synergic Effect of Borneol and Ligustrazine on the Neuroprotection in Global Cerebral Ischemia/reperfusion Injury: a Region-Specificity Study. *Evid Based. Complement. Altern. Med.* 2016, 1–8. doi:10.1155/2016/4072809
- Yu, B., Liang, T., Huang, S. W., and Li, Y. (2017a). The Anti-ischemia Effect of Different Dose of Borneol Combining with Chuanxiong Rhizoma on the Global Cerebral Ischemia Rats in Different Brain Regions. *Chin. J. Gerontol.* 37 (10), 2352–2355. doi:10.3969/j.issn.1005-9202.2017.10.005
- Yu, B., Ruan, M., Liang, T., Huang, S. W., Yu, Y., Cheng, H. B., et al. (2017b). The Synergic Effect of Tetramethylpyrazine Phosphate and Borneol for Protecting against Ischemia Injury in Cortex and hippocampus Regions by Modulating Apoptosis and Autophagy. *J. Mol. Neurosci.* 63 (1), 70–83. doi:10.1007/s12031-017-0958-1
- Yu, B., Shen, X. C., Liang, T., Huang, S. W., Yang, L., Cheng, H. B., et al. (2017c). Research on the Synergy of Different Doses of Borneol and Chuanxiong Rhizoma on the Anti-ischemia Effect in Different Brain Regions. *Chin. J. Hosp. Pharm.* 37 (18), 1792–1796. doi:10.13286/j.cnki.chinhosppharmacy.2017.18.05
- Yu, B., Ruan, M., Xu, L., Liu, S. J., Xu, H. Q., and Sheng, X. C. (2019a). Synergic Effect of Chuanxiong Rhizoma and Borneol on Protecting hippocampus and Hypothalamus of Rats from Global Cerebral Ischemia Reperfusion Injury. *Chin. Pharmacol. Bull.* 35 (9), 1302–1307. doi:10.3969/j.issn.1001-1978.2019.09.022
- Yu, B., Zhong, F. M., Yao, Y., Deng, S. Q., Xu, H. Q., Lu, J. F., et al. (2019b). Synergistic Protection of Tetramethylpyrazine Phosphate and Borneol on Brain Microvascular Endothelium Cells Injured by Hypoxia. *Am. J. Transl Res.* 11 (4), 2168–2180.
- Yu, B., Ruan, M., Liang, T., and Yu, Y. (2020). Synergy between Borneol and Extract of Ligusticum Chuanxiong Hort against Cortex and Striatum Ischemia. *Int. J. Pharmacol.* 16, 104–119. doi:10.3923/ijp.2020.104.119
- Yuan, Z., Zhang, J. P., Liu, Y. F., and Zhang, B. L. (2006). Study on the Relationship between P-Glycoprotein and Borneol Promoting the Physiological Opening of Blood-Brain Barrier. *Tianjin J. Traditional Chin. Med.* 023 (03), 261–262. doi:10.3969/j.issn.1672-1519.2006.03.041
- Zhang, C. A., Liu, Y. M., Xu, Q. Y., and Peng, S. Q. (2002). Effect of Aromatic Herbs for Resuscitation on NO Content and Expression of NOS in Brain Tissue of Rats with Cerebral Schemia and Reperfusion Injury. *J. Guangzhou Univ. Traditional Chin. Med.* 19 (02), 115–118. doi:10.3969/j.issn.1007-3213.2002.02.011
- Zhang, X. Y. (2013). *Cysteinyl Leukotriene CysLT2 Receptor Mediates Neuronal Injury Damage through Activation Microglia*. Hangzhou: Zhejiang University
- Zhang, Q., Wu, D., Wu, J., Ou, Y., Mu, C., Han, B., et al. (2015). Improved Blood-Brain Barrier Distribution: Effect of Borneol on the Brain Pharmacokinetics of Kaempferol in Rats by In Vivo Microdialysis Sampling. *J. Ethnopharmacology* 162, 270–277. doi:10.1016/j.jep.2015.01.003
- Zhang, Q.-L., Fu, B. M., and Zhang, Z.-J. (2017a). Borneol, a Novel Agent that Improves Central Nervous System Drug Delivery by Enhancing Blood-Brain Barrier Permeability. *Drug Deliv.* 24 (1), 1037–1044. doi:10.1080/10717544.2017.1346002
- Zhang, X.-G., Shan, C., Zhu, J.-Z., Bao, X.-Y., Tong, Q., Wu, X.-F., et al. (2017b). Additive Neuroprotective Effect of Borneol with Mesenchymal Stem Cells on Ischemic Stroke in Mice. *Front. Physiol.* 8, 1133. doi:10.3389/fphys.2017.01133
- Zhang, Y.-M., Qu, X.-Y., Tao, L.-N., Zhai, J.-H., Gao, H., Song, Y.-Q., et al. (2019). XingNaofeng Injection Ameliorates Cerebral Ischemia/reperfusion Injury via SIRT1-Mediated Inflammatory Response Inhibition. *Pharm. Biol.* 58 (9), 16–24. doi:10.1080/13880209.2019.1698619

- Zhao, B. S., Xu, Q., Mi, S. Q., and Wang, N. S. (2001). The Relationship between eNOS and the Function of Borneol in Stimulating the BBB's Opening. *J. Brain Nervous Dis.* 9 (4), 207–209. doi:10.3969/j.issn.1006-351X.2001.04.006
- Zhao, J.-y., Lu, Y., Du, S.-y., Song, X., Bai, J., and Wang, Y. (2012). Comparative Pharmacokinetic Studies of Borneol in Mouse Plasma and Brain by Different Administrations. *J. Zhejiang Univ. Sci. B* 13, 990–996. doi:10.1631/jzus.B1200142
- Zhong, M., Chen, H., Jiang, Y., Tu, P. F., Liu, C. L., Zhang, W. X., et al. (2012). Effect of Echinacoside on Striatal Extracellular Level of Amino Acids Neurotransmitter in Cerebral Ischemia Rats. *Chin. Pharmacol. Bull.* (3), 361–365. doi:10.3969/j.issn.1001-1978.2012.03.015
- Zhou, L., and Zhu, D.-Y. (2009). Neuronal Nitric Oxide Synthase: Structure, Subcellular Localization, Regulation, and Clinical Implications. *Nitric Oxide* 20, 223–230. doi:10.1016/j.niox.2009.03.001
- Zou, L., Zhang, Y., Li, W., Zhang, J., Wang, D., Fu, J., et al. (2017). Comparison of Chemical Profiles, Anti-inflammatory Activity, and UPLC-Q-TOF/MS-Based Metabolomics in Endotoxic Fever Rats between Synthetic Borneol and Natural Borneol. *Molecules*. 22 (9), 1446. doi:10.3390/molecules22091446
- Conflict of Interest:** The authors declare that the research was conducted in the absence of any commercial or financial relationships that could be construed as a potential conflict of interest.

Copyright © 2021 Li, Ren, Wang, Ma, Chen, Xie, Li, Li and Wang. This is an open-access article distributed under the terms of the Creative Commons Attribution License (CC BY). The use, distribution or reproduction in other forums is permitted, provided the original author(s) and the copyright owner(s) are credited and that the original publication in this journal is cited, in accordance with accepted academic practice. No use, distribution or reproduction is permitted which does not comply with these terms.

GLOSSARY

5-HT	5-hydroxytryptamine	LFA-1	lymphocyte function-associated antigen-1
5-LOX	5-lipoxygenase	MDA	malondialdehyde
APC	adenomatous polyposis coli	MMP 2	matrix metalloproteinase 2
BBB	blood-brain barrier	MMP 9	matrix metalloproteinase 9
BDNF	brain-derived neurotrophic factor	MPO	Myeloperoxidase
bFGF/FGF2	fibroblast growth factor 2	mTOR	mammalian Target of rapamycin
BMEC	brain micro-vascular endothelial cell	NF-κB	nuclear factor- κ B
Cadm2	cell adhesion molecule 2	NGF	nerve growth factor
CAT	Catalase	NMDA-R	N-methyl-d-aspartate glutamate receptor
CGRP	calcitonin gene-related peptide	nNOS	neuronal nitric oxide synthase
CIR	cerebral ischemia reperfusion	NO	nitric oxide
CNS	central nervous system	NOS	nitric oxide synthase
COX-2	cyclooxygenase-2	O²⁻	superoxide anion
CysLT-2	cysteinyl leukotriene receptor-2	OGD/R	Oxygen-Glucose Deprivation/Reperfusion
Dsh	disheveled	OH⁻	hydroxyl radical
EB	evans blue	p53	tumor protein 53
eNOS	endothelial nitric oxide synthase	p62	sequestosome-1
ET-1	endothelin-1	pBCO	permanent bilateral carotid occlusion
GABA	gamma-aminobutyric acid	pCIR	permanent cerebral ischemia reperfusion
GDNF	glial cell-derived neurotrophic factor	P-gp	P-glycoprotein
Glu	glutamic acid	ROS	reactive oxygen species
GSH-Px	glutathione peroxidase	SOD	superoxide dismutase
GSK-3β	glycogen synthase kinase-3 beta	tBCO	transient bilateral carotid occlusion
H₂O₂	Hydrogen peroxide	TCM	traditional Chinese Medicine
HnnpA1	heterogeneous Nuclear Ribonucleoprotein A1	TTC	2,3,5-Triphenyltetrazolium chloride
ICAM-1	intercellular adhesion molecule-1	tGCIR	transient Global cerebral ischemia reperfusion
IL-10	interleukin-10	TIMP-1	tissue inhibitor of metalloproteinase-1
IL-1β	interleukin-1 β	tMCAO	transient middle cerebral artery occlusion
IL-6	interleukin-6	TNF-α	necrosis factor- α
iNOS	inducible nitric oxide synthase	VEGF	vascular endothelial growth factor
LC3	microtubule-associated protein light chain 3	VEGFR1/FLT1	fms related receptor tyrosine kinase 1
LEF1	lymphoid Enhancer-Binding Factor 1	VEGFR2/KDR	Kinase insert domain receptor
		Wnt3a	wnt family member 3A



Jiedu Tongluo Granules Ameliorates Post-stroke Depression Rat Model via Regulating NMDAR/BDNF Signaling Pathway

Aimei Zhao^{1,2†}, Bo Ma^{1,3†}, Li Xu¹, Mingjiang Yao¹, Yehao Zhang¹, Bingjie Xue¹, Junguo Ren¹, Dennis Chang⁴ and Jianxun Liu^{1*}

¹Beijing Key Laboratory of Pharmacology of Chinese Materia Region, Institute of Basic Medical Sciences, Xiyuan Hospital of China Academy of Chinese Medical Sciences, Beijing, China, ²Graduate School, Beijing University of Chinese Medicine, Beijing, China, ³State Key Laboratory of Bioactive Substance and Function of Natural Medicines, Institute of Materia Medica, Chinese Academy of Medical Sciences and Peking Union Medical College, Beijing, China, ⁴NICM, Western Sydney University, Penrith, NSW, Australia

OPEN ACCESS

Edited by:

Juxian Song,
Guangzhou University of Chinese
Medicine, China

Reviewed by:

Perle Totosen,
Université Bourgogne Franche-
Comté, France
Hady Keita,
University of the South Sierra, Mexico

*Correspondence:

Jianxun Liu
liujx0324@sina.com

[†]These authors have contributed
equally to this work and share first
authorship

Specialty section:

This article was submitted to
Ethnopharmacology,
a section of the journal
Frontiers in Pharmacology

Received: 31 January 2021

Accepted: 28 April 2021

Published: 20 May 2021

Citation:

Zhao A, Ma B, Xu L, Yao M, Zhang Y,
Xue B, Ren J, Chang D and Liu J (2021)
Jiedu Tongluo Granules Ameliorates
Post-stroke Depression Rat Model via
Regulating NMDAR/BDNF
Signaling Pathway.
Front. Pharmacol. 12:662003.
doi: 10.3389/fphar.2021.662003

Post-stroke depression (PSD) is one of the most common stroke complications, which seriously affects stroke's therapeutic effect and brings great pain for patients. The pathological mechanism of PSD has not been revealed. Jiedu Tongluo granules (JDTLG) is an effective traditional Chinese medicine for PSD treatment which is widely used in clinical treatment. JDTLG has a significant therapeutic effect against PSD, but the mechanism is still unclear. The PSD rat model was established by carotid artery embolization combined with chronic sleep deprivation followed by treating with JDTLG. Neurobehavioral and neurofunctional experiments were engaged in studying the neural function of rats. Histomorphology, proteomics, and western blotting researches were performed to investigate the potential molecular mechanisms related to JDTLG therapy. Oral treatment of JDTLG could significantly improve the symptoms of neurological deficit and depression symptoms of PSD rats. Proteomic analysis identified several processes that may involve the regulation of JDTLG on the PSD animal model, including energy metabolism, nervous system, and N-methyl-D-aspartate receptor (NMDAR)/brain-derived neurotrophic factor (BDNF) signal pathway. Our results showed that JDTLG could reduce glutamate (Glu) level and increase gamma-aminobutyric acid (GABA) level via regulating the NMDAR/BDNF pathway, which may play a vital role in the occurrence and development of PSD.

Keywords: post-stroke depression, traditional Chinese medicine, jiedu tongluo granules, NMDAR/BDNF, neuroprotection

INTRODUCTION

Post-stroke depression (PSD) is one of the most common psychiatric complications of stroke, racked up about 33 percent of stroke survivors (Towfighi et al., 2017). The pathogenesis of PSD is very complex, including biological and social psychological mechanisms (Wang et al., 2018). Several researches provided evidence that it may associate with the neurotransmitter system's modulation, neuronal plasticity, neuroendocrine activation, and energy metabolism (Villa et al., 2017). However, the pathophysiological mechanisms of PSD remain far from clearness.

Glutamate, N-methyl-D-aspartate (NMDA) receptors (NMDARs), and brain-derived neurotrophic factor (BDNF) are the critical gene nodes in PSD. Glutamate is the primary excitatory neurotransmitter of the central nervous system (CNS) and plays a crucial role in maintaining the nervous system's homeostasis and function. NMDARs are essential members of the ionic glutamate receptor family. Excess release of glutamate in the brain is one of the causes of ischemic stroke. It is known that excitotoxicity can cause neuronal death after acute stroke and is associated with overactivation of glutamate receptors (Szydłowska and Tymianski, 2010). Increased glutamate-mediated excitotoxicity could also cause PSD (Sanacora et al., 2012), as a previous study suggested that the glutamate may be involved in PSD via infarct formation (Cheng et al., 2014). Besides, BDNF plays a vital role in neuronal plasticity, cognition, learning, and memory. Numerous studies have demonstrated that the BDNF expression level in PSD patients is lower than that without depression. Moreover, antidepressants are known to improve BDNF expression in the brain, which may reduce the symptom of depression (Zhang and Liao, 2020). Inhibition of NMDARs could improve the BDNF function (Tanqueiro et al., 2018). What's more, in central nervous system neurons, CREB phosphorylation is induced by activation of NMDARs, which lies downstream of Ca^{2+} /Calmodulin dependent protein kinase activation (Deisseroth et al., 1996). Calcium-dependent nuclear signaling via CAMK4 and CREB is critical for neuroprotection (Bell et al., 2013). Thus, gaining a clearer understanding of the complex pathogenesis of PSD is essential for developing better treatments.

In recent years, Traditional Chinese Medicine (TCM), as a primary form of complementary and alternative therapy, has been recognized to be effective and safe in treating depression (Jun et al., 2014). The Chinese herbal preparation named Jiedu Tongluo granules (JDTLG) is a patented complex Chinese medicine formulation (No: 201510419571.3) (Zhao et al., 2018). It has shown that JDTLG is effective for the recovery of body function and depression in PSD patients. An earlier study showed that JDTLG could significantly improve depression-like behavior in animal stroke models (SongWT and Ren, 2015). However, the underlying mechanism was poorly understood until now. This study hypothesized that glutamate excitotoxicity is the pathogenic mechanism of PSD, and JDTLG may have an antidepressant effect and neuroprotection function in the PSD animal model. Therefore, the present research explores the therapeutic effects of JDTLG in the PSD animal model and uncovers the potential mechanism of neuroprotection through the NMDAR/BDNF signaling pathway.

MATERIALS AND METHODS

Preparation and Analysis for JDTL Granules

JDTLG was provided by Huashen Pharmaceutical Co., Ltd. (Beijing, China, #20131230), which was composed of *Panax ginseng* C. A. Mey. (Ren Shen) 12.5 g/100 g, *Scutellaria baicalensis* Georgi (Huang Qin) 12.5 g/100 g, *Ginkgo biloba* L. (Yin Xing Ye) 25 g/100 g, *Hypericum perforatum* L. (GuanYe Lian

Qiao) 12.5 g/100 g, *Gardenia jasminoides* J. Ellis (Zhi Zi) 12.5 g/100 g, *Gastrodia elata* Blume (Tian Ma) 12.5 g/100 g, *Conioselinum anthriscoides* “Chuanxiong” (Chuan Xiong) 12.5 g/100 g. The main compounds of JDTLG were identified according to the Chinese Pharmacopeia specifications (2010 Edition). To obtain the bioactive ingredient of ginsenoside (Ma et al., 2017), samples of JDTLG were separated on XB-C18 column (4.6 × 250 mm, 5 μm), mobile phases consisted of solvents A (acetonitrile) and B (pure water). A gradient eluting program was selected as follows: 0–35 min, 19%A with 81%B; 35–55 min, linear-gradient elution 19–29%A and 81–71%B; 55–70 min, maintaining 29%A and 71%B for 15 min; 70–100 min, linear-gradient 29–38%A and 71–62%B. The flow rate was 1.0 ml/min, and the detection wavelength was 203 nm. To obtain Baicalin (Li et al., 2004), samples of JDTLG were separated on a Topsisil™ C18 column (4.6 × 250 mm, 5 μm), and used methanol-water-phosphoric acid (47:53:0.2) as the mobile phase; the detection wavelength is 280 nm, the flow rate is 1.0 ml min⁻¹, the column temperature controlled at 30°C. Reference substances of Ginsenoside Rg1, Ginsenoside Re, and Baicalin bought from the National Institutes for Food and Drug Control (Beijing, China). Reference substances of Ginsenoside Rb1 bought from Chengdu Pusi Biological Technology Co., Ltd. (Beijing, China).

Animals

We used male SD (Sprague Dawley) rats (License No. SCXK 2016-0011) weighing 200–220 g supplied by the Beijing Vital River Laboratory Animal Technology Co., Ltd. Rats were reared at 25 ± 1°C and 65 ± 5% temperature and humidity, with a 12 h light-dark cycle. All rats were adapted to the environment for about one week and had free access to food and water. Try to minimize animal suffering during experiments. The Committee approved the procedures and ethics guidelines for Experimental Animal Use and Care of Xiyuan Hospital, China Academy of Chinese Medical Sciences, Beijing, China.

Rats were randomly assigned to five groups ($n = 10$): control group, model group, fluoxetine (10 mg kg⁻¹) group (Liang et al., 2015; Sun et al., 2017), JDTL low group (2 g kg⁻¹) and JDTL high group (4 g kg⁻¹). The JDTL Granules and fluoxetine were intragastrically administrated from the first day of the surgery until the behavioral test. Rats in the control and the model group were given the same volume of drinking water. The dosage of drugs was updated according to the weight of rats weekly. Fluoxetine hydrochloride obtained from Lilly (NO. 5198A, Suzhou, China).

Microsphere-Induced Cerebral Embolism

Microsphere-induced cerebral embolism was performed using the previously described method (Zhang et al., 2018). After intraperitoneal injection of 40 mg kg⁻¹ chloral hydrate, the right common carotid artery and the rats' external carotid were temporarily clamped with vascular clamps. The microspheres (106–212 μm in diameter, UVPMS-BY2, Cospheric, United States) were suspended in rat serum at a concentration of 1 mg ml⁻¹, and 0.2 ml of this suspension was injected into the right internal carotid artery. After injection,

loosened the clamp and sutured the puncture wound. The right common and external carotid arteries resumed blood supply to the brain after 2–3 s. Rats in the control group were injected with the same volume of rat serum without microspheres.

Chronic Sleep Deprivation

The procedure of chronic sleep deprivation (CSD) was adopted from the previously published method with modifications (Alhaider et al., 2010; Wang et al., 2017; Ma et al., 2018). All rats have received a 7 days adaptation before MCE surgery and taken CSD from the third day after cerebral ischemia except the control group. The animals subjected to CSD were placed in regular containers for 16 h (16:00–8:00) per day for 4 weeks, and each CSD animal was placed on a circular platform. Six platforms were located in a rectangle container filled with room-temperature water, with 150 mm between the two platforms. During sleep deprivation, low muscle tone caused animals to fall into the water, forcing them to climb back onto the platform and stay awake. Animals in the control group were placed in identical rectangle containers without water to allow them to sleep under the same conditions. Animals were transferred to cages for the remaining 8 h/day (8:00–16:00). During the sleep deprivation, rats had free access to water and food, which hang on the container cover.

Evaluation of Neurological Deficit

The neurological deficit scored according to Longa's five-point scale (Longa et al., 1989). Scores were calculated for each group on days 1, 14, 28 during sleep deprivation. The following neurological deficit scoring system was used: 0, no neurological deficit (normal); 1, inability to extend forepaw fully (mild); 2, unable to move linearly and spiraling to one side (moderate); 3, unable to bear weight and fall to one side at rest (severe); and 4, no spontaneous locomotor activity or lose consciousness (critical). An uninformed researcher performed all neurological assessments.

Behavioral Test

Open Field Test

The open-field test was used to assess general activity level, including locomotor activity and exploratory behavior. The test equipment was a black rectangular structure (100 × 100 × 40 cm³) divided into 16 squares. Rats were initially placed in the test chamber center and observed for 5 min. Within 5 min, the total number of squares crossed with all paws was counted to assess the locomotor activity, and the number of forefeet leaving the ground was measured to evaluate exploratory behavior. The equipment was cleaned up with 10% alcohol solution after each session (Arslan et al., 2016).

Tail Suspension Test

The tail suspension test was carried out before and after the sleep deprivation procedure as previous reports (Kumar and Mondal, 2016). The animals were suspended 50 cm above the ground and secured with tape about 1 cm from the tail. The test lasted 6 min, and the animals' immobility was quantified during the last 4 min

of each test. Rats were considered immobile only when they were passively suspended and remained motionless.

Sucrose Preference Test

The sucrose preference test was performed before and after the sleep deprivation procedure as previous reports (Xu et al., 2016). First, all rats were conditioned to 1% sucrose solution, 24 h of exposure to two bottles of sucrose solution, another 24 h of exposure to one bottle of sucrose solution and one bottle of water. After the adaptation, rats were deprived of water and food for 24 h. Then sucrose preference test was conducted for 1 h. During this period, rats were housed in individual cages, with free access to two bottles, one containing 200 ml 1% sucrose solution and the other 200 ml water. The sucrose preference test was measured as a percentage of sucrose solution consumed relative to the total liquid intake.

Hematoxylin-Eosin Staining

Histopathology was performed after the completion of behavioral tests. Rats were sacrificed after deep anesthetization with an intraperitoneal chloral hydrate injection (40 mg kg⁻¹). Brain tissues were fixed in 4% paraformaldehyde at 4°C for 24 h, dehydrated in a graded series of alcohols, then embedded in paraffin, and cut into 5 µm-thick sections (Zhang et al., 2018). The sections were stained with H&E and assessed on a light microscope (Olympus FV1200, Tokyo, Japan).

Electron Microscopy

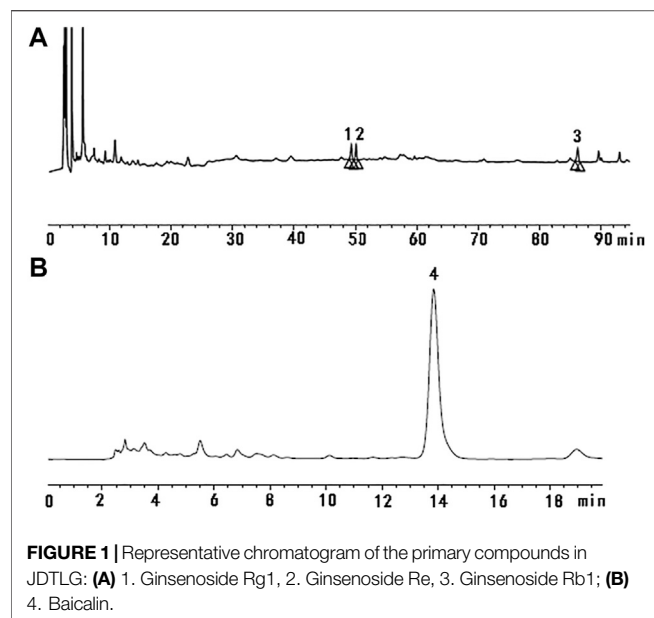
Hippocampus slices of the ischemic hemisphere were cut into 1 mm cubes and were immediately fixed in 2.5% glutaraldehyde at room temperature for 2 h. The pieces were washed with PBS, incubated in PBS solution containing 1% osmium tetroxide for 1 h, dehydrated with ethanol, stained with 1% uranyl acetate for contrast, and embedded in EPON resin. After ultrathin sectioning by Leica EM-UC 6, the specimen sections were stained with uranyl acetate and alkaline lead citrate and observed under a transmission electron microscope (HITACHI-H-7500) (Zhang et al., 2018).

Cerebral Tissue Samples Preparation for LC-MS Analysis

The rats' cerebral tissue was incubated in lysis buffer for 2 h at 4°C, containing NaCl 150 mmol/L, 50 mm Tris-Cl pH 7.5, 1 mm EDTA, and 1% Nonidet P-40. Then the sample was lysed by ultrasound for 3 cycles of 30 s and centrifuged at 12,000 rpm for 15 min. The supernatant was collected and treated with 10 mM of DTT for 30 min followed by 5 mm iodoacetamide for 30 min. After that, the protein sample was digested with trypsin overnight (Fornasiero et al., 2018; Wang et al., 2006).

LC-MS/MS Analysis and Data Analysis

The peptides samples were separated on a column packed with C18 Luna beads and then analyzed using a nanoflow liquid chromatography-tandem mass spectrometry. The solvent system was made up of water (solvent A) and acetonitrile (solvent B). The peptides were eluted from 4% B to 35% B in



90 min. The mass spectrometry data was used for protein identification against the UniProt *Rattus norvegicus* protein database. Protein quantitation was analyzed using MaxQuant software. For the searches, oxidation (M) and acetylation (protein N-term) were set as the variable modifications. Two missed cleavages were allowed. Bioinformatics analysis was performed using Gene Ontology (<http://www.geneontology.org/>), UniProt Database (<https://www.uniprot.org/>), Kyoto Encyclopedia of Genes and Genomes, KEGG Resources (<https://www.genome.jp/kegg/>) and DAVID Bioinformatics Resources (<https://david.ncifcrf.gov/conversion.jsp>) (Ma et al., 2018). The mass spectrometry proteomics data have been deposited to the ProteomeXchange Consortium via the PRIDE (Perez-Riverol et al., 2019) partner repository with the dataset identifier PXD025480.

Glu and GABA Assays

Rats were sacrificed after completion of behavioral tests, and cerebral cortex slices were homogenized and centrifuged according to the manufacturers' instructions. Glu and GABA concentrations in the cerebral cortex were measured with Glu (EGLT-100, BioAssay systems) and GABA (201712, Bio-swamp) ELISA kits. The results are expressed as the means \pm standard deviation.

TABLE 1 | Linear range, R^2 , and limits of quantification of calibration curve used to determine the main identified compounds.

Compounds	Linear range (μ g)	Calibration curve	R^2
Ginsenoside Rg1	0.364~3.64	$Y = 2.5 \times 10^5 X + 2,951$	0.9985
Ginsenoside Re	0.317~3.17	$Y = 3.0 \times 10^5 X - 18,773$	0.9999
Ginsenoside Rb1	0.324~3.24	$Y = 1.7 \times 10^5 X - 13,850$	0.9995
Baicalin	0.0925~0.925	$Y = 4.0 \times 10^6 X - 65,619$	0.9998

Western Blotting

The Western blotting procedures were carried out as previously described (Zhang et al., 2018). The brain tissue protein was extracted by RIPA buffer (Beyotime, China) mixed with protease and phosphatase inhibitor mixture (MCE, United States). Protein concentration was determined by using a protein assay solution (Bio-Rad). Identical quantities of protein were denatured with protein loading buffer, loaded onto 10% SDS-PAGE gels, and transferred to polyvinylidene difluoride (PVDF) membranes by electroblotting. The PVDF membranes were blocked by 5% bovine serum albumin (BSA) in TBST buffer for 1 h, and the following antibodies were used to incubate overnight at 4°C: GRIN2B (Abcam, 1:1,000 dilution), CAMK4 (Abclonal, 1:1,000 dilution), CREB1 (Abclonal, 1:1,000 dilution), BDNF (Abclonal, 1:1,000 dilution), NTRK2 (Proteintech, 1:1,000 dilution) and ACTB (Sigma, 1:5,000). Reactive bands were detected using ECL detection reagent (Thermo Fisher Scientific, MA, United States) following the instructions. All the experiments reported in this study were carried out three times, and the results were repeatable.

qPCR

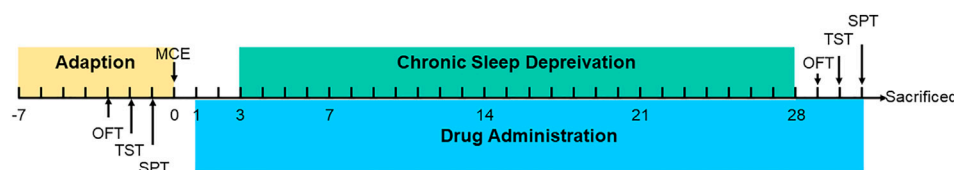
According to the instructions, the total RNA in brain tissue was extracted by using Trizol reagent (Thermo Scientific, United States). A NanoDrop 2000 spectrophotometer (Thermo Scientific, United States) was used to determine the concentration and purity of RNA. The absorbance ratio (A260/280) of all samples ranged from 1.8 to 2.0, and Prime Script RT Master Mix (Takara, Dalian, China) was used to reverse transcribing 2 μ g total RNA into cDNA according to the specification. qPCR was performed using the QuantiFast® SYBR® Green PCR Master Mix (Qiagen, Germany) with specific primers and expression of each sample in Light Cycler® 480 II Real-time PCR instrument (Roche, Swiss), which was internally normalized against Actb. Primers used were as follows: Grin2b: forward 5'- AGCCCCACTAATTCCAAGGC-3' and reverse: 5'- TTGTCCTTCAGGCTCACGCT-3'; Camk4: forward 5'- TGGAGGCAGTTGCTTACCTG-3' and reverse: 5'- GGTTCCACACACCGTCTTCA-3'; Creb1: forward 5'- CCAGGGAGGAGCAATACAGC-3' and reverse: 5'- TGTCCA TCAGTGGTCTGTGC-3'; Bdnf: forward 5'- ATTAGCGAGTGGGTCACAGC-3' and reverse: 5'- TGGCCT TTTGATACCGGGAC-3'; Ntrk2: forward 5'- ACGGGGACCTCAACAAGTTC-3' and reverse: 5'- CTGCGA TTTGCTGAGCGATG-3'; Actb: forward 5'- CCAACCGTG AAAAGATGACC-3' and reverse: 5'- ACCAGAGGCATA CAGGGACA-3'. Relative expression fold change was calculated using the $2^{-\Delta\Delta C_t}$ method (Livak and Schmittgen, 2001).

Statistical Analysis

All statistical data were expressed as mean \pm standard deviation (SD), which were analyzed using GraphPad Prism software (San Diego, CA, United States). One-way analysis of variance (ANOVA), followed by Newman-Keuls post hoc test, was used to compare all groups' differences. Each experiment was repeated at least three times. $p < 0.05$ was considered statistically significant.

TABLE 2 | Contents of the main identified compounds in JDTLG Granules.

Herbs	Compounds	Contents (mg/g)
Panax ginseng C. A. Mey. (<i>Ren Shen</i>)	Ginsenoside Rg1	0.315
	Ginsenoside Re	0.343
	Ginsenoside Rb1	0.968
	Baicalin	13.996
<i>Scutellaria baicalensis</i> Georgi (<i>Huang Qin</i>)		

**FIGURE 2** | Schedule of experimental procedures.

RESULTS

Qualitative Analysis of Bioactive Compounds in JDTLG Granules

High-performance liquid chromatography (HPLC) was used to determine the contents of representative chemical components in JDTLG. **Figure 1** shows the chromatograms of the main identified components of JDTLG. In **Table 1**, the calibration curves' equations and the quantitative limits of these components are determined. All calibration curves showed good linear regression ($R^2 > 0.99$). The results' precision and accuracy tests are listed in **Table 2**. The concentration of the main compound is calculated by using the calibration curve of the internal standard.

JDTLG Granules Ameliorated PSD-Induced Neurological Deficits and Depressive Symptoms

The schedule of our research procedure was shown in **Figure 2**. Body weights of the rats were observed every two weeks during the CSD phase. As shown in **Figure 3A**, MCE + CSD induced bodyweight decrease since the second week compared to the control group ($p < 0.05$). In comparison, JDTLG granules and fluoxetine attenuated the fourth week's bodyweight reduction ($p < 0.01$). Additionally, the model group's neurological deficit scores were higher on the second and the fourth week ($p < 0.05$), which exerted a delayed functional recovery. However, JDTLG granules and fluoxetine treatment significantly ameliorated the neurological deficit ($p < 0.05$, **Figure 3B**).

What's more, several behavioral tests were conducted to determine the antidepressant effects of JDTLG granules on the PSD rats. The horizontal and vertical frequency tested the locomotor activity and exploratory behavior. Rats in the model group displayed a significant decrease in locomotor activity and exploratory behavior ($p < 0.01$ or $p < 0.05$), whereas JDTLG granules and fluoxetine treatment reversed the reduction of

locomotor activity ($p < 0.05$ or $p < 0.01$, **Figure 3C**). As for the TST, rats treated with JDTLG granules and fluoxetine show a shorter immobility time compared with the model group ($p < 0.05$ or $p < 0.01$, **Figure 3D**). We also tested the rats' sucrose preference and found that JDTLG granules and fluoxetine could increase the rats' sucrose preference, compared with the model group ($p < 0.05$, **Figure 3E**).

Histological and Ultrastructural Changes Associated With JDTLG Granules Treatment

Histological changes of brain neurons can reveal the structural and functional changes of the brain. We engaged HE staining of brain neurons for all groups (**Figure 4A**). In the control group, the neurons in the hippocampal CA3 area were normal in morphology, structurally intact. Moreover, the cells were arranged neatly. The cytoplasm was clearly visible. However, in the model group, the cell gap was enlarged with a scattered arrangement. The number of cells was reduced. The nucleus was condensed and deep stained with degeneration and necrosis. Moreover, JDTLG granules and fluoxetine treatment clearly reduced the degree of cell damage in hippocampal neurons.

Morphology study of electron microscopy in the hippocampal area generates a detailed evaluation of the nucleus (**Figure 4B**) and mitochondria (**Figure 4C**). The neurons in the control group were with intact shape and uniform chromatin distribution in the nucleus. The mitochondria were apparent and remained intact. While the nucleus of the model group showed nuclear pyknosis and nuclear membrane structure disintegrates. The mitochondria deform and swell with the sputum rupture and the vacuolization. JDTLG granules treatment reduced brain tissue elements' damage in a dose-dependent manner, and this tissue had a more viable appearance.

LC-MS/MS Analysis

We engaged label-free quantitative proteomic technology to study protein expression levels of PSD rat models' brain tissue.

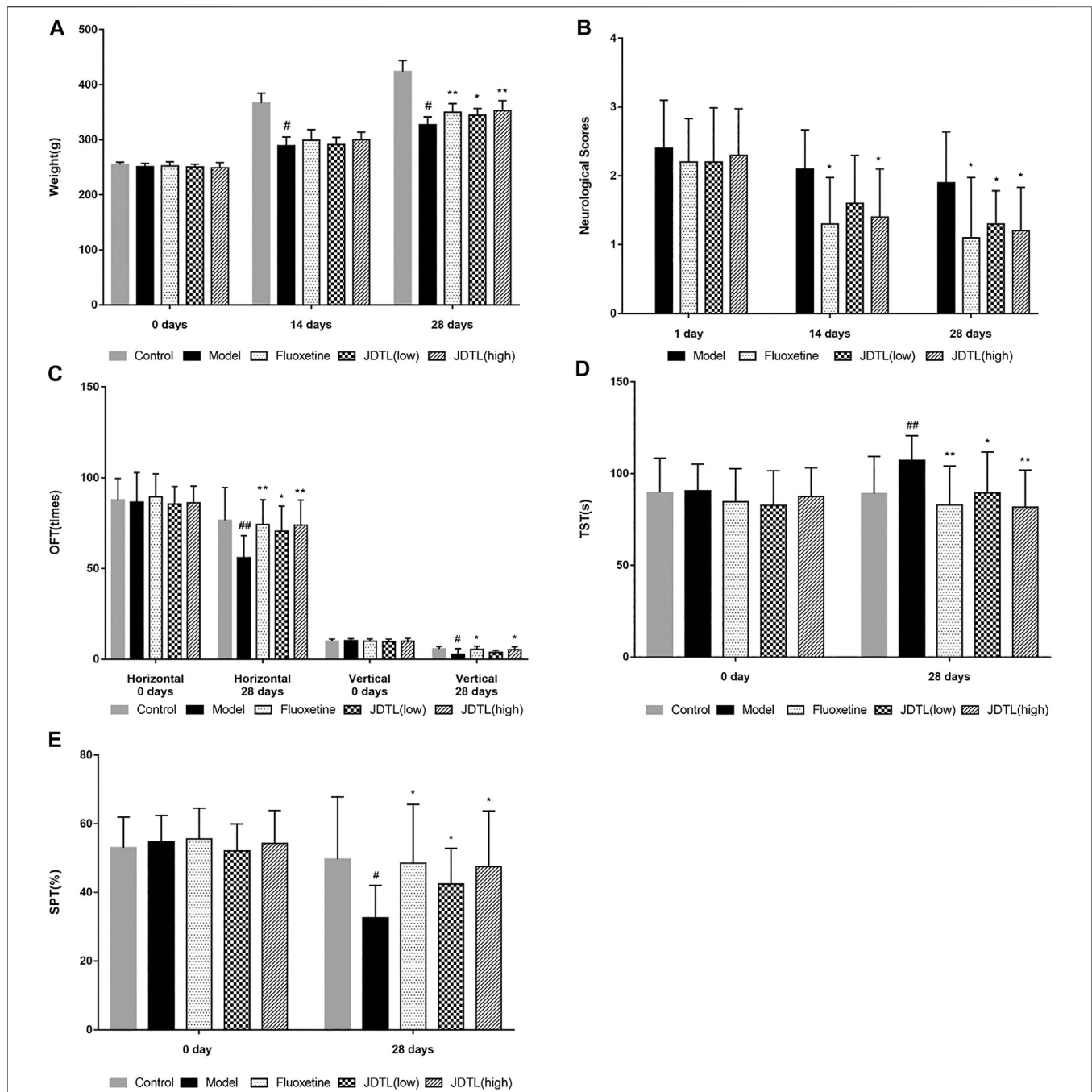


FIGURE 3 | JDTLG Granules Ameliorated PSD-Induced Neurological Deficits and Depressive Symptoms. **(A)** Bodyweight. **(B)** Neurological deficit scores. **(C–E)** Neurobehaviors **(C)** OFT, **(D)** TST, **(E)** SPT. All data were expressed as mean \pm SD, $n = 10$. ^{##} $p < 0.01$, [#] $p < 0.05$ vs. Control group, ^{**} $p < 0.01$, ^{*} $p < 0.05$ vs. Model group.

As the statistics revealed, 3,503 non-redundant proteins were identified in the three groups of rat brain tissue. Among the proteins, 3,254, 3,231, and 3,295 proteins were detected in the control group, the model group, and the JDTLG granules group. 2,969 proteins were detected in all three groups, constituting 84.9% of the total proteins (Figure 5A).

We set 2-folds as the apparent abundance alteration and detected 881 proteins that were up or down-regulated by PSD and recovered by JDTLG granules (Figure 5B). These proteins were identified as the different abundance proteins (DAPs) involving in PSD. Gene ontology analysis revealed that DAPs involving in the molecular function of catalytic activity, protein binding, transporter activity, and so on (Figure 5C). The DAPs

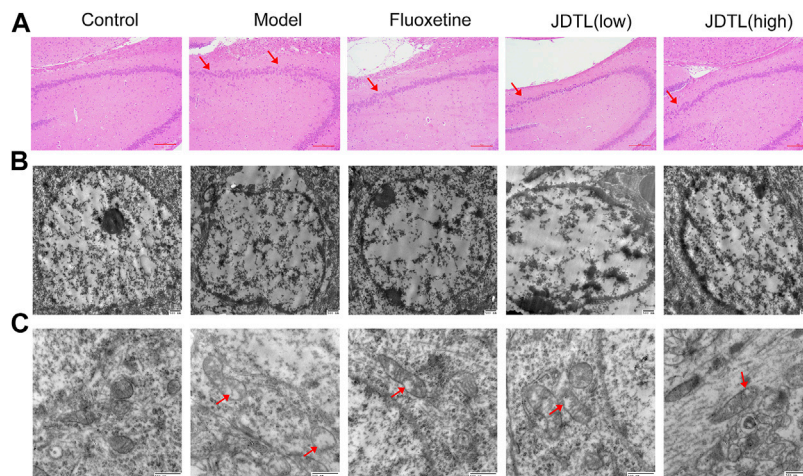


FIGURE 4 | Histological and Ultrastructural Changes Associated with JDTLG Granules Treatment. H&E staining of the hippocampal CA3 area [(A), $\times 40$]. Cells were structurally intact and with clear cytoplasm in the control group. In the model group, degeneration and necrosis occurred with reduced cells, scattered arrangement (arrow), and condensed and deep stained nucleus. Minor damage was observed in JDTLG granules and fluoxetine groups. Ultrastructural characteristics of the nucleus [(B), $\times 20,000$] and mitochondria [(C), $\times 40,000$] in the hippocampal area. The control group neurons were with intact shape and uniform chromatin in the nucleus. Furthermore, the mitochondria were apparent and remained intact. The model group's nucleus showed nuclear pyknosis, and the mitochondria deform, swell, and vacuolization (arrow). The treatment of JDTLG granules and fluoxetine reduced the damage.

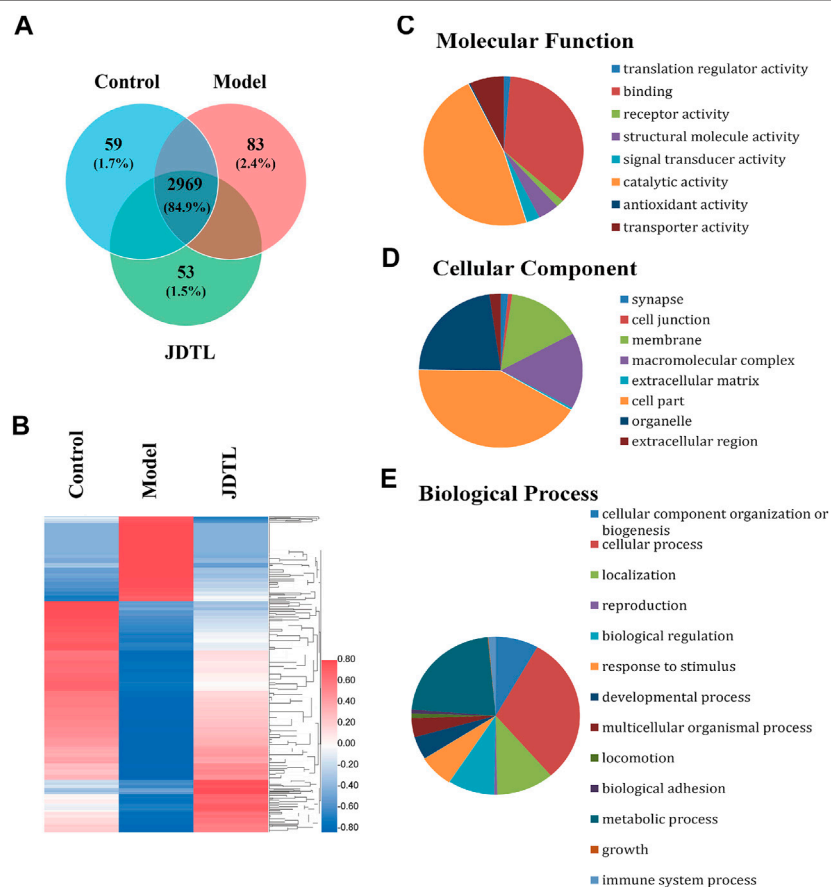
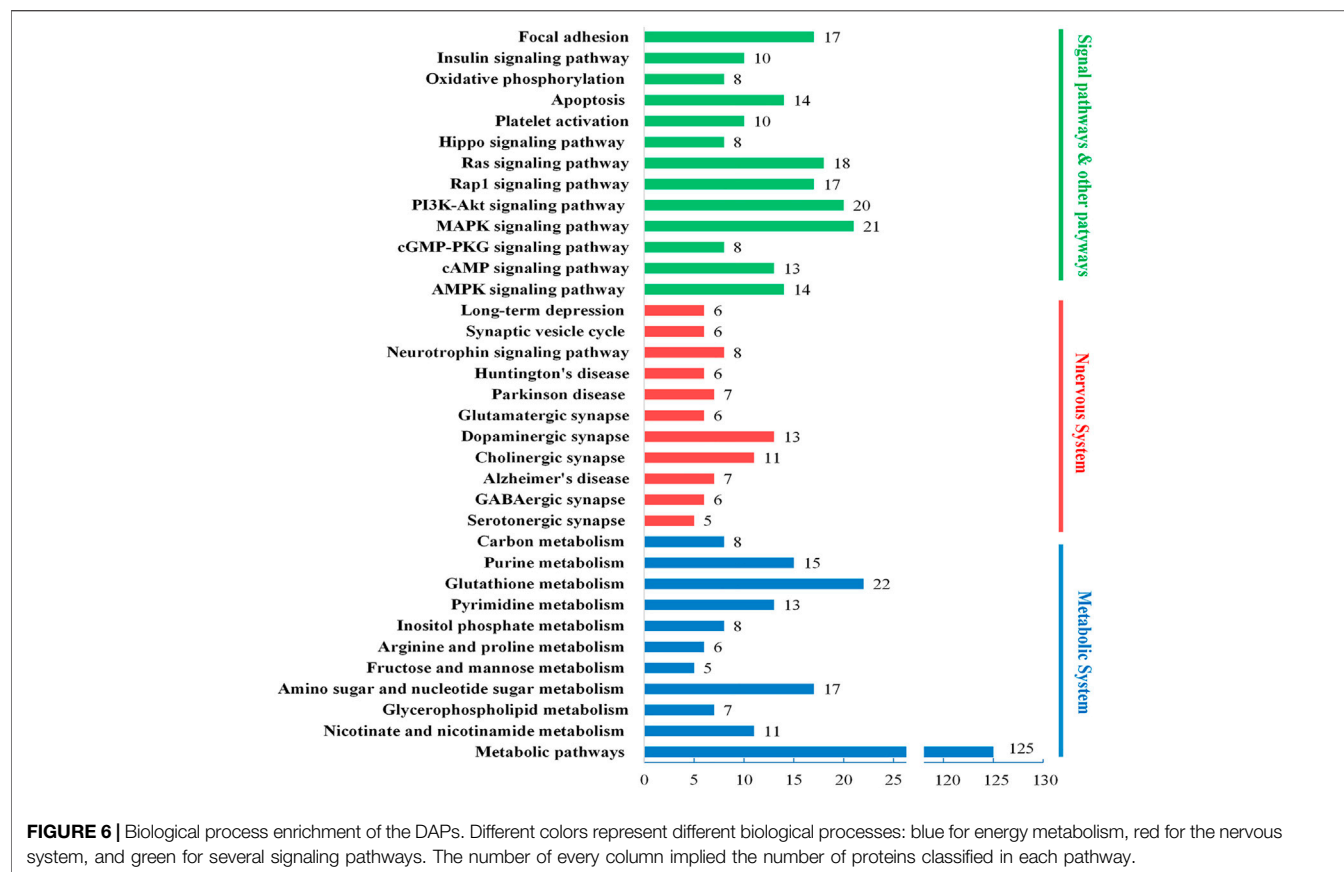


FIGURE 5 | Summary statistics of LC-MS/MS analysis. (A) Area-proportional Venn diagram depicts the overlap of the identified proteins of Control, Model, and JDTLG groups. (B) Heat map analysis of the DAPs among the three groups. (C–E) Molecular functional assignments, cellular component and biological process of the DAPs according to gene ontology analysis.



were located on several parts, including cytoplasm, membrane, organelles, cell junction, and so on (Figure 5D). Biological process analysis demonstrated that PSD might significantly affect metabolism, protein localization, biological regulation, the immune system, and other processes. Furthermore, JDTL granules may involve PSD through these processes (Figure 5E).

Functional Enrichment of the DAPs

To further analyze the biological mechanisms involving in the DAPs, we engaged the DAVID, KEGG, and UniProt databases to study the proteins' biological processes. As shown in Figure 6, the DAPs' biological functions focus on three biological processes, energy metabolism, nervous system, and several signaling pathways. Based on the results of brain histochemical staining and electron microscopy analysis, we focused the therapeutic targets of JDTL granules on nerve cells' energy metabolism and related NMDAR-CAMK4-BDNF pathways. NMDAR-CAMK4-BDNF pathways involve energy metabolism and some signal pathways, including cAMP, PI3K-Akt, Ras, and so on.

JDTL Granules Inhibits GRIN2B and Activates BDNF Pathway in Ipsilateral Cortex

As the functional enrichment in Figure 6 shows, GABAergic synapse, Glutamatergic synapse, Cholinergic synapse, and

dopaminergic synapse are detected. GABAergic synapse dysregulation has been implicated in many brain disorders. We tested the expression levels of Glu and GABA of rat brains using ELISA kits.

The changes in Glu and GABA levels in the brain tissues were illustrated in Figure 7B ($n = 10$). It was found that the Glu levels were significantly higher in the model group ($p < 0.01$, vs. control group). JDTL granules and fluoxetine treatments notably reduced the Glu levels ($p < 0.05$, vs. model group). Additionally, the GABA was remarkably reduced in the model group ($p < 0.01$, vs. control group). JDTL granules and fluoxetine treatments significantly increased the GABA compared to the model group ($p < 0.05$).

We tested the protein expression level of the NMDAR/BDNF pathway-related proteins. And found that GRIN2B protein was significantly increased in model rats ($p < 0.05$), whereas JDTL granules and fluoxetine decreased the expression of GRIN2B ($p < 0.05$). BDNF is a crucial protein on neuron protection, and CAMK4 is a BDNF relative protein. We found that CAMK4 was a reduction in the model rats, while JDTL granules and fluoxetine increased the CAMK4 level ($p < 0.05$). What's more, the expression of the downstream proteins of CREB1, BDNF, and NTRK2 was reduced in the model group ($p < 0.05$), whereas JDTL granules and fluoxetine treatment increased the expression level of CREB1, BDNF, and NTRK2 ($p < 0.05$) (Figures 7A,C-F) ($n = 3$).

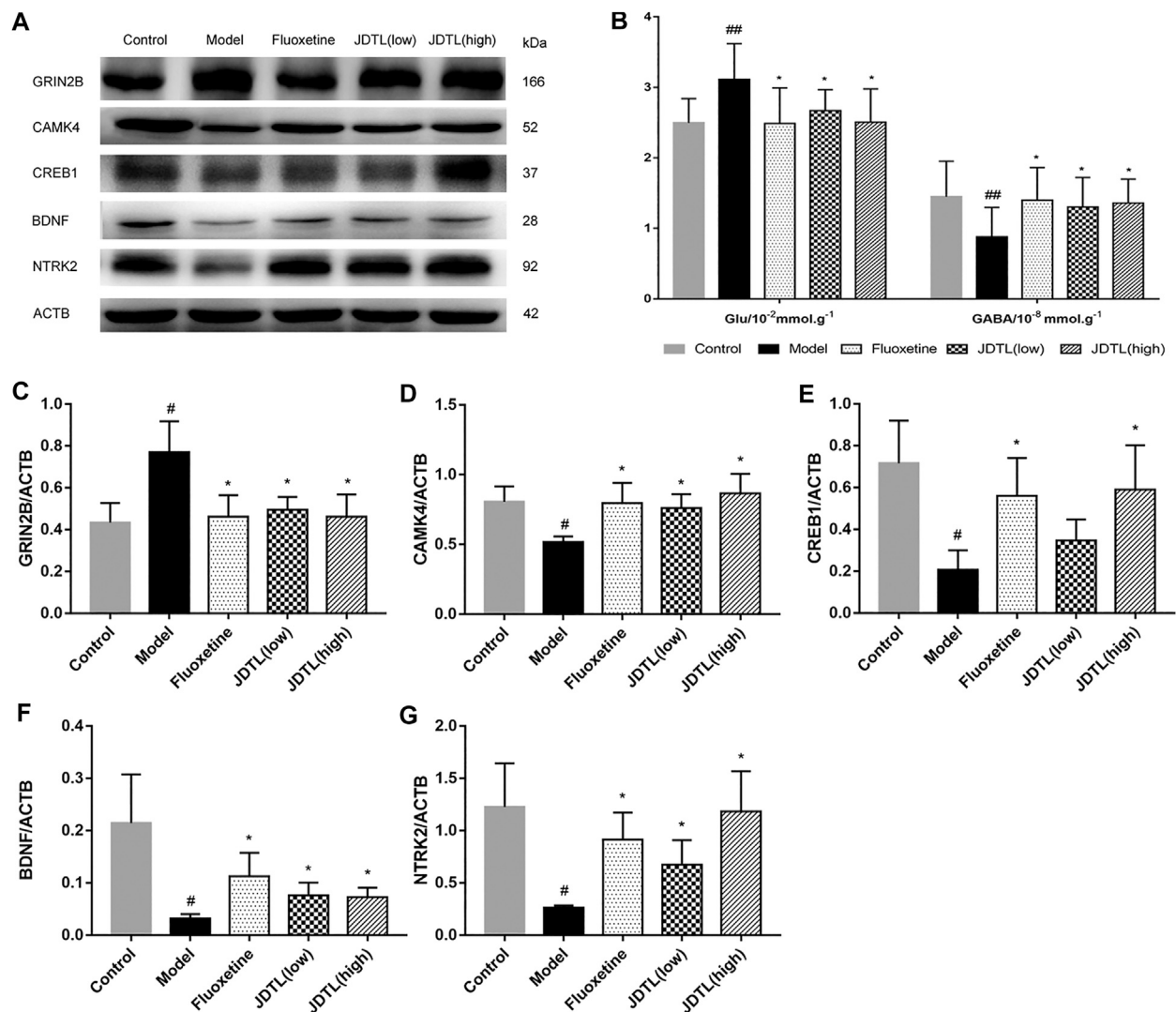


FIGURE 7 | JDTLG Granules Inhibits GRIN2B and Activates BDNF Pathway in Ipsilateral Cortex. **(A,C–F)** Representative immunoblots of GRIN2B, CAMK4, CREB1, BDNF, and NTRK2 in all rats' ipsilateral cortex ($n = 3$). **(B)** The changes in Glu and GABA levels of brain tissues ($n = 10$). Data are described as mean \pm SD. [#] $p < 0.05$, ^{##} $p < 0.01$ vs. control group. ^{*} $p < 0.05$ vs. model group.

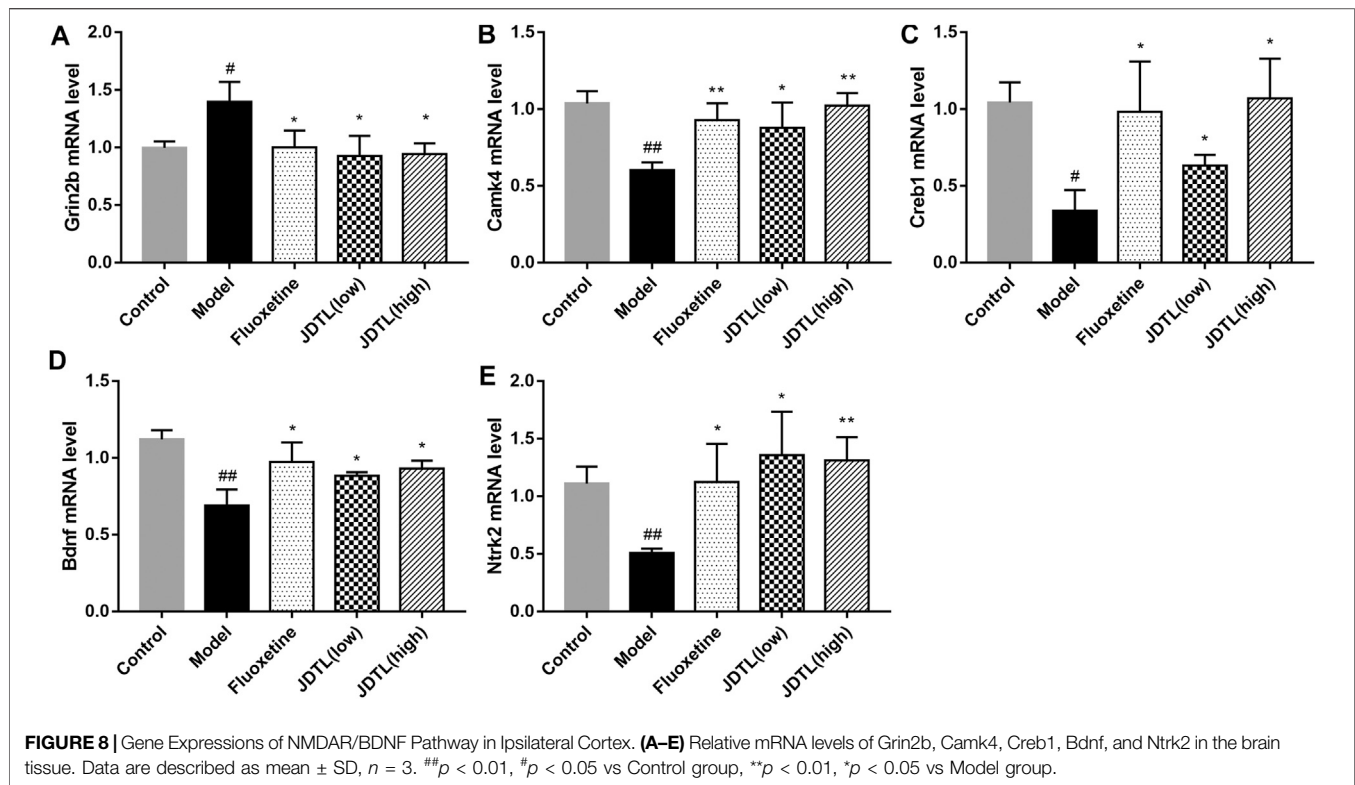
Gene Expressions of NMDAR/BDNF Pathway in Ipsilateral Cortex

The relative mRNA levels of *Grin2b*, *Camk4*, *Creb1*, *Bdnf*, and *Ntrk2* were detected by quantitative reverse transcription-polymerase chain reaction (qRT-PCR). We observed the strong activation of the *Grin2b* in the model group ($p < 0.05$) and a notable reduction in both granules and fluoxetine treatment groups ($p < 0.05$, **Figure 8A**). On the other hand, *Camk4*, *Creb1*, *Bdnf*, and *Ntrk2* were significantly up-regulated in granules and fluoxetine treatment groups ($p < 0.05$, **Figures 8B–E**) ($n = 3$), which was corresponding to the protein levels.

DISCUSSION

In the present study, animals were exposed to chronic sleep deprivation (CSD) after ischemic stroke to elicit experimental

post-stroke depression. Sleep consists of two main stages of non-REM and REM sleep (Acosta, 2019). REM sleep is closely associated with depression. During the REM sleep phase, loss of muscle tone caused rats to fall into the water and wake up, which will cause major depressive disorders involving anxiety, anhedonia, and behavioral despair. What's more, exposure to chronic sleep deprivation after stroke exacerbates neurological deficits, depressive-like symptoms and stimulates excitatory neurotoxicity reactions. Long-term sleep deprivation may lead to sleep disturbance and depression while reducing BDNF levels (Schmitt et al., 2016). The results indicated that the model group suffered from CSD after MCE surgery with apparent depression and neurological deficits. JDTL granules' effect was evaluated and compared with fluoxetine (Jin et al., 2017), which showed JDTL granules had a significant effect on PSD. Our findings demonstrated



that apart from the improvement of neural function recovery, JDTL granules may also notably attenuated depressive-like symptoms. However, the underlying therapeutic mechanism of JDTL granules remains unclear. Therefore, we investigated the excitatory neurotoxicity and NMDAR/BDNF signaling pathway.

We use microsphere-induced cerebral embolism combined with the chronic sleep deprivation model in this study. Embolic stroke models can cause cerebral stroke clinical symptoms, one of the models mimicking human stroke most closely (Fluri et al., 2015; Sommer, 2017). Chronic sleep deprivation can cause disruptions in circadian rhythms (Soreca, 2014), which give rise to the development of depression (Kalmbach et al., 2017; Ma et al., 2019). The combination of these two methods can reflect the disability and depression symptoms of PSD patients.

Glutamate is the primary excitatory neurotransmitter in the brain, while GABA is the primary inhibitory neurotransmitter. The balance of glutamatergic and GABAergic is essential for normal neurologic function (Guerriero et al., 2015). After a stroke, glutamate in the brain increases. Excessive glutamate stimulates glutamate receptors, leading to swelling and apoptosis of nerve cells, which in turn leads to neurological disorders (Castillo et al., 1996; Han et al., 2008). Hence, limiting secondary brain damage accompanied by excessive glutamate concentrations is an important component of stroke management (Gruenbaum et al., 2020). The glutamatergic system similarly plays a key role in mood disorders, such as anxiety (Riaza Bermudo-Soriano et al., 2012), depression (Lin et al., 2019; Sanacora et al., 2012), dementia (Butterfield and Pocernich, 2003), and other psychiatric diseases. Glutamate and GABA

systems are becoming targets for the development of mood disorders drugs (Krystal et al., 2002). We observed that the change of glutamatergic synapse and GABAergic synapse were involved in the brain of post-stroke depression rats. The glutamate level was increased in the brain of MCE + CSD rats. However, the GABA level was decreased on the contrary. Correspondingly, the glutamate receptor (NMDAR) was also over-activated in the model group due to increased glutamate stimulation. Several researches indicated that antidepressants might exert their behavioral effects around the glutamate system (Sanacora et al., 2008; Chen et al., 2019; Duman et al., 2019). Following previous findings, we noticed that JDTL granules could reverse the brain's level alteration of glutamate and GABA. Thus, the results showed that the improvement of JDTLG on PSD should be attributed to its neuroprotection via regulating excitotoxicity.

BDNF is the most abundant and widely distributed neurotrophin in the central nervous system. Animal models have been used to conduct extensive research on behavioral and emotional changes (Duman and Monteggia, 2006; Serra et al., 2017). BDNF serves as a critical transducer of antidepressants that have been linked to the antidepressant drug and the neuroplastic changes of depressive symptoms (Bjorkholm and Monteggia, 2016). The transcription of BDNF mRNA can be regulated by neuronal activity through Ca^{2+} influx, via Ca^{2+} permeable glutamate receptors (mainly NMDAR receptors) and voltage-gated Ca^{2+} channels; Zafra et al., 1991; Ghosh et al., 1994; Osteen et al., 2004). The classical cellular signaling pathway of CaM/CAMK4/CREB is closely associated with neuroprotective function. Ca^{2+} influx triggers phosphorylation of CREB, which binds to the key Ca^{2+}

responsive element. The Ca^{2+} responsive element may activate BDNF transcription. The release of BDNF may stimulate NTRK2 receptors on GABAergic interneurons, which may increase GABA input to neural precursors, thus stimulating their differentiation and maturation into neurons and balancing the glutamate excitotoxicity (Waterhouse et al., 2012). Our observation suggests that GDTL Granules and fluoxetine might protect neurons via modulating the NMDAR/BDNF signaling pathway.

Although therapeutic effects of JDTL granules were observed in PSD rats, there are still some limitations. Firstly, the observation period is not long enough, and a more extended study period and sufficient samples may identify more trusted results. Secondly, fluoxetine is a representative of SSRI antidepressants. Though fluoxetine could also treat glutamate toxicity in the hippocampus (Ludka et al., 2017; Lazarevic et al., 2019), more detection of relative molecular will be better to increase the reliability of the results. Besides, we only explore the pharmacological effects of JDTLG on the glutamatergic system. The mechanism deserves further study in the future.

CONCLUSION

In summary, we observed a significant neurological function recovery and antidepressant effect of JDTLG. The current investigation indicates that JDTLG can modulate excitotoxicity and alleviate depressive behavior. The beneficial effects of JDTLG treatment may be mediated by the activation of the NMDAR/BDNF signaling pathway.

REFERENCES

- Acosta, M. T. (2019). [Sleep, Memory and Learning]. *Medicina (B Aires)* 79 (Suppl. 3), 29–32. Available at: <https://www.ncbi.nlm.nih.gov/pubmed/31603840>.
- Alhaider, I. A., Aleisa, A. M., Tran, T. T., Alzoubi, K. H., and Alkadi, K. A. (2010). Chronic Caffeine Treatment Prevents Sleep Deprivation-Induced Impairment of Cognitive Function and Synaptic Plasticity. *Sleep* 33 (4), 437–444. doi:10.1093/sleep/33.4.437
- Arslan, F. C., Tiriyaki, A., Yildirim, M., Özkorumak, E., Alver, A., Altun, İ. K., et al. (2016). The Effects of Edaravone in Ketamine-Induced Model of Mania in Rats. *Acta Neurobiol. Exp. (Wars)* 76 (3), 192–198. doi:10.21307/ane-2017-019
- Bell, K. F. S., Bent, R. J., Meese-Tamuri, S., Ali, A., Forder, J. P., and Aarts, M. M. (2013). Calmodulin Kinase IV-dependent CREB Activation Is Required for Neuroprotection via NMDA Receptor-PSD95 Disruption. *J. Neurochem.* 126 (2), 274–287. doi:10.1111/jnc.12176
- Björkholm, C., and Monteggia, L. M. (2016). BDNF - a Key Transducer of Antidepressant Effects. *Neuropharmacology* 102, 72–79. doi:10.1016/j.neuropharm.2015.10.034
- Butterfield, D. A., and Pocernich, C. B. (2003). The glutamatergic system and Alzheimer's disease: therapeutic implications. *CNS Drugs* 17 (9), 641–652. doi:10.2165/00023210-200317090-00004
- Castillo, J., Dávalos, A., Naveiro, J., and Noya, M. (1996). Neuroexcitatory Amino Acids and Their Relation to Infarct Size and Neurological Deficit in Ischemic Stroke. *Stroke* 27 (6), 1060–1065. doi:10.1161/01.str.27.6.1060
- Chen, Y.-P., Wang, C., and Xu, J.-P. (2019). Chronic Unpredictable Mild Stress Induced Depression-like Behaviours and Glutamate-Glutamine Cycling

DATA AVAILABILITY STATEMENT

The datasets presented in this study can be found in online repositories. The mass spectrometry proteomics data in this article can be accessed through the following link: Project Webpage; <http://www.ebi.ac.uk/pride/archive/projects/PXD025480>.

ETHICS STATEMENT

The animal study was reviewed and approved by the Committee for Experimental Animal Use and Care of Xiyuan Hospital, China Academy of Chinese Medical Sciences, Beijing, China.

AUTHOR CONTRIBUTIONS

JL and LX designed and supervised the research study. AZ and BM: performed the research, analyzed the data and wrote the manuscript, both contributed equally to the work. MY, YZ, and BX: participated in the performance of the experiment. JR and DC: contributed to the revising of the manuscript.

FUNDING

This study was supported by grants from the National Basic Research Program, China (973 program) (No.2015CB554405) and the National Natural Science Foundation, China (NSFC 82030124, NSFC 81873041).

- Dysfunctions in Both Blood and Brain of Mice. *Pharm. Biol.* 57 (1), 280–286. doi:10.1080/13880209.2019.1598445
- Cheng, S.-Y., Zhao, Y.-D., Li, J., Chen, X.-Y., Wang, R.-D., and Zeng, J.-W. (2014). Plasma Levels of Glutamate during Stroke Is Associated with Development of Post-stroke Depression. *Psychoneuroendocrinology* 47, 126–135. doi:10.1016/j.psyneuen.2014.05.006
- Deisseroth, K., Bito, H., and Tsien, R. W. (1996). Signaling from Synapse to Nucleus: Postsynaptic CREB Phosphorylation during Multiple Forms of Hippocampal Synaptic Plasticity. *Neuron* 16 (1), 89–101. doi:10.1016/s0896-6273(00)80026-4
- Duman, R. S., and Monteggia, L. M. (2006). A Neurotrophic Model for Stress-Related Mood Disorders. *Biol. Psychiatry* 59 (12), 1116–1127. doi:10.1016/j.biopsych.2006.02.013
- Duman, R. S., Sanacora, G., and Krystal, J. H. (2019). Altered Connectivity in Depression: GABA and Glutamate Neurotransmitter Deficits and Reversal by Novel Treatments. *Neuron* 102 (1), 75–90. doi:10.1016/j.neuron.2019.03.013
- Fluri, F., Schuhmann, M. K., and Kleinschmitt, C. (2015). Animal Models of Ischemic Stroke and Their Application in Clinical Research. *Drug Des. Devel Ther.* 9, 3445–3454. doi:10.2147/DDDT.S56071
- Fornasiero, E. F., Mandad, S., Wildhagen, H., Alevra, M., Rammner, B., Keihani, S., et al. (2018). Precisely Measured Protein Lifetimes in the Mouse Brain Reveal Differences across Tissues and Subcellular Fractions. *Nat. Commun.* 9 (1), 4230. doi:10.1038/s41467-018-06519-0
- Ghosh, A., Carnahan, J., and Greenberg, M. (1994). Requirement for BDNF in Activity-dependent Survival of Cortical Neurons. *Science* 263 (5153), 1618–1623. doi:10.1126/science.7907431
- Gruenbaum, B. F., Kutz, R., Zlotnik, A., and Boyko, M. (2020). Blood Glutamate Scavenging as a Novel Glutamate-Based Therapeutic Approach for Post-stroke

- Depression. *Ther. Adv. Psychopharmacol.* 10, 204512532090395. doi:10.1177/2045125320903951
- Guerriero, R. M., Giza, C. C., and Rotenberg, A. (2015). Glutamate and GABA Imbalance Following Traumatic Brain Injury. *Curr. Neurol. Neurosci. Rep.* 15 (5), 27. doi:10.1007/s11910-015-0545-1
- Han, F., Shioda, N., Moriguchi, S., Qin, Z.-H., and Fukunaga, K. (2008). Downregulation of Glutamate Transporters Is Associated with Elevation in Extracellular Glutamate Concentration Following Rat Microsphere Embolism. *Neurosci. Lett.* 430 (3), 275–280. doi:10.1016/j.neulet.2007.11.021
- Jin, H.-J., Pei, L., Li, Y.-N., Zheng, H., Yang, S., Wan, Y., et al. (2017). Alleviative Effects of Fluoxetine on Depressive-like Behaviors by Epigenetic Regulation of BDNF Gene Transcription in Mouse Model of Post-stroke Depression. *Sci. Rep.* 7, 15. doi:10.1038/s41598-017-13929-5
- Jun, J. H., Choi, T.-Y., Lee, J. A., Yun, K.-J., and Lee, M. S. (2014). Herbal Medicine (Gan Mai Da Zao Decoction) for Depression: A Systematic Review and Meta-Analysis of Randomized Controlled Trials. *Maturitas* 79 (4), 370–380. doi:10.1016/j.maturitas.2014.08.008
- Kalmbach, D. A., Arnedt, J. T., Song, P. X., Guille, C., and Sen, S. (2017). Sleep Disturbance and Short Sleep as Risk Factors for Depression and Perceived Medical Errors in First-Year Residents. *Sleep* 40 (3), zsw073. doi:10.1093/sleep/zsw073
- Krystal, J. H., Sanacora, G., Blumberg, H., Anand, A., Charney, D. S., Marek, G., et al. (2002). Glutamate and GABA Systems as Targets for Novel Antidepressant and Mood-Stabilizing Treatments. *Mol. Psychiatry* 7 (Suppl. 1), S71–S80. doi:10.1038/sj.mp.4001021
- Kumar, S., and Mondal, A. C. (2016). Neuroprotective, Neurotrophic and Antioxidative Role of Bacopa Monnieri on CUS Induced Model of Depression in Rat. *Neurochem. Res.* 41 (11), 3083–3094. doi:10.1007/s11064-016-2029-3
- Lazarevic, V., Mantas, I., Flais, I., and Svenningsson, P. (2019). Fluoxetine Suppresses Glutamate- and GABA-Mediated Neurotransmission by Altering SNARE Complex. *Ijms* 20 (17), 4247. doi:10.3390/ijms20174247
- Li, H., Jiang, Y., and Chen, F. (2004). Separation Methods Used for Scutellaria Baicalensis Active Components. *J. Chromatogr. B* 812, 277–290. doi:10.1016/j.jchromb.2004.06.04510.1016/s1570-0232(04)00545-8
- Liang, J. J., Yuan, X., Shi, S., Wang, F., Chen, Y., Qu, C., et al. (2015). Effect and Mechanism of Fluoxetine on Electrophysiology In Vivo in a Rat Model of Postmyocardial Infarction Depression. *Dddt* 9, 763–772. doi:10.2147/dddt.s75863
- Lin, C.-H., Huang, M.-W., Lin, C.-H., Huang, C.-H., and Lane, H.-Y. (2019). Altered mRNA Expressions for N-Methyl-D-Aspartate Receptor-Related Genes in WBC of Patients with Major Depressive Disorder. *J. affective Disord.* 245, 1119–1125. doi:10.1016/j.jad.2018.12.016
- Livak, K. J., and Schmittgen, T. D. (2001). Analysis of Relative Gene Expression Data Using Real-Time Quantitative PCR and the 2^{-ΔΔCT} Method. *Methods* 25 (4), 402–408. doi:10.1006/meth.2001.1262
- Longa, E. Z., Weinstein, P. R., Carlson, S., and Cummins, R. (1989). Reversible Middle Cerebral Artery Occlusion without Craniectomy in Rats. *Stroke* 20 (1), 84–91. doi:10.1161/01.str.20.1.84
- Ludka, F. K., Dal-Cim, T., Binder, L. B., Constantino, L. C., Massari, C., and Tasca, C. I. (2017). Atorvastatin and Fluoxetine Prevent Oxidative Stress and Mitochondrial Dysfunction Evoked by Glutamate Toxicity in Hippocampal Slices. *Mol. Neurobiol.* 54 (5), 3149–3161. doi:10.1007/s12035-016-9882-6
- Ma, B., Chen, J., Mu, Y., Xue, B., Zhao, A., Wang, D., et al. (2018). Proteomic Analysis of Rat Serum Revealed the Effects of Chronic Sleep Deprivation on Metabolic, Cardiovascular and Nervous System. *PLoS one* 13 (9), e0199237. doi:10.1371/journal.pone.0199237
- Ma, G.-D., Chiu, C.-H., Hsu, Y.-J., Hou, C.-W., Chen, Y.-M., and Huang, C.-C. (2017). Changbai Mountain Ginseng (Panax Ginseng C.A. Mey) Extract Supplementation Improves Exercise Performance and Energy Utilization and Decreases Fatigue-Associated Parameters in Mice. *Molecules* 22 (2), 237. doi:10.3390/molecules22020237
- Ma, W., Song, J., Wang, H., Shi, F., Zhou, N., Jiang, J., et al. (2019). Chronic Paradoxical Sleep Deprivation-Induced Depression-like Behavior, Energy Metabolism and Microbial Changes in Rats. *Life Sci.* 225, 88–97. doi:10.1016/j.lfs.2019.04.006
- Osteen, C. L., Giza, C. C., and Hovda, D. A. (2004). Injury-induced Alterations in N-Methyl-D-Aspartate Receptor Subunit Composition Contribute to Prolonged 45calcium Accumulation Following Lateral Fluid Percussion. *Neuroscience* 128 (2), 305–322. doi:10.1016/j.neuroscience.2004.06.034
- Perez-Riverol, Y., Csordas, A., Bai, J., Bernal-Llinares, M., Hewapathirana, S., Kundu, D. J., et al. (2019). The PRIDE Database and Related Tools and Resources in 2019: Improving Support for Quantification Data. *Nucleic Acids Res.* 47 (D1), D442–D450. doi:10.1093/nar/gky1106
- Riaza Bermudo-Soriano, C., Perez-Rodriguez, M. M., Vaquero-Lorenzo, C., and Baca-Garcia, E. (2012). New Perspectives in Glutamate and Anxiety. *Pharmacol. Biochem. Behav.* 100 (4), 752–774. doi:10.1016/j.pbb.2011.04.010
- Sanacora, G., Treccani, G., and Popoli, M. (2012). Towards a Glutamate Hypothesis of Depression. *Neuropharmacology* 62 (1), 63–77. doi:10.1016/j.neuropharm.2011.07.036
- Sanacora, G., Zarate, C. A., Krystal, J. H., and Manji, H. K. (2008). Targeting the Glutamatergic System to Develop Novel, Improved Therapeutics for Mood Disorders. *Nat. Rev. Drug Discov.* 7 (5), 426–437. doi:10.1038/nrd2462
- Schmitt, K., Holsboer-Trachsler, E., and Eckert, A. (2016). BDNF in Sleep, Insomnia, and Sleep Deprivation. *Ann. Med.* 48 (1-2), 42–51. doi:10.3109/0853890.2015.1131327
- Serra, M. P., Poddighe, L., Boi, M., Sanna, F., Piludu, M. A., Corda, M. G., et al. (2017). Expression of BDNF and trkB in the hippocampus of a Rat Genetic Model of Vulnerability (Roman Low-Avoidance) and Resistance (Roman High-Avoidance) to Stress-Induced Depression. *Brain Behav.* 7 (10), e00861. doi:10.1002/brb3.861
- Sommer, C. J. (2017). Ischemic Stroke: Experimental Models and Reality. *Acta Neuropathol.* 133 (2), 245–261. doi:10.1007/s00401-017-1667-0
- Song WT, X. L., and Ren, J. X. (2015). Effect of Jiedu Tongluo Capsule on Qi-Relieving Depression in Rats with Depression after Stroke. *World Sci. Technol.* 7, 1380–1385. Available at: <https://kns.cnki.net/kcms/detail/detail.aspx?dbcode=CJFD&dbname=CJFDLAST2015&filename=SJKX201507012&v=aQUdrWa6z%25mmd2FXwzFakXOSJ7vpRn6CLOREZM99FcJx78Y69HwONj5X1RYfujKKqgr4>
- Soreca, I. (2014). Circadian Rhythms and Sleep in Bipolar Disorder. *Curr. Opin. Psychiatry* 27 (6), 467–471. doi:10.1097/YCO.0000000000000108
- Sun, Y., Sun, X., Qu, H., Zhao, S., Xiao, T., and Zhao, C. (2017). Neuroplasticity and Behavioral Effects of Fluoxetine after Experimental Stroke. *Rnn* 35 (5), 457–468. doi:10.3233/rnn-170725
- Szydlowska, K., and Tymianski, M. (2010). Calcium, Ischemia and Excitotoxicity. *Cell Calcium* 47 (2), 122–129. doi:10.1016/j.ceca.2010.01.003
- Tanqueiro, S. R., Ramalho, R. M., Rodrigues, T. M., Lopes, L. V., Sebastião, A. M., and Diógenes, M. J. (2018). Inhibition of NMDA Receptors Prevents the Loss of BDNF Function Induced by Amyloid β. *Front. Pharmacol.* 9, 237. doi:10.3389/fphar.2018.00237
- Towfighi, A., Ovbiagele, B., El Hussein, N., Hackett, M. L., Jorge, R. E., Kissela, B. M., et al. (2017). Poststroke Depression: A Scientific Statement for Healthcare Professionals from the American Heart Association/American Stroke Association. *Stroke* 48 (2), e30–e43. doi:10.1161/str.0000000000000113
- Villa, R., Ferrari, F., and Moretti, A. (2017). Post-stroke Depression: Mechanisms and Pharmacological Treatment. *Pharmacol. Ther.* 184, 131–144. doi:10.1016/j.pharmthera.2017.11.005
- Wang, H., Qian, W.-J., Chin, M. H., Petyuk, V. A., Barry, R. C., Liu, T., et al. (2006). Characterization of the Mouse Brain Proteome Using Global Proteomic Analysis Complemented with Cysteinyln-Peptide Enrichment. *J. Proteome Res.* 5 (2), 361–369. doi:10.1021/pr0503681
- Wang, Z., Chen, L., Zhang, L., and Wang, X. (2017). Paradoxical Sleep Deprivation Modulates Depressive-like Behaviors by Regulating the MAOA Levels in the Amygdala and hippocampus. *Brain Res.* 1664, 17–24. doi:10.1016/j.brainres.2017.03.022
- Wang, Z., Shi, Y., Liu, F., Jia, N., Gao, J., Pang, X., et al. (2018). Diverseiform Etiologies for Post-stroke Depression. *Front. Psychiatry* 9, 761. doi:10.3389/fpsy.2018.00761
- Waterhouse, E. G., An, J. J., Orefice, L. L., Baydyuk, M., Liao, G.-Y., Zheng, K., et al. (2012). BDNF Promotes Differentiation and Maturation of Adult-Born Neurons through GABAergic Transmission. *J. Neurosci.* 32 (41), 14318–14330. doi:10.1523/jneurosci.0709-12.2012
- Xu, P., Wang, K. Z., Lu, C., Dong, L. M., Le Zhai, J., Liao, Y. H., et al. (2016). Antidepressant-like Effects and Cognitive Enhancement of the Total Phenols Extract of Hemerocallis Citrina Baroni in Chronic Unpredictable Mild Stress Rats and its Related Mechanism. *J. ethnopharmacology* 194, 819–826. doi:10.1016/j.jep.2016.09.023

- Zafra, F., Castrén, E., Thoenen, H., and Lindholm, D. (1991). Interplay between Glutamate and Gamma-Aminobutyric Acid Transmitter Systems in the Physiological Regulation of Brain-Derived Neurotrophic Factor and Nerve Growth Factor Synthesis in Hippocampal Neurons. *Proc. Natl. Acad. Sci.* 88 (22), 10037–10041. doi:10.1073/pnas.88.22.10037
- Zhang, E., and Liao, P. (2020). Brain-derived Neurotrophic Factor and Post-stroke Depression. *J. Neurosci. Res.* 98 (3), 537–548. doi:10.1002/jnr.24510
- Zhang, Y., Liu, J., Yang, B., Zheng, Y., Yao, M., Sun, M., et al. (2018). Ginkgo Biloba Extract Inhibits Astrocytic Lipocalin-2 Expression and Alleviates Neuroinflammatory Injury via the JAK2/STAT3 Pathway after Ischemic Brain Stroke. *Front. Pharmacol.* 9, 518. doi:10.3389/fphar.2018.00518
- Zhao, A.-m., Qiu, W.-r., Mao, L.-j., Ren, J.-g., Xu, L., Yao, M.-j., et al. (2018). The Efficacy and Safety of Jiedu Tongluo Granules for Treating Post-stroke

Depression with Qi Deficiency and Blood Stasis Syndrome: Study Protocol for a Randomized Controlled Trial. *Trials* 19 (1), 275. doi:10.1186/s13063-018-2633-4

Conflict of Interest: The authors declare that the research was conducted in the absence of any commercial or financial relationships that could be construed as a potential conflict of interest.

Copyright © 2021 Zhao, Ma, Xu, Yao, Zhang, Xue, Ren, Chang and Liu. This is an open-access article distributed under the terms of the Creative Commons Attribution License (CC BY). The use, distribution or reproduction in other forums is permitted, provided the original author(s) and the copyright owner(s) are credited and that the original publication in this journal is cited, in accordance with accepted academic practice. No use, distribution or reproduction is permitted which does not comply with these terms.



Branched-Chain Amino Acids Catabolism Pathway Regulation Plays a Critical Role in the Improvement of Leukopenia Induced by Cyclophosphamide in 4T1 Tumor-Bearing Mice Treated With Lvjiaobuxue Granule

OPEN ACCESS

Edited by:

Jia-bo Wang,
Capital Medical University, China

Reviewed by:

Liwen Han,
Shandong First Medical University,
China
Kuo Zhang,
Shenyang Pharmaceutical University,
China

*Correspondence:

Jun-sheng Tian
jstian@sxu.edu.cn
Xiang-ping Xu
xxp@hnjzt.com
Sheng Huang
huangsheng32@126.com

Specialty section:

This article was submitted to
Ethnopharmacology,
a section of the journal
Frontiers in Pharmacology

Received: 22 January 2021

Accepted: 02 August 2021

Published: 25 October 2021

Citation:

Tian J, Zhao H, Gao Y, Wang Q,
Xiang H, Xu X, Huang S, Yan D and
Qin X (2021) Branched-Chain Amino
Acids Catabolism Pathway Regulation
Plays a Critical Role in the
Improvement of Leukopenia Induced
by Cyclophosphamide in 4T1 Tumor-
Bearing Mice Treated With
Lvjiabuxue Granule.
Front. Pharmacol. 12:657047.
doi: 10.3389/fphar.2021.657047

Jun-sheng Tian^{1,2*}, Hui-liang Zhao¹, Yao Gao¹, Qi Wang¹, Huan Xiang³, Xiang-ping Xu^{2*},
Sheng Huang^{2,4*}, Dong-lan Yan² and Xue-mei Qin¹

¹Modern Research Center for Traditional Chinese Medicine, Shanxi University, Taiyuan, China, ²Jiuzhitang Co. Ltd., Changsha, China, ³School of Physical Education, Shanxi University, Taiyuan, China, ⁴School of Life Science and Technology, Xi'an Jiaotong University, Xi'an, China

Background: Cyclophosphamide is a common tumor chemotherapy drug used to treat various cancers. However, the resulting immunosuppression leads to leukopenia, which is a serious limiting factor in clinical application. Therefore, the introduction of immunomodulators as adjuvant therapy may help to reduce the hematological side effects of cyclophosphamide. Lvjiabuxue granule has been widely used in the clinical treatment of gynecological diseases such as anemia and irregular menstruation. Recently, it has been found to increase the function of white blood cells, but its mechanism of action is still unclear. We aimed to reveal the mechanisms of Lvjiabuxue granule against acute leukopenia by an integrated strategy combining metabolomics with network pharmacology.

Methods: Subcutaneously inoculated 4T1 breast cancer cells to prepare tumor-bearing mice, intraperitoneal injection of cyclophosphamide to establish a 4T1 tumor-bearing mice leukopenia animal model, using pharmacodynamic indicators, metabolomics, network pharmacology and molecular biology and other technical methods. To comprehensively and systematically elucidate the effect and mechanism of Lvjiabuxue granule in improving cyclophosphamide-induced leukopenia in 4T1 tumor-bearing mice.

Abbreviations: BCAAs, Branched-chain amino acids; LBG, Lvjiabuxue granule; TCM, Traditional Chinese medicine; DST, Diyu-shengbai tablets; WBC, white blood cell count; NE, neutrophil count; LY, lymphocyte count; MO, monocytes count; RBC, red blood cell count; HGB, hemoglobin; HCT, red blood cell volume; PLT, platelet count; MCV, mean red cell volume; MCH, mean corpuscular hemoglobin; TSP, 2,2,3,3-trimethyl siliconalkyl propionate; PW, pulse width; PCA, principal component analysis; PLS-DA, partial least-squares discriminant analysis; OPLS-DA, Orthogonal-projection to latent structure-discriminant analysis; BCKDHA, branched-chain keto acid dehydrogenase E1, alpha polypeptide; ACADS, Acyl-CoA Dehydrogenase Short Chain; TMAO, Trimethylamine-N-oxide; PC, Phosphocholine; GPC, Glycerophosphocholine.

Results: Lvjiaobuxue granule can improve the blood routine parameters and organ index levels of the leukopenia model of 4T1 tumor-bearing mice. Metabolomics studies revealed that 15 endogenous metabolites in the spleen of mice were considered as potential biomarkers of Lvjiaobuxue granule for their protective effect. Metabonomics and network pharmacology integrated analysis indicated that Lvjiaobuxue granule exerted the leukocyte elevation activity by inhibiting the branched-chain amino acids (BCAAs) degradation pathway and increasing the levels of valine, leucine and isoleucine. The results of molecular biology also showed that Lvjiaobuxue granule can significantly regulate the key enzymes in the catabolism of BCAAs, which further illustrates the importance of BCAAs in improving leukopenia.

Conclusion: Lvjiaobuxue granule exerts obvious pharmacological effects on the leukopenia model of 4T1 tumor-bearing mice induced by cyclophosphamide, which could be mediated by regulating the branched-chain amino acid degradation pathway and the levels of valine, leucine and isoleucine.

Keywords: Lvjiaobuxue granule, leucopenia, metabolomics, biological targets network, branched-chain amino acids

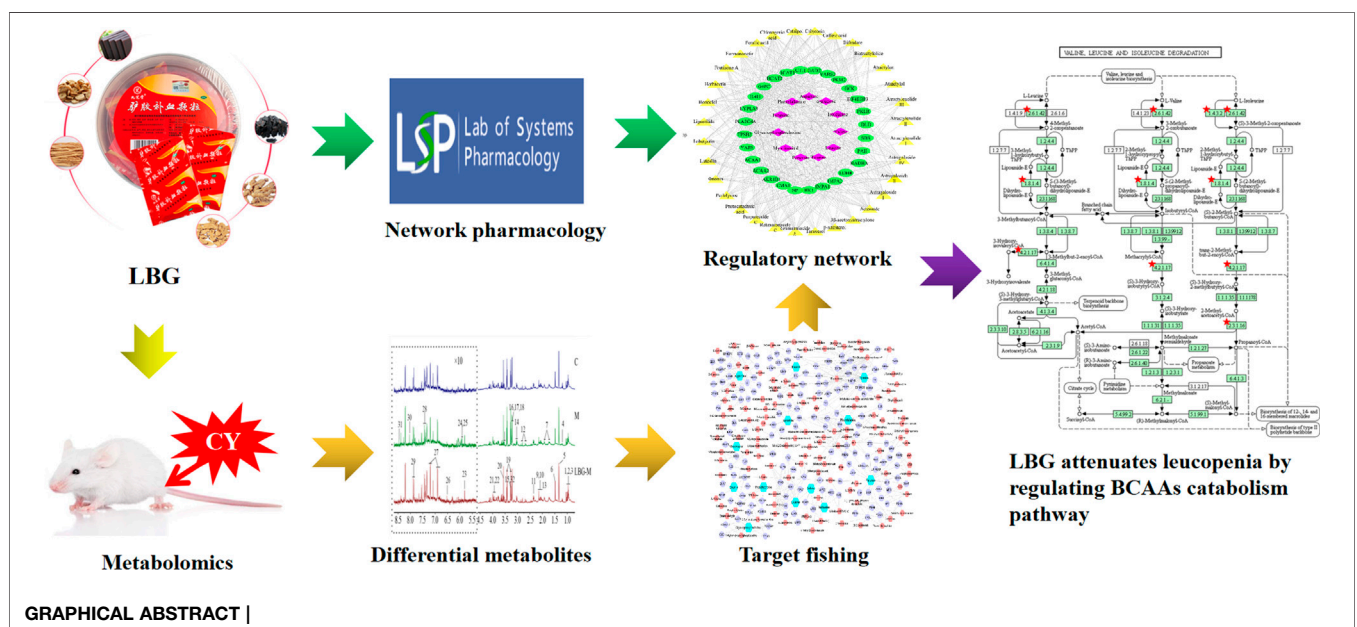
INTRODUCTION

Cyclophosphamide is the most common cancer chemotherapy agent and used in anticancer for various types of cancer, especially breast cancer (Futamura et al., 2017; Hung et al., 2017). Unfortunately, immunosuppression induced by cyclophosphamide causes the occurrence of leukopenia, which is a seriously limiting factor in a clinical application (Deng et al., 2018; Sun et al., 2018). Therefore, introducing immunomodulatory agents as supportive therapy might be useful in alleviating the hematotoxicity side effects of cyclophosphamide.

After constant efforts, the treatment against the side effects of chemotherapy still leaves much to be desired. In recent years, prescriptions are composed of a combination of multiple drugs, which are considered to be a promising treatment strategy to improve

the anti-tumor effect and reduce the side effects of chemotherapy drugs (Mellor et al., 2010). Traditional Chinese Medicine (TCM) prescriptions are usually made up of different kinds of herbs, which have the advantages of low toxicity and multiple targets (Gu et al., 2014). Through overall and multi-target therapies, it has a comprehensive therapeutic effect in multi-factorial diseases.

Lvjiaobuxue granule is a new kind of good medicine for the treatment of Qi and blood deficiency and fatigue. It fills the blank of *Colla corii asini*, *Angelica sinensis* (Oliv.) Diels and other compound preparations in the treatment of deficiency of Qi and blood. It is known as the “Holy Medicine in Blood” and widely used in the clinical treatment of gynecological diseases such as anemia, irregular menstruation and so on. Besides, a large number of clinical studies have found that it has the effect of increasing white blood cells (Li and Fan, 1998; Yu, 1999; He et al.,



2018). However, the research on drug pharmacological effects and mechanism of action is relatively rare. Lvjiaobuxue granule generally comprised of six herbs: *Colla corii asini* (Equidae; *Equus asinus* L. skin), *Astragalus mongholicus* Bunge (Fabaceae; *Astragalus mongholicus* radix), *Codonopsis pilosula* (Franch.) Nannf (Campanulaceae; *Codonopsis pilosula* radix), *Rehmannia glutinosa* (Gaertn.) DC (Orobanchaceae; *Rehmannia glutinosa* root), *Atractylodes macrocephala* Koidz (Asteraceae; *Atractylodes macrocephala* rhizoma) and *Angelica sinensis* (Oliv.) Diels (Apiaceae; *Angelica sinensis* radix) at a ratio of 36:30:30:20:15:10.

Specific immune function can be stimulated by *Colla corii asini* (Equidae; *Equus asinus* L. skin) in cyclophosphamide-induced mice (An et al., 2018). The compatibility of *Astragalus mongholicus* Bunge (Fabaceae; *Astragalus mongholicus* radix) and *Angelica sinensis* (Oliv.) Diels (Apiaceae; *Angelica sinensis* radix) [Such as Danggui-buxue Tang is the famous prescription and could increase the quantity of bone marrow mononuclear cells and peripheral blood leukocytes, enhance immunity and improve microcirculation (Zhang et al., 2019)]. Some other previous studies have also demonstrated that *Codonopsis pilosula* (Franch.) Nannf (Campanulaceae; *Codonopsis pilosula* radix), *Rehmannia glutinosa* (Gaertn.) DC (Orobanchaceae; *Rehmannia glutinosa* root) and *Atractylodes macrocephala* Koidz (Asteraceae; *Atractylodes macrocephala* rhizoma) exhibited effects of leukocyte elevation and immuno-enhancement (Huang et al., 2018; Tang et al., 2018). Moreover, all the above herbs in the Lvjiaobuxue granule are commonly and safely used in the formula of TCM, and rare adverse reactions were reported in clinical applications. However, the action mechanism of Lvjiaobuxue granule in the treatment of leukopenia was still poorly understood.

In recent years, metabolomics is used to clarify the scientific effects related to the effectiveness mechanism, material basis and compatibility of TCM. It will provide the technical support for the evaluation of the effectiveness of TCM, the basis of prescription substances and the understanding essence of TCM syndromes (Hu et al., 2018; Wang et al., 2018; Sun et al., 2019). However, traditional metabolomics could only reflect the terminal variation of disease and treatment (Simón-Manso et al., 2013; Singh et al., 2017). Network pharmacology as an alternative system-level method to find new drug candidates, through the entire drug-disease network, looking for multi-target drugs to reduce side effects. Network pharmacology alone can only predict the possibility of compound-target combinations and pathway analysis (Gertsch, 2011; Zhong et al., 2018). Therefore, we integrated metabolomics with network pharmacology. Metabolomics was applied to determine the influences of Lvjiaobuxue granule on leukopenia and to identify the essential metabolites. Subsequently, network pharmacology was used to analyze the proteins and reactions that regulate metabolites, as well as the targets of Lvjiaobuxue granule. In general, this strategy made up for the lack of experimental verification in network pharmacology and the lack of upstream molecular mechanisms and drug binding targets in metabolomics. This strategy will hopefully contribute to a better understanding of the therapeutic principle of natural compounds for the treatment of leukopenia.

In this study, we firstly constructed a cyclophosphamide induced leukopenia model in 4T1 tumor-bearing mice, and then used pharmacodynamic indicators, metabolomics, network pharmacology, and molecular biology techniques to

comprehensively and systematically clarify Lvjiaobuxue granule improve the effect and mechanism of cyclophosphamide-induced leukopenia in 4T1 tumor-bearing mice.

MATERIALS AND METHODS

Materials

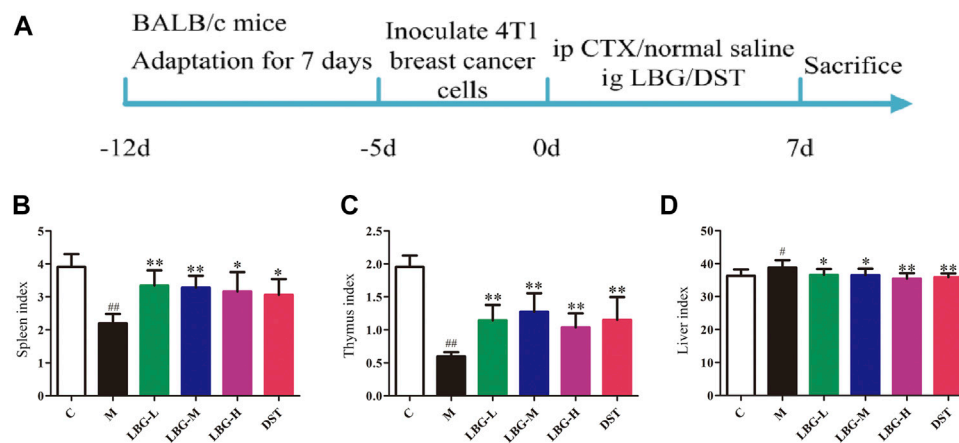
Cyclophosphamide was obtained from Jiangsu Shengdi Pharmaceutical Co., Ltd (Batch No. 18051125, Jiangsu, China). The 0.5 ml EDTA-K₂ anticoagulant tube and DMEM high-glucose medium and EDTA trypsin were purchased from Boshide Bioengineering Co., Ltd. Fetal bovine serum was obtained from Shanghai ShengGong Biological Engineering Co., Ltd. D₂O was purchased from Norell (Landisville, United States). K₂HPO₄·3H₂O and NaH₂PO₄·2H₂O were obtained from Wuhan Yuancheng Technology Development Co., Ltd (Wuhan, China). Lvjiaobuxue granule was purchased from Jiuzhitang Co., Ltd (Batch No. 201802029, Hunan, China), which production method conforms to the standard of Chinese Pharmacopoeia (2015 edition). Diyu-shengbai tablets were obtained from Chengdu Diao Co., Ltd (Batch No. Z20026497, Chengdu, China). The enzyme-linked immunosorbent assay (ELISA) kits were obtained from MEIMIAN (Jiangsu, China).

Animals and Cell Lines

Inbred strain female (6–8 weeks old) BALB/c mice, weighing 18–20 g, provided by Vital River Laboratory Animal Technology Co., Ltd (Beijing) (License number SCXK-2016-0006). The animals were kept at room temperature (24 ± 1)°C, humidity (60 ± 5)%, and freely eating under the natural rhythm of day and night before the experiments. The murine mammary 4T1 cancer cells were supported by Cell Bank of Shanghai, Chinese Academy of Science (CAS, Shanghai, China). All animal experiments were conducted following the NIH Guidelines for Care and Use of Laboratory Animals (U.S.A) and the Prevention of Cruelty to Animals Act (1986) of China, and all experimental procedures tried to minimize the suffering of experimental animals. The animal use protocol listed below has been reviewed and approved by the Committee of Scientific Research at Shanxi University (CSRSX), and the approved number was SXULL2018012.

Establishment and Treatment of Leukopenia Model in 4T1 Tumor-Bearing Mice

Animals were randomly divided into six cyclophosphamide-induced groups: control group (C), model group (M), low dose of Lvjiaobuxue granule group (LBG-L), moderate dose of Lvjiaobuxue granule group (LBG-M), high dose of Lvjiaobuxue granule group (LBG-H), and Diyu-shengbai tablets group (DST), each group was consist of eight mice. Except control group, the mice in other groups were first inoculated with breast cancer cells under the armpits to establish a tumor model, and then cyclophosphamide was given to establish a leukopenia model. Five days after mice were inoculated with 4T1 cells on the right armpit (10⁷ cells per animal), all mice developed subcutaneous tumors. On the first, third, fifth and seventh day,



the model of leukopenia in 4T1 tumor bearing mice was established by intraperitoneal injection of 80 mg/kg cyclophosphamide. The mice in LBG-L, LBG-M, or LBG-H groups were administered Lvjiabuxue granule (3 g/kg, 6 g/kg, 12 g/kg) suspension daily, and the mice in the DST group were administered Diyu-shengbai tablets (0.14 g/kg) suspension daily. Mice in the control and model groups received an equal volume of vehicle orally. During the whole experiment, the drug was administered while modeling. The treatment lasted for 7 days, and the state of the mice was observed daily (Figure 1A).

Sample Collection and Determination

After 1 h of the last treatment on the seventh day, 0.4 ml blood samples were collected into a 1.0 ml tube with EDTA within *via* the orbital blood. Animal blood analyzer (HEMAVET950) was applied to evaluate peripheral blood routine parameters of 400 μ l whole blood: white blood cell count (WBC), neutrophil count (NE), lymphocyte count (LY), monocytes count (MO), red blood cell count (RBC), hemoglobin (HGB), red blood cell volume (HCT), platelet count (PLT), mean red cell volume (MCV) and mean corpuscular hemoglobin (MCH). On the eighth day, mice were sacrificed, and spleen, thymus and liver tissues were immediately weighed and collected. The calculation formula of the organ index is as follows: organ index = organ weight (mg)/body weight (g). The spleen was quickly transferred to a refrigerator at -80°C and used for metabolomics analysis.

Sample Preparation for NMR Measurements

After thawing the spleen tissue, took about 40 mg, cut it (on ice), added 650 μ l of MeOH and H_2O (v/v, 2:1) to a 2 ml centrifuge tube, and homogenized and extracted twice on the ice bath. The homogenate centrifuged at 4°C , 13,000 $\text{r}\cdot\text{min}^{-1}$ for 15 min. The supernatants were combined, transferred to a 2 ml centrifuge tube and blown with nitrogen. The dried sample was dissolved in 700 μ l of phosphate buffer (pH 7.40, containing D_2O , 0.1 mol/L, $\text{Na}_2\text{HPO}_4/\text{NaH}_2\text{PO}_4$, 0.01% TSP), centrifuged at 13°C , 13,000

$\text{r}\cdot\text{min}^{-1}$ for 20 min, 600 μ l supernatant was transferred into a 5 mm NMR tube for ^1H -NMR analysis.

Metabolomics Analysis

The ^1H -NMR spectral data were collected on a Bruker 600 MHz AVANCE III NMR spectrometer (Bruker, Germany). The sample was the Noesygppr 1 day sequence to suppress the water peak. The number of scans was 64 scans, and each scan required an acquisition time of 2.654 s. The specific parameters were as follows: spectral width was 12 345.7 Hz; spectrum size was 65 536 data points; pulse width (PW) was 30° (12.7 μ s); fourier transform was 0.3 Hz and relaxation delay time was 1.0 s. The ^1H -NMR spectrum of the spleen was corrected for chemical shifts using TSP ($\delta 0.00$) as the standard. The spectrum in the region of $\delta 0.60$ to 9.49 was divided into 0.01 equal widths and integrated. All resulting integration data are “mass” normalized to eliminate weight differences of spleen tissue.

Statistical Analysis

Simca-P 14.1 (Umetrics, Sweden) was used to perform multivariate data analysis. Firstly, by principal component analysis (PCA) of the normalized data, to identify the degree of dispersion between the control group and the model group, and the outliers were eliminated. Next, partial least-squares discriminant analysis (PLS-DA) was used to distinguish the differences in metabolic profiles among the control, model and drug groups. Orthogonal-projection to latent structure-discriminant analysis (OPLS-DA) was used to find differential metabolites between the control group and the model group. Finally, GraphPad Prism 7 (GraphPad Software, Inc., La Jolla, CA, United States) and SPSS 21.0 (SPSS Software, Inc., Chicago, IL, United States) were used for statistical analysis by two-way ANOVA and Dunnett multiple comparisons. $\text{VIP} > 1$ and $p < 0.05$ were used as differential metabolites.

The data were expressed as the mean \pm standard deviation (SD) of the mean from at least three independent experiments. $p < 0.05$ was considered to be statistically significant.

Biological Targets Network Analysis

All components of Lvjiaobuxue granule were collected from the TCMSP database (<https://tcmsp.com/tcmssp.php>, Version 2). For all ingredients, the initial structure formats (e.g., mol2 and SDF) were transformed into a unified SDF format using the Open Babel toolkit (version 2.4.1). The ingredients with suitable OB $\geq 30\%$, DL ≥ 0.18 and active or higher contents in the drugs reported in the literature were chosen as candidate ingredients for further research, which were used as a selection criterion for the ingredients in the TCM. All databases and software mentioned above are public.

The PharmMapper server (<http://www.lilab-ecust.cn/pharmmapper/>) was used for potential target prediction analysis. Metabolite data were imported in Metascape, a plugin of Cytoscape 3.7.1 and subjected to metabolic enzyme analysis. Finally, Cytoscape 3.7.1 software was used to construct the “herb-chemical components-targets-pathway-metabolite” regulatory network of Lvjiaobuxue granule for leukopenia treatment.

Determination of the Levels of BCKDHA and ACADS

To further verify the results of biological targets network, the content of the key rate-limiting enzymes BCKDHA (branched-chain keto acid dehydrogenase E1, alpha polypeptide) and ACADS (acyl-CoA dehydrogenase short chain) on the BCAAs degradation pathway were determined. The content of these enzymes will affect the levels and degradation rate of BCAAs. The levels of BCKDHA and ACADS in the liver tissue lysates were determined by ELISA kits according to manufacturer instructions.

RESULTS

Quality Control of Lvjiaobuxue Granule

To ensure the quality control of Lvjiaobuxue granule used in this study, High Performance Liquid Chromatography (HPLC) analysis was performed. The preparation of Lvjiaobuxue granule chemical determination was referred to China Pharmacopoeia (2020 version). The HPLC system consisted of a Dual-Gradient Analytical LC System (UltiMate 3000, Dionex, United States) equipped with DGP-3600SD Pump, SRD-3600 Degasser, WPS-3000SL Autosampler, TCC-3000RS Column Compartment, DAD-3000 Diode Array Detector and Sedex-75 Evaporative Light-Scattering Detector (ELSD). Peak areas were calculated with Chromeleon 6.8 Chromatography Data System. Kromasil C18 (250 mm \times 4.6 mm, 5 μ m). Acetonitrile-water (40:60) was used as the mobile phase. The Carrier-gas velocity was 1.0 ml min⁻¹ and the temperature of drift tube was 45°C. Taking Astragaloside IV as an example, the identified results were shown in **Supplementary Figure S1**.

Effect of Lvjiaobuxue Granule on Blood Routine Parameters and Organ Indexes of 4T1 Tumor-Bearing Mice Induced by Cyclophosphamide

The biochemical indexes of the peripheral blood were observed by evaluating the blood toxicity of cyclophosphamide. The

parameters of WBC, NE, LY, MO, RBC, HGB, HCT, and MCH in the model group were significantly lower than those in the control group ($p < 0.01$; **Table 1**), and the PLT parameters were significantly higher than those in the control group ($p < 0.05$; **Table 1**). The increase and decrease of these peripheral blood routine parameters (especially WBC less than $2.0 \times 10^9/L$, NE significantly reduced) were the main diagnostic criteria of leukopenia, indicating that the model of leukopenia was successfully replicated. Compared to the model group, the expressions of WBC, NE, LY, MO, RBC, HGB, and MCH in the LBG-L, LBG-M and LBG-H were significantly increased ($p < 0.05$; **Table 1**). Compared to the control group, the mice in the model group had an enlargement of the liver ($p < 0.05$; **Figure 1D**), and reduction of the spleen ($p < 0.01$; **Figure 1C**) and thymus ($p < 0.01$; **Figure 1C**). The administration of Lvjiaobuxue granule and DST over 7 days reversed the viscera lesions of mice with hematopoietic dysfunction ($p < 0.05$; **Figure 1**).

¹H-NMR Metabolomics Analysis and Multivariate Data Analysis

Analysis of ¹H-NMR Spectrum of Spleen Tissue

The representative ¹H-NMR spectra of the extracts from spleen tissue of mice in control group, model group and LBG-M group were shown in **Figure 2**. Firstly, the ¹H-NMR data were analyzed by chemical shift values, coupling constants and peak splitting conditions, and further identified by Human Metabolome Database [HMDB (<http://www.hmdb.ca/>)], Biological Magnetic Resonance Data Bank [BMRB (<http://www.bmrwisc.edu/>)] and published literature. In total, 32 endogenous metabolites were identified, belonging to amino acids, organic acids, sugars, lipids, etc. the details of the metabolites were shown in **Table 2**.

Lvjiaobuxue Granule Regulates Metabolic Disorders of Leukopenia Induced by Cyclophosphamide in 4T1 Tumor-Bearing Mice

To explore the metabolites levels in 4T1 tumor-bearing mice with leukopenia induced by cyclophosphamide, the supervised multivariate methods PLS-DA and OPLS-DA were used for processing (**Figure 3**). The PLS-DA pattern recognition analysis of all the group trends was shown in **Figure 3A**, in which the control group was completely separated from the model group, and the LBG-L, LBG-M, LBG-H groups were separated from the model group, with a tendency closer to the control group. It was suggested that CTX caused the disorder of mice spleen metabolites. After administration of LBG, the metabolic profile of the mice's spleen was significantly close to that of the control group, suggesting that LBG may exert a whitening effect by adjusting the metabolites of the spleen.

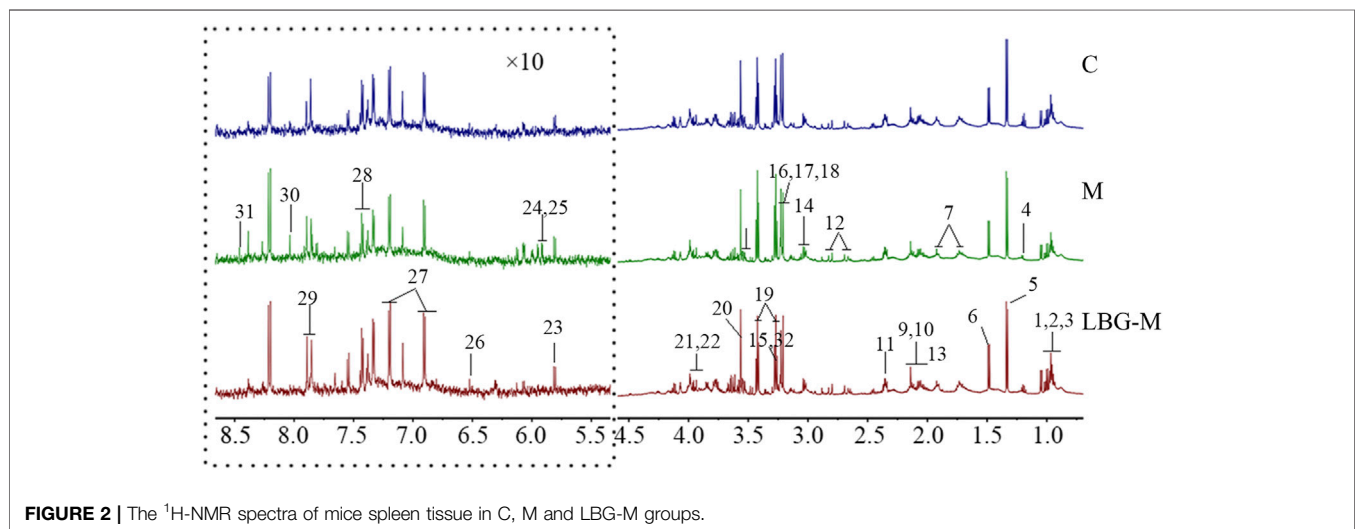
The validity of the analysis was performed by using 200 permutation tests, in which all R^2 and Q^2 values were lower than the original ones (Intercepts: $R^2 = 0.854$, $Q^2 = 0.649$) (**Figure 3B**). Furthermore, differential metabolites between the control and the model groups were discovered by OPLS-DA, which was a supervised pattern recognition method that could improve the discovery effect of differential metabolites (**Figure 3C**). The corresponding loading (S + V)-plot with

TABLE 1 | Changes in indexes of blood routine examination on leukopenia mice with LBG treatment ($n = 8$).

Groups	WBC ($10^9/L$)	NE ($10^9/L$)	LY ($10^9/L$)	MO ($10^9/L$)	RBC ($10^{12}/L$)
C	4.63 \pm 0.58	0.52 \pm 0.11	3.61 \pm 0.42	0.18 \pm 0.04	9.99 \pm 0.43
M	1.83 \pm 0.25 ^{##}	0.25 \pm 0.04 ^{##}	1.45 \pm 0.21 ^{##}	0.13 \pm 0.04 [#]	8.01 \pm 0.23 ^{##}
LBG-L	3.03 \pm 0.44 ^{**}	0.54 \pm 0.12 ^{**}	2.24 \pm 0.35 ^{**}	0.25 \pm 0.04 ^{**}	8.69 \pm 0.18 ^{**}
LBG-M	3.33 \pm 0.48 ^{**}	0.55 \pm 0.14 ^{**}	2.41 \pm 0.38 ^{**}	0.36 \pm 0.10 ^{**}	8.63 \pm 0.12 ^{**}
LBG-H	2.60 \pm 0.20 ^{**}	0.41 \pm 0.16 [*]	1.88 \pm 0.12 ^{**}	0.31 \pm 0.09 ^{**}	8.44 \pm 0.18 ^{**}
DST	2.79 \pm 0.36 ^{**}	0.36 \pm 0.14 [*]	2.08 \pm 0.31 ^{**}	0.30 \pm 0.09 ^{**}	8.00 \pm 0.29

Groups	HGB (g/L)	HCT (%)	PLT ($10^9/L$)	MCV (fL)	MCH (pg)
C	149.50 \pm 2.78	58.69 \pm 1.36	539.13 \pm 54.19	58.66 \pm 0.64	15.56 \pm 0.37
M	124.50 \pm 2.56 ^{##}	49.50 \pm 2.32 ^{##}	615.75 \pm 52.30 [#]	58.89 \pm 0.40	14.28 \pm 0.15 ^{##}
LBG-L	135.00 \pm 5.93 ^{**}	52.11 \pm 2.08 [*]	605.63 \pm 40.60	59.08 \pm 0.48	15.59 \pm 0.24 ^{**}
LBG-M	132.75 \pm 1.04 ^{**}	51.39 \pm 1.03	602.25 \pm 22.28	59.35 \pm 0.61	15.69 \pm 0.24 ^{**}
LBG-H	130.25 \pm 2.82 ^{**}	49.1 \pm 1.59	622.13 \pm 47.92	59.68 \pm 0.53	15.79 \pm 0.14 ^{**}
DST	128.88 \pm 5.06	50.09 \pm 2.25	612.38 \pm 58.24	60.16 \pm 0.59	15.60 \pm 0.33 ^{**}

Data are expressed as mean \pm SD. of eight mice. WBC, white blood cell count; NE, neutrophil count; LY, lymphocyte count; MO, monocytes count; RBC, red blood cell count; HGB, hemoglobin; HCT, red blood cell volume; PLT, platelet count; MCV, mean red cell volume; MCH, mean corpuscular hemoglobin. ^{*} $p < 0.05$ vs. C group; ^{##} $p < 0.01$ vs. C group; ^{*} $p < 0.05$ vs. M group; ^{**} $p < 0.01$ vs. M group.

**FIGURE 2** | The 1H -NMR spectra of mice spleen tissue in C, M and LBG-M groups.

color-coded was illustrated in **Figure 3D**, and the metabolites contributed to the leukocyte elevation effect were identified by corresponding (S + V)-plots and statistical analysis.

The disturbed metabolite variances of the different groups could be related to the decrease and increase of leukocytes. The changes of the differential metabolites between the control and the model groups in mice spleen were shown in **Figure 4**. Compared with the control group, the elevated levels of TMAO, pyruvate, GPC, taurine, aspartate and glutamate in the model group were evident in the spleen samples. Additionally, lower levels of choline, myo-inositol, tyrosine, valine, iso-leucine, PC, α -glucose, leucine, and phenylalanine in the spleen of the model group were observed. The changes of these endogenous metabolites were considered to be a direct result of the leukopenia. Meaningfully, the levels of metabolites were regulated by LBG treatment (**Figure 4**), suggesting that LBG may play a role in leukocyte by adjusting the level of metabolites.

Correlation Analysis of Differential Metabolites, Blood Routine Parameters and Organ Indexes

Blood routine parameters and organ index were used to evaluate important indicators of leukopenia. Through the correlation analysis with different metabolites, it was helpful to screen the key differential metabolites and clarify the regulatory role of different metabolites on the body. Pearson's correlation analysis was used to visualize the different metabolites, blood routine parameters and organ index. The correlation map was shown in **Figure 5A**, where the color reflects the correlation strength and sign, WBC, RBC, HGB, HCT, NE, LY, MO, and MCH were negatively correlated with glutamate, pyruvate, aspartate, GPC, taurine and positive correlations with valine, iso-leucine, leucine, choline, PC, myo-inositol, α -glucose, tyrosine, and phenylalanine. In addition, the fluctuation of spleen index was correlated with different metabolites ($p < 0.01$) (**Figure 5A**). The correlation network of blood routine parameters, organ index and differential metabolites based on Pearson's was shown in

TABLE 2 | ¹H-NMR assignments of major metabolites from mice spleen tissues.

No	Metabolites	Components assignment	Chemical shift (δ ¹ H ppm)
1	Isoleucine	δ -CH ₃ , γ' -CH ₃ , γ -CH ₂ , γ -CH ₂ ', β -CH, α -CH	0.94(t), 1.01(d), 1.27(m), 1.47(m), 1.98(m), 3.68(d)
2	Leucine	δ -CH ₃ , δ' -CH ₃ , β -CH ₂ , γ -CH, β -CH ₂ ', α -CH	0.96(d), 0.97(d), 1.70(m), 1.72(m), 1.74(m), 3.74(m)
3	Valine	γ -CH ₃ , γ' -CH ₃ , β -CH, α -CH	0.99(d), 1.05(d), 2.28(m), 3.62(d)
4	3-hydroxybutyrate	γ -CH ₃ , α -CH ₂ , α -CH ₂ ', β -CH	1.20(d), 2.31(dd), 2.41(dd), 4.16(m)
5	Lactate	β -CH ₃ , α -CH	1.33(d), 4.11(q)
6	Alanine	β -CH ₃ , α -CH	1.48(d), 3.78(d)
7	Lysine	γ -CH ₂ , γ -CH ₂ ', δ -CH ₂ , β -CH ₂ , ϵ -CH ₂ , CH	1.45(m), 1.51(m), 1.73(m), 1.91(m), 3.03(t), 3.76(t)
8	Glutamate	β -CH ₂ , β -CH ₂ ', γ -CH ₂ , CH	2.07(m), 2.13(m), 2.35(m), 3.76 (dd)
9	Methionine	δ -CH ₃ , β -CH ₂ , γ -CH ₂ , α -CH	2.13(s), 2.14(m), 2.64(t), 3.85(m)
10	Glutamine	β -CH ₂ , γ -CH ₂ , CH	2.14(m), 2.46(m), 3.78(t)
11	Pyruvate	CH ₃	2.37(s)
12	Aspartate	CH ₂ , CH ₂ ', CH	2.68(dd), 2.82(dd), 3.90(dd)
13	Acetate	CH ₃	1.93(s)
14	Creatine	CH ₃ , CH ₂	3.04(s), 3.94(s)
15	Myo-inositol	2-CH, 4/6-CH, 1/3-CH, 5-CH	3.29(t), 3.54(dd), 3.63(dd), 4.07(t)
16	Choline	(CH ₃) ₃ , N-CH ₂ , OH-CH ₂	3.21(s), 3.52(m), 4.07(m)
17	Phosphocholine (PC)	CH ₃ , N-CH ₂ , O-CH ₂	3.22(s), 3.59(m), 4.18(m)
18	Glycerophosphocholine (GPC)	CH ₃ , OH-CH ₂ , N-CH ₂ , OH-CH, NCH ₂ CH ₂	3.23(s), 3.68(m), 3.68(m), 3.92(m), 4.33(m)
19	Taurine	S-CH ₂ , N-CH ₂	3.28(t), 3.43(t)
20	Glycine	CH ₂	3.57(s)
21	α -glucose	4-CH, 2-CH, 3-CH, CH ₂ , CH ₂ ', 5-CH, 1-CH	3.41(m), 3.59(m), 3.73(m), 3.73(m), 3.85(m), 3.85(m), 5.26(d)
22	β -glucose	2-CH, 3/5-CH, CH ₂ , CH ₂ ', 1-CH	3.29(m), 3.52(m), 3.74(m), 3.91 (dd), 4.66 (d)
23	Uracil	5-CH, 6-CH	5.81(d), 7.55(d)
24	Uridine	ribose-2-CH, uracil-C-CH, uracil-N-CH	5.90(d), 5.92(d), 7.88(d)
25	Cytidine	ribose-2-CH, ring-5-CH, ring-6-CH	5.92(d), 6.07(d), 7.85(d)
26	Fumarate	CH	6.51(s)
27	Tyrosine	CH ₂ , CH ₂ ', N-CH, 3/5-CH, 2/6-CH	3.06(dd), 3.19(dd), 3.94(dd), 6.90(m), 7.20(m)
28	Phenylalanine	CH ₂ , CH ₂ ', N-CH, o-CH, p-CH, m-CH	3.13(dd), 3.28(dd), 4.00(dd), 7.33(m), 7.38(m), 7.43(m)
29	Xanthine	CH	7.90(s)
30	Hypoxanthine	2-CH, 7-CH	8.20(s), 8.22(s)
31	Formate	HCOOH	8.46(s)
32	Trimethylamine-N-oxide (TMAO)	CH ₃	3.28(s)

Figure 5B, which could be served as differential metabolites for assessing the leukopenia and the effect of Lvjiaobuxue granule.

Establishment of “Spleen Differential Metabolite-Target/Metabolic Enzyme-Related Metabolite” Network

The metabolic networks involved in a series of enzymes and genes were constructed by using the Metscape plug-in running on Cytoscape 3.7.1, that the internal correlation of the differential metabolites based on enzyme or gene levels could be better understood (**Figure 6**). As a result, 154 candidate genes or enzymes related to differential metabolites were tentatively found out, and they will be served as targets for subsequent biological targets network analysis for the construction of targets-metabolites interactions network (**Figure 6**). Finally, to find the metabolic pathway of identified differential metabolites from leukopenia-associated researches, the enrichment analysis was performed and metabolic pathways were obtained for further investigation.

Network Pharmacology and Metabolomics Integration Analysis

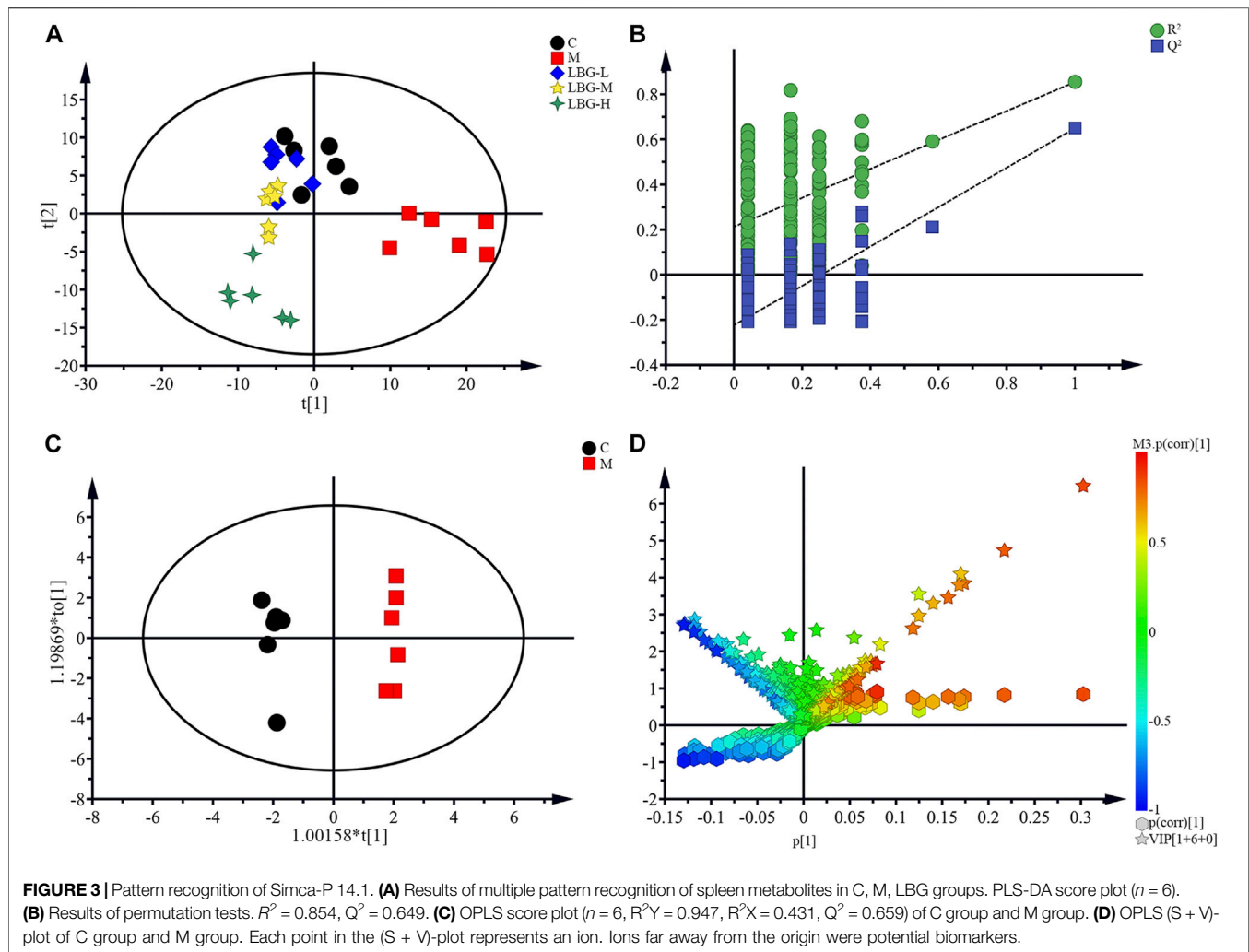
Screening Active Compounds of Lvjiaobuxue Granule

In the current study, two ADME-related parameters, including OB and DL, were employed to screen for active ingredients in Lvjiaobuxue granule. After ADME screening, some ingredients that did not meet

the screening criteria were selected because of their high content and high biological activity. First of all, a gross of 87, 134, 76, 55, and 125 candidate ingredients were obtained from *Astragalus mongholicus* Bunge (Fabaceae; *Astragalus mongholicus* radix), *Codonopsis pilosula* (Franch.) Nannf (Campanulaceae; *Codonopsis pilosula* radix), *Rehmannia glutinosa* (Gaertn.) DC (Orobanchaceae; *Rehmannia glutinosa* root), *Atractylodes macrocephala* Koidz (Asteraceae; *Atractylodes macrocephala* rhizoma) and *Angelica sinensis* (Oliv.) Diels (Apiaceae; *Angelica sinensis* radix) respectively. The ingredients were retrieved from these ingredients via the ADME parameters and literature confirmation. Consequently, a total of 32 active ingredients of Lvjiaobuxue granule were filtered out for further analysis (**Supplementary Table S1**).

Construction of “Chemical Components-Targets-Differential Metabolites” Regulatory Network and Correlative Pathways

490 targets of the 32 active ingredients in Lvjiaobuxue granule were predicted using the PharmMapper server, and 28 of them were closely related to differential metabolites of leukopenia with a total frequency of 496 (**Supplementary Table S2**). Cytoscape software was used to establish the “chemical components-targets-differential metabolites” regulatory network of Lvjiaobuxue granule, which was an indication that the correlations of 32 active ingredients, 28 metabolite-associated target proteins, and 11 differential metabolites were presented in **Figure 7**. Analysis of the “active ingredients-targets” correlation



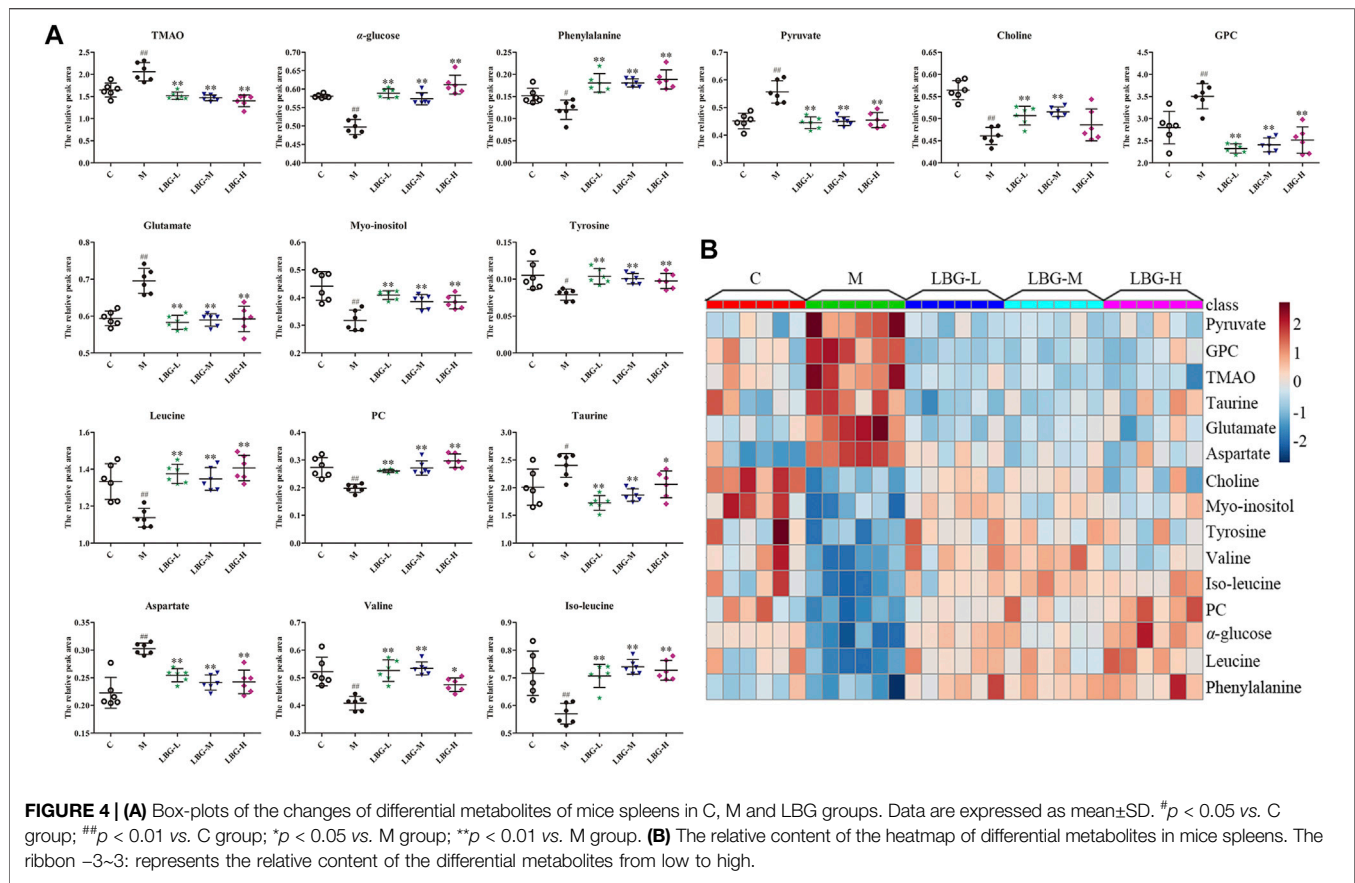
revealed that multiple compounds could act on the same target, and multiple targets could be affected by the same compound. For instance, the L-amino-acid oxidase could be the target of ferulic acid, caffeic acid, biatractylolide simultaneously, while the compound of catalpol could act on Aldo-keto reductase family one member B1, Eukaryotic translation initiation factor 4E-binding protein 3, and Glucose-6-phosphatase at the same time (Figure 7).

To assess the molecular mechanisms of Lvjiaobuxue granule effects on leukopenia, the Cytoscape with its plugin ClueGO was utilized for KEGG pathway analysis, followed by the analysis of target-related pathway. A total of nine significant pathways were predicted ($p < 0.05$), among which the valine, leucine and isoleucine degradation were the most closely related (Table 3). According to the results of biological targets network and metabolomics, the mechanism of increasing leukocyte activity of Lvjiaobuxue granule was preliminarily predicted as follows: Lvjiaobuxue granule can inhibit the valine, leucine and isoleucine degradation and add the levels of valine, leucine and isoleucine (Figure 4A).

Molecular Docking Verification

KEGG pathway analysis revealed that the decomposition pathway of valine, leucine and isoleucine was the most

important way for the Lvjiaobuxue granule to improve cyclophosphamide-induced leukopenia in 4T1 tumor-bearing mice (Table 3), and then constructed the chemical component-target-differential metabolite regulatory network. **Supplementary Figure S2** showed 35 compounds, seven metabolite-related target proteins, and three correlation of different metabolites. Furthermore, the SystemsDock (<http://systemsdock.unit.oist.jp/iddp/home/index>) method was used to evaluate the binding potential between selected valine, leucine and isoleucine degradation pathway targets and the chemical components with top 7[°] (Degree ≥ 5) (**Supplementary Figure S2**). The docking score of SystemsDock can directly indicate the protein-ligand binding potential. The 3D structures and PDB ID of the above seven selected targets were gathered from the PDB database (<https://www.rcsb.org/>) (**Supplementary Table S3**). The results showed that six targets (ACAA2, BCAT1, BCAT2, DLD, HADHA, and IL4I1) had 3D structures, while the 3D structure of ACAA1 did not exist. As shown in **Supplementary Figure S3**, the docking scores of 95 pairs of target-compound combinations were mostly greater than native ligand, which showed that they possessed great binding activity.



Experimental Validation of BCAAs Catabolism Pathway by ELISA

To further confirm the results of the biological targets network, we verified the BCAAs catabolism pathway. Two key and irreversible reactions of BCAAs catabolism require the participation of branched-chain keto acid dehydrogenase (BCKDH) complex and acyl-CoA dehydrogenase (ACAD). The levels of BCKDHA and ACADS were significantly increased ($p < 0.01$) in the model group (Figure 8). After oral administration of Lvjiaobuxue granule, the levels of BCKDHA and ACADS were significantly reduced ($p < 0.05$ or $p < 0.01$). The BCKDHA and ACADS enzyme levels in the model group were significantly increased in the catabolism pathway of BCAAs. Abnormal expression of BCAAs degrading enzymes cause BCAAs to overly decomposed in the model group. Lvjiaobuxue granule can reverse the levels of two enzymes, thereby improving the abnormal metabolism of BCAAs. In the leukopenia model group, the abnormal expression of BCAAs degrading enzyme lead to the excessive decomposition of BCAAs.

DISCUSSION

In this study, we observed the pharmacological effects profiles of low, moderate and high dose Lvjiaobuxue granule on the increase of leukocytes in 4T1 tumor-bearing mice model of leukopenia induced

by cyclophosphamide for the first time. The major new findings were that Lvjiaobuxue granule could improve cyclophosphamide-induced leukopenia in 4T1 tumor-bearing mice, accelerate the recovery of spleen, thymus and liver indices, accelerate the recovery of WBC, NE, LY, Mo, and RBC contents, and the recovery of spleen metabolite levels in the mice spleen caused by leukopenia. Thus, the *in vivo* treatment with Lvjiaobuxue granule accelerated recovery of leukopenia after chemotherapy in mice. In this study, an integrated approach of metabolomics and network pharmacology was performed to explore the biological mechanisms of Lvjiaobuxue granule in the treatment of cyclophosphamide induced leukopenia in 4T1 tumor-bearing mice. According to the results of network pharmacology and metabolomics, that regulation on the BCAAs catabolism pathway may play a key role in cyclophosphamide induced leukopenia in 4T1 tumor-bearing mice after the treatment of a typical TCM of Lvjiaobuxue granule.

Construction of Leukopenia Model in 4T1 Tumor-Bearing Mice and Dosage Screening of Lvjiaobuxue Granule

Cyclophosphamide, a cell cycle non-specific anti-tumor drug, is one of the most commonly used drugs for establishing an animal model of leukopenia (Huyan et al., 2011; Qu et al., 2016). The cyclophosphamide can easily block the division and proliferation

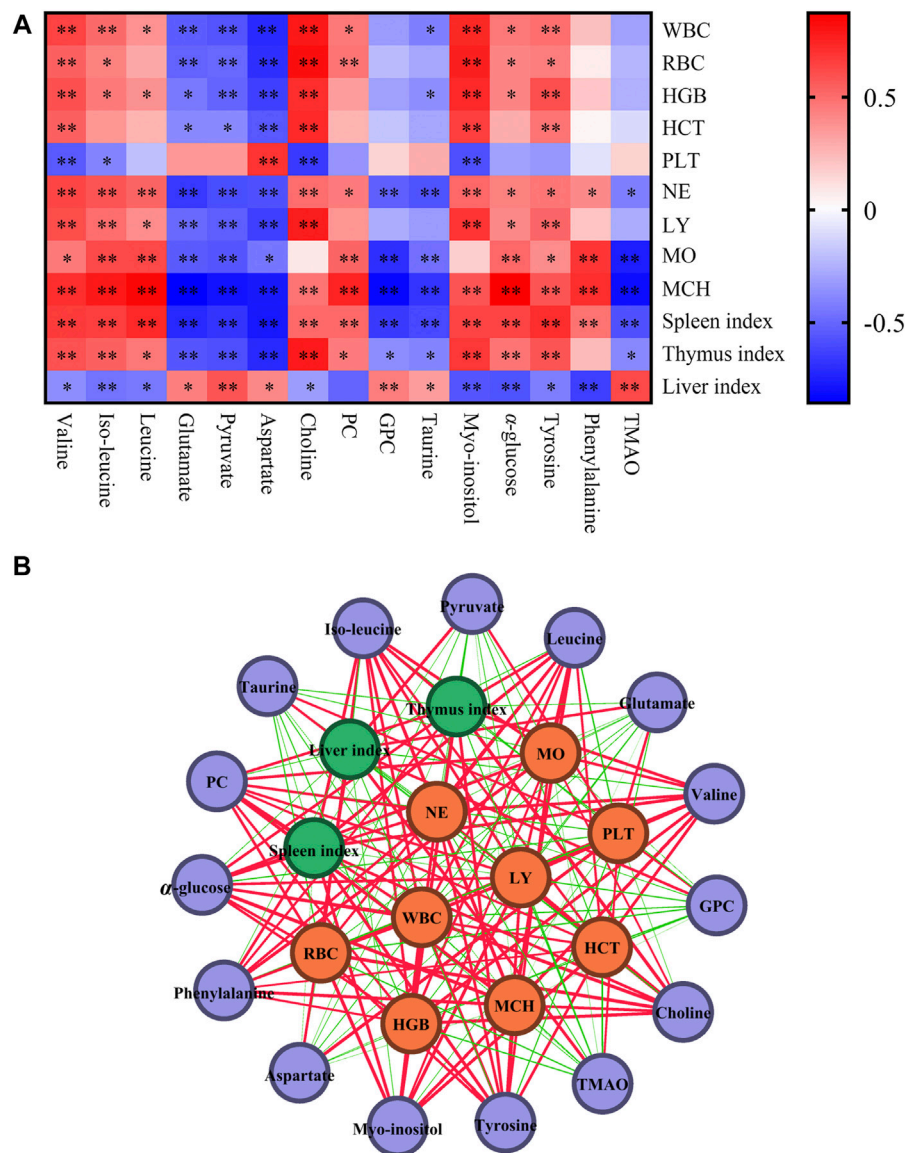
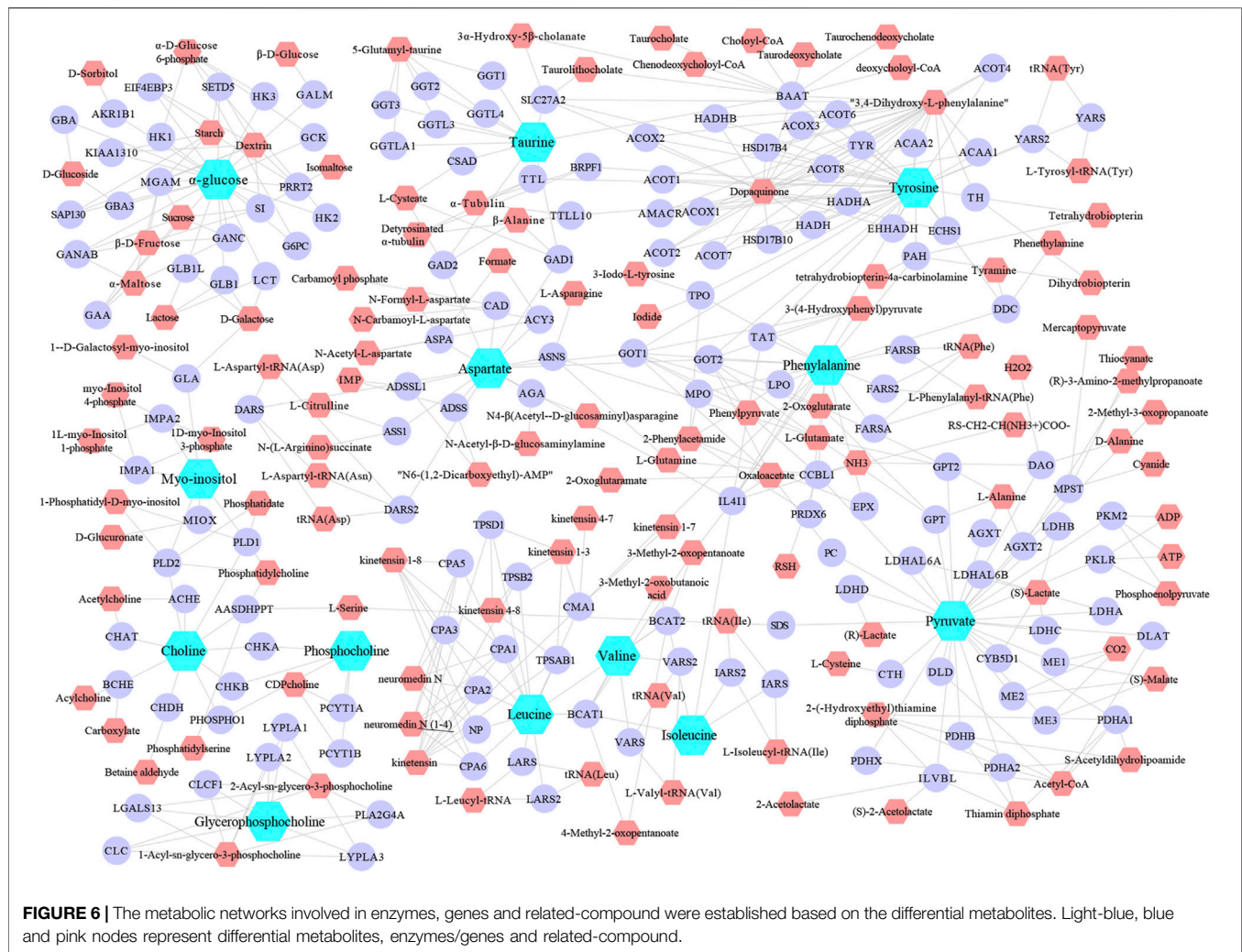


FIGURE 5 | Correlation analysis of differential metabolites, blood routine parameters and organ indexes. **(A)** The correlation map of differential metabolites, blood routine parameters and organ indexes. Red and blue represent positive and negative correlations respectively (* $p < 0.05$, ** $p < 0.01$). **(B)** Correlation network of differential metabolites, blood routine parameters and organ indexes based on Pearson's correlation coefficients. Purple, yellow and green nodes represent differential metabolites, blood routine parameters and organ indexes. Red and green lines represent positive and negative correlations. Line thickness reflects the magnitude of the correlation coefficients.

of normal hematopoietic cells, lead to impaired bone marrow regeneration or damage to the hematopoietic system, decrease the number of bone marrow nucleated cells, and decrease hematopoietic reconstitution activity. Among them, leukopenia is the most common result (Fan et al., 2017; Luo et al., 2017). By combing the references, the cyclophosphamide-induced leukopenia model has been relatively mature, but the mouse species, dosage and duration are different, and it is mostly used to stimulate bone marrow suppression and immunosuppression caused by chemotherapy (Huang et al., 2017; Khan, 2017; Zhang et al., 2017; Sun et al., 2018). However, in clinical practice, the cyclophosphamide is used for chemotherapy in

cancer patients, while animal models are often used in normal mice, which is different from clinical practice. Therefore, in this study, cyclophosphamide was used for the first time to induce a 4T1 tumor-bearing mice leukopenia model to simulate clinical and pathophysiology.

The research previously conducted a dose screening on the cyclophosphamide-induced leukopenia model, and found that the effect of Lvjaobuxue granule in increasing leukocytes was not dose-dependent, and the dose of 24 g/kg Lvjaobuxue granule caused a sharp increase in white blood cells. Exceeding the normal level, affecting the normal level of the body. Among them, 6 g/kg has the most significant effect on white blood cell



improvement. Therefore, during the experiment, we chose 3 g/kg, 6 g/kg, 12 g/kg three doses (He, 2018). DST is a pure Chinese medicine preparation composed of *Sanguisorba officinalis* Linn (Rosaceae; *Sanguisorba officinalis* radix) single medicine, which can stimulate bone marrow hematopoiesis, promote the proliferation and differentiation of hematopoietic stem progenitor cells, increase the number of blood cells produced, and effectively improve the white blood cell level of leukopenia. Radiotherapy and chemotherapy can cause bone marrow suppression in cancer patients, and their hematopoietic microenvironment will also be destroyed. In addition, DST can prevent the DNA damage of bone marrow hematopoietic cells caused by radiotherapy and chemotherapy, and have the effect of protecting the hematopoietic microenvironment (Jia et al., 2012; Zhu et al., 2020). It has a good clinical effect in the treatment of leukopenia without adverse side effects.

Blood Routine Parameters

Hematopoietic dysfunction including leukopenia, hematopoietic suppression and immunosuppression were observed in patients receiving cyclophosphamide with

malignant tumors. The occurrence of leukopenia may be related to hematopoietic stem cell dysfunction, apoptosis of bone marrow cells and imbalance of hematopoietic regulatory factors (Cook and Nutini, 1971; Christen et al., 2017). Thus rebuilding hematopoietic function is the primary problem of adjuvant chemotherapy. In this study, significant decreases in WBC, NE, LY, MO, RBC, and HGB were observed through the impact of cyclophosphamide, and these altered blood routine parameters were regulated by Lvjiabuxue granule treatment. The cyclophosphamide can degrade to amido nitrogen mustard, acrolein and so on, which bind to the DNA of rapidly growing cells and produce strong toxicity in the cells, while Lvjiabuxue granule may play a role in leukocyte elevation through the reduction of DNA damage and improvement of bone marrow hematopoietic function (Stroda et al., 2017). In addition, the results of this study identified 15 differential metabolites in nuclear magnetic metabolomics, and the correlation analysis showed that the decreased content of differential metabolites was positively correlated with blood routine index levels, indicating that blood routine test results were correlated with metabolomics.

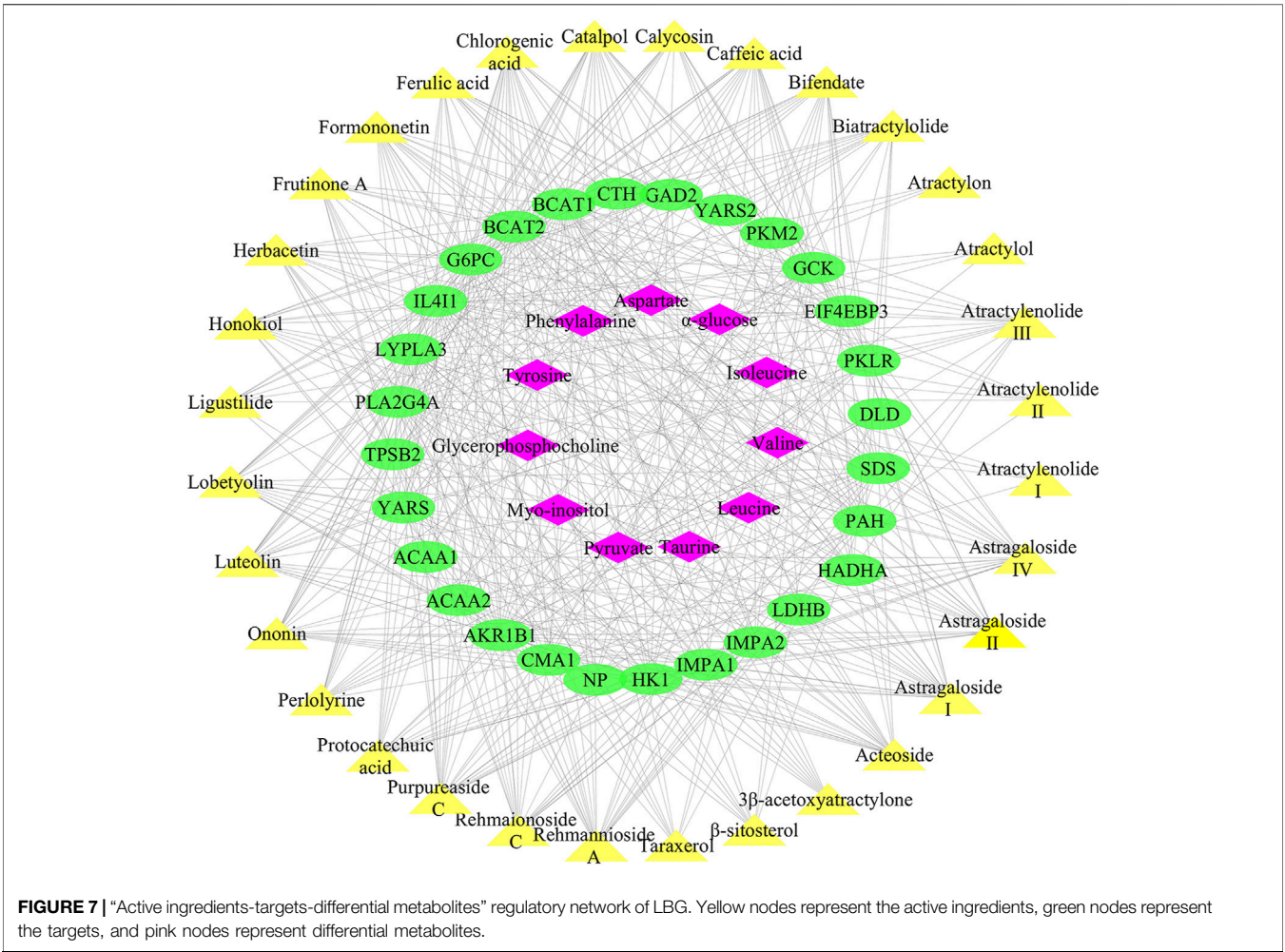


TABLE 3 | The results of KEGG correlative pathways of LBG major active ingredient related targets were analyzed by Cytoscape 3.7.1 software.

Rank	KEGG term	p-value	Associated genes found
1	Valine, leucine and isoleucine degradation	2.76E-10	ACAA1, ACAA2, BCAT1, BCAT2, DLD, HADHA, IL4I1
2	Glycolysis/Gluconeogenesis	3.46E-9	DLD, G6PC, GSK, HK1, LDHB, PKLR, PKM
3	Cysteine and methionine metabolism	1.06E-8	BCAT1, BCAT2, CTH, IL4I1, LDHB, SDS
4	Galactose metabolism	4.41E-6	AKR1B1, G6PC, GSK, HK1
5	Pyruvate metabolism	1.13E-5	DLD, LDHB, PKLR, PKM
6	Propanoate metabolism	2.10E-4	DLD, HADHA, LDHB
7	Starch and sucrose metabolism	2.99E-4	G6PC, GSK, HK1
8	Glycine, serine and threonine metabolism	4.10E-4	CTH, DLD, SDS
9	Fatty acid degradation	5.44E-4	ACAA1, ACAA2, HADHA

The results were consistent, which verified the reliability of metabolomics results to a certain extent.

Organ Indexes

As the most important immune organs in mammals, spleen and thymus are the places where immune cells grow and proliferate (Zhang et al., 2012). The developmental status of the spleen and thymus directly affects immune function and disease resistance (Duan et al., 2017; Sasaguri et al., 2017;

Mahaki et al., 2019). The results of this experiment showed that the spleen and thymus indexes of the high, moderate and low dose Lvjiabuxue granule groups were significantly higher than those of the model group. It was suggested that Lvjiabuxue granule could resist the toxic effects of cyclophosphamide on the development of spleen and thymus. Cyclophosphamide is a commonly used chemotherapeutic drug in clinical practice. It kills tumor cells but also destroys normal cells. It is hydrolyzed by

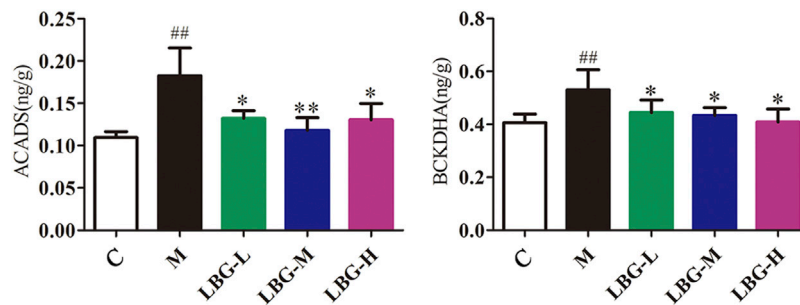


FIGURE 8 | Expression of ACADS and BCKDHA enzyme levels in mice liver tissue using ELISA analysis. Data are expressed as mean \pm SD. ^{##} $p < 0.01$ vs. C group; ^{*} $p < 0.05$ vs. M group; ^{**} $p < 0.01$ vs. M group.

excessive phosphatases or phosphatases in the liver or tumors. Therefore, the liver is the main metabolic site of cyclophosphamide. (Lin et al., 2017; Yang et al., 2018). Moreover, the liver is the main drug metabolism organ in mammals. Metabolized cyclophosphamide causes damage to mitochondria and damage to cellular respiration, which affects the onset of lipid peroxidation and an increase in reactive oxygen species (Stankiewicz and Skrzydlewska, 2003; Olayinka et al., 2015). In this study, significant increases in the liver index were observed through the impact of cyclophosphamide, and these altered were regulated by Lvjiabuxue granule' treatment. Hence, Lvjiabuxue granule may play an important role in improving liver index by reducing lipid peroxidation and reactive oxygen species production.

Integration of Metabolomics and Network Pharmacology

Metabolomics are limited to a listing of potential metabolites and related pathways without further exploration of their direct relationships. Network pharmacology can further validate the therapeutic regulation of metabolic networks and facilitate the identification of key targets and biomarkers. The organic combination of network pharmacology and metabolomics effectively explains how Lvjiabuxue granule can regulate metabolite levels by intervening in metabolic enzymes in the body, thereby improving the mechanism of leukopenia. KEGG analysis results shown that Lvjiabuxue granule may improve leukopenia in mice by regulating the catabolic pathways of valine, leucine and isoleucine.

BCAAs Catabolism

The BCAAs are essential amino acids for human body, which cannot be synthesized *in vivo* and can only be obtained from food. BCAAs catabolism has been focused on a great deal of diseases, especially liver cirrhosis, renal failure, sepsis and cancer (Figure 9) (Holeček, 2018). Numerous studies have shown that BCAAs have a positive effect on regulating body weight, muscle protein synthesis, insulin secretion, the aging process, and prolonging the healthy period (Ikeda et al., 2018; Xu et al., 2018;

Yamada et al., 2018). BCAAs have been shown to an important role in regulating body metabolism and maintaining energy balance by directly affecting body tissues, such as white adipose tissue, liver tissue and muscle tissue (Lashinger et al., 2011). BCAAs can be used as energy substrates in catabolic states, which can be directly oxidized or converted to glycogen isolipoproteins in the muscle. In contrast, BCAAs stimulate protein synthesis and cell growth in anabolic conditions (De Palo et al., 2001).

In the current study, we used 19 potential active ingredients of Lvjiabuxue granule as a probe to conduct molecular docking with potential targets of BCAAs catabolism, and the molecular docking showed that they possessed great binding activity. A study revealed that astragaloside IV, formononetin, calycosin and ferulic acid showed promoting hematopoiesis through regulating cyclin-related proteins, promoting cell cycle transformation, and promoting HSC proliferation (Liu et al., 2015). Another study showed that caffeic acid can down-regulated the expression of TLR-2 and HLA-DR, and inhibited the production of cytokines, then exerted an immunomodulatory action on human monocytes (Búfalo and Sforzin, 2015). Studies of receiver biases suggested that the chemical components of the Lvjiabuxue granule have a better activity of immunity regulation and hematopoiesis. The results of molecular docking showed that there were complex interactions between them, which showed the characteristics of multi-components and multi-targets. In this study, the levels of valine, leucine and isoleucine decreased significantly in the cyclophosphamide-induced mice, which was a suggestion that the leukopenia was associated with the branched-chain amino acids catabolism. Moreover, the branched-chain amino acids were positively correlated with WBC, NE, LY, and MO in the leukopenia mice, which were an indication that they played key roles in the progression of leukopenia. Compared with cyclophosphamide-induced mice, the levels of valine, leucine, and isoleucine can be improved significantly in the Lvjiabuxue granule groups, which was a suggestion that the Lvjiabuxue granule could play a key role in the leukocyte elevation effect by inhibiting the BCAAs catabolism. In this study, two key enzymes, the BCKDHA and ACADS enzyme levels in leukopenia, significantly increased in the BCAAs catabolism pathway. Abnormal expression of BCAAs degrading enzymes causes

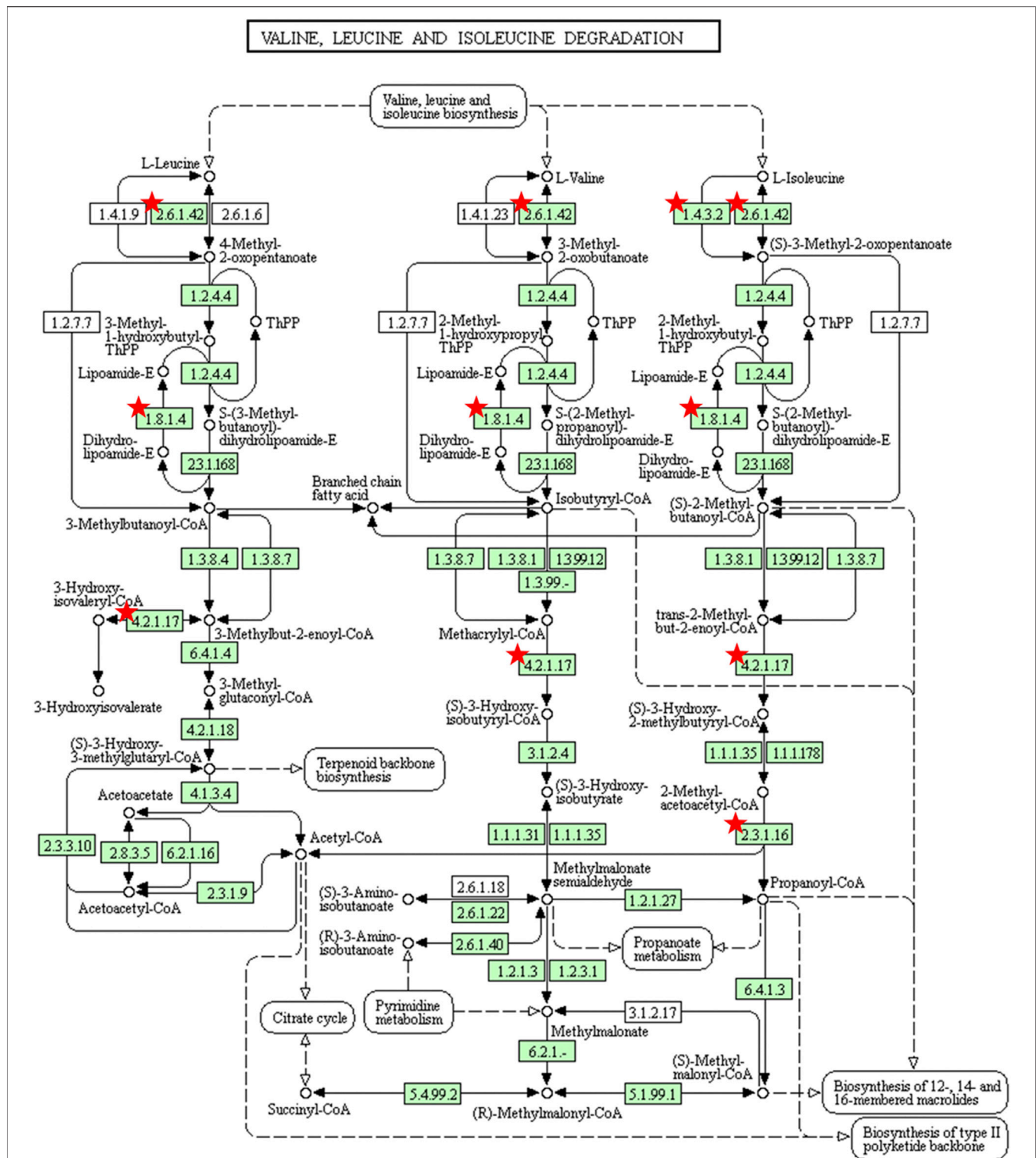


FIGURE 9 | Pathway of branched-chain amino acids catabolism found by KEGG Pathway maps. The organism-specific pathways are colored green, where coloring indicates that map objects exist and are linked to corresponding entries. The red stars mark potential targets of LBG in pathways. It is indicated that *Lyjiaobuxue* granule attenuates cyclophosphamide-induced leukopenia by regulating branched-chain amino acids catabolism pathway.

BCAAs overly decomposed in leukopenia model mice. Lvjiaobuxue granule can reverse the levels of two enzymes, thereby improving the abnormal metabolism of BCAAs.

Although this study had systematically explained the mechanism of Lvjiaobuxue granule, there are still the following aspects worthy of further study:

- 1). At the metabolite level, this study only used ¹H-NMR metabolomics technology to reveal the changes in the level of branched-chain amino acids, and only detected the upstream metabolites leucine, isoleucine and valine in the catabolism of BCAAs. Unable to detect its downstream substances.
- 2). At the genetic level, although this study uses the method of network prediction to find out the genes that affect the changes of metabolites and the genes regulated by Lvjiaobuxue granule, it is still necessary to further determine the accuracy of the prediction results.
- 3). At the level of enzymes and proteins, this study only used ELISA to determine the content of the key metabolic enzymes ACADS and BCKDHA in the BCAAs catabolic pathway, but it is not known whether the enzyme activity changes when the BCAAs catabolic pathway changes.
- 4). At the pathway level, this study conducted a systematic study on the regulation of BCAAs from the metabolite to the molecular level. However, both KEGG pathway analysis and metabolomics results show that Lvjiaobuxue granule have effects on other pathways [amino acid metabolism (glutamine, phenylalanine), energy metabolism and choline metabolism, etc.] and metabolites (choline, tyrosine, phenylalanine, etc.) also have a certain effect. In view of the overall regulatory effect of TCM, it is not comprehensive to study only the decomposition pathway of BCAAs.

CONCLUSION

In summary, we first established a model of leukopenia after chemotherapy, which can be used to study the effect of drugs on leukopenia. Determine the method and dosage of cyclophosphamide. This model can reflect the pathophysiological nature of clinical patients. Based on metabolomics and network pharmacology, a new comprehensive strategy was developed to construct an “active ingredients-targets-differential metabolites” network, which involved 32 active ingredients, 28 potential targets, and 11 differential metabolites. KEGG results showed that Lvjiaobuxue granule can improve leukopenia in mice by regulating the decomposition pathway of valine, leucine and isoleucine (BCAAs). The molecular docking results showed that the active ingredients of Lvjiaobuxue granule and the six targets on the decomposition pathway of BCAAs had a high binding force, indicating the reliability of the biological target network analysis results. Molecular biology verification

results showed that Lvjiaobuxue granule can significantly reduce the key metabolic enzymes ACADS and BCKDHA in the catabolism of BCAAs, thereby playing a role in the treatment of leukopenia. This research provided data and theoretical support for in-depth study of its mechanism, and lay a foundation for clinical application.

DATA AVAILABILITY STATEMENT

The raw data supporting the conclusions of this article will be made available by the authors, without undue reservation, to any qualified researcher.

ETHICS STATEMENT

The animal study was reviewed and approved by The animal use protocol listed below has been reviewed and approved by the Committee of Scientific Research at Shanxi University (CSRSX), and the approved number was SXULL2018012.

AUTHOR CONTRIBUTIONS

JT, HZ, and QW conceived and performed the experiments; JT and HZ wrote the paper; HZ, YG, and QW analyzed the data, HX, XX, SH, and DY assisted in the execution of research; XQ design of the study and writing the protocol; All authors have understood, concurred and approved the final edition of this manuscript.

FUNDING

This work was financially supported by the National S&T Major Projects for “Major New Drugs Innovation and Development” (2017ZX09301047); the China Postdoctoral Science Foundation Funded Project (2016M602414); the Science and Technology of Shanxi Province (201903D321210).

ACKNOWLEDGMENTS

The experiments involved in this institute were completed at the Modern Research Center for Traditional Chinese Medicine, Shanxi University. The authors of this study are grateful for their supporters and funding support.

SUPPLEMENTARY MATERIAL

The Supplementary Material for this article can be found online at: <https://www.frontiersin.org/articles/10.3389/fphar.2021.657047/full#supplementary-material>

REFERENCES

- An, M. P., Zhang, S. Y., Zhang, Y., Zhu, Z. N., Hu, J. F., and Shen, X. P. (2018). Effect of Asini Corii Colla on Immune Function in Hypoimmune Mice. *Drug Eval. Res.* 41, 567–571.
- Búfalo, M. C., and Sforzin, J. M. (2015). The Modulatory Effects of Caffeic Acid on Human Monocytes and its Involvement in Propolis Action. *J. Pharm. Pharmacol.* 67, 740–745. doi:10.1111/jphp.12364
- Christen, D., Brümendorf, T., and Panse, J. (2017). Leukopenie - ein diagnostischer Leitfaden für die Praxis. *Dtsch. Med. Wochenschr.* 142, 1744–1749. doi:10.1055/s-0043-113123
- Cook, E. S., and Nutini, L. G. (1971). Counteraction of Leukopenia Caused by Mechlorethamine and Azathioprine. *J. Surg. Oncol.* 3, 131–141. doi:10.1002/jso.2930030206
- De Palo, E. F., Gatti, R., Cappellin, E., Schiraldi, C., De Palo, C. B., and Spinella, P. (2001). Plasma Lactate, GH and GH-Binding Protein Levels in Exercise Following BCAA Supplementation in Athletes. *Amino Acids* 20, 1–11. doi:10.1007/s007260170061
- Deng, J., Zhong, Y.-F., Wu, Y.-P., Luo, Z., Sun, Y.-M., Wang, G.-E., et al. (2018). Carnosine Attenuates Cyclophosphamide-Induced Bone Marrow Suppression by Reducing Oxidative DNA Damage. *Redox Biol.* 14, 1–6. doi:10.1016/j.redox.2017.08.003
- Duan, X., Gao, S., Li, J., Wu, L., Zhang, Y., Li, W., et al. (2017). Acute Arsenic Exposure Induces Inflammatory Responses and CD4+ T Cell Subpopulations Differentiation in Spleen and Thymus with the Involvement of MAPK, NF- κ B, and Nrf2. *Mol. Immunol.* 81, 160–172. doi:10.1016/j.molimm.2016.12.005
- Fan, C., Georgiou, K. R., Morris, H. A., Mckinnon, R. A., Keefe, D. M. K., Howe, P. R., et al. (2017). Combination Breast Cancer Chemotherapy with Doxorubicin and Cyclophosphamide Damages Bone and Bone Marrow in a Female Rat Model. *Breast Cancer Res. Treat.* 165, 41–51. doi:10.1007/s10549-017-4308-3
- Futamura, M., Nagao, Y., Ishihara, K., Takeuchi, M., Nakada, T., Kawaguchi, Y., et al. (2017). Preoperative Neoadjuvant Chemotherapy Using Nanoparticle Albumin-Bound Paclitaxel Followed by Epirubicin and Cyclophosphamide for Operable Breast Cancer: a Multicenter Phase II Trial. *Breast Cancer* 24, 615–623. doi:10.1007/s12282-016-0748-6
- Gertsch, J. (2011). Botanical Drugs, Synergy, and Network Pharmacology: Forth and Back to Intelligent Mixtures. *Planta Med.* 77, 1086–1098. doi:10.1055/s-0030-1270904
- Gu, J. F., Feng, L., Zhang, M. H., Qin, D., and Jia, X. B. (2014). New Exploration on Effect of Characteristics of Traditional Chinese Medicine Components Structure on Multi-Ingredient/component Pharmacokinetics. *Zhongguo Zhong Yao Za Zhi.* 39, 2782–2786.
- He, X. Y. (2018). *Studies on the Mechanism on Leucopenia of Lvjiao Buxue Granules and its Metabolic Network Regulation Function*. Shanxi: Shanxi University.
- He, X. Y., Yan, L., Xu, X. P., Huang, S., Yan, D. L., Qin, X. M., et al. (2018). Investigation on Positive Effect and Possible Mechanisms of Lvjiao Buxue Granules Treatment on Cyclophosphamide-Induced Leukopenia Mice through 1H-NMR Based Metabolomics Approach. *Chin. Tradit. Herbal Drugs* 49, 2282–2290. doi:10.7501/j.issn.0253-2670.2018.10.008
- Holeček, M. (2018). Branched-chain Amino Acids in Health and Disease: Metabolism, Alterations in Blood Plasma, and as Supplements. *Nutr. Metab. (Lond)* 15, 33. doi:10.1186/s12986-018-0271-1
- Hu, Q.-d., Wu, W.-h., Zeng, Y., Wen, J., Li, X.-j., Pan, W., et al. (2018). Blood Metabolism Study on protection of Residual Renal Function of Hemodialysis Patients by Traditional Chinese Medicine Kidney Flaccidity Compound. *Cell Mol Biol. (Noisy-le-grand)* 64, 107–112. doi:10.14715/cmb/2018.64.5.18
- Huang, J.-q., Pang, M.-r., Li, G.-y., Wang, N., Jin, L., and Zhang, Y. (2017). Alleviation of Cyclophosphamide-Induced Immunosuppression in Mice by Naturally Acetylated Hemicellulose from Bamboo Shavings. *Food Agric. Immunol.* 28, 328–342. doi:10.1080/09540105.2016.1272553
- Huang, Y. Y., Zhang, Y., Kang, L. P., Yu, Y., and Guo, L. P. (2018). Research Progress on Chemical Constituents and Their Pharmacological Activities of Plant from Codonopsis. *Chin. Tradit. Herbal Drugs* 49, 239–250.
- Hung, C.-M., Hsu, Y.-C., Chen, T.-Y., Chang, C.-C., and Lee, M.-J. (2017). Cyclophosphamide Promotes Breast Cancer Cell Migration through CXCR4 and Matrix Metalloproteinases. *Cell Biol Int.* 41, 345–352. doi:10.1002/cbin.10726
- Huyan, X.-H., Lin, Y.-P., Gao, T., Chen, R.-Y., and Fan, Y.-M. (2011). Immunosuppressive Effect of Cyclophosphamide on white Blood Cells and Lymphocyte Subpopulations from Peripheral Blood of Balb/c Mice. *Int. Immunopharmacology* 11, 1293–1297. doi:10.1016/j.intimp.2011.04.011
- Ikeda, T., Jinno, T., Masuda, T., Aizawa, J., Ninomiya, K., Suzuki, K., et al. (2018). Effect of Exercise Therapy Combined with Branched-Chain Amino Acid Supplementation on Muscle Strengthening in Persons with Osteoarthritis. *Hong Kong Physiother. J.* 38, 23–31. doi:10.1142/s1013702518500038
- Jia, L. L., Xi, W., and Jin, G. L. (2012). Effect of Diyu Shengbai Tablets on Bone Marrow Depression Induced by Cyclophosphamide in Mice. *Chin. J. Exp. Tradit. Med. Form* 18, 251–254. doi:10.1007/s11655-011-0950-5
- Khan, M. A. (2017). Immune Potentiating and Antitoxic Effects of Camel Milk against Cyclophosphamide-Induced Toxicity in BALB/C Mice. *Int. J. Health Sci. (Qassim)* 11, 18–22.
- Lashinger, L. M., Malone, L. M., Brown, G. W., Daniels, E. A., Goldberg, J. A., Otto, G., et al. (2011). Rapamycin Partially Mimics the Anticancer Effects of Calorie Restriction in a Murine Model of Pancreatic Cancer. *Cancer Prev. Res.* 4, 1041–1051. doi:10.1158/1940-6207.capr-11-0023
- Li, R. X., and Fan, F. Y. (1998). Clinical Observation on 100 Cases of Primary Leukopenia Treated with Lvjiao Buxue Granules. *Hunan J. Tradit. Chin. Med.* 14, 27–28.
- Lin, S., Hao, G., Long, M., Lai, F., Li, Q., Xiong, Y., et al. (2017). Oyster (*Ostrea Plicatula* Gmelin) Polysaccharides Intervention Ameliorates Cyclophosphamide-Induced Genotoxicity and Hepatotoxicity in Mice via the Nrf2-ARE Pathway. *Biomed. Pharmacother.* 95, 1067–1071. doi:10.1016/j.biopha.2017.08.058
- Liu, M., Li, P., Zeng, X., Wu, H., Su, W., and He, J. (2015). Identification and Pharmacokinetics of Multiple Potential Bioactive Constituents after Oral Administration of Radix Astragali on Cyclophosphamide-Induced Immunosuppression in Balb/c Mice. *Ijms* 16, 5047–5071. doi:10.3390/ijms16035047
- Luo, G. F., Tang, Y. H., Wu, L. F., Liu, X., Xu, Z., Zeng, G. R., et al. (2017). Haematology, Protective Effects of Qiangshengxue Oral Liquid on Chemotherapy-Induced Bone Marrow Suppression in Mice. *Chin. J. New Drugs* 26, 2664–2671.
- Mahaki, H., Jabarivassal, N., Sardarian, K., and Zamani, A. (2019). The Effects of Extremely Low-Frequency Electromagnetic fields on C-Maf, STAT6, and ROR α Expressions in Spleen and Thymus of Rat. *Electromagn. Biol. Med.* 38, 177–183. doi:10.1080/15368378.2019.1608832
- Mellor, D., Prieto, E., Mathieson, L., and Moscato, P. (2010). A Kernelisation Approach for Multiple D-Hitting Set and its Application in Optimal Multi-Drug Therapeutic Combinations. *PLoS One* 5, e13055. doi:10.1371/journal.pone.0013055
- Olayinka, E., Ore, A., Ola, O., and Adeyemo, O. (2015). Ameliorative Effect of Gallic Acid on Cyclophosphamide-Induced Oxidative Injury and Hepatic Dysfunction in Rats. *Med. Sci.* 3, 78–92. doi:10.3390/medsci3030078
- Qu, T., Wang, E., Li, A., Du, G., Li, Z., and Qin, X. (2016). NMR Based Metabolomic Approach Revealed Cyclophosphamide-Induced Systematic Alterations in a Rat Model. *RSC Adv.* 6, 111020–111030. doi:10.1039/c6ra18600a
- Sasaguri, K., Yamada, K., Narimatsu, Y., Oonuki, M., Oishi, A., Koda, K., et al. (2017). Stress-induced Galectin-1 Influences Immune Tolerance in the Spleen and Thymus by Modulating CD45 Immunoreactive Lymphocytes. *J. Physiol. Sci.* 67, 489–496. doi:10.1007/s12576-016-0478-8
- Simón-Manso, Y., Lowenthal, M. S., Kilpatrick, L. E., Sampson, M. L., Telu, K. H., Rudnick, P. A., et al. (2013). Metabolite Profiling of a NIST Standard Reference Material for Human Plasma (SRM 1950): GC-MS, LC-MS, NMR, and Clinical Laboratory Analyses, Libraries, and Web-Based Resources. *Anal. Chem.* 85, 11725–11731. doi:10.1021/ac402503m
- Singh, K., Trivedi, R., Verma, A., D'souza, M. M., Koundal, S., Rana, P., et al. (2017). Altered Metabolites of the Rat hippocampus after Mild and Moderate Traumatic Brain Injury - a Combined *In Vivo* and *In Vitro* 1 H-MRS Study. *NMR Biomed.* 30. doi:10.1002/nbm.3764

- Stankiewicz, A., and Skrzydlewska, E. (2003). Protection against Cyclophosphamide-Induced Renal Oxidative Stress by Amifostine: the Role of Antioxidative Mechanisms. *Toxicol. Mech. Methods* 13, 301–308. doi:10.1080/713857191
- Stroda, K. A., Murphy, J. D., Hansen, R. J., Brownlee, L., Atencio, E. A., Gustafson, D. L., et al. (2017). Pharmacokinetics of Cyclophosphamide and 4-hydroxycyclophosphamide in Cats after Oral, Intravenous, and Intraperitoneal Administration of Cyclophosphamide. *Am. J. Vet. Res.* 78, 862–866. doi:10.2460/ajvr.78.7.862
- Sun, H., Li, X.-n., Zhang, A.-h., Zhang, K.-m., Yan, G.-l., Han, Y., et al. (2019). Exploring Potential Biomarkers of Coronary Heart Disease Treated by Jing Zhi Guan Xin Pian Using High-Throughput Metabolomics. *RSC Adv.* 9, 11420–11432. doi:10.1039/c8ra10557j
- Sun, X., Zhao, Y.-n., Qian, S., Gao, R.-l., Yin, L.-m., Wang, L.-p., et al. (2018). Ginseng-Derived Panaxadiol Saponins Promote Hematopoiesis Recovery in Cyclophosphamide-Induced Myelosuppressive Mice: Potential Novel Treatment of Chemotherapy-Induced Cytopenias. *Chin. J. Integr. Med.* 24, 200–206. doi:10.1007/s11655-017-2754-8
- Tang, B. B., Zhou, D. H., He, X. M., and Zhang, X. P. (2018). Study on Medication Rule of TCM Compound Prescription in Treatment of Leukopenia after Radiotherapy and Chemotherapy for Malignant Tumor. *Acta Chin. Med.* 33, 1838–1842. doi:10.1002/14651858.CD010559.pub2
- Tian, J.-s., Meng, Y., Wu, Y.-f., Zhao, L., Xiang, H., Jia, J.-p., et al. (2019). A Novel Insight into the Underlying Mechanism of Baihe Dihuang Tang Improving the State of Psychological Suboptimal Health Subjects Obtained from Plasma Metabolic Profiles and Network Analysis. *J. Pharm. Biomed. Anal.* 169, 99–110. doi:10.1016/j.jpba.2019.02.041
- Tian, J.-S., Peng, G.-J., Wu, Y.-F., Zhou, J.-J., Xiang, H., Gao, X.-X., et al. (2016). A GC-MS Urinary Quantitative Metabolomics Analysis in Depressed Patients Treated with TCM Formula of Xiaoyaosan. *J. Chromatogr. B* 1026, 227–235. doi:10.1016/j.jchromb.2015.12.026
- Wang, W., Zhao, L., He, Z., Wu, N., Li, Q., Qiu, X., et al. (2018). Metabolomics-based Evidence of the Hypoglycemic Effect of Ge-Gen-Jiao-Tai-Wan in Type 2 Diabetic Rats via UHPLC-QTOF/MS Analysis. *J. Ethnopharmacology* 219, 299–318. doi:10.1016/j.jep.2018.03.026
- Xu, M., Kitaura, Y., Shindo, D., and Shimomura, Y. (2018). Branched-chain Amino Acid (BCAA) Supplementation Enhances Adaptability to Exercise Training of Mice with a Muscle-specific Defect in the Control of BCAA Catabolism. *Biosci. Biotechnol. Biochem.*, 1–4. doi:10.1080/09168451.2018.1440174
- Yamada, T., Matsuzaki, M., and Tanaka, A. (2018). Increase in Insulin Secretion and Decrease in Muscle Degradation by Fat-free Milk Intake Are Attenuated by Physical Exercise. *Clinica Chim. Acta* 484, 21–25. doi:10.1016/j.cca.2018.05.017
- Yang, L., Yan, C., Zhang, F., Jiang, B., Gao, S., Liang, Y., et al. (2018). Effects of Ketoconazole on Cyclophosphamide Metabolism: Evaluation of CYP3A4 Inhibition Effect Using the *In Vitro* and *In Vivo* Models. *Exp. Anim.* 67, 71–82. doi:10.1538/expanim.17-0048
- Yu, S. H. (1999). Overview of Clinical Application of Lvjiao Buxue Granules. *Hunan J. Tradit Chin. Med.* 15, 40–41.
- Zhang, L., Gong, A. G. W., Riaz, K., Deng, J. Y., Ho, C. M., Lin, H. Q., et al. (2017). A Novel Combination of Four Flavonoids Derived from Astragali Radix Relieves the Symptoms of Cyclophosphamide-Induced Anemic Rats. *FEBS Open Bio* 7, 318–323. doi:10.1002/2211-5463.12146
- Zhang, W., Zhu, J. H., Xu, H., Huang, X. P., Liu, X. D., and Deng, C. Q. (2019). Five Active Components Compatibility of Astragali Radix and Angelicae Sinensis Radix Protect Hematopoietic Function against Cyclophosphamide-Induced Injury in Mice and T-BHP-Induced Injury in HSCs. *Front. Pharmacol.* 10, 936. doi:10.3389/fphar.2019.00936
- Zhang, X. L., Lu, Y. S., Jian, J. C., and Wu, Z. H. (2012). Cloning and Expression Analysis of Recombination Activating Genes (RAG1/2) in Red Snapper (*Lutjanus Sanguineus*). *Fish Shellfish Immunol.* 32, 534–543. doi:10.1016/j.fsi.2012.01.001
- Zhong, Y., Luo, J., Tang, T., Li, P., Liu, T., Cui, H., et al. (2018). Exploring Pharmacological Mechanisms of Xuefu Zhuyu Decoction in the Treatment of Traumatic Brain Injury via a Network Pharmacology Approach. *Evid. Based Complement. Alternat Med.* 2018, 8916938. doi:10.1155/2018/8916938
- Zhu, L.-j., Chen, L., Bai, C.-f., Wu, A.-g., Liang, S.-c., Huang, F.-h., et al. (2020). A Rapid and Sensitive UHPLC-MS/MS Method for the Determination of Ziyuglycoside I and its Application in a Preliminary Pharmacokinetic Study in Healthy and Leukopenic Rats. *Biomed. Pharmacother.* 123, 109756. doi:10.1016/j.biopha.2019.109756

Conflict of Interest: JT, XX, SH, and DY were employed by Jiuzhitang Co. Ltd.

The remaining authors declare that the research was conducted in the absence of any commercial or financial relationships that could be construed as a potential conflict of interest.

Publisher's Note: All claims expressed in this article are solely those of the authors and do not necessarily represent those of their affiliated organizations, or those of the publisher, the editors and the reviewers. Any product that may be evaluated in this article, or claim that may be made by its manufacturer, is not guaranteed or endorsed by the publisher.

Copyright © 2021 Tian, Zhao, Gao, Wang, Xiang, Xu, Huang, Yan and Qin. This is an open-access article distributed under the terms of the Creative Commons Attribution License (CC BY). The use, distribution or reproduction in other forums is permitted, provided the original author(s) and the copyright owner(s) are credited and that the original publication in this journal is cited, in accordance with accepted academic practice. No use, distribution or reproduction is permitted which does not comply with these terms.

Advantages of publishing in Frontiers



OPEN ACCESS

Articles are free to read
for greatest visibility
and readership



FAST PUBLICATION

Around 90 days
from submission
to decision



HIGH QUALITY PEER-REVIEW

Rigorous, collaborative,
and constructive
peer-review



TRANSPARENT PEER-REVIEW

Editors and reviewers
acknowledged by name
on published articles

Frontiers

Avenue du Tribunal-Fédéral 34
1005 Lausanne | Switzerland

Visit us: www.frontiersin.org

Contact us: frontiersin.org/about/contact



REPRODUCIBILITY OF RESEARCH

Support open data
and methods to enhance
research reproducibility



DIGITAL PUBLISHING

Articles designed
for optimal readership
across devices



FOLLOW US

@frontiersin



IMPACT METRICS

Advanced article metrics
track visibility across
digital media



EXTENSIVE PROMOTION

Marketing
and promotion
of impactful research



LOOP RESEARCH NETWORK

Our network
increases your
article's readership